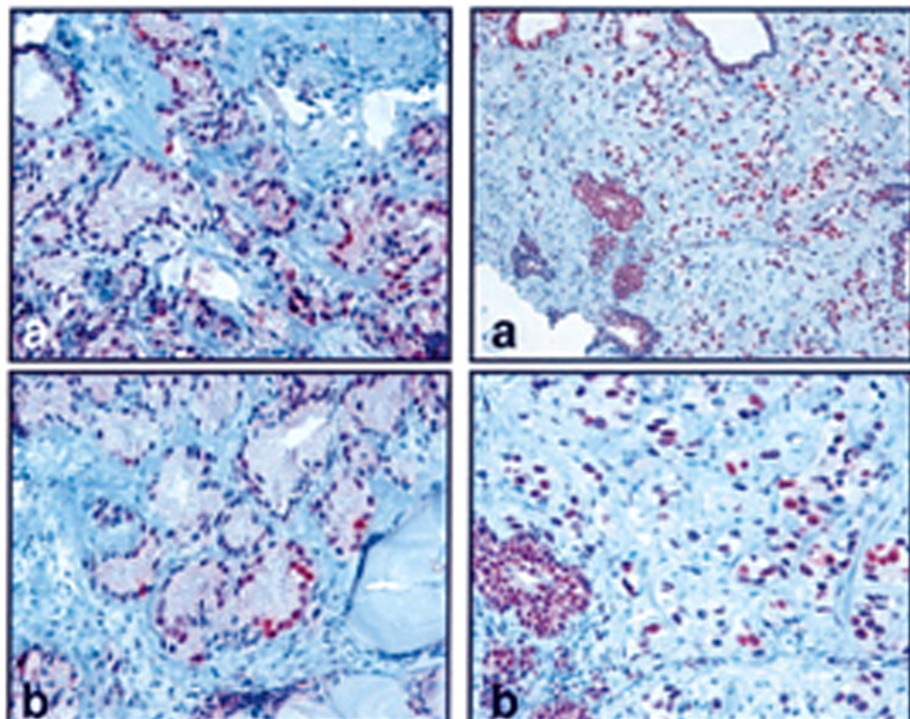Volume **2**

HANDBOOK OF

IMMUNOHISTOCHEMISTRY AND *IN SITU* HYBRIDIZATION OF HUMAN CARCINOMAS

MOLECULAR PATHOLOGY, COLORECTAL CARCINOMA, AND PROSTATE CARCINOMA

Carcinoma low-grade   Carcinoma high-grade

P53

a   a

b   b

EDITED BY **M.A. HAYAT**

Handbook of Immunohistochemistry and *in situ* Hybridization of Human Carcinomas, Volume 2

Handbook of Immunohistochemistry and *in situ* Hybridization of Human Carcinomas

Edited by M. A. Hayat

Volume 1
Molecular Genetics; Lung and Breast Carcinomas

Volume 2
Molecular Pathology, Colorectal Carcinoma, and Prostate Carcinoma

Handbook of Immunohistochemistry and *in situ* Hybridization of Human Carcinomas, Volume 2

Molecular Pathology, Colorectal Carcinoma, and Prostate Carcinoma

Edited by

M.A. Hayat

Distinguished Professor
Department of Biological Sciences
Kean University
Union, New Jersey

ELSEVIER
ACADEMIC
PRESS

Amsterdam • Boston • Heidelberg • London • New York • Oxford
Paris • San Diego • San Francisco • Singapore • Sydney • Tokyo

This book is printed on acid-free paper. ∞

To

Molecular Geneticists/Clinical Pathologists

This Page Intentionally Left Blank

Contents

This Page Intentionally Left Blank

Authors and Coauthors
of Volume 2

N.J. Agnantis (193)
Department of Pathology, Medical School, University of Ioannina, 45110 Ioannina, Greece

Juan Alfaro (399)
Department of Cell Biology and Genetics, University of Alcalá, 28871 Alcalá de Henares, Madrid, Spain

Kazuhiko Aoyagi (1)
Genetics Division, National Cancer Center Research Institute, 1-1, Tsukiji 5-chome, Chuo-ku, Tokyo 104-0045, Japan

María I. Arenas (399)
Department of Cell Biology and Genetics, University of Alcalá, 28871 Alcalá de Henares, Madrid, Spain

Arzu Atalay (113)
Bilkent University, Faculty of Science, Department of Molecular Biology and Genetics, 06800 Ankara, Turkey

Gabriela Aust (201)
University of Leipzig, Institute of Anatomy, Research Laboratories in the Department of Obstetrics and Gynecology, Ph.-Rosenthal-Str.55, 04103 Leipzing, Germany

Jacques Bara (167)
U-482 INSERM, Hôpital St-Antoine, 184, rue du Fbg St-Antoine, 75012 Paris, France

Julian A. Barden (335)
Institute for Biomedical Research, Department of Anatomy and Histology, the University of Sydney, Sydney NSW 2006, Australia

John M.S. Bartlett (423)
Endocrine Cancer Group, Glasgow Royal Infirmary, Glasgow, Scotland, G32 2ER

Ben Beheshti (11)
Ontario Cancer Institute, Princess Margaret Hospital, 610 University Avenue, Room 9-721, Toronto, Ontario, Canada M5G 2M9

Fabio Bucchieri (359)
Sezione di Anatomica Umana, Dipartimento di Medicina Sperimentale, Università degli Studi di Palermo, via del Vespro 129, 90127—Palermo–Italy

Marie-Pierre Buisine (167)
U-560 INSERM 1, Pl de Verdun, 59045 Lille, France

Francesco Cappello (359)
Sezione di Anatomica Umana, Dipartimento di Medicina Sperimentale, Università degli Studi di Palermo, via del Vespro 129, 90127—Palermo–Italy

Eva Carrasco (65)
Clinical Research Department, Eli Lilly & Co., Avenida de la Industria 30, 28108 Alcobendas, Madrid, Spain

Maria Lucia Caruso (65)
Department of Pathology, Scientific Institute for Digestive Diseases "S de Bellis," Via della Resistenza, 70013 Castellana Grotte (BA), Italy

Lisa W. Chu (327)
Division of Life Sciences, Lawrence Berkeley National Laboratory, Berkeley, CA 94720

Angelo De Marzo (83)
Department of Pathology, Ross Research Building, John Hopkins University School of Medicine, 720 Rutland Avenue, Baltimore, MD 21205-2196

James B. DuHadaway (431)
Lankenau Institute for Medical Research, Department of Pathology, Anatomy, and Cell Biology, Thomas Jefferson University, 100 Lancaster Avenue, Wynnewood, PA 19096

Joanne Edwards (423)
Endocrine Cancer Group, Glasgow Royal Infirmary, Glasgow, Scotland, G32 2ER

Pedro L. Fernández (307)
Department of Anatomical Pathology, Hospital Clinic, Villarroel 170, Barcelona 08036, Spain

Eva Fernebro (149)
Department of Oncology, Lund University Hospital,
221 85 Lund, Sweden

Thomas Fixemer (321)
Clinic of Urology and Pediatric Urology, University of
the Saarland, 66421 Homburg/Saar, Germany

Marie-Elisabeth Forgue-Lafitte (167)
U-482 INSERM, Hôpital St-Antoine, 184, rue du Fbg
St-Antoine, 75012 Paris, France

Zheng Fu (471)
Department of Oncology, Mayo Clinic,
200 First Street SW, Rochester, MN 55905

Wesley R. Gage (83)
Department of Pathology, Ross Research Building,
John Hopkins University School of Medicine,
720 Rutland Avenue, Baltimore, MD 21205-2196

Regina Gandour-Edwards (457)
Department of Pathology, University of California
Davis Health System, 4400 V Street,
Sacramento, CA 95817

Ignacio Garcia-Ribas (65)
Clinical Research Department, Eli Lilly & Co.,
Avenida de la Industria 30, 28108 Alcobendas,
Madrid, Spain

J.J. Garrido (227)
Department of Genetics, Campus Rabanales,
Edificio C-5, Spanish Research Council, University of
Córdoba, 14071 Córdoba, Spain

Angus Gidley-Baird (335)
Institute for Biomedical Research, Department of
Anatomy and Histology, University of Sydney,
Sydney NSW 2006, Australia

A.C. Goussia (193)
Department of Pathology, Medical School, University of
Ioannina, 45110 Ioannina, Greece

Jens Hansson (387)
Lund University, Department of Urology, Wallenberg
Laboratory, Building 46, Level 4, Malmö University
Hospital, S-205 02 Malmö, Sweden

M.A. Hayat (129, 279)
Department of Biological Sciences, Kean University,
1000 Morris Avenue, Union, NJ 07083

Annakaisa Herrala (439)
Biocenter Oulu and Research Center for Molecular
Endocrinology, P.O. Box 5000, FIN-90014,
University of Oulu, Finland

Jörg D. Hoheisel (23)
Functional Genome Analysis, Deutsches
Krebsforschungszentrum, Im Neuenheimer Feld 580,
D-69120 Heidelberg, Germany

Simon Hughes (11)
Ontario Cancer Institute, Princess Margaret Hospital,
610 University Avenue, Room 9-717, Toronto, Ontario,
Canada M5G 2M9

Katsumi Imaida (207)
Onco-pathology, Kagawa Medical University, 1750-1
Ikenobe, Miki-cho, Kita-gun, Kagawa 761-0793, Japan

E. Ioachim (193)
Department of Pathology, Medical School, University of
Ioannina, 45110 Ioannina, Greece

Toshiyuki Ishiwata (237)
Department of Pathology, Nippon Medical School,
1-1-5 Sendagi, Bunkyo-ku, Tokyo 113-8602, Japan

Yung-Ming Jeng (139)
Division of Colorectal Surgery, Department of Surgery,
National Taiwan University Hospital, No.7, Chung-Shan
South Road, Taipei, Taiwan

Zhong Jiang (377)
Department of Pathology, University of Massachusetts
Medical School, 55 Lake Avenue North, Worcester,
MA 01655

Volker Jung (321)
Clinic of Urology and Pediatric Urology, University of
the Saarland, 66421 Homburg/Saar, Germany

Jörn Kamradt (321)
Clinic of Urology and Pediatric Urology, University of
the Saarland, 66421 Homburg/Saar, Germany

Kotaro Kasahara (299)
Department of Urology, Kochi Medical School,
Nankoku, Kochi 783-8505, Japan

Evan T. Keller (471)
Rm 5111 CCGC Building, 1500 E. Medical Center Dr.,
University of Michigan, Ann Arbor, MI 48109-0940

Sourabh Kharait (463)
Department of Pathology, 711 Scaife, University of
Pittsburgh, Pittsburgh, PA 15261

Vanessa King (73)
Chemistry and Immunohistochemistry, Dade Behring,
Inc., Box 707, Glasgow Business Community,
P.O. Box 6101, Newark, DE 19714

Noboru Konishi (369)
Department of Pathology, Nara Medical University,
840 Shijo-Cho, Kashihara, Nara 634-8521, Japan

Shigeki Kuriyama (163)
Third Department of Internal Medicine,
Kagawa Medical University, 1750-1 Miki-cho,
Kita-gun, Kagawa 761-0793, Japan

Kazutaka Kurokohchi (163)
Third Department of Internal Medicine,
Kagawa Medical University, 1750-1 Miki-cho,
Kita-gun, Kagawa 761-0793, Japan

Wlad Kusnezow (23)
Functional Genome Analysis, Deutsches Krebsforschungszentrum, Im Neuenheimer Feld 580, D-69120 Heidelberg, Germany

Janine LaSalle (457)
Department of Medical Microbiology and Immunology, University of California Davis, One Shields Avenue, Davis, CA 95616

Christopher Lauer (335)
Missenden Medical Centre, Camperdown, NSW 2050, Australia

Peng Lee (409)
Department of Cancer Biology-Box 173, The University of Texas, M.D. Anderson Cancer Center, 1515 Holocombe Boulevard, Houston, TX 77030-4009

Mathie P.G. Leers (89)
Atrium Medical Center Heerlen, Department of Clinical Chemistry & Hematology, P.O. Box 4446, 6401 CX Heerlen, The Netherlands

Jia-Qing Li (207)
Onco-pathology, Kagawa Medical University, 1750-1 Ikenobe, Miki-cho, Kita-gun, Kagawa 761-0793, Japan

Jan C. Liang (327)
Division of Life Sciences, Lawrence Berkeley National Laboratory, Berkeley, CA 94720

Jin-Tung Liang (139)
Division of Colorectal Surgery, Department of Surgery, National Taiwan University Hospital, No. 7, Chung-Shan South Road, Taipei, Taiwan

Gloria Lim (11)
Ontario Cancer Institute, Princess Margaret Hospital, 610 University Avenue, Room 9-721, Toronto, Ontario, Canada M5G 2M9

D. Llanes (227)
Department of Genetics, Campus Rabanales, Edificio C-5, Spanish Research Council, University of Córdoba, 14071 Córdoba, Spain

C. Lucena (227)
Department of Genetics, Campus Rabanales, Edificio C-5, Spanish Research Council, University of Córdoba, 14071 Córdoba, Spain

Yoshihiko Maehara (55)
Department of Surgery and Science, Graduate School of Medical Sciences, Kyushu University, Fukuoka 812-8582, Japan

Anirban Maitra (83)
Department of Pathology, Ross Research Building, Johns Hopkins University School of Medicine, 720 Rutland Avenue, Baltimore, MD 21205-2196

Paula Marrano (11)
Ontario Cancer Institute, Princess Margaret Hospital, 610 University Avenue, Room 9-721, Toronto, Ontario, Canada M5G 2M9

Tsutomu Masaki (163)
Third Department of Internal Medicine, Kagawa Medical University, 1750-1 Miki-cho, Kita-gun, Kagawa 761-0793, Japan

Alan Meeker (83)
Department of Pathology, Ross Research Building, Johns Hopkins University School of Medicine, 720 Rutland Avenue, Baltimore, MD 21205-2196

Masaru Miyazaki (159)
Department of Gastroenterological Surgery, Chiba Cancer Center Hospital, 666-2 Nitonacho, Chuo-ku, Chiba 260-0801, Japan

A. Moreno (227)
Department of Genetics, Campus Rabanales, Edificio C-5, Spanish Research Council, University of Córdoba, 14071 Córdoba, Spain

Marius Nap (89)
Atrium Medical Center Heerlen, Department of Clinical Chemistry & Hematology, P.O. Box 4446, 6401 CX Heerlen, The Netherlands

Mef Nilbert (149)
Department of Oncology, Lund University of Hospital, 221 85 Lund, Sweden

Shinya Oda (55)
Department of Pathology, Institute for Clinical Research, National Kyushu Cancer Center, Notame 3-1-1, Fukuoka 811-1395, Japan

Ricardo Paniagua (399)
Department of Cell Biology and Genetics, University of Alcalá, 28871 Alcalá de Henares, Madrid, Spain

Jose Luis Perez-Gracia (65)
Medical Oncology Department, Clinica Universitaria de Navarra, Avenida Pio XII, 36, 31008, Pamplona, Spain

Sven Petersen (183)
Department of General and Abdominal Surgery, General Hospatal Dresden-Friedrichstadt, Teaching Hospital Technical University Dresden, Dresden, Germany

Florence Pinet (245)
INSERM Unit 508, Institut Pasteur de Lille, 1 rue du professeur Calmette, 59019 Lille cedex, France

George C. Prendergast (431)
Lankenau Institute for Medical Research, Department of Pathology, Anatomy, and Cell Biology, Thomas Jefferson University, 100 Lancaster Avenue, Wynnewood, PA 19096

Timo Pulli (23)
Functional Genome Analysis, Deutsches Krebsforschungszentrum, Im Neuenheimer Feld 580, D-69120 Heidelberg, Germany

Maria Gloria Ruiz-Ilundain (65)
Medical Oncology Department, Clinica Universitaria de Navarra, Avenida Pio XII, 36, 31008, Pamplona, Spain

Hiroki Sasaki (1)
Genetics Division, National Cancer Center Research Institute, 1-1, Tsukiji 5-chome, Chuo-ku, Tokyo 104-0045, Japan

Latha Satish (463)
Department of Pathology, 711 Scaife, University of Pittsburgh, Pittsburgh, PA 15261

Kimmo J. Savinainen (449)
Laboratory of Cancer Genetics, Institute of Medical Technology, University of Tampere and Tampere Hospital, Tampere, Finland

Taro Shuin (299)
Department of Urology, Kochi Medical School, Nankoku, Kochi 783-8505, Japan

Michael D. Slater (335)
Institute for Biomedical Research, Department of Anatomy and Histology, University of Sydney, Sydney NSW 2006, Australia

Nobuhito Sogawa (159)
Department of Gastroenterological Surgery, Chiba Cancer Center Hospital, 666-2 Nitonacho, Chuo-ku, Chiba 260-0801, Japan

Jeremy A. Squire (11)
Ontario Cancer Institute, Princess Margaret Hospital, 610 University Avenue, Room 9-721, Toronto, Ontario, Canada M5G 2M9

D. Stefanou (193)
Department of Pathology, Medical School, University of Ioannina, 45110 Ioannina, Greece

Yana V. Syagailo (23)
Functional Genome Analysis, Deutsches Krebsforschungszentrum, Im Neuenheimer Feld 580, D-69120 Heidelberg, Germany

Takahiro Taguchi (159)
Department of Anatomy, Kochi Medical School, Nankoku, Kochi 783-8505, Japan

Nobuhiro Takiguchi (159)
Department of Gastroenterological Surgery, Chiba Cancer Center Hospital, 666-2 Nitonacho, Chuo-ku, Chiba 260-0801, Japan

Timothy M. Thomson (307)
Department of Anatomical Pathology, Hospital Clinic, Villarroel 170, Barcelona 08036, Spain

Pirkko Vihko (439)
Biocenter Oulu and Research Center for Molecular Endocrinology, P.O. Box 5000, FIN-90014, University of Oulu, Finland

Tapio Visakorpi (449)
Institute of Medical Technology, University of Tampere, Biokatu 6, FIN-33520, Tampere, Finland

Hanlin L. Wang (267)
Department of Pathology & Immunology, Division of Anatomic Pathology, Campus Box 8118, Washington University School of Medicine, 660 South Euclid Avenue, St. Louis, MO 63110-1093

Zhengxin Wang (409)
Department of Cancer Biology, Box 173, The University of Texas, M.D. Anderson Cancer Center, 1515 Holocombe Boulevard, Houston, TX 77030-4009

Alan Wells (463)
Department of Pathology, 713 Scaife, University of Pittsburgh, Pittsburgh, PA 15261

Nicolas Wernert (255)
Institute of Pathology, University of Bonn, Sigmund-Freud-Str. 25, P.O. Box 2120, 53011 Bonn, Germany

Fei Wu (163)
Third Department of Internal Medicine, Kagawa Medical University, 1750-1 Miki-cho, Kita-gun, Kagawa 761-0793, Japan

Guang-Jer Wu (347)
Department of Microbiology and Immunology and the Winship Cancer Institute, Emory University School of Medicine, 1510 Clifton Rd., NE, Atlanta, GA 30322

Bernd Wullich (321)
Clinic of Urology and Pediatric Urology, University of the Saarland, 66421 Homburg/Saar, Germany

Ichiro Yamasaki (299)
Department of Urology, Kochi Medical School, Nankoku, Kochi 783-8505, Japan

Clayton Yates (463)
Department of Pathology, 711 Scaife, University of Pittsburgh, Pittsburgh, PA 15261

Isik G. Yulug (113)
Bilkent University, Faculty of Science, Department of Molecular Biology and Genetics, 06800 Ankara, Turkey

Lizhi Zhang (471)
Rm 5111 CCGC Building, 1500 E. Medical Center Dr., University of Michigan, Ann Arbor, MI 48109-0940

Isabel Zudaire (37)
Department of Genetics, University of Navarra, C/Irunlarrea s/n, 31008 Pamplona, Spain

Giovanni Zummo (359)
Sezione di Anatomica Umana, Dipartimento di Medicina Sperimentale, Universitá degli Studi di Palermo, via del Vespro 129, 90127—Palermo–Italy

Foreword

According to mortality data from the National Center for Health Statistics, approximately 1,334,100 new cases of cancer will have been diagnosed, and 556,500 people will have died from cancer in the United States by the end of 2003. Though the number of cancer-related deaths has been on the decline since 1992, the incidence has increased over the same period. This increase is largely due to the implementation of improved screening techniques that have in turn been made possible by advances in immunochemical diagnostic testing. As immunochemical techniques such as *in situ* hybridization (ISH) and immunohistochemistry (IHC) continue to be refined, their use in improving patient care through research and improved methods of diagnosis is becoming ever more valuable.

In situ hybridization is a well-established approach for identifying the organization and physical position of a specific nucleic acid within the cellular environment, by means of hybridizing a complementary nucleotide probe to the sequence of interest. The use of deoxyribonucleic acid (DNA) and ribonucleic acid (RNA) as probes to assay biologic material has been in use for approximately 30 years. However, recently, advances in ISH have seen a replacement of radioactive detection by more adaptable colorimetric and fluorescent (FISH) methods for the interrogation of nuclei, metaphase chromosomes, DNA fibers, patient tissue, and, most recently, deriving information from patient samples using DNA microarrays. Technologic advances, including array comparative genomic hybridization, spectral karyotyping, and multicolor banding, have provided a refinement in the study of genome organization and chromosomal rearrangements. In addition, ISH using RNA has allowed for a determination of the expression pattern and the abundance of specific transcripts on a cell-to-cell basis. Advances in DNA and RNA ISH have migrated from the research setting and are becoming routine tests in the clinical setting permitting examination of the steps involved in tumorigenesis, which would not have been possible by the use of classical cytogenetic analysis.

Since the introduction of monoclonal antibodies, immunohistochemistry has developed into a vital tool, which is now extensively used in many research laboratories and for clinical diagnosis. Immunohistochemistry is a collective term for a variety of methods, which can be used to identify cellular or tissue components by means of antigen-antibody interactions. Immunostaining techniques date back to the pioneering work by Albert Coons in the early 1940s, using fluorescein-labeled antibodies. Since then, developments in the techniques have permitted visualization of antigen-antibody interactions by conjugation of the antibody to additional fluorophores, enzyme, or radioactive elements. As there are a wide variety of tissue types, antigen availabilities, antigen-antibody affinities, antibody types, and detection methods, it is essential to select antibodies almost on a case-to-case basis. The consideration of these factors has led to the identification of several key antibodies that have great utility in the study and diagnosis of tumors.

The scientific advances in the field of immunochemistry have necessitated rapid developments in microscopy, image capture, and analytical software in order to objectively quantify results. These cutting-edge experimental systems have already produced many significant differences between cancers that might not have been distinguished by conventional means.

The focus of these volumes is the use of ISH and IHC to study the molecular events occurring at the DNA, RNA, and protein levels during development and progression of human carcinomas. Continued investment of time and expertise by researchers worldwide has contributed significantly to a greater understanding of the disease processes. As the technical requirements for many immunochemical techniques is quite demanding and as the methodology itself poses many pitfalls, the step-by-step methods provided in these volumes will serve as an excellent guide for both clinical and basic researchers studying human malignancies.

Simon Hughes
Ontario Cancer Institute
Princess Margaret Hospital
Toronto, Canada

This Page Intentionally Left Blank

Preface to Volume 2

The primary objectives of this volume remain the same as those of volume 1—that is, discussion of immunohistochemical and *in situ* hybridization (ISH), including fluorescence *in situ* hybridization (FISH) and chromogenic *in situ* hybridization (CISH) procedures as they are used in the field of pathology, especially cancer diagnosis. The practical importance of the antigen retrieval protocols in immunohistochemistry was realized in 1991, and since then they have been used routinely in pathology laboratories. Many chapters in this volume contain the details of these protocols. However, detection of certain antigens even in formalin-fixed tissues can be accomplished without using antigen retrieval methods.

Immunohistochemistry, ISH, FISH, and CISH of two major carcinomas (colorectal and prostate) are presented. The biomarkers of two other major carcinomas (lung and breast) were explained in Volume 1, and others will be discussed in the forthcoming Volume 3. The procedures are explained in maximum details in a step-by-step fashion so that the readers can use them without additional references. Materials required to carry out the procedures are also included. These procedures are also useful in clinical laboratories.

Another objective of this volume is the discussion of the role of molecular pathology (molecular genetics, molecular medicine, molecular morphology) to understand and achieve correct diagnosis and therapy in neoplastic diseases. Molecular pathology/genetics has the advantage of assessing genes directly. Knowledge of the genetic basis of disease will, in turn, allow more specific targeting of the cause, rather than the symptoms only, of the disease. The time is overdue to apply our knowledge of molecular genetics in conjunction with immunohistochemistry and histology to diagnostic, therapeutic, and prognostic decisions.

Genetic information will improve the prognosis used to monitor both the efficacy of treatment and the disease recurrence. Molecular markers, largely from tumors but also from germline, have great potential for diagnosis, for directing treatment, and as indicators of the outcome. In other words, these markers are of considerable importance to clinical practitioners. For this and other reasons the role of gene mutations in cancer is emphasized because the characteristics of the tumor depend on the mutations that lead to their emergence. For example, down-regulation of tumor suppressor genes BRCA1/2 and their proteins is a well-known test for breast cancer susceptibility, resulting in poor prognosis. Indeed, methods of molecular testing of tumors are finally well established and are discussed in this and other volumes of this series of handbooks. Widespread molecular testing is the future for clinical practice.

Unfortunately, clinical practice has lagged behind the current knowledge of research in molecular genetics. Both technicians and pathologists need to be aware of the importance of molecular pathology testing. Somatic mutations are rarely performed, although some histopathology and cytogenetics laboratories have done limited testing such as chromosomal rearrangements in lymphoma. Molecular testing should be regarded as a means of complementing, rather than replacing, established methods such as immunohistochemistry and FISH.

There are several reasons for the limited use of molecular genetics in clinical practice. One reason is the high cost of establishing facilities for molecular techniques; another is our comparatively meager understanding of the nature of many diseases, including cancer. Although equipment for molecular testing is available, some investment is needed. Another reason is the dearth of clinician–scientist training programs, resulting in limited clinician–scientists. Also, an inequity in pay exists between those working in clinical practice versus research faculty. Accordingly, the differential in pay may be a disincentive for choosing a full-time career in medical research. The length of time (8 years as an average) to receive the M.D./Ph.D. is probably also a barrier in the development of new clinician–scientists. Many clinician–scientist trainees are married, or are in stable relationships, and personal time for family life and children is increasingly important.

Narrowing the gap in income between clinical practitioners and full-time medical researchers would provide a positive incentive for this profession.

Pathologists are well advised to adapt to modern therapeutic shifts (i.e., morphologic interpretation needs to be combined with molecular diagnostic modalities). The latter protocols can provide a second level of testing that is particularly useful for the analysis of neoplasms for which histologic and immunophenotypic data are inconclusive. Therapies already are beginning to progress more and more toward specific molecular targets. Examples are deoxyribonucleic acid (DNA) microarrays, differential display of gene expression, serial analysis of gene expression, comparative genomic hybridization, rolling circle amplification, reverse transcription polymerase chain reaction, FISH, Southern Blot hybridization, and specific cloned probes; most of these methods were discussed in Volume 1 and are also discussed in this volume. Flow cytometry technology is also presented. We already are down a path that has the potential to alter oncology clinical practice. My hope, through this series of volumes, is to expedite the translation of molecular genetics into clinical practice.

I am indebted to the authors of the chapters for their promptness and appreciate their dedication and hard work in sharing their expertise with the readers. In most cases the protocols presented were either introduced or refined by the authors and routinely used in their clinical pathology laboratories. The methods presented here offer much more detailed information than is available in scientific journals. Because of its relatively recent emergence from the research laboratory, many molecular pathology protocols are still found in scientific journals only and have not appeared in a book. Each chapter provides unique individual practical knowledge based on the expertise of the author. As with all clinical laboratory testing, the results obtained should be interpreted in conjunction with other established and proven laboratory data and clinical findings.

This volume has been developed through the efforts of 97 authors, representing 15 countries. The high quality of each manuscript made my work as the editor an easy one. The authors were gracious and prompt. This volume is intended for use in research and clinical laboratories by medical technicians and pathologists, especially in the field of oncology. This volume will also be of interest and help to medical students.

I appreciate the cooperation extended to me by Hilary Rowe, a valued, competent publishing editor. As the sponsoring editor, her understanding of the importance of this project in the field of human carcinomas helped me to embark on this uniquely difficult and complex endeavor and bring it to fruition. I am grateful to Dr. Frank Esposito and Dr. Dawood Farahi for their recognition of my teaching and scholarly contributions, and for their help. I acknowledge the hard, efficient work of Denise DeLancey, the production editor. I greatly appreciate receiving indispensable, expert help from Eliza McGovern in the preparation of the manuscript.

M.A. Hayat
February 2004

Contents of Volume 1

IV Breast Carcinoma

This Page Intentionally Left Blank

Prologue

We possess scientific and industrial knowledge in new biotechniques, including human genetic technologies. However, ethical and social implications of these advances must be addressed. Such concerns are especially relevant in some of the applications of genetic engineering, such as pharmacogenetics, gene therapy, predictive diagnostics (including prenatal genetic diagnosis, therapeutic cloning, and cloning of humans and other animals), human tissue banking, transplanting, and patenting of inventions that involve elements of human origin including stem cells. Bioethics should be a legitimate part of governmental control or supervision of these technologies. Scientific and industrial progress in this field is contingent on the extent to which it is acceptable to the cultural values of the public. In addition, in medical research on human subjects considerations related to the well-being of the human subject should take precedence over the interests of science and industry. Any form of discrimination against a person based on genetic heritage is prohibited.

M.A. Hayat

This Page Intentionally Left Blank

Selected Definitions

Ablation: Ablation consists of removal of a body part or the destruction of its function.

Adenocarcinoma: Adenocarcinoma is a malignant neoplasm of epithelial cells in glandular or glandlike pattern.

Adenoma: Adenoma is a benign epithelial neoplasm in which the tumor cells form glands or glandlike structures. It does not infiltrate or invade adjacent tissues.

Adjuvent: Adjuvent is a substance that nonspecifically enhances or potentiates an immune response to an antigen; something that enhances the effectiveness of a medical treatment.

Affinity: Affinity is a measure of the bonding strength (association constant) between a receptor (one binding site on an antibody) and a ligand (antigenic determinant).

Allele: Allele is one of two or more alternative forms of a single gene locus. Different alleles of a gene have a unique nucleotide sequence, and their activities are all concerned with the same biochemical and developmental process, although their individual phenotypes may differ. An allele is one of several alternate forms of a gene at a single locus that controls a particular characteristic.

Alternative Splicing: Genes with new functions often evolve by gene duplication. Alternative splicing is another means of evolutionary innovation in eukaryotes, which allows a single gene to encode functionally diverse proteins (Kondrashov and Koonin, 2001). In other words, the alternative splicing refers to splicing the same pre-mRNA in two or more ways to yield two or more different protein products. Alternative splicing can produce variant proteins and expression patterns as different as the products of different genes. Alternative splicing either substitutes one protein sequence segment for another (substitution alternative splicing) or involves insertion or deletion of a part of the protein sequence (length difference alternative splicing). Thus, alternative splicing is a major source of functional diversity in animal proteins. Very large types and number of proteins are required to perform immensely diverse functions in a eukaryote.

Lack of correlation between the high complexity of an organism and the number of genes can be partially explained if a gene often codes for more than one protein. Individual genes with mutually alternate, alternative exons are capable of producing many more protein isoforms than there are genes in the entire genome. A substantial amount of exon duplication events lead to alternative splicing, which is a common phenomenon. Indeed, alternative splicing is widespread in multicellular eukaryotes, with as many as one (or more) in every three human genes producing multiple isoforms (Mironov *et al.,* 1999). In other words, alternative splicing is a ubiquitous mechanism for the generation of multiple protein isoforms from single genes, resulting in the increased diversity in the proteomic world.

Amplification: Amplification refers to the production of additional copies of a chromosomal sequence, found as intrachromosomal or extrachromosomal DNA. Amplification is selective replication of a gene to produce more than the normal single copy in a haploid genome.

Anaplasia: Anaplasia results in the regression of cells and tissues to undifferentiated state (dedifferentiation) in most malignant neoplasms.

Aneuploidy: Aneuploidy is the abnormal condition in which one or more whole chromosomes of a normal set of chromosomes either are missing or are present in more than the usual number of copies. Aneuploidy refers to not having the normal diploid number of chromosomes.

Annealing of DNA: Annealing of DNA is the process of bringing back together the two separate strands of denatured DNA to re-form a double helix.

Antibody: Antibody (immunoglobulin) is a protein produced by B lymphocytes that recognizes a particular foreign antigenic determinant and facilitates clearance

of that antigen; antigens can also be carbohydrates, even DNA.

Antigen: An antigen is a foreign substance that binds specifically to antibody or T-cell receptors and elicits an immune response.

Antigenic Determinant: Antigenic determinant is the site on an antigenic molecule that is recognized and bound by antibody.

Apoptosis: Apoptosis is the capacity of a cell to undergo programmed cell death. In response to a stimulus, a pathway is triggered that leads to destruction of the cell by a characteristic set of reactions. Failure to apoptose allows tumorigenic cells to survive and thus contribute to cancer.

Avidity: Avidity is referred to the functional binding strength between two molecules such as an antibody and an antigen. Avidity differs from affinity because it reflects the valency of the antigen-antibody interaction.

Carcinoma: Carcinoma is of various types of malignant neoplasm arising from epithelial cells, mainly glandular (adenocarcinoma) or squamous cell. Carcinoma is the most common cancer and displays uncontrolled cellular proliferation, anaplasia, and invasion of other tissues, spreading to distant sites by metastasis. The origin of carcinoma in both sexes is skin, and in prostate in men and in breast in women. The most frequent carcinoma in both sexes is bronchogenic carcinoma.

cDNA (complementary deoxyribonucleic acid): mRNA molecules are isolated from cells, and DNA copies of these RNAs are made and inserted into a cloning vector. The analysis of that cloned cDNA molecule can then provide information about the gene that encoded the mRNA. The end result is a cDNA library.

Chromosomal Aberration: Chromosomal aberration is a change in the structure or number of chromosomes. The variation from the wild-type condition is either chromosome number or chromosome structure. Four major types of aberrations are deletions, duplications, inversions, and translocations. Variations in the chromosome number of a cell give rise to aneuploidy, monoploidy, or polyploidy.

Clinical Guidelines: Clinical guidelines are statements aimed to assist clinicians in making decisions regarding treatment for specific conditions. They are systematically developed, evidence-based, and clinically workable statements that aim to provide consistent and high-quality care for patients. From the perspective of litigation, the key question has been whether guidelines can be admitted as evidence of the standard of expected practice or whether this would be regarded as hearsay. Guidelines may be admissible as

evidence in the United States if qualified as authoritative material or a learned treatise, although judges may objectively scrutinize the motivation and rationale behind guidelines before accepting their evidential value (Samanta *et al.*, 2003). The reason for this scrutiny is the inability of guidelines to address all the uncertainties inherent in clinical practice. However, clinical guidelines should form a vital part of clinical governance.

Clones: A clone is a group of cells that are genetically identical to the original individual cell.

Codon: A codon is a three-base sequence in mRNA that causes the insertion of a specific amino acid into polypeptide, or causes termination of translation.

Concatemers: Concatemers are DNAs of multiple genome length.

Constitutive Gene: A gene whose products are essential to normal cell functioning, regardless of the life-supporting environmental conditions. These genes are always active in growing cells.

Constitutive Mutation: Constitutive mutation is a mutation that causes a gene to be expressed at all times, regardless of normal controls.

Cytokines: Cytokines are a group of secreted low molecular weight proteins that regulate the intensity and duration of an immune response by stimulating or inhibiting the proliferation of various immune cells or their secretion of antibodies or other cytokines.

Deletion: Deletion is a mutation involving a loss of one or more base pairs; a chromosomal segment or gene is missing.

Dendritic Cell: Dendritic cell is a type of antigen-presenting cell that has long membrane processes (resembling dendrites of nerve cells) and is found in the lymph nodes, spleen, thymus, skin, and other tissues.

Determinant: Determinant is the portion of an antigen molecule that is recognized by a complementary section of an antibody of T-cell receptor.

Diagnosis: Diagnosis means the differentiation of malignant from benign disease or of a particular malignant disease from others. A tumor marker that helps in diagnosis may be helpful in identifying the most effective treatment plan.

DNA Methylation: Genetic mutations or deletions often inactivate tumor suppressor genes. Another mechanism for silencing genes involves DNA methylation. In other words, in addition to genetic alterations, epigenetics controls gene expression, which does not involve changes of genomic sequences. DNA methylation is an enzymatic reaction that brings a methyl group to the 5th carbon position of cystine located 5′ to guanosine in a CpG dinucleotide within the gene promoter region. This results in the prevention of transcription. Usually, multiple genes are silenced by DNA methylation in a tumor.

DNA methylation of genes, however, is not common in normal tissues. Gene methylation profiles, almost unique for each tumor type, can be detected in cytologic specimens by methylation-specific polymerase chain reaction (Pu and Douglas, 2003).

In the human genome, ~80% of CpG dinucleotides are heavily methylated, but some areas remain unmethylated in GC-rich CpG island (Bird, 2002). In cancer cells, aberrant DNA methylation is frequently observed in normally unmethylated CpG islands, resulting in the silencing of the function of normally expressed genes. If the silencing occurs in genes critical to growth inhibition, the epigenetic alteration could promote tumor progression as a result of uncontrolled cell growth. However, pharmacologic demythylation can restore gene function and promote death of tumor cells (Shi *et al*., 2003).

ELISA: Enzyme-linked immunosorbent assay in which antibody or antigen can be quantitated by using an enzyme-linked antibody and a colored substance to measure the activity of the bound enzyme.

Encode: Encode refers to containing the information for making an RNA or polypeptide; a gene can encode an RNA or a polypeptide.

Epigenetics: Epigenetics is the study of mitotically and/or meiotically heritable changes in gene function that cannot be explained by changes in DNA sequence. Epigenetic change means an alteration in the expression of a gene but not in the structure of the gene itself. Processes less irrevocable than mutation fall under the umbrella term *epigenetic*. Known molecular mechanisms involved in epigenetic phenomenon include DNA methylation, chromatin remodeling, histone modification, and RNA interference. Patterns of gene expression regulated by chromatin factors can be inherited through the germline (Cavalli *et al*., 1999). The evidence that heritable epigentic variation is common raises questions about the contribution of epigenetic variation to quantitative traits in general (Rutherford and Henikoff, 2003).

Epitope: An epitope is the antigenic determinant or antigen site that interacts with an antibody or T-cell receptor.

Exon: An exon is the region of a gene that is ultimately represented in that gene's mature transcript, in both the DNA and its RNA product.

Familial Trait: A familial trait is a trait shared by members of a family.

FISH: Fluorescent *in situ* hybridization is a technique of hybridizing a fluorescence probe to whole chromosome to determine the location of a gene or other DNA sequence within a chromosome.

Gastritis: Gastritis refers to the inflammation, especially mucosal, of the stomach.

Gene: A gene is the basic unit of heredity and contains the information for making one RNA and, in most cases, one polypeptide.

Gene Cloning: Gene cloning means generating many copies of a gene by inserting it into an organism (e.g., bacterium), where it can replicate along with the host.

Gene Expression: Gene expression is the process by which gene products are made.

Gene Family: Gene family consists of a set of genes whose exons are related; the members were derived by duplication and variation from some ancestral genes.

Gene Mutation: A heritable alteration of the genetic material, usually from one allele form to another. A gene mutation is confined to a single gene.

Genetic Code: Genetic code is the set of 64 codons and the amino acids (or terminations) they stand for. Genetic code is the correspondence between triplets in DNA (or RNA) and amino acids in protein.

Genetic Mapping: Genetic mapping determines the linear order of genes and the distances between them.

Genome: Genome is the total amount of genetic material in a cell. In eukaryotes the haploid set of chromosomes of an organism.

Genomic Instability: It takes many years to get a cancer. Approximately 20 years may elapse from the time of exposure to a carcinogen to the development of a clinically detectable tumor. During this duration, tumors are characterized by genomic instability, resulting in the progressive accumulation of mutations and phenotypic changes. Some of the mutations bypass the host-regulatory processes that control cell location, division, expression, adaptation, and death. Genetic instability is manifested by extensive heterogeneity of cancer cells within each tumor.

Destabilized DNA repair mechanisms can play an important role in genomic instability. Human cells may use at least seven different repair mechanisms to deal with DNA lesions that represent clear danger to survival and genomic stability. For example, homologous recombination repair, nonhomologous end-joining, and mismatch-repair mechanisms normally act to maintain genetic stability, but if they are deregulated, genomic instability and malignant transformation might occur (Pierce *et al*., 2001). Also, because the human genome contains ~500,000 members of the *Alu* family, increased levels of homologous/homologous recombination events between such repeats might lead to increased genomic instability and contribute to malignant progression (Rinehart *et al*., 1981).

In addition, BCR/ABL oncogenic tyrosine kinase allows cells to proliferate in the absence of growth factors, protects them from apoptosis in the absence of growth factors, protects them from apoptosis in the

absence of external survival factors, and promotes invasion and metastasis. The unrepaired and/or aberrantly repaired DNA lesions resulting from spontaneous and/or drug-induced damage can accumulate in BCR/ABL-transformed cells, which may lead to genomic instability and malignant progression of the disease (Skorski, 2002).

Genomic Library: Genomic library is a set of clones containing DNA fragments derived directly from a genome, rather than from RNA. The collection of molecular clones that contain at least one copy of every DNA sequence in the genome.

Genotype: Genotype is the combined genetic material inherited from both parents; also, the alleles present at one or more specific loci. In other words, genotype is the allelic constitution of a given individual.

Germline: Germline is the unmodified genetic material that is transmitted from one generation to the next through the gametes.

Germline Mutations: Mutations in the germline of sexually reproducing organisms may be transmitted by the gametes to the next generation, giving rise to an individual with the mutant state in both its somatic and germline cells.

G1 Phase: G1 phase is the period of the eukaryotic cell cycle between the last mitosis and start of DNA replication.

G2 Phase: G2 phase is the period of the eukaryotic cell cycle between the end of DNA replication and the start of the next mitosis.

Hepatitis: Hepatitis consists of inflammation of the liver caused by viral infection or toxic agents.

Heterozygous: A diploid organism having different alleles of one or more genes. As a result, the organism produces gametes of different genotypes.

Humoral Immunity: Humoral immunity is the immunity that can be transferred by antibodies present in the plasma, lymph, and tissue fluids.

Hybridization: Hybridization is the pairing of complementary RNA and DNA strands to give an RNA–DNA hybrid.

Immunotherapy: Immunotherapy involves delivering therapeutic agents conjugated to monoclonal antibodies that bind to the antigens at the surface of cancer cells. Ideal antigens for immunotherapy should be strongly and uniformally expressed on the external surface of the plasma membrane of all cancer cells. Many solid neoplasms often demonstrate regional variation in the phenotypic expression of antigens. These regional differences in the immunophenotypic profile within the same tumor are referred to as intratumoral heterogeneity. Therapeutic agents that have been used include radioisotopes, toxins, cytokines, chemotherapeutic agents, and immunologic cells.

Kaposi's Sarcoma: Kaposi's sarcoma is a multifocal malignant neoplasm that occurs in the skin and lymph nodes. It consists of cutaneous lesions reddish to dark-blue in color, found commonly in men over 60 years of age or in AIDS patients.

Laser-Capture Microdissection: Tissue heterogeneity and the consequent need for precision before specimen analysis present a major problem in the study of disease. Even a tissue biopsy consists of a heterogenous population of cells and extracellular material, and analysis of such material may yield misleading or confusing results. Cell cultures can be homogenous but not necessarily reflect the *in vivo* condition. Therefore, a strategy is required to facilitate selective purification of relevant homogenous cell types.

The technology of laser-capture microdissection allows extraction of single cells or defined groups of cells from a tissue section. This technique is important for characterizing molecular profiles of cell populations within a heterogeneous tissue. In combination with various downstream applications, this method provides the possibility of cell-type or even cell-specific investigation of DNA, RNA, and proteins (Mikulowska-Mennis *et al*., 2002).

Library: Library is a set of cloned fragments together representing the entire genome.

Ligand: Ligand is a molecule recognized by a receptor structure.

Loss of Heterozygosity: In the majority of cases where the gene mutation is recessive, tumor cells often retain only the mutated allele and lose the wild-type one. This loss is known as loss of heterozygosity.

Lymph: Lymph is the intercellular tissue fluid that circulates through the lymphatic vessels.

Lymphadenopathy: Lymphadenopathy is the enlargement of the lymph nodes.

Lymph Nodes: Lymph nodes are small secondary lymphoid organs containing populations of lymphocytes, macrophages, and dendric cells that serve as sites of filtration of foreign antigens and activation of lymphocytes.

Lymphokines: Lymphokine is a generic term for cytokines produced by activated lymphocytes, especially T cells, that act as intercellular mediators of the immune response.

Lymphoma: Lyphoma is a cancer of lymphoid cells that tends to proliferate as solid tumors.

Malignant: Malignant tumors have the capacity to invade and alter the normal tissue.

Marker (Biomarker): A marker is a mutated gene or its product that serves as a signpost at a known location in the genome.

Metastasis: Initially tumor growth is confined to the original tissue of origin, but eventually the mass

grows sufficiently large enough to push through the basement membrane and invade other tissues. When some cells lose adhesiveness, they are free to be picked up by lymph and carried to lymph nodes and/or may invade capillaries and enter blood circulation. If the migrant cells can escape host defenses and continue to grow in the new location, a metastasis is established. Approximately more than half of cancers have metastasized by the time of diagnosis. Usually it is the metastasis that kills the person rather than the primary (original) tumor.

Metastasis itself is a multistep process. The cancer must break through any surrounding covering (capsule) and invade the neighboring (surrounding) tissue. Cancer cells must separate from the main mass and be picked up by the lymphatic or vascular circulation. The circulating cancer cells must lodge in another tissue. Cancer cells traveling through the lymphatic system must lodge in a lymph node. Cancer cells in vascular circulation must adhere to the endothelial cells and pass through the blood vessel wall into the tissue. For cancer cells to grow, they must establish a blood supply to bring oxygen and nutrients; this usually involves angiogenesis factors. All of these events must occur before host defenses can kill the migrating cancer cells.

If host defenses are to be able to attack and kill malignant cells, they must be able to distinguish between cancer and normal cells. In other words, there must be immunogens on cancer cells not found on normal cells. In the case of virally induced cancer circulating cells, viral antigens are often expressed, and such cancer cells can be killed by mechanisms similar to those for virally infected tissues. Some cancers do express antigens specific for those cancers (tumor-specific antigens), and such antigens are not expressed by normal cells.

As stated earlier, metastasis is the principal cause of death in individuals with cancer, yet its molecular basis is poorly understood. To explore the molecular difference between human primary tumors and metastases, Ramaswany *et al*. (2003) compared the gene-expression profiles of adenocarcinoma metastases of multiple tumor types to unmatched primary adenocarcinomas. They found a gene-expression signature that distinguished primary from metastatic adenocarcinomas. More importantly, they found that a subset of primary tumors resembled metastatic tumors with respect to this gene-expression signature. The results of this study differ from most other earlier studies in that the metastatic potential of human tumors is encoded in the bulk of a primary tumor. In contrast, some earlier studies suggest that most primary tumor cells have low metastatic potential, and cells within large primary tumors rarely acquire metastatic capacity

through somatic mutation (Poste and Fidler, 1980). The emerging notion is that the clinical outcome of individuals with cancer can be predicted using the gene profiles of primary tumors at diagnosis.

Methylation: DNA methylation (an epigenetic change) in mammals occurs at the cytosine residues of cytosine guanine (CpG) dinucleotides by an enzymatic reaction that produces 5-methylcytosine (5-mc). In other words, methylation of normal unmethylated CpG islands in gene-promoter regions is an important method for silencing tumor suppressor genes (TSGs). Methylation results in transcriptional inactivation of several TSGs in human cancer and serves as an alternative for the genetic loss of gene function by deletion or mutation.

One of the first alterations of DNA methylation to be recognized in neoplastic cells is a decrease in overall 5-mc content, referred to as genome-wide or global DNA hypomethylation. Despite the frequently observed cancer-associated increases of regional hypermethylation, the prevalence of global DNA hypomethylation in many types of human cancers suggests that such hypomethylation plays a significant and fundamental role in tumorigenesis.

Microsatellite: Microsatellite is a short DNA sequence (usually 2–4 bp) repeated many times in tendem. A given microsatellite is found in varying lengths, scattered around a eukaryotic genome.

Mitogen: Mitogen is a substance (e.g., hormone growth factor) that stimulates cell division.

Molecular Genetics: Molecular genetics is a subdivision of the science of genetics involving how genetic information is encoded within the DNA and how the cell's biochemical processes translate the genetic information into the phenotype.

Monitoring: Monitoring means repeated assessment if there is an early relapse or other signs of disease activity or progression. If early relapse of the disease is identified, a change in patient management will be considered, which may lead to a favorable outcome for the patient.

Monoclonal Antibody: Monoclonal antibodies are homogeneous antibodies produced by a clone of hybridoma cells.

mRNA Splicing: mRNA splicing is a process whereby an intervening sequence between two coding sequences in an RNA molecule is excised and the coding sequences are ligated (spliced) together.

Multifactorial Trait: A multifactorial trait is a trait influenced by multiple genes and environmental factors. When multiple genes and environmental factors influence a trait, it is difficult to find a simple relationship between genotype and phenotype that exists in discontinuous traits.

Mutagens: Mutagen is a mutation-causing agent. A mutagen is any physical or chemical agent that significantly increases the frequency of mutational events above the rate of spontaneous mutation.

Mutant: A mutant is an organism (or genetic system) that has suffered at least one mutation.

Mutation: Mutation is the original source of genetic variation caused, for example, by a change in a DNA base or a chromosome.

Neoplasia: Neoplasia usually refers to pathologic process that causes the formation and growth of an abnormal tissue. However, the growth could be benign or malignant.

Neoplasm: Neoplasm is an abnormal tissue that grows by cellular proliferation faster than normal, and continues to grow.

Oligonucleotide: An olignucleotide is a short piece of RNA or DNA.

Oncogene: Oncogene is a gene that transforms a normal cell to a tumorous (cancerous) state. Products of oncogenes are capable of causing cellular transformations. Oncogenes derived from viruses are denoted v-onc, while their cellular counterparts, or protooncogenes, are denoted c-onc.

Pancreatitis: Pancreatitis refers to the inflammation of the pancreas. It can be caused by alcoholism, endocrine diseases, hereditary, viral, parasitic, allergic, immunologic, pregnancy, drug effects, and abdominal injury.

Phenotype: Phenotype is the physical manifestation of a genetic trait, resulting from a specific genotype and its interaction with the environment. Genes give only the potential for the development of a particular phenotypic characteristc; the extent to which that potential is realized depends not only on interactions with the other genes and their products but also on environmental influences.

PCNA: Proliferating cell nuclear antigen.

Polymerase Chain Reaction: Polymerase chain reaction (PCR) method is used to selectively and repeatedly replicate defined DNA sequences from a DNA mixture. The starting point for PCR is the DNA mixture containing the DNA sequence to be amplified and a pair of oligonucleotide primers that flank that DNA sequence.

Polymorphism: Polymorphism refers to the simultaneous occurrence in the population of genomes showing allelic variations, which are seen either in alleles producing different phenotypes or, for example, in changes in DNA affecting the restriction pattern. A polymorphic locus is any locus that has more than one allele present within a population.

Prognosis: Prognosis is defined as the prediction of how well or how poorly a patient is likely to fare in terms of response to therapy, relapse, survival time, or other outcome measures.

Protooncogene: A protooncogene is the normal counterpart in the eukaryotic genome to the oncogene carried by some viruses. In other words, protooncogene is a gene that, in normal cells, functions to control the normal proliferation of cells and that, when mutated or changed in any other way, becomes an oncogene.

Repressor Gene: A repressor gene is a regulatory gene whose product is a protein that controls the transcriptional activity of a particular operon. When an operon is repressed, it is turned off and becomes inactive.

Sarcoma: Sarcoma is a connective tissue neoplasm that is usually highly malignant. It is formed by proliferation of mesodermal cells.

Sarcomatoid: Sarcomatoid is a neoplasm that resembles a sarcoma.

Screening: Screening is defined as the application of a test to detect disease in a population of individuals who do not show any symptoms of their disease. The objective of screening is to detect disease at an early stage, when curative treatment is more effective.

Serial Analysis of Gene Expression (SAGE) is an approach that allows rapid and detailed analysis of thousands of transcripts. The LongSAGE method (Saha *et al*., 2002) is similar to the original SAGE protocol (Velculescu *et al.,* 1995) but produces longer transcript tags. The resulting 21 bp consists of a constant 4 bp sequence representing the restriction site at which the transcript has been cleaved, followed by a unique 17 bp sequence derived from an adjacent sequence in each transcript. This improved method was used for characterizing ~28,000 transcript tags from the colorectal cancer cell line DLD-1. The SAGE method was also used for identifying and quantifying a total of 303,706 transcripts derived from colorectal and pancreatic cancers (Zhang *et al*., 1997). Metastatic colorectal cancer showed multiple copies of the PRL-3 gene that was located at chromosome 8q24.3 (Saha *et al*., 2001). Several genes and pathways have been identified in breast cancer using the SAGE method (Porter *et al*., 2001). The SAGE method is particularly useful for organisms whose genome is not completely sequenced because it does not require a hybridization probe for each transcript and allows new genes to be discovered. Because SAGE tag numbers directly reflect the abundance of the mRNAs, these data are highly accurate and quantitative. For further details, see Part II, Chapter 6, in Volume 1 of this series by Dr. Ye.

Signal Transduction: Signal transduction describes the process by which a receptor interacts with a ligand at the surface of the cell and then transmits a signal to trigger a pathway within the cell. The basic principle of

this interaction is that ligand binding on the extracellular side influences the activity of the receptor domain on the cytoplasmic side. The signal is transduced across the membrane. Signal transduction provides a means for amplification of the original signal.

Somatic Mutation: A somatic mutation is a mutation occurring in a somatic cell and therefore affecting only its daughter cells; it is not inherited by decendents of the organism.

Specificity: Specificity is the capacity for discrimination between antigenic determinants by antibody or lymphocyte receptor.

Splicing: Splicing is the process of linking together two RNA exons while removing the intron that lies between them.

Suppressor Gene: A suppressor gene is a gene that suppresses mutations in other genes. The effects of a mutation may be diminished or abolished by a mutation at another site. The latter may totally or partially restore a function lost because of a primary mutation at another site. A suppressor mutation does not result in a reversal of the original mutation; instead, it masks or compensates for the effects of the primary mutation.

Transcription: Transcription is the process by which an RNA copy of a gene is made.

Transduction: Transduction refers to the use of a phage (or virus) to carry host genes from one cell to another cell of different genotype.

Transgenic Animals: Transgenic animals are created by introducing new DNA sequences into the germline via addition to the egg.

Tumor Markers: Tumor markers are molecular entities that distinguish tumor cells from normal cells. They may be unique genes or their products that are found only in tumor cells or they may be genes or gene products that are found in normal cells but are aberrantly expressed in unique locations in the tumor cells, or are present in abnormal amounts, or function abnormally in response to cellular stress or to environmental signals (Schilsky and Taube, 2002). Tumor markers may be located intracellularly (within the nucleus, in the cytoplasm, or on the membrane), on the cell surface, or secreted into the extracellular space, including into the circulation. Tumor markers usually are used for monitoring and detecting early response in asymptomatic patients. For example, tissuebased estrogen receptor and HER-2/neu amplification/overexpression markers in breast cancer have been validated to predict response to therapy in breast cancer. Other examples are PSA, which is a marker for early detection of prostate cancer and carcinoembryonic antigen, which is used for detecting colon cancer.

Viral Oncogene: A viral oncogene transforms a cell it infects to a cancerous state.

Xenograft: Xenograft refers to transferring a graft or tissue from one species to another.

Wild-Type: A strain, organism, or gene of the type that is designated as the standard for the organism with respect to genotype and phenotype.

References

Birch, J.M., Alston, R.D., Kelsey, A.M., Quinn, M.J., Babb, P., and McNally, R.J.Q. 2002. Classification and incidence of cancers in adolescents and young adults in England 1979–1997. *Br. J. Cancer 87*:1267–1274.

Bird, A. 2002. DNA methylation patterns and epigenetic memory. *Genes Dev*. *16*:6–21.

Cavalli, G., and Paro, R. 1999. Epigenetic inheritance of active chromatin after removal of the main transactivator. *Science 286*:955–958.

Kondrashov, F.A., and Koonin, E.V. 2001. Origin of alternative splicing by tandem exon duplication. *Hum. Mol. Genet. 10*: 2661–2669.

Mikulowska-Mennis, A., Taylor, T.B., Vishnu, P., Michie, S.A., Raja, R., Horner, N., and Kunitake, S.T. 2002. High quality RNA from cells isolated by laser capture microdissection. *Biotechniques 33*:1–4.

Mironov, A.A., Fickett, J.W., and Gelfand, M.S. 1999. Frequent alternative splicing of human genes. *Genome Res. 9*:1288–1293.

Pierce, A.J., Stark, J.M., Araujo, F.D., Moynahan, M.E., Berwick, M., and Jasin, M. 2001. Double-strand breaks and tumorigenesis. *Trends Cell Biol*. *11*:S52–S59.

Porter, D.A., Krop, I.E., Nasser, S., Sgroi, D., Kaelin, C.M., Marks, J.R., Riggins, G., and Polyak, K. 2001. A sage (Serial analysis of gene expression) view of breast tumor progression. *Cancer Res. 61*:5697–5702.

Poste, G., and Fidler, I.J. 1980. The pathogenesis of cancer metastasis. *Nature 283*:139–146.

Pu, R.T., and Clark, D.P. 2003. Detection of DNA methylation. Potential applications to diagnostic cytopathology. *Acta. Cytol. 47*:247–252.

Ramaswamy, S., and Golub, T.R. 2002. DNA microarrays in clinical oncology. *J. Clin. Oncol. 20*:1932–1941.

Rinehart, F.P., Ritch, T.G., Deininger, P., and Schmid, C.W. 1981. Renaturation rate studies of a single family of interspersed repeated sequences in human deoxyribonucleic acid. *Biochemistry 20*:3003–3010.

Rutherford, S.L., and Henikoff, S. 2003. Quantitative epigenetics. *Nat. Genetics 33*:6–8.

Saha, S., Bardelli, A., Buckhaults, P., Velculescu, V.E., Rago, C., Croix, B. St., Romans, K.E., Choti, A., Lengauer, C., Kinzler, K.W., and Vogelstein, B. 2001. A phosphate associated with metastasis of colorectal cancer. *Science 294*:1343–1345.

Saha, S., Sparks, A.B., Rago, C., Akmaev, V., Wang, C.J., Vogelstein, B., Kinzler, K.W., and Velculescu, V.E., 2002. Using the transcriptome to annotate the genome. *Nat. Biotechnol. 19*:508–512.

Samanta, A., Samanta, J., and Gunn, M. 2003. Legal considerations of clinical guidelines: Will NICE make a difference? *J. R. Soc. Med. 96*:133–138.

Schilsky, R.L., and Taube, S.E. 2002. Introduction: Tumor markers as clinical cancer tests—are we there yet? *Sem. Oncol. 29*:211–212.

Shi, H., Maier, S., Nimmrich, I., Yan, P.S., Caldwell, C.W., Olek, A., and Huang, T.H.-M. 2003. Oligonucleotide-based microarray for DNA methylation analysis: Principles and applications. *J. Cellular Biochem. 88*:138–143.

Skorski, T. 2002. BCR/ABL regulates response to DNA damage: The role in resistance to genotoxic treatment and in genomic instability. *Oncogene 21:*8591–8604.

Velculescu, V.E., Zhang, L., Vogelstein, B., and Kinzler, K.W. 1995. Serial analysis of gene expression. *Science 270:*484–487.

Zhang, L., Zhou, W., Velculescu, V.E., Kern, S.E., Hruban, R.H., Hamilton, S.R., Vogelstein, B., and Kinzler, K.W. 1997. Gene expression profiles in normal and cancer cells. *Science 276:*1268–1272.

I

Molecular Pathology

This Page Intentionally Left Blank

1

Laser Capture Microdissection-Microarray Technology: Global mRNA Amplification for Expression Profiling on Laser Capture Cells

Kazuhiko Aoyagi and Hiroki Sasaki

Introduction

To understand gene expression in multicellular organisms, purification or enrichment of the cell types of interest is essential. The development of laser capture microdissection (LCM) also allows us to directly procure histologically pure populations of cells from microscopic regions of complex heterogeneous tissues such as cancer tissues (Emmert-Buck *et al.*, 1996). The combined use of LCM and microarray has been reported (Kitahara *et al.*, 2001; Luo *et al.*, 1999; Sgroi *et al.*, 1999). Those reports, however, relied on the T7-transcription alone. Although that standard procedure has been validated to faithfully maintain relative messenger ribonucleic acid (mRNA) levels (Baugh *et al.*, 2001; Wang *et al.*, 2000), only 8–40 μg of complementary ribonucleic acid (cRNA) are obtainable from purified cells (10^3–10^4) by LCM, even after three rounds of amplification (Kitahara *et al.*, 2001).

Therefore, the resolution of gene expression analysis in various physiologic and pathologic conditions in multicellular organisms has been limited by the insufficiency of the T7-based ribonucleic acid (RNA) amplification alone from fewer than 1000 cells.

We describe here an effective method for high-fidelity global mRNA amplification for *in vivo* gene expression profiling of as few as 100 cells obtained by LCM. This method, called TALPAT, is based on *T*7 RNA polymerase-mediated transcription, *a*daptor *l*igation, and *P*CR (*P*olymerase chain reaction) *a*mplification followed by *T*7-transcription (Aoyagi *et al.*, 2003). More than 80% of genes were commonly identified as a more than threefold changed gene among three gastric cancer cell lines using cRNA amplified by both TALPAT and the ordinary *in vitro* T7-transcription. The reproducibility of TALPAT was validated by microarray analysis on 100 breast cancer cells obtained by LCM. For the application of the

LCM-TALPAT method, we successfully obtained expression profiles of gastric cancer cells and the mesenchymal cells, enabling us to understand *in vivo* cell-to-cell cross-talk in the microenvironment.

MATERIALS AND METHODS

LCM And RNA Extraction from Microdissected Samples

1. Procedure of sample preparation for LCM is according to the standard protocol (Sgroi *et al.*, 1999). Surgical specimens of breast and gastric cancer tissues are embedded in TissueTek OCT medium (VWR Scientific Products Corp., Torrance, CA) and snap-frozen in liquid nitrogen.

2. The tissues are sectioned at 5–8 µm in a cryostat, mounted on uncoated glass slides, and immediately stored at –80°C.

3. Slides containing frozen sections are immediately fixed in 70% ethanol for 30 sec; stained with Mayer's hematoxylin solution (MUTO, Tokyo, Japan) and 0.5% eosin alcohol solution (MUTO); and followed by 3-min dehydration steps in 70%, 95%, and 100% of ethanol and a final 5-min dehydration step in xylene.

4. Once air-dried, the sections are laser microdissected with a PixCell II LCM system (Arcturus Engineering, Mountain View, CA) according to the standard protocol (Emmert-Buck *et al.*, 1996).

5. The transfer film and adherent cells are mixed with 500 µl of IsoGen lysis buffer (Nippon Gene Co., Ltd., Toyama, Japan) or TRIZOL Reagent (Invitrogen Corp., Carlsbad, CA) in a 1.5-ml tube. The cells are homogenized by a voltex mixer. Add 1 µl of 20 µg/µl glycogen as a carrier.

6. The homogenized samples are incubated for 5 min at room temperature, and 100 µl of chloroform are added. The tubes are capped and shaken vigorously by hand for 15 sec and incubated for 2–3 min at room temperature. They are centrifuged for 10 min at $14,000 \times g$ to separate the phases, and the upper layer is transferred to a fresh 1.5-ml tube.

7. Equal volumes of isopropanol and voltex are added. They are incubated for 10 min at room temperature and centrifuged at $14,000 \times g$ for 10 min at room temperature.

8. The supernatant is removed and the pellet is overlayed with 0.5 ml of 75% ethanol. It is voltexed and centrifuged at $14,000 \times g$ for 5 min at room temperature. The supernatant is removed and the RNA pellet is dried for 5 min at room temperature.

9. The RNA pellet is resuspended in 17 µl of RNase-free water. Add 1 µl of RNase-free DNAse I

(Takara Shuzo Co., Ltd., Shiga, Japan) and 2 µl of $10\times$ Dnase I buffer (Takara Shuzo Co., Ltd.). The RNA samples are incubated at 37°C for 30 min.

10. The RNA is isolated once again by extraction with IsoGen lysis buffer or TRIZOL Reagent and precipitated in isopropanol (the procedures are according to those previously mentioned).

11. The RNA pellet is then resuspended in 10 µl of RNase-free water.

TALPAT Step 1

1. A Super Script Choice System (Invitrogen Corp.) is used for cDNA synthesis. To initiate first-strand cDNA synthesis, 1 µl of 100 pmole/µl Oligo (dT) 24-T7 primer,

5′-pGGCCAGTGAATTGTAATACGACTCAC-
TATAGGGAGGCG-
GTTTTTTTTTTTTTTTTTTTTTTTTT-3′

is added to 10 µl of a solution containing total RNA corresponding to 100 or 1000 cells, incubated at 65°C for 10 min, and chilled on ice.

2. Four microliters of $5 \times$ first-strand buffer, 2 µl of 0.1 M DTT, 1 µl of 10 mM dNTP and 1 µl of RNase inhibitor are added to the RNA solution and incubated at 37°C for 5 min.

3. One microliter of Superscript RT II is then added and incubated at 37°C for 1 hr.

4. For second-strand complementary deoxyribonucleic acid (cDNA) synthesis, 30 µl of $5 \times$ second-strand synthesis buffer, 3 µl of 10 mM dNTPs, 4 µl of DNA polymerase I, 1 µl of *Escherichia coli* RNase H, 1 µl of *E. coli* DNA ligase, and 91 µl of RNase-free water are added to the first-strand cDNA solution and incubated at 16°C for 2 hr.

5. For end-filling, 2 µl of T4 DNA polymerase is added and incubated at 16°C for 10 min.

6. Phenol (150 µl) saturated by 10 mM Tris-HCl pH 7.5, 0.5 mM ethylenediane tetra-acetic acid (EDTA) buffer is added. The tubes are capped and shaken vigorously by hand for 15 sec. They are centrifuged for 5 min at $14,000 \times g$ to separate the phases. The upper layer (~150 µl) is transferred to a fresh 1.5-ml tube.

7. Phenol (150 µl) is added, saturated by 10 mM Tris-HCl (pH 7.5) 0.5 mM EDTA buffer. The tubes are capped and shaken vigorously by hand for 15 sec. They are centrifuged for 5 min at $14,000 \times g$ to separate the phases. The upper layer (~150 µl) is transferred to a fresh 1.5-ml tube.

8. Then 75 µl of 7.5 M CH_3COOH_4 and 500 µl of isopropanol and voltex are added. They are incubated

for 10 min at room temperature and centrifuged at $14,000 \times g$ for 10 min at room temperature.

9. The supernatant is removed and the pellet is over-layered with 0.5 ml of 75% ethanol. They are vortexed and centrifuged at $14,000 \times g$ for 5 min at room temperature. Remove the supernatant and dry the cDNA pellet for 5 min at room temperature.

10. The cDNA pellet is resuspended in 150 µl of RNase-free water and isolated once again by isopropanol precipitation and 75% ethanol wash (the procedures are according to those previously outlined).

11. The cDNA pellet is then resuspended in 8 µl of RNase-free water.

TALPAT Step 2

12. A MEGAscript *in vitro* Transcription Kit (Ambion Inc., Austin, TX) is used for cRNA production by *in vitro* transcription using T7 RNA polymerase. Two microliters of $10 \times$ reaction buffer; 2 µl each of 100 mM adenosine triphosphate (ATP), cytidine triphosphate (CTP), guanosine triphosphate (GTP), and uridine triphosphate (UTP), and 2 µl of T7 RNA polymerase are added to the 8 µl cDNA solution and incubated at 37°C for 5 hr.

13. One microliter of RNase-free DNase I is added and incubated at 37°C for 15 min.

14. After mixing with 480 µl of IsoGen lysis buffer or TRIZOL Reagent (Invitrogen Corp.) at room temperature, 100 µl of chloroform is added. The tubes are capped and shaken vigorously by hand for 15 sec and incubated for 2–3 min at room temperature. They are centrifuged for 10 min at $14,000 \times g$ to separate the phases. The upper layer is transferred to a fresh 1.5-ml tube.

15. Equal volume of isopropanol and voltex is added. They are incubated for 10 min at room temperature and centrifuged at $14,000 \times g$ for 10 min at room temperature.

16. The supernatant is removed and the pellet is overlayed with 0.5 ml of 75% ethanol. They are vortexed and centrifuged at $14,000 \times g$ for 5 min at room temperature. The supernatant is removed and the cRNA pellet is dried for 5 min at room temperature.

17. The cRNA pellet is then resuspended in 10 µl of RNase-free water.

TALPAT Step 3

18. To initiate first-strand cDNA synthesis, 1 µl of 0.5 µg/µl random hexanucleotide primer is added to 10 µl of the cRNA solution and incubated at 65°C for 10 min, chilled on ice, and equilibrated at room temperature for 10 min.

19. Four microliters of 5× first-strand buffer, 2 µl of 0.1 M DTT, 1 µl of 10 mM dNTP, 1 µl of RNase

inhibitor, and 1 µl of Superscript RT II are added and incubated at room temperature for 5 min followed by incubation at 37°C for 1 hr. For annealing of the primer in second-strand cDNA synthesis, 1 µl of 100 pmole/µl Oligo (dT)24-T7 primer is added and incubated at 65°C for 5 min and 42°C for 10 min.

20. 30 µl of 5× second-strand synthesis buffer, 3 µl of 10 mM dNTPs, 4 µl of DNA polymerase I, 1 µl of *E. coli* RNase H, and 90 µl of RNase-free water are added to the first-strand cDNA solution and incubated at 16°C for 2 hr.

21. For end-filling, 2 µl of T4 DNA polymerase is added and incubated at 37°C for 10 min.

22. Phenol (150 µl) is added, saturated by 10 mM Tris-HCl (pH 7.5) 0.5 mM EDTA buffer. The tubes are capped and shaken vigorously by hand for 15 sec. They are centrifuged for 5 min at $14,000 \times g$ to separate the phases. Transfer the upper layer (~150 µl) to a fresh 1.5-ml tube.

23. 150 µl of chloroform is added. The tubes are capped and shaken vigorously by hand for 15 sec. It is centrifuged for 5 min at $14,000 \times g$ to separate the phases. The upper layer (~150 µl) is transferred to a fresh 1.5-ml tube.

24. Then 75 µl of 7.5 M CH_3COOH_4 and 500 µl of isopropanol and voltex are added and incubated for 10 min at room temperature. It is centrifuged at $14,000 \times g$ for 10 min at room temperature.

25. The supernatant is removed and the pellet is overlayed with 0.5 ml of 75% ethanol. It should be vortexed and centrifuged at $14,000 \times g$ for 5 min at room temperature. The supernatant removed, and the cDNA pellet should be dried for 5 min at room temperature.

26. The cDNA pellet is resuspended in 150 µl of RNase-free water and isolated once again by isopropanol precipitation and 75% ethanol wash (the procedures were according to those outlined previously).

27. The cDNA pellet is then resuspended in 8 µl of RNase-free water.

The second-round T7-transcription as described in TALPAT step 2 is carried out when the starting material is less than 10 ng of total RNA or fewer than 1000 captured cells.

TALPAT Step 4

28. To amplify the cDNA by PCR, *Eco*Rl-*Not*l-*Bam*HI adaptor (Takara Shuzo Co., Ltd., Shiga, Japan),

$5'$-$_{HO}$AATTCGGCGGCCGCGGATCC $3'$-
GCCGCCGGCGCCTAGGp-$5'$

is ligated to the cDNA using T4 DNA ligase (Takara Shuzo CO., Ltd.); 14 µl of cDNA solution (200 ng), 2 µl

of 10 × T4 DNA ligase reaction buffer, 2 µl of 100 pmole/µl *Eco*RI-*Not*l-*Bam*HI adaptor, 0.5 µl 10 mM ATP, and 1 µl T4 DNA ligase (350 units) are mixed and incubated at 16°C for 12 hrs.

29. The adaptor-ligated cDNA was amplified in 20 microcentrifuge tubes by PCR, which is carried out in a total volume of 100 µl : 1 µl of the ligation mixture, 76 µl DNase-free water, 10 µl of 10 × PCR reaction buffer (100 mM Tris-HCl [pH 7.5] 500 mM KCl, 30 mM MgCl$_2$), 3 µl of 100 pmole/µl ER-1 primer,

5′-GGAATTCGGCGGCCGCGGATCC-3′

10 µl of 2.5 mM dNTP, and 1 µl Taq polymerase (2.5 units). Two-step PCR is cycled 30 times (95°C for 1 min, 72°C for 3 min) followed by incubation at 72°C for 10 min.

30. Phenol (100 µl) is added and saturated by 10 mM Tris-HCl (pH 7.5) 0.5 mM EDTA buffer. The tubes are capped and shaken vigorously by hand for 15 sec. They are centrifuged for 5 min at 14,000 × g to separate the phases. The upper layer (~100 µl) is transferred to a fresh 1.5-ml tube.

31. Chloroform (100 µl) is added. The tubes are capped and shaken vigorously by hand for 15 sec. They are centrifuged for 5 min at 14,000 × g to separate the phases. Transfer the upper layer (~100 µl) to a fresh 1.5-ml tube.

32. Then, 1 µl of 20 µg/µl glycogen, 50 µl of 7.5 M CH$_3$COOH$_4$, and 250 µl of isopropanol and voltex are added. They are incubated for 10 min at room temperature and centrifuged at 14,000 × g for 10 min at room temperature.

33. The supernatant is removed and the pellet is overlayed with 0.5 ml of 75% ethanol. They are vortexed and centrifuged at 14,000 × g for 5 min at room temperature. The supernatant is removed and the cDNA pellet is dried for 5 min.

34. The cDNA pellet is resuspended in 100 µl of RNase-free water and isolated once again by isopropanol precipitation and 75% ethanol wash (the procedures are according to those outlined previously).

35. The amplified cDNA pellet is resuspended in 10 mM Tris-HCl (pH 7.5) 0.5 mM EDTA buffer.

TALPAT Step 5

36. The amplified cDNA is then used for T7-transcription, as outlined previously).

Microarray Analysis

We used human U95A oligonucleotide probe arrays (Affymetrix, Santa Clara, CA) for analysis of mRNA expression levels corresponding to 12,626 transcripts. The procedures were conducted according to the supplier's protocols and are described briefly as follows.

1. Every 1 µg of cDNA produced by TALPAT was used to generate a cRNA probe by the T7-transcription.

2. Some fragmented (10 µg) cRNA was hybridized to the microarrays in 200 µl of a hybridization cocktail at 45°C for 16 hr in a rotisserie oven set at 60 rpm.

3. The arrays were then washed with a nonstringent wash buffer (6 × SSPE) at 25°C, followed by a stringent wash buffer (100 mM MES [pH 6.7], 0.1 M NaCl, and 0.01% Tween-20) at 50°C, stained with streptavidin phycoerythrin (Molecular Probes), washed again with 6 × SSPE, stained with biotinylated anti-streptavidin immunoglobulin G, followed by a second staining with streptavidin phycoerythrin and a third wash with 6 × SSPE.

4. The arrays were scanned using the GeneArray scanner (Affymetrix) at 3-µm resolution, and the scanned image was quantitatively analyzed with the computer software Microarray Suite 4.0 (Affymetrix).

5. For normalizing the data to compare mRNA expression levels among samples, we unified 1000 as an average of average distance (AD) scores corresponding to signal intensities of all probe sets in each sample.

RESULTS AND DISCUSSION

The TALPAT method for high-fidelity mRNA amplification for *in vivo* gene expression profiling of a small number of cells is based on a T7 RNA polymerase-mediated RNA amplification reaction combined with an adaptor ligation-mediated PCR. Figure 1 shows a schematic diagram of TALPAT. We usually checked the size of both cDNA and cRNA prior to hybridization because the size of a cRNA probe decreases depending on both the cycles of T7-transcription and the quality of the starting samples. Although the 3′ portions of mRNAs are selectively amplified in the process of Step 3, final products of cDNA after PCR ranged in size from 0.3 to 3.0 kb, which are sufficient for producing cRNA for microarray analysis. In fact, the size of cRNA produced by TALPAT was comparable to, or at least not much smaller than, that of cRNA produced by a single round of the T7-transcription (Figure 1). Some cDNA fragments have high guanine and cytosine (G/C) contents and may form a stable secondary structure, which often prevents PCR amplification at a standard annealing temperature, 50–60°C. To minimize the biased amplification resulting from differences in template sequences, a specific adaptor acting at a high annealing temperature (72°C) was selected by our previously reported system for whole genome DNA amplification

Total RNA (1~100ng)
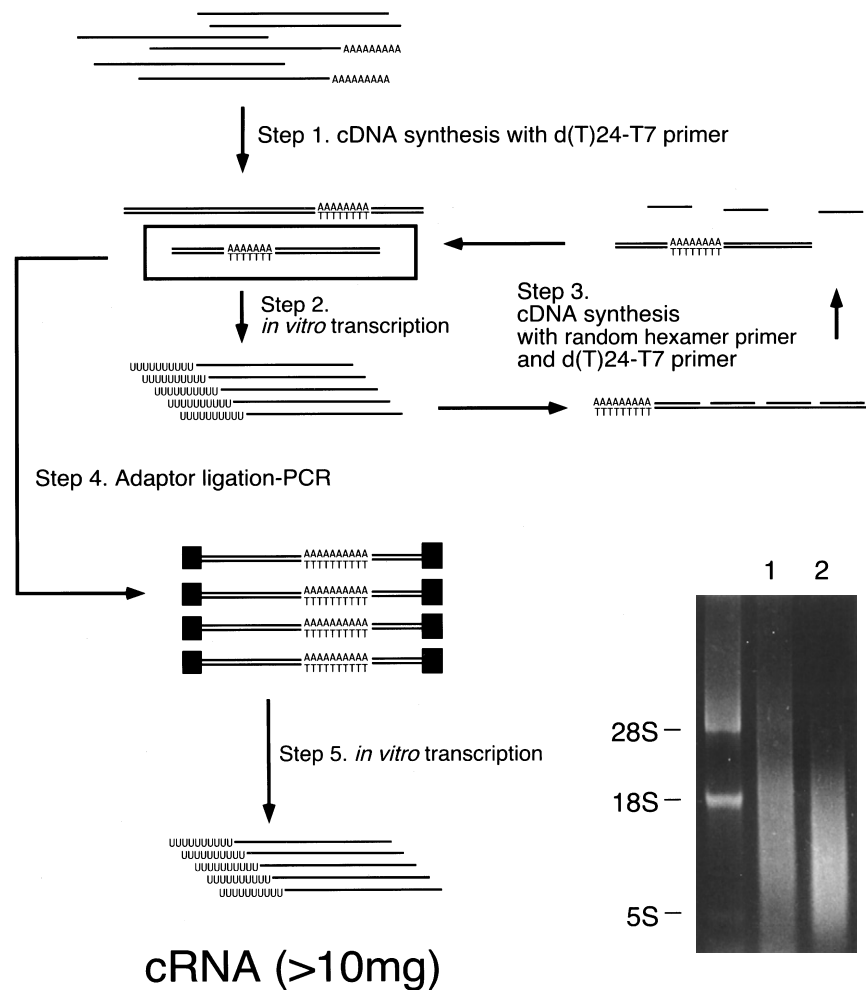
Figure 1 Schematic flow of high-fidelity genome-wide mRNA amplification by TALPAT. TALPAT consists of five steps of enzymatic reactions, as described in Materials and Methods: step 1, complementary deoxyribonucleic acid (cDNA) synthesis with oligo dT-T7 promoter primer; step 2, complementary ribonucleic acid (cRNA) amplification by *in vitro* transcription using T7 ribonucleic acid (RNA) polymerase; step 3, cDNA synthesis with random hexamer primer for the first-strand cDNA and oligo dT-T7 promoter primer for the second-strand cDNA; step 4, adaptor ligation-mediated PCR; step 5, cRNA amplification by *in vitro* transcription using T7 RNA polymerase. cRNA produced by a standard *in vitro* T7-transcription method (lane 1) and by TALPAT (lane 2) were resolved by non-denaturing agarose gel electrophoresis.

(Lucito *et al.*, 1998; Sasaki *et al.*, 1994). The PCR condition was optimized so that it can amplify sheared-genomic DNA fragments ranging in size from 0.3 to 2.0 kb with quite low biases, which was confirmed by test cloning, microsatellite typing, and gene-dosage analysis (Tanabe *et al.*, 2003). Only 1 ng of total RNA is available from 100 cultured cells, whereas TALPAT can generate 5–10 mg of cRNA from this limited amount of sample (data not shown). Milligrams of cRNA thus obtained can be analyzed by slot blot hybridization for quantifying mRNA levels and can be used for construction of a cDNA library of specific cells.

The reproducibility of TALPAT was examined by a scatter plot of a microarray analysis for 12,626 transcripts (human U95A oligonucleotide arrays, Affymetrix) using 10 ng of total RNA extracted from three gastric cancer cell lines as the starting material. A high concordance was observed between the two experiments of mRNA amplification by TALPAT

compared with the duplicate standard procedures of a single round of the T7-transcription using 5 μg of total RNA as the starting materials, which provide the highest reproducibility (Wang *et al.*, 2000) (Figure 2A). The linearity of the scatter plot between the duplicate TALPAT procedures (square of correlation coefficient, $R^2 = 0.9577$ for gastric cancer cell line HSC58, $R^2 = 0.9698$ for HSC59, and $R^2 = 0.9788$ for OCUM2M) was as high as that between the duplicate standard T7-transcription procedures ($R^2 = 0.9832$ for HSC58, $R^2 = 0.9788$ for HSC59, and $R^2 = 0.9835$ for OCUM2M). In all cell lines tested, 90–95% of the signals of detectable genes showed ratios of less than a twofold change between the two TALPAT experiments. These data are comparable to those of the standard T7-transcription using 5 μg of total RNA as the starting materials (Baugh *et al.*, 2001; Wang *et al.*, 2000). In general, signal intensities obtained by hybridization to microarrays are different depending on the cycles
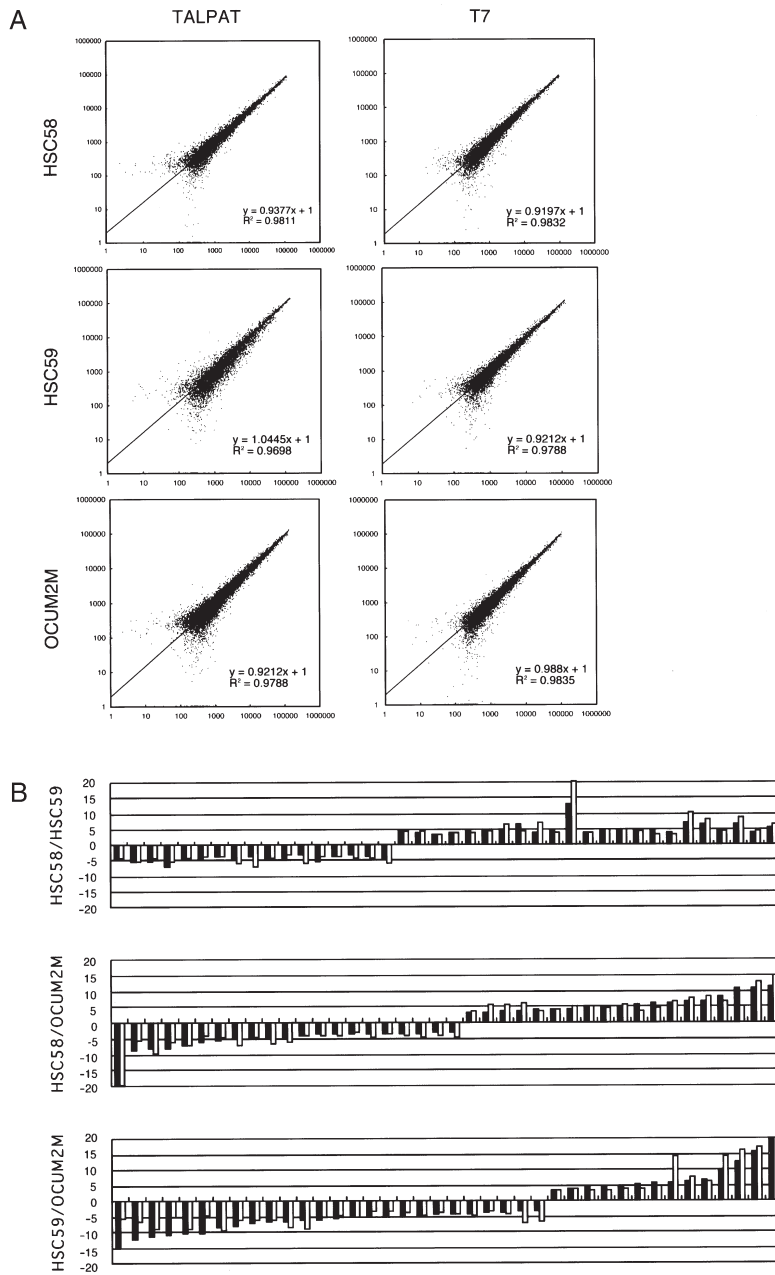
Figure 2 A: Scatter plots to evaluate the reproducibility of messenger ribonucleic acid (mRNA) amplification methods. The duplicate complementary ribonucleic acid (cRNA) samples were prepared by two independent amplification procedures, and the levels of gene expression were analyzed by hybridizations of each cRNA sample to a high-density oligonucleotide microarray. TALPAT using 10 ng total RNA of gastric cancer cell lines HSC58, HSC59, and OCUM2M *(left)* and the standard *in vitro* T7-transcription method using 5 μg of total RNA of same gastric cancer cell lines *(right)*. The genes showing a 1:1 ratio of signal intensities for the duplicate cRNA samples are clustered along the diagonal line. **B:** Comparative ratios of representative genes identified as a more than threefold changed gene between two gastric cancer cell lines by microarray analysis using cRNAs amplified by both TALPAT and the T7-transcription. The comparative ratios of each 40 representative genes (HSC58/HSC59, HSC58/OCUM2M, and HSC59/OCUM2M) are identified by both TALPAT *(solid box)* and the T7-transcription *(open box)*.

of the T7-transcription for producing a cRNA probe because the average size of the cRNAs decreases from cycle to cycle. Therefore, it is impossible to compare the signal intensities obtained by the different procedures.

To demonstrate TALPAT practicability, we compared the efficacy between TALPAT and the T7-transcription on identifying the differentially expressed genes among those gastric cancer cell lines. More than 80% of the genes were commonly identified as a more than threefold changed gene between two different gastric cancer cell lines using cRNAs amplified by

both TALPAT and a single round of the T7-transcription, which faithfully maintains relative mRNA levels (Wang *et al.*, 2000). The comparative ratios of each 40 representative genes (HSC58/HSC59, HSC58/OCUM2M, and HSC59/OCUM2M) identified by both experiments are shown in Figure 2B. The efficiency of the commonly identified genes as a differentially expressed gene by both the T7-transcription and direct reverse transcription is greatly affected by the starting amount of total RNA (85–90% in a single round of the T7-transcription from micrograms of source RNA,

30–70% in the same T7-transcription from 30–100 ng RNA, and 80–85% in a second amplification from 10–30 ng RNA) (Wang *et al.*, 2000). We compared the level of concordance between TALPAT from 10 ng RNA and a single round of the T7-transcription from 5 µg RNA, which is a faithful control. Therefore, TALPAT is concluded to be practicable in identifying the differentially expressed genes among a small amount of samples.

The power of TALPAT-mediated amplification was evaluated by expression profiling on total RNA extracted from a small number of cells obtained by LCM from a surgical specimen. One hundred or 500 breast cancer cells on a frozen tissue section were collected by LCM, as shown in Figure 3A, and total RNA was extracted and amplified by TALPAT. The cRNA was labeled and hybridized to the high-density microarray. The result of the scatter plot analysis is shown in Figure 3B. A strong linear relationship ($R^2 = 0.9735$) was observed between the 100 captured cells and the 500 captured cells as a faithful control, and 89% of the signals of the detectable genes showed ratios of less than a twofold difference between the two samples. This report is the first to demonstrate a successful result of microarray analysis on 100 cells collected by LCM.

For the application of the LCM-TALPAT method, we prepared two sets of fewer than 100 cancer cells and the mesenchymal cells from a section of a well-differentiated gastric adenocarcinoma by LCM (Figure 3C) and performed microarray analysis using their RNA samples amplified by TALPAT. The identity on gene expression levels between the two sets of gastric cancer cells was much higher than that between each set of gastric cancer cells and the mesenchymal cells (Figure 3D). It is noted that TALPAT can be applicable to 1–10 cells for identifying genes specific to one cell type; however, in identifying more than threefold changed genes among samples with a high reproducibility (Figure 2B), 10–100 cells should be required.
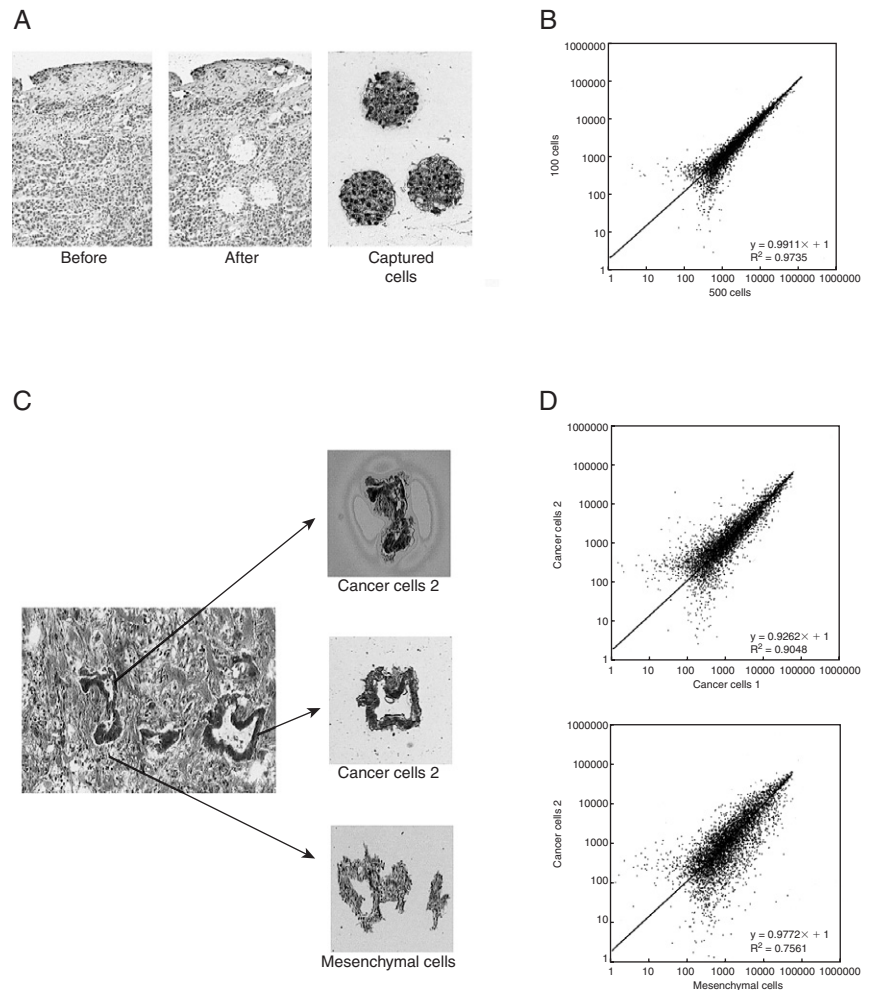
Figure 3 A: Separation of cells from a breast cancer tissue by laser capture microdissection (LCM). Sections (8 µm) were stained with hematoxylin. Breast cancer cells were transferred to a transfer film, as shown on the right. Approximately 40 breast cancer cells were collected by a single laser shot (30 µm in diameter). **B:** A scatter plot showing a high concordance ($R^2 = 0.9735$) of gene expression profiles obtained by hybridization to the human U95A oligonucleotide arrays using cRNAs produced by TALPAT on 100 or 500 captured breast cancer cells (LCM-TALPAT). **C:** Separation of cells from a gastric cancer tissue by LCM. Sections (5 µm) were stained with hematoxylin and eosin (H&E). Cancer cells and the mesenchymal cells were transferred to a transfer film, as shown on the right. Fewer than 100 cells were collected by several laser shots 7.5 µm in diameter. **D:** Scatter plots of gene expression profiles obtained by the microarray hybridization with cRNAs produced by TALPAT. A scatter plot from Set-1 of gastric cancer cells versus Set-2 of gastric cancer cells *(upper)* and Set-2 of gastric cancer cells versus the mesenchymal cells *(lower)*.

Taken together, it is expected that expression analysis with TALPAT using an oligonucleotide microarray and a cDNA microarray (data not shown) will offer a variety of new opportunities in biology and medicine for human beings and other multicellular organisms, whose gene functions are characterized by high regional and temporal diversities.

References

Aoyagi, K., Tatsuta, T., Nishigaki, M., Akimoto, S., Tanabe, C., Omoto, Y., Hayashi, S., Sakamoto, H., Sakamoto, M., Teruhiko, Y., Terada, M., and Sasaki, H. 2003. A faithful method for PCR-mediated global mRNA amplification and its integration into microarray analysis on laser-captured cells. *Biochem. Biophys. Res. Commun. 300*:915–920.

Baugh, L.R., Hill, A.A., Brown, E.L., and Hunter, C.P. 2001. Quantitative analysis of mRNA amplification by in vitro transcription. *Nucl. Acids Res. 29*:E29.

Emmert-Buck, M.R., Bonner, R.F., Smith, P.D., Chuaqui, R.F., Zhuang, Z., Goldstein, S.R., Weiss, R.A., and Liotta, L.A. 1996. Laser capture microdissection. *Science 274*:998–1001.

Kitahara, O., Furukawa, Y., Tanaka, T., Kihara, C., Ono, K., Yanagawa, R., Nita, T.M.E., Takagi, T., Nakamura, Y., and Tsunoda, T. 2001. Alterations of gene expression during colorectal carcinogenesis revealed by cDNA microarrays after laser-capture microdissection of tumor tissues and normal epithelia. *Cancer Res. 61*:3544–3549.

Lucito, R., Nakimura, M., West, J.A., Han, Y., Chin, K., Jensen, K., McCombie, R., Gray, J.W., and Wigler, M. 1998. Genetic analysis using genomic representations. *Proc. Natl. Acad. Sci. USA 95*:4487–4492.

Luo, L., Salunga, R.C., Guo, H., Bittner, A., Joy, K.C., Galindo, J.E., Xiao, H., Rogers, K.E., Wan, J.S., Jackson, M.R., and Eriander, M.G. 1999. Gene expression profiles of laser-captured adjacent neuronal subtypes. *Nature Med. 5*:117–122.

Sasaki, H., Nomura, S., Akiyama, N., Takahashi, A., Sugimura, T., Oishi, M., and Terada, M. 1994. Highly efficient method for obtaining a subtracted genomic DNA library by the modified in-gel competitive reassociation method. *Cancer Res. 54*:5821–5823.

Sgroi, D.C., Teng, S., Robinson, G., LeVangie, R., Hudson, J.R. Jr., and Elkahloun, A.G. 1999. *In vivo* gene expression profile analysis of human breast cancer progression. *Cancer Res. 59*:5656–5661.

Tanabe, C., Aoyagi, K., Sakiyama, T., Kohno, T., Yanagitani, N., Akimoto, S., Sakamoto, M., Sakamoto, H., Yokota, J., Ohki, M., Terada, M., Yoshida, T., and Sasaki, H. 2003. Evaluation of a whole genome amplification method based on adaptor-ligation PCR of randomly sheared genomic DNA. *Genes Chromos. Cancer 38*:168–176.

Wang, E., Miller, L.D., Ohnmacht, G.A., Liu, E.T., and Marincola, F.M. 2000. High-fidelity mRNA amplification for gene profiling. *Nat. Biotechnol. 18*:457–459.

2

Comparative Genomic Hybridization Analysis Using Metaphase or Microarray Slides

Simon Hughes, Ben Beheshti, Paula Marrano,
Gloria Lim, and Jeremy A. Squire

Introduction

Comparative genomic hybridization (CGH; Figure 4) has contributed to our understanding of chromosomal changes by making it possible to study all the chromosomal imbalances associated with tumor development and progression in a single experiment (Forozan *et al*., 1997; James *et al*., 1999). It has the advantage of combining the resolution of *in situ* techniques but eliminating the requirement for cytogenetic preparations from tumors and many of the technical variables associated with specialized cytogenetic analysis.

Chromosomal CGH uses metaphase chromosomes derived from a normal cell population to study and infer the cyto-genetic composition of the tumor of interest. For this approach, equal quantities of tumor and a normal reference genomic deoxyribonucleic acid (DNA) are labeled either directly or indirectly with different fluorescent dyes; the DNAs are then mixed and hybridized in equal amounts to immobilized metaphase targets on microscope slides. Labeled tumor DNA competes with differentially labeled and equimolar concentrations of normal reference DNA for hybridization. The ratio of fluorescence for the two dyes at the target is then used to map out DNA copy-number

changes between the DNA samples using chromosome preparations on glass slides (du Manoir *et al*., 1995; Kallioniemi *et al*., 1992). Inherent in chromosomal CGH is the problem of batch-to-batch variability in the quality of chromosome preparations, which can dramatically influence the fidelity of the CGH results. Factors such as drying rate, relative humidity, and age can profoundly influence the overall success of metaphase CGH. Although not dealt with in this chapter, an approach for optimizing metaphase preparation is described by Karhu *et al*. (1997). Following hybridization the interpretation of fluorescent signals requires sophisticated image analysis equipment and a high level of technical proficiency in identifying each human chromosome; thus, this method may not be suitable for all users.

The technique of "array CGH" has been developed, which combines the examination of chromosome changes with a similar microscope slide substrate platform to that used for microarray expression analysis. For array CGH, well-defined arrayed sequences of DNA have replaced the metaphase chromosomes as the hybridization targets on glass slides. The advantage of this approach is that it enables the researcher to quantitatively measure DNA copy-number changes at high

Handbook of Immunohistochemistry and in situ Hybridization of Human Carcinomas,
Volume 2: Molecular Pathology, Colorectal Carcinoma, and Prostate Carcinoma

11

A   Chromosome CGH   B   Array CGH
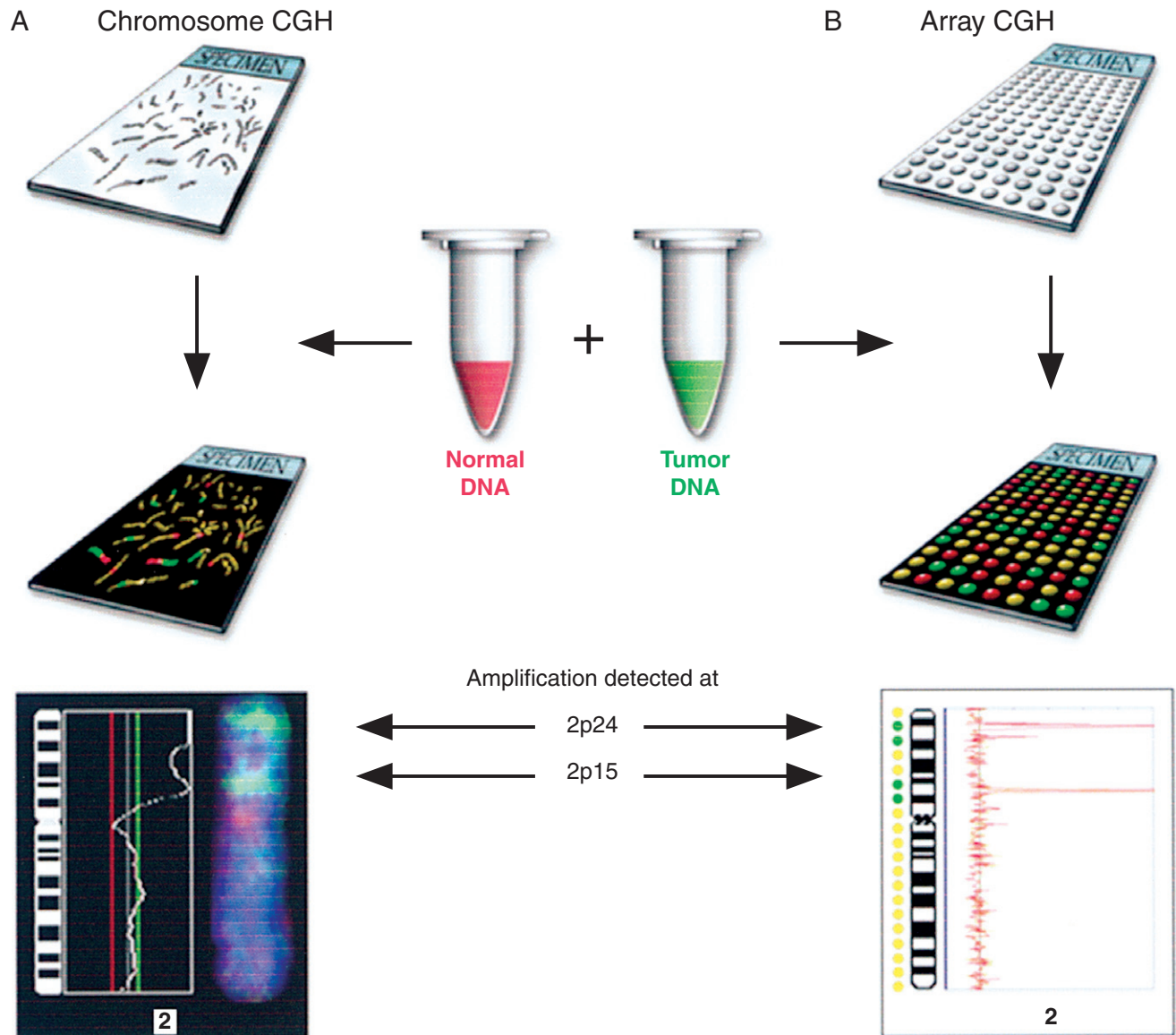
Figure 4 CGH methodology. Equal quantities of normal reference DNA and tumor DNA are labeled either directly or indirectly with different fluorescent dyes. The DNAs are then mixed and hybridized in equal amounts to immobilized targets, either metaphase chromosomes or arrayed DNA sequences. Labeled tumor DNA competes with differentially labeled normal reference DNA for hybridization, and the ratio of fluorescence for the two dyes can then be used to determine whether chromosomal regions have been lost or gained.

resolution and use *in silico* analysis to accurately map them directly to chromosomal locations.

Array CGH with complementary DNA (cDNA) targets makes use of cDNA microarrays to study underrepresentation and overrepresentation in terms of gene copy-number (Beheshti *et al.*, 2003a; Pollack *et al.*, 1999). cDNA array CGH has been used to examine breast cancer cell lines and tissues, which can detect copy-number gains and losses (Pollack *et al.*, 1999). Work performed in our laboratory has demonstrated the utility of cDNA array CGH for detecting MYCN (chromosome region 2p24) amplification in patients with neuroblastoma and cell lines using both cDNA array

CGH and chromosome CGH (Figure 4) (Beheshti *et al.*, 2003b). In addition, we have used cDNA array to analyze recurrent patterns of genomic imbalance in osteosarcomas (Squire *et al.*, 2003). These results show that the two approaches are comparable but also demonstrate the increased resolution provided by cDNA array CGH in contrast to chromosome CGH (Zhao *et al.*, 2002).

The CGH analysis using genomic DNA arrays refers to CGH applied to bacterial artificial chromosome (BAC) and phage artificial chromosome (PAC) targets spotted onto glass slides (Cai *et al.*, 2002). Kraus *et al.* (2003), studying micrometastatic tumor cell lines using a combination of multiplex-FISH (fluorescent *in situ*

hybridization), chromosome CGH, and genomic DNA array CGH, identified genomic regions involved in the evolution of metastasis. In addition, they demonstrated that the resolution obtained for CGH using genomic DNA arrays was superior to that obtained using chromosomes. These findings support earlier studies showing that genomic DNA arrays allow for the detection of several chromosomal alterations that fail to be identified by chromosome CGH (Hui *et al.*, 2001; Solinas-Toldo *et al.*, 1997; Wessendorf *et al.*, 2003).

This chapter will provide an overview of some of the CGH methods that are used in cytogenetic and genomics laboratories, and as an example their usefulness for genomewide analysis of chromosomal imbalances in the neuroblastoma cell line NUB7 is described.

Extraction Of High-Molecular–Weight DNA from Cells and Tissue

MATERIALS

1. Tissue culture cells.
2. Phosphate buffered saline (PBS) (pH 7.0).
3. Trypsin.
4. 15 ml polypropylene centrifuge tube.
5. 10–100 mg of tissue.
6. Proteinase K buffer: 5 ml 1 M Tris-HCl (pH 7.0), 0.2 ml 500 mM ethylenediamine tetra-acetic acid (EDTA) (pH 8.0), 0.5 ml Tween-20, sterile water up to 100 ml.
7. Proteinase K (14 mg/ml).
8. Sterile scalpel blade.
9. Fresh or frozen tissue sections, 10–100 mg.
10. Buffer saturated phenol.
11. Chloroform/isoamyl alcohol (24:1).
12. 3 M sodium acetate (NaAc) (pH 5.3).
13. Ethanol (70% and 100%).

METHODS

Tissue Culture Cells

1. Grow cells to 75–90% confluency.
2. Remove media, wash cells twice with PBS, and treat with trypsin (diluted 1 in 10 with PBS) at 37°C to dislodge cells.
3. Transfer cell suspension to a 15 ml polypropylene centrifuge tube and pellet cells ($200 \times g$ for 5 min). Discard the supernatant.
4. Resuspend cell pellet in 2 ml of proteinase K buffer containing 14 µl of proteinase K (final concentration 100 µg/ml). Incubate overnight at 37°C with constant gentle shaking.
5. Extract DNA using the phenol-chloroform extraction protocol outlined later in this chapter.

Tissue Samples

1. Use a scalpel blade to cut tissue (10–100 mg) into small pieces.
2. Transfer tissue to a 15 ml polypropylene tube containing 2 ml of proteinase K buffer and 14 µl of proteinase K (final concentration 100 µg/ml). Incubate for 24–48 hr at 37°C with constant gentle shaking.
3. Extract DNA using the phenol-chloroform extraction protocol outlined later in this chapter.

Phenol-Chloroform Extraction

1. Add an equal volume of phenol, and mix for 5 min.
2. Spin for 10 min at $16,000 \times g$.
3. Transfer the upper aqueous layer to a fresh tube, and add an equal volume of phenol/chloroform/isoamyl alcohol (in a 24:24:1 ratio). Mix for 5 min.
4. Spin for 10 min at $16,000 \times g$.
5. Transfer the upper aqueous layer to a fresh tube, and add an equal volume of chloroform. Mix for 5 min.
6. Spin for 10 min at $16,000 \times g$.
7. Transfer the upper aqueous layer to a new tube and add one-tenth volume of 3 M NaAc. Mix well.
8. Add 2 volumes of 100% ethanol. Mix gently by inversion. If the DNA is visible in the solution, remove the DNA with a pipette, place in a new tube, and then proceed to Step 10. If no DNA is visible, place solution at 70°C for 20 min or −20°C overnight.
9. Spin at $16,000 \times g$ for 10 min.
10. Remove ethanol and wash pellet with 1 ml of 70% ethanol.
11. Centrifuge at $16,000 \times g$ for 10 min, discard supernatant, and allow pellet to air-dry.
12. Dissolve in 100–300 µl of sterile water (volume depends on the amount of DNA visible after precipitation) and measure concentration using a spectrophotometer.

Metaphase CGH

MATERIALS

1. 5 ml NH$_4$-heparinized blood.
2. Tissue culture medium: RPMI 1640 containing 10% fetal calf serum, 1% L-glutamine, 1% penicillin-streptomycin, and 1% phytohemagglutinin.
3. 75 ml tissue culture flask.
4. Colcemid solution (10 µg/ml).
5. 50 ml polypropylene centrifuge tube.
6. 0.075 M KCl (hypotonic solution).
7. Ice-cold fixative; absolute methanol/acetic acid (in a 3:1 ratio).
8. Glass microscope slides.

9. 10X biotin dNTPs: 1 µl bovine serum albumin (BSA) (10 mg/ml), 10 µl 1 M β-mercaptoethanol, 50 µl 1 M Tris (pH 7.5), 5 µl 1 M MgCl$_2$, 25 µl 0.4 mM biotin 14-dATP, 1 µl 10 mM dATP, 2 µl 10 mM dCTP, 2 µl 10 mM dGTP, 2 µl 10 mM dTTP, sterile water up to 100 µl.

10. 20X digoxigenin (DIG) dNTPs: 25 µl 1mM DIG 11-dUTP, 7.7 µl 10 mM dATP, 7.7 µl 10 mM dCTP, 7.7 µl 10 mM dGTP, 5 µl 10 mM dTTP, sterile water up to 77 µl.

11. 10X DIG incubation buffer: 10 µl BSA (10 mg/ml), 5 ml 1 M Tris (pH 7.5), 0.5 ml 1 M MgCl$_2$, 1 ml 1 M β-mercaptoethanol, sterile water up to 10 ml.

12. BSA, 10 mg/ml.

13. DNAse I dilution buffer: 50 µl 1 M Tris (pH 7.5), 5 µl 1 M MgCl$_2$ 1 µl 1 M β-mercaptoethanol, 10 µl BSA (10 mg/mL), sterile water up to 1 ml.

14. DNAse I (92 units/µl).

15. DNA polymerase I (10 units/µl).

16. 1 kb DNA ladder (1 µg/µl, Invitrogen Corp., Carlsbad, CA).

17. Agarose.

18. 0.5X Tris-Borate-EDTA (TBE) buffer.

19. Ethidium bromide.

20. Sonicated salmon sperm DNA (1 mg/ml).

21. 300 mM EDTA (pH 8.0).

22. 3 M NaAc (pH 5.3).

23. Ethanol (100% and 70%).

24. Human Cot-1 DNA (1 µg/µl).

25. Hybrisol VII (50% formamide-2X SSC pH 7.0).

26. Formamide.

27. 20X saline-sodium citrate (SSC).

28. Denaturation solution: 49 ml of formamide, 7 ml of 20X SSC, and 14 ml of sterile water.

29. 10% Pepsin.

30. HCl.

31. 1X PBS.

32. 22 × 40 mm coverslip.

33. Wash solution 1: 500 ml formamide, 100 ml 20X SSC; sterile water up to 1 L.

34. Wash solution 2: 200 ml 20X SSC, 1 ml Tween-20 (Sigma, St. Louis, MO); sterile water up to 1 L.

35. Blocking solution: 0.3 ml BSA, 10 µl Tween-20 1 ml 20X SSC; sterile water up to 10 ml.

36. Avidin-FITC.

37. Rhodamine anti-DIG (200 µg/ml).

38. Antifade containing DAPI (1 mg/ml).

METHODS

Metaphase Spread Preparation

1. Add 5 ml of NH$_4$-heparinized blood to 45 ml of tissue culture medium in a 75 ml flask and incubate for 72 hrs at 37°C.

2. Add 0.5 ml of colcemid solution and incubate for 20 min at 37°C.

3. Transfer solution to a 50 ml polypropylene tube and pellet cells by centrifugation (200 × g, 5 min). Discard supernatant.

4. Resuspend pellet in 5–10 drops of hypotonic solution and gently mix cells by swirling.

5. Slowly add 2 ml of hypotonic solution dropwise and swirl cells to mix.

6. Add an additional 12 ml of hypotonic solution and swirl to mix. Incubate for 15 min at 37°C.

7. Pellet cells by centrifugation (200 × g, 5 min) and then discard the supernatant.

8. Resuspend pellet in 5–10 drops of ice-cold fixative.

9. Slowly add an additional 5 ml of cold fixative while constantly swirling the cell suspension.

10. Pellet cells by centrifugation (200 × g, 5 min), discard the supernatant, and repeat **Steps 7 and 8**.

11. Incubate the cells on ice for 20–30 min.

12. Pellet cells by centrifugation (200 × g, 5 min at 4°C) and resuspend cells in 0.5–1 ml of cold fixative.

13. Place 2 or 3 drops of cell suspension, depending on the number of cells, onto a wet slide chilled in ice-cold water.

14. Air-dry slides at room temperature, and store slides for at least 2 weeks at room temperature prior to use.

DNA Labelling and Probe Production

1. The source of DNA used can be prepared as outlined in Extraction of High-Molecular–Weight DNA from cells and tissue.[1]

2. For tumor DNA, combine 2 µg of DNA, 10 µl of 10X Biotin dNTPs, 10 µl of DNAse I (diluted 1 in 10,000 in DNAse I dilution buffer), 1 µl of DNA polymerase I, and sterile water up to 100 µl.

3. For normal reference DNA combine 2 µg of DNA, 10 µl of 10X DIG incubation buffer, 5 µl of 20X DIG dNTPs, 10 µl of DNase I (diluted 1 in 10,000 in DNAse I dilution buffer), 1 µl of DNA polymerase I, and sterile water up to 100 µl.

4. Incubate for 90 min at 16°C.

5. Determine the size of the probe by removing a 10 µl aliquot from the reaction mixture and analyzing the aliquot by agarose gel electrophoresis (1% agarose gel

---

[1]The data produced by CGH analysis represent an average of all cells from a sample. If the specimen is a heterogeneous mixture of normal and tumor cells, this will reduce the sensitivity. Thus, in those instances it is important to dissect out the specific cells of interest.

containing 10 ng/ml of ethidium bromide) alongside 1 μl of a mole-cular weight marker (1 kb DNA ladder).

6. Perform the electrophoresis at 100 volts (V) for 30 min in 0.5X TBE.

7. Visualize the DNA fragments using an ultraviolet (UV) transilluminator. Check that the length of the probe DNA (which appears as a smear) is in the range of 500 bp to 2 kb.

8. If the probe size is in optimal range, add 5 μl of 300 mM EDTA (to stop the DNase I activity) and proceed to First Precipitation. If the probe size is too large, add more DNAse I and incubate for a further 15–30 min at 16°C and repeat **Steps 4 and 5**. If the probe size is too small, repeat from step 1 but use less DNAse I.

First Precipitation[2]

1. Add 100 μl of sonicated salmon sperm DNA to the labeled DNA (biotin-labeled tumor DNA and DIG labeled normal DNA) and then add sterile water to give a final volume of 150 μl. Precipitate the DNA by the addition of one-tenth volume of 3 M NaAc and 2 volumes of 100% ethanol.

2. Place at −20°C overnight or at −70°C for 20 min.

3. Centrifuge for 20 min at 16,000 × g and decant supernatant.

4. Wash the pellet with 1 ml of 70% ethanol, centrifuge for 10 min at 16,000 × g, decant the supernatant, and air-dry the pellet (5–10 min).

5. Resuspend the pellet in 200 μl of water to give a final DNA concentration of ~10 ng/μl.

Second Precipitation and Probe Preparation

1. Combine 15 μl of biotin-labeled tumor DNA, 15 μl of DIG-labeled normal DNA (from first precipitation), 10 μl of Human Cot-1 DNA, and 60 μl of sterile water. Precipitate the DNA by the addition of one-tenth volume of 3 M NaAc and 2 volumes of 100% ethanol.

2. Place at −20°C overnight or at −70°C for 20 min.

3. Centrifuge for 20 min at 16,000 × g and decant supernatant.

4. Wash the pellet with 70% ethanol, centrifuge for 10 min at 16,000 × g, decant supernatant, and air-dry the pellet (5–10 min).

5. Resuspend the pellet in 30 μl of Hybrisol VII.

6. Heat denature the probe for 10 min at 75°C and then incubate at 37°C for 1 hr to preanneal.[3]

Slide Pretreatment

1. Dehydrate the slides in an ethanol series: 70%, 90%, or 100% for 5 min in each. Air-dry the slides.

2. Denature the slides for 2 min at 75°C in the denaturation solution.

3. Immediately transfer slides to 70% ice-cold ethanol for 2 min and continue to dehydrate in 90% and 100% ethanol for 2 min each. Air-dry the slides.

4. Pepsin treatment: incubate slides for 7.5 min at 37°C in a solution containing 15 μl of 10% pepsin in 50 ml 0.01 M HCl (preheated to 37°C). Wash the slides in 1× PBS for 5 min at room temperature.

5. Dehydrate the slide through an ethanol series, 70%, 90%, and 100%, 2 min each.

6. Air-dry the slides.[4]

Hybridization and Washing

1. Add the 30 μl prehybridized probe to the pretreated slide, cover with a coverslip (20 × 40 mm), and seal with rubber cement.

2. Hybridize for 72 hr in a humid incubator at 37°C.

3. Remove the rubber cement, being careful not to move the coverslip.

4. Perform all washes in glass Coplin jars.

5. Gently dip slides into and out of wash 1 until coverslip detaches from slide.

6. Wash 3× for 5 min each in wash 1 at 45°C.

7. Wash 3× for 5 min each in 2× SSC at 45°C.

8. Block for 30 min at 37°C with 35 μl of blocking solution under a coverslip (20 × 40 mm).

9. Incubate for 30 min at 37°C with 35 μl of avidin-FITC (1:10) and Rhodamine anti-DIG (1:10) in blocking solution under a coverslip (20 × 40 mm) in a humid chamber.

10. Wash 3× for 5 min each in wash 2 at 45°C.

11. Mount with 30 μl of anti-fade containing DAPI and cover with a coverslip.

12. Store slides in the dark at −20°C.

Chromosome Visualization and Image Analysis

1. Our image capture and analysis is performed using the Vysis Quips SmartCapture imaging system and Quips CGH/Karyotyper and Interpreter software

---

[2]The first precipitation removes unincorporated dNTPs. The addition of salmon sperm in this precipitation is done so that any loss of DNA comes mainly from the salmon sperm rather than the labeled DNA.
[3]Incubation at 37°C allows for annealing of Cot-1 to repetitive sequences within the probe.

[4]It is important to use slides immediately after the final dehydration step because the slide will start to rehydrate.

(Vysis, Downers Grove, IL), so our experience is limited to their use.

2. Scan the slide for metaphase spreads showing good chromosomal separation with an even green and red fluorescent signal and a low background. Capture 10–12 images per slide. Using the protocol outlined previously, the ratio of FITC:rhodamine signal is expressed as green:red ratio, and any deviation from a 1:1 ratio indicates gain or loss of chromosome material. Only analyze gains or losses exceeding the 50% CGH threshold (lower threshold 0.75, upper threshold 1.25). Thus, an increase of green:red ratio indicates a gain of chromosomal material in the tumor; conversely, a decrease in green:red ratio indicates a loss of genomic material in the tumor.

3. For further analysis, refer to specific system information.

CGH Arrays[5]

CGH Analysis on cDNA Microarrays

MATERIALS

1. High-molecular–weight DNA (tumor and normal reference).
2. Sterile water.
3. BioPrime DNA labeling system (Invitrogen).
4. 10× dNTP mixture: 12 µl (final concentration 1.2 mM) 100 mM dATP, 12 µl (final concentration 1.2 mM) 100 mM dGTP, 12 µl (final concentration 1.2 mM) 100 mM dTTP, 6 µl (final concentration 0.6 mM) 100 mM dCTP, and 958 µl Tris-EDTA (pH 8.0).
5. 1 mM Cy5-dCTP and 1 mM Cy3-dCTP.
6. EDTA (pH 8.0).
7. 1× Tris-EDTA buffer (pH 7.4).
8. Microcon 30 filter.
9. Yeast transfer ribonucleic acid (tRNA; 10 mg/ml).
10. Poly(dA-dT) (4 mg/ml).
11. Human Cot-1 DNA (1 mg/ml).
12. DIG Easy Hyb (Roche).
13. 20X SSC (pH 7.0).
14. 10% Sodium dodecyl sulfate (SDS).
15. cDNA array.
16. 24 × 50 mm coverslip.
17. Rubber cement.
18. Hybridization oven.
19. Coplin jars.

20. Wash A: 1 ml 10% SDS, sterile water up to 100 ml.
21. Wash B: 2.5 ml 20X SSC, 0.1 ml 10% SDS, sterile water up to 100 ml.
22. Wash C: 0.3 ml 20X SSC, sterile water up to 100 ml.
23. Slide centrifuge.
24. Scanner.

DNA Labeling[6]

1. The source of DNA used can be prepared as outlined in Extraction of High-Molecular–Weight DNA from Cells and Tissue.
2. In each labeling experiment eight reactions are set up, four containing 2.5 µg of tumor DNA and four containing 2.5 µg of normal DNA.
3. To each tube, add sterile water to bring the volume up to 21.5 µl, then add 20 µl of 2.5X random primers (BioPrime DNA labeling system) and mix by vortexing. Boil tubes for 5 min and then immediately place on ice.
4. To each tube add 5 µl 10× dNTPs (do not use the dNTPs from BioPrime DNA labeling system), 2.5 µl of either Cy3-dCTP (1 mM) or Cy5-dCTP (1 mM) and mix well. Separate labeling reactions for Cy3 and Cy5 are set up for both tumor and normal DNA. Thus, each sample, tumor or normal, will have two duplicate reactions labeled with Cy3 and two duplicate reactions labeled with Cy5.
5. Finally add 1 µl of Klenow Fragment (BioPrime DNA labeling system), mix by tapping, and recollect by brief centrifugation.
6. Incubate for 2 hr at 37°C, and then stop the reaction by the addition of 5 µl 0.5 M EDTA.

Probe Purification and Hybridization

1. Purify each labeling reaction separately using a microcon 30 filter.
2. Add 450 µl TE to each of the labeling reactions.
3. Pipette the solution onto the microcon 30 filter. Centrifuge for 8–10 min at 8000 × g. Invert filter and transfer to a fresh tube. Centrifuge for 1 min at 8000 × g to recover purified probe (20–40 µl volume).
4. Combine one Cy3-labeled tumor sample with one Cy5-labeled normal sample and vice versa (dye-switch experiments).
5. Add 50 µl Human Cot-1 DNA, 20 µl yeast tRNA, and 4 µl Poly(dA-dT) to each combined probe mix.[7]

---

[5]It is possible that there may be a number of clones that are misannotated for both the cDNA and BAC clones. It is therefore important to verify array CGH results by FISH.

[6]Cy3 and Cy5 dyes are light sensitive, so avoid prolonged exposure to light.

[7]Cot-1 DNA blocks hybridization or repetitive sequences. Yeast tRNA blocks nonspecific DNA binding. Poly(dA-dT) blocks hybridization to PolyA tails of cDNA array targets.
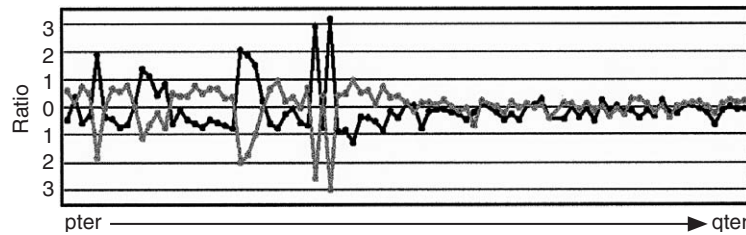
Figure 5 Chromosomal dosage changes across chromosome 6 in the osteosarcoma cell line MG63 using Spectral Genomics BAC-based genomic arrays. Dye-switch experiments are performed and Cy5:Cy3 ratios plotted (standard non–dye-switch, black line; dye-switch, gray line) using the SpectralWare v1.0 software package. The horizontal axes above and below the baseline (0) indicate 1, 2, and 3 copy-number gains and losses, respectively. Regions of copy number gain are indicated wherever the black line above the baseline is mirrored by the gray line below the baseline and vice versa for copy number losses.

6. Use a speed-vac to concentrate down each probe mixture to 10 µl or less.

7. Resuspend one of the duplicate probes in 35 µl of DIG buffer, then transfer it to the next duplicate and resuspend.

8. Denature the hybridization mixture (100°C, 1.5 min), incubate for 30 min at 37°C, then spin at $16,000 \times$ g for 5 min to bring down precipitated material.

9. Add the probe mixture to a 24×50 mm coverslip, then carefully overlay the cDNA array on to the coverslip, trying not to trap air bubbles. Seal with rubber cement.

10. Incubate for 12–16 hr at 37°C in a humid chamber.

Washes

1. Perform all washes in glass Coplin jars.

2. Gently dip slides into and out of wash A until the coverslip detaches from the slide.

3. Wash once for 2 min in wash A at room temperature, followed by successive washes in wash B and wash C at room temperature (2 min each).

4. Centrifuge immediately for 3–5 min at $85 \times$ g at room temperature to dry.

5. The slides are now ready for scanning.[8]

CGH Analysis on Spectral Genomic Arrays

An example of the results obtained for the osteosarcoma cell line MG63 are displayed in Figure 5.

---

[8]Microarray features are often spotted in duplicate or triplicate for assessing result reproducibility. Image acquisition for array CGH involves laser-based scanning of the array.

MATERIALS

1. Sterile water.
2. EcoRI (10,000 units/ml).
3. 1 kb DNA ladder (1 µg/µl).
4. 100 bp DNA ladder (1 µg/µl).
5. Agarose.
6. 0.5X TBE buffer.
7. Ethidium bromide.
8. BioPrime DNA labeling system (Invitrogen).
9. Spectral Random Prime Kit.
10. 1 mM Cy5-dCTP and 1mM Cy3-dCTP.
11. 0.5 M EDTA (pH 8.0).
12. 5 M NaCl.
13. Isopropanol.
14. 70% ethanol.
15. 2–4 Mb human BAC arrays.
16. Hybridization oven.
17. 50 ml polypropylene tubes.
18. 20× SSC (pH 7.0).
19. 10% SDS.
20. Wash buffer I: 50 ml 20× SSC, 2.5 ml 10% SDS, sterile water up to 500 ml (pH 7.5).
21. Wash buffer II: 50 ml 20× SSC, 250 ml formamide, sterile water up to 500 ml (pH 7.5).
22. Wash III: 50 ml 20× SSC, 0.5 ml IGEPAL CA-630, sterile water up to 500 ml (pH 7.5).
23. Wash IV: 5 ml 20× SSC, sterile water up to 500 ml (pH 7.5).
24. 22×60 mm coverslip.
25. Scanner.

DNA Digestion

1. The source of DNA used can be prepared as outlined in Extraction of High-Molecular–Weight DNA from cells and tissue.

2. For tumor or reference DNA combine 2.5 μg of genomic DNA, 5 μl of restriction enzyme reaction buffer (10X), 2 μl of EcoR1, and sterile water up 50 μl.

3. Incubate overnight in a humid chamber at 37°C.

4. Determine the size of the digest products by removing a 5 μl aliquot from the reaction mix and analyzing the aliquot by agarose gel electrophoresis (1% agarose gel containing 10 ng/ml of ethidium bromide) alongside 1 μl of a molecular weight marker (1 kb DNA ladder).

5. Perform the electrophoresis at 100 V for 30 min in 0.5X TBE. Visualize the DNA using a UV transilluminator.

6. If the digestion is complete, stop the reaction by incubating at 72°C for 10 min.

Clean-Up of Digestion Products

1. Bring the digest volume up to 500 μl with TE (pH 8.0) and mix by vortexing.

2. Purify the DNA using the phenol-chloroform extraction protocol outlined earlier.

DNA Labeling

1. In each labeling experiment four reactions are set up, two containing 2.5 μg of tumor DNA and two containing 2.5 μg of normal DNA.

2. To each tube, add sterile water to bring the volume of 25 μl, then add 20 μl of 2.5X random primers (BioPrime DNA labeling system) and mix by vortexing. Boil tubes for 5 min and then immediately place on ice for 5 min.

3. To each tube add 2.5 μl of Spectral labeling buffer (Spectral Random Prime Kit), 1.5 μl of either Cy3-dCTP (1 mM) or Cy5-dCTP (1 mM), and mix well by pipetting. Separate labeling reactions for Cy3 and Cy5 are set up for both tumor and normal DNA. Thus, each sample, tumor or normal, will have one reaction labeled with Cy3 and one reaction labeled with Cy5.

4. Add 1 μl of Klenow Fragment (BioPrime DNA labeling system), mix by gently tapping the tube, and recollect by brief centrifugation.

5. Incubate for 2 hr at 37°C and then place on ice.

6. Determine the probe size by resolving 5 μl of each labeled DNA alongside 1 μl of a molecular weight marker (100 bp DNA ladder) on a 0.8% agarose gel (containing 10 ng/ml of ethidium bromide).

7. Perform the electrophoresis at 100 V for 30 min in 0.5X TBE. Visualize the DNA using a UV transilluminator.

8. Stop the reaction by adding 5 μl 0.5 M EDTA (pH 8.0) and incubating at 72°C for 10 min.

9. Place samples on ice or store at −20°C until required.

Hybridizing Probe to the Spectral Genomics Array

1. Combine the Cy3 labeled tumor sample with the Cy5 labeled normal sample and vice versa (dye-switch experiments).

2. Add 45 μl of Spectral Hybridization Buffer I (Spectral Random Prime Kit) to each tube.

3. Precipitate samples by the addition of 11.3 μl of 5 M NaCl and 110 μl of room-temperature isopropanol. Mix well and incubate in the dark at room temperature for 10–15 min.

4. Centrifuge samples at 16,000 × g for 10 min, and carefully discard the supernatant.[9]

5. Wash the pellet with 500 μl of 70% ethanol.

6. Centrifuge at 16,000 × g for 10 min, discard the supernatant, and allow pellet to air-dry at room temperature in the dark.

7. Add 10 μl of sterile water to the pellet, let stand for 5 min at room temperature in the dark, then resuspend pellet by vortexing.

8. Once resuspended, add 30 μl of Spectral Hybridization Buffer II (Spectral Random Prime Kit) and mix well by pipetting.

9. Denature the hybridization mixture (72°C, 10 min), place on ice for 5 min, and then incubate for 30 min at 37°C.

10. Add the prehybridized probes to the arrays, cover with a 22 × 60 mm coverslip, and incubate for 12–16 hr at 37°C in a humid chamber.

Washes

1. Prewarm wash buffers II–IV to 50°C in separate 50 ml polypropylene tubes.

2. Gently dip slides into and out of wash I until coverslip detaches from slide.

3. Transfer slides to prewarmed wash buffer II.

4. Wash once for 20 min in wash II, followed by successive washes in wash III for 20 min and wash IV for 10 min. All washes are performed at 50°C in a hybridization oven fitted with a rotator.

5. Briefly rinse slides in distilled deionized water for 5–10 sec.

6. Centrifuge immediately for 3–5 min at 85 × g at room temperature to dry.

7. The slides are now ready for scanning.[10]

---

[9]The pellet should have a purplish coloration, indicating that there are equal amounts of Cy3 and Cy5 labeled DNA. If the pellet is too pink or too blue, this suggests that either the tumor or reference DNA was not effectively labeled.

[10]CGH analysis involves three steps: 1) image acquisition, 2) fluorescence intensity quantification, and 3) interpretation. All of these steps can be performed using the software and hardware developed for analysis of expression microarrays. Software required for quantification is usually included with the scanner hardware; however,

RESULTS AND DISCUSSION

The innovation of CGH analysis has allowed for the identification of copy-number changes in a wide range of tumor samples and cell lines. This has greatly simplified the study of many tumors for which obtaining metaphase chromosome or interphase nuclei is technically challenging.

The metaphase and array CGH results depicted in Figure 4, for the neuroblastoma cell line NUB7, were produced using the techniques described in this chapter. For clarity, only changes for chromosomes 1, 2, 6, and 11 are shown. The gains and losses identified by chromosome CGH and array CGH show the same trends; a gain of genetic material at 1p, 1q, 2p, 7q, and 17q and loss of genetic material from 4q, 6q, and 11q. However, the amplification of 2p24, the region containing MYCN, detected by chromosome CGH (Figure 6A) and cDNA array CGH (Figure 6B), is not observed using the genomic DNA arrays (Figure 6C). This part of the genome is poorly represented on the 2–4 Mb arrays, and it appears that MYCN sequences are absent.

When optimal, the resolution for determining copy-number changes using chromosome CGH is typically 10 Mb for a simple loss or gain (Kallioniemi *et al.*, 1992) and approximately 2 Mb for a high copy-number gain. Although this offers a suitable starting point for analysis of chromosomal changes, the limited level of resolution mean that small focal changes that are detected by array CGH may be missed by chromosome CGH, as can be seen for chromosome 11 (Figure 6). Despite the limitations of chromosome CGH, we have been able to show copy-number changes higher than the 50% CGH sensitivity thresholds. The use of microarray technology in this study allowed the regions of chromosomal change identified by chromosome CGH to be studied at a higher resolution. With genomic DNA arrays, this resolution corresponds to chromosomal changes detectable within the resolving power of the array (currently 2–4 Mb). In contrast, for the cDNA arrays it relates to the detection of copynumber changes for individual genes (e.g., MYCN at 2p24) that is highly amplified in the NUB7 cell line.

Although cDNA arrays and genomic DNA arrays provide a clear advantage over chromosome CGH in terms of resolution, they still have certain limitations. cDNA targets lack the intronic and nontranscribed elements present in genomic DNA, resulting in a lack of consistency in hybridization and poor specific signal-to-noise ratios, which as a result cause an overall decrease in sensitivity. This can clearly be seen in Figure 6B; as for cDNA arrays, it is only possible to accurately identify many of the low copy-number chromosomal changes by comparing the cDNA array data to the genomic DNA-array data (Figure 6C). This limitation decreases the potential value of cDNA arrays for detecting single copy changes. In contrast, genomic DNA-based arrays provide a more accurate approach for detecting single copy changes as a result of a greater uniformity in hybridization. However, limitations of BAC size (greater than 100 Kb) and resolution (2–4 Mb in this study) can make it difficult to detect copy-number differences between closely placed genes using this technique. In addition, the low-resolution genomic DNA arrays used in these experiments lack uniform chromosome coverage, resulting in many genomic regions not being represented. This is demonstrated by the absence of a BAC clone covering the region of 2p24 containing MYCN. Progression in this field is ongoing, and a new genomic DNA array platform providing a higher resolution will soon be available; supplementary information can be obtained from the Spectral Genomics Web site (www.spectralgenomics.com). Additionally, genomic oligo-arrays and tiling path genomic arrays are being developed, which will offer an alternative platform offering the same high resolution of cDNA arrays and the uniformity of hybridization of the current low-resolution genomic DNA arrays (Ishkanian *et al.*, 2004; Lucito *et al.*, 2003). Nonetheless, the current array CGH methodologies enable a considerable decrease in target size, from whole chromosomes to considerably shorter DNA sequences. This increase in resolution allows for a more accurate measure of chromosome gains or losses, thus greatly refining the results produced by chromosome CGH.

Because many tumors demonstrate considerable heterogeneity and can contain multiple foci of cancerous and precancerous lesions, a coupling of laser capture microdissection and CGH will allow for independent analysis of each foci. This will potentially allow for the identification of genomic regions of imbalance associated with tumor progression, invasion, and metastasis.

The genetic changes associated with cancer often involve gene loss or gene amplification. The loss of specific regions may reduce gene expression, potentially contributing to inactivation of tumor suppressor genes. In contrast, the amplification of key regions may increase the level of expression of known or novel oncogenes (Hui *et al.*, 2002; Pollack *et al.*, 2002). Screening for these gene-expression alterations using cDNA microarrays has a requirement for high-quality RNA that is not always available. However, obtaining

---

quantified fluorescence intensities require normalization and establishment of the fluorescence ratio baseline (Beheshti *et al.*, 2003). The technical aspects of this procedure are specific to the hardware package and are beyond the scope of this chapter.

Chromosome 1

Chromosome 2

Chromosome 6
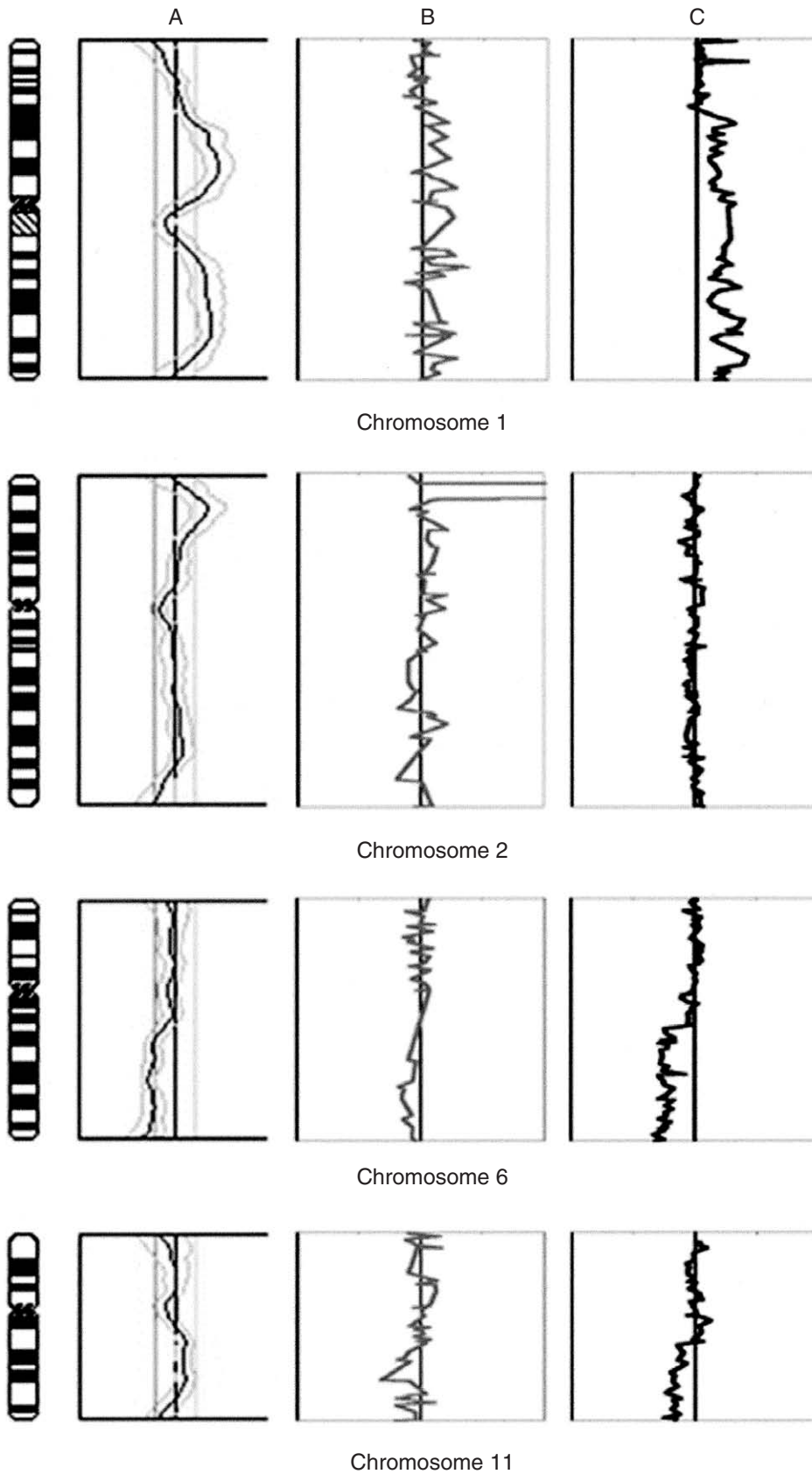
Chromosome 11

Figure 6 Chromosomal dosage changes for the NUB7 cell line. **A:** Chromosomes 1, 2, and 6 are shown to contain chromosomal imbalances, as identified by chromosome CGH. **B**: Changes for chromosomes 1, 6, and 11 are difficult to make out by cDNA array; however, the amplification of MYCN on chromosome 2 is clearly identifiable. **C:** Low-level amplifications on chromosomes 1, 6, and 11, the latter not identified by chromosome CGH, are easily resolved by genomic DNA array CGH; however, amplification of MYCN is not seen as a result of the lack of coverage for this locus. By convention, chromosome and array CGH left of the median line (*horizontal black line*) indicates a loss, whereas right of the median line denotes a gain. In the case of chromosome CGH, only gains or losses exceeding the 50% CGH threshold (lower threshold 0.75, upper threshold 1.25, indicated by horizontal light gray lines) are considered to be significant.

DNA of a quality suitable for CGH analysis is less problematic, thus allowing for detection of alterations at the genomic level that can be suggestive of gene-expression changes. Use of tissue arrays in conjunction with *in situ* hybridization with RNA probes and/or immunohistochemistry will help to show how consistent CGH findings are in a histologic context (Heiskanen *et al.*, 2001). CGH analytic methods have developed rapidly in recent years. With the advent of high-resolution genomic profiling techniques, CGH will be able to precisely define molecular rearrangements of the genome associated with the key functional abnormalities in many classes of tumors.

References

Beheshti, B., Park, P.C., Braude, I., and Squire, J.A. 2003a. Microarray CGH. *Methods Mol. Biol. 204*:191–207.

Beheshti, B., Braude, I., Marrano, P., Thorner, P., Zielenska, M., and Squire, J.A. 2003b. Chromosomal localization of DNA amplifications in neuroblastoma tumors using cDNA microarray comparative genomic hybridization. *Neoplasia 5*:53–62.

Cai, W.W., Mao, J.H., Chow, C.W., Damani, S., Balmain, A., and Bradley, A. 2002. Genome-wide detection of chromosomal imbalances in tumors using BAC microarrays. *Nat. Biotechnol. 20*:393–396.

du Manoir, S., Schrock, E., Bentz, M., Speicher, M.R., Joos, S., Ried, T., Lichter, P., and Cremer, T. 1995. Quantitative analysis of comparative genomic hybridization. *Cytometry 19*:27–41.

Forozan, F., Karhu, R., Kononen, J., Kallioniemi, A., and Kallioniemi, O.P. 1997. Genome screening by comparative genomic hybridization. *Trends Genet. 13*:405–409.

Heiskanen, M., Kononen, J., Barlund, M., Torhorst, J., Sauter, G., Kallioniemi, A., and Kallioniemi, O. 2001. CGH, cDNA and tissue microarray analyses implicate FGFR2 amplification in a small subset of breast tumors. *Anal. Cell Pathol. 22*:229–234.

Hui, A.B., Lo, K.W., Teo, P.M., To, K.F., and Huang, D.P. 2002. Genome wide detection of oncogene amplifications in nasopharyngeal carcinoma by array based comparative genomic hybridization. *Int. J. Oncol. 20*:467–473.

Hui, A.B., Lo, K.W., Yin, X.L., Poon, W.S., and Ng, H.K. 2001. Detection of multiple gene amplifications in glioblastoma multiforme using array-based comparative genomic hybridization. *Lab. Invest. 81*:717–723.

Ishkanian, A.S., Malloff, C.A., Watson, S.K., DeLeeuw, R.J., Chi, B., Coe, B.P., Snijders, A., Albertson, D.G., Pinkel, D., Marra, M.A., Ling, V., MacAulay, C., and Lam, W.L. 2004. A tiling resolution DNA microarray with complete coverage of the human genome. *Nat. Genet. 36*:299–303.

James, L.A. 1999. Comparative genomic hybridization as a tool in tumour cytogenetics. *J. Pathol. 187*:385–395.

Kallioniemi, A., Kallioniemi, O.P., Sudar, D., Rutovitz, D., Gray, J.W., Waldman, F., and Pinkel, D. 1992. Comparative genomic hybridization for molecular cytogenetic analysis of solid tumors. *Science 258*:818–821.

Karhu, R., Kahkonen, M., Kuukasjarvi, T., Pennanen, S., Tirkkonen, M., and Kallioniemi, O. 1997. Quality control of CGH: impact of metaphase chromosomes and the dynamic range of hybridization. *Cytometry 28*:198–205.

Kraus, J., Pantel, K., Pinke, D., Albertson, D.G., and Speicher, M.R. 2003. High-resolution genomic profiling of occult micrometastatic tumor cells. *Genes Chromos. Cancer 36*: 159–166.

Lucito, R., Healy, J., Alexander, J., Reiner, A., Esposito, D., Chi, M., Rodgers, L., Brady, A., Sebat, J., Troge, J., West, J.A., Rostan, S., Nguyen, K.C., Powers, S., Ye, K.Q., Olshen, A., Venkataraman, E., Norton, L., and Wigler, M. 2003. Representational oligonucleotide microarray analysis: A high-resolution method to detect genome copy number variation. *Genome Res. 13*:2291–2305.

Pollack, J.R., Perou, C.M., Alizadeh, A.A., Eisen, M.B., Pergamenschikov, A., Williams, C.F., Jeffrey, S.S., Botstein, D., and Brown, P.O. 1999. Genome-wide analysis of DNA copy-number changes using cDNA microarrays. *Nat. Genet. 23*:41–46.

Pollack, J.R., Sorlie, T., Perou, C.M., Rees, C.A., Jeffrey, S.S., Lonning, P.E., Tibshirani, R., Botstein, D., Borresen-Dale, A.L., and Brown, P.O. 2002. Microarray analysis reveals a major direct role of DNA copy number alteration in the transcriptional program of human breast tumors. *Proc. Natl. Acad. Sci. USA 99*:12963–12968.

Solinas-Toldo, S., Lampel, S., Stilgenbauer, S., Nickolenko, J., Benner, A., Dohner, H., Cremer, T., and Lichter, P. 1997. Matrix-based comparative genomic hybridization: biochips to screen for genomic imbalances. *Genes Chromos. Cancer 20*:399–407.

Squire, J.A., Pei, J., Marrano, P., Beheshti, B., Bayani, J., Lim, G., Moldovan, L., and Zielenska, M. 2003. High-resolution mapping of amplifications and deletions inpediatric osteosarcoma using CGH analysis of cDNA microarrays identifies an association with sigmental duplications. *Genes Chromos. Cancer 38*:215–225.

Wessendorf, S., Schwaenen, C., Kohlhammer, H., Kienle, D., Wrobel, G., Barth, T.F., Nessling, M., Moller, P., Dohner, H., Lichter, P., and Bentz, M. 2003. Hidden gene amplifications in aggressive B-cell non-Hodgkin lymphomas detected by microarray-based comparative genomic hybridization. *Oncogene 22*:1425–1429.

Zhao, J., Roth, J., Bode-Lesniewska, B., Pfaltz, M., Heitz, P.U., and Komminoth, P. 2002. Combined comparative genomic hybridization and genomic microarray for detection of gene amplifications in pulmonary artery intimal sarcomas and adrenocortical tumors. *Genes Chromos. Cancer 34*:48–57.

This Page Intentionally Left Blank

3

Microarray Immunoassay of Complex Specimens: Problems and Technologic Challenges

Wlad Kusnezow, Timo Pulli, Yana V. Syagailo, and Jörg D. Hoheisel

Introduction

DNA-microarrays have become an essential tool for the functional interpretation of the sequence information generated by various genome projects. However, many aspects of modulation and regulation of cellular activity cannot be investigated on the nucleic acids level but require an analysis of the proteome. Several studies in yeast (Gygi *et al.*, 1999) and higher eukaryotes (Anderson *et al.*, 1997), for example, demonstrated a poor correlation between messenger ribonucleic acid (mRNA) and protein levels. This is because of the post-transcriptional control of protein translation, a number of post-translational modifications of proteins, and protein degradation by proteolysis. Because of several hundred possible protein modifications, the complexity in the human proteome is expected to range from a hundred thousand to several million different molecules, which greatly exceeds the estimated number of 32,000 genes. Additionally, the function of a large percentage of the predicted proteins of multicellular organisms is not known. Also, the dynamic range of protein expression ranges widely and could be as large as seven orders of magnitude.

All this has led to a strong demand of analytic procedures on the protein level that correspond in performance to similar studies possible with DNA-microarrays. The existing classical proteomic technology, two-dimensional gel electrophoresis, is rather low-throughput as a result of its complexity and high costs. Even in combination with mass spectrometry, only more abundant proteins can be detected, indicating the need for new technologies. Antibody and antigen microarrays represent a methodology that is compatible to DNA-microarrays, aiming at a simultaneous analysis of several thousand proteins from biologic samples with very good sensitivity and specificity. However, although some microspot immunoassay systems such as antibody miniarrays (Moody *et al.*, 2001) and antigen microarrays (Robinson *et al.*, 2002) have been successful in demonstrating their usefulness to detect protein expression, the sensitivity of the most complex antibody microarrays, containing several hundred features each, has been moderate. The current status of such antibody microarray systems demonstrates the lacking feasibility of getting qualitative data from small quantities of clinical samples (Knezevic *et al.*, 2001). It was found to be impossible to detect signal intensities on most spotted

Handbook of Immunohistochemistry and *in situ* Hybridization of Human Carcinomas,
Volume 2: Molecular Pathology, Colorectal Carcinoma, and Prostate Carcinoma

23

antibodies (Knezevic *et al.*, 2001; Sreekumar *et al.*, 2001). There are also examples of successful protein detection, but unfortunately it was with samples of low complexity (Schweitzer *et al.*, 2002). The development of protein microarrays on the basis of conventional DNA-microarray technology is associated with a number of problems as a result of basic biophysical and chemical properties of proteins. In contrast to DNA, proteins are chemically and structurally much more complex and heterogeneous and they lose more easily their biochemical activity because of denaturation, dehydration, or oxidation. Especially, comprehensive analyses of clinical samples such as tumor biopsies represent the most difficult technologic challenge in the protein microarray area. The difficulties are based on a small volume and high protein complexity of the samples and the requirement for a set of sensor molecules with high specificity and affinity. Currently this approach exhibits low signal to background ratios and quite a few nonspecific signals.

To advance protein microarray analysis of clinical specimens, many technical hurdles in the fields of surface chemistries, microarray processing, large-scale production of specific recombinant binders, and detection strategies have to be overcome. The various technologic issues are reviewed here.

Protein Microarrays: A Generic Term for Various Formats and Analytic Possibilities

Filter Membrane and Microtiter Plate Supports

The first array approach in the initial development phase was the use of array support media of filter membranes and 96-well microtiter plates (Figure 7, top and central panels). Filter membranes enable the production of low-density (Ge, 2000) and high-density protein arrays with up to several hundred features per square centimeter (Bussow *et al.*, 1998; de Wildt *et al.*, 2000). Filters have successfully been used for a variety of investigations such as multiplex detection of cytokines in patient sera and cell culture media (Huang *et al.*, 2001c), screening of a human fetal brain complementary deoxyribonucleic acid (cDNA) expression library for appropriate antibodies (Lueking *et al.*, 1999), and screening of a library of bacterial clones expressing single-chain antibodies (de Wildt *et al.*, 2000). However, limitations of all filter arrays are the relatively low resolution, the considerable background signal leading to limitation of further miniaturization,

and difficulties in automating the analysis process. Because of the relatively large reaction volume required, it is also impracticable to use filter arrays in applications, such as protein expression profiling of tumor biopsies, where only limited sample quantities are available.

In the microtiter plate approach, proteins were printed onto the bottom of a well serving as a reaction vessel (Mendoza *et al.*, 1999). This platform was mainly applied to the detection of cytokines in serum samples using miniarrays with only few antibodies per well (Moody *et al.*, 2001; Wiese *et al.*, 2001). The achievable sensitivity and dynamic range of detection of these arrays were considerably better compared with conventional enzyme linked immunosorbent assays (ELISA). The maximum capacity of these arrays-in-well was up to 250 features per well (Huang *et al.*, 2001a), and commercial system with 50 antibodies per well are available (Genometrix Inc., Houston, TX). The main disadvantage of the microtiter plate format is the inherent limitation for further increase of the assay's multiplex factor and thus sample volume reduction. Advantages of these systems include the possibility to use standard ELISA equipment such as shakers or plate washers and the potential to process various protein samples in parallel.

Chip Format

The chip format enables miniaturization of assays, consequently leading to an increase in multiplexing detection and decreasing sample volume. A number of systems exist, differing by the modes of application, manufacturing, and detection (Figure 7, bottom panel). Some of these differences are described later in this chapter.

One of the first strategies to produce protein chips was developed by the group of Andrei Mirzabekov (Arenkov *et al.*, 2000; Guschin *et al.*, 1997). Arrays were produced by covalent binding of proteins to 150 to 10 μm sized three-dimensional polyacrylamide gel pads that were immobilized on glass plates and separated by hydrophobic silane coatings. This very small reaction vessels array could be analyzed by laser scanning and mass-spectrometric detection and by specially constructed detection/incubation devices. This enabled the study of biochemical reactions under real-time conditions. These chips have been applied to various types of immunoassays and enzymatic reactions and were ideally suited for kinetic studies. The main disadvantage of the gel pads is the complicated production process.

MacBeath and Schreiber (MacBeath *et al.*, 2000) described a strategy that opened perspectives for potentially simple, large-scale protein analysis in
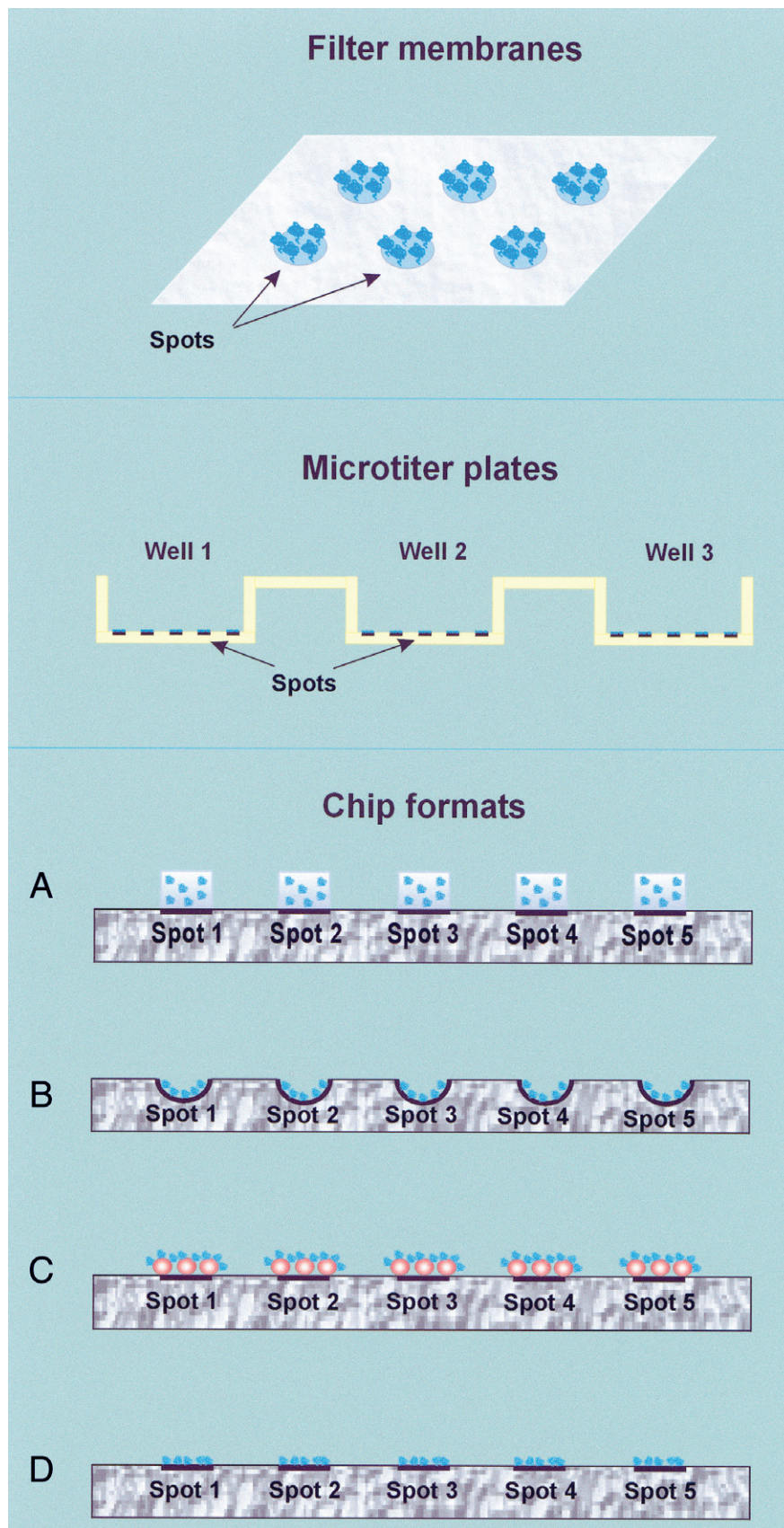
Figure 7 Different formats applied to the construction of protein microarrays. The chip formats depicted are the gel-pads microarray (**A**), nanowell microarray (**B**), particle microarray (**C**), and planar side microarray (**D**).

functional and comparative proteomics. Currently this format involves a large variety of protein microarray applications including antigen (Robinson *et al.*, 2002) and antibody (Sreekumar *et al.*, 2001) micro-arrays, microarray ELISAs (Joos *et al.*, 2000), and microarray Western analysis (Paweletz *et al.*, 2001).

A further modification of this approach is the coating of planar supports with nanoparticles. In a proof-of-concept study, a microarray was constructed containing widely dispersed (about 100 per spot), 0.8 µm sized, antibody-coated particles on a spot (Stevens *et al.*, 2003). Using a specially constructed scanning device, individual particles on a single spot could be detected. This results in multiple replicates of one analyte detection event during a single array scan.

Based on planar waveguide (PWG) technology, Zeptosens has developed a unique microarray system for fluorescence detection (Pawlak *et al.*, 2002). Laser light propagated within the thin (150–300 nm) PWG film of high refractive material (Ta$_2$O$_5$) deposited on a microarray support creates a strong evanescent field, exciting molecules only in the vicinity of the surface (several hundred nanometers), whereas excitation in the bulk medium does not occur. In comparison to a standard laser scanner, the intensity of light near the surface can be increased by a factor of 100. Consequently, this technology results in an increased sensetivity and signal-to-noise ratio and offers the possibility to monitor binding events under real-time conditions. In fact, analytes in biologic samples such as serum can be quantitatively measured at concentrations of down to 1–10 pg/ml with a minimal sample volume of 15–20 µl.

Receptor-Ligand Interactions on Microarrays: Problematic Character and Technologic Solutions

Theoretic Sensitivity and Practical Reality

Although protein microarrays are a new and fast-developing technology today, the history of microspot immunoassays already began in the late 1980s, when Roger Ekins and co-workers created a first microspot multianalyte immunoassay (Ekins, 1994; Ekins, 1998; Ekins *et al.*, 1992). Based on these developments, Ekins proposed a concept describing ligand-receptor interactions on microarray-based assays, the so-called *ambient analyte theory*. This theory arose from two initial physicochemical considerations: 1) all receptor-ligand assays are based on the measurement of the *fractional occupancy of binding sites* (FOB) by the analyte (ligand); and 2) the FOB is relatively
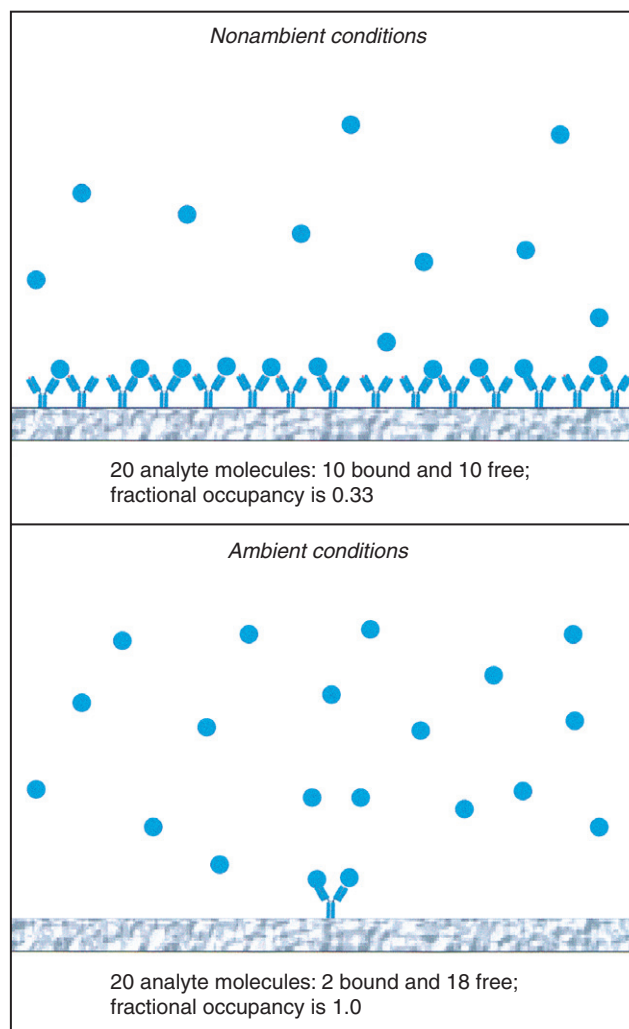
Figure 8 Schematic illustration of ambient analyte theory. In classical immunoassays (*top panel*), analyte molecules are widely depleted from sample solution, which results in establishment of new thermodynamic equilibrium and lower fractional occupancy of binding site (FOB). In ambient analyte assays (*bottom panel*), FOB displays the initial analyte concentration.

independent of the receptor concentration and sample volume, if the concentration of the receptor itself is small enough. Under this *ambient analyte condition*, in which the formation of receptor-ligand complexes does not significantly deplete the initial concentration of the analyte, the theory predicts a much higher FOB in microspot multianalyte assays than in conventional ELISAs and radio immunoassays (Figure 8). Because sample volume is usually a limiting factor, the ambient analyte theory points to the minimization of the binding area with a maximum possible receptor density. Consequently, the miniaturization of the binding area will not only positively affect the multiplex factor of

assays but also may improve its sensitivity by several orders of magnitude.

In contrast to the theory, performance of antibody microarrays in protein profiling has only been moderately productive thus far. Knezevic *et al.* (2001) analyzed protein expression in squamous cell carcinoma of the oral cavity using an microarray of 368 antibodies. Laser capture microdissection (LCM) and ELISA-like detection were used for the preparation and analysis of clinical samples. With only 0.5 µg protein available for each microarray incubation, 11 proteins were found to have a different expression level in either epithelium or stroma in the vicinity of the cancer cells. However, the data could not be presented in a quantitative form. Another example is a microarray with 146 antibodies created by Sreekumar *et al.*, (2001). Protein level alternations were detected in a colon carcinoma cell line that had been treated with ionizing radiation. Dual labeling with Cy3 and Cy5 was used in this system. Radiation-induced up- and down-regulation was demonstrated for several apoptotic regulators. Unfortunately, only the data obtained with 20 of the 146 antibodies were presented. This discrepancy between theory and practice is for most part based on the following technologic difficulties of modern protein microarray analysis.

First Challenge: Minimizing the Spot Size

The Ekins theory suggests a detection limit of approximately 10^{-17} M for a microarray using high-affinity antibodies bound as a monolayer in spots of 100–1000 µm². However, current microarray systems usually have spots with diameters of about 100–400 µm and thus fail to meet this condition. Further developments in biomolecule printing technologies are therefore expected to significantly advance microarray performances. For example, ink-jet technology applied for microarray printing can produce high-quality spots with a diameter of as little as 25 µm (Okamoto *et al.*, 2000). Electrospray deposition—originally developed for molecule ionization—can also be used, resulting in feature sizes of few micrometers (Morozov *et al.*, 1999). The minimization of the spot size is not only limited by printing techniques but also by the capacity of the detector systems (Sapsford *et al.*, 2001).

Second Challenge: Establishment of a Thermodynamic Equilibrium

A prerequisite to high-sensitivity analysis at ambient analyte conditions is the establishment of a thermodynamic equilibrium. Some theoretic analyses of DNA-microarray experiments indicate substantial cross-hybridization effects and "incorrectness" of signal ratios under nonequilibrium conditions (Bhanot *et al.*, 2003; Livshits *et al.*, 1996). Similar effects occur on protein microarrays. When compared to conventional immunoassays such as ELISA, the time required to establish the thermodynamic equilibrium in microspot assays is much longer because of a very low receptor concentration. An analysis of binding kinetics on protein and DNA microarrays demonstrated that the time is strongly dependent on the concentration of analytes (Adey *et al.*, 2002; Sapsford *et al.*, 2001). Additionally, the protein immobilization on surfaces usually leads to a substantial loss of the biologic activity of proteins, which causes subsequent lower reaction velocities and a lower fractional occupancy.

This situation is complicated further by diffusion constraints in a typical microarray experiment. It has been widely recognized that mixing is very important for high association rates on DNA microarrays leading to much higher signal intensities, especially for low abundant molecules (Adey *et al.*, 2002; Scriba *et al.*, 2002). These effects are similar or even worse in the case of protein interactions on microarrays. Because of the lower affinity of most antibodies in comparison to DNA-DNA interaction, the signal intensities on the antibody microarray develop under nonmixing conditions over many days without reaching thermo-dynamic equilibrium (Kusnezow *et al.*, 2004). Additionally, proteins vary strongly in their size and shape, which results in differences in diffusion velocities of particular analytes. Mobility of proteins in interface areas is additionally complicated by amphipathic properties of proteins leading to their continuous adsorption/desorption on a surface.

Therefore, there is a strong demand for technologies enabling a reliable nonlaminar mixing on a chip surface. Because, from the kinetic point of view, dilution of a sample automatically results in reduction of signal intensity, approaches enabling mixing of very small sample volumes will be advantageous. An agitation system facilitating mixing of volumes in the range from 20 µl to about 300 µl on microarrays has been developed by Advalytix (Munich, Germany) (Scriba *et al.*, 2002). Surface acoustic waves produced by nanopumps in this system mix solutions in a nano and micro scale. An application of this system to protein microarray analysis resulted in shorter incubation times and up to tenfold higher signal intensities at low analyte concentrations (Kusnezow *et al.*, 2004). BioMicro Systems produce a system for DNA-microarrays based on two air-driven bubbles that continuously mix 35–40 µl of the incubation solution (Adey *et al.*, 2002). Gains in sensitivity across a DNA-microarray of 6912 spots were twofold to threefold.

Third Challenge: A Low
Protein Adsorption

In contrast to the uniformly structured DNA molecules, which contain a negatively charged backbone with low adsorption affinity to hydrophobic and/or negatively charged surfaces, large amphipathic protein molecules exhibit abundant surface activities (Hlady *et al.*, 1996). The high degree of the protein adsorption is caused by electrostatic, van-der-Waals and Lewis acid-base forces, hydrophobic interactions, and conformational changes and restricted lateral diffusion in the vicinity of a surface. These physical forces often lead to an irreversibility of the protein adsorption process, especially if complex biologic samples are applied.

Protein microarray create a new situation in assay development because all analytes in a directly labeled sample, or all detectable analytes in sandwich assays, produce signals by nonspecific binding. In microspot-sandwich assays, the background increases with the amount and total number of secondary antibodies applied. Because the adsorption process has a competitive character, a low degree of unspecific binding is extremely difficult to achieve if a complex protein sample with thousands of molecules is analyzed, even under optimal blocking conditions. Very low protein adsorption is crucial for the achievement of reliable results. The increasing complexity of multianalyte experiments demands the development of an appropriate surface chemistry.

Protein Immobilization on a Microarray Chip Format

Parameters for an Optimal Protein
Microarray Surface

Surface chemistry is one of the keys to this technology, a fact recognized by the industry, which currently is concentrating mostly on developing and selling slides for protein microarrays (Kusnezow *et al.*, 2002). Applying DNA-microarray surface chemistry directly to proteins was not very feasible because of many problems resulting from fundamental biophysical and biochemical differences between these two classes of biomolecules. Therefore, it is clear that there is a need for new sophisticated immobilization chemistries for proteins. An optimal protein microarray surface should meet the following criteria:

- ▲ High-density and nondenaturing protein attachments.
- ▲ Low protein adsorption.
- ▲ Attachment chemistry, which minimally disturbs different kinds of receptor-ligand interactions.

- ▲ Compatability with manufacturing devices.
- ▲ Spot uniformity.

In practice, no single surface or attachment strategy will satisfy the demands of all protein microarray experiments. Therefore, one has to select the most suitable strategy and may have to accept compromises for the reason of cost.

Performance of Some Conventional
Surface Coatings

Adsorption of biomolecules on poly-L-lysine (PLL) slides is often used for the attachment of nucleic acids and proteins. Using these slides, Haab *et al.* (2001) developed a comparative antibody-antigen microarray analysis, in which the dual fluorescent labeling was applied as known from DNA-microarrays. However, of 115 tested antibody-antigen pairs, only 50% of the antigens and 20% of the arrayed antibodies provided specific and accurate results with a detection threshold of 1 ng/ml. Typical DNA microarray surfaces such as aminosilane or aldehydesilane coatings have also been successfully applied for a variety of protein microarray assays. An antigen microarray printed on aminosilane-coated slides was developed using fluorescence-labeled anti-human immunoglobulin G (IgG) IgM antibodies. This array was able to detect antibodies in human sera with similar reliability as standard ELISAs with a sensitivity of 0.5 pg of antibody per spot (Mezzasoma *et al.*, 2002). In several studies, cyanosilane coating has been used to construct antibody array ELISAs exhibiting a low picomolar sensitivity (Huang *et al.*, 2001a; Tam *et al.*, 2002; Wiese *et al.*, 2001). In these assays, the antibodies have been densely attached in a directed manner *via* electrostatic interactions between glycosyl rests of the Fc regions and cyano-groups on the surface (Falipou *et al.*, 1999). The functional groups introduced by silanization or PLL coating can be further derivatized using monobifunctional or heterobifunctional cross-linkers enabling the fabrication of a variety of surfaces with binding activity toward amino, thiol, or aldehyde groups of proteins. A microarray of 51 cytokine antibodies (Schweitzer *et al.*, 2002) was printed on a thiolsilane-coated surface that had been activated with a maleimido-succinimide cross-linker (GMBS), an often-used attachment method in an immunosensor production (Bhatia *et al.*, 1989). The reported sensitivity was about 1 ng/ml of antigen using a cocktail of about 40 fluorescence-labeled antibodies.

The main advantages of these attachment strategies are the simplicity and the low cost of the derivatization. Several studies comparing the performance parameters of different surface chemistries demonstrated that a

covalent binding on these surfaces usually results in a higher protein binding capacity and a higher signal intensity compared with a protein adsorption on PLL or aminosilane surfaces. In our hands, epoxy-silanization and mercaptosilanization with maleimido-succinimidyl cross-linker (aminoreactive NHS-surface) or aminosilanization with maleimido-succinimidyl cross-linker (thiolreactive maleimid-surface) produced three to four times better signal-to-background ratios compared with PLL slides and high signal intensities using antigen concentrations in the range of few pg/ml at optimal antibody concentrations (Kusnezow *et al.*, 2003). In accordance with our results, other studies also reported epoxy-silanized slides as the ones with the highest sensitivity in this group of surface modifications (Li *et al.*, 2003; Seong, 2002).

One problem caused by most of the surfaces is protein denaturation as a result of relatively high surface hydrophobicity (Li *et al.*, 2003). For this reason, all surface modifications discussed here require the addition of protective substances such as glycerol (MacBeath *et al.*, 2000), disaccharides (trehalose) (Kusnezow *et al.*, 2003), or sucrose (Avseenko *et al.*, 2001), or low–molecular-weight polyethylene glycol (PEG) (Lee *et al.*, 2002a) to the spotting buffer. Hydrophobic surfaces, however, exhibit a higher degree of unspecific binding when compared to hydrophilic support media (Piehler *et al.*, 2000). Therefore, these surfaces, which were successfully applied for functional proteome analysis or even construction of antigen microarrays, are less suited for systems in which highly complex samples, such as fluorescence-labeled protein-lysates from cell lines or tissues, are to be analyzed. Moreover, there may be a larger steric influence on binding events as a result of the close proximity of the surface and the sensor molecules.

Pegylated Surfaces

Surface modifications by neutral hydrophilic polymers have been used for years to prevent a surface fouling by proteins. Mainly they were used in medical applications such as the enhancement of the biocompatibility of implants and drug delivery systems. Among these polymers, PEG is a promising biomaterial exhibiting high resistance to protein adsorption. Several PEG immobilizations strategies have been described and shown to cause a nearly tenfold lower protein adsorption compared to silanized surfaces, thus indicating their potential for protein microarray construction (Lesaicherre *et al.*, 2002b; Piehler *et al.*, 2000). Also, positioning large PEG spacer molecules between protein and support matrix helps to avoid a steric interference and results in a higher analyte capture capacity (Weimer *et al.*, 2000).

One of the key difficulties arising from immobilization of high–molecular-weight PEG molecules is a poor grafting efficiency. An alternative strategy to obtain high-density PEG-modified surfaces is graft-copolymerization of PEG-side chains with a polymer backbone. Metal oxide surfaces coated with poly-L-lysine-grafted polyethylene glycol copolymers (PLL-g-PEG) exhibited more than 100 times lower unspecific protein binding compared with untreated surfaces (Huang *et al.*, 2001b). Biotinylated proteins (Koopmann *et al.*, 2003; Ruiz-Taylor *et al.*, 2001), Mabs and Fab fragments (Peluso *et al.*, 2003), were attached to slides coated with PLL-g-PEG biotin in a first level followed by streptavidin. Extremely low unspecific binding of nonbiotinylated proteins enabled purification of biotinylated proteins from bacterial lysates directly on a microarray (Koopmann *et al.*, 2003; Ruiz-Taylor *et al.*, 2001).

Self-Assembled Monolayers

Self-assembled monolayers (SAMs) are formed by the spontaneous and highly ordered adsorption of amphiphilic surfactant on a surface, resulting in the formation of a stable monolayer film. The most common example is monolayer formation by alkanthiols on gold, quartz, glass, metal, and other surfaces. Alkanthiols can be functionalized with different reactive groups for protein coupling in a desired manner, and termination in short PEG-groups effectively prevents the unspecific adsorption of proteins. The advantage of this chemistry includes the preparation of surfaces with well-defined topographic properties and the control of density and uniform activity of immobilized biomolecules. Because of these properties, SAMs have a very suitable chemistry for label-free detection approaches such as surface plasmon resonance (SPR) or atomic force microscopy (AFM). SAM applications for protein microarrays have been reviewed extensively (Schaeferling *et al.*, 2002). Jones *et al.,* (1998) developed an immunoassay based on the arraying of rabbit IgG molecules with a feature size of 7.5 μm. On addition of a secondary anti-rabbit antibody, binding could be detected by atomic force microassay as an increase in the height of the features. Lee *et al.*, (2002b) constructed protein arrays with 100–350 nm feature sizes for studies on antibody-antigen interactions and cell adhesion. SAM surfaces were also applied in peptide microarrays for screening of protein kinase activities with SPR, fluorescence and phosphorimaging detections (Houseman *et al.*, 2002a), and carbohydrate microarrays for analysis of binding specificities of several lectins and enzymatic activities of galactosyltransferase (SPR detection) (Houseman *et al.*, 2002b).

In both reports, protein interactions and enzymatic activities were detected quantitatively, reflecting the advantageous properties of SAM discussed earlier (Housemann *et al.*, 2002c).

Three-Dimensional Surfaces: Gel and Filter Membrane Coatings

A critical factor for all microarray surfaces described earlier is their protein binding capacity. At best, spotting produces a monolayer of active proteins. Three-dimensional surfaces may provide higher sensitivity and increased dynamic range of measurement. For protein arrays, these immobilization strategies include coating with filter membranes, gel surfaces, and various branched polymers. Long incubation periods to achieve a maximal sensitivity may be a drawback of these surfaces, however.

A covalent immobilization using the three-dimensional matrix structure of polyacrylamide gels, a component of gel pad formats, provides several advantages including increased loading capacity, reduced protein denaturation as a result of the homogenous aqueous environment, and low unspecific binding. Ready-to-use polyacrylamide slides, called HydroGel, are available from *Perkin-Elmer Life Sciences*. Miller *et al.,* (2003) compared the performance of HydroGel slides with PLL slides additionally coated with a photoreactive cross-linker. Performing protein profiling of prostate cancer and control sera, a sixfold higher signal-to-noise ratio was obtained on HydroGel compared with the HSAB (poly-L-lysine/photoreactive bifunctional cross-linker) slides. Because of the almost undetectable background, these slides seem to be a suitable support for a highly complex protein microarray analysis.

Nitrocellulose-coated FAST slides from Schleicher and Schuell are another popular support matrix for protein arrays. The main reason for this is their enormous binding capacity (Kukar *et al.*, 2002) resulting in much higher signal intensities compared with one-dimensional surfaces. Less than 1000 molecules of prostate specific antigens (PSAs) could be detected in a single spot, taking advantage of a signal amplification system (Paweletz *et al.*, 2001). Consequently, FAST slides are a reasonable solid support for studies, in which protein lysates of biologic samples are spotted and subsequently probed with particular antibodies (Madoz-Gurpide *et al.*, 2001; Paweletz *et al.*, 2001). Additionally, proteins adsorbed to the hydrophilic nitrocellulose surface show high biochemical stability, and antibodies spotted on FAST slides can be stored for many months and possibly years. However, this surface seems not to be suitable for the analysis of highly complex protein solutions because of a very high background signal on the nitrocellulose support.

A limited number of other polymer-based three-dimensional surfaces are available. Benters *et al.* (2001), for instance, suggested series of polyamino-functionalized dendritic macromolecules, which were subsequently modified with homobifunctional cross-linkers. Tested mostly for DNA-microarray applications, these surfaces demonstrated better spot morphology and higher signal intensities. *Prolinx Inc. (Bothell, WA)* and *Accelr8 Technology Corporation (Denver, CO)* offer slides coated with three-dimensional polymers, the former modified with salicylhydroxamic acid functional groups. Salicylhydroxamic acid forms a stable complex with phenyldiboronic acid, which is provided in the form of a protein-modifying reagent.

Alternative Sensor Molecules

To date, most antibody microarrays have been produced with several dozens or hundreds of commercially available polyclonal or monoclonal antibodies. Although several tens of thousands of antibodies are commercially available, this number is insufficient. First and foremost, for very many proteins no antibodies are available nevertheless. Also, the number of sensor molecules required for analysis is bigger than the mere number of analytes. In many cases, receptors with different equilibrium dissociation constants and specificities to different epitopes are needed for each protein target. Therefore, mass production of sensor molecules with a minimal cross-reactivity represents a most critical bottleneck. Classical antibody production strategies of monoclonal and polyclonal antibodies, based on animal immunizations, are very laborious to scale up to satisfy the needs for the high-throughput production of sensor molecules. Therefore, future applications may be based on recombinant sensor molecules such as antibody fragments (Borrebaeck *et al.*, 2001); engineered microbial proteins such as staphylococcus protein A domain, called affibody (Nord *et al.*, 1997); or short, single-stranded nucleic acid species or peptides with protein binding properties, entitled as aptamers (James, 2001).

Recombinant antibody display libraries are promising techniques that are based on a direct coupling of each binder molecule to its DNA code. The most favorable phage libraries are limited in their complexity because of the requirement for bacterial host cells. Because bacteria grow in the order of 10^8 cells per milliliter, a big culture volume is needed to prepare a highly complex library (about 10^{11} different antibody fragments) (Sblattero *et al.*, 2000). mRNA (Roberts *et al.*, 1997)

and ribosomal display techniques (Hanes *et al.*, 1997) circumvent this problem because all steps—amplification, transcription, translation, selection, purification, and the maturation of antibody affinity— occur entirely *in vitro*. Using a ribosome display technique, several antibody fragments with affinities in the low picomolar range have been isolated (Hanes *et al.*, 2000). Therefore, the two latter techniques enable the establishment of a complexity that is several orders of magnitude higher than in phage libraries and allows the automation of the production processes.

The mRNA-protein fusion of the mRNA display system has been used elegantly to generate addressable protein microarrays (PROfusion; Weng *et al.*, 2002). mRNA display is based on the translation terminating antibiotic pyromycin, which functions by entering the A site of ribosomes and forming a covalent bond with the nascent peptide. By covalently attached pyromycin in the 3′ end of an mRNA, covalent link between a polypeptide and its encoding mRNA can be achieved during *in vitro* translation. After the translation, the nucleic acid component of the mRNA-protein fusion hybridizes to surface-bound DNA capture probes. In this system the nucleic acid component not only directs the mRNA-protein fusion to the proper coordinate of the microarray but also positions the protein in a uniform orientation. The anchoring of the protein to the chip surface was shown to be robust, and displayed protein was detected without signal amplification in subattomole quantities.

The more recent development in the field of sensor molecules is the engineering of microbial proteins in the way that antibody-like properties can be obtained (Kronvall *et al.*, 1999). One of the most promising alternatives is a phage library made of engineered domains of staphylococcus protein A—called affibodies. Each molecule consists of only 58 amino acids (Nord *et al.*, 1997). This protein has some advantages compared to a classical immunoglobulin domain: smaller size means higher stability and enabling immobilization at higher concentrations. As in the field of recombinant antibody engineering, cell-free display systems are also developed (Abbott, 2002).

Because of the small molecular weight of recombinant proteins, dense attachment to support surface is facilitated. Additionally, recombinant proteins can be generated as fusion proteins using different kinds of affinity tags (reviewed in Terpe, 2003). The affinity tags are widely applied in the purification of recombinant proteins and are also applicable to promote correct oriented binding of recombinant sensor molecules onto microarray surfaces. The specific orientation may also lead to improvement of the stability of attached proteins and increase the sensitivity of the assay.

The most commonly used tags are 5–26 amino acids long, small peptides. The advantage of these small tags is that they interfere less with the correct folding and biologic activity of the fused protein.

To analyze biochemical activities of yeast proteins, Zhu *et al.* produced 5800 fusion proteins with glutathione-S-transferase and a His_6 tag (Zhu *et al.*, 2001) and spotted them on nickel-coated microarray slides at high density. Interestingly, the nickel-coated slides demonstrated much better performance compared to a conventional aldehyde surface. In another study, His-tag fusion proteins were expressed *in vitro* and simultaneously immobilized on solid support (protein *in situ* arrays [PISAs]) (He *et al.*, 2001). An attractive basis for numerous bioanalytical applications is biotin/streptavidin or avidin interaction, which has a very strong affinity ($K_d \approx 10^{-15}$ M) (Lindqvist *et al.*, 1996). Lesaicherre *et al.* (2002a) proposed a new strategy for a site-directed attachment of a fusion protein. Fusion proteins containing an intein-tag with chitin binding domain were purified on columns filled with chitin beads and biotinylated cysteine. Disruption of the protein-intein connection produced biotinylated proteins, which were spotted on avidin-coated slides. This technique may also be used to immobilize recombinant fusion antibodies. Recently, a new protein tag cutinase was introduced (Hodneland *et al.*, 2002). It can be used to immobilize fusion proteins covalently on activated surfaces. Cutinase is a 22 kDa serine esterase that forms a site-specific covalent adduct with phosphonate ligands. Calmodulin-cutinase fusion protein was expressed in *Escherichia coli* and after purification was immobilized covalently on the monolayer of a phosphanate ligand.

As another option, short, single-stranded nucleic acid species with protein binding properties (aptamers) make a strong claim for their use as sensor molecules. Combinatorial aptamer libraries have diversities from 10^{13} to 10^{17}. An aptamer microarray could be constructed using microarray surfaces for covalent DNA attachment or even synthesized *in situ* (James, 2001). In an aptamer microarray scenario, aptamer-ligand complexes will be photo-cross-linked and subsequently washed with high stringency for the reduction of the unspecific binding and background. However, there are some problematic issues. Because of the low chemical diversity of aptamers, 4 nucleotides versus 20 amino acids, electrostatic interactions may dominate the ligand binding of aptamers resulting in a high binding strength but low specificity (James, 2001). Additionally, aptamers are susceptible to nucleases, which could be present in the analyzed protein mixture.

Detection Methods

Possibly the most frequent approach of the detection of the bound target is a sandwich assay format. Using ELISA signal amplification systems, PSA in serum has been detected at a concentration of 200 pg/ml (Wiese *et al.*, 2001), and sensitivities of 1 pg/ml of cytokines in serum have been achieved (Moody *et al.*, 2001). However, these microarray systems contained only a small number of antibodies, and consequently, by increasing assay multiplexity, lower sensitivity would be expected. This application of the ELISA limits also the degree of multiplexing because of an increased spot size at a high analyte concentration (Moody *et al.*, 2001). In this context, fluorescently labeled secondary antibodies (Rowe *et al.*, 1999) may provide a more suitable and sensitive sandwich technique.

As an alternative sandwich technique, the rolling circle DNA amplification method (RCA) has been adapted to the detection of antigens by Schweitzer *et al.* (2002). In the presence of a primer attached to a secondary antibody, DNA-polymerase, and nucleotides, the amplification of circular DNA occurs resulting in a long DNA molecule containing hundreds of copies of the circular template molecule. Using this technique, purified human PSA has been detected on microarray slides at a level of 100 fg/ml (Schweitzer *et al.*, 2000). Although sandwich techniques are suitable for some diagnostic purposes, these methods may be difficult to be applied to a large-scale protein profiling, because of the doubled amount of antibodies required.

A sample labeling with fluorophors, a similar procedure that is routinely used for the transcriptional profiling on cDNA-microarrays, is well suited for a protein profiling on antibody microarrays (Haab *et al.*, 2001; Sreekumar, *et al.*, 2001). Using this method detection limits of a few pg/ml could be achieved when incubating antibody slides with a couple of labeled antigens, whereas sensitivity with a complex protein sample remains in the area of few ng/ml. However, the direct labeling has also drawbacks. A covalent attachment of fluorophors decreases the solubility of proteins. In addition, too high a degree of label incorporation can also interfere with the antigen-antibody recognition. Consequently, an application of nonlabeled detection techniques such as AFM, SPR, and mass spectrometry is advantageous. But still, all detection methods are limited by a degree of nonspecific binding of a complex protein sample on a microarray surface indicating again the significance of the appropriate surface chemistry for an extensive protein profiling of clinical specimens.

Conclusions

Microarray immunoassays of clinical specimens are very promising proteomics approaches for research and diagnostic purposes. The current status of this approach, including a wide spectrum of various fabrication and detection systems, is still in an early stage of development. However, the development of protein microarrays, which occurs mostly on the basis of conventional DNA microarray platforms, is currently associated with a number of problems arisen from common biophysical and chemical properties of proteins. Further advances in surface chemistry, printing techniques, microarray processing devices, and detection methods will contribute to the establishment of the microarray technology as a reliable tool for proteomics in the future (Table 1). Many of the basic problems have been identified, and ongoing research tries to solve them. Then the bottleneck will proceed from mere production issues toward the ability and capacity of identifying and isolating suitable receptor molecules.

Table 1 Problems Associated with Analysis of Highly Complex Samples on Current Protein Microarray Formats

Problems	Potential Technical Solution
Too large binding area (spot size)	Alternative printing technologies (e.g., ink-jet technology)
Establishment of thermodynamic equilibrium; long incubation time	Mixing devices (e.g., ArrayBooster, Advalytix, Germany)
High protein adsorption and denaturation of sensor molecules on microarray surface	Surfaces chemistries such as HydroGel, pegylated surfaces, or self-assembled monolayer
A set of sensor molecules with high specificity and affinity	Recombinant antibody display libraries, affibodies, aptamers
Efficient immobilization of recombinant sensor molecules	Tag-fusion recombinant proteins
Suitable sensitive detection methods	Rolling circle amplification

In summary, protein microarrays have enormous potential for becoming a tool that will enable a global characterization of molecular mixtures, in extent similar to DNA-microarray technology today. However, the biochemical diversity of proteins and the complexity of the proteome and the big dynamic range of particular proteins complicate the development of this new proteomic tool and pose an array of technologic challenges. The initial keys of this technology are a solid support and a sophisticated surface chemistry. Various protein microarray formats enabling different analytic possibilities are described here. Highly multiplexe microarrays represent a big challenge to surface chemistry, requiring extremely low nonspecific binding of proteins, high binding capacity of the sensor molecules, suitability for different receptor-ligand interactions, compatibility with manufacturing devices, and good spot quality. Suitability of the one-, two-, and three-dimensional surfaces reported here depends strongly on the kind of assay, their complexity, and the applied detection system. Additionally, recombinant proteins fused with different tags present another possibility for oriented attachment, which may preserve stability and affinity of proteins on microarray. Sensitivity of microspot immunoassays predicted by the ambient analyte theory is not yet reality, indicating the extent of the challenge that the surface chemistry, printing, and detection technologies are facing.

Acknowledgments

References

Abbott, A. 2002. Betting on tomorrow's chips. *Nature 415*: 112–114.

Adey, N.B., Ley, M., Howard, M.T., Jensen, J.D., Mayo, D.A., Butel, D.L., Coffin, S.C., Moyer, T.C., Slade, D.E., Spute, M.K., Hancock, A.M., Eisenhoffer, G.T., Dalley, B.K., and McNeely, M.R. 2002. Gains in sensitivity with a device that mixes microarray hybridization solution in 25-μm thick chamber. *Anal. Chem. 74*:6413–6417.

Anderson, L., and Seilhamer, J. 1997. A comparison of selected mRNA and protein abundances in human liver. *Electrophoresis 18*:533–537.

Arenkov, P., Kukhtin, A., Gemmell, A., Voloshchuk, S., Chupeeva, V., and Mirzabekov, A. 2000. Protein microchips: use for immunoassay and enzymatic reactions. *Anal. Biochem. 278*:128–131.

Avseenko, N.V., Morozova, T., Ataullakhanov, F.I., and Morozov, V.N. 2001. Immobilization of proteins in immunochemical microarrays fabricated by electrospray deposition. *Anal. Chem. 73*:6047–6052.

Benters, R., Niemeyer, C.M., and Wohrle, D. 2001. Dendrimer-activated solid supports for nucleic acid and protein microarrays. *Chembiochem. 2*:686–694.

Bhanot, G., Louzon, Y., Zhu, J., and DeLisi, C. 2003. The importance of thermodinamic equilibrium for high throughput gene expression arrays. *Biophys. J. 84*:124–135.

Bhatia, S.K., Shriver-Lake, L.C., Prior, K.J., Georger, J., Clavert, J.M., Bredehorst, R., and Ligler, F.S., 1989. Use of thiol-terminal silanes and heterobifunctional crosslinkers for immobilization of antibodies on silica surfaces. *Anal. Biochem. 178*:408–413.

Borrebaeck, C.A., Ekstrom, S., Hager, A.C., Nilsson, J., Laurell, T., and Marko-Varga, G. 2001. Protein chips based on recombinant antibody fragments: a highly sensitive approach as detected by mass spectro-metry. *Biotechniques 30*:1126–1130, 1132.

Bussow, K., Cahill, D., Nietfeld, W., Bancroft, D., Scherzinger, E., Lehrach, H., and Walter, G. 1998. A method for global protein expression and antibody screening on high-density filters of an arrayed cDNA library. *Nucl. Acids Res. 26*:5007–5008.

de Wildt, R.M., Mundy, C.R., Gorick, B.D., and Tomlinson, I.M. 2000. Antibody arrays for high-throughput screening of antibody-antigen interactions. *Nat. Biotechnol. 18*:989–994.

Ekins, R. 1994. Immunoassay: recent developments and future directions. *Nucl. Med. Biol. 21*:495–521.

Ekins, R., and Chu, F. 1992. Multianalyte microspot immunoassay. The microanalytical "compact disk" of the future. *Ann. Biol. Clin. 50*:337–353.

Ekins, R.P. 1998. Ligand assays: from electrophoresis to miniaturized microarrays. *Clin. Chem. 44*:2015–2030.

Falipou, S., Chovelon, J.M., Martelet, C., Margonari, J., and Cathignol, D. 1999. New use of cyanosilane coupling agent for direct binding of antibodies to silica supports. Physicochemical characterization of molecularly bioengineered layers. *Bioconjug. Chem. 10*:346–353.

Ge, H. 2000. UPA, a universal protein array system for quantitative detection of protein-protein, protein-DNA, protein-RNA and protein-ligand interactions. *Nucl. Acids Res. 28*:3e.

Guschin, D., Yershov, G., Zaslavsky, A., Gemmell, A., Shick, V., Proudnikov, D., Arenkov, P., and Mirzabekov, A. 1997. Manual manufacturing of oligonucleotide, DNA, and protein microchips. *Anal. Biochem. 250*:203–211.

Gygi, S.P., Rochon, Y., Franza, B.R., and Aebersold, R. 1999. Correlation between protein and mRNA abundance in yeast. *Mol. Cell. Biol. 19*:1720–1730.

Haab, B.B., Dunham, M.J., and Brown, P.O. 2001. Protein microarrays for highly parallel detection and quantitation of specific proteins and antibodies in complex solutions. *Genome Biol. 2*:10004–10013.

Hanes, J., and Pluckthun, A. 1997. In vitro selection and evolution of functional proteins by using ribosome display. *Proc. Natl. Acad. Sci. USA 94*:4937–4942.

Hanes, J., Schaffitzel, C., Knappik, A., and Pluckthun, A. 2000. Picomolar affinity antibodies from a fully synthetic naive library selected and evolved by ribosome display. *Nat. Biotechnol. 18*:1287–1292.

He, M., and Taussig, M.J., 2001. Single step generation of protein arrays from DNA by cell-free expression and in situ immobilisation (PISA method). *Nucl. Acids Res. 29*:E73–73.

Hlady, V.V., and Buijs, J. 1996. Protein adsorption on solid surfaces. *Curr. Opin. Biotechnol. 7*:72–77.

Hodneland, C.D., Lee, Y.S., Min, D.H., and Mrksich, M. 2002. Selective immobilization of proteins to self-assembled monolayers presenting active site-directed capture ligands. *Proc. Natl. Acad. Sci. USA 99*:5048–5052.

Houseman, B.T., Huh, J.H., Kron, S.J., and Mrksich, M. 2002a. Peptide chips for the quantitative evaluation of protein kinase activity. *Nat. Biotechnol. 20*:270–274.

Houseman, B.T., and Mrksich, M. 2002b. Carbohydrate arrays for the evaluation of protein binding and enzymatic modification. *Chem. Biol. 9*:443–454.

Houseman, B.T., and Mrksich, M. 2002c. Towards quantitative assays with peptide chips: a surface engineering approach. *Trends Biotechnol. 20*:279–281.

Huang, J.X., Mehrens, D., Wiese, R., Lee, S., Tam, S.W., Daniel, S., Gilmore, J., Shi, M., and Lashkari, D. 2001a. High-throughput genomic and proteomic analysis using microarray technology. *Clin. Chem. 47*:1912–1916.

Huang, N.-P., Michel, R., Voros, J., Textor, M., Hofer, R., Rossi, A., Elbert, D.L., Hubbell, J.A., and Spencer, D. 2001b. Poly (L-lysine)-g-poly(ethylene glycol) layers on metal oxide surfaces: Surface-analytical characterization and resistance to serum and fibrinogen adsorption. *Langmuir 17*:489–498.

Huang, R.P., Huang, R., Fan, Y., and Lin, Y. 2001c. Simultaneous detection of multiple cytokines from conditioned media and patient's sera by an antibody-based protein array system. *Anal. Biochem. 294*:55–62.

James, W. 2001. Nucleic acid and polypeptide aptamers: a powerful approach to ligand discovery. *Curr. Opin. Pharmacol. 1*:540–546.

Jones, V.W., Kenseth, J.R., Porter, M.D., Mosher, C.L., and Henderson, E. 1998. Microminiaturized immunoassays using atomic force microscopy and compositionally patterned antigen arrays. *Anal. Chem. 70*:1233–1241.

Joos, T.O., Schrenk, M., Hopfl, P., Kroger, K., Chowdhury, U., Stoll, D., Schorner, D., Durr, M., Herick, K., Rupp, S., Sohn, K., and Hammerle, H. 2000. A microarray enzyme-linked immunosorbent assay for autoimmune diagnostics. *Electrophoresis 21*:2641–2650.

Knezevic, V., Leethanakul, C., Bichsel, V.E., Worth, J.M., Prabhu, V.V., Gutkind, J.S., Liotta, L.A., Munson, P.J., Petricoin, E.F., III., and Krizman, D.B. 2001. Proteomic profiling of the cancer microenvironment by antibody arrays. *Proteomics 1*:1271–1278.

Koopmann, J.-O., and Blackburn, J. 2003. High affinity capture surface for matrix-assisted laser desorption/ionisation compatible protein micro-arrays. *Rapid. Commun. Mass Spectrom. 17*:455–462.

Kronvall, G., and Jonsson, K. 1999. Receptins: a novel term for an expanding spectrum of natural and engineered microbial proteins with binding properties for mammalian proteins. *J. Mol. Recognit. 12*:38–44.

Kukar, T., Eckenrode, S., Gu, Y., Lian, W., Megginson, M., She, J.X., and Wu, D. 2002. Protein microarrays to detect protein-protein interactions using red and green fluorescent proteins. *Anal. Biochem. 306*:50–54.

Kusnezow, W., and Hoheisel, J.D. 2002. Antibody microarrays: promises and problems. *Biotechniques Suppl. Suppl*:14–23.

Kusnezow, W., Jacob, A., Walijew, A., Diehl, F., and Hoheisel, J.D. 2003. Antibody microarrays: An evaluation of production parameters. *Proteomics 3*:254–264.

Kusnezow, W., Pulli, T., Witt, O., and Hoheisel, J.D. 2004. Solid support for protein microarrays and related devices. In Schena, M. (ed) *Protein Microarrays*. Sudbury, MA: Jones and Bartlett Publishers, 247–284.

Lee, C.S., and Kim, B.G. 2002a. Improvement of protein stability in protein microarray. *Biotechnol. Lett. 24*:839–844.

Lee, K.B., Park, S.J., Mirkin, C.A., Smith, J.C., and Mrksich, M. 2002b. Protein nanoarrays generated by dip-pen nanolithography. *Science 295*:1702–1705.

Lesaicherre, M.L., Lue, R.Y., Chen, G.Y., Zhu, Q., and Yao, S.Q. 2002a. Intein-mediated biotinylation of proteins and its application in a protein microarray. *J. Am. Chem. Soc. 124*:8768–8769.

Lesaicherre, M.L., Uttamchandani, M., Chen, G.Y., and Yao, S.Q. 2002b. Developing site-specific immobilization strategies of peptides in a microarray. *Bioorg. Med. Chem. Lett. 12*:2079–2083.

Li, Y., and Reichert, W.M. 2003. Adapting cDNA microarray format to cytokine detection protein arrays. *Langmuir* page est: 9.2. *19(5)*:1557–1566.

Lindqvist, Y., and Schneider, G. 1996. Protein-biotin interactions. *Curr. Opin. Struct. Biol. 6*:798–803.

Livshits, M.A., and Mirzabekov, A.D. 1996. Theoretical analysis of the kinetics of DNA hybridization with gel-immobilized oligonucleotides. *Biophys. J. 71*:2795–2801.

Lueking, A., Horn, M., Eickhoff, H., Bussow, K., Lehrach, H., and Walter, G. 1999. Protein microarrays for gene expression and antibody screening. *Anal. Biochem. 270*:103–111.

MacBeath, G., and Schreiber, S.L. 2000. Printing proteins as microarrays for high-throughput function determination. *Science 289:*1760–1763.

Madoz-Gurpide, J., Wang, H., Misek, D.E., Brichory, F., and Hansh, S.M. 2001. Protein based microarrays: A tool for probing the proteome of cancer cells and tissues. *Proteomics 1*:1279–1287.

Mendoza, L.G., McQuary, P., Mongan, A., Gangadharan, R., Brignac, S., and Eggers, M. 1999. High-throughput microarray-based enzyme-linked immunosorbent assay (ELISA). *Biotechniques 27*:778–780, 782–776, 788.

Mezzasoma, L., Becarese-Hamilton, T., Di Cristina, M., Rossi, R., Bistoni, F., and Crisanti, A. 2002. Antigen microarrays for serodiagnosis of infectious diseases. *Clin. Chem. 48*:121–130.

Miller, J.C., Zhou, H., Kwekel, J., Cavallo, R., Burke, J., Butler E.B., Teh, B.S., and Haab, B.B. 2003. Antibody microarray profiling of human prostate cancer sera: Antibody screening and identification of potential biomarkers. *Proteomics 3*:56–63.

Moody, M.D., Van Arsdell, S.W., Murphy, K.P., Orencole, S.F., and Burns, C. 2001. Array-based ELISAs for high-throughput analysis of human cytokines. *Biotechniques 31*:186–190, 192–184.

Morozov, V.N., and Morozova, T. 1999. Electrospray deposition as a method for mass fabrication of mono- and multicomponent microarrays of biological and biologically active substances. *Anal. Chem. 71*:3110–3117.

Nord, K., Gunneriusson, E., Ringdahl, J., Stahl, S., Uhlen, M., and Nygren, P.A. 1997. Binding proteins selected from combinatorial libraries of an alpha-helical bacterial receptor domain. *Nat. Biotechnol. 15*:772–777.

Okamoto, T., Suzuki, T., and Yamamoto, N. 2000. Microarray fabrication with covalent attachment of DNA using bubble jet technology. *Nat. Biotechnol. 18*:438–441.

Paweletz, C.P., Charboneau, L., Bichsel, V.E., Simone, N.L., Chen, T., Gillespie, J.W., Emmert-Buck, M.R., Roth, M.J., Petricoin, I.E., and Liotta, L.A. 2001. Reverse phase protein microarrays which capture disease progression show activation of prosurvival pathways at the cancer invasion front. *Oncogene 20*:1981–1989.

Pawlak, M., Schick, E., Bopp, M.A., Schneider, M.J., Oroszlan, P., and Ehrat, M. 2002. Zeptosens' protein microarrays: a novel high performance microarray platform for low abundance protein analysis. *Proteomics 2*:383–393.

Peluso, P., Wilson, D.S., Do, D., Tran, H., Venkatasubbaiah, M., Quincy, D., Heidecker, B., Poindexter, K., Tolani, N., Phelan, M., Witte, K., Jung, L.S., Wagner, P., and Nock, S. 2003.

Optimizing antibody immobilization strategies for the construction of protein microarrays. *Anal. Biochem. 312*:113–124.

Piehler, J., Brecht, A., Valiokas, R., Liedberg, B., and Gauglitz, G. 2000. A high-density poly(ethylene glycol) polymer brush for immobilization on glass-type surfaces. *Biosens. Bioelectron. 15*:473–481.

Roberts, R.W., and Szostak, J.W. 1997. RNA-peptide fusions for the in vitro selection of peptides and proteins. *Proc. Natl. Acad. Sci. USA 94*:12297–12302.

Robinson, W.H., DiGennaro, C., Heuber, W., Haab, B.B., Kamachi, M., Dean, E.J., Fournel, S., Fong, D., Genovese, M.C., Neuman de Vegvar, H.E., Skriner, K., Hrischberg, D.L., Morris, R.I., Muller, S., Prujin, G.J., van Venrooij, W.J., Smolen, J.S., Brown, P.O., Steinman, L., and Utz, P.J. 2002. Autoantigen microarrays for multiplex characterization of autoantibody responses. *Nat. Med. 8*:295–301.

Rowe, C.A., Scruggs, S.B., Feldstein, M.J., Golden, J.P., and Ligler, F.S. 1999. An array immunosensor for simultaneous detection of clinical analytes. *Anal. Chem. 71*:433–439.

Ruiz-Taylor, L.A., Martin, T.L., Zaugg, F.G., Witte, K., Indermuhle, P., Nock, S., and Wagner, P. 2001. Monolayers of derivatized poly (L-lysine)-grafted poly(ethylene glycol) on metal oxides as a class of biomolecular interfaces. *Proc. Natl. Acad. Sci. USA 98*:852–857.

Sapsford, K.E., Liron, Z., Shubin, Y.S., and Ligler, F.S. 2001. Kinetics of antigen binding to arrays of antibodies in different sized spots. *Anal. Chem. 73*:5518–5524.

Sblattero, D., and Bradbury, A. 2000. Exploiting recombination in single bacteria to make large phage antibody libraries. *Nat. Biotechnol. 18*:75–80.

Schaeferling, M., Schiller, S., Paul, H., Kruschina, M., Pavlickova, P., Meerkamp, M., Giammasi, C., and Kambhampati, D. 2002. Application of self-assembly techniques in the design of biocompatible protein microarray surfaces. *Electrophoresis 23*:3097–3105.

Schweitzer, B., Roberts, S., Grimwade, B., Shao, W., Wang, M., Fu, Q., Shu, Q., Laroche, I., Zhou, Z., Tchernev, V.T., Christiansen, J., Velleca, M., and Kingsmore, S.F. 2002. Multiplexed protein profiling on microarrays by rolling-cricle amplification. *Nat. Biotechnol. 20*:359–365.

Schweitzer, B., Wiltshire, S., Lambert, J., O'Malley, S., Kukanskis, K., Zhu, Z., Kingsmore, S.F., Lizardi, P.M., and Ward, D.C. 2000. Inaugral article: immunoassays with rolling circle DNA amplification: a versatile platform for ultrasensitive antigen detection. *Proc. Natl. Acad. Sci. USA 97*:10113–10119.

Scriba, J., Tögl, A., and Kirchner, R. 2002. Nanopumpen verbessern die Microarray-Inkunation. *Transkript LABORWELT Nr III*:12–14.

Seong, S.Y. 2002. Microimmunoassay using a protein chip: optimizing conditions for protein immobilization. *Clin. Diagn. Lab. Immunol. 9*:927–930.

Sreekumar, A., Nyati, M.K., Varambally, S., Barrette, T.R., Ghosh, D., Lawrence, T.S., and Chinnaiyan, A.M. 2001. Profiling of cancer cells using protein microarrays: discovery of novel radiation-regulated proteins. *Cancer Res. 61*:7585–7593.

Stevens, P.W., Wang, C.H.J., and Kelso, D.M. 2003. Immobilized particle arrays: coalescence of planar- and suspension-array technologies. *Anal. Chem. 75*:1141–1146.

Tam, S.W., Wiese, R., Lee, S., Gilmore, J., and Kumble, K.D. 2002. Simultaneous analysis of eight human Th1/Th2 cytokines using microarrays. *J. Immunol. Methods 261*:157–165.

Terpe, K. 2003. Overview of tag protein fusions: From molecular and biochemical fundamentals to commercial systems. *Appl. Microbiol. Biotechnol. 60(5)*:523–533.

Weimer, B.C., Walsh, M.K., and Wang, X. 2000. Influence of a poly-ethylene glycol spacer on antigen capture by immobilized antibodies. *J. Biochem. Biophys. Methods 45*:211–219.

Weng, S., Gu, K., Hammond, P.W., Lohse, P., Rise, C., Wagner, R.W., Wright, M.C., and Kuimelis, R.G. 2002. Generating addressable protein microarrays with PROfusion covalent mRNA-protein fusion technology. *Proteomics 2*:48–57.

Wiese, R., Belosludtsev, Y., Powdrill, T., Thompson, P., and Hogan, M. 2001. Simultaneous multianalyte ELISA performed on a microarray platform. *Clin. Chem. 47*:1451–1457.

Zhu, H., Bilgin, M., Bangham, R., Hall, D., Casamayor, A., Bertone, P., Lan, N., Jansen, R., Bidlingmaier, S., Houfek, T., Mitchell, T., Miller, P., Dean, R.A., Gerstein, M., and Snyder, M. 2001. Global analysis of protein activities using proteome chips. *Science 293*:2101–2105.

This Page Intentionally Left Blank

4

Comparative Genomic Hybridization

Isabel Zudaire

Introduction

Comparative genomic hybridization (CGH) is a molecular cytogenetic technique that allows the analysis of deoxyribonucleic acid (DNA) gains and losses in the entire genome in a single hybridization experiment. It is based on the cohybridization of two differentially fluorescence-labeled DNAs to normal human metaphase chromosomes: the target DNA, called test DNA, and a genetically normal DNA used as reference DNA. Equal amounts of both DNAs compete to hybridize proportionally to the copy-numbers of the sequences present in each genome. Comparison of the test fluorescence signals and the reference fluorescence signals allows the detection of chromosomal gains and losses (Figure 9).

This technique was developed by Kallioniemi *et al.* in 1992, and since then it has contributed to the knowledge of the chromosomal aberrations present in constitutional diseases and tumors. CGH has been particularly relevant in the study of solid tumors because it is not dependent on the availability of metaphases from the neoplastic cells. Obtaining metaphases from solid tissue always has been hard work because of the need of specific *in vitro* culture conditions and the low mitotic activity of solid tumors, which forces long culture periods, favoring the acquisition of secondary chromosomal changes and clonal outgrowth of cell subpopulations. Furthermore, when metaphases are obtained, they are usually of poor quality compared with those obtained from blood or bone marrow (James, 1999). In addition, because of the delay in diagnosis, karyotypes are often so complex that it is difficult to describe which aberrations are primary or secondary to the neoplastic process.

In this context, CGH is a useful technique to the study of solid tumors because genomic DNA is the only source required from the tumor specimen. Although CGH requires DNA of a high quality, CGH analysis could be performed either from cell lines or from fresh, frozen, or formalin-fixed and paraffin-embedded (FFPE) tissues.

Hundreds of CGH studies have been published. It has been used as a complementary technique when G-banding was unable to characterize complex karyotypes and unknown markers. Constitutive disease also has been described by CGH, although most studies are of solid tumors. CGH has allowed defining new cancer genes and has provided important information about tumor classification, progression, prognosis, and response to therapy (www.helsinki.fi/cmg/dokumentit/ Minireview.doc). Description of the main aberrations detected by CGH in different neoplasias are found

Tumor tissue

Normal tissue

DNA isolation
and labeling

Test DNA

Cot-1 DNA

Reference DNA

Coprecipitation

Denaturation

Hybridization to the normal metaphase

DAPI stain

Analysis

Loss

Gain

0.85   1.15

1
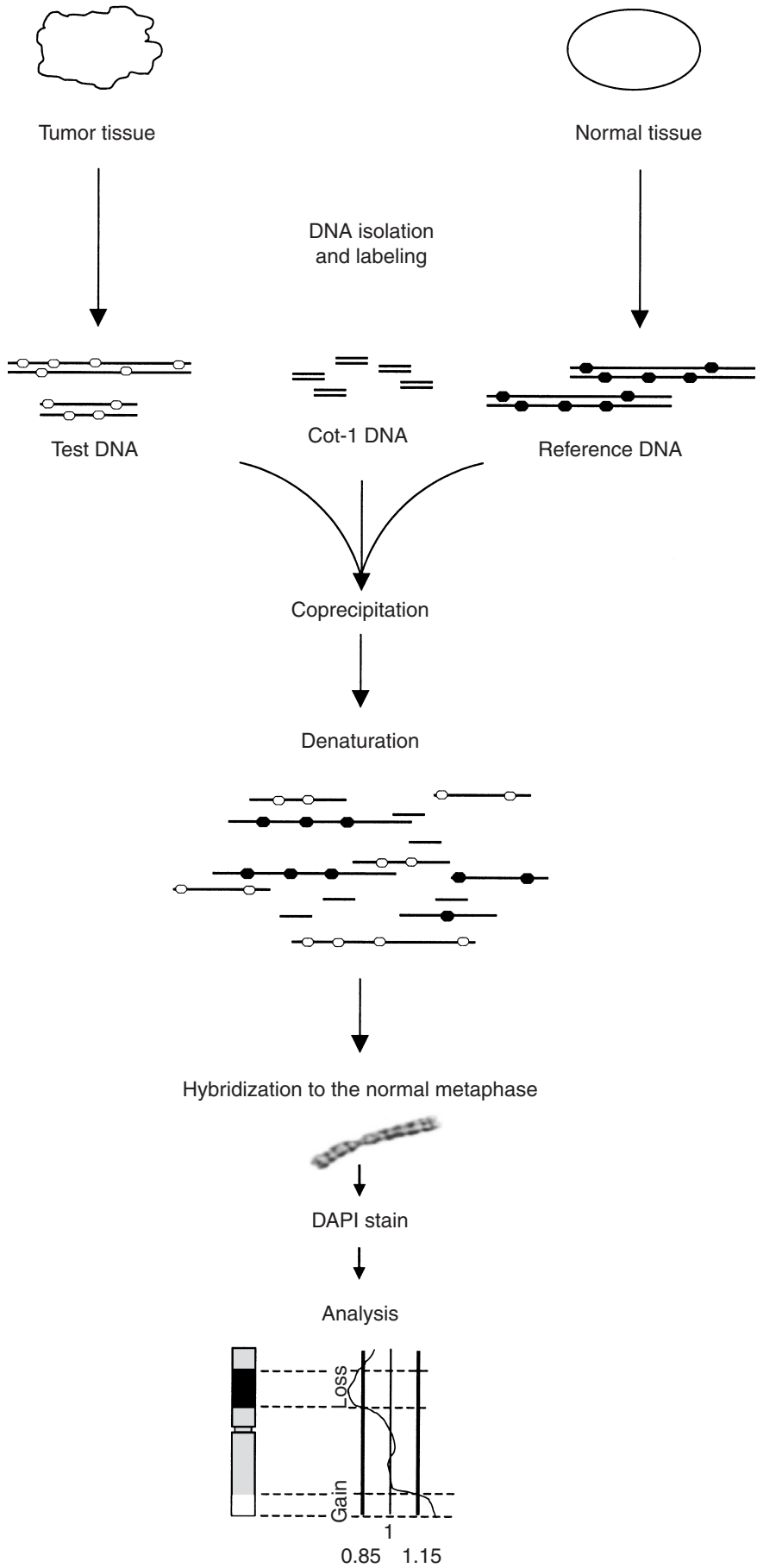
Figure 9 Schematic overview of comparative genomic hybridization.

in many CGH reviews and online CGH databases. The most updated is the CGH database from the University of Helsinki (www.helsinki.fi/cmg/Minireview). Other Web sites also provide useful information, such as www.ncbi.nlm.nih.gov/sky/;amba.charite.de/~ksch/cghdatabase/index.htm; and www.progenetix.net/.

CGH also presents some disadvantages. For instance, it only detects copy-number changes but no balanced aberrations such as translocations or inversions. Pericentromeric, telomeric, and heterochromatic regions cannot be evaluated because CGH hybridization implies the blocking of repetitive sequences. Some specific regions such as 1p32-pter, 16p, 19, and 22 chromosomes are especially conflictive, leading to frequent false-positive results (Struski *et al.,* 2002). Furthermore, because CGH uses the DNA of all cells of the specimen, results could not be reliable in the case of polysomies, genetically different clones, and normal cells present in a percentage up to 50% in the specimen. CGH sensitivity also depends on the level and the size of the copy-number changes. Theoretically the resolution of CGH is 5–10 Mb, but in practice the resolution for deletion detection is 10–20 Mb. A copy-number increase of 50% could be detectable if the region is 2 Mb or larger and a 250 Kb amplified region may present a copy-number increase of 400% to be detected (Weiss *et al.,* 1999).

CGH modifications have been developed to improve CGH sensitivity and specificity. In 1998 Kirchhoff *et al.* published that the use of the standard deviation as a significant threshold improved the sensitivity of CGH results. Every laboratory should estimate the standard deviation of its own CGH experiments in control CGH experiments and apply this standard deviation to its CGH interpretations. With this method, the sensitivity of CGH could be improved to detect deletions involving 3 Mb.

The use of the microdissection of the tumor cells followed by degenerate oligonucleotide primed-polymerase chain reaction (DOP-PCR) amplification of the isolated DNA can minimize normal cell contamination and intratumor genomic heterogeneity (Aubele *et al.,* 2000; Zitzelsberger *et al.,* 1998), improving the CGH sensitivity.

In 1999 Karhü *et al.* developed the four-color CGH. This CGH modification consists of adding a second reference DNA labeled with Cy5 to the conventional mixture. This DNA serves as an internal control in every hybridization. Normalization of the ratio Red-labeled DNA versus Cy5-labeled DNA allows the analysis of complex regions such as 1pter, 19, 22.

The use of normal metaphases as targets limits the CGH resolution to the chromosomal size. For this reason, Solinas-Toldo *et al.* in 1997 and Pinkel *et al.* in 1998 developed the matrix-CGH. Matrix-CGH substitutes the metaphases by small DNA fragments from 90 to 230 Kb length as targets to CGH hybridization. With matrix-CGH, also called array-CGH, low copy-number gains and losses can be detected at a resolution of ~100 kb.

Many different CGH protocols have been described with different complexity and sensitivity. Some of them are available online:

amba.charite.de/cgh/protocol/02/prot02.html
cc.ucsf.edu/people/waldman/Protocols
www.riedlab.nci.nih.gov/protocols.asp
www.patho.unibas.ch/d/fo_neme_mozy_cgh%20_
   prot.html
www.sanger.ac.uk/HGP/methods/cytogenetics/

In this chapter I will present a short review of the different CGH methodologies performed, describing the advantages and disadvantages of all of them.

MATERIALS AND METHODS

The CGH procedure involves the following steps: DNA isolation, DNA labeling, hybridization, washing, and analysis.

DNA Isolation

MATERIALS

1. Proteinase K (Cat. No. 25530-015, Invitrogen Corp., Carlsbad, CA).
2. QIAamp DNA Mini kit (50) (Cat. No. 51304, QIAGEN, Valencia, CA).
3. Xylene (Cat. No. 211769.1611, Panreac, Barcelona, Spain).
4. Ethanol (Cat. No. 1.00983.2500, Merck & C., Whitehouse Station, NJ).
5. Agarose (Cat. No. 8016, Pronadisa, Madrid, Spain).
6. Ethidium bromide 10 mg/ml (Cat. No. E1510, Sigma, St. Louis, MO).
7. Phosphate buffer saline (PBS) tablets (Cat. No. P-4417, Sigma).
8. Tris (Cat. No. 37190, Serva, Heidelberg, Germany).
9. Boric acid (Cat. No. 131015.1211, Panreac).
10. Ethylenediamine tetra-acetic acid (EDTA) (Cat. No. 131669, Panreac).

Solutions

1. Proteinase K 20 mg/ml stock solution: 20 mg proteinase K with 1 ml of distilled water. Make 40 µl aliquots and keep them at −20°C.

2. Ethidium bromide (EtBr) 5 mg/ml solution: dilute EtBr 10 mg/ml with distilled water to 5 mg/ml concentration.

3. EDTA 0.5 M: 93.06 g in 500 ml of distilled water. Store at room temperature.

4. Tris-borate-EDTA (TBE) 1X: 10.8 g Tris, 5.5 g boric acid, 4 ml EDTA, 0.5 M pH 8.0 to 1 L.

5. PBS: dissolve 1 tablet in 200 ml of water. Filter.

METHOD

CGH quality depends mainly on the quality of DNAs used. Concerning reference DNA, normal DNA belonging to the same individual as the test DNA is suitable. Even more, when CGH is performed for the analysis of a tumor sample, variations in CGH results may be minimized if normal DNA is extracted from a histopathologically normal sample from the tumor tissue but distal to the tumoral focus. However, in many cases this reference DNA is not available or we cannot be sure if this phenotypically normal tissue is genetically normal. In those cases, many sources of normal DNA can be used: blood of the same individual whose tumoral sample will be analyzed, blood of healthy donors, or commercial reference DNA.

DNA from fresh or frozen tissue is suitable because of its high quality, but CGH protocols using DNA isolated from FFPE tissue have also been successfully optimized.

DNA could be isolated using a conventional proteinase K/phenol-chloroform method (Isola *et al.,* 1994) or following the use of any commercial kit such as QiAGEN (Zudaire *et al.,* 2002). We have obtained better results with commercial kits; they provide higher DNA concentration.

DNA from Fresh or Frozen Samples

1. Place 60–80 mg of tissue in a Petri dish, add culture media, and slice it in sections.

2. Collect them in a 15 ml tube and centrifuge for 2 min at 1500 rpm.

3. Remove the supernatant and wash twice with PBS.

4. Remove the supernatant and resuspend the DNA in QIAamp DNA kit lysis buffer.

5. Add 20 µl of proteinase K and incubate overnight at 55°C in a water bath.

6. Perform the DNA extraction according to the manufacturer's directions.

DNA form FFPE DNA

Until recently, pathologic laboratories routinely preserved FFPE tissues. Neutral-buffered formalin (10%) contains 4% formaldehyde, which induces the formation of cross-links between proteins or between proteins and nucleic acids. These cross-links decrease the efficiency of DNA isolation and nick translation reaction (see Nick Translation Protocol for Paraffin Samples). The type of fixative used and the fixation time strongly affect the DNA quality. Tissue fixation may be started in the 30 min after removal of the tissue, and the optimal time of fixation may be no less than 24 hr or longer than 48 hr (Werner *et al.,* 2000).

Isola *et al.* (1994) published the first approach to CGH using paraffin-embedded samples. We recommend it but using QIAamp DNA kit. The protocol is as follows:

1. Obtain 20–30 5 µm sections from paraffin tissue block.

2. Incubate them at 65°C for 10 min.

3. Add 1 ml xylene and centrifuge at high speed for 10 min.

4. Remove the supernatant, and repeat **Step 3.**

5. Pipette off supernatant and add 1 ml of 100% ethanol. Vortex and centrifuge at high speed for 10 min.

6. Repeat **Step 5.**

7. Remove the supernatant and let the pellet air-dry.

8. According to the QIAamp DNA kit, add 180 µl of digestion buffer.

9. Add 20 µl of proteinase K (20 mg/ml) and incubate the tube overnight at 55°C in a water bath.

10. The next day, if the tissue is not disintegrated, add 10 µl of additional proteinase K. Digestion can be extended for several days to total digestion of the tissue.

11. At this point, DNA extraction could be performed according to the QIAamp DNA kit directions.

Microdissection

In tumor analysis, DNA extracted from tissue samples does not contain 100% amount of genetically abnormal DNA. Contamination from normal cells such as lymphocytes, macrophages, endothelial cells, and others is common. This "normal" DNA in the test sample dilutes the chromosomal aberrations present in the tumor.

Microdissection of the tumoral suspicious cells avoids this usual contamination. It also allows the analysis of minute subregions of tumors independently (e.g., invasive component versus *in situ* component), making possible the comparison of different stages of tumor progression (Aubele *et al.,* 2000).

Microdissection technique is explained in detail in chapter one of this book. Concerning application to the CGH technique, microdissected material may be processed as described before, with concentration adjusted according to the amount of material obtained. The number of cells that should be collected from a microdissection varies significantly depending on the

tissue source. From frozen tissue approximately 20 cells/µl of extraction buffer is recommended. More cells are needed if microdissection is performed from an FFPE tissue. In any case, PCR amplification of the DNA obtained after microdissection is needed.

After any isolation procedure, because of the equimolecular competition of both DNAs in CGH technique, measurement of the DNA concentration with a spectrophotometer is recommended. Furthermore, to estimate the DNA fragmentation, 2 µl of the DNA solution may be run in a 0.8% agarose gel.

Labeling

Different labeling reactions have been used in CGH experiments: nick translation, random priming, DOP-PCR, and ULS (Universal Linkage System). The most popular is nick translation reaction; random priming is usually chosen when paraffin DNA is used, and DOP-PCR is the best method to label DNA from samples obtained after microdissection. ULS is unpopular, and only a few papers are published using this labeling method (Alers *et al.,* 1999; van Gijlswijk *et al.,* 2001).

In nick translation, random priming, and DOP-PCR protocols, two different subset of labeling molecules could be used:

a. Fluorescence particles link to one of the deoxynucleotide supplied to the reaction. This methodology is called "direct labeling." The most common are TexasRed-dUTP or SpectrumRed-dUTP (red color fluorochromes) and FITC-dUTP or SpectrumGreen-dUTP (green color fluorochromes).

b. Fluorochrome molecules conjugated with haptens will be detected immunohistochemically (indirect labeling*)*. The most commonly used are Biotin-dUTP and Digoxigenin-dUTP.

In conventional CGH, test DNA is labeled with the green fluorochrome and reference DNA is labeled with the red fluorochrome.

Nick Translation Reaction

Nick translation reaction consists of nicking the genome DNA with a limiting concentration of DNAse enzyme. Then DNA polymerase is used to both digest and fill the gaps with the provided nucleotides (among which is the labeled nucleotide).

MATERIALS

CGH Nick Translation Kit from Vysis (Downer's Grove, IL) is an efficient commercial kit for this reaction.

However, high efficient nick translation also can be performed acquiring reagents individually.

If Vysis Kit Is Used

1. CGH Nick Translation Kit, 50 reactions (Cat. No. 32-801024, Vysis).

2. SpectrumRed Female human genomic DNA, 300 ng/µl (Cat. No. 32-804023, Vysis).

3. SpectrumRed Male human genomic DNA, 300 ng/µl (Cat. No. 32-804024, Vysis).

4. SpectrumRed-dUTP, 50 nmol (Cat. No. 30-803400, Vysis).

5. SpectrumGreen-dUTP, 50 nmol (Cat. No. 30-803200, Vysis).

If Nick Translation Kit Is Not Used

1. If direct labeling is performed: FITC-dUTP and TexasRed-5-dUTP (Cat. No. NEL413 and Cat. No. NEL417, Dupont, Wilmington, DE).

2. If indirect labeling is performed: Biotin-16-dUTP and Digoxigenin-11-dUTP (Cat. No. 1093070 and Cat. No. 1093088, Boehringer Mannheim, Indianapolis, IN).

3. dNTPs (regular nucleotides): dATP (Cat. No. 10216.018, dCTP Cat. No. 10217.016, dGTP, Cat. No. 10218.014, dTTP, Cat. No. 10219.012, Invitrogen).

4. DNA Polymerase/DNAse I (Cat. No. 18162-016, Invitrogen).

5. DNApolymerase-1 (Cat. No. 18010-025, Invitrogen).

6. Agarose (see earlier).

7. Lambda HindIII DNA marker 0.5 µg/µl (Cat. No. 15612-03, Invitrogen).

8. Ethidium bromide (see earlier).

9. Glycerol (Cat. No. 5516, Sigma).

10. Orange G (Cat. No. O-1625, Sigma).

Solutions

1. TBE 1X (see earlier).

2. Loading buffer: mix 30% (v/v) of glycerol, 70% (v/v) of distilled water, and 0.25% of orange G.

3. Buffer Tris ethylenediaminetetraacetate (TE): 10 mM Tris ClH (pH 7.4) and 1 mM EDTA (pH 8.0).

4. Lambda HindIII DNA marker: mix 300 µl of 0.5 µg/µl of DNA marker stock, 300 µl of loading buffer, and 900 µl of buffer TE (pH 7.5). Mix well. Store at 4°C between uses.

5. 1% agarose gel: 1 g agarose to 100 ml TBE 1X buffer. Heat the solution in the microwave until the agarose is melted. Cool the agarose, and add 10 µl of ethidium bromide (EtBr) (5 mg/ml).

6. If CGH Nick Translation Kit is used, prepare 0.2 mM SpectrumGreen, 0.2 mM SpectrumRed, 0.1 mM dTTP, and 0.1 mM dNTP mix according to the manufacturer's directions.

METHOD

1. Place a 1.5 ml microcentrifuge tube on ice.
2. Add the reagents to the tube in the following order:
   a. If CGH Nick Translation Kit is used:
      ▲ Nuclease-free water up to 50 µl.
      ▲ x µl of DNA (for 1 µg of DNA).
      ▲ 10 µl dNTPs mix (0.1 mM of dATP, dCTP, dGTP).
      ▲ 5 µl of 0.1 mM dTTP.
      ▲ 5 µl of the 10X nick translation reaction buffer.
      ▲ 10 µl of the nick translation enzyme.
      ▲ 2.5 µl of the 0.2 mM SpectrumGreen (test DNA) or SpectrumRed (reference DNA) dUTP.
   b. If reagents are ordered separately:
      ▲ nuclease-free water up to 50 µl.
      ▲ x µl of DNA (for 1 µg of DNA).
      ▲ 10 µl dNTPs mix (0.2 mM of dATP, dCTP, dGTP and 0.04 mM dTTP).
      ▲ 2 µl of the DNApolymerase-1.
      ▲ 10 µl of the DNA Polymerase/DNAse I mix.
      ▲ 2 µl of the 0.2 mM FITC-dUTP and TexasRed-5-dUTP or Biotin-16-dUTP and Digoxigenin-11-dUTP.

3. Vortex to mix the reagents completely and incubate them for 90 min at 15ºC.

4. Check the DNA fragmentation running an aliquot of 5 µl from each nick translation reaction in a 1% agarose gel together with 5 µl of Lambda HindIII DNA marker (0.1 µg/µl). The optimal length of DNA fragments should range from 600 to 2000 bp. Smaller fragments can result in nonspecific hybridization, and longer fragments can increase background staining (Jeuken *et al.,* 2002).

Digestion time and enzyme concentration may be adjusted for each sample. If the length of DNA fragments is longer than 2 Kb, longer nick reactions may be performed with or without new enzyme addition. Increasing the amount of DNAse could decrease drastically time reactions. However, in our opinion, it is recommended to prolong nick translation reaction without DNAse addition to prevent an excess of DNA fragmentation.

DNA obtained from paraffin-embedded samples is highly fragmented with fragments ranging from 20 kb to 200 pb. Thus, agarose gel images before and after nick translations are quite similar. Furthermore, fragments bigger than 20 Kb are usually present. They are the result of the cross-links between DNA and proteins consequence of the formalin fixation of the tissue. These fragments can never be nicked by nick translation.

Thus, agarose gel does not help to check nick translation reaction. In this case the labeling process can be optimized. As a general rule, nick translation for DNA from paraffin-embedded tissues may be performed with smaller DNAse concentration, a higher amount of DNA, and a shorter period of digestion.

After checking, incubate the nick translation reaction for 15 min at 65°C to stop the labeling.

Random Priming Reaction

In random priming reaction, DNA is denatured in the presence of a high concentration of all possible sequence combinations of short oligonucleotides. Using the Klenow fragment of DNA polymerase, a complementary DNA strand is synthesized incorporating the labeled nucleotides (Feinberg *et al.,* 1983). When using DNA from paraffin samples, random priming is suitable because no DNA fragmentation is performed during labeling reaction. However, this labeling reaction is not usually used in conventional CGH but in matrix-CGH (see later).

DOP-PCR

Microdissected tumor samples do not usually provide enough DNA for standard CGH. In those cases DOP-PCR amplification is usually required. This technique was first described by Speicher *et al.* in 1993. It is based on the amplification of all DNA sequences using degenerate primers in low PCR stringency conditions. Two separate rounds of amplification are performed: the first one (preamplification step) is done in low stringency conditions, and the second one is done in high stringency conditions. DNA labeling may be performed by the incorporation of the labeled nucleotide in the PCR reaction or after PCR, either by nick translation or random priming.

Here we describe the protocol published by Huang *et al.* in 2000 with minor modifications.

MATERIALS

1. ThermoSequenase DNA polymerase (Cat. No. E79000Y, Amersham Biosciences, Piscataway, NJ).
2. ThermoSequenase buffer: 260 mM Tris-HCl, (pH 9.5) 65 mM $MgCl_2$ (Amersham Biosciences).
3. AmpliTAq DNA polymerase (Cat. No. N808-0158, Perkin Elmer, Wellesley, MA).
4. 10X low salt buffer: 500 mM Tris-HCl, 500 mM KCl, (pH 8.9) (Cat. No. N808-0010, Perkin Elmer).
5. Regular nucleotides (dATP, dCTP, dGTP, dTTP). Prepare 10XdNTP (2 mM of dATP, dCTP, dGTP, and 0.5 mM dTTP) (see earlier).

6. If DNA labeling is performed during DOP-PCR, 1 mM dUTP-FITC and 1 mM dUTP-TexasRed are required (see earlier).

7. Universal primer (UN1 primer) is 5′-CCG ACT CGA GNN NNN NAT GTG G-3′ (where N = A, C, G and T in equal amounts; Midland Certified Reagent Co. Telenius 6MW).

METHOD

I. Preamplification step:
  A. Mixture:
    1. ThermoSequenase buffer, 1 µl.
      2 mM 10X dNTP, 1 µl.
      10 µM UNI-primer, 1 µl.
      ThermoSequenase 4 U/µl, 1 µl.
      Sample, 12.5 pg to 1 ng.
      ddH$_2$O, up to 10 µl.
  B. PCR conditions:
    1. 3 min at 95°C.
    2. 4 cycles of the following:
      a. 1 min at 94°C.
      b. 1 min annealing at 25°C.
      c. 3 min ramp at 25–74°C.
      d. 2 min extension at 74°C.
      e. Final extension of 10 min.
II. Second amplification step:
  A. Mixture:
    1. 10X low salt buffer, 4 µl.
    2. 10X dNTP, 4 µl.
    3. 1 mM FITC-dUTP, 2 µl.
    4. 10 µM UNI-primer, 6 µl.
    5. AmpliTaq DNA polymerase 5 U/µl, 1 µl.
    6. Sample, the 10 µl from the first step.
    7. ddH$_2$O, up to 50 µl.
  B. PCR conditions:
    1. 3 min at 95°C.
    2. 35 cycles of the following:
      a. 1 min at 94°C.
      b. 1 min annealing at 56°C.
      c. 2 min extension at 72°C.
      d. Final extension of 10 min.

According to the authors, TexasRed incorporation is low and nick translation after DOP-PCR is recommended.

Huang *et al.* (2000) showed that, to minimize false-negative and false-positive results, if test DNA is labeled by DOP-PCR, reference DNA also may be DOP-PCR amplified. No false results are detected if reference DNA is labeled either during DOP-PCR or by nick translation after PCR reaction. Nevertheless, variation in CGH results is detected if random priming reaction is used after DOP-PCR.

DOP-PCR is a very useful technique when a small amount of DNA is available, but when it is based on the amplification of the whole genome, artifacts may be introduced. Its efficiency is much lower than labeling proceedings without PCR reaction.

Universal Linkage System

ULS was developed as a new strategy to label degraded DNA, as it is in the case of DNA from paraffin samples or PCR products (Alers *et al.,* 1999). In those cases, DNA is so fragmented, and fragments obtained after nick translation may be too small.

ULS uses a special platinum compound. It has two free binding sites: one for the marker molecule as biotin or digoxigenin and the other site to DNA binding, preferentially at the N7 position of guanine groups.

ULS labeling system is very fast and simple, but in our experience its labeling efficiency is quite low, which could be explained by the fact that ULS also can label proteins and RNA, decreasing fluorescence intensity (Jeuken *et al.,* 2002).

MATERIALS

1. The ULS is available in the following:
  ▲ Qbiogene: DGreen Direct labeling kit, Cat. No. DLKG 04, and Rhodamine direct labeling kit, Cat. No. DLKR 05.
  ▲ KREATECH, Amsterdam, The Netherlands (www.kreatech.com/techn/techuls.html).
  ▲ Molecular Probes; ULYSIS Nucleic Acid Labeling Kits: U-21650 (ULS kit with Alexa Fluor 488), U-21654 (ULS kit with Alexa Fluor 594).
2. MicroSpin G-50 Columns (Cat. No. 27-5330-01, Amersham Biosciences).
3. DNAse (Cat. No. 18047-019, Invitrogen).

METHOD

Follow the manufacturer's instructions of Qbiogene ULS kit.

1. Adjust DNA fragments to the CGH fragment range by DNAse digestion or by boiling the DNA 30 min at 95°C in 10 mmol/L Tris (pH 8.0).
2. Add 1 µg of DNA with 1 U (2 µl) of Marker-ULS (DGreen-ULS or Rhodamine-ULS also provided by Qbiogene), and adjust the volume to 20 µl with labeling solution.
3. Incubate at 65°C for 15 min.
4. Purify the labeled DNA using a spin column.

Hybridization

Metaphase Chromosome Preparation

The quality of metaphase highly affects the quality of CGH results. Once again, commercial normal human metaphases are available. However, good-quality metaphase could be prepared from peripheral blood lymphocytes from healthy donors.

MATERIALS

1. Normal metaphase CGH target slides (Cat. No. 30-806010, Vysis) or 5 ml of blood sample from a healthy donor.
2. RPMI 1640 medium.
3. Fetal bovine serum (Cat. No. 10270-106, GIBCO).
4. Glutamine (Cat. No. K0282, BIOCHROM).
5. Gentamicin, 40 mg/ml, Schering-Plough.
6. Phytohemagglutinin (Cat. No. M5030, BIOCHROM).
7. Methanol (Cat. No. 1.06009.10000, Merck).
8. Acetic acid (Cat. No. 1.00063.10000, Merck).
9. KCl (Cat. No. 131494, Panreac).
10. Karyomax colcemid 10 µg/ml (Cat. No. 15212-012, GIBCO).
11. Giemsa stain, ANALEMA.
12. Di-sodium hydrogen phosphate12-hydrate (Cat. No. 131678, Panreac).
13. Potassium di-hydrogen phosphate (Cat. No. 131509, Panreac).
14. Microscopy slides (Cat. No. 21102, Menzel-Glaser).

Solutions

1. Culture medium (for 100 ml): add 20 ml fetal calf serum, 1 ml glutamine, 2 ml phytohemagglutinin, 180 µl gentamicin, and RPMI 1640 up to 100 ml.
2. Carnoy's fixative: Mix methanol and acetic acid reagents in 3:1 proportion. Prepare fresh solution every day.
3. Hypotonic solution (KCl 0.075 M): 2.796 g of KCl in 500 ml of distilled water. Store at 4°C between uses.
4. Di-sodium hydrogen phosphate 12-hydrate 0.07 M: 25.07 g in 1 L of distilled water. Store at 4°C between uses.
5. Potassium d-hydrogen phosphate 0.07 M: 9.78 g in 1 L of distilled water. Store at 4°C between uses.
6. Giemsa stain: 45% (v/v) of di-sodium hydrogen phosphate, 45% (v/v) of potassium d-hydrogen phosphate, 10% Giemsa stain.

METHOD

1. Culture peripheral blood sample in 5 ml of culture medium for 72 hr at 37°C. Cell concentration: 10^6 cells/ml.

2. Add 40 µl of colcemid to arrest cells in metaphase. Incubate at 37°C for 45 min.
3. Centrifuge cell suspension at 2000 rpm for 10 min.
4. Eliminate supernatant and add 5 ml of pre-warmed (37°C) hypotonic solution drop by drop.
5. Incubate the suspension for 12 min at 37°C.
6. Centrifuge cell suspension at 2000 rpm for 10 min.
7. Remove supernatant and resuspend the pellet adding Carnoy's fixative drop by drop.
8. Centrifuge cell suspension again, as in **Step 2**.
9. Repeat fixation procedure twice.
10. Drop the suspension in a cold and clean slide and check the quality of the metaphase using a phase contrast microscope or staining the slide with Giemsa stain. Metaphases may have the following:

▲ Chromosomes with an adequate length to detect chromosomal aberrations with an acceptable sensitivity
▲ A minimal number of overlapping chromosomes
▲ A minimum cytoplasm debris, which can make probe hybridization difficult

Cell suspension may be stored at −20°C between uses.

Our cytogenetic department has considerable experience in G-band cytogenetics. Metaphases of a high quality could be routinely obtained there. Despite the high price of commercial CGH slides, we prefer to use them because of the time consumed preparing and checking the homemade metaphases.

Probe Preparation

Equimolecular amounts of reference DNA and test DNA may be mixed together with Cot-1 DNA. Cot-1 DNA is used to suppress the hybridization of labeled DNA to repetitive sequences, such as centromeres and heterochromatic regions.

MATERIALS

1. Cot-1 Human DNA (1 µg/µl) (Cat. No. 1 581 074, Roche).
2. Ethanol (absolute) (Cat. No. 1.00983.2500, Merck).
3. NaCl (Cat. No. 1064045000, Merck).
4. Sodium acetate anhydrous (Cat. No. 131633, Panreac).
5. Sodium citrate dihydrate (Cat. No. 106432.5000, Merck).
6. Formamide (Cat. No. 344206, CALBIOCHEM).

Solutions

1. 3 M sodium acetate: 24.6 g sodium acetate; bring volume to 100 ml with distilled water. Adjust pH to 5.5. Store at room temperature.

2. 20X saline-sodium citrate (SSC): 87.6 g NaCl, 44.1 g Na citrate; bring to 500 ml with distilled water. Store at room temperature.

3. 4X SSC: dilute from the 20X SSC. Adjust pH to 7.0 and store at room temperature.

4. Dextran sulfate 20%: 20 g of dextran sulfate and 100 ml of 4X SSC. Filter.

5. Master Mix 50%: 50% of dextran sulfate 20% and 50% of deionized formamide.

METHOD

1. Coprecipitate test, reference and Cot-1 preparing the followed mix:
   - ▲ 600 ng test DNA.
   - ▲ 600 ng reference DNA.
   - ▲ 10 μl Cot-1 DNA.
   - ▲ 1/10 volume sodium acetate 3M.
   - ▲ 2.5 × volume 100% ethanol.
2. Store at –80°C for 30 min.
3. Centrifuge the tube for 30 min at 4°C at maximum speed.
4. Remove the supernatant.
5. Dry the pellet at room temperature in darkness.
6. Solve the pellet in 10 μl Master Mix 50% for 15 min to 1 hr at 37°C.

Several publications suggest lower amounts of DNA (e.g., 200 ng; Hidaka *et al.,* 2003). If DNA is of a high quality, 200 ng could be enough for chromosomal aberration detection. However, we prefer to use 600 ng to get brighter fluorescence signals. Related to paraffin DNA, nick translation effectiveness is much lower because of DNA initial fragmentation and because of the presence of DNA cross-linked to proteins. So, the real quantity of labeled DNA is lower. In this case, larger amounts of DNA may be added in each reaction. Recommendations of DNA amounts are shown at Waldman's Web site (cc.ucsf.edu/people/waldman/Protocols/directcgh.html). In our experience, the DNA amount may be optimized in each lab.

Denaturation

MATERIAL

1. NaCl (Cat. No. 1064045000, Merck).
2. Sodium citrate dihydrate (Cat. No. 106432.5000, Merck).
3. Formamide (Cat. No. 344206, CALBIOCHEM).
4. Ethanol (see earlier).

Solutions

1. 20X SSC: 87.6 g NaCl, 44.1 g sodium citrate; bring to 500 ml with distilled water. Store at room temperature.

2. 2X SSC: dilute from the 20X SSC. Adjust pH to 7.0 and store at room temperature.

3. Formamide 70%: 7 ml deionized formamide mixed with 3 ml 2X SSC. Mix well. Aliquot the 10 ml solution in 1 ml and store at –20°C between uses.

4. Ethanol series: 70%, 85%, 100% (v/v).

METHOD

1. Incubate DNA probe for 5 min in a waterbath at 75°C for DNA denaturation. The length of time it takes depends on the DNA. Small variation of ± 2 min or ± 1°C could improve fluorescence intensity. After denaturation, incubate DNA probe at 37°C for 15 min to preannealing.

2. Denaturation of the metaphase spreads could be performed as follows:
   a. In a Coplin jar containing 40 ml of 70% formamide at 75°C for 3 min.
   b. On a hot plate at 75°C: add 100 μl of 70% formamide to the slide, cover it with a 24 × 60 mm coverslip, and incubate for 1.5–2 min.

As in the probe case, denaturation time depends on the metaphase preparation and may be standardized for each batch of metaphase slides. Overdenaturation results in good fluorescence intensity but destroys chromosome morphology, which will result in difficulty in chromosome identification. If insufficient denaturation is performed, hybridization efficiency decreases.

1. To stop denaturation reaction, quickly remove the coverslip, and place the slide in 70% ethanol.
2. Dehydrate the slides by placing them in ascending concentrations of ethanol (70%, 85%, 100%) 2 min each. Air-dry.

Hybridization

MATERIALS

Rubber cement.
18 × 18 mm coverslip, Marienfield.

METHOD

1. Apply 10 μl of the probe to the selected section.
2. Cover with an 18 × 18 mm coverslip and seal with rubber cement.
3. Incubate the slides in a dark, humid chamber at 37°C for 48 hr.

Washes

Direct DNA Labeling

Many CGH washing protocols have been published. All of them could be grouped in two categories: those

performed at 45°C and using 50% formamide solutions and those performed at 74°C and using SSC solutions.

MATERIALS

1. NP-40 (Cat. No. 32-804818, Vysis).
2. DAPI (4′6′diamino-2-phenylindole) (Cat. No. 32-804932, Vysis).

Solutions

1. 2X SSC, 0.4X SSC, and 0.1XSSC (see earlier).
2. 50% formamide: mix 60 ml of deionized formamide with 60 ml of 2X SSC.

METHODS

Protocol A

1. Remove the rubber cement and the coverslip and place the slide immediately in the first solution of formamide.
2. Wash three times with 50% formamide in 2X SSC at 45°C for 10 min each.
3. Wash twice in 2X SSC at 45°C for 10 min.
4. Wash once in 0.1X SSC at 45°C for 10 min.
5. Counterstain with 10 µl of DAPI.

Protocol B

1. Remove the rubber cement and the coverslip and place the slide immediately in the first solution of 0.4X SSC.
2. Wash the slide in 0.4X SSC plus 0.3% NP-40 at 74 ± 1°C for 2 min.
3. Wash the slide in 2X SSC plus 0.1% NP-40 at room temperature for 1 min.
4. Air-dry the slide in darkness.
5. Counterstain with 10 µl of DAPI.

Indirect DNA Labeling

The advantage of indirect labeling is that fluorescence signals can be amplified using any biotin/digoxigenin amplification protocol. However, this method increases the granularity of the signals and the background fluorescence. That is the reason most CGH publications have been performed using direct labeling.

MATERIALS

1. Bovine serum albumin (BSA) (Cat. No. B 2901, Sigma).
2. 20X SSC: see earlier.
3. Formamide: see earlier.

4. Tween 20 (Cat. No. 93773, Fluka).
5. Avidin-FITC (Cat. No. A-2011, Vector Laboratories, Inc., Burlingame, CA).
6. anti-Dig-Rodamine (Cat. No. T-2402, Vector).
7. Tris (hydroxymethyl) aminomethane (Cat. No. 1.08382.0500, Merck).
8. CLNa (Cat. No. 1.06404.5000, Merck).

Solutions

1. 50% formamide (see earlier).
2. 0.1X SSC: dilute from the 20X SSC solution.
3. 4 X SSC/0.1%Tween-20: add 10 ml of 20X SSC solution, 400 ml dH$_2$O, and 0.5 ml of Tween-20.
4. Blocking solution: add 3 g of BSA in 10 ml of 4X SSC/Tween-20.
5. Tris buffered saline (TBS): add 6 g of Trizma and 29 g of ClNa with 1 L of distilled water. Adjust pH to 7.36.
6. Antibody solution: prepare Avidin-fluorescein isothiocyanate (FITC; 1:200) and anti-Dig-Rodamine (1:200) dilution in TBS buffer.

METHOD

1. Remove the rubber cement and the coverslip and place the slide immediately in the first solution.
2. Wash slides 3× for 5 min in 50% formamide/2X SSC at 45°C.
3. Wash slides 2× for 5 min with 0.1X SSC at 60°C.
4. Keep slides in 4X SSC/Tween-20 until the next step.
5. Add 100 µl of blocking solution, cover with a 24 × 60 mm coverslip and incubate at 37°C for 30 min.
6. Remove the coverslip and place the slides in 4X SSC/Tween-20 until the next step.
7. Add 100 µl of antibody solution to coverslip 24 × 60 mm, touch slide to coverslip, and incubate in a humidified chamber at 37°C for 30 min.
8. Wash 3× for 5 min in 4X SSC/Tween at 45°C.
9. Counterstain with DAPI.

Analysis

The basic assumption in CGH is that the hybridization kinetics of test and reference DNA are independent, so the ratio binding of the DNA is proportional to the ratio of the copy-numbers of the sequences in the DNA samples to a specific locus (Piper *et al.,* 1995). Furthermore, the amount of DNA bound from the test or reference DNA is characterized by the intensity with which they fluoresce on the normal chromosomes. So, the evaluation of the signal fluorescence intensities of
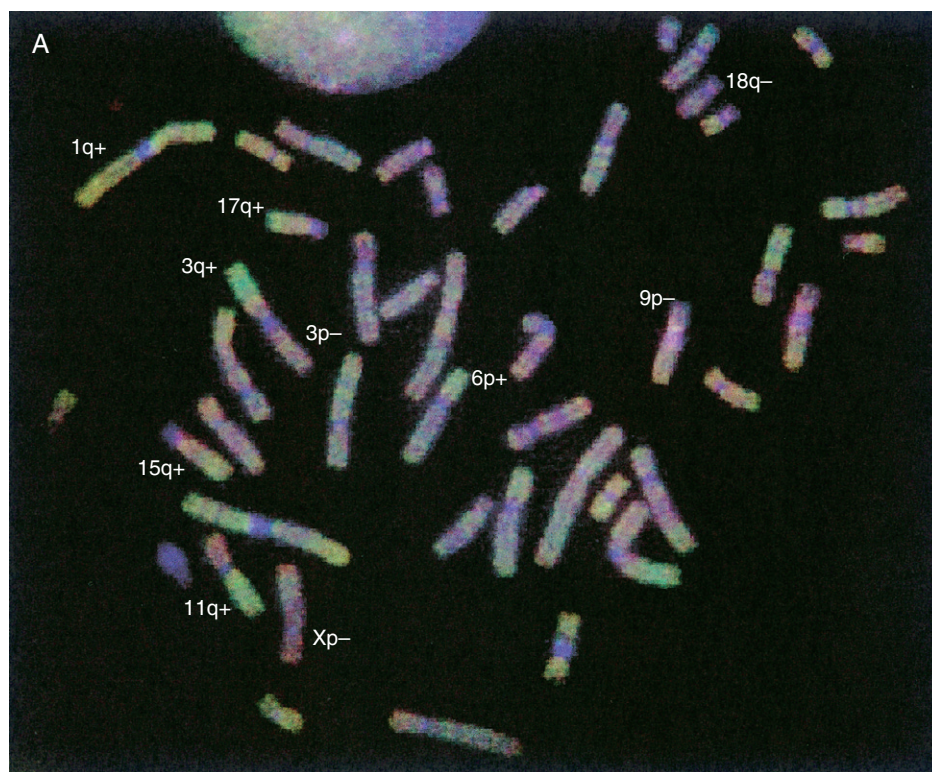
Figure 10 **A:** Metaphase image of a breast cancer tumor analyzed by comparative genomic hybridization (CGH). **B:** Example of partial CGH analysis of the chromosome 8; (*1*) chromosome 8 in green, as a result of the test deoxyribonucleic acid (DNA) hybridization; (*2*) chromosome 8 in red, as a result of the reference DNA hybridization; (*3*) chromosome 8 in blue because of the DAPI (4'6'diamino-2-phenylindole) counterstain; (*4*) image of the chromosome 8 through triple band filter; and (*5*) inverted DAPI image to identify chromosome 8. CGH profile of the two chromosome 8s belonging to one metaphase and final analysis. This tumor case showed a loss in the short arm of chromosome 8 and a gain in the long arm.
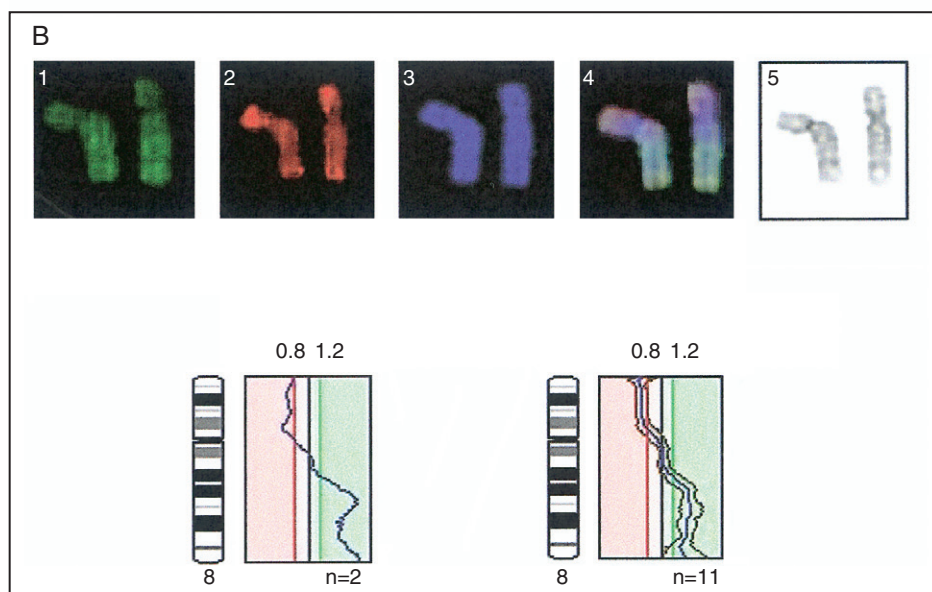
both DNAs allows the characterization of the chromosomal changes present in test DNA (Figure 10A).

CGH analysis requires an epifluorescence microscope equipped with a filter set to green, red, and DAPI fluorescence signals visualization. Filters may be mounted in an automatic filter wheel allowing capturing of each fluorochrome image without overlapping errors (Figure 10B). The microscope also may be equipped with a cooled charge-coupled device (CCD) camera,

a 100W mercury lamp, and 63X and 100X plan-apochromatic or plan-neofluar objective lenses.

Some commercial digital image analysis systems are available. The most popular are the following:

▲ ISIS from MetaSystems (Altlussheim, Germany), www.metasystems.de
▲ Quips XL from Vysis (Downers Grove, IL), www.vysis.com/

▲ Cytovision from Applied Imaging (Newcastle Upon Tyne, UK), www.cytovision.com/international/index.htm.
▲ QCGH from Leica (Cambridge, UK), www.leica-microsystems.com/website/lms.nsf.

Almost 8–10 metaphases with a good quality of fluorescence signal may be captured. The criteria for selecting them are as follows:

▲ Minimal overlapping chromosomes.
▲ Adequate chromosomal condensation.
▲ Low background fluorescence.
▲ Smooth fluorescence signals across the chromosomes.
▲ Adequate probe intensity.
▲ Balanced green–red fluorescence.
▲ Low binding of the probes at the centromeres and heterochromatic regions.
▲ Adequate DAPI banding patterns.

Image analysis systems follow these steps:

▲ Background subtraction.
▲ Segmentation to separate chromosomes from the background.
▲ Chromosomal identification through DAPI banding patterns. Image analysis systems allow inversion of the DAPI image, showing a banding pattern similar to G-bands, which is used to karyotype the metaphases. Although image analysis systems are able to karyotype the metaphases, an expert cytogeneticist is need to correctly identify all the chromosomes.
▲ Normalization of green and red fluorescence.
▲ Determination of the intensity profiles across the axis of each chromosome.
▲ Determination of the ratio profile.

The ratio profile is calculated along the axis of each chromosome. The ratio should be 1 when test and reference DNA have the same amount of DNA. If the ratio value is bigger than 1, this region is considered to have a gain of material. If the ratio is less than 1, a chromosomal loss is defined (Figure 9). Although theoretically the loss or gain of one copy of a chromosome should be 0.5 or 1.5, in practice these ratios range from 0.6 to 0.7 and 1.3 to 1.4 (Karhü *et al.,* 1999). Thus, thresholds are needed to consider a true chromosomal aberration. Three different thresholds are usually used: fixed thresholds, the probability, and the standard deviation.

Fixed thresholds: When Kallioniemi *et al.* described CGH technique in 1992, they suggested the use of 1.25 and 0.75 as thresholds that the ratio may exceed to consider a gain and a loss, respectively. The development of more sensitive methods, such as the use of direct labeling, new wash protocols, and commercial metaphases have addressed the use of, more specifically, upper and lower thresholds (e.g., 0.8 and 1.2; Figure 10B). When excellent hybridization conditions are achieved, 0.85 and 1.15 thresholds are admitted. Amplifications are usually defined when the fluorescence ratio values exceed 1.5. By fixed threshold single-copy deletions can be detected in the range of 10–20 Mb.

In the *probability thresholds,* the significance limits are expressed as statistical probability of 95% or 99%. The distance between the upper and lower limit width is given by the confidence interval. Aberrations are detected if the confidence interval does not include the ratio of 1.0 (Barth *et al.,* 2000).

Using the *standard deviations intervals,* CGH results are highly dependent on the quality of the hybridization, and this hybridization is conditioned by the different material used and the method that follows. Different sources of DNA, fluorochromes from different companies, different batches of metaphases, and different labeling and washes protocols used provide variation in CGH results. These interlaboratory and intralaboratory variabilities are too high to accept universal fixed thresholds.

In 1998, Kirchhoff *et al.* described the use of the standard deviation interval as a significant limit to chromosomal aberration detection. Five control CGH experiments with differentially labeled normal DNAs may be performing to the calculated threshold. t-Student analysis of the profiles along all the chromosomes allows the estimation of the standard deviation of the experiment. In this way, any CGH result may be evaluated considering the significance limit of $1.0 \pm 3\sigma$ (three times the standard deviation) or $1.0 \pm 2\sigma$. Once standard reference interval is estimated in each laboratory it may be changed only if labeling protocol is changed (Kirchhoff *et al.,* 1998).

The standard deviation interval improved the sensitivity and specificity of the CGH analysis. With this modification deletions of 3 Mb could be detected (Kirchhoff *et al.,* 1999). It reduces to the minimum the number of false-positive results, allowing the standardization of the significant limits to one's own laboratory conditions.

Software usually draws red and green bars showing the chromosomal region where ratios profile excess significant thresholds. Nevertheless, aberrations may be evaluated by the expert, who may decide if this aberration is real or not (Figure 11).

Genetics changes affecting specific regions should be analyzed by caution. Those are telomeric regions where the fluorescence intensity could be similar to background levels, the pericentromeric regions on

A Bad Cot-1 blocking:

1(15)   9(10)

B Questionable results:

0.8 1.2

0.8 1.2

4(14)   13(16)

C Quality of the CGH

1. Good hybridization: 2. Low quality hybridization:

4(13)   8(7)
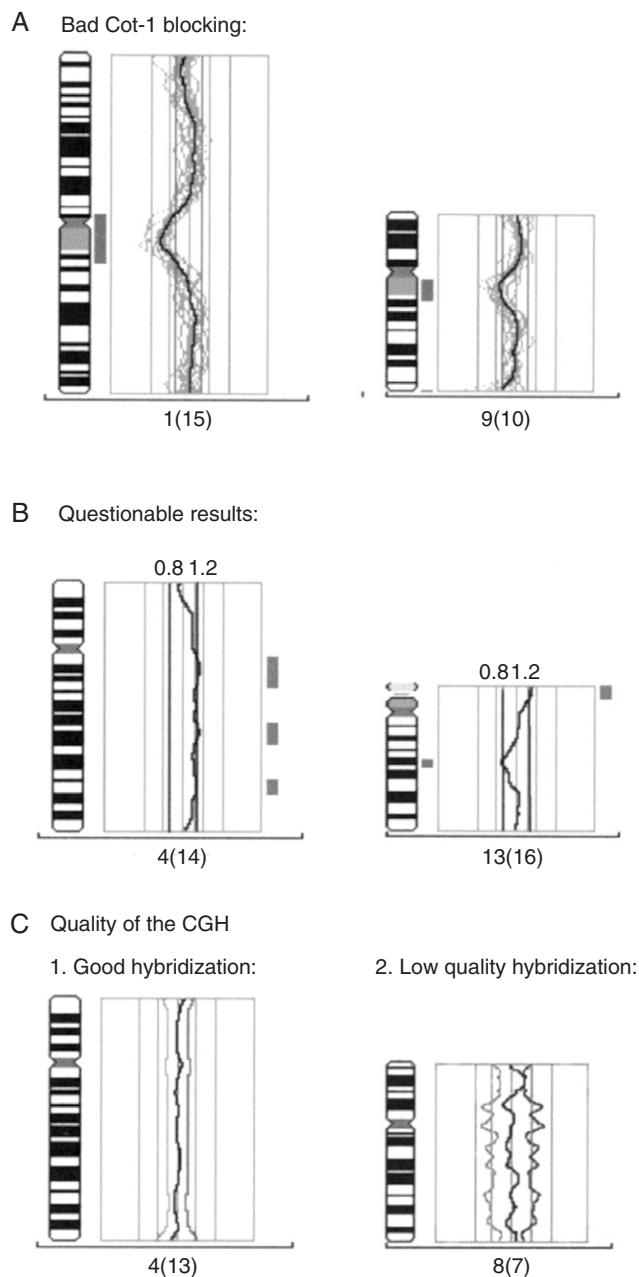
Figure 11 Comparative genomic hybridization (CGH) ratio profiles. Vertical lines on the left side of the chromosome idiograms correspond to losses, and those on the right side correspond to gains. **A:** Profile showing a false-positive result consequence of a bad Cot-1 blocking. **B:** Questionable results: CGH profile is close to the thresholds limit. **C:** Different quality of CGH results: (*1*) a good CGH profile showing a narrow standard deviation interval and (*2*) a CGH profile showing a wide standard deviation interval.

chromosome 1, 9, 16, the heterochromatic region on Y chromosome where fluorescence varies greatly, and GC rich region in 1pter, 19 and 22 ratios where false-positive results are frequent.

Controls

Proper controls should be included in CGH experiments.

▲ Negative controls: The hybridization of two differentially labeled normal DNAs.

▲ Positive controls: Hybridization of the reference DNA used in CGH experiments versus a DNA with known aberrations (e.g., MPE 600 breast cancer cell line, which is also commercially available from Vysis, included in the CGH kit).

▲ Reversed labeling: This control is based on labeling reference DNA with the green fluorochrome and the test DNA with red fluorochrome, inversely to conventional CGH. At the beginning of CGH, some authors suggest that red fluorochrome incorporation is different from green fluorochrome (Larramendy *et al.,* 1998). For this reason, mix probes were prepared, mixing different amounts of red-labeled and green-labeled DNAs. Image analysis systems have solved this problem and no differences are detected if equal amounts of both DNAs are added to the reaction. Despite this, when borderline chromosomal aberrations are detected, reversed labeling could be useful to check the result.

▲ Four-color CGH: In 1999, Karhü *et al*. developed a new CGH method called four-color CGH. This modification is based on the use of a second reference DNA, together with the standard test and reference DNA. This new DNA serves as an internal control of the hybridization dynamics. Four-color CGH hybridization is performed exactly as in the conventional CGH protocol except that an equal amount of the second reference DNA is added. Special software modifications are required for the four-color CGH analysis: four metaphase images may be captured corresponding to the test DNA labeled with dUTP-FITC (green), the first reference DNA labeled with Cy5-dUTP (red), the second reference DNA labeled with TexasRed-dUTP (red) and DAPI image (blue). Software may be able to profile calculation and profile normalization for the three DNAs. The main difference to the conventional CGH is the dynamic range correction applied. To standardize the variation in the hybridization a correction algorithm is applied. The use of the arithmetic mean profile of the two reference DNA profiles when comparing with the tumor DNA profile minimizes the random variation of the fluorescence intensities. The dynamic range correction improves the sensitivity of CGH, making the borderline chromosomal aberrations statistically significant. Mixing sex-mismatched reference DNAs is very useful because

comparison of the reference 1 DNA versus reference 2 DNA allows checking if the dynamic range of the hybridization is decreased or increased. This comparison also allows the visualization of the regions where either reference DNAs have hybridized abnormally.

Although four-color CGH was a promising modification of conventional CGH, it has not been used in CGH assays, perhaps because of the software requirements.

▲ Internal control: Some authors have published the use of reference DNA and test DNA belonging to different sexes. This is a very adequate internal control but only in those cases in which chromosome X aberrations are not expected.

We recommend one negative and one positive CGH control experiment in each set of CGH experiments (e.g., when eight CGH experiments are performed, a control slide, with negative and positive control, could be included).

Matrix-CGH

The sensitivity of the CGH technique depends on the degree of condensation of the chromosomes and the size of the chromosomal aberration. As described earlier, the use of metaphases limits the CGH resolution to 3–20 Mb for low number losses and 1–5 Mb for gains.

A novel CGH approach has been described based on the use of small fragments of DNA arrayed onto a solid support to serve as targets to CGH. This new technique was called Matrix-CGH or Array CGH. These DNA fragments are usually genomic DNA cloned into BAC, PAC, or YAC vectors. cDNA fragments have also been used (Pollack *et al.,* 1999).

CGH arrays can contain thousand of DNA fragments. The length of these DNA fragments could range from 90 to 230 Kb, improving the CGH sensitivity to 100 Kb and several kilobases for high-level amplification (Lichter, 2000; Wang, 2002). Matrix-CGH procedure is basically similar to conventional CGH. Microarray technology will be discussed in detail in this book. For this reason only a technical scheme is described here.

Array Preparation

1. Selection of the DNA clones: Because of the huge amount of information obtained in microarray, the most important step is to perform a good clone selection. There are some commercially available microarrays. They have the advantage in that there is no need to spend time preparing the array; however, they are expensive and the experiment is limited to the clones the company has chosen. Home-array assays are highly time consuming because many control assays are needed before starting the CGH assay; however, they are cheaper. Besides the clones of interest, array may include control clones for normalization of the signal ratios. These may be clones from chromosome X and from the chromosomal region where copy-number changes are not expected.

2. Isolation of the DNA from clones: DNA may be isolated using any commercial kit. This DNA may be sonicated to reduce sample viscosity and size fragments to several hundred nucleotides. Spots from sonicated samples have a more homogenous morphology, resulting in lower standard deviations in the replicas (Wessendorf *et al.,* 2002). In 2003, DOP-PCR primers for the amplification of clones used in microarrays were designed (Fiegler *et al.,* 2003).

3. Spotting: Slides may be pretreated with poly-L-lysin and completely cleaned to minimize background fluorescence. Robots take the DNA from PCR microtiter plates and print four replicas of each target DNA on the slide.

Preparation of the Probe

Test and normal DNA are usually labeled by random priming with Cy3-dCTP (test DNA) and Cy5-dCTP (reference DNA).

Bioprime Kit from Invitrogen (Cat. No. 18095-011) is one of the most popular kits for random priming labeling. Briefly, 500 ng of DNA may be incubated with the random primers solution in a water bath at 100°C. After DNA denaturation dNTP, Cy3 or Cy5 labeled dCTP, and the Klenow fragment are added on ice. The reaction is incubated overnight at 37°C, stopped by adding the stop solution. Unincorporated nucleotides may be removed using purification columns. As in conventional CGH, universal DNA amplification may be performed if a small amount of DNA is available. Probe mixture is prepared mixing 500 ng of both test and reference DNA with 50 µg of Cot-1 DNA. After precipitation, DNA is resuspended in Master Mix 50%.

Hybridization

1. The probe is denatured at 75°C for 5 min and incubated at 37°C for 30–60 min for preannealing. No target DNA denaturation is needed.

2. The hybridization is performed at 37°C during 16–72 hr on a slowly rocking table.

Washes

They are performed as in conventional CGH.

Image Analysis

Software locates the DNA clones by the DAPI image, subtracts the background, and calculates the intensity of the Cy5 and Cy3 signals. Hybridization intensities below an intensity threshold are excluded from the analysis. Ratios of the intensities of both test and reference DNA and the average and the standard deviation of the four replicas of each clone are calculated. Normalization following the results of the control clones is performed. To confirm the results obtained in the CGH array, fluorescence *in situ* hybridization experiments in some positive cases are recommended.

Application and Future

CGH is an essential technique to characterize chromosomal aberrations in solid tumors. Its main contribution has been the description of chromosomal regions where new cancer genes are located. CGH has also helped in the characterization of hematologic tumors with low mitotic index and some constitutional diseases. Complex karyotypes with unknown markers, double minutes, hsr (homogeneous staining regions), or additions of unknown material have been solved by CGH (Teixeira, 2002). Moreover, chromosomal aberrations described by CGH seem to have clinical relevance improving tumoral diagnosis, prognosis, and therapy response.

The characterization of a region frequently amplified has addressed molecular researches to the identification of oncogenes, as in the case of the androgen receptor (*AR*) gene in hormone-refractory recurrent prostate carcinomas (Visakorpi *et al.,* 1995) and the *AIB1* gene in breast cancer (Tanner *et al.,* 1996). In the same way, regions frequently deleted make suspicious the presence of putative suppressor genes, as is the case of the *LKB1* gene in Peutz-Jeghers tumors (Hemminki *et al.,* 1998).

CGH has contributed to a better classification of some tumors. Some examples are the analysis of a series of 109 malignant fibrous histiocytomas, which has allowed the classification of this tumor in two groups: those with similar aberrations to leiomyosarcomas and those characterized by a high-level amplification of bands 12q14~q15 (Chibon *et al.,* 2003).

Chromosomal aberrations detected by CGH have described genetic progression of some tumors. In esophageal squamous cell carcinomas, gains on 3q26qter and loss of 18q22qter are frequent in stage I cancers, whereas 8q24-qter gains are more frequent in stage III and IV (Ueno *et al.,* 2002).

CGH has also contributed to the knowledge of tumor prognosis and therapy response. Lillington *et al.* (2003) described the analysis of 49 retinoblastoma tumors in which losses of 13q, 5q, and 16 were associated with relapse and metastasis. Regarding breast cancer we reported that 17q and 20q gains identify a subgroup of patients with an increased relapse rate within the good prognosis group of women who are lymph node–negative (Zudaire *et al.,* 2002). Branle *et al.* (2002) described the different chromosomal aberration present in three glioma cells lines with different responses to chemotherapy.

Although most CGH publications have been addressed to the field of solid tumors, CGH has been also applied to the analysis of hematologic malignancies with frequent normal karyotypes, failure of karyotype, and metaphases of poor quality or complex karyotypes (Karhü *et al.,* 1997; Odero *et al.,* 2001). Concerning constitutional diseases, Ness *et al.* (2002) have characterized constitutional imbalances present in a series of 66 children with different developmental delays. CGH allowed the identification of duplications and small subtelomeric deletions not identified by G banding. CGH is also contributing to reproductive medicine. Because 90% of chromosomal abnormalities found prenatally are aneuploidies, CGH analysis has been applied to the study of the ploidy of the embryos prior to being transferred to the mother in *in vitro* fecundation (Wells *et al.,* 2003).

Array CGH provides unprecedented high-resolution assessment of genome copy-number changes. However, it has not yet become a widely applied method because of its high price and reproducibility problems. In the future, CGH analysis of a disease-specific array could become a powerful tool to clinical patients' management.

Acknowledgments

References

Alers, J.C., Rochat, J., Krijtenburg, P.J., van Dekken, H., Raap, A.K., and Rosenberg, C. 1999. Universal linkage system: An improved method for labeling archival DNA for comparative genomic hybridization. *Genes Chromos. Cancer* 25:301–305.

Aubele, M., Mattis, A., Zitzelsberger, H., Walch, A., Kremer, M., Welzl, G., Hofler, H., and Werner, M. 2000. Extensive ductal

carcinoma In situ with small foci of invasive ductal carcinoma: Evidence of genetic resemblance by CGH. *Int. J. Cancer* 85:82–86.

Barth, T.F., Benner, A., Bentz, M., Dohner, H., Moller, P., and Lichter, P. 2000. Risk of false positive results in comparative genomic hybridization. *Genes Chromos. Cancer 28*: 353–357.

Branle, F., Lefranc, F., Camby, I., Jeuken, J., Geurts-Moespot, A., Sprenger, S., Sweep, F., Kiss, R., and Salmon, I. 2002. Evaluation of the efficiency of chemotherapy in in vivo orthotopic models of human glioma cells with and without 1p19q deletions and in C6 rat orthotopic allografts serving for the evaluation of surgery combined with chemotherapy. *Cancer 95*:641–655.

Chibon, F., Mariani, O., Mairal, A., Derre, J., Coindre, J.M., Terrier, P., Lagace, R., Sastre, X., and Aurias, A. 2003. The use of clustering software for the classification of comparative genomic hybridization data. An analysis of 109 malignant fibrous histiocytomas. *Cancer Genet Cytogenet. 141*:75–78.

Feinberg, A.P., and Vogelstein, B. 1983. A technique for radiolabeling DNA restriction endonuclease fragments to high specific activity. *Anal. Biochem. 132*:6–13.

Fiegler, H., Carr, P., Douglas, E.J., Burford, D.C., Hunt, S., Smith, J., Vetrie, D., Gorman, P., Tomlinson, I.P., and Carter, N.P. 2003. DNA microarrays for comparative genomic hybridization based on DOP-PCR amplification of BAC and PAC clones. *Genes Chromos. Cancer 36*:361–374.

Hemminki, A., Markie, D., Tomlinson, I., Avizienyte, E., Roth, S., Loukola, A., Bignell, G., Warren, W., Aminoff, M., Hoglund, P., Jarvinen, H., Kristo, P., Pelin, K., Ridanpaa, M., Salovaara, R., Toro, T., Bodmer, W., Olschwang, S., Olsen, A.S., Stratton, M.R., de la Chapelle, A., and Aaltonen, L.A. 1998. A serine/threonine kinase gene defective in Peutz-Jeghers syndrome. *Nature 391*:184–187.

Hidaka, S., Yasutake, T., Fukushima, M., Yano, H., Haseba, M., Tsuji, T., Sawai, T., Yamaguchi, H., Nakagoe, T., Ayabe, H., and Tagawa, Y. 2003. Chromosomal imbalances associated with acquired resistance to fluoropyrimidines in human colorectal cancer cells. *Eur. J. Cancer 39*:975–980.

Huang, Q., Schantz, S.P., Rao, P.H., Mo, J., McCormick, S.A., and Chaganti, R.S. 2000. Improving degenerate oligonucleotide primed PCR-comparative genomic hybridization for analysis of DNA copy number changes in tumors. *Genes Chromos. Cancer 28*:395–403.

Isola, J., DeVries, S., Chu, L., Ghazvini, S., and Waldman, F. 1994. Analysis of changes in DNA sequence copy number by comparative genomic hybridization in archival paraffin-embedded tumor samples. *Am. J. Pathol. 145*:1301–1308.

James, L.A. 1999. Comparative genomic hybridization as a tool in tumour cytogenetics. *J. Pathol. 187*:385–395.

Jeuken, J.W., Sprenger, S.H., and Wesseling, P. 2002. Comparative genomic hybridization: Practical guidelines. *Diagn. Mol. Pathol. 11*:193–203.

Kallioniemi, A., Kallioniemi, O.P., Sudar, D., Rutovitz, D., Gray, J.W., Waldman, F., and Pinkel, D. 1992. Comparative genomic hybridization for molecular cytogenetic analysis of solid tumors. *Science 258*:818–821.

Karhü, R., Knuutila, S., Kallioniemi, O.P., Siltonen, S., Aine, R., Vilpo, L., and Vilpo, J. 1997. Frequent loss of the 11q14-24 region in chronic lymphocytic leukemia: A study by comparative genomic hybridization. Tampere CLL Group. *Genes Chromos. Cancer 19*:286–290.

Karhü, R., Rummukainen, J., Lorch, T., and Isola, J. 1999. Four-color CGH: A new method for quality control of comparative genomic hybridization. *Genes Chromos. Cancer 24*:112–118.

Kirchhoff, M., Gerdes, T., Maahr, J., Rose, H., Bentz, M., Dohner, H., and Lundsteen, C. 1999. Deletions below 10 megabasepairs are detected in comparative genomic hybridization by standard reference intervals. *Genes Chromos. Cancer 25*:410–413.

Kirchhoff, M., Gerdes, T., Rose, H., Maahr, J., Ottesen, A.M., and Lundsteen, C. 1998. Detection of chromosomal gains and losses in comparative genomic hybridization analysis based on standard reference intervals. *Cytometry 31*:163–173.

Larramendy, M.L., El-Rifai, W., and Knuutila, S. 1998. Comparison of fluorescein isothiocyanate and Texas red-conjugated nucleotides for direct labeling in comparative genomic hybridization. *Cytometry 31*:174–179.

Lichter, P. 2000. New tools in molecular pathology. *J. Mol. Diagn. 2*:171–173.

Lillington, D.M., Kingston, J.E., Coen, P.G., Price, E., Hungerford, J., Domizio, P., Young, B.D., and Onadim, Z. 2003. Comparative genomic hybridization of 49 primary retinoblastoma tumors identifies chromosomal regions associated with histopathology, progression, and patient outcome. *Genes Chromos. Cancer 36*:121–128.

Ness, G.O., Lybaek, H., and Houge, G. 2002. Usefulness of high-resolution comparative genomic hybridization (CGH) for detecting and characterizing constitutional chromosome abnormalities. *Am. J. Med. Genet. 113*:125–136.

Odero, M.D., Soto, J.L., Matutes, E., Martin-Subero, J.I., Zudaire, I., Rao, P.H., Cigudosa, J.C., Ardanaz, M.T., Chaganti, R.S., Perucho, M., and Calasanz, M.J. 2001. Comparative genomic hybridization and amplotyping by arbitrarily primed PCR in stage A B-CLL. *Cancer Genet. Cytogenet. 130*:8–13.

Pinkel, D., Segraves, R., Sudar, D., Clark, S., Poole, I., Kowbel, D., Collins, C., Kuo, W.L., Chen, C., Zhai, Y., Dairkee, S.H., Ljung, B.M., Gray, J.W., and Albertson, D.G. 1998. High resolution analysis of DNA copy number variation using comparative genomic hybridization to microarrays. *Nat. Genet. 20*:207–211.

Piper, J., Rutovitz, D., Sudar, D., Kallioniemi, A., Kallioniemi, O.P., Waldman, F.M., Gray, J.W., and Pinkel, D. 1995. Computer image analysis of comparative genomic hybridization. *Cytometry 19*:10–26.

Pollack, J.R., Perou, C.M., Alizadeh, A.A., Eisen, M.B., Pergamenschikov, A., Williams, C.F., Jeffrey, S.S., Botstein, D., and Brown, P.O. 1999. Genome-wide analysis of DNA copy-number changes using cDNA microarrays. *Nat. Genet. 23*:41–46.

Solinas-Toldo, S., Lampel, S., Stilgenbauer, S., Nickolenko, J., Benner, A., Dohner, H., Cremer, T., and Lichter, P. 1997. Matrix-based comparative genomic hybridization: Biochips to screen for genomic imbalances. *Genes Chromos. Cancer 20*:399–407.

Speicher, M.R., du Manoir, S., Schrock, E., Holtgreve-Grez, H., Schoell, B., Lengauer, C., Cremer, T., and Ried, T. 1993. Molecular cytogenetic analysis of formalin-fixed, paraffin-embedded solid tumors by comparative genomic hybridization after universal DNA-amplification. *Hum. Mol. Genet. 2*: 1907–1914.

Struski, S., Doco-Fenzy, M., and Cornillet-Lefebvre, P. 2002. Compilation of published comparative genomic hybridization studies. *Cancer Genet. Cytogenet. 135*:63–90.

Tanner, M.M., Tirkkonen, M., Kallioniemi, A., Isola, J., Kuukasjarvi, T., Collins, C., Kowbel, D., Guan, X.Y., Trent, J., Gray, J.W., Meltzer, P., and Kallioniemi, O.P. 1996. Independent amplification and frequent co-amplification of three nonsyntenic regions on the long arm of chromosome 20 in human breast cancer. *Cancer Res. 56*:3441–3445.

Teixeira, M.R. 2002. Combined classical and molecular cytogenetic analysis of cancer. *Eur. J. Cancer 38*:1580–1584.

Ueno, T., Tangoku, A., Yoshino, S., Abe, T., Toshimitsu, H., Furuya, T., Kawauchi, S., Oga, A., Oka, M., and Sasaki, K. 2002. Gain of 5p15 detected by comparative genomic hybridization as an independent marker of poor prognosis in patients with esophageal squamous cell carcinoma. *Clin. Cancer Res*. 8:526–533.

van Gijlswijk, R.P., Talman, E.G., Janssen, P.J., Snoeijers, S.S., Killian, J., Tanke, H.J., and Heetebrij, R.J. 2001. Universal Linkage System: Versatile nucleic acid labeling technique. *Expert Rev. Mol. Diagn*. 1:81–91.

Visakorpi, T., Hyytinen, E., Koivisto, P., Tanner, M., Keinanen, R., Palmberg, C., Palotie, A., Tammela, T., Isola, J., and Kallioniemi, O.P. 1995. In vivo amplification of the androgen receptor gene and progression of human prostate cancer. *Nat. Genet*. 9:401–406.

Wang, N. 2002. Methodologies in cancer cytogenetics and molecular cytogenetics. *Am. J. Med. Genet*. 115:118–124.

Weiss, M.M., Hermsen, M.A., Meijer, G.A., van Grieken, N.C., Baak, J.P., Kuipers, E.J., and van Diest, P.J. 1999. Comparative genomic hybridisation. *Mol. Pathol*. 52:243–251.

Wells, D., and Levy, B. 2003. Cytogenetics in reproductive medicine: The contribution of comparative genomic hybridization (CGH). *Bioessays* 25:289–300.

Werner, M., Chott, A., Fabiano, A., and Battifora, H. 2000. Effect of formalin tissue fixation and processing on immunohistochemistry. *Am. J. Surg. Pathol. 24:*1016–1019.

Wessendorf, S., Fritz, B., Wrobel, G., Nessling, M., Lampel, S., Goettel, D., Kuepper, M., Joos, S., Hopman, T., Kokocinski, F., Dohner, H., Bentz, M., Schwaenen, C., and Lichter, P. 2002. Automated screening for genomic imbalances using matrix-based comparative genomic hybridization. *Lab. Invest. 82*: 47–60.

Zitzelsberger, H., Kulka, U., Lehmann, L., Walch, A., Smida, J., Aubele, M., Lorch, T., Hofler, H., Bauchinger, M., and Werner, M. 1998. Genetic heterogeneity in a prostatic carcinoma and associated prostatic intraepithelial neoplasia as demonstrated by combined use of laser-microdissection, degenerate oligonucleotide primed PCR and comparative genomic hybridization. *Virchows Arch*. 433:297–304.

Zudaire, I., Odero, M.D., Caballero, C., Valenti, C., Martinez-Penuela, J.M., Isola, J., and Calasanz, M.J. 2002. Genomic imbalances detected by comparative genomic hybridization are prognostic markers in invasive ductal breast carcinomas. *Histopathology 40*:547–555.

This Page Intentionally Left Blank

5

Microsatellite Instability in Cancer: Assessment by High Resolution Fluorescent Microsatellite Analysis

Shinya Oda and Yoshihiko Maehara

Introduction

Microsatellites are one of the most abundant classes of repetitive deoxyribonucleic acid (DNA) sequences dispersed throughout the eukaryotic genome, and they comprise short reiterated motifs varying one to several base pairs. Microsatellites are highly polymorphic in human populations, which suggests that this polymorphism may be derived from relatively high mutation rates in these sequences. However, they appear stable during a relatively short time such as the life span of individuals. Somatic instability of microsatellite sequences has initially been reported in human colorectal cancer (Ionov *et al.*, 1993; Thibodeau *et al.*, 1993) and in the familial cancer-prone syndrome hereditary nonpolyposis colorectal cancer (HNPCC) (Aaltonen *et al.*, 1993; Peltomaki *et al.*, 1993). In 1993, mutations in one of the genes essential for DNA mismatch repair (MMR) were found in HNPCC kindred (Fishel *et al.*, 1993; Leach *et al.*, 1993).

MMR is an important DNA repair system that counteracts base mismatches and strand misalignments that occur during DNA replication and recombination (Modrich and Lahue, 1996). In regions of DNA comprising repeats of simple mononucleotide or dinucleotide motifs, slippage of DNA polymerases occurs frequently, and strand misalignments are formed. If uncorrected by MMR, they are fixed as insertion or deletion of repeat units after a next round of replication. Microsatellites are included in this type of repetitive sequences. Therefore, the phenomenon of unstable microsatellites, microsatellite instability (MSI), is considered to reflect MMR deficiency. MSI is frequently associated with various human malignancies (Arzimanoglou *et al.*, 1998). Because defective MMR is regarded as a risk factor for familial predisposition or second malignancies, analyses of MSI have been prevalent, particularly in the field of oncology. However, in the literature, results of MSI analyses lack consistency (Arzimanoglou *et al.*, 1998).

Although analysis of MSI is now commonplace, a designation of MSI is sometimes difficult. The 1997 National Cancer Institute (NCI) workshop, "Microsatellite Instability and RER Phenotypes in Cancer Detection and Familial Predisposition," concluded that the variety of microsatellites used was a major cause for discrepancies among data in the literature and recommended a panel of five microsatellites as a "working reference panel" (Boland *et al.*, 1998). In addition to selection of markers for analysis, methodologic problems may also account for a part of discrepancies among the data. In many cases, changes in microsatellite lengths are minute—as small as loss

Handbook of Immunohistochemistry and in situ Hybridization of Human Carcinomas,
Volume 2: Molecular Pathology, Colorectal Carcinoma, and Prostate Carcinoma

55

or gain of a single repeat unit. In addition, cell populations carrying changes in microsatellites are not always major in a given sample. Accurate analysis of MSI therefore requires highly sensitive, quantitative, and reproducible characters in an assay system. In the most widely used approach for MSI analysis, microsatellite sequences are amplified by polymerase chain reaction (PCR) using radio-labeled primers. PCR products are run in the conventional sequencing gel and imaged by autoradiography using X-ray films. However, polyacrylamide gel electrophoresis is susceptible to migration errors, and autoradiography is known to have biased detection characteristics. PCR itself also has intrinsic problems. The most widely used thermostable DNA polymerase (*Taq*) has a terminal deoxynucleotidyl transferase (TdT) activity, which adds one additional base to PCR products in a sequence-dependent manner. TdT activity of *Taq* polymerase is variably expressed, depending on the conditions used. This property, in addition to slippage of the polymerase, increases the complexity of PCR products. These factors have been present as a major obstacle against an accurate analysis of MSI.

New electrophoresis techniques using fluorescence labeling and laser scanning have recently evolved. In some systems, each fragment is quantitatively detected, and its mobility is standardized accurately. We have applied such a fluorescent technique for MSI analysis to overcome the above-mentioned methodologic problems (Oda *et al.*, 1997). Application of our new assay system, High Resolution Fluorescent Microsatellite Analysis (HRFMA), has made it possible to describe more detailed microsatellite changes and, consequently, elucidated previously unrecognized aspects of MSI in human cancer.

MATERIALS

Enzymes

For PCR, *Taq* polymerase (*TaKaRa Taq*, TakaRa Bio Inc., Tokyo, Japan) was used. Other equivalent *Taq* products are also available. However, because other thermostable polymerases, including *TaKaRa Ex Taq* (Takara Bio Inc.), *Pfu* (Stratagene, La Jolla, CA), *Vent* (New England Biolabs, Inc., Beverly, MA), and so on, behave differently on repetitive sequences (unpublished data), these polymerases are not recommended.

Oligonucleotides Used for PCR

All the oligonucleotides used as a primer were synthesized and purified by high-performance liquid chromatography (HPLC). The sequences of the oligonucleotide primers are as follows:

D2S123-5′; 5′-AAACAGGATGCCTGCCTTTA, D2S123-3′; 5′-GGACTTTCCACCTATGGGAC, D5S107-5′; 5′-GGCATCAACTTGAACAGCAT, D5S107-3′; 5′-GATCCACTTTAACCCAAATAC, D10S197-5′; 5′-ACCACTGCACTTCAGGTGAC, D10S197-3′; 5′-GTGATACTGTCCTCAGGTCTCC, D11S904-5′; 5′-ATGACAAGCAATCCTTGAGC, D11S904-3′; 5′-GCTGTGTTATATCCCTAAAGTG-GTGA, D13S175-5′; 5′-TGCATCACCTCACATAG-GTTA, D13S175-3′; 5′-GTATTGGATACTTGAA-TCTGCTG.

In the 3′ primers, guanine residues were chosen at the 5′ end of the oligonucleotides, to control TdT activity of *Taq* polymerase (see Discussion). In D11S904, a guanine residue was added artificially at the 5′ end of the 3′ primer.

The 5′ PCR primers were labeled with ROX (6-carboxy-x-rhodamine), HEX (6-carboxy-2′,4′,7′,4,7,-hexachloro-fluorescein), or 6-FAM (6-carboxyfluorescein). Size standards were labeled with TAMRA (N,N,N′,N′-tetramethyl-6-carboxyrhodamine) or ROX.

Preparation of Genomic DNA

1. Tissue specimens.
Tissue specimens were collected immediately after surgery and kept in liquid nitrogen or at −80°C.
2. Digestion buffer: 10 mM Tris-Cl (pH 8.0), 0.1 M ethylenediamine tetra-acetic acid (EDTA) (pH 8.0), 0.5% sodium dodecyl sulfate (SDS).
3. Proteinase K: 20 mg/ml.
4. Buffer-saturated phenol.
5. Chloroform.
6. Ethanol.
7. 1X TE buffer; 10 mM Tris-Cl (pH 7.5), 1 mM EDTA.

Polymerase Chain Reaction

1. 10X PCR buffer; 100 mM Tris-Cl (pH 8.3), 500 mM KCl, 15 mM $MgCl_2$.
2. Deoxyribonucleotide-triphosphate (dNTP) mixture; 2.5 mM for each.

Fragment Analysis Using an Automated Sequencer (1): Gel Plate System—ABI373A, 377, etc.

1. Urea.
2. 10X TBE.
3. 30% 19:1 Acrylamide/N,N′-methylene-bis-acrylamide solution.

4. Formamide.

5. Tracking dye; 25% blue dextran, 25 mM EDTA (pH 8.0).

6. Size standard; GeneScan 500 TAMRA (Applied Biosystems, Foster City, CA).

Fragment Analysis Using an Automated Sequencer (2): Capillary System—ABI310, 3100

1. 47 cm × 50 µm capillary (Applied Biosystems).
2. Sample tubes and gaskets (Applied Biosystems).
3. Buffer vials (Applied Biosystems).
4. Glass syringe (Applied Biosystems).
5. Capillary polymer; 310 POP4 (Applied Biosystems).
6. 10X running buffer; Genetic Analyzer Buffer with EDTA (Applied Biosystems).
7. Template suppression reagent (Applied Biosystems).
8. Size standard; GeneScan 500 ROX (Applied Biosystems).

METHODS

Preparation of Genomic DNA from Tissue Specimens

Preparation of high molecular weight DNA from tissue specimens was done, as described elsewhere.

1. Thaw a tissue specimen and cut off a part in a 3 × 3 mm size, using sterile scissors.
2. Mince using scissors in a 1.5 ml microtube.
3. Add 400 µl lysis buffer and 2 µl of 20 mg/ml Proteinase K.
4. Mix gently.
5. Incubate at 55°C for 1 hr, with shaking.
6. Spin briefly, and add 400 µl buffer-saturated phenol.
7. Shake gently at room temperature for 10 min.
8. Spin at 15,000 rpm for 10 min at room temperature.
9. Collect the aqueous phase in a new microtube.
10. Add 400 µl of buffer-saturated phenol/chloroform/isoamylalcohol (25:24:1).
11. Repeat **Steps 7–9**.
12. Add 400 µl chloroform/isoamylalcohol (24:1).
13. Repeat **Steps 7–9**.
14. Add 40 µl of 10 N ammonium acetate, and mix.
15. Add 1 ml 100% ethanol and mix gently, until high–molecular-weight DNA is completely insolublized.

16. Keep at 4°C for 10 min.
17. Spin at 15,000 rpm for 20 min at 4°C.
18. Decant gently the supernatant and remove traces of ethanol, as much as possible.
19. Add 360 µl of 1X TE (pH 8.0) and dissolve the pellet, without shaking. This step normally takes overnight at 4°C.
20. Repeat **Steps 6–18**.
21. Wash the pellet with 70% ethanol.
22. Decant gently the supernatant, and set the tube with the top open under a vacuum until no trace of 70% ethanol is visible. This step normally takes 3–10 min. Do not allow the pellet to dry completely.
23. Dissolve the pellet completely in an adequate volume of 1X TE (pH 8.0), without shaking.
24. Scan the absorbance at from 220 to 320 nm. Calculate the concentration from OD_{260}. The quality of DNA can also be checked by routine agarose gel electrophoresis.
25. Store at 4°C.

Polymerase Chain Reaction

1. Dilute genomic DNA solution to 5 µg/ml with 1X TE (pH 8.0).
2. Prepare the premix (per tube); 5 µl of 10X PCR buffer (100 mM Tris-Cl (pH 8.3), 500 mM KCl, 15 mM $MgCl_2$), 7 µl of dNTP mix, 5 µl for each of primers, 22.5 µl of dH_2O, 0.5 µl (2.5u) of *Taq* polymerase. If an automated sequencer is a gel-plate system (ABI373A, 377, etc.), use HEX (normal) and ROX (cancer)-labeled primers. If a capillary sequencer (ABI310, 3100, etc.) is used, choose HEX (normal) and 6-FAM (cancer) for primer labeling.
3. Aliquot 45 µl of the premix into a 0.2 ml thin-walled PCR tube.
4. Add 5 µl of 5 µg/ml genomic DNA sample.
5. Mix well, and spin down.
6. Set the tube in a thermal cycler, and carry out the following program:
   One cycle:
     Presoaking at 95°C for 4 min.
   35 cycles:
     Denaturing at 95°C for 30 sec.
     Annealing at 55°C for 30 sec.
     Extension at 72°C for 30 sec.
   One cycle:
     Additional extension at 72°C for 10 min.
     Keep at 4°C.
7. Mix well, and spin briefly.
8. Store at 4°C until loaded onto an automated sequencer.

Fragment Analysis Using an Automated Sequencer (1): Gel Plate System—ABI373A, 377, etc.

1. Clean the gel plates with detergent solution and isopropanol. Assemble the gel mold according to the manual provided by the manufacturer. Make sure that there is no dust or stain on the glass plates, especially in the belts scanned by laser light, and if necessary, clean the surface again.

2. Mix 40 g urea, 8 ml of 10X TBE, 12 ml of 30% 19:1 acrylamide/bis solution, and 20 ml dH$_2$O in a 100 ml beaker. Stir well, heating, until urea has been completely dissolved.

3. Adjust the volume to 100 ml in a messcyllinder.

4. Filtrate the solution using a disposable bottle-top filter (pore size; 0.45 µm), and deaerate in the same filter ware for 10 min after the solution has been completely filtrated.

5. Transfer the solution in a small Erlenmeyer flask.

6. Add 45 µl of TEMED (N,N,N′,N′-tetramethylethylenediamine) and 0.4 ml of 10% APS to the solution and mix by rapid swirling.

7. Slowly pour the solution into the gel mold, using a pipette or a small polyethylene-made washing bottle with a flexible nozzle. The solution should be poured in the continuous stream so that air bubbles are not included in the gel.

8. Place the gel mold horizontally and examine the gel carefully. If any of air bubbles are present in the areas where DNA samples track, remake a gel.

9. Insert the 24 well-comb and pour the excess gel solution on the comb. Spare 0.5–1.0 ml of the gel solution in a microtube as an indicator for polymerization.

10. Set the gel for at least 3 hr. To avoid overdrying the gel, place Kimwipe paper soaked with 1X TBE at the top, and, if necessary, the bottom of the gel mold, and wrap the gel mold with SaranWrap. The gel can be stored at room temperature up to 24 hr after polymerization is complete.

11. When polymerization is complete, wipe away dried urea or acrylamide and clean the surface of the gel plate, especially in the belts scanned by laser light. Remove the comb carefully.

12. Set the gel plate to the automated sequencer according to the manual provided by the manufacturer.

13. Turn on the power of the sequencer and the computer. The analytic software "GeneScan ver. 1.2.2" is automatically started. Check the gel plate ("plate check"), as instructed in the user's manual. If the signal baseline is not straight, due to the dust on the glass plate, remove the gel from the apparatus and clean again the belts scanned by laser light with isopropanol. If this symptom is not improved, analyses may be affected in some lanes.

14. Set the buffer chambers and pour 1X TBE. Prerun the sequencer (1500 V, 20 mM, 30 W) according to the instruction in the manual.

15. In the meantime, prepare samples. Mix 12 µl of ROX-labeled PCR product and 3 µl of HEX-labeled PCR product in a microtube. This ratio has been determined according to the difference in signal strength among fluorescence compounds so that signal levels acquired in the sequencer may be in a similar range.

16. Prepare the premix (per tube): 2.5 µl of formamide, 0.5 µl of tracking dye, and 0.5 µl of GeneScan 500 TAMRA size marker. Aliquot 3.5 µl into each microtube.

17. Add 1.5 µl of the PCR product mixture to the aliquoted premix, and mix well.

18. Heat at 95°C for 5 min, and chill immediately on ice. Spin briefly.

19. Before loading, remove urea crystalized in the well completely by flushing the well using a syringe with a fine needle. Load samples onto the gel using a flatted flexible tip.

20. Start electrophoresis and scan in the sequencer.

21. After entering necessary information in the "sample sheet" and setting "preprocess parameters" and "analysis parameters" start data acquisition (press the "collection" button). This is normally done 1 hr after electrophoresis has been started. Data acquisition should be done for at least 6 hrs.

22. Acquired data are automatically analyzed if the mode has been selected beforehand in the sample sheet. However, when opening the "Gel File," check whether the "Channel" traces each band correctly in each lane. If necessary, correct "Channel Selector Line," according to the manual, and then reanalyze the data.

23. Results are seen in the "Electropherogram." In HRFMA by gel plate system, two independent PCR products labeled with HEX and ROX are electrophoresed in each lane. To adjust the signal level of these two products, use "Dye Scale" command in the "View" menu. Change values for each fluorescence so that two profiles are superimposed on the Electropherogram. If the size standard has been selected, the data will be displayed by fragment size (the horizontal axis), but, to obtain correct fragment size, verify size calculations and reanalyze the data.

Fragment Analysis Using an Automated Sequencer (2): Capillary System—ABI310, 3100

1. Mix 5 µl of 6-FAM-labeled PCR product, 5 µl of HEX-labeled PCR product, and 30 µl dH$_2$O in a microtube.

2. Mix 1 µl of this mixture with 23.5 µl of Template Suppression Reagent and 0.5 µl of GeneScan-500 ROX Size Standard in a new tube.

3. Heat at 95°C for 5 min, and chill immediately on ice. Spin briefly.

4. Transfer the sample into a sample tube.

5. Set and fill the capillary with the POP4 polymer according to the user's manual. Dilute 10X running buffer with dH$_2$O, and set the buffer and dH$_2$O on the auto-sampler.

6. Set sample tubes on the sample tray.

7. Close the front cover and start up "GeneScan ver. 3.1.2." Set the temperature at 60°C.

8. Start up the "Data Collection" program. Fill in the "Sample Sheet."

9. Open the "Injection List." After setting the parameters, click the "Run" button.

10. Acquired data are automatically analyzed if the analysis parameters and the size standard file are selected in the "Injection List" beforehand. In case of reanalyzing the data, start the "GeneScan Analysis" program. After setting parameters in the "Analysis Parameters" window and choosing size standard and analysis parameter files in the "Analysis Control Window," click the Analyze button.

11. Results are seen in the Electropherogram, as in the gelplate system. In HRFMA by capillary system, two independent PCR products labeled with 6-FAM and HEX are electrophoresed in each run. To adjust the signal level of these two products, use "Dye Scale" command in the "Settings" menu, as in the gelplate system.

Criteria for MSI

The criterion for MSI that we apply to data obtained using HRFMA is "appearance of novel peaks in at least one of more than five selected dinucleotide microsatellites." In "inseparable heterozygous" allelotypes (see Results and Discussion), significant changes in the ratio between the major peaks of two parental clusters also can be regarded as MSI. However, in this case, the possibility of "loss of heterozygosity (LOH)" is not excluded (Maehara *et al.*, 2001) (Figure 12E and F). We designate this category as MSI/LOH. We further classify MSI into two subtypes, according to the fragment length of newly appeared peaks (see Results and Discussion; Figure 12C, D, G, and H).
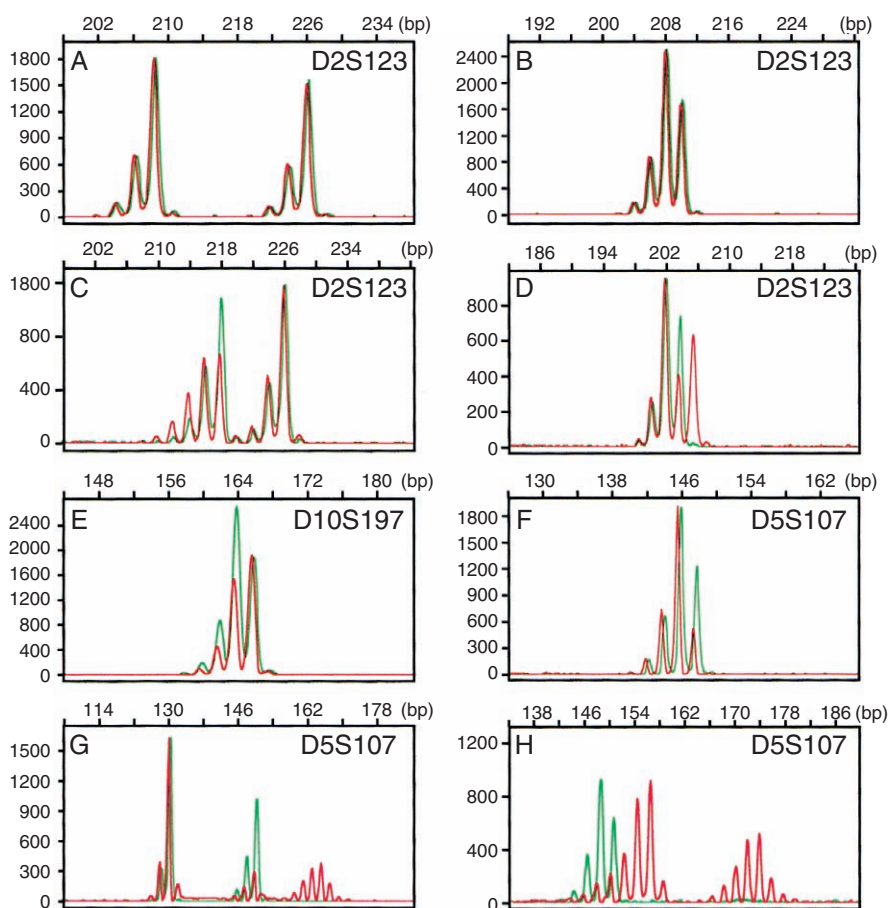
Figure 12 Microsatellite instability determined using HRFMA. A: Normal in a heterozygous allelotype. **B:** Normal in an inseparable heterozygous allelotype. **C:** Type A microsatellite instability (MSI) in a heterozygous allelotype. **D:** Type A MSI in an inseparable heterozygous allelotype. **E, F:** Type A MSI indistinguishable from LOH (inseparable heterozygous allelotype). **G:** Type B MSI in a heterozygous allelotype. **H:** Type B MSI in an inseparable heterozygous allelotype.

RESULTS AND DISCUSSION

Selection of the Microsatellite Markers

Selection of microsatellites is always controversial. A wide variety of microsatellites has been used as a marker for MSI analysis. This circumstance raised a considerable confusion in this field. In 1997, the National Cancer Institute (NCI) sponsored a workshop to review and unify this field (Boland *et al*., 1998). In this workshop, it was concluded that the diversity in data derives mainly from the variety of microsatellites used, a panel of five microsatellites was recommended as a "working reference panel." This panel consists of two mononucleotide microsatellites and three dinucleotide microsatellites.

In selecting markers for MSI assay, repeat length and unit size appear important. Repeat length determines the susceptibility of DNA polymerases to slippage (Greene and Jinks-Robertson, 1997; Tran *et al*., 1997), and unit size determines workability of an MMR system on repeat units looping out of the strand (Sia *et al*., 1997). Indeed, the rare alteration of microsatellite sequences in *Drosophila* cells is thought to derive from their shortness (Schug *et al*., 1997), and eukaryotic MMR is known to work mainly on relatively short repeat units varying from one to several bases (Genschel *et al*., 1998). We have selected five dinucleotide microsatellites located in five independent chromosomes, which contain different repeat lengths varying from 16 to 58 (see Materials). To confer validity on this set of markers, we tested whether they show instability in cells deficient in MMR. Oki *et al*. (1999) have shown that these sequences were highly unstable in cells with a known mutation in *hMSH2* or *hMLH1* and that even cells defective in *hMSH6* (*GTBP*) exhibit a low level of MSI. In addition to MutSα (i.e., hMSH2/hMSH6 heterodimer) MutSβ comprising hMSH2 and hMSH3 functions on nucleotides looped out of the strand in eukaryotic MMR (Genschel *et al*., 1998; Marsischky *et al*., 1996). Therefore, we concluded that this set of markers is highly sensitive to changes derived from defective MMR.

In the NCI workshop mentioned earlier two mononucleotide microsatellites were included in the working reference panel. However, as discussed later in this chapter, use of mononucleotide microsatellites appears problematic. Behavior of *Taq* polymerase on this variety of repeats is unknown because this problem has not been addressed using an artificially synthesized template. In addition, the effect of TdT activity in *Taq* polymerase will be more critical in mononucleotide repeats. Although mononucleotide repeats were known to be a sensitive marker for MSI, correlation between instability in mononucleotide microsatellites and mutation in MMR genes has not been confirmed (Percesepe *et al*., 1998).

In the NCI workshop, MSI phenotypes were classified into two categories: MSI-H and MSI-L (Boland *et al*., 1998). The first is defined as ones showing microsatellite alterations in "the majority (40%) of markers" and the second exhibiting changes only in "a minority (<40%) of markers." In this workshop, the number of markers required for microsatellite analysis was intensively discussed because the sensitivity of assay may depend on the number of markers examined. Indeed, recent studies using more than 10 microsatellites are not rare. However, to answer this problem, it may be more pertinent to test whether a given set of markers exhibits instability in established cell lines deficient in MMR. As mentioned earlier, our five dinucleotide markers detected changes even in cells defective in hMSH6 (Oki *et al*., 1999), which may indicate that at least five markers are required for a sensitive assay. Indeed, the NCI workshop recommended five markers.

Electrophoretic Profiles of Amplified Microsatellite Sequences

Microsatellite sequences amplified by PCR show a complicated cluster of fragments with different lengths and amounts, due to modifications by polymerases used. In addition, microsatellite sequences are highly polymorphic in human populations, which implies that, in many cases, cells are heterozygous for the length of each microsatellite allele. These facts have been in part an obstacle against an accurate microsatellite analysis. *Taq* polymerase is a major thermostable bacterial DNA polymerase used for PCR. This enzyme has TdT activity, in addition to the template-dependent 5′-3′ DNA polymerase activity. Modification of PCR products by TdT activity has been reported in detail (Hu, 1993). TdT activity of *Taq* polymerase adds one additional base to the 3′ end of synthesized strands in a sequence-dependent manner. In many cases, this activity is variably expressed, which leads to a variety with a one-base pair difference in PCR products. This phenomenon is known as a "stuttering" in microsatellite analysis. In addition, *Taq* polymerase is highly susceptible to slippage on repetitive sequences. Slippage of *Taq* polymerase also confers a repeat unit-pitched variety to PCR products of microsatellite sequences.

To analyze *Taq*-dependent modifications in PCR products of microsatellite sequences, we used artificially synthesized microsatellite sequences (Oda *et al*., 1997). The 105-bp region of an artificially synthesized D13S175 human dinucleotide microsatellite was

amplified as a complex of several fragments with different lengths. The highest peak corresponded to 108 bp and was accompanied by shorter peaks different by one base. Because heterogeneity of templates was excluded in this case, this multiplicity of peaks is derived from slippage and TdT activity of *Taq* polymerase. As shown in Figure 13, the major PCR products were fragments with an insertion of one additional repeat unit, and next to these products fragments of the correct size were present. Those lacking one repeat unit were also detectable. In addition to these modifications by polymerase slippage, TdT activity adds one additional base to PCR products, the result being a cluster of fragments the size of which varies from −2 to +3. Thus, when *Taq* polymerase is used, we observe microsatellite alterations through these modifications.

Slippage of *Taq* polymerase on repetitive sequences is not avoidable, although it is known that this activity can be partially controllable by altering Mg^{++} concentration
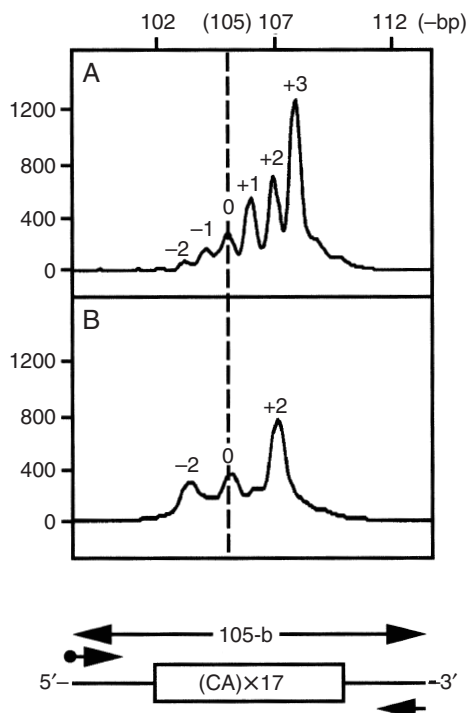
Figure 13 *Taq* **polymerase-dependent modification of polymerase chain reaction (PCR)-amplified microsatellite sequences**. Dinucleotide microsatellite, D13S175, which contains 17 repeats of CA, was artificially synthesized and its 105-bp region was amplified by PCR using *Taq* polymerase. Six peaks, +3, +2, +1, 0, −1, and −2, were observed in **A**. The 3′ exonuclease activity of T4 DNA polymerase removed 3′-protruded nucleotides from the PCR products and simplified them into three peaks, +2, 0, and −2, which were generated by polymerase slippage in **B**. (Adapted from Maehara *et al*., 2000, with permission.)

in PCR. TdT activity of *Taq* polymerase is considered to be a major cause for the low reproducibility seen in PCR products of microsatellite sequences, because this activity is easily altered not only by primer sequences but also by reaction conditions. Efforts to control TdT activity of *Taq* polymerase have been reported. Brownstein *et al*. (1996) have reported that modifications at the bottom sequence of PCR primers are useful to control TdT activity, whereas use of 3′ exonuclease activity in some DNA polymerases to remove additional nucleotides has also been reported (Ginot *et al*., 1996; Oda *et al*., 1997). We once used T4 DNA polymerase. However, enzymatic treatment after PCR may appear complicated. According to the report by Hu *et al*. (1993), Oki *et al*. (1999) found that addition of single guanine residue at the 5′ end of 3′ (nonlabeled) primer induces TdT activity completely at the 3′ end of labeled strands and consequently removes "stuttering" efficiently (unpublished data). In this case, all of the labeled strands are one base longer than their real lengths. At present, we use this method. Thus, as shown in Figure 13, the most simplified profile of amplified dinucleotide microsatellite sequences is a two bases-pitched cluster of peaks showing an increasing pattern; the amount of fragments increases in proportion to their length. When using genomic DNA template, two clusters of peaks derived from paternal and maternal alleles are seen in many cases (i.e., heterozygous) (Figure 12 A, C, and G; *green lines*) and, in some cases, they cross (i.e., "inseparable" heterozygous) (Figure 12B, D–F, and H, *green lines*) or coincide (i.e., homozygous). In MSI analysis, it is essential that this basic pattern is always being obtained in the normal control.

In addition to clusters of peaks included in the basic pattern, additional peaks may be seen in some cases. The sources of these artifacts are mainly secondary structures in the electrophoresed DNA fragments and incorrect calculation files in the analysis program. Artifacts derived from secondary structures in PCR products often form a cluster of peaks shorter than their real lengths. In this case, more stringent denaturing before loading is necessary. Immediate chilling after denaturing is also important. In case the artifacts do not disappear by these procedures, the optical system in a sequencer, particularly the laser axis, should be checked. The ranges of laser emission by various fluorescence compounds used in this system cross each other. Therefore, the analysis program requires a calculation file in which overlapped emission is subtracted in each fluorescence. This calculation file is named "Matrix File" and originally is installed by the manufacturer, according to the combination of fluorescence labels used. However, in some cases, trails by other fluorescence labels, particularly ones used in a

coelectrophoresed size standard, form small peaks that are indistinguishable from peaks that appear as a result of MSI. In this case, a new Matrix File should be originally prepared according to the manual. In MSI analysis, an assay system should be completely free from these artifacts.

Advantages in High Resolution Fluorescent Microsatellite Analysis

As discussed earlier, PCR products of a dinucleotide microsatellite sequence are composed of fragments the size of which varies from −2 to +2 bp. In microsatellite-unstable cells, this sequence fluctuates by 2 bp in some populations. Therefore, in MSI analysis, an accurate electrophoresis is needed. However, in the conventional assay system, sequencing gel electrophoresis has been used. Affected by various conditions, migration of DNA fragments is error-prone in a sequencing gel. Use of an automated sequencer for microsatellite analysis is on the increase. However, in many cases, labeling is done using a single fluorescence and samples are run on separate lanes. In some systems, migration of each DNA fragment is standardized, using a coelectrophoresed size marker with a different fluorescence. However, even in such systems, it appears difficult to standardize migration absolutely because there is no calculation file that corrects mobility differences among fluorescence compounds. To exclude migration errors completely, it appears more pertinent to run two samples labeled with different fluorescent labels in one lane. We have established this dual fluorescence coelectrophoresis system. We examined electrophoretic mobilities and specific intensity of DNA fragments labeled with various fluorescence compounds and found the combinations and the ratios in which their electrophoretic profiles match completely (Figure 12A and B). This improvement has obviously facilitated a precise comparison of two independent PCR products.

Application of fluorescent labeling to microsatellite analysis has another advantage. In the conventional MSI assay, PCR products are radio-labeled and imaged by autoradiography. However, X-ray films often used in autoradiography have biased detection characteristics, which leads to wrong estimate of the signal magnitude and, sometimes, to a loss of bands, particularly in ones with a low signal. From this point of view, laser scanning of fluorescent-labeled fragments seems to be more feasible for microsatellite analysis because it has highly linear detection characteristics in addition to a high sensitivity for detection (Oda *et al.*, 1997). This should lead to a correct detection of DNA fragments both in number and in signal magnitude.

This property of the detection system is essential because, in designating MSI, changes in signal magnitude in each peak are important as are changes in the number of peaks (see Methods) (Maehara *et al.*, 2001). This quantitative character of the detection system has also lead to a sensitive assay of MSI.

In detecting minute changes, one may be concerned about the reproducibility in results. To test whether results obtained using HRFMA are highly reproducible, we electrophoresed the same PCR products more than 10 independent times. We also performed PCR of normal tissue DNA more than 10 independent times, and eletrophoresed them. Results were highly reproducible. In all of these data, no additional peak was observed and the electrophoretic profiles were identical (data not shown). These findings imply that in HRFMA, appearance of novel peaks can be regarded as MSI. The ratio between two neighboring peaks did not vary more than 5% in independent PCR products, which implies that changes in the signal magnitude in each peak can be interpreted as a change in template DNA. When mixing genomic DNA samples with different microsatellite lengths in various ratios, the system detected the existence of template with a different microsatellite length at 10% (Oda *et al.*, 1997). These data may guarantee sensitive detection of MSI in HRFMA.

Qualitatively Different Subtypes of Microsatellite Instability in Human Cancer

Development of a sensitive and quantitative MSI assay has shed light on qualitative differences in MSI in human cancer. Using HRFMA, we have observed two qualitatively different subtypes of MSI in various human malignancies. We define Type A alterations as length changes of ≤6-base pairs (Figure 12C and D). Type B changes are more drastic and involve alterations of ≥8-base pairs, and they sometimes appear as if a "third" allele is present in addition to the parental alleles (Figure 12G and H). In our panel of more than 100 patients with colorectal cancer, the frequencies of Type A and Type B MSI were approximately 30% and 10%, respectively. Inspection of published data reveals that microsatellite changes thus far reported in various tumors, including ones in HNPCC, are largely Type B, possibly related to the fact that in the conventional microsatellite assay it is less difficult to detect Type B changes. More subtle Type A MSI might have remained undetected in many cases.

When dinucleotide MSI in cancer was first reported by Thibodeau *et al.* (1993), the patterns of alterations were classified into two categories: Type I mutation with "a significant increase or decrease in the apparent

fragment size" and Type II mutation with "minor alteration" such as changes within 2 bp. Type A MSI appears similar to their Type II mutation. On the other hand, Type I mutations may correspond to our Type B instability. Microsatellite changes determined using HRFMA in human or mouse cells with a known defect in MMR genes were within 6 bp (Oki *et al.*, 1999 and unpublished data), which implies that MSI observed in these cells are Type A. Indeed, examination of published microsatellite changes in cells of MMR gene-knock out mice clearly indicates that most changes are of Type A. These findings strongly suggest that Type A is a direct consequence of defective MMR. Nevertheless, Type B MSI is noted in various tumors, including HNPCC. The problem is that mutations in MMR genes have been reported in tumors displaying this type of instability. However, the reported frequencies of mutation in the two major MMR genes, *hMSH2* and *hMLH1*, in HNPCC kindred are not always high. Additional and previously unrecognized molecular abnormalities may underlie Type B instability. Thus, application of a sensitive and quantitative technique has elucidated qualitative differences in MSI in human cancer. Such techniques will precisely distinguish tumors with different molecular backgrounds.

References

Aaltonen, L.A., Peltomaki, P., Leach, F.S., Sistonen, P., Pylkkanen, L., Mecklin, J.P., Jarvinen, H., Powell, S.M., Jen, J., Hamilton, S.R., Petersen, G.M., Kinzler, K.W., Vogelstein, B., and de la Chapelle, A. 1993. Clues to the pathogenesis of familial colorectal cancer [see comments]. Comment in: *Science* 1993 May 7;260(5109):751. *Science 260*:812–816.

Arzimanoglou, I.I., Gilbert, F., and Barber, H.R. 1998. Microsatellite instability in human solid tumors. [Review] [132 refs]. *Cancer 82*:1808–1820.

Boland, C.R., Thibodeau, S.N., Hamilton, S.R., Sidransky, D., Eshleman, J.R., Burt, R.W., Meltzer, S.J., Rodriguez-Bigas, M.A., Fodde, R., Ranzani, G.N., and Srivastava, S. 1998. A National Cancer Institute Workshop on Microsatellite Instability for cancer detection and familial predisposition: Development of international criteria for the determination of microsatellite instability in colorectal cancer. [Review] [119 refs]. *Cancer Res. 58*:5248–5257.

Brownstein, M.J., Carpten, J.D., and Smitha, J.R. 1996. Modulation of non-templated nucleotide addition by Taq DNA polymerase: Primer modifications that facilitate genotyping. *Biotechniques 20*:1004–1010.

Fishel, R., Lescoe, M.K., Rao, M.R., Copeland, N.G., Jenkins, N.A., Garber, J., Kane, M., and Kolodner, R. 1993. The human mutator gene homolog MSH2 and its association with hereditary nonpolyposis colon cancer [published erratum appears in Cell 1994 Apr 8;77(1):167]. *Cell 75*:1027–1038.

Genschel, J., Littman, S.J., Drummond, J.T., and Modrich, P. 1998. Isolation of MutSbeta from human cells and comparison of the mismatch repair specificities of MutSbeta and MutSalpha. *J. Biol. Chem. 273*:19895–19901.

Ginot, F., Bordelais, I., Nguyen, S., and Gyapay, G. 1996. Correction of some genotyping errors in automated fluorescent microsatellite analysis by enzymatic removal of one base overhangs. *Nucleic Acids Res. 24*:540–541.

Greene, C.N., and Jinks–Robertson, S. 1997. Frameshift intermediates in homopolymer runs are removed efficiently by yeast mismatch repair proteins. *Mol. Cell. Biol. 17*:2844–2850.

Hu, G. 1993. DNA polymerase-catalyzed addition of nontemplated extra nucleotides to the 3′ end of a DNA fragment. *DNA Cell Biol. 12*:763–770.

Ionov, Y., Peinado, M.A., Malkhosyan, S., Shibata, D., and Perucho, M. 1993. Ubiquitous somatic mutations in simple repeated sequences reveal a new mechanism for colonic carcinogenesis. *Nature 363*:558–561.

Leach, F.S., Nicolaides, N.C., Papadopoulos, N., Liu, B., Jen, J., Parsons, R., Peltomaki, P., Sistonen, P., Aaltonen, L.A., Nystrom-Lahti, M., Guan, X.-Y., Zhang, J., Meltzer, P.S., Yu, J.-W., Kao, F.-T., Chen, D.J., Cerosaletti, K.M., Fournier, R.E.K., Todd, S., Lewis, T., Leach, R.J., Naylor, S.L., Weissenbach, J., Mecklin, J.-P., Jarvinen, H., Petersen, G.M., Hamilton, S.R., Green, J., Jass, J., Watson, P., Lynch, H.T., Trent, J.M., de la Chapelle, A., Kinzler, K.W., and Vogelstein, B. 1993. Mutations of a mutS homolog in hereditary nonpolyposis colorectal cancer. *Cell 75*:1215–1225.

Maehara, Y., Oda, S., and Sugimachi, K. 2001. The instability within: Problems in current analyses of microsatellite instability. [Review] [108 refs]. *Mutation Res. 461*:249–263.

Marsischky, G.T., Filosi, N., Kane, M.F., and Kolodner, R. 1996. Redundancy of Saccharomyces cerevisiae MSH3 and MSH6 in MSH2-dependent mismatch repair. *Genes Dev. 10*:407–420.

Modrich, P., and Lahue, R. 1996. Mismatch repair in replication fidelity, genetic recombination, and cancer biology. *Ann. Rev. Biochem. 65*:101–133.

Oda, S., Oki, E., Maehara, Y., and Sugimachi, K. 1997. Precise assessment of microsatellite instability using high resolution fluorescent microsatellite analysis. *Nucleic Acids Res. 25*:3415–3420.

Oki, E., Oda, S., Maehara, Y., and Sugimachi, K. 1999. Mutated gene-specific phenotypes of dinucleotide repeat instability in human colorectal carcinoma cell lines deficient in DNA mismatch repair. *Oncogene 18*:2143–2147.

Peltomaki, P., Lothe, R.A., Aaltonen, L.A., Pylkkanen, L., Nystrom-Lahti, M., Seruca, R., David, L., Holm, R., Ryberg, D., Haugen, A., Brogger, A., Borresen, A.-L., and de la Chapelle, A. 1993. Microsatellite instability is associated with tumors that characterize the hereditary non-polyposis colorectal carcinoma syndrome. *Cancer Res. 53*:5853–5855.

Percesepe, A., Kristo, P., Aaltonen, L.A., Ponz de Leon, M., de la Chapelle, A., and Peltomaki, P. 1998. Mismatch repair genes and mononucleotide tracts as mutation targets in colorectal tumors with different degrees of microsatellite instability. *Oncogene 17*:157–163.

Schug, M.D., Mackay, T.F., and Aquadro, C.F. 1997. Low mutation rates of microsatellite loci in Drosophila melanogaster. *Nat. Genet. 15*:99–102.

Sia, E.A., Kokoska, R.J., Dominska, M., Greenwell, P., and Petes, T.D. 1997. Microsatellite instability in yeast: Dependence on repeat unit size and DNA mismatch repair genes. *Mol. Cell. Biol. 17*:2851–2858.

Thibodeau, S.N., Bren, G., and Schaid, D. 1993. Microsatellite instability in cancer of the proximal colon [see comments]. Comment in: *Science* 1993 May 7;260(5109): 751. *Science 260*:816–819.

Tran, H.T., Keen, J.D., Kricker, M., Resnick, M.A., and Gordenin, D.A. 1997. Hypermutability of homonucleotide runs in mismatch repair and DNA polymerase proofreading yeast mutants. *Mol. Cell. Biol. 17*:2859–2865.

This Page Intentionally Left Blank

6

The Role of Extreme Phenotype Selection in Cancer Research

Jose Luis Perez-Gracia, Maria Gloria Ruiz-Ilundain, Ignacio Garcia-Ribas, and Eva Carrasco

Introduction

The availability of modern techniques of molecular biology has opened a new era in the field of genetics. These techniques are used in a pure laboratory environment and in the setting of translational research, which represents the integration of basic science and clinical findings to improve our understanding of the biology underlying the clinics. In the field of cancer research, many of those studies have been focused on correlating the genetic characteristics of patients with cancer, either from normal or tumoral tissue, with their prognosis or with the efficacy of the treatments that are used. These studies follow the hypothesis that different individuals or tumors might harbor diverse genetic characteristics that may correlate with their prognosis. The selection of the genetic characteristics that are studied is usually based on theoretic hypotheses that correlate preclinical knowledge with tumor biology or with the mechanisms of action of antitumor agents. Nonetheless, with the incorporation of high-throughput techniques, such as microarrays or serial analysis of gene expression (SAGE), it has become common to screen the expression of large numbers of genes at the same time, with or without potential correlation with the end point studied.

The validity of such an approach is unquestionable, as reflected by some outstanding results that have been achieved with it. Some relevant examples are the correlation between the level of expression of thymidylate synthase and the efficacy of 5-fluorouracil in digestive tumors (Johnston *et al.*, 1994) or the identification through microarrays of different gene-expression patterns in patients with diffuse large B-cell lymphoma (Alizadeh *et al.*, 2000). This new methodology for classification of lymphoma offers important advantages over traditional clinical and pathologic classifications. However, it is clear that not all trials have achieved relevant results, and during the last few years we have seen an enormous proliferation of studies that reach conclusions of uncertain clinical significance, sometimes even contradicting previous results from similar studies. This fact has resulted in the need to design specific guidelines to validate the quality of such studies prior to publication (Editor, 1999). Several factors underlie this problem, and their detailed review is out of the scope of the present work, so we will focus on some of the most relevant ones.

First, there is the possibility that, even if the genetic alterations studied are truly related to the outcome of the disease, they may not be the only or the main prognostic factor. In contrast with diseases caused by fully

Handbook of Immunohistochemistry and in situ Hybridization of Human Carcinomas,
Volume 2: Molecular Pathology, Colorectal Carcinoma, and Prostate Carcinoma

65

penetrant genetic alterations, such as cystic fibrosis, in which the presence of the genetic alteration is inexorably linked with the development of the disease, cancer is usually a complex and multifactorial disease. Therefore, cancer prognosis depends on the interaction of many intrinsic and extrinsic factors. Consequently, the identification of genetic alterations that are truly associated with a significantly different prognosis becomes a difficult task because most of them have a reduced penetrance.

Second, in most cases the patients selected for these studies do not have a truly characteristic phenotype. Instead, they belong to a general patient population that is classified in terms of their good or bad prognosis using conventional efficacy parameters such as survival or clinical response. This complicates the process of identifying genetic factors that correlate with a characteristic prognosis because in many instances none of the patients have a truly characteristic outcome. Moreover, a large part of the variability observed might be explained by clinical factors.

Third, many studies are of retrospective nature and have a low potential to establish relationships of causality. Instead, they are just valid for generation of hypotheses. Moreover, the thresholds to define the relations between the factors studied and the prognosis are frequently based on retrospective statistical calculations, which may lead to additional biases.

Last, technical and methodologic differences in the way that laboratory work is performed, and the intrinsic heterogeneity of any technique, contribute to more confusion in the interpretation of the results.

The possibility to solve most of the previously mentioned issues is somewhat remote. We cannot change the nature of the disease, and the techniques that we have today, although constantly improving, have some limitations. Similarly, although some prospective studies are moving forward, cost and time will always limit their feasibility and perhaps their value. Yet, the inadequate selection of the phenotypes studied could provide a valid frame to improve the design of current trials. Indeed, a potentially more efficient strategy to isolate the genetic features associated with characteristic outcomes could be to focus research in few subjects with extreme, truly differentiated phenotypes. Such individuals may have a greater chance of carrying characteristic genotypes that are responsible for their distinctive prognosis than the general population. Such an approach is not new in medical research and has been used successfully before, including in oncology. The study of individuals either affected by multiple tumor syndromes, and/or with a markedly increased familiar risk of developing cancer, has led to the discovery of genetic alterations that explain such situations. Some well-known examples are the detection of *p53*

germ-line mutations in patients with the Li-Fraumeni syndrome (Malkin *et al*., 1990), described through the identification of an excess in the risk of death by rhabdomyosarcoma in siblings (Li *et al*., 1969; Miller, 1968), or the finding that patients with hereditary retinoblastoma present an inactivation of both copies of the *retinoblastoma tumor-suppressor gene* (Cavenee *et al*., 1983), as was wisely predicted by Knudson (1971). Nonetheless, the selection of phenotypes with increased risk to develop cancer is not the only approach that has led to successful results. The identification of complete deficiency of dihydropyirimidine dehydrogenase activity in peripheral blood mononuclear cells of a patient who developed severe toxicity after administration of 5-fluorouracil is an illustrative example (Diasio *et al*., 1988). Although in the initial report the molecular explanation for such deficiency was not identified, subsequent studies have demonstrated that genetic alterations are associated with this deficiency of enzymatic activity (Van Kuilenburg *et al*., 1999).

The common factor for all the previous examples is that the key step that led to the final discovery was the identification and the study of a characteristic phenotype. As seen, the yield of this strategy is very high because only a few patients—or even just one—need to be studied to identify which factors determine the phenotype. This is logical because the only hypothesis tested is whether the observed phenotype (which is so unique that chance does not play a part in it) is related with a determined cause. In contrast, the hypothesis that a specific alteration confers a determined prognosis, either improved or worsened, is more uncertain because it actually implies two hypotheses: that the patients studied really have a characteristic prognosis and that the factor being studied explains such difference. Therefore, it is more difficult to achieve reliable conclusions.

Quite surprisingly, the success achieved by these and other similar studies has not led to the development of a research methodology to obtain the maximum benefit of this strategy. Rather than from a systematic and solid scientific approach, the identification of characteristic phenotypes has mostly been based on isolated observations from bright clinicians. Another interesting consideration is that the selection of characteristic phenotypes has usually been limited to subjects with negative phenotypes, mainly those presenting an increased risk to develop one or multiple tumors. This is logical because such individuals or families are relatively easy to identify because their high incidence of cancer is unusual. Nonetheless, the possibility that subjects with positive phenotypes exist should also be considered as an alternative to optimize the strategy of studying extreme phenotypes.

As we have seen in the previous examples, the strategy of correlating very characteristic phenotypes with their respective genotypes has been very successful. Therefore, it is clear that a consistent methodology should be developed to standardize and to obtain the maximum benefit from this strategy. This methodology should not only be directed to the identification of negative phenotypes but should also contemplate the possibility of identifying individuals with markedly positive phenotypes, either because of unusually positive outcomes from diseases of bad prognosis or because of a low risk to develop those diseases. In the following sections we will develop these possibilities.

Phenotype Selection of Patients with Cancer with Long-Term Survival

Nowadays, a majority of advanced solid tumors are considered to be incurable with current treatment alternatives, and their median survival is very low. However, even in the tumor types with lowest survivals, there are some rare exceptions. Some case reports of unexplained long-term survivors of diseases, such as gastric cancer (Miyaji *et al.*, 1996), colon cancer (Mukai *et al.*, 2000), pancreatic cancer (Silberstein *et al.*, 2000), or myeloma (Dutcher *et al.*, 1984), in apparently incurable situations can be found in the medical literature. Therefore, these individuals could represent examples of extreme phenotypes because their prolonged survival is highly unusual, considering their disease, and it is unlikely that this is a consequence of the treatment that they received.

If the existence of patients with cancer presenting an unusually prolonged survival would be confirmed, their study perhaps would explain the causes underlying that fact. These causes could be related to tumoral factors (such as alterations in mechanisms of drug resistance or cell-cycle regulation) or host factors (such as differences in drug metabolism, immunologic response, or deoxyribonucleic acid [DNA] repair mechanisms) in addition to other potential external factors. Although these and other potential explanations represent many hypotheses to study, their limitation to one or few subjects would represent a great advantage to the efficiency of this research. Evidently, the finding of more than one individual within the same family with unexpected long-term survival following a confirmed diagnosis of a tumor with a very poor prognosis would strongly argue in favor of the hypothesis that such phenotype is characteristic and that it is secondary to genetic factors.

Obviously, the histologic diagnosis and the disease staging of these individuals should be based on solid evidence because it is possible that some of them may have been erroneously staged or even diagnosed of cancer, that being the underlying explanation for their characteristic prognosis.

Phenotype Selection of Individuals Potentially Protected from Developing Cancer

It is well known that the risk of developing cancer is not uniform. Today we know that several genetic or environmental factors may increase the risk of individuals to develop certain types of cancer. Moreover, we also know that such increase in the risk is not uniform, but gradual. Whereas some of the factors such as passive or active smoking lead to mild or moderate increases, respectively, in the risk of cancer, other factors such as inactivation of both retinoblastoma tumor-suppressor genes markedly increase the risk of developing cancer.

Therefore, assuming that the risk of cancer is not uniform, one further step would be to hypothesize that just as some individuals present an increased risk, other subjects may have lower risk than would be expected because of their environment and habits and that this decrease may also be gradual. These subjects would represent the left tail of a gaussian distribution showing the risk to develop cancer. If these individuals exist, their identification and the study of the causes of such protection would increase our knowledge about cancer and perhaps could also yield potentially useful treatments against it. This decrease in the risk to develop cancer could be secondary, for example, to factors related to improved mechanisms of DNA repair, cell-cycle regulation, metabolism of carcinogens, or immunologic response.

Theoretically, the potential existence of such individuals could be supported by the intrinsic nature of the evolution process. Indeed, because cancer is a frequent and ancient disease (probably, inherent to life) organisms have developed mechanisms to protect themselves against neoplastic disorders, and probably the most efficient mechanisms have been selected during the course of evolution. However, the question remains whether individuals with genetic characteristics that confer them a significant protection against certain neoplastic disorders really exist. It is interesting to note that, if we look to diseases different than cancer, we will see that this is the case and that such an approach is again not new in medicine. Some intriguing examples can be used to illustrate that individuals with genetic alterations that confer protection against some diseases may exist, and, moreover, the use of an adequate methodology of phenotype selection may

lead to identifying such alterations. Probably one of the most outstanding examples has been the identification of genetic alterations that confer to individuals that carry them a complete protection against infection by certain strains of the human immunodeficiency virus (HIV). The chemokine coreceptor CCR-5 allows the entry of HIV into its target cells, and it is well known that some alterations in the gene encoding CCR-5 confer to the individuals bearing them complete protection against the infection by certain strains of HIV. This phenotype has been observed in individuals with different genotypes: homozygotic deletions in the gene encoding *CCR-5* (Liu *et al*., 1996) and heterozygotic mutations in *CCR-5*, when associated with the mentioned deletion in the other allele (Quillent *et al*., 1998). Quite interestingly, the discovery of these genotypes was based on the identification of the characteristic phenotypes of the individuals bearing them. Because the *CCR-5* mutations had not been associated with any abnormalities, an astute observation that some individuals highly exposed to HIV never developed the infection gave the impetus to identify them (Rowland-Jones *et al*., 1995). Secondary to this observation, *CCR-5* and other coreceptors for HIV have become a relevant target in the investigation of HIV infection.

Another interesting example in which a characteristic phenotype has been successfully used to identify the underlying genotype is the relation between certain factor VII genotypes and the risk of myocardial infarction (Girelli *et al*., 2000). Elevated plasmatic levels of coagulation factor VII have been suggested to correlate with the risk of death as a result of coronary artery disease, and polymorphisms in the factor VII gene are associated with variations in levels of factor VII. Therefore, these polymorphisms were studied in 311 individuals with severe, angiographically documented coronary atherosclerosis, of whom 175 had a history of previous myocardial infarction and the rest did not. Among patients with no history of previous myocardial infarction, there was a significantly higher number of patients with determined genotypes than among patients with myocardial infarction. Therefore, this finding suggests that those genotypes confer a protection against developing myocardial infarction. This type of study must always be interpreted with because it is subject to a potentially high risk of bias, as reviewed by Gambaro *et al*. (2000). However, this example is of particular interest because the individuals that were found to be protected against ischemic disease had not developed myocardial infarction despite having a strong risk factor to develop it—documented coronary atherosclerosis—rather than being just normal healthy subjects (although the study did include a control

group formed by healthy subjects). Therefore, there was a greater chance of finding true protective factors, rather than just absence of disease, as could be expected in a group formed by individuals with a normal population risk.

The bottom line of both examples is that the study of subjects with a lower than normal risk of developing a disease may unveil protective host factors for that disease, just as the study of subjects with an elevated risk of developing cancer can lead to the discovery of cancer-related genetic alterations, as we have seen in some of the examples presented before.

In the field of cancer, preclinical evidence is available that does provide a proof for the potential existence of cancer-protective genetic alterations. One outstanding example is the development of a "super p53" mice model, which carries supernumerary copies of the *p53 gene* in the form of large genomic transgenes (Garcia-Cao *et al*., 2002). These mice show a decreased risk to develop tumors in comparison with wild-type mice, as was shown in several tumor-induction models using chemical carcinogens. These mice present completely normal phenotypes, including a normal lifespan and aging process, in contrast with other mice models that also overexpress p53 and show premature aging. This is probably because the additional *p53* copies inserted are under normal regulatory control, as opposed to the other mice models. Although the insertion of additional copies of *p53* in the genotype of these mice was artificially induced, their normal phenotype raises the question of whether this same phenomenon could have taken place through spontaneous mechanisms. In that case, the individuals affected would be partially protected against the development of certain tumors.

In the clinical setting, several studies have targeted the identification of genetic profiles that might be associated with a decrease in the risk to develop cancer, although, as summarized later in this chapter, the results of most of them have not been encouraging. Some polymorphisms in the *methylenetetrahydrofolate reductase* gene have been associated with a decreased risk of developing acute lymphocytic leukemia (Skibola *et al*., 1999) or colorectal cancer (Chen *et al*., 1996) in certain population subsets. Polymorphisms of enzymes such as microsomal epoxide hydrolase (London *et al*., 2000), myeloperoxidase (London *et al*., 1997), or *NAD(P)H*:quinone reductase (Chen *et al*., 1999), which are involved in the metabolism of determined carcinogens, have also been related to some protection against lung cancer or colorectal cancer (Harth *et al*., 2000) in some population subsets and/or ethnic groups. However, other studies, such as that of *microsomal epoxide hydrolase*, have shown no

association (Smith *et al.*, 1997) or even an inverse relationship (Benhamou *et al.*, 1998). Determined genotypes of some cytochrome P450 enzymes, such as CYP1A1 or CYP2D6, have also been correlated with a decreased risk of lung cancer. Nonetheless, meta-analyses have failed to confirm this observation (Christensen *et al.*, 1997; Houlston *et al.*, 2000) or have just described a small protective effect with a nonappreciable relationship to individual susceptibility (Rostami-Hodjegan *et al.*, 1998). Two common polymorphisms of the *p21WAF1/Cip1* gene have been correlated with a potential protective role against ovarian cancer (Milner *et al.*, 1999). Certain genotypes of the glutathione S-transferase M1 have also been related with the risk of lung cancer and other aerodigestive tract cancers, but again a meta-analysis has failed to confirm such results (Houlston *et al.*, 1999). Some human leukocyte antigen (HLA) alleles have been linked in cases and control studies with a decreased susceptibility to renal cell carcinoma (Ozdemir *et al.*, 1997), melanoma (Ichimiya *et al.*, 1996), or lung cancer (Tokumoto *et al.*, 1998). Finally, even women who are homozygotic for determined polymorphic alleles of the *BRCA-1* gene have been associated with a decreased risk of breast cancer (Dunning *et al.*, 1997).

The ambiguous and clinically not very relevant results of some of these studies may be explained by methodologic flaws, as detailed elsewhere (Gambaro *et al.*, 2000), but may also be related in part with an inadequate selection of the populations studied. In contrast with the former studies in which subjects were selected by a very characteristic phenotype—a definite protection against developing HIV or myocardial infarction was observed despite high risk factors. The later studies compared the risk of patients who have developed cancer with a control group formed by normal subjects. In these subjects, the risk of developing cancer was probably neither increased nor decreased, perhaps the only exception being that some groups were formed by smokers, and it was therefore unlikely that clinically relevant information would be discovered. A potentially more efficient approach would be to study individuals with a truly characteristic phenotype that indicates that they have a markedly reduced familiar or individual risk to develop cancer. Families with a very low or ideally null incidence of cancer over several generations (perhaps despite crossing with high-risk families), could be considered to have a reduced familiar risk. Subjects that do not develop cancer despite important exposure to widely recognized intrinsic factors or extrinsic ones could be considered to have a reduced individual risk. An example of individuals protected against cancer despite high intrinsic risk factors could

be potential subjects with familiar adenomatous polyposis developing cancer significantly later than would be expected or not developing it at all. Also, an example of an individual protected against cancer despite high extrinsic risk factors could be a subject that does not develop a tumor despite heavy exposure to radiation.

Different combinations of these and other strategies or different ones could also be pursued, always realizing that if such families or individuals exist, it would be naive to attribute their characteristic phenotype to chance, at least until other causes have been ruled out. Evidently, the chance of yielding positive results always will be directly related to the discrepancy between the risk of developing cancer and the actual phenotype.

This methodology raises a number of issues. The main one is obviously how to select the individuals to study. In some cases, such as the selection of patients with cancer with long-term survival, it is clear that the best way would be to do it through the physicians that see those patients, and, therefore, appropriate training and awareness should be created among them. However, in the case of individuals potentially protected from cancer, patient selection becomes more complicated because they are in fact healthy subjects. Therefore, quite complex epidemiologic studies would be required.

A second issue is what should be studied in these subjects, if they are identified. As we have hypothesized, in the case of long-term survivors, their phenotype may be the result of either intrinsic factors (related to the tumor or to the host) or to external ones. Therefore, all of them should be analyzed, and ideally samples from the tumor, the host, and environmental factors should be studied. In the case of individuals potentially protected from cancer, only host and environmental factors would need to be studied. One important limitation is the kind of samples that can be collected. Evidently, the availability of fresh tissue would be preferred because it makes it possible to perform a greater variety of studies, including high-throughput techniques, which would be useful for this kind of research, given their high potential to screen the expression of numerous genes. Nonetheless, it is clear that these samples or even others, such as paraffin-embedded tissue, will not always be available. Therefore, access to adequate material might be an important limitation to perform these type of studies.

Lastly, ethical issues are another potential point of concern because the study and the storage of genetic materials are subject to strict regulations to protect the privacy and the rights of the individuals. This becomes even more problematic if we consider the possibility

that some of the target individuals might have been lost to follow-up, or they may not even be alive. Moreover, one additional ethical problem would be to approach individuals and try to estimate their risk to develop cancer as being high or low without being certain about it and without knowing the consequences that this may imply for those people.

In summary, the study of individuals with very characteristic phenotypes has been useful to describe the mechanisms underlying them. This has been confirmed in subjects with high risk to develop determined diseases and in others who seem to be protected against certain diseases. Therefore, it seems logical to pursue this strategy as a valid methodology for the study of other diseases, including cancer. We propose to create databases compiling clinical and environmental information and appropriate samples from individuals who are either long-term survivors of theoretically incurable tumors or who seem to be protected against certain neoplastic disorders. The study of such data could perhaps help to provide a useful interpretation of the information that the sequencing of the human genome is yielding and could help to increase our current knowledge of cancer and to discover new therapeutic strategies against this disease. Even in the age of computer-aided molecular biology, observation should remain a better way to generate valid hypothesis than speculation.

References

Alizadeh, A.A., Eisen, M.B., Davis, R.E., Ma, C., Lossos, I.S., Rosenwald, A., Boldrick, J.C., Sabet, H., Tran, T., Yu, X., Powell, J.I., Yang, L., Marti, G.E., Moore, T., Hudson, J. Jr., Lu, L., Lewis, D.B., Tibshirani, R., Sherlock, G., Chan, W.C., Greiner, T.C., Weisenburger, D.D., Armitage, J.O., Warnke, R., Levy, R., Wilson, W., Grever, M.R., Byrd, J.C., Botstein, D., Brown, P.O., and Staudt, L.M. 2000. Distinct types of diffuse large B-cell lymphoma identified by gene expression profiling. *Nature* 403:503–511.

Benhamou, S., Reinikainen, M., Bouchardy, C., Dayer P., and Hirvonen, A. 1998. Association between lung cancer and microsomal epoxide hydrolase genotypes. *Cancer Res.* 58:5291–5293.

Cavenee, W.K., Dryja, T.P., Phillips, R.A., Benedict, W.F., Godbout R., Gallie, B.L., Murphree, A.L., Strong, L.C., and White, R.L. 1983. Expression of recessive alleles by chromosomal mechanisms in retinoblastoma. *Nature* 305:779–784.

Chen, H., Lum, A., Seifried, A., Wilkens, L.R., and Le Marchand, L. 1999. Association of the NAD(P)H:quinone oxidoreductase 609C—>T polymorphism with a decreased lung cancer risk. *Cancer Res. 59*:3045–3048.

Chen, J., Giovanucci, E., Kelsey, K., Rimm, E.B., Stampfer, M.J., Colditz, G.A., Spiegelman, D., Willett, W.C., and Hunter, D.J. 1996. A methylenetetrahydrofolate reductase polymorphism and the risk of colorectal cancer. *Cancer Res. 56*:4862–4864.

Christensen, P.M., Gotzsche, P.C., and Brosen, K. 1997. The sparteine/debrisoquine (CYP2D6) oxidation polymorphism and the risk of lung cancer: A meta-analysis. *Eur. J. Clin. Pharmacol.* 51:389–393.

Diasio, R.B., Beaveres, T.L., and Carpenter, J.T. 1988. Familial deficiency of dihydropyrimidine dehydrogenase. Biochemical basis for familial pyrimidinemia and severe 5-fluorouracil-induced toxicity. *J. Clin. Invest. 81*:47–51.

Dunning, A.M., Chiano, M., Smith, N.R., Dearden, J., Gore, M., Oakes, S., Wilson, C., Stratton, M., Peto, J., Easton, D., Clayton, D., and Ponder, B.A. 1997. Common BRCA1 variants and susceptibility to breast and ovarian cancer in the general population. *Hum. Mol. Genet. 6*:285–289.

Dutcher, J.P., and Wiernik, P.H. 1984. Long-term survival of a patient with multiple myeloma—a cure? A case report. *Cancer 53*:2069–2072.

Editor. 1999. Freely associating. *Nat. Genet. 22*:12

Gambaro, G., Anglani, F., and D'Angelo, A. 2000. Association studies of genetic polymorphisms and complex disease. *Lancet 355*:308–311.

Garcia-Cao, I., Garcia-Cao, M., Martin-Caballero, J., Criado, L.M., Klatt, P., Flores, J.M., Weill, J.C. Blasco, M.A., and Serrano, M. 2002. "Super P 53" mice exhibit enhanced DNA damage response, are tumor resistant and age normally. *EMBO. J. 21*: 6225–6235.

Girelli, D., Russo, C., Ferraresi, P., Olivieri, O., Pinotti, M., Friso, S., Manzato, F., Mazzucco, A., Bernardi, F., and Corrocher, R. 2000. Polymorphisms in the factor VII gene and the risk of myocardial infarction in patients with coronary artery disease. *N. Engl. J. Med. 343*:774–780.

Harth, V., Donat, S., Ko, Y., Abel, J., Vetter, H., and Bruning, T. 2000. NAD(P)H quinone oxidoreductatse 1 codon 609 polymorphism and its association to colorectal cancer. *Arch. Toxicol. 73*:528–531.

Houlston, R.S. 2000. CYP1A1 polymorphisms and lung cancer risk: a metaanalysis. *Pharmacogenetics 10*:105–114.

Houlston, R.S. 1999. Glutathione S-transferase M1 status and lung cancer risk: a meta-analysis. *Cancer Epidemiol. Biomarkers Prev.* 8:675–682.

Ichimiya, M., Muto, M., Hamamoto, Y., Ohmura, A., Tateno, H., and Asagami, C. 1996. Putative linkage between HLA class I polymorphism and the susceptibility to malignant melanoma. *Australas. J. Dermatol. 37 Suppl* 1:S39.

Johnston. P.G., Fisher, E.R., Rockette, H.E., Fisher, B., Wolmark, N., Drake, J.C., Chabner, B.A., and Allegra, C.J. 1994. The role of thymidylate synthase expression in prognosis and outcome of adjuvant chemotherapy in patients with rectal cancer. *J. Clin. Oncol. 12*:2640–2647.

Knudson, A.G. Jr. 1971. Mutation and cancer: Statistical study of retinoblastoma. *Proc. Natl. Acad. Sci. U.S.A. 68*:820–823.

Li, F.P., and Fraumeni, J.F. Jr. 1969. Rhabdomyosarcoma in children: Epidemiologic study and identification of a familial cancer syndrome. *J. Natl. Cancer. Inst. 43*:1365–1373.

Liu, R., Paxton, W.A., Choe, S., Ceradini, D., Martin, S.R., Horuk, R., MacDonald, M.E., Stuhlmann, H., Koup, R.A., and Landau, N.R. 1996. Homozygous defect in HIV-1 correceptor accounts of resistance of some multiply-exposed individuals to HIV-1 infection. *Cell 86*:367–377.

London, S.J., Lehman, T.A., and Taylor, J.A. 1997. Myeloperoxidase genetic polymorphism and lung cancer risk. *Cancer Res. 57*: 5001–5003.

London, S.J., Smart, J., and Daly, A.K. 2000. Lung cancer risk in relation to genetic polymorphisms of microsomal epoxide hydrolase among African-Americans and Caucasians in Los Angeles County. *Lung Cancer 28*:147–155.

Malkin, D., Li, F.P., Strong, L.C., Fraumeni, J.F. Jr., Nelson, C.E., Kim, D.H., Kassel, J., Gryka, M.A., Bischoff, F.Z., and Tainsky, M.A. 1990. Germ line p53 mutations in a familial syndrome of breast cancer, sarcomas, and other neoplasms. *Science 250*:1233–1238.

Miller, R.W. 1968. Deaths from childhood cancer in sibs. *N. Engl. J. Med. 279*:122–126.

Milner, B.J., Brown, I., Gabra, H., Kitchener, H.C., Parkin, D.E., and Haites, N.E. 1999. A protective role for common p21WAF1/Cip 1 polymorphisms in human ovarian cancer. *Int. J. Oncol. 15*:117–119.

Miyaji, M., Ogoshi, K., Kajiura, Y., Nakamura, K., Kondo, Y., Tajima, T., and Mitomi, T. 1996. A case of advanced gastric cancer with liver metastasis with no recurrence and long survival. *Gan. To. Kagaku Ryoho 23*:915–918.

Mukai, M., Tokunaga, N., Yasuda, S., Mukohyama, S., Kameya, T., Ishikawa, K., Iwase, H., Suzuki, T., Ishida, H., Sadahiro, S., and Makuuchi, H. 2000. Long-term survival after immunochemotherapy for juvenile colon cancer with peritoneal dissemination: A case report. *Oncol. Rep. 7*: 1343–1347.

Ozdemir, E., Kakehi, Y., Nakamura, E., Kinoshita, H., Terachi, T., Okada, Y., and Yoshida, O. 1997. HLA-DRB1*0101 and *0405 as protective alleles in Japanese patients with renal cell carcinoma. *Cancer Res. 57*:742–746.

Quillent, C., Oberlin, E., Braun, J., Rousset, D., Gonzalez-Canali, G., Métais, P., Montagnier, L., Virelizier, J.L., Arenzana-Seisdedos, F., and Beretta, A. 1998. HIV-1-resistance phenotype conferred by combination of two separate inherited mutations of CCR5 gene. *Lancet 351*:14–18.

Rostami-Hodjegan, A., Lennard, M.S., Woods, H.F., and Tucker, G.T. 1998. Meta-analysis of studies of the CYP2D6 polymorphism in relation to lung cancer and Parkinson's disease. *Pharmacogenetics 8*:227–238.

Rowland-Jones, S., Sutton, J., Ariyoshi, K., Dong, T., Gotch, F., McAdam, S., Whitby, D., Sabally, S., Gallimore, A., and Corrah, T. 1995. HIV-specific cytotoxic T-cells in HIV-exposed but uninfected Gambian women. *Nat. Med. 1*:59–64.

Silberstein, E., Walfisch, S., Lupu, L., and Sztarkier, I. 2000. Twelve-year survival after the diagnosis of locally advanced carcinoma of the pancreas: A case report. *J. Surg. Oncol. 75*:142–145.

Skibola, C.F., Smith, M.T., Kane, E., Roman, E., Rollinson, S., Cartwright, R.A., and Morgan, G. 1999. Polymorphisms in the methylenetetrahydrofolate reductase gene are associated with susceptibility to acute leukemia in adults. *Proc. Natl. Acad. Sci. U.S.A. 96*:12810–12815.

Smith, C.A., and Harrison, D.J. 1997. Association between polymorphism in gene for microsomal epoxide hydrolase and susceptibility to emphysema. *Lancet 350*:630–633.

Tokumoto, H. 1998. Analysis of HLA-DRB1-related alleles in Japanese patients with lung cancer-relationship to genetic susceptibility and resistance to lung cancer. *J. Cancer Res. Clin. Oncol. 124*:511–516.

Van Kuilenburg, A.B., Vreken, P., Abeling, N.G., Bakker, H.D., Meinsma, R., Van Lenthe, H., De Abreu, R.A., Smeitink, J.A., Kayserili, H., Apak, M.Y., Christensen, E., Holopainen, I., Pulkki, K., Riva, D., Botteon, G., Holme, E., Tulinius, M., Kleijer, W.J., Beemer, F.A., Duran, M., Niezen-Koning, K.E., Smit, G.P., Jakobs, C., Smit, L.M., Moog, U., Spaapen, L.J., and Van Gennip, A.H. 1999. Genotype and phenotype in patients with dihydropyrimidine dehydrogenase deficiency. *Hum. Genet. 104*:1–9.

This Page Intentionally Left Blank

7

Rolling Circle Amplification

Vanessa King

Introduction

Rolling circle amplification (RCA) is a versatile technology that has been used successfully to detect nucleic acid and protein targets. The versatility of this technology arises from the numerous platforms that have been developed for the amplification of specific targets or its use as a signal amplification methodology. Assays for detecting single nucleotide polymorphisms (SNPs) have been developed with the use of less than 100 padlock probes (Thomas *et al.*, 1999). Although the process consists of several steps, it can be carried out in a homogenous format that uses either genomic deoxyribonucleic acid (DNA) (Faruqi *et al.*, 2001) or polymerase chain reaction (PCR) amplified DNA as starting material and can exist as either real-time or end-point (Pickering *et al.*, 2002). Thus SNP detection using RCA is far less laborious than gel-based methods such as restriction fragment length polymorphism (RFLP). An alternative method of RCA uses covalently closed circles. The circles can range from 28 to 74 nucleotides and function as excellent templates for a number of different polymerases (Fire and Xu, 1995; Kool, 1996). As a result, the potential of RCA in diagnostics has been developed for the detection of DNA (Nallur *et al.*, 2001) and proteins (Schweitzer *et al.*, 2000, 2002) on both microarrays and tissues (Gusev *et al.*, 2001) as a signal amplification technology. Regardless of the platform, the isothermal nature in conjunction with either linear or geometric kinetics makes this technology particularly attractive.

The isothermal feature of RCA as a nucleic acid amplification method has shown great potential for *in situ* (IS) applications. Several IS-RCA approaches have been developed that can provide improved detection of a desired target via signal or target amplification. Initial work involved the use of padlock probes for *in situ* haplotyping. As with the solution format, this is a multistep process that requires hybridization of the padlock probe to the desired target sequence. Padlock probes generally consist of 100 nucleotides with approximately 30 bases that hybridize to the region of interest. This region is split in two for hybridization, discrimination, and ultimately ligation to occur. Discrimination of the mismatch is accomplished with the use of DNA Ampligase. As a result, the probe is now circularized and topologically connected to the target sequence, as was originally designed (Nilsson *et al.*, 1994). The likelihood of false-positive results is theoretically eliminated by the ligation because replication can only occur if the padlock probe has been ligated, and with the addition of high stringency washes following the ligation any unligated or nonspecifically bound probe can be removed. After ligation, synthesis begins with the addition of the polymerase and a primer for initiation. The RCA product is detected in a step termed *decoration*, in which labeled oligonucleotides that are complementary to the RCA product are annealed; alternatively, direct incorporation of nucleotide analogues (such as biotin or digoxigenin) can be used during polymerization and subsequently detected with streptavidin

Handbook of Immunohistochemistry and in situ Hybridization of Human Carcinomas,
Volume 2: Molecular Pathology, Colorectal Carcinoma, and Prostate Carcinoma

73

or antibody conjugates. Success with padlock probes has been demonstrated *in situ* for the detection of cystic fibrosis transmembrane conductance regulator (CFTR) and TP53 (Christian *et al.*, 2001; Lizardi *et al.*, 1998) with some important procedural alterations in their protocols. In both cases cells underwent a hypotonic lysis to leave only "haloed" nuclei. An alternative probe design was used by Zhong *et al.* (2001) for allele discrimination, which did not involve target amplification. Similar results for allele discrimination were accomplished for CFTR using this method and, as with padlock probes, the protocol used "haloed" nuclei. One potential problem associated with padlock probes is the issue of topologic constraints, which would more than likely exist in a fixed cell or tissue and thus make padlock probes very sensitive to different fixatives or fixation processes. It is believed that, to maximize the potential of RCA with padlock probes, the target strand must have a free end within 1 kb of the probe (Baner *et al.*, 1998). This result may explain why padlock probes have not worked successfully in formalin-fixed cells or tissues, which results in cross-linking of proteins and nucleic acids thus constricting free ends. It is interesting to note that detection of RNA targets was successful with padlock probes using ethanol as a fixative and required no additional treatment of the cells (Christian *et al.*, 2001). Therefore, one of the problems associated with padlock probes and their use in diagnostics is that the protocols are fixation-dependent and have not been successfully used in paraffin-embedded formalin-fixed tissues.

Signal amplification strategies for the detection of nucleic acid targets can use either ImmunoRCA or bispecific probes. ImmunoRCA for the detection of nucleic acid targets uses hapten-labeled probes, which are detected via an antibody–oligonucleotide conjugate. Following the binding of the antibody conjugate, the circle hybridizes to the primer and initiates rolling on the addition of the polymerase. ImmunoRCA approaches have been used to detect messenger ribonucleic acid (mRNA) transcripts in paraformaldehyde fixed cells (Zhou *et al.*, 2001). An alternative approach to ImmunoRCA for the detection of nucleic acid targets uses bispecific probes.

For the purpose of this review linear RCA with bispecific probes will be the primary focus of RCA as a signal amplification technology. Linear RCA is a multistep process that starts with a bispecific probe comprising two functional regions and is synthesized as a single oligonucleotide of 60–70 bp. The first region is complementary to the DNA or RNA target of interest, and the second region is complementary to a portion of a single-stranded DNA circle. On the addition of the enzyme mix, DNA synthesis is initiated. The RCA product is a single-stranded piece of DNA made up of tandem repeats that are complementary to the circle, of which 10^4 copies of the circle may be produced at a single site (Zhong *et al.*, 2001). Following synthesis, the RCA product is detected via the decoration step, where labeled oligonucleotides are hybridized to the product.

The versatility and potential advantages of this platform become more apparent with respect to decorating the RCA product (which can be fluorescent or colorimetric) and providing the most attractive feature of RCA: the ability to multiplex. Multiplexing is a feature that is becoming increasingly more important and necessary in diagnostic assays. Linear RCA lends itself to multiplexing because the product remains tethered to the detection sandwich. This is in contrast to other signal amplification technologies such as enzyme labeled fluorescence (ELF) and tyramide signal amplification (TSA) methods, in which the products are distributed in the general vicinity of the original signal. In addition, although the ability to multiplex has been demonstrated (Breininger and Baskin, 2000; Zaidi *et al.*, 2000), the protocol is cumbersome as a result of the sequential rounds of hybridizations and development. *In situ* RCA (IS-RCA) can exist in a single-step multiplexed format where the only limitation is the availability of circles and spectrally separable fluorophores.

Molecular cytogenetics is important for the determination of *de novo* chromosomal rearrangements, detecting abnormalities of chromosomes in nondividing cells and studying structure and function of specific chromosomal regions. *In situ* hybridization (ISH) is an important technique for providing information regarding gene amplification such as HER-2/neu for the pathogenesis and prognosis of numerous solid tumors (Tanner *et al.*, 2000) and gene expression analysis. Although other technologies exist that can accomplish similar results in less time, the major advantage that ISH and immunohistochemistry (IHC) have over these technologies is the fact that they can indicate which specific organelles or cells are undergoing these changes in the context of a whole cell or tissue. PCR and other solution-based assays can determine the presence of a particular mutation or transcript but not which cell has undergone a potentially damaging event or infection with viral sequences.

ISH protocols need to accomplish sufficient levels of sensitivity without loss of specificity while allowing for penetration of the probes into cells and tissues without significant loss of morphology. The majority of ISH protocols use probes in excess of 100 nucleotides. However, with the aid of signal amplification technologies such as TSA, ELF, branched DNA (bDNA), and EnVision[+], the size of these probes can be reduced,

which may result in increased ease of penetration into the cell and increased sensitivity. Although these signal amplification techniques can provide an increase in sensitivity, they may also cause an increase in background, loss of morphology, and less signal localization (Schmidt *et al*., 1997). The current limits of detection for ISH have been determined to be about 40 kb of target DNA and 10–20 copies of mRNA or viral DNA/cell (Speel, 1999).

Catalyzed reporter deposition (CARD) systems, also referred to as TSA, are based on the peroxidase-mediated deposition of haptenized tyramine molecules (Bobrow *et al*., 1989). It has demonstrated the greatest potential for providing increased sensitivity for ISH applications while providing versatility with respect to either colorimetric or fluorescent visualization. During the amplification reaction, the tyramine is converted into reactive oxidized intermediates by peroxidase, which then covalently binds to cell-associated proteins at or near the site of the horseradish peroxidase (HRP)–conjugated probe or protein. Although some diffusion does still occur, the spatial resolution is superior with peroxidase substrates rather than alkaline phosphatase substrates, but the products from the amplification reaction are still not tethered to the exact site. There are several different approaches for using TSA. The first is the use of biotin-labeled probes, which are detected by streptavidin-HRP conjugates, followed by the tyramine conjugated molecule (Schmidt *et al*., 1997). The second approach is to conjugate the HRP directly to the oligonucleotide (Leuhrsen *et al*., 2000; van de Corput *et al*., 1998), which has resulted in a reduction in noise. The increase in sensitivity provided by TSA remains somewhat controversial with numbers of up to 1000-fold improvement with respect to antibody dilution; in reality, however, improvements of 5- to 50-fold are more commonly observed (Speel, 1999). This increase in sensitivity is similar to EnVision[+], developed by Dako. EnVison[+] uses a dextran polymer to which HRP and an antibody are conjugated. This complex recognizes biotinylated probes and may provide an increase in signal of up to 40-fold (Wiedorn *et al*., 2001). Although this method has fewer steps than TSA, it is not as sensitive. Single-copy detection has been achieved with TSA (Adler *et al*., 1997; Schmidt *et al*., 1997) and does not appear to be as sensitive to fixation as *in situ* PCR. TSA has also been used to detect RNA and protein in frozen and paraffin-embedded formalin-fixed tissues (Zaidi *et al*., 2000) and alcohol fixed cells (Samama *et al*., 2002). The multiplexing capability of TSA has been examined, and, although it is possible, multiplexing requires sequential rounds of development after destroying residual peroxidase with 0.3% H_2O_2 (van Gijlswijk *et al*., 1997).

In situ PCR was successfully used for the detection of lentiviral DNA (Haase *et al*., 1990) and has been further studied and developed for the detection of human papilloma virus (HPV) DNA in formalin fixed tissues (Bernard *et al*., 1994) and metalloproteinases (Nuovo, 1997). *In situ* PCR protocols can use conventional ISH following amplification to detect the amplified sequence or incorporate reporter nucleotides, such as biotin or digoxigenin, during the amplification step. The incorporation of biotin or digoxigenin appears to only be successful when using frozen tissues (Nuovo, 2001). Although the development of *in situ* PCR protocols for use in clinical settings has been attempted for many years, the protocols have invariably ended up being cumbersome and fail to consistently reproduce the levels of sensitivity required (Speel *et al*., 1999). The result of successive rounds of high-temperature denaturation may not only contribute to the loss of morphology but also the loss of sensitivity as a result of the diffusion of the PCR product. This diffusion is dependent on fixation and increases significantly when cells are fixed in acetone or ethanol.

Assays of b-DNA hybridization have been used for quantitation of nucleic acid targets with a sensitivity of less than 100 molecules/ml (Collins *et al*., 1997) using linear signal amplification. The assay was developed to detect human immunodeficiency virus (HIV) viral load and consists of several rounds of hybridization of a series of oligonucleotide probes. It consists of the following: 1) the capture extenders, which capture the target and attach it to the solid support; 2) the label extenders, which hybridize to the captured target sequence; 3) preamplifiers, which anneal to the label extenders; 4) amplifier oligonucleotides, which anneal to the label extenders; and 5) the alkaline phosphatase-conjugated oligonucleotides (Collins *et al*., 1997). For the HIV assay, a total of 74 separate oligonucleotides to the HIV polymerase sequence were required. The b-DNA technology has since been adapted for use *in situ*, with the ability to detect single-copy targets such as HPV genomes in cervical carcinoma cell lines (Player *et al*., 2001) and HPV RNA and DNA sequences in paraffin-embedded tissues (Kenny *et al*., 2002). However, to achieve this level of sensitivity, as with the solution assay, a cocktail of up to 30 oligonucleotides was required, which does raise the question of how much increase in sensitivity is truly provided when single copy sensitivity can be accomplished with the use of TSA and a single probe of 619 bp (Adler *et al*., 1997). In addition, the likelihood of successfully being able to multiplex is severely reduced.

The purpose of this review is to demonstrate the utility of IS-RCA in a clinical setting. Although other laboratories have demonstrated the use of padlock

probes and other ligase-mediated methods for target and signal amplification, these methods are unlikely to be incorporated into existing clinical diagnostic protocols in the immediate future because of their sensitivity to fixation and duration of the protocol. Therefore, the constraints on this work were to develop assays that could be easily introduced into existing clinical diagnostic tests without requiring additional equipment and could be used easily. The assays needed to provide increased sensitivity without loss of specificity and have a wide dynamic range while being compatible with conventional fixatives. As a result, the protocols presented are compatible with clinically relevant fixatives and permeabilization procedures with no more than two to three additional steps when compared to conventional ISH protocols.

MATERIALS AND METHODS

Protocol for Detection of Lambda and Kappa RNA in Formalin-Fixed Paraffin-Embedded Tissues

MATERIALS

1. 20X SSC stock solution.
2. 1 M Tris (pH 7.4).
3. 50X Denhardt's solution.
4. 1 M potassium glutamate.
5. 1 M magnesium acetate.
6. 10 mM each dATP, dCTP, dGTP, dTTP.
7. 1 M HEPES (pH 7.4); pH with potassium hydroxide.
8. 1 M DTT.
9. 3% H_2O_2.
10. Proteinase K: 5 µg/ml in 50 mM Tris pH 7.5.
11. 10% CHAPS: Dissolve 1 g of CHAPS in water. Aliquot and store at −20°C.
12. 50% dextran sulfate: Dissolve 50 g of dextran sulfate in 40 ml deionized water; stir until dissolved. Bring volume to 100 ml with deionized water.
13. 10 mg/ml bovine serum albumin (BSA): Dissolve 10 mg of BSA in 1 ml water and store at −20°C.
14. Hybridization buffer: 25% formamide, 20 mM HEPES (pH 7.4), 300 mM NaCl, 1X Denhardt's, 10% dextran sulfate.
15. TBST: 50 mM Tris (pH 7.4), 150 mM NaCl, 0.1% Triton X-100.
16. −Magnesium mix: 200 mM potassium glutamate, 35 mM HEPES (pH 7.4), 7 mM DTT, 70 µg/ml BSA, 5% glycerol, 400 µM dATP, dCTP, dGTP, dTTP, 150 nM phi 29.
17. +Magnesium mix: 200 mM potassium glutamate, 35 mM HEPES (pH 7.4), 20 mM Mg acetate,

7 mM DTT, 70 µg/ml BSA, 5% glycerol, 400 µM dATP, dCTP, dGTP, dTTP.
18. Decoration buffer: 0.5% CHAPS, 10 mM Tris pH 7.5, 2X SSC, 2X Denhardt's, 10% dextran sulfate.

METHOD

1. Bake slides for 60 min at 65°C.
2. Deparaffinize slides by incubating for 2 min each through the following series.
3. 3X Xylene, 2X 100% ethanol, 2X 95% ethanol, 2X deionized water.
4. Quench slides in 3% H_2O_2 for 10 min.
5. Wash slides in water.
6. Treat with proteinase K for 30 min at 37°C, at 5 µg/ml.
7. Rinse slides in water.
8. Dehydrate slides in 95% ethanol followed by 100% ethanol for 2 min each.
9. Air-dry slides before applying probes.
10. Denature probe and circle mixture by incubating at 90°C for 2 min and quenching on ice.
11. Apply denatured probe mix, coverslip, and incubate for 2 hrs at 37°C.
12. Wash slides 3× for 5 min each in TBST at room temperature.
13. Rinse slides with 0.1 M potassium glutamate.
14. Apply −Mg mix and incubate for 30 min at 31°C.
15. Remove hybrislip, add +Mg mix and incubate for 60 min at 31°C.
16. Remove hybrislip, apply decorator (50 nM HRP-conjugated oligonucleotide), and incubate for 30 min at 37°C.
17. Remove hybrislips and wash 2–5 min in 0.2X SSC at room temperature.
18. Apply staining solution and incubate for 5 min.
19. Counterstain.
20. Rinse slides in deionized water and air dry.
21. Mount slides in Vectamount.

Protocol for the Detection of Human Papillomavirus DNA in Cervical Carcinoma Cell Lines

MATERIALS

1. PreservCyt.
2. Acetone.
3. Phosphate buffer saline (PBS).
4. 100%, 95% ethanol.

5. 1 M Tris (pH 7.5).

6. 1 M potassium glutamate.

7. 1 M magnesium acetate.

8. 1 M HEPES (pH 7.4).

9. 1 M DTT.

10. 50X Denhardt's.

11. 50% dextran sulfate.

12. 20X SSC stock solution.

13. 10 mM each dATP, dCTP, dGTP, dTTP.

14. Hybridization mix: 25% formamide, 20 mM HEPES (pH 7.4), 300 mM NaCl, 1X Denhardts, 10% dextran sulfate, 1 mM EDTA.

15. Formamide wash buffer: 50% formamide, 2X SSC.

16. TBST: 50 mM Tris (pH 7.4), 150 mM NaCl, 0.1% Triton X-100.

17. Enzyme delivery buffer: 200 µg/ml BSA, 400 µM each dATP, dCTP, dGTP, dTTP, 10 mM ammonium sulfate, 50 mTris pH 8.0, 150 nM phi29.

18. +Magnesium mix: 200 mM potassium glutamate, 35 mM HEPES pH 7.4, 20 mM Mg acetate, 7 mM DTT, 70 µg/ml BSA, 5% glycerol, 400 µM dATP, dCTP, dGTP, dTTP.

19. Decoration buffer: 0.5% CHAPS, 10 mM Tris pH 7.5, 2X SSC, 2X Denhardt's, 10% dextran sulfate.

20. DAPI counterstain.

21. Prolong Antifade (Molecular Probes).

METHOD

1. Rehydrate slides in PBS followed by deionized water for 3 min each.

2. Dehydrate slides in 95% ethanol, 100% ethanol for 3 min each.

3. Air-dry slides.

4. Dip slides in acetone for 5 seconds at −20°C, and allow slides to air-dry for 10 min.

5. Apply probe-circle (5 nM bispecific probe and 5 nM circle) mixture and coverslip.

6. Denature slides for 2 min at 95°C.

7. Hybridize at 37°C for 30 min.

8. Soak slides in formamide wash buffer to remove coverslips.

9. Wash in formamide wash buffer for 5 min at room temperature.

10. Wash 2× for 5 min each in TBST at 50°C.

11. Rinse slides in −Mg buffer.

12. Apply enzyme delivery mix and incubate for 10 min at 4°C.

13. Remove hybrislip apply +Magnesium mix, and incubate at 31°C for 16 hrs.

14. Remove hybrislip, apply fluorescent decorator (200 nM), and incubate for 30 min at 37°C.

15. Wash 2–5 min in 0.2X SSC.

16. Counterstain.

17. Rinse with PBS.

18. Air-dry slides and mount in Prolong antifade.

Protocol for Fixing Cervical Carcinoma Cell Lines in PreservCyt

MATERIALS

1. Cytocentrifuge (Wescor).

2. Dulbecco's PBS.

3. PreservCyt.

4. Superfrost Plus slides.

5. Trypsin.

METHOD

1. Trypsinize and wash cells.

2. Rinse in Dulbecco's PBS.

3. Resuspend at 1×10^5 cells/mL in PreservCyt.

4. Spin onto slides.

5. Allow slides to air-dry.

RESULTS

The goal was to develop molecular diagnostic assays that could provide increased sensitivity without loss of specificity or morphology. In addition, given the number of amplification technologies available, it was necessary to benchmark RCA with the most sensitive technology currently available, which appeared to be TSA. Several model systems have been used to develop IS-RCA protocols. For the detection of DNA targets the detection of HPV was used. The HPV system is used commonly to benchmark new technologies for *in situ* assays because it provides the opportunity to examine sensitivity and specificity simultaneously as a result of the availability of different cervical cell lines that vary with respect to copy number and type of HPV integrated. HPV has clinical relevance and applications because certain serotypes of HPV have been linked with the onset of cervical cancer. With the introduction of the Pap test there has been a 74% decline in cervical cancer–related deaths. The Pap test is graded according to the morphology of the cells. Even with the success of the Pap test, 4 million smears are classified as ASCUS (atypical squamous cells of undetermined significance), which invariably results in these women undergoing unnecessary colposcopy. Current testing relies on a homogenate of the entire cellular sample

and is separate from the diagnostic slide. Therefore, from a clinical perspective the ability to combine HPV testing with cytologic screening could be beneficial for better triaging women diagnosed with ASCUS or low-grade lesions. RNA targets were also examined, which included epidermal growth factor receptor and lambda or kappa immunoglobulin light chains. The development of an IS-RCA protocol required numerous factors to be addressed such as fixation, permeabilization, delivery and hybridization of the probe and circle, choice of polymerase, maximizing the decoration of the RCA product, and the multiplexing capability.

In a clinical laboratory the issue of fixation is critical. For tissues, the use of formalin and paraffin embedding is the conventional method. For the development of an HPV assay, the use and optimization of formalin fixed cells would not necessarily be of much use because the majority of cervical specimens are fixed in PreservCyt, a methanol-based fixative. The three fixatives used were paraformaldehyde, formalin, and PreservCyt. As a different result, methods of permeabilization needed to be examined to maximize the delivery of the probe and circle without the loss of morphology. Proteinase K was determined to be optimal for tissues, whereas pepsin was used for paraformaldehyde fixed cells; for PreservCyt fixed cells, acetone treatment resulted in maximal permeabilization.

The issue of probe hybridization is paramount in all ISH protocols, and RCA is no different. Unlike the majority of ISH protocols, RCA has three distinct DNA hybridization events: the hybridization of the bispecific probe to the target, the circle to the probe, and the decorator to the product. Hybridization of the bispecific probe to the target sequence used to be a separate event from the circle hybridization. Following optimization, it was found that equimolar amounts of the circle and bispecific probe could be hybridized simultaneously, thus reducing the number of steps but also the amount of circle by 40-fold. The combination of the circle and probe hybridization events resulted in no loss of sensitivity or specificity and was determined by both RCA and TSA. An additional minimizing step was attempted by combining the decorator into the RCA mix. However, although it was possible to decorate the RCA product during synthesis, maximum sensitivity was achieved by separating these steps. One reason for this could be because the RCA mix may not have provided optimum hybridization conditions, which could be especially true when using the enzyme-conjugated decorators.

The choice of polymerases for use in the RCA reactions has been studied extensively. For IS-RCA and IHC applications, native T7 and phi29 polymerases were found to provide the greatest sensitivity. Although both enzymes behaved in a similar manner for ImmunoRCA applications and some RNA detection assays in tissues, phi29 was found to consistently provide greater levels of sensitivity. Therefore, for all protocols in this review, phi29 is the enzyme of choice. In addition to the increased sensitivity, phi29 does not require any accessory proteins, in contrast to T7, which requires SSB for maximal synthesis. The DNA polymerase from the *Bacillus subtilis* bacteriophage phi29 is a monomeric protein of 66 kDa and is one of the smallest known replicases (Blanco and Salas, 1996). It is an incredibly processive enzyme capable of producing products of up to 70 kb in length at a rate of 80–200 nucleotides per second, with strand displacement activity (Blanco *et al*., 1989), but it lacks strand-switching capabilities (Canceill *et al*., 1999), an essential feature for the linear RCA reaction. Enzymes with the tendency to strand-switch, such as Klenow, may reduce the sensitivity of the linear RCA reaction because the final RCA product would be partially double-stranded. In addition to the processivity and strand displacement activity, the polymerization reaction can last for at least 12 hrs (Baner *et al*., 1998). Unlike PCR, RCA requires no temperature cycling, which can be advantageous when trying to maintain morphology. However, as a result of the lack of cycling, RCA has only one opportunity to achieve maximum specificity, and because of the processivity of phi29, once it is bound to a DNA target, it is unlikely to release. Therefore the ability to deliver the enzyme to the "correct" 3′-end is critical when working with cells and tissues because the opportunity for phi29 to bind to a multitude of targets is very great. The optimization of an enzyme delivery buffer that lacks magnesium proved to be extremely beneficial when attempting to deliver the enzyme into the nucleus, which resulted in an increase of the number of cells that had signal and the total amount of signal. One hypothesis is the absence of magnesium serves to destabilize the enzyme and reduce its affinity for DNA; thus, it successfully loads the enzyme onto more probe-circle complexes. On the addition of the magnesium mix the pre-loaded enzymes are primed and start synthesizing simultaneously. Depending on the level of sensitivity required the reaction time could be increased to run overnight. Running the reaction overnight enabled the detection of single HPV sequences.

Decoration is another step in which versatility was built into the protocol. The IS-RCA protocols have the opportunity to use fluorescent or colorimetric detection systems. When a fluorescent endpoint is desired, the decorator oligonucleotides can be labeled with the desired fluorophore. Alternatively, for tissue systems

requiring a colorimetric HPV assay, the use of HPR- or alkaline phosphotase (AP)-conjugated oligonucleotides was indicated. In both cases multiplexing is possible, which would not be the case were labeled nucleotides incorporated into the RCA product during the synthesis. For fluorescent multiplexing protocols it has been possible to detect RNA and DNA targets simultaneously within the same cell without the loss of sensitivity, specificity, or the addition of steps to the protocol. This is a distinct advantage compared to multiplexing with TSA.

For the HPV model system, cells were treated in a manner that would closely emulate the handling of patient samples. The cells were fixed in PreservCyt and cytocentrifuged onto slides. In contrast to bDNA protocols, which require cocktails of up to 30 target oligonucleotides, IS-RCA was able to accomplish similar levels of sensitivity by detecting single copies of HPV 16 sequences in SiHa cells. Both fluorescent and colorimetric assays have been used with similar levels of sensitivity. Maximal signal was observed in SiHa cells after polymerization had run for 16 hrs. Although this amount of time was not necessary for the detection of HPV sequences in CaSki cells, it demonstrated the wide dynamic range of RCA.

Initial experiment for the detection of RNA used bispecific probes to epidermal growth factor receptor (EGFR). Sense and antisense probes to EGFR were designed, and EGFR mRNA was only detected in A431 cells followed by numerous tissue sections with an improved level of sensitivity with the sense probe. When comparing IS-RCA with TSA, serial dilutions of the bispecific probe were made and run with either TSA or RCA protocols. Signal was still observed at 25 pM probe using RCA, whereas the signal with TSA was barely detectable at 2.5 nM. Similar results were obtained in both paraformaldehyde fixed cells and formalin fixed tissues. Therefore RCA resulted in a 10- to 100-fold improvement in sensitivity with respect to probe concentration over TSA.

DISCUSSION

The ability to study molecular events within the confines of a cellular environment has become more feasible and capable of providing more information. As a result, the demand for ISH procedures in clinical diagnostics has significantly increased (Becich, 2000). Amplification technologies that can provide improved sensitivity in conjunction with the opportunity to study multiple events within live or fixed cells are improving. Multiparameter testing is becoming essential when studying pathologic events because few cellular events are carried out by single-step processes or proteins.

The use of spectrally separable fluorescent dyes has enabled the detection of multiple targets simultaneously.

An alternative to fluorescent dyes is the use of nanocrystals or quantum dots (Mitchell, 2001). Quantum dots (QDs) can be 1.5–10 nm in diameter, and when compared with fluorophores such as rhodamine, can provide signals that are at least 20 times as bright and 100 times as photostable and spectral width that is one-third as wide; also, because of their inert coating, they are less toxic (Wu *et al*., 2003). QDs provide an alternative to green fluorescent protein for studying events in live cells (Jaiswal *et al*., 2003), and they have been used successfully in fixed cells. The use of an immunoglobulin G–conjugated QD enabled the detection of Her2 protein in paraformaldehyde fixed cells (Wu *et al*., 2003), whereas detection of DNA targets has been achieved using oligonucleotide-conjugated QDs (Dubertret *et al*., 2002).

The move toward cellular and functional genomics has begun, and the incorporation of new technologies such as QDs and RCA into ISH protocols will provide more information to the pathologist. Single-cell gene expression profiling using multiple labeled probes and computational fluorescence microscopy has made it possible to simultaneously visualize the specific transcription sites for 11 genes (Femino *et al*., 1998; Levsky *et al*., 2002). As a result transcription site analysis can enable the monitoring of allele silencing, analysis of active regions of the chromatin, determination of ploidy, and detection of changes in gene expression regardless of total transcript abundance. In contrast, microarray analysis will measure stability and abundance levels of transcripts (Levsky *et al*., 2002).

ISH is an important diagnostic technique that enables the detection of viral sequences, chromosomal rearrangements, and gene expression analysis at the subcellular level for numerous developmental, inflammatory, metabolic, infectious, and neoplastic diseases. Sensitivity and specificity are the criteria that will continue to determine the success of any technology being developed for ISH. As a result of the heterogeneity of tumors, the detection of gene expression in cells and tissues will affect diagnostic accuracy and classification. The advent of laser microdissection along with the development of tissue microarrays is providing the ability for high throughput screening of tissues by comparing expression profiles of normal and cancerous cells. Whereas the size of the collected samples has decreased, the amount of information has increased, to the point where new specimen handling the conjunction with improved ISH detection procedures are affecting the management of treatment from diagnosis and prognosis through choice of therapy and monitoring the success of the chosen therapy.

References

Adams, J.C. 1992. Biotin amplification of biotin and horseradish peroxidase signals in histochemical stains. *J. Histochem. Cytochem. 40*:1457–1463.

Adler, K., Erickson, T., and Bobrow, M. 1997. High sensitivity detection of HPV-16 in SiHa and CaSki cells utilizing FISH enhanced by TSA. *Histochem. Cell Biol. 108*:321–324.

Baner, J., Nilsson, M., Mendel-Hartvig, M., and Landegren, U. 1998. Signal amplification of padlock probes by rolling circle replication. *Nucleic Acids Res. 26*:5073–5078.

Becich, M.J. 2000. Information management: Moving from test results to clinical information. *Clin. Leadersh. Manag. Rev. 14*:296–300.

Bernard, C., Mougin, C., Bettinger, D., Didier, J.M., and Lab, M. 1994. Detection of human papillomavirus by *in situ* polymerase chain reaction in paraffin-embedded cervical biopsies. *Mol. Cell. Probes 8*:337–343.

Blanco, L., and Salas, M. 1996. Relating structure to function in phi29 DNA polymerase. *J. Biol. Chem. 271*:8509–8512.

Blanco, L., Bernad, A., Lazaro, J.M., Martin, G., Garmendia, C., and Salas, M. 1989. Highly efficient DNA synthesis by the phage phi29 DNA polymerase. *J. Biol. Chem*. *264*:8935–8940.

Bobrow, M.N., Harris, T.D., Shaughnessy, K.J., and Litt, G.J. 1981. Catalyzed reporter deposition, a novel method of signal amplification. Application to immunoassays. *J. Immunol. Methods 125*:279–285.

Breininger, J.F., and Baskin, D.G. 2000. Fluorescence in situ hybridization of scarce leptin receptor mRNA using the enzyme-labeled fluorescent substrate method and tyramide signal amplification. *J. Histochem. Cytochem. 48*:1593–1599.

Canceill, D., Viguera, E., and Ehrlich, S.D. 1999. Replication slippage of different DNA polymerases is inversely related to their strand displacement efficiency. *J. Biol. Chem. 274*:27481–27490.

Christian, A.T., Pattee, M.S., Attix, C.M., Reed, B.E., Sorensen, K.J., and Tucker, J.D. 2001. Detection of DNA point mutations and mRNA expression levels by rolling circle amplification in individual cells. *Proc. Natl. Acad. Sci. USA 98*:14238–14243.

Collins, M.L., Irvine, B., Tyner, D., Fine, E., Zayati, C., Chang, C., Horn, T., Ahle, D., Detmer, J., Shen, L., Kolverg, J., Bushnell, S., Urdea, M.S., and Ho, D.D. 1997. A branched DNA signal amplification assay for quantification of nucleic acid targets below 100 molecules/ml. *Nucleic Acids Res. 25*:2979–2984.

Dubertret, B., Skourides, P., Norris, D.J., Noireaux, V., Brivanlou, A.H., and Libchaber, A. 2002. In vivo imaging of quantum dots encapsulated in phospholipid micelles. *Science 298*:1759–1762.

Faruqi A.F., Hosono S., Driscoll M.D., Dean F.B., Alsmadi O., Bandaru R., Kumar G., Grimwade B., Zong Q., Sun Z., Du Y., Kingsmore S., Knott T., and Lasken R.S. 2001. High-throughput genotyping of single nucleotide polymorphisms with rolling circle amplification. *BMC Genomics 2*:4.

Femino, A.M., Fay, F.S., Fogarty, K., and Singer, R.H. 1998. Visualization of single RNA transcripts *in situ*. *Science 280*:585–590.

Fire, A., and Xu, S. 1995. Rolling replication of short DNA circles. *Proc. Natl. Acad. Sci. USA 92*:4641–4645.

Gusev, Y., Sparkowski, J., Raghunathan, A., Ferguson, H., Montano, J., Bogdan, N., Schweitzer, B., Wiltshire, S., Kingsmore, S.F., Maltzman, W., and Wheeler, V. 2001. Rolling circle amplification: A new approach to increase sensitivity for immunohistochemistry and flow cytometry. *Am. J. Pathol. 159*:63–69.

Haase, A.T., Retzel, E.F., and Staskus, K.A. 1990. Amplification and detection of lentiviral DNA inside cells. *Proc. Natl. Acad. Sci. USA 87(13)*:4971–4975.

Jaiswal, J.K., Mattoussi, H., Mauro, J.M., and Simon, S.M. 2003. Long-term multiple color imaging of live cells using quantum dot bioconjugates. *Nature Biotech. 21*:47–51.

Kenny, D., Shen, L., and Kolberg, J.A. 2002. Detection of viral infection and gene expression in clinical tissue specimens using branched DNA (bDNA) *in situ* hybridization. *J. Histochem. Cytochem. 50*:1219–1227.

Kool, E.T. 1996. Circular oligonucleotides: New concepts in oligonucleotide design. *Annu. Rev. Biophys. Biomol. Struct. 25*:1–28.

Leuhrsen, K.R., Davidson, S., Lee, Y.J., Rouhani, R., Soleimani, A., Raich, T., Cain, C.A., Collarini, E.J., Yamanishi, D.T., Pearson, J., Magee, K., Madlansacay, M., Bodepudi, V., Davoudzadeh, D., Schueler, P.A., and Mahoney, W. 2000. High-density hapten labeling and HRP conjugation of Oligonucleotides for use as in situ hybridization probes to detect mRNA targets in cells and tissues. *J. Histochem. Cytochem. 48*:133–145.

Levsky, J.M., Shenoy, S.M., Pezo, R.C., and Singer, R.H. 2002. Single-cell gene expression profiling. *Science. 297*:836–840.

Lizardi, P.M., Huang, Z., Zhu, Z., Bray-Ward, P., Thomas, D.C., and Ward, D.C. 1998. Mutation detection and single-molecule counting using isothermal rolling-circle amplification. *Nat. Genet. 19*:225–232.

Mitchell, P. 2001. Turning the spotlight on cellular imaging. *Nature Biotech. 19:*1013–1017.

Nilsson, M., Malmgren, H., Samiotaki, M., Kwiatkowski, M., Chowdhary, B.P., and Landegren, U. 1994. Padlock probes: circularizing oligonucleotides for localized DNA detection. *Science 265*:2085–2088.

Nallur, G., Luo, C., Fang, L., Cooley, S., Dave, V., Lambert, J., Kukanskis, K., Kingsmore, S., Lasken, R., and Schweitzer, B. 2001. Signal amplification by rolling circle amplification on DNA microarrays. *Nucleic Acids Res. 29*:E118.

Nuovo, G.J. 1997. *In situ* detection of PCR-amplified metalloproteinase cDNAs, their inhibitors and human papillomavirus transcripts in cervical carcinoma cell lines. *In. J. Cancer. 71*:1056–1060.

Nuovo, G.J., Gallery, F., Hom, R., MacConnell, P., and Block, W. 1993. Importance of different variables for enhancing *in situ* detection of PCR-amplified DNA. *PCR Methods Appl. 2*:305–312.

Pickering, J., Bamford, A., Godbole, V., Briggs, J., Scozzafava, G., Roe, P., Wheeler, C., Ghouze, F., and Cuss, S. 2002. Integration of DNA ligation and rolling circle amplification for the homogeneous, end-point detection of signal nucleotide polymorphisms. *Nucleic Acids Res. 30*:1–7.

Player, A.N., Shen, L., Kenny, D., Antao, V.P., and Kolberg, J.A. 2001. Single-copy detection using branched DNA (bDNA) *in situ* hybridization. *J. Histochem. Cytochem. 49*:603–611.

Samama, B., Plas-Roser, S., Schaeffer, C., Chateau, D., Fabre, M., and Boehm, N. 2002. HPV DNA detection by *in situ* hybridization with catalyzed signal simplification on thin-layer cervical smears. *J. Histochem. Cytochem. 50*:1417–1420.

Schmidt, B.F., Chao, J., Zhu, Z., DeBiasio, R.L., and Fisher, G. 1997. Signal amplification in the detection of single-copy DNA and RNA by enzyme-catalyzed deposition (CARD) of the novel fluorescent reporter substrate Cy3.29-tyramide. *J. Histochem. Cytochem. 45*:365–373.

Schweitzer, B., Roberts, S., Grimwade, B., Shwo, W., Wang, M., Fu, Q., Shu, Q., Laroche, I., Zhou, Z., Tchernev, V.T., Christiansen, J., Velleca, M., and Kingsmore, S.F. 2002. Multiplexed protein profiling on microarrays by rolling-circle amplification. *Nature Biotech. 20*:359–365.

Schweitzer, B., Wiltshire, S., Lambert, J., O'Malley, S., Kukanskis, K., Zhu, Z., Kingsmore, S.F., Lizardi, P.M., and Ward, D.C. 2000. Immunoassays with rolling circle DNA amplification: A versatile platform for ultrasensitive antigen detection. *Proc. Natl. Acad. Sci.USA 97*:10113–10119.

Speel, E.J.M. 1999. Detection and amplification systems for sensitive, multiple-target DNA and RNA *in situ* hybridization: Looking inside cells with a spectrum of colors. *Histochem. Cell Biol. 112*:89–113.

Speel, E.J.M., Hopman, A.H.N., and Komminoth, P. 1999. Amplification methods to increase the sensitivity of *in situ* hybridization: Play CARD(S). *J. Histochem. Cytochem. 47*:281–288.

Tanner, M., Gancberg, D., Di Leo, A., Larsimont, D., Rouas, G., Piccart, M.J., and Isola, J. 2000. Chromogenic *in situ* hybridization: A practical alternative for fluorescence *in situ* hybridization to detect HER-2.neu oncogene amplification in archival breast cancer samples. *Am. J. Pathol. 157*:1467–1472.

Thomas, D.C., Nardone, G.A., and Randall, S.K. 1999. Amplification of padlock probes for DNA diagnostics by cascade rolling circle amplification or the polymerase chain reaction. *Arch. Pathol. Lab. Med. 123*:1170–1176.

van de Corput, M.P.C., Dirks, R.W., van Gijlswijk, R.P.M., van Binnendijk, E., Hattinger, C.M., de Paus, R.A., Landegent, J.E., and Raap, A.K. 1998. Sensitive mRNA detection by fluorescence *in situ* hybridization using horseradish peroxidase-labeled oligodeoxynucleotides and tyramide signal amplification. *J. Histochem. Cytochem. 46*:1249–1259.

van Gijlswijk, R.P.M., Zijlmans, H.J.M.A.A., Wiegant, J., Bobrow, M.N., Erickson, T.J., Adler, K.E., Tanke, H.J., and Raap, A.K. 1997. Fluorchrome-labeled tyramides: Use in immunocytochemistry and fluorescence *in situ* hybridization. *J. Histochem. Cytochem. 45*:375–382.

Wiedorn, K.H., Goldmann, T., Henne, C., Kuhl, H., and Vollmer, E. 2001. EnVision+, a new dextran polymer-based signal enhancement technique for *in situ* hybridization (ISH). *J. Histochem. Cytochem. 49*:1067–1071.

Wu, X., Liu, H., Liu, J., Haley, K.N., Treadway, J.A., Larson, J.P., Ge, N., Peale, F., and Bruchez, M.P. 2003. Immunofluorescent labeling of cancer marker Her2 and other cellular targets with semiconductor quantum dots. *Nature Biotech. 21*: 41–46.

Zaidi, A.U., Enomoto, H., Milbrandt, J., and Roth, K.A. 2000. Dual fluorescent *in situ* hybridization and immunohistochemical detection with tyramide signal amplification. *J. Histochem. Cytochem. 48*:1369–1375.

Zhong, X., Lizardi, P.M., Huang, X., Bray-Ward, P.L., and Ward, D.C. 2001. Visualization of oligonucleotide probes and point mutations in interphase nuclei and DNA fibers using rolling circle DNA amplification. *Proc. Natl. Acad. Sci. USA 98*:3940–3945.

Zhou, Y., Calciano, M., Hamann, S., Leamon, J.H., Strugnell, T., Christian, M.W., and Lizardi, P.M. 2001. *In situ* detection of messenger RNA using digoxigenin-labeled oligonucleotides and rolling circle amplification. *Exptl. Mol. Pathol. 70*:281–288.

This Page Intentionally Left Blank

8

Direct, *in situ* Assessment of Telomere Length Variation in Human Cancers and Preneoplastic Lesions

Alan Meeker, Wesley R. Gage, Angelo De Marzo, and Anirban Maitra

Introduction

Grossly abnormal karyotypes, displaying both numeric and structural changes, are a nearly universal finding in human epithelial malignancies, reflecting either a transient or ongoing state of chromosomal instability (Lengauer *et al*., 1998). This observation may be interpreted as a manifestation of a mutator phenotype acting at the chromosomal level and likely appears early in tumorigenesis (Shih *et al*., 2001). Several genes involved in the maintenance of chromosomal stability have been identified, and, as such, they represent candidate mutational targets for karyotype destabilization (Hartwell, 1992). However, defects in such genes have so far been implicated in only a small subset of human cancer cases, and these primarily affect chromosome number. Thus, the molecular mechanisms underlying chromosomal instability, particularly those involved in the generation of complex chromosomal rearrangements, in the majority of human cancers remain a mystery.

The transition from normal to cancer is thought to require the accumulation of multiple somatic genomic alterations in key cancer-associated genes (Fearon and Vogelstein, 1990). Given the extremely low basal mutation rate of normal human somatic cells, it has been proposed that an underlying genetic instability must exist in cancer progenitor cells, resulting in the generation of a sufficient number of such clonal genetic changes (Loeb, 1991). Although it is well recognized that tumor-associated genetic instability operates at the level of the chromosomes (Lengauer *et al*., 1998; Loeb, 2001), the precise timing of chromosomal instability during tumorigenesis has not been well characterized.

One path to chromosomal instability is via telomere dysfunction (Gisselsson *et al*., 2000). Telomeres are composed of specialized deoxyribonucleic acid (DNA) tandem repeats complexed with telomere-binding proteins, located at the ends of linear chromosomes (Blackburn, 1991). Telomeres stabilize chromosomes by preventing deleterious recombinations and fusions; they also keep cells from recognizing their chromosomal termini as DNA double-strand breaks. Telomeric DNA tracts are dynamic entities, subject to shortening during cell division as a result of their incomplete replication

Handbook of Immunohistochemistry and in situ Hybridization of Human Carcinomas,
Volume 2: Molecular Pathology, Colorectal Carcinoma, and Prostate Carcinoma

83

(referred to as the "end replication problem") (Levy *et al*., 1992). In addition, telomeres may shorten as a result of cell turnover in the presence of unrepaired DNA strand breaks caused by oxidative damage (von Zglinicki, 2000).

Critically short telomeres become dysfunctional and, as demonstrated more than 50 years ago, loss of telomere function can be a major mechanisms for the generation of chromosomal abnormalities (McClintock, 1941). Chromosome end-to-end fusions ensue, producing dicentric, multicentric, and ring chromosomes that missegregate or break during mitosis, leading to a series of so-called breakage-fusion-bridge (BFB) cycles capable of generating aneusomies and the various types of structural abnormalities typically seen in human solid tumor karyotypes (Blasco *et al*.,1997; O'Hagan *et al*., 2002). It has been postulated that dysfunctional telomeres could play a causal role in tumorigenesis by instigating chromosomal instability, thus promoting neoplastic transformation (Bacchetti, 1996; Hastie *et al*., 1990). Results from telomerase knockout mouse models, in which animals possessing critically short telomeres exhibit an increased cancer incidence, support this concept (Blasco *et al*., 1997; Rudolph *et al*., 2001).

The combined observations of short telomeres, plus the frequent activation of telomerase in human cancers, suggest that the majority of tumors undergo critical telomere shortening at some point during their development. This could simply be a consequence of the end-replication problem combined with extensive cell turnover occurring during tumor expansion. However, if telomere shortening occurs early, it could be playing an important role during the initiation stage of tumorigenesis. Thus, the timing of the occurrence of telomere shortening during human cancer development is a critical question.

The vast majority of epithelial malignancies appear to develop from morphologically defined precursor lesions, termed intraepithelial neoplasia (IEN). Examinations to date have revealed evidence of gross genetic instability in IEN lesions, supporting an early role for genetic changes in malignant transformation (Qian *et al*., 1999; Shih *et al*., 2001). If telomere dysfunction is a major cause of this genetic instability, then signs of this dysfunction should likewise be evident in these early premalignant lesions. To test this, we developed and validated an *in situ* method for telomere length assessment telomere length fluorescent *in situ* hybridization (TEL-FISH) in formalin-fixed and paraffin-embedded (FFPE) human tissues (Meeker *et al*., 2002a). Application of this method to preinvasive precursor lesions of several human epithelial cancers—including those of prostate, pancreas, breast, large intestine, bladder, uterine cervix, esophagus, and oral cavity—demonstrated its utility (Meeker *et al*., 2004). We found clear evidence of telomere length abnormalities, primarily telomere shortening, and telomere length heterogeneity in the majority of IEN lesions from these human epithelial tissues (Figure 14). In this review we describe the detailed method for analyzing telomere lengths in archival tissue sections using this fluorescence *in situ* hybridization (FISH) protocol.

MATERIALS

1. ChemMate slides (Cat. No. 12-548-6A, Fisher Scientific, Newark, DE).
2. Xylene.
3. Ethanol (absolute, 95%, 70%).
4. A source of deionized water.
5. 1% Tween-20 detergent.
6. Citrate buffer (Target unmasking solution; Cat. No. H-3300, Vector Laboratories, Inc., Burlingame, CA).
7. Capillary gap tray (automated processor slide holder, or equivalent, Dako Corp., Carpinteria, CA).
8. Black and Decker Handy Steamer Plus (Black and Decker, Towson, MD).
9. Phosphate buffer saline with Tween (PBST) (Cat. No. P-3563, Sigma, St. Louis, MO).
10. Protease Type VIII (Cat. No. P-5380, Sigma) (*optional*; see later in this chapter).
11. Prolong Anti-fade Mounting Media (Cat. No. P-7481, Molecular Probes, Eugene, OR).
12. 1 M Tris (pH 7.5) (Cat. No. 15567-027, Gibco/BRL, Grand Island, NY).
13. B/M Blocking Reagent (10% in maleic acid; as per manufacturer's instructions; Cat. No. 1096-176, Boehringer-Mannheim, Indianapolis, IN).
14. 100% Formamide (Cat. No. 1814-320, Boehringer-Mannheim).
15. Bovine-albumin solution (Cat. No. A-7284, Sigma).
16. DAPI[4′-6-diamidino-2-phenylindole] (Cat. No. D-8417, Sigma).
17. Anti-mouse immunoglobulin G (IgG) fraction Alexa Fluor 488 (Molecular Probes, Cat. No. A-11029), or anti-rabbit IgG fraction Alexa Fluor 488 (Molecular Probes, Cat. No. A-11034) secondary antibody.
18. Peptide nucleic acid (PNA) telomere-specific hybridization probe, custom synthesized. Sequence = (N-terminus to C-terminus) CCCTAACCCTAACCC-TAA with an N-terminal covalently linked fluorescent dye—here we use Cy3. (Applied Biosystems, Framingham, MA).
19. Fluorescence microscope equipped with appropriate fluorescence filter set. Here, we use Omega Optical, XF38 filter set (Omega Optical Inc., Brattleboro, VT) for Cy3 visualization.
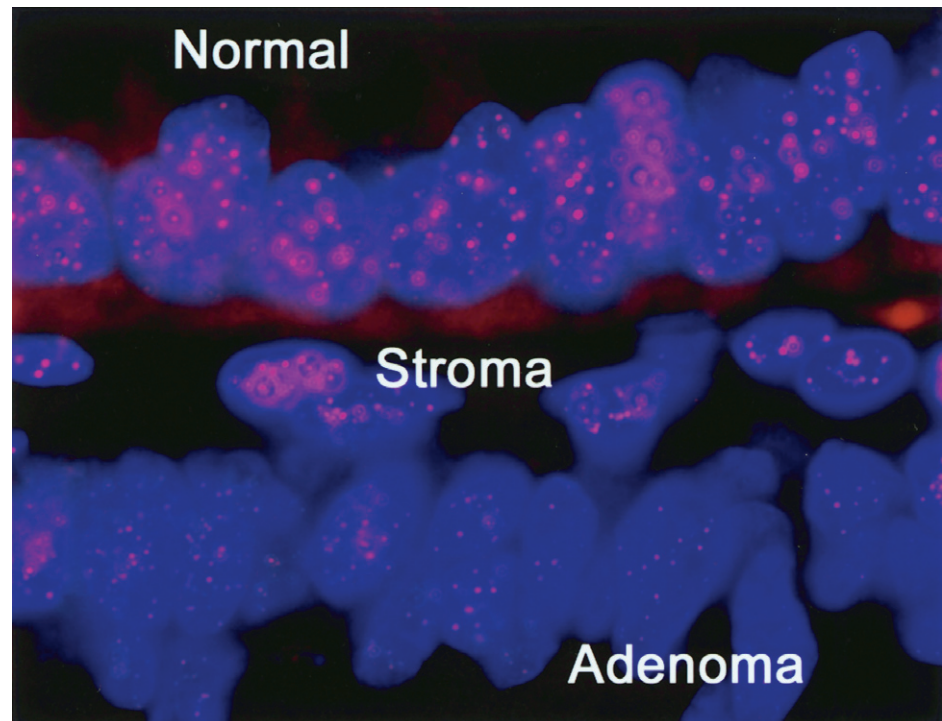20. Slide warmer.

Figure 14 Telomeric fluorescence *in situ* hybridization) (TEL-FISH) for telomere signal intensities demonstrate intense fluorescent signals in normal colonic epithelium and in stromal fibroblasts, whereas striking reduction in telomere signal intensity is observed in adenomatous (precancerous) epithelium.

METHOD

1. Prepare unstained slides. The specimens used are tissues that have undergone routine neutral-buffered formalin fixation followed by paraffin embedding. Ethanol-fixed tissues are also suitable. Typically, 4 or 5 μM thick sections are cut from the paraffin blocks and applied to ChemMate slides. These slides are suitably treated and marked to allow for capillary gap formation during stream treatment. Heating at high temperature or for prolonged periods should be avoided because this can cause increased background auto fluorescence.

2. Preheat slides to 65°C for 10 min to melt paraffin.

3. Transfer slides to staining rack and place them in xylene 2 × for 5 min each to remove paraffin (at this time, turn on slide rack warmer and steamer to preheat).

4. Hydrate slides through a graded ethanol series—absolute × 2, 95% × 2, and one change of 70%—and dip until clear (DUC).

5. Place slides in one change of deionized water, then place them in one change of deionized water with 0.1% Tween, DUC.

6. Pair slides to form capillary gaps between tissue sides, and then place into a cap gap tray (automated processor slide holder, Dako or equivalent) containing citrate buffer (target unmasking solution); steam for 14 min (Black and Decker Handy Steamer Plus).

7. Remove slides from steamer and let cool to room temperature (~5 min).

8. Place slides into PBS with Tween (PBST) × 5 min.

If you are not digesting the tissue with protease: Rinse in deionized water, 70% ethanol, 95% ethanol, and let air-dry. Then, proceed to Denaturation (*Step 9*). Otherwise, perform protease steps (a–d), and then proceed to Denaturation.

Protease Treatment

Depending on the tissue, degree of fixation, or particular antibody being used, the incubation time, protease type, and concentration may require optimization.

a. Place slides in protease solution (Protease Type VIII, 0.5 mg/ml in PBST) for 1 min at room temperature in a Coplin (50 ml) or PAP jar (holds 4 slides, 20 ml).

b. Rinse slides thoroughly with deionized water 4–5 times.

c. Place slides in 95% EtOH for 5 min.

d. Air-dry slides.

Sample Denaturation

Adjust temperature on slide warmer to prepare for denaturation. Do this by placing a small box (e.g., slide box) upside down over the heater surface with a surface-reading thermometer underneath the box. Cover the box with aluminum foil and allow to

equilibrate to temperature. Check thermometer, and adjust setting of slide warmer as necessary to obtain proper denaturation temperature under the enclosure. Remove tube of Prolong Anti-fade Mounting Media (Molecular Probes) from freezer to thaw.

Note: For this and all subsequent steps, keep slide(s) in darkness.

9. Dilute PNA telomere hybridization probe in PNA diluent buffer to a final concentration of 300 ng/ml. Carefully, so as to avoid introducing bubbles, place 35 μl of diluted PNA probe onto the specimen. Apply coverslip, again without introducing air bubbles, and denature at 83°C × 4 min in the dark (inverted slide box on preheated slide warmer).

PNA Diluent:

(recipe makes 1 ml; 35 μl required per slide)
0.29 ml distilled water
10 μl 1 M Tris (pH 7.5) (Cat. No. 15567-027, Gibco/BRL)
5 μl B/M Blocking Reagent, prepared as per manufacturer
0.7 ml 100% Formamide

10. Move slides to a dark closed container and hybridize for 2 hrs at room temperature. To thawed tube of Prolong, add 1 ml glycerol (supplied) and mix well. Mix occasionally to dissolve solid.

11. Carefully remove coverslips from slides and wash in darkness with PNA Wash Solution: 2 × 15 min each.

PNA Wash Solution:

(50 ml)
35 ml formamide
15 ml distilled water
0.5 ml 1 M Tris (pH 7.5)
165 μl 30% bovine serum albumin

12. TBST wash 3 × 5 min each.
   Note: If NOT conducting a double label (FISH + fluorescent antibody), skip to **Step 17** of this protocol.

Immunofluorescence Section
(for Antibody/FISH Double Label)

13. Rinse slides 1 × in PBST.

14. Apply appropriately diluted primary antibody. Incubate 45 min at room temperature or overnight at 4°C.

15. Rinse slides in PBST.

16. Apply appropriate fluorescent secondary antibody diluted 1:100 in Dulbecco's PBS. Incubate for 30 min at room temperature.

17. Rinse slides in PBST.

18. Drain slides and stain with DAPI for 1 min (1:10,000 dilution in water of a 5 mg/ml stock solution).

19. Rinse with PBST.

20. Rinse slides well in distilled water.

21. Drain slides and mount while still wet with coverslip using 1–2 drops of Prolong. Anti-fade Mounting Media solution or equivalent anti-fade solution. Avoid bubbles.

   Viewing: Fluorescent telomere signals are best viewed with 40X or higher oil immersion objectives. For Cy3-labeled PNA probes, we find we get good signals using an Omega Optical XF38 filter set (Omega Optical Inc.):
   Emission: OG 590 (Omega XF3016)
   Dichroic: DRLP 570 (Omega XF2015)
   Excitation: DF10 546 (Omega XF3016)

   Storage: Slides kept refrigerated (4°C) in the dark will retain signals for at least several weeks.

RESULTS AND DISCUSSION

The method described herein was developed to allow high-resolution telomere length assessment in human FFPE tissue sections, thus making the vast resources of archival tissues available for telomere length analysis. Validation of the method (Meeker *et al.*, 2002a) showed that intensity of the fluorescent telomeric (TEL-FISH) signals is linearly related to telomere length as determined independently via Southern blot analysis of telomeric restriction fragments. Unlike Southern analysis, TEL-FISH can be performed on very small, fixed specimens. Furthermore, providing single cell resolution completely avoids the confounding effects of cell type heterogeneity typically present in clinical specimens. It is important to note that because TEL-FISH can be combined with standard immunofluorescence and tissue architecture is maintained, direct comparisons between different regions or specific cell types are easily accomplished. Further information regarding regions of interest can be obtained by performing standard hematoxylin and eosin (H&E) staining following examination of the TEL-FISH slides by fluorescence microscopy. Finally, because the telomeric signal intensity is directly related to telomere length, quantitation is possible via standard image analysis techniques (Meeker *et al.*, 2002a).

TEL-FISH has proved useful in assessing telomere length abnormalities in cancerous and precancerous lesions. The vast majority (~95%) of IEN lesions examined, the earliest identifiable cancer precursors, are composed largely of cells possessing telomere length abnormalities, with most lesions displaying abnormally

short telomeres (Figure 14). It therefore appears that the telomere shortening frequently observed in malignant epithelial tumors has already occurred by the preinvasive stage (Meeker *et al.*, 2002a,b; Meeker *et al.*, 2004; van Heek *et al.*, 2002). Indeed, when both were present, invasive cancers and accompanying IEN lesions exhibited similar degrees of telomeric shortening.

Telomere length status may provide utility in predicting prognosis, as a novel endpoint for cancer chemoprevention studies, in the pathologic diagnosis of human cancer precursor lesions, and for prediction and monitoring patient response to anti-telomerase therapies. It is our hope that the method described here will prove to be a useful research tool for addressing these questions.

References

Bacchetti, S. 1996. Telomere maintenance in tumor cells. *Cancer Surv.* 28:197–216.

Blackburn, E.H. 1991. Structure and function of telomeres. *Nature* 350:569–572.

Blasco, M.A., Lee, H.W., Hande, M.P., Samper, E., Lansdorp, P.M., DePinho, R.A., and Greider, C.W. 1997. Telomere shortening and tumor formation by mouse cells lacking telomerase RNA. *Cell 91(1)*:25–34.

Fearon, E.R. and Vogelstein, B. 1990. A genetic model for colorectal tumorigenesis. *Cell 61(5)*:759–767.

Gisselsson, D., Pettersson, L., Hoglund, M., Heidenblad, M., Gorunova, L., Wiegant, J., Mertens, F., Dal, C., in, P., Mitalman, F., and Mandanl, N. 2000 Chromosomal breakage-fusion-bridge events cause genetic intratumor heterogeneity. *Proc Natl. Acad Sci. USA 97(10)*:5357–5362.

Hartwell, L. 1992. Defects in a cell cycle checkpoint may be responsible for the genomic instability of cancer cells. *Cell 71(4)*:543–546.

Hastie, N., Dempster, M. Dunlop, M., Thompson, A.M., Green D.K., and Allshire, R.C. 1990. Telomere reduction in human colorectal carcinoma and with ageing. *Nature 346*:866–868.

Lengauer, C., Kinzler, K.W. 1998. Genetic instabilities in human cancers. *Nature 396(6712)*:643–649.

Levy, M.Z., Allsopp, R.C., Futcher, A.B., Greider, C.B., and Hartey, C.B., 1992. Telomere end-replication problem and cell aging. *J. Mol. Biol. 225(4)*:951–960.

Loeb, L.A. 1991. Mutator phenotype may be required for multistage carcinogenesis. *Cancer Res. 51(12)*:3075–3079.

Loeb, L.A. 2001. A mutator phenotype in cancer. *Cancer Res. 61(8)*:3230–3239.

McClintock, B. 1941. The stability of broken ends of chromosomes in Zea mays. *Genetics 26*:234–282.

Meeker, A.K., Gage, W.R. Hicks, J.L., Simon, I., Cottman, J.R., Platz, E.A., March, G.E., and De Marzo A.M. 2002. Telomere length assessment in human arichival tissues: Combined telomere fluorescence in situ hybridization and immunostaining. *Am. J. Pathol. 160(4)*:1259–1268.

Meeker, A.K., Hicks, J.L., Platz, E.A., March, G. E., Bennett, C. J., Delannay, M.J., De Marzo, A.M. 2002b. Telomere shortening is an early somatic DNA alteration in human prostate tumorigenesis. *Cancer Res. 62(22)*:6405–6409.

Meeker, A.K., Hicks, J.L., Iacobuzio-Donahue, C.A., Montgomery, E.A., Westra, W.H., Chan, T.Y., Ronnett, B.M., and De Marzo, A.M., 2004. Telomere length abnormalities occur early in the initiation of epithelial carcinogenesis. *Clin. Cancer Res. 10(10)*:3317–3326.

O'Hagan, R.C., Chang, S., Maser, R.S., Mohan, R., Artandi, S.E., Chin, L., and DePinho, R.A. 2002. Telomere dysfunction provokes regional amplification and deletion in cancer genomes. *Cancer Cell 2(2)*:149–155.

Qian, J., Jenkins, R.B., and Bostwick, D.G. 1999. Genotic and chromosomal alterations in prostatic intraepithelial neoplasia and carcinoma detected by fluorescence in situ hybridization. *Eur. Urol. 35(5–6)*:479–483.

Rudolph, K.L., Millard, M., Bosenberg, M.W., and DePinho, R.A. 2001. Telomere dysfunction and evolution of intestinal carcinoma in mice and humans. *Nat. Genet. 28(2)*:155–159.

Shih, I.M., Zhou, W., Goodman, S.N., Lengauer, C., Kinzler, K.W., and Vogelstein, B. 2001. Evidence that genetic instability occurs at an early stage of colorectal tumorigenesis. *Cancer Res. 61(3)*:818–822.

van Heek, N.T., Meeker, A.K., Kern, S.E., Yeo, C.J., Lillemoe, K.D., Cameron, J.L., Offerhaus, G.J., Hicks, J.L., Wilentz, R.E., Goggins, M.G., De Marzo, A.M., Hruban, R.H., and Maitra, A. 2002. Telomere shortening is nearly universal in pancreatic intraepithelial neoplasia. *Am. J. Pathol. 161(5)*: 1541–1547.

von Zgylinicki, T. 2000. Role of oxidative stress in telomere length regulation and replicative sensescence. *Ann. N. Y. Acad. Sci. 908*:99–110.

This Page Intentionally Left Blank

9

Clinical Flow Cytometry of Solid Tumors

Mathie P.G. Leers and Marius Nap

Introduction

In surgical pathology, cytologic or histologic examinations are the most essential parts of daily practice to discriminate among benign, premaligant, and malignant cell proliferations. Although the clinical value of these examinations is not in doubt and despite the fact that in the majority of cases the diagnosis can be reliably established in this way, several attempts have been made to improve the cytologic and histologic diagnosis over the past 30 years. There is a continuous search for additional parameters, such as "predictors" for response to therapy or prognosis of the disease. In the past three decades it has been shown that immunophenotyping of tumor cells is very useful for the diagnosis, classification, prognostic evaluation, and detection of residual disease in patients with certain malignancies. Quantitative analysis of stained cells has played an important role in this respect. However, immunohistochemistry as an additional tool for the surgical pathologist is not always satisfactory. For example, clonality assessment in B-cell lymphomas is still difficult to perform with immunohistochemistry because of lack of staining contrast between surface-immunoglobulins and extracellular immunoglobulins (Taylor and Cote, 1994).

In addition, solid tumors are heterogeneous of composition. They consist of a mixture of normal stromal, inflammatory, and malignant cells. This heterogeneous cell composition is one of the limiting factors for reproducible quantification, for example, of steroid hormone receptor expression in breast carcinomas. In addition, immunohistochemistry is sensitive to many external factors interfering with accurate quantification of receptor content. For instance, staining intensity is influenced by the kind and duration of fixation, thickness of the tissue section, incubation conditions of the primary antibodies, choice and concentration of the chromogens, and often, subjective scoring by the investigators.

Furthermore, despite the high technical level of these tools, their application leads to qualitative results. The determination of a quantitative interrelationship of the various cell constituents making up the tumor tissue still remains a task with a high level of subjective influence. Yet, accurate quantification of certain cell biologic parameters can be of importance to improve the diagnosis and predict therapy response (e.g., the assessment of steroid hormone receptors for patients with breast cancer). The three most important keystones of tissue homeostasis, controlling expansion or regression in tumors, are cell proliferation, differentiation, and cell death (apoptosis). Carcinogenesis can be viewed as a process of cellular evolution in which individual cells acquire mutations that increase the survival

89

and/or proliferative capacity or decrease the apoptotic activity. The growth potential and behavior of human neoplasms is the net result of an imbalance between cell proliferation and cell death. Methods that allow the specific quantification of such cell biologic parameters may contribute to our understanding of the mutual relationship between these factors in tumor growth and aid in the management of malignancies. Moreover, tumors in general consist of more than one cell population, each with their own characteristics and behavior. It is very difficult to investigate the different tumor cell populations by light microscopy because of admixture with nonrelevant normal cells (e.g., inflammatory cells, stromal component). The previously mentioned aspects lead us to the conclusion that in a situation in which quantitative interpretation of cell characteristics is important, a different approach should be looked for. Flow cytometry is a technique that can tackle these problems.

MATERIALS AND METHODS

Principles of Flow Cytometry: The Hardware

Whereas immunohistochemistry and related techniques primarily deal with qualitative identification of phenotypic characteristics of cell components, flow cytometry is focused on the simultaneous detection, measurement, and registration of multiple parameters of thousands of cells that pass the laser beam.

Flow cytometers are instruments constructed to measure and record fluorescence intensity. The basic components of a flow cytometer include a light source, a flow chamber, and optical assembly. The measurements are usually performed on cells stained with an appropriate flurochrome, flowing past an excitation source. The emitted fluorescence level of the stained cell is captured by a photomultiplier tube and digitally converted to an electronic pulse.

The Light Source

A variety of light sources have been used in clinical flow cytometers. The most commonly used are Arc sources (mercury compact arc lamp) and laser sources. Laser sources include continuous wave, argon-ion gas laser (UV, blue and green light), krypton ion gas laser (yellow and red light), helium–neon gas laser (red light), and the diode (red light) laser. Laser sources are principally used in modern flow cytometers. The advantages of a laser source are that they consist of a single color of light or an extremely narrow range of wavelengths. In addition, the waves comprising a laser beam are in "phase." As a result the beam of laser light is much more intense than that produced from incoherent light sources. The third advantage of laser light is directionality. The beam of light emerging from a laser is narrow and highly arranged in one direction, whereas light from ordinary sources is emitted in all directions.

The Flow Chamber

The cells to be measured flow in a laminar nonturbulent fluid stream through the flow cell or flow chamber. This laminar flow is achieved by injecting the core fluid containing the sample particles into the center of another smoothly flowing stream (i.e., sheath stream); the two streams will maintain their relative positions and not mix much, a condition called laminar flow. This enables a sequential flow of primarily single cells, sufficiently separated to measure one cell at a time. The sheath stream rate is constant. Increasing the pressure or pump speed for the core fluid (sample) results in larger core diameter: More cells can be measured in a given time. However, precision is likely to be decreased because the illumination from a Gaussian laser beam is less uniform over a large diameter core. Less speed for the core stream gives a smaller core diameter and a slower measurement, but precision is higher. When measuring deoxyribonucleic acid (DNA) content, precision is important; in immunofluorescence measurement precision is usually of much less concern. The cells within the stream pass next a measurement station where they are illuminated by a light source. The point at which the laser beam and the cell stream meet is called the laser interrogation point. Alignment is critical to successful operation of flow cytometers; suboptimal alignment can result in erroneous data collection, presentation, and interpretation. The newer clinical flow cytometers are constructed to reduce or eliminate the need for daily alignment.

Optical Assembly

Once a cell passes the light beam two events occur, assuming that fluorochromes are in or on the cell. The first event is that cells will scatter light from the beam at the incident wavelength in 360 degrees. If one collects light scattered along the axis of the laser beam, a parameter known as forward angle light scatter, the quantity of the light is proportional to the size of the cell. If the scattered light is collected orthogonally at right angles to the light beam, the parameter is named 90 degrees, light scatter, or side scatter. The side scatter has been shown to be composed primarily of

light reflected by internal structures or membrane undulations. Therefore, this parameter correlates with cell granularity. The properties of forward and side scatter are called intrinsic properties because they can be measured by the flow cytometer without the use of exogenous reagents. Those properties requiring additional reagents for analysis are called extrinsic properties.

The second event that occurs at the laser interrogation point is that fluorochromes present on or in the cell absorb the laser light and reemit the light at a lower energy and a longer wavelength. This property is known as fluorescence. Each fluorochrome possesses a distinctive spectral pattern of excitation and emission. Typically, with argon-ion lasers, the excitation wavelength used is 488 nm, a blue to blue–green light. The fluorochrome must also emit light at a wavelength sufficiently longer than the excitation wavelength so that the two colors of light may be optically separated with selective filters. The difference between the peak wavelength of the excitation light and the peak wavelength of the emitted fluorescence light is a constant factor referred to as the "Stokes shift." The most popular fluorochromes used in immunofluorescence analysis are fluorescein isothiocyanate (FITC) and r-phycoerythrein (RPE). If multiple fluorochromes are used, their emission spectra must have minimal overlap so as to be separately quantitated. By using appropriate excitation and emission filters and dichroic mirrors, the emission spectra of distinct fluorochromes can be separated, and thereby simultaneous analysis of different stainings can be performed.

Signal Detection and Amplification

The detection system of a flow cytometer consists of a variety of photocells that collect light and convert it into integrated pulses. Because the burst of light from the particle lasts for only microseconds, the detector must be capable of rapidly processing signals from the detection zone, usually at a rate exceeding 10,000 pulses per second. Because the intensity of fluorescent light emitted by a cell is much less than that of light scatter signals, different types of photocells are used for each parameter. Photodiodes are used as detectors for light scatter signals, whereas photomultiplier tubes are used to detect fluorescence light. The photomultiplier tube (PMT) detects fluorescent signals as well as amplifies the weak signals to a useful level. Amplification of the peak or integrated pulses can be used to accentuate the differences between the peaks. Logarithmic amplification increases the difference between small pulses much more than that between larger peaks, and is ideal for differentiating

between events with similar but slightly different fluorescence signals. Linear amplification accentuates all peaks by the same amount and is preferable when examining events with large fluorescence differences. As a result of overlap between the emission spectra, a correction step called compensation is necessary.

Compensation

The goal of compensation is to remove the spillover fluorescence of a particular fluorochrome from the wrong channel (Baumgarth and Roederer, 2000). For example, FITC emits mainly green light, which is usually measured in the FL1 (FITC)-channel. However, FITC also emits a significant portion of light with a yellow component, which will appear in the FL2(r-PE)-channel. The appropriate choice of optical filters (band pass and long pass filters) can greatly reduce collection of light from other fluorochromes. Because of this spectral overlap, each fluorochrome will contribute a signal to more than one detector; therefore the contribution of signals in detectors not assigned to that fluorochrome must be subtracted from the total signal in those detectors. Compensation between detectors can be performed either by hardware (electronic) detection but before logarithmic conversion and/or digitization or afterward by software. Although compensation is one of the most important steps required for proper data analysis in flow cytometry, it is also perhaps the least well understood. Proper compensation is absolutely necessary to obtain antigen density measurements and to distinguish very weak (dim) positive populations from negative populations. Undercompensation will result in overestimating the frequency of the dim cells; overcompensation will result in underestimating this frequency. As the number of parameters increases, the complexity and costs of electronic or "hardware" compensation increases; therefore, software compensation becomes a more attractive alternative. For a proper compensation control, stains are very important. The higher the number of fluorochromes and antibodies used in each assay, the greater the risk for artifacts introduced by compensation errors and/or reagent interactions. In general, two types of controls should be included and data collected with every experiment irrespective of the kind of compensation (electronic or software-based): compensation controls and staining controls (Baumgarth and Roederer, 2000).

For each fluorochrome used in an assay, one should include a compensation control (i.e., a single color stain for which data are collected). For example, in a two-parameter flow cytometric assay using FITC and r-PE as fluorochromes, one should include two compensation

controls: a tube of cells labeled only with the FITC-label and another tube of cells labeled with r-PE. Ideally, the reagents used for the compensation sample should be the same as that used in the two-colored sample.

In addition, one must include staining control tubes in which the cells are labeled as in the double-staining assay. However, one of the two primary antibodies must be replaced by an isotype- and species-matched negative control immunoglobulin (staining control). In this way, one can control for background staining of the "unstained" cells (which can be at very different levels). By using the aforementioned controls, the spillover of the fluorescence signals in the different channels can be determined and can be compensated (before actual acquisition [electronically or software-based] or afterward [software-based]).

Calibration and Maintenance

A good quality-control scheme for flow cytometric analysis must be designed to assess the major instrument parameters that affect the reliability and reproducibility of data and must consist of two groups of procedures. The first group of procedures is carried out at relatively large intervals (one or two times a year) by qualified service personnel and includes examination of the efficiency and performance of the laser tube, optical filters, logarithmic and linear amplifiers, and PMTs. The second group of procedures consists of frequent (every new use of the machine, such as daily) monitoring of instrument performance by the flow cytometer operator to identify both immediate and potential problems. The operator can use labeled beads for this purpose. These beads can be classified into three major categories: alignment beads, reference beads, and calibration beads.

Alignment beads include particles used to align the optics of the flow cytometer. Although many of the modern flow cytometers do not require daily optical alignment because they have fixed optical systems, it is strongly recommended to check regularly instrument alignment when samples appear to be shifted or when peaks are broader than normal. Proper use of the alignment beads ensures the highest resolution between sample populations by allowing the adjustment of the positions of the flow cell and optical components. Alignment maximizes the fluorescence and scatter signal (maximum mean channel number) while minimizing signal variability (minimum coefficient of variation [CV]).

Reference beads refer to particles with a given fluorescence intensity that are used to set up the instrument. A recommended approach for achieving a unified instrument setup is the establishment of a common window of analysis or analysis region. This is accomplished by using beads with a high stability of fluorescence signals to prevent drift of the position of the fluorescence window of analysis over time as a result of decay of the fluorochrome on the bead. Daily monitoring with these reference beads ensures reproducibility of the analysis range and also standardizes the position of cell clusters in histograms obtained from different instruments.

Calibration beads encompass the fluorescence particles with multiple populations used to calibrate the response of the instrument and to quantify the fluorescence signal of samples. The ability to resolve or distinguish fluorescence signals of different intensities is the basis of determining negative from positive cell populations. These differences in resolution across the intensity range can be conveniently monitored using calibration beads. At least, these calibration beads consist of four types of beads with different fluorescence intensity and one group of nonfluorescent beads. The fluorescence intensities of these beads should cover that part of the fluorescence scale in which a linear response of the instrument to fluorescence signals can be expected.

The Technique of Flow Cytometric DNA Analysis

Software

Acquisition and Analysis: Data Display

When a cell hits the laser beam, it scatters light and/or fluorescence: these light signals generated from the cell can be detected by one of the photodetectors, dependent on the direction of the scattered light and the wavelength of the fluorescence. Photodiode detectors are generally used for detection of forward scattered light, because this light is bright and sensitivity is not an issue. PMTs are generally used for detection of side scatter light and of fluorescence because the high voltage applied to them increases their gain. Fluorescence signals obtained from cells immunocytochemically stained for protein expression show a wide variation in amplitude, which, when plotted on a logarithmic scale, approach a Gaussian distribution. For this reason, logarithmic amplification is most frequently used for the analysis of protein expression.

The electronic pulses generated by these photodetectors become digitized and displayed on the monitor screen or stored in the computer for further analysis. The data generated by most commercial flow cytometers is stored in FCS-format (*F*low *C*ytometry *S*tandard). Within this standard the most common mode

of storage is List Mode. This means that the correlated data are digitized and directly stored on disk while the sample is being analyzed. Selection of the most discriminative parameters and gated analysis of the data may then be performed later. List Mode data files have a text header followed by the data values, stored in a sequential fashion, as they were generated by each cell as it passed through the instrument. These FCS-format data generated by a certain flow cytometer can be read and further analyzed by other analysis software programs that can handle FCS-format data.

These digitized data are processed by a computer system and can be displayed on a monitor screen as one-parameter frequency distribution (univariate, histograms) or as two-parameter dot plots (also known as bivariate or scattergram). This type of display plots one point in this dotplot related to the amount of parameter *x* and *y* for each cell that hits the corresponding detectors. Dotplots are excellent for detecting small numbers of events that are well separated from the main population of the cells present but give little or no information of the relative density or number of events in a certain population. This is particularly true for large data files. This is one reason for using a contour or density plot. Contour plots are a two-dimensional display of relative *x* and *y* amounts of two parameters, with contour lines being drawn to form *x* and *y* coordinates that have a similar number of cells. Density plots simulate a three-dimensional display of events with the third parameter being the number of events (indicated by colors or shades of gray).

Cell Cycle Analysis

Development, growth, renewal, and maintenance of organisms are dependent on the formation of new cells out of parent cells. In other words, the cells need to be copied. This takes place through a process known as the cell cycle. The normal cell cycle is divided into four phases:

1. G_1-phase: the cells have a diploid or 2N DNA content (equivalent to 46 chromosomes in humans).
2. S-phase: the cycling cells replicate their DNA and have an amount of DNA varying between 2N and 4N. The fraction of cells in the S-phase (SPF) is often used as indication of proliferative status of a tissue.
3. G_2-phase: the cells have a double (4N) or tetraploid DNA content.
4. M-phase: mitosis, the cell divides, thus forming the two daughter cells.

The only stage recognizable to the microscopist is the mitotic phase. Cells produced at mitosis reenter the G_1-phase, which is the most variable in duration, and there are a number of biochemical events that occur during this phase that regulate exit from this phase. A separate G_0-phase was proposed by Lajtha to account for cells that do not divide unless stimulated to do so (Lajtha, 1963). It is currently not possible to separate a very long G_1 from G_0. At a certain point after entering the G_1 phase the cells begin to duplicate their DNA. This phase, during which DNA is synthesized, is termed the S-phase. This phase has duration in the order of 6–16 hr. When the cells have completely doubled their DNA content, they enter a second phase—G_2. This phase typically lasts 4–8 hr. After this phase the cells enter mitosis.

In any tissue, there are proliferating and nonproliferating cells; the latter are either end-stage, differentiated, or resting. The cells, which are actively involved in the cell cycle, make up the proliferation fraction. The proliferation fraction and the cell cycle time determine the growth activity of any tissue. The discovery of the existence of fluorochromes that bind to DNA in a stoichiometric manner (see "DNA Staining") was an important development in quantitative flow cytometric DNA analysis. This type of DNA analysis is the study of the distribution of cells into different phases of the cell cycle based on the DNA staining among the cells of a population. These analyses provide clinicians with two potentially important cellular parameters of information. First, it gives information about the size of the fraction of cells that are in the S-phase of the cell cycle. Second, it provides information about the presence and degree of abnormal DNA content in the investigated cell population. DNA histogram analysis requires mathematic analysis to extract the underlying G_1, S, and $G_2 + M$ phase distribution; methods for this analysis have been developed and refined over the past two decades. Methods to derive cell cycle information from DNA histograms range from simple graphic approaches to more complex deconvolution methods using curve-fitting. The two software programs most widely used for DNA histogram analysis are ModFit (from Bruce Bagwell; Verity Software House) and MultiCycle (from Peter Rabinovitch; Phoenix Flow Systems).

In normal tissue or a DNA diploid tumor, the great majority of cells is in the G_0/G_1 phase and have a diploid DNA content. This is reflected in the DNA histogram, which shows a single large peak of cells, the G_0/G_1 peak, with 2N DNA content. Normally a smaller peak of cells, which are in the G_2- and M-phase of the cell cycle, is present on the *x*-axis at twice the distance of the G_0/G_1 peak (4N). The compartment in between those two peaks is the SPF with DNA content between 2N and 4N. In 1992 a DNA cytometry consensus conference was held, and a nomenclature for DNA cytometry was recommended (Shankey *et al*., 1993b).

For ploidy, only the terms DNA diploid and DNA aneuploid should be used, with identification of the degree of DNA content abnormality given by the use of the DNA-index (DI). The DI is the ratio of mean or mode of sample G_0/G_1 population divided by mean or mode of diploid reference cells. The definition of DNA aneuploidy includes the requirement that two distinct peaks are present in the DNA histogram (Hiddemann *et al.*, 1984). Furthermore, it was stated that tumors with a DI of 2.0 (DNA "tetraploidy") should be recorded separately as a distinct group of DNA aneuploidy because they may have a distinct prognostic significance in some types of tumors (bladder, prostate). The working definition for DNA tetraploidy is DI values between 1.9 and 2.1 with proportions of cells greater than the G_2M fraction of normal tissue samples, after correction for aggregates. Many flow cytometric studies have used mainly the calculation of the proportion of cells in the S-phase of the cell cycle to predict the clinical behavior of human tumors. The assumption of these studies is that the fraction of cells, which synthesize DNA (SPF), is a direct reflection of tumor proliferation and hence aggressive behavior (Shankey *et al.*, 1993a). However, the assessment of SPF by DNA flow cytometry encounters some limitations. In many studies, the SPF could not be determined in a considerable number of cases. Because of technical reasons (e.g., wrong fixatives, prolonged fixation time, delayed time of fixation), only some of the DNA histograms were suitable for analysis by these computer programs. Another possible danger is the underestimation of the SPF in DNA diploid, mixed DNA diploid/aneuploid, or DNA peridiploid tumors. Solid tumors are in fact a heterogeneous mixture of benign (normal epithelial, stromal, endothelial, and inflammatory cells) and malignant (viable, necrotic, and apoptotic) cells. Furthermore, the malignant cells also show intratumoral heterogeneity in DNA content. All these factors adversely affect DNA ploidy and SPF determinations. Proliferating nonneoplastic cells have in general a lower SPF value than malignant cells, causing an underestimation of SPF in DNA diploid or DNA peridiploid tumors (Hedley *et al.*, 1987). In addition, dilution with nonneoplastic cells impairs sensitivity for detection of minor aneuploid stem lines (Frei *et al.*, 1994).

Multiparameter Flow Cytometric Analyses

One of the powers of flow cytometry is the ability to measure simultaneously more than one parameter on single cells. Ormerod and co-workers showed that light scatter/volume measurements could help to distinguish normal from malignant nuclei isolated from paraffin sections, even when both are diploid

(Ormerod *et al.*, 1995). To increase the accuracy of ploidy and cell cycle analysis, Ramaekers and co-workers demonstrated in 1984 in a tumor model the use of monoclonal antibodies directed against cytokeratin in combination with DNA content measurements (Ramaekers *et al.*, 1984). Cytokeratins can be considered as epithelium-specific intermediate filament proteins expressed in normal and neoplastic conditions (Moll *et al.*, 1982). Exclusion of nonepithelial cells after selecting only the cytokeratin-positive cells in a gated flow cytometric DNA histogram increases the accuracy of SPF and DNA index determination. Otsuka *et al.*, (2001) showed after filtering out the nonrelevant fibroblasts and leukocytes that the SPF increased significantly in DNA-diploid tumors. Futhermore, they showed that some tumors were aneuploid, whereas they were originally classified as DNA-diploid. Multiparameter flow cytometry could offer much more to clinical studies than simply helping to distinguish between normal and malignant cells. DNA content analysis can also be coupled to immunofluorescence staining of a variety of potentially biologically relevant cellular constituents to analyze tissue homeostasis and tumor biodynamics. An example is the combined measurement of the expression of BrdU and DNA (Schutte *et al.*, 1995). This technique can give kinetic information and static indices of proliferation. An example of a multiparameter flow cytometric analysis of a breast carcinoma is shown in Figure 15. From this figure the power of selection of cell populations with different expression of a certain parameter becomes clear.

When performing a DNA flow cytometric analysis, one has to exclude cell aggregates because these interfere with the accuracy of flow cytometric measurements. For instance, when two G_0/G_1 cells form a doublet, they will yield the same fluorescence signal as a single G_2M cell. A method to reduce the contribution of cell aggregates to the acquired DNA histogram is the use of hardware doublet detection called pulse processing: a kind of electronic gating. In this technique, the signals of the width of the propidium iodide electronic pulses are displayed on the *x*-axis of a dotplot (e.g., Figure 15A), and the area of these pulses on the *y*-axis. Because single cells have a linear relationship between these parameters, cells in the G_0/G_1, S, and G_2/M phases of the cell cycle fall on a diagonal line between the axes (Figure 15A). A gate can be set (R1 in Figure 15A) along the diagonal to exclude cell doublets, based on the fact that cell doublets show an increased width signal as compared to G_2-phase cells. The DNA histogram of this tumor (Figure 15B) show two cell populations: a DNA diploid and an aneuploid one. In the next step the nonrelevant single

cells (inflammatory cells, stromal compartment, etc.) are excluded from the analysis. This is performed by selection of cytokeratin-positive cells.

In a dotplot of DNA content (*x*-axis) versus cytokeratin signal (*y*-axis), a region is set around the cytokeratin-positive cells (Figure 15C; upper parts of the dotplot R2). The cutoff value for determining the threshold for immunoreactivity is based on the signal from the negative control (a single cell suspension incubated with a nonrelevant immunoglobulin). Figure 15D shows a dotplot of DNA content (*x*-axis) versus the expression of the progesterone receptor (*y*-axis) of the total single cell population. Figures 15E and 15F show the dotplot (of DNA content versus PR-expression) and DNA histogram, respectively, for the cytokeratin-negative cell population (all cells that are excluded from the region from Figures 15C). From these figures it becomes clear that this compartment comprises almost only the DNA diploid cell population, whereas the DNA aneuploid population is found in the cytokeratin-positive selection (Figure 15G and 15H; all cells that are situated in the region of Figure 15C). Here also the highest immunoreactivity for the progesterone receptor is found. This example shows that by using more than one parameter simultaneously, plus the possibility of making selections (gates) based on the differential expression of markers, a more defined and possibly a more reliable quantification of specific characteristics can be performed in the cell population of interest.

Quality of the Analysis

In the ideal case, signals from cells in a certain phase of the cell cycle, with the same DNA content, will accumulate in the same channel of the DNA histogram. However, because of small differences in chromatin compactness between individual cells (which affects the binding of a DNA stain), minor instrumental errors, and preparation artifacts, a Gaussian (normal) distribution is observed (Corver, 2001). A Gaussian distribution is characterized by a mean and a standard deviation (SD). Precision and resolution of DNA-histogram analysis is usually monitored by the use of CV and gives an impression of the width of the peak. The CV of the DNA diploid G_0/G_1-peak is usually calculated by the following equation:

$$CV = W/(M \times 2.35)$$

where W = full width of the G_0/G_1-peak at the half-maximum height and M = peak channel number of the G_0/G_1-peak. The result is expressed as a percentage. The lower the CV of the peaks in the DNA histogram,

the better the quality. In practice, CVs of less than 1% are exceptional. The quality of the DNA histogram can be affected by, for example, debris and aggregates. The CV significantly affects the accuracy of S-phase calculations. In a DNA cytometry consensus conference it has been stated that the CV of normal diploid cells in a histogram should be less than 8% (Shankey, *et al.*, 1993a). If the CV is greater than 8%, the peak may be composed of two or more populations of cells that cannot be resolved by the software program and estimation of the S-phase fraction should not be attempted. Our experience is that as a rule one should always try to have CVs of less than 5%.

Technical Controls

The fluorescence signal strength of a cell nucleus stained with propidium iodide is many times greater than that of an intact cell stained with a fluorochrome-labeled antibody against a certain cell constituent. In addition, fluorescence intensity of the DNA-staining dye must be measured on a linear scale, rather than on a logarithmic scale, because of the direct stoichiometric relationship of DNA content to fluorescence. However, lack of linearity of the amplifier for this signal is a common problem in many instruments. One of the frequent consequences of this nonlinearity is the situation in which G_2/M phase cells, which have twice the amount of DNA in G_0/G_1 phase cells, appear to have substantially more or less DNA. Signal amplifier linearity should be checked on a regular basis, using standard particles (standard fluorescent beads, polyploidy liver cells) and/or suitable methods. A common method for fresh or frozen tissue samples involved the addition of both chicken erythrocytes (CRBC; with a DNA content of 35% of the human diploid value) and rainbow trout erythrocytes (TRBC; with a DNA content of 80% of the human diploid value) to the sample (Vindelov *et al.*, 1983b). The use of two standards eliminates technical errors resulting from nonlinearity. Next to this control for linearity, the CRBCs and TRBCs serve as an internal diploid standard to detect staining variations. In practice, normal human lymphocytes and CRBCs are added to the sample. After flow cytometric analysis, the presence of the G_0/G_1 peak produced by the lymphocytes is a valuable landmark in verifying the position of the diploid G_0/G_1 peak of the clinical sample. The CRBC peak is essential for verifying the linearity of the DNA channel.

For formalin-fixed and paraffin-embedded (FFPE) tissues (variability in fixation [time] and DNA-dye accessibility) this control is complicated because of the lack of a known DNA diploid reference population. This makes the identification of the diploid G_0/G_1 peak
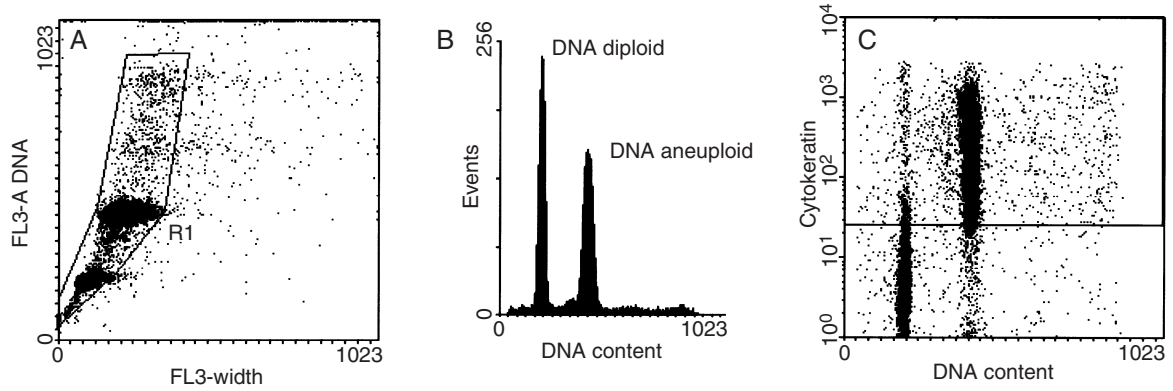
Marker expression vs DNA content

CK-negative
single cells

CK-positive
single cells
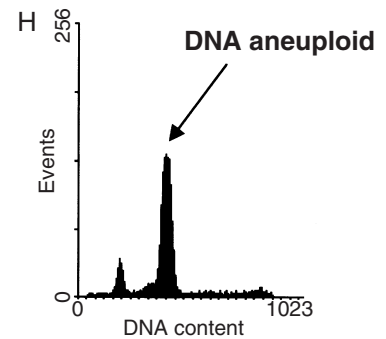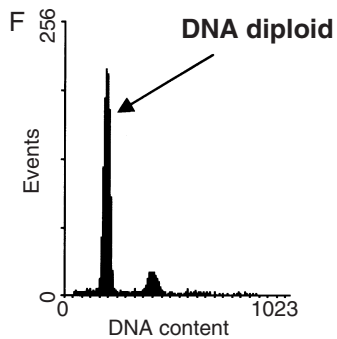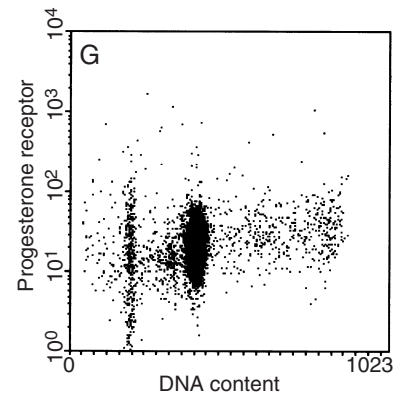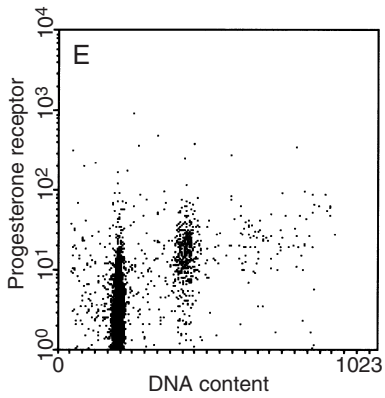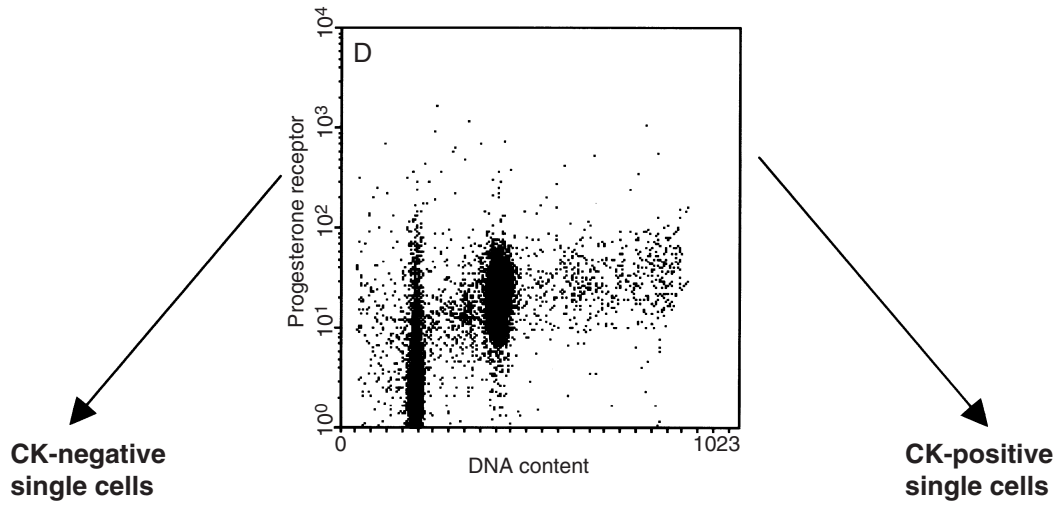
of the clinical sample difficult. It is possible to add CRBCs to the tissue specimen prior to fixation and paraffin embedding in the event that future flow cytometric DNA analysis may be required; however, this has several logistical problems. Therefore, the DNA cytometry consensus conference pointed out that because of the rare finding of hypoploid tumors, it is recommended that the leftmost peak in the DNA-histogram from paraffin-embedded tissue samples may be assumed to represent the DNA diploid population (Shankey *et al*., 1993a).

Principles of Cell Preparation

Dissociation Methods for Isolation of Cells or Nuclei from Human Solid Tumors

A single cell suspension is an essential prerequisite of the flow cytometric technique. When analyzing solid tumors, a cell suspension must be prepared by dissociating the samples of fresh or FFPE tissues. The most used dissociation techniques (or combinations of these) are based on chemical, mechanical, enucleation, and enzymatic dissociation principles. Difficulties in obtaining single cell suspensions vary with the tissue: fresh or fresh frozen lymphoid tissues require only minimal disruption by mechanical ways (mincing, sieving, etc.), whereas most epithelial tissues and paraffin-embedded solid tissues require careful disaggregation, usually by enzymatic techniques.

Mechanical dissociation techniques have been criticized as selective of cell populations with weak cell-to-cell adhesions, whereas enzymatic digestion may destroy labile cell populations and preferentially isolate cells with strong cell-to-cell contacts. The most common method for dissociation of single cells from fresh or frozen tissue is based on mechanical disruption of the tissue (e.g., by a combination of gentle mincing and teasing with one or two scalpel blades). Ottesen and co-workers described a technique based on an automated mechanical disaggregation method using the "Medimachine" (Ottesen *et al*., 1996). With this automated method for tissue disaggregation, the same resolution of the DNA histograms and the same

frequency of aneuploidy were obtained as compared to the manual mechanical dissociation method. In addition, automated mechanical disaggregation resulted in DNA histograms with significantly less debris and with lower S-phase fractions. The authors stated that this automated mechanical disaggregation also has the advantages of rapidity, ease, and safety because of minimal handling of the unfixed tissue compared to the manual mechanical dissociation of the tissue (Ottesen *et al*., 1996).

For enzymatic dissociation, three categories of enzymes can be used: nonspecific proteases, proteases specific for elastic and collagenous fibers, and hydrolytic enzymes specific for mucopolysaccharides. Examples of enzymes frequently used are trypsin and pepsin. Trypsin is a serine protease that hydrolyzes peptide bonds involving carboxyl groups of arginine and lysine. Pepsin has a broad range of nonspecific proteolytic activities. Among the many cleavage sites, pepsin preferentially cleaves bonds between hydrophobic residues and the amino acids leucine, phenylalanine, methionine, and tryptophan. The most used enzymatic method for the isolation of bare nuclei from fresh or frozen solid tumor specimens is that described by Vindelov *et al*. (1983a). This method is based on a combined trypsin-digestion and a detergent lysis of cell membranes and produces stained nuclei in monodisperse suspension in a single step. Although there are many dissociation techniques for fresh or frozen tissue, most pathology laboratories process their tissue routinely by formalin fixation and paraffin embedding. This type of tissue requires a different approach for the isolation of single cells because of, for example, the cross-links of many proteins within the tissue by formalin fixation. In 1983 Hedley and co-workers described an enzymatic method to prepare single cells from FFPE tissues (Hedley *et al*., 1983) by use of pepsin. Since then, there has been a plethora of investigations using these techniques for both prognostic and diagnostic implications. The use of paraffin blocks facilitates retrospective studies determining the prognostic significance of DNA content and cell proliferation in well-defined patient groups with known clinical follow-up (Hedley, 1989; Hedley, *et al*., 1983). However, it is important to

Figure 15 Example of a multiparameter flow cytometric cytokeratin/progesterone receptor (PR)/deoxyribonucleic acid (DNA) analysis of an aneuploid breast carcinoma (see text on page 95 for explanation; CK=cytokeratin). Panel **A** shows the selection of the single cells (exclusion of doublets, triplets, and aggregates), whereas in Panel **B** the DNA histogram of the ungated cells is depicted. Panels **C** and **D** show the dotplots of DNA (*x*-axis) versus cytokeratin (*y*-axis) and DNA (*x*-axis) versus PR (*y*-axis), respectively, for the **total** cell population. The solid line in Panel **C** denotes the thresholds for immunoreactivity as determined based on the negative controls. Panels **E** and **F** show the dotplot (DNA versus PR) and the DNA histogram, respectively, of the cytokeratin-negative cells. Gating for cytokeratin positivity resulted in the dotplot (DNA versus PR) and DNA histogram, as depicted in Panels **G** and **H**.

recognize that fixation artifacts may arise in some paraffin-embedded tissues, particularly in the generation of near-diploid DNA peaks, which are not necessarily derived from DNA aneuploid tumor nuclei (Joensuu *et al.*, 1990). Excessive fixation times (more than 48 hr) and elevated fixation temperatures (higher than 20°C) should be avoided to minimize potential DNA content artifacts (Joensuu *et al.*, 1990: Shankey, *et al.*, 1993a). For that reason a lot of investigations have been performed to improve or to modify the original Hedley method by using different pepsin concentrations (ranging from 0.05–1.0%) and different enzyme solutions for the dissociation of the rehydrated tissues (trypsin [Schutte *et al.*, 1985]; proteinase K [Albro *et al.*, 1993]; and pronase [van Driel-Kulker *et al.*, 1985]).

Overton and co-workers showed that the disadvantageous effects of formalin fixation could be reversed by heating the resuspended enzymatic dissociated cells for at least 1 hr at 75°C in phosphate buffer saline (PBS) before DNA-staining (Overton and McCoy, 1994; Overton *et al.*, 1996). This heating step restores the staining of the DNA to approximately the same fluorescence intensity as that of fresh tissue. This finding was the basis of a recently developed technique for multiparameter flow cytometry of FFPE tissue combining heat-induced antigen retrieval (2 hr in a ctirate solution at 80°C) followed by a very mild enzymatic digestion step (5–10 min with pepsin at 37°C). This protocol solves a lot of the previously mentioned problems (Leers *et al.*, 1999b). In addition, this new method has several advantages when compared to the Hedley method, for example:

▲ The recovery of single cells from the paraffin section is doubled by the heat-pretreatment step.
▲ The limited time of proteolysis results in a decreased cell debris.
▲ DNA histograms prepared from cell suspensions obtained according to this heat-induced antigen retrieval method show a significantly improved resolution, leading to a better identification of peridiploid cell populations.
▲ The isolated cells retain enough cytoskeletal and even cell membrane remnants allowing immunocytochemical labeling of a variety of proteins with monoclonal or polyclonal antibodies.
▲ Compared to the Hedley method, an increased fraction of cells becomes cytokeratin-positive, whereas these immunocytochemical stained cells also exhibit a higher mean fluorescence intensity.

Next to the previously mentioned modifications, which are all principally based on an enzymatic dissociation step, other approaches also are investigated.

Gonchoroff and co-workers performed a sonication of the cells after extraction from paraffin and rehydration. They showed a reduction in background staining and disaggregation of nuclear clumps, and improved accuracy of SPF determination (Gonchoroff *et al.*, 1990).

Staining

DNA Staining

A major development in quantitative cytometry came with the discovery of a cytochemical stain specific for DNA. In the early 1960s and 1970s the Feulgen technique was adapted for flow cytometry. During the years several other DNA staining dyes (ethidium bromide, propidium iodide, acridine orange) appeared to be more sensitive and easier to use. The most commonly used DNA-staining dyes are propidium iodide and ethidium bromide. Both show intercalation between base pairs in double-stranded DNA or ribonucleic acid (RNA). When staining DNA for flow cytometric analysis, those DNA staining dyes are used under so-called equilibrium conditions (i.e., cells are resuspended in the dye solution, allowed to take up stain, and analyzed by flow cytometry while suspended in dye solution). In theory, the fluorescence intensity of individual cells stained with DNA-specific dyes is proportional to the DNA content of the cells. Therefore, for accurate quantitation, the dye must be used at a saturating concentration. However, it should be remembered that binding of dyes to DNA depends on chromatin configuration. Only a portion of total DNA is ordinarily accessible to DNA binding fluorochromes (Bertuzzi *et al.*, 1990), and accessibility may be influenced by cell type, cell cycle phase, cell differentiation, and cell viability. In addition, blocking or an enzymatic digestion step is required for dyes that show nonspecific or unwanted staining reaction. For example, RNA must be removed by RNAse treatment when staining with propidium iodide because this dye binds to both DNA and RNA. The spectral characteristics of propidium iodide make it a popular choice for flow cytometry because it is readily excited by the 488 nm line of the argon-ion laser and it fluoresces with a maximum of around 620 nm, which makes it suitable for combination with FITC in multiparametric measurements.

Other DNA staining dyes are the ultraviolet excited dyes Hoechst and DAPI (4′-6-diamidino-2-phenylindole). The Hoechst dyes act as DNA-specific fluorochromes when bound to sequences of three A-T base pairs in DNA. DAPI shows also a strong A-T preference and does not require RNAse treatment. There are several reports that state that DAPI

yields DNA histograms with CVs lower than those obtained using other dyes (Otto and Tsou, 1985). This lower CV is probably because the DAPI staining is less affected by the state of chromatin condensation than staining with other dyes. However, DAPI requires ultraviolet (UV) excitation, which is not a common light source in most standard equipped flow cytometers.

Many new DNA dyes have been developed, and some of these dyes are also useful in flow cytometry. For example, deep-red antraquinone-5 (DRAQ-5) is a recently developed DNA stain, which has an optimal excitation at 647 nm and fluorescence emission extending from 670 nm into the low infrared (Smith *et al*., 2000; Wiltshire *et al*., 2000). It shows also excitation at suboptimal wavelengths, among the 488 nm line from the argon-ion laser. The advantage claimed by these investigators is that this new DNA stain has a very large "Stokes shift" (see "Optical Assembly"), so that no compensation is required when used in combination with FITC-and R-PE-labeled cells.

Immunocytochemistry

It is well-known that solid tumors exhibit considerable cellular heterogeneity. For example, on average, colon cancer specimens may contain less than 27% neoplastic cells (Crissman *et al*., 1989). The majority of cells are stromal, endothelial, and inflammatory. This example, which may typify the situation in many or most solid tumors, argues that single-parameter DNA flow cytometry measurements can primarily reflect nonneoplastic elements. Since the development of monoclonal antibodies, many studies have appeared in the literature that advocate the use of immunofluorescence analysis of intracellular (e.g., intermediate filament proteins) or cell membrane–bound antigens (e.g., epithelial cell adhesion molecule [Ep-CAM] or HER-2) to enrich for neoplastic eells from carcinomas under such circumstances. In 1984, Ramaekers and co-workers demonstrated in a tumor model the use of monoclonal antibodies against keratin labeled with a FITC-conjugated secondary antibody, in combination with DNA content measurements using propidium iodide as DNA stain. This approach allowed the discrimination between cultured bladder carcinoma cells and Molt-4 leukemia cells based on protein expression and DNA content (Ramaekers *et al*., 1984). This approach was later successfully applied to fresh or frozen tissue samples of many other human solid carcinomas. In this way tumor cells could be distinguished from normal stromal cells and inflammatory cells in solid human tumors by flow cytometry. The groups of Frei (Frei and Martinez, 1993) and Nylander (Nylander *et al*., 1994) demonstrated that the bivariate keratin-DNA labeling technique could also be applied

to cells extracted from routinely processed FFPE tumor samples. In 1999 we introduced heating in citrate buffer (which is an accepted technique for heat-induced epitope retrieval in an acidic environment for FFPE tissue sections for immunohistochemistry [Hayat, 2002]), prior to dissociation (Leers *et al*., 1999b). This strongly improved DNA-histogram quality (better CVs of the G_0/G_1-peaks of the first peak in the DNA-histogram, reduction in background and debris, and caused release of more single cells, while expression of many epitopes (among which keratin) was retained or restored for identification of tumor cell subpopulations (Leers *et al*., 1999b) resulting in higher fluorescence signals. In later studies we demonstrated the utility of three-parameter analysis in which cytokeratin was used for labeling of the epithelial compartment (conjugated with r-PE) and antibodies against steroid hormone receptor, HER-2 or apoptosis-related proteins (conjugated with FITC) and DNA content using propidium iodide in several types of cancer specimens (Leers and Nap, 2001; Leers *et al*., 2000a; Leers *et al*., 2003; Morsi *et al*., 2000; Nap *et al*., 2001; Rupa *et al*., 2003).

Direct conjugated primary antibodies with appropriate label/protein ratios will enable the most efficient and economical application of true multiparameter flow cytometric analysis of solid tumors, next to the availability of a straightforward relation of different aspects within the same cell suspension. Indirect, two-step procedures may offer more signal; however, they limit the possibility of using certain combinations of antibodies (species differences, isotype-differences, etc.).

Tissue Material

As described previously, multiparameter FCM analysis allows quantification of cellular parameters in the relevant (i.e., malignant) subpopulation of cells. In almost all surgical pathology laboratories most of the material is routinely processed for formalin fixation and paraffin embedding. As mentioned before, the use of fresh material offers logistic problems in a routine setting. The use of fresh material also has other drawbacks: the danger of biohazardous contamination and the long time period needed to collect material when performing a study in rare tumors. In addition, in a routine setting standardization of the technique on fresh material confronts the investigator with several problems. However, routinely processed FFPE material has the advantage that retrospective studies can be performed easier because of the huge archives of paraffin-embedded material in almost each routine pathology laboratory. In addition, the use of parrafin-embedded tissue allows the evaluation of the routinely made hematoxylin and eosin (H&E) stained

section so that the investigator is informed about the possible admixture with other tissues. Using this section, the investigator can decide to perform microdissection in case of extensive admixture with nonrelevant or contaminating tissue. So, the preferred method of analysis is that of single cell suspensions prepared from FFPE material. A method has become available that allows the use of archival paraffin blocks for studies of most antigens that can be detected after antigen retrieval (Leers *et al*., 1999b). After dewaxing and rehydrating 50 μm thick paraffin sections, heat-induced antigen retrieval is carried out by incubating these sections in an antigen retrieval solution for 2 hr at 80°C. After a cooling-down period of 15 min at room temperature only a short enzymatic pepsin digestion is necessary to release enough cells for multiparameter DNA-flow cytometric analysis. These cells have retained enough cytoskeletal remnants, which allows immunocytochemical labeling with a variety of antibodies (polyclonal and/or monoclonal), which can detect their epitopes after heat-induced antigen retrieval in routine immunohistochemistry on FFPE thin tissue sections. However, to perform a successful multiparameter flow cytometric analysis, several important features must be kept in mind:

▲ Maintain the correct pH of the antigen retrieval buffer (citrate pH = 6.0 and ethylenediamine tetraacetic acid [EDTA] pH 8.5). An incorrect pH will result in worse quality of the DNA histograms.
▲ Ensure the current temperature of the enzyme solution: do not preheat this solution because of excessive and unwanted damage to or a rapid digestion of the cells.
▲ Promote mechanical dissociation of the tissue sections by firmly vortexing the suspension after incubation with the enzyme solution. If this is not done properly, too many aggregates will remain.
▲ Correctly label the antibodies: for labeling cells derived from archival tissues, FITC-conjugated antibodies with a high F/P ratio (± 5) must be used.
▲ Use the right isotype-negative controls for setting up the instrument (compensation and threshold determination).
▲ When one is interested in *possible* weak expression of a protein (e.g., estrogen receptor, progesterone receptor, Her2/neu oncogene protein), it is advisable to visualize the bound antibodies with a FITC-labeled secondary antibody. It is better to use the RPE-labeled secondary antibodies for the visualization of proteins, which are abundant in their expression pattern (e.g., cytokeratin, vimentin).
▲ The RPE-fluorochrome is a large molecule that penetrates with difficulty into the nucleus. For the

visualization of nuclear-bound epitopes it is advisable to use an immunocytochemical labeling with FITC.

When performing semiquantitative flow cytometry, be aware of the fact that antibodies directed against the same protein but a different epitope can result in different sizes of fractions.

Protocol for Pure Enzymatic Cell Dissociation (Original Hedley Method)

1. Cut 30 μm thick paraffin sections and place them in a glass tube.
2. Deparaffinize by rinsing in xylene (2× for 10 min).
3. Rehydrate in decreasing series of ethanol:
    a. Ethanol 100%, 10 min
    b. Ethanol 95%, 10 min
    c. Ethanol 70%, 10 min
    d. Ethanol 50%, 10 min
4. Wash sections twice in distilled water.
5. Resuspend the sections in 1 ml 0.5% pepsin/0.9% NaCl (pH 1.5, adjust with 2 N HCl).
6. Place the tube in a waterbath of 37°C for 30 min.
7. Add 2 ml cold PBS to the suspension and vortex thoroughly. Prepare as much as possible single cells by firm mechanical pipetting with a micropipette.
8. Wash the cells with PBS by centrifugation, 3 times at 400 g.
9. Stain DNA with DAPI (1 μg/ml RPMI 1640).
10. Allow the cells to incubate for a minimum of 30 min at room temperature.
11. Filter cells through nylon gauze.

General Protocol for Formalin-Fixed and Paraffin-Embedded Epithelial Tumors (Combined Heat/Enzymatic Digestion)

1. Cut for each assay two 50 μm thick paraffin sections and put them in a glass tube.
2. Deparaffinize by rinsing in xylene (2× for 30 min).
3. Rehydrate in decreasing series of ethanol:
    a. Ethanol 96%, 2× for 30 min
    b. Ethanol 70%, 30 min
    c. PBS, 30 min
4. Add 2 ml cold citrate solution (2 g/L aqua dest, pH 6.0) to the sections and heat for 120 min in a waterbath of 80°C.
5. Allow the sections to cool for 15 min at room temperature, and tap off the citrate solution.
6. Digest the tissue sections by adding 2 ml **cold** pepsin solution (1 mg/ml 0.1 N HCl) and place the tube for a **maximum** of 10 min in an oven of 37°C.
7. Add 2 ml cold PBS to the suspension and vortex very thoroughly. Prepare as much as possible single cells by firm mechanical pipetting with micropipette.

8. Wash the cells with PBS by centrifugation, 3 times at 400 g.

9. Incubate the cells overnight at room temperature with properly diluted primary antibody/ies.

10. Wash the cells with PBS by centrifugation, 3 times at 400 g.

11. Incubate the cells for 90 min at room temperature with properly diluted fluorochrome-labeled secondary antibody/ies.

12. Wash the cells with PBS by centrifugation, 3 times at 400 g.

13. Stain DNA by adding 2 ml propidium iodide-solution (1.0 µg PI/ml and 0.1 mg/ml RNAse).

14. Allow the cells to incubate for a minimum of 60 min 4°C in the dark.

15. Analyze the cells.

Advantages
▲ High DNA-histogram resolution
▲ Excellent technique for the detection of intermediate filaments (e.g., cytokeratin)
▲ High yield of isolated cells after pepsin digestion

Disadvantages
▲ Pepsin digestion destroys most, if not all, cell surface bound epitopes and for example, the nuclear epitope for Ki-67 (detected by MIB-1)

General Protocol for Formalin-Fixed and Paraffin-Embedded Lymphoid Tissues (Combined Heat/Enzymatic Digestion)

1. Cut for each assay two 50 µm thick paraffin sections and place them in a glass tube.

2. Deparaffinize by rinsing in xylene (2× for 30 min).

3. Rehydrate in decreasing series of ethanol:
   a. Ethanol 96%, 2× for 30 min
   b. Ethanol 70%, 30 min
   c. PBS, 30 min

4. Add 2 ml cold EDTA solution (0.29 g/L aqua dest, pH 8.5) to the sections and heat for 120 min in a waterbath of 80°C.

5. Allow the sections to cool for 15 min at room temperature and tap off the EDTA solution.

6. Digest the tissue sections by adding 2 ml **cold** trypsin solution (1 mg trypsin/ml and 1 mg $CaCl_2$/ml Tris/HCl buffer, pH = 7.6) and place the tube for a **maximum** of 10 min in an oven of 37°C.

7. Add 2 ml cold TBS (Tris-buffered saline) to the suspension and vortex thoroughly. Prepare as much as possible single cells by firm mechanical pipetting with a micropipette.

8. Wash the cells with TBS by centrifugation, 3 times at 400 g.

9. Incubate the cells overnight at room temperature with properly diluted primary antibody/ies.

10. Wash the cells with PBS by centrifugation, 3 times at 400 g.

11. Incubate the cells for 90 min at room temperature with properly diluted fluorochrome-labeled secondary antibody/ies.

12. Wash the cells with PBS by centrifugation, 3 times at 400 g.

13. Stain DNA by adding 2 ml propidium iodide-solution (1.0 µg PI/ml & 0.1 mg/ml RNAse).

14. Allow the cells to incubate for a minimum of 60 min at 4°C in the dark.

15. Analyze the cells.

Advantages
▲ Most cell surface-bound epitopes stay intact after the mild trypsin-digestion.
▲ The nuclear epitope Ki-67 can be detected by the antibody clones MIB-1 as well as by Ki-S5.

Disadvantages
▲ DNA-histogram resolution is suboptimal (higher CV values).
▲ Number of isolated cells is lower after trypsin digestion.

RESULTS

Applications of Multiparameter Flow Cytometry in Clinical Pathology

The application of this technique in routine clinical pathology can primarily be found in those cases where immunophenotyping is normally associated with semiquantitation of subpopulations of cells in immunohistochemistry. In the following paragraphs several applications of the implementation of multiparameter flow cytometry in surgical pathology will be highlighted.

Qualitative Identification of Tissue Components

Selection of Rare Events: Micrometastasis in Lymph Nodes and Bone Marrow

Axillary lymph node status is the most important prognostic factor for patients with breast cancer. Therefore axillary lymph node dissection has been considered an essential component of breast cancer management. However, axillary dissection can result in significant morbidity. This fact has led to a search

for a new method that can stage the axillary lymph nodes accurately but that is associated with minor postoperative consequences. The sentinel lymph node procedure is such a new method emerging as an alternative for the staging of the axillary lymph nodes. The sentinel lymph node (SLN) is the first lymph node in a nodal basin to drain the primary tumor. This lymph node could be removed by limited surgery and examined to determine whether more extensive lymph node excision should be performed. Conceptually, because the SLN is the first lymph node to receive lymphatic drainage from a tumor, it should be the first to show metastatic tumor. The sensitivity of the procedure for detection of occult micrometastatic tumor cells in the SLN has been variable. The methods most often used for the identification of mircometastases in lymph nodes are H&E serial sectioning and immunohistochemical staining (IHC) of the SLN for a pan-ctyokeratin epitope. More recently, single-mRNA marker reverse transcription polymerase chain reaction (RT-PCR) assays have been tested for the detection of micrometastatic cells in SLN. A problem of this technique is the relatively high level of false-positive reactions resulting from the presence in lymph nodes of nonepithelial cytokeratin-positive elements (Bostick *et al*., 1998). In a recent study, it was shown that

multiparameter DNA flow cytometry could be used for this analysis (Leers *et al*., 2002).

It appeared that multiparameter flow cytometry was more sensitive than both multilevel histology and immunohistochemistry in the analysis of 238 lymph nodes. In addition, it was reported that the majority of micrometastases (smaller than 2 mm) presented themselves with a diploid DNA content, irrespective of the DNA profile of the primary tumor (Figure 16). Approximately 30% of SLN micrometastasis proved to be accompanied by additional non-SLN metastasis. The size of the aneuploid fraction (>60%) in the primary tumor may influence the risk of having both SLN and non-SLN metastases. Also, primary tumors in which the aneuploid fraction was larger than 60% showed aneuploid macrometastasis more often (Figure 16). Furthermore, in this group additional metastases were more often found in non-SLNs. It seems that the chance of finding aneuploid lymph node metastasis and/or macrometastasis is directly related to the size of the aneuploid fraction in the primary tumor: when this fraction increases, the chance of developing aneuploid and/or lymph node metastasis also increases. By applying this technique for more than 3 years in the Atrium Medical Center Heerlen in the Netherlands, some follow-up data for these patients
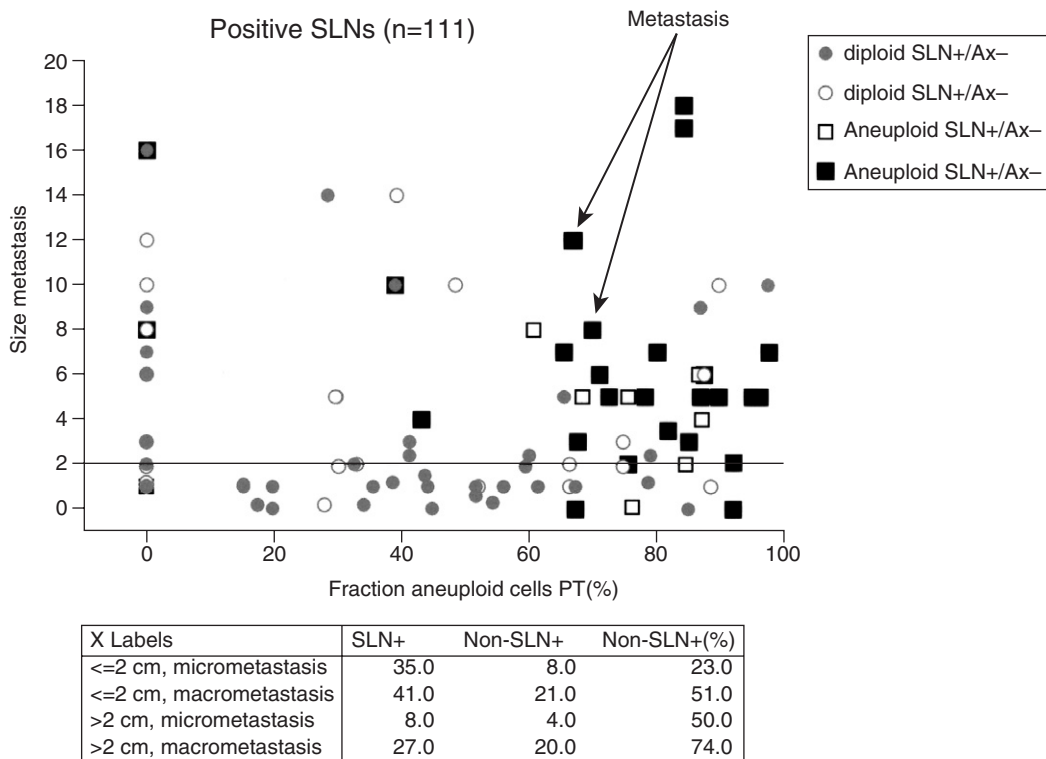

X Labels	SLN+	Non-SLN+	Non-SLN+(%)
<=2 cm, micrometastasis	35.0	8.0	23.0
<=2 cm, macrometastasis	41.0	21.0	51.0
>2 cm, micrometastasis	8.0	4.0	50.0
>2 cm, macrometastasis	27.0	20.0	74.0

Figure 16 Comparison of the size and ploidy of the sentinel lymph node (SLN) metastasis with the fraction of aneuploid tumor cells and the N-stage of the primary tumor (Ax = axillary lymph node dissection; PT = primary tumor).

became available. It appeared that only two patients developed distant metastasis after a positive SLN procedure and an axillary lymph node dissection. Both patients had an aneuploid primary breast tumor in which the aneuploid fraction was larger than 60% (Figure 16). Further studies and more patient follow-up are necessary to clarify the relation found between the size of the aneuploid fraction in the primary tumor and the size and the possible prediction for having the chance of non-SLN involvement.

This technique can also be extrapolated to detecting isolated tumor cells in bone marrow samples of patients with, for example, breast cancer. Cabioglu and co-workers removed the epithelial cells in a bone marrow sample with the aid of magnetic microbeads conjugated with a monoclonal antibody directed against cytokeratin to enrich tumor cells in bone marrow samples (Cabioglu *et al.* 2002). Using gating strategies they could demonstrate isolated tumor cells in 53% of patients with stage I/II breast cancer. Although this technique needs some optimization and further investigation, this approach might increase its reliability in the detection of occult metastatic tumor cells and might be useful in selecting patients with higher risk of relapse regarding tumor load to determine the need for adjuvant therapies. Zhang and co-workers have described a protocol for immunophenotyping disseminated breast tumor cells and their microenvironment in fresh bone marrow samples (Zhang *et al.*, 2003).

Correlation of Phenotypes with Size and Contour: Large Cell Neoplasms in Reactive Background

Measurements of the light scatter properties of cells are widely used in flow cytometry to distinguish subpopulations of cells. Because forward and side scatter signals differentiate cells on the basis of cell size and internal complexity, they are often used together to differentiate major cell populations. The combination of these signals can be used, for example, to distinguish different types of cells in blood and bone marrow. When using optimized cell preparation techniques, a complete separation of the granulocytes, monocytes, and granular and nongranular lymphocytes can be made. There are several reports describing the use of light scatter properties in hematologic malignancies (Bertram *et al.*, 2001; Duque *et al.*, 1990; Gong *et al.*, 2002; Gorczyca *et al.*, 2002). In most of the studies using light scatter analysis of cells from hematologic origin, it appeared that a relationship existed between cell size and genomic size: large cells in these tumors were mostly presynthetic aneuploid cells (Braylan *et al.*, 1984).

Besides the application of scatter signals in hematology, the quality of a DNA histogram as recorded by a flow cytometer can often be improved by gating on forward and side scatter light signals. This may be helpful when measuring DNA histograms from FFPE material (Ormerod, *et al.*, 1995). The light scatter signals can be used to exclude cells that are not of interest or to enrich cells that are of interest. Nuclei from malignant cells are larger and scatter more light in a forward direction than stromal cells and lymphocytes. Moreover, granulocytes have disproportionately high side scatter. Gating on light scatter enabled the DNA histogram from the tumor to be recorded with reduced contamination from normal cells. However, different cellular factors such as nuclear morphologic heterogeneity of the neoplastic cells, intratumoral variability, histologic origin, dysplasia grade, necrosis, and size of the tumoral piece analyzed constitute important problems in ploidy studies, and, consequently, residual or underrepresented clones with different ploidy levels can be masked by populations with a large cell number. Eriksen and co-workers demonstrated in ovarian carcinoma of low malignant potential that the combination of DNA-content analysis (with propidium iodide) and forward light scatter detection improves the detection of DNA-aneuploid (15 out of 45 cases) as compared to single parameter DNA flow cytometric analysis (7 out of 45 cases) (Eriksen *et al.*, 1991). In all 15 cases a single peridiploid peak was observed.

Petriz and co-workers showed that an alternative methodology can be used for aneuploidy detection because populations coinciding with DNA content may be different with respect to morphologic criteria (Petriz *et al.*, 1996). The discrimination of aggregates and background noise by using peak or logarithmic fluorescence signal, and backgating in side scatter/forward scatter histograms, permits the establishment of specific bounds through complete scatterplot mapping and helps to distinguish between scarce or minor populations in association with small or abnormal DNA peaks.

These and other reports have suggested that the use of light scatter signals can lead to improvement of the detection of malignant cells or, if present, the detection of heterogeneity (and existence of different clones) of the tumor. However, caution must be taken when using light scatter signal for exclusion of nonrelevant cells because this can prevent the accurate application of debris and aggregate modeling in cell cycle analysis (most cell cycle analyses need a certain amount of debris and aggregates for proper curve fitting). Also, the use of an immunofluorescence label (e.g., cytokeratin labeling of epithelial cells) is almost always a more sensitive method of improving the analysis in most common situations.

Semi-Quantification of Composing Fractions in Solid Tumors

Diagnostic Classification: Clonality Assessment in Lymphoproliferative Disorders

Another field of diagnostic application can be found in the assessment of clonality in lymphoproliferative disorders, which plays a key diagnostic role in distinguishing neoplastic from reactive B-cell lymphocytosis. An ever-pending problem for many laboratories is the staining for light chain-immunoglobulins (kappa and lambda) as a result of their intrinsic presence in serum and tissue fluids. To circumvent this problem phenotyping by FCM has been used, offering high-speed multiparameter analysis and statistical accuracy.

Identification of subtypes of lymphoid cells is possible when using CD-markers that function well on paraffin material after heat-induced epitope retrieval (e.g., CD3, CD20, and CD79a). Using these antibodies for labeling certain lineage-specific cell types (T-lymphocytes, B-lymphocytes, etc.) in combination with antibodies directed against one of the light chain immunoglobulins (kappa and lambda) it is possible to calculate the ratio of the expression of both kappa- and lambda-light chains in the relevant cell population. From haematologic studies it is known that a range between 0.5 and 3 is acceptable for reactive conditions (Witzig *et al.*, 1991). For example, see Figure 17. In a pilot study this was confirmed and ratios were found below and above these borders in 9 out of 10 malignant
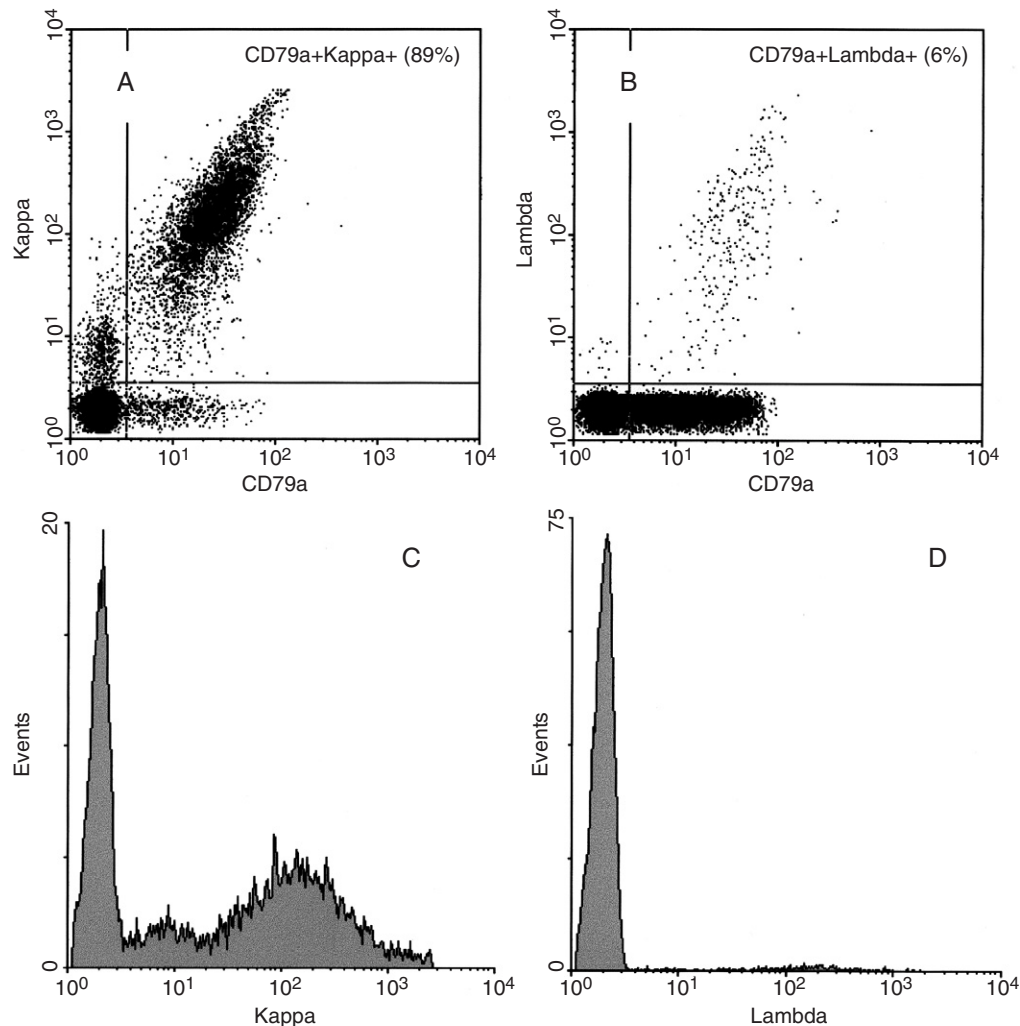

Figure 17 An example of a multiparameter flow cytometric analysis of a formalin fixed, paraffin embedded non-Hodgkin's B-cell lymphoma. The tumor cells were stained in suspension with a monoclonal antibody directed against CD79a and polyclonal antibodies directed against kappa- and lambda-light chain immunoglobulins. Panel **A** and **B** show the dotplots of the expression of kappa-light chains (*y*-axis) versus CD79a (*x*-axis, B-lymphocyte lineage marker) and lambda-light chains (*y*-axis) versus CD79a (*x*-axis), respectively. The majority of CD79a-positive cells show expression of kappa-light chain immunoglobulins (85%). The kappa/lambda ratio in the CD79a-positive fraction is 14.8 (89%/6%), indicative for a kappa-light chain-expressing B-lymphocyte clone. In Panels **C** and **D** the histograms of the immunofluorescence signals of the kappa- and lambda-light chains are depicted.

B-cell lymphomas. The only case that did not fit in this range was a case without light chain expression (Leers *et al*., 2000b).

An advantage of this approach is that when using multiparameter flow cytometry, neoplastic clones can be found by selecting cell populations by including the cell size information. These clones were otherwise obscured by reactive nonmalignant B- or T-lymphocytes. In addition, ploidy information and proliferative activity of the reactive and malignant lymphocytes can be obtained within the same assay. In the literature there is large variation in reported percentages of cases with aneuploidy found by FCM. This varies from a small number (Braylan and Benson, 1989) up to 57% of the non-Hodgkin's lymphomas (Winter *et al*., 1996). Overall, DNA aneuploidy is encountered in 30% of non-Hodgkin's lymphomas when single parameter DNA FCM analyses are used (Macartney and Camplejohn, 1993). However, when using multiparameter FCM analyses, combining a B-lymphocyte and a light chain-marker on fresh tissue samples, Braylan and Benson (1989) found abnormal DNA contents in 80% of their cases. These results emphasize the importance of a multiparameter approach for the detection of ploidy abnormalities in non-Hodgkin's lymphomas.

Prediction of Biologic Behavior and Therapeutic Sensitivity

Expression of Steroid Hormone Receptor Expression in Breast and Endometrial Cancer

Breast cancer is the most frequent type of cancer in women in the Western world. It accounts for 22% of all cancer deaths. The clinical presentation has radically changed in the last 10 years. Improvements in education and mass screening programs have produced substantial effects. One of these effects is the reduction of the average size of the primary tumor at first diagnosis. Despite this, the most important prognostic factor for patients with breast cancer is still the axillary lymph node status (Jatoi *et al*., 1999). Other prognostic factors are steroid hormone receptor status, DNA ploidy, and proliferative fraction (as determined, for example, by Ki67 immunostaining, thymidine labeling, or S-phase fraction determination) (Arnesson *et al*., 1992; Klijn *et al*., 1993; Stal *et al*., 1993).

The value of steroid hormone receptor analysis in the management of patients with breast cancer has been demonstrated clearly. Patients with estrogen receptor (ER)-positive tumors have a longer disease-free interval and better survival (McGuire, 1991) than those with receptor-negative cancers. In addition, these patients are clearly more likely to respond to endocrine

therapies (Nicholson *et al*., 1995; Ravdin *et al*., 1992). During the last decades several techniques have been developed to determine steroid hormone receptor expression (e.g., dextran-coated charcoal, enzyme immunoassays, immunochemistry, or by flow cytometry) (Schutte *et al*., 1992). However, the heterogeneous cell composition of most tumor samples is one of the limiting factors for both quantitative and semiquantitative receptor assays. Multiparameter FCM analysis of cytoplasmic markers (cytokeratin), hormone receptors (ER or PR [progesterone receptor]) and DNA content facilitate the semiquantitative measurement of hormone receptors in the relevant subpopulation of cells by focusing on the epithelial cells. Furthermore, receptor content can be analyzed in relation to DNA ploidy and growth potential, which is reflected by the percentage of tumor cells in the S-phase of the cell cycle (Hedley *et al.*, 1993). Both DNA ploidy and the SPF have shown to be important prognostic parameters in cancer. This approach is already part of the routine diagnostic protocol of breast carcinomas in the Atrium Medical Center Heerlen in the Netherlands for 4 years. The association between DNA aneuploidy and the high SPF observed by others (Batsakis *et al*., 1993) could be confirmed even more explicitly in relation to aneuploid subfractions with this multiparameter approach (Leers *et al*., 2000a). In a recently published study it became clear that in the majority of nondiploid tumors a diploid tumor cell subpopulation could also be detected (Leers and Nap, 2001). Multiparameter FCM has broad potentials in objectifying tumor heterogeneity with respect to cytoplasmic and nuclear proteins in combination with DNA. Information on steroid hormone receptor expression can not only be provided for the entire epithelial (cytoplasmic) compartment of the tumor but also separately for the diploid and aneuploid (DNA) epithelial fractions within the same tumor (Leers and Nap, 2001). It appeared that the aneuploid subpopulation within the same tumor showed a significant loss of receptor expression (nuclear) as opposed to the diploid epithelial tumor compartment. This finding, next to the fact that more than half of the tumors are composed of both diploid and aneuploid subfractions, stipulates the possibility of heterogeneous reactions to therapeutic agents. The combination of this information with clinical course of the tumor will eventually result in a more precise classification of possible sensitivity for hormonal treatment.

Another type of tissue that is hormonal under the influence of steroid hormones is endometrial tissue. During the reproductive years of life, steroid hormones govern the cyclic changes of endometrium. The expression of steroid hormone receptors in endometrial glandular and stromal cells is considered to be a reflection

of the differential functions with different requirements of hormonal effects. The cyclic changes in expression of steroid hormone receptors in normal endometrial tissue has been extensively studied by immunohistochemistry (Mertens *et al*., 2001; Snijders *et al*., 1992). Mertens and co-workers also used multiparameter CK/steroid hormone receptor/DNA FCM to demonstrate this cyclic pattern in the expression of steroid hormone receptors with an additional advantage of the direct relation to ploidy status and proliferative activity (as assessed by S-phase fraction) (Mertens *et al*., 2003a). In a study they used this approach to investigate endometrial hyperplasia with or without atypia. In this study it was demonstrated that there was no significant difference in steroid hormone receptor content and SPF between these two pathologic entities (Mertens *et al*., 2003b). Steroid hormone receptors were strongly elevated in hyperplastic endometrium compared to inactive postmenopausal endometrium. However, the SPF did not change. With increasing histologic grade of the endometrial cancer, ER and PR decreased, whereas androgen receptor (AR), SPF, and the percentages of aneuploid cells increased.

Morsi and co-workers evaluated the quantitative relation between apoptosis (M30-expression, a caspase-cleavage product of cytokeratin 18 [Leers *et al*., 1999a]), antiapoptosis (bcl-2), and proliferation (SPF) in benign and malignant endometrium using multiparameter FCM. They found a strong increase in bcl-2 expression and a moderate increase of apoptotic activity in complex hyperplasia as compared to simple hyperplasia. Within the carcinomas, well-differentiated tumors showed the highest bcl-2 expression next to a small M30-positive fraction. However, poorly differentiated tumors showed the highest M30-positivity and almost no bcl-2 expression (Morsi *et al*., 2000).

Expression of c-erbB-2 (HER-2/neu) in Breast Cancer in Relation to Cell-Cycle Characteristics

The HER-2/neu oncogene is a member of the human epidermal growth factor receptor family and is located on chromosome 17q21. Amplification of this oncogene or overexpression of HER-2/neu protein has been identified in 10–34% of breast carcinomas. These abnormalities are currently considered not only as an important possible marker of poor prognosis but also as a useful determinant of susceptibility to chemotherapy. Recently, a recombinant humanized monoclonal antibody against HER-2/neu protein (Herceptin) has been administered to patients whose breast carcinomas demonstrate HER-2/neu amplification or overexpression, with clinical effectiveness (Baselga *et al*., 1998; Pegram and Slamon, 1999). A prerequisite to enroll in this Herceptin-protocol is a moderate to strong (membranous) expression of HER-2/neu on the breast carcinoma cells. There are several possible techniques to study this expression. The most used and approved detection techniques are immunohistochemistry (IHC; overexpression), fluorescence *in situ* hybridization (FISH; amplification), chromogenic *in situ* hybridization (CISH) (Dandachi *et al*., 2002; Zhao *et al*., 2002), and PCR assays (O'Malley *et al*., 2001). Because of the semiquantitative aspect of the assessment of HER-2/neu expression, we investigated the possibilities of multiparameter FCM performed on routinely processed paraffin-embedded breast tumor samples. This technique showed a significant correlation with IHC and CISH, which were also applied to the same paraffin-embedded blocks (Leers *et al*., 2003). Furthermore, it has the advantage of giving additional combined information on the DNA histogram, an additional criterion for determining patients of high risk, which cannot be derived from the information obtained with IHC alone. Moreover, FCM determined HER-2/neu expression can be related to steroid hormone receptor expression, DNA ploidy, and proliferative activity (as determined by SPF). A more precise identification of subgroups with co-expression of different receptors involved in therapeutic interventions, in combination with cell growth parameters, may help in the selection of the most efficient application of individual therapeutic support.

DNA and Cell Cycle Analysis and Their Relation to Metastatic Offspring

Numerous investigators have compared flow cytometric DNA content and proliferative activity (as determined by SPF) with histomorphologic classification, grade of differentiation, clinical stage, and a variety of other features. Generally, tumors with model patterns close to diploid appear to have a more favorable prognosis than tumors with tetraploid, aneuploid, or mosaic DNA distribution. DNA aneuploidy has been associated with poor tumor differentiation, high proliferative activity, and lack of certain differentiation markers (e.g., steroid hormone receptors in breast or endometrial carcinomas). Although there are numerous articles in the literature demonstrating the prognostic importance of these two parameters, there is also an unsettling number of articles that have failed to demonstrate DNA ploidy or S phase as significant independent prognostic factors for solid tumors (Belessi *et al*., 2003; Dreinhofer *et al*., 2002; Ikonen *et al*., 1999; Lee *et al*., 2001; Orbo *et al*., 2002). Much of this disagreement is the result of a lack of standardized methods to prepare and analyze cells and to analyze data. In addition, much disagreement exists because of not restricting the analysis to the relevant tumor cell. Another problem with these DNA histogram

parameters is that their relationship with patient clinical outcome is nebulous and inconsistently applied by laboratories throughout the world (Bagwell *et al.*, 2001). The precise value of these measurements has not been adequately established, and for many organs and tumor types, multiparameter FCM prospective studies are still needed to confirm the predictive value of DNA analysis. For example, in recent reports of Rupa *et al.*, 2003 the combined measurement of apoptotic activity (using a monoclonal antibody against a caspase-cleavage product of cytokeratin 18) (Leers *et al.*, 1999a) and S-phase determination in the relevant epithelial compartment (using a polyclonal antibody against pan-cytokeratin) of colorectal carcinomas led to a better separation of low- and high-turnover tumors and improved the assessment of prognosis, leading to a better stratification of patients for adjuvant chemotherapy.

Bagwell and co-workers proposed 10 adjustments derived from a single large study of breast carcinomas (n=961 cases) that optimized the prognostic strength of both DNA ploidy and SPF and classified patients into two groups: low-risk and high-risk ploidy patterns. Afterward, these adjustments were consolidated positively when tested on two other large multicenter studies. This study may bring us closer to a universal and standardized prognostic model derived from a DNA histogram (Bagwell *et al .,* 2001).

Mannweiler *et al.,* 2002, used the DNA index of the primary tumor to predict the presence of lymph node metastases in invasive ductal breast carcinomas. They demonstrated that in invasive ductal carcinoma larger than 2 cm and with a DNA index higher than 1.44, the prediction of having lymph node metastases at the time of operation had a specificity of 100% and a sensitivity of 89%, a negative predictive value of 91%, and a positive predictive value of 100%.

However, when using the DNA index of the metastasis, we showed in our study of sentinel lymph nodes in breast carcinomas that the majority of micrometastases (<2 mm) had a diploid DNA content, irrespective of the DNA profile of the primary tumor (Leers *et al.*, 2002). In addition, the chance of finding aneuploid lymph node metastases was related to the size of the fraction of aneuploid epithelial cells in the primary tumor: Primary tumors in which the aneuploid fraction was larger than 60% showed (aneuploid) macrometastases (>2 mm) more often (Figure 16).

DISCUSSION

Immunophenotyping by multiparameter FCM can provide a rapid accurate method for both identifying unique cell populations and describing their functional status. This can be achieved because antibodies to cellular proteins can be conjugated or labeled with different-colored fluorochromes and combined in panels for staining heterogeneous cell populations. Traditionally, FCM has never been the core business of surgical pathology. Although in certain institutes, DNA ploidy measurements have been applied. The value of this technique has often been questioned with regard to the additional information obtained. This doubt is a logical consequence of the existence of several bottle necks if we apply isolated DNA FCM to fresh tissue or cells. The preparation of single cell suspensions from solid tumors is complicated by the fact that we have only limited information about the composition of the different contributing populations in the solid tumor. If a frozen section is made to obtain this information, artifacts introduced by freezing and thawing will impair cell and tissue morphology. In the case of an FFPE sample, the morphology is probably better, but, even with this knowledge available, single parameter DNA analysis does not take into account the contribution of inflammatory and other stromal cells to the result of cell cycle parameter calculations. The use of multiparameter flow cytometric analysis, using a combination of immunophenotyping and DNA, allows the separation of the data related to specific immunophenotypes, collection of data from a variety of different classes in the same run, and relating these specifically to the population of interest from those in the total population. This software mediated precision analysis brings within reach what is otherwise not possible. We can virtually visualize the presence and distribution of multiple cell characteristics directly and make calculations with them in relation to each other. By gating and eventually also sorting we can tell the proliferative activity even in subsets of tumor cells and relate that to the distribution of other markers of biologic activity. Sorting even allows the relative enrichment of rare events to prepare them for further analysis at a molecular level (Bonsing *et al.*, 2000).

If this is all so easy and within reach and would contribute so much to the contents of a pathology report, why is it that not every institute of pathology has implemented this fine technique alongside IHC and other forms of molecular pathology? One of the main reasons is probably that there are not yet sufficient data available that show the complementary possibilities of this approach to conventional morphology. Similar to the introduction of new technologic applications in any profession, there has to be a good reason for their implementation. Scientific or quality interest and concern are not enough. This is a logical consequence of the financial and labor limitations that also have to be dealt within surgical pathology.

As soon as the prediction of tumor behavior in relation to therapeutic sensitivity, tumor-free survival, and overall survival appears to be better possible by multi-parameter FCM or any other method, clinicians will start asking for it. At that moment it will become a matter of time, training, and money before the new technique enters the list of indispensable instruments of every pathology institute. However, before we have reached this stage, many things have to be taken care of.

In the first place a solid quality control and management system have to be set up to guarantee that the data obtained are robust and reliable. A prerequisite for this is that one is not only informed about the specificity of the reagents and machinery but that one also knows the composition and preservation characteristics of the tissue to be analyzed. This is where the routine skills of the histopathology lab are needed. The use of FFPE tissue blocks allows the introduction of routine H&E stained sections for evaluation of tissue components and the preselection of the area of interest by trimming the paraffin block. Tissue preservation is another important item. Formalin fixation seems to be simple and easy to control. Basically this is correct and it is still the most widespread and probably cheapest way of tissue fixation and preservation. At the same time there are many factors that can interfere with correct fixation and not all of them are within reach for the pathology staff to monitor. The whole process starts at the moment of tissue removal and the conditions under which the sample is stored and transported to the pathology laboratory. Good and robust logistics are necessary from the very start. If no special measurements are taken to assure complete penetration of the fixative in the tissue, the center of samples more than 1 cm thick will not be easily preserved properly before the autolysis has done part of its destructive work. Proper fixation for at least 24 hr has been shown to be a minimum time to obtain complete cross-linking of most proteins in the tissue. The second step to preservation of the tissue in paraffin follows a process that will remove all water and, with that, all water soluble reagents such as formalin. If the fixation process was not completed, there is still a possibility that the degradation of proteins and DNA will slowly continue. Longer fixation is not necessary but, from several experiments with formalin fixation at room temperature up to 72 hr, we have seen no negative effect on DNA histograms (Leers *et al*., 1999b).

Another argument in favor of complete fixation is a bit contradictory, but those familiar with immunohistochemistry will probably recognize it. After incomplete fixation, preservation of optimal morphology will interfere with antigen retrieval methods in a way of destructing cell membranes and blurring nuclear shapes. In addition, endogenous biotin, if available, will become reactive again for avidin or streptavidin, resulting in an unwanted background staining (Hayat, 2002). Because the preparation process of single cells from FFPE tissue includes a 2-hour-long heating step at 80°C, these negative effects will also influence the quality of the flow cytometric results. Wide CVs for the DNA histogram and increased background and debris will be the result.

The combination of immunophenotyping with DNA still is a rather unusual policy. Whereas in hemato-oncology immunophenotyping without DNA is a standard procedure, application of DNA ploidy alone is the rule in pathology. It has serious advantages, however; the combination of these two approaches also serves as a quality indicator in two directions. In contrast to regular IHC, in which morphology and external QC is an important tool, multiparameter FCM has a strong intrinsic advantage to monitor the quality of the sample that is offered for analysis. Once the CV of the DNA histogram becomes wider than usual and the amount of debris before the G_0/G_1 peak increases, this is an indication of inferior sample quality. This advantage has another effect. If very narrow DNA peaks are obtained and low debris level are observed, this means that the tissue was rather well preserved and that a negative immunologic reaction is more likely to be a correct observation; if high CVs are seen in combination with an increased amount of debris, a stronger than usual positive signal needs to be mistrusted. If, like in our routine applications, multiple tubes are sampled from the same suspension with repetitive reagents, such as PE-labeled cytokeratins, as a first group, in combination with FITC-labeled ER, PR or HER-2/neu, the reproducibility of the results from the first group of reagents (e.g., the size of the cytokeratin-positive fraction) will also give more value to the presence or absence of reactivity for the second group of reagents.

Standardization is another problem that needs attention. Whereas results obtained on fresh material often give reproducible information, the results that are obtained in FCM studies on FFPE material, suspended primarily by enzymatic digestion procedures, often show wide variations in CVs and cell cycle characteristics. Before we introduced the prolonged heating step in our routine procedures we also investigated the effect of this technical modification on the stability of DNA analysis. We could show that the variation in results did not exceed the 5% boundary, which is generally accepted as an intrinsic level of variation in biologic samples (Leers *et al*., 1999b). This means that the results from consecutively performed tests have to

be monitored, and changes in the mean values and the occurrence of outliers need to be signaled. Explanations need to be looked for, and corrections of procedures or adjustment of calibration values must be taken care of.

In the previous paragraphs we have discussed mostly the quality of the sample and how to monitor this. In a similar way it is important to be informed about the possible influence of the hardware and software components and the experience of the operator at the instrument and the one who is involved in the analysis of the data.

During a period of training inside the lab we encountered the situation that, although we used the same data files, the same version of the analysis software but different hardware components, the calculated percentage of reactive material was sometimes more than the cut-off value on one machine and less than this threshold on the other machine. If the same sample was then analyzed by two different individuals on the same machine, the outcome of each analysis was identical. If the same samples were analyzed by the same operator on two different computers, the aberrant results showed again. We do not yet have a good explanation for this, but it underlines the need for objectification of analytic procedures.

The present interactive approach with a user interface that allows the operator to move demarcation lines in a graphical presentation field of the data might be one of the reasons for the occurrence of discrepancies. The resolution of the screen and the internal settings of the computer may cause slight deviations in the screen display. Selections made by demarcation lines on screen in a data-rich area can easily result in serious changes of the numbers that fall inside the population of interest. Theoretically, this could be a post-acquisition event. The data collected by the flow cytometer have not been changed. One can imagine that in such a situation it becomes very important that the analysis is done by an experienced, preferably the same, operator who intuitively follows the same way of working all the time. It also takes more than an average effort to reach this state of experience before such a technique can then be introduced as a routine procedure. In addition, if new combinations of parameters from the same dataset are to be analyzed, this must be done by the same operator again; otherwise the contents of the previous analysis cannot be compared with the new results. These are all complicating factors before introducing multiparameter FCM into everyday routine in a general pathology institute.

Once the quality control and maintenance programs have been established and data analysis rendered less operator dependent, a broad field of possible applications for FCM comes within reach. Preanalytic separation of cells from body fluids, based on size, shape, DNA, and/or immunophenotype, might enhance the possibilities to study the contribution of small numbers of aberrant expression patterns to our understanding of pathogenetic processes or to the course of disease in case of minimal residual pathologic elements. In this way multiparameter FCM completed with advanced sorting facilities might become a serious and economical favorable competitor of other more laborious methods, such as laser capturing or automated image analysis, in which only the image is retained and not the actual cell.

References

Albro, J., Bauer, K.D., Hitchcock, C.L., and Wittwer, C.T. 1993. Improved DNA content histograms from formalin-fixed, paraffin-embedded liver tissue by proteinase K digestion. *Cytometry* *14*:673–678.

Arnesson, L.G., Smeds, S., Hatschek, T., Nordenskjold, B., and Fagerberg, G. 1992. Hormone receptors, ploidy and proliferation rate in breast cancers up to 10 mm. *Eur. J. Surg. Oncol.* *18*:235–240.

Bagwell, C.B., Clark, G.M., Spyratos, F., Chassevent, A., Bendahl, P.O., Stal, O., Killander, D., Jourdan, M.L., Romain, S., Hunsberger, B., and Baldetorp, B. 2001. Optimizing flow cytometric DNA ploidy and S-phase fraction as independent prognostic markers for node-negative breast cancer specimens. *Cytometry 46*:121–135.

Baselga, J., Norton, L., Albanell, J., Kim, Y.M., and Mendelsohn, J. 1998. Recombinant humanized anti-HER2 antibody (Herceptin) enhances the antitumor activity of paclitaxel and doxorubicin against HER2/neu overexpressing human breast cancer xenografts. *Cancer Res. 58*:2825–2831.

Batsakis, J.G., Sneige, N., and el-Naggar, A.K. 1993. Flow cytometric (DNA content and S-phase fraction) analysis of breast cancer. *Cancer 71*:2151–2153.

Baumgarth, N., and Roederer, M. 2000. A practical approach to multicolor flow cytometry for immunophenotyping. *J. Immunol. Methods 243*:77–97.

Belessi, C.J., Parasi, A.S., Manioudaki, H.S., Laoutaris, N.P., Legakis, N.C., Peros, G.T., and Androulakis, G.A. 2003. Prognostic impact of DNA ploidy pattern, S-phase fraction (SPE), and proliferating cell nuclear antigen (PCNA) in patients with primary gastric lymphoma. *J. Surg. Oncol. 82*:247–255.

Bertram, H.C., Check, I.J., and Milano, M.A. 2001. Immunophenotyping large B-cell lymphomas. Flow cytometric pitfalls and pathologic correlation. *Am. J. Clin. Pathol. 116*:191–203.

Bertuzzi, A., D'Agnano, I., Gandolfi, A., Graziano, A., Starace, G., and Ubezio, P. 1990. Study of propidium iodide binding to DNA in intact cells by flow cytometry. *Cell Biophys. 17*:257–267.

Bonsing, B.A., Corver, W.E., Fleuren, G.J., Cleton-Jansen, A.M., Devilee, P., and Cornelisse, C.J. 2000. Allelotype analysis of flow-sorted breast cancer cells demonstrates genetically related diploid and aneuploid subpopulations in primary tumors and lymph node metastases. *Genes Chromos. Cancer 28*:173–183.

Bostick, P.J., Chatterjee, S., Chi, D.D., Huynh, K.T., Giuliano, A.E., Cote, R., and Hoon, D.S. 1998. Limitations of specific reverse-transcriptase polymerase chain reaction markers in the detection of metastases in the lymph nodes and blood of breast cancer patients. *J. Clin. Oncol. 16*:2632–2640.

Braylan, R.C., and Benson, N.A. 1989. Flow cytometric analysis of lymphomas. *Arch. Pathol. Lab. Med. 113*:627–633.

Braylan, R.C., benson, N.A., and Nourse, V.A. 1984. Cellular DNA of human neoplastic B-cells measured by flow cytometry. *Cancer Res. 44*:5010–5016.

Cabioglu, N., Igci, A., Yildirim, E.O., Atkas, E., Bilgic, S., Yavuz, E., Muslumanoglu, M., Bozfakioglu, Y., Kecer, M., Ozmen, V., and Denzig, G. 2002. An ultrasensitive tumor enriched flow-cytometric assay for detection of isolated tumor cells in bone marrow of patients with breast cancer. *Am. J. Surg. 184*:414–417.

Corver, W.E. 2001. Multiparameter DNA flow cytometry of human solid tumors: Technical improvements and applications. Thesis, University of Leiden, The Netherlands, Leiden, 191.

Crissman, J.D., Zarbo, R.J., Ma, C.K., and Visscher, D.W. 1989. Histopathologic parameters and DNA analysis in colorectal adenocarcinomas. *Pathol. Annu. 24*:103–147.

Dandachi, N., Dietze, O., and Hauser-Kronberger, C. 2002. Chromogenic in situ hybridization: A novel approach to a practical and sensitive method for the detection of HER-2 oncogene in archival human breast carcinoma. *Lab. Invest. 82*: 1007–1014.

Dreinhofer, K.E., Baldetorp, B., Akerman, M., Ferno, M., Rydholm, A., and Gustafson, P. 2002. DNA ploidy in soft tissue sarcoma:comparison of flow and image cytometry with clinical follow-up in 93 patients. *Cytometry 50*:19–24.

Duque, R.E., Everett, E.T., and Iturraspe, J. 1990. Biclonal composite lymphoma. A multiparameter flow cytometric analysis. *Arch. Pathol. Lab. Med. 114*:176–179.

Eriksen, B., Miller, D.S., Murad, T.M., Lurain, J.R., and Bauer, K.D. 1991. Dual-parameter flow cytometric analysis coupling the measurements of forward-angle light scatter and DNA content of archival ovarian carcinomas of low malignant potential. *Anal. Quat. Cytol. Histol. 13*:45–53.

Frei, J.V., and Martinez, V.J. 1993. DNA flow cytometry of fresh and paraffin-embedded tissue using cytokeratin staining. *Mod. Pathol. 6*:599–605.

Frei, J.V., Rizkalla, K., and Martinez, V.J. 1994. Proliferative cell indices measured by DNA flow cytometry in node-negative adenocarcinomas of breast: Accuracy and significance in cytokeratin-stained archival specimens. *Mod. Pathol. 7*:925–929.

Gonchoroff, N.J., Ryan, J.J., Kimlinger, T.K., Witzig, T.E., Greipp, P.R., Meyer, J.S., and Katzmann, J.A. 1990. Effect of sonication on paraffin-embedded tissue preparation for DNA flow cytometry. *Cytometry 11*:642–646.

Gong, J.Z., Williams, D.C., Jr., Liu, K., and Jones, C. 2002. Fine-needle aspiration in non-Hodgkin lymphoma: Evaluation of cell size by cytomorphology and flow cytometry. *Am. J. Clin. Pathol. 117*:880–888.

Gorczyca, W., Weisberger, J., Liu, Z., Tsang, P., Hossein, M., Wu, C.D., Dong, H., Wong, J.Y., Tugulea, S., Dee, S., Melamed, M.R., and Darzynkiewicz, Z. 2002. An approach to diagnosis of T-cell lymphoproliferative disorders by flow cytometry. *Cytometry 50*:177–190.

Hayat, M.A. 2002. *Microscopy, Immunohistochemistry, and Antigen Retrieval Methods: For Light and Electron Microscopy,* New York: Kluwer Academic/Plenum Publishers.

Hedley, D.W. 1989. Flow cytometry using paraffin-embedded tissue: Five years on. *Cytometry 10*:229–241.

Hedley, D.W., Friedlander, M.L., Taylor, I.W., Rugg, C.A., and Musgrove, E.A. 1983. Method for analysis of cellular DNA content of paraffin-embedded pathological material using flow cytometry. *J. Histochem. Cytochem. 31*:1333–1335.

Hedley, D.W., Rugg, C.A., and Gelbert, R.D. 1987. Association of DNA index and S-phase fraction with prognosis of nodes positive early breast cancer. *Cancer Res. 47*:4729–4735.

Hedley, D.W., Shankey, T.V., and Wheeless, L.L. 1993. DNA cytometry consensus conference. *Cytometry 14*:471.

Hiddemann, W., Schumann, J., Andreef, M., Barlogie, B., Herman, C.J., Leif, R.C., Mayall, B.H., Murphy, R.F., and Sandberg, A.A. 1984. Convention on nomenclature for DNA cytometry. Committee on Nomenclature, Society for Analytical Cytology. *Cancer Genet. Cytogenet. 13*:181–183.

Ikonen, J.T., Ojala, A., Salenius, J.P., Mattila, J., Riekkinen, H., and Wigren, T. 1999. DNA flow cytometry in surgically treated lung cancer – prognostic significance. *Scand. Cardiovasc. J. 33*:228–233.

Jatoi, I., Hilsenbeck, S.G., Clark, G.M., and Osborne, C.K. 1999. Significance of axillary lymph node metastasis in primary breast cancer [published erratum appears in *J. Clin. Oncol.* 1999 Oct; 17(10):3365]. *J. Clin. Oncol. 17*:2334–2340.

Joensuu, H., Alanen, K.A., Klemi, P.J., and Aine, R. 1990. Evidence for false aneuploid peaks in flow cytometric analysis of paraffin-embedded tissue. *Cytometry 11*:431–437.

Klijn, J.G., Berns, E.M., and Foekens, J.A. 1993. Prognostic factors and response to therapy in breast cancer. *Cancer Surv. 18*:165–198.

Lajtha, L.G. 1963. On the concept of the cell cycle. *J. Cell. Comp. Phys. 62*:143–145.

Lee, J.H., Noh, S.H., Lee, K.Y., Choi, S.H., and Min, J.S. 2001. DNA ploidy patterns in advanced gastric carcinoma; is it a clinically applicable prognosticator? *Hepatogastroenterology 48*:1793–1796.

Leers, M.P.G., Hoop, J., and Nap, M. 2003. Her2/neu analysis in formalin fixed, paraffin embedded breast carcinomas: Comparison of immunohistochemistry and multiparameter DNA flow cytometry. *Anticancer Res.* 23.

Leers, M.P.G., Kolgen, W., Bjorklund, V., Bergman, T., Tribbick, G., Persson, B., Bjorklund, P., Ramaekers, F., Bjorklund, B., Nap, M., Jornvall, H., and Schutte, B. 1999a. Immunocytochemical detection and mapping of a cytokeratin 18 neo-epitope exposed during early apoptosis. *J. Pathol. 187*:567–572.

Leers, M.P.G., and Nap, M. 2001. Steroid receptor heterogeneity in relation to DNA-index in breast cancer: A multiparameter flow cytometric approach on paraffin embedded tumor samples. *Breast J. 7*:249–259.

Leers, M.P.G., Schoffelen, R., Theunissen, P., Oosterhuis, J., Bijl, H.V., Rahmy, A., Tan, W., and Nap, M. 2002. Multiparameter flow cytometry as a tool for the detection of micrometastatic tumor cells in the sentinel lymph node procedure. *J. Clin. Pathol. 55*:359–366.

Leers, M.P.G., Schutte, B., Theunissen, P.H., Ramaekers, F.C., and Nap, M. 1999b. Heat pretreatment increases resolution in DNA flow cytometry of paraffin-embedded tumor tissue. *Cytometry 35*:260–266.

Leers, M.P.G., Schutte, B., Theunissen, P.H., Ramaekers, F.C., and Nap, M. 2000a. A novel flow cytometric steroid hormone receptor assay for paraffin-embedded breast carcinomas: An objective quantification of the steroid hormone receptors and direct correlation to ploidy status and proliferative capacity in a single-tube assay. *Hum. Pathol. 31*:584–592.

Leers, M.P.G., Theunissen, P.H., Ramaekers, F.C., Schutte, B., and Nap, M. 2000b. Clonality assessment of lymphoproliferative disorders by multiparameter flow cytometry of paraffin-embedded tissue: An additional diagnostic tool in surgical pathology. *Hum. Pathol. 31*:422–427.

Macartney, J., and Camplejoh, R. 1993. In: Crocker J., ed. *Cell Proliferation in Lymphomas*. Blackwell Scientific Publications, Oxford.

Mannweiler, S., Tsybrovskyy, O., and Regauer, S. 2002. The flow cytometric DNA index can predict the presence of lymph node metastases in invasive ductal breast carcinoma. *Apmis* 110:580–586.

McGuire, W.L. 1991. Breast cancer prognostic factors: Evaluation guidelines. *J. Natl. Cancer. Inst.* 83:154–155.

Mertens, H.J., Heineman, M.J., Theunissen, P.H., de Jong, F.H., and Evers, J.L. 2001. Androgen, estrogen and progesterone receptor expression in the human uterus during the menstrual cycle. *Eur. J. Obstet. Gynecol. Reprod. Biol.* 98:58–65.

Mertens, H.J.M.M., Heineman, M.J., and Evers, J.L.H. 2003a. Steroid hormone receptor analysis in human endometrium: Comparison of immunohistochemistry and flow cytometry. *Gy. Obstet. Invest.* accepted.

Mertens, H.J.M.M., Leers, M.P.G., Nap, M., Kisters, N., Stoot, J.E.G.M., Heinerman, M.J., and Evers, J.L.H. 2003b. Steroid receptor content and its heterogeneity in relation to DNA ploidy in benign and malignant endometrium. *Submitted*.

Moll, R., Franke, W.W., Schiller, D.L., Geiger, B., and Krepler, R. 1982. The catalog of human cytokeratins: Patterns of expression in normal epithelia, tumors and cultured cells. *Cell* 31:11–24.

Morsi, H.M., Leers, M.P., Radespiel-Troger, M., Bjorklund, V., Kabarity, H.E., Nap, M., and Jager, W. 2000. Apoptosis, bcl-2 Expression, and Proliferation in Benign and Malignant Endometrial Epithelium: An Approach Using Multiparameter Flow Cytometry. *Gynecol. Oncol.* 77:11–17.

Nap, M., Brockhoff, G., Brandt, B., Knuechel, R., Leers, M.P., Schmidt, H., De Angelis, G., Eltze, E., and Semjonow, A. 2001. Flow cytometric DNA and phenotype analysis in pathology. A meeting report of a symposium at the annual conference of the German Society of Pathology, Kiel, Germany, 6–9 June 2000. *Virchows Arch.* 438:425–432.

Nicholson, R.I., McClelland, R.A., and Gee, J.M. 1995. Steroid hormone receptors and their clinical significance in cancer. *J. Clin. Pathol.* 48:890–895.

Nylander, K., Stenling, R., Gustafsson, H., and Roos, G. 1994. Application of dual parameter analysis in flow cytometric DNA measurements of paraffin-embedded samples. *J. Oral. Pathol. Med.* 23:190–192.

O'Malley, F.P., Parkes, R., Latta, E., Tjan, S., Zadro, T., Mueller, R., Arneson, N., Blackstein, M., and Andrulis, I. 2001. Comparison of HER-2/neu status assessed by quantitative polymerase chain reaction and immunohistochemistry. *Am. J. Clin. Pathol.* 115:504–511.

Orbo, A., Rydningen, M., Straume, B., and Lysne, S. 2002. Significance of morphometric, DNA cytometric features, and other prognostic markers on survival of endometrial cancer patients in northern Norway. *Int. J. Gynecol. Cancer* 12:49–56.

Ormerod, M.G., Titley, J.C., and Imrie, P.R. 1995. Use of light scatter when recording a DNA histogram from paraffin-embedded tissue. *Cytometry* 21:294–299.

Otsuka, H., Funai, S., Tsuda, H., Azumi, T., Hara, S., Okuno, K., and Yasutomi, M. 2001. The significance of bivariate cytokeratin and DNA flow cytometry in paraffin-embedded specimens of non-small cell lung cancer. *Int. J. Clin. Oncol.* 6:229–235.

Ottesen, G.L., Christensen, I.J., Larsen, J.K., Hansen, B., and Andersen, J.A. 1996. Tissue disaggregation for flow cytometric DNA analysis: Comparison of fine-needle aspiration and an automated mechanical procedure. *Cytometry* 26:65–68.

Otto, F., and Tsou, K.C. 1985. A comparative study of DAPI, DIPI, and Hoechst 33258 and 33342 as chromosomal DNA stains. *Stain Technol.* 60:7–11.

Overton, W.R., Catalano, E., and McCoy, J.P., Jr. 1996. Method to make paraffin-embedded breast and lymph tissue mimic fresh tissue in DNA analysis. *Cytometry* 26:166–171.

Overton, W.R., and McCoy, J.P., Jr. 1994. Reversing the effect of formalin on the binding of propidium iodide to DNA. *Cytometry* 16:351–356.

Pregram, M.D., and Slamon, D.J. 1999. Combination therapy with transtuzumab (Herceptin) and cisplatin for chemoresistant metastatic breast cancer: Evidence for receptor-enhanced chemosensitivity. *Semin. Oncol.* 26:89–95.

Petriz, J., Tugues, D., and Garcia-Lopez, J. 1996. Relevance of forward scatter and side scatter in aneuploidy detection by flow cytometry. *Anal. Cell Pathol.* 10:243–252.

Ramaekers, F.C., Beck, H., Vooijs, G.P., and Herman, C.J. 1984. Flow-cytometric analysis of mixed cell populations using intermediate filament antibodies. *Exp. Cell. Res.* 153:249–253.

Ravdin, P.M., Green, S., Dorr, T.M., McGuire, W.L., Fabian, C., Pugh, R.P., Carter, R.D., Rivkin, S.E., Borst, J.R., Belt, R.J., and *et al.* 1992. Prognostic significance of progesterone receptor levels in estrogen receptor-positive patients with metastatic breast cancer treated with tamoxifen: Results of a prospective Southwest Oncology Group study. *J. Clin. Oncol.* 10:1284–1291.

Rupa, J.D., De Bruine, A.P., Gerbers, A.J., Leers, M.P., Nap, M., Kessels, A.G., Schutte, B., and Arends, J.W. 2003. Simultaneous detection of apoptosis and proliferation in colorectal carcinoma by multiparameter flow cytometry allows separation of high and low-turnover tumors with distinct clinical outcome. *Cancer* 97:2404–2411.

Schutte, B., Reynders, M.M., Bosman, F.T., and Blijham, G.H. 1985. Flow cytometric determination of DNA ploidy level in nuclei isolated from paraffin-embedded tissue. *Cytometry* 6:26–30.

Schutte, B., Scheres, H.M., De Goeij, A.F., Rousch, M.J., Blijham, G.H., Bosman, F.T., and Ramaekrs, F.C. 1992. Flow cytometric steroid receptor analysis. *Prog. Histochem. Chytochem.* 26:68–76.

Schutte, B., Tinnemans, M.M., Pijpers, G.F., Lenders, M.H., and Ramaekers, F.C. 1995. Three parameter flow cytometric analysis for simultaneous detection of cytokeratin, proliferation associated antigens and DNA content. *Cytometry* 21: 177–186.

Shankey, T.V., Rabinovitch, P.S., Bagwell, B., Bauer, K.D., Duque, R.E., Hedley, D.W., Mayall, B.H., Wheeless, L., and Cox, C. 1993a. Guidelines for implementation of clinical DNA cytometry. International Society for Analytical Cytology. *Cytometry* 14:472–477.

Shankey, T.V., Rabinovitch, P.S., Bagwell, B., Bauer, K.D., Duque, R.E., Hedley, D.W., Mayall, B.H., Wheeless, L., and Cox, C. 1993b. Guidelines for implementation of clinical DNA cytometry. International Society for Analytical Cytology [published erratum appears in Cytometry 1993 Oct; 14(7):842]. *Cytometry* 14:472–477.

Smith, P.J., Blunt, N., Wiltshire, M., Hoy, T., Teesdale-Spittle, P., Craven, M.R., Watson, J.V., Amos, W.B., Errington, R.J., and Patterson, L.H. 2000. Characteristics of a novel deep red/infrared fluorescent cell-permeant DNA probe, DRAQ5, in intact human cells analyzed by flow cytometry, confocal and multiphoton microscopy. *Cytometry* 40:280–291.

Snijders, M.P., de Goeij, A.F., Debets-Te Baerts, M.J., Rousch, M.J., Koudstaal, J., and Bosman, F.T. 1992. Immunocyto-chemical analysis of oestrogen receptors and progesterone receptors in the human uterus throughout the menstrual cycle and after the menopause. *J. Reprod. Fertil*. *94*:363–371.

Stal, O., Dufmats, M., Hatschek, T., Carstensen, J., Klintenberg, C., Rutqvist, L.E., Skoog, L., Sullivan, S., Wingren, S., and Nordenskjold, B. 1993. S-phase fraction is a prognostic factor in stage I breast carcinoma. *J. Clin. Oncol*. *11*:1717–1722.

Taylor, C.R., and Cote, J. 1994. *Immunomicroscopy: A Diagnostic Tool for the Surgical Pathologist*, Vol. 19. Philadelphia: W.B. Saunders Co., 71–106.

van Driel-Kulker, A.M., Mesker, W.E., van Velzen, I., Tanke, H.J., Feichtinger, J., and Ploem, J.S. 1985. Preparation of monolayer smears from paraffin-embedded tissue for image cytometry. *Cytometry 6*:268–272.

Vindelov, L.L., Christensen, I.J., and Nissen, N.I. 1983a. A deter-gent-trypsin method for the preparation of nuclei for flow cyto-metric DNA analysis. *Cytometry 3*:323–327.

Vindelov, L.L., Christensen, I.J., and Nissen, N.I. 1983b. Standardization of high-resolution flow cytometric DNA analy-sis by the simultaneous use of chicken and trout red blood cells as internal reference standards. *Cytometry 3*:328–331.

Wiltshire, M., Patterson, L.H., and Smith, P.J. 2000. A novel deep red/low infrared fluorescent flow cytometric probe, DRAQ5NO, for the discrimination of intact nucleated cells in apoptotic cell populations. *Cytometry 39*:217–223.

Winter, J.N., Andersen, J., Variakojis, D., Gordon, L.I., Fisher, R.I., Oken, M.M., Neiman, R.S., Jiang, S., and Bauer, K.D. 1996. Prognostic implications of ploidy and proliferative activity in the diffuse, aggressive non-Hodgkin's lymphomas. *Blood 88*:3919–3925.

Witzig, T.E., Gonchoroff, N.J., Therneau, T., Gilbertson, D.T., Wold, L.E., Grant, C., Grande, J., Katzmann, J.A., Ahmann, D.L., and Ingle, J.N. 1991. DNA content flow cytometry as a prognostic factor for node-positive breast cancer. The role of multiparameter ploidy analysis and specimen sonication. *Cancer 68*:1781–1788.

Zhang, J., Shen, K.W., Liu, G., Zhou, J., Shen, Q., Shen, Z.Z., and Shao, Z.M. 2003. Antigenic profiles of disseminated breast tumour cells and microenvironment in bone marrow. *Eur. J. Surg. Oncol*. *29*:121–126.

Zhao, J., Wu, R., Au, A., Marquez, A., Yu, y., and Shi, Z. 2002. Determination of HER2 gene amplification by chromogenic in situ hybridization (CISH) in archival breast carcinoma. *Mod. pathol*. *15*:657–665.

10

Suppression Subtractive Hybridization Technology

Isik G. Yulug and Arzu Atalay

Introduction

It is important to understand where and when each gene is expressed when trying to identify gene function. Although there have been many studies to determine which genes are preferentially expressed in a particular cell or tissue, it has been difficult until recent years to evaluate differences concerning the whole genome. We are now able to study gene expression at the whole-genome level by using modern techniques.

Alterations in gene expression lie at the root of many human diseases and normal and abnormal processes. These alterations can be studied with many different methods including display differential, serial analysis of gene expression (SAGE) (Ye, 2004), representational difference analysis (RDA), gene expression microarrays, and suppression subtractive hybridization (SSH). All of these methods are useful in comparing and identifying differentially expressed genes between two populations. Subtractive hybridization is a frequently used and attractive method for enriching differentially expressed genes. The method was first described in the early 1980s to create complementary deoxyribonucleic acid (cDNA) libraries (Sargent and Dawid, 1983) and generate probes (Davis *et al*., 1984) of differentially expressed genes. Originally a large quantity of messenger ribonucleic acid (mRNA) was required to drive hybridization to

completion and it was difficult to clone the minute amount of DNA that remained after hybridization, limiting the method's usefulness. However, the method was improved greatly when Duguid and Dinauer (1990) adapted generic linkers to cDNA, which allowed the selective polymerase chain reaction (PCR) amplification of tester cDNA between hybridization cycles. Diatchenko *et al*. (1996, 1999) then introduced the technique of SSH PCR, where it was possible to normalize and enrich the differentially expressed genes more than 1000-fold in a single round of hybridization. With Clontech's introduction of the commercial PCR-Select cDNA Subtraction Kit (Clontech Laboratories, Palo Alto, CA), SSH rapidly became a popular method in biologic research and took its rightful place in the molecular biologist's armamentarium (Atalay *et al*., 2002; Li *et al*., 2001; Liu *et al*., 2002; Stassar *et al*., 2001; Uchijima *et al*., 2001). The SSH technology is a PCR-based cDNA subtraction method and can be used to compare two mRNA populations and obtain cDNAs of genes that are either overexpressed or exclusively expressed in one population compared to another. Genes up-regulated in one sample (referred to as tester) relative to the other sample (called the driver) can be identified. The technique has the advantage of isolating expressed sequences without prior knowledge of their sequence, and its use does not require specialized equipment or

Handbook of Immunohistochemistry and in situ Hybridization of Human Carcinomas,
Volume 2: Molecular Pathology, Colorectal Carcinoma, and Prostate Carcinoma

113

analyses other than those commonly used with molecular biology techniques (Desai *et al*., 2000).

Subtractive hybridization has been applied successfully to clone cDNA sequences that are expressed differentially in two cDNA populations (Hedrick *et al*., 1984; Sargent and Dawid, 1983; Wang and Brown, 1991). The method is designed to selectively amplify differentially expressed transcripts and suppress the amplification of abundant transcripts at the same time; it also normalizes the target transcripts to approximately equal abundance. It thus eliminates the need to separate single- and double-stranded molecules.

The Principle of Suppression Subtractive Hybridization

SSH (Diatchenko *et al*., 1996) is a recently developed technique. The basic principle of the SSH method combines normalization of abundant and rare cDNAs with efficient subtraction of common cDNAs between two populations. It is based on the specific suppression PCR that allows for the exponential amplification of differentially expressed genes and suppression of equally expressed genes. This technique is widely used to compare the gene expression profile of two tissues or cell populations. Figure 18 shows the schematic diagram of the SSH procedure. mRNA from both populations are converted to cDNA. The cDNA population, which contains the differentially expressed transcripts, is named "tester" (cDNA1), and the reference cDNA population is named "driver" (cDNA2).

The SSH process entails two rounds of hybridization followed by two PCR reactions. Poly A+ mRNA is isolated from total RNA and reverse transcribed to give a double-stranded cDNA pool. The cDNAs are digested by a restriction enzyme into fragments of a narrow size range. For cDNA subtraction, the tester pool is divided into two equal parts and different adaptors are ligated to 5′ ends of each fragment (Ad1 and Ad2R). In the first set of hybridizations, an excess of driver cDNA without linkers is denatured and hybridized separately with each tester cDNA pool and the reactions are allowed to proceed under identical conditions. Among species present at the same concentration in the tester, those present in similar or higher levels in the driver will form duplexes at a faster rate than those whose concentration in the driver is lower. In the second hybridization, both samples are mixed together with addition of excess single-stranded driver for further subtraction. The resulting pool is a mixture of single-stranded, double-stranded with only one linker, double-stranded like the original pools, and double-stranded with both linkers corresponding to the tester-specific fragments. After the hybridization reaction, filling the ends of the

adaptors allows the creation of templates to be amplified by PCR. The cDNA possessing the same kind of adaptor on both sides will form a hairpin structure, thus preventing the amplification of this type of product. Those duplexes in which the two strands have different adaptors are exponentially amplified in the PCR reactions. The resulting final PCR product is enriched in tester-specific cDNAs. The products are then ligated into vectors that are used to transform *Escherichia coli*. The clones are characterized to confirm their specificity. To identify genes that are down-regulated in the sample used as the tester, a reverse SSH is carried out by switching the samples used as tester and driver.

After the subtraction, specificity must be confirmed because the resulting PCR product is only enriched in differentially expressed cDNAs. To screen a large number of candidates, the cDNAs are arrayed on nitrocellulose, nylon membrane, or glass and hybridized with probes made from the original tissues. In the case of very low expression genes, the use of subtracted probes may prove to be useful because relative abundance is normalized during the suppressive PCR amplifications. Finally, Northern blot analysis or quantitative PCR standardized to the level of a stable known housekeeping gene are needed to precisely measure the levels in differential expression between the samples.

The following materials are available as a kit from Clontech Laboratories (PCR-Select cDNA Subtraction Kit).

MATERIALS

1. Oligonucleotides:
cDNA synthesis primer: 5′-TTTTGTACAAGCTT$_{30}$-3′
(GTAC-*Rsa* I, AAGCTT-*Hin*d III restriction enzyme digestion sites)
Adaptor 1 (Ad1):
5′-CTAATACGACTCACTATAGGGCTCGAGCGGCCGCCCGGGCAGGT-3′
3′-GGCCCGTCCA-5′
Adaptor 2R (Ad2R):
5′-GTAATACGACTCACTATAGGGCAGCGTGGTGGTCGCGGCCGAGGT-3′
3′-GCCGGCTCCA-5′
PCR Primer 1 (P1): 5′-CTAATACGACTCACTATAGGGC-3′
Nested PCR Primer 1 (NP1): 5′-TCGAGCGGCCGCCCGGGCAGGT-3′
Nested PCR Primer 2R (NP2R): 5′-AGCGTGGTCGCGGCCGAGGT-3′
Control Primers: Glyceraldehyde 3-phosphate dehydrogenase (G3PDH)
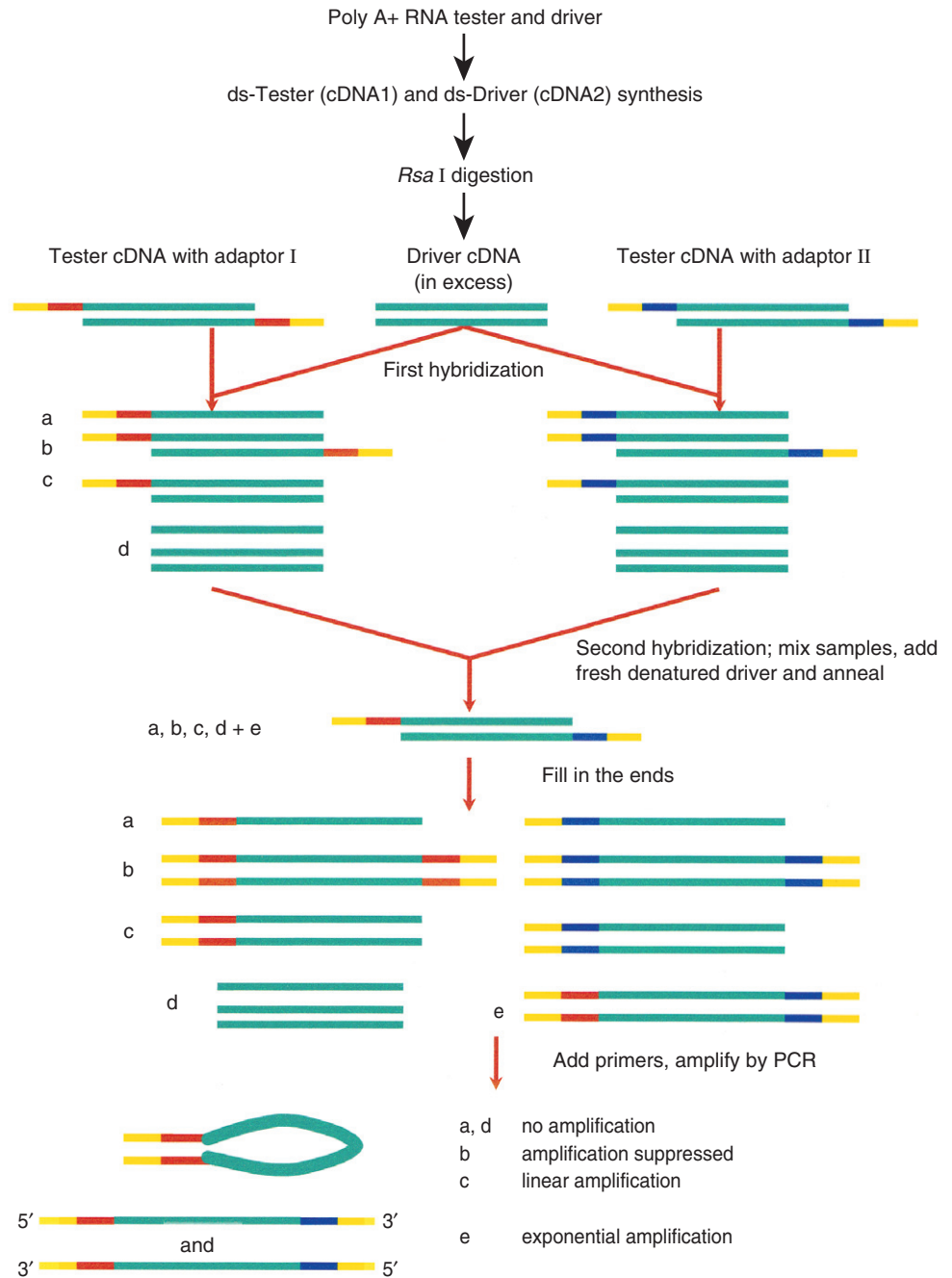G3PDH 5′ Primer: 5′-ACCACAGTCCATGCCATCAC-3′

Poly A+ RNA tester and driver

ds-Tester (cDNA1) and ds-Driver (cDNA2) synthesis

Rsa I digestion

Tester cDNA with adaptor I   Driver cDNA   Tester cDNA with adaptor II
                                    (in excess)

First hybridization

a
b
c
d

Second hybridization; mix samples, add
fresh denatured driver and anneal

a, b, c, d + e

Fill in the ends

a
b
c
d   e

Add primers, amplify by PCR

a, d   no amplification
b   amplification suppressed
c   linear amplification

5′   3′   e   exponential amplification
          and
3′   5′

Figure 18 Principle of suppression subtractive hybridization.

G3PDH 3′ Primer: 5′-TCCACCACCCTGTTGCT-GTA-3′

2. Blocking solution: A mixture of the cDNA synthesis primer, nested primers (NP1 and NP2R), and their respective complementary oligonucleotides (2 mg ml⁻¹ each).

3. Buffers and enzymes:

   a. First-strand synthesis: AMV (avian myeloblastosis virus) reverse transcriptase (20 units μl⁻¹), 5X first-strand buffer (250 mM Tris-HCl [pH 8.5], 4.0 mM MgCl$_2$, 150 mM KCl, 5 mM Dithiothreitol).

b. Second-strand synthesis: 20X second-strand enzyme cocktail (DNA polymerase I, 6 units μl⁻¹, RNAse H, 0.25 units μl⁻¹, *E. coli* DNA ligase, 1.2 units μl⁻¹), 5X second-strand buffer (500 mM KCl, 50 mM ammonium sulfate, 25 mM MgCl$_2$, 0.75 mM beta-nicotinamide adenine dinucleotide (B-NAD), 100 mM Tris-HCl [pH 7.5], 0.25 mg ml⁻¹ bovine serum albumin [BSA] and T4 DNA polymerase [3 units μl⁻¹]).

c. Endonuclease digestion: 10X *Rsa* I restriction buffer, 100 mM Bis Tris propane-HCl [pH 7.0], 100 mM MgCl$_2$, 1 mM DTT, (100 mM Bis Tris

propane-HCl [pH 7.0], 100 mM MgCl$_2$, 1 mM DTT) *Rsa* I (10 units μl^{-1}).

d. Adaptor ligation: T4 DNA ligase (400 units μl^{-1}; contains 3 mM ATP), 5X DNA ligation buffer (250 mM Tris-HCl [pH 7.8], 50 mM MgCl$_2$, 10 mM DTT, 0.25 mg ml^{-1} BSA), 10 μM adaptor 1, 10 μM adaptor 2R.

e. Hybridization: 4X hybridization buffer (4M NaCl, 200 mM HEPES [pH 8.3], 4 mM cetyltrimethyl ammonium bromide CTAB), dilution buffer (20 mM HEPES-HCl [pH 8.3], 50 mM NaCl, 0.2 mM EDTA [pH 8.0]).

f. PCR amplification: use of Advantage cDNA PCR mix (Clontech) is strongly recommended. Alternatively, normal Taq DNA polymerase can be used, but five additional PCR cycles will be needed in both the primary and secondary PCR, and the use of manual hot start or hot start wax beads is strongly recommended to reduce nonspecific DNA synthesis.

g. General reagents: dNTP mix (10 mM each dATP, dCTP, dGTP, dTTP), 20X EDTA/glycogen mix (0.2M EDTA; 1 mg ml^{-1} glycogen), 4M NH$_4$OAc, sterile H$_2$O. DNA size marker *Hae* III digest of bacteriophage φX174, RNAse-free DNAse (MessageClean Kit, GenHunter Corporation, MA).

h. General solutions: 80% and 96% ethanol, phenol:chlorphorm:isoamyl alcohol (25:24:1), 50X TAE electrophoresis buffer (242 g Tris base, 57.l g glacial acetic acid, 37.2 g Na$_2$EDTA.2H$_2$O, add H$_2$O to 1 L).

Radioisotope [α-^{32}P]dCTP (10 mCi ml^{-1} 3000 Ci/mmol) usage is optional.

Note: All the cycling parameters are given for the Perkin-Elmer DNA Thermal Cycler 9600/2400 (Perkin-Elmer). The cycling parameters must be optimized for each PCR machine.

METHODS

Isolation of poly(A)$^+$ RNA from Sample Tissue or Cultured Cells

SSH requires high-quality, intact, and pure mRNA for the synthesis of high-quality cDNA. It is more efficient to isolate total RNA from the samples that will be used as tester and driver and then isolate poly(A)$^+$ RNA from the total RNA. The general procedure for total RNA isolation can be found in the book by Sambrook *et al*. (1989). The total RNA is then used to isolate poly(A)$^+$ RNA by using a commercial mRNA purification kit (such as polyA Spin isolation kit [New England Biolabs Inc., MA]).

It is highly recommended to examine the total and poly(A)$^+$ RNA integrity by electrophoresing samples on a formaldehyde denaturing agarose/ethidium bromide gel. Total mammalian RNA typically shows two bright bands, which correspond to ribosomal 28S and 18S at ~ 4.5 and 1.9 kb, respectively, and the ratio of band intensities are ~ 1.5–2.5:1. Mammalian poly(A)$^+$ RNA appears as a smear from approximately 0.5–12 kb with weak ribosomal bands. It is also recommended to remove the contaminating DNA to improve the efficiency of SSH by treating the RNA samples with RNAse-free DNAse (the MessegeClean Kit can efficiently remove the DNA without degrading the RNA samples).

The following protocol is recommended for generating a subtracted library from 2–4 μg of poly(A)$^+$ RNA. Using a PCR block for all reactions is strongly recommended.

First-Strand cDNA Synthesis

The following procedure should be applied to each individual tester and driver poly(A)$^+$ RNA sample.

1. For each tester and driver sample (name the tubes cDNA1 and cDNA2, respectively) combine the following components into a sterile 0.5 ml microcentrifuge tube (do not use a polystyrene tube): 2–4 μg poly(A)$^+$ RNA to 2–4 μl, 10 μM cDNA synthesis primer to 1 μl. If necessary add sterile H$_2$O to a final volume of 5 μl.

2. Heat a thermal cycler to 70°C and incubate tubes for 2 min at 70°C.

3. Cool the tubes on ice for 2 min and briefly centrifuge the tubes.

4. In each tube, add 2 μl 5X first-strand buffer, 1 μl dNTP (deoxyribonucleotide-triphosphate) mix, 1 μl sterile H$_2$O, 1 μl AMV reverse transcriptase (20 units μl^{-1}). (Optional: to monitor the progress of cDNA synthesis, dilute 1 μl of [α-^{32}P]dCTP [10 mCi ml^{-1} 3000 Ci/mmol] with 9 μl of H$_2$O, and replace H$_2$O with 1 μl of diluted label.)

5. Gently vortex and briefly centrifuge the tubes.

6. Incubate the tubes at 42°C for 1.5 h in an air incubator to avoid any evaporation.

7. Place the tubes on ice to terminate first-strand cDNA synthesis and immediately proceed to second-strand synthesis.

Second-Strand cDNA Synthesis

1. Combine the following components into the first-strand cDNA sample tubes (from previous section, **Step 7**): 48.4 μl H$_2$O, 16 μl 5X second-strand buffer,

1.6 μl dNTP mix, 4 μl 20X second-strand enzyme cocktail.

2. Mix the contents and briefly centrifuge the tubes. The final volume should be 80 μl.

3. Incubate the tubes at 16°C for 30 min in a thermal cycler.

4. Add 4 μl of 20X EDTA/glycogen mix to terminate the second-strand synthesis reaction.

5. Add 100 μl of phenol:chlorophorm:isoamyl alcohol (25:24:1).

6. Vortex thoroughly, and centrifuge the tubes at 14,000 rpm for 10 min at room temperature.

7. Carefully remove the top aqueous layer and place in a sterile 0.5 ml microcentrifuge tube. Discard the interphase and lower phase.

8. Add 100 μl of chlorophorm:isoamyl alcohol (24:1) to the aqueous layer.

9. Repeat **Steps 6 and 7**.

10. Add 40 μl of 4M NH$_4$OAc and 300 μl of 95% ethanol.

11. Without waiting, vortex the tubes thoroughly and precipitate the pellet at 14,000 rpm for 20 min at room temperature.

12. Remove the supernatant carefully (if you used [α-^{32}P]dCTP check for presence of the pellet using a Geiger counter).

13. Wash the pellet with 500 μl of 80% ethanol without excessively disturbing the pellet.

14. Air-dry the pellet for ~10 min to evaporate the remaining ethanol.

15. Dissolve the pellet in 50 μl H$_2$O.

16. Transfer 6 μl from each sample to fresh tubes and store these samples at −20°C.

Rsa I Digestion

The *Rsa* I digestion step is performed to generate shorter, blunt-ended double-strand (ds) cDNA fragments that are optimal for subtractive hybridization and also necessary for the adaptor ligation step later in the protocol.

The following protocol should be performed for each experimental ds tester (cDNA1) and driver (cDNA2) cDNA:

1. Add the following reagents into each tube: 43.5 μl ds cDNA, 5 μl 10X *Rsa* I restriction buffer, 1.5 μl *Rsa* I (10 units μl^{-1}).

2. Mix by vortexing and centrifuge briefly.

3. Incubate at 37°C for 1.5 hr.

4. Set aside 5 μl of the digested mixture and analyze on a 2% agarose/EtBr gel run in 1 × TAE buffer along with undigested cDNA (from previous section, **Step 16**) to determine the efficiency of *Rsa* I digestion.

The ds cDNA preparation appears as a smear, and after *Rsa* I digestion, the average cDNA size is smaller.

Note: During this procedure continue the digestion reaction and terminate it only after you are satisfied with the result of your digestion.

5. Add 2.5 μl of 20X EDTA/glycogen mix to terminate the reaction.

6. Add 50 μl of phenol:chloroform:isoamyl alcohol (25:24:1) and vortex thoroughly.

7. Centrifuge the tubes at 14,000 rpm for 10 min to separate the phases.

8. Remove the top aqueous layer and place in a clean 0.5 ml tube.

9. Add 50 μl of phenol:chloroform (24:1) and vortex thoroughly.

10. Centrifuge the tubes at 14,000 rpm for 10 min to separate phases.

11. Transfer the top aqueous layer to a clean 0.5 ml tube.

12. Add 25 μl of 4M NH$_4$OAc and 187.5 μl of 95% ethanol.

13. Without waiting, vortex the mixture thoroughly and precipitate the pellet at 14,000 rpm for 20 min at room temperature.

14. Remove the supernatant carefully and gently overlay 200 μl of 80% ethanol on the pellet.

15. Centrifuge at 14,000 rpm for 5 min and remove the supernatant carefully (if you used [α-^{32}P]dCTP, check for presence of the pellet using a Geiger counter).

16. Air-dry the pellet for about 10 min to evaporate the remaining ethanol.

17. Dissolve the pellet in 5.5 μl of H$_2$O (the pellets can be stored at −20°C at this step).

Adaptor Ligation

It is strongly recommended that subtraction be performed in both directions for each tester/driver cDNA pair. The forward subtraction reaction is designed to enrich for differentially expressed sequences present in tester (cDNA1) but not in driver (cDNA2); reverse subtraction is designed to enrich differentially expressed sequences present in driver (cDNA2) but not in tester (cDNA1). Both forward and reverse subtracted cDNAs will be useful as probes for differential screening of the resulting tester cDNA library. Tester cDNAs are ligated separately to Ad1 (tester 1-1 and 2-1) and Ad2R (tester 1-2 and 2-2). It is highly recommended that a third ligation of both adaptors 1 and 2R to the tester cDNAs (unsubtracted tester control) be performed and used as a negative control for subtraction.

Important Note: The adaptors are not ligated to the driver cDNA; for example, if you are using *Rsa* I digested cDNA1 as a tester for subtraction, *Rsa* I digested driver cDNA2 should not be used for ligation, and vice versa.

1. Label four 0.5 ml tubes as tester 1-1, tester 1-2 (for cDNA1 as a tester), tester 2-1, and tester 2-2 (for cDNA2 as a tester).

2. Dilute 1 μl of each *Rsa* I digested tester cDNA 1 and cDNA2 from the previous section, **Step 17**, with 5 μl sterile H_2O.

3. Prepare a master ligation mix by combining the following reagents in a 0.5 ml tube: 3 μl sterile H_2O, 2 μl 5X ligation buffer, 1 μl adenosine triphosphate (ATP) (3 mM), 1 μl T4 DNA ligase (400 units $μl^{-1}$).

4. For each tester cDNA mixture, the reagents are combined in a 0.5 ml tube in the following order:

Component	Tube 1, Tester 1-1[a] (μl)	Tube 2, Tester 1-2[a] (μl)
Diluted tester cDNA	2	2
Adaptor Ad1 (10 μM)	2	-
Adaptor Ad2R (10 μM)	-	2
Master ligation mix	6	6
Final volume	10	10

[a]The same setup also is used for Tester 2-1 and Tester 2-2.

Tester 1-1: cDNA1 ligated to adaptor 1; **Tester 1-2**: cDNA1 ligated to adaptor 2

Tester 2-1: cDNA2 ligated to adaptor 1; **Tester 2-2**: cDNA2 ligated to adaptor 2

The two adaptors provide different PCR primer annealing sites. This way, two tester cDNA populations from the same cDNA are created with different adaptors.

5. In a fresh microcentrifuge tube, mix 2 μl of tester 1-1 (from tube 1) and 2 μl of tester 1-2 (from tube 2). This will be your unsubtracted tester control. Do the same reaction for tester 2-1 and 2-2.

6. Centrifuge the tubes briefly and incubate at 16°C overnight.

7. Stop the ligation reaction by adding 1 μl of 0.2 M EDTA.

8. Heat the samples at 72°C for 5 min to inactivate the ligase (use a thermal block) and briefly centrifuge the tubes. The adaptor ligation step is now completed for tester cDNAs 1-1 and 1-2.

9. Remove 1 μl of each unsubtracted tester control and dilute in 1 ml of H_2O. These samples will be used for PCR amplification.

Analysis of Ligation Efficiency

It is recommended to perform the following PCR experiment to verify that at least 25% of the cDNAs have adaptors at both ends.

1. Dilute 1 μl of each ligated cDNA (from previous section, **Step 4**) into 200 μl of H_2O.

2. Set up the PCR reaction as follows:

Component	Tube#	1	2	3	4
Tester 1-1 or 2-1		1	1	-	-
Tester 1-2 or 2-2		-	-	1	1
G3PDH 3′ primer (10 μM)		1	1	1	1
G3PDH 5′ primer (10 μM)		-	1	-	1
PCR Primer 1 (10 μM)[a]		1	-	1	-
Total volume (μl)		3	3	3	3

[a]Primer 1 (P1) contains 22 nucleotides corresponding to the 5′ end sequence of both adaptors Ad1 and Ad2R.

3. Prepare a master mix for all the tubes plus one additional tube. For each reaction, combine the reagents in the order:

Reagent	Amount per reaction tube (μl)
Sterile H_2O	18.5
10X PCR reaction buffer	2.5
dNTP mix (10 mM)	0.5
50X Advantage cDNA PCR mix	0.5
Total volume	22

Alternatively, normal Taq DNA polymerase can be used instead of Advantage cDNA PCR polymerase chain reaction mix, but additional PCR cycles will be needed.

4. Mix the reagents thoroughly and briefly centrifuge the tubes.

5. Aliquot 22 μl of master mix into each reaction tube from **Step 2**.

6. Put 50 μl of mineral oil into each tube (if oil-free thermal cycler is used, omit this step).

7. Incubate the reaction mixture in a thermal cycler at 75°C for 5 min to extend the adaptors.

8. Without removing the samples from the cycler, immediately commence 20 cycles of 94°C, 30 seconds; 65°C, 30 seconds; 68°C, 2.5 min.

9. Analyze 5 μl from each reaction on a 2% agarose/EtBr gel run in 1X TAE buffer.

If the product is not visible after 20 cycles, an additional five cycles can be carried out and step 9 can be repeated.

The PCR reactions with G3PDH 3′ and primer 1 primers where tester 1-1 (adaptor 1 ligated) or tester 1-2 (adaptor 2R ligated) are used as the template should generate 0.75 kb PCR product (tubes 1 and 3). The PCR reactions with G3PDH 3′ and 5′ primers where tester 1-1 or tester 1-2 are used as the template should generate 0.4 kb PCR product (tubes 2 and 4). The efficiency of adaptor 1 and adaptor 2R ligation is determined by comparing the relative intensities of the bands for the products of tube 2 to 1 and tube 4 to 3, respectively.

Note: If the result of the ligation is not satisfactory, you should repeat the ligation with fresh samples before proceeding to the hybridization steps.

First Hybridization

During first hybridization, hybridization kinetics lead to equalization and enrichment of differentially expressed sequences. In the first hybridization, each tester (1-1, 1-2, etc.) cDNA is hybridized with excess driver cDNA. Single-strand cDNAs are enriched for differentially expressed sequences because nontarget cDNAs present in the tester and driver cDNA form hybrids.

1. For each tester sample, combine the reagents in 0.5 ml tubes in the following order:

Important note: 4X hybridization buffer should be warmed to room temperature before use.

Component	Hybridization sample 1 (μl)	Hybridization sample 2 (μl)
Rsa I digested driver cDNA (from *Rsa* I Digestion section, Step 17)	1.5	1.5
Ad1-ligated tester 1-1[a] (from Adaptor Ligation section, Step 4)	1.5	-
Ad2R-ligated tester 1-2 (from Adaptor Ligation section, Step 4)	-	1.5
4X hybridization buffer	1	1
Final volume	4	4

[a]Use the same setup for tester 2-1 and 2-2.

2. Put one drop of mineral oil into each tube and centrifuge briefly.

3. Incubate the samples in a thermal cycler at 98°C for 1.5 min and then at 68°C for 8–12 hr.

4. Proceed immediately to the second hybridization step.

Important note: Do not remove the hybridization samples from the thermal cycler for longer than necessary to add fresh driver for the second hybridization.

Second Hybridization

In the second hybridization, two samples from the first hybridization are mixed together and excess driver cDNA is added. New hybrid molecules consisting of differentially expressed cDNAs with different adaptors on each end that can be used for PCR are formed.

The following steps should be repeated for each experimental driver cDNA:

1. Add the following reagents in a tube: 1 μl driver cDNA (from *Rsa* I Digestion section, **Step 17**), 4X hybridization buffer, 2 μl sterile H₂O. Mix gently and briefly centrifuge the contents of the tube.

2. Place 1 μl of this mixture in a 0.5 ml microcentrifuge tube and overlay with one drop of mineral oil. Incubate in a thermal cycler at 98°C for 1.5 min.

3. To this tube of freshly denatured driver cDNA, add hybridized sample 1 and hybridized sample 2 (prepared in First Hybridization section, **Step 4**).

Note: For efficient hybridization, the two hybridization samples should be mixed together only in the presence of freshly denatured driver. To achieve this, using a 20 μl micropipettor draw the hybridization sample 2 (4 μl) into the pipette tip, provide a little air space in the tip, and then draw freshly denatured driver cDNA (1 μl) without mixing the samples. Then add the whole content of the tip into the hybridization sample 1 (4 μl).

4. Mix the entire mixture and briefly centrifuge the tube.

5. Incubate the hybridization reaction in a thermal cycler at 68°C for 14–16 hr.

6. Add 200 μl of dilution buffer to the tube and mix well by pipetting.

7. Incubate the hybridization reaction in a thermal cycler at 68°C for 7 min.

8. Store the sample at −20°C.

PCR Amplification for the Selection of Differentially Expressed cDNAs

In this step differentially expressed cDNAs are selectively amplified. Adaptors Ad1 and Ad2R contain the sequence for PCR primer P1 at their 5′ ends. Therefore it is essential to extend the 5′ ends of the adaptors. All the cycling parameters are given for the Perkin-Elmer DNA Thermal Cycler 9600/2400 (Perkin-Elmer). The cycling parameters must be optimized for each PCR machine. Use of Advantage cDNA PCR mix (Clontech) is strongly recommended. Alternatively, normal Taq DNA polymerase can be used, but five additional PCR cycles will be needed in both the primary and secondary PCR and the use of manual hot start or hot start wax beads is strongly recommended to reduce nonspecific DNA synthesis. Each amplification should have at least four reactions: 1) forward subtracted tester cDNAs; 2) unsubtracted tester control; 3) reverse subtracted tester cDNAs; and 4) unsubtracted driver control for the reverse subtraction.

Primary PCR

1. Aliquot 1 μl of each diluted cDNA into an appropriately labeled tube (each subtracted sample from Second Hybridization section, **Step 8** and the corresponding diluted unsubtracted tester control from Adaptor Ligation section, **Step 9**).

2. Prepare a master mix sufficient for all the reaction tubes by combining the following reagents in order (amount per reaction): 19.5 μl H₂O, 2.5 μl 10X PCR buffer, 0.5 μl dNTP mix (10 mM),1 μl PCR primer

P1 (10 µM), 0.5 µl Advantage cDNA polymerase mix for a total volume of 24 µl.

3. Mix the reagents well and briefly centrifuge the tube.

4. Aliquot 24 µl of master mix into each reaction tube from **Step 1.**

5. Overlay 50 µl of mineral oil into each tube (if oil-free thermal cycler is used, omit this step).

6. Incubate the reaction mixture in a thermal cycler at 75°C for 5 min to extend the adaptors.

7. Immediately commence one cycle of 94°C, 25 seconds and 27 cycles of 94°C, 30 seconds; 66°C, 30 seconds; 72°C, 1.5 min.

8. Analyze 8 µl from each reaction on a 2% agarose/EtBr gel run in 1X TAE buffer.

Secondary PCR

1. Dilute each primary PCR mixture in 27 µl of H$_2$O.

2. Aliquot 1 µl of each diluted primary PCR product mixture from **Step 1** into appropriately numbered tubes.

3. Prepare a master mix for the secondary PCR enough for all the reaction tubes by combining the following reagents in order (amount per reaction): 18.5 µl H$_2$O, 2.5 µl 10X PCR buffer, 0.5 µl dNTP mix (10 mM), 1 µl nested PCR primer NP1 (10 µM), 1 µl nested PCR primer NP2R (10 µM), 0.5 µl 50X Advantage cDNA polymerase mix for a total volume of 24 µl.

4. Mix the reagents well and briefly centrifuge the tube.

5. Aliquot 24 µl of master mix into each reaction tube from **Step 2**.

6. Overlay 50 µl of mineral oil into each tube (if oil-free thermal cycler is used, omit this step).

7. Immediately commence 12 cycles of 94°C, 30 seconds; 68°C, 30 seconds; 72°C, 1.5 min.

8. Analyze 8 µl from each reaction on a 2% agarose/EtBr gel run in 1X TAE buffer.

9. Store reaction products at 4°C for the Thymine/Adenine (T/A) cloning procedure. Freezing and thawing the PCR products decreases the efficiency of cloning.

The PCR mixture is now enriched for differentially expressed sequences.

The secondary PCR products of subtracted samples usually look like smears. If no product is observed after 12 cycles, increase the number of cycles cautiously because too many cycles increase the background.

Subtraction Efficiency Test

To compare the abundance of known cDNAs before and after subtraction and to analyze the efficiency of subtraction, a quick PCR-based assay can be performed. PCR is performed for a ubiquitously expressed gene (such as G3PDH) between the two RNA sources under comparison. Figure 19 shows the results of the subtraction efficiency test for the forward and reverse subtracted libraries. In a successfully subtracted mixture, G3PDH abundance is reduced. In the subtracted samples the G3PDH PCR product should be observed 5–15 cycles later than the unsubtracted samples. In the unsubtracted sample, G3PDH product is observed after 18–23 cycles.

PCR Analysis of Subtraction

1. Dilute the subtracted and unsubtracted (unsubtracted tester control 1 and 2) secondary PCR products tenfold in H$_2$O.

2. Combine the following reagents in 0.5 ml microcentrifuge tubes in the following order:

Tube no.	1 (µl)	2 (µl)
Diluted subtracted cDNA (2nd PCR product)	1	-
Diluted unsubtracted control (2nd PCR product)	-	1
G3PDH 5′ primer (10 µM)	1.2	1.2
G3PDH 3′ primer (10 µM)	1.2	1.2
Sterile H$_2$O	22.4	22.4
10× PCR reaction buffer	3	3
dNTP mix (10 mM)	0.6	0.6
50× Advantage cDNA PCR Mix	0.6	0.6
Total volume	30	30

3. Mix and briefly centrifuge the tubes.

4. Overlay with one drop of mineral oil (if oil-free thermal cycler is used, omit this step).
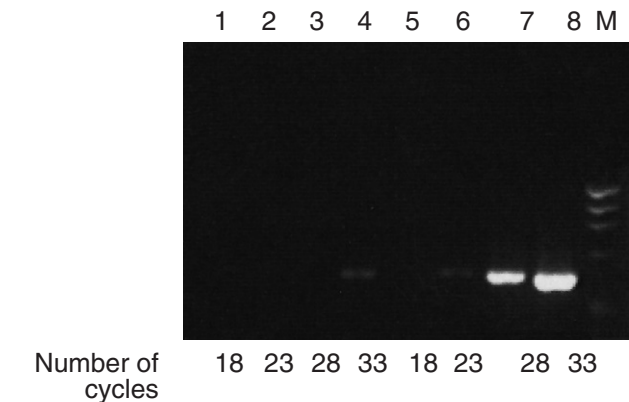
Figure 19 Analysis of subtraction efficiency test: Tester complementary deoxyribonucleic acid (cDNA) was prepared from MCF7 breast carcinoma cells transfected with *BRCA*1 cDNA carrying expression vector and driver cDNA was prepared from MCF7 cells transfected only with the expression vector. M: *Hae*III digested φX174 (Sigma) (1.3, 1.1, 0.9, 0.6, 0.3 kb). Secondary polymerase chain reaction (PCR) was performed on forward subtracted experimental cDNA (lanes 1–4) and unsubtracted tester control for forward subtraction (lanes 5–8) with G3PDH 5′ and 3′ primers.

5. Use the following thermal cycling program for 18 cycles; 94°C, 30 seconds; 60°C, 30 seconds; 68°C, 2 min.

6. Remove 5 µl from each reaction, place it in a clean tube, and store on ice. Put the rest of the reaction back into the thermal cycler for three more cycles.

7. Repeat **Step 6** three times (i.e., remove 5 µl after 23, 28, and 33 cycles).

8. Examine the 5 µl samples (the aliquots that were removed from each reaction after 18, 23, 28, and 33 cycles) on a 2.0% agarose/EtBr gel (Figure 19).

A gene known to be expressed in the tester RNA but not in the driver RNA can be used as a positive control, and the previous procedure can be performed with the primers specific to this gene. This cDNA should become enriched by the subtraction procedure.

Cloning of Subtracted cDNAs

The uncloned subtracted cDNA mixture can be used to screen various libraries such as genomic, cDNA, YAC, or cosmid. The subtracted cDNA library can be made by subcloning the PCR products (secondary PCR products from the Secondary PCR section) into plasmid vectors using conventional cloning procedures.

The following details describe a method that is commonly applied for cloning the subtracted cDNAs.

T/A Cloning

1. Use 3 µl of the secondary PCR product (from Secondary PCR section, **Step 7**) for cloning with a T/A-based system, such as the Advantage PCR Cloning Kit (Clontech) or Promega PGEM-T Easy Vector system, according to the manufacturer's protocols.

2. After ligating the secondary PCR products into the vector, the library is transformed into a bacterial strain such as *E. coli* JM109 strain of high-efficiency competent cells (1×10^8 cfu/µg DNA) by heat shock treatment. Alternatively, electrocompetent cells can be transformed by electroporation using 1.8 kV pulse with a pulser (BioRad Gene Pulser).

Other host strains can be used, but they should be compatible with blue/white color screening and standard ampicillin selection.

It is important to optimize the cloning efficiency because low efficiency will cause high background and low representation of the subtracted clones.

3. The transformed cells are plated onto agar plates containing X-gal (50 mg l^{-1}) and IPTG (isopropyl-D-thiogaloctopyranoside) (100 mM).

4. Recombinant white clones are randomly picked and inoculated in 100 µl of ampicillin-containing LB-medium in 96-well microtiter plates.

5. Bacteria should be allowed to grow at 37°C for at least 4 hr before insert amplification or alternatively grown overnight.

cDNA Insert Analysis by PCR

It is recommended to check for the presence of cDNA inserts in a small number of colonies first and then analyze a large number of colonies. PGEM-T Easy Vector has universal T7 and SP6 primers that can be used to amplify inserts cloned into this plasmid. The bacterial culture can be used directly for PCR amplification of the cDNA inserts.

1. Prepare a master mix for 100 PCR reactions:

	Per reaction (µL)
$10\times$ PCR reaction buffer	2
MgCl$_2$ (25 mM)	1.2
SP6 Primer (20 pmol/µl)^a	1
T7 primer (20 pmol/µl)^a	1
dNTP Mix (10 mM)	0.4
H$_2$O	13.2
Taq DNA Polymerase	0.2
Total volume	19.0

^{a}Alternatively nested PCR primer 1 and 2R can be used in PCR amplification of the inserts.

2. Aliquot 19 µl of the master mix into each tube.

3. Transfer 1 µl of each bacterial culture (from **Step 5**) to each tube containing the master mix.

4. Perform PCR in an oil-free thermal cycler with the following conditions: 1 cycle: 94°C, 2 min and then 30 cycles: 94°C, 1 min; 55°C, 1 min; 72°C, 1 min.

5. Analyze 5 µl from each reaction on a 2.0% agarose/EtBr gel (Figure 20).

It is important to detect clones carrying cDNA inserts before proceeding to the differential screening procedure. The number of differentially expressed

Figure 20 Insert screening analysis. White colonies were randomly picked from forward subtracted library of MCF7 breast carcinoma cells ectopically expressing the *BRCA*1 gene and polymerase chain reaction amplified with T7-Sp6 primers.
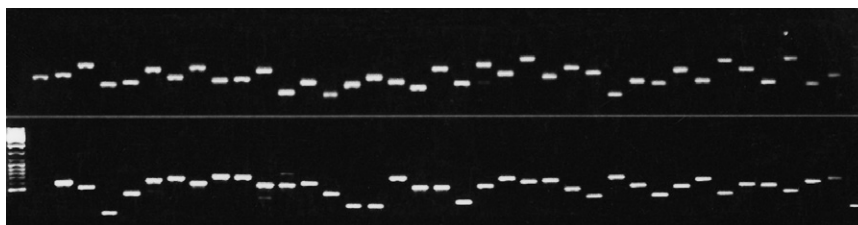
genes can differ between the two tissue types under comparison. This effects the number of independent clones obtained from the subtracted samples. The subtraction and the cloning efficiencies are other important parameters that directly influence the colony numbers. In general, 500–1000 colonies are recommended for the screening procedure.

Differential Screening of the Subtracted Library

Several factors are responsible for the sensitivity of the whole experiment. Screening the subtracted library is very important for the sensitivity. The PCR-based SSH technology greatly enriches the differentially expressed genes, but the subtracted samples may still have some cDNAs common to both the tester and driver samples. Differential screening of subtracted library with subtracted probes will increase the sensitivity for detecting true differentially expressed sequences and decrease the chance of getting false-positive transcripts, which may still be present in the subtracted library.

The following differential screening technique will greatly increase the sensitivity for detecting the differentially expressed sequences, even those that correspond to low-abundance differentially expressed mRNAs. The subtracted library is hybridized with forward and reverse subtracted cDNA probes. The reverse subtracted probe is made by performing the subtraction with original tester cDNA as a driver and the driver as a tester. Truly differentially expressed sequences will hybridize only with the forward subtracted probe, and clones that hybridize with reverse subtracted probe are considered to be background. To screen the subtracted library, the PCR products of the cDNA clones can be arrayed as dots on nylon filters.

Preparation of cDNA Dot Blots by Arraying the PCR Products

MATERIALS

PCR products from each clone, 0.6N NaOH, 0.5M Tris-HCl [pH 7.5], 2X SSC (300 mM NaCl and 30 mM Na$_3$. Citrate.2H$_2$O [pH 7.0]) are required.

METHODS

For high-throughput analysis, it is easier to use a 96-well microtiter plate for formatting the PCR products as arrays.

1. Transfer 5 μl of PCR product of each cDNA clone in a 96-well microtiter plate and add 5 μl of freshly made 0.6N NaOH to denature the DNA for hybridization.

2. Mix the combination by slowly spinning the plate.

3. Transfer 1 or 2 μl of each mixture to a nylon membrane by using a micropipettor. This process can be accomplished by using a 96-well replicator or alternatively with a multichannel micropipettor.

4. Make at least two identical blots for hybridization with subtracted and reverse subtracted probes (see the Adaptor Ligation section).

5. Neutralize the blots for 2–4 min in 0.5M Tris-HCl (pH 7.5) and wash in 2X SSC.

6. Cross-link cDNA on the membrane by baking the blots at 80°C for 2 hours or alternatively use a ultraviolet UV crosslinking device (such as Strategene's UV Stratalinker) under 120 mJ.

Preparation of cDNA Probes

The arrays prepared from the previous step are hybridized with forward and reverse subtracted cDNA probes. Before the hybridization step, the adaptors from the forward and reverse subtracted cDNA probes should be removed to reduce the background that can be caused by these sequences on the arrayed subtracted library. Therefore the subtracted cDNA mixtures are digested with restriction enzymes that have specific restriction sites in the adaptor sequences. Some of the following materials are also available as a kit from Clontech Laboratories (PCR-Select Differential Screening Kit).

MATERIALS

The following enzymes can be obtained from New England BioLabs: *Rsa* I, *Eag* I, and *Sma* I restriction enzymes (10 unit μl^{-1}), 10X restriction buffer 4 (for *Rsa* I, *Eag* I), and 10X restriction buffer 3 (for *Sma* I).

1. Each of the forward and reverse subtracted secondary PCR products (~40 μl) should be purified before the restriction enzyme digestion using a PCR purification kit or alternatively using a silica matrix-based purification system. You can set up more than one reaction to ensure enough cDNA as a probe for the hybridization steps.

2. After purification adjust the volume of both products to 28 μl with H$_2$O. Remove 3 μl of this sample for agarose gel electrophoresis. Make sure that the concentration of PCR products in each sample is the same.

3. To remove the adaptor sequences add 3 μl 10X restriction buffer 4 and 1.5 μl *Rsa* I.

Note: To control the restriction reaction efficiency you can use a plasmid that contains an *Rsa* I restriction site as a control. In separate tubes, mix 3 µl of each restriction digest sample (From **Step 3**) and add 25 ng of plasmid DNA.

4. Incubate the tubes for 1 hr at 37°C.

5. While this digestion reaction is still in incubation, electrophorese 3 µl of each undigested cDNA, 3 µl of each digested cDNA, and 3 µl of each digested cDNA plus digested plasmid on a 2% agarose/EtBR gel.

6. After analyzing the first digestion efficiency, add 1 µl of *Sma* I into each reaction (from **Step 4**) and incubate for another hour at room temperature.

7. Add 61 µl of H_2O, 10 µl of 10X restriction buffer 3, and 1 µl of *Eag* I to each tube and incubate the tubes for another hour at 37°C.

8. Remove the adaptors from the cDNA using a PCR purification kit or alternatively using a silica matrix-based purification system.

Random Primer Labeling of cDNA Probes

The tester and driver cDNA probes can be labeled with radioisotope [α-^{32}P]dCTP (10 mCi ml^{-1} 3000 Ci/mmol) by using a commercially available random primer labeling kit. Tester-specific subtracted probe (forward subtracted probe) and driver-specific subtracted probe (reverse subtracted probe) are used for differential screening hybridization.

Differential Hybridization with Forward and Reverse Subtracted Probes

In this section, the ^{32}P-labeled probes will be hybridized to the subtracted clones arrayed on nylon membranes.

MATERIALS

The required reagents include the following:
▲ Hybridization solution: 0.5 M phosphate buffer (pH 7.2), 7% SDS, 1 mM EDTA (pH 8.0), 1% BSA, 10 µg ml^{-1} sheared salmon sperm DNA (added after boiling).
▲ Blocking solution: 2 mg ml^{-1} of NP1, NP2R, cDNA synthesis primers, and their complementary oligonucleotides.
▲ Wash buffers: Low-stringency (2X SSC/0.5% SDS) and high-stringency (0.2X SSC/0.5% SDS) washing buffers, prewarmed to 68°C.
▲ Hybridization probes: 20X SSC (3M NaCl and 0.3M Na_3 Citrate.$2H_2O$ [pH 7.0]), 50 µl of sheared salmon sperm DNA (10 µg ml^{-1}), 10 µl blocking solution, purified probe (at least 10^7 cpm. per 100 ng of subtracted cDNA).

METHODS

1. Prepare a prehybridization solution for each membrane:
   a. Mix 50 µl of 20X SSC, 50 µl of sheared salmon sperm DNA (10 µg ml^{-1}) and 10 µl of blocking solution.
   b Boil this mixture for 5 min, then chill on ice.
   c. Combine the chilled mixture with 5 ml of hybridization solution (prewarmed to 68°C).
2. Place each membrane in the prehybridization solution prepared in **Step 1**.
3. Prehybridize for 2–4 hr with continuous agitation at 68°C.

Note: It is important that you add blocking solution to the prehybridization solution because subtracted probes contain the same adaptor sequences as arrayed clones.

4. Prepare hybridization probes:
   a. Mix 50 µl of 20X SSC, 50 µl of sheared salmon sperm DNA (10 µg ml^{-1}), and 10 µl blocking solution and purified probe.
   b. Boil the probe for 5 min, then chill on ice.
   c. Add the chilled probe solution to the hybridization solution.
5. Hybridize overnight with continuous agitation at 68°C.

Note: Avoid adding the probe directly to the membrane.

6. Prepare low-stringency (2X SSC/0.5% SDS) and high-stringency (0.2X SSC/0.5% SDS) washing buffers, prewarmed to 68°C.

7. Wash membranes with low-stringency buffer (4×20 min at 68°C), then wash with high-stringency buffer (2×20 min at 68°C)

8. Expose the membrane to X-ray film (Kodak) overnight with an intensifying screen at −70°C. (You can expose the membrane to X-ray film for varying lengths of time.)

RESULTS

Interpretation of Hybridization Results

The results of a differential screening experiment are shown in Figure 21. These results show different types of hybridization:

1. Clones hybridized with the forward subtracted probe but not with the reverse subtracted probe (e.g., C3, G3, and E1) are most likely to correspond to differentially expressed mRNAs that are worth pursuing.

2. Clones that are hybridized equally to both subtracted probes (e.g., E2 and F1) do not represent
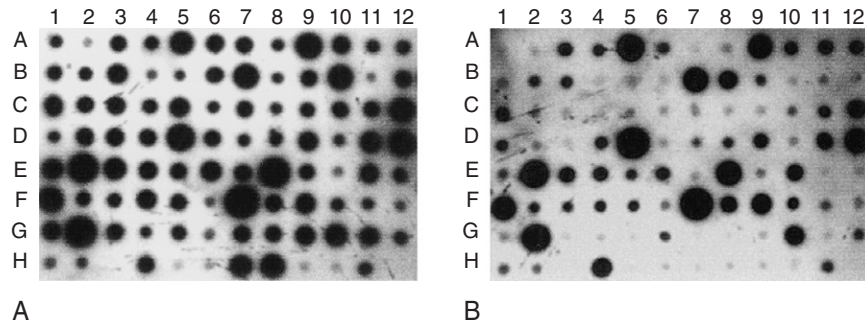
Figure 21 Differential screening of suppression subtractive hybridization (SSH)-selected complementary deoxyribonucleic acid (cDNA)-clones with forward (**A**) and reverse (**B**) subtracted probes. Selected cDNA inserts were PCR-amplified from the forward subtracted cDNA library, enriched for *BRCA*1 upregulated sequences, spotted in two identical membranes, and hybridized with [α-^{32}P]dCTP-labeled forward (Tester; MCF7 breast carcinoma cells ectopically expressing *BRCA*1) or reverse subtracted (Tester; MCF7 cells transfected only with the vector that was used to clone *BRCA*1) cDNA probes. **Rows A–H**: test cDNA samples, **H3**: negative PCR control, **H5–H6**: cDNA1 and **H9–10**: cDNA2 as negative control cDNAs, **H7–8**: *BRCA*1, **H12**: NaOH + water). For example, E2 cDNA showed no significant increase (1.76-fold), but C3 cDNA (zinc finger protein, LZK1) displayed sevenfold increase. The signal intensities were measured by a phosphorimager (Atalay *et al*., 2002).

differentially expressed mRNAs and do not need further analysis.

3. Clones that are hybridized equally to both subtracted probes, but where the intensity of the hybridization signals is different: If the intensity difference is ≥ fivefold (e.g., E3), the clone probably corresponds to differentially expressed mRNAs and should be analyzed further. If the intensity difference is ≤ threefold (e.g., F2), it is more likely the result of a random fluctuation in the efficiency of the forward and reverse subtractions.

4. Clones that are not hybridized with either of the subtracted probes (e.g., A2 and F12) usually represent nondifferentially expressed cDNAs present in the PCR select library.

Confirmation of Differential Screening Results

There are several ways to confirm the differential expression of the candidate clones identified by differential screening, such as Northern blot hybridization, Virtual Northern blot analysis, or quantitative-reverse transcription PCR. Northern blot analysis is a direct way to analyze the expression between two samples populations under comparison. It not only shows the expression difference but also the amount of transcript present in the samples and the full transcript size of the gene. This analysis requires at least 2 μg of poly A$^+$ RNA.

Virtual Northern blots can be used if the amount of starting poly A$^+$ RNA is not sufficient for Northern blot analysis. To carry out a Virtual Northern blot, the SMART PCR cDNA synthesis kit (Clontech) can be used to make cDNAs from the poly A$^+$ RNA sample,

which can be transferred onto a nylon membrane. Although it is an informative method, for some cDNA clones it may give multiple bands.

RT-PCR analysis is extremely sensitive for detecting the expression differences between the samples and can be performed either as a semi-quantitative or quantitative method. To use this approach, the candidate cDNA clones should be sequenced and specific PCR primers should be designed. However, it is not a technique for high-throughput analysis because it is time consuming.

Sequence Analysis of Differentially Expressed Clones

To determine the nature of the transcripts, sequence analysis should be carried out from the 5′-end of the selected transcripts. The sequences can then be analyzed by using the freely available databases such as Genbank/EMBL and Expressed Sequence Tag (EST). The result of the sequence analysis may assign each transcript to a known tissue-specific transcript or a transcript known to be expressed preferentially in target tissue or a novel transcript with known or recognizable motifs. The last case may also provide clues to whether the sequence is a member of a protein family.

DISCUSSION

SSH PCR is a sophisticated cDNA subtraction method to enrich and isolate differentially expressed genes. SSH accomplishes normalization and subtraction by taking advantage of the different rates of hybridization of cDNA strands for different genes depending on

their abundance level and the degree of (differential) expression (Desai *et al*., 2000). Effective enrichment of a target gene by SSH PCR is determined by the concentration ratio between tester and driver and is more efficient the higher this value (Ji *et al*., 2002). SSH is generally better suited for the identification of sizable differences (approximately fivefold or greater) in rare transcripts, but arrays can detect smaller differences. The two techniques are complementary if the goal is a comprehensive detection of even small differences.

SSH, unfortunately, can be used only for pairwise treatment comparisons and must be replicated with the tester and driver reversed to identify gene expression changes in both directions. It also is not a quantitative method for measuring expression differences. SSH is best used for identifying genes that are completely absent, rather than expressed less abundantly, in the driver sample (Moody, 2001). In general, one of the major problems associated with specific cellular characterization is the low amount of sample. However, problems associated with tissues in small quantities can be solved by a restricted PCR amplification step prior to cDNA subtraction. When the amount of starting material is limited it is possible to start with only a few ng of total RNA and produce enough double-stranded cDNA of both tester and driver to subtract two specific cell populations by using PCR technology (SMART PCR cDNA Synthesis Kit, Clontech).

There are some other methods such as DNA chip/microarray, which is a very powerful method when used to identify differentially regulated genes on a genomewide scale (Kurian *et al*., 1999) but may not be able to detect transcripts present in the mRNA (or cDNA) populations in low quantity, making SSH a useful complementary approach (Yang *et al*., 1999).

SSH has been widely used in the study of cell differentiation (Du *et al*., 2001; Hofsaess and Kapfhammer, 2003) and development in animals (Cobellis *et al*., 2001; Fellenberg *et al*., 2003; Lee *et al*., 2002; Yao *et al*., 2003) and cancer diagnosis in humans because differentially expressed genes are often important in disease pathogenesis (Atalay *et al*., 2002; Kostic and Shaw, 2000; Wang *et al*., 2001; Zhou *et al*., 2002). It has even been used for the study of rice development (Liu *et al*., 2001) and algae (Zhang *et al*., 2002). SSH is applicable to many studies in which the cDNAs derived from the differentially expressed genes of a particular tissue of cell type are being analyzed. The method reviewed here is a powerful technology that expands the study of gene expression from single genes to the genomic level. The genomic information from different species continues to be sequenced at great speed and SSH technology is one of the approaches that will be very much in demand for comparing the genomic structure of cells in the coming years. This type of genomic technique and the rapidly developing bioinformatics field will enable researchers to investigate gene expression and gain a better understanding of the genomic regulation of biologic processes that will have important applications in human and animal health and improvement of livestock production.

References

Atalay, A., Crook, T., Ozturk, M., and Yulug, I.G. 2002. Identification of genes induced by BRCA1 in breast cancer cells. *Biochem. Biophys. Res. Commun. 299*:839–846.

Cobellis, G., Missero, C., Simionati, B., Valle, G., and Di Lauro, R. 2001. Immediate early genes induced by H-Ras in thyroid cells. *Oncogene 20*:2281–2290.

Davis, M.M., Cohen, D.I., Nielsen, E.A., Steinmetz, M., Paul, W.E., and Hood, L. 1984. Cell-type specific cDNA probes and the murine I region: The localization and orientation of Ad alpha. *Proc. Natl. Acad. Sci. USA. 81*:2194–2198.

Desai, S., Hill, J., Trelogan, S., Diatchenko, L., Siebert, P.D. 2000. Identification of differentially expressed genes by suppression subtractive hybridization. In: *Functional Genomics: A Practical Approach.* Hunt, S.P., and Livesey, F.J. (eds), pp. 81–112. Oxford, Oxford University Press, 81–112.

Diatchenko, L., Lau, Y.F., Campbell, A.P., Chenchik, A., Moqadam, F., Huang, B., Lukyanov, S., Lukyanov, k., Gurskaya, N., Sverdlov, E.D., and Siebert, P.D. 1996. Suppression subtractive hybridization: A method for generating differentially regulated or tissue-specific cDNA probes and libraries. *Proc. Natl. Acad. Sci. USA. 93*:6025–6030.

Diatchenko, L., Lukyanov, S., Lau, Y.F., and Siebert, P.D. 1999. Suppression subtractive hybridization: A versatile method for identifying differentially expressed genes. *Methods Enzymol. 303*:349–380.

Du, Z., Cong, H., and Yao, Z. 2001. Identification of putative downstream genes of Oct-4 by suppression-subtractive hybridization. *Biochem. Biophys. Res. Commun. 282*:701–706.

Duguid, J.R., and Dinauer, M.C. 1990. Library subtraction of in vitro cDNA libraries to identify differentially expressed genes in scrapie infection. *Nucleic Acids Res. 18*:2789–2792.

Fellenberg, J., Dechant, M.J., Ewerbeck, V., and Mau, H. 2003. Identification of drug-regulated genes in osteosarcoma cells. *Int. J. Cancer 105*:636–643.

Hedrick, S.M., Cohen, D.I., Neilson, E.A., and Davis, M.M. 1984. Isolation of cDNA clones encoding T cell-specific membrane-associated proteins. *Nature 308*:149–153.

Hofsaess, U., and Kapfhammer, J.P. 2003. Identification of numerous genes differentially expressed in rat brain during postnatal development by suppression subtractive hybridization and expression analysis of the novel rat gene rMMS2. *Brain Res. Mol. Brain Res. 113*:13–27.

Ji, W., Wright, B.M., Cai, L., Flament, A., and Lindpaintner, K. 2002. Efficacy of SSH PCR in isolating differentially expressed genes. *BMC Genomics 3*:12.

Kostic, C., and Shaw, P.H. 2000. Isolation and characterization of sixteen novel p53 response genes. *Oncogene 19*:3978–3987.

Kurian, K.M., Watson, C.J., and Wyllie, A.H. 1999. DNA chip technology. *J. Pathol. 187*:267–271.

Lee, K.F., Yao, Y.Q., Kwok, K.L., Xu, J.S., and Yeung, W.S. 2002. Early developing embryos affect the gene expression patterns in the mouse oviduct. *Biochem. Biophys. Res. Commun. 292*:564–570.

Li, P., and Rossman; T.G. 2001. Genes upregulated in lead-resist-ant glioma cells reveal possible targets for lead-induced devel-opmental neurotoxicity. *Toxicol. Sci. 64*:90–99.

Liu, C., Zhang, L., Shao, Z.M., Beatty, P., Sartippour, M., Lane, T.F., Barsky, S.H., Livingston, E., and Nguyen, M. 2002. Identification of a novel endothelial-derived gene EG-1. *Biochem. Biophys. Res. Commun. 290*:602–612.

Liu, J., Liu, J., Yuan, Z., Qian, X., Qian, M., and Yang, J. 2001. Isolation and identification of genes expressed differentially in rice inflorescence meristem with suppression subtractive hybridization. *Chinese Sci. Bull. 46*:98–101.

Moody, D.E. 2001. Genomics techniques: An overview of methods for the study of gene expression. *J. Anim. Sci. 79* (E. Suppl.):E128–E135.

Sambrook, J., Fritsch, E.F., and Manistis, T., 1989. *Molecular Cloning: A Laboratory Manual*, 2nd ed. New York, Cold Spring Harbor Laboratory.

Sargent, T.D., and Dawid, I.B., 1983. Differential gene expression in the gastrula of Xenopus laevis. *Science 222*:135–139.

Stassar, M.J., Devitt, G., Brosius, M., Rinnab, L., Prang, J., Schradin, T., Simon, J., Petersen, S., Kopp-Schneider, A., and Zoller, M. 2001. Identification of human renal cell carcinoma associated genes by suppression subtractive hybridization. *Br. J. Cancer 85*:1372–1382.

Uchijima, M., Raz, E., Carson, D.A., Nagata, T., and Koide, Y., 2001. Identification of immunostimulatory DNA-induced genes by suppression subtractive hybridization. *Biochem. Biophys. Res. Commun. 286*:688–691.

Wang, Q., Yang, C., Zhou, J., Wang, X., Wu, M., and Liu, Z. 2001. Cloning and characterization of full-length human ribosomal protein L15 cDNA which was overexpressed in esophageal cancer. *Gene 263*:205–209.

Wang, Z., and Brown, D.D. 1991. A gene expression screen. *Proc. Natl. Acad. Sci. USA. 88*:11505–11509.

Yang, G.P., Ross, D.T., Kuang, W.W., Brown P.O., and Weigel, R.J. 1999. Combining SSH and cDNA microarrays for rapid identi-fication of differentially expressed genes. *Nucleic Acids Res. 27*:1517–1523.

Yao, Y.Q., Xu, J.S., Lee, W.M., Yeung, W.S., and Lee, K.F. 2003. Identification of mRNAs that are up-regulated after fertilization in the murine zygote by suppression subtractive hybridization. *Biochem. Biophys. Res. Commun. 304*:60–66.

Ye, S.Q. 2004. Serial analysis of gene expression in human diseases. In Hayat, M.A. (ed) Immunohistochemistry and *in situ* Hybridization of Human Carcinomas. Vol. 1. San Diego: Elsevier Academic, 85–98.

Zhang, X.N., Qu, Z.C., Wan, Y.Z., Zhang, H.W., and Shen, D.A. 2002. Application of suppression subtractive hybridization (SSH) to cloning differentially expressed cDNA in Dunaliella salina (Chlorophyta) under hyperosmotic shock. *Plant. Mol. Biol. Report 20*:49–57.

Zhou, J., Wang, H., Lu, A., Hu, G., Luo, A., Ding, F., Zhang, J., Wang, X., Wu, M., and Liu, Z. 2002. A novel gene, NMES1, downregulated in human esophageal squamous cell carcinoma. *Int. J. Cancer 101*:311–316.

II

Colorectal Carcinoma

This Page Intentionally Left Blank

1

Colorectal Carcinoma: An Introduction

M.A. Hayat

Introduction

Colorectal cancer constitutes a major public health problem. This disease affects one in 20 people in Western countries, and more than 155,000 new cases are diagnosed in the United States each year, with 56,700 deaths for the year 2001. On average, 25% of the patients with resectable disease at the time of diagnosis will have recurrent disease, presumably from local, regional, and peritoneal seeding (Sanchez-Cespedes *et al.,* 1999). The prognosis of patients with this disease has not changed during the last 30 years. Unfortunately, the incidence of colorectal carcinoma is increasing worldwide. The current main treatment is surgical resection of the primary lesion. However, distant metastases in the liver and lung in colorectal carcinoma are not uncommon and local recurrence in rectal carcinoma sometimes is observed in advanced cases in patients who are node-positive and serosa-positive. To prevent distant metastasis, systemic treatment as the postoperative adjuvant chemotherapy is being tried.

Of all cancer types, the molecular changes leading to malignant growth are perhaps best known in colorectal carcinoma. Considerable progress has been made in defining critical mutations and gene expression changes in colorectal cancer pathogenesis. Several of the genetic alterations identified thus far are frequently seen in the most common type of malignant colorectal tumors (i.e., the overtly glandular, moderately to well-differentiated adenocarcinomas).

In common with other cancers, colorectal carcinomas arise through a multistep process in which repeated cycles of somatic mutation of cellular genes and clonal selection of variant-progeny with increasingly aggressive growth properties play a prominent role. A stepwise accumulation of genetic changes involving tumor suppressive genes and oncogenes results in the transformation of normal to malignant cells. In other words, tumor development occurs through activation of oncogenes and inactivation of tumor suppressor genes. Mutations in the *adenomatous polyposis coli* (*APC*) gene is thought to be the initiating event in most colorectal cancers (Jen *et al.*, 1994). These mutations occur at the *APC* loci 5q and q22 and generally lead to a truncated *APC* protein or take the form of allele loss. In addition to the *APC*, tumor suppressor genes *p53* and *DCC* and the dominant oncogene *K-ras* play key roles in the progression of colon cancer. An estimated 10–20 genetic events may occur in the interval between initiation and presentation of frank colorectal carcinoma.

The majority of colorectal tumors (85%) are sporadic in origin, yet they exhibit close similarities to tumors resulting from inherited colorectal cancer syndromes. A common feature of colorectal tumors is genetic instability, with a frequency of allele loss of up to 20% in evaluable chromosome arms. The chromosomal

Handbook of Immunohistochemistry and in situ Hybridization of Human Carcinomas,
Volume 2: Molecular Pathology, Colorectal Carcinoma, and Prostate Carcinoma

129

instability phenotype, which accounts for 85% of sporadic cases, exhibits gross chromosomal abnormalities such as aneuploidy and loss of heterozygosity. The microsatellite instability phenotype is not as prevalent in sporadic colorectal cancer, accounting for 15% of such malignancies, and is linked to a faulty deoxyribonucleic acid (DNA) mismatch repair system. *APC* or *β-catenin* mutations are the most common initial molecular lesions in the chromosomal instability phenotype (Kinzler and Vogelstein, 1996). A link between microsatellite instability and mutant DNA repair genes has been established.

A minority of colorectal carcinomas harbor DNA mismatch repair defects and manifest a phenotype in which there is a high frequency of instability at microsatellite sequence tracts. Microsatellite instability is observed in essentially all colorectal cancers arising in patients with hereditary nonpolyposis colorectal cancer and in ~10–15% of sporadic colorectal cancers. Defects in mismatch repair function are thought to increase the rate at which cells acquire the mutations critical in malignant transformation.

Germline mutations in several human DNA mismatch repair genes, including *MSH2*, *MLH1*, *PMS1*, *PMS2*, and *MSH6/GTBP*, have been identified in patients with hereditary nonpolyposis colorectal cancer (Lynch and de la Chapelle, 1999). Such nonpolyposis accounts for ~2–5% of colorectal cancers. Identification of a specific germline DNA mismatch repair gene mutation is successful in 50–70% of families with classical hereditary nonpolyposis colorectal cancer and allows predictive genetic testing of relatives at risk. The finding of tumor microsatellite instability in patients with suspected colorectal cancer was demonstrated to be the best predictor of a germline DNA mismatch repair gene mutation (Liu *et al*., 2000). Microsatellite instability analysis can be carried out by direct fluorescent polymerase chain reaction (PCR) amplification using hematoxylin-eosin–stained colorectal cancer specimen slides (Trojan *et al*., 2002).

In addition, loss of heterozygosity (LOH) at loci on chromosomes 5q, 17q, and/or 18q is frequent in colorectal carcinomas. In the case of chromosomes 5q and 17q, LOH is presumed to inactivate the *APC* and *p53* genes, respectively, whereas the gene(s) targeted for inactivation by 18q LOH remains poorly understood (Kinzler and Vogelstein, 1996).

Several of the genetic alterations that contribute to initiation and progression of colorectal tumors have been identified. An important role in colorectal oncogenesis is played by the mutations of specific oncogenes such as *p53* and *APC*. Mutations of the *p53* gene are the most frequent genetic alterations identified in human tumors. The p53 protein expression, either secondary to *p53* gene mutation or because of adhesion to other cellular or viral proteins, can be detected by immunohistochemistry. This gene has a central role in the regulation of cell cycle and apoptosis by modulating the expression of *p21*, *Bcl-2*, and *bax* genes. There is evidence that *p53* downregulates the expression of the anti-apoptotic *Bcl-2* gene and up-regulates the expression of *bax* that is an inducer of apoptosis. Immunohistochemical studies demonstrate that p53, p21, Bcl-2, bax, Rb, and Ki-67 proteins play an important role in colorectal oncogenesis (Akino *et al*., 2002). The *APC* plays a key role not only in the familial adenomatous polyposis but also in the majority of sporadic colorectal cancer by activating the Wnt signal transduction pathways and by causing chromosomal instability.

Alterations in *CDX2*, a caudal-related homebox gene encoding a transcription factor, are also implicated in colorectal tumor development (Yagi *et al*., 1999). Immunohistochemistry has been used for determining the role of *CDX2* in colorectal carcinoma (Hinoi *et al*., 2001). This study indicates that *CDX2* alterations have a particularly prominent role in the development of a subset, large cell, minimally differentiated colon carcinomas.

Immunohistochemical studies demonstrate that the expression of vascular endothelial growth factor C at the deepest site of tumor invasion can be a useful predictor of poor prognosis in advanced colorectal carcinoma (Furudoi *et al*., 2002). Based on immunohistochemical studies, Habel *et al*. (2002) indicate that targeting of the epidermal growth factor receptor is justified not only for therapeutic purposes but also in the prevention of malignant colorectal tumors. Beta catenin also represents a key molecule in the development of colorectal carcinoma (Wong and Pignatelli, 2002). MUC1 and sialyl-Lewis immunoreactivity exhibits statistically significant correlation with established markers for tumor progression. However, only MUC1 presents an independent prognostic factor of colorectal adenocarcinoma (Baldus *et al.*, 2002).

The *FHIT* (fragile histidine triad) gene, a member of the histidine triad family, has been identified as a putative tumor suppressor gene. This gene is located on chromosome 3p14.2. Alterations of the FHIT transcripts have been identified not only in colorectal cancer but also in other epithelial cancers such as lung, head and neck, breast, digestive tract, uterine cervix, and pancreas. Overexpression of *FHIT* is directly proportional to the apoptotic rate in tumors. According to Mady and Melhem (2002), computerized image analysis provides an accurate assessment of the staining patterns and generates numeric data evaluating

staining intensity better than depending on subjective light microscopy alone.

Ras mutations occur in an early stage of progression from adenoma to carcinoma. *Ras* mutations are present in 40–50% of human colorectal tumors (Spandidos *et al*., 1995). Physiologically, the *ras* gene leads to the production of p21-ras, a protein that catalyzes the hydrolysis of guanosine triphosphate to guanosine diphosphate, thus controlling the cell proliferation by regulating signal transduction pathways. Inhibition of expression of mutated *ras* causes tumor growth inhibition and apoptosis.

Cancer invasion and metastasis also involve the degradation of extracellular matrix components by proteolytic enzymes. Urokinase type plasminogen activator (uPA) converts inactive zymogen plasminogen into plasmin, which can activate some prometalloproteinases and degrade extracellular matrix (Schmitt *et al*., 1997). A high level of uPA is an important predictor of colorectal cancer development, liver metastasis, and overall survival and is regarded as a strong prognostic marker in this disease (Przybylowska *et al.*, 2002).

In summary, molecular markers that have been associated with a worse prognosis include 18q deletions, overexpression of thymidylate synthase, *Ki-ras* mutations, *p53* overexpression, absence of *p27*, microsatellite instability, and absence of *Bcl-2* overexpression. However, the correlation of these and other individual molecular abnormalities with prognosis is conflicting.

The following different molecular pathways are recognized in colorectal carcinoma; this information allows not only the separation of hereditary from sporadic forms, but also the separation within these groups of several major subgroups (Jass *et al*., 2002). These subgroups differ in clinical features, morphology, and prognosis and thus should be useful in deciding specific treatments.

1. Carcinomas in patients with familial adenomatous polyposis. In these patients the *APC* gene is mutated, leading to chromosomal instability and the activation of mutated tumor suppressor genes (*DCC*, *TP53*) by allelic loss (LOH).

2. Sporadic microsatellite instability-stable with acquired *APC*-mutation, LOH, and tumor suppressor gene involvement.

3. Carcinomas in patients with hereditary nonpolyposis colorectal cancer. In these patients a DNA mismatch repair gene is mutated in the germline, leading to high levels of microsatellite instability.

4. Sporadic microsatellite instability-high carcinomas, without a germline mutation of a DNA mismatch repair gene, no LOH, but with methylation of *MLH1* and mutations in several genes.

5. Sporadic microsatellite instability-low carcinomas, with LOH, involvement of a tumor suppressor gene and methylation of *MGMT*, but no widespread DNA methylation.

The prognosis of patients with colorectal cancer who undergo surgical resection ranges between favorable and grave depending on the specific properties of the patient's tumor. The parameters of T factor (depth of tumor invasion), N factor (lymph node invasion), and M factor (distant metastasis) are well-established as important prognostic variables. In addition, independent prognostic variables that are generally used in patient management include histologic type, serum *carcinoembryonic antigen* (*CEA*) level, and vascular invasion.

Colorectal Carcinoma Biomarkers

The detection of clinically useful tumor markers whose expression predicts tumor stage or clinical outcome is an important priority in cancer. The identification of markers is a major advance in the understanding of cancer because their alterations result in a high predisposition to malignancy. The elucidation of the effect of candidate tumor markers can be used to derive biologic insight regarding the mechanisms underlying tumor initiation and progression. Furthermore, early detection of a marker can lead to prevention of certain cancers.

It is established that gene mutations confer increased risk of cancer. The majority of mutations found in tumor cells occur in signal transduction pathways that ultimately regulate transcription factors involving a large number of genes and their transcription patterns. Therefore, abnormalities in gene expression are characteristic of neoplastic tissues. Adenocarcinomas are correlated with specific sequential genetic mutations. Although the total accumulation of mutations is the principal factor in most colorectal cancers, the causative mutations in tumor suppressor and oncogenes occur in a specific order. These events include *APC* gene mutations, global hypomethylation, *K-ras* mutations, *DCC* gene mutations, and mutations in the *p53* gene (Houlston, 2001; Kaserer *et al*., 2000). However, cancer is a complex disease that refers to conditions that emerge as a result of the interaction of genes and environment. Genes impart susceptibility of protection, which is neither necessary nor sufficient for disease to develop. Environmental factors are required, and these can promote, delay, or prevent disease.

Not only gene–environment interactions but also gene–gene (e.g., *p53-MDM2*) interactions play a role in complex disease genetics.

Differences in gene expression between the chromosomal instability phenotype and microsatellite instability phenotype in sporadic colorectal cancer are detailed by Dunican *et al*. (2002). Housekeeping gene variability in normal and carcinomatous colorectal tissues has been reported by Blanquicett *et al*. (2002). De Lange *et al*. (2001) have compared the transcriptional profile of 5600 full-length genes in the nonmetastatic colon cell lines and in the metastatic cell lines. This study presents data on which genes are up- or down-regulated in the metastatic cell lines.

Another important advantage of detecting markers is to elucidate their behavior when tumors are exposed to the stress of cytotoxic therapy. Proportions of cells expressing a particular marker profile in a heterogeneous tumor can change in response to this stress (Crane *et al*., 2003). The question is: Will identifying or targeting altered marker expression in response to cytotoxic therapy be of prognostic or therapeutic value? Such information is available with regard to some markers. For example, the short half-life of p53 protein is substantially increased following genotoxic stress such as irradiation and chemically induced DNA damage. It has been shown that radiation-induced DNA damage causes p53 to arrest the cell cycle in G_1 or (depending on cell type and external stimuli) triggers apoptosis (Ko and Prives, 1996).

Ideally, a tumor marker should have clinical utility in the management of cancer. For a marker to be clinically relevant, it must be notably overexpressed or underexpressed in the majority of the tumor samples of a given histology. For a marker to have prognostic significance, it should also show expression alterations concordant with tumor stage or clinical outcome. Most of the markers for colorectal cancer are given in Table 2. Although not all of them have demonstrated clinical utility, most have proved useful and some require further testing. The protocols of immunohistochemistry and *in situ* hybridization for some of these markers are detailed in Part II of this volume.

Other Colorectal Cancer Biomarkers

Cytokeratins

The immunohistochemistry of cytokeratins (cytoplasmic intermediate filaments) has been used for diagnosing poorly differentiated carcinomas with minimal morphologic differentiation. Different epithelia and carcinomas express different subsets of cytokeratin filaments in different amounts and arranged in different patterns. Metastatic carcinomas tend to retain the cytokeratin profile of the primary tumors (Lagendijk *et al.*, 1998). Cytokeratin 7 expression is positive in rectal adenocarcinomas associated with perianal Paget disease but not in those unassociated with perianal Paget disease (Ramalingan *et al.*, 2001). In contrast with colorectal adenocarcinomas, anal gland adenocarcinoma is typically CK 7-positive and CK 20-negative. A recent immunohistochemical study demonstrates a significantly increased frequency of CK7 and CK 7/CK 20 profile in rectal glandular neoplasms relative to those arising in a more proximal region (Zhang *et al.*, 2003).

Beta Catenin

In addition to other functional properties of β-catenin, this protein plays a direct role in colorectal tumorigenesis because it binds to the product of the tumor suppressor gene *APC*. Because *APC* is inactivated in most colorectal cancers, *β-catenin* nuclear location would be expected in these tumors. A recent immunohistochemical study demonstrates that the activation of β-catenin signaling pathway plays a significant role during the initiation and progression stages of colon carcinogenesis (Yamada *et al.*, 2003). Another immunohistochemical study suggests that reciprocal interactions between the changing tumor environment and the tumor cell regulate the dynamic intracellular *β-catenin* distribution and *E-cadherin* expression, resulting in tumor morphogenesis and progression (Brabletz *et al.*, 2002).

The location of β-catenin also depends on the processing method used. Immunohistochemical studies indicate the absence of β-catenin in the nuclei of normal or tumor cells in frozen tissue sections. Beta-catenin, in contrast, is detected in the nuclei of tumor cells but not in normal cells in paraffin-embedded tissue sections. This evidence indicates the superiority of paraffin-embedded sections over frozen sections because the former avoids loss of this protein.

MUC1

MUC1 belongs to the group of membrane-bound mucins and plays various roles in tumor immunology. It is involved in cell adhesion, especially by interaction with β-catenin, the cell–cell contacts involving E-cadherin, and the formation of complexes with the intercellular adhesion molecule 1. Immunohistochemical studies, using monoclonal antibody HMFG-2, demonstrate that *MUC1* is an independent prognostic parameter in colorectal cancer (Baldus *et al.*, 2002). Therefore, it can be considered as a potential target of immunotherapeutic strategies.

Table 2 Colorectal Cancer Biomarkers

[a]Actin	Adegboyega *et al.* (2002)	IGF2R	Boland *et al.* (2000)
ApoE	Watson *et al.* (2003)	IGF-I/IGFBP-3	Le Marchand *et al.* (2002)
[a]Angiotensin II receptor	Hirasawa *et al.* (2002)	Interleukin-6	Nakagoe *et al.* (2003)
[a]APC (adenomatous polyposis coli)	Scheenstra *et al.* (2003)	[a]IQGAP1	Nabeshima *et al.* (2002)
[a]Bak	Suzuki *et al.* (2002)	[a]Ki-67	Suzuki *et al.* (2002)
[a]BAX	Tateyama *et al.* (2002)	K-ras	Brink *et al.* (2003)
[a]Beta catenin	Chiang *et al.* (2002)	Lymphangiogenic markers	Parr and Jiang (2003)
[a]Bcl-2	Tateyama *et al.* (2002)	MGMT	Esteller *et al.* (2000)
BTF3, H2AZ, PTPD1, RanBP2, CCNA2, HDAC2	Dunican *et al.* (2002)	[a]Minichromosome maintenance (MCM) protein 2	Scott *et al.* (2003)
[a]CA242	Murphy *et al.* (2001)	[a]MLH1	Miyakura *et al.* (2003)
Carcinoembryonic antigen	Duffy *et al.* (2003)	[a]MUC1	Murphy *et al.* (2001)
Caspase	Schwartz *et al.* (1999)	[a]MUC2	Baldus *et al.* (2002)
[a]CD10	Ogawa *et al.* (2002)	[a]MUC5AC	Kocer *et al.* (2002)
[a]CD31/MIB-1	Hasebe *et al.* (2001)	[a]Nuclear factor-κB/Re1A	Yu *et al.* (2004)
[a]CD34	Furudoi *et al.* (2002)	Nuclear matrix protein	Brünagel *et al.* (2002)
[a]CD44	Sökmen *et al.* (2001)	Oligophrenin	Pinheiro *et al.* (2001)
[a]CD45	Adegboyega *et al.* (2002)	Osteopontin	Agrawal *et al.* (2002)
[a]CD95 (Fas)	Tateyama *et al.* (2002)	PGHS-2	Kargman *et al.* (1995)
[a]CD151	Hashida *et al.* (2003)	Polyamines	Linsalata *et al.* (2002)
[a]CDX2	Hinoi *et al.* (2001)	PRL-3 protein tyrosine phosphatase gene	Saha *et al.* (2001)
[a]Claudin-1	Miwa *et al.* (2001)	[a]p21 (WAF1)	Akino *et al.* (2002)
[a]COX-2, IL-1beta, IL-6	Maihöfner *et al.* (2003)	[a]p27	Akino *et al.* (2002)
CRD-BP	Ross *et al.* (2001)	p35	Akino *et al.* (2002)
[a]Cyclin A	Li *et al.* (2002)	[a]p53 (TP53)	Jourdan *et al.* (2003)
[a]Cyclin D1	Utsunomiya *et al.* (2001)	[a]p65	Maihöfner *et al.* (2003)
[a]Cytokeratin 20	Vlems *et al.* (2002)	p73	Sun (2002)
[a]E-cadherin/catenin	El-Bahrawy *et al.* (2001)	[a]Renin	Hirasawa *et al.* (2002)
[a]EGFR	Goldstein and Armin (2001)	[a]Sialyl-Lewis[a], Sialyl-Lewis[x]	Baldus *et al.* (2002)
[a]Endothelin-1	Eberl *et al.* (2003)	[a]Seprase	Iwasa *et al.* (2003)
[a]Ephrin-Bs	Liu *et al.* (2002)	[a]Smad 5	van Beijnum *et al.* (2002)
[a]Ese-3b, Fls353, PBEF, SPARC	van Beijnum *et al.* (2002)	STK II	Jass (1999)
[a]Estrogen receptor β	Witte *et al.* (2001)	[a]RACK 1	Saito *et al.* (2002)
[a]FHIT	Mady and Melhem (2002)	Telomerase subunits (hTERT)	Liu *et al.* (2001)
GAPDH, Beta actin	Zhong and Simons (1999)	TGFbetaRII	Boland (2000)
[a]Heat shock protein 70	Murphy *et al.* (2001)	[a]TGFα	Habel *et al.* (2002)
[a]HER-2/neu	Knösel *et al.* (2002)	Thioredoxin reductase1	Lechner *et al.* (2003)
[a]hMLH1, hMSH2, hMSH6	Fogt *et al.* (2002)	Thymidine phosphorylase	Mimori *et al.* (2002)
hPMS1, hPMS2, hMSH2, hMSH6	Petersen *et al.* (1999)	Thymidylate synthase	van Triest and Peters (1999)
		[a]Trypsin	Solakidi *et al.* (2003)
		[a]VEGF	Wendum *et al.* (2003)

[a]These biomarkers have been identified with IHC or ISH, or both.

Caspases

Caspases play a crucial role as apoptotic effectors, and their potential implication in tumorogenesis remains to be clarified. Some members of the caspase family show their down-regulation in colonic cancer, whereas other members either remain unchanged or exhibit slight up-regulation. Another function of caspases is down-regulation of *β-catenin*. Caspase activation tends to down-regulate β-catenin (Rice *et al.*, 2003).

Bcl-2

Apoptosis or programmed cell death deletes cells that have sustained DNA damage. The *Bcl-2* proto-oncogene is an inhibitor of apoptosis and may therefore allow the accumulation of genetic alterations that become propagated by cell division and potentially contribute to tumor development. In other words, *Bcl-2* expression enhances genetic instability by inhibiting apoptosis in colorectal neoplasms (Sinicrope *et al.*, 1995). Phenotypic expression of *Bcl-2* can be used as

a molecular marker in molecular staging of specific subgroups of colorectal cancers (Grizzle *et al.*, 2002).

Thymidylate Synthase

Thymidylate synthase (TS) protein has been extensively studied as a prognostic molecular marker in a variety of cancers. High levels of this protein are found in patients with colorectal and other cancers. Some studies indicate that TS enzyme expression is a powerful prognostic marker of colorectal cancer recurrence and survival in epithelial malignancies. However, the value of this protein as a prognostic indicator is somewhat controversial. To pursue this uncertainty, polyclonal antibody (hTS7.4) and monoclonal antibody TS 106 have been developed (Johnston *et al.*, 1995). An immunohistochemical study, using TS 106 antibody, was carried out for characterizing TS in the primary colorectal carcinoma (Corsi *et al.*, 2002). This study suggests that high TS levels in resected metastases of colorectal cancer are associated with a poor outcome after surgery.

AP-2

The transcription factor AP-2 is involved in the regulation of various genes, including those encoding p21, HER-2/neu, and cytokeratins. AP-2 shows reduced expression in colorectal carcinomas, and such reduction is inversely correlated with the malignancy of this carcinoma. Post-translational events are thought to effectively regulate the expression of *AP-2*, although its growth-suppressive mechanisms remain largely unknown.

Nuclear Factor-κB/Re1A

Nuclear factor-κB/Re1A (NF-κB) is a pleiotropic transcription factor that plays an important role in controlling cell proliferation and apoptosis and hence oncogenesis. Immunohistochemical studies demonstrate that increased expression of this factor contributes to tumor angiogenesis in colorectal cancer (Yu *et al.*, 2004). A significant association is found between NF-κB and vascular endothelial growth factor (VEGF) in that increased expression of the former is accompanied by increased expression of the latter.

Vascular Endothelial Growth Factor

VEGF is a growth factor involved in the regulation of angiogenesis, a process that plays a central role in tumor growth. Up-regulation of VEGF is not uncommon in colorectal cancer. It is also known that mutations of *p53* or activation of the Ras/MAPK pathway contribute to the up-regulation of VEGF expression and induction of angiogenesis. Immunohistochemical studies, using anti-VEGF-C polyclonal antibody, show VEGF-C expression at the site of deepest colorectal

tumor invasion (Furudoi *et al.*, 2002). This finding may help to identify subpopulations of colorectal cancer cells that have a higher malignant potential and to detect patients who should undergo further treatment.

Seprase

Seprase is a membrane-bound serine protease with gelatinase activity. Immunohistochemistry and immunoblotting have been carried out for investigating the relationship of seprase with clinicopathological factors (Iwasa *et al.*, 2003). These studies suggest that an abundant expression of seprase in colorectal cancer tissue is associated with lymph node metastasis. Seprase is also overexpressed in the invasive ductal carcinoma cells of human breast cancers (Kelly *et al.*, 1998). Inhibition of seprase may be effective in preventing the development of metastases in colorectal cancer.

Extracellular Matrix

It is known that organ-specific extracellular matrix (ECM) determines metastasis formation by regulating tumor cell proliferation. For example, hepatocyte-derived ECM enhances proliferation of colon cancer cell lines by increasing the expression of tyrosine kinase receptors of the HER-2. Not only hepatocyte-derived heparan sulfate but also disaccharide molecules derived from heparan sulfate can affect colon cancer cell proliferation; their effect is mediated by modulation of the HER-2 signal transduction (Fishman *et al.*, 2002).

Angiogenesis

It is known that angiogenesis process leads to the formation of new blood vessels, which plays a central role in the survival of cancer cells, in local tumor growth, and in the development of distant metastasis. Massive formation of blood vessels at the tumor site facilitates tumor cells to enter the circulation. The formation of tumor microvessels is stimulated by angiogenic factors such as VEGF. NK-κB/RelA is also involved in tumor angiogenesis. Immunohistochemical studies demonstrate that this factor contributes to tumor angiogenesis in colorectal cancer (Yu *et al.*, 2004). Increased expression of this factor is mediated by VEGF. In fact, increased expression of NF-κB/RelA is accompanied by increased VEGF expression. NF-κB/RelA is a pleiotropic transcription factor that plays an important role in controlling cell proliferation and apoptosis and hence oncogenesis.

The identification of tumor markers, however, is not a simple biologic problem. Unlike clonal cell cultures, the molecular analysis of human tissue specimens necessarily involves heterogeneous cell populations

whose messenger ribonucleic acid (mRNA) composition is proportionally complex. Similarly, the variability in gene expression from one individual tissue sample to another is substantial and may obscure common patterns of gene expression that are predictive of clinical outcome. Furthermore, because a gene may be responsible for a variety of tumor types, its value as an independent prognostic factor is considerably diminished. For example, *p53* amplification is not likely to be an independent marker for colorectal cancer. *p53* mutations occur not only in colorectal cancer but also in many other cancers, including endometrial and ovarian cancers. Genes exert different effects in different populations (genetic heterogeneity). Therefore, identifying the targets, developing target-specific interventions, and validating biologic effects of an intervention are daunting tasks. Molecular target expression is certainly a dynamic phenomenon. Nevertheless, the future of oncology undoubtedly involves the detection, validation, and targeting of tumor-specific molecules. In fact, cancer risk assessment has developed into a distinct discipline.

The question is to what extent is it possible to predict phenotypes from genotypes. This can be accomplished relatively easily for monogenic diseases such as genetic disorders of hemoglobin (e.g., thalassemias), muscular dystrophy (muscle weakness), cystic fibrosis, Gaucher's disease, and familial adenomatous polyposis. In contrast, attempts to identify the genes in the multigenic diseases are fraught with difficulty. These diseases include diabetes and asthma. A wide variety of approaches is being used to dissect the genetic factors in these diseases. Many different classes of genetic markers have been used including candidate genes, microsatellite DNA, and single nucleotide polymorphisms. Some of these approaches are detailed in this volume. There is a need of closely integrated partnership between the clinical and basic biomedical sciences.

The era of molecular medicine has dawned for cancer. Progress in prevention and early cancer detection will be delayed by the failure to adopt a critical and nondogmatic approach to the pathogenesis of cancer. The advent of DNA chip technology will catalyze the development of revised paradigms. Specifically, modern genomics will allow cancers to be grouped within pathogenic pathways on the basis of shared gene expression profiles.

References

Adegboyega, P.A., Mifflin, R.C., DiMari, J.F., Saada, J.I., and Powell, D.W. 2002. Immunohistochemical study of myofibroblasts in normal colonic mucosa, hyperplastic polyps, and adenomatous colorectal polyps. *Arch. Pathol. Lab. Med.* 126:829–836.

Agrawal, D., Chen, T., Irby, R., Quackenbush, J., Chambers, A.F., Szabo, M., Cantor, A., Coppola, D., and Yeatman, T.J. 2002. Osteopontin identified as lead marker of colon cancer progression, using pooled sample expression profiling. *J. Natl. Cancer Inst.* 94:513–521.

Akino, F., Mitomi, H., Nakamura, T., Ohtani, Y., Ichinoe, M., and Okayasu, I. 2002. High apoptotic activity and low epithelial cell proliferation with underexpression of p21(WAF1/CIP1) and p27Kip1 of mucinous carcinomas of the colorectum: Comparison with well-differentiated type. *Am. J. Clin. Pathol.* 117:908–915.

Baldus, S.E., Monig, S.P., Hanisch, F.G., Zirbes, T.K., Flucke, U., Oelert, S., Zilkens, G., Madejczik, B., Thiele, J., Schneider, P.M., Holscher, A.H., and Dienes, H.P. 2002. Comparative evaluation of the prognostic value of MUC1, MUC2, sialyl-Lewis(a) and sialyl-Lewis(x) antigens in colorectal adenocarcinoma. *Histopathology* 40:440–449.

Blanquicett, C., Johnson, M.R., Heslin, M., and Diasio, R.B. 2002. Housekeeping gene variability in normal and carcinomatous colorectal and liver tissues: Applications in pharmacogenomic gene expression studies. *Anal. Biochem.* 303:209–214.

Boland, C.R., Sinicrope, F.A., Brenner, D.E., and Carethers, J.M. 2000. Colorectal cancer prevention and treatment. *Gastroenterology* 118:S115–128.

Brabletz, T., Jung, A., and Kirchner, T. 2002. β-Catenin and the morphogenesis of colorectal cancer. *Virchows Arch.* 441:1–11.

Brink, M., de Goeij, A.F., Weijenberg, M.P., Roemen, G.M., Lentjes, M.H., Pachen, M.M., Smits, K.M., de Bruine, A.P., Goldbohm, R.A., and van den Brandt, P.A. 2003. K-ras oncogene mutations in sporadic colorectal cancer in The Netherlands cohort study. *Carcinogenesis* 24:703–710.

Brünagel, G., Vietmeier, B.N., Bauer, A.J., Schoen, R.E., and Getzenberg, R.H. 2002. Identification of nuclear matrix protein alterations associated with human colon cancer. *Cancer Res.* 62:2437–2442.

Chiang, J.M., Chou, Y.H., Chen, T.C., Ng, K.F., and Lin, J.L. 2002. Nuclear beta-catenin expression is closely related to ulcerative growth of colorectal carcinoma. *Br. J. Cancer* 86:1124–1129.

Corsi, D.C., Ciaparrone, M., Zannoni, G., Mancini, M., Cassano, A., Specchia, M., Pozzo, C., Martin, M., and Barone, C. 2002. Predictive value of thymidilate synthase expression in resected metastases of colorectal cancer. *Eur. J. Cancer* 38:527–534.

Crane, C.H., Thames, H.D., and Hamilton, S.R. 2003. Will identifying or targeting altered marker expression in response to cytotoxic therapy be of prognostic or therapeutic value? *J. Clin. Oncol.* 21:3381–3382.

Duffy, M.J., van Dalen, A., Haglund, C., Hansson, L., Klapdor, R., Lamerz, R., Nilsson, O., Sturgeon, C., and Topolcan, O. 2003. Clinical utility of biochemical markers in colorectal cancer: European Group on Tumour Markers (EGTM) guidelines. *Eur. J. Cancer* 39:718–727.

Dunican, D.S., McWilliam, P., Tighe, O., Parle-McDermott, A., and Croke, D.T. 2002. Gene expression differences between the microsatellite instability (MIN) and chromosomal instability (CIN) phenotypes in colorectal cancer revealed by high-density cDNA array hybridization. *Oncogene* 21:3252–3257.

Eberl, L.P., Bovey, R., and Juillerat-jeanneret, L. 2003. Endothelin-receptor antagonists are proapoptotic and antiproliferative in human colon cancer cells. *Br. J. Cancer* 88:788–795.

El-Bahrawy, M.A., Poulsom, R., Jeffery, R., Talbot, I., and Alison, M.R. 2001. The expression of E-cadherin and catenins in sporadic colorectal carcinoma. *Hum. Pathol.* 32:1216–1224.

Esteller, M., Toyota, M., Sanchez-Cespedes, M., Capella, G., Peinado, M.A., Watkins, D.N., Issa, J.P., Sidransky, D.,

Baylin, S.B., and Herman, J.G. 2000. Inactivation of the DNA repair gene O6-methylguanine-DNA methyltransferase by promoter hypermethylation is associated with G to A mutations in K-ras in colorectal tumorigenesis. *Cancer Res. 60*:2368–2371.

Fishman, S., Brill, S., Papa, M., Halpern, Z., and Zvibel, I. 2002. Heparin-derived disaccharides modulate proliferation and EBR-B2-Mediated signal transduction in colon cancer cell lines. *Int. J. Cancer 99*:179–184.

Fogt, F., Zimmerman, R.L., Poremba, C., Noffsinger, A.E., Alsaigh, N., and Rueschoff, J. 2002. Immunohistochemical screening of mismatch repair genes hMLH1, hMSH2, and hMSH6 in dysplastic lesions of the colon. *Appl. Immunohistochem. Mol. Morphol. 10*:57–61.

Furudoi, A., Tanaka, S., Haruma, K., Kitadai, Y., Yoshihara, M., Chayama, K., and Shimamoto, F. 2002. Clinical significance of vascular endothelial growth factor C expression and angiogenesis at the deepest invasive site of advanced colorectal carcinoma. *Oncology 62*:157–166.

Goldstein, N.S., and Armin, M. 2001. Epidermal growth factor receptor immunohistochemical reactivity in patients with American Joint Committee on Cancer Stage IV colon adenocarcinoma: Implications for a standardized scoring system. *Cancer 92*:1331–1346.

Grizzle, W.E., Manne, U., Weiss, H.L., Jhala, N., and Talley, L. 2002. Molecular staging of colorectal cancer in African-American and Caucasian patients using phenotypic expression of p53, BCL-2, MUC-1, and p27. *Int. J. Cancer 97*:403–409.

Habel, O., Bertario, L., Andreola, S., Sirizzotti, G., and Marian, B. 2002. Tissue localization of TGFalpha and apoptosis are inversely related in colorectal tumors. *Histochem. Cell Biol. 117*:235–241.

Hasebe, T., Sasaki, S., Sugitoh, M., Ono, M., Saitoh, N., and Ochiai, A. 2001. Highly proliferative intratumoral fibroblasts and a high proliferative microvessel index are significant predictors of tumor metastasis in T3 ulcerative-type colorectal cancer. *Hum Pathol. 32*:401–409.

Hashida, H., Takabayashi, A., Tokuhara, T., Hattori, N., Taki, T., Hasegawa, H., Satoh, S., and Kobayashi, N. 2003. Clinical significance of transmembrane 4 superfamily in colon cancer. *Br. J. Cancer 89*:158–167.

Hinoi, T., Tani, M., Lucas, P.C., Caca, K., Dunn, R.L., Macri, E., Loda, M., Appelman, H.D., Cho, K.R., and Fearon, E.R. 2001. Loss of CDX2 expression and microsatellite instability are prominent features of large cell minimally differentiated carcinomas of the colon. *Am. J. Pathol. 159*:2239–2248.

Hirasawa, K., Sato, Y., Hosoda, Y., Yamamoto, T., and Hanai, H. 2002. Immunohistochemical localization of angiotensin II receptor and local renin-angiotensin system in human colonic mucosa. *J. Histochem. Cytochem. 50*:275–282.

Houlston, R.S. 2001. What we could do now: Molecular pathology of colorectal cancer. *Mol. Pathol. 54*:206–214.

Iwasa, S., Jin, X., Okada, K., Mitsumata, M., and Ooi, A. 2003. Increased expression of serpase, a membrane-type serine protease, is associated with lymph node metastasis in human colorectal cancer. *Cancer Lett. 199*:91–98.

Jass, J.R. 1999. Towards a molecular classification of colorectal cancer. *Int. J. Colorectal Dis. 14*:194–200.

Jass, J.R. 2002. Pathogenesis of colorectal cancer. *Surg. Clin. North Am. 82*:891–904.

Jen, J., Powell, S.M., Papadopoulos, N., Smith, K.J., Hamilton, S.R., Vogelstein, B., and Kinzler, K.W. 1994. Molecular determinants of dysplasia in colorectal lesions. *Cancer Res. 54*: 5523–5526.

Johnston, P.J., Lenz, H.J., Leichman, C.G., Danenberg, K.D., Allegra, C.J., Danenberg, P.V., and Leichman, L. 1995.

Thymidilate synthase gene and protein associated with response to 5-fluorouracil in human colorectal and gastric tumors. *Cancer Res. 55*:1407–1412.

Jourdan, F., Sebbagh, N., Comperat, E., Mourra, N., Flahault, A., Olschwang, S., Duval, A., Hamelin, R., and Flejou, J.F. 2003. Tissue microarray technology: Validation in colorectal carcinoma and analysis of p53, hMLH1, and hMSH2 immunohistochemical expression. *Virchows Arch. 443*:115–121.

Kargman, S.L., O'Neill, G.P., Vickers, P.J., Evans, J.F., Mancini, J.A., and Jothy, S. 1995. Expression of prostaglandin G/H synthase-1 and -2 protein in human colon cancer. *Cancer Res. 55*:2556–2559.

Kaserer, K., Schmaus, J., Bethge, U., Migschitz, B., Fasching, S., Walch, A., Herbst, F., Teleky, B., and Wrba, F. 2000. Staining patterns of p53 immunohistochemistry and their biological significance in colorectal cancer. *J. Pathol. 190*: 450–456.

Kelly, T., Kechelava, S., Rozypal, T.L., West, K.W., and Korourian, S. 1998. Separase, a membrane-bound protease, is overexpressed by invasive ductal carcinoma cells of human breast cancers. *Mod. Pathol. 11*:855–863.

Kinzler, K.W., and Vogelstein, B. 1996. Lessons from hereditary colorectal cancer. *Cell 87*:159–170.

Knösel, T., Yu, Y., Stein, U., Schwabe, H., Schluns, K., Schlag, P.M., Dietel, M., and Petersen, I. 2002. Overexpression of c-erbB-2 protein correlates with chromosomal gain at the c-erbB-2 locus and patient survival in advanced colorectal carcinomas. *Clin. Exp. Metastasis 19*:401–407.

Ko, L.J., and Prives, C. 1996. p53: Puzzle and paradigm. *Genes Dev. 10*:1054–1072.

Kocer, B., Soran, A., Erdogan, S., Karabeyoglu, M., Yildirim, O., Eroglu, A., Bozkurt, B., and Cengiz, O. 2002. Expression of MUC5AC in colorectal carcinoma and relationship with prognosis. *Pathol. Int. 52*:470–477.

De Lange, R., Burtscher, H., Jarsch, M., and Weidle, U.H. 2001. Identification of metastasis-associated genes by transcriptional profiling of metastatic versus non-metastatic colon cancer cell lines. *Anticancer Res. 21*:2329–2339.

Lagendijk, J., Mullink, H., VanDiest, P.J., Meijer, G.A., and Meijer, C.J. 1998. Tracing the origin of adenocarcinomas with unknown primary using immunohistochemistry. *Hum. Pathol. 5*:491–497.

Lechner, S., Muller-Ladner, U., Neumann, E., Spöttl, T., Schlottmann, K., Rüschoff, J., Schölmerich, J., and Kullmann, F. 2003. Thioredoxin reductase 1 expression in colon cancer: Discrepancy between in vitro and in vivo findings. *Lab. Invest. 83*:1321–1331.

Le Marchand, L., Donlon, T., Seifried, A., Kaaks, R., Rinaldi, S., and Wilkens, L.R. 2002. Association of a common polymorphism in the human GH1 gene with colorectal neoplasia. *J. Natl. Cancer Inst. 94*:454–460.

Li, J.Q., Miki, H., Wu, F., Saoo, K., Nishioka, M., Ohmori, M., and Imaida, K. 2002. Cyclin A correlates with carcinogenesis and metastasis, and p27(kip1) correlates with lymphatic invasion, in colorectal neoplasms. *Hum. Pathol. 33*:1006–1015.

Linsalata, M., Caruso, M.G., Leo, S., Guerra, V., D'Attoma, B., and Di Leo, A. 2002. Prognostic value of tissue polyamine levels in human colorectal carcinoma. *Anticancer Res. 22*:2465–2469.

Liu, B.C., LaRose, I., Weinstein, L.J., Ahn, M., Weinstein, M.H., and Richie, J.P. 2001. Expression of telomerase subunits in normal and neoplastic prostate epithelial cells isolated by laser capture microdissection. *Cancer 92*:1943–1948.

Liu, T., Wahlberg, S., Burek, E., Lindblom, P., Rubio, C., and Lindblom, A. 2000. Microsatellite instability as a predictor of a

mutation in a DNA mismatch repair gene in familial colorectal cancer. *Genes Chromos. Cancer* 27:17–25.

Liu, W., Ahmad, S.A., Jung, Y.D., Reinmuth, N., Fan, F., Bucana, C.D., and Ellis, L.M. 2002. Coexpression of ephrin-Bs and their receptors in colon carcinoma. *Cancer* 94:934–939.

Lynch, H.T., and de la Chapelle, A. 1999. Genetic susceptibility to non-polyposis colorectal cancer. *J. Med. Genet.* 36:801–818.

Mady, H.H., and Melhem, M.F. 2002. FHIT protein expression and its relation to apoptosis, tumor histologic grade and prognosis in colorectal adenocarcinoma: An immunohistochemical and image analysis study. *Clin. Exp. Metastasis* 19:351–358.

Maihöfner, C., Charalambous, M.P., Bhambra, U., Lightfoot, T., Geisslinger, G., Gooderham, N.J., and Colorectal Cancer Group. 2003. Expression of cyclooxygenase-2 parallels expression of interleukin-1beta, interleukin-6 and NF-kappaB in human colorectal cancer. *Carcinogenesis* 24:665–671.

Mimori, K., Matsuyama, A., Yoshinaga, K., Yamashita, K., Masuda, T., Inoue, H., Ueo, H., and Mori, M. 2002. Localization of thymidine phosphorylase expression in colorectal carcinoma tissues by in situ RT-PCR assay. *Oncology* 62:327–332.

Miyakura, Y., Sugano, K., Konishi, F., Fukayama, N., Igarashi, S., Kotake, K., Matsui, T., Koyama, Y., Maekawa, M., and Nagai, H. 2003. Methylation profile of the MLH1 promoter region and their relationship to colorectal carcinogenesis. *Genes Chromos. Cancer* 36:17–25.

Miwa, N., Furuse, M., Tsukita, S., Niikawa, N., Nakamura, Y., and Furukawa, Y. 2001. Involvement of claudin-1 in the beta-catenin/Tcf signaling pathway and its frequent upregulation in human colorectal cancers. *Oncol. Res.* 12:469–476.

Murphy, K.J., Nielson, K.R., and Albertine, K.H. 2001. Defining a molecularly normal colon. *J. Histochem. Cytochem.* 49:667–668.

Nabeshima, K., Shimao, Y., Inoue, T., and Koono, M. 2002. Immunohistochemical analysis of IQGAP1 expression in human colorectal carcinomas: Its overexpression in carcinomas and association with invasion fronts. *Cancer Lett.* 176:101–109.

Nakagoe, T., Tsuji, T., Sawai, T., Tanaka, K., Hidaka, S., Shibasaki, S-I., Nanashima, A., Yamaguchi, H., Yasutake, T., Sugawara, K., Inokuchi, N., and Kamihira, S. 2003. The relationship between circulating interleukin-6 and carcinoembryonic antigen in patients with colorectal cancer. *Anticancer Res.* 23:3561–3564.

Ogawa, H., Iwaya, K., Izumi, M., Kuroda, M., Serizawa, H., Koyanagi, Y., and Mukai, K. 2002. Expression of CD10 by stromal cells during colorectal tumor development. *Hum. Pathol.* 33:806–811.

Parr, C., and Jiang, W.G. 2003. Quantitative analysis of lymphangiogenic markers in human colorectal cancer. *Int. J. Oncol.* 23:533–539.

Petersen, G.M., Brensinger, J.D., Johnson, K.A., and Giardiello, F.M. 1999. Genetic testing and counseling for hereditary forms of colorectal cancer. *Cancer* 86:2540–2550.

Pinheiro, N.A., Caballero, O.L., Soares, F., Reis, L.F., and Simpson, A.J. 2001. Significant overexpression of oligophrenin-1 in colorectal tumors detected by cDNA microarray analysis. *Cancer Lett.* 172:67–73.

Przybylowska, K., Smolarczyk, K., Kulig, A., Romanowicz-Makowska, H., Dziki, A., Ulanska, J., Pander, B., and Blasiak, J. 2002. Antigen levels of the urokinase-type plasminogen activator and its gene polymorphisms in colorectal cancer. *Cancer Lett.* 181:23–30.

Ramalingam, P., Hart, W.R., and Goldblum, J.R. 2001. Cytokeratin subset immunostaining in rectal adenocarcinoma and normal anal glands. *Arch. Pathol. Lab. Med.* 125:1074–1077.

Rice, P.L., Kelloff, J., Sullivan, H., Driggers, L., ScottBeard, K., Kuwada, S., Piazza, G., and Ahnen, D.J. 2003. Sulindac metabolites induce caspase and proteaseome-dependent degradation of β-catenin protein in human colon cancer. *Mol. Cancer Ther.* 2:885–892.

Ross, J., Lemm, I., and Berberet, B. 2001. Overexpression of an mRNA-binding protein in human colorectal cancer. *Oncogene* 20:6544–6550.

Rice, P.L., Kelloff, J., Sullivan, H., Driggers, L., ScottBeard, K., Kuwada, S., Piazza, G., and Ahnen, D.J. 2003. Sulindac metabolites induce caspase and proteasome-dependent degradation of β-catenin protein in human colon cancer. *Mol. Cancer Ther.* 2:885–892.

Saha, S., Bardelli, A., Buckhaults, P., Velculescu, V.E., Rago, C., St. Croix, B., Romans, K.E., Choti, M.A., Lengauer, C., Kinzler, K.W., and Vogelstein, B. 2001. A phosphatase associated with metastasis of colorectal cancer. *Science* 294:1343–1346.

Saito, A., Fujii, G., Sato, Y., Gotoh, M., Sakamoto, M., Toda, G., and Hirohashi, S. 2002. Detection of genes expressed in primary colon cancers by in situ hybridisation: Overexpression of RACK 1. *Mol. Pathol.* 55:34–39.

Sanchez-Cespedes, M., Esteller, M., Hibi, K., Cope, F.O., Westra, W.H., Piantadosi, S., Herman, J.G., Jen, J., and Sidransky, D. 1999. Molecular detection of neoplastic cells in lymph nodes of metastatic colorectal cancer patients predicts recurrence. *Clin. Cancer Res.* 5:2450–2454.

Scheenstra, R., Rijcken, F.E., Koornstra, J.J., Hollema, H., Fodde, R., Menko, F.H., Sijmons, R.H., Bijleveld, C.M., and Kleibeuker, J.H. 2003. Rapidly progressive adenomatous polyposis in a patient with germline mutations in both the APC and MLH1 genes: The worst of two worlds. *Gut* 52:898–899.

Schmitt, M., Harbeck, N., Thomssen, C., Wilhelm, O., Magdolen, V., Reuning, U., Ulm, K., Hofler, H., Janicke, F., and Graeff, H. 1997. Clinical impact of the plasminogen activation system in tumor invasion and metastasis: prognostic relevance and target for therapy. *Thromb. Haemost.* 78:285–296.

Schwartz, S. Jr., Yamamoto, H., Navarro, M., Maestro, M., Reventos, J., and Perucho, M. 1999. Frameshift mutations at mononucleotide repeats in caspase-5 and other target genes in endometrial and gastrointestinal cancer of the microsatellite mutator phenotype. *Cancer Res.* 59:2995–3002.

Scott, I.S., Morris, L.S., Bird, K., Davies, R.J., Vowler, S.L., Rushbrook, S.M., Marshall, A.E., Laskey, R.A., Miller, R., Arends, M.J., and Coleman, N. 2003. A novel immunohistochemical method to estimate cell-cycle phase distribution in archival tissue: Outcome in colorectal cancer. *J. Pathol.* 201:187–197.

Sinicrope, F.A., Ruan, S.B., Cleary, K.R., Stephens, L.C., Lee, J.J., and Levin, B. 1995. Bcl-2 and p53 oncoprotein expression during colorectal tumorigenesis. *Cancer Res.* 55:237–241.

Sökmen, S., Lebe, B., Sarioglu, S., Fuzun, M., Terzi, C., Kupelioglu, A., and Ellidokuz, H. 2001. Prognostic value of CD44 expression in colorectal carcinomas. *Anticancer Res.* 21:4121–4126.

Solakidi, S., Tiniakos, D.G., Petraki, K., Stathopoulos, G.P., Markaki, I., Androulakis, G., and Sekeris, C.E. 2003. Co-expression of trypsin and tumor-associated trypsin inhibitor (TATI) in colorectal adenocarcinomas. *Histol. Histopathol.* 18:1181–1188.

Spandidos, D.A., Glarakis, I.S., Kotsinas, A., Ergazaki, M., and Kiaris, H. 1995. Ras oncogene activation in benign and malignant colorectal tumours. *Tumori.* 81:7–11.

Sun, X.F. 2002. p73 overexpression is a prognostic factor in patients with colorectal adenocarcinoma. *Clin. Cancer Res.* 8:165–170.

Suzuki, Y., Honma, T., Hayashi, S., Ajioka, Y., and Asakura, H. 2002. Bcl-2 expression and frequency of apoptosis correlate with morphogenesis of colorectal neoplasia. *J. Clin. Pathol.* *55*:212–216.

Tateyama, H., Li, W., Takahashi, E., Miura, Y., Sugiura, H., and Eimoto, T. 2002. Apoptosis index and apoptosis-related antigen expression in serrated adenoma of the colorectum: The saw-toothed structure may be related to inhibition of apoptosis. *Am. J. Surg. Pathol. 26*:249–256.

Trojan, J., Raedle, J., Herrmann, G., Brieger, A., and Zeuzem, S. 2002. Detection of microsatellite instability from archival, hematoxylin-eosin-stained colorectal cancer specimen. *Arch. Pathol. Lab. Med. 26*:202–204.

Utsunomiya, T., Doki, Y., Takemoto, H., Shiozaki, H., Yano, M., Sekimoto, M., Tamura, S., Yasuda, T., Fujiwara, Y., and Monden, M. 2001. Correlation of beta-catenin and cyclin D1 expression in colon cancers. *Oncology 61*:226–233.

Van Beijnum, J.R., Moerkerk, P.T., Gerbers, A.J., De Bruine, A.P., Arends, J.W., Hoogenboom, H.R., and Hufton, S.E. 2002. Target validation for genomics using peptide-specific phage antibodies: A study of five gene products overexpressed in colorectal cancer. *Int. J. Cancer 101*:118–127.

Van Triest, B., and Peters, G.J. 1999. Thymidylate synthase: A target for combination therapy and determinant of chemotherapeutic response in colorectal cancer. *Oncology 57*:179–194.

Vlems, F.A., Diepstra, J.H., Cornelissen, I.M., Ruers, T.J., Ligtenberg, M.J., Punt, C.J., van Krieken, J.H., Wobbes, T., and van Muijen, G.N. 2002. Limitations of cytokeratin 20 RT-PCR to detect disseminated tumour cells in blood and bone marrow of patients with colorectal cancer: Expression in controls and downregulation in tumour tissue. *Mol. Pathol. 55*:156–163.

Watson, M.A., Gay, L., Stebbings, W.S., Speakman, C.T., Bingham, S.A., and Loktionov, A. 2003. Apolipoprotein E gene polymorphism and colorectal cancer: Gender-specific modulation of risk and prognosis. *Clin. Sci. 104*:537–545.

Wendum, D., Boelle, P.Y., Rigau, V., Sebbagh, N., Olschwang, S., Mourra, N., Parc, R., Trugnan, G., Masliah, J., and Flejou, J.F. 2003. Mucinous colon carcinomas with microsatellite instability have a lower microvessel density and lower vascular endothelial growth factor expression. *Virchows Arch. 442*:111–117.

Witte, D., Chirala, M., Younes, A., Li, Y., and Younes, M. 2001. Estrogen receptor beta is expressed in human colorectal adenocarcinoma. *Hum. Pathol. 32*:940–944.

Wong, N.A., and Pignatelli, M. 2002. Beta-catenin–a linchpin in colorectal carcinogenesis? *Am. J. Pathol. 160*:389–401.

Yagi, O.K., Akiyama, Y., and Yuasa, Y. 1999. Genomic structure and alterations of homeobox gene CDX2 in colorectal carcinomas. *Br. J. Cancer 79*:440–444.

Yamada, Y., Oyama, T., Hirose, Y., Hara, A., Sugie, S., Yoshida, K., Yoshini, N., and Mori, H. 2003. β-catenin mutation is selected during malignant transformation in colon carcinogenesis. *Carcinogenesis 24*:91–97.

Yu, H-G., Zhong, X., Yang, Y-N., Luo, H-S., Yu, J-P., Meier, J.J., Schrader, H., Bastian, A., Schmidt, W.E., and Schmitz, F. 2004. Increased expression of nuclear factor-κB/Re1A is correlated with tumor angiogenesis in human colorectal cancer. *Int. J. Colorect. Dis. 19*:18–22.

Zhang, P.J., Shah, M., Spiegel, G.W., and Brooks, J.J. 2003. Cytokeratin 7 immunoreactivity in rectal adenocarcinomas. *Appl. Immunohistochem. Mol. Morphol. 11*:306–310.

Zhong, H., and Simons, J.W. 1999. Direct comparison of GAPDH, beta-actin, cyclophilin, and 28S rRNA as internal standards for quantifying RNA levels under hypoxia. *Biochem. Biophys. Res. Commun. 259*:523–526.

2

Role of Immunohistochemical Expression of p53 in Colorectal Carcinoma

Jin-Tung Liang and Yung-Ming Jeng

Introduction

The p53 protein was initially identified as a protein forming a stable complex with the SV40 (simian vacuolating virus 40) large T antigen and was originally suspected to be an oncogene (Watson *et al*., 1992). Subsequent studies demonstrated that p53 is a transcription factor that is located at 17p13.1 and is mutated in 50% of primary human tumors, including tumors of the gastrointestinal tract (Ko *et al*., 1996). The protein encoded by *p53* has been structurally divided into four domains: 1) an acidic amino-terminal domain (codons 1–43) required for transcriptional activation; 2) a central core sequence-specific deoxyribonucleic acid (DNA)-binding domain (codons 100–300); 3) a tetramerization domain (codons 324–355); and 4) a C-terminal regulatory domain (codons 363–393) rich in basic amino acids and believed to regulate the core DNA-binding domain (Ko *et al*., 1996). The spectrum of mutations in *p53* seen in colon cancer appears similar to that seen in other tumors, with mutations of *p53* clustering at four hot spots in highly conserved regions (domains II–V) (Figure 22). *p53* is mutated in more than 50% of colon adenocarcinomas, and the mutations localize primarily to exons 5–8 (Vogelstein *et al*., 1988, 1989). The mutations occurring commonly in colon carcinoma are G:C to A:T transitions at CpG dinucleotide repeats and in general interfere with the DNA-binding activity of the protein (Hollstein *et al*., 1991; Ko *et al*., 1996). The mutation of *p53* in colon cancer is commonly accompanied by allelic loss at 17p consistent with its role as a tumor-suppressor gene (Baker *et al*., 1990). The half-life of wild-type p53 protein is ~20 min. Most *p53* gene mutations in human cancers are missense changes (Ko *et al*., 1996). Such missense mutations result in a *p53* product with a longer half-life than the wild-type protein. This allows the immunohistochemistry (IHC) of p53 in the nuclei of the affected cells and was generally recognized as "p53 overexpression."

There is general acceptance of the important role of *p53* as "guardian of genome" (i.e., as regulator of cell proliferation, differentiation, DNA repair [response to DNA damage], and apoptosis [Lane, 1992; Levine, 1997]). Moreover, according to the "molecular paradigm" of colorectal carcinogenesis, as pointed out by Fearon and Vogelstein (1990), *p53* mutation is involved in the later stage of adenoma–carcinoma sequence. Therefore, we have good reasons to speculate that colorectal cancers with *p53* mutations might be more aggressive in biologic behavior. In fact, numerous investigators have attempted to correlate this important molecular maker with the clinical outcome

Handbook of Immunohistochemistry and in situ Hybridization of Human Carcinomas,
Volume 2: Molecular Pathology, Colorectal Carcinoma, and Prostate Carcinoma

139
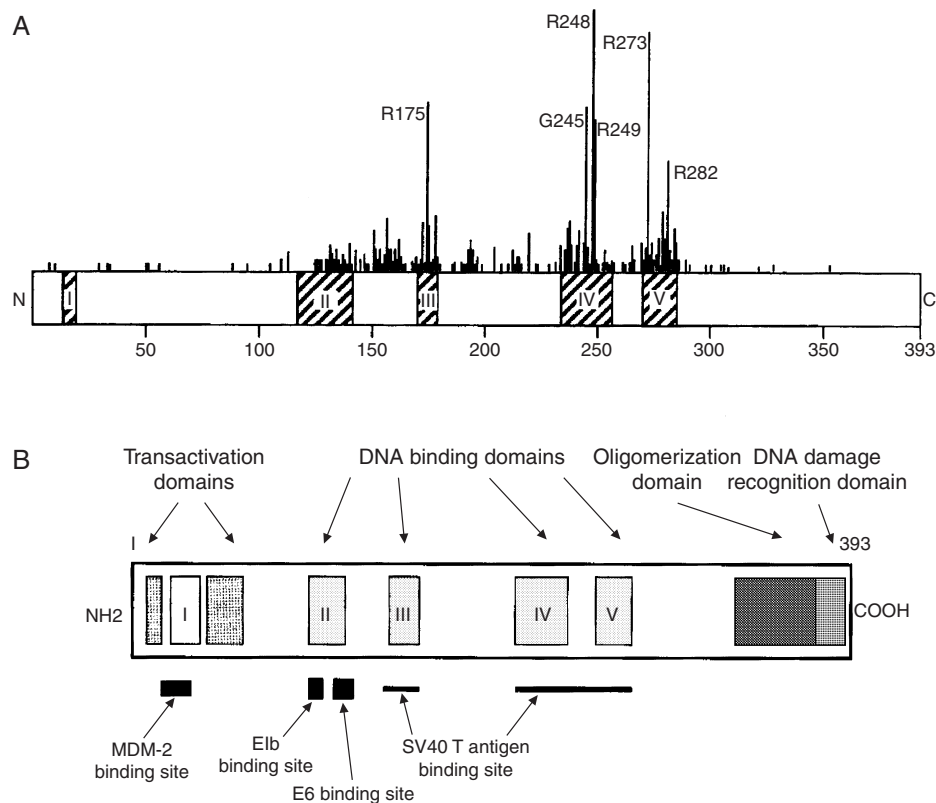
Figure 22 **A:** p53 mutations found in human cancer. Hatched boxes represent evolutionarily conserved regions. Vertical lines represent the frequency at which mutations are found at each particular residue and are clustered in conserved regions II–V. Several hot spots for mutations R175, G245, R248, R249, R273, and R282 are also indicated. **B:** The p53 protein has two transactivation domains near the amino terminus, oligomerization, and deoxyribonucleic acid (DNA) binding domains, which overlap at the carboxy terminus, and five evolutionarily conserved domains conserved (I–V), which are important in sequence-specific DNA binding. The DNA binding domain recognizes damaged DNA, which activates the p53 protein to exert its transactivation function via its transactivating domain in part by enabling p53 to bind to the DNA of genes via its evolutionarily conserved regions. Viral proteins such as the SV40 T antigen, human papilloma virus E6 protein, and adenovirus E1b proteins, and amplified cellular proteins such as MDM2 may bind to the evolutionarily conserved regions, thus preventing p53's transactivating function.

of colorectal cancers (Kirsch *et al*., 1998; Lowe, 1995). However, results reported to date have been controversial (Compton *et al*., 2000; Kressner *et al*., 1999). The inconsistency of the clinical relevance of *p53* mutations in different studies resulted from different methodology and interpretation criteria used for the assessment of *p53* status (Baas *et al*., 1994; Wynford-Thomas, 1992); different clinical treatment modalities used for patients (Hermanek, 1999a); and the variations in clinicopathologic characteristics of the included patients, in particular in regard of pTNM, stage grouping, and residual tumor (R) classification (Hermanek *et al*., 1994, 1999b; UICC, 1997).

Furthermore, theoretically, tumor prognosis is determined by intrinsic aggressiveness and/or potential sensitivity to chemotherapy. However, although our previous study (Liang *et al*., 1999a) and some other authors (Benhatter *et al*., 1996; Pereira *et al*., 1997;

Pricolo *et al*., 1997) strongly advocated that colorectal cancers with *p53* mutations were associated with poor clinical prognosis, we are not fully convinced whether it is because of their chemotherapeutic insensitivity and/or more biologic invasiveness (Figure 23A). Therefore, the clinical implications of *p53* alterations remain obscure and deserve further investigation. Further clarification of the prognostic significance of *p53* status will rely on the implementation of large, population-based studies and prospective clinical trials (Elsaleh *et al*., 2000a; Hermanek, 1999c; McLeod, 1999).

In continuation of our previous study (Liang *et al*., 2002a), we further determined the clinical relevance of *p53* overexpression in stage IV colorectal cancer, based on a large group of patients with long-term, prospective follow-up. The major purpose of this study was focused on exploring whether *p53* overexpression
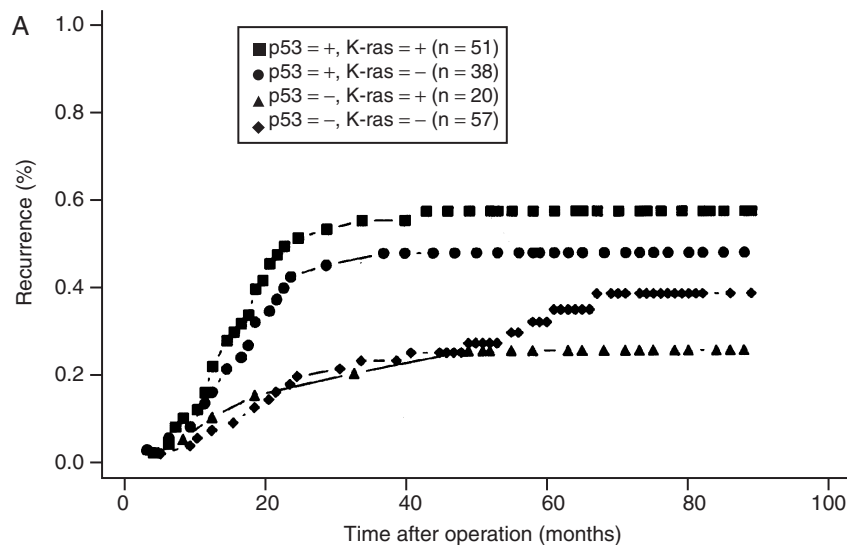
Figure 23 A: Kaplan-Meier Curve indicated that p53 overexpression predicted higher recurrences rate ($p = 0.0013$) and shorter median recurrence time. **B:** Kaplan-Meier survival curves for the study population based on the status of p53 overexpression and the implementation of high-dose 5-fluorouracil plus leucovorin chemotherapy (HDFL). In patients receiving chemotherapy, the subgroup of patients with normal *p53* expression survived significantly longer than those with *p53* overexpression [p = 0.0043, log-rank test, p53 (normal) HDFL (–) versus p53 (overexpression) HDFL (–)]. In contrast, in patients without chemotherapy, there was no significant difference of survival between the two subgroups of *p53* normal expression and overexpression [p = 0.2820, log-rank test, p53 (normal) HDFL (–) versus *p53* (overexpression) HDFL (–)].
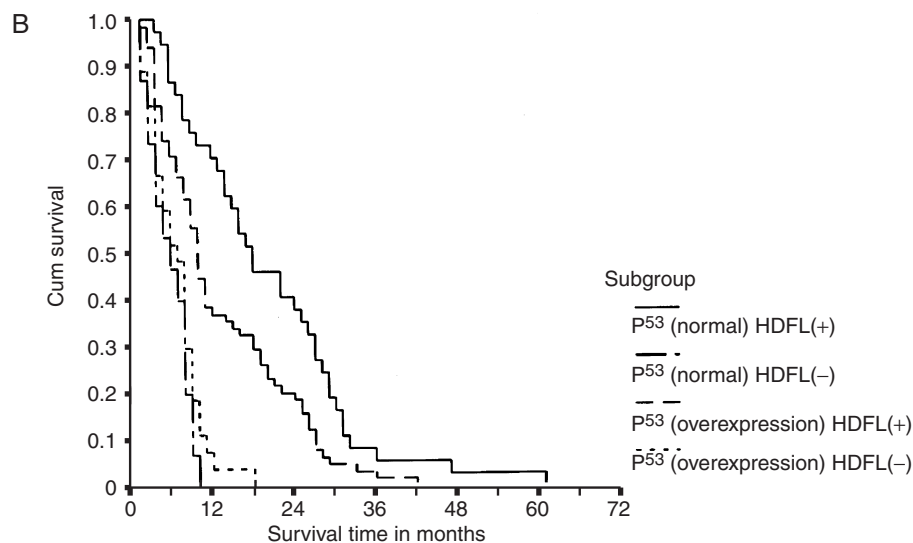
interacted with chemosensitivity and/or biologic aggressiveness in predicting the clinical outcome of stage IV colorectal cancers. We believe that the clinical significance of p53 overexpression in colorectal cancer will be better clarified through this study.

MATERIALS

Patients

The patients recruited met the following eligibility criteria: 1) the primary bowel lesion could be palliatively resected and pathologically confirmed as colorectal adenocarcinoma; 2) the metastatic lesions were measurable but unresectable; 3) Karnofsky performance status was ≥50%; 4) the life expectancy was greater than 12 weeks; and 5) white blood cell (WBC) count was ≥4,000/µl, platelet count was ≥100,000/µl, serum bilirubin was ≥2.0 mg/dl, and serum glucose and electrolyte were normal. Patients with evident carcinosis peritonitis were excluded from this study because their bowel function could not be restored through palliative operation and their prognosis was considered to be very poor. The location of the tumors was classified into right-sided colon cancer, left-sided colon cancer, and rectal cancer. Right-sided colon cancer was defined as tumors proximal to the splenic flexure of colon. Tumors at splenic flexure, descending colon, and sigmoid colon were recognized as left-sided colon cancers. Informed consent was obtained from all patients entering this study. The details of treatment protocol were explained to all of

the patients. However, some patients rejected the high-dose 5-fluorouracil plus leucovorin chemotherapy (HDFL) and favored only supportive care. Therefore, the allocation of patients to treatment arms was non-randomized. However, the *p53* status of each patient was determined by immunostaining of stored specimens from a palliatively resected bowel lesion. The patients were then stratified according the implementation of HDFL and *p53* status. Therefore, there were four subgroups of patients in this study and designated as follows: *p53* (overexpression) HDFL (+), p53 (normal) HDFL (+), *p53* (overexpression) HDFL (−), and *p53* (normal) HDFL (−), respectively. The clinico-pathologic data and overall survival were recorded, analyzed, and compared among subgroups of patients.

Treatments

The HDFL regimen consisted of 5-FU 2600 mg/m^2/week and leucovorin (LV) 300 mg/m^2/week (maximum 500 mg) in a 24-hr intravenous infusion. 5-FU and LV were mixed together to a final volume of 250 ml with 0.9% normal saline. An ambulatory Lifecare Provider 5500 infusion pump system (Abbott Laboratories, North Chicago, IL) was used to perform weekly 24-hr infusions via a single-lumen catheter in an outpatient setting. This method of drug administration has proved to be safe and without adverse precipitation (Ardalan *et al.*, 1991; Yeh *et al.*, 1994, 1997). Chemotherapy was continued until objective evidence of disease progression or unacceptable toxicity developed. When ≥ Eastern Cooperative Oncology Group (ECOG) Grade 3 diarrhea or stomatitis developed, chemotherapy was discontinued temporarily (Oken *et al.*, 1982). HDFL was then resumed with prolonged interval after diarrhea and stomatitis subsided (i.e., rest for 2 weeks after every 4-weekly HDFL). All patients who received a minimum of 4 weeks of treatment were eligible for response evaluation.

Evaluation of Response and Toxicity

Complete blood count with WBC differential classification and biochemical screening test were examined every 1–2 weeks. Chest X-ray and *carcinoembryonic antigen* (*CEA*), if elevated, were studied every 4 weeks. Abdominal sonography and computed tomographic (CT) scan were performed every 2–3 months. Whole body bone scan and other necessary examinations (such as ascites or effusion cytology) were examined as indicated. Complete response (CR) was defined as disappearance of all objective evidence of disease, including all necessary imaging studies, lasting for more than 4 weeks. Partial response (PR) was defined

as a decrease of greater than 50% in the sum of the products of the diameters of all measurable lesion(s) without evidence of new lesion(s), lasting for more than 4 weeks. Progressive disease (PD) was defined as an increase of greater than 25% in the sum of the products of the diameters of all measurable lesion(s) or the appearance of new lesion(s). All other patients were considered to have stable disease (SD). The duration of follow-up was calculated from the date of entry to the cutoff date of the study. Duration of survival was the interval from the date of starting treatment with HDFL to the date of death or last follow-up. The treatment toxicity was recorded according to the ECOG criteria (Oken *et al.*, 1982).

METHODS

Immunohistochemistry of p53

1. Surgical specimens are formalin-fixed and paraffin-embedded (FFPE).
2. 4-μm sections are taken and baked overnight in a 60°C oven.
3. The slides are deparaffinized in fresh reagents, 30 min in xylene, 2 min in 100% ethanol, 1 min in 90% ehanol, 1 min in 70% ethanol, and 1 min in 50% ethanol.
4. The slides are rinsed in running water for 5 min.
5. The slides are placed in citric acid buffer (pH 6.0) and heated to boiling point for 10 min.
6. After heating, the slides are allowed to cool for 1 hr.
7. Slides are rinsed in phosphate buffer saline (PBS) for 5 min.
8. Endogenous peroxidase is blocked with 3% H$_2$O$_2$ for 10 min.
9. Slides are rinsed twice with PBS.
10. The slides are placed in incubation chamber and 3–6 drops of 5% normal goat serum are applied. The slides are incubated for 20 min.
11. Normal goat serum is shaken off and carefully dried around the etched area; the slides are placed in the incubation chamber, and anti-p53 antibody (clone: DO1; dilution: 1:50, Santa Cruz, CA) is applied. The slides are incubated for 1 hr at room temperature.
12. The slides are placed in a PBS bath for 10 min.
13. The slides are placed in incubation chamber and 3–6 drops of biotinated secondary antibody are applied. The slides are incubated for 10 min.
14. The slides are placed in a PBS bath for 10 min.
15. The slides are placed in incubation chamber and 3–6 drops of peroxidase-conjugated streptavidin are applied. The slides are incubated for 10 min.
16. The slides are placed in a PBS bath for 10 min.

17. The peroxidase reaction is developed using diaminobenzidine for 5 min.

18. They are counterstained with hematoxylin for 1 min.

19. The slides are dehydrated for 1 min in 50% ethanol, 1 min in 70% ethanol, 1 min in 90% ethanol, 2 min in 100% ethanol, and 2 min in xylene; then the slide is mounted.

20. The staining intensity is scored as follows: –: negative staining, ±: scattered positive cells (less than 10% of the specimen); +: intermediate positive staining; (10–49% of the specimen); and ++: diffuse positive staining (more than or equal to 50% of the specimen). Tumors with immunostaining of more than 10% of the cells are considered positive for p53 (Hsu *et al.*, 1993; Liang *et al.*, 1999a) (Figure 24).

Statistics

The prognostic significance of p53 overexpression and various clinicopathologic factors were evaluated by multivariate analysis using Cox proportional hazards model. The background clinicopathologic variables of these four subgroups of patients were compared by Chi-square test. Kaplan-Meier curves were constructed, with the patient death as the primary
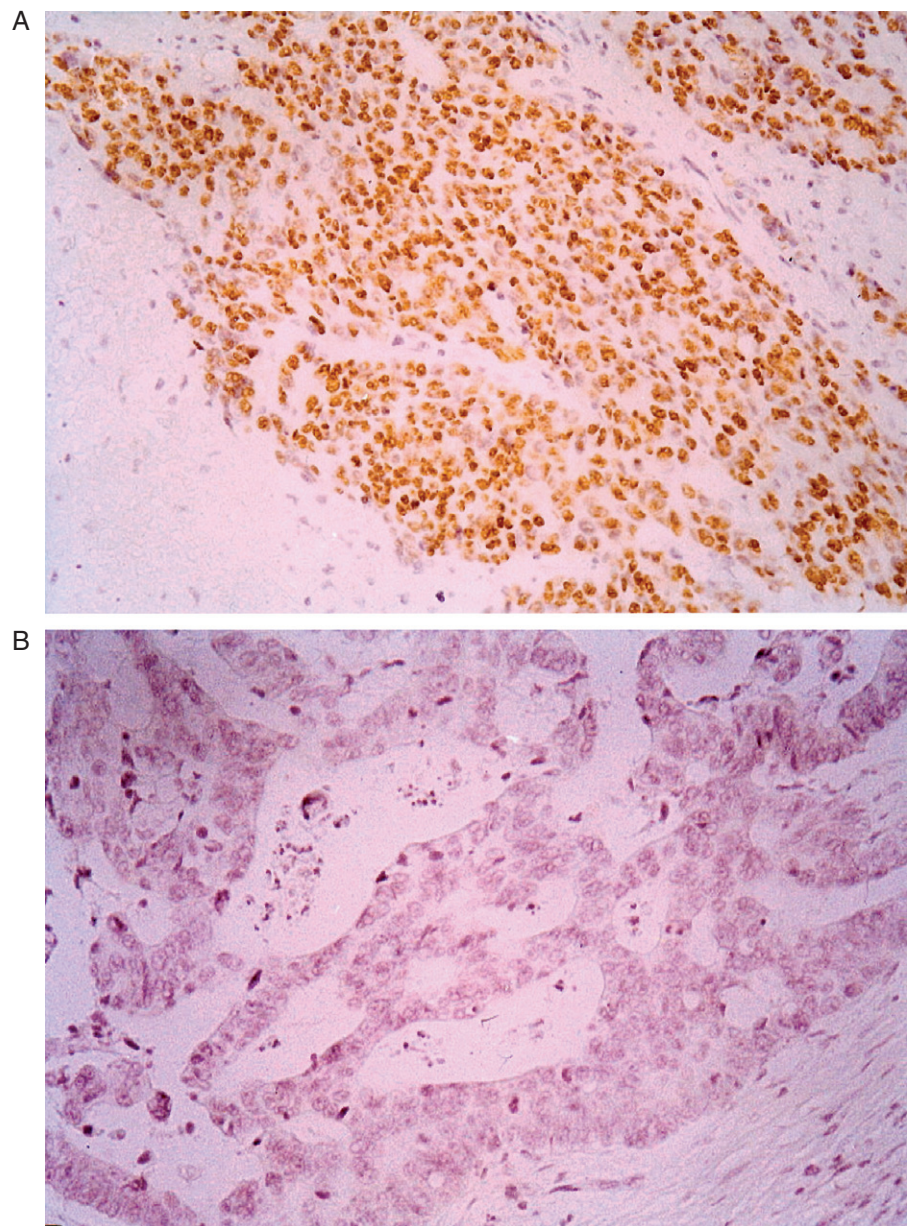
Figure 24 Immunohistochemical stains of p53 using DO.1 antibody in colonic adenocarcinomas. **A:** the positive control, which shows grade (+ +) nuclear staining of p53 (200X magnification). **B:** the negative control, which shows grade (−) intranuclear staining of p53 (400X magnification).

end point. Differences in overall survival among subgroups of patients were assessed by log-rank test. P values of less than 0.05 were considered statistically significant.

RESULTS

Between January 1994 and June 1997, a total of 144 patients were enrolled into this study, with n = 65 in subgroup p53 (overexpression) HDFL (+), n = 37 in subgroup p53 (normal) HDFL (+), n = 27 in subgroup p53 (overexpression) HDFL (–), and n = 15 in subgroup p53 (normal) HDFL (–), respectively. All patients were followed until April 2001. There was no significant difference of background clinicopathologic data among the four subgroups of patients stratified by $p53$ status and the implementation of chemotherapy (p > 0.05). Multivariate analysis for the whole 144 patients indicated that age 60 years or older, poor differentiation, mucin production, CEA >100 ng/ml, $p53$ overexpression, and no chemotherapy were the significant (p < 0.05) poor prognostic factors for survival (Liang *et al.*, 2002a). In contrast, the patient survival was not significantly (p > 0.05) affected by the gender, tumor location, performance status, lymphatic/vascular permeation, and number of organs metastasized. Survival analyses indicated that the patients of subgroup $p53$ (normal) HDFL (+) survived significantly longer (p = 0.0043, log-rank test) than those of subgroup $p53$ (overexpression) HDFL (+), with mean survival time (95% confidence interval [CI]) of 20.24 (16.24–24.25) and 13.29 (10.98–15.60) months, respectively. In contrast, there was no significant difference of survival (p = 0.2820, log-rank test) between subgroup p53 (overexpression) HDFL (–) and subgroup $p53$ (normal) HDFL (–), with mean survival time (95% CI) of 6.85 (5.47–8.23) and 5.87 (4.48–7.26) months, respectively. These findings implied that in patients with HDFL therapy, $p53$-normal group had better survival than $p53$-overexpression group.

However, in patients without HDFL therapy, the prognosis was similarly poor regardless of their p53 status. This can translate into the fact that the prognostic significance of $p53$ overexpression for stage IV colorectal cancers lies in its prediction of poor chemosensitivity rather than the more biologic aggressiveness (Figure 23B). The better chemosensitivity in cancers with normal $p53$ expression was further demonstrated by the direct evidence that the response rate to HDFL was significantly higher (p < 0.005) in subgroup $p53$ (normal) HDFL (+) (mean 67.57%, 95%, CI: 52.18–82.96%) than in subgroup $p53$ (overexpression) HDFL (+) (mean 35.38%, 95% CI: 23.52–47.24%). Remarkably, the data also showed that

patients with chemotherapy survived significantly longer than patients without chemotherapy, irrespective of their $p53$ status [$p53$ (normal) HDFL (+) versus $p53$ (normal) HDFL (–), p < 0.0001; $p53$ (overexpression) HDFL (+) versus $p53$ (overexprssion) HDFL (–), p = 0.0001, log-rank test]. This finding indicates that both $p53$-normal and $p53$-overexpression patients seem to benefit from the HDFL chemotherapy. Additionally, we found that the toxicity to HDFL was minimal and there was no correlation of chemotherapeutic toxicity with $p53$ status (p > 0.05).

DISCUSSION

With the progress of molecular biology, more and more molecular targets of chemotherapeutic of chemopreventive agents have been recognized (Nicoll *et al.*, 1999; Offit, 2000). The clinical applicability of all these molecular markers should only be confirmed through the way of evidence-based medicine (i.e., the population-based, well-controlled, prospective study). $p53$ is one of the molecular markers of which the prognostic significance has been intensively studied. However, to the best of our knowledge, very few articles published were based on a well-controlled prospective study (Kirsch *et al.*, 1998; Petersen *et al.*, 2001). Therefore, the present study provides another sound conclusion in this respect. However, one may argue that the impact of this study was reduced because the allocation of patients into treatment arms was not randomized (McLeod, 1999).

Actually, because HDFL was generally accepted as the mainstay treatment for patients with metastatic colorectal cancers (Ardalan *et al.*, 1991; Yeh *et al.*, 1997), randomization of patients was thus ethically impossible in our clinical setting. Nevertheless, in this study all the patients assigned to either treatment arm were based on the same eligibility criteria. Actually, there was no significant difference of various clinicopathologic factors between the two treatment arms: HDFL (+), n=102, and HDFL (–), n=42. When these two groups of patients were further divided to four subgroups according to their $p53$ status, we again found that there was no significant difference among the four subgroups regarding their clinicopathologic characteristics. Therefore, we believe that the potential bias of case selection has been reduced. Furthermore, the patients in this study were followed up completely and long term. Thus, although one might suggest that the conclusion would be more convincing if more cases were recruited, we believe that the conclusion of this study, in its present status, is clear and solid (Hermanek, 1999c). Whether the results of this study can be extrapolated to stage II and III colorectal

cancers remains to be elucidated. However, because the necessity for adjuvant chemotherapy in patients with stage II colorectal cancer is still controversial, the ethical problems regarding the randomization of patients into treatment groups with or without chemotherapy could be avoided. Therefore, the successful conduction of this study should facilitate further studies in patients with stage II colorectal cancer, thus promoting further understanding of the prognostic role of *p53*.

The determination of *p53* status in this study was based on the immunostaining using *p53* DO.1 antibody. These results are controversial because of the differences in the methodology and criteria for the interpretation of a nonfunctional *p53*. Technically, *p53* status can be assessed by IHC and genomic analysis with direct DNA or cDNA sequencing (Wynford-Thomas, 1992). IHC is used to assess accumulation of p53 protein, both wild-type and mutant. Therefore, the evaluation of p53 staining cannot be taken as definite evidence of gene mutation. A positive result could be caused either by an up-regulated expression of wild-type gene or by the binding of normal p53 to a variety of cellular proteins. Moreover, detectable levels of *p53* may exist, for example, as a result of normal cell-cycle fluctuation, response to DNA damage, or stabilization caused by interaction with *MDM 2* (Amundson *et al*., 1998; Kirsch *et al*., 1998). The results with IHC can vary because of different antibodies, variations in the technique of incubation and antigen fixation, subjectivity in scoring, and absence of uniform cutoff value for definition of positive tumors (Baas *et al*., 1994). Finally, as pointed out by Wynford-Thomas (1992), there are two conditions when loss of *p53* activity may not be accompanied by the expected accumulation of the protein and led to a "false-negative" result: 1) the underlying lesion of *p53* gene may not be a missense point mutation but a gross deletion, which abolishes all p53 protein production; and 2) the point mutation may not stabilize the protein sufficiently for its level to reach detectability by IHC.

Because of these shortcomings inherent in IHC, genomic analysis is being increasingly used for evaluation. However, in most of the articles reporting DNA-based techniques, only the core regions were screened so that mutations at the ends of the molecule would have remained undetected. In fact, the highest frequency of *p53* mutations is described in exon 5–8, but *p53* mutations have been identified in more than 100 different codons (Wallace-Brodeur *et al*., 1999). In addition, the evaluation of one mutant allele in polymerase chain reaction (PCR) and the single-strand conformation polymorphism (SSCP) method do not prove the lack of production of wild-type *p53*. Because of these reasons, it is no wonder that most researchers

found a relative weak concordance of both techniques, ranging from 53% to 74% (Kressner *et al*., 1999; Leahy *et al*., 1996). The report by Smith *et al*. (1996), describing a strong association of detectable levels of immunoreactive p53 and DNA mutations using the antibody Pab 240, represented only a rare case. In the present study, we persisted in the use of IHC for the determination of *p53* status because we noted that IHC using p53 DO.1 antibody was technically highly reproducible and its result was highly concordant with that of genomic analysis, based on our previous studies (Hsu *et al*., 1993; Liang *et al*., 1999a).

In our study comparing IHC with direct genomic analysis, we found that *p53* overexpression and genetic mutation were present in 50% (n=83) and 53.6% (n=89) of 166 resected Dukes' B_2 rectal cancers, respectively (Liang *et al*., 1999a). In this context, there were no false-positive cases of IHC, but six patients with false-negative results were detected. Four of these six false-negative cases were considered to exhibit mutations in their *p53* genes, which completely abolished the expression of the full-length *p53*. The causes of false-negative results in the remaining two patients were undetermined. Moreover, although direct genomic analyses of *p53* gene are theoretically more precise, they are less practical and cumbersome than IHC if used on a large scale in the day-to-day management of patients with colorectal cancer. Therefore, we believe that the prognostic significance of *p53* overexpression is more important than that of direct *p53* mutation analysis.

The interaction of *p53* overexpression and chemosensitivity is thought provoking. Superficially, one may speculate that a normal *p53* is required for efficient execution of the death program in cancer cells with genotoxicity induced by chemotherapeutic agents (Amundson *et al*., 1998; Bristow *et al*., 1996). Remarkably, however, Johnston (2000) indicated that there was a correlation between thymidylate synthetase (TS) and *p53* mutations, suggesting an overexpression of TS in *p53* mutated tumors and therefore less responsiveness to 5-FU–based chemotherapy. Although this is an encouraging explanation for the poor chemosensitivity of the *p53*-overexpression cancers, the relationship between TS and *p53* needs to be further investigated at the molecular level. Based on our data, however, both *p53*-normal and *p53*-overexpression patients seem to benefit from HDFL chemotherapy.

The survival benefit of chemotherapy for patients with *p53* overexpression implied that there might exist other *p53*-independent apoptosis pathways in colorectal cancers undergoing HDFL (Luna-Perez *et al*., 1998; Paradiso *et al*., 1996). Furthermore, correlating the apoptosis regulator proteins with HDFL was thus

needed to clarify this issue. It is interesting that the study by Arango *et al*. (2001) was helpful in gaining insights into this respect. They elegantly demonstrated that only patients with both amplified *c-myc* and wild-type *p53* in their primary tumors would be responsive to 5-FU–based therapy. Remarkably, however, patients with amplified *C-Myc* and mutant *p53* also appeared to have an intermediate response to 5-FU–based treatment, although their survival was not statistically significant as compared to the untreated patients. The amplification of *C-Myc,* as pointed out by the authors, was a *p53*-independent process and could affect the chemosensitivity of tumor cells.

We incidentally found that at age 60 years and older, poor differentiation, mucin production, and CEA level >100 ng/ml were the independent prognostic factors. In these four factors, only age has not been fully clarified as a poor prognostic factor and needs to be further adressed.

Our study has indicated that colorectal cancer of young patients tended to present with microsatellite instability (MSI) (Liang *et al*., 1999b, 2003). Several studies have advocated that MSI is associated with favorable chemosensitivity (Elsaleh *et al*., 2000b; Gryfe *et al*., 2000; Liang *et al*., 2002b). Therefore, it is conceivable that better responsiveness to HDFL in younger patients than that in the older patients may be related to the presence of MSI. Further investigation of the prognostic significance of MSI in these early-onset colorectal cancers is thus mandatory to clarify this point. However, one may argue that younger patients tend to be more robust and thus are able to survive longer with a larger tumor burden than the elderly patients. Because all patients in this study were selected by the same eligibility criteria, we did not consider this as the major reason. Additionally, this study further documented that HDFL is an effective and safe regimen for patients with stage IV colorectal cancer, as pointed out in our previous phase II clinical trials (Yeh *et al*., 1997).

In conclusion, the present study indicates that the poorer prognosis of stage IV colorectal cancers with *p53* overexpression is not so much associated with their intrinsic tumor aggressiveness as with their poorer chemosensitivity. This study should facilitate further randomized, prospective clinical trials to prove that *p53* status can be applied in a routine clinical setting alongside factors such as T stage, nodal status, and residual tumor, whose prognostic value has been well established.

References

Amundson, S.A., Myers, T.G., and Fornace, A.J. Jr. 1998. Roles for p53 in growth arrest and apoptosis: Putting the brakes after genotoxic stress. *Oncogene 17*:3287–3299.

Arango, D., Corner, G.A., Wadler, S., Catalano, P.J., and Augenlicht, L.H. 2001. C-myc/p53 interaction determines sensitivity of human colon carcinoma cells to 5-Fluorouracil in vitro and in vivo. *Cancer Res. 61*:4910–4915.

Ardalan, B., Chua, L., Tian, E., Reddy, R., Sridhar, K., Benedetto, P., Richman, S., Legaspi, A., Waldman, S., and Morrell, L. 1991. A phase II study of weekly 24-hour infusion with high-dose fluorouracil with leucovorin in colorectal carcinoma. *J. Clin. Oncol. 9*:625–630.

Baas, I.O., Mulder, J.W.R., Offerhaus, G.J.A., Vogelstein, B., and Hamilton, S.R. 1994. An evaluation of six antibodies for immunohistochemistry of mutant p53 gene product in archival colorectal neoplasms. *J. Pathol. 172*:5–12.

Baker, S.J., Preisinger, A.C., Jessup, J.M., Paraskeva, C., Markowitz, S., Willson, J.K., Hamilton, S., and Vogelstein, B. 1990. p53 gene mutations occur in combination with 17P allelic deletions as late events in colorectal tumorigenesis. *Cancer Res. 50*:7717–7722.

Benhatter, J., Cerottini, J.P., Saraga, E., Mettez, G., and Givel, J.C. 1996. p53 mutations as a possible predictor of response to chemotherapy in metastatic colorectal carcinomas. *Int. J. Cancer 69*:190–192.

Bristow, R.G., Benchimol, S., and Hill, R.P. 1996. The p53 genes as a modifier of intrinsic radiosensitivity: Implications for radiotherapy. *Radiother Oncol. 40*:197–223.

Compton, C., Fenoglio-Preiser, C.M., Pettigrew, N., and Fielding, L.P. 2000. American Joint Committee on Cancer Prognostic Factors Consensus Conference. Colorectal Working Group. *Cancer 88*:1739–1757.

Elsaleh, H., Joseph, D., Grieu, F., Zeps, N., Spry, N., and Iacopetta, B. 2000b. Association of tumor site and sex with survival benefit from adjuvant chemotherapy in colorectal cancer. *Lancet 355*:1745–1750.

Elsaleh, H., Powell, B., Soontrapornchai, P., Joseph, D., Goria, F., Spry, N., and Iacopetta, B. 2000a. p53 mutation, microsatellite instability and adjuvant chemotherapy: Impact survival of 388 patients with Dukes' C colon carcinoma. *Oncology 58*:52–59.

Fearon, E.R., and Vogelstein, B. 1990. A genetic model for colorectal tumorigenesis. *Cell 61*:759–767.

Gryfe, R., Kim, H., Hsieh, E.T.K., Aronson, M.D., Holowaty, E.J., Bull, S.B., Redston, M., and Gallinger, S. 2000. Tumor microsatellite instability and clinical outcome in young patients with colorectal cancer. *N. Engl. J. Med. 342*:69–77.

Hermanek, P., Wittekind, C. 1994. Residual tumor (R) classification and prognosis. *Semin. Surg. Oncol. 10*:12–20.

Hermanek, P. 1999a Impact of surgeon's technique on outcome after treatment of rectal carcinoma. *Dis. Colon Rectum 42*: 559–562.

Hermanek, P., Sobin, L.H., and Wittekind, C. 1999b. How to improve the present TNM staging system. *Cancer 86*:2189–2191.

Hermanek, P. 1999c. Prognostic factor research in oncology. *J. Clin. Epidemiol. 52*:371–374.

Hollstein, M., Sidransdy, D., Vogelstein, B., and Harris, C.C. 1991. p53 mutations in human cancers. *Science 253*:49–53.

Hsu, H.C., Tseng, H.W., Lai, P.L., Lee, P.H., and Peng, S.Y. 1993. Expression of p53 gene in 184 unifocal hepatocellular carcinomas: Association with tumor growth and invasiveness. *Cancer Res. 53*:4691–4694.

Johnston, P. 2000. Molecular markers as prognostic factors to determine treatment. [Proceedings of 2nd Annual European Conference on Perspectives in Colorectal Cancer]. *J. Natl. Cancer Inst. 92*:1976–1977.

Kirsch, D.G., and Kastan, M.B. 1998. Tumor-suppressor p53: Implications for tumor development and prognosis. *J. Clin. Oncol. 16*:3158–3168.

Ko, L.J., and Prives, C. 1996. p53: Puzzle and paradigm. *Genes Dev. 10*:1054–1072.

Kressner, U., Inganäs, M., Byding, S., Blikstad, I., Påhlman, L., Glimelius, B., and Lindmark, G. 1999. Prognostic value of p53 genetic changes in colorectal cancer. *J. Clin. Oncol. 17*:593–599.

Lane, P.P. 1992. p53: Guardian of the genome. *Nature 358*:15–16.

Leahy, D.T., Salman, R., Mulcahy, H., Sheahan, K., O'Donoghue, D.P., and Parfrey, N.A. 1996. Prognostic significance of p53 abnormalities in colorectal carcinoma detected by PCR-SSCP and immunohistochemical analysis. *J. Pathol. 180*:364–370.

Levine, A.J. 1997. p53, the cellular gatekeeper for growth and division. *Cell 88*:323–331.

Liang, J.T., Chang, K.J., Chen, J.C., Lee, C.C., Cheng, Y.M., Hsu, H.C., Chien, C.T., and Wang, S.M. 1999b. Clinicopathologic and carcinogenetic appraisal of DNA replication error in sporadic T3NoMo stage colorectal cancer after curative resection. *Hepato-Gastroenterol. 46*:883–890.

Liang, J.T., Cheng, Y.M., Chang, K.J., Chien, C.T., and Hsu, H.C. 1999a. Reappraisal of K-ras and p53 gene mutations in the recurrence of Dukes' B2 rectal cancer after curative resection. *Hepato-Gastroenterol. 46*:830–837.

Liang, J.T., Huang, K.C., Cheng, A.L., Jeng, Y.M., Wu, M.S., and Wang, S.M. 2003. Clinicopathological and molecular biological features of colorectal cancer in patients less than 40 years of age. *Br. J. Surg. 90*:205–214.

Liang, J.T., Huang, K.C., Cheng, Y.M., Hsu, H.C., Cheng, A.L., Hsu, C.H., Yeh, K.H., Wang, S.M., and Chang, K.J. 2002a. p53 overexpression predicts poor chemosensitivity to high-dose 5-fluorouracil plus leucovorin chemotherapy for stage IV colorectal cancers after palliative bowel resection. *Int. J. Cancer 97*:451–457.

Liang, J.T., Huang, K.C., Lai, H.S., Lee, P.H., Cheng, Y.M., Hsu, H.C., Cheng, A.L., Hsu, C.H., Yeh, K.H., Wang, S.M., Tang, C., and Chang, K.J. 2002b. High-frequency microsatellite instability predicts better chemosensitivity to high-dose 5-fluorouracil plus leucovorin chemotherapy for stage IV colorectal cancers after palliative bowel resection. *Int. J. Cancer 101*:519–525.

Lowe, S.W. 1995. Cancer therapy and p53. *Current Opinion in Oncology 7*:547–553.

Luna-Perez, P., Arriola, E.L., Cuadra, Y., Alvarado, I., and Quintero, A. 1998. p53 protein overexpression and response to induction chemoradiation therapy in patients with locally advanced rectal adenocarcinoma. *Ann. Surg. Oncol. 5*:203–208.

McLeod, R.S. 1999. Issues in surgical randomized controlled trials. *World. J. Sur. 23*:1210–1214.

Nicoll, I.D., and Dunlop, M.G. 1999. Molecular markers of prognosis in colorectal cancer. *J. Natl. Cancer. Inst. 91*:1267–1269.

Offit, K. 2000. Genetic prognostic markers for colorectal cancer. *N. Engl. J. Med. 342*:124–125.

Oken, M.M., Creech, R.H., Tormey, D.C., and Horton, J. 1982. Toxicity and response criteria of the Eastern Cooperative Oncology Group. *Am. J. Clin. Oncol. 5*:649–655.

Paradiso, A., Rabinovich, M., Vallejo, C., Machiavelli, M., Romen, A., Perez, J., Lacava, J., Cuevas, M.A., Rodriguez, R., Leone, B., Sapia, M.G., Simone, G., and Lena, M.D. 1996. p53 and PCNA expression in advanced colorectal cancer: Response to chemotherapy and long-term prognosis. *Int. J. Cancer 69*:437–441.

Pereira, H., Silva, S., Juliao, R., Carcia, P., and Perpetua, F. 1997. Prognostic markers for colorectal cancer: Expression of p53 and BCL 2. *World J. Surg. 21*:210–213.

Petersen, S.P., Thames, H.D., Nieder, C., Petersen, C., and Baumann, M. 2001. The results of colorectal treatment by p53 status. *Dis. Colon Rectum 44*:322–334.

Pricolo, V.E., Finkelstein, S.D., Hansen, K., Cole, B.F., and Bland, K.I. 1997. Mutated p53 gene is an independent adverse predictor of survival in colon carcinoma. *Arch. Surg. 132*:371–375.

Smith, D.R., Ji, C.Y., and Goh, H.S. 1996. Prognostic significance of p53 overexpression and mutation in colorectal adenocarcinomas. *Br. J. Cancer 74*:216–223.

UICC. 1997. *TNM Classification of Malignant Tumors*, 5th ed. Sobin, L.H., Wittekind, C.H. (eds.) New York: Wiley and Sons.

Vogelstein, B., Fearon, E.R., Hamilton, S.R., Kern, S.E., Preisinger, A.C., Leppert, M., Nakamura, Y., White, R., Smits, A.M., and Bos, J.L. 1988. Gonetic alterations during colorectal tumor development. *N. Engl. J. Med. 319*:525–532.

Vogelstein, B., Fearon, E.R., Kern, S.E., Hamilton, S.R., Preisinger, A.C., Nakamura, Y., and White, R. 1989. Allelotype of colorectal carcinomas. *Science 244*:207–211.

Wallace-Brodeur, R.R., and Lowe, S.W. 1999. Clinical implications of p53 mutations. *Cell Mol. Life Sci. 55*:64–75.

Watson, J.D., Gilman, M., Witkowski, J., and Zoller, M. 1992. Oncogenes and antioncogenes. In Watson, J.D., Gilman, M., Witkowski, J., and Zoller, M. (eds.) *Recombinant DNA*. New York, W.H. Freeman and Company, 335–367.

Wynford-Thomas, D. 1992. p53 in tumor pathology: Can we trust immunocytochemistry? *J. Pathol. 166*:329–330.

Yeh, K.H., and Cheng, A.L. 1994. An alternative method to overcome central venous portable external infusion pump blockage in patients receiving weekly 24-hour high-dose fluorouracil and leucovorin. *J. Clin. Oncol. 12*:875–876.

Yeh, K.H., Cheng, A.L., Lin, M.T., Hong, R.L., Hsu, C.H., Lin, J.F., Chang, K.J., Lee, P.H., and Chen, Y.C. 1997. A phase II study of weekly 24-hour infusion of high-dose 5-fluorouracil and leucovorin (HDFL) in the treatment of recurrent or metastatic colorectal cancers. *Anticancer Res. 17*:3867–3872.

This Page Intentionally Left Blank

3

Applying Tissue Microarray in Rectal Cancer: Immunostaining of Ki-67 and p53

Mef Nilbert and Eva Fernebro

Introduction

Colorectal Cancer

Colorectal cancer represents one of the most common malignancies with an estimated annual incidence of almost 1 million cases worldwide (Parkin, 2001). Approximately one-third of these tumors are located within the rectum (i.e., the lower 15 cm of the large bowel). Rectal cancer differs from colon cancer with regard to clinical behavior, histology, and molecular genetic alterations. During the last decades an improved surgical technique (total mesorectal excision), the introduction of preoperative or post-operative radiation, and the use of adjuvant chemotherapy have reduced the previously high local recurrence rate and improved survival in these patients. Despite these improvements 4 out of 10 patients still die from the disease. Although the sequential accumulation of genetic changes in genes such as adenomatous polyposis coli (APC), *K-ras*, and *TP53* that characterize the adenoma-carcinoma sequence of colorectal cancer development applies also to rectal cancer, few studies have separately analyzed these tumor types. Rectal cancer has been associated with high *Ki-67* proliferative indices and frequent aneuploidy, loss of heterozygozity at 17p and 18q, mutation/overexpression of *p53*, and overexpression of *C-Myc* (Bazan *et al*., 2002; Hoos *et al*., 2002; Kapiteijn *et al*., 2001; Samowitz *et al*., 2002; Soong *et al*., 1997). Consequently, diploid tumors and microsatellite instability (MSI) occur less frequently in rectal cancers than in colon cancers (Kapiteijn *et al*., 2001; Nilbert *et al*., 1999). Because the frequencies of the different genetic alterations vary depending on the tumor location within the large bowel, studies aiming to investigate a possible prognostic role of biologic parameters should optimally analyze these tumor types separately.

Prognostic Markers Assessed by Immunostaining

Identification of biologically aggressive tumors is of clinical value to identify high-risk patients who could benefit from adjuvant therapy. Identification of tumor-specific markers also provides a basis for development of future targeted therapies. However, studies of single molecular markers have not yet revealed any consistent and independent prognostic or predictive factor in rectal cancer. Considering the complex biology in this tumor type with gross aneuploidy and variable expression of multiple targets involved in, for example, cell-cycle regulation, deoxyribonucleic acid (DNA) repair, proliferation, and apoptosis in most tumors, the lack of a single important marker is perhaps expected rather than surprising. Immunostaining for the proliferation marker *Ki-67* and the tumor suppressor protein p53 have, among many other alterations, been thoroughly investigated in colorectal cancer.

Handbook of Immunohistochemistry and *in situ* Hybridization of Human Carcinomas,
Volume 2: Molecular Pathology, Colorectal Carcinoma, and Prostate Carcinoma

149

Ki-67 has been shown to be a prognostic marker in several tumor types, but no consistent association between *Ki-67* expression and survival has been identified in colorectal cancer. Although some studies have suggested that a high fraction of *Ki-67* expressing cells is associated with a better outcome for the patient (Allegra *et al.*, 2002, 2003), other investigators have not found such an association (Bhatavdekar *et al.*, 2001; Hoos *et al.*, 2002). A high *Ki-67* labeling index has been described in colorectal cancers with MSI, and this observation could constitute a possible explanation for the survival advantage observed among patients with MSI tumors (Michael-Robinson *et al.*, 2001; Takagi *et al.*, 2002). Because the appearance of nuclear Ki-67 staining reflects cells in the various stages of the cell cycle, a high *Ki-67* index does not necessarily correspond to actively dividing tumor cells. We assessed the mitotic rate and the S-phase in rectal cancers with high (>70% expressing nuclei) Ki-67 staining and generally found less than 1 mitosis per high power field (40X) and a low S-phase in these tumors (Fernebro *et al.*, unpublished observations). Thus, a high fraction of Ki-67 staining cells may in rectal cancer also reflect slow-growing tumors with many cells in the different stages of the cell cycle, which stands in contrast to other tumor types (e.g., lymphomas), in which a high fraction of Ki-67–positive nuclei is associated with highly proliferative tumors with a high mitotic rate.

The *TP53* gene, in addition to its tumor suppressor properties, also plays an important role in cell-cycle regulation and apoptosis. Normal p53 protein has a short half-life and is normally expressed at very low levels and cannot be detected using immunohistochemistry. In tumor cells mutant p53 products are not ubiquitinated and therefore accumulate at amounts detectable using immunohistochemical staining. A high degree, 60–80%, of p53 positive immunostaining has been reported in rectal cancer, and *TP53* has been shown to carry somatic mutations in about 50% of colorectal cancers and in 40–70% of rectal cancers (Elsaleh *et al.*, 1999; Kandioler *et al.*, 2002; Kapiteijn *et al.*, 2001; Samowitz *et al.*, 2001). Studies of the prognostic value of *p53* expression in relation to prognosis in colorectal cancer have reached contradictory results (Allergra *et al.*, 2002; Bazan *et al.*, 2002; Hoos *et al.*, 2002; Resnich *et al.*, 2004; Tollenaar *et al.*, 1998). Even in studies separately analyzing rectal cancer there is as yet no consensus about the prognostic role of *p53*. An association between *TP53* mutation and/or positive immunostaining for p53 in the tumor tissue and poor prognosis has been found in some studies of rectal cancer (Cascinu *et al.*, 2002; Gervaz *et al.*, 2001; Kapiteijn *et al.*, 2001; Schwandner *et al.*, 2000;

Tollenaar *et al.*, 1998). Other investigators have found an association between *TP53* mutation or immunostaining and poor response to radiotherapy (Kandioler *et al.*, 2002; Rebischung *et al.*, 2002). However, several large studies have failed to demonstrate that *p53* confers any consistent and significant prognostic impact in rectal cancer (Elsaleh *et al.*, 1999; Fernebro *et al.*, 2004; Hoos *et al.*, 2002).

Traditionally, novel tumor markers have been investigated in one type of tumor, followed by subsequent evaluation in other histopathologic types of tumors. This process is laborious and thereby delays the time from discovery of a novel marker until it has been validated in large tumor series. Thus, there is a strong demand for novel techniques that allow simultaneous analysis of multiple biologic markers in large tumor series. The tissue microarray (TMA) technique was developed in 1998 for high-throughput analysis of multiple tumor samples in a single experiment (Kononen *et al.*, 1998). The TMA technology uses 0.6-mm core needle biopsies, which are obtained from archival paraffin-embedded tissue blocks and thereafter re-embedded in a novel paraffin array block. The introduction of TMA facilitates studies of molecular alterations at the DNA, ribonucleic acid (RNA), and protein level in large tumor materials and thereby provides a powerful tool to detect associations between molecular markers, histopathologic subsets, and clinical end points (Andersen *et al.*, 2002; Rimm *et al.*, 2001; Schraml *et al.*, 1999).

The conflicting data on the clinical correlations for several biologic markers reached by different investigators may be caused by differences in methodology and interpretations rather than by a true variation in tumor biology. Thus, there is a strong need for guidelines on how to perform and interpret immunostaining and how to apply the recently introduced TMA technique. The aim of this chapter is to review the TMA technique for immunohistochemistry with respect to reproducibility and technical advantages, to provide detailed methodologic data, and to discuss our experiences from applying TMA and immunostaining in rectal cancer with specific focus on the proliferation marker *Ki-67* and the tumor suppressor protein p53.

MATERIALS

Tissue Microarray

1. Representative paraffin-embedded tumor blocks are selected. Optimally, well-preserved tissue without necrosis should be selected and the tumor blocks should contain tumor throughout the block. Block selection is important and the thickness of the tumor

tissue will determine the number of sections that can be obtained from the block.

2. A fresh section is made and is stained with Mayer's hematoxylin and erythrosin B (H&E) (0.3%) (as applied for routine morphology).

3. Representative tumor areas, and if applicable also an area containing normal tissue, are hand-marked by a pathologist on the H&E-stained slide. The number of areas depends on the design of the study. In order not to lose information most investigators aim at taking three cylinder biopsies from each tumor. However, tumor heterogeneity influences this decision (see Discussion).

Immunohistochemistry

1. Tris buffered saline (TBS) stock buffer (10X): 60.55 g Tris, 84.7 g NaCl. Bring to volume 500 ml using deionized distilled water. Adjust pH to 7.6 using HCl. Bring volume to 1 L.

2. TBS buffer to use: dilute stock solution (10X TBS) 1:10 using deionized distilled water (to a final concentration of 0.05 M Tris, 0.145 M NaCl, pH 7.6).

3. Citrate buffer: 2.1 g citric acid is dissolved in 900 ml distilled water. pH 6.0 is obtained through addition of 2 M NaOH (approximately 25 ml needed). Bring volume to 1 L.

4. The TechMate automated immunostainer (Dako cytomation, Glostrup, Denmark) requires specific buffers. Buffer 1: 0.5% bovine serum albumin (BSA) in $1 \times$ TBS (a 1:10 dilution of the stock solution) + 0.1% Triton X-100. Buffer 2 and 3: 0.1% Triton X-100 in 1 $\times$ TBS. Buffer 4: H_2O + 0.1% Triton X-100.

METHODS

Tissue Microarray

1. A novel paraffin block, referred to as the array block, is made. Ideally, the array block should be thicker than the blocks used for routine histopathology to allow the entire length of the cylinder biopsy to be introduced into the array block.

2. A manual tissue arrayer (Beecher Instruments, Sun Prairie, WI) was used according to the manufacturer's instructions. The instrument uses two separate core needles to punch the donor and the recipient tumor blocks. A hole is punched in the newly made array block using the smaller (S, 0.6-mm) cylinder, after which the larger (L, 0.8-mm) cylinder is used to obtain a biopsy from the original, donor, tumor block.

The tumor-containing (L) cylinder is introduced into the hole leaving a small part of the tumor cylinder above the surface of the array block. Care should be taken not to introduce the cylinders too low in the array block.

3. The next cylinder biopsy is made 0.8 mm from the first one leaving 0.1-mm spacing between the samples. The system uses a micrometer-precise coordinate system for the assembly of the array, and 500 specimens or more can be assembled in an array block, but we have generally (for practical purposes) used array blocks containing 200–400 cylinder biopsies. When constructing the array block, asymmetric positioning (e.g., with half a row at one end or inclusion of an empty row) is important for correct orientation during analysis. Between 30 and 70 core biopsies can generally be arrayed per hour. Empty slots or rows are included to facilitate orientation when analyzing the stained TMA sections.

4. When the array block is full, it is incubated at 37°C for 15 min. Thereafter a glass slide is placed on top of the array block and gentle pressure is applied to ensure that the cylinders are at the same level and to obtain an even surface. The heating step will improve the quality of the tissue arrays.

5. A regular microtome was used for sectioning. Sections of 3–4 µm were used for immunohistochemistry and placed on glass slides developed for optimal results according to the automated immunohistochemical staining method used (see later in this chapter).

Immunohistochemistry

1. 4-µm sections of the tissue array blocks were mounted on Dako ChemMate Capillary Gap Microscope Slides (S2024, Dako A/S BioTek Solutions). The slides were dried at room temperature overnight followed by incubation at 60°C for 1–2 hr.

2. The sections were deparaffinized in xylene 2× for 5 min each. Rehydration was obtained through incubation in descending concentrations of ethanol (5 min in 99.5% ethanol followed by 5 min in 95% ethanol), followed by rinsing in distilled water.

3. Antigen retrieval was achieved by microwave treatment. The sections were incubated in 0.01 M citrate buffer (pH 6.0) and treated in a microwave oven at 900 W for 8–10 min to bring the buffer to boiling, followed by treatment at 300 W for 15 min. The slides were then allowed to cool at room temperature for 20 min in the citrate buffer and were thereafter rinsed in distilled water.

4. Monoclonal antibodies against *p53* and *Ki-67* were used; for p53 DO-7, clone 7 (Dako, code #M7001) at a concentration of 1:300 and for Ki-67 clone MIB-1

(Dako, #M7240) at a dilution of 1:1000. The Chem-Mate Antibody Dilutent (Dako, code #M2022) was used for the dilutions.

5. The slides were stained in an automatic immunostainer (TechMate 500 Plus, Dako) according to the manufacturer's instructions using the streptavidin-biotin (Dako ChemMate Detection Kit, peroxidase diaminobenzadine [DAB], rabbit/mouse) method with diaminobenzidine as the chromogen. The program MSIP was used, and all steps were performed at room temperature. These steps include the following:

a. Rinse in buffer 1 (0.5% BSA in TBS [pH 7.6] + 0.1% Triton X-100).
b. Incubate in primary antibody (AB1) for 25 min.
c. Rinse in buffer 1.
d. Incubate in biotinylated secondary antibodies (AB2) (Biotinylated goat anti-mouse and anti-rabbit immunoglobulins).
e. Rinse in buffer 1.
f. Rinse in buffer 2 (TBS, pH 7.6, 0.1% Triton X-100).
g. Incubate in streptavidin peroxidase (HRP) (streptavidin conjugated to horseradish peroxidase) for 25 min.
h. Rinse in buffer 2.
i. Rinse in buffer 3.
j. Incubate in DAB for 1 min.
k. Rinse in buffer 3.
l. Counterstain in Mayer's hematoxylin for 1 min.
m. Rinse in buffer 4.
n. Rinse in running tap water for 10 min.
o. Dehydrate in 95% ethanol for 5 min and in 99.5% ethanol for 5 min, followed by incubation in xylol for 5 min.

6. The slides were mounted with coverslips using Pertex mounting medium and allowed to rest for 1 week before being stored in dark boxes to avoid fading of the immunohistochemical staining (Figure 25).
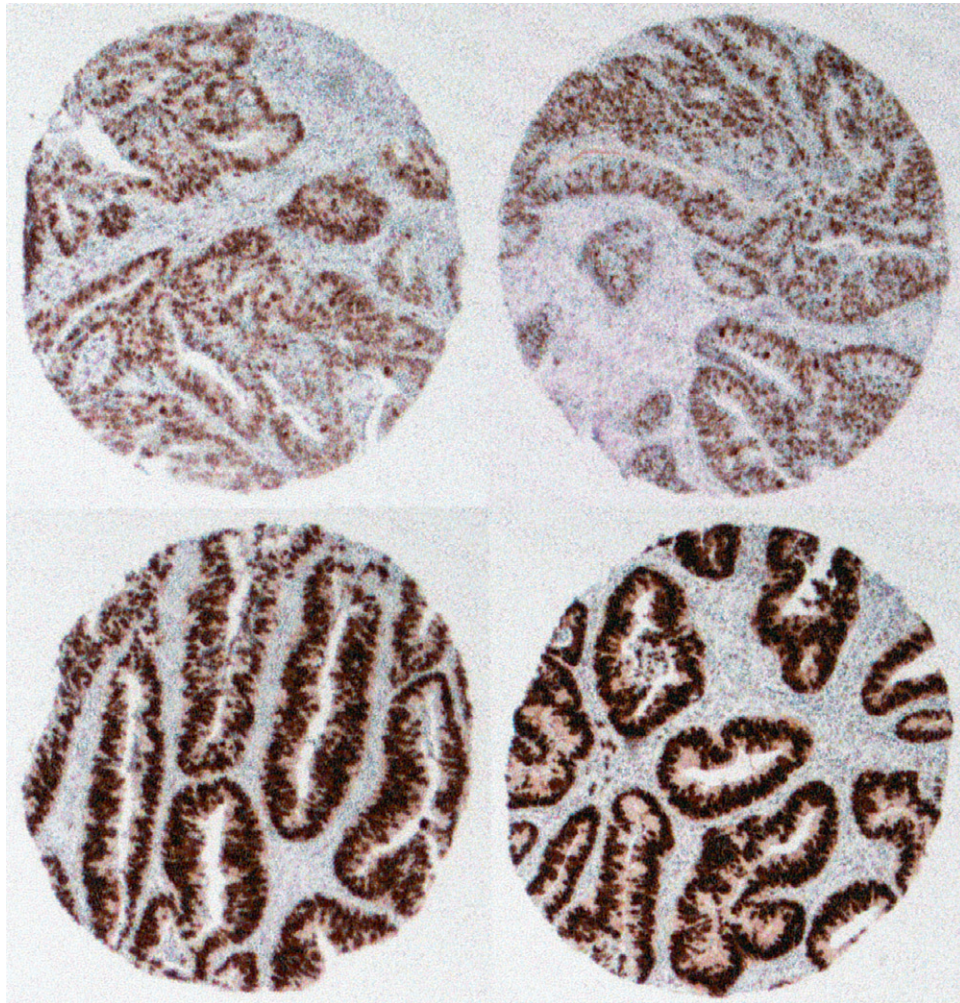
Figure 25 Rectal cancer tissue microarray sections stained with MIB-1 for Ki-67 (*top*) and DO-7 for p53 (*bottom*).

RESULTS AND DISCUSSION

Reproducibility of the TMA Technology

When TMA was introduced, concern was raised regarding the reproducibility of a method that analyzed only a minute sample of tumor tissue. Indeed, each cylinder section encompasses only about $0.3\,mm^2$. However, TMA data have been found to reproduce information gained from studies that have used large tissue sections and have confirmed clinicopathologic correlations reported from studies applying immunostaining on large tissue sections or using DNA isolated from entire tumor pieces or from paraffin sections. These studies have included different tumor types, such as colorectal cancer, breast cancer, bladder cancer, and soft-tissue sarcoma (Camp *et al*., 2001; Engellau *et al*., 2001; Fernebro *et al*., 2002; Hendriks *et al*., 2003; Kononen *et al*., 1999; Nocito *et al*., 2001; Schraml *et al*., 1999; Torhorst *et al*., 2001). We used immunohistochemical staining for Ki-67 and p53 to evaluate the TMA technique in rectal cancer (Fernebro *et al*., 2002). In this study the results from analysis of 10 high-power fields (HPFs) from large tissue sections were compared to the results obtained evaluating at least two TMA sections from each tumor. The mean fraction of nuclear Ki-67 expression was 0.81 in the large tissue sections and 0.85 in the TMA sections. Immunostaining for p53 revealed nuclear staining in the same 15/20 tumor whether analyzed using large tissue sections of TMA. The two methods thus correlated well with only slightly higher Ki-67 values for the TMA technique.

Perhaps even more important than the correlation between the results using TMA and large tissue sections is the observation that TMA data can be used to determine previously identified clinicopathologic associations. It is important in this regard to remember that the TMA technology was developed to survey large tumor populations rather than to characterize expression patterns in individual tumors. In a TMA study applying fluorescence *in situ* hybridization (FISH) to study oncogene amplification in different histopathologic types of tumors, 73% of the amplification data collected through multiple previous investigations could be reproduced in one single experiment (Schraml *et al*., 1999). Studies applying TMA to breast cancer have confirmed clinicopathologic correlations such as amplification of *HER-2/neu* and *MYC* in steroid receptor–negative tumors and *p53*-expressing tumors (Kononen *et al*., 1998; Torhorst *et al*., 2001), evaluated TMA-based immunostaining for the estrogen receptor (ER), the progesterone receptor (PR), and *p53* in breast cancer. Analysis of a single core biopsy identified

95% of the information for ER, 75–81% for PR, and 74% for *p53*, but the combined data using these three antibodies on four different core biopsies yielded as significant correlations with clinical end points as data obtained from large tissue sections. In studies applying TMA to bladder cancer Nocito *et al*. (2001) assessed the correspondence between histologic grade and *Ki-67* labeling index using four replica TMA sections versus large tissue sections. Despite discrepancies in individual cases, the same clinicopathologic associations as found in studies using large sections could be demonstrated using TMA. Identification of colorectal cancers with defective mismatch repair (MMR) is valuable for prognostic purposes or for identification of patients with hereditary nonpolyposis colorectal cancer (HNPCC). Immunostaining applied on TMA sections has been shown to identify MMR-deficient tumors with a sensitivity of 89% with a concordance of 75–95% for the different MMR proteins as compared to large tissue sections (Hendriks *et al*., 2003). TMA can thus reliably be used also to screen large tumor series for defective MMR.

The TMA technique has technical limitations such as nonuniform staining results, presence of necrosis or benign tissue within the biopsy, and loss of cylinder sections in the array process. The thickness of the donor block influences the number of usable slides obtained from the array block. Therefore, tumor blocks that have not been sectioned for multiple routine stainings should, if possible, be selected. Studies aiming to determine the number of core needle biopsies needed to successfully reproduce the results from large tissue staining generally suggest obtaining core biopsies should be obtained in triplicate from each tumor. Camp *et al*. (2001) obtained an accuracy rate of >95% if two to three core biopsies were used to study immunohistochemical expression of ER, PR, and *HER-2/neu* in breast cancer. Depending on the marker studied and the quality of the material within the array sections one to two array sections are generally required to evaluate the staining.

Regarding the immunohistochemical staining, nuclear staining and patterns evaluated based on the presence or absence of staining can be determined from one TMA section containing representative tumor tissue of good quality. In contrast, staining that is dominantly cytoplasmic or markers that produce heterogeneous staining patterns or are evaluated in three or more categories will result in a higher number of nonassessible tumors as a result of discordant readings, and may thus require two or more TMA sections to obtain an acceptable level of reproducibility (Fernebro *et al*., 2004; Hoos *et al*., 2001).

Loss of TMA sections during the array process is another reason for obtaining three to four replica

biopsies from each tumor. Most TMA series report loss of about 10–15% of the sections, either because of empty spots on the slide or because of sections of poor technical quality, most commonly necrotic, thorn, or folded sections. If three core biopsies are obtained from each tumor, 98% of the tumors are estimated to be successfully analyzed using immunostaining (Fernebro *et al*., 2004; Hoos *et al*., 2002). The recommendation of using triplicate TMA sections for analysis is in accordance with the results of other investigators validating the TMA technique and will minimize loss of data, ensure concordant readings in most cases, and thereby provide a reliable immunohistochemical expression profile. Studies that have applied FISH analysis to TMA sections generally report a somewhat lower rate of successful analysis and concordant results than studies applying immunostaining (Andersen *et al*., 2002; Schraml *et al*., 1999). However, the gene amplification surveys report successful analysis of many tumor types, good correlations with previously identified amplifications, and identification of clinicopathologic correlations based on TMA data.

Heterogeneous staining patterns and discordant readings between the TMA sections influence the number of assessable tumors. The fraction of tumors with heterogeneous findings is probably dependent on the tumor type and on the type of marker studied. In our experience heterogeneous immunostaining most often affects tumors with an intermediate staining intensity, whereas the truly positive or negative tumors tend to display a more uniform expression pattern (Fernebro *et al*., unpublished observations). We used Ki-67 staining to calculate how intratumor heterogeneity may affect the immunostaining results in studies applying TMA. Because the area of one TMA section is approximately the size of a $40L \times HPF$, we assessed the standard error of the mean (SEM) according to the number of HPFs analyzed. The SEM values for *Ki-67* gave a variability of 6.1% for 1 HPF, 3.7% for 2, 3.0% for 3, 2.6% for 4, and 2.3% for 5 HPFs analyzed (Fernebro *et al*., 2002). From these data (which show that analysis of an increasing number of HPFs is beneficial up to 3–4 areas and where after the additional areas studied have a marginal impact on the SEM values) we suggest that the core biopsies should, when possible, be obtained in triplicate. Furthermore, retrieval of core biopsies from multiple paraffin-embedded tumor blocks may provide an even better estimate of the tumor's biology, with lower SEM values compared to analysis of multiple biopsies from the same block (Engellau *et al*., 2000). Markers with a high degree of intratumor heterogeneity and with different staining patterns in the periphery and in the

center of the tumor are likely to be more vulnerable to TMA interpretations. Thus, obtaining core biopsies from the periphery and the center of the tumor may be required for a correct immunohistochemical characterization of certain markers (Camp *et al*., 2000). Furthermore, careful identification of informative tumor areas and distinction between *in situ* cancer and invasive tumor areas may be difficult but is crucial because antigen expression may differ between these tumor components. These approaches will be important to maximize the number of evaluable TMA sections, to reduce the impact of tumor heterogeneity, and to provide a true estimate of the immunohistochemical expression.

Once the defined tumor material has been collected, TMA is performed at a speed of 30–70 biopsies per hour, and 500–1000 biopsies can be evaluated on a single microscope slide. Retrieval of the 0.6-mm tumor biopsies used for TMA results in minor, usually negligible, damage to the donor block. Such multiple biopsies can therefore be obtained from most paraffin blocks, which allow construction of several replicate array blocks, each containing the same tumor at a given coordinate. Indeed, applying TMA to a 10-mm diameter tumor will allow >10.000 analyses (Schraml *et al*., 1999). TMA thereby increases the number of markers that can be investigated within the same tumor set and contributes to tissue preservation. Whereas 100–200 sections can generally be obtained from a regular paraffin-embedded tissue block, several thousands of TMA sections can be generated from a paraffin block.

The impressive number of new candidate markers identified using the novel techniques applied in genomics and proteomics will require evaluation in large and clinically well-characterized tumor series to diagnose markers with diagnostic, prognostic, and therapeutic possibilities. Tissue preservation will in this regard be fundamental to evaluate potentially important markers. Many studies investigating molecular markers in various tumor types have been small and thus have not been powered to detect possible clinicopathologic associations. Use of multi-tumor TMAs constructed to contain different histopathologic tumor types within the array will probably provide a quick and efficient means to evaluate involvement of newly discovered markers in different tumor types.

Because TMA offers the possibility to study large tumor cohorts with long follow-up, the question of antigen durability was studied by Camp *et al*. (2000). This study demonstrated that most 50–70-year-old tumors are suitable for immunohistochemical analysis. However, antigen preservation may depend on fixation,

paraffin embedding, block storage, and the method applied for antigen retrieval (Rimm *et al.*, 2001). Previous handling of the tumor tissue may also affect the structure and consistency of the tissue and may thereby also influence the sectioning of the array block. For these reasons a validation of the results obtained in older archival specimens may be needed from each institution.

Optimization of the TMA technique will increase the success rate. Therefore, each laboratory should optimally apply a standard procedure for the construction of tissue microarrays. Such an effort could include obtaining a standardized number of core biopsies from the tumors, retrieving tissue from the periphery and the center of the tumor and optimally from normal surrounding tissue, and having the TMAs constructed by experienced laboratory personnel. In our experience, the number of successful arrays and staining thereof increases with experience. The regular arrangement of the arrayed specimens facilitates efficient evaluation of the stained sections and allows for automated array construction and analysis. Automated TMA will probably also minimize the technical problems recognized using manual arrayers. The samples will be automatically positioned at equal levels within the array block, which will presumably reduce the number of folded, or thorn, arrays and the number of empty spots on the TMA sections. The possibility or evaluating multiple samples simultaneously also has the advantage that all specimens are processed under identical conditions in a single experiment, which should facilitate a standardized and homogenous evaluation of the results.

Tissue Microarray in Rectal Cancer

Hitherto, relatively few biomarkers have been implemented in clinical decision making in rectal cancer, but for several markers routine clinical application depends on the outcome or awaits confirmation of the findings in large-scale studies of well-characterized tumor series with complete clinical follow-up. Hoos *et al.* (2002) used TMA for immunohistochemical characterization of 100 primary T2–T3 rectal cancers. The tumors were assessed for immunostaining using seven different antibodies against cell-cycle–regulatory proteins. The study revealed a high *Ki-67* proliferative index in 61% of the adenocarcinomas and an increased expression of *p53* in 58%, *MDM2* in 58%, *cyclin D1* in 8%, *Bcl-2* in 25%, and an increased expression of *p21* in 48% of the tumors. However, no significant correlation between the molecular expression profile and disease status was found, although down-regulation of the cyclin-dependent kinase inhibitor and tumor suppressor *p27* showed a trend toward reduced survival. This study concluded that even in the relatively homogenous group of patients with early-stage rectal cancer, the tumors as a group display heterogeneous expression profiles. A combination of an increased *p53* expression without detectable *Bcl-2* expression has been associated with poor prognosis of colorectal cancer (Schwandner *et al.*, 1999). This observation could not be reproduced in the TMA study of early-stage rectal cancer, in which neither *p53* alone, *Bcl-2* alone, or a combination of the two revealed any prognostic significance. We have performed a study applying TMA to a series of 269 preoperative biopsies from rectal cancers (Fernebro *et al.*, 2004). The patients had received standardized treatment (including 25 Gy preoperative radiotherapy and surgery using total mesorectal excision). In line with the observations by Hoos *et al.* (2002), our study did not show any significant prognostic correlations between the immunostaining for *p53* or *Ki-67* and prognosis, but indicated a prognostic role for expression of β-catenin and E-cadherin (Fernebro *et al.*, 2004).

The different conclusions reached in different studies of the prognostic importance of markers such as *p53* and *Ki-67* in rectal cancer are probably the result of differences in patient materials, staining techniques, and evaluation protocols. The lack of prognostic information contributed by these markers in the large (n=100 and n=269) studies by Hoos *et al.* (2002) and by Fernebro *et al.* (2004) suggests that none of the single markers identified and investigated so far yield consistent independent prognostic information in rectal cancer. Furthermore, Samowitz *et al.* (2001) evaluated *p53* gene mutations in a population-based series of more than 1400 colon cancers. Although *p53* mutations were found to be associated with distal, high-stage tumors without *MSI* and *K-ras* mutations, the overall *TP53* mutation status was not an independent prognostic marker in multivariate analysis. However, specific hot spot mutations correlated with prognosis in cancers of the proximal colon. Immunostaining for p53 correlated well with *TP53* mutation status in colorectal tumors, but if only a specific subset of *TP53* mutations influences prognosis and furthermore does so only in a subset of the colorectal cancers, the lack of prognostic value reported in several studies applying *p53* immunostaining to rectal cancer is expected rather than surprising. The lack of prognostic importance for several of the tumor-associated factors so far identified and tested in colorectal cancer could also reflect the fact that a

broad range of abnormalities have accumulated already in the early-stage tumors. Several of these alterations may not persist during clonal evolution and may thus not represent characteristics of aggressive tumor behavior. The lessons learned from *TP53* mutation analysis and immunostaining in colorectal cancer emphasize the need to perform detailed mutation analysis, to correlate the different techniques (mutation analysis versus immunostaining), and to validate the findings in independent tumor materials. TMA will contribute to this labor-intensive work because the ease and feasibility of applying TMA will allow an efficient validation of tumor markers in large materials.

In summary, the minute tumor samples obtained using TMA have in several studies been found to reproduce data obtained from studies of large tissue sections and to be sufficiently representative of the tumor to allow establishment of previously identified associations between molecular alterations, pathologic characteristics, and clinical end points. Several large-scale studies have also applied TMA to determine expression patterns using immunohistochemical staining and FISH analysis. However, as yet no single tumor-associated marker has shown a consistent and independent correlation to clinicopathologic factors such as response and prognosis in rectal cancer, and the role of *Ki-67* and *p53* in this regard is uncertain. Because a major aim of tumor marker studies is to predict treatment response and to tailor therapy to improve outcome, standardization of the methodology and the interpretations is fundamental. The technological developments that allow genome-wide expression studies will put forward a large number of potentially interesting diagnostic and prognostic markers. The possibility to combine the different array techniques is a fundamental step toward the application of novel markers in clinical decision making. TMA offers a challenging potential to accelerate translational research because it allows rapid evaluation of the basic research findings in different tumor types and marker validation in large and clinically well-characterized tumor materials.

Acknowledgments

References

Allegra, C.J., Paik, S., Colangelo, L.H., Parr, A.L., Kirsch, I., Kim, G., Klein, I., Johnston, P.G., Wolmark, N., and Wieland, H.S. 2003. Prognostic value of thymidylate synthase, Ki-67, and p53 in patients with Dukes' B and C colon cancer: A national cancer institute-national surgical adjuvant breast and bowel project collaborative study. *J. Clin Oncol. 21*:241–250.

Allegra, C.J., Parr, A.L., Wold, L.E., Mahoney, M.R., Sargent, D.J., Johnston, P., Klein, P., Behan, K., O'Connell, M.J., Levitt, R., Kugler, J.W., Tria Tirona, M., and Goldberg, R.M. 2002. Investigation of the prognostic and predictive value of thymidylate synthase, p53, and Ki-67 in patients with locally advanced colon cancer. *J. Clin. Oncol. 20*:1735–1743.

Andersen, C.L., Monni, O., Wagner, U., Kononen, J., Bärlund, M., Bucher, C., Haas, P., Nocito, A., Bissing, H., Sauter, G., and Kallioniemi, A. 2002. High-throughput copy number analysis of 17q23 in 3520 tissue specimens by fluorescence in situ hybridization to tissue microarrays. *Am. J. Pathol. 161*:73–79.

Bazan, V., Migliavacca, M., Zanna, I., Tubiolo, C., Corsale, S., Calo, V.V., Amato, A., Cammareri, P., Latteri, F., Grassi, N., Fulfaro, F., Porcasi, R., Morello, V., Nuara, R.B., Dardanoni, G., Salerno, S., Valerio, M.R., Dusonchet, L., Gerbino, A., Gebbia, N., Tomasino, R.M., and Russo, A. 2002. DNA ploidy and S-phase fraction, but not p53 or NM23-H1 expression, predict outcome in colorectal cancer patients. Results of a 5-year prospective study. *J. Cancer. Res. Clin. Oncol. 128*:650–658.

Bhatavdekar, J.M., Patel, D.D., Chikhlikar, P.R., Shah, N.G., Vora, H.H., Ghosh, N., and Trivedi, T.I. 2001. Molecular markers are predictors of recurrence and survival in patients with Dukes B and Dukes C colorectal adenocarcinoma. *Dis. Colon. Rectum 44*:523–533.

Camp, R.L., Charette, L.A., and Rimm, D.L. 2000. Validation of tissue microarray technology in breast carcinoma. *Lab. Invest. 80*:1934–1949.

Cascinu, S., Graziano, F., Catalano, V., Staccioli, M.P., Rossi, M.C., Baldelli, A.M., Barni, S., Brenna, A., Seconcino, S., Muretto, P., and Catalano, G. 2002. An analysis of p53, BAX and vascular endothelial growth factor expression in node-positive rectal cancer. Relationship with tumor recurrence and event-free survival of patients treated with adjuvant chemoradiation. *Br. J. Cancer 86*:744–749.

Elsaleh, H., Soontrapornchai, P., Grieu, F., Joseph, D., and Iacopetta, B. 1999. p53 alterations have no prognostic or predictive significance in Dukes' C rectal carcinomas. *Int. J. Oncol. 15*:1239–1243.

Engellau, J., Åkerman, M., Andersson, H., Domanski, H.A., Rambech, E., Alvegård, T.A., and Nilbert, M. 2001. Tissue-array technique in soft tissue sarcoma; immunohistochemical Ki-67 expression in malignant fibrous histicytoma. *Appl. Immunohist. Mol. Morphol. 9*:358–363.

Fernebro, E., Bendahl, P-O., Dictor, M., Persson, A., Fernon, M., and Nilbert, M. 2004. Immunohistochemical patterns in rectal cancer: Application of tissue microarray with prognostic correlations. *Int. J. Cancer 111*:421–428.

Fernebro, E., Dictor, M., Bendahl, P-O., Fernö, M., and Nilbert, M. 2002. Evaluation of the tissue microarray technique for immunohistochemical analysis in rectal cancer. *Arch. pathol. Lab. Med. 126*:702–705.

Gervaz, P., Bouzourene, H., Cerottini, J-P., Chaubert, P., Benhattar, J., Secic, M., Wexner, S., Givel, J-C., and Belin, B. 2001. Dukes B colorectal cancer. Distinct genetic categories and clinical outcome based on proximal or distal tumor location. *Dis. Colon Rectum. 44*:364–373.

Hendriks, Y., Franken, P., Dierssen, J.W., de Leeuw, W., Wijenen, J., Dreef, E., Trops, C., Breuning, M., Bröcker-Vriends, A., Vasen, H., Fodde, R., and Morreau, H. 2003. Conventional and tissue microarray immunohistochemical expression analysis of mismatch repair in hereditary colorectal tumors. *Am. J. Pathol. 162*:469–477.

Hoos, A., Nissan, A., Stojadinovic, A., Shia, J., Hedvat, C.V., Leung, D.H.Y., Paty, P.B., Klimstra, D., Cordon-Cardo, C., and Wong, W.D. 2002. Tissue microarray molecular profiling of early, node-negative adenocarcinoma of the rectum: A comprehensive analysis. *Clin. Cancer Res. 8*:3841–3849.

Hoos, A., Urist, M.J., Stojadinovic, A., Mastorides, S., Dudas, M.E., Leung, D.H.Y., Kuo, D., Brennan, M.F., Lewis, J.J., and Cordon-Cardo, C. 2001. Validation of tissue microarrays for immunohistochemical profiling of cancer specimens using the example of human fibroblastic tumors. *Am. J. Pathol. 158*:1245–1251.

Kandioler, D., Zwrtek, R., Ludwig, C., Janschek, E., Ploner, M., Hofbauer, F., Kuhrer, I., Kappel, S., Wrba, F., Horvath, M., Karner, J., Renner, K., Bergmann, M., Karner-Hanusch, J., Potter, R., Jakesz, R., Teleky, B., and Herbst, F. TP53 genotype but not p53 immunohistochemical result predicts response to preoperative short-term radiotherapy in rectal cancer. *Ann. Surg. 235*:493–498.

Kapiteijn, E., Liefers, G.J., Los, L.C., Kranenbrag, E.K., Herman, J., Tollenaar, R.A.E.M., Moriya, Y., van de Velde, C.J.H., and van Krieken, J.H.J.M. 2001. Mechanisms of oncogenesis in colon cancer versus rectal cancer. *J. Pathol. 195*:171–178.

Kononen, J., Bubendorf, L., Kallionemi, A., Bärlund, M., Schraml, P., Leighton, S., Torhorst, J., Mihatsch, M.J., Sauter, G., and Kallioniemi, O-P. 1998. Tissue microarrays for high throughput molecular profiling of tumor specimens. *Nat. Med. 7*:844–847.

Michael-Robinson, J.M., Reid, L.E., Purdie, D.M., Biemer-Huttmann, A.E., Walsh, M.D., Pandeya, N., Simms, L.A., Young, J.P., Leggett, B.A., Jass, J.R., and Radford-Smith, G.L. 2001. Proliferation, apoptosis, and survival in high-level microsatellite instability sporadic colorectal cancer. *Clin. Cancer Res. 8*:2347–2356.

Nilbert, M., Planck, M., Fernebro, E., Borg, Å., and Johnson, A. 1999. Microsatellite instability is rare in rectal carcinomas and signify hereditary cancer. *Eur. J. Cancer 35*:942–945.

Nocito, A., Bubendorf, L., Tinner, E.M., Suess, K., Wagner, U., Forster, T., Kononen, J., Fijan, A., Bruderer, J., Schmid, U., Ackermann, D., Maurer, R., Alund, G., Knönagel, H., Rist, M., Anabitarte, M., Hernig, F., Hardmeie, T., Schoenenberger, A.J., Flury, R., Jäger, P., Fehr, J.L., Schraml, P., Moch, H., Mihatsch, M.J., Gasser, T., and Sauter, G. 2001. Microarrays of bladder cancer tissue are highly representative of proliferation index and histological grade. *J. Pathol. 195*:349–357.

Parkin, D.M. 2001. Global cancer statistics in the year 2000. *Lancet Oncol. 2*:533–543.

Rebischung, C., Gérard, J.P., Gayet, J., Thomas, G., Hamelin, R., and Laurent-Puig, P. 2002. Prognostic value of p53 mutations in rectal carcinoma. *Int. J. Cancer 100*:131–135.

Resnick, M.B., Ronthier, J., Konkin, T., Sabo, E., and Pricolo, V.E. 2004. Epidermal growth factor receptor, C-MET, β-catenin, and p53 expression as prognostic indicators in stage II colon cancer: A tissue microarray study. *Clin. Cancer Res.* 10:3069–3075.

Rimm, D.L., Camp, R.L., Charette, L.A., Costa, J., Olsen, D.A., and Reiss, M. 2001. Tissue microarray: A new technology for amplification of tissue resources. *Cancer J. 7*:24–31.

Samowitz, W.S., Curtin, K., Ma, K.N., Edwards, S., Schaffer, D., Leppert, M.F., and Slattery, M.L. 2002. Prognostic significance of p53 mutations in colon cancer at the population level. *Int. J. Cancer 99*:597–602.

Schraml, P., Kononen, J., Bubendorf, L., Moch, H., Bissig, H., Nocito, A., Mihatsch, J.M., Kallioniemi, O-P., and Sauter, G. 1999. Tissue microarrays for gene amplification surveys in many tumor types. *Clin. Cancer Res. 5*:1966–1975.

Schwandner, O., Schiedeck, T.H., Bruch, H.P., Duchrow, M., Windhoevel, U., and Broll, R. 2000. p53 and Bcl-2 as significant predictors of recurrence and survival in rectal cancer. *Eur. J. Cancer 36*:348–356.

Soong, R., Grieu, F., Robbins, P., Dix, B., Chen, D., Parsons, R., House, A., and Iacopetta, B. 1997. p53 alterations are associated with improved prognosis in distal colonic carcinomas. *Clin. Cancer Res. 3*:1405–1411.

Takagi, S., Kumagai, S., Kinouchi, Y., Hiwatashi, N., Nagashima, F., Takahashi, S., and Shimosegawa, T. 2002. High Ki-67 labeling index in human colorectal cancer with microsatellite instability. *Anticancer Res. 22*:3241–3244.

Tollenaar, R.A., van Krieken, J.H., van Slooten, H.J., Bruinvels, D.J., Nelemans, K.M., van den Broek, L.J., Hermans, J., and van Dierendonck, J.H. 1998. Immunohistochemical detection of p53 and Bcl-2 in colorectal carcinoma: No evidence for prognostic significance. *Br. J. Cancer 77*:1842–1847.

Torhorst, J., Bucher, C., Kononen, J., Haas, P., Zuber, M., Köchi, O.R., Mross, F., Dieterich, H., Moch, H., Mihatsch, M., Kallioniemi, O-P., and Sauter, G. 2001. Tissue microarrays for rapid linking of molecular changes to clinical endpoints. *Am. J. Pathol. 159*:2249–2256.

This Page Intentionally Left Blank

4

Role of Immunohistochemical Expression of p21 in Rectal Carcinoma

Nobuhiro Takiguchi, Nobuhito Sogawa, and Masaru Miyazaki

Introduction

Recent molecular biologic studies suggested certain molecular markers might be useful as prognostic factors in patients with colorectal cancer. The *WAF1/CIP1* gene encodes p21 protein, a cyclin-dependent kinase (CDK) inhibitor whose activation is crucial for cell-cycle progression (Sherr *et al.*, 1995). The expression of *p21* is activated by wild-type *p53* gene product in response to deoxyribonucleic acid (DNA) damage. The gene *p53*, located on the short arm of chromosome 17, is a tumor suppressor gene that encodes a transcription factor that plays a role in DNA repair and that either arrests cell growth in G1 or induces apoptototic cell death. Both *p53* and *p21* might play important roles in regulating the induction of apoptosis in radiosensitive tumor cells. Wild-type p53 protein functions as a transcription factor that regulates the expression of a variety of genes (Levine *et al.*, 1997). For example, the *WAF1* gene is transactivated by the wild-type p53 protein as a result of the binding of p53 DNA to its promoter region but not by mutant p53 proteins commonly found in human cancers (El-Deiry *et al.*, 1993). Recent studies have suggested that *p21* is also induced by other *p53*-independent factors, such as *p73* (Lee *et al.*, 1998).

Apoptosis is a genetically mediated physiologic process that occurs in a variety of different cell types and results in cell death. Apoptosis can be inhibited by cellular protooncogenes such as *p53* and *Bcl-2* and can be induced by chemotherapy and irradiation.

We have studied the levels of expression of *p21* and *p53*, and the degree of apoptosis, in the patients with advanced rectal cancer, some of whom received preoperative radiochemotherapy (Sogawa *et al.*, 2002), and discuss the role of immunohistochemical expression of *p21* in rectal carcinoma.

MATERIALS AND METHODS

Clinical Materials

Tissues from a total of 75 patients with advanced middle or lower rectal cancer were examined. Of these, 40 received preoperative radiochemotherapy (irradiation group), whereas the remainder received neither chemotherapy nor radiation therapy (control group). Indications for preoperative radiochemotherapy were as follows: 1) tumor invasion beyond the proper muscularis layer as determined by imaging studies; and 2) extruding mucinous carcinoma diagnosed at biopsy. Preoperative radiochemotherapy was performed using a linear accelerator with the shrinking field technique. The total dose 42.6 Gy: 30.6 Gy (1.8 Gy/fraction × 5 sessions per week for 4 weeks) was delivered to the whole pelvis from both the anterior and posterior portals, and additional 12 Gy (3.0 Gy/fraction daily for 4 days) was boosted to the pelvic canal. In addition,

Handbook of Immunohistochemistry and in situ Hybridization of Human Carcinomas,
Volume 2: Molecular Pathology, Colorectal Carcinoma, and Prostate Carcinoma

159

patients receiving radiotherapy were also given chemotherapy via the anus for 4 weeks using tegafur suppositories (750 mg per day).

Immunohistochemical Staining and Scoring Method for Gene Expression

MATERIALS

1. Routinely processed 10% formalin-fixed and paraffin-embedded (FFPE) blocks containing primary tumor were serially sectioned at 4 μm through their maximal cross-sectional area.

2. Paraffin-embedded sections were placed on poly-L-lysine–coated glass slides.

3. Immunohistochemical staining for antigens was performed by the standard avidin-biotin-peroxidase complex technique using a Dako LSAB2 kit (Dako Japan Ltd., Kyoto, Japan).

METHODS

1. Sections were deparaffinized and rehydrated.

2. Deparaffinized and rehydrated sections were heated three times in a microwave oven for 5 min each in citrate buffer (pH 6.0) to unmask antigenic activity and then finally cooled for 60 min at room temperature.

3. Endogenous peroxidase activity was inhibited by incubation with 3% hydrogen peroxide in water for 5 min at room temperature.

4. The sections were incubated overnight with either the p53 antibody (DO-7; Dako Japan Ltd.) or p21 antibody (SC-187; Dako Japan Ltd.) at a dilution of 1:50.

5. The sections were then incubated with either biotinylated anti-rabbit or anti-mouse immunoglobulins for 10 min followed by a 10-min incubation with streptavidin-peroxidase complex.

6. Color development was induced by diaminobenzidine, and the sections were lightly counterstained with hematoxylin and mounted on glass slides.

7. Negative controls for each of the antibodies were performed using phosphate buffer saline (PBS) instead of the primary antibody.

For *p53* expression, samples with <50% of positively stained tumor cells were defined as negative, and all others were defined as positive. In the case of *p21* expression, samples with <5% of positively stained tumor cells were defined as negative, and all others were defined as positive. The percentages of *p53*- and *p21*-positive cells were estimated by counting more

than 1000 cells at random and were recorded as the *p53*-labeling index (*p53*-LI) and *p21*-labeling index (*p21*-LI), respectively.

Detection of Apoptosis and Determination of the Apoptotic Index

Apoptotic carcinoma cells were identified using the Apop Tag *in situ* Apoptosis Detection Kit (Oncor, Inc., Gaithersburg, MD), which is based on the terminal deoxynucleotidyl I transferase (TdT)–mediated dUTP-biotin nick end labeling (TUNEL) method (Gavrieli *et al.*, 1992). The percentage of apoptotic cells was calculated as the number of TUNEL-positive cancer cells per 1000 cancer cells. The apoptotic index (AI) was expressed as the ratio of positively stained tumor cells to all other tumor cells. The index gives a percentage for each case as determined according to the criteria described previously (Lu *et al.*, 1997). For apoptosis detection, cases with <1% positively stained tumor cells were considered negative.

RESULTS

Immunohistochemical Staining

p53 Immunostaining

The overall positive staining ratio for p53 was 81.3%. The nuclear p53 staining was present in 27 of 35 samples (77%) from the control group and in 34 of 40 samples (85%) from the irradiated group. There was no correlation between p53 expression and several clinicopathologic parameters.

p21 Immunostaining

The gene *p21* was expressed in the nuclei of terminally differentiated epithelial cells in normal surface mucosa. The cells at the base of the crypts did not contain detectable *p21* staining. Although most tumor cell nuclei of high *p21* expression showed high *p53* expression, there were *p21*-stained cells that showed very low expression of *p53* (Figure 26). The overall percentage of positive *p21* staining was 41.3%. The nuclear *p21* staining was present in 23 of 40 samples (57.5%) from the irradiation group and in 8 of 35 samples (2.3%) from the control group. The difference in the *p21*-LI between the irradiation and control groups was significant (8% versus 3%, respectively; p = 0.03), and *p21* expression was significantly reduced in samples derived from patients with lymph nodal metastasis (p = 0.0002). There was no correlation
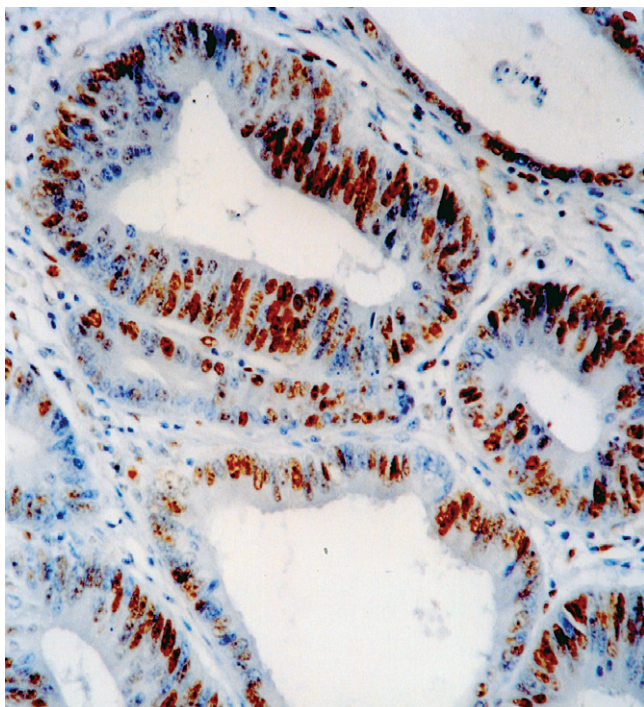
Figure 26 Immunostaining of *p21* in advanced lower rectal cancer tissue treated with preoperative radiochemotherapy: Immunostaining with *p21* reveals that more than 80% of tumor cells have positive nuclei. The expression of *p21* and the apoptotic index were significantly higher in the irradiated group. There was a significant correlation between *p21* immunoreactivity and survival rate.

between *p21* and *p53* expression and the clinicopathologic features of the tumor. However, there was a significantly greater *p21* expression in the invaded muscularis compared to that in the invaded serosa. Expression of *p21* staining in samples from Dukes A patients was significantly higher than that from Dukes C patients (p = 0.0009).

Detection of Apoptosis

The mean percentage of apoptosis in all tumors was 50.6%. Apoptosis was present in 25 of 40 (62.5%) samples from the irradiation group and in 13 of 35 (37.1%) samples from the control group. There was a significant correlation of AI between these two groups (2% versus 1.2%; p = 0.05).

Analysis of Prognostic Usefulness of *p21*, *p53*, and Apoptosis

The overall 5-year survival rates for *p53*-positive cases (62.6%) were less than those for *p53*-negative cases (70.7%), but the difference was not significant (p = 0.58). The overall 5-year survival rates for apoptosis-positive cases (74.5%) were higher than those for apoptosis-negative cases (53.5%), but the difference again was not significant (p = 0.09). The overall 5-year survival rates for *p21*-positive cases (92.0%) were higher than those for *p21*-negative cases (49.6%), and this difference was significant (p = 0.002).

Multivariate Cox proportional hazard modeling demonstrated that *p21* expression (relative ratio [RR]: 0.09, 95% confidence interval [CI]: 0.01~0.78, p = 0.03) as well as lymph nodal metastasis (RR: 3.63, 95% CI: 1.06~12.37, p = 0.04) was an independent predictor of overall survival.

DISCUSSION

The most commonly mutated gene in human colorectal carcinomas is *p53* (Remvikos *et al.*, 1992). In cells with a wild-type *p53* gene, exposure to ionizing radiation produces a rapid increase in *p53* protein levels and transcriptional activation of *p21* and other *p53*-responsive genes, leading to either cell-cycle arrest or apoptosis (Brugarolas *et al.*, 1995). Several studies have found a significant association between *p53* immunostaining and rectal cancer radiosensitivity (Fu *et al.*, 1998). Our results showed no radiosensitive and prognostic significance of *p53* expression in individual patients in agreement with some other studies (Scott *et al.*, 1998).

Tumor growth is thought to depend on the requisite balance between cellular proliferation and apoptosis (Kerr *et al.*, 1994, LaCasse *et al.*, 1998). Our results also showed that apoptosis was induced by radiochemotherapy.

The *p21* tumor suppressor gene, which regulates the cell cycle, may play a major role in tumor responsiveness to cytotoxic agents such as radiation and chemotherapy (El-Deiry *et al.*, 1994). Our results demonstrated a significant correlation of *p21* expression between the irradiation group and the control group. Expression of *p53* was significantly reduced in patients with lymph nodal metastasis. Despite the preoperative patient selection as tumor invasion beyond the muscle layer, *p21* expression was significantly higher in patients with muscle invasion in the irradiated group, compared to that in the control group. The ratio of positive *p21* cells in tumors with muscle invasion of the irradiation group was especially higher. These results suggested that p21 expression was related to down-staging induced by radiochemotherapy. The theories that *p21* and *Bcl-2* are activated following *p53* activation, in response to radiation-induced DNA damage, and that it plays an important

role in rectal cancer radiosensitivity are supported by the results of our study (Levine *et al.*, 1997). In colorectal cancer the induction of *p21* may occur mostly in *p53*-dependent pathways, and *p21* may also inhibit the activity of *cyclins* such as *cyclin D1* (Grazyna *et al.*, 2001). Both *p21* and *p53* immunostaining were demonstrable in 33.3% of all of the cases we studied, suggesting that *p21* was induced by a *p53*-dependent pathway. Interestingly, this was not reported to be the case for *p73*, a homologue of *p53* that was found to lie within 1p36 chromosomal region, suggesting that it, too, may be a tumor suppressor (Kaghad *et al.*, 1997). However, a report showing that *p73* is activated by *c-Abl*, a tyrosine kinase, by cisplatin and gamma radiation treatment, suggests that *p53*-independent *p21* expression may have occurred in response to the induction of *p73* (Gong *et al.*, 1999).

Although there have been some reports that *p21* plays an important role in tumor radiosensitivity (Qui *et al.*, 2000), it has not yet been clarified whether there is an independent prognostic factor in patients with rectal cancer who undergo preoperative radiochemotherapy. In this study, the multivariate Cox proportional hazard model showed that *p21* expression was confirmed as a significant independent predictor of survival, which supports a role for *p21* as an independent prognostic factor in patients with rectal cancer who receive preoperative radiochemotherapy.

References

Brugarolas, J., Chandrasekaran, C., Gordon, J.I., Beach, D., Jacks, T., and Hannon, G.J. 1995. Radiation-induced cell cycle arrest compromised by 21 deficiency. *Nature 377*:552–557.

El-Deiry, W.S., Harper, J.W., and O'Connor, P.M. 1994. WAF1/CIP1 is induced in p53 mediated G1 arrest and apoptosis. *Cancer Res. 54*:1169–1174.

El-Deiry, W.S., Tokino, T., Velculescu, V.E., Lewy, D.B., Persons, R., Trent, J.M., Lin, D., Mercer, W.E., Kinzler, K.W., and Vogelstein, B. 1993. WAF1, a potential mediator p53 tumor suppression. *Cell 75*:817–825.

Fu, C.G., Tominaga, O., Nagawa, H., Nita, M.E., Masaki, T., Ishimaru, G., Higuchi, Y., Tsuruo, T., and Muto, T. 1998. Role of p53 and p21/WAF1 detection in patient selection for preoperative radiotherapy in rectal cancer patients. *Dis. Colon. Rectum 41*:68–74.

Gavrieli, Y., Sherman, Y., and Ben-Sasson, S.A. 1992. Identification of programmed cell death in situ via specific labeling of nuclear DNA fragmentation. *J. Cell. Biol. 119*:493–501.

Gong, J.G., Costanzo, A., Yang, H.Q., Melino, G., Kaelin, W.G., Jr, Levrero, M., and Wang, J.Y. 1999. The tyrosine kinase c-Abl regulates p73 in apoptotic response to cisplatin-induced DNA damage. *Nature 399*:806–809.

Grazyna, P.W., Radzislaw, K., and Marcin, F. 2001. p21 (WAF1) expression in colorectal cancer: Correlation with p53 and cyclin D1 expression, clinicopathological parameters and prognosis. *Pathol. Res. Pract. 197*:683–689.

Kaghad, M., Bonnet, H., Yang, A., Creancier, L., Biscan, J.C., Valent, A., Minty, A., Chalon, P., Lelias, J.M., Dumont, X., Ferrara, P., McKeon, F., and Caput, D. 1997. Monoallelically expressed gene related to p53 at 1p36, a region frequently deleted in neuroblastoma and other human cancers. *Cell 90*:809–819.

Kerr, J.F., Winterford, C.M., and Harmon, B.V. 1994. Apoptosis. Its significance in cancer and cancer therapy. *Cancer 73*:2013–2026.

LaCasse, E.C., Baird, S., Korneluk, R.G., and MacKenzie, A.E. 1998. The inhibitors of apoptosis (IAPs) and their emerging role in cancer. *Oncogene 17*:3247–3259.

Levine, A.J. 1997. p53, the cellular gatekeeper for growth and division. *Cell 88*:323–331.

Lu, C., and Tanigawa, N. 1997. Spontaneous apoptosis is inversely related to intramural microvessel density in gastric carcinoma. *Cancer Res. 57*:221–224.

Qiu, H., Sirivongs, P., Rothenberger, M., Rothenberger, D.A., and Garcia-Aguilar, J. 2000. Molecular prognostic factors in rectal cancer treated by radiation and surgery. *Dis. Colon Rectum 43*:451–459.

Remvikos, Y., Tominaga, O., Hammel, P., Laurent-Puig, P., Salmon, R.J., Dutrillaux, B., and Thomas, G. 1992. Increased p53 protein content of colorectal tumours correlates with poor survival. *Br. J. Cancer 66*:758–764.

Scott, N., Hale, A., Deakin, M., Hand, P., Adab, F.A., Hall, C., Williams, G.T., and Elder, J.B. 1998. A histopathological assessment of the response of rectal adenocarcinoma to combination chemo-radiotherapy: Relationship to apoptotic activity, p53 and bcl-2 expression. *Eur. J. Surg. Oncol. 24*:169–173.

Sherr, C.J., and Roberts, J.M. 1995. Inhibitors of mammalian G1 cyclin-dependent kinases. *Genes Dev. 9*:1149–1163.

Sogawa, N., Takiguchi, N., Koda, K., Oda, K., Satomi, D., Kato, K., Ishikura, H., and Miyazaki, M. 2002. Value of expression of p21[WAF1/CIP1] as a prognostic factor in advanced middle and lower rectal cancer patients treated with preoperative radiochemotherapy. *Int. J. Oncol. 21*:787–793.

5

Role of p107 Expression in Colorectal Carcinoma

Tsutomu Masaki, Kazutaka Kurokohchi, Fei Wu, and Shigeki Kuriyama

Introduction

Retinoblastoma (Rb), *p107*, and *p130* belong to the RB gene family, which has been proved to be a tumor suppressor (Grana *et al*., 1998). Loss of Rb protein (pRb) frequently occurs in various kinds of cancers and is widely associated with carcinogenesis and cancer development (Paggi *et al*., 1996). Reduction of *p130* is associated with the pathogenesis and progression of several kinds of cancers (Claudio *et al*., 2000; Zamparelli *et al*., 2001) and strongly predicts a poor prognosis in endometrial carcinoma (Susini *et al*., 1998) and choroidal melanoma (Massaro-Giordano *et al*., 1999).

Similarly, *p107* expression varies abnormally in lung cancer (Baldi *et al*., 1997), lymphoma (Cinti *et al*., 2000; Leoncini *et al*., 1999), melanoma (Massaro-Giordano *et al*., 1999), mesothelioma (De Luca *et al*., 1997), and colorectal carcinoma (Wu *et al*., 2002), suggesting that *p107* may also play a role in carcinogenesis and cancer progression. The *p107* gene is located at the human chromosome region 20q11.2 and codes for a nuclear protein of 1068 amino acids, with a molecular weight of 120 kDa (Paggi *et al*., 1996). The gene *p107* includes a unique structural domain composed of subdomains A and B separated by a space region. Through the space region, p107 protein links to cyclin E and cyclin-dependent kinase 2 (Cdk2) in S phase, to regulate the progression of the cell cycle

(Grana *et al*., 1998). Levels of p107 protein are low in G0 and early G1, and rise rapidly from mid-G1 through the G1/S transition to mitosis (Paggi *et al*., 1996). In this chapter, we introduce the methodology (step-by-step) of p107 immunostaining and discuss the clinical significance of *p107* expression in colorectal carcinoma based on our results (Wu *et al*., 2002).

MATERIALS

Samples were resected endoscopically or surgically from the patients with colorectal tumors at the Kagawa Medical University. Samples obtained were formalin-fixed and paraffin-embedded to be immunostained for p107.

Paraffin Section

1. Fix the samples with 10% (v/v) formalin for 6 hr.
2. Immerse the samples in 80% ethanol for 1 hr each.
3. Immerse the samples in 95% ethanol 2× for 1 hr each.
4. Immerse the samples in 100% ethanol 2× for 1 hr each.
5. Immerse the samples in acetone for 2 hr.
6. Immerse the samples in 100% xylene 2× for 1 hr each.
7. Immerse the samples in xylene + paraffin (1:1) for 2 hr.

8. Infiltrate the samples with paraffin 3× for 2 hr each.

9. Embed the samples in paraffin, cut 2 μm thick sections, and mount them on glass slides.

METHODS

Deparaffin

1. Wash the sections in 100% xylene 3× for 15 min each.

2. Wash the sections in 100% ethanol 2× for 15 min each.

3. Wash the sections once in 95% ethanol for 10 min.

4. Wash the sections once in 90% ethanol for 10 min.

5. Wash the sections once in 80% ethanol for 10 min.

6. Wash the sections once in 70% ethanol for 10 min.

7. Wash the sections once in 50% ethanol for 10 min.

8. Rinse the sections once with distilled water for 15 min.

Immunostaining Procedure

1. Treat the sections with 0.1% Triton X-100 in phosphate buffer saline (PBS) for 1 hr.

2. Wash the sections with PBS 3× for 5 min each.

3. Treat the sections with 0.3% hydrogen peroxide in PBS for 30 min.

4. Wash the sections with PBS 3× for 5 min each.

5. Place the sections in a glass jar filled with 10 mM citrate buffer (10 mM citric acid monohydrate, pH 6.5 adjusted with 2N NaOH).

6. Heat the sections for 10 min at 120°C in the citrate buffer. Slides should not dry during the incubation in the microwave. If necessary, stop the incubation and add the citrate buffer to replace the evaporated volume.

Note: Antigen unmasking may be performed at this point. Certain antigenic determinants are masked by formalin fixation. In such cases the antigens may often be exposed by heat treatment. This step is very important for fixed-embedded tissues to allow the antigen to react with the p107 monoclonal antibody.

7. Let sections cool down in the tray at room temperature for 2 hr.

8. Wash the sections with PBS 3× for 5 min each.

9. Incubate the sections with a blocking reagent (3% normal goat/horse serum) at room temperature for 30 min.

10. Incubate the sections with the primary monoclonal antibody against p107 (sc-318; Santa Cruz Biotechnology, Santa Cruz, CA; 1:3000) at 4°C for 12 hr.

11. Wash the sections with PBS 3× for 5 min each.

12. The secondary antibody is the biotylated mouse immunoglobulin (IgG) from the Vectastain Elite ABC kit (Vector Laboratories, Burlingame, CA). Pour 1 drop of the biotylated mouse IgG with 10 ml PBS, and then add 3 drops of 1.5% horse normal serum. Incubate the sections with the secondary antibody at room temperature for 1 hr.

13. Wash the sections with PBS 5× for 5 min each.

14. The ABC reagent is prepared according to the protocol provided with the ABC kit (i.e., pour 2 drops of the reagent A and 2 drops of the reagent B in the bottle with 5 ml PBS). This mixed reagent must be prepared approximately 30 min before use. Incubate the sections with this solution at room temperature for 1 hr.

Color Development

▲ Prepare 0.1% DAB (3,3′-diaminobenzidine tetrahydrochloride) in 100 mM Tris HCl (pH 7.2) and 0.02% hydrogen peroxide in distilled water. Prepare these solutions separately and in equal volume. Then, just before use, mix them and immerse into it the sections until the desired stain intensity develops. Stop the reaction with tap water for at least 10 min.

Counterstain and Mount

1. Counterstain the sections for 1 min with Mayer's hematoxylin.

2. Wash the counterstained sections with tap water for 30 min.

3. Dehydrate through ethanol and xylene as follows: in 70%, 80%, 90%, and 95% ethanol for 2 min for each, in 100% ethanol 2× for 3 min, then in xylene 2× for 2 min. Let the sections dry. Mount a coverslip using a permanent mounting medium and observe under light microscopy.

Immunohistochemical Evaluation

One author, without knowledge of clinical and pathologic parameters of the cases, evaluated and scored all of the sections. Only the cells with nuclear staining were scored as positively stained ones. At least 1000 cells were randomly counted at 10 high-power fields for each section. Then, the ratio of the cells positive for p107 staining to the cells counted was calculated as a labeling index (LI). In addition, to study the relationship between p107 expression and prognosis, the patients were divided into two groups.

One is with high p107 expression and the other is with low p107 expression. The median of p107 LI of colorectal carcinoma was 13.5% in our previous report (Wu *et al.*, 2002). Therefore, cancerous p107 expression was regarded as low when the p107 LI was less than or equal to 13.5% and high when the p107 LI was greater than 13.5%.

RESULTS AND DISCUSSION

Cells positive for p107 staining were detected only in the lower part of the crypt of normal colonic epithelia and scattered heterogeneously in the whole area of early colorectal carcinoma. In the adenomas, cells with p107-positive were observed more frequently in the upper one-third of each crypt and had a moderate-staining intensity (Figure 27). In the process to the early carcinoma from normal epithelia, the staining intensity of p107 was enhanced, indicating that p107 levels were increased progressively during the carcinogenesis of the colon. However, such increase does not persist. The p107-positive cells were significantly decreased not only in primary carcinomas with a large size, poorly differentiated type or advanced stage, but also in those invading veins, lymphatic vessels, deep layers of the intestinal wall, lymph nodes, or liver. In addition, low p107 expression in colorectal carcinoma was associated with a shorter survival (Wu *et al.*, 2002). Based on these results, the role of p107 in colorectal carcinoma may be divided into two processes; one is the development of early colorectal carcinoma from normal epithelia, and the other is the progression of colorectal carcinoma from the early carcinoma.

Role of p107 in the Process of the Development of Early Colorectal Carcinoma from Normal Epithelia and Adenoma

What role does p107 play in the process of early colorectal carcinoma from normal epithelia? The answer is still far from clear, although pRb has widely been confirmed to inhibit cell-cycle progression (Grana *et al.*, 1998). In our study, we observed p107 expression in the process of early colorectal carcinoma from normal epithelia as follows: 1) p107 protein always appeared in the proliferative zones of normal epithelia; 2) it increased steadily in carcinogenesis; 3) its elevation was associated with high *Ki67* expression, a marker of rapid proliferation; and 4) its rise was concurrently associated with the increase of cyclin A, cyclin E, and Cdk2 expression (Wu *et al.*, 2002). These results are inconsistent with the hypothesis that
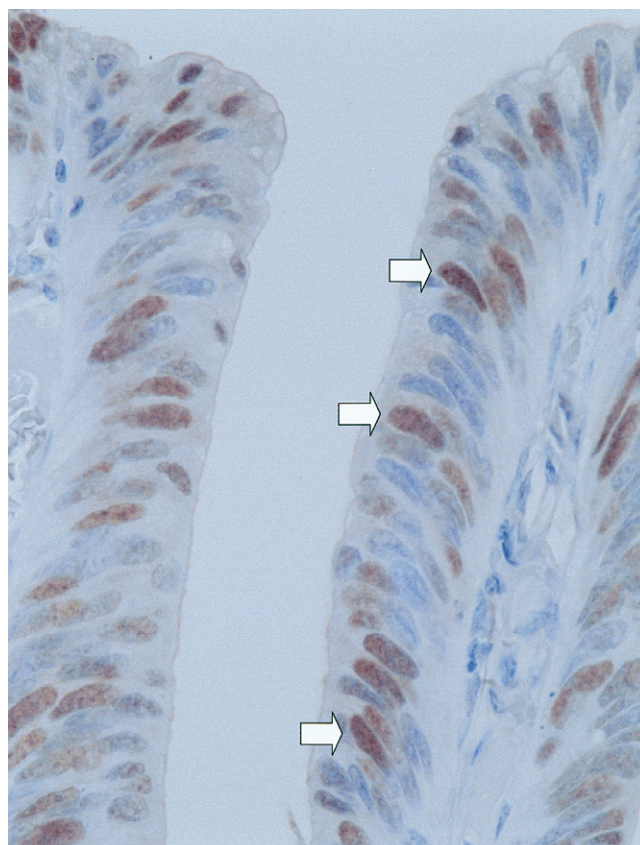
Figure 27 Immunohistochemical staining of p107 in colorectal adenoma. The staining of p107 is confined to nuclei (*arrows*). In colorectal adenoma, cells with p107-positive nuclei were observed frequently in the upper one-third of each crypt and had a moderate staining intensity.

elevated p107 inhibits cellular proliferation. As is true in the case of *p53*, an inhibitor of cell cycle, which becomes an oncogene after mutation in carcinoma (Baker *et al.*, 1990), unknown variations of p107 might also arise in tumors. Consequently, abnormally increased p107 may play a positive role in cellular proliferation, at least in the process of the development of early colorectal carcinoma from normal epithelia.

Role of p107 in the Process of the Progression of Early Colorectal Carcinoma

It is important to note that p107 expression was decreased not only in primary colorectal carcinomas with a large size, poorly differentiated type, or advanced stage, but also in those invading veins, lymphatic vessels, deep layers of the intestinal wall, lymph nodes, or liver. In terms of clinical involvement, low p107 expression was associated with a shorter survival (Wu *et al.*, 2002). These events demonstrated that p107

expression was progressively decreased as primary carcinomas invaded local tissues, indicating 1) primary colorectal carcinomas with low p107 expression had the strong invasive ability along with the high malignancy; 2) the decrease of p107 protein in cancer might enhance the invasive ability of cancer cells after carcinogenesis; and 3) patients with colorectal carcinoma with low p107 expression might need more aggressive treatment.

In summary, through the immunohistochemical staining of normal mucosae and primary colorectal carcinomas, we found that colorectal carcinomas abnormally expressed p107 protein and that such expression was increased gradually during carcinogenesis but apparently decreased during invasion associated with rapid cell proliferation. Clinically, we also demonstrated that patients with colorectal carcinoma with low p107 expression had a poor prognosis. Finally, the assessment of the p107 status in colorectal carcinoma may provide significant information for the treatment of patients with colorectal carcinoma.

References

Baker, S.J., Markowitz, S., Fearon, E.R., Willson, J.K., and Vogelstein, B. 1990. Suppression of human colorectal carcinoma cell growth by wild-type p53. *Science 249*:912–915.

Baldi, A., Esposito, V., De Luca, A., Fu, Y., Meoli, I., Giordano, G.G., Caputi, M., Baldi, F., and Giordano, A. 1997. Differential expression of Rb2/p130 and p107 in normal human tissues and in primary lung cancer. *Clin. Cancer Res. 3*:1691–1697.

Cinti, C., Leoncini, L., Nyongo, A., Ferrari, F., Lazzi, S., Bellan, C., Vatti, R., Zamparelli, A., Cevenini, G., Tosi, G.M., Claudio, P.P., Maraldi, N.M., Tosi, P., and Giordano, A. 2000. Genetic alterations of the retinoblastoma-related gene RB2/p130 iden-

tify different pathogenetic mechanisms in and among Burkitt's lymphoma subtypes. *Am. J. Pathol. 156*:751–760.

Claudio, P.P., Howard, C.M., Pacilio, C., Cinti, C., Romano, G., Minimo, C., Maraldi, N.M., Minna, J.D., Gelbert, L., Leoncini, L., Tosi, G.M., Hicheli, P., Caputi, M., Giordano, G.G., and Giordano, A. 2000. Mutations in the retinoblastoma-related gene RB2/p130 in lung tumors and suppression of tumor growth in vivo by retrovirus-mediated gene transfer. *Cancer. Res. 60*:372–382.

De Luca, A., Baldi, A., Esposito, V., Howard, C.M., Bagella, L., Rizzo, P., Caputi, M., Pass, H.I., Giordano, G.G., Baldi, F., Carbone, M., and Giordano, A. 1997. The retinoblastoma gene family pRb-p105, p107, pRb2-p130 and Simian virus-40 large T-antigen in human mesotheliomas. *Nat. Med. 3*:913–916.

Grana, X., Garriga, J., and Mayol, X. 1998. Role of the retinoblastoma protein family, pRB, p107 and p130 in the negative control of cell growth. *Oncogene 17*:3365–3383.

Massaro-Giordano, M., Baldi, G., De Luca, A., Baldi, A., and Giordano, A. 1999. Differential expression of the retinoblastoma gene family members in choroidal melanoma: Prognostic significance. *Clin. Cancer. Res. 5*:1455–1458.

Paggi, M.G., Baldi, A., Bonetto, F., and Giordano, A. 1996. Retinoblastoma protein family in cell cycle and cancer: A review. *J. Cell. Biochem. 62*:418–430.

Susini, T., Baldi, F., Howard, C.M., Baldi, A., Taddei, G., Massi, D., Rapi, S., Savino, L., Massi, G., and Giordano, A. 1998. Expression of the retinoblastoma-related gene Rb2/p130 correlates with clinical outcome in endometrial cancer. *J. Clin. Oncol. 16*:1085–1093.

Wu, F., Li, J.Q., Miki, H., Nishioka, M., Fujita, J., Ohmori, M., Imaida, K., and Kuriyama, S. 2002. p107 Expression in colorectal tumours rises during carcinogenesis and falls during invasion. *Eur. J. Cancer 38*:1838–1848.

Zamparelli, A., Masciullo, V., Bovicelli, A., Santini, D., Ferrandina, G., Minimo, C., Terzano, P., Costa, S., Cinti, C., Ceccarelli, C., Mancuso, S., Scambia, G., Bovicelli, L., and Giordano, A. 2001. Expression of cell-cycle-associated proteins pRB2/p130 and p27kip in vulvar squamous cell carcinomas. *Hum. Pathol. 32*:4–9.

6

Expression of Gastric MUC5AC Mucin During Colon Carcinogenesis

Jacques Bara, Marie-Elisabeth Forgue-Lafitte, and Marie-Pierre Buisine

Introduction

Mucins and Gastrointestinal Carcinogenesis

Secretory gel-forming mucins are high–molecular-weight glycoproteins secreted by specialized mucous cells throughout the gastrointestinal tract. These mucins are the main components of the mucous gel, which is a barrier against potential injurious luminal agents including acids, enzymes, toxins, and infectious organisms. Secretory mucins can be regarded also as specific differentiation markers for each of the mucous cells of the digestive epithelium (i.e., gastric surface and neck cells, gastric and Brünner's mucous gland cells, and intestinal goblet cells). This last characteristic is of importance to study the modifications of cell differentiation during the carcinogenesis processes. Thus, these mucins can also be of interest as potential tumor markers.

Mucin Gastric Antigens

More than 30 years ago, using polyclonal antibodies, a first immunohistochemical approach characterized gastric mucin antigenically different from intestinal mucin (Hakkinen *et al.*, 1968; Kawasaki *et al.*, 1974). The abnormal expression of mucins during gastrointestinal carcinogenesis has been described by several authors before the cloning of the mucin genes. In gastric carcinoma, intestinal sulphomucin antigen was expressed (Hakkinen *et al.*, 1968), and in the colonic adenocarcinomas the ectopic expression of gastric mucin was reported (Kawasaki *et al.*, 1974). Later, the expression of oncofetal mucins was detected during colonic carcinogenesis: the small intestine mucin antigen (Ma *et al.*, 1980) and the gastric M1 antigen (Bara *et al.*, 1980). In fact, the gastric M1 mucin was more strongly expressed in adenomas (Bara *et al.*, 1983) and in the mucosa adjacent to adenocarcinomas, rather than in colon adenocarcinomas themselves (Bara *et al.*, 1983, 1984a), and could be regarded as an early marker of colonic carcinogenesis. This observation was confirmed by the expression of gastric M1 mucin during carcinogenesis induced by dimethyl hydrazine (DMH) in the rat. Indeed, the expression of gastric M1 mucin in colon goblet cells occurs early, 2 weeks after the DMH treatment (Decaens *et al.*, 1983). For a better characterization of the M1 mucin, 11 monoclonal antibodies (MAbs) against gastric mucin were raised (Bara *et al.*, 1986; 1991a; Nollet *et al.*, 2002). The originality of these MAbs is the unusual method of the selection of hybridomas secreting anti-M1 antibodies. Using immunohistology, we selected the clones secreting antibodies, which showed on serial sections the same immunostaining pattern as the polyclonal anti-M1

Handbook of Immunohistochemistry and in situ Hybridization of Human Carcinomas,
Volume 2: Molecular Pathology, Colorectal Carcinoma, and Prostate Carcinoma

167

antibodies: strong staining of colonic adenomatous glands and normal surface gastric epithelium but negative on the normal colon (Bara *et al.*, 1986). When the complete sequence of the *MUC5AC* gene became available, it was possible to show that 8 of these 11 anti-gastric M1 MAbs immunoreacted with the product of this *MUC5AC* gene. The epitopes recognized by the three other MAbs were precipitated by each of eight anti-M1/MUC5AC MAbs, which immunoreacted with the product of *MUC5AC* gene. Consequently, the link between gastric M1 mucin and the *MUC5AC* gene was clearly established. The results obtained in the past by immunohistochemistry using the anti-M1 antibodies (polyclonal and monoclonal) can be now correctly interpreted with a *MUC5AC* gene reference. Consequently, these anti-M1 antibodies can be regarded as relevant tools to characterize the expression of gastric *MUC5AC* gene during colon carcinogenesis.

The *MUC5AC* Gene

The human *MUC5AC* was characterized 8 years ago. Initially, two complementary deoxyribonucleic acid (cDNA) fragments called *MUC5A* and *MUC5C* were cloned from a tracheobronchial cDNA library. Further investigations demonstrated that these two cDNA fragments were parts from the same gene called, for this reason, *MUC5AC* (Guyonnet Duperat *et al.*, 1995). The *MUC5AC* gene was mapped to 11p15.3–15.5, where a mucin gene cluster is localized near the gene encoding the v oncogene Ha-ras, extended by ~400 kb, and which contains also *MUC2*, *MUC5B,* and *MUC6*. The cDNA sequence of the *MUC5AC* gene has been elucidated showing a length of ~17.5 kb (Escande *et al.*, 2001). The N- and C-terminal regions of apomucin are large, cysteine-rich, globular domains that are poorly glycosylated. These domains share significant amino acid similarity with the pro-von Willebrand factor as well as with the N- and C-terminal domains of the MUC5B, MUC2, and MUC6 mucins. Moreover, these domains appear to be relatively well conserved in different animal species. The central

region, which is encoded by a single large exon of ~10.5 kb, shows nine cysteine-rich domains called Cys-domains 1 to 9, interspersed by highly glycosylated threonine/serine/proline domains (Figure 28). Each Cys domain has ~110 amino acid residues and contains 10 cysteine residues (Escande *et al.*, 2001). There is 98% sequence identity between the Cys2 and Cys4 domain and 95–99% identity between Cys3 and Cys5–Cys9. The Cys1–5 domains are separated by nonrepetitive sequences rich in threonine/serine/ proline residues (TSP1 to TSP4). The Cys 5–9 domains are separated by four domains (TR1–TR4) composed of various numbers of MUC5AC-specific tandem repeat domains of eight amino acids having a consensus sequence TTSTTSAP (GTTPSPVP is also frequently observed).

The Antibodies Against MUC5AC Apomucin

Polyclonal or monoclonal antibodies against anti-MUC5AC apomucin have been obtained using three main strategies of immunization: 1) with native gastric mucin, 2) with deglycosylated mucin, or 3) with a synthetic peptide deduced from the *MUC5AC* cDNA sequence. In this last case, a software predicting the immunogenic peptide sequence was used. Each strategy has its advantages and pitfalls. Concerning the antibodies against native gastric mucin, it is necessary to demonstrate that these antibodies recognize the product of the *MUC5AC* gene and that they do not react with products of other mucin genes. However, these MAbs have the advantages of high affinity and specificity and they recognize native mucin without the need for reduction or deglycosylation. These antibodies are therefore suitable for enzyme linked immunosorbent assay (ELISA) or immunoradiometric assay (IRMA) of MUC5AC mucin in biologic fluids. In contrast, some of these antibodies raised against the deglycosylated MUC5AC mucin do not recognize well the native mucin, and sometimes they immunoreact with native mucin only after deglycosylation. Moreover, it is necessary to demonstrate that these antibodies recognize
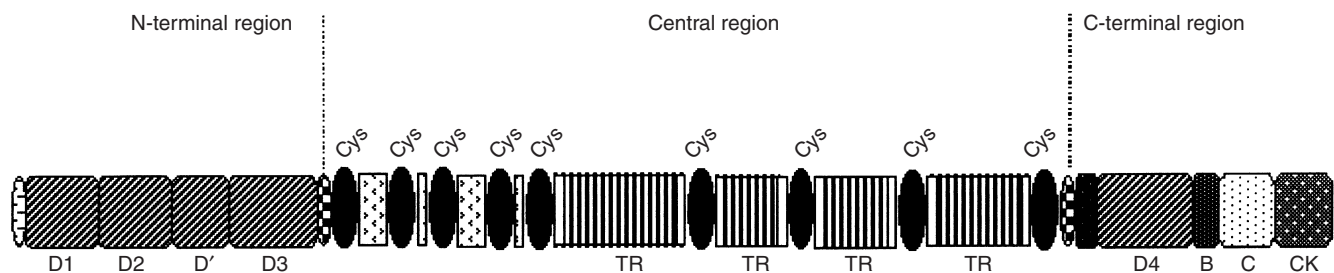
Figure 28 Schematic representation of MUC5AC apomucin.

the product of the *MUC5AC* gene. The advantage of antibodies against synthetic peptides is that the biochemical structure of the mucin epitope is known with great precision. Similar to antibodies raised against deglycosylated mucin, they may recognize the native mucin only after reduction or deglycosylation and are therefore unsuitable for assays in biologic fluids but useful for biochemical studies of mucins. Moreover, it is of crucial importance to check the accuracy of each MAb used in terms of specificity using the different methods available, such as ELISA, Western Blot, and immunohistology.

Polyclonal Antibodies

Antibodies Against Native Mucin

The anti-M1 antibodies have been obtained by immunization of rabbit with native mucin isolated from ovarian mucinous cyst fluids of pure endocervical type (Bara *et al.*, 1980) according to the Fenoglio's classification. They were absorbed by red blood cells to remove antibodies against blood group antigens and by human colon tissue extracts to obtain a gastric specificity. These antibodies showed a good cross-reactivity with rat gastric mucin (Bara *et al.*, 1983; Decaens *et al.*, 1983). Other anti-M1 polyclonal antibodies were raised in the chicken by immunization with a recombinant MUC5AC apomucin produced in the baculovirus/insect cell system (Bara *et al.*, 1998). When tested on serial sections of colon adenoma, these antibodies showed an identical immunoreactivity as the anti-M1 monoclonal or rabbit polyclonal antibodies (Bara *et al.*, 1998).

Antibodies Against Deglycosylated Mucin

The polyclonal antibodies F-HF were obtained by rabbit immunization against deglycosylated gastric mucin purified from normal human fundic mucosa. This mucin was deglycosylated by exposure to hydrogen fluoride, removing essentially all the oligosaccharide side chains (Toribara *et al.*, 1993). By immunohistology this antiserum showed a perinuclear staining pattern in the surface gastric epithelium. It was used for immunoscreening of a human gastric cDNA library to isolate a *MUC5AC* partial cDNA.

Antibodies Against Synthetic Peptide

The LUM5-1 rabbit polyclonal antibodies were obtained after rabbit immunization with a synthetic peptide coupled to a KLH (keyhole limpet hemacyanin) carrier (Nordman *et al.*, 2002). The peptide used was a 12-amino acid sequence (RNQDQQGPFKMC) that is repeated six times in Cys domains (Cys3 and Cys5–9). However, these antibodies slightly cross-reacted with pooled fractions of mucin MUC5B (either unreduced or reduced) and with MUC6 on ELISA plates (www.gene.ucl.ac.uk/mucin/ResMuc/lum51.html). No cross-reactivity was observed with blood group antigens (A, Le[a], Le[b], H) obtained from ovarian cyst fluid (see Web site). Using immunohistology, these antibodies displayed the same immunoreactivities as the anti-M1 monoclonal and polyclonal antibodies when tested in normal gastrointestinal tract and colon tumors (Nordman *et al.*, 2002).

Antibodies PH1426 were obtained by immunization of mice with a KLH-coupled synthetic peptide (Asker *et al.*, 1998). The peptide of 18 amino acids (CHRPHPTPTTVGPTTVGS) is located at the end of the D4 domain of the C-terminal region of the MUC5AC apomucin. To our knowledge, the histologic immunoreactivity of these antibodies has not been tested.

Antibodies M5P-c1 and M5P-b1 were obtained in the chicken and rabbit, respectively, after immunization with a 17-amino acids synthetic peptide containing the consensus sequence units of the MUC5AC-specific tandem repeat region with a terminal lysine (KTTSAPTTSTTTSAPTTS) (Ho *et al.*, 1995). These antibodies were made to screen a human gastric cDNA expression library. However, they immunoreacted against deglycosylated mucin showing an immunoreactivity in the supranuclear area of the mucous cells. Apical mucus droplets were only slightly positive, probably because of the more extensive glycosylation of the mature MUC5AC mucin.

A murine antiserum (antibodies PDM5) was raised against a synthetic peptide corresponding to the consensus motif TTSTTSAP of the MUC5AC tandem repeat region (Thornton *et al.*, 1996).

A goat antiserum produced by QCB (Hopkinton, MA) was raised against a mixture of two peptide sequences (KTTHSQPVTRD and PSPGPHGGKETYNN) corresponding to the Cys3/Cys5–9 domains (Jumblatt *et al.*, 1999).

Antibody 791 was raised in chickens against a synthetic peptide mimicking the deduced amino acid sequence from the D3 region of the MUC5AC mucin (CDFATRSRSVVGDVLEFGNS) (Argueso *et al.*, 2002). This antiserum recognized native MUC5AC mucin. Using immunohistology, this antiserum stained specifically conjunctival goblet cells and was used in ELISA with MUC5AC native mucin.

Monoclonal Antibodies

Antibodies Against Native Mucin

Eleven anti-M1 MAbs have been obtained after mouse immunization with native mucin isolated from ovarian mucinous cyst fluids of pure endocervical type (MAb 1-13M1, 2-11M1, 2-12M1, 9-13M1,

58M1, 19M1, 21M1, 45M1) or from human (62M1) or rat (463M and 589M) gastric mucosa. After cell fusion of Sp₂O myeloma cells with spleen cells of an immunized mouse, the antibodies present in the supernatant of hybridomas were selected by immunohistology screening on serial sections of colon adenomas, one of them being stained by the anti-M1 serum. Antibodies secreted by hybridomas were selected by their ability to stain the same adenomatous glands as the anti-M1 antiserum. Their positive immunoreactivity on normal gastric surface epithelium and the lack of immunoreactivity on normal colon were controlled. All these MAbs belong to the immunoglobulin G_1 (IgG$_1$) isotype, and all of them immunoreacted with the same gastric MUC5AC mucin, as demonstrated by immunoprecipitation experiments. Six different fragments of *MUC5AC* cDNA have been shown to encode the epitopes characterized by 8 of the 11 anti-M1 MAbs. The 19M1/21M1 and 463/589M immunoreacted with the same (or neighboring) epitope, as demonstrated by competition experiments. In the N-terminal region of the MUC5AC apomucin, the 2-11M1 MAb immunoreacted with the product of *MUC5AC* cDNA fragment encoding the D1/D2 domain (AJ298318, nt 275 to nt 2232 and nt 3312 to nt 3692) (Escande *et al.*, 2001) (see Figure 28), and the 9-13M1 immunoreacted with the fragment encoding the D3 domain (nt 2232 to nt 3312). The 1-13M1 MAb immunoreacted with the product of the *MUC5AC* cDNA fragment encoding the Cys2 and Cys4 domains (Nollet *et al.*, 2004).

In the C-terminal region of MUC5AC, the 19M1 and 21M1 MAbs reacted with the fragment encoding a region of the MUC11p15-type domain (Z48314, nt 216 to nt 495) (Lesuffleur *et al.*, 1995), the 453M and 589M MAbs with a part of the fragment encoding the D4-like domain (nt 705 to nt 1320), and the 62M1 with a part of the fragments C- and CK-like domain (nt 2061 to nt 2899) (Nollet *et al.*, 2002). The 2-12M1, 45M1, and 58M1 epitopes have not yet been mapped on the MUC5AC apomucin. Nevertheless, the antibodies against the M1/MUC5AC mapped epitopes immunoprecipitated by these three unmapped M1 epitopes. It has been clearly demonstrated that cells producing several MUC apomucins formed single species of disulfide-linked homooligomers (Asker *et al.*, 1998) and not heterodimers (Lidell *et al.*, 2003). Consequently, it is most likely that the 2-12M1, 45M1, and 58M1 epitopes are actually encoded by the *MUC5AC* gene. These anti-M1 MAbs cross-reacted with the gastric mucin from different animal species, showing that these Cys domains are well conserved during evolution (Bara *et al.*, 1992). In contrast, the tandem repeat regions are specific for a given animal species. For instance, the 45M1 epitope is conserved in the monkey, cat, mouse, rat, rabbit, pig, hedgehog, and bird. Sometimes, a partial

deglycosylation is necessary to allow the antibodies to recognize an epitope (Bara *et al.*, 1992). Reduction using β-mercaptoethanol destroyed the M1 immunoreactivities (except for the 19/21M1 epitope).

The MAb 96-RA has been obtained after immunization of a mouse with mucin isolated from pancreatic adenocarcinomas. The corresponding epitope is immunoprecipitated with the 1-13M1 MAb, an anti-MUC5AC MAb (Bara *et al.*, 1991a). Consequently, the 96-RA is probably associated with the MUC5AC apomucin. This MAb is specific for human gastric mucin and does not cross-react with monkey gastric mucin or with mucins of other animal species (Bara *et al.*, 1992).

The MAb Nd2 was obtained after immunization with mucins isolated from xenografts of the human pancreatic SW 1990 cell line (Ho *et al.*, 1995). Its immunoreactivity is inhibited by the 45M1 MAb and, consequently, this MAb can be regarded as an anti-MUC5AC apomucin. The Nd2 immunoreactivity with native and partially deglycosylated mucin is lost after pretreatment with protease and β-mercaptoethanol. The immunostaining pattern on normal and neoplastic gastrointestinal epithelium is similar to the anti-M1/MUC5AC staining.

Antibodies Raised Against Deglycosylated Mucin

SOMU1 MAb was obtained after immunization with human gastric mucin deglycosylated with trifluoromethanesulfonic acid (Sotozono *et al.*, 1996). SOMU1 MAb recognized both deglycosylated and native mucin. By screening a human stomach cDNA library with SOMU1 MAb, a cDNA clone containing the MUC5AC tandem repeat domain has been isolated. Furthermore, this antibody immunoreacted with the product of a short cDNA fragment encoding the Cys5 domain (Nollet *et al.*, 2004). Because the five other Cys domains (Cys3 and Cys6–9) show 95–99% of homology with the Cys5 domain, the SOMU1 epitope is likely to be repeated six times in the Cys domains of the large tandem repeat domain, as is the RNQDQQGPFKMC peptide immunoreacting with the LUM5-1 polyclonal antibodies. Using serial sections, we demonstrated that the SOMU1 MAbs immunoreacted with normal and cancerous gastrointestinal mucosae similar to the anti-M1 MAbs (Nollet *et al.*, 2004).

Antibodies Raised Against Synthetic Peptide

The CLH2 MAb was obtained after mouse immunization with synthetic peptide containing the tandem repeat sequence PTTPTTAP specific for the MUC5AC apomucin (Reis *et al.*, 1997). This antibody strongly immunoreacted in ELISA with the PTTPTTAP peptide. However, using immunohistology this antibody did not recognize the native mucin but only the deglycosylated mucin, staining specifically the Golgi apparatus area

where the mucins are poorly glycosylated (Nordman *et al.*, 2002). It reacted strongly after deglycosylation of the native mucin. Visit http://ifr31w3.toulouse.inserm.fr.mucines/ for more information.

MUC5AC cDNA Probes

Until 1994, only cDNA fragments corresponding to the central repetitive region of *MUC5AC* were isolated (Guyonnet Duperat *et al.*, 1995). It is the principal reason why a majority of the *MUC5AC* probes used still correspond to this region. As other cDNA fragments of *MUC5AC* were cloned, additional probes corresponding to parts of the 3′ region and then to the 5′ region of *MUC5AC* became available to analyze *MUC5AC* expression at the messenger ribonucleic acid (mRNA) level (Escande *et al.*, 2001; Lesuffleur *et al.*, 1995; Li *et al.*, 1998). However, as mentioned earlier, *MUC5AC* shows extensive sequence similarity to other chromosome 11p15 MUC genes and especially to *MUC5B*, in its nonrepetitive regions (5′ and 3′ regions and sequences corresponding to the Cys-domains within the central region). Also, a high sequence similarity exists with its animal homologues in these regions. In contrast, tandem repeats are specific for a given mucin gene and animal species, differing significantly in sequence and size. Consequently, probes corresponding to the tandem repeat domains of *MUC5AC* present the advantage of the greatest specificity, whereas probes corresponding to nonrepetitive regions of *MUC5AC* may cross-hybridize with *MUC5B, MUC2*, and/or *MUC6* and their animal homologues. Moreover, probes corresponding to the tandem repeats are able to hybridize several times with the repetitive domains, enhancing the sensitivity of the method. Some variations in the signal intensity can be observed between individuals using such repetitive probes as a result of genetically determined variations in the number of copies of the tandem repeat motif (VNTR, variable number of tandem repeats). However, such variations are minor in *MUC5AC* compared with most of other mucin genes (Escande *et al.*, 2001), and the impact on the signal intensity thus remains very low. Probes corresponding to nonrepetitive regions of *MUC5AC* that are composed of unique sequences are, nevertheless, more suitable for strict quantitative studies of *MUC5AC* mRNA expression than probes corresponding to tandem repeat regions.

Studies of MUC5AC Expression

MUC5AC expression was largely studied by Northern blot, dot or slot blot, RNAse protection assay, and/or *in situ* hybridization. cDNA fragments corresponding either to the tandem repeat region or to nonrepetitive regions of *MUC5AC* are used in Northern Blot and slot or dot blot experiments. cDNA fragments are also commonly used to generate RNA probes for RNase protection assay and *in situ* hybridization studies. Antisense oligonucleotide probes chosen in the tandem repeat region of *MUC5AC* are excellent tools for *in situ* hybridization and are very easy to use compared to RNA probes. One of the *MUC5AC* oligonucleotide probes often used is as follows: 5′ AGGGGCA-GAAGTTGTGCTCGTTGTGGGAGCAGAG-GTTGTGCTGGTTGT 3′ (Audie *et al.*, 1993).

The anti-M1/*MUC5AC* antibodies are useful tools to investigate the final product of the *MUC5AC* gene by immunohistology. In this paper we discuss data obtained by immunohistology and *in situ* hybridization techniques, focusing at the expression of *MUC5AC* gene as an early event occurring during colon carcinogenesis, including the relevance and the differences in the results obtained by these two methodologies.

Immunohistochemistry

MATERIALS

1. Phosphate buffer saline (PBS): 0.15 M phosphate buffer with 0.9% NaCl (pH 7.2–7.4).

2. Fixative: 95% ethanol: add 5 ml of distilled water to 95 ml pure ethanol, kept at room temperature.

3. Primary antibody diluted in PBS containing 0.1% Tween-20.

4. Horse peroxidase secondary antibody (goat anti-IgG mouse antibody) (Santa Cruz, CA), diluted in PBS-Tween-20 (1/1000).

5. Hydrogen peroxide (H_2O_2) 30%.

6. Amino-ethyl carbazol (AEC)—toxic—possible carcinogen (Sigma, St. Louis, MO).

7. N, N-dimethylformamide (Carlo Erba, Milano, Italia).

8. Mayer's hematoxylin (light-sensitive).

9. 2M Acetate buffer (pH 5.6) (this buffer is diluted 20 times in injectable H_2O, just before use).

10. Sterile distilled H_2O.

11. Kaiser's glycerol gelatin (Merck, Darmstadt, Germany).

METHODS

Immunoperoxidase Labeling of Gastrointestinal Mucosae

1. Rinse the colon tissues with PBS and cut with a scalpel longitudinal strips of 1×20 cm of mucosae containing a bulk of tumor.

2. Separate the mucosa with a scalpel to remove the muscularis mucosae layer from the macroscopically normal tissue adjacent to the tumor.

3. Pin the mucosa on a cork plate placed in the bottom of a glass box (20 cm × 45 cm × 6 cm).

4. Immerse the mucosae in 95% ethanol for 24 hr. Cut 1 × 20 cm longitudinal strips of mucosae with a scalpel.

5. Coil the mucosae into "Swiss rolls" around the tumor (when present) and bind with cotton yarn.

6. Embed the samples in paraffin, and cut 3-μm thick sections.

7. Deparaffinize the sections in three successive baths of xylene and ethanol incubating for 10 min in each bath.

8. Rinse with PBS-Tween-20 for 3 min and then incubate the sections for 30 min with anti-MUC5AC MAbs.

9. Wash the sections with PBS-Tween-20 three times for 3 min each, add peroxidase-labeled anti-IgG antibodies (diluted 1/200), and incubate for 30 min.

10. Wash the sections with PBS-Tween-20 three times for 3 min each.

11. Dilute 60 mg of AEC in 5 ml of N,N-dimethylformamide and then diluted with 95 ml acetate buffer (50 mM, pH 5.0) (from a solution of acetate buffer 2 M, pH 5.0). Then, add then 100 μl of H_2O_2.

12. Incubate the sections for 4 min with the AEC reagent.

13. Rinse the sections with water, incubate 2 min in hematein solution, and mount using Kaiser's glycerol gelatine.

Note: If you use paraformaldehyde fixative, it may be difficult to coil the mucosae into "Swiss rolls" and the immunoreactivity of anti-MUC5AC MAbs is weaker than that with ethanol fixative. To obtain better results, a microwave or protease treatment may be necessary.

in situ Hybridization

MATERIALS

1. Antisense 48-mer-oligonucleotide corresponding to the tandem repeat of *MUC5AC*: 5′ AGGGGCA-GAAGTTGTGCTCGTTGTGGGAGCAGAG-GTTGTGCTGGTTGT 3′.

2. Sterile deionized glass-distilled water.

3. 10X Terminal desoxynucleotidyl transferase (TdT) buffer: 1.54 mg dithiothreitol, 1.97 mg $MnCl_2$, 0.95 mg $MgCl_2$, and 2.14 g sodium cacodylate in 10 ml sterile water.

4. DEPC water: 100 μl diethylpyrocarbonate in 100 ml sterile water; agitate vigorously and let repose for 24 hr before autoclaving.

5. Gelatin covered slides: 5 g gelatin in 1 L sterile water; incubate in a waterbath at 55ºC until complete dissolution; equilibrate the temperature at 43ºC, add 4 g chromium (III) potassium sulfate duodecahydrate, and incubate at 40ºC until complete dissolution; immerse slides in the preparation and let them dry in a ventilated incubator at 37ºC.

6. 30%, 70%, and 100% ethanol.

7. Glycin buffer: 24 g Tris-HCl, 7.5 g glycin; bring volume to 1 L with sterile water; adjust pH to 7.4 with HCl; autoclave.

8. 10X proteinase K buffer: 12.1 g Tris-HCl, 18.6 g ethylenediamine tetra-acetic acid (EDTA); bring volume to 100 ml with sterile water (pH 8.0).

9. PBS: 8 g NaCl, 200 mg KCl, 1.78 g Na_2HPO_4. $2H_2O$, 240 mg KH_2PO_4; bring volume to 1 L with sterile water; adjust pH to 7.4 with HCl; autoclave.

10. 4% paraformaldehyde: 4 g paraformaldehyde in 100 ml PBS; incubate in a waterbath at 55ºC until complete dissolution; filtrate on 0.45 μm filter units; add 0.5 ml $MgCl_2$.

11. 20X SSPE (sodium chloride sodium phosphate + EDTA): 174 g NaCl, 27.6 g Na_2HPO_4. $2H_2O$, 7.4 g EDTA; bring volume to 1 L with sterile water; adjust pH to 7.4 with NaOH; autoclave.

12. Acetylation buffer: 20 ml 20X SSPE in 100 ml sterile water, 1.3 ml triethanolamin; adjust pH to 8.0 with HCl; add 250 μl acetic anhydride.

13. 50X Denhardt's: 1 g Ficoll 400, 1 g polyvinyl-pyrrolidone, 1 g bovine serum albumin; bring volume to 100 ml with sterile water; filtrate on 0.22 μm filter units.

14. 1.2 *M* phosphate buffer: solution A: 5.34 g Na_2HPO_4. $2H_2O$ in 25 ml sterile water; solution B: 1.87 g Na_2HPO_4. $2H_2O$ in 10 ml sterile water; Mix solutions A and B and adjust pH to 7.2.

15. 20X Sarcosyl: 2 g *N*-lauroylsarcosine sodium salt in 100 ml sterile water; filtrate on 0.22 μm filter units.

16. Prehybridization mixture: 15 mg dithiothreitol, 300 μl DEPC water, 200 μl 20X SSPE, 500 μl deionized formamide, 100 μl 1.2 *M* phosphate buffer, 50 μl 20 X sarcosyl, 20 μl 50X Denhardt's buffer, 30 μg calf thymus DNA, 30 μg yeast transfer RNA (tRNA).

17. Hybridization mixture: 15 mg dithiothreitol, 300 μl DEPC water, 200 μl 20X SSPE, 500 μl deionized formamide, 100 μl 1.2 *M* phosphate buffer, 50 μl 20X sarcosyl, 20 μl 50X Denardt's buffer, 3 μg yeast tRNA.

18. Developer: 500 mg *p*-methylaminophenol hemisulfite salt, 2.25 g hydroquinone, 18 g sodium sulfite, 12 g sodium carbonate, 1 g potassium bromide in 250 ml water.

19. Fixative: 80 g sodium thiosulfate in 250 ml water.

METHODS

Tissue

1. Immerse the tissue samples immediately after removal either in fresh 4% paraformaldehyde or 10% phosphate buffered formalin for 3–24 hr depending on specimen size.

Note: Tissues must be fixed for 30 min after removal to avoid mRNA degradation and tissue lysis.

2. Embed the samples in paraffin.

3. Cut 3-μm thick sections and mount onto gelatin-covered slides; store at 4ºC until use.

Labeling of the Probe

1. Heat denatured 60 ng oligonucleotide in DEPC water (to final volume 15 μl) for 5 min in boiling water; rapidly cool on ice.

2. On ice, add 1.5 μl 10X TdT buffer, 35 μCi α-(^{35}S-dATP), 20 U terminaldeoxynucleotidyl-transferase.

3. Incubate at 37ºC for 1.5–2 hr.

4. Stop the reaction by adding 1 μl 0.5 M EDTA.

5. Purify the probe by gel permeation chromatography using a Sephadex G-25 type spin column according to the manufacturer's instructions.

6. Determine the labeling efficiency of the probe and store at –80ºC until use.

In situ Hybridization Procedure

1. Immerse the slides in xylene at room temperature for 10 min; repeat using fresh xylene.

2. Rinse the slides in 100% ethanol for 5 min and rehydrate in an ethanol series (100%, 70%, 30%) and sterile water at room temperature for 3 min each.

3. Immerse the slides in glycine buffer at room temperature for 10 min.

4. Incubate the slides with 2 μg/ml proteinase K in X proteinase K buffer at 37ºC for 20 min. Rinse in water.

5. Immerse the slides in fresh 4% paraformaldehyde at room temperature for 15 min. Rinse in PBS.

6. Immerse the slides in fresh acetylation buffer at room temperature for exactly 10 min. Rinse in water.

7. Dehydrate the slides in an ethanol series (30%, 70%, 100%) and air dry at 37ºC.

8. Place the slides horizontally in a humidified chamber prewarmed to 42ºC and apply prehybridization mixture on specimen area.

9. Cover and incubate the slides at 42ºC for at least 45 min.

10. Dehydrate the slides in an ethanol series (30%, 70%, 100%) and air-dry at 37ºC.

11. Replace the slides in the humidified chamber and apply between 20 and 120 μl (depending on specimen size) hybridization mixture containing 7.5×10^3 dpm/ml of ^{35}S-labeled probe previously denatured on specimen area.

12. Cover and incubate the slides overnight at 42°C.

13. Rinse the slides gently with 4X SSPE containing 2.5 mg/ml dithiothreitol.

14. Wash the slides in 4X SSPE containing 2.5 mg/ml dithiothreitol and in 4X SSPE at room temperature for 30 min each.

15. Wash the slides in X SSPE at room temperature and at 42ºC for 30 min each.

16. Wash the slides in 0.1X SSPE at 42ºC for 2 × 30 min.

17. Dehydrate the slides in an ethanol series (30%, 70%, 100%) and air-dry at 37°C.

18. Dip the slides in the dark in photographic emulsion prewarmed to 43°C and air-dry in a vertical position in a dark chamber for at least 2 hr.

19. Transfer the slides into a dark box and store at 4°C.

20. Develop the slides for 1–3 weeks after exposure by immersion in developer and in fixative 5 min each.

21. Rinse the slides in water and counterstain with methyl green pyronin.

22. Controls consist of the following: 1) competition studies by treatment of specimen with a large excess (50X) of unlabeled oligonucleotide identical to or distinct from the ^{35}S-labeled-probe; 2) verification of the absence of background by careful examination of nonepithelial structures (vessels, muscle, and connective tissue); and 3) analysis of specimen tested and a specimen positive for *MUC5AC* expression (stomach) in parallel, under the same conditions.

RESULTS

Normal Adult Gastrointestinal Tract

For a better characterization of the abnormal expression of MUC5AC mucin during colon carcinogenesis, it is important to analyze its expression in the normal colon. An extensive study has been performed using normal tissues removed from 40 organ donors (age range: 15–48 years) just after the kidneys were removed for transplantation, using anti-M1 MAbs (polyclonal and monoclonal antibodies giving identical results) (Bara *et al.*, 1986). The M1/MUC5AC apomucin is expressed in the gastric surface epithelium but not in the mucous cells of the deep glands. In the duodenum, this mucin is faintly expressed in some goblet cells near the pylorus/duodenum junction.

The remaining gastrointestinal tract epithelium did not react with anti-M1 antibodies (jejunum: 0/17; ileum: 0/24). However, mucous cells of Wirsung's duct near the duodenal mucosa (seven of seven cases) were positive. Extensive studies were performed on 40 normal colon mucosae. Four mucosal samples of 1×10 cm were studied for each individual, in the right, transversal, sigmoidal, and rectal region. Then, approximately 16 meters of colon coiled into "Swiss rolls" were studied. Of individuals, 70% showed less than 0.01% M1 positive goblet cells, 19% contained between 0.01% and 0.1% M1-positive cells, and 11% contained between 0.1% and 0.3%. The M1-positive cells were mainly located in the upper part of colon crypts. Small mucinous hyperplasia (corresponding probably to aberrant crypt foci, or ACF) containing M1-positive goblet cells also located in the upper part of the colon glands was observed in three individuals and in three small tubular M1+ adenomas in one individual. Such alterations were not included in these estimations. Recently, using 45M1 MAb, M1/MUC5AC apomucin was found in three of 10 normal rectal mucosae of the anus and six of six anal glands obtained after hemorrhoidectomy. Anal glands are special glands present in variable number and extend to the transitional zone. They are characterized by basal squamoid epithelium overlined by columnar mucus cells. The surface mucus cells were positive for M1/MUC5AC (Kuan *et al.*, 2001).

MUC5AC expression was also studied at the RNA level by *in situ* hybridization using the 48-mer tandem repeat-oligonucleotide probe in various specimens of normal gastrointestinal tissues obtained from patients without evidence of neoplastic or inflammatory bowel disease (Buisine *et al.*, 1998, 2000a,b). (See Table 3.) High mRNA expression of *MUC5AC* was detected in gastric specimens, in the cardia (1/1), fundus (5/5), and antrum (5/5). *MUC5AC* mRNA were observed in epithelial cells of the surface and pits and in mucous neck cells but not in glands, irrespective of the region examined. In contrast, no *MUC5AC* mRNA expression was detected in any region of the intestine (duodenum [0/3], jejunum [0/3], ileum [0/6], colon [0/10]). This result was confirmed by others using the same technique (Sylvester *et al.*, 2002). Only minimal amounts of *MUC5AC* mRNA were detected by dot blot, slot blot, and RNase protection assay (Bartman *et al.*, 1999; Buisine *et al.*, 1996).

Fetal Gastrointestinal Tract

Using immunohistologic methods, in a study including 65 fetuses between 2 and 7.5 months of gestation, 4 stillborn infants, and 8 newborn (premature or term) (Bara *et al.*, 1986), M1/MUC5AC positive goblet cells were observed from the fourth months of gestation. The gastric mucin expression was maximal during the sixth month of gestation showing Lieberkühn glands containing nearly 95% M1-positive cells. Goblet cells located near the surface epithelium were most strongly stained. After the sixth month, few mucosae were positive; however, some rare M1-positive goblet cells, located in the upper part of the glands, were strongly stained.

MUC5AC gene expression was also analyzed by *in situ* hybridization in intestinal tissues (duodenum, jejunum, ileum, and colon) obtained from 5 human embryos and 27 human fetuses ranging in age from 6.5 to 27 weeks of gestation (Buisine *et al.*, 1998, 2000a,b). The mRNA expression of *MUC5AC* was detected as early as 8 weeks of gestation in the primitive intestine. At 12 weeks, *MUC5AC* mRNA was detected in the ileum but not in the colon. After 12 weeks, *MUC5AC* was not detected again in any region of the intestine, except in the duodenum at 23 weeks (one case), where it was focally expressed (Buisine *et al.*, 1998, 2000b). Expression of *MUC5AC* was nevertheless reported in the colon at 17 weeks (one case) by other authors (Reid *et al.*, 1998).

Macroscopically Normal Colon Mucosa Adjacent to Colon Tumors

In the area adjacent to colonic adenocarcinomas (called transitional mucosa), the mucosa is thicker owing to the elongation of crypts that are often branched. In more than 90% of patients operated on for colon cancer, a great number of goblet cells present at this area are strongly stained with the anti-M1/MUC5AC (Bara *et al.*, 1984a). In the macroscopically normal mucosa, dispersed histologically normal glands displaying some strongly positive M1 goblet cells were observed at distance from the adenocarcinoma. These glands are common in patients with a synchronous or metachronous adenocarcinoma (Bara *et al.*, 1984a). Moreover, by *in situ* hybridization using a tandem repeat-oligonucleotide probe, *MUC5AC* was detected in some cases (4/22, or 14%) on biopsies taken at a distance (about 5 cm) from the villous adenomas, in areas previously considered as normal by endoscopic and histologic examination (Buisine *et al.*, 1996). This finding was not confirmed by other authors who analyzed the expression of *MUC5AC* on biopsies of macroscopically normal rectal mucosae obtained 5 cm proximal to villous or tubulovillous by immunohistology, using anti-M1/MUC5AC MAbs (21M1) (Longman *et al.*, 2000). "De novo" expression of MUC5AC was not detected in any of the mucosal biopsies adjacent to either villous (11 cases) or

Table 3 *MUC5AC* **Expression in Normal and Pathologic Gastrointestinal Tract**

Tissues	IP	References	ISH	References
Normal Adult				
Stomach	+++	(1)	+++	(10)
Duodenum	+/−	(1) (2)	−	(11)
Jejunum	−	(2)	−	(10) (12)
Ileum	−	(2)	−	(10) (12)
Colon	−	(1) (2)	−	(10) (12)
Rectum	−	(1) (2)	nd	
Distal region	+	(3)	nd	
Anal glands	+++	(3)	nd	
Fetal				
Stomach	+++	(2)	+++	(13)
Colon	+	(2)	+	(12) (14)
Inflammatory Diseases	+/−	(4)	+	(15) (16)
Colon Carcinogenesis				
Transitional mucosa	+++	(5) (6)	nd	
Histologic normal mucosa				
Adjacent to adenomas	nd		+/−	(17) (18)
Adjacent to adenocarcinomas	+++	(6)	nd	
ACF	+++	(7)	nd	
Hyperplastic polyps	++++	(8)	nd	
Adenomas tubular	+	(8)	+	(19)
Tubulovillous	++	(8)	++	(19)
Villous	+++	(8)	+++	(18) (19)
Adenocarcinomas				
Right colon	+++	(9)	nd	
Left colon	+	(9)	+/−	(17) (18)

IP, immunoperoxidase method; ISH, *in situ* hybridization; ACF, abberant crypt foci.

References: (1) Bara *et al.*, 1980a; (2) Bara *et al.*, 1986; (3) Kuan *et al.*, 2001; (4) Nap *et al.*, 1985; (5) Bara *et al.*, 1980b; (6) Bara *et al.*, 1984a; (7) Bara *et al.*, 2003; (8) Bara *et al.*, 1983b; (9) Bara *et al.*, 1984b; (10) Audié *et al.*, 1993; (11) Buisine *et al.*, 2000a; (12) Buisine *et al.*, 1998; (13) Buisine *et al.*, 2000b; (14) Reid *et al.*, 1998; (15) Longman *et al.*, 2000; (16) Buisine *et al.*, 2001; (17) Sylvester *et al.*, 2001; (18) Buisine *et al.*, 1996; (19) Bartman *et al.*, 1999.

tubulovillous adenomas (11 cases). Another study on 25 cases of "normal" tissue adjacent to colorectal cancer did not show *MUC5AC* transcripts (Sylvester *et al.*, 2001).

More recently, we observed that the aberrant crypt foci (ACF), which are considered to be precursors of the precancerous lesions such as adenomas, produced a large quantity of M1/MUC5AC in goblet cells located in the upper part of the crypts, as ascertained by immunohistochemistry using anti-M1 MAbs (Bara *et al.*, 2003).

Hyperplastic Polyps

Using anti-M1 MAbs, we demonstrated the expression of M1/MUC5AC mucin in hyperplastic polyps (30/30) (Bara *et al.*, 1983, 1986). Generally 80–95% of goblet cells were strongly stained. Another recent study using anti-M1 MAb (45M1) showed that 12 of 12 hyperplastic polyps studied

presented a staining of the goblet cells but also a staining of the cytoplasm of columnar cells (Biemer-Huttmann *et al.*, 1999). However, using an anti-MUC5AC raised against tandem repeat *MUC5AC* sequence, only one of nine hyperplastic polyps showed *MUC5AC*-producing cells (Bartman *et al.*, 1999). An interesting observation in a patient with six M1/MUC5AC-positive "serrated adenocarcinomas" (using 45M1 MAb) showed four hyperplastic polyps and six serrated adenomas producing M1/MUC5AC mucin (Yao *et al.*, 2000). To our knowledge, no study has been yet undertaken by *in situ* hybridization in hyperplastic polyps.

Adenomas

The highest level of expression of M1/MUC5AC mucin in the colon is found in adenomas (92 of 139, or 66%) and is more closely associated with those

showing a villous differentiation (41 of 47, or 87%) (Figure 29A) than with those having a tubular pattern (51 of 92, or 55%) (Bara *et al.*, 1983). The M1/*MUC5AC* expression depended neither on the size nor on the degree of cytologic atypia of the adenomas (Bara *et al.*, 1983; Myerscough *et al.*, 2003). However, M1/MUC5AC mucin is found in 94% (35/37) of adenomas concomitant with adenocarcinoma, versus 56% (55/102) of adenomas observed on the noncancerous mucosa. The expression of this MUC5AC mucin in adenomas and especially those showing a villous differentiation has been reported by other authors (Bartman *et al.*, 1999; Longman *et al.*, 2000). However, the percentage of adenomas expressing this gastric mucin depends on the antibodies and the tissue fixation procedure used.

    MUC5AC gene expression was also analyzed at the RNA level by dot blot with a cDNA probe corresponding to the tandem repeat region and by *in situ* hybridization with a tandem repeat-oligonucleotide probe in rectosigmoid villous adenomas (Figure 29B) obtained from 22 patients (Buisine *et al.*, 1996).
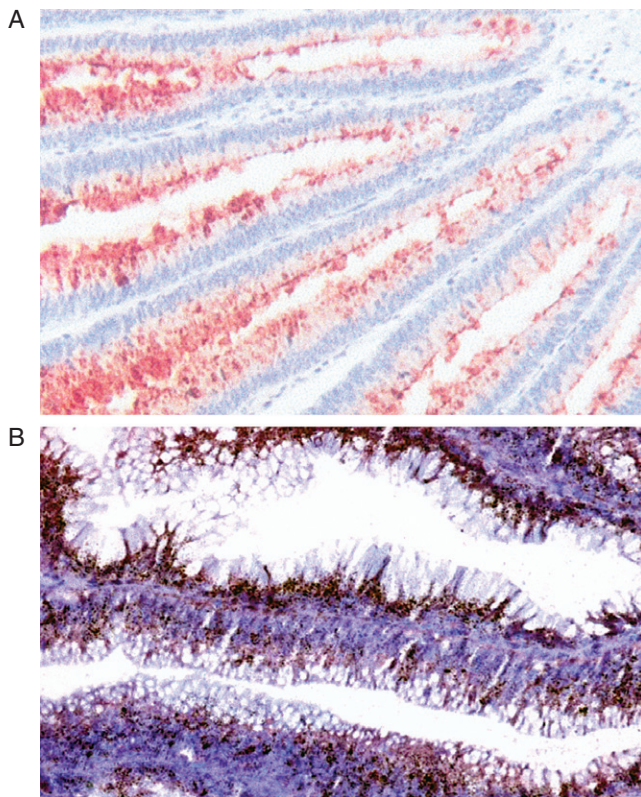
Figure 29 Villous adenomas: **A:** Immunoperoxidase staining with anti-M1/MUC5AC MAbs; hematein counterstain; magnification (250X). **B:** *In situ* hybridization with a ^{35}S-labeled *MUC5AC*-oligonucleotide probe; methyl green pyronin counterstain; magnification (400X).

Abnormal expression of *MUC5AC* was detected in 100% of specimens (22/22) analyzed by *in situ* hybridization with a higher expression level in villous adenomas presenting low-grade dysplasia than in those cases with high-grade dysplasia (Buisine *et al.*, 1996). In a larger study increased expression of *MUC5AC* was found in the majority of colonic adenomas tested (26/45, or 58%) as ascertained by slot blot analysis with a cDNA probe corresponding to the tandem repeat region and by RNase protection assay using a nonrepetitive riboprobe (Bartman *et al.*, 1999). *MUC5AC* mRNA expression was present more frequently and at higher levels in adenomas with intermediate size and villous histology and with low-grade dysplasia (Bartman *et al.*, 1999). Other authors, using *in situ* hybridization, have also reported *MUC5AC* expression in rectal adenomas but without correlation with adenoma size or grade of dysplasia. (Myerscough *et al.*, 2003).

Adenocarcinomas

    A study including 100 proximal and 200 distal colon adenocarcinomas showed a difference in the expression of M1/MUC5AC mucin according to the location of tumors (Bara *et al.*, 1984b). Indeed, the MUC5AC mucin is more expressed in the right side (55%) than in the left side (13%). The high percentage of MUC5AC-positive cancers in the right side could be explained by the higher percentage of 1) mucous-producing tumours, such as signet ring cell (6% versus 1%) or mucinous adenocarcinomas (29% versus 11%); and 2) M1/MUC5AC (+) well-differentiated adenocarcinomas (45% versus 8.5%) and the presence of undifferentiated carcinoma producing MUC5AC mucin (12% versus 0%). These later carcinomas were found in older patients (mean age 78 years versus 66 years). The difference of the expression of M1/MUC5AC mucin between these two sides of the colon has been reported by others (Biemer-Huttmann *et al.*, 2000). Moreover, the M1/MUC5AC immunoreactivity is present in a higher proportion of the high microsatellite instability (MSI) group (Biemer-Huttmann *et al.*, 2000). Analysis of *MUC5AC* gene expression by *in situ* hybridization using a tandem repeat-oligonucleotide probe in a small series of colorectal carcinomas showed abnormal expression of *MUC5AC* in rare cases only (1/8) (Buisine *et al.*, 1996 and unpublished data). Moreover, increased *MUC5AC* expression was found only rarely (1/14) by reverse transcription-polymerase chain reaction (RT-PCR) analysis (Buisine, unpublished data). In a more recent study on a larger series of 36 colorectal adenocarcinomas developed in

the left colon or rectum, *MUC5AC* transcripts were not detected by *in situ* hybridization using the same oligonucleotide probe, whereas the MUC5AC mucin product was observed in most cases (23/36, or 64%) by immunohistochemistry using the LUM5-1 antibody (Sylvester *et al.*, 2001).

Ovary Metastasis

Extraovarian carcinomas that metastasize to the ovaries can mimic primary ovarian tumors and require additional study for differential diagnosis. M1/MUC5AC (MAb 45M1) is not expressed in these metastases but is highly expressed in the primary ovarian tumors and, consequently, is a useful marker in the distinction between colonic carcinoma metastatic to the ovary and primary ovarian carcinoma (Albarracin *et al.*, 2000).

Inflammatory Bowel Disease

Few studies have been published about the M1 expression in inflammatory bowel disease. A preliminary study of Drs. M. Nap and G. Maes showed that this gastric M1/MUC5AC mucin was abnormally expressed in Crohn's disease (10 cases) and in ulcerative colitis (seven cases). Traces of this mucin were observed in the other types of colitis (indeterminate and acute self-limiting) (unpublished data, 1985). More recently, the expression of MUC5AC was analyzed in the ileal mucosa of patients with Crohn's disease independently in two laboratories by *in situ* hybridization using the tandem repeat-oligonucleotide probe and immunohistochemistry using the LUM5-1 polyclonal antibody. *MUC5AC* mRNA and peptides were detected in involved ileal mucosa close to the ulcer margin in distal ductular and surface elements of the ulcer-associated cell lineage (Buisine *et al*., 2001; Longman *et al*., 2000). Moreover, MUC5AC mucin was detected in a small number of cases (5/40) in biopsies of ileoanal reservoir of patients, whereas no *MUC5AC* mRNA were detected in these biopsies. In one of the positive pouch biopsies, MUC5AC protein product was present in ulcer-associated cell lineage (Sylvester *et al.*, 2002).

DISCUSSION

The apparently discrepant results obtained using molecular biology techniques (*in situ* hybridization) and immunochemistry (immunoperoxidase method) can be partially explained by the differences in the reagents and the tissues used.

Variability of Results Using Immunohistochemistry

Concerning immunohistochemistry, the discrepancy of results is often the result of the quality of antibodies against mucin. As described in the Introduction section, some antibodies raised against tandem repeat domain did not recognize the native mucin but only naked apomucin. For instance, the expression of M1/MUC5AC in hyperplastic polyps is observed in 100% of cases using anti-M1 antibodies raised against native mucin (Bara *et al.*, 1986; Biemer-Huttmann *et al.*, 1999; Yao *et al.*, 2000) and in only 11% of cases (1/9) with antibodies raised against tandem repeat domains (antibody M5P-b1) (Bartman *et al.*, 1999). Unfortunately, to our knowledge no observation on hyperplastic polyps using *in situ* hybridization has been reported yet. Such an observation could confirm this interpretation. In the tumor, however, the mucin can be differently glycosylated, and some epitopes can be masked by the polysaccharide moieties.

The tissue preparation itself can also be a source for the discrepancy in the results obtained because of the fixation procedure. Usually, paraformaldehyde is used as fixative, permitting both immunohistochemistry and *in situ* hybridization methods. However, in this case of mucin characterization, when using immunohistochemical approach, it is important to perform a pretreatment (pronase or microwaves) to obtain better results; as a result, variability in the immunoreactivity of antibodies could be observed, however. On the contrary, ethanol does not necessitate any pretreatment and is therefore an excellent fixative to study glycoprotein immunochemistry. However, this fixative cannot be used for *in situ* hybridization.

Variability of Results Using in situ Hybridization

Concerning *in situ* hybridization, results can vary between the studies depending on the probe and the procedure used. The importance of the probe was discussed in the Introduction of this chapter. Differences in stringency conditions during the hybridization and washing steps (temperature and composition of the hybridization mixture and washing buffers) can also explain some discrepancies that depend on the balance between the intensity of the signal and background and thus interpretation of the data. Finally, some of the discrepancies between the results obtained by *in situ* hybridization and by immunohistochemistry are likely the result of a lower sensitivity of the *in situ* hybridization technique and a low stability of mucin mRNA

compared with the corresponding peptides. This may explain why it is sometimes difficult to detect *MUC5AC* mRNA in tissues that are shown in other respects by immunohistology to contain MUC5AC apomucin in mucus lakes containing only residual non–mucus-secreting epithelium as observed in mucinous adenocarcinomas.

MUC5AC Expression in Normal Colon

A careful study of the expression of the MUC5AC mucin in the normal colon is essential for establishing the relevance of its abnormal expression in colonic carcinogenesis. Colon specimen specified as "normal" generally comes from resection margins of colon neoplasms. However, the "histologically normal" mucosa distant from colon tumors may express modified mucin, as was reported in the past by histochemistry (Filipe, 1979) and later by immunohistology (Bara *et al.*, 1984a), and was recently observed in ACF (Bara *et al.*, 2003) that are often present in this mucosa and are suspected to be implicated in the carcinogenesis process. These mucosae should not be regarded as "normal," and the results obtained using these specimens are questionable. Only a few studies have been undertaken on genuine "normal." These studies included colonic mucosae otained from the following: 1) 40 relatively young individuals (15–54 years old) without gastrointestinal disease, after accidental death (Bara *et al.*, 1986), 2) from hemorrhoidectomy specimen containing well-preserved rectal mucosa (Kuan *et al.*, 2001), or 3) from biopsies consisting of histologically normal colon obtained from patients in whom no abnormalities of colonic mucosa were detected during colonoscopy (Bartman *et al.*, 1999). The absense of *MUC5AC* gene expression in the normal colon was confirmed at the RNA level by *in situ* hybridization (Bartman *et al.*, 1999; Buisine *et al.*, 1996). All these studies show that the MUC5AC apomucin is not expressed in the normal adult human colon, except perhaps in the distal part of rectal mucosa (3/10) (Kuan *et al.*, 2001).

MUC5AC Expression in Fetal Colon

In the fetus, the expression of *MUC5AC* is not very clear because the period of gestation during which *MUC5AC* is expressed differs according to the method used. Using immunohistochemistry, M1/MUC5AC mucin was detected at high levels in the human colon at the 24th week. Using *in situ* hybridization, however, *MUC5AC* mRNA was detected at 17 weeks (Reid *et al.*, 1998). Other authors did not find *MUC5AC*

expression between 18 and 27 weeks (Buisine *et al.*, 1998). The discrepancy between these results is not well understood. The sensitivity of the *in situ* hybridization technique is perhaps lower than that of immunohistology. Another explanation is that the *MUC5AC* gene could be expressed during a very short period during gestation. Indeed, in the rat colon, gastric mucin was expressed only 1 day after the birth (Decaens *et al.*, 1983). Consequently, the number of fetuses studied by *in situ* hybridization is probably too small to observe the MUC5AC expression. However, both methods (*in situ* hybridization and immunohistology) suggest that *MUC5AC* is expressed in the colon during fetal development and is not expressed after the birth. Thus, its expression during colon carcinogenesis can be regarded as of an oncofetal nature.

MUC5AC Expression in Colon Carcinogenesis

Histologically Normal Mucosa Adjacent to Colon Tumor

The transitional mucosa adjacent to colorectal cancer is often thickened and is formed of elongated and branched crypts lined by tall epithelium. Secretory mucins show loss of sulphatation and/or increased sialylation (Filipe, 1979), reduced O-acetylation of sialic acid (Hutchins *et al.*, 1988), as well as abnormal expression of small intestinal mucin antigen (Ma *et al.*, 1980) and M1/MUC5AC mucin (Bara *et al.*, 1986). Two hypotheses have been evoked to attempt to explain these mucin changes: 1) reactive process, because similar structural and functional alterations occur adjacent to metastases and in colorectal mucosa undergoing prolapse and 2) premalignant change. This last hypothesis is more likely because the expression of gastric mucin is an early event occurring during rat colon carcinogenesis, already 2 weeks after the first injection of carcinogen (Decaens *et al.*, 1983), and we have never observed *MUC5AC* expression in colon mucosa adjacent to metastasis (unpublished observation). In addition, the expression of M1/MUC5AC mucin is observed in ACF, which are now considered as precursors of adenomas (Bara *et al.*, 2003).

Macroscopically Normal Mucosa Distant from Colon Tumors

The macroscopically normal mucosa distant from adenocarcinomas expressed MUC5AC as observed using immunohistology (Bara *et al.*, 1984a) and was also expressed distant from villous adenomas, as

observed by *in situ* hybridization (Buisine *et al.*, 1996). Using immunoperoxidase, M1/MUC5AC mucin was observed in goblet cells of crypts as scattered patches (Bara *et al.*, 1984a) sometimes at several centimeters distance from the tumor. This observation could explain why it was not possible to find any MUC5AC-positive goblet cells in biopsies, which included a very few number of crypts (Longman *et al.*, 2000). Indeed, in another study, *MUC5AC* transcripts were observed infrequently and only in rare goblet cells of rare crypts in such biopsies taken at several centimeters from adenomas (Buisine *et al.*, 1996). Such mucosa could be compared with the rat colon mucosa several weeks after injection of carcinogen (DMH or MNNG), which displayed isolated glands and ACF-containing goblet cells secreting gastric M1/MUC5AC mucin (Bara *et al.*, 2003). This assumption is strengthened by the fact that patients showing a greater amount of gastric M1 mucin in their macroscopically normal colon have synchronous or metachronous adenocarcinomas.

Polyps

The majority of colon polyps are classified as either hyperplastic polyps or adenomas. In general, these have been considered as fundamentally different lesions, with only the adenomas being neoplastic and having a potential for progression to malignancy. However, the abnormal expression of MUC5AC, an early marker of colon carcinogenesis, in both lesions has challenged this view (Bara *et al.*, 1983, 1986), and this observation is strengthened by the description of mixed polyps. Indeed, mixed polyps have been described as combining hyperplastic and adenomatous features and now are called "serrated adenomas." It has been suggested that hyperplastic polyps may develop into serrated adenomas as a separate histogenetic pathway of colon carcinogenesis (Biemer-Huttmann *et al.*, 1999). The study of a patient having six adenocarcinomas, eight serrated adenomas, and four hyperplastic polyps strongly expressing gastric M1/MUC5AC mucin is a good argument in favor of a possible common lineage among hyperplastic polyps, adenomas, and cancer (Yao *et al.*, 2000).

Adenomas

Concerning adenomas, which are the uncontestable precancerous lesions, both immunohistochemistry and *in situ* hybridization show similar results (see Figure 29). Indeed, MUC5AC expression increases with the degree of villous architecture and decreases with the presence of severe dysplasia (Bara *et al.*, 1983, 1986; Bartman *et al.*, 1999; Buisine *et al.*, 1996). The expression of *MUC5AC* depending on the size is not clear. Some authors described an increase of MUC5AC according to the size (Bartman *et al.*, 1999), whereas others claimed absence of association between MUC5AC expression and adenoma size in distal adenomas (Bara *et al.*, 1983, 1986; Myerscough *et al.*, 2003). The slight discrepancy between the different results can be explained by the anatomic location (proximal or distal colon) of adenomas or by their eventual association with adenocarcinomas, details that are not always reported. These results demonstrate that the M1/MUC5AC mucin could be regarded as an early marker of colon carcinogenesis. In fact, the M1/MUC5AC is also expressed in the ACF, precursors of adenomas (Bara *et al.,* 2003). Such behavior of gastric mucin during colon carcinogenesis is also observed in DMH-treated rat. Indeed, gastric mucin is expressed 2 weeks after the first carcinogen injection and the number of colon mucous cells increased during carcinogenesis until the appearance of tumors (Decaens *et al.*, 1983). After malignant transformation, this M1/MUC5AC mucin is less expressed, especially in the distal adenocarcinomas. Therefore, this M1/MUC5AC mucin could be regarded as an excellent marker of precancerous progression toward malignant transformation, rather than a tumor marker of colon adenocarcinomas.

This gastric MUC5AC apomucin, present in these precancerous colon mucosae, is expressed in colon epithelial cells containing specific glycosyltransferases not present in the stomach, such as sialyltransferases. Thus, these colon goblet cells are able to synthesize gastric apomucin in which the oligosaccharides chains display elongation that can be truncated by eventual premature sialylations (Bara 1991b; Capon *et al.*, 1992). Such mucin could show specific glycotopes (recognizing both peptidic and saccharidic moieties) not found in the normal gastrointestinal tissue. MAbs against these putative glycotopes will be useful for a more specific characterization of the aberrant mucin expression during colon carcinogenesis.

Regulation of the *MUC5AC* Gene

The molecular mechanisms responsible for the control of secretory mucin transcription and expression are beginning to be elucidated as gene promoters (Li *et al.*, 1998), and regulatory regions have been characterized (for review, see Van Seuningen *et al.*, 2001). These include the following: 1) activation of mucin secretion/expression by exogenous factors (Th-1 pro-inflammatory cytokines, Th-2 pleiotropic cytokines,

growth factors, bacterial exoproducts) via specific receptors, 2) by exogenous factors (proinflammatory cytokines, hormones, phorbol esters) via G-protein-associated receptors, and 3) epigenetic silencing through the methylation of CpG islands within the promoter regions. However, little information is available about the mechanisms responsible for the control of *MUC5AC* expression, especially in the colon and provided from *in vitro* experimentation, which is not necessary representative of the situation *in vivo*. Regulation of the expression of *MUC5AC* has been explored in mucous-secreting colon cancer cell lines T84, HT-29/A1, and HM3 and was shown to be subject to proteine kinase C (PKC)-dependent stimuli. Induction of *MUC5AC* expression by phorbol 12-myristate 13-acetate is associated with an increase in secretion of mucin-associated carbohydrate antigens and an increase in metalloproteinase activity. It has been shown to be mediated by the Ca^{2+}-independent PKC-ε isoform of PKC. Nevertheless, such components, which regulate the MUC5AC expression, can hardly explain the early and continuous expression of MUC5AC during colon carcinogenesis because these molecules act via binding to specific membrane receptors and have a short-term effect.

It is interesting that expression of the *MUC2* gene was shown recently to correlate well with the methylation status of the proximal region of the promoter. Indeed, abundant MUC2 expression in normal goblet cells and in mucinous colorectal carcinomas is associated with low methylation of the *MUC2* promoter, whereas suppression of MUC2 expression in other colorectal carcinomas and metastases is associated with high methylation. The expression of MUC5AC in the colon may involve the same type of mechanism, as shown in gastric cancer cells KATO-III (Van Seuningen *et al.*, 2001). Importance of methylation in the regulation of the *MUC5AC* gene expression, however, was turned down in pancreatic cancer cells.

Although altered expression of M1/MUC5AC is observed in human colorectal adenomas and adenocarcinomas, the role of this mucin in colon carcinogenesis remains to be established. Generation of mice overexpressing *MUC5AC* in the colon will be of importance to investigate the functions of this mucin in colon carcinogenesis.

In adenomas, the colonic expression of the MUC5AC gene, of fetal type, suggests a relationship with other early events described in colon carcinogenesis. The clonality of colon cancer is well established. However, this tumor may develop via different molecular pathways, gradually accumulating genetic changes that enhance the clonal expansion of initiated cells and affect their positioning in the epithelium,

inducing a loss of proliferative and cell death controls (by the inactivation of tumor suppressor genes, including *APC* and *p53*, and activation of protooncogenes, including *Ras*, or by inactivation of mismatch repair genes). Although our past and present studies on M1/MUC5AC aberrant and "displaced" expression in human colon carcinogenesis do not prove a direct role of this mucin in the oncogenic transformation, the expression of M1/MUC5A*C* is nevertheless an early event and is thus a useful marker for colon cancer.

Putative Clinical Applications

The results of the fundamental research clearly show that gastric M1/MUC5AC mucin is an excellent tumor marker of early colon and pancreas carcinogenesis. Consequently, it is logical to explore whether this tumor marker might be used to detect patients implicated in colon carcinogenesis before the cancer appears and becomes invasive, and it may be useful to estimate quantitatively the progression of the mucosal changes leading to precancerous lesions. It could be of interest in following patients with a family history of colorectal cancer. An IRMA is used in our laboratory to detect gastric mucin in the fluids of pancreatic cysts to improve the diagnosis of mucinous cystadenomas, a precancerous lesion necessitating surgery (Hammel *et al.*, 1997). It would be useful to detect and quantify the M1/MUC5AC mucin in the lumen of the intestine by a simple, noninvasive method for the detection of this aberrant mucin in colonic washings and subsequently in stools from patients with colon cancer and from high-risk subjects. Such a method, along with other assays for detecting specific markers of colon cancer in fecal material (Traverso *et al.*, 2002), should contribute to improve early screening, leading to a successful reduction of the mortality from colon cancer.

Acknowledgments

References

Albarracin, C.T., Jafri, J., Montag, A.G., Hart, J., and Kuan, S.F. 2000. Differential expression of MUC2 and MUC5AC mucin genes in primary ovarian and metastatic colonic carcinoma. *Hum. Pathol. 31*:672–677.

Argueso, P., Balaram, M., Spurr-Michaud, S., Keutmann, H.T., Dana, M.R., and Gipson, I.K. 2002. Decreased levels of the goblet cell mucin MUC5AC in tears of patients with Sjogren syndrome. *Invest. Ophthalmol. Vis. Sci. 43*:1004–1011.

Asker, N., Axelsson, M.A., Olofsson, S.O., and Hansson, G.C. 1998. Human MUC5AC mucin dimerizes in the rough

endoplasmic reticulum, similarly to the MUC2 mucin. *Biochem. J. 335*:381–387.

Audie, J.P., Janin, A., Porchet, N., Copin, M.C., Gosselin, B., and Aubert, J.P. 1993. Expression of human mucin genes in respiratory, digestive, and reproductive tracts ascertained by in situ hybridization. *J. Histochem. Cytochem. 41*:1479–1485.

Bara, J. 1991b. Expression of gastric and small intestine mucin antigens in colonic carcinogenesis. *Frontiers in mucosal immunology 1*:295–298.

Bara, J., Andre, J., Gautier, R., and Burtin, P. 1984a. Abnormal pattern of mucus-associated M1 antigens in histologically normal mucosa adjacent to colonic adenocarcinomas. *Cancer Res. 44*:4040–4045.

Bara, J., Chastre, E., Mahiou, J., Singh, R.L., Forgue-Lafitte, M.E., Hollande, E., and Godeau, F. 1998. Gastric M1 mucin, an early oncofetal marker of colon carcinogenesis, is encoded by the MUC5AC gene. *Int. J. Cancer 75*:767–773.

Bara, J., Decaens, C., Loridon-Rosa, B., and Oriol, R. 1992. Immunohistological characterization of mucin epitopes by pretreatment of gastro-intestinal sections with periodic acid. *J. Immunol. Methods 149*:105–113.

Bara, J., Forgue-Lafitte, M.E., Maurin, N., Flejou, J.F., and Zimber, A. 2003. Abnormal expression of gastric mucin in human and rat aberrant crypt foci (ACF) occuring during colon carcinogenesis. *Tumor Biol. 24*:109–115.

Bara, J., Gautier, R., Daher, N., Zaghouani, H., and Decaens, C. 1986. Monoclonal antibodies against oncofetal mucin M1 antigens associated with precancerous colonic mucosae. *Cancer Res. 46*:3983–3989.

Bara, J., Gautier, R., Mouradian, P., Decaens, C., and Daher, N. 1991a. Oncofetal mucin M1 epitope family: characterization and expression during colonic carcinogenesis. *Int. J. Cancer 47*:304–310.

Bara, J., Languille, O., Gendron, M.C., Daher, N., Martin, E., and Burtin, P. 1983. Immunohistological study of precancerous mucus modification in human distal colonic polyps. *Cancer Res. 43*:3885–3891.

Bara, J., Loisillier, F., and Burtin, P. 1980. Antigens of gastric and intestinal mucous cells in human colonic tumours. *Br. J. Cancer 41*:209–221.

Bara, J., Nardelli, J., Gadenne, C., Prade, M., and Burtin, P. 1984b. Differences in the expression of mucus-associated antigens between proximal and distal human colon adenocarcinomas. *Br. J. Cancer 49*:495–501.

Bartman, A.E., Sanderson, S.J., Ewing, S.L., Niehans, G.A., Wiehr, C.L., Evans, M.K., and Ho, S.B. 1999. Aberrant expression of MUC5AC and MUC6 gastric mucin genes in colorectal polyps. *Int. J. Cancer 80*:210–218.

Biemer-Huttmann, A.E., Walsh, M.D., McGuckin, M.A., Ajioka, Y., Watanabe, H., Leggett, B.A., and Jass, J.R. 1999. Immunohistochemical staining patterns of MUC1, MUC2, MUC4, and MUC5AC mucins in hyperplastic polyps, serrated adenomas, and traditional adenomas of the colorectum. *J. Histochem. Cytochem. 47*:1039–1048.

Biemer-Huttmann, A.E., Walsh, M.D., McGuckin, M.A., Simms, L.A., Young, J., Leggett, B.A., and Jass, J.R. 2000. Mucin core protein expression in colorectal cancers with high levels of microsatellite instability indicates a novel pathway of morphogenesis. *Clin. Cancer Res. 6*:1909–1916.

Buisine, M.P., Desreumaux, P., Leteurtre, E., Copin, M.C., Colombel, J.F., Porchet, N., and Aubert, J.P. 2001. Mucin gene expression in intestinal epithelial cells in Crohn's disease. *Gut 49*:544–551.

Buisine, M.P., Devisme, L., Degand, P., Dieu, M.C., Gosselin, B., Copin, M.C., Aubert, J.P., and Porchet, N. 2000a. Developmental

mucin gene expression in the gastroduodenal tract and accessory digestive glands. II. Duodenum and liver, gallbladder, and pancreas. *J. Histochem. Cytochem. 48*:1667–1676.

Buisine, M.P., Devisme, L., Maunoury, V., Deschodt, E., Gosselin, B., Copin, M.C., Aubert, J.P., and Porchet, N. 2000b. Developmental mucin gene expression in the gastroduodenal tract and accessory digestive glands. I. Stomach. A relationship to gastric carcinoma. *J.Histochem.Cytochem. 48*:1657–1666.

Buisine, M.P., Devisme, L., Savidge, T.C., Gespach, C., Gosselin, B., Porchet, N., and Aubert, J.P. 1998. Mucin gene expression in human embryonic and fetal intestine. *Gut 43*:519–524.

Buisine, M.P., Janin, A., Maunoury, V., Audie, J.P., Delescaut, M.P., Copin, M.C., Colombel, J.F., Degand, P., Aubert, J.P., and Porchet, N. 1996. Aberrant expression of a human mucin gene (MUC5AC) in rectosigmoid villous adenoma. *Gastroenterology 110*:84–91.

Capon, C., Laboisse, C.L., Wieruszeski, J.M., Maoret, J.J., Augeron, C., and Fournet, B. 1992. Oligosaccharide structures of mucins secreted by the human colonic cancer cell line CL.16E. *J.Biol.Chem. 267*:19248–19257.

Decaens, C., Bara, J., Rosa, B., Daher, N., and Burtin, P. 1983. Early oncofetal antigenic modifications during rat colonic carcinogenesis. *Cancer Res. 43*:355–362.

Escande, F., Aubert, J.P., Porchet, N., and Buisine, M.P. 2001. Human mucin gene MUC5AC: Organization of its 5′-region and central repetitive region. *Biochem. J. 358*:763–772.

Filipe, M.I. 1979. Mucins in the human gastrointestinal epithelium: A review. *Invest. Cell. Pathol. 2*:195–216.

Guyonnet Duperat, V., Audie, J.P., Debailleul, V., Laine, A., Buisine, M.P., Galiegue-Zouitina, S., Pigny, P., Degand, P., Aubert, J.P., and Porchet, N. 1995. Characterization of the human mucin gene MUC5AC: A consensus cysteine-rich domain for 11p15 mucin genes? *Biochem. J. 305*:211–219.

Hakkinen, I., Jarvi, O., and Gronroos, J. 1968. Sulphoglycoprotein antigens in the human alimentary canal and gastric cancer. An immunohistological study. *Int. J. Cancer 3*:572–581.

Hammel, P.R., Forgue-Lafitte, M.E., Levy, P., Voitot, H., Vilgrain, V., Flejou, J.F., Molas, G., Gespach, C., Ruszniewski, P., Bernades, P., and Bara, J. 1997. Detection of gastric mucins (M1 antigens) in cyst fluid for the diagnosis of cystic lesions of the pancreas. *Int. J. Cancer 74*:286–290.

Ho, S.B., Roberton, A.M., Shekels, L.L., Lyftogt, C.T., Niehans, G.A., and Toribara, N.W. 1995. Expression cloning of gastric mucin complementary DNA and localization of mucin gene expression. *Gastroenterology 109*:735–747.

Hutchins, J.T., Reading, C.L., Giavazzi, R., Hoaglund, J., and Jessup, J.M. 1988. Distribution of mono-, di, and tri-O-acetylated sialic acids in normal and neoplastic colon. *Cancer Res. 48*:483–489.

Jumblatt, M.M., McKenzie, R.W., and Jumblatt, J.E. 1999. MUC5AC mucin is a component of the human precorneal tear film. *Invest Ophthalmol. Vis. Sci. 40*:43–49.

Kawasaki, H., and Kimoto, E. 1974. Mucosal glycoproteins in carcinoma cells of gastrointestinal tract, as detected by immunofluorescence technique. *Acta Pathol. Jpn. 24*:481–494.

Kuan, S.F., Montag, A.G., Hart, J., Krausz, T., and Recant, W. 2001. Differential expression of mucin genes in mammary and extramammary Paget's disease. *Am. J. Surg. Pathol. 25*: 1469–1477.

Lesuffleur, T., Roche, F., Hill, A.S., Lacasa, M., Fox, M., Swallow, D.M., Zweibaum, A., and Real, F.X. 1995. Characterization of a mucin cDNA clone isolated from HT-29 mucus-secreting cells. The 3′ end of MUC5AC? *J. Biol. Chem. 270*:13665–13673.

Li, D., Gallup, M., Fan, N., Szymkowski, D.E., and Basbaum, C.B. 1998. Cloning of the amino-terminal and 5′-flanking region of

the human MUC5AC mucin gene and transcriptional up-regulation by bacterial exoproducts. *J. Biol. Chem. 273*: 6812–6820.

Lidell, M.E., Johansson, M.E., Morgelin, M., Asker, N., Gum, J.R., Kim, Y.S., and Hansson, G.C. 2003. The recombinant C-terminus of the human MUC2 mucin forms dimers in CHO cells and heterodimers with full-length MUC2 in LS 174T cells. 2003. *Biochem. J. 372(Pt 2)*:335–345.

Longman, R.J., Douthwaite, J., Sylvester, P.A., O'Leary, D., Warren, B.F., Corfield, A.P., and Thomas, M.G. 2000. Lack of mucin MUC5AC field change expression associated with tubulovillous and villous colorectal adenomas. *J. Clin. Pathol. 53*:100–104.

Ma, J., de Boer, W.G., Ward, H.A., and Nairn, R.C. 1980. Another oncofoetal antigen in colonic carcinoma. *Br. J. Cancer 41*:325–328.

Myerscough, N., Sylvester, P.A., Warren, B.F., Biddolph, S., Durdey, P., Thomas, M.G., Carlstedt, I., and Corfield, A.P. 2003. Abnormal subcellular distribution of mature MUC2 and de novo MUC5AC mucins in adenomas of the rectum: Immunohistochemical detection using non-VNTR antibodies to MUC2 and MUC5AC peptide. *Glycoconj. J. 18*:907–914.

Nollet, S., Escande, F., Buisine, M.P., Forgue-Lafitte, M.E., Kirkham, P., Okada, Y., and Bara, J. 2004. Mapping of SOMU1 and M1 Epitopes on the Apomucin Encoded by the 5′ End of the MUC5AC Gene. *Hybridoma and Hybridomics: 23 (2)*:93–99.

Nollet, S., Forgue-Lafitte, M.E., Kirkham, P., and Bara, J. 2002. Mapping of two new epitopes on the apomucin encoded by MUC5AC gene: Expression in normal GI tract and colon tumors. *Int. J. Cancer 99*:336–343.

Nordman, H., Davies, J.R., Lindell, G., de Bolos, C., Real, F., and Carlstedt, I. 2002. Gastric MUC5AC and MUC6 are large oligomeric mucins that differ in size, glycosylation and tissue distribution. *Biochem. J. 364*:191–200.

Reid, C.J., and Harris, A. 1998. Developmental expression of mucin genes in the human gastrointestinal system. *Gut 42*:220–226.

Reis, C.A., David, L., Nielsen, P.A., Clausen, H., Mirgorodskaya, K., Roepstorff, P., and Sobrinho-Simoes, M. 1997. Immuno-histochemical study of MUC5AC expression in human gastric carcinomas using a novel monoclonal antibody. *Int. J. Cancer 74*:112–121.

Sotozono, M., Okada, Y., Sasagawa, T., Nakatou, T., Yoshida, A., Yokoi, T., Kubota, M., and Tsuji, T. 1996. Novel monoclonal antibody, SO-MU1, against human gastric MUC5AC apomucin. *J. Immunol. Methods 192*:87–96.

Sylvester, P.A., Myerscough, N., Warren, B.F., Carlstedt, I., Corfield, A.P., Durdey, P., and Thomas, M.G. 2001. Differential expression of the chromosome 11 mucin genes in colorectal cancer. *J. Pathol. 195*:327–335.

Sylvester, P.A., Walsh, M., Myerscough, N., Warren, B.F., Corfield, A.P., Thomas, M.G., and Durdey, P. 2002. Mucin gene expression in the ileoanal reservoir is altered and may be relevant to the risk of inflammation and dysplasia. *Gut 51*:386–391.

Thornton, D.J., Carlstedt, I., Howard, M., Devine, P.L., Price, M.R., and Sheehan, J.K. 1996. Respiratory mucins: Identification of core proteins and glycoforms. *Biochem. J. 316*:967–975.

Toribara, N.W., Roberton, A.M., Ho, S.B., Kuo, W.L., Gum, E., Hicks, J.W., Gum, J.R., Jr., Byrd, J.C., Siddiki, B., and Kim, Y.S. 1993. Human gastric mucin. Identification of a unique species by expression cloning. *J. Biol. Chem. 268*:5879–5885.

Traverso, G., Shuber, A., Levin, B., Johnson, C., Olsson, L., Schoetz, D.J., Jr., Hamilton, S.R., Boynton, K., Kinzler, K.W., and Vogelstein, B. 2002. Detection of APC mutations in fecal DNA from patients with colorectal tumors. *N. Engl. J. Med. 346*:311–320.

Van Seuningen, I., Pigny, P., Perrais, M., Porchet, N., and Aubert, J.P. 2001. Transcriptional regulation of the 11p15 mucin genes. Towards new biological tools in human therapy, in inflammatory diseases and cancer? *Front. Biosci. 6*:D1216–1234.

Yao, T., Nishiyama, K., Oya, M., Kouzuki, T., Kajiwara, M., and Tsuneyoshi, M. 2000. Multiple 'serrated adenocarcinomas' of the colon with a cell lineage common to metaplastic polyp and serrated adenoma. Case report of a new subtype of colonic adenocarcinoma with gastric differentiation. *J. Pathol. 190*: 444–449.

7

Role of Cyclooxygenase2 Expression in Colorectal Cancer

Sven Petersen

Introduction

Since their discovery four decades ago prostaglandins (PGs) have been assumed to be precursors for formation and growth of malignant tumors. Thus, the manipulation of PG pathways and their impact on cancer growth and treatment have become important in cancer research.

The purpose of this study is to determine whether the expression pattern of cyclooxygenase2 (COX2) in a series of human rectal tumors is linked to the outcome in a well-defined cohort of patients who underwent surgery for rectal cancer.

Prostaglandins

PGs became of interest for experimental research after they were discovered as a group of mediators in the 1960s. The precursor of all PGs is arachidonic acid, a polyunsaturated fatty acid, which is liberated from the cell membrane phospholipids by the phospholipase A_2. Arachidonic acid then is catalyzed by the COX enzyme to an unstable precursor PG G_2. This intermediate form is transferred to PG H_2, which is the precursor for all resulting prostaglandins including PG E_2, PG F_{2a}, PG D_2, PG I_2, thromboxane TX A_2 and TX B_2. Prostaglandins serve as critical mediators in mammalian physiology affecting a variety of functions, including blood vessel tone, platelet aggregation, and immune responses. The maintenance of the gastric mucosa is regulated by PGs as well as regulation of cell growth and differentiation. PGs are involved in many pathologic conditions such as inflammatory reactions or rheumatoid disease (Kargman *et al.,* 1995; Kutchera *et al.,* 1996). PGs have also been implicated in cancer development with a number of tumor types found to produce more PGs than the normal tissues from which they arise (Hida *et al.*, 1998; Kutchera *et al.*, 1996). PGs stimulate angiogenesis and, in addition, are vasoactive agents, which may influence tumor growth and response to cytotoxic agents (Ziche *et al.*, 1982). Therefore, tumor characteristics such as rapid growth and metastatic spread might be linked to the effect of increased intratumoral PG levels.

COX1 and COX2

The rate-limiting enzyme in the synthesis of PGs from arachidonic acid is COX. The PG synthase COX1 was first cloned in 1988 (Fosslien, 2000). Since 1991 it has been known that two isoforms of COX exist (Kujubu *et al.,* 1991). COX1 is constitutively expressed in most tissues and mediates the synthesis of PGs required for normal physiologic functions. In contrast, COX2 is typically not expressed or expressed at relatively low

levels in undisturbed healthy tissues but is inducible by an assortment of agents including proinflammatory stimuli, mitogens, and/or hormones depending on the tissue (DuBois *et al.,* 1994; Kujubu, *et al.,* 1991). COX1 and COX2 are encoded by genes mapping to chromosomes 9 and 1, respectively. The COX1 gene extends for 22 kilobases (kb) and includes 11 exons, producing a 2.7 kb message. COX2 is an 8.3 kb gene of 10 exons that generates a 4.3–4.5 kb message. Although the intron/exon structure of the genes is nearly identical and the encoded proteins are ≈70% homologous, the regulatory elements within the genes are quite different. Whereas COX1 represents a housekeeping gene, which lacks a TATA box (Kraemer *et al.,* 1992), the promotor of the immediate-early gene COX2 contains a TATA box and binding sites for several transcription factors including nuclear factor-κB, the nuclear factor for interleukin-6 expression and the cyclic adenosine monophosphate response element binding protein (Appleby *et al.*, 1994). COX2 was shown to be moderately overexpressed in a large variety of tumor types including head and neck, colon, breast, and pancreatic cancers. In addition, there is considerable evidence available indicating that COX2 promotes carcinogenesis and growth of established tumors (Eberhart *et al.*, 1994; Fujita *et al.*, 2000; Taketo, 1998; Tsujii *et al.,* 1997).

In most tumors, COX2 expression was detected in ~40–80% of tumor cells. However, even some normal tumor cell infiltrates, particularly epithelial cells, may express COX2. Although the relationship between COX2 and tumor aggressiveness is not fully established, it seems that COX2 overexpression is related to poor patient prognosis and enhanced propensity for metastatic spread (Achiwa *et al*., 1999; Sheehan *et al*., 1999). Enhanced COX2 expression might also be related to the grade of differentiation of the tumors. For instance, in some well-differentiated adenocarcinomas of the lung an increased COX2 level was found (Wolff *et al.,* 1988), but COX2 was also found in other forms of lung cancer (Hida *et al.*, 1998; Khuri *et al.*, 2001). Probably the largest number of publications deals with COX2 expression in colorectal adenomas and carcinomas, and in this case the potential clinical application of nonsteroidal anti-inflammatory drugs has been debated for decades. Most of colorectal cancer cells express COX2. The level of COX2 expression varies depending on the detection methods, and the published data suggest that according to the tumor site, COX2 expression might be more pronounced in rectal tumors compared to the colonic tumors (Dimberg *et al.,* 1999; Sano *et al.,* 1995).

It is controversial whether COX2 expression in itself is a prognostic factor for local recurrence and/or survival of patients with colorectal cancer. Some authors found a significantly higher incidence of local recurrence and increased cancer-specific mortality associated with higher COX2 expression in tumor cells (Tomozawa *et al.,* 2000), whereas others could not confirm these observations (Fujita *et al.,* 1998).

The aim of this synopsis is to determine the influence of COX2 expression in colorectal carcinoma on tumor recurrence and survival. In this context the COX2 expression in tumors of patients treated surgically for rectal cancer in our department were analyzed. The COX2 immunohistochemistry staining technique will be described in detail. Of special interest is to analyze whether there were significant differences in the group with low COX2 expression compared to the high COX2 group with reference to well-known prognostic factors (Fielding *et al.,* 1991). In addition, our data will be compared with currently available data on COX2 expression in colorectal cancer.

COX2 Immunohistochemistry

MATERIALS

1. Tissue samples embedded in paraffin.
2. For deparaffinization: 2X xylene 400 ml; isopropanol, 2X 400 ml; ethanol solution 96% in distilled water, 2X 400 ml; ethanol solution 70%, 2X 400 ml; ethanol solution 50%, 2X 400 ml; distilled water, 2X 400 ml. Phosphate buffer saline (PBS): 100 mg anhydrous calcium chloride, 200 mg monobasic potassium phosphate, 100 mg magnesium chloride, 8 g sodium chloride, and 2.16 g dibasic sodium phosphate; bring volume to 1 L with deionized distilled water (pH 7.4).
3. Solution for unmasking the antigens: citrate buffer solution: 450 ml distilled water, 9 ml of 100 mmol/L citrate, and 41 ml of 100 mmol/L sodium citrate. Tris buffer solution: 900 ml of 154 mmol/L NaCl and 100 ml Tris–buffer stock solution.
4. For endogenous peroxidase blocking: ~400 ml of 3% hydrogen peroxide solution.
5. Incubation with primary antibody. Tris buffer solution: 900 ml of 154 mmol/L NaCl and 100 ml Tris–buffer stock solution. Primary antibody: rabbit polyclonal antibody specific for human recombinant prostaglandin H synthase Form-2 (COX2) diluted 300-fold in antibody dilution (Dako, Code No. S3022, DakoCytomation GmbH, Hamburg, Germany). The antibody was provided by Oxford Biomedical Research Inc., Michigan.
6. For immunostaining, the Dako kit EnVision System was used. The immunostaining kit was provided by DakoCytomation GmbH. Incubation with secondary antibody alkaline phosphatase labeled polymer and

substrate chromogen solution (Fast Red) was used. Distilled water, 2X 400 ml.

8. Counterstaining: hematoxylin.

9. For the dehydration of the samples, the same materials as in **Step 2** were used.

METHODS

Tissue samples were fixed with 4% formaldehyde in PBS, embedded in paraffin, and cut in 4 µm thick sections. The sections were deparaffinized, hydrated through xylene and ethanol, and microwaved. The following steps were performed:

1. Rinse the samples two times in xylene for 10 min each.

2. Rinse the samples two times in isopropanol for 2–3 min each.

3. Hydrate the samples by rinsing first two times in 96% ethanol for 2–3 min each, followed by rinsing in 70% ethanol once for 2–3 min and 50% ethanol once for 2–3 min. Finally, rinse the samples two times in distilled water for 2–3 min each.

4. Microwave the samples two times for 5 min each.

5. Rinse the samples in Tris buffer two times for 5 min each.

6. Endogenous peroxidase was blocked by immersion of the samples in 3% hydrogen peroxide for 30 min at room temperature. Estimated 100 µl peroxidase solution for each sample.

7. Rinse the samples in Tris buffer two times for 5 min each.

8. Incubation with the COX2 antibody, for this rabbit polyclonal antibody specific for human COX2 (Oxford) diluted 300-fold, was applied and sections were incubated at 4ºC overnight. Estimated 100 µl antibody solution for each sample.

9. Rinse the samples in Tris buffer two times for 5 min each.

10. Incubation with alkaline phosphatase labeled polymer from the Dako EnVision kit for 30 min at room temperature. Estimated 100 µl polymer solution for each sample.

11. Rinse the samples in Tris buffer two times for 5 min each.

12. Apply substrate chromogen solution (Fast Red) from the Dako EnVision kit for 8 min at room temperature. Estimated 100 µl chromogen solution for each sample.

13. Rinse the samples in distilled water two times for 5 min each.

14. The sections were counterstained with hematoxylin (HE); incubate the samples shortly in the HE solution just until the nuclears start staining (~5–10 seconds).

15. Rinse the samples with room temperature distilled water until the HE staining changes color from brown to blue.

16. Dehydrate the samples by rinsing two times in distilled water for 2–3 min each. Apply 50% ethanol for 2–3 min once and ethanol 70% for 2–3 min one time. Rinse the samples twice for 2–3 min in 96% ethanol solution. After that, rinse the samples with isopropanol twice for 2–3 min, and finally rinse the samples twice in xylene for 10 min each.

17. Mount the samples.

Nonimmunized rabbit serum was used as negative control.

Evaluation of COX2 Immunostaining

The specimens immunostained for COX2 were evaluated according to the intensity and extent of positive reaction of tumor cells on a semiquantitative scale. The number of stained versus not stained epithelial cells was counted in at least 500 cancer cells in the area of the most intense staining. A labeling index of COX2 staining was calculated by dividing the number of stained cells by all counted tumor cells. The median labeling index was the base of the calculations for the Chi-square test and the univariate and multivariate analyses; patients were classified in two groups, one above and one below the median COX2 labeling index. In addition, in all tumor samples the staining intensity of COX2 was divided semiquantitatively into grades 1–4, from grades 1 (low), 2 (mild), 3 (moderate), to 4 (high). In 46 of all specimens simultaneous evaluation of the staining intensity of normal tissue mucosa was possible.

Patient Samples

Specimens from 62 consecutive patients with International Union Against Cancer (UICC) stage I–III rectal cancer received radical surgical treatment at the Department of General and Abdominal Surgery at the Hospital Dresden-Friedrichstadt, in the period 1995–1996, were evaluated. None of the patients underwent neoadjuvant chemotherapy or radiotherapy. The mean follow-up period was 42 months (standard deviation [SD] ±17 months). The tumor was curatively resected in all patients; however, no mesorectal excision was performed in general. The mean number of examined lymphnodes was 10 (SD ±8).

Survival

The survival of patients was quantified in two different endpoints: overall survival and disease-specific survival. The overall survival excluded all dead

patients independent of cause of death. The disease-specific survival was defined as cumulative survival for patients with curative resection, excluding patients who died from cancer-related causes, with a proven local recurrence, distant metastasis, or both. Survival time was counted starting at the day of surgery.

Local Recurrence and Distant Metastasis

All 62 patients had a curative resection, defined as complete removal of all macroscopically evident tumor and cancer-free resection margins on histologic examination. Patients who developed a histologically proven local recurrence, an anastomotic recurrence, or combined local recurrence with distant metastasis were included in the group of local recurrence. Distant metastasis was defined as newly discovered evidence of tumor recurrence using standard follow-up for colorectal cancer. Pulmonary metastases were detected by routine chest X-ray.

Tumor Classification and Histologic Categorization

According to the World Health Organization (WHO) categorization, only adenocarcinomas (International Classification of Diseases Manual [ICDM] 8140/3 or 8480/3) were included in this study. Mucinous tumors (ICDM 8480/3) were defined as more than 50% mucin in the extracellular matrix. The tumor classification was based on the TNM (tumor, lymph nodes, metastasis) staging system, including L category for lymph vessel invasion and the V1 classification for microscopic venous invasion (Hermanek *et al.,* 1997).

Statistical Methods

Statistical analysis was performed using the SPSS 10.0.7 software package (SPSS, Inc., Chicago, IL). Actuarial survival curves were calculated and plotted according to the Kaplan-Meier life-table method. For univariate analysis, comparison between the survival curves was made using the log-rank test. Variables with *p*-value less than 0.05 were considered to be significant.

RESULTS AND DISCUSSION

Tumor Staining

All of the 62 specimens were stained positively for COX2 with a cytoplasmic immunoreactivity. There was a typical staining pattern of granular immunoreactivity in the apical part of the epithelial
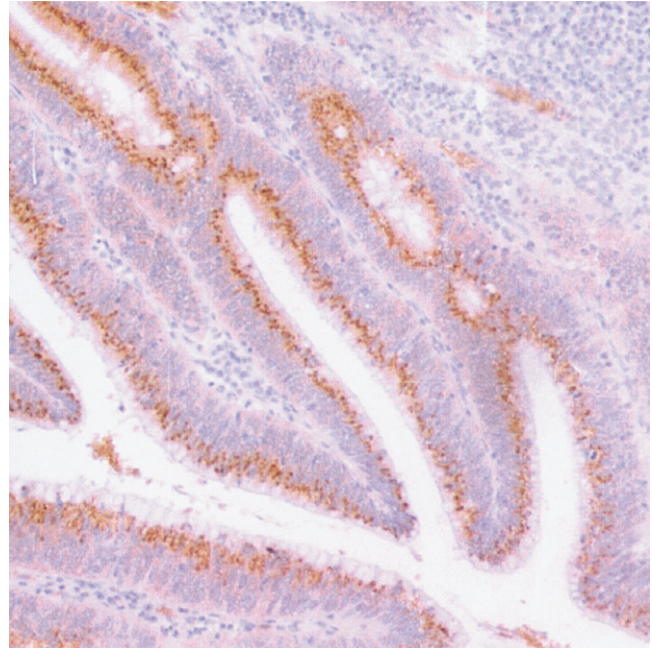
Figure 30 COX2 staining in a highly differentiated tubulopapillar rectal adenocarcinoma (G1): intensive immunoreactivity in perinuclear granular of the epithelial tumor cells, nuclei with hematoxylin counterstaining (original magnification 100X).

cells (Figure 30). No staining of the nucleus was observed. This is in agreement with other publications, which also found the staining pattern predominantly localized in the cytoplasm and the nuclear envelope (Tomozawa *et al.,* 2000; Yamauchi *et al.,* 2002). In this study, no staining of stroma cells was observed. This finding is supported by other authors who also found no stroma staining (Yamauchi *et al.,* 2002). In contrast, there are also publications showing COX2 staining in stroma cells (Konno *et al.,* 2002; Tomozawa *et al.,* 2000). The median COX2 labeling index was 0.58 (SD ±0.25). Low staining intensity was observed in 10 specimens (16%); it was mild in 18 (29%), moderate in 28 (45%), and high in 6 cases (10%).

Mucosa Staining

In 46 specimens (74%), mucosa could be evaluated. In the normal tissue the COX2 staining was evaluated as high in 1 specimen (2%); the staining was moderate in 19 cases (41%), mild in 18 cases (39%), and low in 8 specimens (17%). The distribution of staining in tumor versus normal mucosa showed no difference. There was an increase of staining intensity from the distant parts of the mucosa to the tumor-adjacent mucosal areas in 17 cases (37%). These findings are in good agreement with other studies, which found COX2 staining of adjacent mucosa only in a minority of samples

(Tomozawa *et al.,* 2000; Zhang and Sun, 2002). However, it is emphasized that COX2 is eventually detectable in normal tissue. Thus, the simple paradigm that COX2 is found only in inflammatory- and cancer-related tissues is not always true. Whether this investigation is of relevance needs to be evaluated in further studies.

COX2 as Prognostic Factor for Survival

The follow-up of 62 patients with rectal carcinoma revealed that 25 patients (40.3%) died. Using the median labeling index to distinguish low from high COX2 expression for survival analysis showed that 12 patients died after a mean of 48.6 months in the group of low COX2 expression and 13 patients died in the overexpression group after 44.2 months. These results are obviously not significant in the Kaplan-Meier survival statistics ($p = 0.69$). However, using a much higher threshold of a labeling index of 0.74 for COX2 overexpression provided significant results in the survival analysis, where 13 patients in the overexpression group only had a follow-up of 34.6 months compared to 49.7 months of survival in 49 patients with low COX2 expression ($p < 0.01$).

In the case of colorectal cancer and survival, a large variety of potential prognostic factors are available. Besides the well-established prognostic factors, the number of biologic and molecular markers that characterize carcinomas is increasing (Ratto *et al.,* 1998). In addition, there are surgery-related factors, such as the extent of mesorectal excision in rectal surgery, the surgeon himself, or complicating events, which affect prognosis (Hermanek, 1999a; Marusch *et al.,* 2002).

Thus, Hermanek postulated the following recommendation for prognostic factors using immunohistochemistry: 1) standardization of methods to increase the acceptance of potential prognostic or predictive factors; 2) analysis of potential new markers must include the established prognostic factors with the highest statistical power (pT, pN, UICC stage, and curative resection R) (comments in Petersen *et al.,* 2001).

According to the value of prognostic factors, the Colorectal Working Group published the "American Joint Committee on Cancer Prognostic Factors Consensus Conference." In this survey, prognostic factors were classified into four groups (Compton *et al.,* 2000). Category I includes prognostic factors that are well evaluated by published data and on which treatment strategies are based and which can modify the established TNM classification. In category IIa, factors from clinical or histologic evaluations with prognostic value might be added to the histopathologic characterization tumors. Category IIb includes well-studied prognostic factors that are not sufficiently established for category I or IIa. Prognostic variables, which are not yet established to meet criteria for category I and II, are summarized in category III. Category IV includes prognostic factors that show no consistent prognostic significance.

The most important prognostic factors in category I are variables, which are included into TNM classification and the UICC stage (Compton *et al.,* 2000; Fielding *et al.,* 1991; Hermanek, 1999b).

According to relevance of COX2 expression and survival analyses only data on immunohistochemistry (IHC) evaluation of COX2 are available (Table 4). Three studies found significant impact of COX2

Table 4 Published Data of Prognostic Influence of COX2 in Colorectal Cancer

Author	Patients	Therapy	COX2 Detection	Antibody (Dilution)	Cutoff (No. Patient: Negative versus Positive)	Overall Survival	Disease-Specific Survival
Konno *et al.* (2002)	56	Surgery	IHC	IBL (1:20)	>5% (42 versus 14)	Significant	n.s.
Masunaga *et al.* (2000)	100	Surgery (n = 58 postoperative chemotherapy)	IHC	Cayman (1:300)	>0% (24 versus 76)	Significant	n.s.
Öhd *et al.* (2003)	61	Surgery	IHC	Cayman (1:500)	Low/moderate versus high/very high (n.s.)	Insignificant	n.s.
Sheehan *et al.* (1999)	76	Surgery	IHC	Cayman (1:500)	>1% (14 versus 62)	Significant	n.s.
Tomozawa *et al.* (2000)	63	Surgery	IHC	IBL (1:40)	>50% (50 versus 13)	n.s.	Significant
Yamauchi *et al.* (2002)	232	Surgery	IHC	Alexis (1:1000)	>70% (66 versus 166)	n.s.	Significant
Zhang *et al.* (2002)	112	n.s.	IHC	Dako (1:400)	n.s. (31 versus 81)	Insignificant	n.s.

IHC, immunohistochemistry; n.s., not stated.

expression on the overall survival (Konno *et al.,* 2002; Masunaga *et al.,* 2000; Sheehan *et al.,* 1999); two additional studies provided evidence that COX2 overexpression reduced the disease-specific survival (Tomozawa *et al.,* 2000; Yamauchi *et al.,* 2002). Their results are inconsistent with the results reported here. Using the median COX2 labeling index as a cutoff point, no significant influence on local recurrence or survival was found. The data presented here, however, are in good agreement with the results presented by Zhang *et al.* (2002) and Öhd *et al.* (2003). In a study including 112 patients with colorectal cancer, Zhang found no impact of COX2 expression on survival (Zhang and Sun, 2002). The authors concluded that COX2 overexpression is more likely linked to cancer differentiation rather than to prognostic value. Öhd *et al.* also could not confirm the relevance of COX2 overexpression on overall survival in 61 patients with colorectal cancer; they only found an impact of COX2 on survival in a subgroup of UICC-stage II patients (Öhd *et al.,* 2003).

The results with IHC can vary because of different antibodies, variations in the technique of incubation and antigen fixation, subjectivity in scoring, and absence of uniform cutoff value for definition of positive tumors. Accordingly, reasons for divergent results from different publication are mainly the result of differences of the immunohistochemical staining techniques (Garewal *et al.,* 2003). As stated in Table 4, techniques for assessing the COX2 activation vary extensively (e.g., dilution of the antibody or the incubating time). In this study the Oxford polyclonal antibody was used. In contrast, other published data on COX2 in colorectal cancer and prognostic evaluation used other antibodies. Two studies used the IBL antibody (Konno *et al.,* 2002; Tomozawa *et al.,* 2000); three used the Cayman antibody (Masunaga *et al.,* 2000; Öhd *et al.,* 2003; Sheehan *et al.,* 1999). In one study the Dako antibody was used (Zhang and Sun, 2002); in another study the staining analysis was performed using the Alexis antibody (Yamauchi *et al.,* 2002).

Another methodologic problem is the cutoff point to distinguish COX2 overexpression. The threshold varies substantially among different studies. Masunaga *et al.* (2000) and Sheehan *et al.* (1999) considered tumors with a minimal COX2 staining as positive. In contrast, Tomozawa *et al.* (2000) regarded IHC as COX2 overexpressed when 50% of all tumor cells showed staining pattern. Using the median labeling index as cutoff, the data presented here provide no impact of COX2 expression on local recurrence or overall survival. In contrast, there was a significant increased number of isolated pulmonary metastasis in the COX2 overexpression group.

Changing the cutoff point of the labeling index to 0.74, only 13 patients showed COX2 overexpression. However, in this group the disease-specific and the overall survival were significantly decreased. This result of negative impact of very high COX2 expression is in good agreement with other studies. Konno *et al.* (2002) and Masunaga *et al.* (2000) found also a decreased overall survival associated with COX2 overexpression. Tomozawa *et al.* (2000) and Yamauchi *et al.* (2002) were able to show this effect of high COX2 levels on disease-specific survival. Thus, low COX2 expression in colorectal tumors does not seem to be linked to malign potential of carcinoma. In contrast, severe COX2 overexpression indicates increased malign potency of a tumor and an increased risk of potential metastatic spread. Only a small number of data is published according to the relevance of COX2 overexpression on local recurrence of colorectal cancer (Tomozawa *et al.,* 2000). The data presented here provide evidence that COX2 overexpression is not linked to local failure following curative resection of rectal carcinoma.

COX2 and Metastasis

One of the potential reasons of decreased survival associated with COX2 overexpression is an increased capability of the overexpressing tumor for metastatic spread. The data presented here show a higher incidence of lung metastasis in the group with increased levels of COX2 expression in the tumor samples. Using the median labeling index of 0.58, isolated lung metastasis was observed in five patients; all of these metastatic events happened in the overexpression group, which was obviously statistically significant in the Kaplan-Meier analysis ($p = 0.04$). In eight patients the rectal carcinoma recurred locally—five times in the lower expression group and only three times in the group with COX2 overexpression. These results were insignificant ($p = 0.41$). The outcome presented here gives evidence that increased levels of COX2 expression in rectal carcinoma are associated with higher potency of hematogenous metastatic spread. The latter effect of COX2 is most likely linked to higher levels of PGs that are known to cause increased metastatic events (Honn *et al.,* 1981).

Metastatic events are the result of a complicated interaction between tumor and host. Primary tumor growth is followed by tumor cell translation to the location of metastasis; this event is closely related to angiogenesis (Hejna *et al.,* 1999; Liotta *et al.,* 1993). Thus, increased COX2-associated neoangionenesis might explain higher rates of hemateneous metastasis

in tumors with COX2 overexpression (Cianchi *et al.,* 2001; Costa *et al.,* 2002; Gallo *et al.,* 2001). Cianchi *et al.* (2001) reported a strong correlation between COX2 and vascular endothelial growth factor (VEGF) expression in human colorectal cancer specimens, and Gallo *et al.* (2001) showed head and neck tumors with high levels of VEGF and COX2 expression and significantly higher vascularization. Tomozawa *et al.* (2000) also reported increased rates of hematogenous metastasis in patients with COX2 overexpression in the tumor samples. These data were supported by experimental results from the same group. In a mouse model, they evaluated the number of lung metastases following intravenous tumor injection. The number of pulmonary metastases was significantly reduced by application of selective COX2 inhibitor (Tomozawa *et al.,* 1999).

The biologic background of the influence of COX2 expression on tumor growth and metastatic potential is a focus of investigation. There is evidence that high COX2 expression is associated with mutant p53 (Leung *et al.,* 2001) or with EGF and nuclear factor-κB expression (Saha *et al.,* 1999; Sato *et al.,* 1997). In addition, data are available from cell culture and *in vivo* studies indicating that elevated levels of COX2 promote angiogenesis, which might influence the metastatic behavior of tumor cells (Kishi *et al.,* 2000; Sawaoka *et al.,* 1999). Another mechanism that might be involved in COX2-associated metastatic spread is the connection of COX2 and the matrix-metalloproteinase 2 (MMP-2). MMP-2 modulates cell surface integrity and was shown to be associated with increased metastatic spread in a variety of tumors (Baker *et al.,* 2000; Barozzi *et al.,* 2002). Using COX2 transfected colorectal cancer cell in *in vitro* experiments it was shown that COX2 induced increased MMP-2 activity (Tsujii *et al.,* 1997). Other metastasis-inducing factors that might be linked to COX2 overexpression are urokinase-type plasminogen activator (uPA) and interleukins (Fosslien, 2000; Konno *et al.,* 2002).

Because there is increasing emphasis to stratify treatment modalities according to molecular parameters, the critical evaluation of prognostic molecular factors has become essential (Petersen *et al.,* 2001). According to COX2 overexpression in tumor samples, and the data presented here, the conclusion can be drawn that COX2 overexpression is linked to increased tumor aggressiveness. However, the immunohistochemical detection of COX2 is not yet an established prognostic factor. According to the American Joint Committee on Cancer Prognostic Factors Consensus Conference, at present COX2 overexpression can be classified as level IIb to III prognostic factor (Compton *et al.,* 2000).

CONCLUSIONS

The data presented here indicate that COX2 overexpression, detected with IHC analysis, has a marginal impact on the survival of surgically treated patients with colorectal cancer, but there is need for standardization of the technical approach to assess COX2 overexpression. Presently, there is not enough evidence that COX2 mutation is a predictive factor for response to adjuvant treatment. One of the major questions is how to treat patients with an immunohistochemical COX2 overexpression, cannot be answered sufficiently from the data. The role of COX2 as a predictive factor in colorectal cancer, therefore, needs to be addressed in appropriate clinical trials.

Since selective COX2 inhibitors became available, the detection of COX2 expression has played an emerging role in the stratification of treatment with COX2 inhibitors in human malignant tumors. Experimental data show that COX2 inhibition, especially in combination with other treatment modalities, might be one part of cancer treatment in the future (Milas, 2001; Petersen *et al.,* 2000). Studies are ongoing to evaluate the role of COX2 inhibition in human malignant neoplasms (Chang, 2002; VICTOR, 2000). The results of these studies will soon give evidence whether COX2 needs to be focused more in cancer treatment.

Acknowledgments

References

Achiwa, H., Yatabe, Y., Hida, T., Kuroishi, T., Kozaki, K., Nakamura, S., Ogawa, M., Sugiura, T., Mitsudomi, T., and Takahashi, T. 1999. Prognostic significance of elevated cyclooxygenase 2 expression in primary, resected lung adenocarcinomas. *Clin. Cancer Res. 5*:1001–1005.

Appleby, S.B., Ristimaki, A., Neilson, K., Narko, K., and Hla, T. 1994. Structure of the human cyclo-oxygenase-2 gene. *Biochem. J. 302*:723–727.

Baker, E.A., Bergin, F.G., and Leaper, D.J. 2000. Matrix metalloproteinases, their tissue inhibitors and colorectal cancer staging. *Br. J. Surg. 87*:1215–1221.

Barozzi, C., Ravaioli, M., D'Errico, A., Grazi, G.L., Poggioli, G., Cavrini, G., Mazziotti, A., and Grigioni, W.F. 2002. Relevance of biologic markers in colorectal carcinoma: A comparative study of a broad panel. *Cancer 94*:647–657.

Chang, E.L. 2002. Phase I study of VIOXX and radiation therapy for brainstem gliomas. Study ID 01-460: M.D. Anderson Cancer Center, Houston TX.

Cianchi, F., Cortesini, C., Bechi, P., Fantappie, O., Messerini, L., Vannacci, A., Sardi, I., Baroni, G., Boddi, V., Mazzanti, R., and Masini, E. 2001. Up-regulation of cyclooxygenase 2 gene expression correlates with tumor angiogenesis in human colorectal cancer. *Gastroenterology 121*:1339–1347.

Compton, C., Fenoglio-Preiser, C.M., Pettigrew, N., and Fielding, L.P. 2000. American Joint Committee on Cancer Prognostic Factors Consensus Conference: Colorectal Working Group. *Cancer 88*:1739–1757.

Costa, C., Soares, R., Reis-Filho, J.S., Leitao, D., Amendoeira, I., and Schmitt, F.C. 2002. Cyclo-oxygenase 2 expression is associated with angiogenesis and lymph node metastasis in human breast cancer. *J. Clin. Pathol. 55*:429–434.

Dimberg, J., Samuelsson, A., Hugander, A., and Soderkvist, P. 1999. Differential expression of cyclooxygenase 2 in human colorectal cancer. *Gut 45*:730–732.

DuBois, R.N., Awad, J., Morrow, J., Roberts, L.J., 2nd, and Bishop, P.R. 1994. Regulation of eicosanoid production and mitogenesis in rat intestinal epithelial cells by transforming growth factor-alpha and phorbol ester. *J. Clin. Invest. 93*:493–498.

Eberhart, C.E., Coffey, R.J., Radhika, A., Giardiello, F.M., Ferrenbach, S., and DuBois, R.N. 1994. Up-regulation of cyclooxygenase 2 gene expression in human colorectal adenomas and adenocarcinomas. *Gastroenterology 107*:1183–1188.

Fielding, L.P., Arsenault, P.A., Chapuis, P.H., Dent, O., Gathright, B., Hardcastle, J.D., Hermanek, P., Jass, J.R., and Newland, R.C. 1991. Clinicopathological staging for colorectal cancer: an International Documentation System (IDS) and an International Comprehensive Anatomical Terminology (ICAT). *J. Gastroenterol. Hepatol. 6*:325–344.

Fosslien, E. 2000. Molecular pathology of cyclooxygenase-2 in neoplasia. *Ann. Clin. Lab. Sci. 30*:3–21.

Fujita, M., Fukui, H., Kusaka, T., Ueda, Y., and Fujimori, T. 2000. Immunohistochemical expression of cyclooxygenase (COX)-2 in colorectal adenomas. *J. Gastroenterol. 35*:488–490.

Fujita, T., Matsui, M., Takaku, K., Uetake, H., Ichikawa, W., Taketo, M.M., and Sugihara, K. 1988. Size- and invasion-dependent increase in cyclooxygenase 2 levels in human colorectal carcinomas. *Cancer Res. 58*:4823–4826.

Gallo, O., Franchi, A., Magnelli, L., Sardi, I., Vannacci, A., Boddi, V., Chiarugi, V., and Masini, E. 2001. Cyclooxygenase-2 pathway correlates with VEGF expression in head and neck cancer. Implications for tumor angiogenesis and metastasis. *Neoplasia 3*:53–61.

Garewal, H., Ramsey, L., Fass, R., Hart, N.K., Payne, C.M., Bernstein, H., and Bernstein, C. 2003. Perils of immunohistochemistry: Variability in staining specificity of commercially available COX-2 antibodies on human colon tissue. *Dig. Dis. Sci. 48*:197–202.

Hejna, M., Raderer, M., and Zielinski, C.C. 1999. Inhibition of metastases by anticoagulants. *J. Natl. Cancer Inst. 91*:22–36.

Hermanek, P. 1999a. Impact of surgeon's technique on outcome after treatment of rectal carcinoma. *Dis. Colon Rectum 42*:559–562.

Hermanek, P. 1999b. Prognostic factor research in oncology. *J. Clin. Epidemiol. 52*:371–374.

Hermanek, P., Hutter, R.V.P., Sobin, L.H., Wagner, G., and Wittekind, C. 1997. *TNM atlas,* 4th Edition. Berlin, Heidelberg, New York: Springer.

Hida, T., Yatabe, Y., Achiwa, H., Muramatsu, H., Kozaki, K., Nakamura, S., Ogawa, M., Mitsudomi, T., Sugiura, T., and Takahashi, T. 1998. Increased expression of cyclooxygenase 2 occurs frequently in human lung cancers, specifically in adenocarcinomas. *Cancer Res. 58*:3761–3764.

Honn, K.V., Bockman, R.S., and Marnett, L.J. 1981. Prostaglandins and cancer: a review of tumor initiation through tumor metastasis. *Prostaglandins 21*:833–864.

Kargman, S.L., O'Neill, G.P., Vickers, P.J., Evans, J.F., Mancini, J.A., and Jothy, S. 1995. Expression of prostaglandin G/H synthase-1 and -2 protein in human colon cancer. *Cancer Res. 55*:2556–2559.

Khuri, F.R., Wu, H., Lee, J.J., Kemp, B.L., Lotan, R., Lippman, S.M., Feng, L., Hong, W.K., and Xu, X.C. 2001. Cyclooxygenase-2 overexpression is a marker of poor prognosis in stage I non-small cell lung cancer. *Clin. Cancer Res. 7*:861–867.

Kishi, K., Petersen, S., Petersen, C., Hunter, N., Mason, K., Masferrer, J.L., Tofilon, P.J., and Milas, L. 2000. Preferential enhancement of tumor radioresponse by a cyclooxygenase-2 inhibitor. *Cancer Res. 60*:1326–1331.

Konno, H., Baba, M., Shoji, T., Ohta, M., Suzuki, S., and Nakamura, S. 2002. Cyclooxygenase-2 expression correlates with uPAR levels and is responsible for poor prognosis of colorectal cancer. *Clin. Exp. Metastasis 19*:527–534.

Kraemer, S.A., Meade, E.A., and DeWitt, D.L. 1992. Prostaglandin endoperoxide synthase gene structure: Identification of the transcriptional start site and 5′-flanking regulatory sequences. *Arch. Biochem. Biophys. 293*:391–400.

Kujubu, D.A., Fletcher, B.S., Varnum, B.C., Lim, R.W., and Herschman, H.R. 1991. TIS10, a phorbol ester tumor promoter-inducible mRNA from Swiss 3T3 cells, encodes a novel prostaglandin synthase/cyclooxygenase homologue. *J. Biol. Chem. 266*:12866–12872.

Kutchera, W., Jones, D.A., Matsunami, N., Groden, J., Mclntyre, T.M., Zimmerman, G.A., White, R.L., and Prescott, S.M. 1996. Prostaglandin H synthase 2 is expressed abnormally in human colon cancer: Evidence for a transcriptional effect. *Proc. Natl. Acad. Sci. USA. 93*:4816–4820.

Leung, W.K., To, K.F., Ng, Y.P., Lee, T.L., Lau, J.Y., Chan, F.K., Ng, E.K., Chung, S.C., and Sung, J.J. 2001. Association between cyclo-oxygenase-2 overexpression and missense p53 mutations in gastric cancer. *Br. J. Cancer 84*:335–339.

Liotta, L.A., and Stetler-Stevenson, W.G. 1993. *Principles of Molecular Cell Biology of Cancer: Cancer Metastasis*, 4th ed. Philadelphia: J.B. Lippincott.

Marusch, F., Koch, A., Schmidt, U., Zippel, R., Geissler, S., Pross, M., Roessner, A., Kockerling, F., Gastinger, I., and Lippert, H. 2002. "Colon-/rectal carcinoma" prospective studies as comprehensive surgical quality assurance. *Chirurg 73*:138–145.

Masunaga, R., Kohno, H., Dhar, D.K., Ohno, S., Shibakita, M., Kinugasa, S., Yoshimura, H., Tachibana, M., Kubota, H., and Nagasue, N. 2000. Cyclooxygenase-2 expression correlates with tumor neovascularization and prognosis in human colorectal carcinoma patients. *Clin. Cancer Res. 6*:4064–4068.

Milas, L. 2001. Cyclooxygenase-2 (COX-2) enzyme inhibitors as potential enhancers of tumor radioresponse. *Semin. Radiat. Oncol. 11*:290–299.

Öhd, J.F., Nielsen, C.K., Campbell, J., Landberg, G., Lofberg, H., and Sjolander, A. 2003. Expression of the leukotriene D4 receptor CysLT1, COX-2, and other cell survival factors in colorectal adenocarcinomas. *Gastroenterology 124*:57–70.

Petersen, C., Petersen, S., Milas, L., Lang, F.F., and Tofilon, P.J. 2000. Enhancement of intrinsic tumor cell radiosensitivity induced by a selective cyclooxygenase-2 inhibitor. *Clin. Cancer Res. 6*:2513–2520.

Petersen, S., Thames, H.D., Nieder, C., Petersen, C., and Baumann, M. 2001. The results of colorectal cancer treatment by p53 status. *Dis. Colon Rectum 44*:322–334.

Ratto, C., Sofo, L., Ippoliti, M., Merico, M., Doglietto, G.B., and Crucitti, F. 1998. Prognostic factors in colorectal cancer.

Literature review for clinical application. *Dis. Colon Rectum* *41*:1033–1049.

Saha, D., Datta, P.K., Sheng, H., Morrow, J.D., Wada, M., Moses, H.L., and Beauchamp, R.D. 1999. Synergistic induction of cyclooxygenase-2 by transforming growth factor- beta1 and epidermal growth factor inhibits apoptosis in epithelial cells. *Neoplasia 1*:508–517.

Sano, H., Kawahito, Y., Wilder, R.L., Hashiramoto, A., Mukai, S., Asai, K., Kimura, S., Kato, H., Kondo, M., and Hla, T. 1995. Expression of cyclooxygenase-1 and -2 in human colorectal cancer. *Cancer Res. 55*:3785–3789.

Sato, T., Nakajima, H., Fujio, K., and Mori, Y. 1997. Enhancement of prostaglandin E2 production by epidermal growth factor requires the coordinate activation of cytosolic phospholipase A2 and cyclooxygenase 2 in human squamous carcinoma A431 cells. *Prostaglandins 53*:355–369.

Sawaoka, H., Tsuji, S., Tsujii, M., Gunawan, E.S., Sasaki, Y., Kawano, S., and Hori, M. 1999. Cyclooxygenase inhibitors suppress angiogenesis and reduce tumor growth in vivo. *Lab. Invest. 79*:1469–1477.

Sheehan, K.M., Sheahan, K., O'Donoghue, D.P., MacSweeney, F., Conroy, R.M., Fitzgerald, D.J., and Murray, F.E. 1999. The relationship between cyclooxygenase-2 expression and colorectal cancer. *JAMA 282*:1254–1257.

Taketo, M.M. 1998. Cyclooxygenase-2 inhibitors in tumorigenesis (Part I). *J. Natl. Cancer Inst. 90*:1529–1536.

Tomozawa, S., Nagawa, H., Tsuno, N., Hatano, K., Osada, T., Kitayama, J., Sunami, E., Nita, M.E., Ishihara, S., Yano, H., Tsuruo, T., Shibata, Y., and Muto, T. 1999. Inhibition of haematogenous metastasis of colon cancer in mice by a selective COX-2 inhibitor, JTE-522. *Br. J. Cancer 81*: 1274–1279.

Tomozawa, S., Tsuno, N.H., Sunami, E., Hatano, K., Kitayama, J., Osada, T., Saito, S., Tsuruo, T., Shibata, Y., and Nagawa, H. 2000. Cyclooxygenase-2 overexpression correlates with tumour recurrence, especially haematogenous metastasis, of colorectal cancer. *Br. J. Cancer 83*:324–328.

Tsujii, M., Kawano, S., and DuBois, R.N. 1997. Cyclooxygenase-2 expression in human colon cancer cells increases metastatic potential. *Proc. Natl. Acad. Sci. USA. 94*:3336–3340.

VICTOR 2000. VIOXX in colorectal cancer therapy: definition of optimal regime. CRC Trial Unit, Institute for Cancer Studies Clinical Research Block, The Medical School Edgbaston, Birmingham B15 2TT.

Wolff, H., Saukkonen, K., Anttila, S., Karjalainen, A., Vainio, H., and Ristimaki, A. 1998. Expression of cyclooxygenase-2 in human lung carcinoma. *Cancer Res. 58*:4997–5001.

Yamauchi, T., Watanabe, M., Kubota, T., Hasegawa, H., Ishii, Y., Endo, T., Kabeshima, Y., Yorozuya, K., Yamamoto, K., Mukai, M., and Kitajima, M. 2002. Cyclooxygenase-2 expression as a new marker for patients with colorectal cancer. *Dis. Colon Rectum 45*:98–103.

Zhang, H., and Sun, X.F. 2002. Overexpression of cyclooxygenase-2 correlates with advanced stages of colorectal cancer. *Am. J. Gastroenterol. 97*:1037–1041.

Ziche, M., Jones, J., and Gullino, P.M. 1982. Role of prostaglandin E1 and copper in angiogenesis. *J. Natl. Cancer Inst. 69*:475–482.

This Page Intentionally Left Blank

8

Role of Immunohistochemical Expression of Bcl-2 in Colorectal Carcinoma

N.J. Agnantis, A.C. Goussia, E. Ioachim, and D. Stefanou

Introduction

Sequential studies of transformation in a variety of colorectal lesions (ranging from reactive to neoplastic or from adenoma to carcinoma) indicate that carcinogenesis is a stepwise process associated with the accumulation of multiple clonally selected genetic alterations (Fearon and Vogelstein, 1990). These alterations result in accelerated rates of cell division, decreased rates of cell death, or both. An imbalance between cell division and cell death is believed to underlie colorectal cancer development and progression.

Apoptosis or programmed cell death is a tightly regulated mechanism, existing in all multicellular organisms, with importance to a variety of physiologic procedures by eliminating unnecessary cells. During fetal development and morphogenesis, apoptosis is instrumental as the organism acquires its normal shape after the deletion of the excessive cells. During adulthood the maintenance of tissue homeostasis is regulated by a balance between apoptosis and cell proliferation. Obligatory coupling of cell proliferation with cell death provides a potent innate mechanism that suppresses neoplasia.

At the molecular level, the best understood cell death pathways involve those initiated by "death receptors" including Fas (or Apo 1 or CD95) and tumor necrosis factor receptor 1 (TNFR1; or p55 or CD120a).

Deoxyribonucleic acid (DNA) damage can also induce apoptosis through a central player, *p53*, although *p53*-independent pathways also exist. *p53* transmits the apoptotic signal by a complicated mechanism that involves its ability to transactivate target genes, such as *Bax*. In addition, the *Bcl-2* family of genes has a central role in the control of cell death. Since the identification about 20 years ago of the *Bcl-2* gene, a group of genes with homology to *Bcl-2* has been identified. The list of these important effectors of apoptotic pathway continues to grow, and the determination whether a given cell will die in response to an apoptotic stimulus is carefully regulated through a network of positive and negative elements. To date, more than 20 proteins encoded by genes of the Bcl-2 family exist that either suppress (Bcl-x$_L$, Bcl-w, Mcl-1, Boo/DIVA, Bcl-b, A1/Bfl-1) or promote (Bax, Bad, Bak, Bcl-x$_s$, Bik/Nbk, Bid, Bag-1, Bim/Bod, Bok/Mtd, Blk, Bcl-Rambo, Bcl-g) apoptosis by interacting with and/or functionally antagonizing each other (Evan *et al.*, 2001). Disturbances in these pathways have been identified in several types of tumors.

Relevant to the function of several members of the Bcl-2 family is their ability to homodimerize and heterodimerize with each other. Homodimerization or heterodimerization is important for the apoptosis-regulating function and especially the dimerization that takes place between the anti-apoptotic Bcl-2 and

Handbook of Immunohistochemistry and *in situ* Hybridization of Human Carcinomas,
Volume 2: Molecular Pathology, Colorectal Carcinoma, and Prostate Carcinoma

193

the pro-apoptotic Bax protein (Reed, 2000). Some Bcl-2 family proteins also possess dimerization-independent functions. For example, $Bcl-x_L$ has been reported to bind the CED-4–like domain of Apaf-1, which binds to and activates pro-caspase-9 (Pan *et al*., 1998). Some pro-apoptotic members of this family appear to induce alterations in mitochondrial permeability barrier function (Eskes *et al*., 1998). Other biochemical functions of Bcl-2 family proteins have also been described, suggesting that these molecules are multifunctional proteins and the regulation of apoptosis by them occurs through several potential mechanisms. It is interesting that several proteins with anti-apoptotic function, in addition to cell death blocking, have an inhibitory effect on cell proliferation. Mutagenesis studies, however, indicate that both actions may be dissociated from each other (Reed and Krajewski, 1998).

The *Bcl-2* gene was primarily investigated in hematologic malignancies and concretely in follicular B-cell lymphomas, where it contributed to tumorigenesis by preventing cell death (Tsujimoto *et al*., 1985). In these lymphomas, overproduction of both Bcl-2 messenger ribonucleic acid (mRNA) and protein was associated with a t (14;18) chromosomal translocation. However, Bcl-2 overexpression was also found in lymphomas and other malignancies lacking the 14;18 translocation. It has been suggested that this overexpression may prevent or delay normal cell turnover caused by apoptosis, thus prolonging cellular life span, which may increase the risk of secondary genetic alteration resulting in malignant transformation. Subsequent studies showed that high levels of the protein can suppress the initiation of apoptosis in response to a number of stimuli, including chemical oxidative injury, heat shock, ionizing radiation, and chemotherapeutic agents (Miyashita and Reed, 1992). The molecular function of Bcl-2 remains elusive. One idea is that it may regulate the levels of lipid peroxidation products and reactive oxygen species (ROS) within cells, although Bcl-2 can also inhibit anaerobic cell death. In addition, Bcl-2 may inhibit apoptosis by altering Ca2+ fluxes through intracellular organelles or by regulating cell-cycle proteins such as p53.

The recent availability of reagents able to detect Bcl-2 and related proteins in tissues has contributed to the understanding of some mechanisms that regulate apoptotic pathways. The role of Bcl-2 expression in oncogenesis is currently being investigated in a number of studies in many cancerous tissues, using immunohistochemical approaches (Hanaoka *et al*., 2002; Ioachim *et al*., 2000). Bcl-2 in colorectal cancer biology has also been explored. Because adenoma–carcinoma sequence represents the process by which most, if not all, colorectal cancers arise, many investigators have focused their interest on this aspect of colorectal tumorigenesis involving Bcl-2 expression. This chapter summarizes the main findings of recent immunohistochemical studies, including our experience, and relates Bcl-2 expression to clinicopathologic parameters, expression of proliferation or apoptosis-related proteins, and clinical outcome.

MATERIALS

1. Xylene.
2. Absolute alcohol.
3. Alcohol 96%: 480 ml absolute alcohol and 20 ml double-distilled water (DDW) to make 500 ml.
4. Tris-buffered saline (TBS). It contains Tris-base, Tris-HCl, and NaCl; bring volume to 1 L with DDW (pH 7.4).
5. 0.01 M citric acid antigen retrieval solution: 0.01 citric acid, 1 N NaOH (pH 6.0).
6. 1% bovine serum albumin (BSA): 1 g BSA and 100 ml TBS; and BSA to buffer with stirring.
7. 3% hydrogen peroxidase (H_2O_2): 1 ml of 30% H_2O_2 and 99 ml methanol.
8. Primary antibodies diluted in TBS with 1% BSA: anti-Bcl-2 (M0887, clone 124, Dako [Glostrup, Germany], dilution 1:40); anti-p53 (clone DO-7, Dako, dilution 1:50); anti-Ki-67 (MIB-1, Dako, dilution 1:50).
9. Diaminobenzidine (DAB) tetrahydrochloride chromogen: add 20 µl DAB chromogen in 1 ml substrate buffer.
10. Mounting media.

METHOD

1. Place the sections in xylene for 5 min, twice for deparaffinization.
2. Place the sections through a series of graded alcohols (absolute alcohol; 96% alcohol) for 5 min, twice, for rehydration.
3. Rinse the sections in running tap water for 2 min.
4. Rinse the sections in DDW.
5. Place the sections in a Coplin jar of microwave-compatible plastic, filled with preheated 0.01 M citric acid antigen retrieval solution.
6. Heat the jar in a microwave oven at 300 W for 15 min.
7. Check the antigen retrieval fluid levels and replenish, if necessary. Place the jar in the microwave oven for an additional heating cycle of 15 min.
8. Allow the sections to cool at room temperature for 20 min.
9. Rinse the sections in DDW.

10. Incubate the sections with 3% H_2O_2 for 30 min to block endogenous peroxidase.

11. Rinse the sections in DDW three times.

12. Place the sections in TBS for 10 min.

13. Incubate the sections overnight at 4°C with primary antibodies diluted in TBS containing 1% BSA.

14. Rinse the sections with TBS and place them in TBS for 10 min.

15. Incubate the sections with EnVision/HRP (hydrogen peroxidase) kit (Dako) for 30 min at room temperature.

16. Place the sections in TBS.

17. Incubate the sections with DAB chromogen solution for color development. Check the slides under optical microscope for the color development.

18. Rinse the sections in DDW three times.

19. Place the sections in 10% Harris hematoxylin in DDW for 2 min for counterstaining.

20. Rinse the sections in running tap water.

21. Place the sections into 96% alcohol for 5 min, twice, and subsequently twice in absolute alcohol for 5 min each.

22. Mount the sections with mounting media. They are now ready for final examination in the optic microscope.

RESULTS AND DISCUSSION

As mentioned earlier, the majority of studies in colorectal tumors have used immunohistochemical methods for Bcl-2 detection. In these studies, Bcl-2 was detectable mainly in the cell cytoplasm, and lymphocytes were always used as an internal positive control. However, differences in methodologies used, including estimation of immunostaining and cutoff values chosen by various investigators, provoke differences in the results. Studies have used antigen retrieval methods for adequate detection of Bcl-2 because it has been found that protein expression levels are typically lowered using routine immunohistochemistry (Manne et al., 1997). In a series of 134 colorectal tumors, Manne et al. showed Bcl-2 expression in only 7% of the cases with a concomitant weak staining intensity in the absence of antigen retrieval. The use of antigen retrieval resulted in an increase of the number of stained cells and of staining intensity. In addition, it has been reported that staining intensity is decreased significantly during storage of cut tissue sections (Hayat, 2002) and improvements of storage conditions are proposed by many investigators. Sectioning just prior to immunostaining avoids some of these problems.

Different ways of Bcl-2 estimation including the percentage of stained cells or the staining intensity or both are responsible for the conflicting results in various studies. However, the estimation of stained cells seems to be the most commonly used methodology. According to Baretton et al. (1996) and Buglioni et al. (1999), more than 30% of cells were Bcl-2-immuno-labeled, and this cutoff was chosen to distinguish Bc1-2-negative and Bcl-2-positive cases. Other investigators considered positive protein expression when >5% or >10% of tumor cells were stained (Giatromanolaki et al., 1999; Goussia et al., 2000). Because of tumor heterogeneity, various degrees of staining were also observed. Manne et al. (1997) have discussed the semiquantitative immunostaining score for Bcl-2 using a scale from 0 to 4+ (4+ = the strongest staining intensity), and a score of ≥0.5 was chosen to be positive for protein expression. Bukholm et al. (2000) have mentioned three grades of immunoreactivity (+, ++, +++) that corresponded to 5–10%, 10–50%, and >50% positive cells.

In the existing studies, including ours, the immuno-histochemical expression of Bcl-2 was apparent in normal colonic tissue adjacent to tumor. It is known that during the developmental period Bcl-2 is expressed in every tissue; however, in adults it is expressed only in the proliferating or reserve cells. In colonic tissue, the physiologic expression of Bcl-2 is confined especially to the stem cells and the proliferative zone (i.e., the base of crypts) (Hockenbery et al., 1991). Evidently, the role of Bcl-2 is to protect the stem cells and the renewal and repair abilities of epithelium from apoptosis (Hockenbery et al., 1991).

Sinicrope et al. (1995) reported for the first time the importance of Bcl-2 in colorectal carcinogenesis; 71% of adenomas and 67% of adenocarcinomas showed Bcl-2 immunoreactivity. Subsequent studies revealed similar results, although the reduction of Bcl-2 expression in carcinomas compared with adenomas was more apparent. In most of the relative studies the incidence of Bcl-2 expression ranges from 59% to 86% in adenomas (Baretton et al., 1996; Dursun et al., 2001) and from 31% to 67% in carcinomas (Elkablawy et al., 2001; Giatromanolaki et al., 1999). We also observed a reduction of Bcl-2 expression from adenomas to carcinomas, but the positive cases in our series of tumors were much less than those reported in the literature. Bcl-2 expression was detected in 30.8% of adenomas and only 16.7% in carcinomas (Goussia et al., 2000). Similarly, Leahy et al. (1999) reported Bcl-2 gene product in 22% and Nomura et al. (2000) reported it in 11% of colorectal cancers. Perhaps these discrepancies may be related to differences in methodologic procedures. However, in the majority of the studies the authors suggest that Bcl-2 is involved in the prevention of apoptosis in large bowel epithelium and that if overexpression is important in the carcinogenesis process,

it seems to occur as an early event. In addition, it has been suggested that there may be more than one pathway to malignancy, which could permit carcinomas to arise with down-regulated Bcl-2.

In adenomas, Bcl-2 expression has not been correlated with histologic growth type or grade of dysplasia (Goussia *et al.*, 2000), although a more diffuse staining pattern of higher levels of expression was noted in adenomas of the tubular type and those with mild dysplasia (Yang *et al.*, 1999). However, in other studies Bcl-2 expression showed an inverse decrease along with the degree of dysplasia (Sada *et al.*, 1999). In carcinomas, decreased or lack of Bcl-2 expression has been correlated with high tumor grade, lymph node involvement, advanced Dukes' stage, or distant metastases, whereas high Bcl-2 expression has been observed more frequently in tumors without lymph node or distant metastases (Giatromanolaki *et al.*, 1999; Kim *et al.*, 2002). These observations suggest that Bcl-2–expressing tumors have a less aggressive phenotype than those that do not express, or express in low levels, the protein. This concept has been supported by further studies correlated with patient clinical outcome. However, other studies, including ours, did not show any association of Bcl-2 status with the conventional clinicopathologic parameters (Bukholm *et al.*, 2000; Goussia *et al.*, 2000), whereas a significant correlation of high Bcl-2 expression with Dukes' stage and lymph node metastases has also been described (Zhang *et al.*, 2002).

Differences of Bcl-2 expression according to the macroscopic form of colorectal tumors have been reported. Suzuki *et al.* (2002) showed a significantly lower Bcl-2 expression in flattened or depressed tumors than that in polypoid tumors, suggesting that Bcl-2 may play an important role in the morphogenesis of colorectal neoplasia; Nomura *et al.* (2000) showed contradicting results. Nonpolypoid tumors tend to be *de novo* carcinomas without having adenomatous component or showing *ras* mutations. They are easily invasive neoplasms and therefore are considered as important precursors for advanced colorectal carcinomas. The effect of Bcl-2 on the colorectal tumors at the macroscopic level remains unelucidated. This effect may be clarified when detailed mechanisms of apoptosis become available. From the existing studies, there is no evidence of a relationship between Bcl-2 expression and patient characteristics, such as sex or age, although a rather weaker expression in cancer tissues from the elderly compared with those from the younger patients has been described (Tanaka *et al.*, 2002).

The complex pattern of interrelations among variables related to apoptotic activity, proliferative potential, and

Bcl-2 expression has been studied extensively in colorectal tumors. The TUNEL (terminal deoxynucleotidyl transferase-mediated triphosphotase-biotin nick-end-label staining) technique is the most widely used method to study apoptotic activity because it enables *in situ* detection of fragmented DNA at the single-cell level. The apoptotic process is often described by means of the apoptosis index (AI). It has been demonstrated that apoptosis is reduced during the malignant transformation of colorectal adenoma to carcinoma (Valentini *et al.*, 1999). But it is yet uncertain whether further decrease in apoptosis occurs along with the progression of colorectal carcinomas. However, an increased frequency of apoptosis from Dukes' stages A–D has been reported in established cancers (Evertsson *et al.*, 1999). A close relationship between apoptosis and cell proliferation observed in some colorectal tumors suggests common regulatory mechanisms (Evertsson *et al.*, 1999). This suggestion seems paradoxical because neoplasms with greater AI are slow-growing tumors. Apoptosis is a complex phenomenon, and some potent inducers of cell proliferation (such as C-Myc and the adenovirus oncoprotein E1A) have also pro-apoptotic properties (Adams *et al.*, 1996). In addition, previous reports have speculated that increased cell proliferation might induce apoptosis, probably because of the lack of nutrients, competition for growth factors, or oxygen starvation resulting from the deregulated proliferation (Fearon and Vogelstein, 1990; Sinicrope *et al.*, 1996).

In theory, Bcl-2 inhibits apoptosis, and the relationship found in some colorectal cancer studies supports this aspect (Baretton *et al.*, 1996; Kim *et al.*, 2002). In a series of 57 rectal cancers, Kim *et al.* (2002) showed that the mean AI of tumors without Bcl-2 expression was significantly higher than that of tumors with Bcl-2 expression. In a previous investigation of Barretton *et al.* (1996), Bcl-2 expression was inversely correlated with AI (in a statistically significant manner) in carcinomas only, whereas in adenomas a trend toward a negative correlation was observed. The results seem similar with those observed in other types of tumors, such as breast cancer. Lipponen *et al.* (1995) reported an AI ~30% lower in Bcl-2–positive breast cancers than in Bcl-2–negative tumors. The staining intensity for Bcl-2 was also inversely correlated with the AI. These data suggest that the physiologic function of Bcl-2 for the regulation of apoptosis is preserved not only in normal colonic epithelium but also in cancerous tissue.

In contrast, no significant relationship between AI and Bcl-2 was revealed in several studies (Evertsson *et al.*, 1999; Nomura *et al.*, 2000), whereas opposite results were also reported by others (Elkablawy *et al.*, 2001;

Schwandner *et al.*, 2000). In the study of Elkablawy *et al.* (2001), an increased AI was associated with Bcl-2 expression, in terms of both the percentage of Bcl-2–positive cells and the staining intensity. In contrast, the authors found an inverse correlation of Bcl-2 with mitotic index. Similarly, Schwandner *et al.* (2000) reported a mean AI of 5.13% in Bcl-2–negative rectal cancers compared with 6.5% in Bcl-2–positive tumors. The findings suggest that Bcl-2 is unlikely to be the main reason for the reduction of apoptosis in colorectal tumors. These results were explained by hypothesizing that many other regulators may interact with Bcl-2 to affect cell death. Bcl-2 regulates apoptosis through dimerization, and its influence may be dependent on its association with some other members of the Bcl-2 family (i.e., Bax protein or other unknown proteins controlling the complex molecular pathways leading to apoptosis). The activation of apoptosis in colorectal cancer through pathways different from that of Bcl-2 could be another explanation.

Apoptosis and mitosis are closely interrelated, and several investigations have studied the relationship between Bcl-2 expression and cell proliferation antigens. Ki-67 is considered a powerful marker to differentiate between proliferating and nonproliferating cells. Data regarding this relationship are variable, with some studies showing an inverse correlation between Bcl-2 and Ki-67 indices (Saleh *et al.*, 2000), and others, like ours, revealing no similar relation (Goussia *et al.*, 2000; Kim *et al.*, 2002).

The *p53* tumor suppressor gene is a crucial gene to regulate cell-cycle progression and apoptosis. Apoptosis response after DNA damage is p53-dependent for some cell types. The effect may be partially mediated by Bcl-2 because p53 is capable of down-regulating the transcription of Bcl-2 and up-regulating the apoptosis-promoting protein Bax (Miyashita *et al.*, 1994). Wild-type p53 has been found to decrease Bcl-2 protein levels both *in vivo* and *in vitro*, and mutant p53 has been shown to inhibit Bcl-2 expression in some cancer cell lines (Miyashita *et al.*, 1994). Currently available data on the correlation of Bcl-2 with p53 are often controversial. p53 overexpression has been reported to be inversely correlated with Bcl-2 expression in colorectal cancers (Schwandner *et al.*, 2000), and tumors with low p53 expression frequently showed high levels of Bcl-2, whereas tumors with high p53 expression exhibited low levels of Bcl-2. These results mean that mutant p53 protein may inhibit Bcl-2 gene expression. Sinicrope *et al.* (1995) suggested that this inverse correlation was confined only in adenomas. Being in good accordance with other studies (Elkablawy *et al.*, 2001; Manne *et al.*, 1997), we did not observe any correlation between p53 and Bcl-2 protein, suggesting

that p53 is not involved in the regulation of apoptosis in colorectal tumors. Moreover, it is possible that Bcl-2 expression, as an early event in colorectal carcinogenesis, may occur before changes of p53 take place.

Data regarding the relationship of Bcl-2 expression with other apoptosis-related proteins are scarce. Correlations between Bcl-2 and the proapoptotic protein Bax have been proved inverse (Bukholm *et al.*, 2000). Low levels of Bax protein have been correlated inversely with lymph node involvement, suggesting that it plays a role in the later stages of colorectal cancers. Theoretically, the prognostic significance of both proteins should be reflected by a balance between them, but only limited information is available in this regard.

A large number of studies have been conducted on the possible prognostic value of Bcl-2 in colorectal cancer, and in most of them, Bcl-2 overexpression is considered as a favorable prognostic factor (Buglioni *et al.*, 1999; Manne *et al.*, 1997). Manne *et al.* (1997) have demonstrated in all tumor stages an association of Bcl-2 expression with longer survival. Previously, Sinicrope *et al.* (1995) reported Bcl-2 as a prognostic marker in Dukes' stage B cancers, and in proximal tumors Bcl-2 expression was the most important predictor for overall survival in node-negative colon cancers. In a large study of 171 patients, increased Bcl-2 expression was an independent marker of advanced disease-free survival and overall survival (Buglioni *et al.*, 1999). A correlation of decreased Bcl-2 expression with a high risk of recurrence has also been reported (Schwandner *et al.*, 2000). In contrast, other studies did not show any prognostic significance of Bcl-2 expression (Giatromanolaki *et al.*, 1999), and in a small group of cancers high Bcl-2 levels had been correlated with poor prognosis (Bhatavdekar *et al.*, 1997). Because of contradictory results, we suggest that the prognostic importance of Bcl-2 expression in colorectal cancer may be limited to subgroups of patients or may be related to geographic and/or ethnic variations or to dietary differences in the patient population (Manne *et al.*, 1997). However, in a very interesting meta-analysis study of Grizzle *et al.* (2002), in which ~2000 patients were included, Bcl-2 was revealed as a useful prognostic marker in colorectal cancer.

When the combined effect of Bcl-2 and p53 was examined, patients whose tumors demonstrated Bcl-2 expression but no p53 expression had a better survival, whereas patients whose tumors exhibited p53 nuclear accumulation but not Bcl-2 expression had a worse survival (Buglioni *et al.*, 1999; Schwandner *et al.*, 2000). Taking into account several pathologic parameters, we found that tumors with Bcl-2–positive and p53-negative phenotypes were frequently associated

with negative lymph node status, suggesting that this subgroup of cancers may have a less aggressive behavior. Buglioni *et al.* (1999) showed two different clinicopathologic profiles of colorectal cancers. The first, characterized by Bcl-2 positivity, p53 negativity, diploidy, and low Ki-67 index, was associated with non-recurrent, well-differentiated, and low-stage tumors. The second one, defined by Bcl-2 negativity, p53 positivity, aneuploidy, and high Ki-67 index, was correlated with recurrent, poorly differentiated, and advanced cancers. A significantly shorter disease-free and overall survival were observed in patients bearing p53-positive and Bcl-2–negative tumors. Similar results have been reported by other studies, suggesting that the combined evaluation of p53 and Bcl-2 may be useful for identifying patients to be enrolled in adjuvant setting therapy (Manne *et al.*, 1997).

Bcl-2 protein, as an inhibitor of apoptosis, should be associated with an aggressive tumor phenotype; therefore it should be a predictive factor of a worse clinical course. According to this point of view, the observation that Bcl-2–positive patients have better prognosis and an overall better survival rate, when compared with Bcl-2–negative patients, seems paradoxical. There are some possible explanations for this phenomenon. An inhibitory effect of Bcl-2 on cell proliferation has been suggested. Proliferating cells overexpressing Bcl-2 resist DNA damage–induced apoptosis but undergo growth arrest in G_0/G_1 or G_2/M phases, which promotes tumor cell survival and oncogenic process but does not enhance cell proliferation. Studies by Pietentol *et al.* (1994) of colorectal cancer cell lines also demonstrated growth inhibition as a result of Bcl-2 protein overexpression. The presence of Bcl-2 antagonists, which inhibit its cytoprotective function, or the presence of an anti-proliferative domain in Bcl-2, which would lower the rate of cell proliferation, has also been suggested (Buglioni *et al.*, 1999). The inverse correlation between Bcl-2 and Ki-67 observed in some series of tumors supports the latter hypothesis (Buglioni *et al.*, 1999; Saleh *et al.*, 2000).

The clinical relevance of Bcl-2 expression with regard to patient outcome following chemotherapy is still under investigation and validation. In several neoplasms, Bcl-2 overexpression has been associated with resistance to chemotherapeutic or irradiation treatment. However, in patients with locally advanced, recurrent, or metastatic colorectal cancers who were submitted to undergo different chemotherapeutic agents including methotrexate and fruorouracil/leucovorin, Bcl-2 status was unrelated to clinical outcome (Paradiso *et al.*, 2001).

In conclusion, the role of Bcl-2 in colorectal tumors remains elusive. It is suggested that Bcl-2 expression

appears early in colorectal carcinogenesis. Its immuno-histochemical detection in colorectal cancers may define a subgroup of patients with a favorable clinical outcome. The evaluation of Bcl-2 and p53 together seems to be a better prognostic indicator than the status of either marker alone. At present, there is insufficient evidence to modify treatment recommendations based on Bcl-2 regarding systemic therapy and irradiation. Further studies are needed, especially in a prospective manner, with uniform methods of measurement and cutoff points to assess the potential value of Bcl-2 in clinical practice. Moreover, as more anti-apoptotic mechanisms are uncovered, development of therapeutic strategies that modulate its occurrence in disease process can be expected.

Acknowledgment

References

Adams, P.D., and Kaelin, W.G. Jr. 1996. The cellular effects of E2F overexpression. *Curr. Top. Microbiol. Immunol. 208*:79–93.

Baretton, G.B., Diebold, J., Christoforis, G., Vogt, M., Muller, Chr., Dopfer, K., Schneiderbanger, K., Schmidt, M., and Lohr, U. 1996. Apoptosis and Immunohistochemical bcl-2 expression in Colorectal Adenomas and Carcinomas. Aspects of Carcinogenesis and Prognostic Significance. *Cancer 77*: 255–264.

Bhatavdekar, J.M., Patel, D.D., Ghosh, N., Chikhlikar, P.R., Trivedi, T.I., Suthar, T.P., Doctor, S.S., Shah, N.G., and Balar, D.B. 1997. Coexpression of Bcl-2, c-Myc, p53 onco-proteins as prognostic discriminants in patients with colorectal carcinoma. *Dis. Colon. Rectum 40*:785–790.

Buglioni, S., Agnano, I.D., Cosimelli, M., Vasselli, S., Angelo, C.D., Tedesco, M., Zupi, G., and Mottolese, M. 1999. Evaluation of multiple bio-pathological factors in colorectal adenocarcinomas: Independent prognostic role of p53 and bcl-2. *Int. J. Cancer 84*:545–552.

Bukholm, I.K., and Nesland, J.M. 2000. Protein expression of p53, p21 (WAF1/CIP1), bcl-2, Bax, cyclin D1 and pRb in human colon carcinomas. *Virchows Arch. 436*:224–228.

Dursun, A., Poyraz, A., Suer, O., Sezer, C., and Akyol, G. 2001. Expression of Bcl-2 and c-ErbB-2 in colorectal neoplasia. *Pathol. Oncol. Res. 7*:24–27.

Elkablawy, M.A., Maxwell, P., Williamson, K., Anderson, N., and Hamilton, W. 2001. Apoptosis and cell-cycle regulatory proteins in colorectal carcinoma: Relationship to tumor stage and patient survival. *J. Pathol. 194*:436–443.

Eskes, R., Antonsson, B., Osen-Sand, A., Montessuit, S., Richter, C., Sadoul, R., Mazzei, G., Nichols, A., and Martinous, J.-C. 1998. Bax-induced cytochrome C release from mitochondria is independent of the permeability transition pore but highly dependent on Mg^{2+} ions. *J. Cell Biol. 143*:217–224.

Evan, G.I., and Vousden, K.H. 2001. Proliferation, cell cycle, and apoptosis in cancer. *Nature 411*:342–348.

Evertsson, S., Bartik, Z., Zhang, H., Jansson, A., and Sun, X.F. 1999. Apoptosis in relation to proliferating cell nuclear antigen

and Dukes' stage in colorectal adenocarcinoma. *Int. J. Oncol. 15*:53–58.

Fearon, E.R., and Vogelstein, B. 1990. A genetic model for colorectal tumorigenesis. *Cell 61*:759–767.

Giatromanolaki, A., Stathopoulos, G.P., Tsiobanou, E., Papadimitriou, C., Georgoulias, V., Gatter, K.C., Harris, A.L., and Koukouralis, M.I. 1999. Combined role of tumor angiogenesis, bcl-2 and p53 expression in the prognosis of patients with colorectal carcinoma. *Cancer 86*:1421–1430.

Goussia, A.C., Ioachim, E., Agnantis, N.J., Mahera, M., and Tsianos, E. 2000. Bcl-2 expression in colorectal tumours. Correlation with p53, mdm-2, Rb proteins and proliferating indices. *Histol. Histopathol. 15*:667–672.

Grizzle, W.E., Manne, U., Weiss, H., Jhala, N., and Talley, L. 2002. Molecular staging of colorectal cancer in African-American and Caucasian patients using phenotypic expression of p53, Bcl-2, MUC-1 and p27KIP-1. *Int. J. Cancer 97*:403–409.

Hanaoka, T., Nakayama, J., Hanouda, M., and Sato, T.A. 2002. Immunohistochemical demonstration of apoptosis-regulated proteins, Bcl-2 and Bax, in resected non-small-cell lung cancers. *Int. J. Clin. Oncol. 7*:152–158.

Hayat, M.A. 2002. *Microscopy, Immunohistochemistry, and Antigen Retrieval Methods: For Light and Electron Microscopy*. New York: Kluwer Academic/Plenum Publisher, 1–355.

Hockenbery, D.M., Zutter, M., Hickhey, B., Nahm, M., and Korsmeyer, S.J. 1991. Bcl-2 expression is topographically restricted in tissues characterised by apoptotic cell death. *Proc. Natl. Acad. Sci. USA. 88*:6961–6965.

Ioachim, E., Malamou-Mitsi, V.M., Kamina, S.A., Goussia, A.C., and Agnantis, N.J. 2000. Immunohistochemical expression of bcl-2 protein in breast lesions: Correlation with Bax, p53, Rb, c-erbB-2, EGFR and proliferation indices. *Anticancer Res. 20*:4221–4226.

Kim, Y.-H., Lee, J.H., Chun, H., Nam, S.-J., Lee, W.Y., Song, S.-Y., Kwon, O.J., Hyun, J.G., Sung, I.K., Son, H.J., Rhee, P.L., Kim, J.J., Paik, S.W., Rhee, J.C., and Choi, K.W. 2002. Apoptosis and its correlation with proliferative activity in rectal cancer. *J. Surg. Oncol. 79*:236–242.

Leahy, D.T., Mulcahy, H.E., O'Donoghue D.P., and Parfrey, N.A. 1999. Bcl-2 protein expression is associated with better prognosis in colorectal cancer. *Histopathology 35*:360–367.

Lipponen, P., Pietilainen, T., Kosma, V.-M., Aaltomaa, S., Eskelinen, M., and Syrjanen, K. 1995. Apoptosis suppressing protein bcl-2 is expressed in well-differentiated breast carcinomas with favourable prognosis. *J. Pathol. 177*:49–55.

Manne, U., Myers, R.B., Moron, C., Poczatec, R.B., Dillard, S., Weiss, H., Brown, D., Srivastana, S., and Grizzle, W.E. 1997. Prognostic significance of bcl-2 expression and p53 nuclear accumulation in colorectal adenocarcinoma. *Int. J. Cancer 74*:346–358.

Miyashita, T., and Reed, J.C. 1992. Bcl-2 gene transfer increases relative resistance in S49.1 and WEH17.2 lymphoid cells to cell death and DNA fragmentation induced by glycocorticosteroids and multiple chemotherapeutic drugs. *Cancer Res. 52*:5407–5411.

Miyashita, T., Krajewski, S., Krajewska, M., Wang, H.G., Lin, H.K., Liebermann, D.A., Hoffman, B., and Reed, J.C. 1994. Tumor suppressor p53 is a regulator of bcl-2 and bax gene expression *in vitro* and *in vivo*. *Oncogene 9*:1799–1805.

Nomura, M., Watari, J., Yokota, K., Saitoh, Y., Obara, T., and Kohgo, Y. 2000. Morphogenesis of nonpolypoid colorectal adenomas and early carcinomas assessed by cell proliferation and apoptosis. *Virchows Arch. 437*:17–24.

Pan, G., O'Rourke, K., and Dixit, V.M. 1998. Caspase-9, Bcl-XL, and apaf-1 form a ternary complex. *J. Biol. Chem. 273*:5841–5845.

Paradiso, A., Simone, G., Lena, M.D., Leone, B., Vallego, C., Lacava, J., Dellpasqua, S., Daidone, M.G., and Costa, A. 2001. Expression of apoptosis-related markers and clinical outcome in patients with advanced colorectal cancer. *Br. J. Cancer 84*:651–658.

Pietentol, J., Papadopoulos, N., Markowitz, S., Willson, J., Kinzler, K., and Vogelstein, B. 1994. Paradoxical inhibition of solid tumor cell growth by bcl-2. *Cancer Res. 54*:3714–3717.

Reed, J., and Krajewski, S. 1998. Apoptosis research: Life in the fast lane. *DAKO Research Connection 3*:6–11.

Reed, J.C. 2000. Mechanisms of apoptosis. *Am. J. Pathol. 157*:1415–1430.

Sada, M., Mitomi, H., Igarashi, M., Katsumata, T., Saigenji, K., and Okayasu, I. 1999. Cell kinetics, p53 and bcl-2 expression and c-Ki-ras mutations in flat-elevated tubulovillous adenomas and adenocarcinomas of the colorectum: Comparison with polypoid lesions. *Scand. J. Gastroenterol. 34*:798–807.

Saleh, H.A., Jackson, H., and Banerjee, M. 2000. Immunohistochemical expression of bcl-2 and p53 oncoproteins: Correlation with Ki67 proliferation index and prognostic histopathologic parameters in colorectal neoplasia. *Appl. Immunohistochem. Mol. Morphol. 8*:175–182.

Schwandner, O., Schiedeck, T.H., Bruch, H.P., Duchrow, M., Windhoevel, U., and Broll, R. 2000. p53 and Bcl-2 as significant predictors of recurrence and survival in rectal cancer. *Eur. J. Cancer 36*:348–356.

Sinicrope, F.A., Ruan, S.B., Cleary, K.R., Stephens, L.C., Lee, J.J., and Levin, B. 1995. Bcl-2 and p53 oncoprotein expression during colorectal carcinogenesis. *Cancer Res. 55*:237–241.

Sinicrope, F.A., Rodde, G., McDonnell, T.J., Shen, Y., Cleary, K.R., and Stephens, L.C. 1996. Increased apoptosis accompanies neoplastic development in the human colorectum. *Clin. Cancer Res. 2*:1999–2006.

Suzuki, Y., Honma, T., Hayashi, S., Ajioka, Y., and Asakura, H. 2002. Bcl-2 expression and frequency of apoptosis correlate with morphogenesis of colorectal neoplasia. *J. Clin. Pathol. 55*:212–217.

Tanaka, K., Nagaoka, S., Takemura, T., Atai, T., Sawabe, M., Takubo, K., Sugihava, K., Kitagawa, M., and Hirokawa, K. 2002. Incidence of apoptosis increases with age in colorectal cancer. *Exp. Gerontol. 37*:1469–1479.

Tsujimoto, Y., Cossman, J., Jaffe, E., and Croce, C. 1985. Involvement of the bcl-2 gene in human follicular lymphoma. *Science 228*:1440–1443.

Valentini, A.M., Caruso, M.L., Armentano, R., Pirrelli, M., Rizzi, E., Lopen, F., and Renna, L. 1999. Programmed cell death in colorectal carcinogenesis. *Anticancer Res. 19*:3019–3024.

Yang, H.B., Chow, N.H., Sheu, B.S., Chan, S.H., Chien, C.H., and Su, I.J. 1999. The role of bcl-2 in the progression of the colorectal adenoma-carcinoma sequence. *Anticancer Res. 19*:727–730.

Zhang, M.S., Yuan, H.Y., Xong, B., Deng, Q., Tang, Z.J., and Xia, D. 2002. Expression and clinical significance of IGF-II mRNA and bcl-2 protein in colorectal adenocarcinomas. *Ai. Zheng. 21*:1226–1230.

This Page Intentionally Left Blank

9

Immunohistochemical Detection of CD97 Protein in Colorectal Carcinoma

Gabriela Aust

Introduction

CD97 is a member of a small subfamily of class II G-protein-coupled receptors (GPCRs) referred to as EGF-TM7 (McKnight *et al*., 1998; Stacey *et al*., 2000). These proteins possess N-terminal and a variable number of epidermal growth factor (EGF)-like domains coupled to a seven-span transmembrane (TM7) moiety via an extended stalk region. The varying numbers of EGF-like domains in EGF-TM7 molecules result from alternative splicing of the precursor transcript. CD97 isoforms possessing either three (EGF 1,2,5), four (EGF 1,2,3,5), or five (EGF 1,2,3,4,5) EGF-like domains have been detected (Figure 31). These isoforms always seem to be coexpressed on CD97-positive cells.

CD97 has been implicated in cellular adhesion through its interaction with other cell surface proteins or extracellular matrix proteins. CD55, a membrane-bound molecule acting as a regulatory protein of the complement cascade, has been identified as cellular ligand with the highest affinity to the shortest CD97 isoform (EGF 1,2,5) (Hamann *et al*., 1996). Recently, dermatan sulfate glucosaminoglycan was detected as a ligand for the largest CD97 isoform (EGF 1,2,3,4,5) (Stacey *et al*., 2003).

MATERIALS AND METHODS

Monoclonal Antibodies (MAbs) Against CD97

Antibodies to various epitopes of CD97 vary strongly in their staining pattern and cross-reactivity to other EGF-TM7 molecules. The first group of MAbs, which includes BL-Ac/F2 (Eichler *et al*., 1994), CLB-CD97/1 (Hamann *et al*., 1996), and VIM-3b (Pickl *et al.,* 1995), binds to the first N-terminal EGF-domain of CD97 and is named in this article as the CD97[EGF] MAbs (Table 5). BL-Ac/F2 and CLB-CD97/1 compete for the same epitope. All these MAbs also detect EMR2, another member of the EGF-TM7 family (Lin *et al*., 2000). In most cases, this cross-reactivity to EMR2 will not influence the results obtained for CD97 staining in carcinomas because EMR2 is strongly restricted to myeloid cells (Kwakkenbos *et al*., 2002a). Using 2A1 (Kwakkenbos *et al*., 2002a), the only EMR2-specific MAb available up to now, all gastric, pancreatic, and esophageal carcinomas examined were negative for EMR2 (Aust *et al*., 2002). Only a subpopulation of tumor-infiltrating leukocytes, probably macrophages, was EMR2-positive in tumor tissues. In colorectal carcinomas, we found low staining for

Handbook of Immunohistochemistry and in situ Hybridization of Human Carcinomas,
Volume 2: Molecular Pathology, Colorectal Carcinoma, and Prostate Carcinoma

201
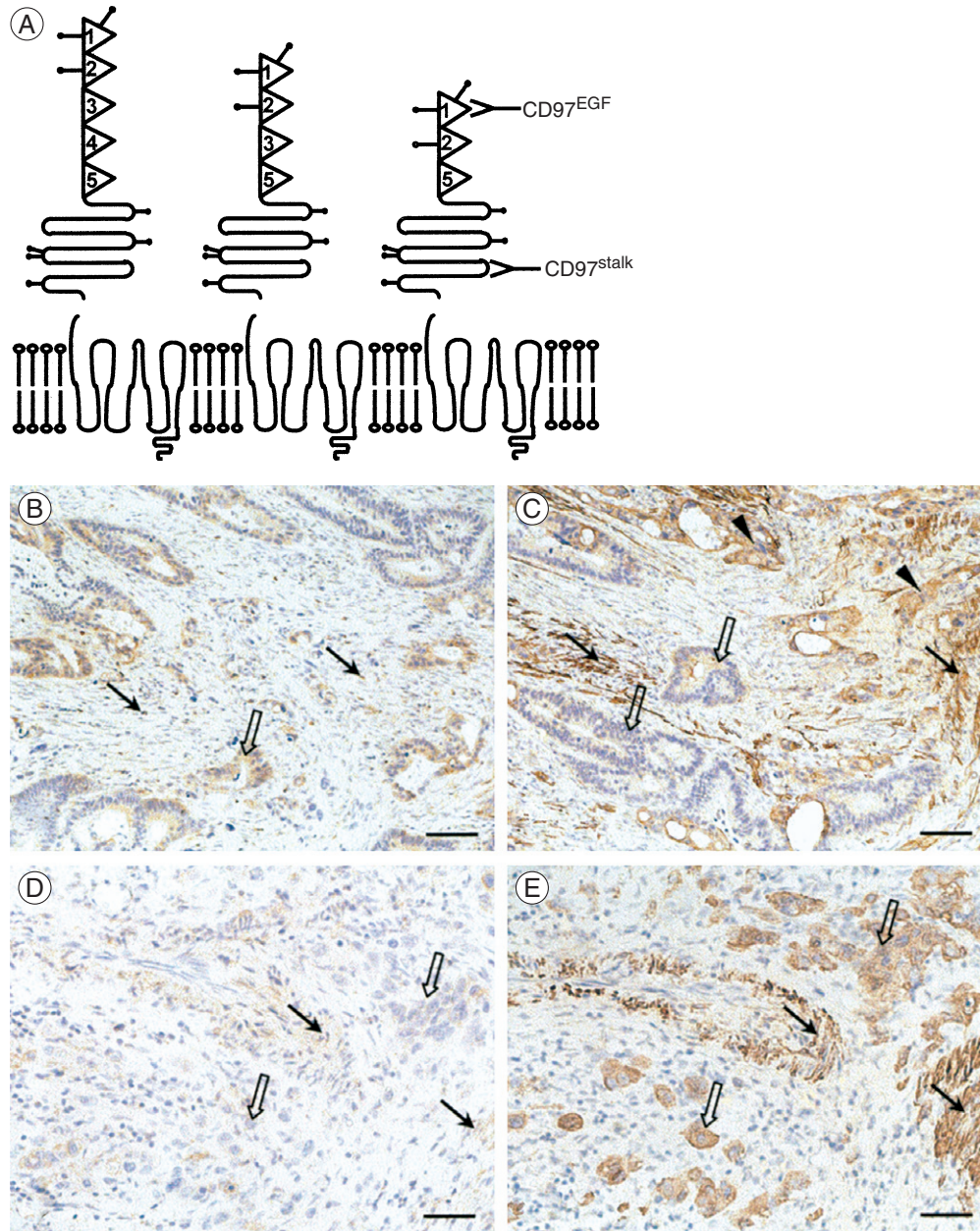
Figure 31 **A:** Schematic presentation of CD97. The molecule is expressed at the cell surface as a heterodimer of an extracellular chain noncovalently associated to a TM7 (transmembrane)/cytoplasmic chain. Different isoforms have been identified that vary in the number of epidermal growth factor (EGF) domains. The binding region of CD97^{EGF} and CD97^{stalk} monoclonal antibodies (MAbs) is indicated. **B–E:** Immunohistologic staining patterns of different CD97 MAbs in sections of colorectal carcinomas. **B,C:** Rectal carcinoma. **B:** Homogenous staining of tumor cells by a CD97^{EGF} MAb (*open arrow*). A few leukocytes located in the stroma were also CD97^{EGF}-positive (*arrow*). **C:** Stronger cytoplasmic and membranous expression of CD97^{stalk} in scattered dedifferentiated tumor cells (*arrow head*) compared to tumor cells located in tumor glands (*open arrow*). Smooth-muscle cells strongly express CD97^{stalk} (*arrow*). **D,E:** Colon carcinoma: Scattered tumor cells did not express CD97^{EGF} (**D**) but CD97^{stalk} (**E**, *open arrow*). Smooth-muscle cells were CD97^{EGF}-negative but CD97^{stalk}-positive (*arrow*). Scale bar: **B,C:** 100 μm; **D,E:** 50 μm.

Table 5 Available CD97 Monoclonal Antibodies

Name of the Monoclonal Antibody	First Description	Commercially Available	Cross-reactivity To	Epitope Within
BL-Ac/F2	(Eichler *et al.*, 1994)	—	EMR2	First EGF-like domain
VIM3b	(Pickl *et al.*, 1995)	BD Biosciences Europe, Erembodegem, Belgium	EMR2	First EGF-like domain
CLB-CD97/1/	(Hamann *et al.*, 1996)	—	EMR2	First EGF-like domain
CLB-CD97/3	(Kwakkenbos *et al.*, 2002b)	—	—	Stalk region
MEM-180	(Kwakkenbos *et al.*, 2002b)	Serotec Ltd, Oxford, UK	—	Stalk region

EMR2 in 10% of the tumors, which clearly contrasts to the known high number of CD97-positive tumors (Aust *et al.*, 2003).

CD97 MAbs MEM-180 (Pickl *et al.*, 1995) and CLB-CD97/3 (Kwakkenbos *et al.*, 2002b) bind to the stalk region of CD97 (CD97^{stalk} MAbs), compete for the same epitope, and do not show any reactivity to EMR2 (Jaspars *et al.*, 2001).

The epitope specificity of CD97^{EGF} and CD97^{stalk} MAbs is strongly correlated with their binding pattern in human normal tissues and cancer specimens. The reason for the varying accessibility among the respective epitopes has been clarified very recently (Wobus *et al.*, 2004). Neither mRNA or protein truncation, varying affinities of the MAbs, cross-reactivity of one of the MAbs with another molecule, or modulation of the molecule conformation by Ca^{2+} could explain the observed differences (own unpublished results). However, as shown by site-directed mutagenesis, deletion of the N-glycosylation sites located within the EGF domains efficiently disturbed CD97^{EGF} MAb immunoreactivity and, more importantly, binding of CD55. In conclusion, CD97^{EGF} epitope accessibility for MAbs and ligand binding is influenced by cell type-specific N-glycosylation. Thus the selection of the CD97 MAb strongly influences the result in immunohistologic studies focused on the correlation between CD97 and histopathologic subtypes, diagnosis, progression, or prognosis. It is important to indicate which CD97 MAb has been used (Table 5).

CD97 mRNA Detection in Tissues

Detection and quantitation of *CD97* messenger ribonucleic acid (mRNA) by competitive or real-time reverse transcription polymerase chain reaction (RT-PCR) in colorectal tumor tissues are not recommended for gaining information on CD97 expression in tumor cells. There are several reasons for this restriction; first, in some of the colorectal carcinomas, a subpopulation of tumor-infiltrating leukocytes, mainly macrophages, are positive for CD97 (and EMR2). Until now, the correlation between the number and distribution of these CD97-positive tumor-infiltrating leukocytes and the clinicopathologic features of the tumor patients has never been investigated. Second, smooth-muscle cells often located between the tumor cells strongly express CD97. Third, discrepancies between the *CD97* mRNA and protein expression levels have been observed (Aust *et al.*, 1997) that suggest post-transcriptional regulation of CD97. *In situ* hybridization allowing the mRNA signal to be matched to a specific cell type may help overcome some of these problems.

CD97 Immunostaining in Tissues

Up to now, CD97 MAbs have only been successfully used on cryostat sections (see Table 5) (Hamann *et al.*, 1999; Visser *et al.*, 2002). None of the MAbs are suitable for paraffin-embedded tissues. Antigen retrieval as 1) pretreatment of the sections with antigen unmasking solutions or 2) heat or ultrasound treatment that induce change in the protein conformation and/or facilitate access to the antibody have not worked. Apart from this restriction, all common immunohistochemical staining methods work well for CD97. Indirect methods are very sensitive, particularly when the avidin–biotin system is used. The use of nonfluorescent conjugates, such as horseradish peroxidase, allows the simultaneous detection of the protein localization and tissue morphology analysis. Here, we will describe one easy method that is sufficient for colorectal carcinomas. Double-labeling techniques enabling the identification of the stained cell type have been published elsewhere (Hamann *et al.*, 1999; Jaspars *et al.*, 2001; Visser *et al.*, 2002).

MATERIALS

1. Phosphate buffer saline (PBS).
2. Primary antibody diluted in PBS.
3. Negative control mouse (DakoCytomation GmbH, Hamburg, Germany; Code-No.: N1698).
4. Biotin blocking system (Dako; code-No.: X0590).
5. Supersensitive detection kit (Vectastain Elite ABC kit; mouse kit; Vector Laboratories, Burlingame, CA; code-No.: PK-6102).
6. 3,3′ diaminobenzidine (DAB; DAB substrate kit, Vector, code-No.: SK-4100).
7. Nonaqueous mounting medium (VectaMount; permanent mounting media, Vector; code-No.: H5000).

METHOD

Sampling

Tissues were snap-frozen in liquid nitrogen. Serial frozen sections were cut at 5 μm, fixed in ice-cold methanol for 10 min, and briefly rinsed in PBS.

Single Staining

Blocking

1. If a horseradish peroxidase (HRP)-conjugated system is used to detect the signal, quenching endogenous peroxidase activity is required by incubating the sections in 0.5% H_2O_2/methanol for 30 min at room temperature. Incubation in H_2O_2 can be increased in tissues with high levels of endogenous peroxidase activity. Normal serum from the species in which the secondary antibody has been raised is generally used to inhibit nonspecific binding of antibodies to cellular components (2–5%/1X PBS; 30 min).

2. In cases where the avidin–biotin amplification system binds nonspecifically to the tissue, avidin–biotin blocking steps can be introduced into the protocol. This procedure ensures that all endogenous biotin, biotin receptors, and avidin-binding sites present in tissues are blocked prior to the addition of the labeled avidin reagent. The Dako biotin-blocking system contains an avidin and a biotin solution and is very efficient.

Incubation of Primary Antibody

1. After the blocking steps, the primary antibody is added to the slides and incubated overnight (4°C) in a humidified chamber. The standard working concentration should be 1–10 μg/ml. In negative control sections, an irrelevant MAb (e.g., a negative control mouse, Dako)

was applied at the same concentration as the primary antibody.

2. Several washes in 1X PBS are then performed to remove the excess of primary antibody that did not bind specifically to its antigen.

Secondary System

1. Bound antibody was detected using a supersensitive detection kit including biotinylated anti-mouse immunoglobulin (Ig) and HRP-conjugated streptavidin. Sections were incubated using the biotinylated secondary antibody for 1 hr at room temperature in a humidified chamber, and the signal was then amplified with a preformed avidin–biotin complex conjugated with HRP.

2. Sections are then incubated with the corresponding enzyme substrate solution for about 10 min in the dark. Oxidase substrates are available in several colors. Here, we used 3,3′ DAB. The tissue staining must be followed under a microscope by checking the level of specific staining to background intensity. When the specific staining is dark enough and before the background has reached too high a level, staining is halted by immersing the slides in 1X PBS.

3. Sections are rinsed several times in 1X PBS before counterstaining the nuclei with hematoxylin. Sections should be dehydrated with an ethanol series (50%, 70%, 95%, 100% for 10 min each) and permanently mounted with nonaqueous mounting medium for indefinite storage.

Double Staining

Double staining for CD97 and a cell-type specific antigen or extracellular matrix protein allows clear identification of the CD97-positive cell or structure. Two different techniques, double immunofluorescence staining and classic double immunohistochemistry, have been used (Hamann *et al.*, 1999; Jaspars *et al.*, 2001; Visser *et al.*, 2002). Because the methods have not been used for the examination of CD97 in tumors, only the principles are described here. Double immunofluorescence staining using a mixture of two secondary goat-anti-mouse antibodies directed against the different Ig subtypes of the two primary mouse MAbs works out well (Jaspars *et al.*, 2001). One of these secondary antibodies was labeled with biotin, and the other was coupled to alkaline phosphatase (AP). After incubation with these secondary antibodies, the slides were first incubated with a biotin–streptavidin complex coupled to HRP (sAB-HRP; Dako) and exposed to Cy-3 tyramide with 0.03% H_2O_2 (bright-red fluorescence).

The secondary AP substrate-coupled antibody was visualized using an enzyme-labeled immunofluorescence method (bright-yellow fluorescence).

Classic double immunohistochemistry is a smooth and easy method if two primary antibodies from different species are used (Visser *et al*., 2002). The secondary system is then adjusted to the first species and coupled to either HRP or alkaline phosphatase. Through the use of different substrates, 2-amino-9-ethyl-carbazol for HRP resulting in a bright-red precipitate and naphthol-AS-MX phosphate/fast blue BB base to reveal AP activity resulting in a blue precipitate; the cells expressing one marker were stained red or blue, whereas those expressing both were stained violet.

RESULTS AND DISCUSSION

CD97 Expression in Normal Tissues

In the hematopoietic system, CD97 is present at low levels on resting lymphocytes but is strongly up-regulated within a few hours after lymphocyte activation (Eichler *et al*., 1994), which is consistent with CD97's suspected role in adhesion. CD97 is constitutively expressed on monocytes and granulocytes (Eichler *et al*., 1994). These first results published on CD97 were all obtained using the BL-Ac/F2 MAb (CD97^{EGF}). In normal tissues, abundant expression of CD97 is only detected in macrophages and dendritic cells except for glial cells and some T- and B-cells (Jaspars *et al*., 2001). The most striking difference between staining with CD97^{EGF} and CD97^{stalk} MAbs was found on smooth-muscle cells. The cells were strongly positive for CD97^{stalk}, whereas CD97^{EGF} MAbs only weakly stained them, if at all. The same is true for duct cells in secretory glands. In contrast, CD97^{EGF} MAbs are more useful in detecting CD97 in macrophages and dendritic cells through immunohistology.

CD97 Expression in Carcinomas

The presence of CD97 in several carcinomas suggests that the expression of this molecule may be a common feature in tumors. However, the studies that have been published on CD97 immunohistology have the disadvantage that only one MAb directed against either the CD97^{EGF} or the CD97^{stalk} region has been used (Table 6). Where available, we completed the results using a MAb against the second CD97 region not yet examined (Table 6).

In thyroid tumors, strong CD97^{EGF} immunostaining was exclusively found in anaplastic carcinomas, which were highly dedifferentiated, whereas well-differentiated papillary and follicular carcinomas were CD97^{EGF}-negative or expressed CD97^{EGF} at lower levels (Aust *et al*., 1997; Hoang-Vu *et al*., 1999).

Nearly all of the colorectal carcinomas were positive for CD97^{stalk} (Steinert *et al*., 2002). In half of these positive carcinomas, CD97 was strongly localized in isolated tumor cells or small tumor cell clusters at the invasion front, whereas the opposite was the case in central parts of the tumor (i.e., low or even absent CD97^{stalk} expression). Such colorectal carcinomas containing strongly CD97^{stalk}-positive tumor cells at the invasion front showed significantly more often lymph-vessel invasion and a more advanced clinical stage, which are strong prognostic factors in colorectal carcinomas (Compton *et al*., 2000), compared to carcinomas with homogenous CD97^{stalk} staining. The idea that CD97 plays a role in tumor-cell migration and invasion has been strengthened by *in vitro* tests and by the observation that the ligands CD55 and dermatan sulphate glucosaminoglycan are overexpressed in the tumor environment of colorectal carcinomas (Li *et al*., 2001). CD97 is preferentially present on the tumor cells here at the tumor–stroma interface. By direct receptor-ligand interaction, CD97 may enable cancer

Table 6 Differences in Immunostaining of Carcinomas Between CD97^{stalk} and CD97^{EGF} Monoclonal Antibodies

Carcinoma	Number of CD97-Positive Tumors	Monoclonal Antibody Used	Reference
Thyroid	2 out of 4 (2/4) follicular; 3/6 papillary, 12/13 anaplastic	BL-Ac/F2 (CD97^{EGF})	(Aust *et al*., 1997)
Colorectal	75/81	CLB-CD97/3 (CD97^{stalk})	(Steinert *et al*., 2002)
	40/81	VIM3b (CD97^{EGF})	—
Pancreatic	14/18	CLB-CD97/3 (CD97^{stalk})	(Aust *et al*., 2002)
	7/18	VIM3b (CD97^{EGF})	—
	0/50	BL-Ac/F2 (CD97^{EGF})	(Boltze *et al*., 2002)
Gastric	44/50	CLB-CD97/3 (CD97^{stalk})	(Aust *et al*., 2002)
	5/50	VIM3b (CD97^{EGF})	—

cells to invade the surrounding matrix and survive through foreign microenvironments through cell–cell and cell–extracellular matrix. There was no correlation between CD97[stalk] staining intensity or number of stained cells and clinicopathologic features of the patients in gastric carcinomas (Aust *et al.*, 2002), which was mainly caused by the heterogeneity of the patient groups in combination with the small number of patients analyzed. Analyzing the same colorectal and gastric carcinomas again with an CD97[EGF] MAb, a significant lower number of tumors was positive for CD97[EGF] compared to CD97[stalk] (Table 6).

References

Aust, G., Eichler, W., Laue, S., Lehmann, I., Heldin, N.E., Lotz, O., Scherbaum, W.A., Dralle, H., and Hoang-Vu, C. 1997. CD97: A dedifferentiation marker in human thyroid carcinomas. *Cancer Res. 57*:1798–1806.

Aust, G., Hamann, J., Schilling, N., and Wobus, M. 2003. Detection of alternatively spliced EMR2 mRNAs in colorectal tumor cell lines but rare expression of the molecule in the corresponding adenocarcinomas. *Virchows Arch. 443*:32–37.

Aust, G., Steinert, M., Schütz, A., Wahlbuhl, M., Hamann, J., and Wobus, M. 2002. CD97, but not its closely related EGF-TM7 family member EMR2, is expressed on gastric, pancreatic and esophageal carcinomas. *Am. J. Clin. Pathol. 118*:699–707.

Boltze, C., Schneider-Stock, R., Aust, G., Mawrin, C., Dralle, H., Roessner, A., and Hoang-Vu, C. 2002. CD97, CD95 and Fas-L clearly discriminate between chronic pancreatitis and pancreatic ductal adenocarcinoma in perioperative evaluation of cryocut sections. *Pathol. Int. 52*:83–88.

Compton, C.C., Fielding, L.P., Burgart, L.J., Conley, B., Cooper, H.S., Hamilton, S.R., Hammond, M.E., Henson, D.E., Hutter, R.V., Nagle, R.B., Nielsen, M.L., Sargent, D.J., Taylor, C.R., Welton, M., and Willett, C. 2000. Prognostic factors in colorectal cancer. College of American Pathologists Consensus Statement 1999. *Arch. Pathol. Lab. Med. 124*:979–994.

Eichler, W., Aust, G., and Hamann, D. 1994. Characterization of the early activation-dependent antigen on lymphocytes defined by the monoclonal antibody BL-Ac(F2). *Scand. J. Immunol. 39*:111–115.

Hamann, J., Vogel, B., van Schijndel, G.M., and van Lier, R.A. 1996. The seven-span transmembrane receptor CD97 has a cellular ligand (CD55, DAF). *J. Exp. Med. 184*:1185–1189.

Hamann, J., Wishaupt, J.O., van Lier, R.A., Smeets, T.J., Breedveld, F.C., and Tak, P.P. 1999. Expression of the activation antigen CD97 and its ligand CD55 in rheumatoid synovial tissue. *Arthritis Rheum. 42*:650–658.

Hoang-Vu, C., Bull, K., Schwarz, I., Krause, G., Schmutzler, C., Aust, G., Köhrle, J., and Dralle, H. 1999. Regulation of CD97 protein in thyroid carcinoma. *J. Clin. Endocrinol. Metab. 84*:1104–1109.

Jaspars, L.H., Vos, W., Aust, G., van Lier, R.A., and Hamann, J. 2001. Tissue distribution of the human CD97 EGF-TM7 receptor. *Tissue Antigens 57*:325–331.

Kwakkenbos, M.J., Chang, G.W., Lin, H.H., Pouwels, W., de Jong, E.C., van Lier, R.A., Gordon, S., and Hamann, J. 2002a. The human EGF-TM7 family member EMR2 is a heterodimeric receptor expressed on myeloid cells. *J. Leukoc. Biol. 71*:854–862.

Kwakkenbos, M.J., van Lier, R.A., and Hamann, J. 2002b. Characterization of EGF-TM7 family members by novel monoclonal antibodies. In Mason, D., (ed) *Leucocyte Typing VII. White cell Differentiation Antigens*. Oxford, England: Oxford University Press, 381–383.

Li, L., Spendlove, I., Morgan, J., and Durrant, L.G. 2001. CD55 is over-expressed in the tumour environment. *Br. J. Cancer 84*:80–86.

Lin, H.H., Stacey, M., Hamann, J., Gordon, S., and McKnight, A.J. 2000. Human EMR2, a novel EGF-TM7 molecule on chromosome 19p13.1, is closely related to CD97. *Genomics 67*:188–200.

McKnight, A.J., and Gordon, S. 1998. The EGF-TM7 family: Unusual structures at the leukocyte surface. *J. Leukoc. Biol. 63*:271–280.

Pickl, W.F., Majdic, O., Mai, I., Gadd, S., and Knapp, W. 1995. Overview of CD97. In Schlossman, S.F., Boumsell, L., Gilks, W., Halan, J.M., Morimoto, C., Ritz, J., Shaw, S., Silverstein, R., Springer, T., Tedder, T.F., and Todd, R.F., (eds) *Leucocyte Typing V*. Oxford, England: Oxford University Press, 1151–1153.

Stacey, M., Chang, G.W., Davies, J., Kwakkenbos, M.J., Sanderson, R., Hamann, J., Gordon, S., and Lin, H.H. 2003. The epidermal growth factor-like domains of the human EMR2 receptor mediate cell attachment through chondroitin sulphate glycosaminoglycans. *Blood 102*:2916–2924.

Stacey, M., Lin, H.H., Gordon, S., and McKnight, A.J. 2000. LNB-TM7, a group of seven-transmembrane proteins related to family-B G-protein-coupled receptors. *Trends Biochem. Sci. 25*:284–289.

Steinert, M., Wobus, M., Boltze, C., Schütz, A., Wahlbuhl, M., Hamann, J., and Aust, G. 2002. Expression and regulation of CD97 in colorectal carcinoma cell lines and tumor tissues. *Am. J. Pathol. 161*:1657–1667.

Visser, L., de Vos, A.F., Hamann, J., Melief, M.J., van Meurs, M., van Lier, R.A.W., Laman, J.D., Hintzen, R.Q. 2002. Expression of the EGF-TM7 receptor CD97 and its ligand CD55 (DAF) in multiple sclerosis brain lession. *J. Neuroimmunol. 132*:156–163.

Wobus, M., Vogel, B., Schmücking, E., Hamann, J., and Aust, G. 2004. N-glycosylation of CD97 within the EGF domains is crucial for epitope accessibility in normal and malignant cells as well as CD55 ligand binding. *Int. J. Cancer* (in press).

10

Roles of Immunohistochemical Expression of Cyclin A and Cyclin-Dependent Kinase 2 in Colorectal Tumors

Jia-Qing Li and Katsumi Imaida

Introduction

Cyclin A and cyclin-dependent kinase 2 (CDK2) play important roles in many human tumors including colorectal neoplasms. Elucidation of the *in situ* expression of the two proteins by immunohistochemistry (Figures 32 and 33) is very useful, especially for clarification of carcinogenic mechanisms and for chemotherapeutic research. Genetic discoveries are already resulting in the development of many new drugs to treat cancer, one important example being flavopiridol, which inhibits CDK2.

The human gene for cyclin A maps to chromosome region 4q27 and encodes a nuclear protein of 432 amino acids, which binds to CDK2 in S phase and is linked with p34 CDC2 in the G_2/M phase (Brechot, 1993). The protein level remains zero from G_0 to late G_1, increases rapidly to a peak in G_2 phase, and then decreases quickly to zero before metaphase (Desdouets *et al*., 1995). In cells, cyclin A is involved in apoptosis induced by Myc (Hoang *et al*., 1994), promotes cells passage through the S phase by participating in the replication and repair of deoxyribonucleic acid (DNA), and regulates the G_2/M transition by preventing entry into mitosis before cells complete DNA replication (Desdouets *et al*., 1995). Overexpression of cyclin A accelerates entry into S phase, and this entry is inhibited by antisense complementary DNA (cDNA) or antibodies targeted against cyclin A (Desdouets *et al*., 1995).

Cyclin A has been linked with carcinogenesis. Genetic transfection of cyclin A leads to the anchorage-independent growth, which marks oncogenetic transformation (Guadagno *et al*., 1993). In a hepatoma, gene of cyclin A is inserted by the DNA of hepatitis B virus (Wang *et al*., 1990), chronic infection with which it is strongly linked with hepatocellular carcinoma by epidemiology. Cyclin A binds to the E1A oncoprotein of adenovirus in transformed cells (Pines, 1995), and is abnormally increased in immortalized fibroblasts (Ohashi *et al*., 1999), dysplastic lesions of the ureter (Furihata *et al*., 1997), and some primary cancers (Chao *et al*., 1998; Furihata *et al*., 1996; Huuhtanen *et al*., 1999a). Cyclin A has also been associated with cancerous invasion. The levels of the protein increase significantly when esophageal carcinoma reaches an advanced stage (Furihata *et al*., 1997) or when soft-tissue sarcoma

Handbook of Immunohistochemistry and in situ Hybridization of Human Carcinomas,
Volume 2: Molecular Pathology, Colorectal Carcinoma, and Prostate Carcinoma

207
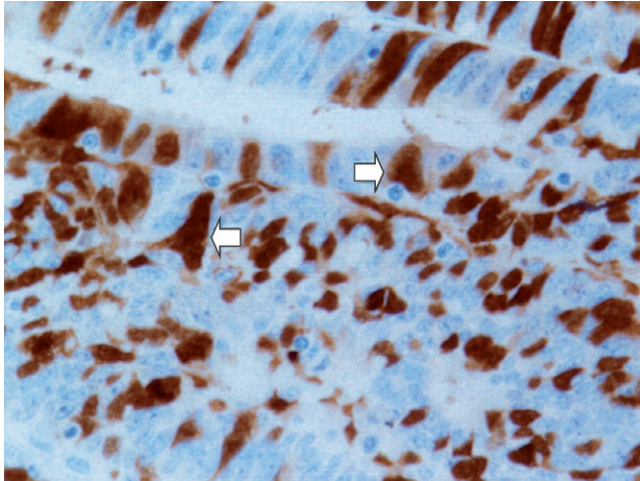
Figure 32 Staining of cyclin A in a colorectal carcinoma. Cyclin A staining, usually moderate or strong, is located in nuclei *(arrows)*, and positive cells are scattered widely and heterogeneously. Immunohistochemical staining; original magnifications, 400X.

(Huuhtanen *et al.*, 1999a) belongs to a poorly differentiated type that usually exhibits strong invasion. Elevation of cyclin A protein is linked with short survival in patients with cancers of the esophagus (Furihata *et al.*, 1996), soft tissue (Huuhtanen *et al.*, 1999a), or liver (Chao *et al.*, 1998). In addition, increase of cyclin A has been linked to rapid proliferation of cells in several kinds of cancers (Chao *et al.*, 1998; Huuhtanen *et al.*, 1999a).

The human gene for CDK2 is located in chromosome region 12q13 (Demetrick *et al.*, 1994), coding
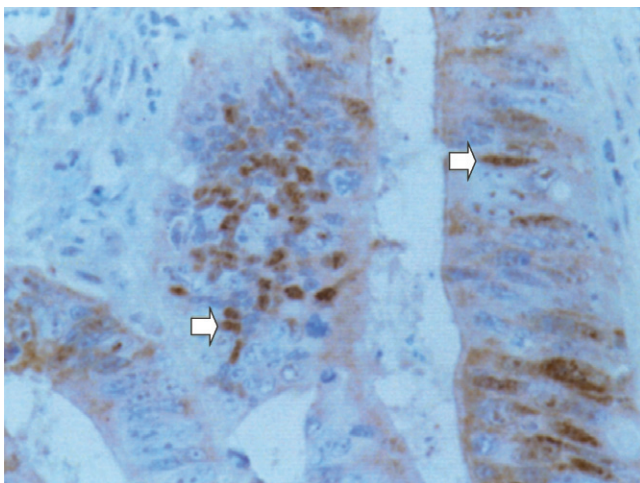
Figure 33 Staining of CDK2 in a colorectal carcinoma. CDK2 staining, often weak or moderate, is limited to nuclei *(arrows)* and is distributed heterogeneously. Immunohistochemical staining; original magnifications, 400X.

for a polypeptide of 298 amino acids, which links to cyclin E during G_1/S transition and binds to cyclin A during S phase. Although protein level remains unchanged, kinase activity of CDK2 fluctuates throughout G_1, S, G_2, and M phases. CDK2 propels movement through the G_1/S transition after activation by cyclin E and promotes G_1/S and G_2/M transitions after linking to cyclin A (Wadler, 2001). Elevation of kinase activity initiates both centrosome duplication and DNA synthesis (Hinchcliffe *et al.*, 2002). Also, CDK2 appears to participate in cellular apoptosis: Its inhibition efficiently blocks cellular death via certain apoptotic pathways, but its overexpression accelerates apoptosis (Gil-Gomez *et al.*, 1998).

The *CDK2* gene has been found to be amplified and rearranged in colorectal carcinomas (Kitahara *et al.*, 1995), and its ribonucleic acid (RNA) is increased in ovarian cancer (Marone *et al.*, 1998). Protein expression also increases from normal mucosa through dysplastic epithelium to squamous cell carcinoma of the mouth (Mihara *et al.*, 2001). CDK2 is linked with SV40 T antigen and associates with oncoproteins of adenovirus, papillomavirus, and cytomegalovirus (Wadler, 2001). Overexpression of CDK2 protein accompanies high kinase activity in lung carcinomas (Dobashi *et al.*, 1998) and is correlated with lymph node metastases, poor differentiation, strong invasion, and short survival in cases of oral squamous cell carcinomas (Mihara *et al.*, 2001). Additionally, increased CDK2 has been linked to rapid proliferation of cells in several sorts of cancers.

For studies of genetic alterations during human neoplastic development, colorectal tumors provide an excellent system (Fearon *et al.*, 1990). Cellular proliferation can be accurately monitored with reference to Ki-67 (Diebold *et al.*, 1994). Tumors in various stages of development can be obtained, unlike the situation in most other types of human neoplasms. The adenoma–carcinoma sequence is a typical model for human carcinogenesis because there are abundant clinicopathologic data indicating that most colorectal carcinomas arise from preexisting adenomas (Fearon *et al.*, 1990). Colorectal primary carcinoma has a high incidence and causes a high mortality rate (Landis *et al.*, 1999). Compared with the primary, the lymph node-metastatic focus displays different variations in genic expression (McKay *et al.*, 2000), whose identification may provide therapeutic opportunities (McLeod *et al.*, 2000).

This chapter details findings for the expression of cyclin A and CDK2 in multistage development of colorectal tumors and assesses the value of the expression for predicting prognosis. Because cyclin A and CDK2 are closely related to cellular proliferation (Huuhtanen *et al.*, 1999a) and Ki-67 can be used to

monitor proliferative cells reliably (Diebold *et al.*, 1994), it was also investigated.

MATERIALS

Specimens

Between 1991 and 1999 at Kagawa Medical University Hospital, 200 colorectal samples embedded in paraffin were consecutively collected and divided into four groups: normal mucosa ($n = 10$), adenoma ($n = 32$), primary carcinoma ($n = 143$), and lymph node-metastatic focus ($n = 15$). Normal mucosa was sampled at >10 cm distance from edges of primary carcinomas. Adenomas were classified as tubular ($n = 8$), tubulovillous ($n = 20$), or villous ($n = 4$) and were graded as having mild ($n = 6$), moderate ($n = 13$), or severe dysplasia ($n = 13$), according to the criteria of the World Health Organization in 1989. Primary carcinomas were evaluated by the classification system of Tumor-Node-Metastasis, 5th edition, Union Internationale Contre le Cancer in 1997 and were divided into mucinous and nonmucinous types, based on the criteria of the World Health Organization in 1989. Among all patients undergoing curative surgery, 123 cases were followed up for at least 5 years; 19 patients were grouped as early carcinoma, which, at the deepest, invaded into but not beyond submucosa. Lymph-nodal metastases were paired with primary carcinomas. Both primary and metastatic carcinomas did not receive preoperative chemotherapy or radiotherapy. From each specimen, four serial sections of 3 μm thickness were made, and were fixed on silane-S-coated slides (5116, MUTO Pure Chemicals Co., Tokyo, Japan). To confirm the histologic diagnosis for each specimen, one section was stained with hematoxylin and eosin.

Reagents

1. Xylene: 244-00081 (Wako Pure Chemical Industries Ltd., Osaka, Japan).
2. 99.5% ethanol: 057-00451 (Wako Pure Chemical Industries Ltd.).
3. 80% ethanol: 99.5% ethanol 800 ml, bring volume to 1 L with deionized glass-distilled water.
4. 0.3% hydrogen peroxide-methanol: 100% methanol 148.5 ml, add 30% hydrogen peroxide 1.5 ml.
5. Phosphate buffer saline (PBS): 120 g sodium chloride, 17.25 g disodium hydrogenphosphate, 3 g potassium dihydrogenphosphate, and 3 g potassium chloride; bring volume to 15 L with deionized glass-distilled water (pH 7.4).

6. 0.01 M citrate buffer solution: 189.1 mg citric acid monohydrate, and 1205.8 mg tri-sodium citrate dihydrate; bring volume to 500 ml with deionized glass-distilled water.
7. 0.1% bovine serum albumin (BSA): 0.1 g BSA of immunohistochemical grade and 100 ml PBS.
8. Mouse Vectastain Elite ABC kit: PK-6102 (Vector Laboratories, Burlingame, CA).
9. Blocking serum: add 150 μL horse normal serum (from the ABC kit) to 10 ml PBS.
10. 1:100 anti-cyclin A antibody: 6E6 (Novocastra Laboratories, Newcastle upon Tyne, UK); add 10 μL anti-cyclin A antibody to 10 ml 0.1% BSA.
11. 1:2500 anti-CDK2 antibody: C18520 (Transduction Laboratories, Lexington, KY); add 10 μL anti-CDK2 antibody to 10 ml 0.1% BSA.
12. 1:300 anti-Ki-67 antibody: IM0505 (Immunotech, Marseille, France); add 10 μL anti-Ki-67 antibody to 10 ml 0.1% BSA.
13. Biotinylated antibody: add 150 μL horse normal serum (from the ABC kit) and 50 μL biotinylated antibody targeting mouse (from the ABC kit) to 10 ml PBS.
14. Vectastain Elite ABC Reagent: add exactly two drops of "Reagent A" (from the ABC kit) to 5 ml PBS in a mixing bottle, add exactly two drops of "Reagent B" (from the ABC kit) to the same mixing bottle; mix immediately, and allow the Vectastain Elite ABC Reagent to stand for about 30 min before use.
15. DAB (diaminobenzidine tetrahydrochloride) solution: dissolve 30 mg DAB in 30 ml PBS, and then add 30% hydrogen peroxide 20 μL.
16. Mayer's hematoxylin solution: 131-09665 (Wako Pure Chemical Industries Ltd.).
17. Malinol: 2009-3 (MUTO Pure Chemicals Co.).

METHOD

Staining Procedure

1. Deparaffinize 3 μm sections in xylene (4× for 10 min each).
2. Rehydrate sections, in order, using 100% ethanol (3× for 2 min each) and 80% ethanol (few seconds).
3. Incubate slides in 0.3% hydrogen-peroxide methanol (30 min at room temperature).
4. Rinse slides in tap water (1 min), distilled water (1 min), and PBS (2× for 5 min each), respectively.
5. Heat sections in 0.01 M citrate buffer solution (10 min at 120°C).
6. Cool sections.
7. Rinse sections in PBS (2× for 5 min each).
8. Incubate sections in blocking serum (20 min at room temperature).
9. Rinse sections in PBS (few seconds).

10. Incubate sections in 1:100 anti-cyclin A, 1:2500 anti-CDK2, and 1:300 anti-Ki-67 antibodies, respectively (overnight at 4°C).

11. Rinse sections in PBS (3× for 5 min each).

12. Incubate sections in biotinylated antibody (30 min at room temperature).

13. Rinse sections in PBS (3× for 5 min each).

14. Incubate sections in the Vectastain Elite ABC Reagent (30 min at room temperature).

15. Rinse slides in PBS (3× for 5 min each).

16. Incubate sections in the DAB solution (5 min at room temperature).

17. Rinse slides in tap water (5 min).

18. Counterstain sections in Mayer's hematoxylin (1 min).

19. Rinse slides in tap water (10 min).

20. Dehydrate sections, in order, using 80% ethanol (few seconds) and 100% ethanol (3× for 2 min each).

21. Clear sections in xylene (4× for 2 min each).

22. Mount sections using malinol.

Staining Evaluation

Only the cells with unclear staining were considered as positive for cyclin A (Dobashi *et al*., 1998), CDK2 (Dobashi *et al*., 1998), and Ki-67 (Diebold *et al*., 1994). At least 1000 cells were randomly counted in 10 high-power fields for each section to provide a labeling index (LI): the percentage of positive cells in the total counted (Dobashi *et al*., 1998). To determine the intensity of stained cells, all sections were also compared with positive controls stained strongly, and results were divided into strong, moderate, and weak expression. To analyze prognosis of primary carcinoma cases, the mean of cyclin A LIs, 29.5%, served as the cutoff value in primary carcinomas: Cyclin A staining was regarded as low when the LIs were less than or equal to 29.5% and high when the LIs were more than 29.5%. The cutoff value for CDK2 LIs was set at 1.5%—the mean of primary carcinomas. CDK2 staining was considered low when the percentage of positive cells was less than or equal to 1.5% and high when the LIs were more than 1.5%.

Statistical Analysis

A one-sample Kolmogorov-Smirnov test was used to check for normality of distribution. Differences between two groups were evaluated by an unpaired *t*-test for cyclin A but by the Mann-Whitney U-test for CDK2. Variation among three or more groups was assessed by one-way analysis of variance (one-way

ANOVA) for cyclin A and by Kruskal-Wallis test for CDK2. If significance was observed, multiple comparisons were further conducted by the Bonferroni method if there were three and four groups or by the Student-Newman-Keuls method if there were six groups. Survival rates were analyzed using the Breslow-Gehan-Wilcoxon method in the Kaplan-Meier test, whereas the influence of each variable on survival was evaluated with the Cox proportional hazards model. The paired *t*-test was used to compare cyclin A levels between primary carcinomas and lymph-nodal metastases, whereas the Wilcoxon signed rank test was used in the CDK2 case. The association between cyclin A and Ki67 was evaluated by a linear correlation test because their LIs demonstrated a normal distribution, whereas the relation between cyclin A and CDK2 was analyzed by the Spearman rank correlation test because CDK2 LIs showed a nonnormal distribution. All tests were performed using SPSS version 10.0 software (SPSS Inc., Chicago, IL). *P* values <0.05 were considered to be statistically significant.

RESULTS AND DISCUSSION

Increase of Cyclin A and CDK2 during Carcinogenesis

Situated in nuclear, cyclin A staining was moderate or severe and increased only slightly from normal mucosa through adenomas to carcinomas. The stained cells were limited to the lower regions of the crypts in normal mucosa, were also present in the upper parts of the crypts in adenomas, and were heterogeneously scattered throughout the entire epithelial area in early carcinomas. Cyclin A LIs demonstrated a normal distribution in adenomas and primary carcinomas. The mean ± standard error (SE) of cyclin A LIs increased significantly from 9.1% ± 1.3% in normal mucosa (range, 4.5–16.8%; median, 7.9%) through 22.4% ± 1.3% in adenomas (range, 10.7–39.8%; median, 22.1%) to 32.0% ± 2.3% in early carcinomas (range, 9.0–42.0%; median, 37.0%; *P* < 0.0001, by one-way ANOVA). Multiple comparisons displayed significant differences between normal mucosa and adenomas (*P* < 0.0001), between adenomas and early carcinomas (*P* < 0.0001), and between normal mucosa and early carcinomas (*P* = 0.0001, by Bonferroni method).

In adenomas, cyclin A was apparently correlated with the degree of dysplasia. The range of cyclin A LIs continuously expanded from mild (13.5–28.8%; median, 15.0%) through moderate (10.7–29.0%; median, 20.7%) to severe dysplasia (16.8–39.8%; median, 22.8%). The mean ± SE of cyclin A LIs also increased significantly

from moderate (20.7% ± 1.7%) to severe (26.2% ± 2.2%) dysplasia, although only little elevation was evident from mild (18.0% ± 2.5%) to moderate dysplasia (by one-way ANOVA and Bonferroni method). When the Student-Newman-Keuls method was used to compare the means among normal mucosa, mild dysplasia, moderate dysplasia, severe dysplasia, and early carcinoma, the difference was significant between normal mucosa and mild dysplasia but not between severe dysplasia and early carcinoma. In addition, cyclin A LIs were not related to the histologic type of adenoma: ranges did not clearly vary among tubular (15.2–39.8%; median, 25.3%), tubulovillous (10.7–35.1%; median, 22.3%), and villous types (16.8–22.2%; median, 18.8%). The mean ± SE values also did not display significant variation ($P = 0.4228$, by one-way ANOVA) among tubular (25.0% ± 2.8%), tubulovillous (22.1% ± 1.8%), and villous adenomas (19.1% ± 1.4%).

In colorectal epithelium, CDK2 staining was limited to the nuclei and the intensity was generally weak or moderate, although it increased slightly from normal mucosa to adenomas to early carcinomas. CDK2-positive cells were confined to the lower regions of the crypts in normal mucosa, were also found in the upper parts of the crypts in adenomas, and were heterogeneously distributed in early carcinomas. CDK2 LIs displayed a nonnormal distribution in adenomas and primary carcinomas. The median was significantly elevated (by Kruskal-Wallis test and Bonferroni method) from 0.7% in normal mucosa (range, 0–10%; mean ± standard deviation [SD], 2.1% ± 3.0%) to 8.6% in adenomas (range, 1.2–26.0%; mean ± SD, 10.6% ± 6.5%) and then decreased to 2.4% in early carcinomas (range, 0–20.8%; mean ± SD, 4.0% ± 5.2%).

In adenomas, the range of CDK2 LIs remained unchanged from mild (1.2–24.0%; mean ± SD, 8.9% ± 8.4%) through moderate (1.2–17.0%; mean ± SD, 8.8% ± 4.6%) to severe dysplasia (2.0–26.0%; mean ± SD, 13.2% ± 6.8%), but the median values increased significantly (by Kruskal-Wallis test and Bonferroni method) from moderate (7.4%) to severe dysplasia (12.8%) despite only minor elevation from mild (6.2%) to moderate dysplasia. When the Student-Newman-Keuls method was used to compare the medians among normal mucosa, mild dysplasia, moderate dysplasia, severe dysplasia, and early carcinoma, the difference was significant not only between normal mucosa and mild dysplasia but also between severe dysplasia and early carcinoma. However, the range of CDK2 LIs did not change from tubular (1.2–24.0%; mean ± SD, 10.1% ± 7.2%) through tubulovillous (1.2–26.0%; mean ± SD, 10.8% ± 6.8%) to villous adenomas (6.8–16.2%; mean ± SD, 10.4% ± 4.4%), and the median values also did not display significant differences (by Kruskal-Wallis

test) among tubular (7.5%), tubulovillous (10.2%), and villous adenomas (9.3%).

The aforementioned results indicated that expression of cyclin A and CDK2 is limited to proliferating cells of colorectal epithelium because the proliferative zone also appears only in the lower part of each crypt in normal mucosa, but includes the upper part of the crypt in adenoma, and is widely scattered in the epithelial areas of cancers (Johnston *et al.*, 1989). During the carcinogenic process, the staining intensity for cyclin A and CDK2 was slightly enhanced, the range of cyclin A LIs and CDK2 LIs increased, and the mean or median of cyclin A LIs and CDK2 LIs increased. The distributional variation and proteinous elevation demonstrated that overexpression of cyclin A and CDK2 is involved in colorectal carcinogenesis.

Decrease of Cyclin A and CDK2 during Invasion

In colorectal primary carcinomas, the mean of cyclin A LIs significantly declined in the mucinous type (mean ± SE, 19.7% ± 2.5%; median, 20.7%; range 8.8–28.4%) compared with that in the nonmucinous type (mean ± SE, 30.0% ± 0.7%; median, 29.6%; range 8.8–51.4%). It also declined in carcinomas with venous invasion (mean ± SE, 28.2% ± 0.8%; median, 27.4%; range 8.8–51.4%), compared with the value for tumors without invasion (mean ± SE, 31.7% ± 1.4%; median, 32.1%; range 8.8–51.2%). The mean significantly decreased in the carcinomas with lymph node metastases (mean ± SE, 26.9% ± 1.3%; median, 25.6%; range 8.8–51.2%) in contrast to that in tumors without metastases (mean ± SE, 31.0% ± 0.9%; median, 30.7%; range 9.0–51.4%). When primary carcinomas progressed from stages 0/I to IV, the mean ± SE decreased from 32.2% ± 1.4% (median, 31.4%; range 9.0–43.8%) to 26.4% ± 2.1% (median, 25.6%; range 11.4–51.2%) significantly. However, cyclin A expression did not correlate with age, sex, maximum tumor size, lymph-vessel invasion, or tumorous grade.

In the 123 patients undergoing a curative operation, the 5-year survival rate significantly declined from the group expressing high cyclin A (93.9%) to the group expressing low cyclin A (73.2%, Breslow-Gehan-Wilcoxon method). Univariate analysis showed that maximum size, grade, stage, and reduction of cyclin A were factors significantly affecting patient prognosis. Multivariate analysis indicated that only stage and reduced cyclin A were independent prognostic factors.

In colorectal primary carcinomas, the median CDK2 LI was decreased significantly in moderately and poorly differentiated carcinomas (median, 0.2%;

mean ± SD, 1.0% ± 1.9%; range 0–8.6%), as compared with the value for well-differentiated lesions (median, 0.4%; mean ± SD, 2.1% ± 3.6%; range 0–20.1%). When primary carcinomas invaded from submucosa to serosa, the median CDK2 LI decreased significantly from 1.8% (mean ± SD, 3.8% ± 5.1%; range 0–20.8%) to 0.2% (mean ± SD, 1.1% ± 2.1%; range 0–12.0%). Compared to the value (0.6%) in tumors without lymph-vessel invasion (mean ± SD, 3.3% ± 5.0%; range, 0–20.8%), the median was significantly lower in carcinomas with venous invasion (median, 0.2%; mean ± SD, 1.3% ± 2.3%; range, 0–12.0%). When primary carcinomas developed from stages 0/I to stage IV, the median decreased significantly from 1.2% (mean ± SD, 3.1% ± 4.3%; range, 0–20.8%) to 0.2% (mean ± SD, 0.6% ± 0.8%; range, 0–2.6%). CDK2 expression was not associated with age, sex, tumorous position, tumor-maximum size, histologic type, venous invasion, and lymph node metastasis. The 5-year survival rate was 79.8% in the group expressing low CDK2, whereas it was 95.7% in the group expressing high CDK2 ($P = 0.059$, Breslow-Gehan-Wilcoxon method).

The results thus demonstrate that overexpression of cyclin A and CDK2 becomes progressively weakened as primary carcinomas invade local tissues, indicating the following: 1) primary carcinomas losing cyclin-A or CDK2 overexpression develop a strong invasive ability and high malignancy; 2) such carcinomas require more aggressive treatment; and 3) the invasive ability of carcinomas may be enhanced by the reduction of overexpression of cyclin A and CDK2. Such reduction can be explained from two aspects. Firstly, cyclin A expression varies greatly among normal organs, exhibiting organ specificity (Muller-Tidow et al., 2001). This specificity might be able to explain why cyclin A expression decreases in colorectal malignancies but increases in cancers from other organs when the primary cancer progresses (Chao et al., 1998; Furihata et al., 1996). Second, whereas the reduction indicates that cell proliferation decreases, cellular apoptosis also reduces significantly in advanced carcinomas (Evertsson et al., 1999). Net growth of advanced colorectal carcinoma may thus continue, with slowing of proliferation playing a minor role, as confirmed for prostate cancers (Denmeade et al., 1996).

Increase of CDK2 in Metastases

Lymph node metastases displayed cyclin A-staining features similar to those of primary carcinomas, with cyclin A LIs ranging from 6.4% to 45.4% (median, 26.0%). When primary carcinomas invaded the lymph nodes, the mean ± SE increased nonsignificantly (by paired t-test) from 26.4% ± 2.6% to 27.6% ± 3.2%. The staining features of CDK2 in nodal foci were similar to those in primary carcinomas. From the paired primary carcinomas to the nodal foci, the median of CDK2-LIs increased significantly (by Wilcoxon signed rank test) from 0.2% (range, 0–2.0%; mean ± SD, 0.4% ± 0.5%) to 2.0% (range, 0.4–14.4%; mean ± SD, 3.0% ± 3.7%).

The results thus indicate that, whereas levels of cyclin A remain unchanged, expression of CDK2 increases clearly when primary carcinomas metastasize to lymph nodes. At the same time, expression of Ki67 (Tatebe et al., 1996) and cyclin D1 (McKay et al., 2000) increases. Because progression of cell cycle is inhibited by p21[WAF1/CIP1] and p27[KIP1] (Lloyd et al., 1999) but is propelled by cyclin A and CDK2 (Sherr, 1996), both loss of inhibitors and increase of propellers can enhance the proliferative ability of cells (Sherr, 1996). Indeed, the nodal foci lose p21[WAF1/CIP1] (McKay et al., 2000) and p27[KIP1] (Li et al., 2002) but contain elevated cyclin D1 (McKay et al., 2000) and CDK2. Therefore, elevated CDK2—like elevated cyclin D1, reduced p21[WAF1/CIP1], and reduced p27[KIP1]—may be an important factor to promote the rapid proliferation of cancerous cells in lymph nodes, whereas cyclin A may not play a key role.

Associations Among Cyclin A, CDK2 and Ki67

In adenomas, elevated cyclin A LIs tended to be related to high CDK2 LIs ($r_s = 0.318$, $P = 0.0766$) and were highly associated with increased Ki-67 LIs ($r_s = 0.764$, $P < 0.0001$), although CDK2 LIs were not correlated with Ki-67 LIs ($r_s = 0.249$, $P = 0.1665$). In primary carcinomas, increased cyclin A LIs were apparently linked with elevated Ki-67 LIs ($r_s = 0.356$, $P < 0.0001$), although there was not significant association between cyclin A LIs and CDK2 LIs ($r_s = 0.027$, $P = 0.7435$) or between CDK2 LIs and Ki-67 LIs ($r_s = 0.105$, $P = 0.2118$).

These results reveal that elevated cyclin A is linked with increased CDK2 and Ki-67. In the present results, staining of CDK2 and Ki-67 showed the same characteristics as reported earlier (Diebold et al., 1994; Kim et al., 1999). The linkage between cyclin A and CDK2 resembles that in lung carcinoma (Dobashi et al., 1998); the association between cyclin A and Ki-67 is consistent with that in soft-tissue sarcomas (Huuhtanen et al., 1999a). The linkage between elevated cyclin A and increased CDK2 is in line with the report that cyclin A binds to and activates CDK2 in colorectal tumors, whereas active CDK2 promotes

cell-cycle progression and cellular proliferation (Pines, 1995; Sherr, 1996). The association of cyclin A with *Ki-67* and the linkage of *Ki-67* with proliferation suggest that cyclin A overexpression is linked with rapid proliferation of cells. Thus, elevated cyclin A, by activating CDK2, may accelerate cellular proliferation in colorectal tumors.

Regulation of Cyclin A and CDK2

There have been reports for variation of cyclin A at the DNA (De Mitri *et al.*, 1993; Paterlini *et al.*, 1995), RNA (Paterlini *et al.*, 1995), and protein (Chao *et al.*, 1998) levels in hepatocellular carcinoma. Colorectal tumors might also feature gene amplification and transcription leading to overexpression of cyclin A protein, but the exact mechanism should be further investigated because cyclin A expression shows different characteristics in various organs (Muller-Tidow *et al.*, 2001). This study demonstrated CDK2 overexpression in 17.2% of carcinomas (35/203), but Kitahara found genic amplification in only 5.6% of cases (3/53) (Kitahara *et al.*, 1995). Frequent overexpression but infrequent amplification might suggest that both translational and post-translational mechanisms may cause overexpression of CDK2 in colorectal tumors. However, it remains unclear why overexpression for cyclin A and CDK2 increases during tumorigenesis but abates during invasion. Because regulation for cyclin A involves many factors such as p21[WAF1/CIP1] (Sherr, 1996), p53 (Shiozawa *et al.*, 1997), p57[KIP2] (Sherr, 1996), p107 (Grana *et al.*, 1998), and HuR (Wang *et al.*, 2000), the situation is clearly very complex. Expression of CDK2 is also influenced by many factors (Porter *et al.*, 1997). To elucidate mechanisms, cyclin A and CDK2 should be examined concurrently at the gene, RNA, and protein levels in various stages of colorectal tumors.

Significance of Cyclin A and CDK2 Staining

The data presented in this chapter indicate that overexpression of cyclin A and CDK2 is involved in colorectal carcinogenesis and cellular proliferation. Additionally, cyclin A can mark the cell-cycle phase most sensitive to chemotherapy (Mattern *et al.*, 1986), and application of this feature apparently improved the chemotherapeutic effects in soft tissue sarcomas (Huuhtanen *et al.*, 1999b). Cyclin A staining might provide a sound basis for chemotherapeutic research. Furthermore, some lymph nodes in post-operative patients

often contain residual micrometastases—obvious targets of chemotherapy—and the first CDK inhibitor, flavopiridol, has entered clinical trials (Stadler *et al.*, 2000). The high CDK2 LIs demonstrate that lymph node metastases and early primary carcinomas are suited to anti-CDK2 chemotherapy. Conversely, low CDK2 LIs indicate that advanced primary carcinomas are not suitable for such therapy. Moreover, reduction of cyclin A may indicate a poorer prognosis in patients with colorectal carcinoma.

In summary, through the immunohistochemical staining of normal mucosa, adenomas, primary carcinomas, and lymph-nodal metastases, this chapter has clarified that 1) levels of cyclin A and CDK2 increase during carcinogenesis; 2) the two proteins decrease during invasion; and 3) CDK2 expression is elevated during lymph node metastasis. These findings indicate that overexpression of cyclin A and CDK2 is involved in colorectal carcinogenesis and cellular proliferation, and staining characteristics of cyclin A and CDK2 provide a sound basis for chemotherapeutic research. Clinically, low expression of cyclin A may indicate a poorer prognosis in patients with colorectal carcinoma.

References

Brechot, C. 1993. Oncogenic activation of cyclin A. *Curr. Opin. Genet. Dev. 3*:11–18.

Chao, Y., Shih, Y.L., Chiu, J.H., Chau, G.Y., Lui, W.Y., Yang, W.K., Lee, S.D., and Huang, T.S. 1998. Overexpression of cyclin A but not Skp 2 correlates with the tumor relapse of human hepatocellular carcinoma. *Cancer Res. 58*:985–990.

De Mitri, M.S., Pisi, E., Brechot, C., and Paterlini, P. 1993. Low frequency of allelic loss in the cyclin A gene in human hepatocellular carcinomas: A study based on PCR. *Liver 13*:259–261.

Demetrick, D.J., Zhang, H., and Beach, D.H. 1994. Chromosomal mapping of human CDK2, CDK4, and CDK5 cell cycle kinase genes. *Cytogenet. Cell Genet. 66*:72–74.

Denmeade, S.R., Lin, X.S., and Isaacs, J.T. 1996. Role of programmed (apoptotic) cell death during the progression and therapy for prostate cancer. *Prostate 28*:251–265.

Desdouets, C., Sobczak-Thepot, J., Murphy, M., and Brechot, C. 1995. Cyclin A: Function and expression during cell proliferation. *Prog. Cell Cycle Res. 1*:115–123.

Diebold, J., Dopfer, K., Lai, M., and Lohrs, U. 1994. Comparison of different monoclonal antibodies for the immunohistochemical assessment of cell proliferation in routine colorectal biopsy specimens. *Scand. J. Gastroenterol. 29*:47–53.

Dobashi, Y., Shoji, M., Jiang, S.X., Kobayashi, M., Kawakubo, Y., and Kameya, T. 1998. Active cyclin A-CDK2 complex, a possible critical factor for cell proliferation in human primary lung carcinomas. *Am. J. Pathol. 153*:963–972.

Evertsson, S., Bartik, Z., Zhang, H., Jansson, A., and Sun, X.F. 1999. Apoptosis in relation to proliferating cell nuclear antigen and Dukes' stage in colorectal adenocarcinoma. *Int. J. Oncol. 15*:53–58.

Fearon, E.R., and Vogelstein, B. 1990. A genetic model for colorectal tumorigenesis. *Cell 61*:759–767.

Furihata, M., Ishikawa, T., Inoue, A., Yoshikawa, C., Sonobe, H., Ohtsuki, Y., Araki, K., and Ogoshi, S. 1996. Determination of the prognostic significance of unscheduled cyclin A over-expression in patients with esophageal squamous cell carcinoma. *Clin. Cancer Res. 2*:1781–1785.

Furihata, M., Ohtsuki, Y., Sonobe, H., Shuin, T., Yamamoto, A., Terao, N., and Kuwahara, M. 1997. Cyclin A overexpression in carcinoma of the renal pelvis and ureter including dysplasia: Immunohistochemical findings in relation to prognosis. *Clin. Cancer Res. 3*:1399–1404.

Gil-Gomez, G., Berns, A., and Brady, H.J. 1998. A link between cell cycle and cell death: Bax and Bc1-2 modulate Cdk2 activation during thymocyte apoptosis. *Embo. J. 17*:7209–7218.

Grana, X., Garriga, J., and Mayol, X. 1998. Role of the retino-blastoma protein family, pRB, p107 and p130 in the negative control of cell growth. *Oncogene 17*:3365–3383.

Guadagno, T.M., Ohtsubo, M., Roberts, J.M., and Assoian, R.K. 1993. A link between cyclin A expression and adhesion-dependent cell cycle progression. *Science 262*:1572–1575.

Hinchcliffe, E.H., and Sluder, G. 2002. Two for two: Cdk2 and its role in centrosome doubling. *Oncogene 21*:6154–6160.

Hoang, A.T., Cohen, K.J., Barrett, J.F., Bergstrom, D.A., and Dang, C.V. 1994. Participation of cyclin A in Myc-induced apoptosis. *Proc. Natl. Acad. Sci. U S A. 91*:6875–6879.

Huuhtanen, R.L., Blomqvist, C.P., Bohling, T.O., Wiklund, T.A., Tukiainen, E.J., Virolainen, M., Tribukait, B., and Andersson, L.C. 1999a. Expression of cyclin A in soft tissue sarcomas correlates with tumor aggressiveness. *Cancer Res. 59*:2885–2890.

Huuhtanen, R.L., Wiklund, T.A., Blomqvist, C.P., Bohling, T.O., Virolainen, M.J., Tribukait, B., and Andersson, L.C. 1999b. A high proliferation rate measured by cyclin A predicts a favourable chemotherapy response in soft tissue sarcoma patients. *Br. J. Cancer 81*:1017–1021.

Johnston, P.G., O'Brien, M.J., Dervan, P.A., and Carney, D.N. 1989. Immunohistochemical analysis of cell kinetic parameters in colonic adenocarcinomas, adenomas, and normal mucosa. *Hum. Pathol. 20*:696–700.

Kim, J.H., Kang, M.J., Park, C.U., Kwak, H.J., Hwang, Y., and Koh, G.Y. 1999. Amplified CDK2 and cdc2 activities in primary colorectal carcinoma. *Cancer 85*:546–553.

Kitahara, K., Yasui, W., Kuniyasu, H., Yokozaki, H., Akama, Y., Yunotani, S., Hisatsugu, T., and Tahara, E. 1995. Concurrent amplification of cyclin E and CDK2 genes in colorectal carcinomas. *Int. J. Cancer 62*:25–28.

Landis, S.H., Murray, T., Bolden, S., and Wingo, P.A. 1999. Cancer statistics, 1999. *CA Cancer J. Clin. 49*:8–31.

Li., J.Q., Miki, H., Wu, F., Saoo, K., Nishioka, M., Ohmori, M., and Imaida, K. 2002. Cyclin A correlates with carcinogenesis and metastasis, and p27(kip1) correlates with lymphatic invasion, in colorectal neoplasms. *Hum. Pathol. 33*:1006–1015.

Lloyd., R.V., Erickson, L.A., Jin, L., Kulig, E., Qian, X., Cheville, J.C., and Scheithauer, B.W. 1999. p27kip1: A multifunctional cyclin-dependent kinase inhibitor with prognostic significance in human cancers. *Am. J. Pathol. 154*:313–323.

Marone, M., Scambia, G., Giannitelli, C., Ferrandina, G., Masciullo, V., Bellacosa, A., Benedetti-Panici, P., and Mancuso, S. 1998. Analysis of cyclin E and CDK2 in ovarian cancer: Gene amplification and RNA overexpression. *Int. J. Cancer 75*:34–39.

Mattern, J., Wayss, K., and Volm, M. 1986. Predicting chemo-sensitivity of tumors. *Breast Cancer Res. Treat. 8*:157–159.

McKay, J.A., Douglas, J.J., Ross, V.G., Curran, S., Ahmed, F.Y., Loane, J.F., Murray, G.I., and McLeod, H.L. 2000. Expression of cell cycle control proteins in primary colorectal tumors does not always predict expression in lymph node metastases. *Clin. Cancer Res. 6*:1113–1118.

McLeod, H.L., McKay, J.A., Collie-Duguid, E.S., and Cassidy, J. 2000. Therapeutic opportunities from tumour biology in metastatic colon cancer. *Eur. J. Cancer 36*:1706–1712.

Mihara, M., Shintani, S., Nakahara, Y., Kiyota, A., Ueyama, Y., Matsumura, T., and Wong, D.T. 2001. Overexpression of CDK2 is a prognostic indicator of oral cancer progression. *Jpn. J. Cancer Res. 92*:352–360.

Muller-Tidow, C., Bornemann, C., Diederichs, S., Westermann, A., Klumpen, S., Zuo, P., Wang, W., Berdel, W.E., and Serve, H. 2001. Analyses of the genomic methylation status of the human cyclin A1 promoter by a novel real-time PCR-based methodology. *FEBS Lett. 490*:75–78.

Ohashi, R., Miyazaki, M., Fushimi, K., Tsuji, T., Inoue, Y., Shimizu, N., and Namba, M. 1999. Enhanced activity of cyclin A-associated kinase in immortalized human fibroblasts. *Int. J. Cancer 82*:754–758.

Paterlini, P., Flejou, J.F., De Mitri, M.S., Pisi, E., Franco, D., and Brechot, C. 1995. Structure and expression of the cyclin A gene in human primary liver cancer. Correlation with flow cytometric parameters. *J. Hepatol. 23*:47–52.

Pines, J. 1995. Cyclins, CDKs and cancer. *Semin. Cancer Biol. 6*:63–72.

Porter, P.L., Malone, K.E., Heagerty, P.J., Alexander, G.M., Gatti, L.A., Firpo, E.J., Daling, J.R., and Roberts, J.M. 1997. Expression of cell-cycle regulators p27Kip1 and cyclin E, alone and in combination, correlate with survival in young breast cancer patients. *Nat. Med. 3*:222–225.

Sherr, C.J. 1996. Cancer cell cycles. *Science 274*:1672–1677.

Shiozawa, T., Xin, L., Nikaido, T., and Fujii, S. 1997. Immunohistochemical detection of cyclin A with reference to p53 expression in endometrial endometrioid carcinomas. *Int. J. Gynecol. Pathol. 16*:348–353.

Stadler, W.M., Vogelzang, N.J., Amato, R., Sosman, J., Taber, D., Liebowitz, D., and Vokes, E.E. 2000. Flavopiridol, a novel cyclin-dependent kinase inhibitor, in metastatic renal cancer: A University of Chicago Phase II Consortium study. *J. Clin. Oncol. 18*:371–375.

Tatebe, S., Ishida, M., Kasagi, N., Tsujitani, S., Kaibara, N., and Ito, H. 1996. Apoptosis occurs more frequently in metastatic foci than in primary lesions of human colorectal carcinomas: Analysis by terminal-deoxynucleotidyl-transferase-mediated dUTP-biotin nick end labeling. *Int. J. Cancer 65*:173–177.

Wadler, S. 2001. Perspectives for cancer therapies with cdk2 inhibitors. *Drug Resist. Updat. 4*:347–367.

Wang, J., Chenivesse, X., Henglein, B., and Brechot, C. 1990. Hepatitis B virus integration in a cyclin A gene in a hepato-cellular carcinoma. *Nature 343*:555–557.

Wang. W., Caldwell, M.C., Lin, S., Furneaux, H., and Gorospe, M. 2000. HuR regulates cyclin A and cyclin B1 mRNA stability during cell proliferation. *Embo. J. 19*:2340–2350.

11

Role of Mismatch Repair Proteins and Microsatellite Instability in Colon Carcinoma

Maria Lucia Caruso

Introduction

Because cancer cells harbor a corrupted genome, cancer is considered a genetic disease (Loeb, 2001). However, we owe to the science of epidemiology the knowledge that most human cancers are related to environmental factors.

Both of these concepts are correct because cancer is the result of a complex interaction between genetics and the environment. Colorectal cancer (CRC) has long been regarded largely as an environmentally determined human cancer, with dietary factors playing a major role in its initiation and/or promotion. It is only recently that genetic factors have emerged as significant in the understanding of this disease (Fearon *et al.*, 1990). The high-fidelity replication of the human genome represents a very important biologic goal, which requires the cooperation of many systems. The spontaneous basal mutation rate in normal human cells is not high enough to account for the number of mutations that accumulate in cancer cells. Therefore, the neoplastic cells must acquire and tolerate mutations faster than the basal rates in normal cells (Loeb, 1991). CRC is probably the best model system for analyzing the roles of selection and genomic instability in tumors because of the stepwise nature of their progression, from aberrant crypt foci to early adenoma to late adenoma to adenocarcinoma. Each of these steps is accompanied by a specific genetic alteration (Vogelstein *et al.*, 1989).

CRC may be classified as hereditary when analysis of the family tree shows a pattern of Mendelian (vertical) transmission, familial when there is a cluster of a given cancer or cancers in the kindred, or "sporadic" when no familial predisposition is identified.

Genomic instability in colorectal tumors can involve one of the two apparently different and independent mechanisms: chromosomal instability and genetic instability (Redston, 2001). For sporadic colorectal carcinomas, a multistep model of carcinogenesis has been proposed, which describes somatic mutations and loss of heterozygosity (LOH) in a number of tumor suppressor genes, as well as activation of oncogenes during the malignant transformation of normal colon mucosa to invasive and metastasizing adenocarcinoma (Fearon *et al.*, 1990; Vogelstein *et al.*, 1989). The adenoma–carcinoma sequence is a major mechanism in the development of colorectal cancer via adenomas. The genes that are most frequently affected in sporadic CRC are *APC, Ki-ras,* and *p53*. Additionally, hypermethylation of the deoxyribonucleic acid (DNA) increasing aneuploidy and chromosomal aberration are observed. This pathway accounts for ~80% of

Handbook of Immunohistochemistry and in situ Hybridization of Human Carcinomas,
Volume 2: Molecular Pathology, Colorectal Carcinoma, and Prostate Carcinoma

215

CRC and encompasses most sporadic cancers (suppressor pathway). Failure of the caretakers, genes that safeguard genomic stability by controlling the rate of accumulation of genetic alterations and maintaining replication fidelity, will result in the "mutator" phenotype. Mutations in genetic stability genes could produce additional mutations throughout the genome, leading to a cascade of mutations as the cancer evolves (Loeb, 2001). The mutator pathway accounts for ~15% of CRCs (Edmonston *et al.*, 2000; Redston, 2001).

Although the genome is a database of information that is constantly monitored for both large- and small-scale defects, errors in DNA replication pose one of the greatest threats to cells. Among the DNA repair mechanisms that operate in response to the presence of DNA base damage, three biochemical pathways result in excision of damaged or inappropriate bases. These are called 1) base excision repair (BER); 2) nucleotide excision repair (NER) for the repair of large, bulky DNA lesions; and 3) DNA mismatch repair (MMR), an enzymatic system coded by MMR genes. These systems work primarily on misaligned strands or misincorporated bases and cooperatively prevent insertion/deletion mutations or base substitutions derived from errors caused by replicational polymerases (Loeb, 2001).

The homology between bacterial (*Escherichia coli*) and human proteins deputed to repair errors in DNA replication shows how the structure and functions of the MMR system have been conserved during evolution. Some of the eukaryotic MMR proteins are named MutS and MutL proteins for this reason. The MMR proteins are MSH2 (MutS homologue 2), MLH1 (MutL homologue 1), PMS1 (Postmeiotic segregation 1), PMS2 (Postmeiotic segregation 2), MSH3, and MSH6 (MutS homologue 3 and 6) (Fishel *et al.*, 1997; Kolodner *et al.*, 1999). However, in contrast to the homodimeric structure of bacterial MutL and MutS, eukaryotic MMR is mediated by heterodimeric complexes. In human cells, the recognition of small loops generated by insertion or deletion of nucleotides, as well as simple base mismatches (A:X), is primarily accomplished by a complex called MUTS-α, a heterodimer of MSH2 and MSH6. Another heterodimer, MUTS-β, comprising MSH2 and MSH3, can also be involved in the recognition of small loops during mismatch repair. Thus, the two different complexes MutS-α and MutS-β are responsible for mismatch recognition (Fishel *et al.*, 1997), but it is important to note that, whereas MSH2 must necessarily be present in the complexes, MSH3 can replace MSH6 in the repair of insertion–deletion mismatches, but not in single-base mispairs. On the contrary, the MSH2–MSH6 complex has a role in the repair of single-base pair mispairs, rather than larger insertion–deletion mispairs.

Following mismatch binding, MutL-α complex, a heterodimeric complex of MutL-related proteins, MLH1-PMS2 (and possibly another alternative complex formed by MLH1-MLH3) is recruited, and this larger complex, together with numerous other proteins, accomplishes MMR. Interaction of the two MutLa subunits is mediated by the carboxy-terminal regions of the two proteins. Mutations in this domain result in reduced affinity of the heterodimeric partners and consequent MMR impairment. Then, MMR genes correct nucleic base anomalies and alterations in short repeat units (microsatellites) that occur during DNA replication.

Correction of biosynthetic errors in the newly synthesized DNA is not the only function of the DNA mismatch repair system. It is also able to recognize lesions caused by exogenous mutagens and has been shown to participate in transcription-coupled repair. The MMR proteins also appear to be involved in other biologic activities, including induction of apoptosis in response to DNA damage, acting as a molecular switch. The triggering of the apoptotic response requires the cell to be able to recognize the presence of DNA damage, produced by cytotoxic agents (Zhang *et al.*, 1999). The current hypothesis is that, when mismatch repair is disabled, the cell cannot sense DNA lesions and cannot generate the signals that eventually result in apoptosis. Such cells may survive on the basis that they are tolerant of additions in their DNA. The DNA MMR system also provides a crucial contribution to the toxicity of DNA-damaging drugs that are used in cancer chemotherapy because most anticancer drugs act by causing cell death via apoptosis.

Dysfunction of the repair machinery results in an accumulation of mutations throughout the genome, especially in loci that contain short tandem repeats (Boland *et al.*, 1998), and leads to the mutator phenotype, characterized by frequent length alterations of microsatellites. Microsatellites are one of the most abundant classes of intergenic repetitive sequences dispersed on eukaryotic genomes as part of the coding regions of genes and in interspersed (noncoding) stretches of DNA. These sequences vary from one individual to the next and are the basis for the precise DNA fingerprinting used in forensics. Microsatellites are normally relatively stable, and microsatellite instability (MSI) is defined as a relatively frequent change of any length of these loci resulting from either insertion or deletion of repeated units. These are normally repaired, but in the absence of an efficient MMR function, they become permanent. Alleles of different sizes will be formed and can be revealed by polymerase chain reaction (PCR) by comparing the PCR products from tumor tissue with those from normal tissue. Moreover, microsatellites may constitute chromosome

fragile sites with high sensitivity to some genotoxic agents, as has been demonstrated by studies on humans living in regions contaminated by the release of radioactive material after the explosion at Chernobyl power station in 1986 (Dubrova *et al*., 1997).

In 1993, a class of microsatellites was found to exhibit instability at the level of somatic cells in cases of CRC and in cancers occurring in patients with one of the cancer-prone syndromes, hereditary nonpolyposis colorectal cancer (HNPCC) (Ionov *et al*., 1993; Peltomäki *et al*., 1993; Thibodeau *et al*., 1993). HNPCC is an autosomal-dominant inherited condition predisposing to cancer, characterized by early onset CRC with a proximal location, increased risk of neoplasia of other organs (endometrium, urothelium, small intestine, and ovary), and synchronous and metachronous CRC (Lynch *et al*., 1993). The HNPCC syndrome is responsible for 3–13% of all CRCs (Samowitz *et al*., 2001). The interest in MMR genes is related to the discovery of germline mutations in some MMR genes in HNPCC kindred (Peltomäki *et al*., 1993; Thibodeau *et al*., 1993). Patients with HNPCC inherit one mutant copy of one of the MMR genes from the affected parent and one wild-type copy (normal) from the unaffected parent. The wild-type allele allows expression of the normal protein and maintains MMR activity in normal cells. In tumor cells, the wild-type allele is inactivated by mutation, deletion, or methylation (Raedle *et al*., 2001), leaving the cells with no functional protein and, hence, a deficiency in MMR.

The most important genes of the MMR system are *MSH2* and *MLH1*. The *MSH2* gene has 2805 nucleotides in 16 exons localized on chromosome 2p21. The *MLH1* gene has 19 exons and comprises 58 Kb of genome DNA codifying sequence, featuring 2268 nucleotides, localized in 3p21-23. So far, more than 332 germline mutations in DNA MMR genes have been identified (IGC-HNPCC database), the majority being found in *MLH1* (49%) and *MSH2* (38%). In HNPCC kindred, *MSH2* and *MLH1* mutations are more rarely associated with *MSH3* (2%) or *MSH6* (9%) mutations (Peltomäki, 2001). The hot spots of mutation in germline and somatic mutation of these genes have not yet been fully determined. The exon–intron junction of exon 5 in *MSH2* is suspected to be one of these hot spots. Mutations of other MMR genes (*PMS1* 0.3%; *PMS2* 2%) have also been detected, although they do not seem to have an important role in cancer predisposition. Thus, microsatellite instability, now considered the hallmark of HNPCC, is secondary to mutations of several specific genes implicated in the DNA MMR system, such as *MLH1, MSH2, MSH6, MSH3, PMS2*, and *PMS1*.

After these initial pioneering studies, which did not make a clear distinction between MSI Low (MSI-L),

MSI High (MSI-H), and microsatellite stable (MSS) cancers, international guidelines were defined. The panel (minimum) of five microsatellite markers recommended by the National Cancer Institute and the International Collaborative Group for HNPCC (Boland *et al*., 1998) includes the dinucleotide CA repeat markers, such as D2S123, D5S346, D17S250, and two poly A markers: BAT25 and BAT26 (a poly-A tract localized in the fifth intron of MSH2).

MSI tumors are defined as high (H) when they show instability at two or more markers and low (L) when this occurs at only one marker. When more than five markers are adopted, tumors showing more than 30% instability at the markers used were defined as unstable (Thibodeau *et al*., 1998). MSS cancer did not show instabilities at any marker.

Because high frequency microsatellite instability (MSI-H) is the phenotypical manifestation of an MMR defect, a genomic-based classification of CRC can be used to guide clinical decision management, distinguishing MSI cancer from MSS, because MSI-L has almost the same behavior as MSS (Boland *et al*., 1998; Thibodeau *et al*., 1998; Togo *et al*., 2001).

Several studies have recognized differences in epidemiologic, pathologic, prognostic, molecular, and therapeutic aspects between MSS CRC and MSI-H CRC (Hemminki *et al*., 2000; Jass *et al*., 1998; Mayer *et al*., 2002; Perrin *et al*., 2001; Watanabe *et al*., 2001). MSI-H CRC has been associated with age (younger patients), tumor site (right), sex (female), ploidy status (euploid), stage (more favorable), and family history (positive) (Boland *et al*., 1998; Chapusot *et al*., 2002; Loeb, 2001; Peltomäki, 2001; Togo *et al*., 2001). MSI is demonstrable in 15% of sporadic CRC (Thibodeau *et al*., 1993). Recognition of sporadic MSI CRC is of importance because of its different prognosis, possible increased likelihood of multiple tumors, different profile of molecular tumorigenesis, and possible different response to chemotherapy (Claij *et al*., 1999; Jacob *et al*., 2001; Perrin *et al*., 2001; Yamashita *et al*., 2000). Because tumors arising in HNPCC are phenotypically characterized by a high level of genetic instability, it has been suggested that the name HNPCC should be changed to the more appropriate name, "hereditary MMR deficient syndrome," but no consensus has been reached on this issue (Boland *et al*., 1998). In any case, MSI is demonstrable by PCR in more than 80% of HNPCC (Aaltonen *et al*., 1993; Ionov *et al*., 1993). Furthermore, from 57% to 93% of cases of HNPCC adenoma also show MSI. Promotion from MSI-L to MSI-H has also been demonstrated in adenoma progression in HNPCC, as well as a significant association of MSI-H status with high-grade dysplasia. On the contrary, a low level of MSI was evident in

hyperplastic and in serrated adenomas, suggesting a mild mutator pathway for these lesions (Iino *et al*., 2000; Jass *et al*., 2000). However, MSI is not specific to HNPCC and occurs in other tumors as well: gastric, endometrial, hepatic (Peirò *et al*., 2001; Wang *et al*., 2001). Moreover, HNPCC and sporadic MSI-H cancer, which share a parallel tumorigenesis pathway (mutator pathway), generally have a better stage-for-stage prognosis than sporadic MSS-CRC (Boland *et al*., 1998; Perrin *et al*., 2001). However, both HNPCC tumors and sporadic CRCs with MSI are thought to exhibit a faster tumor progression rate from adenoma to carcinoma (Kinzler *et al*., 1996). In addition, the MSI phenotype has been demonstrated to be useful in predicting the likelihood of developing recurrent disease after surgical resection (Boland *et al*., 1998; Cawkwell *et al*., 1999). Several studies have examined the histopathology of MSI-H CRC and found these tumors to be high-grade, cribriform, mucin-rich tumors displaying a Crohn-like reaction, extensive necrosis, and well-defined borders with an increased number of tumor-infiltrating lymphocytes (CD3+) (Boland *et al*., 1998; Jass *et al*., 1998; Lothe *et al*., 1993).

At the molecular level, whereas HNPCC-MSI cases show germline mutation in MMR genes, methylation of the promoter region of *MLH1* is regarded as the usual pathogenetic basis for nonfamilial examples of MSI-H CRC (Ahuja *et al*., 1997; Raedle *et al*., 2001). The methylation, analyzed by methylation-specific PCR using bisulfite sequencing, occurs at the cytosine residues of CpG islands (CGC- and CpG-rich areas) in the proximity of the promoter region. The DNA methylation inhibits the start of transcription by reducing the binding affinity of transcription factors. Inactivation of *MLH1* as a result of epigenetic methylation of its promoter region has been shown to be age- and sex-related and modulated by carcinogen exposure (Ahuja *et al*., 1997). If MMR genes are mutated, mismatch errors also may affect other genes with an important role in cancer progression, such as tumor suppressor genes (*APC* = *adenomatous polyposis coli*), resulting in the development of malignancy (from adenoma to carcinoma). Moreover, the alterations that accumulate during progression of both hereditary and sporadic neoplasms characterized by MSI-H include mutations in microsatellites within the coding region of some genes involved in growth control and apoptosis, such as *TGFβRII, IGFR,* and *BAX* (Edmonston *et al*., 2000; Rampino *et al*., 1997; Togo *et al*., 2001). In fact, the coding sequence of the type II TGF-β receptor contains an A8 repeat, and *BAX* harbors a poly G tract, making them preferential targets for mutations in MMR-deficient tumors. The gene encoding TGF-βRII is mutated in 90% of CRCs with MSI (Parsons *et al*.,

1995). *BAX*, which encodes a protein that has a central role in the induction of apoptosis, is altered in more than 50% of MSI tumors (Rampino *et al*., 1997).

Most, but not all, studies on colon cancer suggest that mutations in MMR genes and the resulting MSI are early events in the pathogenesis of these tumors (Iino *et al*., 2000; Shih *et al*., 2001). The studies on the spectrum of *APC* gene mutations in tumors that exhibit MSI, and those that do not, provide strong evidence that MMR alterations occur prior to mutation in the APC gene, a marker for colon cancer. In either sporadic or HNPCC MSI-H cancers, *p53* mutation loss of heterozygosity in 17p and 18p are infrequent (Edmonston *et al*., 2000). It has also been shown that wild-type p53 has the ability to bind insertion deletion loops, cooperating with MSH2 in lesion recognition (Toft *et al*., 2002). The defective MMR machinery at the germline level in HNPCC and the specific organ (colon) involvement in tumorigenesis is more difficult to explain. It is tempting to suggest that food-borne alkylating agents may be involved in the selection of colon cells with MMR gene mutations, acting through inactivation of the second allele (Fishel *et al.*, 1999). Because of lack of specific clinicopathologic phenotypical features in HNPCC, a clinical diagnosis is impossible in the individual patient and the suspicion relies heavily on a positive family history.

In practice, the first approach for the stratification and allocation of patients to the appropriate category of putative genetic risk is inquiry about the incidence of all cancers in first-degree relatives, especially in young individuals, and multiple cancer cases. It has proved to be very difficult to formulate diagnostic criteria for HNPCC that can select as many patients as possible with pathogenetic germline mutations in one of the MMR genes while reducing screening in those cases, without such mutations, to a minimum (Raedle *et al*., 2001; Terdiman *et al*., 2001; Vasen *et al*., 1999).

Furthermore, the modern smaller family makes it difficult to find three first-degree relatives affected by cancer and to perform linkage analysis; also "de novo" germline mutations, the existence of phenocopies (individuals affected by sporadic CRC in a family with HNPCC), and the nonpenetrance of a mutation make it more difficult to identify eligible candidates for molecular testing. Nevertheless, genetic testing of individuals at high risk of developing certain hereditary conditions remains a powerful emerging strategy for the prevention of the disease. The detection of pathogenic mutations in persons at high risk of developing CRC, from families with HNPCC, has made presymptomatic diagnosis possible. However, although genetic testing for HNPCC is available, the high cost

and fear of insurance and social discrimination remain major barriers to full implementation.

The majority of mutations occurring in the *MLH1* and *MSH2* genes consist of splice-site, frameshift, and nonsense changes, which lead to the formation of a truncated protein and loss of protein function (Togo *et al.*, 2001). Analysis of constitutional DNA for *MSH2* and *MLH1* mutations is not straightforward because both genes are relatively large and mutations are scattered throughout each gene (Stone *et al.*, 2001). Persistent ambiguity regarding the functional significance of missense codons identified by gene sequencing will severely impair the utility of the genetic tests. Three classes of missense codons have been defined: complete loss of functions (mutations), variants indistinguishable from wild-type protein (silent polymorphisms), and functional variants that reduce the MMR efficiency (efficiency polymorphisms). In these cases, it is necessary to validate the sequencing results with complementary techniques, which can detect the protein products of genes. Moreover, the sequencing method adopted to search for a germline mutation is sometimes unable to show MMR gene alteration. In fact, some cases with loss of both proteins (MSH2 and MLH1) do not show gene alterations. This is possible because of the mutation type, such as the deletion of entire exons, or alterations in the promoter region that cannot be detected by the genetic methods adopted. In addition, some cases without the MSI phenotype can harbor germline mutations in MMR genes, such as *MSH6*. In fact, the MSH6 protein, related to correction of single base mispairs, is not responsible for MSI and is not searched for.

The specific mutation analysis is performed only when a positive tumoral MSI status is revealed. Germline mutations of *MSH6* would be searched for in cases of suspected HNPCC without MSI because the *MSH6* mutation can cause an attenuated mutator phenotype (Berends *et al.*, 2001). Finally, screening for mutations is time consuming and expensive because of the heterogeneity of the mutations in DNA MMR genes. Instead, several studies have demonstrated that MSI status detected by the immunohistochemical method has a high predictive value and high sensitivity (ranging from 72% to 96%) for underlying germline mutations of *MSH2* and *MLH1* (Marcus *et al.*, 1999; Stone *et al.*, 2001; Thibodeau *et al.*, 1996).

In fact, when the MMR system is working well, the protein products involved in the DNA repair are normally expressed in the tissue and can be demonstrated by immunohistochemical analysis in the nuclei of the cells. Because MMR-defective cells in MSI cancers are unable to produce normal MMR proteins, immunohistochemical analysis can reveal the lack of expression of MSH2 and/or MLH1, and other related proteins,

providing rapid and relatively inexpensive proof of the existence of an antigenically different protein (truncated protein) caused by mutation of the corresponding gene. In this way, it is possible to infer a genetic alteration of the MMR system in a tumor on the basis of the effects of its malfunction, using a more rapid, practical, and convenient method, albeit indirect.

MATERIALS

1. Fixative: 10% neutral buffered formalin (NBF): 100 ml formalin, 4 g NaH_2PO_4 monohydrate, 6.5 g anhydrous NaH_2PO_4, bring vol to 1 L.

2. 0.5% Tween-20/phosphate buffer saline (PBS): 7.75 g NaCl, 1.5 g K_2HPO_4, 0.2 g KH_2PO_4, 0.5 ml Tween-20; bring vol to 1 L with deionized water, pH 7.6.

3. Tris-buffered saline (TBS): 2.4 g Tris-HCl and 8.76 g NaCl; bring vol to 1 L with deionized water, pH 7.4.

4. 0.05 M Tris: 6.1 g tris-hydroxy-methylamino-methane in 50 ml of deionized water. Add 37 ml 1 N HCl; bring vol to 1 L with deionized water, pH 7.6.

5. 3-aminopropyltriethoxysilane (APS): 2 g 3-aminopropyltriethoxysilane in 100 ml acetone.

6. Glass slides: Clean in alcohol before use.

7. Ethyl alcohol: 50%, 70%, and 95%.

8. 3% peroxidase blocking solution: 20 ml 30% H_2O_2 in 180 ml methanol.

9. 10 mM citrate buffer solution (this should be freshly made): Stock solution A: 0.1 M citric acid (21.01 g in 1000 ml deionized water); stock solution B: 0.1 M sodium citrate (29.41 g in 1000 ml deionized water); store at 2–8°C, 9 ml of A + 41 ml of B, add deionized water to a final volume of 500 ml.

10. 10% normal rabbit serum: 10 ml normal goat serum (Dako, Glostrup, Denmark) + 90 ml Tween-20-PBS.

11. Primary antibodies: MSH2 (clone FE11, Oncogene Research Product, Boston, MA), MLH1 (Clone G168-728, Pharmingen, San Diego, CA), MSH6 (polyclonal rabbit antiserum, Oncogene Research Products) diluted 1:50 in 0.5% Tween-20%-PBS to a final concentration of 10 µg/ml, 2 µg/ml, 10 µg/ml, respectively. PMS2 (clone A16-4, Pharmingen) Polyclonal antibodies anti MSH3, MLH3, PMS1 (Santa Cruz Biotechnology, CA).

12. Negative control: nonimmune mouse serum (Dako) diluted in 0.5% Tween-20/PBS at a protein concentration of 10 µg/ml.

13. Biotinylated secondary antibody (anti-mouse for monoclonal primary antibodies and anti-rabbit for polyclonal primary antibodies) (Dako) diluted 1:300 in 0.5% Tween-20%-PBS to a final concentration of 340 µg/ml.

14. Endogenous biotin block: avidin solution (0.1% avidin in PBS), biotin solution (0.01% biotin in PBS).

15. Peroxidase streptavidin (Dako): diluted 1:500 in 0.5% Tween-20%-PBS to a final concentration of 1.5 mg/L. Diaminobenzidine (DAB) substrate solution: Dissolve 6 mg DAB in 10 ml 0.05 Tris buffer, pH 7.6. Add 0.1 ml 3% hydrogen peroxide, mix and filter if precipitate forms. (Solution is stable for 2 hr at room temperature).

METHOD

Current formalin-fixed and paraffin-embedded specimens from colorectal carcinomas can be used for immunohistochemical analysis. Old paraffin-embedded block can be used for immunohistochemistry (IHC) if a good technical handling of the tissue in all the processing steps, especially duration of the fixation, is warranted. Ideal working conditions consist of the use of three paraffin blocks of the same tumor, two of which would be specular of samples supplied for the PCR method and the third would include adjacent normal mucosa, serving as internal control.

1. Fix tissue blocks ($30 \times 25 \times 4$ mm) in NBF for up to 24 hr.

2. Wash in running water for 2 hr.

3. Proceed with dehydration and paraffin embedding.

4. Cut three sections 4 microns thick per case, mount on sylanized slides, and dry overnight at 37°C or at room temperature for 48 hr.

5. Remove paraffin in xylene (2 changes of 20-min each).

6. Rehydrate partially by two 3-min immersions in 95% ethanol.

7. Quench the endogenous peroxidase by 20-min incubation in 3% hydrogen peroxide in methanol.

8. Completely rehydrate by 3-min immersion in 70% ethanol and two 5-min immersions in 0.5% Tween-20-PBS, pH 7.6.

9. Perform antigen retrieval with a steel pressure cooker: Fill the cooker with citrate buffer solution and bring to the boil without the lid. When boiling is observed, wholly dip the slides (stacked in a metal rack) in the buffer. At the greatest pressure wait for 1 min 30 seconds. Remove the cooker from the electric plate and let out all the steam through the opposite valve. Open the lid and cool the slides with running water.

10. Soak the slides in 0.5% Tween-20-PBS, pH 7.6 in a Coplin jar (2 changes of 5 min each). Perform all remaining incubations with 200 µl of reagent per slide at room temperature in a humid chamber.

11. Blot excess liquid from around specimens.

12. Treat the section with 10% normal rabbit serum for 10 min.

13. Blot as in **Step 11**.

14. Incubate with avidin solution for 20 min.

15. Rinse as in **Step 10**.

16. Incubate with biotin solution for 20 min.

17. Rinse as in **Step 10**.

18. Blot as in **Step 11**.

19. Incubate with primary antibody or with nonimmune normal serum (negative control) for 30 min.

20. Rinse as in **Step 10**.

21. Blot as in **Step 11**.

22. Incubate with secondary antibody biotinylated F(ab′)2 fragment of anti-mouse Ig or anti-rabbit Ig diluted 1:300 in 0.5% Tween-20-PBS, pH 7.6, for 30 min.

23. Rinse as in **Step 10.**

24. Blot as in **Step 11**.

25. Incubate with streptavidine-peroxidase for 30 min.

26. Rinse as in **Step 10**.

27. Blot as in **Step 11**.

28. Incubate with DAB substrate solution, freshly made before use.

29. Rinse briefly in running water.

30. Counterstain lightly with hematoxylin, dehydrate in graded alcohols, clear in xylene, and coverslip.

Clone FE11 is a mouse monoclonal antibody generated with a COOH-terminal fragment of the MSH2 protein, whereas clone G168-728 was prepared with a full-length MLH1 protein. Clone A16-4 is a monoclonal mouse antibody generated against a COOH-terminal fragment of the PMS2 protein (aa 431-862). The polyclonal rabbit antisera are raised against the full-length MSH6 protein, purified over a protein A column, against the epitope corresponding to amino acids 1228-1453 mapping at the carboxyl terminus of MLH3 and against the epitope corresponding to amino acids 633-932 mapping at the carboxyl terminus of PMS1. The normal staining pattern for both MLH1 and MSH2 (Figure 34) and for other MMR proteins is nuclear. Lack of expression of MLH1 and/or MSH2 and other MMR proteins is defined as complete absence of detectable nuclear staining in the tumor cells. Intact nuclear staining of colonic crypts of the peritumoral normal mucosa, stromal cells, endothelial cells, and lymphocytes represents the internal positive control and is required for adequate evaluation. When normal tissue is not stained, the sample is considered ambiguous. Specimens with positive staining even in a small cluster of neoplastic cells must be considered to express the proteins, so regional positivity should be reported as demonstrating the presence of an antigenically normal protein.
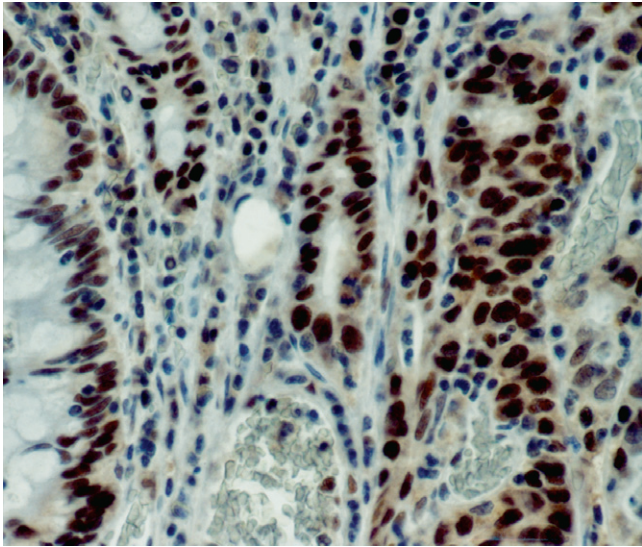
Figure 34 The immunohistochemical nuclear expression of MSH2 in colorectal cancer cells. (Final magnification 250X.)

These results justify the classification of the immunoreactivity as focal or diffuse. Moreover, the intensity of staining in the single-cell nucleus would be graded as weak or strong to obtain a more precise correlation between protein expression and their functional ability. It is possible that the amount of normal protein produced and the affinity (normal or reduced) of the heterodimeric partners of MMR complexes could affect the function and therefore the intensity of the staining.

RESULTS AND DISCUSSION

Dysfunction of the DNA MMR system, as a result of mutations or inactivation of genes, is responsible for causing cells to become cancerous in HNPCC and for some cases of sporadic colon cancer. Unfortunately, there are technical limitations to the detection of mutations in the MMR genes, be they germline or somatic. These large genes have no mutation hot spots; hence no simple strategies can be used to detect mutations. Detection of *MLH1* promoter hypermethylation with methylation-specific PCR also suffers from a number of drawbacks (Yuen *et al*., 2002). However, the phenotypic expression of an MMR defect is the presence of novel alleles at microsatellite loci, demonstrable at molecular level by PCR amplification, which is considered the gold standard for MSI recognition.

The practical importance of microsatellite status assessment is related to the fact that in addition to HNPCC, 15% of all sporadic cancers show the MSI phenotype and 30–35% of unselected proximal colon cancers also show MSI and abnormal MMR protein

expression, resulting in a distinctive pathologic and clinical phenotype (Perrin *et al*., 2001). Hence, detection of MSI in tumors can provide a practical method of identifying those patients whose mutational analysis is appropriated and those featuring different prognostic and hence therapeutic patterns. But MSI assessment in tumor samples requires microdissection procedures and molecular biologic laboratory techniques that are complex, labor intensive, and expensive. Moreover, the MSI status identified by molecular approaches is not ideally suited for routine clinical practice in the pathology department.

Because DNA determines the phenotype and hence protein expression, DNA mutations can often be detected or inferred by indirect means. It has been shown that in tumor tissues loss of DNA MMR protein expression, detected by IHC, one of the two major MMR proteins may correlate with MSI and germline mutation of the corresponding gene (Cawkwell *et al*., 1999; Chapusot *et al*., 2002; Marcus *et al*., 1999). Since the role of germline mutations in the MMR genes *MLH1* and *MSH2* was recognized to cause HNPCC, numerous studies have evaluated the usefulness of IHC as a method of identifying CRCs with MSI caused by inactivation of the *MSH2* or *MLH1* genes (Dieumegard *et al*., 2000; Marcus *et al*., 1999; Stone *et al*., 2001; Thibodeau *et al*., 1996). The sensitivity of this methodologic approach ranges from 72% (Thibodeau *et al*., 1996) to 97% (Marcus *et al*., 1999); the negative predictive value (NPV) ranges from 50% (Thibodeau *et al*., 1996) to 97% (Marcus *et al*., 1999). These values for NPV make mutation analysis necessary in cases with high probability of HNPCC but with normal expression of the two proteins (Perrin *et al*., 2001).

In a recent study on different mechanisms of MMR deficiency, loss of one or the other protein was evident in all MSI-H tumors arising in patients with a family history, in 80% of sporadic early-onset tumors, and 70% of sporadic late-onset tumors (Yuen *et al*., 2002). In contrast, the proteins were invariably expressed in tumors without MSI-H. Germline mutation in *MLH1* or *MSH2* was detectable in 93% of cases. Germline *MSH2* mutation was detected in the majority of tumors with deficient MSH2 protein expression (75%), including 91% of familial and 40% of sporadic early-onset tumors (Yuen *et al*., 2002).

In our experience, in colon cancer, in patients with sporadic and familial tumors, the concordance rate between the microsatellite status identified by PCR as MSS or MSI, and immunohistochemical detection of the MSH2 and MLH1 proteins, was 80%. Protein expression was demonstrated in the normal mucosa in all cases, being more evident in the proliferative zone

of the crypts and in the germinal center of lymphoid follicles. This compartmentalized enhancement suggests that there is transcriptional control of MMR protein expression, as occurs for other proteins involved in DNA replication. Moreover, no difference was found regarding the staining of both proteins in normal tissue, confirming the good preservation of antigenicity in the materials under study (Valentini *et al.*, 2002).

A preponderance of *MLH1* abnormalities with respect to *MSH2* defects in sporadic CRC have generally been reported (Cawkwell *et al.*, 1999; Chapusot *et al.*, 2002; Thibodeau *et al.*, 1998), whereas in HNPCC it is mainly the MSH2 protein that is lost (65%) (Yuen *et al.*, 2002). It is hypothesized that an excess of *MLH1* abnormalities could be because the *MSH2* promoter is less likely to be inactivated by methylation (Cawkwell *et al.*, 1999). In fact, lack of MLH1 protein expression in immunohistochemical analysis can also occur in the absence of germline or somatic mutations of genes in cancers without the familial stigmata (sporadic tumors) because of inactivation of the gene expression as a result of methylation to the promoter. For some gene loci, such as the ER and *IGF2* loci, the CpG island methylation actually begins in normal cells as a function of aging, and these aged cells may be selected during tumor formation. This suggestion is in agreement with the finding of a greater number of elderly patients with MSI-sporadic CRC. In addition, hypermethylation of the promoter region may be reversed *in vitro,* with subsequent reexpression of the protein; this raises the possibility of its clinical application as a future target of possible therapy (Wheeler *et al.*, 1999). In a recent study, methylation of the biallelic promoter in region 2 was identified in 83% of tumors that lacked MLH1 protein expression (Yuen *et al.*, 2002).

However, not all MSI-positive cases will be detected by the IHC research of MSH2 and MLH1 either for missense mutation of the two genes or for mutations in other genes (Redston, 2001). In fact, MSI status may not be concordant with the loss of protein pattern, when the MMR defect is related to a functional mutation rather than to an antigenic alteration of the proteins. In any case, IHC helps to identify the functional significance of a DNA mutation when a novel germline mutation in either *MSH2* or *MLH1* is detected in a patient with cancer whose family history satisfies the Amsterdam Criteria. Immunohistochemical findings showing lack of expression of the proteins suggest that the mutation is a disease-causing mutation.

In some families with only the suspicion of HNPCC but displaying MSS or MSI-low status, *MSH6*, essential in the repair of single nucleotide mismatches, shows germline mutations. In fact, *MSH6* mutations are responsible for a subset of HNPCC family cancers with an atypical pedigree, a low level of microsatellite instability, proximal localization, later age at diagnosis, and an association with extracolonic tumors. In other cases of *MSH6* germline mutation, MSI-H is the result of association with a truncating MLH1 mutation (Berends *et al.*, 2001; Boland *et al.*, 1998).

Because a small number of MSI CRCs are caused by mutations in MMR genes other than *MSH2* and *MLH1,* belonging to the MMR system, the usefulness of IHC as an initial screening tool will be extended by the use of antibodies against MSH6, MSH3, PMS1, and PMS2, which are now commercially available. Furthermore, polymorphisms of certain genes (cyclin D1, N-acetyltransferase) not associated with the MMR system affect the expression of MMR gene mutations, causing differences in the mean age at diagnosis of CRC in HNPCC and making it more difficult to recognize a suspicious pedigree (Kong *et al.*, 2000).

Because adenoma with MSI progresses more quickly to carcinoma and more often contains cancer foci in patients with HNPCC (Boland *et al.*, 1998), it is also important to assess MSI in the precursors of cancers to detect high-risk patients. Most colorectal adenomas show loss of MLH1 or MSH2 proteins; although additional secondary mutations in *MSH3* and *MSH6* may rarely be present, immunohistochemical staining of the prevalent abnormal proteins can aid in risk assessment of individual patients (Iino *et al.*, 2000). Thus, IHC detection of MMR proteins in patients with HNPCC with both newly diagnosed adenoma and CRC can be considered useful and cost-effective, especially if the benefits to their immediate relatives are also considered.

Because IHC evaluation of protein expression indirectly highlights a mutator phenotype by demonstrating the absence of staining, the main problem is the question of how reliable this is as an indication of the real existence of an MMR malfunction. In fact, using the IHC method the MMR system of a tumor is defined as deficient when, in concurrence with the immunoreactivity of normal tissue, no nuclear staining of carcinoma cells is seen for at least one of the MMR proteins. Thus, the reliability of the methodologic criteria for immunohistochemical staining and the accuracy of evaluation of the results are very important. In most studies, MSI is correlated with the lack of protein staining, defined as complete absence of staining in colon cancer cells, although in some studies on CRC and on multiple primary cancers of the gastrointestinal tract, reduced (weak) staining expression of MHL1 and/or MSH2 is considered to be associated with MSI (Yamashita *et al.*, 2000). Yamashita's study also demonstrated intertumoral heterogeneity in

75% of the cases with the MSI phenotype, in agreement with the concept that other carcinogenetic processes can act concurrently in multiple cancer cases, whether or not they belong to the HNPCC syndrome. This emphasizes the need for a detailed, precise report of immunohistochemical staining as a result of the existence of intratumoral heterogeneity so that in the future better correlations with clinicopathologic and molecular data are revealed. Intratumoral heterogeneity, a very important issue in IHC field, has not aroused great interest in literature, although Chapusot *et al*. (2002) showed discrepancy between the two methods, according to the area analyzed, by examining the concordance rate between the PCR and IHC methods. In fact, the authors found 95% concordance when the same tissue sample was used for both techniques and only moderate concordance (73.7%) when different tissue samples from the same tumor were studied. It is important to bear in mind the regional variability of MMR protein expression at the time of evaluation because heterogeneous cases do not show the significant pathologic characteristics that distinguish them from other nonheterogeneous cases. Thus, the number and the processing quality of the samples to be used are important issues that must be taken into account.

In the section on methods, the use of at least three blocks of tissue for each tumor is suggested. By using three samples for IHC analysis, a relatively high percentage (52%) of focal staining is found in both MSI and MSS cases, with a significant association between MSI and MLH1 focal expression. Because the homogeneous staining throughout the entire tumor was the prevalent pattern in MSS cancers, the focal immunoreactivity remains a possible subthreshold condition for detection with the IHC method in MSI cases (unpublished data). The problem of overestimation of MMR deficiencies also remains when we have to use IHC to evaluate bioptic material from patients before surgery. The focal loss of MLH1 expression highlighted in the study by Chapusot *et al*. (2002) was associated with regional variability of the MSH6 protein, suggesting that the latter represents a secondary event acquired after MLH1 deficiency. In fact, mutation of some mutator genes leads to further mutation of other mutator genes. Furthermore, missense mutations of *MSH2/MLH1* or single amino acid changes may not impair protein function or may be only partially inactivating leading to a reduction rather than loss of protein expression (Krüger *et al*., 2002) as revealed by Western Blot analysis (Kim *et al*., 1998). This is the reason why IHC results need to be fully documented, with details of the amount and distribution of nuclear staining in the tumor and its intensity in single cells. The main reasons for careful performance and

evaluation of IHC analysis to avoid overestimation of the incidence of MSI include the following: 1) the possible existence of genuine mixed tumors exhibiting heterogeneous MMR deficiency; 2) the existence of regional variability of expression of some or all the MMR proteins; and 3) the risk of poor technical handling of tissues precluding their binding to antigenic epitopes. In this regard, the major responsibility is attributed to incorrect fixation because the monoclonal antibody for MLH1 is very sensitive to overfixation (Edmonston *et al*., 2000). Another important technical issue is antigen retrieval, which poses some difficulty in old tissue blocks and is better obtained using a steel pressure cooker (Manavis *et al*., 2003). Because of tumor heterogeneity, cell clones may exist in cases with no MSI phenotype, alongside MSI-positive clones (Shibata *et al*., 1994). By sampling different areas of a tumor, it is possible to avoid underestimating the MSI incidence and place confidence in the evaluation of the immunoreactivity of a tumor.

The usefulness of IHC for patient management decisions regarding therapy in CRC with MMR defects has been emphasized in several studies (Claij *et al*., 1999; Mayer *et al*., 2002; Peltomäki *et al*., 2001).

MMR-deficient cells have been shown to be resistant to mutagens through alteration of their apoptotic response, which could represent an obvious selective advantage because most anti-cancer drugs act by causing cell death via apoptosis. MMR inactivation desensitizes the intestinal cell to DNA damage inducing apoptosis and allowing initial clonal expansion (Zhang *et al*., 1999). In experimental systems, MMR-deficient cells are highly tolerant of the methylating chemotherapy drugs streptozocin and temozolamide and, albeit to a lesser extent, to cisplatin and doxorubicin. These drugs are therefore expected to be less effective on MMR-deficient tumors (Claij *et al*., 1999; Mayer *et al*., 2002). Furthermore, CRCs that arise in the setting of MSI also have reduced or absent COX2 expression, indicating that COX2 inhibitors may be of limited use in these patients (Peltomäki *et al*., 2001). Even tumors that are exquisitely chemosensitive (testicular germ cell tumors) are associated with chemotherapy resistance (cisplatin) when there is MMR malfunction (Mayer *et al*., 2002). Instead, CRC cell lines with defective DNA MMR exhibit increased sensitivity to both camptothecin (CPT), a topoisomerase I inhibitor, and etoposide, a topoisomerase II inhibitor. In fact, patients with metastatic CRC and defective MMR have better responsiveness to camptothecin (Jacob *et al*., 2001). Well-targeted specific chemopreventive therapy may be developed in CRC treatment, thanks to the demonstration of increased sensitivity of CRC cells

with MSI to 5-fluorouracyl and the results of treatment of MMR-defective cells with aspirin or Sulindac, which suppressed the mutator phenotype (Ruschoff *et al*., 1998). Therefore, immunohistochemical staining highlighting an MMR deficiency can be a valid tool for use as a predictor for the purposes of drug optimization or prognosis assessment in patients with CRC before chemotherapy.

CONCLUSION

In conclusion, in view of its high correlation with molecular analysis, IHC can replace the sophisticated molecular technique, providing the first data on expression of the most important proteins of the MMR machinery and accurately identifying CRC with MSI. In addition, careful performance of the method and precise evaluation criteria are observed. The greatest value of the immunohistochemical test may be in the management of patients with MSI CRC, both hereditary and sporadic, and it could significantly influence the level of surveillance of the relatives of patients with HNPCC. In patients with suspected HNPCC, IHC specifically identifies the underlying mutated gene and therefore directs guideline mutation analysis to one of the two more frequently affected genes, saving unnecessary random searches for mutations in all the MMR genes. Moreover, because the IHC test is able to recognize the final gene product, the enzymatic protein, it also serves to identify sporadic MSI-H cases of CRC induced by the epigenetic effect, in which the promoter region of *MLH1* is hypermethylated. IHC is a diagnostic test that is able to differentiate between pathogenic mutations and silent polymorphisms in CRC occurring in patients suspected to have a familial cancer syndrome harboring a germline mutation in mutator genes. In addition, IHC can help in the study of families with suspected HNPCC, allowing the detection of MMR deficiency on archived material (old tumoral tissue blocks) of deceased relatives, whereas DNA obtained from old formalin-fixed material often fails to adequately amplify during PCR. Loss of expression of MMR proteins seems to be an early phenomenon in the MSI pathway of CRC carcinogenesis, and IHC is a sensitive and specific method for detecting both the adenoma and the carcinoma phenotype. IHC can contribute to providing new monoclonal antibody-targeted cancer therapies, and on the basis of different sensitivity to radiation and anticancer drugs of MMR competent and defective cells, it may influence treatment decisions before and after surgery.

One minor limitation is that IHC is unable to differentiate somatic from constitutional mutations of one allele (followed by inactivation of the other allele) and

to recognize HNPCC with subtly mutated proteins that retain antigenicity while losing function. In any case, IHC offers a relatively convenient and rapid method for prescreening tumors with defects in the expression of MMR genes that is suitable in all pathology laboratories. This simple and inexpensive ancillary study increases the efficacy of the histopathologic report, offering to the pathologist the opportunity to integrate, even in the presurgical bioptic samples, the standard histopathologic assessment with an indirect evaluation of an important genetic alteration. In short, IHC provides important adjunctive indications of prognostic and therapeutic value.

References

Aaltonen, L.A., Peltomaki, P., Leach, F.S., Sistonen, P., Pylkkanen, L., Mecklin, J.P., Jarvinen, H., Powell, S.M., Jen, J., Hamilton, S.R., Petersen, G.M., Kinzler, K.W., Vogelstein, B., and de la Chapelle, A. 1993. Clues to the pathogenesis of familial colorectal cancer. *Science 260*:812–816.

Ahuja, N., Mohan, A.L., Li, Q., Stolker, J.M., Herman, J.G., Hamilton, S.R., Baylin, S.B., and Issa, J.P. 1997. Association between CpG island methylation and microsatellite instability in colorectal cancer. *Cancer Res. 57*:3370–3374.

Berends, M.J.W., Wu, Y., Sijmons, R.H., Hofstra, R.M.W., van der Zee, A.G.J., Buys, C.H.C.M., and Kleibeuker, J.H. 2001. Clinical definition of hereditary non-polyposis colorectal cancer: A search for the impossible? *Gastroenterology 36* Suppl 234:61–67.

Boland, C.R., Thibodeau, S.N., Hamilton, S.R., Sidransky, D., Eshleman, J.R., Burt, R.W., Meltzer, S.J., Rodriguez-Bigas, M.A., Fodde, R., Ranzani, G.N., and Srivastava, S. 1998. A national cancer institute workshop on microsatellite instability for cancer detection and familial predisposition: Development of international criteria for the determination of microsatellite instability in colorectal cancer. *Cancer Res. 58*:5248–5257.

Cawkwell, L., Gray, S., Murgatroyd, H., Sutherland, F., Haine, L., Longfellow, M., O'Loughlin, S., Cross, D., Kronborg, O., Fenger, C., Mapstone, N., Dixon, M., and Quirke, P. 1999. Choice of management strategy for colorectal cancer based on a diagnostic immunohistochemical test for defective mismatch repair. *Gut 45*:409–415.

Chapusot, C., Martin, L., Bouvier, A.M., Bonithon-Kopp, C., Ecarnot-Laubriet, A., Rageot, D., Ponnelle, T., Laurent Puig, P., Faivre, J., and Piard, F. 2002. Microsatellite instability and intratumoral heterogeneity in 100 right-sided sporadic colon carcinomas. *Br. J. Cancer 87*:400–404.

Claij, N., and te Riele, H. 1999. Microsatellite instability in human cancer: A prognostic marker for chemotherapy? *Exp. Cell Res. 246*:1–10.

Dieumegard, B., Grandjouan, S., Sabourin, J.C., Le Bihan, M.L., Lefrere, I., Bellefqih, Pignon, J.P., Rougier, P., Lasser, P., Benard, J., Couturier, D., and Bressac-de Paillerets, B. 2000. Extensive molecular screening for hereditary non-polyposis colorectal cancer. *Br. J. Cancer 82*:871–880.

Dubrova, Y.E., Nesterov, V.N., Krouchinsky, N.G., Ostapenko, V.A., Vergnaud, G., Giraudeau, F., Buard, J., and Jeffrey, A.J. 1997. Further evidence for elevated human minisatellite mutation rate in Belarus eight years after the Chernobyl accident. *Mut. Res. 381*:267–278.

Edmonston, T.B., Cuesta, K.H., Burkholder, S., Barusevicius, A., Rose, D., Kovatich, A.J., Boman, B., Fry, R., Fishel, R., and Palazzo, J.P. 2000. Colorectal carcinomas with high microsatellite instability: Defining a distinct immunologic and molecular entity with respect to prognostic markers. *Hum. Pathol. 31*:1506–1514.

Ellison, A.R., Lofing, J., and Bitter, G.A. 2001. Functional analysis of human MLH1 and MSH2 missense variants and hybrid human-yeast MLH1 proteins in Saccharomyces cerevisiae. *Hum. Mol. Genet. 10*:1889–1900.

Fearon, E.R., and Volgestein, B. 1990. A genetic model for colorectal tumourigenesis, *Cell 61*:759–767.

Fishel, R., and Wilson, T. 1997. MutS homologs in mammalian cells. *Curr. Opin. Genet. Dev. 7*:105–113.

Fishel, R. 1999. Signaling mismatch repair in cancer. *Nat. Med. 5*:1239–1241.

Hemminki, A., Mecklin, J.P., Jarvinen, H., Aaltonen, L.A., and Joensuu, H. 2000. Microsatellite instability is a favorable prognostic indicator in patients with colorectal cancer receiving chemotherapy. *Gastroenterology 119*:921–928.

Iino, H., Simms, L., Young, J., Arnold, J., Winship, I.M., Webb, S.I., Furlong, K.L., Leggett, B., and Jass, J.R. 2000. DNA microsatellite instability and mismatch repair protein loss in adenomas presenting in hereditary non-polyposis colorectal cancer. *Gut 47*:37–42.

Ionov, Y., Peinado, M.A., Malkhosyan, S., Shibata, D., and Perucho, M. 1993. Ubiquitous somatic mutations in simple repeated sequences reveal a new mechanism for colonic carcinogenesis. *Nature 363*:558–561.

Jacob, S., Aguado, M., Fallik, D., and Praz, F. 2001. The role of the DNA mismatch repair system in the cytotoxicity of the topoisomerase inhibitors camptothecin and etoposide to human colorectal cancer cells. *Cancer Res. 61*:6555–6562.

Jass, J.R., Do, K.A., Simms, L.A., Iino, H., Wynter, C., Pillay, S.P., Searle, J., Radford-Smith, G., Young, J., and Leggett, B. 1998. Morphology of sporadic colorectal cancer with DNA replication errors. *Gut 42*:673–679.

Jass, J.R., Iino, H., Ruszkiewicz, A., Painter, D., Solomon, M.J., Koorey, D.J., Cohn, D., Furlong, K.L., Walsh, M.D., Palazzo, J., Bocker Edmonston, T., Fishel, R., Young, J., and Leggett, B.A. 2000. Neoplastic progression occurs through mutator pathways in hyperplastic polyposis of the colorectum. *Gut 47*:43–49.

Kim, H., Piao, Z., Kim, J.W., Choi, J.S., Kim, N.K., Lee, J.M., and Park, J.H. 1998. Expression of hMSH2 and hMLH1 in colorectal carcinomas with microsatellite instability. *Pathol. Res. Pract. 194*:3–9.

Kinzler, K.W., and Vogelstein, B. 1996. Lesson from hereditary colorectal cancer. *Cell 87*:159–170.

Kolodner, R.D., and Marisischky, G.T. 1999. Eukaryotic DNA mismatch repair. *Curr. Opin. Genet. Dev. 9*:89–96.

Kong, S., Amos, C.I., Luthra, R., Lynch, P.M., Levin, B., and Frazier, M.L. 2000. Effects of cyclin D1 polymorphism on age of onset of hereditary nonpolyposis colorectal cancer. *Cancer Res. 60*:249–252.

Krüger, S., Plaschke, J., Pistorius, S., Jeske, B., Haas, S., Krämer, H., Hinterseher, I., Bier, A., Kreuz., F.R., Theissig, F., Saeger, H.D., and Schackert, H.K. 2002. Seven novel *MLH1* and *MSH2* germline mutations in hereditary nonpolyposis colorectal cancer. *Hum. Mutat. 19*:82.

Loeb, L.A. 1991. Mutator phenotype may be required for multi-stage carcinogenesis. *Cancer Res. 51*:3075–3079.

Loeb, L.A. 2001. A mutator phenotype in cancer. *Cancer Res. 61*:3230–3239.

Lothe, R.A., Peltomäki, P., Meling, G.I., Aaltonen, L.A., NyströmLahti, M., Pylkkänen, L., Heimdal, K., Anderson, T.I.,

Moller, P., Rognum, T.O., Fossa, S.D., Haldorsen, T., Langmark, F., Brogger, A., De la Chapelle, A., and Borrensen, A. 1993. Genomic instability in colorectal cancer: Relationship to clinicopathological variables and family history. *Cancer Res. 53*:5849–5852.

Lynch, H.T., Smyrk, T.C., Watson, P., Lanspa, S.J., Lynch, J.F., Lynch, P.M., Cavalieri, R.J., and Boland, C.R. 1993. Genetics, natural history, tumor spectrum and pathology of hereditary nonpolyposis colorectal cancer: An updated review. *Gastroenterology 104*:1535–1549.

Manavis, J., Gilham, P., Davies, R., and Ruszkiewicz, A. 2003. The immunohistochemical detection of mismatch repair gene proteins (MLH1, MSH2, MSH6, and PMS3): Practical aspects in antigen retrieval and biotin blocking protocols. *Appl. Immunohistochem. Mol. Morphol. 11*:73–77.

Marcus, V.A., Madlensky, L., Gryfe, R., Kim, H., So, K., Millar, A., Temple, L.K., Hsieh, E., Hiruki, T., Narod, S., Bapat, B.V., Gallinger, S., and Redston, M. 1999. Immunohistochemistry for hMLH1 and hMSH2: A practical test for DNA mismatch repair-deficient tumors. *Am. J. Surg. Pathol. 23*:1248–1255.

Mayer, F., Dinjens, W., Oosterhuis, J.W., Bokemeyer, C., and Looijenga, L.H. 2002. Microsatellite instability of germ cell tumors is associated with resistance to systemic treatment. *Cancer Res. 62*:2758–2760.

Parsons, R., Myeroff, L.L., Liu, B., Willson, J.K., Markovitz, S.D., Kinzler, K.W., and Vogelstein, B. 1995. Microsatellite instability and mutations of the transforming growth factor β type II receptor gene in colorectal cancer. *Cancer Res. 55*:5548–5550.

Peirò, G., Diebold, J., Mayr, D., Baretton, G.B., Kimming, R., Schmidt, M., and Lohrs, U. 2001. Prognostic relevance of hMLH1, hMSH2, and BAX protein expression in endometrial carcinoma. *Mod. Pathol. 14*:777–783.

Peltomäki, P. 2001. Deficient DNA mismatch repair: A common etiologic factor for colon cancer. *Hum. Mol. Gen. 10*:735–740.

Peltomäki, P., Lothe, R.A., Aaltonen, L.A., Pylkkanen, L., Nystrom-Lahti, M., Seruca, R., David, L., Holm, R., Ryberg, D., Haugen, A., Brogger, A., Borresen, A., and De la Chapelle, A. 1993. Microsatellite instability is associated with tumors that characterize the hereditary non-polyposis colorectal carcinoma syndrome. *Cancer Res. 53*:5853–5855.

Perrin, J., Gouvernet, J., Parriaux, D., Noguchi, T., Giovannini, M-H., Giovannini, M., Delpero, J-R., Birnbaum, D., and Monges, G. 2001. MSH2 and MLH1 immunodetection and the prognosis of colon cancer. *Int. J. Oncol. 19*:891–895.

Raedle, J., Trojan, J., Brieger, A., Weber, N., Schafer, D., Plotz, G., Staib-Sebler, E., Kriener, S., Lorenz, M., and Zeuzem, S. 2001. Bethesda guidelines: Relation to microsatellite instability and MLH1 promoter methylation in patients with colorectal cancer. *Ann. Intern. Med. 135*:566–576.

Rampino, N., Yamamoto, H., Ionov, Y., Li, Y., Sawai, H., Reed, J.C., and Perucho, M. 1997. Somatic frameshift mutations in the *BAX* gene in colon cancers of the microsatellite mutator phenotype. *Science 275*:967–969.

Redston, M. 2001. Carcinogenesis in the GI tract: From morphology to genetics and back again. *Mod. Pathol. 14*:236–245.

Ruschoff, J., Wallinger, S., Dietmaier, W., Bocker, T., Brockhoff, G., Hofstadter, F., and Fishel, R. 1998. Aspirin suppresses the mutator phenotype associated with hereditary nonpolyposis colorectal cancer by genetic selection. *Proc. Natl. Acad. Sci. 95*: 11301–11306.

Samowitz, W.S., Curtin, K., Lin, H.H., Robertson, M.A., Schaffer, D., Nichols, M., Gruenthal, K., Leppert, M., and Slattery, M.L. 2001. The colon cancer burden of genetically defined hereditary nonpoliposis colon cancer. *Gastroenterol. 121*:830–838.

Shibata, D., Peinado, M.A., Ionov, Y., Malkhosyan, S., and Perucho, M. 1994. Genomic instability in repeated sequences is an early somatic event in colorectal tumorigenesis that persists after transformation. *Nat. Genet. 6*:273–281.

Shih, I.M., Zhou, W., Goodman, S.N., Lengauer, C., Kinzler, K.W., and Vogelstein, B. 2001. Evidence that genetic instability occurs at an early stage of colorectal tumorigenesis. *Cancer Res. 61*:818–822.

Stone, J.G., Robertson, D., and Houlston, R.S. 2001. Immunohistochemistry for MSH2 and MHL1: A method for identifying mismatch repair deficient colorectal cancer. *J. Clin. Pathol. 54*:484–487.

Terdiman, J.P., Gum, J.R. Jr., Conrad, P.G., Miller, G.A., Weinberg, V., Crawley, S.C., Levin, T.R., Reeves, C., Schmitt, A., Hepburn, M., Sleisenger, H., and Kim, Y.S. 2001. Efficient detection of hereditary nonpoliposis colorectal cancer gene carriers by screening for tumor microsatellite instability before germline genetic testing. *Gastroenterology 120*:21–30.

Thibodeau, S.N., Bren, G., and Schaid, D. 1993. Microsatellite instability in cancer of the proximal colon. *Science 260*:816–819.

Thibodeau, S.N., French, A.J., Roche, P.C., Cunningham, J.M., Tester, D.J., Lindor, N.M., Moslein, G., Baker, S.M., Liskay, R.M., Burgart, L.J., Honchel, R., and Halling, K.C. 1996. Altered expression of hMSH2 and hMLH1 in tumors with microsatellite instability and genetic alterations in mismatch repair genes. *Cancer Res. 56*:4836–4840.

Thibodeau, S.N., French, A.J., Cunningham, J.M., Tester, D., Burgart, L.J., Roche, P.C., McDonnell, M.J., Schaid, D.J., Walsh Vockley, C., Michels, V.V., Farr, G.H. Jr., and O'Connell, M.J. 1998. Microsatellite instability in colorectal cancer: Different mutator phenotypes and the principal involvement of *hMLH1*. *Cancer Res. 58*:1713–1718.

Toft, N.J., Curtis, L.J., Sansom, O.J., Leitch, A.L., Wyllie, A.H., te Riele, H., Arends, M.J., and Clarke, A.R. 2002. Heterozygosity for *p53* promoter microsatellite instability and tumorigenesis on a MSH2 deficient background. *Oncogene 21*:6299–6306.

Togo, G., Shiratori, Y., Okamoto, M., Yamaji, Y., Matsumura, M., Sano, T., Motojima, T., and Omata, M. 2001. Relationship between grade of microsatellite instability and target genes of mismatch repair pathways in sporadic colorectal carcinoma. *Dig. Dis. Sci. 46*:1615–1622.

Valentini, A.M., Renna, L., Armentano, R., Pirrelli, M., Di Leo, A., Gentile, M., and Caruso, M.L. 2002. Mismatch repair, p53 and β-catenin proteins in colorectal cancer. *Anticancer Res. 22*:2083–2088.

Vasen, H.F.A., Watson, P., Mecklin, J.P., and Lynch, H.T. 1999. New clinical criteria for hereditary nonpolyposis colorectal cancer (HNPCC, Lynch syndrome) proposed by the International Collaborative Group on HNPCC. *Gastroenterology 116*: 1453–1456.

Vogelstein, B., Fearon, E.R., Kern, S.E., Hamilton, S.R., Preisinger, A.C., Nakamura, Y., and White, R. 1989. Allelotype of colorectal carcinomas. *Science 244*:207–211.

Wang, L., Bani-Hani, A., Montoya, D., Roche, P.C., Thibodeau, S.N., Burgart, L.J., and Roberts, L.R. 2001. hMLH1 and hMSH2 expression in human hepatocellular carcinoma. *Int. J. Oncol. 19*:567–570.

Watanabe, Y., Koi, M., Hemmi, H., Hoshai, H., and Noda, K. 2001. A change in microsatellite instability caused by cisplatin-based chemotherapy of ovarian cancer. *Br. J. Cancer 85*:1064–1069.

Wheeler, J.M.D., Beck, N.E., Kim, H.C., Tomlinson, I.P.M., Mortensen, N.J., McC., and Bodmer, W.F. 1999. Mechanisms of inactivation of mismatch repair genes in human colorectal cancer cell lines: The predominant role of *hMLH1*. *Proc. Natl. Acad. Sci. 96*:10296–10301.

Yamashita, K., Arimura, Y., Kurokawa, S., Itoh, F., Endo, T., Hirata, K., Imamura, A., Kondo, M., Sato, T., and Imai, K. 2000. Microsatellite instability in patients with multiple primary cancers of the gastrointestinal tract. *Gut 46*:790–794.

Yuen, S.T., Chan, T.L., Ho, J.W., Chan, A.S., Chung, L.P., Lam, P.W., Tse, C.W., Wyllie, A.H., and Leung, S.Y. 2002. Germline, somatic and epigenetic events underlying mismatch repair deficiency in colorectal and HNPCC-related cancers. *Oncogene 21*:7585–7592.

Zhang, H., Richards, B., Wilson, T., Lloyd, M., Cranston, A., Thorburn, A., Fishel, R., and Meuth, M. 1999. Apoptosis induced by overexpression of hMSH2 or hMLH1. *Cancer Res. 59*:3021–3027.

12

Role of CD-61 (Beta-3 Integrin) Glycoprotein in Colon Carcinoma

A. Moreno, C. Lucena, D. Llanes, and J.J. Garrido

Introduction

Adhesion molecules are widely expressed on the cell surface, basement membrane, and extracellular matrix (ECM). Adhesion molecules include ligands and receptors. Together they provide cells with anchorage and traction for migration, and the receptors also mediate signals that control cell polarity, survival, growth, differentiation, and gene expression (Ruoslahti, 1997). Cell surface adhesion receptors have been studied extensively, and how cells interact with and function within their different environments has become a primary focus of cell biology (Seftor, 1998). Adhesion molecules include several distinct families such as integrins, cadherins, members of the immunoglobulin superfamily, selectins, and some cell surface proteoglycans. They are critical for a variety of physiologic and pathologic processes such as cell growth, differentiation, embryogenesis, inflammation, blood coagulation, and immune response (Huang *et al.*, 1997). They also function as signal transducers to regulate various cellular functions through G-proteins, phospholipids, and protein kinases (Parsons, 1996).

Integrins are a major group of versatile adhesion molecules having both adhesive and signaling functions. They are heterodimeric integral cell surface receptors composed of alpha and beta chains and serve as cell membrane receptors with various extracellular matrix ligands. Eight different beta-chain and 18 alpha-chains have been described, accounting for at least 20 combinations of the heterodimeric receptor. Integrins contain large extracellular domains and short transmembrane and cytoplasmic tails (Seftor, 1998). The short beta-cytoplasmic tail contains regions capable of binding to cytoskeletal-associated proteins that link the integrins to the actin cytoskeletal system.

Integrins mediate cell-to-cell interaction and cell-to-extracellular matrix proteins in intercellular spaces and basement membranes. They also regulate cellular entry in the cell cycle. Binding of integrins by their extracellular matrix ligands induces a cascade of intracellular signals as an expression of immediate early genes. The prevention of integrin-ligand interactions suppresses cellular growth or induces apoptotic cell death (Varner and Cheresh, 1996). Integrins have also been associated with several biologic processes such as cell proliferation, anoikis, embryogenesis, inflammation and immunity, angiogenesis, and hemostasis and as points of entry for infectious agents.

The binding of integrins with extracellular matrix proteins has been associated with the activation of members of the Rho-family small GTPases. Rho- and Ras-family proteins can influence the ability of integrins to bind their ligands, controlling cell motility (Parise *et al.*, 2000). Integrins have been found on practically all cells and tissues studied. During development, they

Handbook of Immunohistochemistry and in situ Hybridization of Human Carcinomas,
Volume 2: Molecular Pathology, Colorectal Carcinoma, and Prostate Carcinoma

227

are ubiquitously expressed and tend to decrease gradually during differentiation as adult structures emerge (Mizejewski, 1999).

The beta-3 (β3) integrin (CD61 or gpIIIa) is a protein that, on the cell surface membrane, gives rise to non-covalent Ca(II)-dependent heterodimeric complexes with the proteins alpha-IIb (CD41 or gpIIb) or alpha-v (CD51) to form the αIIbβ3 and αvβ3 receptors, the two components of the beta-3 integrin subfamily. Alpha-IIb beta-3 integrin is chiefly located in platelets and megakariocytes, whereas alpha-v beta-3 is expressed in endothelial cells and other nucleated cells such as monocytes, macrophages, vascular smooth-muscle cells, and osteoclasts. These integrins recognize the tripeptide Arg-Gly-Asp (RGD) of several ligands such as fibrinogen, fibronectin, vitronectin, or the von Willebrand factor, among others. Beta-3 (β3) integrin is a polypeptide with a molecular weight of 92 Kda. The mature protein has 762 amino acids and contains a large extracellular domain (residues 1–689), a single transmembrane segment (residues 690–715), and a short carboxyterminal cytoplasmic domain (residues 716-762). One region implicated in ligand binding (residues 109–171) is involved in RGD motif recognition. This segment is highly conserved among the beta-subunits of the integrin family (Llanes *et al*., 2002).

As integrins are involved in the interaction of cells with the surrounding extracellular matrix and the behavior of neoplastic cells is strongly influenced by these interactions, the role of integrins in tumor development is evident. Alterations in their expression or function may contribute to the uncontrolled proliferation and metastasis of malignant cells (Pignatelli and Wilding, 1996) and apoptosis, angiogenesis, adhesion, spreading, motility, and invasion (Trikha, 2002a).

A cascade process in the progression of cancer involving adhesion molecules has been suggested by several authors (Huang *et al*., 1997). Initially, the normal cell–cell and cell–matrix adhesion is disrupted, causing neoplastic cells to be released from primary tumors, a process in which integrins appear to be involved. The tumor cells must subsequently migrate into the vascular system. In studies with melanomas it has been shown that the αvβ3 is required at this time. Tumor cells are protected from circulating immune cells by binding to platelets through αIIbβ3 integrin and P-selectin. Tumor cells then manifest a preference for binding to the endothelium in specific organs, depending on the expression pattern of integrins and other adhesion molecules. Later, the interaction of tumor cells with adhesion receptors on the basal surface of endothelial cells and extracellular matrix proteins mediate the extravasation of these cells. Finally, the activation of adhesion molecules is required in the invasion of the

subendothelial matrix, migration into the tissue, neovascularization, and the formation of metastasis. Experiments with Chinese hamster ovary (CHO) cells suggest that integrins can influence tumor metastasis either favorably or unfavorably according to the activity and the balance of various integrins (Ota *et al*., 1997). Therefore, the development of an integrin cell expression profile for individual tumors may have further potential in identifying cell surface signature for a specific tumor type and/or stage.

Several authors have found that the altered expression of integrins on tumor cells can change their adhesive properties and biologic behavior. Thus, integrin expression, along with histopathologic criterion, can be a prognostic marker for malignant tumors and may indicate the site of subsequent metastasis. These observations may have clinical utility and suggest areas for future research (Hieken *et al*., 1999). Accordingly, many experiments have been carried out on different types of cancer. Human cutaneous melanoma, for example, has been useful in studying the involvement of integrins in tumors because it generally follows a sequential series of definable stages. We shall now go on to review some of these studies before turning our attention specifically to colon cancer because these investigations are of interest and can be applied to the subject of our chapter.

Integrin αvβ3 in tumor cells can bind to matrix metalloproteinase-2 (MMP-2) in a proteolytically active form and facilitate cell-mediated collagen degradation and thus invasion (Brooks *et al*., 1996). An increase in its expression can therefore be positively correlated with increased malignancy in melanomas. Furthermore, an association between α2β1 and the positive regulation of MMP expression has also been described. Filardo *et al*. (1995) have identified the NPXY sequence within the beta-3 subunit (residues 744–747) as essential for cell morphologic and migratory response *in vivo* and *in vitro*. Tumor cells transfected with a beta-3 complementary deoxyribonucleic acid (cDNA) containing a mutated NPXY sequence are unable to metastasize, in contrast to tumor cells transfected with an intact beta-3 subunit.

Overexpression of the fibronectin receptor α5β1, which results in the assembly of additional fibrone matrix, reduces the tumorigenicity of cultured tumor cells (Ruoslahti, 1997). Likewise, αvβ3 integrins play a direct role in the progression of human primary melanoma from the nontumorigenic, nonmetastatic radial growth phase to the tumorigenic, metastatically competent vertical growth phase (Hsu *et al*., 1998). This integrin also plays a major role in melanoma cell survival in human skin because it may interact with denatured collagen (generated *in vivo*) to regulate the Bcl-2:Bax ratio (Petitclerc *et al*., 1999). In this regard,

it has been suggested that cell survival is regulated in part by the expression of Bcl-2 and Bax.

Trikha *et al*. (2002a) have obtained similar results for αvβ3 and αIIbβ3 using well-characterized monoclonal antibodies to αIIbβ3 that do not cross-react with αvβ3. They found that the co-expression of αvβ3 and αIIbβ3 enhanced cell survival and promoted growth *in vivo*. Furthermore, they showed by immunocytochemistry that the expression of αIIbβ3 displaced αvβ3 from the focal contact point. They also demonstrated that when SCID (severe combined immunodeficient) mice are implanted subcutaneously with human melanoma cells (in cells which express αvβ3 but not αIIbβ3) transfected with αIIbβ3, the αIIbβ3 (+) cells developed an approximately fourfold larger tumor than their mock counterparts and the level of apoptosis was reduced. Other authors have associated malignant potential with β3 integrin expression in ovarian tumors and melanomas. In melanomas, and in the subset of tumorigenic vertical growth phase melanoma, expression of αvβ3 integrin increased with thickness (Van Belle *et al*., 1999).

The fact that few patients are successfully cured can be attributed to the inability to cure tumors that have spread from their primary anatomic site to dictal sites (metastases) because once solid tumors have formed metastases, no therapies are available to effectively cure them. Several authors have associated integrin expression with cancer metastases in different types of tumors.

Using two different human prostate cancer lines (PC-3 and DU-145), Trikha *et al*. (1998) found that αIIbβ3 integrin participates in the metastatic progression of prostate adenocarcinoma. The more invasive DU-145 cells localize αIIbβ3 in adhesion sites on the cell periphery, whereas in PC-3 cells the integrin is predominantly intracellular. They propose that the differential utilization of the integrin by tumor cells could also be an important parameter in regulating the metastatic phenotype of prostate cancer. Moreover, when they used a function-blocking monoclonal antibody to αIIbβ3, the lung colonization of DU-145 cells in mice was inhibited. In human breast cancer it has been found that the activated αvβ3 integrin, but not the nonactivated type, promotes tumor-cell arrest through interaction with platelets during blood flow. Thus breast cancer can exhibit a platelet-interactive metastatic phenotype that is mediated by the activation of αvβ3. Consequently, alterations that lead to the aberrant control of integrin activation are expected to adversely affect the course of cancer (Felding-Haberman *et al*., 2001).

Several authors have studied the role of β3 integrin in the metastasis of melanoma (Hieken *et al*., 1996, Trikha *et al*., 2002b). Trikha *et al*. (2002b) indicate that the combined blockade of αIIbβ3 and αvβ3 with specific monoclonal antibodies provides a significant antiangiogenic and antimetastatic benefit. However, in analyses with two melanoma cell lines lacking the β3 integrin, it has been found that these cells can grow *in vivo* and metastasize, suggesting that certain types of melanomas may grow and spread in the absence of the αvβ3 integrin complex. Pecheur *et al*. (2002) have also found that αvβ3 expression increases the propensity of tumor cells to metastasize to bone, presumably through the increased invasion of and adhesion to bone.

Angiogenesis is another issue to take into account in studies regarding tumor progression in which integrins are extensively involved. Angiogenesis, or the formation of new blood vessels from preexisting ones, plays a key role in development, wound repair, and inflammation and also contributes to pathologic conditions such as cancer. The growth and metastatic properties of solid tumors are directly influenced by the process of angiogenesis. Primary tumor growth depends on nutrients supplied by blood vessel infiltration, whereas these same vessels will also serve as a conduit for invasive cells and thereby hasten the metastatic process (Brooks *et al*., 1994).

Perhaps the most significant aspect of the physiologic roles played by αvβ3 in cancer is its critical role in the process of angiogenesis and the fact that it is up-regulated in vascular cells within human tumors (Varner and Cheresh, 1996). Max *et al*. (1997) studied αvβ3 expression in colon, pancreas, lung, and breast carcinomas, finding the up-regulation of αvβ3 expression on the vasculature in each case. In some carcinomas, the vasculature that is within and surrounding inflammatory infiltrates showed more intensely stained vessels with a monoclonal antibody against αvβ3 compared with the rest of the section. Because tumor-induced angiogenesis may be initiated by the release of angiogenic factors from tumor and inflammatory cells, this appears to indicate that angiogenesis might be enhanced by inflammatory cells. Gasparini *et al*. (1998) found that αvβ3 plays a critical role in the progression of tumors in breast cancer. They suggest that this integrin is an endothelial cell marker with a significant prognostic value. Indeed, the expression of αvβ3 was significantly higher in tumors of patients with metastasis than in those without metastasis.

In contrast to these experiments, Reynolds *et al*. (2002) found that mice lacking β3 integrin or both β3 and β5 integrins not only support tumorgenesis but also present enhanced tumor growth and angiogenesis. They also observed elevated levels of the vascular endothelial growth factor (VEGF) receptor-2 in β3 null endothelial cells. VEGF has been identified as a major angiogenic factor acting through the endothelial

cell-specific receptor, including the VEGF receptor-2. It has been suggested that the VEGF/VEGF-2 system plays a very important role in the development of angiogenesis, thus indicating the need for the further evaluation of the mechanisms of action of the β3 integrin.

Although much has been published in the literature with regard to the role of integrins in the development and progression of different tumors, little research has been carried out on the role that these adhesion molecules play in colon cancer. There is general consensus that cell–cell and cell–matrix interactions determine, at least in part, the behavior of colon cancer and that cell adhesion molecules are the biologic mediators responsible for these interactions, including the family of integrins (Agrez, 1996). Changes in the levels of integrin expression on tumor cells have been identified with more advanced disease, suggesting that either loss or gain of cell surface receptors may contribute to the progression of colon cancer.

The expression of αvβ6, which is a fibronectin receptor in colon cancer, has been shown to enhance colon cancer proliferation both *in vivo* and *in vitro* in mice (Agrez *et al*., 1994). These same authors found that this integrin expression leads to a relative increase in secretion of the MMP gelatinase B. This phenomenon is associated with the increased proteolysis of denatured collagen on the cell surface, suggesting that αvβ6-mediated gelatinase B secretion is important in the progression of human colon cancer (Agrez *et al*., 1999). Furthermore, it has been shown that the inhibition of integrin αvβ6 expression in colon cancer cells suppresses the secretion of MMP-9. This event depends on the direct binding between the β6 and extracellular signal regulated kinase-2, a member of the MAP kinases (Gu *et al*., 2002).

The integrin α5β1 has been studied by Gong *et al*. (1997) in two distinct phenotypes of colon carcinoma cell lines, showing that highly invasive colon cell lines expressed higher levels of this integrin. To test if the high expression of α5β1 contributes to malignant progression, they transfected the poorly invasive colon cell lines that did not express α5 integrin with an α5 subunit. The transfected cells expressed the cell surface α5β1 protein and were more tumorigenic when injected into athymic nude mice. In contrast, other authors found that colon carcinoma exhibits a loss of β1 integrin compared to normal cells (Mizejewski, 1999). Pouliot *et al*. (2000) have reported that the transforming growth factor-α (TGF-α) and laminin-10 synergize to induce the spreading of human colon carcinoma cells (LIM1215) in low-density cultures and suggest a critical role for α3β1 integrin in this response.

Using immunofluorescence microscopy and flow cytometry analysis, it has been demonstrated that αIIβ3 and αvβ3 are present on the surface of SW-480 human colon adenocarcinoma cells. When the SW-480 cell line is exposed to thrombin, the cells exhibit increased adhesion to both endothelium and extracellular matrix components. The effect of thrombin resulted in the up-regulated cell surface expression of the β3 integrin involving the activation of protein kinase C (PKC). Hence, PKC inhibitors may serve as inhibitory agents in the prevention of thrombin-enhanced metastasis (Chiang *et al*., 1996). The αvβ3 appears to be important in tumor growth because antibodies against this protein blocked the intercellular adhesion of colon carcinoma cells, resulting in the rapid apoptosis of these tumor cells.

The role and clinical significance of β3 integrin expression in the metastasis of colorectal cancer has been studied by Sato *et al*. (2001). They examined primary tumor and lung metastasis for the immuno-chemical detection of β3 integrin. They found that this integrin is located in small-caliber blood vessels and that the vascular integrin β3 index was significantly higher in tumors of patients with lung metastasis than those without lung metastasis. Furthermore, a significant association was observed between stromal Ets-1 (a tissue-specific transcription factor that plays an important role in cell proliferation, differentiation, angiogenesis, and apoptosis) immunoreactivity, and vascular β3 integrin expression. In a multivariate analysis model, vascular integrin β3 and stromal Est-1 over-expression was found to be related to lung metastasis.

The αvβ3 integrin has been identified as a marker of angiogenesis because it is expressed by newly formed blood vessels in disease and neoplasia. In colon carcinoma, this integrin has been studied by Vonlaufen *et al*. (2001) to investigate a possible correlation between vascular αvβ3 integrin expression and clinical parameters such as survival and relapse-free intervals. They found that the risk of death was 10 times higher for patients with a high expression of integrin when compared to patients with low expression. Moreover, tumors that had developed metastasis in the liver generally showed a higher level of αvβ3 integrin expression than tumors without metastasis.

Little information is available regarding the role of β3 in colon cancer and the biologic significance of the change in receptor expression during tumor progression and metastasis. Thus, further research is needed because, like many other cancers, the study of this molecule can aid us in understanding tumor pathogenesis for diagnostic purposes and for the development of anti-integrin approaches to improve cancer therapy.

MATERIALS

1. Phosphate buffer saline (PBS): 8 g sodium chloride, 200 mg monobasic potassium, 1.42 g dibasic potassium phosphate; bring vol to 1 L with distilled water (pH 7.4).

2. Fixative: 10% formalin in PBS.

3. Xylene and graded alcohols (100%, 96%, 70%).

4. 0.1% (w/v) aqueous poly-L-lysine.

5. 3% hydrogen peroxide: 3 ml hydrogen peroxide and 97 ml distilled water.

6. 10 mM citrate buffer, stock solution: 19.2 g citric acid anhydrous, bring vol to 1 L with distilled water (solution A); 29.41 g tri-sodium citrate. $2H_2O$, bring vol to 1 L with distilled water (solution B). For working solution take 18 ml sol A and 82 ml sol B; bring vol to 1 L with distilled water, pH 6.0.

7. 1% albumin-PBS: 1 g bovine serum albumin and 100 ml PBS. Stir albumin in buffer.

8. Normal goat serum: 1:20 v/v in 1% albumin-PBS.

9. JM2E5 antibody diluted in 1% albumin-PBS.

10. Anti-mouse immunoglobulin (Ig)-biotinilated secondary antibody: diluted 1/50 v/v in 1% albumin-PBS.

11. Avidin-biotin-peroxidase complex (ABC): 1/400 dilution in PBS; mix immediately and allow ABC reagent to stand for ~30 min before use.

12. 3.3′-diaminobenzidine (DAB) solution: 5 mg DAB in 10 ml PBS. Prepare 10 min before developing.

13. Carazzi's hematoxylin: 500 mg hematoxylin, 100 mg potassium iodate, 25 g potassium sulfate, 100 ml glycerol, and 400 ml distilled water; slowly add glycerol and stir in distilled water. Let the solution stand for about 2 weeks in dark flask and filtrate before use.

14. Aqueous mounting medium.

METHOD

1. Rinse the surgical samples in PBS and fix for 12–24 hr at room temperature in 10% buffered formalin.

2. After fixation, rinse the samples three times for 30 min in PBS.

3. Dehydrate the samples in alcohol, clear in benzene, and embed in paraffin.

4. Cut the resulting blocks and mount 5 μm sections on poly-L-lysine coated slides and let them stand overnight at 37°C.

5. Dewax in xylene for 20 min.

6. Hydrate the sections by passage through graded alcohols, finishing in distilled water.

7. Inhibit endogenous peroxidase activity with 3% hydrogen peroxide in distilled water. Stir carefully for 30 min at room temperature.

8. Rinse the slides three times in PBS for 15 min.

9. Immerse the samples in 10 mM citrate buffer (pH 6.0) and microwave for 5 min at medium power and twice (3 min each one) at maximum power (800 W).

10. After cooling, cover the sections with distilled water for 20 min.

11. Repeat **Step 8**.

12. Incubate the samples with normal goat serum for 30 min at room temperature.

13. Remove the serum, cover the sections with JM2E5 primary antibody or 1% albumin-PBS (as negative control), and incubate for 18 hr at 4°C in a wet chamber.

14. Repeat **Step 8**.

15. Incubate the slides with biotinilated secondary antibody for 30 min at room temperature.

16. Repeat **Step 8**.

17. Cover the sections with avidin-biotin-peroxidase complex for 1 hr at room temperature in a wet chamber.

18. Repeat **Step 8**.

19. Develop with a DAB solution.

20. Repeat **Step 8**.

21. Counterstain the sections with hematoxylin.

22. Rinse in distilled water to remove the remaining dye.

23. Mount the slides with aqueous medium.

RESULTS AND DISCUSSION

Carcinomas show integrin type and distribution patterns that differ from normal tissue as a result of the altered expression of some of them during tumor development. Thus, it is of interest to determine specific cell integrin expression profiles in both normal and tumor cells from the same tissue. The expression of β3 integrin in cultured tumor cell lines is well documented. On this basis, we propose whether the expression of this molecule observed in cultures of tumor cells can also be found *in vivo*. With that aim, the immunohistochemical expression of β3 integrin using the monoclonal antibody JM2E5 was investigated in formalin-fixed and paraffin-embedded surgical samples of human colon carcinoma, as well as other tissues, and its metastasis in liver. Paraffin-embedded sections were preferred to frozen tissue sections because of their widespread use in diagnostic immunohistochemistry. The monoclonal antibody JM2E5 was prepared in our laboratory (Pérez de la Lastra *et al*., 1997) from mice immunized with pig platelets. It is cross-reactive with human cells. Our results confirm previous data that indicate that adhesion molecules can be detected with antibodies against platelet glycoproteins.

Weak staining of β3 integrin was mainly observed in normal colon mucosa using JM2E5 (data not shown)

and the monoclonal antibody stained epithelial cells. Histologic distribution of JM2E5 in colon carcinoma presented an atypical glandular structure, infiltrating normal tissue and staining in an intracytoplasmic fashion with a membranous pattern, although some samples exhibited an apical cell expression of β3 integrin (Figure 35). In liver metastasis, β3 integrin is distributed heterogeneously. The percentage of stained cells was greater than 50% in the colon carcinoma samples and between 25–50% in liver metastasis. In all cases, staining was intense. These results demonstrate a high expression of β3 integrin in colon cancer and their metastasis in liver.

Likewise, JM2E5 stained the endothelial blood vessel cells surrounding the infiltrated tissue. Our results are in accordance with Voulaufen et al. (2001), who demonstrated that colorectal cancer often induces metastasis in liver. They also found that tumors that have spread to the liver show a level of αvβ3 integrin expression that is nearly double the level of nonmetastatic colon cancer. In our study, we analyzed samples of the primary tumors and metastasis from the same patient. All the colon cancers examined presented a high expression of β3 integrin. The results of these authors indicate that tumors with a marked angiogenic activity metastasize more easily. Brooks et al. (1994) have demonstrated that αvβ3 integrin is involved in this process because after induction of angiogenesis in vivo, the inhibitors of this integrin selectively promote the apoptosis of αvβ3-bearing blood vessels.

Trikha et al. (2002a) have found that the presence of αIIβ3 integrins in a melanoma cell line decreases the apoptosis rate and that larger tumors develop in mice injected subcutaneously with these cells. They assay the presence of αIIbβ3 and αvβ3 in tumor cells by immunohistochemistry, finding that αvβ3 expression
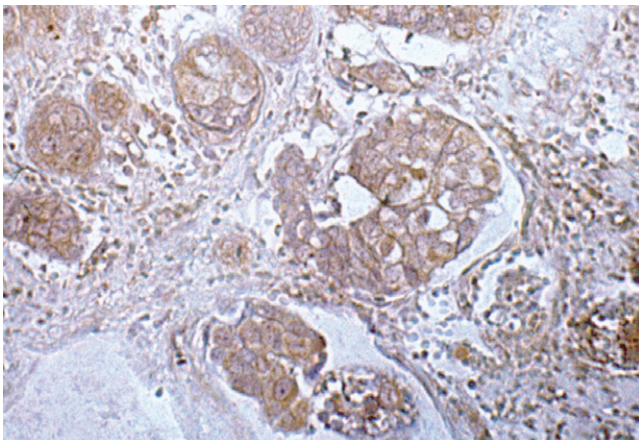
is an early event in melanoma progression and αIIbβ3 is expressed later. Moreover, in adherent melanoma cells, αIIbβ3 staining occurred at focal contact points, whereas αvβ3 immunoreactivity was diffuse. In our case, using a monoclonal antibody against beta-3 integrin, which can stain both αIIbβ3 and αvβ3 integrins, we found immunoreactivity in the intracytoplasma and apical sites of the cells. This apical reactivity is stronger in the same section of colon cancer. These results could be in accordance with Trikha et al. (1998), who found that in a highly invasive prostate cell line, αIIbβ3, is located on the periphery, whereas in a slightly invasive cell line, the integrin is predominantly located intracellulary. They interpret that the differential utilization of this integrin by tumor cells may be an important parameter in regulating the metastatic phenotype of prostate cancer cell. The varying immunoreactivity found in our study between different colon samples could be because they present different levels of progression and/or invasive activity.

However, it should be stressed that we have studied only five primary tumors. Therefore, it is necessary to investigate with further samples having different levels of progression and metastatic capacity because it is very important to understand the genetic changes associated with the acquisition of metastatic phenotype. The aim of our experiments was to check the presence of beta-3 integrin in colon cancer and liver metastasis and to demonstrate that immunohistochemistry is a highly suitable method for the study of integrin expression and location. This was done with a view to establishing phenotypes given that quantitative and qualitative alterations in integrin cell surface patterns have been observed in vitro and in vivo. Thus, the formulation of the integrin expression cell signature from biopsies may have potential as a diagnostic tool for the detection of both tumor transformation and progression (Mizejewski et al., 1999).

The major limitation of immunohistochemistry is the availability of antibodies that recognize integrin subunits in paraffin-embedded tissues. Therefore, greater numbers of antibodies are needed that recognize integrins in tissues because antibodies that detect functionally active integrin conformations will further the study of the role of integrins in biology and tumor pathology (Hieken et al., 1999). Moreover, they can be very useful in clinical studies, for example, as prognostic markers.

Thus, in a study of 97 patients with breast cancer, Gasparini et al. (1998) found that αvβ3 is the most significant prognostic factor in predicting relapse-free survival in both node-negative and node-positive patients and is useful as a target for specific therapy. This finding is in accordance with the observations by

Figure 35 Expression of JM2E5 in colon carcinoma.

Voulaufen *et al*. (2001) in colon carcinoma. They found αvβ3 integrin expression to be the best prognostic factor when compared to tumor grading, node status, depth of invasion, and inflammatory response because patients with high vascular expression of this integrin present a significantly lower relapse-free interval. Van Belle *et al*. (1999) suggest that αvβ3 integrin be used as a prognostic marker. In the subset of tumorigenic vertical growth phase melanomas they found that αvβ3 integrin expression increased with thickness. The ligation of this integrin has been shown *in vitro* to have several properties that may be related to the malignant phenotype.

Together these studies contribute to the growing body of work that clearly identifies the importance of integrin analysis in the diagnosis and prognostic evaluation of cancer, which can be directly correlated to the progression of the clinically defined disease (Seftor *et al*., 1998). This is explained by the fact that integrin-mediated interaction of cells with their extracellular environment can then generate physical and biochemical signaling events that contribute to a change in cell behavior resulting in an aggressive, pathologic phenotype.

The importance of integrins in tumor growth, invasion, and metastasis provides a rationale for developing selective molecular therapy for cancer. Thus, for example, by preventing tumor cells from interacting with one another or with their microenvironments, tumor growth and metastasis should be suppressed. Furthermore, the use of integrin antagonists can induce the apoptosis of proliferating angiogenic blood vessels without affecting preexisting vessels. It is with this objective that several approaches aimed at inhibiting integrin activity have been studied *in vivo* and *in vitro*. Therefore, antibodies, peptide antagonists, and disintegrins may provide viable options for nontoxic therapeutic treatment, which might also eliminate drug resistance—a confounding factor that has emerged in cancer chemotherapy.

As described earlier, αvβ6 integrin expression in colon cancer cells suppresses MMP-9 secretion. Hence, targeting beta 6 to inhibit MMP-9 activity may offer a useful therapeutic approach in preventing the growth and spread of colon cancer. Kumar *et al*. (2001) have described a nonpeptide small molecule (SCH221153) that is a potent inhibitor of both αvβ3 and αvβ5 integrin receptors. They demonstrate that this antagonist inhibits vascular endothelial cell adhesion and proliferation mediated by two different growth factors (Fibroblast growth factor 2 [FGF2] and VEGF). SCH221153 inhibited FGF2-induced angiogenesis in chick choriallantic membrane (CAM) and inhibited the growth of human tumor xenografts in SCID mice.

Because of their specificity and unlimited availability, the most common approach to inhibit integrin is to use monoclonal antibodies that recognize these molecules. Many integrins can serve as signal transducing molecules, and thus monoclonal antibodies against adhesion molecules may induce negative signals in tumor cells resulting in apoptosis or growth arrest (Huang *et al*., 1997). Currently, anti-integrin antibodies, disintegrins, and synthetic peptides have been reported to be effective anti-metastatic agents. Blocking the binding of tumor cells to platelets is also regarded as a potential method to inhibit metastasis (Mizejewski, 1999). Trikha *et al*. (2002b), for example, found that the treatment of human melanoma cells with c7E3 Fab (chimeric antibody against αIIbβ3 platelets) inhibits lung colonization by tumor cells in SCID mice. Trikha *et al*. (1998) also obtained similar results with prostate cancer cell lines where the function-blocking monoclonal antibody to αIIbβ3 inhibits the lung colonization of tumor cells in SCID mice. They suggest several reasons for this event: Monoclonal antibody inhibits platelet function and so platelet–tumor interaction or monoclonal antibodies can block the interaction of cells with the host by binding to the αIIbβ3 integrin expressed by tumor cells, or a combination of both events can occur.

There is wide consensus among authors regarding the important role that the vascular αvβ3 integrin plays in angiogenesis. Thus, this integrin could be a target for anti-αvβ3 therapy. Its antagonists (monoclonal antibodies, peptide inhibitors, antisense β3 oligonucleotides, etc.) could induce the regression of preestablished human tumor xenografts in animals and ultimately prove effective in human patients (Mizejewski, 1999). This strategy has been shown to be effective in different human tumors where the interruption of αvβ3 ligand binding induces apoptosis in the proliferative angiogenic vascular cells without affecting preexisting quiescent blood vessels. Histologic examination of the anti-αvβ3 treated and control-treated tumors revealed that few, if any, viable tumor cells remained in the anti-αvβ3 treated tumors. In fact, these treated tumors contained no viable blood vessels (Brooks *et al*., 1994). These authors suggest that once angiogenesis begins, individual vascular cells divide and begin to move toward the angiogenic source. After this time, αvβ3 ligation provides a signal allowing continued cell survival, leading to the differentiation and formation of mature blood vessels. If αvβ3 is prevented, the cells fail to receive this molecular cue and go into apoptosis by default. This hypothesis would also predict that after differentiation has occurred, mature blood vessels no longer require αvβ3 signaling for survival and are therefore refractory to the antagonist of this integrin.

Other approaches to inhibit tumor growth and metastasis involved the development of synthetic peptides. Thus, adhesive interaction between cells and the extracellular matrix can be inhibited by these peptides or soluble proteins derived from extracellular matrix components or cell membrane. The RGD sequence is critical for many of these interactions, and peptides containing this sequence have been used to inhibit lung metastasis of melanoma in mice (Huang *et al.*, 1997). Cyclic RGD peptides or polymers containing repeating RGD sequences were much more effective in inhibiting experimental lung or liver metastasis of various murine and human tumors (Saiki *et al.*, 1996). Via the up-regulation of beta-3 integrin cell surface expression, thrombin-enhanced metastasis can be inhibited by rhodostomin and Arg-Gly-Asp–containing anti-platelet snake venom peptide that antagonizes the binding of extracellular matrix toward beta-3 integrin on human colon adenocarcinoma cells. Because PKC is involved in this process, the PKC inhibitor may also serve to prevent thrombin-enhanced metastasis (Chiang *et al.*, 1996). Other studies have suggested that anti-integrin therapy in combination with chemotherapy might result in additional anti-tumor activity. Moreover, the presence of several cytokines such as tumor necrosis factor (TNF) and IL-4 can induce changes in integrin expression and the adhesive properties of tumor cells and subsequently decrease the metastatic potential of colon carcinoma cells (Herzberg *et al.*, 1996).

CONCLUSIONS

In conclusion, integrins participate in cell–cell and cell–matrix interactions and transduce the signal between the extracellular matrix and cell interior. These events determine the behavior of cancer in general and colon cancer in particular. Carcinomas show integrin type and distribution patterns that differ from normal colon activity because of the altered expression of several integrins during tumor development. Hence, a systematic study of integrins in normal tissue and carcinoma will provide us with an integrin cell expression profile for a tumor and the changes associated with tumorigenicity and tumor progression. Immunohistochemistry using the appropriate monoclonal antibodies is probably the most suitable technique to do this, although antigenic epitopes may be masked in paraffin-embedded sections. The differential expression of integrins during tumor transformation, progression, and metastasis suggests that integrins may be a prognostic marker and a target for cancer therapy. However, the importance of investigating the signaling mechanism by which integrins regulate cell proliferation,

differentiation, apoptosis, angiogenesis, and metastasis in colon cancer should not be overlooked.

References

Agrez, M. 1996. Cell adhesion molecules and colon cancer. *Aust. N. Z. J. Surg. 66*:791–798.

Agrez, M., Chen, A., Cone, R., Pytela, R., and Sheppard, D. 1994. The αvβ6 integrin promotes proliferation of colon carcinoma cells through a unique region of the beta 6 cytoplasmic domain. *J. Cell. Biol. 127*:547–556.

Agrez, M., Cu, X., Turton, J., Meldrum, C., Niu, J., Antalis, T., and Howard, E. 1999. The αvβ6 integrin induces gelatinase B secretion in colon cancer cells. *Int. J. Cancer 81*:90–97.

Brooks, P., Montgomery, A., Rosenfeld, M., Reisfeld, R., Hu, T., Klier, G., and Cheresh, A. 1994. Integrins αvβ3 antagonists promote tumor regression by inducing apoptosis of angiogenic blood vessels. *Cell 79*:1157–1164.

Brooks, P., Stromblad, S., Sander, L., von Schalscha, T., Aimes, R., and Cheresh, D. 1996. Localization of matrix metalloproteinase MMP-2 to the surface of invasive cells by interaction with αvβ3. *Cell 85*:638–693.

Chiang, H., Yang, R., and Huang, T. 1996. Thrombin enhances the adhesion and migration of human colon adenocarcinoma cells via increased beta-3 integrin expression on the tumor cell surface and their inhibition by the snake venom peptide rhodostomin. *Br. J. Cancer 73*:902–908.

Felding-Habermann, B., O'Toole, T., Smith, J., Fransvea, E., Rugge, Z., Ginsberg, M., Hughes, P., Pampori, N., Shattil, S., Saven, A., and Mueller, B. 2001. Integrin activation controls metastasis in human breast cancer. *Proc. Natl. Acad. Sci. USA 98*:1853–1858.

Filardo, E., Brooks, P., Derning, S., and Cheresh, D. 1995. Requirement of the NPXY motif in the integrin beta 3 subunit cytoplasmic tail for melanoma cell migration in vitro and in vivo. *J. Cell. Biol. 130*:441–450.

Gasparini, G., Brooks, P., Biganzoli, E., Vermeulen, P., Bonoldi, E., Dirix, L., Rani, G., Oliceli, R., and Cheresh, D. 1998. Vascular integrin αvβ3: A new prognostic indicator in breast cancer. *Clin. Cancer Res. 4*:2625–2634.

Gong, J., Wang, D., Sun, L., Zborowska, E., Wilson, J., and Brattain, M. 1997. Role of α5β1 integrin in determining malignant properties of colon carcinoma cells. *Cell. Growth Differ. 8*:83–90.

Gu, X., Niu, J., Dorothy, D., Scott, R., and Agrez, M. 2002. Integrin αvβ6-associated ERK2 mediates MMP-9 secretion in colon cancer cells. *Br. J. Cancer 87*:348–351.

Herzberg, F., Schoning, M., Schirner, M., Topp, M., Thiel, E., and Kreuser, E. 1996. IL-4 and TNF-α induce changes in integrin expression and adhesive properties and decrease the lung-colonizing potential of HT-29 colon carcinoma cells. *Clin. Exp. Metast. 14*:165–175.

Hieken, T., Farolan, M., Ronan, S., Shilkaitis, A., Wild, L., and Das Gupta, T. 1996. Beta 3 integrin expression in melanoma predicts subsequent metastasis. *J. Surg. Res. 63*:169–173.

Hieken, T., Ronan, S., Farolan, M., Shilkaitis, A. and Das Gupta, T. 1999. Molecular prognostic markers in intermediate thickness cutaneous malignant melanoma. *Cancer 85*:375–382.

Hsu, M., Ski, D., Meier, F., van Belle, P., Hsu, J., Elder, D., Buck, C., and Herlyn, M. 1998. Adenoviral gene transfer of beta 3 integrin subunit induces conversion from radial to vertical growth phase in primary human melanoma. *Am. J. Pathol. 45*:1435–1442.

Huang, Y., Baluna, R., and Vitetta, E. 1997. Adhesion molecules as targets for cancer therapy. *Histol. Histopathol. 12*:467–477.

Kumar, C., Malkowski, M., Yin, Z., Tanghetti, E., Yaremko, B., Nechuta, T., Varner, J., Liu, M., Smith, E., Neustadt, B., Presta, M., and Armstrong, L. 2001. Inhibition of angiogenesis and tumor growth by SCH221153, a dual αvβ3 and αvβ5 integrin receptor antagonist. *Can. Res. 61*:2232–2238.

Llanes, D., Morera, L., Garrido, J., and Barbancho, M. 2002. CD61, CD51, CD41. In *Wiley Encyclopedia of Molecular Medicine*. New York: John Wiley and Sons, Inc., 649–654.

Max, R., Gerritsen, R., Nooijen, P., Goodman, S., Sutter, A., Keilhollz, U., Ruite, D., and de Waal, R. 1997. Immunohistochemical analysis of integrin αvβ3 expression on tumor-associates vessel of human carcinomas. *Int. J. Cancer 71*:320–324.

Mizejewski, G. 1999. Role of integrins in cancer: Survey of expression patterns. *Proc. Soc. Exp. Biol. Med. 222*:124–138.

Ota, I., and Matsuura, S. 1997. Adhesion molecules and cancer metastasis. *Rinsho Byori. 45*:528–533.

Parise, L., Weon Lee, J., and Juliano, R. 2000. New aspects of integrins signaling in cancer. *Can. Biol. 10*:407–414.

Parsons, J. 1996. Integrin-mediating signaling: Regulation by protein tyrosine kinase and small GTP-binding proteins. *Curr. Opin. Cell. Biol. 8*:146–152.

Pecheur, I., Peyruchaud, O., Serre, C., Guglielmi, J., Voland, C., Bour Marge, C., Cohen-Solal, M., Buffet, A., Kieffer, N., and Clezardin, D. 2002. Integrin αvβ3 expression confers on tumor cells a greater propensity to metastasize to bone. *FASEB J. 16*:1266–1268.

Pérez de la Lastra, J., Moreno, A., Pérez, J., and Llanes, D. 1997. Characterization of the porcine homologue to human platelets glycoprotein IIb-IIIa by a monoclonal antibody. *Tiss. Antig. 49*:588–594.

Petitclerc, E., Stromblad, S., von Schalscha, T., Mitjans, F., Pinlats, J., Montgomery, A., Cheres, D., and Brooks, P. 1999. Integrin αvβ3 promotes M21 melanoma growth in human skin by regulating tumor cell survival. *Cancer Res. 59*:2724–2730.

Pignatelli, M., and Wilding, J. 1996. Adhesion receptors in epithelial tumors. In Horton, M.A., (ed) *Adhesion Receptors as Therapeutic Targets*. Boca Raton: CRC Press, 199–220.

Pouliot, N., Connolly, L., Moritz, R., Simpson, R., and Burgess, A. 2000. Colon cancer cells adhesion and spreading on autocrine laminin-10 is mediated by multiple integrin receptors and modulated by EGF receptor stimulation. *Exper. Cell. Res. 261*:360–371.

Reynolds, L., Wyder, L., Lively, J., Taverna, D., Robimson, S., Huang, X., Sheppard, D., Hynes, R., and Hodivala-Dilke, K. 2002. Enhanced pathological angiogenesis in mice lacking beta3 integrin or beta3 and beta5 integrins. *Nat. Med. 8*:27–34.

Ruoslahti, E. 1997. Integrins as signaling molecules and targets for tumors therapy. *Kidney Int. 51*:1413–1417.

Saiki, I., Kioike, C., Obata, A., Fujii, H., Murata, J., Kiso, M., Hasegawa, A., Komazawa, H., Tsukada, H., Azxuma, I., Okada, S., and Oku, N. 1996. Functional role of the sialyl Lewis X and fibronectin-derived RGDS peptide analogue on tumor-cell arrest in lung followed by extravasation. *Int. J. Cancer. 65*:833–839.

Sato, T., Konoski, K., Kimura, H., Maeda, K., Yabushita, K., Tsuji, M., and Miwu, A. 2001. Vascular integrin beta 3 and its relation to pulmonary metastasis of colorectal carcinoma. *Anticancer Res. 21*:643–647.

Seftor, R. 1998. Role of the beta 3 integrin in human primary melanoma progression. *Amer. J. Path. 153*:1347–1351.

Trikha, M., Raso, E., Cai, Y., Fazakas, Z., Paku, S., Porter, A., Timar, J., and Honn, K. 1998. Role of αIIβ3 integrin in prostate cancer metastasis. *Prostate 35*:185–192.

Trikha, M., Timar, J., Zacharek, A., Nemeth, J., Cai, Y., Dome, B., Somlai, B., Raso, E., Ladanyi, A., and Honn, K. 2002a. Role of beta 3 integrin in human melanoma growth and survival. *Int. J. Cancer 101*:156–167.

Trikha, M., Zhou, Z., Timar, J., Raso, E., Kennel, M., Emmell, E., and Makada, M. 2002b. Multiple role for platelets αIIβ3 and αvβ3 integrins in tumor growth, angiogenesis and metastasis. *Cancer Res. 62*:2824–2833.

Varner, J., and Cheresh, D. 1996. Integrins and cancer. *Curr. Opin. Cell. Biol. 8*:724–730.

Van Belle, P., Elenitsas, R., Satyamoorthy, K., Wolfe, J., Guerry, D., Schuchter, L., Van Belle, T., Albelda, S., Tahin, P., Herlyn, M., and Elder, D. 1999. Progression-related expression of beta3 integrin in melanomas and nervi. *Hum. Pathol. 30*:562–567.

Vonlaufen, A., Wiedle, G., Borisch, B., Birrer, S., Luder, P., and Imhof, B. 2001. Integrin αvβ3 expression in colon carcinoma correlates with survival. *Mod. Pathol. 14*:1126–1132.

This Page Intentionally Left Blank

13

Immunohistochemical and *in situ* Hybridization Analysis of Lumican in Colorectal Carcinoma

Toshiyuki Ishiwata

Introduction

Members of the small leucine-rich proteoglycan (SLRP) family have relatively small molecular size, with core proteins of 40 kD, and possess 6–10 leucine-rich repeating units between the flanking cysteine-rich disulfide-bonded domains at the N and C termini of the core protein (Blochberger *et al*., 1992). SLRP proteins are considered to modulate cellular behavior, including cell migration and proliferation during embryonic development, tissue repair, and tumor growth, in addition to their extracellular matrix functions as regulators of tissue hydration and collagen fibrillogenesis (Iozzo *et al*., 1997). The SLRP members include keratocan, mimecan, decorine, biglycan, fibromodulin, epiphycan, osteoadherin, and lumican (Wendel *et al*., 1998).

The human lumican protein has 338 amino acids, including a putative 18-residue signal peptide, and the central region of the molecule possesses four asparagine residues capable of participating in N-linked glycosylation (Chakravarti *et al.,* 1995). Different types of glycosylation leads to core protein, glycoprotein, and proteoglycan forms of lumican. The human *lumican* gene is located on chromosome 12q21.3-q22. Lumican was first reported to colocalize with fibrillar collagens in the corneal stroma, and it was reported to regulate the assembly and diameter of collagen fibers in the cornea (Blochberger *et al*., 1992). In addition to the cornea, lumican messenger ribonucleic acid (mRNA) was reported to be expressed in various tissues including the skeletal muscle, kidney, dermis, pancreas, brain, placenta, liver, heart, lung, uterus, aorta, and intervertebral discs (Grover *et al*., 1995; Sztrolovics *et al*., 1999; Ying *et al*., 1997). In the adult cornea, most of the lumican exists as keratan sulfate (KS) proteoglycan, and the KS side chains are considered to affect collagen fibrillogenesis and hydration (Cornuet *et al*., 1994; Ying *et al*., 1997). In contrast, lumican is reported to exist primarily in the glycoprotein form in noncorneal tissues (Funderburgh *et al*., 1991; Grover *et al*., 1995). Mice that are homozygous for a null mutation in *lumican* displayed corneal opacification and skin laxity as a result of the inhomogeneous collagen bundles (Chakravarti *et al*., 1998). In pathologic conditions, lumican was reported to be overexpressed during wound healing of the cornea, in the ischemic and reperfused heart, in atherosclerotic arteries, and in several types of cancer tissues (Onda *et al*., 2002; Saika *et al*., 2000).

Fibrous tissues adjacent to cancer cells mainly consist of collagen fibers and fibroblasts and are considered

Handbook of Immunohistochemistry and in situ Hybridization of Human Carcinomas,
Volume 2: Molecular Pathology, Colorectal Carcinoma, and Prostate Carcinoma

237

to affect cancer cell proliferation, migration, and spread (Hardingham *et al.*, 1992; Yeo *et al.*, 1991). The expression of lumican in fibrous tissues around cancer cells was reported in breast cancer (Leygue *et al.*, 1998, 2000). Lumican mRNA was expressed specifically in breast cancer tissues but not in normal breast tissues. The expression levels of other SLRPs, including *decorin, biglycan*, and *fibromodulin*, were not increased in breast cancer tissues. Lumican mRNA was expressed in fibroblasts adjacent to breast cancer cells but not in cancer cells. A high expression level of lumican is associated with a high tumor grade, low estrogen receptor levels, and young patients. Furthermore, low levels of lumican expression in invasive breast cancer cases were associated with rapid cancer progression and a low survival rate (Troup *et al.*, 2003). These findings may indicate that the lumican protein influences the growth of breast cancer tissues.

We reported that cancer cells themselves synthesize lumican mRNA in pancreatic cancer, uterine cervical cancer, and colorectal cancer, in addition to adjacent fibroblasts (Lu *et al.*, 2002a; Lu *et al.*, 2002b; Naito *et al.*, 2002). In these cancer tissues, lumican protein was prominently localized in cancer cells and stromal tissues close to the cancer cells. Immunohistochemistry is an effective method to determine the localization of target proteins in tissues, but it is difficult to identify the cells that synthesize such proteins. To clarify the cell types that synthesize lumican mRNA, *in situ* hybridization analysis was performed. Immunohistochemical analysis with anti-lumican antibody and *in situ* hybridization with a complementary RNA (cRNA) probe for lumican mRNA were effective in detecting the location of the lumican protein and identifying the cell types that synthesize it. We determined the localization of lumican protein and its mRNA in colorectal cancer tissues by immunohistochemistry and *in situ* hybridization analysis using formalin-fixed and paraffin-embedded sections (Lu *et al.*, 2002b).

MATERIALS AND METHODS

Prior to performing serial staining for immunohistochemical and *in situ* hybridization analysis on formalin-fixed and paraffin-embedded tissues, confirm the effectiveness of each staining method separately. Prepare 10–15 serial sections of 3–5 μm thickness, number the sections, and then perform immunohistochemical analysis using 3–5 different concentrations of primary antibody. Then, perform *in situ* hybridization with three different concentrations of probe using mild hybridization conditions, followed by more stringent conditions at the suitable probe concentration. Perform *in situ* hybridization using the optimum

hybridization conditions, and carry out immunohistochemical analysis on the next set of sections.

Preparation of Tissue Sections for Immunohistochemistry and *in situ* Hybridization

Materials for Preparation of Tissue Sections

1. Ultrapure water: distilled water filtered by Milli-Q Jr. (Millipore, Tokyo).
2. Silane-coated slides.
   a. Soak clean glass slides for 1 min in silane solution (2% of 3-aminoproxytriethoxysilane (Sigma, St. Louis, MO) in acetone).
   b. Wash the slides for 10 sec in acetone.
   c. Repeat **Step 2** with fresh acetone.
   d. Wash the slides in ultrapure water for 1 min.
   e. Dry them overnight at 37°C.

Method for Preparation of Tissue Sections

1. Fix the colorectal cancer tissues in 20% formalin for 18–20 hr and then embed in paraffin.
2. Cut 3–5 μm thick sections, float them on ultrapure water, and place them on silane-coated slides.
3. Bake the slides overnight at 60°C.

Immunohistochemical Staining of Lumican in Colorectal Cancer Tissues

Materials for Immunohistochemistry

1. Xylene.
2. Graded ethanol (70%, 80%, 90%, and 100%).
3. Distilled water.
4. Phosphate buffer saline (PBS), pH 7.6: 7.75 g of NaCl, 1.50 g of K_2HPO_4, and 0.20 g of KH_2PO_4 in 1 L of distilled water.
5. Hydrogen peroxide (H_2O_2).
6. Absolute methanol.
7. Polyclonal rabbit anti-human lumican antibody. This antibody is an affinity-purified rabbit polyclonal antibody raised against a peptide corresponding to amino acids 211-227 of human lumican (Baba *et al.*, 2001; Qin *et al.*, 2001).
8. N-Histofine Simple Stain MAX PO (R) kit (Nichirei Corp., Tokyo, Japan). This kit includes the labeled polymer prepared by combining amino acid polymers with peroxidase and goat anti-rabbit immunoglobulin (Ig), which are reduced to Fab'.

9. Mayer's hematoxylin.

10. 3,3′-Diaminobenzidine tetrahydrochloride (DAB).

11. Malinol mounting medium (MUTO Pure Chemicals Ltd., Tokyo, Japan).

Method for Immunohistochemical Analysis

1. Immerse the slides in xylene. Remove after 10 min and shake off the excess xylene.

2. Repeat **Step 1** twice using fresh xylene.

3. Immerse slides in 100% ethanol. Remove after 3 min and shake off the excess 100% ethanol.

4. Repeat **Step 3** twice with fresh 100% ethanol.

5. Then, treat the slides with 90%, 80%, and 70% ethanol in the same way as described earlier.

6. After immersion in water, immerse in PBS for 5 min.

7. Immerse the slides in a 0.3% solution of H_2O_2 in absolute methanol for 30 min at room temperature.

8. Rinse them in PBS three times for 5 min each time.

9. Wipe areas around the sections on the slides.

10. Apply 100 µl of rabbit anti-human lumican antibody (1:500) in PBS containing 1% bovine serum albumin (BSA) to specimen slides.

11. Incubate them overnight at 4°C in a moist chamber.

12. Rinse the slides in PBS three times for 5 min each time.

13. Wipe areas around the sections on the slides.

14. Apply 2–3 drops of Simple Stain MAX PO (R) reagent to each slide to completely cover the sections on the slides. Incubate at room temperature for 30 min in a moist chamber.

15. Rinse the slides in PBS 3 times for 5 min each time.

16. Wipe areas around the sections on the slides.

17. Apply 2–3 drops of DAB solution (20 µg of DAB powder and 100 µl of 5% H_2O_2 in 100 ml of Tris-HCl, pH 6.5) to each slide to completely cover the sections. Incubate the slides at room temperature for 5–10 min, and observe them under a microscope.

18. Rise the slides in distilled water for 5 min.

19. Immerse them in Mayer's hematoxylin for 2 min.

20. Wash them well in tap water.

21. Immerse them in PBS for 2–3 min.

22. Wash them in tap water.

23. Immerse in graded ethanol (70%, 80%, 90%, and 100%).

24. Clear in xylene 4 times for 3 min each time.

25. Mount with mounting medium.

In situ Hybridization Analysis of Lumican in Colorectal Cancer Tissues

Materials for *in situ* Hybridization

1. Takara RNA PCR kit (AMV) Ver. 2.1 (Takara Bio, Shiga, Japan).

2. pGEM-T vector (Promega Biotechnology, Madison, WI).

3. Digoxigenen (DIG) RNA labeling kit (SP6/T7) (Roche, Diagnostic GmbH, Penzberg).

4. Glassware: Apply RNase AWAY (Molecular BioProducts, San Diego, CA) to the surface of glassware, rub the wet surface with an RNase-free laboratory wipe, rinse with ultrapure water, then dry with a fresh RNase-free wipe.

5. Ultrapure water.

6. Diethyl pyrocarbonate (DEPC) (Sigma)-treated ultrapure water: Add DEPC to milli Q water to give a final concentration of 0.1%; mix, incubate at 37°C for 2–6 hr, and autoclave.

7. Graded ethanol (70%, 80%, and 90%) prepared with DEPC-treated ultrapure water: Add the indicated amount of DEPC-treated ultrapure water to absolute ethanol.

8. Autoclaved PBS (pH 7.6): 7.75 g of NaCl, 1.50 g of K_2HPO_4, and 0.20 g of $KH_2 PO_4$ in 1 L of DEPC-treated ultrapure water.

9. Hydrochloric acid (HCl, 0.2 M): Dilute concentrated HCl with ultrapure water 60-fold.

10. PAP PEN (Daido Sangyo Co., Tokyo, Japan).

11. Proteinase K (Sigma).

12. PFA (4%) in PBS: Add 4 g of PFA to autoclaved PBS, then incubate at 60°C.

13. Glycine/PBS (2 mg/ml): Add 600 mg of glycine to 300 ml of autoclaved PBS.

14. 20X saline-sodium citrate (SSC): Dissolve 175.3 g of NaCl and 88.2 g of sodium citrate in 800 ml of ultrapure water, adjust pH to 7.2, then adjust the volume to 1 L with ultrapure water and autoclave.

15. Hybridization buffer (0.6 M NaCl, 1 mM ethylenediamine tetra-acetic acid [EDTA], 10 mM Tris-HCl [pH 7.6], 0.25% sodium dodecyl sulfate [SDS], 200 µg/ml transfer RNA [tRNA], 1X Denhardt's, 10% dextran sulfate, 40% formamide).

16. DIG nucleic acid detection kit (Roche).

17. Tween-20 (Wako Pure Chemical Ind. Ltd. Osaka, Japan).

18. Buffer 1 (0.1 M Tris-HCl, 0.15 M NaCl (pH 7.5): To prepare 1 L of buffer 1, mix 100 ml of 1 M Tris-HCl (pH 7.5), 150 ml of 1 M NaCl, and 750 ml of ultrapure water.

19. Buffer 2 (1% blocking reagent in buffer 1): Add 1 g of blocking reagent to 100 ml of buffer 1 and incubate at 60°C.

20. Buffer 3 (100 mM Tris-HCl, 100 mM NaCl, 50 mM $MgCl_2$, pH 9.5): To prepare 500 ml, mix 50 ml of 1 M Tris-HCl (pH 9.5), 50 ml of 1 M NaCl, 25 ml of 1 M $MgCl_2$, and 375 ml of ultrapure water.

21. Tris Ethylenediaminetetraacetic acid (TE) buffer (10 mM Tris-HCl and 1 mM EDTA, pH 8.0): To prepare 1 L of TE buffer, mix 10 ml of 1 M Tris-HCl (pH 8.0), 5 ml of 0.2 M EDTA, and 985 ml of ultrapure water.

22. Mount-quick "aqueous" mounting medium (Daido Sangyo Co., Ltd.).

Method for *in situ* Hybridization

Probe Preparation

Short probes are required for *in situ* hybridization because the probes have to infiltrate and diffuse into cells. Usually, complementary deoxyribonucleic acid (cDNA) lengths between 200 and 400 nucleotides give the best results in *in situ* hybridization using a cRNA probe.

1. To amplify a cDNA fragment, corresponding to nucleotides 663-858 of human *lumican* cDNA, synthesize *Eco* RI or *Bam* HI adaptor added primers as follows:

5′-CGG-AAT-TCC-TCA-ACC-AGG-GAT-GAC-ACA-T-3′,

5′-CGC-GGA-TCC-CAA-TCA-GAT-AGC-CAG-ACT-GC-3′

2. Generate a 215-bp *Bam* HI-*Eco* RI cDNA fragment by reverse transcription polymerase chain reaction (RT-PCR) from human placental RNA with the Takara RNA PCR kit.

3. After subcloning the cDNA fragment into the pGEM-T vector, linearize the circular vector with a restriction enzyme, which cuts the multiple cloning sites at two orientations (*Bam* HI or *Eco* RI), allowing sense and antisense synthesis.

To synthesize *in vitro* transcripts, use restriction enzymes that create a 5′-overhang to linearize the template vector.

4. Purify linearized plasmid by phenol-chloroform extraction and ethanol precipitation.

5. Resuspend the linearized plasmid in DEPC-treated ultrapure water.

6. Generate DIG-labeled RNA probes in both sense and antisense directions by *in vitro* transcription with the DIG RNA labeling kit.

7. Purify the probes by ethanol precipitation and resuspend in DEPC-treated ultrapure water.

8. Monitor the transcription reaction by 2% agarose gel electrophoresis to check for the correct cRNA probe length.

9. Monitor probe labeling by spotting diluted aliquots of the labeled cRNA probes on nylon membranes and analyzing with the DIG nucleic acid detection kit.

10. Adjust the concentration of the labeled sense and antisense probes so that they contain equal amounts of label.

Pretreatment of Sections

1. Immerse the colorectal cancer slides in xylene. Remove after 10 min and shake off the excess xylene.

2. Repeat **Step 1** twice using fresh xylene.

3. Immerse slides in 100% ethanol. Remove after 3 min and shake off the excess 100% ethanol.

4. Repeat **Step 3** twice with fresh 100% ethanol.

5. Then, rehydrate the sections with 90%, 80%, and 70% ethanol in DEPC-treated ultrapure water in the same way as described earlier.

6. Wash the slides twice with autoclaved PBS for 15 sec each time, using a vibrator (Sakura Finetek Co. Ltd., Tokyo, Japan).

7. Incubate them in 0.2 M HCl for 20 min at room temperature.

8. Wash them in autoclaved PBS for 3 min.

9. Encircle the tissues on slides with PAP PEN.

10. Apply 2–3 drops of 100 µg/ml proteinase K in PBS on the tissues encircled by PAP PEN, and then incubate for 15 min at 37°C in an OmniSlide Moist Chamber (A Thermo BioAnalysis Company, Teddington, UK). Protease treatment increases target accessibility by digesting the protein that surrounds the target mRNA. For formalin-fixed and paraffin-embedded materials, using 10–150 µg/ml for 15 min gives good results.

11. Wash the slides with PBS for 5 min at room temperature using the vibrator.

12. Incubate them with 4% PFA/PBS for 5 min at room temperature.

13. Wash them with PBS for 5 min at room temperature using the vibrator.

14. Immerse the slides twice in 2 mg/ml glycine/PBS at room temperature for 15 min each time.

15. Wash them with PBS for 5 min at room temperature with the vibrator.

16. Incubate the slides with 50% formamide/2X SSC for 60 min at 42°C.

Hybridization

1. Mix 500 ng/ml of labeled probe and hybridization buffer.

2. Denature the labeled probe with hybridization buffer for 10 min at 60°C and cool on ice.

3. Apply 100–150 µl of the denatured probe onto the slides and incubate overnight (O/N) at 42°C in the OmniSlide Moist Chamber.

Washes and Detection of mRNA

1. Wash the slides with 2X SSC for 20 min at 42°C in an OmniSlide Washing Module (A Thermo Bio-Analysis Company).

2. Wash them with 0.2X SSC for 20 min at 42°C in an OmniSlide Washing Module.

3. Incubate the slides with Buffer 1 for 1 min at room temperature.

4. Incubate them with Buffer 2 for 60 min at room temperature.

5. Incubate them with Buffer 1 for 1 min at room temperature.

6. Centrifuge alkaline phosphatase-conjugated anti-DIG antibody for 2 min at 12,000 rpm at 4°C, and use the supernatant. Centrifuging the antibody precipitates the concentrated particles at the bottom of the tube.

7. Incubate the slides for 30 min with the anti-DIG antibody diluted 1:2000 in Buffer 1 containing 0.2% Tween-20 at room temperature.

8. Wash the slides twice with Buffer 1 containing 0.2% Tween-20 for 15 min each time at room temperature using the vibrator.

9. Incubate the slides with Buffer 3 for 2 min at room temperature.

10. Prepare a color solution containing 10 ml of Buffer 3, 45 µl of nitroblue tetrazolium (NBT) solution, and 35 µl of 5-bromo-4-chloro-3-indolyl-phosphate (BCIP).

11. Cover the slides with 100–150 µl of the color solution, and incubate them in a humidified chamber for 0.5–3 hr in the dark.

12. Observe the slides under a microscope every 30 min, and stop the color reaction by incubating the slides in TE buffer.

13. Mount the sections with aqueous mounting medium.

RESULTS AND DISCUSSION

In normal colorectal tissues, lumican immunoreactivity was observed in mucosal and submucosal stromal tissues, stromal fibroblasts, and peripheral nerve cells in muscular layers and lumican mRNA was expressed in a few stromal fibroblasts but not in epithelial cells. Lumican immunoreactivity was strongly localized in cancer cells and proliferated fibroblasts adjacent to cancer cells (Figure 36A), and lumican mRNA was overexpressed in cancer cells and the stromal fibroblasts adjacent to cancer cells (Figure 36B). Sense probe did not yield any positive signals (Figure 36C). In colorectal epithelial cells with mild dysplasia adjacent to cancer cells, faint lumican protein and its mRNA were detected.
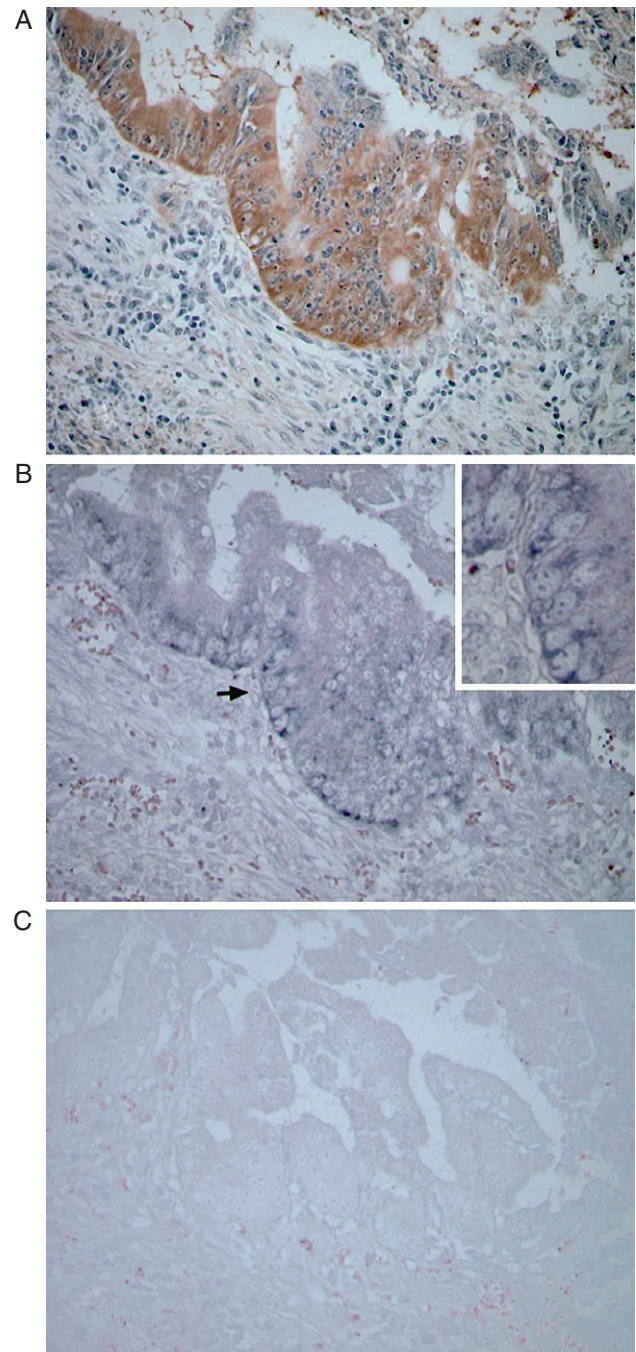
Figure 36 Immunohistochemical and *in situ* hybridization analysis of lumican expression in human colorectal cancer tissues. **A:** Strong lumican immunoreactivity is detected in cancer cells and stromal cells. **B:** Strong lumican messenger ribonucleic acid (mRNA) signals are detected in cancer cells and stromal fibroblasts using the antisense complementary RNA (cRNA) probe in a serial tissue section. Arrows denote the area magnified in inset. **C:** Sense probe reveals no positive signals.

Lumican has a signal sequence for secretion and was localized in the stromal tissues close to cancer cells. In breast cancer tissues, lumican is only synthesized by fibroblasts adjacent to cancer cells (Leygue *et al.*, 1998). In contrast, lumican is synthesized by cancer cells and adjacent fibroblasts in the pancreas, uterine cervix, and colorectum (Lu *et al.*, 2002a; Lu *et al.*, 2002b; Naito *et al.*, 2002). Lumican is strongly expressed in the cancer cells in approximately 70% of colorectal cancer cases. Lumican expression in the invasive front of tumors has been detected in some cancers. Lumican was found to accumulate at the periphery of cancer cell nests of the uterine cervix (Naito *et al.*, 2002). In breast cancer, increased lumican deposition was observed in the collagenous stroma of tumors, particularly at the margins of invasive tumors (Leygue *et al.*, 2000). This accumulation of lumican in tumor invasive fronts may play an important role in cancer cell growth.

However, lumican mRNA and lumican itself were weakly detected in colorectal epithelial cells with mild reactive dysplasia and fibroblasts adjacent to the cancer cells (Lu *et al.*, 2002b). Lumican is not found in normal colorectal epithelial cells distantly located from cancer cells, suggesting that lumican is ectopically synthesized in epithelial cells adjacent to cancer cells. Lumican is expressed ectopically and transiently in the corneal epithelium during the early phase of corneal wound healing and in cardiomyocytes after ischemic and reperfusion injury of the rat heart (Baba *et al.*, 2001; Saika *et al.*, 2000). Furthermore, lumican was ectopically synthesized by acinar cells adjacent to pancreatic cancer cells (Lu *et al.*, 2002b). These findings indicate that epithelial cells close to cancer cells may modulate the extracellular components around the cancer cells.

Lumican is reported to undergo different types of glycosylation, which generate the core protein, glycoprotein, and proteoglycan forms of lumican. In corneal tissues, lumican was reported to be predominantly in the proteoglycan form possessing KS side chains, whereas lumican in other tissues was reported to be mainly in the glycoprotein form. We found prominent expression of the proteoglycan form of lumican that has nonsulfated or poorly sulfated polylactosamine side chains in human pancreatic cancer cell lines or colorectal cancer cell lines (Lu *et al.*, 2002a; Lu *et al.*, 2002b). The lumican in cancer tissues possesses polylactosamine side chains rather than KS side chains, and these glycosylated forms of lumican or the side chains themselves may contribute to cancer cell proliferation.

During the growth of a primary tumor or the establishment of metastatic foci, there is a continuous remodeling of the extracellular matrix characterized by various degrees of biosynthesis and degradation (Iozzo *et al.*, 1995). The proteoglycans are important constituents of the extracellular matrix and regulate cancer cell growth and invasion (Iozzo *et al.*, 1985). Isoforms of transforming growth factor (TGF)-β interact with members of the SLRP family, such as decorin, biglycan, and fibromodulin (Hildebrand *et al.*, 1994). Colon cancer cells transfected with the *decorin* gene exhibited suppressed cell growth *in vitro* and *in vivo* (Santra *et al.*, 1995). Lumican expression was reported to be up-regulated by TGF-β2, which is one of the growth inhibitory factors for epithelial cells (Saika *et al.*, 2003). Lumican was reported to suppress the transformation induced by v-src and v-K-ras in primary rat embryonic fibroblasts, and tumorigenicity in nude mice induced by these oncogenes was also suppressed in these lumican-expressing clones (Yoshioka *et al.*, 2000). We recently found that human embryonic kidney (HEK) 293 cells transfected with the morpholino antisense oligonucleotide against lumican mRNA exhibited a higher growth rate than control cells (Ishiwata *et al.*, 2004). These lines of evidence suggest that the growth of cancer cells is modulated by the SLRPs including lumican, and the functions of SLRPs are closely related to those of other growth factors or cytokines.

In the immunohistochemical method used, the use of a labeled polymer prepared by combining amino acid polymers with peroxidase and goat rabbit Ig eliminates the need to use biotin to form a streptavidin-biotin complex. The use of this method results in the generation of less nonspecific signals as a result of intrinsic biotin. The *in situ* hybridization methods allow specific mRNA to be detected in morphologically preserved tissue sections. The preparation of a cRNA probe (ribo probe) requires time and effort, but its use results in higher sensitivity than the use of oligonucleotide probes. In combination with immunohistochemical analysis, *in situ* hybridization can relate microscopic topologic information to gene activity at mRNA and protein levels. In the present study, we performed the immunohistochemical staining and *in stiu* hybridization analysis on formalin-fixed and paraffin-embedded tissue sections. This method results in the higher resolution of histologic features than when frozen sections are used. Moreover, we can use routine surgical tissue sections. This type of study may help to clarify the biosythsesis and role of various extracellular matrices, growth factors, and cytokines close to cancer cells.

In summary, we found that lumican is synthesized by colorectal cancer cells and by adjacent fibroblasts and epithelial cells with mild reactive dysplasia using immunohistochemical and *in situ* hybridization analysis of serial tissue sections. Lumican may play a role in the growth of human colorectal cancer cells.

References

Baba, H., Ishiwata, T., Takashi, E., Xu, G., and Asano, G. 2001. Expression and localization of lumican in the ischemic and reperfused rat heart. *Jpn. Circ. J.* 65:445–450.

Blochberger, T.C., Vergnes, J.P., Hempel, J., and Hassell, J.R. 1992. cDNA to chick lumican (corneal keratan sulfate proteoglycan) reveals homology to the small interstitial proteoglycan gene family and expression in muscle and intestine. *J. Biol. Chem.* 267:347–352.

Chakravarti, S., Magnuson, T., Lass, J.H., Jepsen, K.J., LaMantia, C., and Carroll, H. 1998. Lumican regulates collagen fibril assembly: Skin fragility and corneal opacity in the absence of lumican. *J. Cell Biol.* 141:1277–1286.

Chakravarti, S., Stallings, R.L., SundarRaj, N., Cornuet, P.K., and Hassell, J.R. 1995. Primary structure of human lumican (keratan sulfate proteoglycan) and localization of the gene (LUM) to chromosome 12q21.3-q22. *Genomics* 27:481–488.

Cornuet, P.K., Blochberger, T.C., and Hassell, J.R. 1994. Molecular polymorphism of lumican during corneal development. *Invest. Ophthalmol. Vis. Sci.* 35:870–877.

Funderburgh, J.L., Funderburgh, M.L., Mann, M.M., and Conrad, G.W. 1991. Arterial lumican. Properties of a corneal-type keratan sulfate proteoglycan from bovine aorta. *J. Biol. Chem.* 266:24773–24777.

Grover, J., Chen, X.N., Korenberg, J.R., and Roughley, P.J. 1995. The human lumican gene. Organization, chromosomal location, and expression in articular cartilage. *J. Biol. Chem.* 270:21942–21949.

Hardingham, T.E., and Fosang, A.J. 1992. Proteoglycans: Many forms and many functions. *FASEB. J.* 6:861–870.

Hildebrand, A., Romaris, M., Rasmussen, L.M., Heinegard, D., Twardzik, D.R., Border, W.A., and Ruoslahti, E. 1994. Interaction of the small interstitial proteoglycans biglycan, decorin and fibromodulin with transforming growth factor beta. *Biochem. J.* 302:527–534.

Iozzo, R.V. 1985. Neoplastic modulation of extracellular matrix. Colon carcinoma cell release polypeptides that alter proteoglycan metabolism in colon fibroblasts. *J. Biol. Chem. 260:* 7464–7473.

Iozzo, R.V. 1995. Tumor stroma as a regulator of neoplastic behavior. Agonistic and antagonistic elements embedded in the same connective tissue. *Lab. Invest.* 73:157–160.

Iozzo, R.V. 1997. The family of the small leucine-rich proteoglycans: Key regulators of matrix assembly and cellular growth. *Crit. Rev. Biochem. Mol. Biol.* 32:141–174.

Ishiwata, T., Fujii, T., Ishiwata, S., Ikegawa, S., and Naito, Z. 2004. Effect of morpholino antisense oligonucleotide against lumican mRNA in human embryonic kidney (HEK) 293 cells. *Pathol. Int.* 54:77–81.

Leygue, E., Snell, L., Dotzlaw, H., Hole, K., Hiller-Hitchcock, T., Roughley, P.J., Watson, P.H., and Murphy, L.C. 1998. Expression of lumican in human breast carcinoma. *Cancer Res.* 58:1348–1352.

Leygue, E., Snell, L., Dotzlaw, H., Troup, S., Hiller-Hitchcock, T., Murphy, L.C., Roughley, P.J., and Watson, P.H. 2000. Lumican and decorin are differentially expressed in human breast carcinoma. *J. Pathol.* 192:313–320.

Lu, Y.P., Ishiwata, T., and Asano, G. 2002a. Lumican expression in alpha cells of islets in pancreas and pancreatic cancer cells. *J. Pathol.* 196:324–330.

Lu, Y.P., Ishiwata, T., Kawahara, K., Watanabe, M., Naito, Z., Moriyama, Y., Sugisaki, Y., and Asano, G. 2002b. Expression of lumican in human colorectal cancer cells. *Pathol. Int.* 52:519–526.

Naito, Z., Ishiwata, T., Kurban, G., Teduka, K., Kawamoto, Y., Kawahara, K., and Sugisaki, Y. 2002. Expression and accumulation of lumican protein in uterine cervical cancer cells at the periphery of cancer nests. *Int. J. Oncol. 20:943–948.

Onda, M., Ishiwata, T., Kawahara, K., Wang, R., Naito, Z., and Sugisaki, Y. 2002. Expression of lumican in thickened intima and smooth muscle cells in human coronary atherosclerosis. *Exp. Mol. Pathol.* 72:142–149.

Qin, H., Ishiwata, T., and Asano, G. 2001. Effects of extracellular matrix on lumican expression in rat aortic smooth muscle cells in vitro. *J. Pathol.* 195:604–608.

Saika, S., Miyamoto, T., Tanaka, S., Tanaka, T., Ishida, I., Ohnishi, Y., Ooshima, A., Ishiwata, T., Asano, G., Chikama, T., Shiraishi, A., Liu, C.Y., Kao, C.W., and Kao, W.W. 2003. Response of lense epithelial cells to injury: Role of lumican in epithelial-mesenchymal transition. *Invest. Ophthalmol. Vis. Sci. 44:* 2094–2102.

Saika, S., Shiraishi, A., Liu, C.Y., Funderburgh, J.L., and Kao, C.W. 2000. Role of lumican in the corneal epithelium during wound healing. *J. Biol. Chem.* 275:2607–2612.

Santra, M., Skorski, T., Calabretta, B., Lattime, E.C., and Iozzo, R.V. 1995. De novo decorin gene expression suppresses the malignant phenotype in human colon cancer cells. *Proc. Natl. Acad. Sci. USA 92:*7016–7020.

Sztrolovics, R., Alini, M., Mort, J.S., and Roughley, P.J. 1999. Age-related changes in fibromodulin and lumican in human intervertebral discs. *Spine 24:*1765–1771.

Troup, S., Njue, C., Kliewer, E.V., Parisien, M., Roskelley, C., Chakravarti, S., Roughley, P.J., Murphy, L.C., and Watson, P.H. 2003. Reduced expression of the small leucine-rich proteoglycans, lumican, and decorin is associated with poor outcome in node-negative invasive breast cancer. *Clin. Cancer Res.* 9:207–214.

Wendel, M., Sommarin, Y., and Heinegard, D. 1998. Bone matrix proteins: Isolation and characterization of a novel cell-binding keratan sulfate proteoglycan (osteoadherin) from bovine bone. *J. Cell Biol.* 141:839–847.

Yeo, T.K., Brown, L., and Dvorak, H.F. 1991. Alterations in proteoglycan synthesis common to healing wounds and tumors. *Am. J. Pathol. 138:*1437–1450.

Ying, S., Shiraishi, A., Kao, C.W., Converse, R.L., Funderburgh, J.L., Swiergiel, J., Roth, M.R., Conrad, G.W., and Kao, W.W. 1997. Characterization and expression of the mouse lumican gene. *J. Biol. Chem.* 272:30306–30313.

Yoshioka, N., Inoue, H., Nakanishi, K., Oka, K., Yutsudo, M., Yamashita, A., Haruka, A., and Nojima, H. 2000. Isolation of transformation suppressor genes by cDNA subtraction: Lumican suppress transformation induced by v-src and v-K-ras. *J. Virol.* 74:1008–1013.

This Page Intentionally Left Blank

14

Role of Immunohistochemical Expression and *in situ* Hybridization Expression of Endothelin in Colon Carcinoma

Florence Pinet

Introduction

The potent vasoconstrictor peptide endothelin (ET)-1 was identified by Yanagisawa *et al*. (1988). It belongs to a family of three 21-amino acid peptides, the endothelins (ETs), which regulate vascular tone. The ETs act on two distinct high-affinity ET receptor sub-types, ETA (Hosoda *et al*., 1991) and ETB (Sakamoto *et al*., 1991), which are seven-transmembrane G protein-coupled receptors. ETA receptors bind ET-1 and ET-2, but not ET-3, at physiologic concentrations, whereas ETB receptors bind all three ETs with similar affinity. ETs are initially synthesized as large precursor polypeptides, prepro-ETs (PPETs), that are cleaved at two pairs of basic amino acids to generate interme-diate peptides, the big ETs. The big ETs are then cleaved by ET-converting enzyme (ECE) (Shimada *et al*., 1995) to produce the mature ETs. ECE is a key enzyme in the synthesis of the ETs because big ETs have negligible biologic activities (Kashiwabara *et al*., 1989). Two ECE-encoding genes have been cloned—*ECE-1* and *ECE-2*. Their sequences are 59% identical, but only *ECE-1*, the most abundant, has been studied in detail (see Turner and Tanzawa 1997,

for a review). Targeted inactivation studies on *ECE-1* in mice showed that although there was still ET-1 in the plasma because of ECE-2, it did not rescue the mutant developmental phenotype, indicating that mature ETs must be produced at specific sites to influence development (Yanagisawa *et al*., 1998). Also, the cleavage of other substrates, vasoactive intestinal peptide (VIP) and neurotensin, by ECE-1 cannot be excluded, because ECE-1 has been shown to have a relatively broad specificity (Johnson *et al*., 1999).

ET-1 was initially believed to be a vasoconstrictor peptide, but it has a variety of other biologic activities, such as stimulation of hormone release and regulation of central nervous system activity (Masaki, 1995), in nonvascular tissues. ET-1 is also a potent mitogen in many cell types, playing a fundamental role in cardiovascular system development (Kurihara *et al*., 1995). Shortly after the discovery of ET-1, Whittle and Esplugues (1988) reported that ET could be pro-ulcerogenic in the rat, in the pathogenesis of gastric damage and ulceration, and a nonselective ET receptor antagonist was found to reduce injury in a rat model of colitis (Hogaboam *et al*., 1996).

There have been few reports on the distribution of ET in the human colon. Inagaki *et al*. (1992) found ET-like immunoreactivity and binding sites for ET-1 in the human colon. In a previous study, we showed that ECE-1 messenger ribonucleic acid (mRNA) and its protein are present in the adult human colon (Korth *et al*., 1999). We used *in situ* hybridization (ISH) and immunohistochemistry to demonstrate large amounts of ECE-1 in the epithelium and enteric ganglia of the normal human colon. ET-1 has also been reported to stimulate proliferation of various types of neoplastic cells (Bagnato *et al*., 1997).

The growth of malignant tumors depends on neovascularization. Tumor angiogenesis requires angiogenic factors, such as vascular endothelial growth factor (VEGF), provided by cancer cells and affecting the host tissues (Folkman *et al*., 1971). The mechanisms involved in maturation of tumor vascularization are not well defined. Endothelial cells are a critical element responsible for new vessel formation, but other cellular elements such as smooth-muscle cells/pericytes are necessary. Maturation of the vascular system involves the recruitment of perivascular supporting cells that do not bear cell-specific markers, but which do contain α-smooth-muscle actin (α-SMA). A report suggests that migration of endothelial cells is promoted by ET-1 via the ETB receptor (Ziche *et al*., 1995) and ET binding sites have been found in human colon cancer tissue (Inagaki *et al*., 1992). However, none of these studies determined the receptor subtype, substrate, and enzyme of the ET system in the same tissue, and most of the studies were carried out at low resolution so that the cellular distribution was not obtained.

The present study was therefore carried out to determine the precise cellular locations of all components of the ET-1 system in the human normal colon and so gain insight into the possible role of ET-1 in gastrointestinal physiology. The distributions of PPET-1, ECE-1, ETA, and ETB receptor mRNAs were studied by ISH. The cells containing the mRNAs were further examined by comparing the distribution of these mRNAs with the markers of endothelial cells, smooth-muscle cells, and macrophages. Also, we compared the expression of mRNAs and proteins of all components of the ET-1 system in the human normal colon, adenoma, and adenocarcinoma colon to assess their potential role in tumor vascularization. In addition, we also used an experimental rat model of colon cancer, with or without bosentan (a mixed antagonist of ETA and ETB receptors) treatment, to further evaluate the influence of ET-1 receptors and α-SMA–positive cells in stromal angiogenic responses. *In situ* hybridization and immunohistochemistry techniques allow a precise

localization of the components of the ET system linked to cellular marker in tumor tissue.

MATERIALS

Human Tissues

1. Human colon tissues were obtained at the Institute of Pathology (Lausanne, Switzerland) at surgery from patients (n = 18) undergoing colectomy for cancer.

2. Samples from 18 patients (41–84 years old, 8 women and 10 men) were examined.

3. Nine samples were from cecum and nine were from the sigmoid colon; all were at the T3 or T4 stage.

4. Tissues were either snap-frozen in liquid nitrogen and stored at −80°C (eight samples) or fixed in 4% buffered paraformaldehyde for at least 25 hr, processed, and embedded in paraffin (10 samples).

METHODS

mRNA Analysis

1. Total RNA was isolated from frozen adenocarcinoma colon sections and control regions and excised at least 1 cm from the lesion, using the protocol of Chomczinkski *et al*. (1987).

2. Complementary deoxyribonucleic acid (cDNA) was prepared with 0.5 μg of total RNA, 10 pmol oligodT using Moloney leukemia virus reverse transcriptase (Life Technologies, Inc., Rockville, MD) according to the manufacturer's instructions.

3. Polymerase chain reaction (PCR) was performed using 3 μl of cDNA solution and 1.25 U of Taq Polymerase (Roche Diagnostics, Meylan, France) according to the manufacturer's instructions.

4. Control reactions for reverse transcriptase-polymerase chain reaction (RT-PCR) were performed from nonreverse–transcribed RNA samples. No amplification was observed for any RNA samples tested (not shown).

5. Specific primers (10 pmol) for *ECE-1* (Shimada *et al*., 1995), *PPET-1* (Itoh *et al*., 1988), *ETA* (Hosada *et al*., 1991) and *ETB* receptors (Sakamoto *et al*., 1991), and *glyceraldehyde-3-phosphate dehydrogenase* (GAPDH) (Tso *et al*., 1985) were added as previously described (Egidy *et al*., 2000a). The primers used were designed to avoid false-positive reactions from genomic DNA contamination.

6. Thirty cycles were performed, consisting of denaturation at 94°C (30 seconds), annealing at 58°C (PPET-1, ETA and ETB receptors) or 55°C (ECE-1 and GAPDH) (30 seconds) and extension at

72°C (30 seconds) with a final extension step of 10 min at 72°C.

7. Amplified products were analyzed on 2% agarose.

Preparation of Radiolabeled Riboprobes

1. The human *PPET-1* partial cDNA, corresponding to the nucleotide sequence 70–630, was subcloned into pBK-CMV (Stratagene, La Jolla, CA) as described previously (Egidy *et al.*, 2000a).

2. The recombinant plasmid was linearized by digestion with *Sac*I to obtain antisense or with *Kpn*I to obtain the sense probe.

3. Probes for human *ECE-1* (Shimada *et al.*, 1995) were prepared as described in Korth *et al.* (1999). Briefly, the *ECE-1* partial cDNA corresponding to the nucleotides 304–1666 was linearized by digestion with *Hind*III to obtain the antisense or with *Xba*I to obtain the sense RNA.

4. Probes for human *ETA* (Hosoda *et al.*, 1991) and *ETB* (Sakamoto *et al.*, 1991) receptors, subcloned into pcDNA3, were linearized by digestion with *Xba*I to obtain the sense probe.

5. *In vitro* transcription and labeling with ^{35}S-UTP (Amersham, Les Ulis, France) were performed with T7 or SP6 RNA polymerase (Roche Diagnostics).

6. Probes were precipitated with ammonium acetate and ethanol, dried by centrifugation-evaporation (speed-vac), and dissolved in 10 mmol/L Tris, 1 mmol/L ethyl-enediamine tetra-acetic acid (EDTA), 20 mmol/L dithiothreitol (DTT).

in situ Hybridization

1. The *in situ* hybridization protocol used for paraffin sections involved microwave pre-treatment to enhance the hybridization signal (Sibony *et al.*, 1995).

2. Paraffin-embedded sections (5 μm) were cut, and two adjacent sections were mounted on each silane-coated slide.

3. Deparaffinized sections were immersed in 0.01 mol/L citric acid (pH 6.0) and heated in a microwave oven for 12 min.

4. The sections were then incubated with proteinase K (2 μg/ml, Roche Diagnostics) for 20 min and dehydrated.

5. *In situ* hybridization performed on frozen sections used 7-μm sections fixed in paraformaldehyde/phosphate-buffered saline and dehydrated without microwaving.

6. The following protocol was subsequently used for both frozen and paraffin-embedded sections.

7. Sections were incubated overnight at 50°C with the respective antisense and sense riboprobes (3–4 × 10 cpm per section).

8. The slides were washed with increasingly stringent solutions and treated with RNase A (20 μg/ml, Sigma, Saint-Quentin, France).

9. The sections were then dehydrated and placed in contact with Biomax film (Kodak, Rochester, NY) for 1–3 days.

10. They were subsequently dipped in NTB2 liquid emulsion (Kodak) and exposed for 2 weeks (*ECE-1* or *PPET-1* probes) or for 4 weeks (*ETA* and *ETB* probes).

11. Sections were counterstained with toluidine blue.

^{125}I ET-1 Binding

1. Sections (7 μm) were cut using a cryostat, thaw-mounted on silane-coated slides, and stored overnight under vacuum at 4°C.

2. Consecutive sections were fixed for 10 min in 4% formaldehyde/phosphate-buffered saline and then incubated for 15 min in 50 mmol/L Tris-HCl buffer (pH 7.5), containing 120 mmol/L NaCl, 5 mmol/L MgCl$_2$, and 40 mg/ml bacitracin.

3. Sections were then incubated with 100 pmol/L ^{125}I ET-1 (2, 125 Ci/mmol) in the previous buffer containing 1% bovine serum albumin (fraction V, protease-free, Sigma Chemical Co.) and 1 mmol/L phosphoramidon for 90 min at room temperature.

4. Sections were given four 1-minute washes in ice-cold 50 mmol/L Tris-HCl, pH 7.4, dipped in ice-cold distilled water, air-dried, and placed in contact with Biomax MR films (Kodak).

5. Nonspecific binding was determined in consecutive sections incubated as described earlier with 1 μmol/L unlabeled ET-1 (Bachem, Bubendorf, Switzerland).

6. The receptor subtypes were identified by incubating consecutive sections as described earlier with 1 μmol/L BQ 123 (ETA antagonist), 10 nmol/L ET-3 (natual ETB agonist), or 0.2 μmol/L sarafotoxin 6c (S6c) (selective ETB agonist).

7. The sections were then fixed in paraformaldehyde at 80°C for 2 hr, dipped in NTB2 photographic emulsion (Kodak), exposed for 4 days, and counterstained with toluidine blue.

Immunohistochemistry

1. Paraffin-embedded tissue sections (5 μm) were incubated with xylene (to remove paraffin), rehydrated

in a graded ethanol series, and their endogenous per-oxidase was inactivated with 3% hydrogen peroxide in methanol for 10 min.

2. They were then washed in water and incubated with monoclonal antibodies to CD31, CD68 (both from Dako, Hamburg, Germany), α-SMA (Sigma) and Ki-67 antigen (MIB-1, Dianova, Hamburg, Germany) according to the manufacturer's instructions.

3. The antiserum 473-17-A (Korth *et al.*, 1997) was used to stain ECE-1.

4. The bound anti-CD31 and anti–α-SMA antibodies were reacted with peroxidase-antiperoxidase (Dako).

5. Sections were treated with 0.035% diaminoben-zidine (Fluka, Buch, Switzerland) for 30 min, counter-stained with hematoxylin (according to Mayer), and mounted.

6. Control sections without first antibody showed no nonspecific staining (not shown).

Quantification

1. The tumors were scored semi-quantitatively for mRNA expression in epithelial and stroma cells by assessing both the grade of labeling (low, moderate, high, and scattered) and the frequency of signal in each cell type considering 50 cells in the field of a 40 objective.

2. The distribution of markers (CD31, α-SMA, ETA, and ETB mRNA) in stroma was evaluated in three different typical regions of normal, adenoma, and adenocarcinoma.

3. The field was chosen in longitudinal sections of crypts and polyps or in vascularized invasive areas.

4. The paired *t*-test was used for statistical analysis.

Animal Experimentation

Bosentan Treatment

1. Peritoneal carcinomas (solid tumors) were induced in inbred BDIX rats (300 g males or females) purchased from IFFA Credo (l'Arbresle, France) by intraperitoneal injection of 10^6 syngeneic PROb cells.

2. The PROb cells were derived from a colon ade-nocarcinoma chemically induced in BDIX rats. Under these conditions, all rats developed peritoneal carcino-matosis and hemorrhagic ascites (Jeannin *et al.*, 1991).

3. Control rats ($n = 10$) were fed normal rat chow (UAR, Epinay-sur-oise, France), and another group ($n = 10$) were fed bosentan (a gift from Dr. M. Clozel, Actelion, Switzerland) incorporated into the pellets of chow at 100 mg/kg/day, assuming that each animal ate 15 g chow per day.

4. Bosentan treatment started the day before the injection of PROb cells.

5. Animals were examined at the time of their death or sacrifice, which was day 30 after implantation.

6. Tumors were evaluated according to class 0, no nodules detected; class I, few 0.1–0.2-cm nodules; class II, numerous 0.1–0.5-cm nodules; class III, 1-cm nodules invaded peritoneal cavity; class IV, peritoneal cavity has been completely invaded.

7. Nodules were characterized as viable tumor area.

8. Treatment efficacy was evaluated by morpho-logic analysis of the tumors in control and bosentan-treated rats.

Analysis of Tumors

1. Sections (10 μm) of tumors were cut using a cryostat, thaw-mounted, and treated as human samples.

2. ^{125}I ET-1 binding was assessed as described for the human tissues.

3. Immunohistochemistry was performed with anti-bodies against cytokeratin-18 (ICN, Costa Mesa, CA), α-SMA (Sigma), and rat von Willebrand factor (vWF) (Cederlane, Hornby, Canada) as for human tissues.

4. Collagen was visualized with hematoxylin-eosin-safranin staining.

5. The number of nodules (viable tumors areas) and necrotic areas were assessed in a 40 objective field of keratin and hematoxylin-eosin-safranin staining slides.

6. Quantification of markers (vWF and α-SMA) in tumors was evaluated in three different areas of each control and bosentan-treated animals considering all of the positive cells in the field of the 40X objective.

7. The impaired *t*-test was used for statistical analysis.

RESULTS AND DISCUSSION

Expression of The ET System in Human Myofibroblasts and Colon Carcinoma Cells

Myofibroblasts are thought to play a role in mucosal contraction and the differentiation and proliferation of colon cells. It has been proposed that myofibroblast contraction affects epithelial restitution and the propul-sion of absorbed material in the lamina propria (Valentich *et al.*, 1997). We found all the components of the endothelin system in primary cultures of human subepithelial myofibroblasts, CDD-18Co (not shown). PPET-1, ECE-1, ET-A, and ETB receptors mRNAs were present to the same level. Egidy *et al.* (2000a) have shown the physiologic role of ET in the gut. The entire ET system is present in the normal colonic

mucosa, suggesting its implication in some characteristic function of the colon and its secretion as both neuroactive and vasoactive peptides. The presence of components of the ET system was also found in the three epithelial cell lines from human colorectal carcinoma available, HCT 116, Caco-2, and HT-29 with the highest expression for ECE-1 mRNA. Both receptors were lower expressed with ETA absent in Caco-2 and HT-29 cell lines.

Expression of the ET System mRNAs in Human Colon Carcinoma

The ET system was more abundant in adenocarcinoma than in normal colon tissue. In particular, the concentrations of mRNA for *PPET-1* and *ECE-1* were higher in the cancer than in normal tissue.

Tissue architecture of samples was analyzed by Ki-67 immunohistochemistry using MIB-1 antibody showing the typical immunostaining in the epithelial monolayer at the base of the crypts of normal colon mucosa, whereas adenoma-disrupted crypts and adenocarcinoma had an anarchical MIB-1 staining pattern mainly in neoplastic epithelial cells.

We located the cellular distribution of the ET system by *in situ* hybridization (Egidy *et al.*, 2000b). The whole ET system showed greater expression in cancer tissue than in normal colon with the same distribution in neoplastic tissue and normal tissue. *PPET-1* and *ECE-1* mRNA was found mainly in the epithelium, and *ETA receptor* mRNA was found in the stroma. The distribution of *ETA receptor* mRNA was comparable to that of α-SMA immunoreactive cells along the normal crypts and tumor vasculature. *ETB receptor* mRNA was abundant in the cancer stroma, associated with the α-SMA–stained cells. However, neither α-SMA signal nor *ETA* or *ETB* mRNAs were detected where nests of tumor cells were invading the submucosa or the muscularis propria without a stromal reaction. Receptor mRNAs seemed to be much less abundant than mRNA for *PPET-1* and *ECE-1*, with *ETB* mRNA being the least abundant, considering that ETA- and ETB-hybridized sections were exposed for twice as long *PPET-1* and *ECE-1* probes.

In situ hybridization showed that the stroma surrounding the cancer had highly vascularized regions with larger concentration of PPET-1 and ECE-1 than the stroma in normal tissue. PPET-1 and ECE-1 mRNAs were mainly found in epithelial and endothelial cells in the adenomas, with labeling being fourfold to fivefold more frequent in adenoma endothelial cells than in the normal colon. Thus, both the substrate, PPET-1, and its converting enzyme, ECE-1, have the same distribution, so that active ET-1 can be produced in tumors. ET-1 is less present in the endothelial cells, tumor cells, and myofibroblasts of colorectal liver metastasis (Shankar *et al.*, 1998). To our knowledge, it was the first study on the expression of cellular distribution of ECE-1 in human tumors.

The cellular distribution of receptor transcripts is almost exclusively in the stroma of adenoma and adenocarcinoma (Figure 37). *ETA* mRNA (Figure 37A, G) was found associated with a subpopulation of α-SMA–positive cells (Figure 37B, E, H, K) probably subepithelial myofibroblasts and also CD31-positive cells (Figure 37J–L). The vessels of adenoma were strongly labeled for ETB (Figure 37C, F), which were also immunostained for α-SMA and the proliferation marker MIB-1 (Figure 37D). ETB labeling was present in adenocarcinomas in the endothelial cells that were immunostained with CD31 antibody (Figure 37I) and in myofibroblasts that were immunostained with α-SMA antibody (Figure 37K). Thus, labeling for *ETA* and *ETB* mRNAs was more intense in regions with pronounced vascularization containing abundant α-SMA–positive cells.

Localization of ET Binding Sites

The distribution of ETA and ETB receptors in human colon adenocarcinomas was assessed by autoradiography of ^{125}I ET-1 binding to frozen samples from eight patients (Figure 38). There was considerable specific binding in the lamina propria of the mucosa, but there was very little over the epithelium of the normal colon (Figure 38A). The distribution of binding in tumor tissue was heterogeneous and was concentrated over clusters of fibroblasts adjacent to cancer cells (Figure 38B). Receptor subtypes were identified in consecutive sections in normal mucosa and adenocarcinomas with a higher proportion of ETB in the myofibroblasts adjacent to the cancer cell foci. The same pattern of expression was obtained by *in situ* hybridization in adjacent sections.

There were also more targets for ET-1 and the ETA and ETB receptors in colorectal cancer than in normal tissue, both the mRNA and the protein, as defined by RT-PCR and *in situ* hybridization and ET-1 binding, respectively. ETA receptors were increased in myofibroblasts. ETB receptors were almost undetectable in normal colon mucosa, but they were abundant in all vascularized areas of the cancer stroma. We found *ETB* mRNA in endothelial cells and in vessel-surrounding myofibroblasts in the vessels of cancer stromas. The myofibroblasts contain four times more labeled cells than in normal colon.
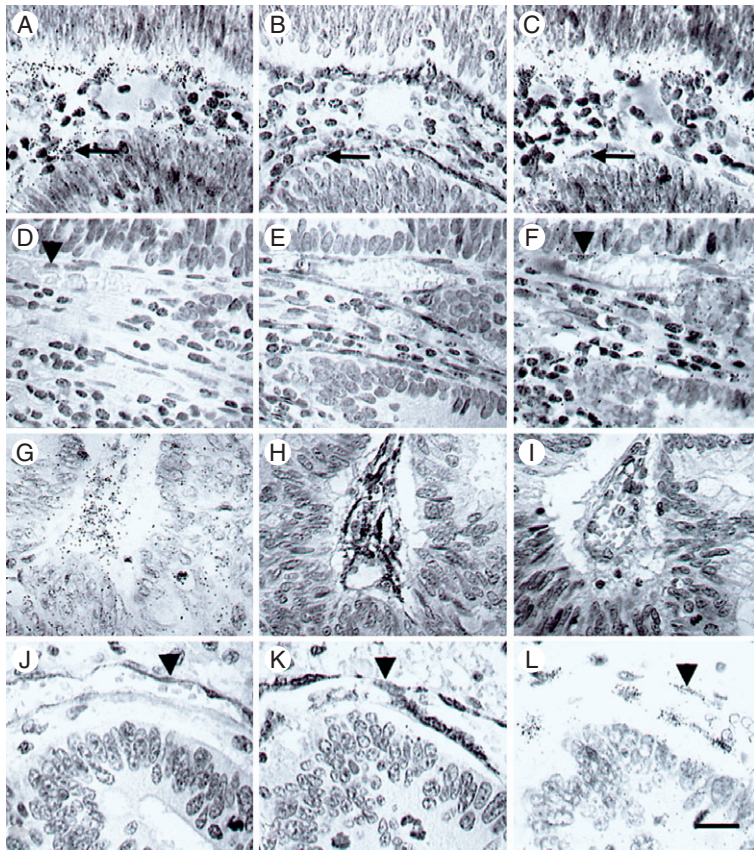
Figure 37 Distribution of specific markers in the stroma. *In situ* hybridization was performed in consecutive sections of adenoma (**A–F**) and adenocarcinoma (**G–L**) with the antisense probes for endothelin A (*ETA*) (**A** and **G**) and *ETB* (**C, F** and **L**) receptors. Immunohistochemistry was performed with anti-α-smooth muscle actin (SMA) (**B, E, H**, and **K**) (smooth-muscle marker), anti-Ki-67 (**D**) (proliferation marker) and anti-CD31 (**I–J**) and **J** (endothelial cell marker) antibodies to identify the cells labeled with ETA and ETB probes. There was intense labeling endothelial (CD31-positive) cells and myofibroblasts (α-SMA positive) with both probes.

Counting of α-SMA–positive cells demonstrated a redistribution of α-SMA–stained cells below the epithelium to around the vasculature in adenocarcinomas. Benjamin *et al*. (1999) showed the importance of α-SMA–positive cells as an index of vessel maturation in human brain and prostate tumors. Our data suggest that the ET system is important as modulator of the colon tumor vascularization causing interaction of myofibroblasts with endothelial cells and ETB receptor induction. Tumor-infiltrating myofibroblasts are α-SMA–positive fibroblasts that are believed to be involved in tumor invasiveness (Powell *et al*., 1999). They are different from the subepithelial α-SMA–positive cells in the human normal colon.

in vivo Effect of Bosentan Blockade in an Experimental Rat Model

Rats implanted with tumors and treated with 100 mg/kg for 30 days of bosentan were killed and the tumors were analyzed. Peduto Eberl *et al*. (2000) have shown that bosentan-treated animals tend to have lower tumor grades than controls but without complete control of tumor progression. Morphologic analysis of the tumors (Figure 39) by hematoxylin-eosin-safranin staining showed a decrease in collagen matrix around the nodules (*insert*) in bosentan-treated animals (Figure 39B) than in controls (Figure 39A). In addition, tumors were less dense in bosentan-treated animals compared with controls, in agreement with the observation that the tumors in the treated rats were less cohesive at the time of sacrifice. Surprisingly, there was no differences in ^{125}I ET-1 sites for both ET subtype receptors in tumors of treated and untreated rats despite bosentan treatment for 30 days.

Analysis of keratin-positive cells showed that the tumor cells in bosentan-treated animals (Figure 39D) were more dispersed than in control rats (Figure 39C). Staining for α-SMA demonstrated a few smooth-muscle cells in the tumors of untreated rats (Figure 39E). In contrast, the tumors of bosentan-treated animals contained α-SMA–positive cells (Figure 39F). Endothelial cells identified by staining for vWF antigen were present in tumors of both groups (Figure 39G, H). The histologic score on hematoxylin-eosin-safranin–stained sections performed on seven different samples for each group of rats showed that the tumors in bosentan-treated rats had significantly less necrotic areas than the controls ($p > 0.05$) (Figure 39I). Quantification of
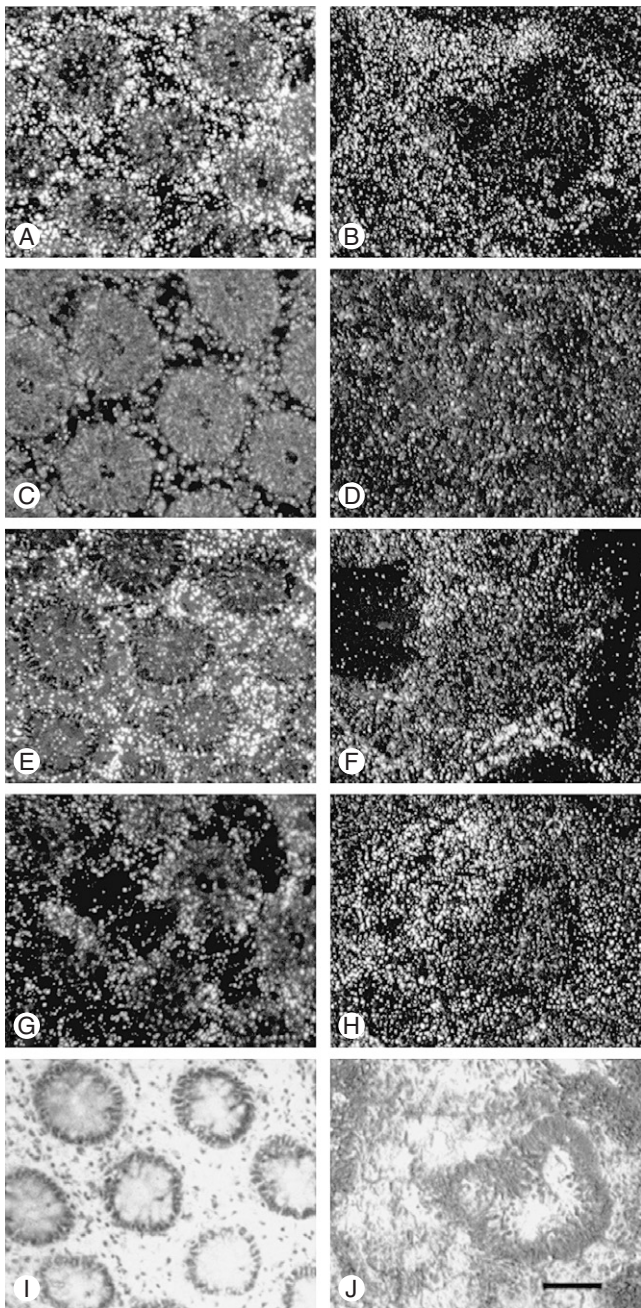
Figure 38 Autoradiographic ^{125}I endothelin (ET)-1 binding sites in human colon adenocarcinoma. ^{125}I ET-1 (100 pmol/L binding was performed in frozen consecutive sections. Dark-field illuminations are shown of transversal sections of normal colon (**A**, **C**, **E**, **G**, and **I**) and adenocarcinoma (**B**, **D**, **F**, **H**, and **J**). **A**, **B**: Total binding. **C**, **D**: Nonspecific binding incubated as in **A** and **B** in the presence of 1 μmol/L ET-1 or both 1 μmol/L BQ123 and 0.2 μmol/L S6c. **E**, **F**: ETA binding, after incubation as in **A** and **B** in the presence of 0.2 μmol/L S6c as competitor. **G**, **H**: ETB binding, after incubation as in **A** and **B** in the presence of 1 μmol/L BQ123. **I**, **J**: toluidine blue counterstaining. Scale bar, 100 μm.

vascular markers showed no significant difference on vWF-positive cells between the two groups and a strong but not significant difference on α-SMA–positive cells, suggesting an exclusive vascular presence of these markers, whereas in bosentan-treated rats α-SMA cells outnumbered vWF cells, indicating the presence of nonvascular myofibroblasts.

By these experiments, we have attempted to elucidate the phenotypic changes that occur during the colon tumor vascularization. We have tried to see whether the induction of ET receptors, in particular ETB, and the redistribution of α-SMA–positive cells were simultaneous or successive events using an experimental rat model of induced colon carcinoma. We blocked ET receptors using bosentan (a mixed antagonist of both ET receptors) showing incomplete control of tumor progression *in vivo* using the same experimental model (Peduto Eberl *et al.*, 2000). There were structural modifications within the tumors in bosentan-treated animals; the tumors were less dense with less collagen around the nodules. Bosentan also reduced deposition of collagen I and III in the extracellular matrix in a murine model of glomerulonephritis (Chatziantoniou *et al.*, 1998). We found a tendency of an increased ratio of α-SMA–positive cells in the tumors of bosentan-treated animals, suggesting that ET-1 acts negatively on α-SMA myofibroblasts. The treatment modified cell phenotypes and the cohesion of the tumor nodules, and necrosis was decreased. Bosentan has been shown to also decrease necrosis in a murine model of myocarditis (Ono *et al.*, 1999). We found no apparent difference in the amount of ETA and ETB receptors in treated and control animals after 30 days on bosentan, however, suggesting a dissociation in time between myofibroblast recruitment and ETB induction or the existence of at least two populations of α-SMA–positive cells. In accordance with this, we did not find ETB receptors in all of the α-SMA–stained cells in human colon tumors.

Our findings of various components of the ET system in specific cells of colon cancers suggest that ET-1 and its receptors could play a role in colon cancer progression. Increased ECE-1 and PPET-1 in endothelial and tumor cells provide a local source of ET-1, which might act in an autocrine role in tumor cell survival and most likely in a paracrine role on the proliferation of tumor stroma cells. ET-1 seems to be functioning as a negative modulator of the stromal angiogenic response, which may be primarily directed through the repression of fibroblast differentiation and may in turn or concomitantly induce the appearance of ETB receptors.

In conclusion, the availability of cDNA microarrays will provide a large-scale approach with the purpose of identifying biomarkers relevant to cancer progression. This technology has been used by Zou *et al.* (2002) to

antibody (**C**, **D**). Smooth-muscle cells were identified with anti-α-smooth muscle actin (SMA) (**E**, **F**) and endothelial cells with an anti-vWF antibody (**G**, **H**). Histologic scores (**I**) were obtained by counting the number of necrotic areas and nodules in the field of the 4X objective in control (*white bars*) and bosentan-treated animals (*black bars*). **J**: Distribution of specific markers in rat nodules. The cells stained for von Willebrand factor and α-SMA were counted in the field of the 40X objective in control (*white bars*) and bosentan-treated animals (*black bars*). The results averaged values of seven different samples that are representative of all of the specimens analyzed. Significant differences ($p < 0.05$) are indicated by an *. Scale bar, 100 μm.

discover global gene expression patterns characterizing subgroups of colon cancer. Two hundred and fifty genes were identified as being involved in colon cancer. This technology could provide invaluable insights into the role of specific genes in the development and progression of colon cancer. The new data should then be confirmed by other techniques: quantitative, real-time RT-PCR, immunohistochemistry, and *in situ* hybridization.

References

Bagnato, A., Tecce, R., Di, C.V., and Catt, K.J. 1997. Activation of mitogenic signaling by endothelin 1 in ovarian carcinoma cells. *Cancer Res. 57*:1306–1311.

Benjamin, L.E., Golijanin, D., Itin, A., Pode, D., and Keshet, E. 1999. Selective ablation of immature blood vessels in established human tumors follows vascular endothelial growth factor withdrawal. *J. Clin. Invest. 103*:159–165.

Chatziantoniou, C., Boffa, J.J., Ardaillou, R., and Dussaule, J.C. 1998. Nitric oxide inhibition induces early activation of type I collagen gene in renal resistance vessels and glomeruli in transgenic mice. Role of endothelin. *J. Clin. Invest. 101*:2780–2789.

Chomczynski, P., and Sacchi, N. 1987. Single-step method of RNA isolation by acid guanidinium thiocyanate-phenol-chloroform extraction. *Anal. Biochem. 162*:156–159.

Egidy, G., Juillerat-Jeanneret, L., Korth, P., Bosman, F.T., and Pinet, F. 2000a. The endothelin system in normal human colon. *Am. J. Physiol. Gastrointest. Liver 279*:G211–G222.

Egidy, G., Juillerat-Jeanneret, L., Jeannin, J.F., Korth, P., Bosman, F.T., and Pinet, F. 2000b. Modulation of human colon tumor-stromal interactions by the endothelin system. *Am. J. Pathol. 157*:1863–1874.

Folkman, J. 1971. Tumor angiogenesis: Therapeutic implications. *N. Engl. J. Med. 285*:1182–1186.

Hogaboam, C.M., Muller, M.J., Collins, S.M., and Hunt, R.H. 1996. An orally active non-selective endothelin receptor antagonist, bosentan, markedly reduces injury in a rat model of colitis. *Eur. J. Pharmacol. 309*:261–269.

Hosoda, K., Nakao, K., Hiroshi, A., Suga, S., Ogawa, Y., Mukoyama, M., Shirakami, G., Saito, Y., Nakanishi, S., and Imura, H. 1991. Cloning and expression of human endothelin-1 receptor cDNA. *FEBS Lett. 287*:23–26.

Inagaki, H., Bishop, A.E., Eimoto, T., and Polak, J.M. 1992. Autoradiographic localization of endothelin-1 binding sites in human colonic cancer tissue. *J. Pathol. 168*:263–267.

Figure 39 Morphology of the colon tumors in the experimental rat model. Immunohistochemistry was performed in consecutive sections of tumors from control (**A**, **C**, **E**, and **G**) and bosentan-treated rats (**B**, **D**, **F**, and **H**). Photographs are presented in brightfield illumination. Eosin-hematoxylin-safran staining (**A**, **B**) was performed for assessing the tumor appearance. Collagen characterized with the safranin staining (*orange*) was shown at higher magnification (insert in **A**, **B**). Tumor epithelial cells bound anti-keratin

Itoh, Y., Yanagisawa, M., Ohkubo, S., Kimura, C., Kosaka, T., Inoue, A., Ishida, N., Mitsui, Y., Onda, H., Fujino, M., Masaki, T. 1988. Cloning and sequence analysis of cDNA encoding the precursor of a human endothelium-derived vasoconstrictor peptide, endothelin: Identity of human and porcine endothelin. *FEBS. Lett. 231*:440–444.

Jeannin, J.F., Onier, N., Lagadec, P., von Jeney, N., Stutz, P., and Liehl, E. 1991. Antitumor effect of synthetic derivatives of lipid A in an experimental model of colon cancer in the rat. *Gastroenterology 101*:726–733.

Johnson, G.D., Stevenson, T., and Ahn, K. 1999. Hydrolysis of peptide hormones by endothelin-converting enzyme-1. A comparison with neprilysin. *J. Biol. Chem. 274*:4053–4058.

Kashiwabara, T., Inagaki, Y., Ohta, H., Iwamatsu, A., Nomizu, M., Morita, A., and Nishikori, K. 1989. Putative precursors of endothelin have less vasoconstrictor activity in vitro but a potent pressor effect in vivo. *FEBS Lett. 247*:73–76.

Korth, P., Bohle, R.M., Corvol, P., and Pinet, F. 1999. Cellular distribution of endothelin-converting enzyme-1 in human tissues. *J. Histochem. Cytochem. 47*:447–462.

Korth, P., Egidy, G., Parnot, C., LeMoullec, J.M., Corvol, P., and Pinet, F. 1997. Construction, expression and characterization of a soluble form of human endothelin-converting enzyme-1. *FEBS Lett. 417*:365–370.

Kurihara, Y., Kurihara, H., Oda, H., Maemura, K., Nagai, R., Ishikawa, T., and Yazaki, Y. 1995. Aortic arch malformations and ventricular septal defect in mice deficient in endothelin-1. *J. Clin. Invest. 96*:293–300.

Masaki, T. 1995. Possible role of endothelin in endothelial regulation of vascular tone. *Annu. Rev. Pharmacol. Toxicol. 35*:235–255.

Ono, K., Matsumori, A., Shioi, T., Furukawa, Y., and Sasayama, S. 1999. Contribution of endothelin-1 to myocardial injury in a murine model of myocarditis: Acute effects of bosentan, an endothelin receptor antagonist. *Circulation 100*:1823–1829.

Peduto Eberl, L., Valdenaire, O., Saintgiorgio, V., Jeannin, J.F., and Juillerat-Jeanneret, L. 2000. Endothelin receptor blockade potentiates FasL-induced apoptosis in rat colon carcinoma cells. *Int. J. Cancer 86*:182–187.

Powell, D.W., Mifflin, R.C., Valentich, J.D., Crowe, S.E., Saada, J.I., and West, A.B. 1999. Myofibroblasts. I. Paracrine cells important in health and disease. *Am. J. Physiol. 277*:C1–C9.

Sakamoto, A., Yanagisawa, M., Sakurai, T., Takuwa, Y., Yanagisawa, H., and Masaki, T. 1991. Cloning and functional expression of human cDNA for the ETB endothelin receptor. *Biochem. Biophys. Res. Commun. 178*:656–663.

Shankar, A., Loizidou, M., Aliev, G., Fredericks, S., Holt, D., Boulos, P.B., Burnstock, G., and Taylor, I. 1998. Raised endothelin 1 levels in patients with colorectal liver metastases. *Br. J. Surg. 85*:502–506.

Shimada, K., Matsushita, Y., Wakabayashi, K., Takahashi, M., Matsubara, A., Iijima, Y., and Tanzawa, K. 1995. Cloning and functional expression of human endothelin-converting enzyme cDNA. *Biochem. Biophys. Res. Commun. 207*:807–812.

Sibony, M., Commo, F., Callard, P., and Gasc, J.M. 1995. Enhancement of mRNA in situ hybridization signal by microwave heating. *Lab. Invest. 73*:586–591.

Tso, J.Y., Sun, X.H., Kao, T.H., Reece, K.S., and Wu, R. 1985. Isolation and characterization of rat and human glyceraldehyde-3-phosphate dehydrogenase cDNAs: Genomic complexity and molecular evolution of the gene. *Nucleic Acids Res. 13*:2485–2502.

Turner, A.J., and Tanzawa, K. 1997. Mammalian membrane metallopeptidases: NEP, ECE, KELL, and PEX. *FASEB J. 11*:355–364.

Valentich, J.D., Popov, V., Saada, J.I., and Powell, D.W. 1997. Phenotypic characterization of an intestinal subepithelial myofibroblast cell line. *Am. J. Physiol. 272*:C1513–C1524.

Whittle, B.J., and Esplugues, J.V. 1988. Induction of rat gastric damage by the endothelium-derived peptide, endothelin. *Br. J. Pharmacol. 95*:1011–1013.

Yanagisawa, H., Yanagisawa, M., Kapur, R.P., Richardson, J.A., Williams, S.C., Clouthier, D.E., de Wit, D., Emoto, N., and Hammer, R.E. 1998. Dual genetic pathways of endothelin-mediated intercellular signaling revealed by targeted disruption of endothelin converting enzyme-1 gene. *Development 125*:825–836.

Yanagisawa, M., Kurihara, H., Kimura, S., Tomobe, Y., Kobayashi, M., Mitsui, Y., Yazaki, Y., Goto, K., and Masaki, T. 1988. A novel potent vasoconstrictor peptide produced by vascular endothelial cells. *Nature 332*:411–415.

Ziche, M., Morbidelli, L., Donnini, S., and Ledda, F. 1995. ETB receptors promote proliferation and migration of endothelial cells. *J. Cardiovasc. Pharmacol. 26 Suppl. 3:*S284–S286.

Zou, T.T., Selaru, F.M., Xu, Y., Shustova, V., Yin, J., Mori, Y., Shibata, D., Sato, F., Wang, S., Olaru, A., Deacu, E., Liu, T.C., Abraham, J.M., and Meltzer, S.J. 2002. Application of cDNA microarrays to generate a molecular taxonomy capable of distinguishing between colon cancer and normal colon. *Oncogene 21*:4855–4862.

This Page Intentionally Left Blank

15

Role of Fibroblastic Stroma in Colon Carcinoma

Nicolas Wernert

Introduction

When single cells were evolved into multicellular organisms, interactions with other cells and the surroundings were a basic requirement for the development and maintainance of ordered morphologic structures and their functions at the levels of tissues and organs. Mesodermal cells and the extracellular matrix still play a pivotal role during this cross-talk. Gastrulation, which leads to the formation of the mesoderm, has been a common feature of embryologic animal development until today. Studies in lower animals such as sponges, sea urchins, and cnidarians, have shown that collagen fibers, proteoglycans, and adhesion molecules, such as fibronectin, tenascin, or laminin, are remarkably conserved (Garronne *et al.*, 1993).

Dynamic interactions between stromal and epithelial cells affect fundamental cell functions such as adhesion, proliferation, differentiation, and migration not only in developing and mature tissues but also under many pathologic conditions such as wound healing and repair, inflammation, and tumor development and progression (Wernert, 1997). Remarkably, a small array of conserved signaling molecules, their receptors, and signal transduction pathways are used by different species during both normal development and pathologic processes.

The idea that tumor stroma may have an important impact on the biologic behavior of neoplasms is as old as the first histologic description of tumors (Dhom,

1994). However, for a long time only neoplastic cells were studied in cancer research, whereas the stroma was considered a reactive component without major significance. This view has now been abandoned. Today tumor stroma is considered to play an important role during tumorgenesis and metastasis. Tumor vascularization by stromal capillaries is necessary for continuous tumor growth (Carmeliet and Jain, 2000), and stromal fibroblasts participate in tumor invasion through the secretion of different proteases involved in the degradation of the extracellular matrix. Transcripts of the interstitial or type 1 collagenase, the two (M_r 72,000 and 92,000) type 4 collagenases, stromelysin 1 and 3 as well as of the serine protease urokinase-type plasminogen activator (uPA, which is implicated in the downstream activation of metalloproteinases), have been found within stromal fibroblasts of human carcinomas including skin, lung, breast, ovarian, and colon cancers (Wernert *et al.*, 1994; Wolf *et al.*, 1994). The activity of these proteases is tightly regulated at several levels.

These levels include the induction by different cytokines and growth factors (such as epidermal growth factor [EGF], basic fibroblast growth factor [bFGF], or tumor necrosis factor alpha [TNFα]), which can be expressed by neoplastic or stromal cells (Wernert, 1997) and the activation of secreted matrix metalloproteinases (MMP)-proenzymes by a proteolytic cleavage. At the same time inhibition occurs through several naturally occurring inhibitors such as TIMP1 and 2

Handbook of Immunohistochemistry and in situ Hybridization of Human Carcinomas,
Volume 2: Molecular Pathology, Colorectal Carcinoma, and Prostate Carcinoma

255

(tissue inhibitors of metalloproteinases) (Blavier *et al.*, 1999; Curran and Murray, 1999). An important level of regulation is transcription. Transcription factors known to be involved at this level are AP1 (Angel *et al.*, 1987; Nerlov *et al.*, 1991) and in particular ETs-1.

Invasion is of great importance in colon carcinoma, which represents one of the most common malignancies in industrialized nations. We found that conditioned medium of Colo 320 colon cancer cells induces the transcription of *ETs-1* in cultured human fibroblasts (Gilles *et al.*, 1996; Wernert *et al.*, 1994). Moreover, using a two-chamber cell culture system, we could show that the colon carcinoma cell line Caco 2 secrets ETs-1-inducing factors toward the stroma (Wardelmann *et al.*, 2003). In cultured human fibroblasts we found a correlation between the transcription of *ETs-1* and its target genes encoding collagenase 1, stromelysin 1, and uPA after stimulation by bFGF, platelet-derived growth factor (PDGF), or TNFα (Wernert *et al.*, 1994). Using ETs-1 -/- fibroblasts from an ETs-1 knock-out mouse (Bories *et al.*, 1995) we could finally prove the role of ETs-1 for transactivation of various proteases genes through transient ETs-1 expression (unpublished results).

Although most colon carcinomas are sporadic tumors, up to 5% occur as part of hereditary syndromes, such as familial adenomatous polyposis (FAP) and hereditary nonpolyposis colorectal cancer (HNPCC) syndrome (Lynch, 1999). Defects of mismatch repair (MMR) genes, such as *MSH2* and *MLH1*, have been found in recent years to be responsible for HNPCC (Aaltonen and Peltomaki, 1994; Bocker *et al.*, 1996). Compared to sporadic colorectal cancers, HNPCC tumors display several distinct features (e.g., less invasive and metastatic properties), which are linked to a more favorable prognosis (Bertario *et al.*, 1999). These less invasive and metastatic properties are observed despite the less-differentiated morphologic phenotype with a lower frequency of glandular differentiation in most HNPCC tumors compared to sporadic colorectal cancers. The reasons for these contradictory features of HNPCC tumors are unknown. High levels of MMP-1 expression have been associated with a poor prognosis in sporadic colorectal cancers (Murray *et al.*, 1996).

In the findings presented here we focus on the expression of ETs-1 and of several of its protease encoding target genes (Behrens *et al.*, 2003). We have investigated by *in situ* hybridization and immunohistochemistry the expression of these genes in the fibroblastic stroma of sporadic colorectal cancers and of HNPCC tumors. The goal was to study differences in the regulation of matrix degrading proteases in the stroma of HNPCC compared to sporadic tumors.

We analyzed resection specimens of 10 sporadic and 10 HNPCC carcinomas that had been sent to the Institute of Pathology, University of Bonn, for diagnostic purposes (Table 7). HNPCC cancers were presented with germline mutations of either *MLH1* or *MSH2* genes (Table 7). We also included 18 adenomas from non-HNPCC patients with low grade (n = 9) or high grade (n = 9) dysplasias. Microsatellite analysis in sporadic tumors was performed with a set of five markers (BAT25, BAT26, D2S123, D5S346, D17S250), according to Lamberti *et al.* (1999), using fluorescence-labeled primers and fragment analysis on an ABI 377 sequencer. In the 10 HNPCC tumors microsatellite instability and mutations have been determined previously (Lamberti *et al.*, 1999).

For *in situ* hybridization and immunohistochemistry we fixed specimens immediately in 4% paraformaldehyde (for 24 hr at 4°C) and embedded them routinely in paraffin. Sections were cut from paraffin blocks at 4 μm, mounted on positively charged slides (Superfrost), and air-dried overnight at 42°C. ^{35}S-labeled ETs-1 antisense and sense riboprobes (negative control) were synthesized by *in vitro* transcription from an 825 bp human ETs-1 complementary deoxyribonucleic acid (cDNA) template (nucleotide 260 to 1086) that had been cloned into a pSP64 plasmid vector (Wernert *et al.*, 1994).

We used monoclonal anti-human mouse antibodies for the detection of the MMR enzymes MSH2 and MLH1 (Pharmingen). Antibodies had been generated using the full-length recombinant protein. For the detection of ETs-1 protein, both a monoclonal mouse antibody (Dianova, against amino acids 122-288) and a polyclonal rabbit antiserum were used (Santa Cruz, against amino acids 422-441). Collagenases 1 (MMP-1) and IV (MMP-9) were demonstrated by monoclonal mouse antibodies (Chemicon, El Segundo, CA). For the evaluation of immunohistochemical results we used a semiquantitative scoring system (number of positive cells × staining intensity) to evaluate ETs-1 and MMP-1 and 9 expression. The number of positive cells was graded as negative (0), <10% (1), <50% (2), <80% (3), and >80% (4). The staining intensity was graded as negative (0), weak (1), medium (2), and strong (3). Three randomly chosen microscopic fields were semiquantitatively evaluated by two independent pathologists.

Generation of Radioactive Probes for *in situ* Hybridization

MATERIALS

1. Enzyme buffer: 10 mM Tris, 10 mM MgCl$_2$, 50 mM NaCl, and 0.1 mg/ml bovine serum albumin (BSA); adjust pH to 7.5 with HCl.
2. Enzymes: XHO I, PVU II.

Table 7 MSI and Mutations of MMR Genes *MLH1* and *MSH2* in 10 HNPCC and 10 Sporadic Colorectal Cancers

Age (Years)	Loci with MSI/Loci Investigated	Loss of MMR Protein	Germline Mutation
28	5/7	MSH2	MSH2; c.942 + 3a → t
44	4/6	MSH2	MSH2; c.1226delAG
53	2/2	MSH2	MSH2; c.187delG
48	4/5	MLH1	MLH1; c.1640 T→AL547X
44	NI	MLH1	MLH1; c.2T→A
23	7/10	MLH1	MLH1; c.184C→T,Q62X
38	5/6	MLH1	MLH1; c.791delATCG
52	4/6	MLH1	MLH1; c.1489insC
53	5/7	MLH1	MLH1; c.1622delC
41	NI	None	MLH1; c.1068-1075delTGGGGAGA
65	0/5	None	Sporadic carcinoma
63	0/5	None	Sporadic carcinoma
75	0/5	None	Sporadic carcinoma
79	0/5	None	Sporadic carcinoma
57	0/5	None	Sporadic carcinoma
68	0/5	None	Sporadic carcinoma
85	0/5	None	Sporadic carcinoma
38	0/5	None	Sporadic carcinoma
58	0/5	None	Sporadic carcinoma

HNPCC, hereditary nonpolyposis colorectal cancer; MMR, mismatch repair; MSI, microsatellite instability; NI, not investigated.

Int. J. Cancer (2003) (Copyright 2003 Wiley-Liss, Inc.).

3. 1% agarose: Dissolve 1 g of agarose powder in 100 ml of 1 × TAE buffer (see next step) by heating in a microwave.

4. 50 × TAE buffer: 242 g Tris, 57 ml of acetic acid, and 18.61 g of ethylenediaminetetraacetic acid (EDTA); adjust pH to 8.0.

5. 2 M NaAc: 164.06 g sodium acetate in millipore water, adjust pH to 5.2.

6. AUG mix: 5 µl 5 × transcription buffer, 2 µl dithiothreitol (DTT), 1 µl 10 mM adenosine triphosphate (ATP), 1 µl 10 mM uridine triphosphate (UTP), 1 µl of 10 mM guanosine triphosphate (GTP) (provided by PROMEGA).

7. 0.1 M DTT: 309 mg DTT and 20 µl of 0.2 M EDTA; bring vol to 20 ml DEPEC-treated water; adjust pH to 6.0.

8. 0.2 M EDTA: Dissolve 37.22 g of EDTA in 500 ml of DEPEC-treated water.

9. Transfer ribonucleic acid (tRNA) *Escherichia coli*: 5 mg tRNA in 100 ml of millipore water.

10. ^{35}S CTP (200 µCi).

11. Diluted SP6 polymerase: Dilute the polymerase with millipore water 1:1(v/v).

12. 10 mM Tris/10 mM NaCl/6 mM $MgCl_2$: 1.21 g Tris, 0.585 g NaCl, and 1.22 g $MgCl_2$; bring vol to 1 L with DEPEC-treated water; adjust pH to 7.9 with HCl.

13. 0.1 M sodium carbonate buffer: solution 1: dissolve 0.084 g of $NaHCO_3$ in 10 ml of DEPEC-treated water. Solution 2: dissolve 0.106 g of Na_2CO_3 in 10 ml of DEPEC-treated water; adjust pH of solution 2 to 10.2 by addition of solution 1.

14. 96% ethanol: 960 ml ethanol; bring vol to 1 L with millipore water.

15. 70% ethanol: 700 ml ethanol; bring vol to 1 L with millipore water.

16. 30% ethanol: 300 ml ethanol; bring vol to 1 L with millipore water.

17. 0.1 M glycine/0.2 M Tris: 0.75 g glycine and 0.25 g Tris; bring vol to 1 L with DEPEC-treated water; adjust pH to 7.4 with HCl.

18. Proteinase K buffer: 12 mg Tris and 18.6 mg of EDTA; bring vol to 1 L with millipore water, adjust pH to 8.0 with HCl.

19. Proteinase K: Prepare a solution of 1 µg proteinase K in 1 ml of proteinase K buffer.

20. Phosphate buffer saline (PBS): 100 mg anhydrous calcium chloride, 200 mg potassium chloride, 200 mg monobasic potassium phosphate, 100 mg magnesium chloride · $6H_2O$, 8 g sodium chloride, and 2.16 g dibasic sodium phosphate · $7H_2O$; bring vol to 1 L with deionized glass-distilled water; adjust pH to 7.4.

21. 4% paraformaldehyde: Dissolve 24 g para-formaldehyde in 600 ml PBS by heating to 70°C; adjust pH to 7.0 with 1 M NaOH.

22. 0.1 M triethanolamine buffer: 7.45 g triethanolamine; bring vol to 500 ml with millipore water; adjust pH to 8.0 with HCl.

23. 0.1 M triethanolamine buffer (pH 8.0)/0.25% acetic acid anhydrid: Mix 625 µl of 0.25% acetic acid anhydrid with 250 ml 0.1 M triethanolamine buffer, pH 8.0.

24. 1 M Tris HCl (pH 8.0): 121.14 g Tris; bring vol to 1 L with DEPEC-treated water; adjust pH to 8.0 with HCl.

25. 0.5 M EDTA: 93.5 g EDTA; bring vol to 500 ml with DEPEC-treated water.

26. 50% dextran sulfate (sodium salt): Dissolve 25 g dextran sulfate in 25 ml DEPEC-treated water; heat the suspension to 80°C and vortex gently; centrifuge at 3000 rpm and add again 25 ml of DEPEC-treated water. Store in 1 ml aliquots at −20°C.

27. $50 \times$ Denhardt's solution: 0.1 g Ficoll 400, 0.1 g polyvinylpyrolidon, and 0.1 g BSA; bring volume to 10 ml with millipore water. Store in 1 ml aliquots at −20°C.

28. Hybridization cocktail: 702 mg NaCl, 20 mg tRNA *E. coli*, 616.8 mg DTT, 800 µl 1 M Tris HCl pH 8, 400 µl 0.5 M EDTA, 8 ml 50% dextran sulfate (sodium salt), and 800 µl $50 \times$ Denhardt's solution; bring vol to 16 ml with 2 ml millipore water.

29. Deionized formamide: Mix 100 ml formamide with 5 mg resin for 12 hr; filtrate the solution and store at −20°C.

30. $20 \times$ saline-sodium citrate (SSC) buffer: 175.3 g NaCl and 88.2 g tri-sodium-citrate; bring volume to 1 L with DEPEC-treated water.

31. DEPEC-treated water: Mix 10 ml diethylpyrocarbonate with 1 L aqua bidest for 1 hr under stirring; autoclave the solution.

32. $2 \times$ SSC buffer: Add 10 ml $20 \times$ SSC to 90 ml of DEPEC-treated water.

33. $4 \times$ SSC buffer/10 mM DTT: Dissolve 0.31 g of DTT in 40 ml $20 \times$ SSC; add 160 ml of DEPEC-treated water.

34. Washing buffer: Dissolve 17.6 g NaCl in 40 ml 1 M Tris-HCl (pH 8.0) and 20 ml 0.5 M EDTA; bring volume to 1 L with millipore water.

35. $10 \times$ RNAse buffer: Dissolve 233.8 g of NaCl in 100 ml of 1 M Tris-HCl (pH 7.5) and 100 ml of 0.5 M EDTA; bring volume to 1 L with millipore water.

36. RNAse-A: Prepare a solution of 1 µg RNAse-A in 1 ml $1 \times$ RNAse buffer.

37. Dye-Solution Hoechst 33258: Dissolve 1 mg of Hoechst 33258 in 250 ml of PBS.

38. Photoemulsion NTB2 (Kodak), store at 4°C.

METHODS

Restriction

1. Prepare the following mixture for plasmid restriction:

       10 µg nonlinearized plasmid.

       4 µl $10 \times$ enzyme buffer.

       3 µl enzyme.

       Add millipore H_2O to a final volume of 10 µl.

2. Incubate the plasmid restriction for 1 hr 30 min at 37°C.

3. Run the sample in a 1% agarose gel to verify restriction.

4. If restriction was not successful add new enzyme aliquot to the tube.

5. Store cut plasmid at −70°C.

6. Thaw the frozen plasmid in waterbath at 37°C before use.

Plasmid Precipitation

1. Add 15 µl of 2 M NaAc (pH 5.2) and 100 µl of ice-cold 100% EtOH to the plasmid sample prepared as described in **Step 1**.

2. Centrifuge the sample at 13,000 rpm for 30 min.

3. Discard the supernatant and resuspend the pellet in 45 µl of millipore H_2O.

Synthesis of Probe

1. Mix in a siliconized tube as follows:

       10 µl AUG mix.

       1 µl RNAsin.

       1 µl tRNA *E. coli* (conc.: 5 mg/ml).

       9 µl plasmid (containing 2 µg DNA).

       3 µl ^{35}S CTP (200 µCi).

       1 µl diluted SP6 polymerase.

2. Incubate the mixture for 1 hr 30 min in a waterbath at 37–39°C.

3. Add 1 µl polymerase and incubate for 1 hr in a waterbath at 39°C.

4. After addition of 175 µl 10 mM Tris (pH 7.9)/10 mM NaCl/6 mM $MgCl_2$ and 5 µl DNAse RQ1, incubate the reaction for 30 min in a waterbath at 39°C.

5. Vortex and centrifugate at 5000 rpm for 2 min.

6. Place the upper phase (aquaous phase) in a new siliconized tube.

7. Add 100 µl millipore H_2O to the lower phase (organic phase); mix and centrifuge at 5000 rpm for 2 min.

8. Add the new upper phase to the old upper phase and discard the lower phase.

9. Mix the combined upper phases with 20 µl tRNA, 40 µl 1 M DTT, 40 µl 2 M NaAc (pH 5.2), and 950 µl 100% EtOH; work on ice.

10. Precipitate the plasmid by incubation for 20 min at −70°C

11. Centrifugate the probe at 8000–10000 rpm for 30 min.

12. Discard the supernatant.

13. Resuspend the pellet in 67 µl 0.1 M sodium phosphate buffer (pH 10.2) (chilled at −20°C) and add 7 µl 1 M DTT.

Reduction of Probe Length

1. If probe length is below 300 bp, a reduction is not necessary; simply add 10 µl tRNA, 5 µl DTT, and 35 µl millipore H_2O.

2. Calculation of incubation time:

original length (ol) = length of probe before reduction
final length (fl) = length of probe after reduction
$$k = 0.11 \text{ kb/min}$$
$$\frac{\text{ol} - \text{fl}}{K \times \text{ol} \times \text{fl}} = \text{incubation time}$$

3. Perform the incubation at 60°C for the calculated time.

4. Add 7 µl 2 M NaAc (pH 5.2) and 8 µl 5% acetic acid.

Purification of Probe with Quick Spin Columns (Qiagen)

1. Work according to the manufacturer's protocol.

2. Mix the column overhead.

3. Empty the column, remove buffer, and keep the column upright.

4. Put the column in a collection tube, and put this tube in a 1.5 ml centrifugation tube.

5. Centrifugate at 3000 rpm for 5 min in a swing-out rotor.

6. Discard the collection tube together with the buffer.

7. Place a new collection tube under the column.

8. Add 30 µl millipore H_2O and 100 µl RNA-probe centrally onto the column.

9. Centrifugate at 3000 rpm for 5 min in a swing-out rotor.

10. Place cleaned probe in a new siliconized tube.

11. Activity input can be checked.

12. Add 20 µl tRNA, 15 µl 2 M NaAc (pH 5.2), 15 µl 1 M DTT, and 325 µl ethanol to the probe.

13. Incubate the mixture for 20–60 min at −20°C.

14. Centrifuge the probe at 10,000 rpm for 30 min.

15. Discard the supernatant and dry the pellet for 5 min.

16. Resuspend the pellet in 5 µl 1 M DTT, 10 µl tRNA, and 35 µl millipore H_2O.

17. Store the resuspended RNA −70°C until use.

In situ Hybridization of Paraffin Sections with Radiolabeled Probes

1. Cut sections at 4 µm, mount them on positively charged slides, and air-dry them in an incubator at 42°C overnight.

2. Incubate sections twice in toluene for 10 min.

3. Incubate sections in 100% ethanol for 5 min.

4. Incubate sections in 96% ethanol for 5 min.

5. Incubate sections in 70% ethanol for 5 min.

6. Incubate sections in 30% ethanol for 5 min.

7. Incubate sections twice in millipore H_2O for 5 min.

8. Incubate sections in 0.1 M glycine/0.2 M Tris-HCl (pH 7.4) for 10 min.

9. Incubate sections in proteinase K buffer for 5 min.

10. Add 1 µg/ml proteinase K into the proteinase K buffer and incubate the sections at 37°C for 15 min.

11. Rinse sections in millipore H_2O.

12. Incubate sections in PBS containing 4% paraformaldehyde and 5 mM $MgCl_2$ for 15 min.

13. Rinse the sections in PBS for 5 min.

Acetylation

1. Incubate sections in 0.1 M triethanolamine buffer (pH 8.0) under shaking for 10 min.

2. Incubate sections in 0.1 M triethanolamine buffer (pH 8.0)/0.25% acetic acid anhydride under shaking for 10 min.

3. Rinse sections with $2 \times$ SSC.

4. Incubate sections twice in millipore H_2O for 5 min.

Dehydration

1. Incubate sections in 30% ethanol for 5 min.

2. Incubate sections in 70% ethanol for 5 min.

3. Incubate sections in 97% ethanol for 5 min.

4. Incubate sections in 100% ethanol for 5 min.

5. Dry sections for 20 min.

Hybridization

1. Thaw an aliquot of the hybridization cocktail, which had been frozen at −70°C.

2. The volume of hybridization mixture needed depends on the size of the section (the same holds true for the size of the gel-bond membrane needed for covering of the sections). Calculate as follows:

(Size)
Section 11 × 11 mm: 15 µl.
Section 18 × 18 mm: 18 µl.
Section 22 × 22 mm: 30 µl.
Section 22 × 40 mm: 50 µl.

3. Calculate the total volume of solution needed for all probes (number of sections × volume = total volume of probe solution) as follows:

5/10 deionized formamide.
4/10 hybridization cocktail.
1/10 radiolabeled probe; final concentration: 20,000 cpm/µl (measure at the counter).

Note: Usually probes are so hot that the needed activity is present in a smaller volume (not 1/10 of the probe solution).

4. Denaturate the prepared solution from **Step 3** by heating to 80°C for 2 min. Place the probe immediately on ice until use.

5. Prepare a humid chamber by mixing 40 ml 100% formamide (not deionized), 16 ml 20 × SSC buffer, and 24 ml millipore H_2O.

6. Clean the desk with 70% ethanol and place slides on the desk.

7. Separate the sense/antisense areas on the slide by an isolation band.

8. Cover the sections with the probe solution.

9. Cover the sections with the hydrophobic half of a gel-bond membrane.

10. Put the sections into the humid chamber at 60°C for 16 hr.

Washing

1. Incubate the samples four times with 4 × SSC (containing 10 mM DTT) for 20 min.

2. Incubate the samples in a mix of 50 ml washing buffer, 50 ml deionized formamide, and 1.54 g DTT at 62°C for 30 min.

3. Incubate the samples twice in RNAse buffer at 37°C for 10 min.

RNAse A Digest

1. Dissolve 2 ml RNAse A in 98 ml 1 × RNAse buffer.
2. Incubate sections at 37°C for 30–60 min.

3. Incubate sections in RNAse buffer at 37°C for 5 min.

4. Incubate sections in 2 × SSC buffer at 60°C for 15 min.

5. Incubate sections in 0.1 × SSC buffer at 60°C for 15 min.

6. Incubate sections in 30% ethanol for 5 min.

7. Incubate sections in 70% ethanol for 5 min.

8. Incubate sections in 97% ethanol for 5 min.

9. Incubate sections in 100% ethanol for 5 min.

10. Dry the sections for 5 min.

Autoradiography (Without Light)

1. Bring the photoemulsion NTB2 to room temperature before use.

2. Incubate the photoemulsion for 30 min in a waterbath at 45°C.

3. Prepare an ice box for the slides; be careful with melting ice; cover the ice box with tin foil.

4. Dip slides into the photoemulsion and put them on the ice box.

5. Dry slides for 1 hr.

6. Place slides in an empty box; store overnight at room temperature.

7. Put slides in an empty slide box together with silica gel with moisture indicator (blue gel, for drying) in a small package.

8. Store slides at 4°C and expose them for 10–15 days.

Develop (Without Light)

1. Incubate slides for 30 min at room temperature.

2. Develop slides with Kodak developing reagent for 150 seconds.

3. Wash slides with water for 30 seconds.

4. Fix slides with Kodak fixation reagent for 10 min.

5. Wash slides with water for 10 min.

6. Incubate sections for 5 min in Hoechst 33258.

7. Incubate sections for 10 min in PBS.

8. Cover slides with mounting medium.

9. Visualize positive signals by dark-field illumination of the slides.

Immunohistochemistry

MATERIALS

1. Tris buffer.
2. 10 mM sodium citrate buffer (pH 6.0).
3. 1% hydrogen peroxide diluted in methanol.

4. PBS: 100 mg anhydrous calcium chloride, 200 mg potassium chloride, 200 mg monobasic potassium phosphate, 100 mg magnesium chloride $\times$ 6 H_2O, 8 g sodium chloride, and 2.16 g dibasic sodium phosphate $\times$ 7 H_2O; bring vol to 1 L with deionized glass-distilled water, (pH 7.4).

5. Blocking solution: 5% (w/v) nonfat dry milk and 2% (v/v) normal rabbit serum in PBS.

6. PBS with 0.1% (v/v) Triton X-100.

METHOD

1. Deparaffinize fresh paraffin sections in xylene, rehydrate in graded alcohols, and wash in Tris buffer prior to immunohistochemistry.

2. Use heat-induced epitope retrieval (600-W microwave treatment for 2 $\times$ 15 min in prewarmed 10 mM sodium citrate buffer (pH 6.0) prior to MSH2- and MLH1-staining (heat-induced epitope retrieval—400 W microwave treatment for 8 min—was used prior to staining of both MMP-1 and MMP-9).

3. Add primary antibodies (dilution: MSH2 1:50, MLH1 1:75, both ETs-1 antibodies 1:500, and both MMP-1 and MMP-9 antibodies 1:25) and incubate slides overnight at 4°C.

4. Incubate slides 30 min at room temperature in 1% hydrogen peroxide diluted in methanol to block endogenous peroxidase activity.

5. Wash slides in PBS.

6. Incubate slides for 30 min at room temperature in blocking solution (PBS with 5% nonfat dry milk and 2% normal rabbit serum) and apply avidin/biotin blocking kit for 2 $\times$ 15 min (Vector Laboratories, Inc., Burlingame, CA).

7. Remove solution from the slides using a filter paper. Then add primary antibodies and incubate slides overnight at 4°C.

8. Wash slides with PBS and PBS containing 0.1% Triton X-100.

9. Detect bound antibodies using the ABC method (Dako) with 3-amino-9-ethylcarbazole (AEC) as a visualizing reagent.

10. Counterstain sections slightly with hematoxylin, mount slides in aqueous mounting media, and analyze by standard light microscopy.

11. Use replacement of the first antibody with PBS as a negative control to assess specificity of antibodies. Staining of adjacent normal colon mucosa, stromal cells and/or lymphocytes, serves as internal positive control for the detection of the MMR enzymes MSH2 and MLH1.

RESULTS AND DISCUSSION

Sporadic colorectal carcinomas and HNPCC differ in their biologic behavior, with patients with HNPCC presenting generally with fewer metastases at time of diagnosis (Bertario *et al.*, 1999). These differences remain unexplained in view of the generally poorer differentiation of HNPCC tumors compared to sporadic carcinomas. A possible explanation is an immunologic response of cytotoxic T-lymphocytes against the neoplastic cells of HNPCC (Dolcetti *et al.*, 1999). Another mechanism may be the participation of stromal fibroblasts in tumor invasion via the production of matrix degrading proteases (Wernert, 1997). We therefore examined expression of ETs-1 and its target genes MMP-1 and MMP-9 in sporadic and HNPCC tumors.

Table 7 shows the age of the 20 patients and microsatellite instability (MSI) and mutations of MMR genes *MLH1* and *MSH2* in the 10 HNPCC tumors.

None of the sporadic cancers had a family history suggestive of HNPCC. The tumors had developed in the descending and sigmoid colon and rectum and exhibited moderate to poor differentiation. Seven of the 10 cases were pT3 tumors, and lymph node metastases were found in seven cases. Liver metastases were present in one case. None of the sporadic cancers showed MSI or lack of MLH1 or MSH2 proteins.

We compared expression of ETs-1, MMP-1, and MMP-9 in normal colon mucosa, adenomas with different degrees of dysplasias, and sporadic colorectal cancers (Table 8). The medium score values of the cases are given in brackets. We found no or only weak signals for either ETs-1 [1,2] or MMP-1 [1,2] and MMP-9 [1] in stromal cells and capillary endothelia of normal mucosa (Figure 40 A–C). In contrast, in adenomas 20–30% of stromal fibroblasts and capillaries expressed ETs-1 messenger ribonucleic acid (mRNA) and ETs-1 protein [3,2] as well as MMP-1 [3,4] and -9 [3] (Figure 40 D–F). ETs-1 protein was expressed both in the cytoplasm and in the nucleus. No relation was evident between the degree of dysplasia in the adenomas and expression of ETs-1, MMP-1, or -9. We noted further significant up-regulation of ETs-1 transcripts, ETs-1 protein [9,2], and both MMP-1 [8,6] and MMP-9 [8,8] in the stroma of sporadic cancers. About 70–80% of fibroblasts and endothelial cells were positive (Figure 41 A–C).

The 10 HNPCC tumors were located in the cecum, the ascending colon, and the rectum and exhibited moderate to poor differentiation. The average age of the patients was 42 years. Five cases were pT3 tumors. Lymph node metastases were present in three cases; distant metastases occurred in one. Microsatellite instability was demonstrated in all cases tested. Table 7 shows the detailed germline mutations in *MLH1* and *MSH2* genes. MLH-1 protein was absent in 7 of 10 cases, and MSH-2 was absent in 3 of 10 cases. HNPCC tumors exhibited a significantly lower expression of both ETs-1 (average score 4,4) and MMP-1 [4] and

Table 8 Semiquantitative Immunohistochemical Evaluation of ETs-1, MMP-1, and MMP-9 Expression in Normal Colonic Mucosa, Adenomas, HNPCC, and Sporadic Colorectal Carcinomas[a]

		ETs-1	MMP-1	MMP-9
Normal	1	1 × 1	1 × 1	1 × 1
	2	1 × 1	1 × 1	1 × 1
	3	1 × 1	2 × 1	1 × 1
	4	1 × 2	1 × 1	1 × 1
	5	1 × 1	1 × 1	1
	Average	1,2	1,2	1
Adenoma	1	1 × 1	2 × 2	2 × 1
	2	3 × 2	2 × 2	2 × 2
	3	2 × 2	2 × 2	2 × 2
	4	1 × 2	2 × 1	2 × 2
	5	2 × 1	2 × 1	2 × 1
	6	2 × 1	2 × 2	1 × 2
	7	2 × 2	3 × 2	2 × 2
	8	3 × 2	3 × 2	3 × 2
	9	1 × 1	2 × 1	1 × 2
	10	2 × 1	2 × 1	2 × 1
	11	2 × 1	1 × 2	1 × 2
	12	2 × 2	2 × 2	2 × 2
	13	2 × 1	2 × 2	2 × 1
	14	2 × 2	2 × 2	2 × 1
	15	2 × 2	1 × 2	2 × 2
	16	3 × 2	3 × 2	2 × 2
	17	3 × 1	2 × 1	2 × 1
	18	2 × 1	1 × 2	2 × 1
	Average	3,2	3,4	3
Sporadic	1	3 × 3	3 × 2	4 × 3
	2	4 × 2	4 × 2	3 × 2
	3	3 × 3	4 × 3	4 × 3
	4	4 × 3	4 × 2	4 × 3
	5	4 × 3	4 × 3	3 × 3
	6	3 × 2	3 × 2	4 × 2
	7	3 × 3	3 × 3	3 × 2
	8	3 × 3	3 × 3	4 × 2
	9	4 × 3	4 × 2	3 × 3
	10	2 × 3	3 × 3	3 × 2
	Average	9,2	8,6	8,8
HNPCC	1	2 × 1	2 × 2	2 × 1
	2	2 × 1	2 × 1	2 × 1
	3	2 × 2	2 × 2	2 × 2
	4	3 × 2	2 × 2	3 × 2
	5	3 × 2	3 × 2	3 × 2
	6	3 × 2	3 × 2	2 × 2
	7	3 × 2	2 × 2	2 × 2
	8	2 × 2	2 × 1	2 × 1
	9	2 × 2	3 × 2	3 × 2
	10	2 × 2	2 × 1	3 × 2
	Average	4,4	4	4,2

HNPCC, hereditary nonpolyposis colorectal cancer.

[a]The immunohistochemical staining scores (percentage of stained cells × staining intensity) for ETs-1 protein and matrix degrading proteases (MMP-1 and MMP-9) are given for each case after semiquantitative evaluation by two independent observers. The following scores have been used: Percentage of stained cells: 0, <10% (1), <50% (2), <80% (3), >80% (4). Staining intensity: negative (0), weak (1), medium (2), strong (3).

Int. J. Cancer (2003) (Copyright 2003 Wiley-Liss, Inc.).

MMP-9 [4,2] in the stroma compared to invasive sporadic carcinomas. We found highest expression in small vessel endothelia and lymphocytes. In contrast, positive reactions were only partly located in stromal fibroblasts (Figure 41 D–F).

Both MMP-1 and MMP-9, investigated in the present study and other proteases known to be involved in matrix degradation (such as uPA and stromelysin 1), have been found to be mainly expressed in the fibroblastic stroma of sporadic colorectal cancers and to be transcriptionally regulated by ETs-1 (Otani *et al.*, 1994; Pyke *et al.*, 1993). We have previously reported that uPA-1 collagenase 1, and stromelysin 1 are topographically co-expressed with ETs-1 in the stroma of colon carcinomas (Wernert *et al.*, 1994). In the present study, we additionally found that ETs-1 and its target genes *MMP-1* and *MMR-9* are up-regulated during the adenoma–carcinoma sequence. Significantly lower levels of ETs-1 transcripts, ETs-1 protein, and MMP-1 and MMR-9 were seen in the stromal fibroblasts of HNPCC carcinomas. In previous studies we have shown that ETs-1 is involved in the transcriptional regulation during tumor vascularization (Wernert *et al.*, 1992; Wernert *et al.*, 1994; Wernert *et al.*, 1999). In line with these findings, in the present study no ETs-1 expression was found in capillary endothelial cells of normal colon mucosa. However up-regulation occurred in adenomas and maximal expression in the stromal capillaries of both invasive sporadic and HNPCC tumors. As in stromal fibroblasts, ETs-1 expression in endothelial cells correlated with that of MMP-1 and MMP-9, proteases known to be involved in matrix remodeling during early steps of angiogenesis (Wernert, 1997). No differences of ETs-1 expression in stromal capillaries were evident comparing sporadic with HNPCC tumors. Therefore, ETs-1 probably promotes both invasion and vascularization of sporadic colorectal cancers. In HNPCC tumors, which express significantly lower levels of ETs-1 and MMP-1 and MMR-9 in their fibroblastic stroma, ETs-1 seems to be more important for angiogenesis. In line with this assumption, MMP-1 expression has been found to be related to poor prognosis of sporadic colon cancer, and tumor progression is reduced by inhibitors of metalloproteinases (Murray *et al.*, 1996; Schmitt *et al.*, 1992). Thus, the lower invasive and metastatic potential of HNPCC tumors compared to sporadic colorectal cancers could in part be the result of a difference in matrix degradation by fibroblasts in HNPCC carcinomas. The present results in colon carcinomas are in line with our previously published findings relating expression of ETs-1 and several proteases to invasion in other human tumors, such as lung and breast cancers (Behrens *et al.*, 2001a; Behrens *et al.*, 2001b; Wernert *et al.*, 1994).
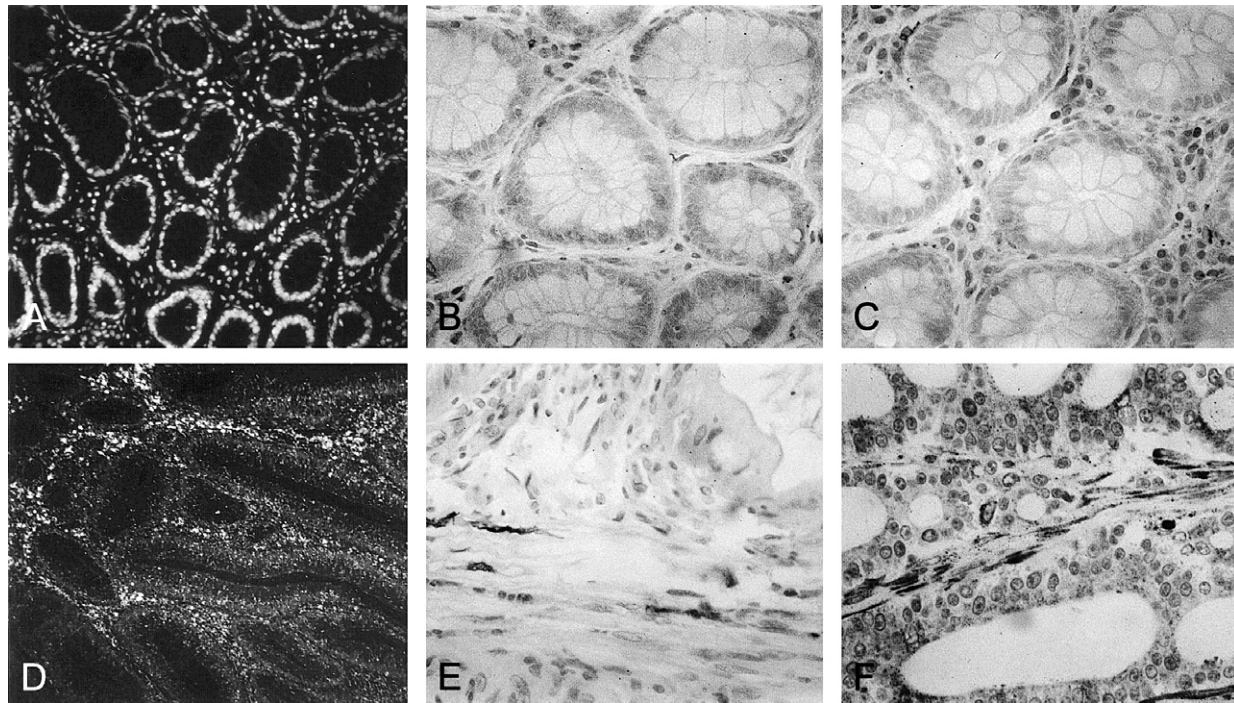
Figure 40 **Expression of ETs-1 and of MMPs-1 and 9 in normal colon mucosa and colorectal adenomas.** Neither ETs-1 messenger ribonucleic acid (**A**) nor ETs-1 (**B**) or MMP-1 protein (**C**) are found in normal colon mucosa (**A**, *in-situ* hybridization, **B** and **C**, immunohistochemistry). In contrast, expression of ETs-1 (**D** and **E**) and of MMP-9 (**F**) is demonstrated in stromal fibroblasts of colorectal adenomas by *in situ* hybridization (**D**) and immunohistochemistry (**E** and **F**). **A** and **D** illustrate dark-field illuminations of the slides after fluorescent counterstaining of the nuclei with Hoechst 33258. Magnification, 200X (**A** and **D**) and 400X (**B**, **C**, **E**, and **F**). (*Int. J. Cancer,* 2003.) (Copyright 2003 Wiley-Liss, Inc.).

Although stroma is today considered a reactive component that is induced by tumor cell–derived growth factors such as VEGF (vascular endothelial growth factor), acidic fibroblast growth factor, and bFGF or PDGF (Wernert, 1997), the neoplastic nature of stromal fibroblasts was a matter of discussion in the early days of histology (Dhom, 1994). Recent findings show that *in vitro* transitions of epithelial tumor cells into fibroblast-like cells can be actually induced through interference with adhesion molecules, signaling via tyrosine kinases, oncogene expression, or stimulation by growth factors (Birchmeier *et al*., 1996; Boyer *et al*., 1997). These two results suggest that tumor cell–mesenchyme transitions might contribute to stroma generation also *in vivo*. During embryonic development, interconversions between organ parenchyma and mesenchymal cells are frequent (Hay, 1995; Sun *et al*., 1998; Viebahn, 1995). In view of this debate we have decided in a previous study to investigate by laser-assisted microdissection whether frequent genetic alterations of invasive human colon and breast carcinomas (loss of heterozygosity, MSI, and *Tp53* mutations) are restricted to the tumor cells or also occur within the adjacent fibroblastic stroma and whether both components share clonal features (Wernert *et al*., 2001). In 20 nonhereditary colon cancers we found both loss of heterozygosity (LOH) (14 tumors) and MSI (3 tumors); LOH alone was present in breast carcinomas (12 of 15 tumors). Separate evaluation of microdissected tumor and adjacent stromal areas revealed that allelic losses were not restricted to the neoplastic epithelial cells but also occurred in the fibroblastic stroma. To evaluate whether tumor and adjacent stromal areas share clonal features, we analyzed the allelic site in cases with LOH in both components. In several colon and breast carcinomas LOH involved the same alleles. In one colon carcinoma, MSI (at D 18S60) was present within the tumor and adjacent fibroblastic stromal area with an identical banding pattern. Among the 20 colon cancers, seven mutations of *TP53* exons 5 and 8 were identified. Four involved malignant epithelium and three microdissected fibroblastic stroma. Theoretically, allelic losses and mutations of tumor suppressor genes could contribute to hyperplasia of the fibroblastic stroma in breast and colon carcinomas and thereby enhance its invasion-promoting properties. The ways in which these genetic changes come about, however,
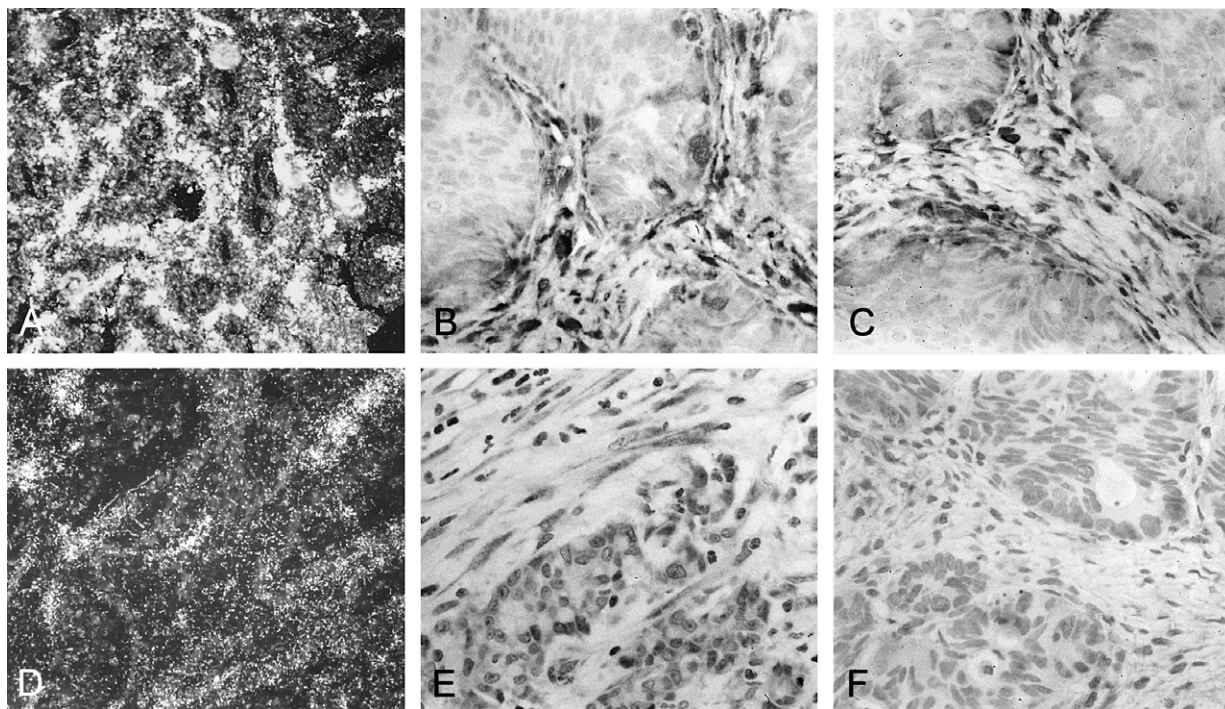
Figure 41 **Expression of ETs-1 and of MMP-1 in the stroma of hereditary nonpolyposis colorectal cancer (HNPCC) and sporadic colorectal cancers.** ETs-1 transcripts **(A)**, ETs-1 protein **(B),** and MMP-1 **(C)** are strongly expressed within stromal fibroblasts of a sporadic colorectal carcinoma. In contrast, expression of ETs-1 messenger ribonucleic acid **(D),** ETs-1 protein, **(E)** and MMP-1 **(F)** is significantly lower in HNPCC. **A** and **D** illustrate dark-field illuminations of the slides after *in situ* hybridization and fluorescent counterstaining of the nuclei with Hoechst 33258. Magnification, 200X (**A** and **D**) and 400X (**B**, **C**, **E**, and **F**). (*Int. J. Cancer,* 2003.) (Copyright 2003 Wiley-Liss, Inc.).

could be different. Carcinogen-induced genetic alterations might affect not only epithelial cells but also the adjacent stromal cells. Genetic alterations could accumulate in the stroma during long-lasting growth stimulation by tumor-cell–derived growth factors. Finally, neoplastic epithelial cells might actually differentiate into mesenchymal fibroblastic cell types, as has been shown *in vitro* (Bellusci *et al*., 1994; Boyer *et al*., 1997). Loss of the same alleles at different loci within both tumor and adjacent fibroblastic stromal areas of several tumors investigated in our study would be in line with clonality of tumor and stroma and support this possibility. Further work along the line of this study could help to better understand the relationship between tumor and stroma in invasive colon carcinomas.

References

Aaltonen, L.A., and Peltomaki, P. 1994. Genes involved in hereditary nonpolyposis colorectal carcinoma. *Anticancer Res. 14*:1657–1660.

Angel, P., Baumann, I., Stein, B., Delius, H., Rahmsdorf, H.J., and Herrlich, P. 1987. 12-*0*-Tetradecanoyl-phorbol-13-acetate induction of the human collagenase gene is mediated by an inducible enhancer element located in the 5′ flanking region. *Mol. Cell Biol. 7*:2256–2266.

Behrens, P., Mathiak, M., Mangold, E., Kirdorf, S., Wellmann, A., Fogt, F., Rothe, M., Florin, A., and Wernert, N. 2003. Stromal expression of invasion-promoting, matrix-degrading proteases MMP-1 and -9 and the ETs 1 transcription factor in HNPCC carcinomas and sporadic colorectal cancers. *Int. J. Cancer 107*:183–188.

Behrens, P., Rothe, M., Florin, A., Wellmann, A., and Wernert, N. 2001a. Invasive properties of serous human epithelial ovarian tumors are related to ETs-1, MMP-1 and MMP-9 expression. *Int. J. Mol. Med. 8*:149–154.

Behrens, P., Rothe, M., Wellmann, A., Krischler, J., and Wernert, N. 2001b. The ETs-1 transcription factor is up-regulated together with MMP 1 and MMP 9 in the stroma of pre-invasive breast cancer. *J. Pathol. 194*:45–50.

Bellusci, S., Moen, G., Gaudino, G., Comoglio, P., Nakamura, T., Thiery, J.P., and Jouanneau, J. 1994. Creation of an hepatocyte growth factor/scatter factor autocrine loop in carcinoma cells induces invasive properties associated with increased tumorigenicity. *Oncogene 9*:1091–1099.

Bertario, L., Russo, A., Sala, P., Eboli, M., Radice, P., Presciuttini, S., Andreola, S., Rodriguez-Bigas, M.A., Pizzetti, P., and Spinelli, P.

1999. Survival of patients with hereditary colorectal cancer: Comparison of HNPCC and colorectal cancer in FAP patients with sporadic colorectal cancer. *Int. J. Cancer 80*: 183–187.

Birchmeier, C., Birchmeier, W., and Brand-Saberi, B. 1996. Epithelial-mesenchymal transitions in cancer progression. *Acta Anat. (Basel) 156*:217–226.

Blavier, L., Henriet, P., Imren, S., and Declerck, Y. 1999. Tissue inhibitors of matrix metalloproteinases in cancer. *Ann. N. Y. Acad. Sci. 878*:108–119.

Bocker, T., Schlegel, J., Kullmann, F., Stumm, G., Zirngibl, H., Epplen, J.T., and Ruschoff, J. 1996. Genomic instability in colorectal carcinomas: Comparison of different evaluation methods and their biological significance. *J. Pathol. 179*: 15–19.

Bories, J.C., Willerford, D.M., Grevin, D., Davidson, L., Camus, A., Martin, P., Stehelin, D., and Alt, F.W. 1995. Increased T-cell apoptosis and terminal B-cell differentiation induced by inactivation of the ETs-1 proto-oncogene. *Nature 377*:635–638.

Boyer, B., Roche, S., Denoyelle, M., and Thiery, J.P. 1997. Src and Ras are involved in separate pathways in epithelial cell scattering. *EMBO. J. 16*:5904–5913.

Carmeliet, P., and Jain, R.K. 2000. Angiogenesis in cancer and other diseases. *Nature 407*:249–257.

Curran, S., and Murray, G. 1999. Matrix metalloproteinases in tumour invasion and metastasis. *J. Pathol. 189*:300–308.

Dhom, G. 1994. Die Krebszelle und das Bindegewebe. *Pathologe 15*:271–278.

Dolcetti, R., Viel, A., Doglioni, C., Russo, A., Guidoboni, M., Capozzi, E., Vecchiato, N., Macri, E., Fornasarig, M., and Boiocchi, M. 1999. High prevalence of activated intraepithelial cytotoxic T lymphocytes and increased neoplastic cells apoptosis in colorectal carcinomas with microsatellite instability. *Am. J. Pathol. 154*:1805–1813.

Garronne, R., Exposito, J., Franc, J., Franc, S., Humbert-David, N., Qint, L., and Tillet, E. 1993. La phylogenese de la matrice extracellulaire. *C. R. Seances Soc. Biol. Fil. 187*:114–123.

Gilles, F., Raes, M.B., Stéhelin, D., Vandenbunder, B., and Fafeur, V. 1996. The c-ETs-1 proto-oncogene is a new early response gene differentially regulated by cytokines and growth factors in human fibroblasts. *Exp. Cell Res. 222*:370–378.

Hay, E.D. 1995. An overview of epithelio-mesenchymal transformation. *Acta Anat. Basel 154*:8–20.

Lamberti, C., Kruse, R., Ruelfs, C., Caspari, R., Wang, Y., Jungck, M., Mathiak, M., Malayeri, H.R.H., Friedl, W., Sauerbruch, T., and Propping, P. 1999. Microsatellite instability—a useful diagnostic tool to select patients at high risk for hereditary non-polyposis colorectal cancer: A study in different groups of patients with colorectal cancer. *Gut 44*:839–843.

Lynch, H. 1999. Hereditary nonpolyposis colorectal cancer (HNPCC). *Cytogenet. Cell Genet. 86*:130–135.

Murray, G., Duncan, M., O'Neil, P., Melvin, W.T., and Fothergill, J.E. 1996. Matrix metalloproteinase-1 is associated with poor prognosis in colorectal cancer. *Nat. Med. 2*:461–462.

Nerlov, C., Rorth, P., Blasi, F., and Johnsen, M. 1991. Essential AP-1 and PEA3 binding elements in the human urokinase enhancer display cell type-specific activity. *Oncogene 6*:1583–1592.

Otani, Y., Okazaki, I., Arai, M., Kameyama, K., Wada, N., Maruyama, K., Yoshino, K., Kitajima, M., Hosoda, Y., and Tsuchiya, M. 1994. Gene expression of interstitial collagenase (matrix metalloproteinase 1) in gastrointestinal tract cancers. *J. Gastroenterol. 29*:391–397.

Pyke, C., Ralfkiær, E., Tryggvason, K., and Danø, K. 1993. Messenger RNA for two type IV collagenases is located in stromal cells in human colon cancer. *Am. J. Pathol. 142*:359–365.

Schmitt, M., Janicke, F., Moniwa, N., Chucholowski, N., Pache, L., and Graeff, H. 1992. Tumor-associated urokinase-type plasminogen activator: Biological and clinical significance. *Biol. Chem. Hoppe. Seyler 373*:611–622.

Sun, D., Mcalmon, K.R., Davies, J.A., Bernfield, M., and Hay, E.D. 1998. Simultaneous loss of expression of syndecan-1 and E-cadherin in the embryonic palate during epithelial-mesenchymal transformation. *Int. J. Dev. Biol. 42*:733–736.

Viebahn, C. 1995. Epithelio-mesenchymal transformation during formation of the mesoderm in the mammalian embryo. *Source 154*:79–97.

Wardelmann, E., Kiriakidis, S., Dreschers, S., Behrens, P., Heim, I., Krischler, J., Pfeifer, U., and Wernert, N. 2003. Colorectal carcinoma cells (Caco-2) secrete stroma-inducing growth factors in a stroma-oriented direction. *Anticancer Res. 23*:137–141.

Wernert, N. 1997. The multiple roles of tumour stroma. *Virchows Arch. 430*:433–443.

Wernert, N., Gilles, F., Fafeur, V., Bouali, F., Raes, M.B., Pyke, C., Dupressoir, T., Seitz, G., Vandenbunder, B., and Stéhelin, D. 1994. Stromal Expression of c-ETs 1 transcription factor correlates with tumor invasion. *Cancer Res. 54*:5683–5688.

Wernert, N., Löcherbach, C., Behrens, P., Wellmann, A., and Hügel, A. 2001. Presence of genetic alterations in microdissected stroma of human colon and breast cancers. *Anticancer Res. 21*:2259–2264.

Wernert, N., Raes, M.B., Lasalle, P., Gosselin, B., Vandenbunder, B., and Stéhelin, D. 1992. The c-*ets* 1 proto-oncogene is a transcription factor expressed in endothelial cells during tumor vascularization and other forms of angiogenesis in man. *Am. J. Pathol. 140*:119–127.

Wernert, N., Stanjek, A., Kiriakidis, S., Hügel, A., Jha, H.C., Mazitschek, R., and Giannis, A. 1999. Inhibition of angiogenesis in vivo by ETs-1 antisense oligonucleotides—inhibition of ETs-1 transcription factor expression by the antibiotic Fumagillin. *Angew. Chem. Int. Ed. 38*:3228–3231.

Wolf, C., Levebvre, O., Rouyer, N., Chenard, M.P., Bellocq, J.P., Rio, M.C., Chambon, P., and Basset, P. 1994. Protéases d'origine stromale et progression tumorale. *Médecine/Sciences 10*:507–515.

This Page Intentionally Left Blank

16

Role of Immunohistochemical Expression of p53, Rb, and p16 Proteins in Anal Squamous Cell Carcinoma

Hanlin L. Wang

Introduction

Anal squamous cell carcinoma originates from the epithelium lining the anal canal and anal margin. Anal canal carcinomas involve the terminal portion of the large intestine beginning at the upper surface of the anorectal ring and ending at the anal verge (Fenger *et al*., 2000). Histologically, tumors from this region may be keratinizing or nonkeratinizing (basaloid or cloacogenic), but they are similarly managed with chemoradiation therapy and do not differ significantly in prognosis. In contrast, anal margin carcinomas arise from the perianal skin and behave more like skin cancers. They usually bear a favorable prognosis by local excision. In practice, however, the distinction between anal canal and anal margin carcinomas may not be always possible, particularly when different definition for anal canal is used by clinicians (Fenger, 1988).

Anal squamous cell carcinomas are uncommon malignancies, accounting for approximately 1.5% of all digestive system cancers in the United States (Ryan *et al*., 2000). However, the incidence has increased considerably in recent years (Frisch, 2002; Melbye *et al*., 1994). The current estimates of incidence per

100,000 person-years are 0.38–0.5 for men and 0.74–1.0 for women, reflecting a 1.5- to 2.5-fold and a 2.6-fold to fivefold increase for men and women, respectively, during the second half of the 20th century. Population-based case–control studies have linked the increase to changes in sexual behavior (Frisch *et al*., 1997; Frisch, 2002), indicating that the etiopatho-genetic mechanisms underlying the development of anal cancers are similar to those established for cervical cancers occurring in women (Ryan *et al*., 2000). That is, a sexually transmitted infectious agent is likely to play an important role in anal carcinogenesis (Frisch *et al*., 1997), although other risk factors such as cigarette smoking may also contribute (Ryan *et al*., 2000).

As demonstrated in cervical cancers, a number of studies have established a strong etiologic association of human papillomavirus (HPV) with the development of anal squamous cell carcinoma (zur Hausen, 2000). Similar to that seen in the cervix, HPV infection in the anus may cause squamous intraepithelial neoplasia or dysplasia, which may progress from low grade to high grade and eventually to invasive cancer (Fenger, 1991). In a case–control study, Frisch and colleagues (1997) detected HPV deoxyribonucleic acid (DNA) in 340

of 388 cases (88%) of anal squamous cell carcinoma but in none of the 20 control cases of rectal adenocarcinoma. The vast majority of the cases were found to harbor high-risk HPVs, as defined by their documented association with invasive carcinomas in the cervix (Lorincz *et al*., 1992), with type 16 being the most prevalent, detected in 73% of the cases. These observations have been substantiated by several other studies that have investigated smaller numbers of patients with anal cancers (Crook *et al*., 1991; Heino *et al*., 1993; Holm *et al*., 1994; Indinnimeo *et al*., 1999; Lu *et al*., 2003; Shroyer *et al*., 1995; Vincent-Salomon *et al*., 1996; Youk *et al*., 2001). It is interesting that high-risk HPV DNA is more likely to be detected in tumors occurring in the anal canal than in those arising from the anal margin. For example, in the study by Frisch *et al*. (1999), who studied 302 women and 84 men with anal cancer, 95% and 83% of anal canal carcinomas seen in women and men, respectively, were positive for high-risk HPVs, in contrast to 80% and 28% of anal margin carcinomas.

The carcinogenic effect of high-risk HPVs has been mainly attributed to two viral oncoproteins, E6 and E7 (Figure 42). Both E6 and E7 are encoded by the early region of the viral genome, which are always preserved and expressed when the virus integrates into the host genome while other open reading frames of the virus may be deleted or disrupted (Stoler, 2000; von Knebel Doeberitz, 2002). *In vitro* studies have shown that the high-risk HPV E6 and E7 proteins can immortalize primary human keratinocytes and can also collaborate with *ras* oncogene to transform primary or established rodent cells. As illustrated in Figure 42, the oncogenic effects of the E6 and E7 proteins are thought to be mediated by targeting two important cellular tumor suppressors, p53 and Rb, which leads to abnormal cell-cycle control, chromosomal alterations, and eventual neoplastic transformation (Fehrmann and Laimins, 2003; Stoler, 2000; zur Hausen, 2000).

The tumor suppressor p53 is a multifunctional nuclear protein that, under physiologic conditions, acts as a guardian of the genome by coordinating DNA repair with G1 phase arrest of the cell cycle and apoptosis (Adimoolam and Ford, 2003; Sherr and McCormick, 2002). It is normally present at low levels within cells because of its very short half-life (~20 minutes). When a cell is exposed to genotoxic stress such as ionizing radiation, however, p53 protein
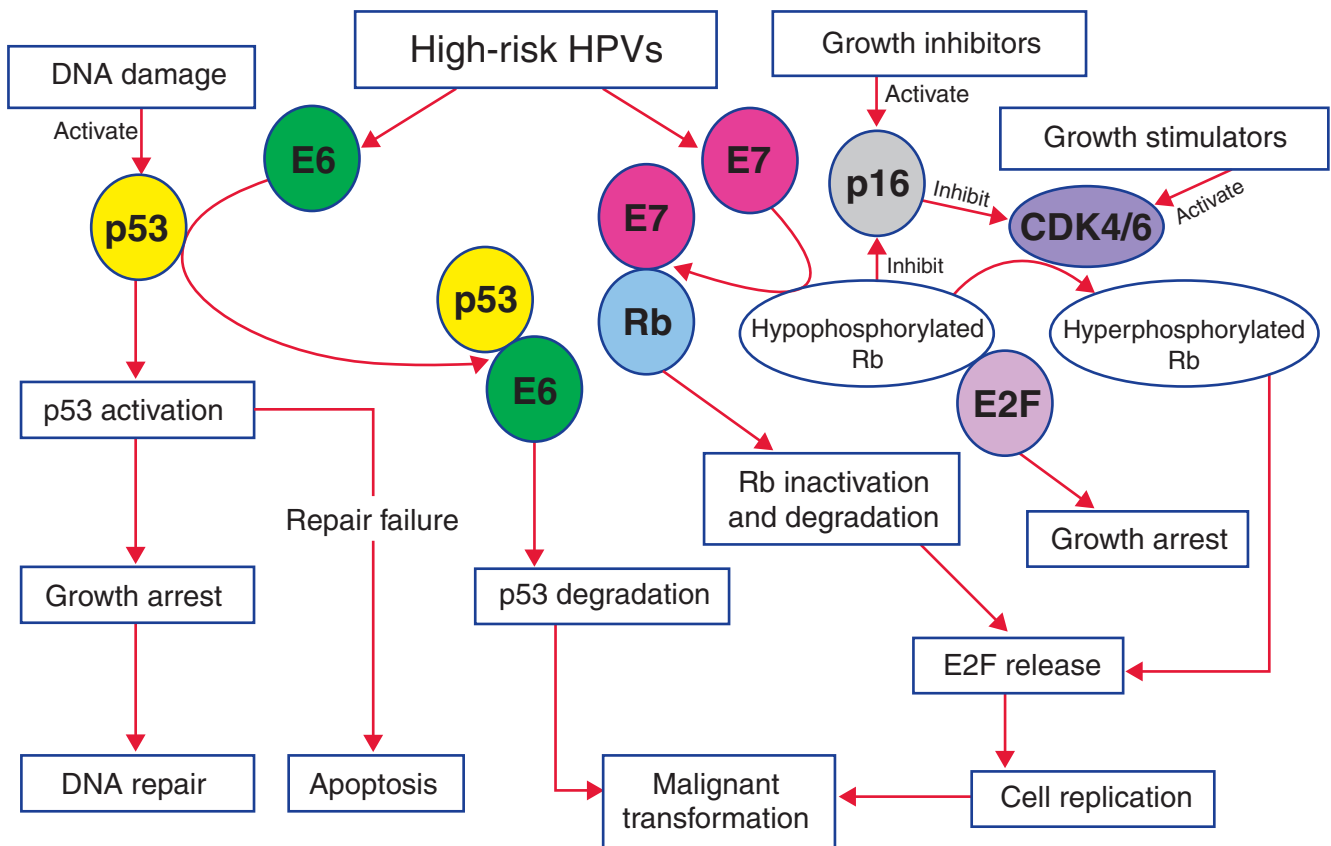
Figure 42 Oncogenic effects of high-risk types of human papillomavirus.

is stabilized via post-translational modifications and regulates the transcription of a number of genes that are necessary for blocking cell-cycle progression to allow damaged DNA repair. If the damage is irreparable, p53 induces the activation of apoptosis cascade to eliminate genetically damaged cells. Therefore, p53 serves a crucial role in maintaining genomic stability by preventing the propagation of genetically damaged cells. The importance of p53 in tumor suppression is also evidenced by the fact that it is the single most common target for genetic alteration in human cancers. Mutations in its gene have been demonstrated in more than 50% of human cancers (Levine, 1997), which most frequently disable the DNA-binding ability so that the p53-dependent transcription of genes is prevented. In this regard, immunohistochemistry has been shown to be an indirect but useful method to detect *p53* mutations (Baas *et al.*, 1994; Hall and Lane, 1994). This is so because the wild-type p53 protein has a very short half-life, as mentioned earlier, that is essentially undetectable by immunohistochemical staining. Mutant p53, however, has a prolonged half-life (several hours), which leads to the abnormal accumulation and allows immunohistochemical detection. It is interesting to note, however, that in HPV-associated malignancies, the molecular mechanism by which p53 is deregulated is not through gene mutations but rather via an epigenetic pathway at the protein level. It has been well established that the HPV E6 oncoprotein interacts directly with p53 protein to promote its degradation via the ubiquitin–proteasome pathway (Scheffner *et al.*, 1993). In fact, an early study by Crook *et al.* (1991) demonstrated no *p53* gene mutations in a limited number of HPV-positive anal squamous cell carcinomas, suggesting that *p53* mutations and HPV infection are mutually exclusive.

Another important tumor suppressor that is also targeted by HPV is Rb, a nuclear phosphoprotein that plays a central role in regulating the cell cycle (Sherr and McCormick, 2002). In the cells, wild-type Rb protein exists in both hypophosphorylated (active) and hyperphosphorylated (inactive) forms. In the active form, Rb blocks the entry into S phase of the cell cycle by inhibiting the E2F transcriptional program. The phosphorylation status of Rb protein is regulated by D-type cyclins and cyclin-dependent kinases, mainly CDK4 and CDK6. Thus, when cyclin D/CDK4 and cyclin D/CDK6 are activated by growth stimulators, Rb undergoes phosphorylation, which leads to the liberation of the E2F factors necessary for the regulation of genes involved in DNA replication. Similar to *p53,* the *Rb* gene is also frequently mutated or deleted in human cancers. Unlike *p53,* however, when *Rb* is mutated, its protein becomes undetectable

by immunohistochemical staining (Cagle *et al.*, 1997; Gouyer *et al.*, 1994). The HPV E7 oncoprotein preferentially binds to the hypophosphorylated Rb, the active form, resulting in a functional inactivation and an acceleration of protein degradation (Boyer *et al.*, 1996; Dyson *et al.*, 1989; Giarrè *et al.*, 2001). In addition, E7 interacts with two other members of the Rb family, p107 and p130, which also negatively control the transcriptional activity of E2F factors (Davies *et al.*, 1993; Dyson *et al.*, 1989). These observations thus demonstrate that HPV E7 oncoprotein simulates the action of CDK-mediated Rb phosphorylation that leads to E2F release. Similar to what has been reported for *p53* gene, no gross rearrangement or loss of the *Rb* locus was observed in squamous cell carcinomas of the anus in one early study by Southern blotting analysis (Crook *et al.*, 1991).

The anti-proliferative function of the Rb protein is modulated by a complicated network of cell-cycle regulators (Sherr and McCormick, 2002; Sherr and Roberts, 1999). Among them, p16, also known as p16[INK4a], CDKN2, CDKN2A, and MTS1, directly inhibits the activities of CDK4 and CDK6 to maintain Rb in its hypophosphorylated state. Therefore, p16 also functions as a tumor suppressor by enhancing the inhibitory effect of Rb on cell-cycle progression. Not unexpectedly, the *p16* gene is also a common target of inactivation in human cancers via deletion, mutation, or hypermethylation (Cairns *et al.*, 1995; Clurman and Groudine, 1998; Sherr and McCormick, 2002). Whether these genetic and epigenetic alterations in the *p16* gene occur in anal squamous cell carcinomas has not been investigated.

MATERIALS

1. Microtome.
2. Waterbath.
3. Drying oven.
4. Microwave oven.
5. pH meter.
6. Light microscope.
7. Flat humid chamber.
8. Staining jars.
9. Wash bottles.
10. Timer.
11. Clean precoated glass slides (e.g., Snowcoat X-tra microslides from Surgipath, Winnipeg, Manitoba, Canada).
12. Coverslips (e.g., Gold Seal cover glass from Fisher Scientific, Pittsburgh, PA).
13. Absorbent wipes.
14. Xylene.
15. Ethanol, absolute and 95%.

16. Hydrogen peroxide, 3% in water.

17. Distilled water.

18. Hematoxylin (e.g., hematoxylin 7211 from Richard-Allan Scientific, Kalamazoo, MI, or Mayer's hematoxylin).

19. Mounting medium (e.g., xylene-based Cytoseal XYL from Richard-Allan Scientific).

20. 10 mM citrate buffer: Dissolve 1.92 g citric acid (anhydrous) in 800 ml distilled water, adjust pH to 6.0 with concentrated NaOH, and bring vol to 1 L with distilled water.

21. 0.05 M phosphate buffer saline (PBS): Dissolve 6.17 g sodium phosphate dibasic (Na_2HPO_4), 0.89 g sodium phosphate monobasic ($NaH_2PO_4 \cdot H_2O$), and 9 g sodium chloride (NaCl) in 800 ml distilled water; adjust pH to 7.4 using 1N HCl, and bring vol to 1 L with distilled water.

22. 0.05 M Tris-buffered saline (TBS) containing 50 mM Tris-HCl, 150 mM NaCl and 0.05% Tween-20, pH 7.6 (commercially available, e.g., Dako or Signet Pathology Systems, Inc., Dedham, MA).

23. Dako LSAB + kit, HRP. This kit contains link (secondary) antibodies that are biotinylated anti-mouse, anti-rabbit, and anti-goat immunoglobulins in PBS with carrier protein and sodium azide and streptavidin conjugated to horseradish peroxidase in PBS with carrier protein and anti-microbial agents.

24. Dako liquid DAB + substrate-chromogen system. This contains 3,3′-diaminobenzidine (DAB) in chromogen solution, and buffered substrate (imidazole-HCl buffer, pH 7.5, with hydrogen peroxide and anti-microbial agents).

25. Primary antibodies: mouse immunoglobulin G2b (IgG2b) against p16 (clone 6H12) from Novocastra Laboratories Ltd. (Newcastle upon Tyne, UK), mouse IgG1, against Rb (clone IF8), and mouse IgG2a against p53 (clone DO-1) from Santa Cruz Biotechnology, Inc. (Santa Cruz, CA).

26. Antibody diluent (e.g., from Dako).

27. Nonhuman reactive mouse IgG (e.g., from Dako).

28. Automated immunostainer (e.g., Dako autostainer).

METHOD

1. Formalin-fixed and paraffin-embedded tissue blocks are cut at 4 μm thick onto precoated glass slides using a microtome and a waterbath.

2. Dry slides in 56ºC oven for 45 min.

3. Deparaffinize sections in xylene with three changes, 3 min each.

4. Rehydrate sections as follows:
   a. Absolute ethanol with three changes, 15–20 dips each.
   b. 95% ethanol with two changes, 15–20 dips each.
   c. Distilled water with two changes, 15–20 dips each.

5. Incubate slides in 3% hydrogen peroxide for 15 min at room temperature.

6. Rinse slides with distilled water.

7. Place slides in 10 mM citrate buffer (pH 6.0) and heat in a microwave oven for 10 min.

8. Allow slides to cool in the buffer for ~20 min.

9. Rinse slides with distilled water.

10. Incubate slides in 0.05 M PBS (pH 7.4) for 10 min at room temperature.

11. Drain slides and wipe carefully around the tissue with absorbent wipes. Leave a fine film of PBS and do not let tissue dry.

12. Apply enough (usually 100–200 μL depending on the size of the tissue section) primary antibody diluted in antibody diluent to each slide to cover the entire tissue (1:40 dilution for anti-p16 antibody and 1:100 for anti-Rb and anti-p53 antibodies).

13. Place slides (with primary antibody) in flat, humid chamber lined with wet paper towels to maintain a moist environment, and incubate at room temperature for 1 hr.

14. Remove the primary antibody and wash slides with PBS in a wash bottle with three changes, 5 min each.

15. Drain and wipe slides as described in **Step 11**.

16. Apply enough biotinylated link (secondary) antibodies to each slide to cover the entire tissue.

17. Incubate in flat, humid chamber at room temperature for 30 min.

18. Remove the link antibodies and wash slides with PBS in a wash bottle with three changes, 5 min each.

19. Drain and wipe slides as described earlier.

20. Apply enough streptavidin-horseradish peroxidase solution to each slide to cover the entire tissue.

21. Incubate in flat, humid chamber at room temperature for 30 min.

22. Remove the streptavidin-horseradish peroxidase solution and wash slides with PBS in a wash bottle with three changes, 5 min each.

23. Drain and wipe slides as described earlier.

24. Apply enough substrate-chromogen solution to each slide to cover the entire tissue. This solution is prepared before use by mixing 1 drop (~20 μL) of DAB chromogen solution with 1 ml of buffered substrate.

25. Incubate at room temperature for 30 sec to 10 min until desired brown color is developed, as determined by examination under a light microscope.

26. Wash slides with tap water for 5 min, with two changes, to completely remove DAB.

27. Counterstain slides with hematoxylin for 3 min in a staining jar.

28. Rinse in running tap water until water becomes clear.

29. Dehydrate slides as follows:
    a. 95% ethanol with two changes, 15–20 dips each.
    b. Absolute ethanol with three changes, 15–20 dips each.
    c. Xylene with three changes, 3 min each.

30. Mount slides with xylene-based permanent medium (such as Cytoseal XYL) and coverslips.

31. Analyze slides under a light microscope.

If an automated immunostainer is used, slides are loaded into the machine after deparaffinization and antigen retrieval with 10 mM citrate buffer. The procedure may then be programmed as 3% hydrogen peroxide treatment for 5 min, primary antibody incubation for 1 hr, link antibody 15 min, streptavidin-horseradish peroxidase 15 min, and substrate-chromogen 5 min. The volume used for each reagent is 200 μL. The wash solution used between steps is 0.05 M TBS instead of PBS. The counterstaining and mounting procedures are performed manually as described earlier.

Ideally, tissue sections from anal squamous cell carcinomas selected for immunohistochemical studies should contain both tumor and histologically normal-appearing squamous or rectal mucosa so that a comparison between tumor and normal tissue can be made. Normal squamous and rectal mucosa also serve as "built-in" negative controls for the expression of p16 and p53 and positive controls for Rb. Squamous cell carcinoma of the uterine cervix and adenocarcinoma of the colon are excellent positive controls for p16 and p53, respectively. Another negative control should also always be included with each experiment, in which the primary antibody is omitted (only antibody diluent is used) or replaced by nonhuman reactive mouse IgG.

RESULTS AND DISCUSSION

Positive expression of p53, Rb, and p16 proteins is indicated by nuclear staining. Although a variable degree of cytoplasmic immunoreactivity is almost always present, cytoplasmic staining only should be interpreted with caution, which may represent nonspecific staining. The expression of p53 and p16 in normal-appearing squamous and colonic epithelial cells as well as inflammatory cells adjacent to anal cancers is usually undetectable by immunohistochemistry. In contrast, nuclear staining for Rb should be observed in these nonneoplastic cells.

There has been no consensus regarding how many tumor cells are needed to show nuclear staining for a tumor to be considered positive. The criteria described in the literature vary widely (from 5% to 50%) and are dependent on different investigators. As discussed later, this variation may be problematic in interpreting p53 immunostaining data. In our laboratory, we generally use 10% as a cutoff (i.e., a tumor is recorded positive if more than 10% of the tumor cells exhibit immunoreactivity to a specific antibody).

The p53 Protein

A number of studies have investigated the expression of p53 protein in anal squamous cell carcinomas by immunohistochemistry (Lu *et al*., 2003). These studies are primarily based on the observations that there is a very close correlation between overexpression of the p53 protein and mutation of its gene (Hall and Lane, 1994). As mentioned in the Introduction, in addition to abolishing the tumor suppressor function, mutations of the *p53* gene also stabilize the protein, allowing detection by immunohistochemistry.

The reported frequency of positive p53 protein expression in anal squamous cell carcinomas ranges from 21% to 82%. This wide variation does not appear to result from different antibodies used in different studies because most anti-p53 antibodies give the same or similar results (Baas *et al*., 1994; Ogunbiyi *et al*., 1993). Rather, different criteria used by different investigators in interpreting the immunostaining results may be a better explanation. For example, in the study by Wong *et al*. (1999), 40 of 49 cases (82%) of squamous cell carcinoma of the anal canal showed positive nuclear immunostaining for p53. However, among these positive cases, 13 had <5% of the tumor cells positively stained, 9 stained 5% to <10%, and 18 stained 10–50% of the tumor cells. The median positive staining was 5%, and none of the positive cases were described to involve >50% of the tumor cell population. In a few other studies where semiquantitative criteria have also been used to define the positivity (Behrendt and Hansmann, 2001; Bonin *et al*., 1999; Lu *et al*., 2003), the expression of p53 protein in anal squamous cell carcinomas is almost always focal and seen in <10% of the tumor cells. In fact, there is only one study (Tanum and Holm, 1996) that has described diffuse positive p53 staining in anal squamous cell carcinomas as defined by >50% of the tumor cells showing nuclear immunoreactivity. By using >50% as a cutoff, the authors found 33 of 97 cases (34%) to be positive for p53 expression.

Correlation of p53 expression with HPV status in anal squamous cell carcinomas has also been examined in several studies. It has been demonstrated that in 10–64% of the tumors investigated, p53 protein expression and evidence of HPV infection coexist. The discrepancy among different studies appears to be largely attributed to the sensitivity of the techniques used to detect HPV. When immunohistochemical staining for HPV16 and 18 E6 proteins is used, the detection rate is very low (Jakate and Saclarides, 1993). In contrast, a much higher detection rate is achieved by polymerase chain reaction (PCR) analysis for the presence of HPV DNA (Indinnimeo *et al.*, 1999; Ogunbiyi *et al.*, 1993). Despite the focal nature of positive p53 immunostaining in many of the cases, most of these studies have concluded that there is no clear association between p53 expression and HPV status. This is so because a similar or higher frequency of positive p53 immunostaining is also demonstrated in tumors where HPV DNA or E6 protein is not detected. Interestingly, Behrendt and Hansmann (2001) reported a higher frequency of p53 expression in carcinomas of the anal margin than in those of the anal canal. Although the HPV status in their cases was not examined, it has been shown that tumors arising from the anal margin are less likely to be HPV-related when compared to those occurring in the anal canal (Frisch *et al.*, 1999). However, the difference observed in this report between the two types of anal cancers may not be statistically significant because only a limited number of tumors were examined. In addition, among the 8 of 17 anal canal carcinomas (47%) and 4 of 5 anal margin carcinomas (80%) that were considered positive for p53 expression, 7 were described to have nuclear staining in <5% of the tumor cells and 1 in 5–10% of the tumor cells. In the remaining 4 cases (all from the anal canal), the positivity was described as the presence of tumor cell islands with >70% of the nuclei stained. These islands were usually located at the tumor border and the rest of the tumor contained only occasional (<5%) positive cells (Behrendt and Hansmann, 2001). However, the study by Indinnimeo *et al.* (1999) found nuclear accumulation of p53 protein to be exclusively associated with the presence of HPV. In that study, 14 cases of anal squamous cell carcinoma were investigated. Positive p53 protein expression, as defined by the presence of at least one focus of positively stained tumor cells by immunohistochemistry, was observed in all 9 tumors that were also positive for HPV DNA detected by PCR analysis. In the remaining 5 cases, p53 and HPV were concordantly negative.

The conflicting observations described illustrate the importance of carefully evaluating p53 immunostaining data. It has been well established that immunohisto-chemistry may detect wild-type p53 protein stabilized by the interruption of normal degradation pathway in the absence of gene mutations (Wynford-Thomas, 1992). It is essential to not only evaluate the staining intensity but also the staining extent. As pointed out by Hall and Lane (1994), only the presence of a strong nuclear staining in the majority of the tumor cells is frequently associated with underlying gene mutations. This staining pattern should be evident in positive controls included in the study (such as colorectal adenocarcinoma), which always exhibit a diffuse and strong nuclear staining. However, the occurrence of only occasional strongly positive cells in a tumor does not appear to correlate with abnormality at the gene level. Rather, this may simply represent normal activation process that leads to the accumulation of wild-type p53 protein in response to genetic errors that occur at a higher frequency in tumor cells than in adjacent nonneoplastic cells.

Lu *et al.* (2003) studied 29 cases of squamous cell carcinoma of the anal canal. All the cases were found to harbor high-risk type HPV DNA by PCR analysis, with type 16 being most prevalent (86%). Six cases (21%) showed p53 nuclear expression in scattered tumor cells. In none of the cases was the positivity diffuse or seen in >10% of the tumor cells. These cases were to be thus considered negative for p53 expression. These observations, together with those described earlier, suggest that mutations of the *p53* gene, as frequently seen in many types of human cancers (Levine, 1997), do not appear to serve a major role in HPV-induced carcinogenesis in the anal region. This notion is also in line with the fact that HPV E6 oncoprotein facilitates p53 protein degradation (Scheffner *et al.*, 1993).

The prognostic value of p53 protein expression in anal squamous cell carcinomas has been controversial. The studies by Tanum and Holm (1996) and Indinnimeo *et al.* (1999) showed no correlation of p53 expression with patient outcome. The study by Bonin *et al.* (1999) showed a trend for patients whose tumors expressed p53 to have an inferior locoregional control and overall survival, but a statistical significance was not achieved. By multivariate analysis, tumor stage was the only predictive factor for the outcome. However, the study by Wong *et al.* (1999) demonstrated that in patients managed with chemoradiation therapy, percent p53 protein expression is an independent prognostic factor. Specifically, for patients with p53 expression in <5% of the tumor cells, survival and disease-free survival at 5 years were 90% and 67%, respectively. For those with p53 ≥10%, the 5-year survival and disease-free survival were 69% and 52%, respectively. When adjusted for T stage, histology, and gender, p53 was significant as a continuous variable for disease-free survival.

The Rb Protein

Tanum and Holm (1996) studied 97 anal squamous cell carcinomas by immunohistochemistry and observed a heterogeneous Rb nuclear staining in 92 (95%) cases. Only 5 cases (5%) exhibited a complete loss of nuclear Rb immunoreactivity. Despite nuclear Rb staining being detected in the vast majority of the tumors they studied, the authors suggest that the Rb protein may be functionally inactivated by HPV E7 oncoprotein because many of these tumors are associated with HPV infection (Holm *et al*., 1994). In addition, the 5 cases with negative Rb expression showed positive immunoreactivity to anti-Ki-67 antibody known to react with cells in the proliferating phase, further suggesting that Rb is not functioning in these tumors.

By studying 29 anal squamous cell carcinomas, we demonstrated that loss of Rb nuclear immunostaining was frequently associated with high-risk HPV infection (Lu *et al*., 2003). Our results show that nuclear staining for Rb protein was universally present in nonneoplastic cells in every case, but was only observed in nine tumors (31%). Twenty cases (69%) exhibited a loss of nuclear immunoreactivity while a weak cytoplasmic staining was noted. These observations, and the results reported by Tanum and Holm (1996), support the concept that Rb protein is deregulated through two different mechanisms in HPV-related anal cancers; that is, in a subset of the tumors, Rb is inactivated by the HPV E7 oncoprotein at the functional level and thus the nuclear Rb protein remains detectable by immunohistochemistry. In other tumors, however, Rb inactivation is achieved through accelerated protein degradation as evidenced by the loss of nuclear staining. This concept is indirectly supported by the study on p16 protein expression in these tumors as discussed below.

The p16 Protein

In all 29 cases of anal squamous cell carcinoma we studied, a strong and diffuse immunostaining pattern for p16 was observed (Lu *et al*., 2003). The staining was predominantly nuclear, but a variable degree of cytoplasmic positivity was noted. The nonneoplastic squamous epithelium and colonic mucosa adjacent to tumors were either completely nonimmunoreactive or exhibited only weak membranous or cytoplasmic positivity. No nuclear staining was evident in nonneoplastic epithelial cells in any of the cases.

Because all anal tumors we examined were high-risk-HPV-related, we have also similarly studied 12 HPV-positive and 21 HPV-negative squamous cell carcinomas from the upper aerodigestive tract for comparison. The results demonstrated that all 12 HPV-positive tumors exhibited strong and diffuse nuclear staining for p16, but the similar pattern was observed in only 2 HPV-negative tumors (10%).

Our observations described earlier are similar to what has been reported in HPV-related cervical cancers, where overexpression of the p16 protein is also detected (Sano *et al*., 1998), but are paradoxical to the fact that p16 functions as a tumor suppressor and is frequently inactivated in human cancers (Cairns *et al*., 1995; Clurman and Groudine, 1998; Sherr and McCormick, 2002). This may be explained by a negative feedback control mechanism secondary to Rb deregulation (Khleif *et al*., 1996; Li *et al*., 1994). It has been shown that there exists an inverse relationship between the expression of p16 and the presence of functional Rb in many cell systems and that Rb represses the transcription of the *p16* gene. Once the inhibitory effect of Rb is abolished by either functional inactivation or protein degradation, as seen in HPV-infected cells, the transcriptional activity and the protein expression level of p16 are expected to increase. However, it appears that p16 cannot effectively inhibit cell-cycle progression in the absence of functional Rb, even if it is overexpressed (Giarrè *et al*., 2001; Medema *et al*., 1995). Therefore, the observation of p16 overexpression supports the notion that in HPV-related anal squamous cell carcinomas, the tumor suppressor function of the Rb protein is nullified even if it remains detectable immunohistochemically in a subset of the tumors.

A number of studies have attempted to determine whether HPV infection bears any prognostic significance in squamous cell carcinomas of the genital areas and upper aerodigestive tract (Li *et al*., 2003; Schwartz *et al.*, 2001). Although the available data are inconclusive and controversial, it may be useful to separate tumors that harbor HPV DNA from those that do not because different etiopathogenetic pathways are involved. In general, the detection of HPV DNA requires sophisticated laboratory facilities and experienced personnel, and it is costly. It thus may not be feasible to be implemented into daily practice. From this perspective, the presence of p16 overexpression, as detected by simple immunohistochemical staining, may serve as a good surrogate marker (Keating *et al*., 2001; von Knebel Doebertz, 2002). This marker may be particularly pertinent when used in combination with negative Rb and p53 nuclear staining, suggesting the presence of protein degradation by HPV oncoproteins and the absence of *p53* gene mutations.

In conclusion, anal squamous cell carcinoma is a high-risk HPV-related malignancy. Its pathogenesis involves inactivation of tumor suppressors p53 and Rb. Immunohistochemistry is a useful technique to investigate the roles of p53, Rb, and p16 proteins in these tumors. Overexpression of p16 protein, in combination with loss of nuclear Rb staining and lack of p53 overexpression, may be a useful surrogate biomarker for identifying anal squamous cell carcinomas associated with HPV infection.

References

Adimoolam, S., and Ford, J.M. 2003. p53 and regulation of DNA damage recognition during nucleotide excision repair. *DNA Repair 2*:947–954.

Baas, I.O., Mulder, J.W., Offerhaus, G.J., Vogelstein, B., and Hamilton, S.R. 1994. An evaluation of six antibodies for immunohistochemistry of mutant p53 gene product in archival colorectal neoplasms. *J. Pathol. 172*:5–12.

Behrendt, G.C., and Hansmann, M.L. 2001. Carcinomas of the anal canal and anal margin differ in their expression of cadherin, cytokeratins and p53. *Virchows Arch. 439*:782–786.

Bonin, S.R., Pajak, T.F., Russell, A.H., Coia, L.R., Paris, K.J., Flam, M.S., and Sauter, E.R. 1999. Overexpression of p53 protein and outcome of patients treated with chemoradiation for carcinoma of the anal canal: A report of randomized trial RTOG 87-04. *Cancer 85*:1226–1233.

Boyer, S.N., Wazer, D.E., and Band, V. 1996. E7 protein of human papilloma virus-16 induces degradation of retinoblastoma protein through the ubiquitin-proteasome pathway. *Cancer Res. 56*:4620–4624.

Cagle, P.T., el-Naggar, A.K., Xu, H.J., Hu, S.X., and Benedict, W.F. 1997. Differential retinoblastoma protein expression in neuroendocrine tumors of the lung: Potential diagnostic implications. *Am. J. Pathol. 150*:393–400.

Cairns, P., Polascik, T.J., Eby, Y., Tokino, K., Califano, J., Merlo, A., Mao, L., Herath, J., Jenkins, R., Westra, W., Rutter, J.L., Buckler, A., Gabrielson, E., Tockman, M., Cho, K.R., Hedrick, L., Bova, G.S., Isaacs, W., Kock, W., Schwab, D., and Sidransky, D. 1995. Frequency of homozygous deletion at *p16/CDKN2* in primary human tumours. *Nat. Genet. 11*:210–212.

Clurman, B.E., and Groudine, M. 1998. The CDKN2A tumor-suppressor locus—a tale of two proteins. *N. Engl. J. Med. 338*:910–912.

Crook, T., Wrede, D., Tidy, J., Scholefield, J., Crawford, L., and Vousden, K.H. 1991. Status of c-myc, p53 and retinoblastoma genes in human papillomavirus positive and negative squamous cell carcinomas of the anus. *Oncogene 6*:1251–1257.

Davies, R., Hicks, R., Crook, T., Morris, J., and Vousden, K. 1993. Human papillomavirus type 16 E7 associates with a histone H1 kinase and with p107 through sequences necessary for transformation. *J. Virol. 67*:2521–2528.

Dyson, N., Howley, P.M., Munger, K., and Harlow, E. 1989. The human papilloma virus-16 E7 oncoprotein is able to bind to the retinoblastoma gene product. *Science 243*:934–937.

Fehrmann, F., and Laimins, L.A. 2003. Human papillomaviruses: Targeting differentiating epithelial cells for malignant transformation. *Oncogene 22*:5201–5207.

Fenger, C. 1988. Histology of the anal canal. *Am. J. Surg. Pathol. 12*:41–55.

Fenger, C. 1991. Anal neoplasia and its precursors: Facts and controversies. *Semin. Diagn. Pathol. 8*:190–201.

Fenger, C., Frisch, M., Marti, M.C., and Parc, R. 2000. Tumours of the anal canal. In Hamilton, S.R., and Aaltonen, L.A., (eds) *World Health Organization Classification of Tumours. Pathology and Genetics of Tumours of the Digestive System.* Lyon, France: IARC Press, 147–155.

Frisch, M. 2002. On the etiology of anal squamous carcinoma. *Dan. Med. Bull. 49*:194–209.

Frisch, M., Fenger, C., van den Brule, A.J., Sorensen, P., Meijer, C.J., Walboomers, J.M., Adami, H.O., Melbye, M., and Glimelius, B. 1999. Variants of squamous cell carcinoma of the anal canal and perianal skin and their relation to human papillomaviruses. *Cancer Res. 59*:753–757.

Frisch, M., Glimelius, B., van den Brule, A.J., Wohlfahrt, J., Meijer, C.J., Walboomers, J.M., Goldman, S., Svensson, C., Adami, H.O., and Melbye, M. 1997. Sexually transmitted infection as a cause of anal cancer. *N. Engl. J. Med. 337*:1350–1358.

Giarrè, M., Caldeira, S., Malanchi, I., Ciccolini, F., Leão, M.J., and Tommasino, M. 2001. Induction of pRb degradation by the human papillomavirus type 16 E7 protein is essential to efficiently overcome p16^{INK4a}-imposed G$_1$ cell cycle arrest. *J. Virol. 75*:4705–4712.

Gouyer, V., Gazzeri, S., Brambilla, E., Bolon, I., Moro, D., Perron, P., Benabid, A.L., and Brambilla, C. 1994. Loss of heterozygosity at the RB locus correlates with loss of RB protein in primary malignant neuro-endocrine lung carcinomas. *Int. J. Cancer 58*:818–824.

Hall, P.A., and Lane, D.P. 1994. p53 in tumour pathology: Can we trust immunohistochemistry?—Revisited! *J. Pathol. 172*:1–4.

Heino, P., Goldman, S., Lagerstedt, U., and Dillner, J. 1993. Molecular and serological studies of human papillomavirus among patients with anal epidermoid carcinoma. *Int. J. Cancer 53*:377–381.

Holm, R., Tanum, G., Karlsen, F., and Nesland, J.M. 1994. Prevalence and physical state of human papillomavirus DNA in anal carcinomas. *Mod. Pathol. 7*:449–453.

Indinnimeo, M., Cicchini, C., Stazi, A., Giarnieri, E., French, D., Limiti, M.R., Ghini, C., and Vecchione, A. 1999. Human papillomavirus infection and p53 nuclear overexpression in anal canal carcinoma. *J. Exp. Clin. Cancer Res. 18*:47–52.

Jakate, S.M., and Saclarides, T.J. 1993. Immunohistochemical detection of mutant p53 protein and human papillomavirus-related E6 protein in anal cancers. *Dis. Colon Rectum 36*: 1026–1029.

Keating, J.T., Ince, T., and Crum, C.P. 2001. Surrogate biomarkers of HPV infection in cervical neoplasia screening and diagnosis. *Adv. Anat. Pathol. 8*:83–92.

Khleif, S.N., DeGregori, J., Yee, C.L., Otterson, G.A., Kaye, F.J., Nevins, J.R., and Howley, P.M. 1996. Inhibition of cyclin D-CDK4/CDK6 activity is associated with an E2F-mediated induction of cyclin kinase inhibitor activity. *Proc. Natl. Acad. Sci. USA 93*:4350–4354.

Levine, A.J. 1997. p53, the cellular gatekeeper for growth and division. *Cell 88*:323–331.

Li, W., Thompson, C.H., O'Brien, C.J., McNeil, E.B., Scolyer, R.A., Cossart, Y.E., Veness, M.J., Walker, D.M., Morgan, G.J., and Rose, B.R. 2003. Human papillomavirus positivity predicts favourable outcome for squamous carcinoma of the tonsil. *Int. J. Cancer 106*:553–558.

Li, Y., Nichols, M.A., Shay, J.W., and Xiong, Y. 1994. Transcriptional repression of the D-type cyclin-dependent kinase inhibitor p16 by the retinoblastoma susceptibility gene product pRb. *Cancer Res. 54*:6078–6082.

Lorincz, A.T., Reid, R., Jenson, A.B., Greenberg, M.D., Lancaster, W., and Kurman, R.J. 1992. Human papillomavirus infection of the cervix: Relative risk associations of 15 common anogenital types. *Obstet. Gynecol. 79*:328–337.

Lu, D.W., El-Mofty, S.K., and Wang, H.L. 2003. Expression of p16, Rb, and p53 proteins in squamous cell carcinomas of the anorectal region harboring human papillomavirus DNA. *Mod. Pathol. 16*:692–699.

Medema, R.H., Herrera, R.E., Lam, F., and Weinberg, R.A. 1995. Growth suppression by p16^{ink4} requires functional retinoblastoma protein. *Proc. Natl. Acad. Sci. USA 92*:6289–6293.

Melbye, M., Rabkin, C., Frisch, M., and Biggar, R.J. 1994. Changing patterns of anal cancer incidence in the United States, 1940-1989. *Am. J. Epidemiol. 139*:772–780.

Ogunbiyi, O.A., Scholefield, J.H., Smith, J.H., Polacarz, S.V., Rogers, K., and Sharp, F. 1993. Immunohistochemical analysis of p53 expression in anal squamous neoplasia. *J. Clin. Pathol. 46*:507–512.

Ryan, D.P., Compton, C.C., and Mayer, R.J. 2000. Carcinoma of the anal canal. *N. Engl. J. Med. 342*:792–800.

Sano, T., Oyama, T., Kashiwabara, K., Fukuda, T., and Nakajima, T. 1998. Expression status of p16 protein is associated with human papillomavirus oncogenic potential in cervical and genital lesions. *Am. J. Pathol. 153*:1741–1748.

Scheffner, M., Huibregtse, J.M., Vierstra, R.D., and Howley, P.M. 1993. The HPV-16 E6 and E6-AP complex functions as a ubiquitin-protein ligase in the ubiquitination of p53. *Cell 75*:495–505.

Schwartz, S.M., Daling, J.R., Shera, K.A., Madeleine, M.M., McKnight, B., Galloway, D.A., Porter, P.L., and McDougall, J.K. 2001. Human papillomavirus and prognosis of invasive cervical cancer: A population-based study. *J. Clin. Oncol. 19*:1906–1915.

Sherr, C.J., and McCormick, F. 2002. The RB and p53 pathways in cancer. *Cancer Cell 2*:103–112.

Sherr, C.J., and Roberts, J.M. 1999. CDK inhibitors: Positive and negative regulators of G$_1$-phase progression. *Genes Dev. 13*:1501–1512.

Shroyer, K.R., Brookes, C.G., Markham, N.E., and Shroyer, A.L. 1995. Detection of human papillomavirus in anorectal squamous cell carcinoma: Correlation with basaloid pattern of differentiation. *Am. J. Clin. Pathol. 104*:299–305.

Stoler, M.H. 2000. Human papillomaviruses and cervical neoplasia: A model for carcinogenesis. *Int. J. Gynecol. Pathol. 19*:16–28.

Tanum, G., and Holm, R. 1996. Anal carcinoma: A clinical approach to p53 and RB gene proteins. *Oncology 53*:369–373.

Vincent-Salomon, A., de la Rochefordiere, A., Salmon, R., Validire, P., Zafrani, B., and Sastre-Garau, X. 1996. Frequent association of human papillomavirus 16 and 18 DNA with anal squamous cell and basaloid carcinoma. *Mod. Pathol. 9*:614–620.

von Knebel Doeberitz, M. 2002. New markers for cervical dysplasia to visualise the genomic chaos created by aberrant oncogenic papillomavirus infections. *Eur. J. Cancer 38*:2229–2242.

Wong, C.S., Tsao, M.S., Sharma, V., Chapman, W.B., Pintilie, M., and Cummings, B.J. 1999. Prognostic role of p53 protein expression in epidermoid carcinoma of the anal canal. *Int. J. Radiat. Oncol. Biol. Phys. 45*:309–314.

Wynford-Thomas, D. 1992. p53 in tumour pathology: Can we trust immunocytochemistry? *J. Pathol. 166*:329–330.

Youk, E.G., Ku, J.L., and Park, J.G. 2001. Detection and typing of human papillomavirus in anal epidermoid carcinomas: Sequence variation in the E7 gene of human papillomavirus type 16. *Dis. Colon Rectum 44*:236–242.

zur Hausen, H. 2000. Papillomaviruses causing cancer: Evasion from host-cell control in early events in carcinogenesis. *J. Natl. Cancer Inst. 92*:690–698.

This Page Intentionally Left Blank

III

Prostate Carcinoma

This Page Intentionally Left Blank

1

Prostate Carcinoma: An Introduction

M.A. Hayat

Introduction

Prostate cancer is a very common malignancy in men, ranking second in cancer mortality exceeded only by lung cancer. The prostate gland is divided anatomically into four zones: anterior fibromuscular stroma, central zone, peripheral zone, and preprostatic region that includes the periurethal ducts and transition zone. The central zone is located at the base of the prostate and surrounds the ejaculatory ducts. Information on the histology of the central zone is important because of its frequency in prostate needle biopsy and radical prostatectomy specimens. Histologic features of this zone also distinguish it from high-grade prostatic intraepithelial neoplasia (PIN). Key features of the central zone histology include the presence of tall columnar cells with eosinophilic cytoplasm (Srodon and Epstein, 2002).

The development of prostate cancer depends on the strict balance between the rate of proliferation and programmed cell death (apoptosis). It is the most commonly diagnosed noncutaneous tumor and confers considerable morbidity and mortality to the general population of men. In recent years, prostate cancer has shown an approximately 3% annual increase worldwide. In American men this cancer is clinically diagnosed in one of every 11 men; one-third of those diagnosed will develop significant life-threatening disease. In 2000, an estimated 180,400 new patients were

diagnosed with prostate cancer and 31,900 deaths were attributed to this malignancy (American Cancer Society, 2001). The most important risk factors are age and ethnicity.

Prostate cancer is rare before age 40, but the rate of increase with aging is greater than that for any other cancer, peaking in men older than 80 years of age. This cancer, however, can be present in some men in their 30s and 40s and even in younger men. In the United States, the incidence of prostate cancer is significantly higher in African Americans than in white Americans and Asian Americans. This difference is discussed later in this chapter.

Unlike benign prostate hyperplasia or prostatitis, prostate cancer may not show symptoms in its early, curable stage, and therefore it is often diagnosed in the advanced stages of the disease. Prostate cancer poses other unique problems in terms of treatment and prognosis because of the frequent histologic heterogeneity encountered. In fact, this carcinoma is genetically multicentric and histologically multifocal. Both genetic and epigenetic events occur independently in intratumor foci, and hypermethylation-induced loss of gene function may be as critical as specific genetic mutations in prostate carcinogenesis.

Because of the poor success rate in the treatment of advanced prostate cancer, an intervention at an early stage may reduce the progression of small localized carcinoma to a large metastatic lesion, thereby

reducing disease-related deaths. The prostate specific antigen (PSA) test has enhanced the detection and awareness of this malignancy. The disagreement regarding the specificity of the PSA screening is discussed later in this chapter.

The relative increase in the incidence of prostate cancer is related primarily to progressive aging of the male population. Such an increase is also the result of widespread use of PSA testing and digital rectal examination, resulting in the detection of many more cancers at an early stage and of precursor lesion-like PINs. The increased incidence of both silent prostate cancer and precursor lesions also has increased the need for reliable prognostic indicators to identify clinically relevant tumors (which require aggressive treatment) and preneoplastic lesions (which will become invasive cancers) (Boccardo *et al.,* 2003). Some progress has been made to identify such prognostic indicators, which are summarized later.

Analysis of prostate cancer by comparative genomic hybridization and by whole-genome allelotyping indicates frequent loss of (part of) chromosome arms 6q, 8p, 10q, 13q, and 16q (Visakorpi *et al.,* 1995). Among these deletions, chromosome 6 alteration (proximal part) is most common. Recently, Verhagen *et al.* (2002) have carried out analysis of chromosome 6 aberrations in tumor cell lines and tumor tissue specimens. This study indicated that chromosome region 6q14-16 was deleted in ~50% of the prostate cancer specimens. This high percentage of loss emphasizes the importance of genes within this region. Thirty-five genes and candidate genes have been mapped within the 6q14-16 region. It should be noted that deletion of 6q is not unique for prostate cancer; for example, deletion of the long arm of this chromosome has been found in adult T-cell leukemia (Hatta *et al.,* 1999).

Benign Prostatic Hyperplasia

Benign prostatic hyperplasia (BPH) is defined as enlargement of the prostate gland. This is a common condition in aging men, and approximately one-fourth of those aged 50 years and older experience problems resulting directly or indirectly from BPH. In fact, BPH occurs in more than 70% of men age 70 years or older. As a result of its anatomic location, an enlarged prostate may cause pressure on the urethra, causing considerable morbidity through the lower urinary tract. This condition includes acute urinary retention (outflow obstruction), urinary tract infections, bladder stones, renal failure, and unintended adverse effect caused by medical or surgical attempts to treat the underlying condition (Clifford and Farmer, 2000).

However, not all cases of BPH are associated with lower urinary tract obstructive symptoms. Nevertheless, although BPH is not a lethal condition, it may have an adverse effect on quality of life and on psychologic general well-being. Histologically, BPH can be recognized in simple (enucleations and transurethral resections) and radical prostatectomy specimens. Hyperplasia is typically confined to the transition zone, although uncommon examples of modular hyperplasia within the peripheral zone have been reported (Kerley *et al.,* 1997).

The weight of the prostate gland in adult males varies between 11 g and 60 g (Foster, 2000). Hyperplastic prostate glands are increased in weight, with some glands exceeding 100 g. In the normal prostate, the ratio of stroma to glands to luminal parts is approximately 11:5:8. In BPH, these ratios are altered such that the stromal component increases out of proportion to the epithelium, yielding relationships on the order of 45:9:21 (Foster, 2000).

For many years, surgery (particularly transurethral resection of the prostate) was the only effective treatment for symptomatic BPH. However, surgery is accompanied by considerable morbidity and complications. Therefore, a number of less invasive alternatives were developed, which include use of α-blockers and 5α-reductase inhibitors, urethral stents, balloon dilation, hyperthermia, and thermotherapy (e.g., microwave, laser coagulation, and needle ablation). The common principle of these techniques is the use of heat energy causing coagulative necrosis of prostate tissue. One disadvantage of these treatments is that no tissue is recovered for the detection of incidental carcinomas. Also, the durability of their therapeutic effect has yet to be confirmed.

For the degree of symptom improvement, the surgical interventions are most effective, followed by α-blockers. However, substantial improvement can also be seen for patients who do not undergo active treatment. In follow-up studies (1–4 years) of untreated BPH, the majority of patients remained stable, whereas 22–33% showed deterioration and 8–26% reported spontaneous improvement (Barry *et al*., 1997). These and other data show considerable variability in individual patients. Treatment choice, depending on the symptoms, is left to the physician's judgment and patient's preference. For a detailed review of this subject, the reader is referred to Stoevelaar and McDonnell (2001).

Prostatic Intraepithelial Neoplasia

The condition PIN is characterized by intraluminal proliferation of epithelial cells and can be divided into

high-grade and low-grade lesions. High-grade prostate intraepithelial neoplasia (HPIN) is the most likely precursor of prostate cancer. A PIN can be used as a predictive marker for this cancer, and HPIN is especially useful in this regard because it is the earliest accepted stage in prostatic carcinogenesis. Patients with HPIN are diagnosed by a prostate needle core biopsy, and if left untreated, the condition of such patients could progress to invasive carcinoma. Can chromosomal instability increase the predictive value of HPIN diagnosis? Interphase fluorescence *in situ* hybridization (FISH) studies show that although no single numeric chromosomal abnormality could be assigned as a predictor of HPIN progression to carcinoma, the overall level of numeric chromosomal abnormalities reveals a trend of elevation in patients with HPIN whose condition subsequently may progress to carcinoma (Al-Maghrabi *et al.,* 2002).

Prostate Cancer in African American Men

In the United States, the incidence of prostate cancer is significantly higher in African Americans than in white people or Asian Americans. In fact, the incidence and mortality for this cancer is approximately twofold higher in African Americans than in whites; the former experience the highest rates worldwide. African Americans are more likely to develop prostate cancer at an earlier age with a higher grade and stage of the disease, and have a higher rate of metastasis and poorer survival than white Americans. These racial differences result from differences in genetics, diet, body size, socioeconomic status, lifestyle, physical activity, and access to medical care (Whittemore and Ross, 1997).

Although molecular mechanisms responsible for racial differences in prostate tumors are not completely known, some information to elucidate these mechanisms is available. Differences in gene promoter hypermethylation may potentially underlie racial differences in prostate cancer pathogenesis (Woodson *et al.*, 2003). Deoxyribonucleic acid (DNA) hypermethylation is an aberrant methylation often found in neoplastic cells. Promoter regions of genes that are normally unmethylated become methylated in cancer cells. This occurs by the covalent binding of a methyl group to the 5′-cytosine of the dinucleotide pair (CpG), resulting in silencing the expression of tumor suppressor and other regulator genes.

In 2003 Woodson *et al.* studied differences in DNA methylation of three genes (*GSTP1*, *CD44*, and *E-cadherin*) in prostate cancers from African Americans and whites in the United States. In this study no racial difference was found in the prevalence of GSTP1 hypermethylation, *CD44* hypermethylation was significantly increased in black men, and *E-cadherin* was not hypermethylated in any of the tumor specimens. The gene *GSTP1* hypermethylation is specific to cancer and occurs early in carcinogenesis, but it is not detected in BPH and normal prostatic tissues. *E-cadherin* and *CD44* inactivation occurs later in prostate cancer development.

An interesting hypothesis is that the uptake of zinc may be different in racial groups. This suggestion is based on the evidence that normal prostate contains high amounts of free zinc ions that are secreted into the seminal fluid. Long-term low serum concentration of zinc deprives the prostate gland of its essential source of vital trace mineral ingredient, resulting in prostate metaplasia and neoplasia. In other words, the loss of the ability to retain normal intracellular levels of zinc is an important factor in the development and progression of prostate cancer.

Rishi *et al.* (2003), using reverse transcription (RT) *in situ* polymerase chain reaction (PCR) method, have compared the relative levels of expression of the two zinc transporters (hZ1P1 and hZ1P2) in African Americans and white people. This study showed a lower degree of the expression of these transporters in African American patients compared with that in age-matched white men. The observation that the uptake of zinc may be different in racial groups can be used as a preventive maneuver for some people. The advantage is that dietary zinc supplements are relatively nontoxic. Further examination of this concept in larger studies is needed. Relatively increased rates of PSA progression after undergoing radical prostatectomy in African American men are discussed elsewhere in this chapter.

Prostate Specific Antigen

A PSA is a 33-kDa glycoprotein and a member of the kallikrein family of serine proteases. It is encoded by the *KLK3* gene located on chromosome 19q13.4. It is secreted by normal, hyperplastic, and cancerous prostatic epithelia. One of its roles is to degrade high–molecular-weight seminal vesicle proteins that otherwise would form seminal coagulates. Alternatively, it appears to be involved in prostate growth regulation by cleaving insulin-like growth factor–binding proteins and thereby increasing the bioavailability of these factors. Elevated levels of PSA occur in patient sera in cases of prostate cancer, BPH, and prostatitis.

A PSA is generally the most valuable tool for early detection, staging, and monitoring of patients with

prostate cancer. Because PSA is almost organ specific (but not cancer specific), its increased concentrations are found in patients with prostate cancer. It is a sensitive indicator of tumor burden and is regarded as a reliable surrogate marker for survival and disease progression for patients with androgen-independent prostate cancer. The pretreatment serum PSA level correlates with tumor burden and is an independent prognostic variable for disease-free survival. The widespread use of serum PSA levels in the follow-up of patients undergoing definitive treatment for prostate cancer has allowed earlier detection of recurrent disease (Banerjee *et al.,* 2002). In fact, one explanation for the rapid increase in the incidence of prostate cancer diagnosis has been the advent of PSA screening. Screening for PSA has led to earlier detection of this cancer even in younger men.

An early detection of prostate cancer is essential for a curative cancer therapy, and PSA is a powerful serum marker for the early diagnosis of this carcinoma. In fact, the diagnosis of prostate cancer increased dramatically in the late 1980s and early 1990s as a result of earlier diagnosis without any symptoms through the increased use of PSA screening. Since 1992 there has been a steady decrease in the incidence rate of prostate cancer, and mortality rates have declined ~2.5% annually between 1992 and 1996 (American Cancer Society, 2000). However, caution is warranted in reaching the diagnosis based on the serum PSA test in all cases because false-positive test results are observed in nonmalignant, prostatic diseases (such as BPH), inflammation, and after manipulations, which limit the clinical utility of PSA. In addition, not all patients with prostate cancer have elevated serum PSA concentrations (Catalona, 1996).

It should be noted that PSA is not specific for the prostate gland and is also found in breast, ovary, endometrial, kidney, adrenal, and salivary gland cancer tissues. Gene expression and production of PSA protein in nonprostatic tissues, as is true in the prostate gland, are regulated by steroid hormones via their receptors. Androgens, glucocorticoids, mineralocorticoids, and progestins up-regulate the PSA production. However, estrogens down-regulate indirectly the PSA production induced by androgens (Zarghami *et al.,* 1997). Androgen, progesterone, and estrogen receptors are also found in colorectal cancer tissues (Korenaga *et al.,* 1997). It has been demonstrated that serum total and free PSA levels are higher in women with colorectal carcinoma than those in healthy women; this difference is especially marked with respect to free PSA levels (Duraker *et al.,* 2002). This and other evidence indicates a relationship between the presence of steroid hormones and prostate and other cancers.

Although the role of PSA in normal and neoplastic prostate cells is not well understood, the information on the regulatory mechanism responsible for PSA expression in prostate cancer cells could be useful for constructing a tissue-specific vector to target metastatic cells (Yu *et al.,* 2001). The PSA promoter contains two sequence elements, one of ~550 base pairs in length flanking the PSA gene, and the other of ~800 base pairs located 3.9 kb upstream of the former.

A PSA forms complexes with protease inhibitors such as α_1-antichymotrypsin (ACT). Approximately 70–90% of the total PSA (tPSA) in serum is complexed with ACT, whereas 10–30% of tPSA is unbound and called free PSA (fPSA). Patients with prostate cancer have lower proportions of fPSA than those in patients with BPH. The ratio of fPSA/tPSA shows reliable discrimination between prostate cancer and BPH. The ACT-PSA assay developed by Lein *et al.* (2000) has demonstrated that ACT-PSA determination alone or the ACT-PSA/tPSA ratio did not improve the diagnostic power compared with that obtained with tPSA and fPSA/tPSA ratio.

According to Hoffman *et al.* (2002), in general the free-to-total PSA ratio results have only a modest effect on revising the probability for cancer. They suggest using multiple cutpoints for the free-to-total PSA ratio, which should increase the discriminating power of the test. The generalization of these data can be further improved by stratifying the free-to-total PSA ratio results by patient demographic and clinical characteristics.

Normal human prostate secretory epithelial cells and almost all prostatic adenocarcinomas produce PSA. The concentration of serum PSA correlates with the age of the patient, size of the prostate without demonstrable prostate carcinoma, volume of carcinoma in both primary and metastatic prostate carcinoma, and the stage of prostate cancer. The presumed mechanism, for the observation that serum PSA levels in men with prostate carcinoma are significantly higher (as an average) than levels in men without carcinoma demonstrable by prostate needle biopsies, is that PSA leaks from malignant cells and glands into the interstitium and thus into the blood instead of being confined to the ductal excretory system (Swanson *et al.,* 2001).

Nevertheless, the correlation between serum PSA and stage of cancer is less than accurate, and the variance is high in patients with prostate carcinoma. It is also known that a major limitation of the serum PSA test is lack of prostate cancer sensitivity and specificity, especially in the intermediate range (gray zone) of PSA detection (4–10 ng/ml). In this range the specificity in differentiating prostate cancer from BPH is only 25–30%. Such lack of sensitivity can lead to

many unnecessary prostate biopsies, particularly for gray zone values. This debate on the degree of lack of specificity emanates from the fact that PSA production is influenced by many factors, including the volume of benign epithelium, the grade of adenocarcinoma, inflammation status of the tissue, androgen levels of individuals, growth factors, extracellular matrix, and ethnicity differences. Furthermore, a decline in PSA levels may not correlate with decrease in tumor growth *in vivo.* These limitations of the PSA test are evidence of the need to identify reliable biomarkers if improvement in diagnosis and prognosis of prostate cancer are to be realized.

The variance mentioned earlier, including low specificity of total PSA for the detection of this disease, has led to the development of various approaches to improve the diagnostic accuracy of serum PSA levels. These modifications include the use of age or race-specific reference ranges, PSA density, PSA transition zone density, and PSA velocity or doubling time. Prostate specific antigen density is the serum PSA value divided by the ultrasound-determined volume of the prostate (Lin *et al.,* 1998). Prostate specific antigen velocity is the rate of increase in serum PSA concentrations throughout time (Carter *et al.,* 1995).

Measurements of different molecular forms of PSA also improve the specificity over total PSA alone (Chan, 1999; Stenman *et al.,* 1991). The molecular forms of PSA that are produced in different ratios in patients with prostate cancer than in those without demonstrable cancer include complexed PSA and fPSA. The difference in ratios between fPSA and tPSA has also been reported to discriminate between benign prostatic hyperplasia and prostate cancer (Lein *et al.,* 2000). Use of the percentage of fPSA in the total PSA range of 4–10 µg/L can eliminate ~20–25% of unnecessary biopsies (Catalona *et al.,* 1998).

In 1994, an artificial neural network (ANN) was used for improving the prostate detection rate (Snow *et al*., 1994). This model includes clinically relevant data and can add substantial information for detecting prostate cancer while avoiding unnecessary biopsies in patients with benign prostates. Stephan *et al.* (2002a; 2002b) developed a diagnostic algorithm based on both immunoassay data and clinical data of age, prostate volume, and digital rectal examination status for enhancing the performance of percentage of fPSA for further reducing the number of unnecessary biopsies within the tPSA range of 2–10 µg/L and for reducing the number of repeat biopsies at 10.1–20.0 µg/L total PSA. However, the hope that the aforementioned modifications would provide more accurate information than that obtained from simple serum PSA has been only partially fulfilled.

Diagnostic Indicators

To understand the mechanism responsible for prostate cancer development, various avenues have been explored: mutations in oncogenes (e.g., *Ras*), tumor suppressor genes (e.g., *p53* and *PTEN*), and androgen receptor and androgen signals. The mechanism of the genetic changes in hormone-refractory growth, however, remains unclear. It is important, therefore, to identify genes related to prostate cancer, which are up- or down-regulated. Such information is important for the diagnosis and therapy of this cancer. The achievement of this goal can be attempted by investigating prostate cancer–specific gene expression. Differential display method is useful for the isolation of up- or down-regulated genes by comparing the expression of messenger ribonucleic acids (mRNAs).

Differential display method has been used for detecting several novel genes in prostate cancer cells; examples are listed later. The *DD3* gene is highly expressed in prostate cancer (Bussemakers *et al.,* 1999). The differentiation-related gene 1 (*Drg 1*) is markedly up-regulated by androgens in prostate adenocarcinoma cells (Ulrix *et al*., 1999). Genes *PAG-1* and *GAGE-7* are expressed in the LNCaP prostatic adenocarcinoma cells (Chen *et al.,* 1998). Using differential display method, Ishiguro *et al.* (2003) identified a specific up-regulated gene encoding a 55 kDa nuclear matrix protein (nmt55) in human prostate cancer tissues. This protein and androgen receptor showed a positive correlation. Also, the transcriptional activity of the PSA promoter was up-regulated by nmt55. It means that PSA is activated by nmt55 expression, which also shows a positive correlation with androgen receptor expression. This information suggests that nmt55 has a cause-and-effect relationship with hormone-dependent and hormone-independent prostate cancer growth. Loss of nmt55 expression in estrogen receptor–negative human breast cancer has been reported (Traish *et al.,* 1997). Further information is awaited to clarify biologic function of nmt55 in prostate cancer growth.

Alterations of important protein pathways, including loss of prostate secretory granules and disruption of the prostatic secretory pathway, have been identified as early events in malignancy. Using immunohistochemistry and Western Blotting, Meehan *et al.* (2002) have mapped the differences in protein expression between normal and malignant human prostate tissues. They identified 20 proteins that were lost in malignant transformation; these proteins included PSA, ACT, haptoglobin, and lactoylglutathione lyase. The expression of NEDD8, calponin, and follistatin-related protein was found in normal prostate tissues. The role of

these functional proteins in normal prostate and their loss or reduced expression in prostate malignancy requires further investigation. Other prostate biomarkers are discussed next.

Prostate Cancer Biomarkers

Although prostate cancer is fairly well characterized at the histopathologic level, the molecular mechanisms leading to cell transformation are beginning to be elucidated. Identification of key players in the process of cellular transformation is a crucial step toward our understanding of prostate cancer progression and toward the development of new, effective cancer therapies. There is an urgent need to determine such players (prostate cancer biomarkers). The use of inherited genetic markers to evaluate prostate cancer outcome could enhance our ability to identify those men who are more likely to develop clinically significant prostate cancer and to intervene in these men to reduce morbidity resulting from this disease. A number of prognostic biomarkers, with varying degrees of specificity, have been determined. Most of these markers, including those at the experimental stage, are summarized as follows and enumerated in Table 9. The expression of most of them can be assessed with reliability in formalin-fixed and paraffin-embedded prostate tissue specimens using immunohistochemistry (IHC) and FISH.

It should be noted that some of these markers (e.g., p53, PTEN, and HER-2) are involved not only in prostate cancer but also in other cancers such as breast cancer and ovarian cancer. Despite the multitargets of a biomarker, immunohistochemical specificity can be obtained by using monoclonal antibodies. Immuno-histochemical expression of many of these markers is reported in other chapters of Part III in this volume. A list of inherited genotypes characteristic of prostate cancers has been presented by Rebbeck (2002).

Prostate Specific Antigen

Expression of PSA is associated with prostate cancer, tumor stage and progression, tumor responsiveness, and patient age and race. However, the precise relationship between tumor volume and the level of serum marker remains elusive for several reasons. A quantity of PSA is released not only from tumor but also from normal tissues, and its level increases with the size of the prostate and with patient age. Also, the amount of PSA present in a tumor seems to vary with the histologic grade of the tumor. In addition, there is an indirect and unspecified relationship between the prostate tissue

compartment and the serum compartment (Vollmer and Humphrey, 2003).

Two aspects of the concentration of the serum marker at any time need to be considered: how much marker is entering the serum and how much is leaving. Understanding the relationship between tumor volume and serum concentration of PSA requires consideration of the kinetics of how PSA moves through the aforementioned compartments. Despite these limitations, PSA testing in asymptomatic men is increasing, mainly because of its simplicity and noninvasiveness as a screening tool. However, with respect to reduction of prostate cancer mortality, no conclusion can be drawn yet regarding the beneficial effects of PSA screening. Advantages and limitations of PSA testing have been discussed earlier in this chapter.

Kallikrein Genes

Besides PSA, other structurally similar kallikrein genes are also related to prostate cancer. Human glandular Kallikrein (hK2 encoded by the *KLK2* gene) is an emerging tumor marker for prostate cancer. The gene *KLK4* is highly expressed in the prostate and is under steroid hormonal regulation in prostate and breast cancer cell lines (Nelson *et al.,* 1999). Human kallikrein gene 5 (*KLK5*) is a relatively recently cloned member of this family, and is located adjacent to *KLK4, KLK2,* and *PSA* genes, sharing a high degree of homology with these kallikreins (Yousef *et al.,* 1999). In 2002, using the quantitative RT-PCR LightCycler technology, Yousef *et al.* (2002) compared the expression of *KLK5* in histologically confirmed normal and prostate cancer tissues. This study shows that *KLK5* expression (at the mRNA level) is lower in prostate cancer tissues compared to their normal counterparts. Lowest levels of expression are found in late stage tumors, indicating down-regulation of this gene in prostate cancer and inhibitory effect on cell growth. Also, a significant negative correlation is found between Gleason score and *KLK5* expression. This gene is also differentially regulated in ovarian cancer (Kim *et al*., 2001). The aforementioned results suggest that *KLK5* is a potential prognostic marker in prostate cancer, whose expression is negatively correlated with cancer aggressiveness.

Epidermal Growth Factor Receptor

The epidermal growth factor receptor (EGFR) and its ligands (epidermal growth factor [EGF] and transforming growth factor alpha [TGFα]) play a critical role during tumorigenesis of the prostate gland. The stimulation of EGFR by its ligands, through autocrine

Table 9 Prostate Cancer Biomarkers 285

[a]Alpha-methylacyl-coenzyme racemase	Kunju *et al.* (2003)
[a]Androgen	Vagundova *et al.* (2004)
[a]Androgen receptor cofactors	This volume
[a]34βE12	Halushka *et al.* (2004)
[a]Bcl-2	Augustin *et al.* (2003)
[a]Bin1/amphiphysin II	This volume
Calpain-2	Mamoune *et al.* (2003); this volume
CD44	Gao *et al.* (1997)
[a]Chromogranin A	Augustin *et al.* (2003)
[a]CXCR4 protein	Sun *et al.* (2003)
[a]Cyclooxygenase	Tanji *et al.* (2002)
CYP1B1 gene	Chang *et al.* (2003)
Cytochrome P-450c17α (CYP17)	Gsur *et al.* (2000)
DD3 gene	Verhaegh *et al.* (2000)
E-cadherin	Köksal *et al.* (2003)
[a]Estrogen	del Carmen *et al.* (2003)
[a]Estrogen receptor-binding fragment-associated gene 9 (EBAG9)	Takahashi *et al.* (2003)
GGN	Platz *et al.* (1998)
[a]Glandular kallikrein 2	This volume
[a]Hepsin protein	Dhanasekaran *et al.* (2001)
[a]HER-2 oncogene	Oxley *et al.* (2002); this volume
[a]Hyaluronan	Simpson *et al.* (2002)
Insulin-like growth factor β	Woodson *et al.* (2003)
KAL1	Dong *et al.* (1996)
Kallikrein gene 5	Yousef *et al.* (2002)
[a]Ki-67	Rubin *et al.* (2002b)
Lipoxygenase	Gao *et al.* (1995)
Mammary tumor 8 kDa protein	Grzmil *et al.* (2004)
Maspin gene	Umekita *et al.* (2002)
[a]MUC18	This volume
Myc	Buttyan *et al.* (1987)
Nuclear matrix proteins	Boccardo *et al.* (2003)
[a]P14	This volume
[a]P16	This volume
P21	Martinez *et al.* (2002)
[a]P504s/α-methylacyl CoA racemase	This volume
P53 gene	van Veldhuizen *et al.* (1993)
P65 gene	Balcerczak *et al.* (2003)
PMEPA1	Xu *et al.* (2003)
[a]Progesterone	del Carmen *et al.* (2003)
Prostate specific antigen (PSA)	Sokoll *et al.* (1997); Xue *et al.* (2000)
Prostate specific membrane antigen	Israeli *et al.* (1997)
Prostate stem cell antigen	Reiter *et al.* (1998)
[a]PSA	Augustin *et al.* (2003)
PSA-positive circulating prostate cells	Tombal *et al.* (2003)
PSGR	Xu *et al.* (2000)
PTEN	George *et al.* (2001); Suzuki *et al.* (1998)
PTX1 gene	Liu *et al.* (2003)

Table 9 Prostate Cancer Biomarkers—cont'd

[a]PTX1 protein	Kwok *et al.* (2001)
Ras oncogene	Konishi *et al.* (1997)
[a]Retinoid X receptors	This volume
[a]Somatostatin receptors	This volume
SRD5A2 gene	Luo *et al.* (2003)
[a]Thromboxane synthase	Nie *et al.* (2004)
Transcription factor early growth response-1 (Egr-1)	Baron *et al.* (2003)
[a]Transforming growth factor-β1 (TGF-β1)	Park *et al.* (2003); Song *et al.* (2003)
[a]trp-p8	Henshall *et al.* (2003a)
[a]Vimentin	Singh *et al.* (2003)
[a]WIFI	Wissmann *et al.* (2003)
[a]ZnT4	Henshall *et al.* (2003b)

[a] These biomarkers have been identified with immunohistochemistry or *in situ* hybridization, or both.

and paracrine pathways, leads to the activation of different signaling cascades involving mitogen-activated protein kinase (MAPK) response element. A study by Mimeault *et al.* (2003) indicates that the blockade of EGFR tyrosine kinase and protein kinase A (PKA) signaling pathways by specific inhibitors (PD153035) leads to a synergistic inhibition of EGF- and serum-stimulated growth of prostatic cancer cells. This inhibitory pathway, which leads to an arrest of the growth and apoptotic death of metastatic prostate cancer cells, represents a promising adjuvant combinatory strategy for the development of more effective treatments against invasive and recurrent forms of prostate cancer.

Guanosine Phosphate Binding Protein Receptors

Guanosine phosphate binding protein (G protein)-coupled receptors are expressed in malignant prostate cells and normal cells. They mediate growth of androgen-independent prostate cancer cells *in vitro* via activation of the ERK pathway (Kue and Daaka, 2000). Expression of these receptors (e.g., prostate-specific gene receptor) is more increased in advanced prostate cancer specimens than in benign tissues (Xu *et al.,* 2000). Enzymes regulating the expression of G protein-coupled receptors (lysophosphatidic acyl transferase) are also increased in advanced prostate cancer (Faas *et al.*, 2001). Kue *et al.* (2002) have shown that lysophosphatidic acid and EGF cooperate to induce mitogenic signaling in prostate cancer cells in metalloproteinase-regulated activation of the ERK pathway. These and other data suggest that characterization

of signal transduction pathways leading to ERK activation can be important for the identification of targets effective in the treatment of prostate malignancy.

Early Growth Response-1 Factor

Another biomarker for prostate cancer is transcription factor early growth response-1 (Egr-1). This nuclear phosphoprotein of 5q kDa is the prototype member of a family of transcription factors, which includes at least four members (Egr-1 to Egr-4). The biomarker Egr-1 is induced by many different stimuli ranging from growth factors and cytokines to stress signals such as ultraviolet light, ionizing radiation, apoptosis-promoting factors, and injury. Thus, it is involved in a variety of cell processes including growth, differentiation, neurite outgrowth, wound healing, apoptosis, and survival.

The biomarker Egr-1 is present at much higher levels in all the human prostate tumors tested so far, as opposed to normal cells (Eid *et al.,* 1998). It promotes growth of prostate cancer cells, and blocking of its function impedes cancer progression. This suggestion is supported by the observation that the mRNA encoding Egr-1 is expressed at much higher levels in prostate adenocarcinoma compared with those in normal tissues. This is also true in the case of protein levels (Thigpen *et al.,* 1996). Moreover, the levels of protein expression correlate with Gleason scores and inversely correlate with the degree of differentiation of carcinoma cells (Eid *et al.,* 1998). In addition, NAB2, which represses the transcriptional activity of Egr-1, is down-regulated in primary prostate carcinomas

(Abdulkadir *et al.,* 2001). Both up-regulation of Egr-1 and loss of its repressor NAB2 may play roles in determining the level of Egr-1 activity in prostate cancer. Baron *et al*. (2003) developed a series of antisense oligonucleotides that specifically block Egr-1 expression at the levels of both mRNA and protein. Colony formation and growth of cancer cell lines in soft agar were inhibited by the antisense oligonucleotide. This and other studies clearly indicate that Egr-1 plays a functional role in the transformed phenotype and may represent a valid target for prostate cancer therapy.

Cyclooxygenase

Cyclooxygenase (COX) is a key enzyme in the conversion of arachidonic acid to prostaglandins and other eicosanoids. Two forms of COX have been characterized: an ubiquitously expressed form (COX1) and a mitogen-inducible form (COX2). Both have similar activities. Cyclooxygenases are generally up-regulated in carcinogenesis. Immunohistochemical studies have demonstrated the expression of COX in normal as well as cancerous prostate, suggesting its role in homeostasis and tumor development of the prostate (Tanji *et al.,* 2000). Expression of COX1 protein is found mainly in stromal cells of human prostate, with or without prostatic adenocarcinoma.

The constitutive expression of COX1 protein in stromal cells suggests its involvement in the actions of prostatic contractility. The finding that only poorly differentiated adenocarcinoma cells express COX1 protein suggests that this protein plays a vital role in the later stages of tumor development. COX specifically plays an important part in the regulation of angiogenesis associated with prostate tumor development. The possibility of new cancer treatment through a COX cascade is suggested.

REPS2/POB1

REPS2/POB1 is an EH domain-containing protein involved in signaling via Ra1Bp1 and plays a role in endocytosis of EGFRS. This protein is relatively highly expressed in androgen-dependent as compared to androgen-independent human prostate cancer cell lines (Oosterhoff *et al.,* 2003). Decreased expression of REPS2/POB1 during prostate cancer progression is thought to result in loss of control of growth factor signaling and, consequently, in loss of control of cell proliferation. Further information on the role of REPS2/POB1 in controlling prostate cancer progression will improve our understanding of androgen-independent tumor growth.

Tenascin

Tenascin has been proposed as a marker for the prostate invasive process. However, inconsistent results have been obtained when protein expression levels have been measured, possibly as a result of epitope masking. According to some studies, tenascin is involved in the maintenance of normal prostatic stromal-epithelial homeostasis and protects against the effects of neoplasia (Xue *et al.,* 1998). This view is supported by studies showing that tenascin is secreted by stromal cells and fibroblasts, but not by prostate cancer cells (Doi *et al.,* 1996). Similarly, some other studies have shown that patients with high tenascin expression levels have a better long-term survival than those with weak or absent tenascin expression (Iskaros *et al.,* 1997). In contrast, some other studies report that tenascin is secreted by cancer cells, and that the expression of this protein is required for stromal invasion (Yoshida *et al.,* 1999).

A study in 2003 indicates that tenascin is strongly expressed in the extracellular matrix and acinar basement membrane in normal and PIN tissues (Slater *et al.,* 2003). In prostate cancer tissue, tenascin expression does not correlate with Gleason score but is markedly deexpressed, whereas purinergic receptor and telomerase-associated protein expression is increased. It is important to note that decreased tenascin expression and increased expression of telomerase-associated protein and purinergic receptor are apparent before any histologic abnormalities become visible in the hematoxylin-eosin-stained sections. Therefore, the two latter proteins can be used as markers for early and developing prostate cancer. Tenascin expression can also be used as a marker of early neoplastic transformation, whereas E-cadherin is ineffective as a marker.

E-Cadherin

E-cadherin is a cancer invasion suppressor gene. It is mapped to chromosome 16q22.1, encoding a transmembrane 120-kDa glycoprotein belonging to the group of Ca^{2+}-dependent cell-to-cell adhesion molecules. E-cadherin has been studied as a potential marker for tumor progression. It is the prime mediator of intercellular adhesion in epithelial cells. Perturbation of E-cadherin–mediated cell adhesion is involved in tumor progression and metastasis. E-cadherin expression has been studied in formalin-fixed and paraffin-embedded surgical specimens from radical retropubic prostatectomies and cancomitant pelvic lymph node dissections; monoclonal antibody

HECD-1 was used in this study (Köksal *et al.,* 2002). Although any significant correlation between E-cadherin staining pattern and tumor invasion could not be demonstrated, aberrant staining patterns of this protein may be a significant predictor for disease recurrence following radical prostatectomies if supported by large-scale studies.

As is true in the case of tenascin, E-cadherin expression in cancers has been contradictory. It has been proposed that prostate cancer cells induce deexpression or loss of E-cadherin, which is associated with dedifferentiation, invasion, and metastasis (Bussemakers *et al.,* 2000). Conversely, some other studies have shown that E-cadherin expression is increased in metastatic prostate cancer (De Marzo *et al.,* 1999). A study in 2003 indicated that E-cadherin was a poor marker, so it was expressed in all lesions except prostatic carcinomas of the highest Gleason score (Slater *et al.,* 2003).

Nuclear Matrix Protein

In 1993, nuclear matrix protein patterns were determined in BPH and prostate cancer; this nuclear protein was referred to as PC-1 (Partin *et al.,* 1993). Changes in the proteic components of the nuclear matrix are associated with malignant transformations and thus have potential clinical applications (Hughes and Cohen, 1999). Subsequently, several other nuclear matrix proteins associated with prostate cancer were identified (Lakshmanan *et al.,* 1998). In 2003, nine tumor-associated nuclear matrix proteins were reported to be present in a significantly higher percentage in prostate cancer tissue specimens than in normal prostatic tissue adjacent to frankly neoplastic tissue (Boccardo *et al.*, 2003). Although the pattern of expression of these proteins can be associated with poor prognostic features of prostate cancer, the clinical usefulness of this determination is limited because of the complexity of the method. Also, the information obtained from these proteins does not significantly add to the prognostic information provided by the Gleason score. Nevertheless, changes in the structure and appearance of these nuclear matrix proteins are potentially important in understanding the process of tumorigenesis.

NKX3•1 and PTEN

Mouse models of prostate carcinogenesis based on the loss of function of genes known to be important for human cancer, including *NKX3•1* and *PTEN*, have been developed (Abate-Shen *et al.,* 2002). Another study has found that a majority of NKX3•1$^{+/-}$, PTEN$^{+/-}$ mice older than 1 year of age develop invasive adenocarcinoma that is frequently accompanied by metastases to lymph nodes (Abate-Shen *et al.,* 2003). This study also reports androgen independence of high-grade PIN lesions after androgen ablation of NKX3•1$^{+/-}$, PTEN$^{+/-}$ mice. (Adenocarcinoma of the prostate undergoes a characteristic progression from precursor lesions [e.g., PIN] to invasive carcinoma and ultimately to metastases.) These mice recapitulate key features of advanced prostate cancer and represent a useful model for investigating associated molecular mechanisms and for evaluating therapeutic approaches. However, these mice do not yet recapitulate all aspects of advanced prostate cancer.

Fatty Acid Synthase

Increased expression of fatty acid synthase (FAS) is one of the earliest and most common events in the development of prostatic cancer. FAS is a key metabolic enzyme that plays a central role in the *de novo* biosynthesis of fatty acids. One of the molecular changes reported in various cancers is overexpression of oncogenic antigen-519 (OA-519). This gene is the marker designation for a protein sharing epitope with a haptoglobin-related protein (Hrp), found to be overexpressed in breast cancer with a high risk of tumor recurrence (Kuhajda *et al.,* 1989). This protein corresponds to FAS. The preferential expression of FAS in cancer cells has lead to its use as a potential target for anti-neoplastic therapy. Inhibition of FAS activity induces apoptosis in FAS-overexpressing cancer cell lines (Pizer *et al.,* 1998).

Immunohistochemistry using frozen needle biopsies has been used for further examining the link between OA-519/FAS expression and prostate cancer development and progression (Swinnen *et al.*, 2002). Needle biopsies have the advantage of being taken and processed more rapidly, avoiding tissue deterioration. Furthermore, tissue antigen preservation by snap freezing is superior to formalin fixation and paraffin embedding. This study demonstrated increased immunohistochemical signal very early in prostate cancer development and was further elevated in invasive cancer. An epigenetic basis of increased FAS expression in cancer cells is proposed.

Endoglin

Endoglin gene is identified as a regulator of cell adhesion, motility, and invasion in human prostate. Loss of expression of this gene is thought to be associated with cancer progression, at least *in vitro* (Liu *et al.,* 2002). Endoglin is known to bind transforming growth factor beta (TGFβ) and has the potential to

interact with integrin proteins. Integrins, TGFβ, and integrin-associated protein (focal adhesion kinase) have been associated with prostate cancer progression. Because changes in adhesion and motility are pre-requisites for development of prostate cancer metastasis, it is important to evaluate endoglin's role *in vivo* in metastasis.

MOST-1

Preliminary studies indicate that a novel human *MOST-1* (*C8orf17*) gene exhibits tissue-specific expression and is amplified in high-grade cancers of the prostate and breast (Tan *et al.,* 2003). In this study the gene was isolated via rapid amplification of complementary DNA (cDNA) ends (RACE) and cycle sequencing. *MOST-1* gene is located on chromosome 8q24.2, which is noteworthy because this region is known to be amplified mainly in breast and prostate cancers and also in ovarian, testicular, renal, bladder, and colorectal tumors (e.g., Knuutila *et al.,* 1999; Tsuchiya *et al.,* 2002). Tan *et al.* (2003) have performed quantitative PCR experiments for determining MOST-1 RNA and DNA values in frozen breast cancer tissues and archival prostate tumors compared with normal tissues. These findings suggest that this gene may serve as a potential marker of prostate and breast tumor progression. Possible role of the gene in cellular differentiation, proliferation, and tumorigenesis is implied.

MMR Protein

DNA mismatch repair (MMR) is involved in the post-replication correction of errors resulting from misincorporated nucleotides or DNA slippage during DNA synthesis. Reduction or loss of MMR protein expression in human prostate cancer cell lines and some primary prostate tumors is known. Immunohistochemical analysis of formalin-fixed and paraffin-embedded human prostate tumors has shown reduction or loss of MMR protein (MLH1, MSH2, and PMS2) expression in the epithelium of the tumor compared to normal adjacent prostate tissue (Chen *et al.,* 2003). Poorly differentiated tumors show greater loss of MSH2 and PMS2 than that in the well-differentiated tumors. Defects in MMR may also result in microsatellite instability in the secondary genes in prostate cancer (Chen *et al*., 2003). Based on these results, it is suggested that loss of MMR function can produce microsatellite instability and target some secondary genes containing microsatellites in their coding regions. Thus, these events may play a role in the development of human prostate cancer.

BRG1

Tumor suppressor genes in chromosomal region 19p13 have been purported to be present in hereditary and sporadic prostate cancer. The *BRG1* gene in this region is one of the possible candidates. Valdman *et al.* (2003) have carried out a complete mutation analysis of all *BRG1* exons in tumor and constitutional DNA samples from 21 patients with prostate cancer. This study indicates absence of common *BRG1* mutations in prostate cancer.

Glucose Transporter Protein

Glucose transporter proteins (GLUT1 and GLUT12) are expressed in human prostate carcinoma cells. Transport of polar glucose molecules across the non-polar membrane depends on these proteins, and GLUT12 is potentially a regulator of glucose utilization in malignant cells. Increased glucose consumption is a basic characteristic of malignant cells. Glucose uptake is increased in prostate carcinoma cells, and higher rates of glucose consumption are required for the rapid proliferation of both androgen-dependent and androgen-independent prostate cancer cells (Singh *et al.,* 1999). A large study of human breast carcinomas has also demonstrated that GLUT1 expression is increased in these cells with a higher grade and proliferative activity (Younes *et al.,* 1995).

Immunohistochemistry, RT-PCR, Western Blot analysis, and immunoflourescence studies indicate GLUT1 and GLUT12 expression in human prostate carcinoma cells (Chandler *et al*., 2002). However, evaluation of a large number of prostate biopsy specimens needs to be carried out to obtain a better understanding of the expression of these proteins in benign and malignant prostate tissues. It is important to determine whether an increase in tumor aggression is accompanied by an alteration in the expression of these proteins. A significant increase in GLUT1 and GLUT12 expression may prove to be a useful diagnostic marker of early prostate malignancy.

8p21-22

Many chromosomal and genetic anomalies are involved in the initiation and progression of prostate cancer. Specifically, loss of 8p21-22 is a common alteration in this cancer (Bova *et al.,* 1993). The percentage of 8p22 is up to 69% and 100% in clinically organ-confined and metastatic prostate cancers, respectively. Up to 50% of PIN lesions also show loss of 8p22. The commonly deleted region of 8p22 includes the *LPL* (lipoprotein lipase) gene, and this

region is thought to be responsible for the initiation or early event in prostate tumorigenesis. Another relevant genetic alteration in prostate cancer is 8q24 over-representation (Nupponen *et al.,* 1998). This anomaly is commonly found in advanced, metastatic, and androgen-independent prostate cancer. The frequency of this anomaly is 8% and 21% in primary tumors and metastatic lymph nodes, respectively (Jenkins *et al.,* 1997). This region contains the oncogene C-Myc that is known to regulate cell proliferation and apoptosis.

The FISH procedure has been used for demonstrating overrepresentation of 8q24, especially concurrent with 8p22 loss (Sato *et al.,* 1999). Dual probe FISH was used for evaluating the copy number changes of 8p22, centromere 8, and 8q24 in a large cohort of patients who had pathologic organ-confined prostate cancer (Tsuchiya *et al.*, 2002). This and other studies suggest that loss of 8q22 is associated with poorer clinical progression-free survival of patients, and overrepresentation of 8q24 is associated with an increased risk of disease progression in organ-confined prostate cancer.

WIFI Protein

The evolutionary conserved protein WIFI binds to Wnt proteins and inhibits their activities. It is known that different Wnt genes are up-regulated in various cancers, including breast, colorectal, and prostate carcinomas and malignant melanoma. Immunohistochemical analysis, using a polyclonal antibody, has revealed strong cytoplasmic perinuclear WIFI expression in normal epithelial cells of the prostate, breast, lung, and urinary bladder (Wissmann *et al.,* 2003). However, strong reduction of WIFI expression is found in prostate carcinoma. No significant association is found between WIFI down-regulation and prostate tumor stage or grade, indicating that loss of WIFI expression may be an early event in tumorigenesis in this tissue. However, down-regulation of WIFI is correlated with higher tumor stage in urinary bladder. Use of microdissection is recommended because the fraction of tumor cells is small and often less than 30% of the entire cell mass. In prostate cancer, one can distinguish different tumor foci exhibiting different differentiation and grades within the same patient.

Alpha-Methylacyl-Coenzyme A Racemase

Alpha-methylacyl-coenzyme A racemase (AMACR) has been identified as a leading candidate gene by differential display and cDNA substraction microarray analysis and is consistently expressed in prostate cancer but not in benign prostate tissue (Rubin *et al.,* 2002a). It encodes a cytoplasmic protein involved in

β-oxidation of branched chain fatty acids. Recent immunohistochemical studies, using monoclonal antibody P504S, demonstrate detection of AMACR in prostate cancer (Kunju *et al.,* 2003). These studies also indicate low sensitivity for detecting foamy prostate cancer. Most high-grade PIN shows diffuse moderate staining. Based on these results, it is recommended to use P504S in conjunction with basal cell markers (34βE12 and p63) and morphologic examination.

Thromboxane Synthase

Human prostate cancer cells express enzymatically active thromboxane synthase (TxS) that is involved in cell motility. Immunohistochemical analysis of tumor specimens reveals that expression of TxS is weak or absent in normal differentiated luminal or secretory cells, significantly elevated in less differentiated or advanced prostate tumors, and markedly increased in tumors with perineural invasion (Nie *et al.,* 2004). It is suggested that this enzyme may contribute to prostate cancer progression through modulating cell motility.

Arachidonate 12-Lipoxygenase

Alterations in arachidonate 12-lipoxygenase (12-LOX) expression or activity have been reported in various carcinomas including prostate carcinoma. It was reported in 2003 that increased expression of 12-LOX in PC-3 cells caused a significant change in cell adhesiveness, spreading, motility, and invasiveness (Nie *et al.,* 2003). A clinical study of prostate carcinoma specimens has found the elevation of 12-LOX mRNA expression frequently in advanced-stage, high-grade prostate cancer, suggesting that such expression or activity may be associated with carcinoma progression and invasion *in vivo*. Based on the available information, it is suggested that an increase in 12-LOX expression enhances the metastatic potential of human prostate cancer cells. The expression of 12-LOX has been detected in a growing list of tumors, especially of epithelial origin, such as prostate cancer, pancreatic cancer, breast cancer, lung cancer, and gastric cancer.

Mast Cells

Some information is available indicating a relationship between the distribution and number of mast cells and prostate tumors. Mast cells are widely distributed in connective tissues adjacent to vessels and nerves and also beneath the epithelial surfaces. Among many other functions, mast cells play a role in the pathogenesis of chronic inflammation and fibrosis (Yakanaka *et al.,* 2000). Some evidence is available affirming the

presence of mast cells in various malignancies and the role of these cells in tumor growth (Sari *et al.*, 1999). Peripheral distribution of mast cells around a variety of human tumors suggests a protective role of them against tumors (Fisher and Fisher, 1965). Aydin *et al.* (2002) determined the utility of mast cell number in evaluating benign and malignant prostate lesions and ascertaining whether there are variations in the number of mast cells with the Gleason grade. This study indicates absence or low presence of mast cells in prostate adenocarcinoma compared with BPH. However, further studies using a larger series are needed to substantiate the use of mast cell count as a diagnostic tool.

Steroid Hormones

Epidemiologic evidence suggests that steroid hormones are involved as initiators or promoters in prostate carcinogenesis, and the hormonal factors are associated with some prostate cancer risk factors. The intraautocrine-perinatal period and maternal estrogen and testosterone levels have also been proposed to be of etiologic importance (Shibata and Minn, 2000). Although prostate tumors grow androgen dependently or androgen independently, androgens act as strong tumor promoters via androgen receptor (Ar)-mediated mechanisms to enhance the carcinogenic activity of strong endogenous genotoxic carcinogens, including reactive estrogen metabolites and estrogen- and prostatitis-generated reactive oxygen species (Medeiros *et al.*, 2003). These processes are modulated by a variety of environmental factors, such as diet, and by genetic determinants, including hereditary susceptibility genes and polymorphic genes that encode receptors and enzymes involved in the metabolism and action of steroid hormones.

As explained earlier, steroid hormones are important determinants in the development of prostate cancer because the prostate is an androgen-regulated organ. Therefore, polymorphism in genes involved in androgen metabolism influences prostate cancer risk. The cytochrome P-450c17α (*CYP17*) gene is the rate-limiting step in androgen biosynthesis. The gene maps to chromosome 10q24.3. A polymorphic T→c substitution creates a recognition site for the restriction enzyme MspAl (Carey *et al.,* 1994). MspAl digestion of a PCR fragment permits the designation of the wild-type (A1) and the polymorphic allele (A2). The A2 allele may result in an increased rate of transcription, and elevated steroid hormone levels may be associated with the risk of prostate cancer (Kadonaga *et al.*, 1986). The important role of CYP17 enzyme in mediating androgen biosynthesis makes it an important

candidate for a susceptibility gene for prostate cancer. A study in 2000 also indicates that the CYP17 polymorphism is a useful biomarker for this cancer (Gsur *et al.,* 2000).

Estrogen receptor–binding fragment-associated gene 9 (*EBAG9*) is a primary estrogen-responsive gene from MCF-7 human breast cancer cells (Watanabe *et al.,* 1998). This gene is also abundantly expressed in the prostate cancer cells compared with the normal epithelial cells. Strong and diffuse immunostaining is found in the cytoplasm of prostatic cancerous tissue samples (Takahashi *et al.*, 2003). The gene *EBAG9/RCAS1* plays an important role in prostate cancer progression via an immune escape system. (RCAS1 is a receptor-binding cancer antigen expressed on SiSo cells; it is a cancer cell surface antigen implicated in immune escape [Nakashima *et al.,* 1999].) Expression of *EBAG9* significantly correlates with advanced prostate cancer and high Gleason score. Furthermore, positive EBAG9 immunoreactivity strongly correlates with poor PSA failure-free survival.

The transition from androgen-dependent to androgen-independent growth during prostate cancer progression is a serious problem because the androgen-independent tumors are incurable. One possible mechanism responsible for this transition is a switch from androgens to growth factors as primary regulators of prostate cancer cell proliferation. Examples of such growth factors are epidermal growth factor, insulin-like growth factors, and fibroblast growth factors. These autocrine factors stimulate growth of advanced, androgen-independent prostate cancer (Russell *et al.,* 1998).

Treatment of Prostate Cancer: A Summary

Prostate cancer is among the most common causes of death because no effective therapeutic treatment allows the abrogation of the progression of localized prostate caner to advanced, invasive forms of malignancies. Our understanding of the molecular genetic changes responsible for the progression of prostate cancer remains at an early stage because this cancer exhibits both intertumor and intratumor genotypic and phenotypic heterogeneity that complicates molecular and histopathologic assessment and outcome prediction.

Knowledge of the factors responsible for initiation and progression of prostate cancer remains incomplete, although androgens are the primary contributors to the disease. Androgen action in prostate cancer and in normal prostate gland is mediated by activation of the androgen receptor, a ligand-controlled nuclear transcription factor. Although prostate cancer grows

primarily in a hormone (androgen)-dependent manner, most patients show hormone-independent growth after several years of hormone therapy.

Primary treatment modalities for early (nonmetastatic) prostate cancer include radical prostatectomy, external-beam radiation therapy, cryotherapy, and brachytherapy (radioactive seed implants). Most men develop severe, permanent erectile dysfunction after any local treatment and enduring urinary incontinence or bowel symptoms, depending on the treatment modality. Approximately more than two decades ago it was reported that avoiding transection of periprostatic neurovascular bundles reduced the previous certainty of post-prostatectomy impotence (Walsh *et al.*, 1982), and so the frequency of this operation increased sixfold from 1984 to 1990 (Lu-Yao *et al.*, 1991). Subsequently, the enthusiasm for surgery has dampened, especially for older men, and dissemination of the percutaneous technique for delivering radiation to the prostate through brachytherapy has become popular.

However, during the last decade physicians began to treat men with asymptomatic early and advanced prostate cancer with androgen deprivation therapy (ADT) (Wasson *et al.*, 1998). Androgen ablation therapy is achieved by surgical or chemical castration of the patient. Although certain prostate cancer cells are sensitive to the effects of androgen deprivation therapies and chemotherapy, other metastatic prostatic cancer cell types acquire multiple oncogenic phenotypes that confer to them resistance to ionizing radiation and most of the anticarcinogenic agents. Patients treated with ADT may develop reduced physical role functioning and vitality, breast swelling, and hot flashes, and they are more than twice as likely to become impotent. Men treated with ADT also may develop palpable tumors, more poorly differentiated tumors, and baseline PSA values higher than 10 ng/dl (Potosky *et al.*, 2002). Prolonged survival has been reported, under certain conditions, when adjuvant ADT is followed by external-beam radiation for locally advanced prostate cancer (Bolla *et al.*, 1999). Many of these treatments invariably fail and the cancer reappears. For example, cancer reappears as androgen-insensitive lesions, suggesting that other factors also contribute to the growth of the prostate cancer; some of such factors are summarized later and elsewhere in this chapter.

Peptide growth factors, such as epidermal growth factor (EGF), induce mitogenesis of the prostate by activating intracellular growth signal networks, including the MAP kinase family of proteins. Malignant prostate specimens have been shown to contain elevated levels of specific activated MAP kinases (the extracellular signal-regulated kinases 1 and 2 [ERK] compared to those in benign tissue)

(Price *et al.,* 1999). Activated ERKs are most prevalent in advanced stage tumors and tumors that have recurred after androgen ablation therapy. Inhibition of ERK activation abrogates peptide growth factor –mediated proliferation of androgen-independent prostate cancer cells. This and other evidence suggests a potential role of these enzymes in the progression of prostate cancer.

The use of screening tools to detect prostate cancer at an early stage has beneficial effects on an individual's prognosis. However, the intense use of these screening modalities also detects tumors that may have a relatively benign course and for which intensive treatment is not necessary. In addition, unlike most cancers, a fairly large proportion of prostate tumors exist without producing symptoms. This fact is supported by the evidence that the prevalence of prostate cancer in autopsied men with no clinical evidence of disease is substantial depending on the age of the man. It should be noted that a substantial portion of PSA-detected cancers are biologically not aggressive and should probably not be treated. At present, however, it is not possible to predict accurately which cancers need treatment. Because advanced prostate cancer is resistant to hormone therapy, radiation, and conventional chemotherapy, new strategies for treatment are needed. A better understanding of the molecular mechanisms involved in this cancer should result in determining reliable prognostic factors and effective therapeutic regimens for metastatic prostate cancer.

As Talcott (2002) has aptly pointed out, prostate cancer provides an example of a central paradox in medicine–the more a patient appears to require treatment, the less successful treatment is likely to be. The treatment choices in early prostate cancer are less heroic than those faced by critically ill patients, but even in the former the diagnosis is chilling, the choices are complex and difficult, and the consequences are enduring. Better and prompt information from randomized clinical trials is deservedly needed to help patients make the decisions. Molecular genetics can play a key role in this effort.

References

Abate-Shen, C., and Shen, M.M. 2002. Mouse models of prostate carcinogenesis. *Trend Genet. 18*:S1–S5. Review.

Abate-Shen, C., Banach-Petrosky, W.A., Sun, X., Economides, K.D., Desai, N., Gregg, J.P., Borowsky, A.D., Cardiff, R.D., and Shen, M.M. 2003. PTEN mutant mice develop invasive prostate adenocarcinoma and lymph node metastases. *Cancer Res. 63*:3886–3890.

Abdulkadir, S.A., Carbone, J.M., Naughton, C.K., Humphrey, P.A., Catolona, W.J., and Milbrandt, J. 2001. Frequent and early loss

of the EGR1 corepressor NAB2 in human prostate carcinoma. *Human Pathol. 32*:935–939.

Al-Maghrabi, J., Vorobyova, L., Toi, A., Chapman, W., Zielenska, M., and Squire, J.A. 2002. Identification of numerical chromosomal changes detected by interphase fluorescence in situ hybridization in highgrade prostate intraepithelial neoplasia as a predictor of carcinoma. *Arch. Pathol. Lab. Med. 126*:165–169.

Augustin, H., Hammerer, P.G., Graefen, M., Palisaar, J., Daghofer, F., Huland, H., and Erbersdobler, A. 2003. Characterization of biomolecular profiles in primary high-grade prostate cancer treated by radical prostatectomy. *J. Cancer Res. Clin. Oncol. 129*:662–668.

Aydin, O., Dusmez, D., Cinel, L., Doruk, E., and Kanik, A. 2002. Immunohistological Analysis of mast cell numbers in the intratumoral and peritumoral regions of prostate carcinoma compared to benign prostatic hyperplasia. *Pathol. Res. Prac. 198*:261–271.

Balcerczak, E., Mirowski, M., Sasor, A., and Wierzbicki, R. 2003. Expression of p65, DD3 and C-erbB2 genes in prostate cancer. *Neoplasma 50*:97–101.

Banerjee, M., Powell, I.S., George, J., Biswas, D., Bianco, F., and Severson, R.K. 2002. Prostate specific antigen progression after radical prostatectomy in African-American men versus White men. *Cancer 94*:2577–2583.

Baron, V., Gregorio, G.D., Krones-Herzig, A., Virolle, T., Calogero, A., Urcis, R., and Mercola, D. 2003. Inhibition of Egr-1 expression reverses transformation of prostate cancer cells in vitro and in vivo. *Oncogene 22*:4194–4204.

Barry, M.J., Fowler, F.J. Jr., Bin, L., Pitts, J.C. 3rd., Harris, C.J., and Mulley, A.G. Jr. 1997. The natural history of patients with benign prostatic hyperplasia as diagnosed by North American urologists. *J. Urol. 157*:10–15.

Boccardo, F., Rubagotti, A., Carmignani, G., Romagnoli, A., Nicolo, G., Barboro, P., Parodi, S., Patrone, E., and Balbi, C. 2003. Nuclear matrix proteins changes in cancerous prostate tissues and their prognostic value in clinically localized prostate cancer. *Prostate 55*:259–264.

Bolla, M., Gonzalez, D., Warde, P., Dubois, J.B., Mirimanoff, R.O., Storme, G., Bermier, J., Kuten, A., Sternberg, C., Gil, T., Collette, L., and Pierart, M. 1997. Improved survival in patients with locally advanced prostate cancer treated with radiotherapy and goserelin. *N. Engl. J. Med. 337*:295–300.

Bova, G.S., Carter, B.S., Bussemakers, M.J., Emi, M., Fujiwara, Y., Kyprianou, N., Jacobs, S.C., Robinson, J.C., Epstein, J.I., Walsh, P.C., and Isaacs, W.B. 1993. Homozygous deletion and frequent allelic loss of chromosome 8p22 loci in human prostate cancer. *Cancer Res. 53*:3869–3873.

Bussemakers, M.J., van Bokhoven, A., Tomita, K., Jansen, C.F., and Schalken, J.A. 2000. Complex cadherin expression in human prostate cancer cells. *Int. J. Cancer 85*:446–450.

Bussemakers, M.J., van Bokhoven, A., Verhaegh, G.W., Smit, F.K., Karthaus, H.F., Schalken, J.A., Debruyne, F.M., Ru, N., and Isaacs, W.B. 1999. DD3: A new prostate-specific gene, highly overexpressed in prostate cancer. *Cancer Res. 59*:5975–5979.

Buttyan, R., Sawczuk, I.S., Benson, M.C., Siegal, J.D., and Olsson, C.A. 1987. Enhanced expression of the c-myc protooncogene in high-grade human prostate cancers. *Prostate 11*:327–337.

Carey, A.H., Waterworth, D., Patel, K., White, D., Little, J., Novelli, P., Franks, S., and Williamson, R. 1994. Polycystic ovaries and premature male pattern baldness are associated with one allele of the steroid metabolism gene. *Hum. Mol. Genet. 3*:1873–1876.

Carter, H.B., Pearson, J.D., Waclawiw, Z., Metter, E.J., Chan, D.W., Guess, H.A., and Walsh, P.C. 1995. Prostate-specific antigen variability in men without prostate cancer: Effect of sampling interval on prostate-specific antigen velocity. *Urology 45*:591–596.

Catalona, W.J. 1996. Clinical utility of measurements of free and total prostrate-specific antigen (PSA): A review. *Prostate 7*:65–69.

Catalona, W.J., Partin, A.W., Slawin, K.M., Brawer, M.K., Flanigan, R.C., Patel, A., Richie, J.P., deKernion, J.B., Walsh, P.C., Scardino, P.T., Lange, P.H., Subong, E.N., Parson, R.E., Gasior, G.H., Loveland, K.G., and Southwick, P.C. 1998. Use of the percentage of free prostate-specific antigen to enhance differentiation of prostate cancer from benign prostatic disease: A prospective multicenter clinical trial. *JAMA 279*:1542–1547.

Chan, D.W. 1999. Prostate specific antigen: Advances and challenges. *Clin. Chem. 45*:755–756.

Chandler, J.D., Williams, E.D., Slavin, J.L., Best, J.D., and Rogers, S. 2002. Expression and localization of GLUT 1 and GLUT 12 in prostate carcinoma. *Cancer 97*:2035–2042.

Chang, B.L., Zheng, S.L., Isaacs, S.D., Turner, A.R., Hawkins, G.A., Wiley, K.E., Bleecker, E.R., Walsh, P.C., Meyers, D.A., Isaacs, W.B., and Xu, J. 2003. Polymorphisms in the CYP1B1 gene are associated with increased risk of prostate cancer. *Br. J. Cancer 89*:1524–1529.

Chen, M.E., Lin, S.H., Chung, L.W., and Sikes, R.A. 1998. Isolation and characterization of PAGE-1 and GAGE-7. New genes expressed in the LNCaP prostate cancer progression model that share homology with melanoma-associated antigens. *J. Biol. Chem. 273*:17618–17625.

Chen, Y., Wang, J., Fraig, M.M., Henderson, K., Bissada, N.K., Watson, D.K., and Schweinfest, C.W. 2003. Alterations in PMS2, MSH2 and MLH1 expression in human prostate cancer. *Int. J. Oncol. 22*:1033–1043.

Clifford, G.M., and Farmer, R.D. 2000. Medical therapy for benign prostatic hyperplasia: A review of the literature. *Eur. Urol. 38*:2–19.

del Carmen, M.G., Sehder, A.E.S., Fader, A.N., Zahurak, M.L., Richardson, M., Fruehauf, J.P., Montz, F.J., and Bristow, R.E. 2003. Endometriosis-associated ovarian carcinoma. *Cancer 98*:1658–1663.

De Marzo, A.M., Knudsen, B., Chan-Tack, K., and Epstein, J.I. 1999. E-cadherin expression as a marker of tumour aggressiveness in routinely processed radical prostatectomy specimens. *Urology 53*:707–713.

Dhanasekaren, S.M., Barrette, T.R., Ghosh, D., Shah, R., Varambally, S., Kurachi, K., Pienta, K.J., Rubin, M.A., and Chinnalyan, A.M. 2001. Delineation of prognostic biomarkers in prostate cancer. *Nature 412*:822–826.

Doi, D., Araki, T., and Asano, G. 1996. Immunohistochemical localization of tenasin, estrogen receptor and transforming growth factor-Beta 1 in human endometrial carcinoma. *Gynocol. Obstet. Invest. 41*:61–66.

Dong, J.T., Suzuki, H., Pin, S.S., Bova, G.S., Schalken, J.A., Isaacs, W.B., Barrett, J.C., and Isaccs, J.T. 1996. Downregulation of the KAI1 metastasis suppressor gene during the progression of human prostatic cancer infrequently involves gene mutation or allelic loss. *Cancer Res. 56*:4387–4390.

Duraker, N., Can, D., and Parilti, M. 2002. Measurement of serum total and free prostate-specific antigen in women with colorectal carcinoma. *Br. J. Cancer 86*:203–206.

Eid, M.A., Kumar, M.V., Iczkowski, K.A., Bostwick, D.G., and Tindall, D.J. 1998. Expression of early growth response genes in human prostate cancer. *Cancer Res. 58*:2461–2468.

Faas, F.H., Dang, A.Q., White, J., Schaefer, R., and Johnson, D. 2001. Increased prostatic lysophosphatidylcholine acyltransferase activity in human prostate cancer: A marker for malignancy. *J. Urol. 165*:463–468.

Fisher, E.R., and Fisher, B. 1965. Role of mast cells in tumor growth. *Arch. Pathol. 79*:185–191.

Foster, C.S. 2000. Pathology of benign prostatic hyperplasia. *Prostate Suppl. 9*:4–14.

Gao, X., Grignon, D.J., Chbihi, T., Zacharek, A., Chen, Y.Q., Saker, W., Porter, A.T., Crissman, J.D., Pontes, J.E., and Powell, I.J., Honn, K.V. 1995. Elevated 12-lipoxygenase mRNA expression correlates with advanced stage and poor differentiation of human prostate cancer. *Urology 46*:227–237.

Gao, A.C., Lou, W., Dong, J.T., and Isaccs, J.T. 1997. CD44 is a metastasis suppressor gene for prostatic cancer located on human chromosome 11p13. *Cancer Res. 57*:849–864.

George, D.J., Shepard, T.F., Ma, J., Giovannucci, E., Kantoff, P.W., and Stampfer, M.J. 2001. PTEN polymorphism (1VS4) is not associated with risk of prostate cancer. *Cancer Epidemiol. Biomark. Prev. 10*:411–412.

Grzmil, M., Voigt, S., Thelen, P., Hemmerlein, B., Helmke, K., and Burfeind, P. 2004. Up-regulated expression of the MAT-8 gene in prostate cancer and its siRNA-mediated inhibition of expression induces a decrease in proliferation of human prostate carcinoma cells. *Int. J. Oncol. 24*:97–105.

Gsur, A., Bernhofer, G., Hinteregger, S., Haidinger, G., Schatzl, G., Madersbacher, S., Marberger, M., Vutuc, C., and Micksche, M. 2000. A polymorphism in the CYP17 gene is associated with prostate cancer risk. *Int. J. Cancer 87*:434–437.

Halushka, M., Kahane, H., and Epstein, J.I. 2004. Negative 34βE12 staining in a small focus of atypical glands on prostate needle biopsy: A follow-up study of 332 cases. *Hum. Pathol. 35*:43–46.

Hatta, Y., Yamada, Y., Tomonaga, M., Miyoshi, I., Said, J.W., and Koeffler, H.P. 1999. Detailed deletion mapping of the long arm of chromosome 6 in adult T cell leukemia. *Blood 93*:613–616.

Henshall, S.M., Afar, D.E.H., Hiller, J., Horvath, L.G., Quinn, D.I., Rasiah, K.K., Gish, K., Willhite, D., Kench, J.G., Gardiner-Garden, M., Stricker, P.D., Scher, H.I., Grygiel, J.J., Agus, D.B., Mack, D.H., and Sutherland, R.L. 2003a. Survival analysis of genome-wide gene expression profiles of prostate cancers identifies new prognostic targets of disease relapse. *Cancer Res. 63*:4196–4203.

Henshall, S.M., Afar, D.E.H., Rasiah, K.K., Horvath, L.G., Gish, K., Caras, I., Ramakrishnan, V., Wong, M., Jeffry, U., Kench, J.G., Quinn, D.I., Turner, J.J., Delprado, W., Lee, C.-H., Golovsky, D., Brenner, P.C., O'Neill, G.F., Kooner, R., Stricker, P.D., Grygiel, J.J., Mack, D.H., and Sutherland, R.L. 2003b. Expression of the zinc transporter ZnT4 is decreased in the progression from early prostate disease to invasive prostate cancer. *Oncogene 22*:6005–6012.

Hoffman, R.M., Clanon, D.L., Chavez, M., and Peirce, J.C. 2002. Using multiple cutpoints for the free-to-total prostate specific antigen ratio improves the accuracy of prostate cancer detection. *Prostate 52*:150–158.

Hughes, J.H., and Cohen, M.B. 1999. Nuclear matrix proteins and their potential applications to diagnostic pathology. *Am. J. Clin. Pathol. 11*:267–274.

Ishiguro, H., Uemura, H., Fujinami, K., Ikeda N., Ohta, S., and Kubota, Y. 2003. 55 kDa nuclear matrix protein (nmt 55) mRNA is expressed in human prostate cancer tissue and is associated with the androgen receptor. *Int. J. Cancer 105*:26–32.

Iskaros, B.F., Tanaka, K.E., Hu, X., Kadish, A.S., and Steinberg, J.J. 1997. Morphologic pattern of tenascin as a diagnostic biomarker in colon cancer. *J. Surg. Oncol. 64*:98–101.

Israeli, R.S., Grob, M., and Tair, W.R. 1997. Prostate-specific membrane antigen and other prostatic tumor markers on the horizon. *Urol. Clin. North Am. 24*:439–450.

Jenkins, R.B., Qian, R.B., Lieber, M.M., and Bostwick, D.G. 1997. Detection of c-myc oncogene amplification and chromosomal anomalies in metastatic prostatic carcinoma. *Cancer Res. 57*:524–531.

Kadonaga, J.T., Jones, K.A., and Tjian, R. 1986. Promotor-specific activation of RNA poly-merase II transcription by SP1. *Trends Biochem. Sci. 11*:20–23.

Kerley, S.W., Corica, F.A., and Qian, J. 1997. Peripheral zone involvement by prostatic hyperplasia. *J. Urol. Pathol. 6*:87–94.

Kim, H., Scorilas, A., Katsaros, D., Massobrio, M., Yosuf, M.G., Fracchioli, S., Piccinno, R., Gordini, G., and Diamandis, E.P. 2001. Human kallikrein gene 5 (KLK 5) expression is an indicator of poor prognosis in ovarian cancer. *Br. J. Cancer 84*:643–650.

Knuutila, S., Aalto, Y., Autio, K., Björkqvist, A.-M., El-Rifai, W., Hemmer, S., Huhta, T., Kettunen, E., Kiuru-Kuhlefelt, S., Larramendy, M.L., Lushnikova, T., Monni, O., Pere, H., Tapper, J., Tarkkanen, M., Varis, A., Wasenius, V.-M., Wolf, M., and Zhu, Y. 1999. DNA copy number losses in human neoplasms. *Am. J. Pathol. 155*:683–694.

Köksal, I.T., Özcan, F., Kilicaslan, I., and Tefekli, A. 2002. Expression of E-Cadherin in prostate cancer in formalin-fixed, paraffin-embedded tissues: Correlation with pathological features. *Pathology 34*:233–238.

Konishi, N., Hiasa, Y., Tsuzuki, T., Tao, M., Enomoto, T., and Miller, G.J. 1997. Comparison of ras activation in prostate carcinoma in Japanese and American men. *Prostate 30*: 53–57.

Korenaga, D., Orita, H., Maekawa, S., Hasaka, H., Ikeda, T., and Sugimachi, K. 1997. Relationship between hormone receptor levels and cell-kinetics in human colorectal cancer. *Hepato-Gastroenterology 44*:78–83.

Kue, P.F., and Daaka, Y. 2000. Essential role of G proteins in prostate cancer cell growth and signaling. *J. Urol. 164*:2162–2167.

Kue, F.F., Taub, J.S., Harrington, L.B., Polakiewicz, R.D., Ullrich, A., and Daaka, Y. 2002. Lysophosphatidic acid-regulated mitogenic, ERK signaling in androgen-insensitive prostate cancer PC-3 cells. *Int. J. Cancer 102*:572–579.

Kuhajda, F.P., Piantadosi, S., and Pasternack, G.R. 1989. Haptoglobin-related protein (Hrp) epitopes in breast cancer as a predictor of recurrence of the disease. *N. Engl. J. Med. 321*:636–641.

Kunju, L.P., Rubin, M.A., Chinnaiyan, A.M., and Shah, R.B. 2003. Diagnostic usefulness of monoclonal antibody P504S in the workup of a typical prostatic glandular proliferations. *Am. J. Clin. Pathol. 120*:737–745.

Kwok, S.C.M., Liu, X., and Daskal, I. 2001. Molecular cloning, expression, localization, and gene organization of PTX1, a human nuclear protein that is downregulated in prostate cancer. *DNA Cell Biol. 20*:349–357.

Lakshmanan, Y., Subong, E.N., and Partin, A.W. 1998. Differential nuclear matrix protein expression in prostate cancers: Correlation with pathologic stage. *J. Urol. 159*:1354–1358.

Lein, M., Jung, K., Elgeti, U., Brux, B., Sinha, P., Schnorr, D., and Loening, S.A. 2000. Ratio of alpha 1-antichymotrypsin-prostate specific antigen to total prostate specific antigen in prostate cancer diagnosis. *Anticancer Res. 20*:4997–5002.

Lin, D.W., Gold, M.H., Ransom, S., Ellis, W.J., and Brawer, M.K. 1998. Transition zone prostate specific antigen: Lack of use in prediction of prostate carcinoma. *J. Urol. 160*:77–81.

Liu, Y., Jovanovic, B., Pins, M., Lee, C., and Bergan, R.C. 2002. Over expression of endoglin in human prostate cancer suppresses cell detachment, migration and invasion. *Oncogene 21*:8272–8281.

Liu, Y., Mangini, J., Saad, R., Silverman, A.R., Abell, A., Tung, M.Y., Graner, S.R., and Silverman, J.F. 2003. Diagnostic value of microtubule-associated protein-2 in markel cell carcinoma. *Appl. Immunohistochem. Mol. Morphol. 11*:326–329.

Lu-Yao, G.L., McLerran, D., Wasson, J., and Wennberg, J.E. 1993. An assessment of radical prostectomy: Time trends, geographic variation and outcomes. The Prostate Patients Outcomes Research Team. 1993. *JAMA 269*:2633–2636.

Mamoune, A., Luo, J.H., Lauffenburger, D.A., and Wells, A. 2003. Calpain-2 as a target for limiting prostate cancer invasion. *Cancer Res. 63*:4632–4640.

Martinez, L.A., Yang, J., Vazquez, E.S., Rodriguez-Vargas, Mdel, C., Olive, M., Hsieh, J.T., Logothetis, J.L., and Navone, N.M. 2002. p21 modulates threshold of apoptosis induced by DNA-damage and growth factor withdrawal in prostate cancer cells. *Carcinogenesis 23*:1289–1296.

Medeiros, R., Vasconcelos, A., Costa, S., Pinto, D., Morais, A., Oliveira, J., and Lopees, C. 2003. Steroid hormone genotypes ARStul and ER 325 are linked to the progression of human prostate cancer. *Cancer Genet. Cytogenet. 141*:91–96.

Meehan, K.L., Holland, J.W., and Dawkins, H.J. 2002. Proteomic analysis of normal and malignant prostate tissue to identify novel proteins lost in cancer. *Prostate 50*:54–63.

Mimeault, M., Pommery, N., and Hénichart, J.P. 2003. Synergistic antiproliferative and apoptotic effects induced by epidermal growth factor receptor and protein kinase A inhibitors in human prostatic cancer cell lines. *Int. J. Cancer 106*:116–124.

Nakashima, M., Sonoda, K., and Watanabe, T. 1999. Inhibition of cell growth and induction of apoptotic cell death by the human tumor-associated antigen RCAS1. *Nat. Med. 5*:938–942.

Nelson, P.S., Gan, L., Ferguson, C., Moss, P., Gelinas, R., Hood, L., and Wang, K. 1999. Molecular cloning and characterization of prostase, an androgen-regulated serine protease with prostate-restricted expression. *Proc. Natl. Acad. Sci. USA 96*:3114–3119.

Nie, D., Che, M., Zacharek, A., Qiao, Y., Li, L., Li, X., Lamberti, M., Tang, K., Cai, Y., Guo, Y., Grignon, D., and Honn, K.V. 2004. Differential expression of thromboxane synthase in prostate carcinoma. *Am. J. Pathol. 164*:429–439.

Nie, D., Nemeth, J., Qiao, Y., Zacharek, A., Li, L., Hanna, K., Tang, K., Hillman, G.G., Cher, M.L., Grignon, D.J., and Honn, K.V. 2003. Increased metastatic potential in human prostate carcinoma cells by overexpression of arachidonate 12-lipoxygenase. *Clin. Exp. Metast. 20*:657–663.

Nupponen, N., Hyytinen, E., Kallioniemi, A., and Visakorpi, T. 1998. Genetic alterations in prostate cancer cell lines detected by comparative genomic hybridization. *Cancer Genet. Cytogenet. 101*:53–57.

Oosterhoff, J.K., Penninkhof, F., Brinkmann, A.O., Grootegoed, J.A., and Blok, L.J. 2003. REPS2/POB1 is downregulated during human prostate cancer progression and inhibits growth factor signalling in prostate cells. *Oncogene 22*:2920–2925.

Oxley, J.D., Winkler, M.H., Gillatt, D.A., and Peat, D.S. 2002. HER-2/neu oncogene amplification in clinically localized prostate cancer. *J. Clin. Pathol. 55*:118–120.

Park, J.I., Lee, M.G., Cho, K., Park, B.J., Chae, K.S., Byun, D.S., Ryu, B.K., Park, Y.K., and Chi, S.G. 2003. Transforming growth factor-β1 activates interleukin-6 expression in prostate cancer cells through the synergistic collaboration of the Smad 2, p38-NF-kB, JNK, and Ras signaling pathways. *Oncogene 22*:4314–4332.

Partin, A.W., Getzenberg, R.H., Carmichael, M.J., Vindivich, D., Yoo, J., Epstein, J.H., and Coffey, D.S. 1993. Nuclear matrix protein patterns in human benign prostatic hyperplasia and prostate cancer. *Cancer Res. 53*:744–746.

Pizer, E.S., Chrest, F.J., DiGiuseppe, J.A., and Han, W.F. 1998. Pharmacological inhibitors of mammalian fatty acid synthase suppress DNA replication and induce apoptosis in tumor cell lines. *Cancer Res. 58*:4611–4615.

Platz, E.A., Giovannucci, E., Dahl, D.M., Krithivas, K., Hennekens, C.H., Brown, M., Stampfer, M.J., and Kantoff, P.W. 1998. The androgen receptor gene GGN microsatellite and prostate cancer risk. *Cancer Epidemiol. Biomark. Prev. 7*:379–384.

Potosky, A.L., Reeve, B.B., Clegg, L.X., Hoffman, R.M., Stephensen, R.A., Albertsen, P.C., Gilliland, F.D., and Stanford, J.L. 2002. Quality of life following localized prostate cancer treated initially with androgen deprivation therapy or no therapy. *J. Natl. Cancer Inst. 94*:430–437.

Price, D.T., Rocca, G.D., Guo, C., Ballo, M.S., Schwinn, D.A., and Luttrell, L.M. 1999. Activation of extracellular signal-regulated kinase in human prostate cancer. *J. Urol. 162*:1537–1542.

Rebbeck, T.R. 2002. Inherited genotype and prostate cancer outcomes. *Cancer Epidemiol. Biomark. Prev. 11*:945–952.

Reiter, R.E., Zhennen, G., Watabe, T., Thomas, G., Szigeti, K., Davis, E., Wahl, M., Nisitani, S., Yamashiro, J., Le Beau, M.M., Loda, M., and Witte, O.N. 1998. Prostate stem cell antigen: A cell surface marker overexpressed in prostate cancer. *Proc. Natl. Acad. Sci. 95*:1735–1740.

Rishi, A.K., Zhang, L., Boyanapalli, M., Wali, A., Mohammad, R.M., Yu, Y., Fontana, J.A., Hatfield, J.S., Dawson, M.I., Majumdar, A.P., and Reichert, U. 2003. Identification and characterization of a cell cycle and apoptosis regulatory protein-1 as a novel mediator of apoptosis signaling by retinoid CD437. *J. Biol. Chem. 278*:33422–33435.

Rubin, M.A., Dunn, R., Strawderman, M., and Pienta, K.J. 2002b. Tissue microarray sampling strategy for prostate cancer biomarker analysis. *Am. J. Surg. Pathol. 26*:312–319.

Rubin, M.A., Zhou, M., Dhanasekaran, S.M., Varambally, S., Barrette, T.R., Sando, M.G., Pienta, K.J., Gosh, D., and Chinnaiyan, A.M. 2002a. alpha-Methylacyl coenzyme A racemase as a tissue biomarker for prostate cancer. *JAMA. 287*:1662–1670.

Russel, P.J., Bennett, S., and Strieker, P. 1998. Growth factor involvement in progression of prostate cancer. *Clin. Chem. 44*:705–723.

Sari, A., Serel, T.A., Candir, Ö., Özturk, A., and Kosar, A. 1999. Mast cell variations in tumor tissue and with histopathological grading in specimens of prostatic adenocarcinoma. *BJU. International 84*:851–853.

Sato, K., Qian, J., Slezak, J.M., Lieber, M.M., Bostwick, D.J., Bergstralh, E.J., and Jenkins, R.B. 1999. Clinical significance of alterations of chromosome 8 in high-grade, advanced, non-metastatic prostate carcinoma. *J. Natl. Cancer Inst. 91*:1574–1580.

Shibata, A., and Minn, A.Y. 2000. Perinatal sex hormones and risk of breast and prostate cancers in adulthood. *Epidemiol. Rev. 22*:239–248.

Simpson, M.A., Wilson, C.M., and McCarthy, J.B. 2002. Inhibition of prostate tumor cell hyaluronan synthesis impairs subcutaneous growth and vascularization in immunocompromised mice. *Am. J. Pathol. 161*:849–857.

Singh, G., Lakkis, C.L., Laucirica, R., and Epner, D.E. 1999. Regulation of prostate cancer cell division by glucose. *J. Cell Physiol. 180*:431–438.

Singh, S., Sadacharan, S., Su, S., Belldegrun, A., Persad, S., and Singh, G. 2003. Overexpression of Vimentin: Role in the invasive phenotype in an androgen-independent model of prostate cancer. *Cancer Res. 63*:2306–2311.

Slater, M.D., Lauer, C., Gidley-Bird, A., and Barden, J.A. 2003. Markers for the development of early prostate cancer. *J. Pathol. 199*:368–377.

Sokoll, L.J., and Chan, D.W. 1997. Prostate-specific antigen: Its discovery and biochemical characteristics. *Urol. Clin. North Am. 24*:253–259.

Song, K., Cornelius, S.C., and Danielpour, D. 2003. Development and characterization of DP-153, a nontumorigenic prostatic cell line that undergoes malignant transformation by expression of dominant-negative transforming growth factor β receptor type II. *Cancer Res. 63*:4358–4367.

Srodon, M., and Epstein, J.I. 2002. Central zone histology of the prostate: A mimicker of high-grade prostatic intraepithelial neoplasia. *Hum. Pathol. 33*:518–523.

Stenman, U.H., Leinonen, J., Alfthan, H., Rannikko, S., Tuhkanen, K., and Alfthan, O. 1991. A complex between prostate-specific antigen and α1-antichymotrypsin is the major form of prostate-specific antigen in serum of patients with prostatic cancer: Assay of the complex improves clinical sensitivity for cancer. *Cancer Res. 51*:222–226.

Stephan, C., Cammann, H., Semjonow, A., Diamandis, E.P., Wymenga, L.F.A., Lein, M., Sinha, P., Loening, S.A., and Jung, K. 2002a. Multicenter evaluation of an artificial neural network to increase the prostate cancer detection rate and reduce unnecessary biopsies. *Clin. Chem. 48*:1279–1287.

Stephan, C., Jung, K., Cammann, H., Vogel, B., Brux, B., Kristiansen, G., Rudolph, B., Hauptmann, S., Lein, M., Schnorr, D., Sinha, P., and Loening, P.A. 2002b. An artificial neural network considerably improves the diagnostic power of percent free prostate specific antigen in prostate cancer diagnosis: Results of a five year prospective investigation. *Int. J. Cancer 99*:466–473.

Stoevelaar, H.J., and McDonnell, J. 2001. Changing therapeutic regimens in benign prostatic hyperplasia. *Pharmacoeconomics 19*:131–153.

Sun, Y.X., Wang, J., Shelburne, C.E., Lopatin, D.E., Chinnaiyan, A.M., Rubin, M.A., Pienta, K.J., and Taichman, R.S. 2003. Expression of CXCR4 and CXCL12 (SDF-1) in human prostate cancers (PCa) in vivo. *J. Cellular Biochem. 89*:462–473.

Suzuki, H., Freije, D., Nusskern, D.R., Okami, K., Cairns, P., Sidransky, D., Isaacs, W.B., and Bova, G.S. 1998. Interfocal heterogeneity of PTEN/MMAC1 gene alterations in multiple metastatic prostate cancer tissues. *Cancer Res. 58*:204–209.

Swanson, K.R., True, L.D., Lin, D.W., Buhler, K.R., Vessella, R., and Murray, J.D. 2001. A quantitative model for the dynamics of serum prostate-specific antigen as a marker for cancerous growth. *Am. J. Pathol. 158*:2195–2199.

Swinnen, J.V., Roskams, T., Joniau, S., Poppel, H.V., Oyen, R., Baert, L., Heyns, W., and Verhoeven, G. 2002. Overexpression of fatty acid synthase is an early and common event in the development of prostate cancer. *Int. J. Cancer 98*:19–22.

Takahashi, S., Urano, T., Tsuchiya, F., Fujimura, T., Kitamura, T., Ouchi, Y., Muramatsu, M., and Inoue, S. 2003. EBAG9/RCAS1 expression and its prognostic significance in prostatic cancer. *Int. J. Cancer 106*:310–315.

Talcott, J.A. 2002. Androgen deprivation as primary treatment for early prostate cancer: Should we "just do something"? *J. Natl. Cancer Inst. 94*:407–409.

Tan, J.M.M., Tock, E.P.C., and Chow, V.T.K. 2003. The novel human MOST-1 (C8 or F 17) gene exhibits tissue specific expression, maps to chromosome 8q 24.2, and is overexpressed/amplified in high grade cancers of the breast and prostate. *Mol. Pathol. 56*:109–115.

Tanji, N., Kikugawa, T., and Yokoyama, M. 2000. Immunohistochemical study of cyclooxygenases in prostatic adenocarcinoma: Relationship to apoptosis and bcl-2 protein. *Anticancer Res. 20*:2313–2320.

Thigpen, A.E., Cala, K.M., Guileyardo, J.M., Molberg, K.H., McConnell, J.D., and Russell, D.W. 1996. Increased expression of early growth response-1 messenger ribonucleic acid in prostatic adenocarcinoma. *J. Urol. 155*:975–981.

Tombal, B., Van Cangh, P.J., Loric, S., and Gala, J.L. 2003. Prognostic value of circulating prostate cells in patients with a rising PSA after radical prostatectomy. *Prostate 56*:163–170.

Traish, A.M., Huang, Y.H., Ashba, J., Pronovost, M., Pavao, M., McAneny, D.B., and Moreland, R.B. 1997. Loss of expression of a 55 kDa nuclear matrix protein (nm 55) in estrogen receptor-negative human breast cancer. *Diagn. Mol. Pathol. 6*: 2009–2021.

Tsuchiya, N., Slezak, J.M., Lieber, M.M., Bergstralh, E.J., and Jenkins, R.B. 2002. Clinical significance of alterations of chromosome 8 detected by fluorescence in situ hybridization analysis in pathologic organ-confined prostate cancer. *Genes Chromos. Cancer 34*:363–371.

Ulrix, W., Swinner, J.V., Heyns, W., and Verhoeven, G. 1999. The differentiation-related gene 1, Drg 1, is markedly upregulated by androgens in LNCaP prostatic adenocarcinoma cells. *FEBS Lett. 455*:23–26.

Umekita, Y., Ohi, Y., Sagara, Y., and Yoshida, H. 2002. Expression of maspin predicts poor prognosis in breast cancer patients. *Int. J. Cancer 100*:452–455.

Vagundova, M., Vagunda, I., Vermousek, I., and Rovny, A. 2003. Androgen receptor in prostate carcinoma: Immunohistochemical and ligand saturation analyses. *Neoplasma 50*:287–290.

Valdman, A., Nordenskjold, A., Fang, X., Naito, A., Al-Shukri, S., Larsson, C., Ekman, P., and Li, C. 2003. Mutation analysis of the BRG1 gene in prostate cancer clinical samples. *Int. J. Oncol. 22*:1003–1007.

van Veldhuizen, P.J., Sadasvian, R., Garcia, F., Austenfeld, M.S., and Stephens, R.L. 1993. Mutant p53 expression in prostate carcinoma. *Prostate 22*:22–30.

Verhagen, P.C., Hermans, K.G., Brok, M.O., van Weerden, W.M., Tilanus, M.G., De Weger, R.A., Boon, T.A., and Trapman, J. 2002. Deletion of chromosomal region 6q14-16 in prostate cancer. *Int. J. Cancer 102*:142–147.

Verhaegh, G.W., van Bokhoven, A., Smith, F., Schalken, J.A., Bussemakers, M.J.G. 2000. Isolation and characterization of the promoter of the human prostate-cancer-specific DD3 gene. *J. Biol. Chem. 275*:37496–37503.

Visakorpi, T., Kallioniemi, A.H., Syvanen, A.C., Hyytinen, E.R., Karhu, R., Tammela, T., Isola, J.J., and Kallioniemi, O.P. 1995. Genetic changes in primary and recurrent prostate cancer by comparative genomic hybridization. *Cancer Res. 55*:342–349.

Vollmer, R.T., and Humphrey, P.A. 2003. Tumor volume in prostate cancer and serum prostate-specific antigen. *Am. Soc. Clin. Pathol. 119*:80–89.

Walsh, P.C., and Donker, P.J. 1982. Impotence following radical prostectomy: Insight into etiology and prevention. *J. Urol. 128*: 492–497.

Wasson, J.H., Fowler, F.J., and Bary, M.J. 1998. Androgen deprivation therapy for asymptomatic advanced prostate cancer in prostate specific antigen era: A national survey of urologist beliefs and practices. *J. Urol. 159*:1993–1996; discussion 1996–1997.

Watanabe, T., Inoue, S., Hiroi, H., Orimo, A., Kawashima, H., and Muramatsu, M. 1998. Isolation of estrogen-responsive genes with a CpG island library. *Mol. Cell Biol. 18*:442–449.

Whittemore, A.S., and Ross, R.K. 1997. Why do African-American men suffer more prostate cancer? *J. Natl. Cancer Inst. 889*: 188–189.

Wissmann, C., Wild, P.J., Kaiser, S., Roepcke, S., Stoehr, R., Woenckhaus, M., Kristiansen, G., Hseieh, J.C., Hofstaedter, F., Hartmann, A., Knuechel, R., Rosenthal, A., and Pilarsky, C. 2003. WIFI, a component of the Wnt pathway, is downregulated in prostate, breast, lung, and bladder cancer. *J. Pathol. 201*: 204–212.

Woodson, K., Tangrea, J.A., Pollak, M., Copeland, T.D., Taylor, P.R., Virtamo, J., and Albanes, D. 2003. Serum insulin-like growth factor I: Tumor marker or etiologic factor? A prospective study of prostate cancer among Finnish men. *Cancer Res. 63*:3991–3994.

Xu, L.L., Shi, Y., Petrovics, G., Sun, C., Makarem, M., Zhang, W., Sesterhenn, I.A., McLeod, D.G., Sun, L., Moul, J.W., and Srivastava, S. 2003. PMEPA1, an androgen-regulated NEDD4-binding protein, exhibits cell growth inhibitory function and decreased expression during prostate cancer progression. *Cancer Res. 63*:4299–4304.

Xu, L.L., Stackhouse, B.G., Florence, K., Zhang, W., Shanmugam, N., Sesterhenn, I. A., Zou, Z., Srikantan, V., Augustus, M., Roschke, V., Carter, K., McLeod, D.G., Moul, J.W., Soppett, D., and Srivastava, S. 2000. PSGR, a novel prostate-specific gene with homology to a G protein-coupled receptor, is overexpressed in prostate cancer. *Cancer Res. 60*:6568–6572.

Xue, W., Irvine, R.A., Yu, M.C., Ross, R.K., Coetzee, G.A., and Ingles, S.A. 2000. Susceptibility to prostate cancer: Interaction between genotypes at the androgen receptor and prostate-specific antigen loci. *Cancer Res. 60*:839–841.

Xue, Y., Li, J., Latijnhouwers, M.A., Smedts, F., Umbas, R., Aalders, T.W., Debruyne, F.M., De La Rosette, J.J., and Schalken, J.A. 1998. Expression of periglandular tenascin-C and basement membrane laminin in normal prostate, benign prostatic hyperplasia and prostate carcinoma. *Br. J. Urol. 81*:844–851.

Yakanaka, K., Fujisawa, M., Tanaka, H., Okada, H., Arakawa, S., and Kamidono, S. 2000. Significance of human testicular mast cells and their subtypes in male infertility. *Hum. Reprod. 15*:1543–1547.

Yoshida, T., Yoshimura, E., Numata, H., Sakakura, Y., and Sakakura, T. 1999. Involvement of tenascin-C in proliferation and migration of laryngeal carcinoma cells. *Virchows Arch. 435*:496–500.

Younes, M., Brown, R.W., Modi, D.R., Fernandez, L., and Laucirica, R. 1995. GLUT1 expression in human breast carcinoma: Correlation with known prognostic markers. *Anticancer Res. 15*:2895–2898.

Yousef, G.M., Luo, L.Y., and Diamandis, E.P. 1999. Identification of novel human kallikrein-like genes on chromosome 19q13.3 - q13.4. *Anticancer Res. 19*:2843–2852.

Yousef, G.M., Scorilas, A., Chang, A., Rendl, L., Diamandis, M., Jung, K., and Diamandis, E.P. 2002. Down-regulation of the human kallikrein gene 5 (KLK5) in prostate cancer tissues. *Prostate 51*:126–132.

Yu, D., Chen, D., Chiu, C., Razmazma, B., Chow, Y.H., and Pang, S. 2001. Prostate-specific targeting using PSA promoter-based lentiviral vectors. *Cancer Gene Therapy 8*:628–635.

Zarghami, N., Grass, I., and Diamandis, E.P. 1997. Steroid hormone regulation of prostate-specific antigen gene expression in breast cancer. *Br. J. Cancer 75*:579–588.

This Page Intentionally Left Blank

2

Genetic Alterations in Prostate Cancer

Kotaro Kasahara, Takahiro Taguchi, Ichiro Yamasaki, and Taro Shuin

Introduction

Prostate cancer is one of the most common malignancies among men in Western countries. Hereditary and environmental factors play an important role in the development of prostate cancer, but the etiology and risk factors have remained largely obscure. Over the past decades, there has been a rapid increase in understanding of the basic molecular events underlying tumorigenesis. A useful working model is the hypothesis that cancer results from an accumulation of genetic changes that affect the expression of certain critical genes. Present knowledge supports the notion that most tumors, regardless of the site of origin, develop after the accumulation of multiple genetic alterations, and progression of a tumor depends on the successive acquisition of specific genetic abnormalities (Fearon *et al.,* 1990). Such genetic alterations are beginning to be known in prostate cancer (Kallioniemi *et al.,* 1996). Chromosomal aberrations in prostate cancer have been studied with several techniques, including both classical and molecular cytogenetics. This chapter describes the most common techniques of molecular cytogenetics, such as fluorescence *in situ* hybridization (FISH) and comparative genomic hybridization (CGH), and also considers their utility in the analysis of prostate cancer.

Fluorescence *in situ* Hybridization

The FISH method has become a widely used experimental technique over the past 10 years, particularly for application to gene mapping and molecular cytogenetics. Fluorochrome-labeled probes have been used most commonly instead of biotin or digoxigenin-labeled probes. In prostate cancer a recent alternative approach to evaluating genetic change has been the use of molecular cytogenetic technologies, such as FISH, to ascertain gross aneusomies (Kasahara *et al.,* 2001; Pinkel *et al.,* 1986; Van Dekken *et al*., 1990). In the following, we present the FISH protocol with centromere-specific probes that enable the copy number of chromosomes to be determined and also their numeric changes.

MATERIALS

1. Glass slides with chromosome or cell preparations.
2. Fluorochrome-labeled centromere-specific probes (Roche Diagnostics GmbH, Mannheim, Germany).
3. Hybridization solution (Sigma, St. Louis, H-7782).
4. Denaturation solution: 70% deionized formamide, 2× saline-sodium citrate (SSC); adjust to pH 7.0 with HCl.
5. Ice-cold ethanol: 70%, 90%, and 100%.
6. Wash solution A: 50% formamide, 2× SSC (17.53 g NaCl and 8.82 g sodium citrate), pH 7.0.
7. Wash solution B: 2× SSC; add deionized glass distilled water to make 1 L and adjust to pH 7.0.
8. Wash solution C: 1× saline: Tween-20 (ST20): 1 L 20× SSC and 2.5 ml Tween 20 (Sigma P-1397).
9. Vectashield (Vector Laboratories, Burlingame, CA).

Handbook of Immunohistochemistry and in situ Hybridization of Human Carcinomas,
Volume 2: Molecular Pathology, Colorectal Carcinoma, and Prostate Carcinoma

299

METHODS

1. Combine 1.0 µl of a centromere-specific probe and 9 µl of hybridization solution per slide.

2. Denature the probe mixture at 70°C for 5 min, then cool at 4°C immediately.

3. Fill a Coplin jar with the denaturation solution and place in a water bath heated to 70°C. Before denaturation, check the temperature of the denaturation solution with a thermometer inside the jar.

4. Transfer the slides to a Coplin jar with the denaturation solution for 2 min.

5. Transfer the slides immediately into Coplin jars with 70%, 90%, and 100% ice-cold ethanol (on ice) for 2 min each.

6. Pipette a 10 µl aliquot of the probe mixture onto the slide and then place an 18×18 mm coverslip on top of the hybridization droplet. Seal the edge of the coverslip with rubber cement and place the slides in a wet chamber.

7. Hybridize overnight in a moist chamber at 37°C.

8. Prewarm the washing solution A in a 45°C water bath.

9. After removal from the wet chamber, carefully remove the rubber cement and coverslip from the slides using forceps.

10. Transfer the slides into a Coplin jar containing washing solution A prewarmed to 45°C for 20 min.

11. Transfer the slides into a Coplin jar with washing solution B and incubate twice for 4 min at room temperature.

12. Wash the slides for 3–4 min at room temperature in washing solution C.

13. Remove each slide from the Coplin jar, add 20–30 µl of Vectashield, and cover the slide with a 22×40 mm coverslip. Store the slides at 4°C in the dark.

14. Observe with an epifluorescence photomicroscope using an fluoroscein isothiocyanate (FITC) and propidium iodide (PI) excitation filter cube.

Comparative Genomic Hybridization

An approach using FISH was introduced in 1992 that permits a comprehensive analysis of imbalanced chromosomal material of entire genome (Kallioniemi *et al*., 1992). This procedure, called comparative genomic hybridization (CGH), is a molecular cytogenetic approach with the potential to detect chromosomal imbalances in previously nonassessable specimens because only deoxyribonucleic acid (DNA) is required for the procedure. Therefore, many studies analyzing genetic alterations in tumor tissues have

been carried out. Furthermore, even minute amounts of DNA prepared from very few cells can be studied by combining CGH with universal polymerase chain reaction (PCR) amplification techniques (Speicher *et al.,* 1993). In CGH, tumor DNA is labeled with one fluorochrome and hybridized to normal metaphase chromosomes together with a normal DNA labeled with another fluorochrome. Differences in the DNA sequence copy number between the tumor and normal DNAs are seen as fluorescence intensity differences on the metaphase chromosomes. The theoretic limit for the detection of copy number changes by CGH is ~1–2 Mb. For example, a tenfold amplification of 100–200 kb regions should be detectable by CGH (Nupponen *et al.,* 2000). The CGH protocol is very similar to many standard FISH protocols. However, special care has to be taken at many points to obtain good CGH results. This protocol, with particular emphasis on the critical steps, is described as follows.

Probe Labeling

Nick translation is the most frequently used method for labeling DNA probes for FISH. The only difference refers to the length of the labeled probe that is optimal for CGH experiments. As a standard procedure, test DNA might be labeled with fluorescein-dUTP, whereas control DNA is labeled with rhodamine-dUTP.

MATERIALS

1. Nick translation system (GIBCOBRL 18160-010).

2. DNA polymerase I/DNAse I (GIBCOBRL 18162-016).

3. Fluorescein-12-dATP (MEN, Life Science Products, Inc., Boston, MA).

4. Rhodamine-4-dUTP (Amersham Pharmacia Biotech, Amersham, UK).

METHODS

1. Prepare a labeling reaction according to the following pipetting scheme:

Solution containing 1 µg of genomic test or control DNA	x µl
10 × nick translation system	5 µl
DNA polymerase I/ DNAse I	5 µl (5 units/µl)
Rhodamine-4-dUTP or fluorescein-12-dATP	5 µl
Double distilled water	y µl
Total volume	50 µl

2. Incubate for 3 hr at 15°C and place it on ice.

3. Check the length of the probe molecules by gel electrophoresis.

4. Adjust the length of the labeled probe molecules to a size between 500 and 1000 bp. Depending on the result of the gel, proceed as follows.

a. If the probe size is within the desired range, proceed to the probe mixture and denaturation.

b. If the probe size is larger, add more DNAse I, incubate at 15°C, and repeat **Step 3**.

c. If part of the probe is less than 100 bp in length, start the reaction again using less DNAse I.

Probe Mixture and Denaturation

MATERIALS

1. 3 M sodium acetate (pH 5.2).
2. Hybridization solution (Sigma, H-7782).
3. Cot-1 DNA (Roche Diagnostics Corporation, Indianapolis, IN).
4. 100% ethanol.

METHOD

1. Combine 500 ng each of labeled test and control DNA and 50–100 µg of Cot-1 DNA. Precipitate by adding 1/10 volume of 3 M sodium acetate and 2 volumes of 100% ethanol. Mix well and incubate at −80°C for 20 min.

2. Spin in an Eppendorf centrifuge at 15,000 rpm for 20 min at 4°C. Discard the supernatant.

3. After air-drying for 30 min, add 8 µl of hybridization solution and vortex for more than 1 min. At this step, proceed with denaturation of the DNA on the slide.

4. Denature DNA at 75°C for 10 min and preanneal the probe solution at 37°C for 15 min.

Denaturation of Chromosomal DNA on Slides

MATERIALS

1. Denaturation solution: 70% deionized formamide, 2× SSC; adjust to pH 7.0 by adding HCl.
2. Ice-cold ethanol: 70%, 90%, and 100%.

METHODS

1. Select appropriate area on the slide for hybridization and mark it from underneath with a diamond pen.

2. Fill a Coplin jar with the denaturation solution and place it in a waterbath heated to 70°C. Before denaturation, check the temperature of the denaturation solution with a thermometer inside the jar.

3. Transfer the slides into Coplin jar with the denaturation solution for 2 min.

4. Immediately transfer the slides into Coplin jars with 70%, 90%, and 100% ice-cold ethanol for 2 min each.

5. After air-drying, the slides are ready for hybridization.

Hybridization

1. Apply 8 µl of hybridization mixture with the denatured and preannealed probe to the denatured chromosomes on the slides.

2. Place an 18 × 18 mm coverslip on top of the hybridization droplet. Take care not to trap air bubbles.

3. Seal the edge of the coverslip with rubber cement and place the slides in a wet chamber. Incubate for 48–72 hr at 37°C.

Detection

MATERIALS

1. Wash solution A: 50% formamide, 2× SSC (pH 7.0).
2. Wash solution B: 2× SSC.
3. Wash solution C: 1× ST20.
4. Vectashield (Vector Laboratories).

METHODS

During the entire protocol, the slides must not become completely dry.

1. Prewarm washing solution A in a 45°C waterbath.

2. After taking the slides out of the wet chamber, carefully remove the rubber cement and cover glass using forceps.

3. Transfer the slides into a Coplin jar containing washing solution prewarmed to 45°C for 20 min.

4. Transfer the slides into a Coplin jar with washing solution B and incubate twice for 4 min each at room temperature.

5. Transfer the slides into a Coplin jar with washing solution C and incubate 3 times for 4 min each at room temperature.

6. Take each slide out of the Coplin jar, add 20–30 µl of Vectashield, and cover with a 22 × 40 mm coverslip. Place the slides in suitable boxes, which should be kept at 4°C for long-term storage.

Comparative Genomic Hybridization Digital Image Analysis

For a comprehensive assessment of all chromosomal imbalances present in the tumor genome, quantitative measurement and analysis of fluorescence intensities are necessary. For this purpose, digitized images should be obtained using a sensitive device, such as a cooled CCD (charged-coupled device) camera. In our laboratory we use an Olympus BX-50 fluorescence microscope equipped with single band-pass filters for fluorescein, rhodamine, and DAPI and with a cooled CCD camera (KAF 1400, Photometrics, USA). All optical settings, as well as exposure times, must be kept constant for images obtained in a series of metaphase spreads acquired for a single case. Owing to slight variations in hybridization quality among different metaphase spreads, averaging of these ratio profiles over several metaphase spreads (~10–15) is necessary to reliably detect imbalances involving smaller chromosomal regions. For the detection of such imbalances, a high sensitivity is critical. This parameter depends largely on the threshold criteria selected; in our laboratory, a fixed range threshold (fixed ratio values defining overrepresentation [e.g., 1.15] and underrepresentation [e.g., 0.85]) has been extensively tested. If the mean green or red ratio exceeded 1.5 in a small segment of the chromosome arm, these regions were considered to represent high-level amplification. Telomeric and heterochromatic regions were excluded from the analysis.

Genetic Alterations

Several studies investigating prostate cancer by CGH have been published (Cher *et al.,* 1994; Cher *et al.,* 1996; Cher *et al*., 1998; Joos *et al.,* 1995; Nupponen *et al.,* 1998). These studies have also indicated that primary prostate cancer contains mainly losses of the genetic material (Visakorpi *et al.,* 1995b). However, advanced tumors and recurrent tumors also show gains suggesting that amplifications of oncogenes occur as rather late events in prostate tumor progression (Nupponen *et al.,* 1998; Visakorpi *et al.,* 1995a). In the following we discuss important genetic alterations in prostate carcinoma.

Chromosome 8q

Gain of the 8q arm has been reported in prostate cancer (Cher *et al.,* 1996; Kasahara *et al.,* 2002; Visakorpi *et al.,* 1995b). Cher *et al.* (1996) detected frequent gain in metastatic and androgen-independent prostate cancer. Visakorpi *et al.* (1995b) found that

gain of 8q occurred far more frequently in locally recurrent cancer than in the primary cancer. Using FISH with centromeric probes, some studies found that gain of chromosome 8 was the most frequent chromosomal anomaly in metastatic prostate cancer (Kasahara *et al.,* 2001; Qian *et al.,* 1995). Kasahara *et al.* (2002) also reported that the most frequent partial gain was seen at chromosome arm 8q in prostate cancer with bone metastases. In general, gain of 8q is among the most frequent alterations that occur in prostate cancer. A natural candidate target gene for the 8q24 amplification is thought to be the gene *C-Myc,* which plays significant roles in the regulation of cellular proliferation, differentiation, and apoptosis (Cher *et al.,* 1996; Henriksson *et al.,* 1996; Visakorpi *et al.,* 1995b). Overexpression of *C-Myc* has also been reported in prostate cancer (Buttyan *et al.,* 1987; Fleming *et al.,* 1986). These data suggest that *C-Myc* is one of the candidate oncogenes associated with prostate cancer progression. Other putative oncogenes on 8q include *eif3* at 8q23 (Nupponen *et al.,* 1999) and the prostate stem cell antigen (*PSCA*) at 8q24 (Reiter *et al.,* 2000), both of which are frequently coamplified with *myc*. Amplification and overexpression of the *eif3* gene was found in ~30% of recurrent hormone refractory prostate cancers by FISH (Nupponen *et al.,* 1999). Overexpression of *PSCA* has been observed in all malignant prostate cancers, especially in poorly differentiated tumors and bone metastases (Reiter *et al.,* 2000).

Chromosome 8p

Chromosome 8p has been the most intensively studied region of loss in prostate cancer to date, and 8p22 has been the most intensively studied regions. The rate of 8p22 loss ranges from 29% to 50% in prostate intraepithelial neoplasia (PIN), 32% to 69% in primary tumors, and 65% to 100% in metastatic cancer (Bova *et al.,* 1993; MacGrogan *et al.,* 1994; Macoska *et al.,* 1995; Vocke *et al.,* 1996). Bostwick *et al.* (1998) detected loss of 8p12-21 in 37% of PIN foci and 46% of cancer foci using allelic imbalance. Emmert-Buck *et al.* (1995) found loss of 8p12-21 in 63% of PIN foci and 91% of cancer foci using microdissected frozen tissue. It is thought that 8p loss may be an early event in prostate tumor formation, and this is supported by the finding of loss in PIN lesions.

Chromosome 13q

Deletion of 13q is a frequent event in prostate cancer. Whereas deletion at 13q has been detected in PIN regions by CGH (Zitzelsberger *et al.,* 2001),

many studies have shown that deletion at 13q is related to clinical aggressiveness of prostate cancer (Dong *et al.,* 2000; Zitzelsberger *et al.,* 2001). At least two regions of deletion occur on 13q in prostate cancer. One is at 13q14, the other at 13q12 (Dong *et al.,* 2000; Dong *et al.,* 2001; Hyytinen *et al.,* 1999). Two known tumor suppressor genes important in some types of carcinoma are located on 13q, such as *BRCA2* at 13q12 and *RB1* at 13q14, although BRCA2 appears not to be involved in the development of prostate cancer (Cooney *et al.,* 1996; Ittmann *et al.,* 1996; Latil *et al.,* 1996; Melamed *et al.,* 1997). Allelic loss and somatic mutations of the *RB1* gene have been detected in some prostate tumors (Brooks *et al.,* 1995; Kubota *et al.,* 1995).

Chromosome 10q

Deletion of 10q is found in ~45% of prostate tumors (Cher *et al.,* 1996; Nupponen *et al.,* 1998). Loss of 10q is thought to be a late change, seen more commonly in metastatic and advanced tumors (Ittmann *et al.,* 1996; Trybus *et al.,* 1996). The two known tumor suppressor genes are located at 10q, *MXI1* (10q25), and *PTEN* (10q23). *MXI1* is a negative regulator of *MYC* and thus may have a tumor-suppressing function (Schreiber-Agus *et al.,* 1998). However, Gray *et al.* (1995) showed that *MXI1* maps outside the minimal region of deletion on 10q, and, in addition, found no mutations in the gene. Mutations of *PTEN* have been found, especially in late-stage prostate carcinomas (Cairns *et al.,* 1997; Dong *et al.,* 1998; Wang *et al.,* 1998).

Chromosome 16q

Cher *et al.* (1995) found that 50% of localized prostate carcinoma samples had loss of 16q24, with the area of deletion distal to 16q23.1–16q23.2, whereas Suzuki *et al.* (1996) found loss of 16q in metastatic prostate carcinomas. Visakorpi *et al.* (1995b) found that loss of 16q was seen in 19% of primary tumors compared with 56% of recurrent tumors. The known tumor suppressor gene in the region is *E-cadherin*, which is located at 16q22; its dysfunction has been associated with an invasive tumor phenotype in prostate cancer (Umbas *et al.,* 1994). Nevertheless, analysis of the gene has not shown any mutations. The minimal commonly lost region is distal to *E-cadherin,* suggesting the presence of other tumor suppressor genes (Cher *et al.,* 1996; Nupponen *et al.,* 1998).

Chromosome 17p

Loss of 17p has been found predominantly by CGH (Cher *et al.,* 1994; Cher *et al.,* 1996). It has been found

in 50% of metastases, but in 65% of metastases that have become androgen-resistant (Cher *et al.,* 1996), suggesting that it may be important in advanced disease. A candidate gene is *p53* (17q13.1). Inactivation of *p53* has been implicated in the progression of prostate cancer. The frequency of *p53* mutations in primary prostate cancer is quite low (10–20%), whereas they are found more often in advanced stage disease (Bookstein *et al.,* 1993; Navone *et al.,* 1993; Navone *et al.,* 1999).

Chromosome 7

Gain of chromosome 7 has also been observed in 30–56% of cases in CGH studies in prostate cancer (Cher *et al.,* 1996; Joos *et al.,* 1995; Visakorpi *et al.,* 1995). FISH studies have demonstrated that aneusomy of chromosome 7 is frequent in prostate cancer and is associated with a higher tumor grade, advanced pathologic stage, and early patient death from prostate cancer (Alcaraz *et al.,* 1994; Bandyk *et al.,* 1994; Takahashi *et al.,* 1994; Takahashi *et al.,* 1996). Although the gain of chromosome 7 usually comprises the entire chromosome, two minimal regions of gains, 7q13 and 7q31, have been identified (Jenkins *et al.,* 1998; Nupponen *et al.,* 1998; Visakorpi *et al.,* 1995).

Chromosome 10q

High-level amplification of chromosome q has been found in about one-third of the hormone refractory prostate cancer and CGH-demonstrated amplification of the region Xp11-13 (Nupponen *et al.,* 1998). Because the androgen receptor (*AR*) gene had already been mapped to Xq12, it emerged as a candidate target gene. Some studies have shown that the *AR* gene is amplified in ~30% of hormone refractory prostate carcinomas (Bubendorf *et al.,* 1999; Visakorpi *et al.,* 1995). The elevated copy number is associated with enhanced *AR* gene transcription, which facilitates tumor cell growth (Visakorpi *et al.,* 1995). In contrast, some of the hormone refractory prostate carcinomas show higher *AR* gene expression even without gene amplification (Kinoshita *et al.,* 2000; Koivisto *et al.,* 1997). The mechanism by which overexpression and amplification of the *AR* gene are involved in the androgen-independent prostate carcinoma growth, however, is not understood.

In conclusion, the use of molecular cytogenetic methods, especially CGH, has revealed common chromosomal alterations in prostate cancer. Studies on the genetic basis of prostate cancer have provided important information regarding the mechanisms responsible for the development and progression of the disease.

However, the target genes for many of the chromosomal aberrations are not known. Genetic alterations as detected by CGH may not be sufficient for correctly identifying the relevant chromosomal regions important in tumor progression. It is hoped that by recognizing and understanding molecular mechanisms, better tools for the prevention, diagnosis, prognostic evaluation, and treatment of malignancies may be developed. As techniques are improving and examination of archival material is now possible, it should be easier to correlate clinical data with tumor studies. This approach will yield important information for the prognosis of patients with prostate cancer.

References

Alcaraz, A., Takahashi, S., Brown, J.A., Herath, J.F, Bergstralh, E.J., Larson-Keller, J.J., Lieber, M.M., and Jenkins, R.B. 1994. Aneuploidy and aneusomy of chromosome 7 detected by fluorescence in situ hybridization are markers of poor prognosis in prostate cancer. *Cancer Res. 54*:3998–4002.

Bandyk, M.G., Zhao, L., Troncoso, P., Pisters, L.L., Palmer, J.L., von Eschenbach, A.C., Chung, L.W., and Liang, J.C. 1994. Trisomy 7: A potential cytogenetic marker of human prostate cancer progression. *Genes Chromos. Cancer 9*:19–27.

Bookstein, R., MacGrogan, D., Hilsenbeck, S.G., Sharkey, F., and Allred, D.C. 1993. p53 is mutated in a subset of advanced-stage prostate cancers. *Cancer Res. 53*:3369–3373.

Bostwick, D.G., Shan, A., Qian, J., Darson, M., Maihle, N.J., Jenkins, R.B., and Cheng, L. 1998. Independent origin of multiple foci of prostatic intraepithelial neoplasia: Comparison with matched foci of prostate carcinoma. *Cancer 83*:1995–2002.

Bova, G.S., Carter, B.S., Bussemakers, M.J., Emi, M., Fujiwara, Y., Kyprianou, N., Jacobs, S.C., Robinson, J.C., Epstein, J.I., and Walsh, P.C. 1993. Homozygous deletion and frequent allelic loss of chromosome 8p22 loci in human prostate cancer. *Cancer Res. 53*:3869–3873.

Brooks, J.D., Bova, G.S., and Isaacs, W.B. 1995. Allelic loss of the retinoblastoma gene in primary human prostatic adenocarcinomas. *Prostate 26*:35–39.

Bubendorf, L., Kononen, J., Koivisto, P., Schraml, P., Moch, H., Gasser, T.C., Willi, N., Mihatsch, M.J., Sauter, G., and Kallioniemi, O.P. 1999. Survey of gene amplifications during prostate cancer progression by high-throughout fluorescence in situ hybridization on tissue microarrays. *Cancer Res. 59*:803–806.

Buttyan, R., Sawczuk, I.S., Benson, M.C., Siegal, J.D., and Olsson, C.A. 1987. Enhanced expression of the *c-myc* protooncogene in high-grade human prostate cancers. *Prostate 11*:327–337.

Cairns, P., Okami, K., Halachmi, S., Halachmi, N., Esteller, M., Herman, J.G., Jen, J., Isaacs, W.B., Bova, G.S., and Sidransky, D. 1997. Frequent inactivation of *PTEN/MMAC1* in primary prostate cancer. *Cancer Res. 57*:4997–5000.

Cher, M.L., MacGrogan, D., Bookstein, R., Brown, J.A., Jenkins, R.B., and Jensen, R.H. 1994. Comparative genomic hybridization, allelic imbalance, and fluorescence in situ hybridization on chromosome 8 in prostate cancer. *Genes Chromos. Cancer 11*:153–162.

Cher, M.L., Bova, G.S., Moore, D.H., Small, E.J., Carroll, P.R., Pin, S.S., Epstein, J.I., Isaacs, W.B., and Jensen, R.H. 1996. Genetic alterations in untreated metastases and androgen-independent prostate cancer detected by comparative genomic hybridization and allelotyping. *Cancer Res. 56*: 3091–3102.

Cher, M.L., Lewis, P.E., Banerjee, M., Hurley, P.M., Sakr, W., Grignon, D.J., and Powell, I.J. 1998. A similar pattern of chromosomal alterations in prostate cancers from African-Americans and Caucasian Americans. *Clin. Cancer Res. 4*:1273–1278.

Cooney, K.A., Wetzel, J.C., Merajver, S.D., Macoska, J.A., Singleton, T.P., and Wojno, K.J. 1996. Distinct regions of allelic loss on 13q in prostate cancer. *Cancer Res. 56*:1142–1145.

Dong, J.T., Sipe, T.W., Hyytinen, E.R., Li, C.L., Heise, C., McClintock, D.E., Grant, C.D., Chung, L.W., and Frierson, H.F. Jr. 1998. PTEN/MMAC1 is infrequently mutated in pT2 and pT3 carcinomas of the prostate. *Oncogene 17*:1979–1982.

Dong, J.T., Chen, C., Stultz, B.G., Isaacs, J.T., and Frierson, H.F. Jr. 2000. Deletion at 13q21 is associated with aggressive prostate cancers. *Cancer Res. 60*:3880–3883.

Dong, J.T., Boyd, J.C., and Frierson, H.F. Jr. 2001. Loss of heterozygosity at 13q14 and 13q21 in high grade, high stage prostate cancer. *Prostate 49*:166–171.

Emmert-Buck, M.R., Vocke, C.D., Pozzatti, R.O., Duray, P.H., Jennings, S.B., Florence, C.D., Zhuang, Z., Bostwick, D.G., Liotta, L.A., and Linehan, W.M. 1995. Allelic loss on chromosome 8p12-21 in microdissected prostatic intraepithelial neoplasia. *Cancer Res. 55*:2959–2962.

Fearon, E.R., and Vogelstein, B. 1990. A genetic model for colorectal tumorigenesis. *Cell 61*:759–767.

Fleming, W.H., Hamel, A., MacDonald, R., Ramsey, E., Pettigrew, N.M., Johnston, B., Dodd, J.G., and Matusik, R.J. 1986. Expression of the *c-myc* protooncogene in human prostatic carcinoma and benign prostatic hyperplasia. *Cancer Res. 46*:1535–1538.

Gray, I.C., Phillips, S.M., Lee, S.J., Neoptolemos, J.P., Weissenbach, J., and Spurr, N.K. 1995. Loss of the chromosomal region 10q23-25 in prostate cancer. *Cancer Res. 55*:4800–4803.

Henriksson, M., and Lusher, B. 1996. Proteins of the Myc network: essential regulators of cell growth and differentiation. *Adv. Cancer Res. 68*:109–182.

Hyytinen, E.R., Frierson, H.F. Jr., Boyd, J.C., Chung, L.W., and Dong, J.T. 1999. Three distinct regions of allelic loss at 13q14, 13q21-22, and 13q33 in prostate cancer. *Genes Chromos. Cancer 25*:108–114.

Ittmann, M.M., and Wieczorek, R. 1996. Alterations of the retinoblastoma gene in clinically localized, stage B prostate adenocarcinomas. *Hum. Pathol. 27*:28–34.

Ittmann, M.M. 1996. Allelic loss on chromosome 10 in prostate adenocarcinoma. *Cancer Res. 56*:2143–2147.

Jenkins, R.B., Qian, J., Lee, H.K., Huang, H., Hirasawa, K., Bostwick, D.G., Proffitt, J., Wilber, K., Lieber, M.M., Liu, W., and Smith, D.I. 1998. A molecular cytogenetic analysis of 7q31 in prostate cancer. *Cancer Res. 58*:759–766.

Joos, S., Bergerheim, U.S., Pan, Y., Matsuyama, H., Bentz, M., du Manoir, S., and Lichter, P. 1995. Mapping of chromosomal gains and losses in prostate cancer by comparative genomic hybridization. *Genes Chromos. Cancer 14*:267–276.

Kallioniemi, A., Kallioniemi, O.P., Sudar, D., Rutovitz, D., Gray, J.W., Waldman, F., and Pinkel, D. 1992. Comparative genomic hybridization for molecular cytogenetic analysis of solid tumors. *Science 258*:818–821.

Kallioniemi, A., Visakorpi, T., Karhu, R., Pinkel, D., and Kallioniemi, O.P. 1996. Gene copy number analysis by fluorescence in situ hybridization and comparative genomic hybridization. *Methods 9*:113–121.

Kasahara, K., Taguchi, T., Yamasaki, I., Kamada, M., Yuri, K., and Shuin, T. 2002. Detection of genetic alterations in advanced prostate cancer by comparative genomic hybridization. *Cancer Genet. Cytogenet. 137*:59–63.

Kasahara, K., Taguchi, T., Yamasaki, I., Karashima, T., Kamada, M., Yuri, K., and Shuin, T. 2001. Fluorescence in situ hybridization to assess transitional changes of aneuploidy for chromosomes 7, 8, 10, 12, 16, X and Y in metastatic prostate cancer following anti-androgen therapy. *Int. J. Oncol. 19*:543–549.

Kinoshita, H., Shi, Y., Sandefur, C., Meisner, L.F., Chang, C., Choon, A., Reznikoff, C.R., Bova, G.S., Friedl, A., and Jarrard, D.F. 2000. Methylation of the androgen receptor minimal promoter silences transcription in human prostate cancer. *Cancer Res. 60*:3623–3630.

Koivisto, P., Kononen, J., Palmberg, C., Tammela, T., Hyytinen, E., Isola, J., Trapman, J., Cleutjens, K., Noordzij, A., Visakorpi, T., and Kallioniemi, O.P. 1997. Androgen receptor gene amplification: A possible molecular mechanism for androgen deprivation therapy failure in prostate cancer. *Cancer Res. 57*:314–319.

Kubota, Y., Fujinami, K., Uemura, H., Dobashi, Y., Miyamoto, H., Iwasaki, Y., Kitamura, H., and Shuin, T. 1995. Retinoblastoma gene mutations in primary human prostate cancer. *Prostate 27*:314–320.

Latil, A., Cussenot, O., Fournier, G., and Lidereau, R. 1996. The BRCA2 gene is not relevant to sporadic prostate tumours. *Int. J. Cancer 66*:282–283.

MacGrogan, D., Levy, A., Bostwick, D., Wagner, M., Wells, D., and Bookstein, R. 1994. Loss of chromosome arm 8p loci in prostate cancer: Mapping by quantitative allelic imbalance. *Genes Chromos. Cancer 10*:151–159.

Macoska, J.A., Trybus, T.M., Benson, P.D., Sakr, W.A., Grignon, D.J., Wojno, K.D., Pietruk, T., and Powell, I.J. 1995. Evidence for three tumor suppressor gene loci on chromosome 8p in human prostate cancer. *Cancer Res. 55*:5390–5395.

Melamed, J., Einhorn, J.M., and Ittmann, M.M. 1997. Allelic loss on chromosome 13q in human prostate carcinoma. *Clin. Cancer Res. 3*:1867–1872.

Navone, N.M., Troncoso, P., Pisters, L.L., Goodrow, T.L., Palmer, J.L., Nichols, W.W., von Eschenbach, A.C., and Conti, C.J. 1993. p53 protein accumulation and gene mutation in the progression of human prostate carcinoma. *J. Natl. Cancer Inst. 85*:1657–1669.

Navone, N.M., Labate, M.E., Troncoso, P., Pisters, L.L., Conti, C.J., von Eschenbach, A.C., and Logothetis, C.J. 1999. p53 mutations in prostate cancer bone metastases suggest that selected p53 mutants in the primary site define foci with metastatic potential. *J. Urol. 161*:304–308.

Nupponen, N.N., Kakkola, L., Koivisto, P., and Visakorpi, T. 1998. Genetic alterations in hormone-refractory recurrent prostate carcinomas. *Am. J. Pathol. 153*:141–148.

Nupponen, N.N., Porkka, K., Kakkola, L., Tanner, M., Persson, K., Borg, A., Isola, J., and Visakorpi, T. 1999. Amplification and overexpression of p40 subunit of eukaryotic translation initiation factor 3 in breast and prostate cancer. *Am. J. Pathol. 154*:1777–1783.

Nupponen, N.N., and Visakorpi, T. 2000. Molecular cytogenetics of prostate cancer. *Microsc. Res. Tech. 51*:456–463.

Pinkel, D., Straume, T., and Gray, J.W. 1986. Cytogenetic analysis using quantitative, high sensitivity, fluorescence hybridization. *Proc. Natl. Acad. Sci. USA 83*:2934–2938.

Qian, J., Bostwick, D.G., Takahashi, S., Borell, T.J., Herath, J.F., Lieber, M.M., and Jenkins, R.B. 1995. Chromosomal anomalies in prostatic intraepithelial neoplasia and carcinoma detected by fluorescence in situ hybridization. *Cancer Res. 55*:5408–5414.

Reiter, R.E., Sato, I., Thomas, G., Qian, J., Gu, Z., Watabe, T., Loda, M., and Jenkins, R.B. 2000. Coamplification of prostate stem cell antigen (*PSCA*) and *MYC* in locally advanced prostate cancer. *Genes Chromos. Cancer 27*:95–103.

Schreiber-Agus, N., Meng, Y., Hoang, T., Hou, H. Jr., Chen, K., Greenberg, R., Cordon-Cardo, C., Lee, H.W., and DePinho, R.A. 1998. Role of *Mxi1* in ageing organ systems and the regulation of normal and neoplastic growth. *Nature 393*:483–487.

Speicher, M.R., du Manoir, S., Schrock, E., Holtgreve-Grez, H., Schoell, B., Lengauer, C., Cremer, T., and Ried, T. 1993. Molecular cytogenetic analysis of formalin-fixed, paraffin-embedded solid tumors by comparative genomic hybridization after universal DNA-amplification. *Hum. Mol. Genet. 2*:1907–1914.

Suzuki, H., Komiya, A., Emi, M., Kuramochi, H., Shiraishi, T., Yatani, R., and Shimazaki, J. 1996. Three distinct commonly deleted regions of chromosome arm 16q in human primary and metastatic prostate cancers. *Genes Chromos. Cancer 17*:225–233.

Takahashi, S., Alcaraz, A., Brown, J.A., Borell, T.J., Herath, J.F., Bergstralh, E.J., Lieber, M.M., and Jenkins, R.B. 1996. Aneusomies of chromosomes 8 and Y detected by fluorescence in situ hybridization are prognostic markers for pathological stage C (pt3N0M0) prostate carcinoma. *Clin. Cancer Res. 2*:137–145.

Takahashi, S., Qian, J., Brown, J.A., Alcaraz, A., Bostwick, D.G., Lieber, M.M., and Jenkins, R.B. 1994. Potential markers of prostate cancer aggressiveness detected by fluorescence in situ hybridization in needle biopsies. *Cancer Res. 54*:3574–3579.

Trybus, T.M., Brugess, A.C., Wojno, K.J., Glover, T.W., and Macoska, J.A. 1996. Distinct areas of allelic loss on chromosomal regions 10p and 10q in human prostate cancer. *Cancer Res. 56*:2263–2267.

Umbas, R., Isaacs, W.B., Bringuier, P.P., Schaafsma, H.E., Karthaus, H.F., Oosterhof, G.O., Debruyne, F.M., and Schalken, J.A. 1994. Decreased E-cadherin expression is associated with poor prognosis in patients with prostate cancer. *Cancer Res. 54*:3929–3933.

Van Dekken, H., Pizzolo, J.G., Reuter, V.E., and Melamed, M.R. 1990. Cytogenetic analysis of human solid tumors by in situ hybridization with a set of 12 chromosome-specific DNA probes. *Cytogenet. Cell Genet. 54*:103–107.

Visakorpi, T., Hyytinen, E., Koivisto, P., Tanner, M., Keinanen, R., Palmberg, C., Palotie, A., Tammela, T., Isola, J., and Kallioniemi, O.P. 1995a. In vivo amplification of the androgen receptor gene and progression of human prostate cancer. *Nat. Genet. 9*:401–406.

Visakorpi, T., Kallioniemi, A.H., Syvanen, A.C., Hyytinen, E.R., Karhu, R., Tammela, T., Isola, J.J., and Kallioniemi, O.P. 1995b. Genetic changes in primary and recurrent prostate cancer by comparative genomic hybridization. *Cancer Res. 55*:342–347.

Vocke, C.D., Pozzatti, R.O., Bostwick, D.G., Florence, C.D., Jennings, S.B., Strup, S.E., Duray, P.H., Liotta, L.A., Emmert-Buck, M.R., and Linehan, W.M. 1996. Analysis of 99 microdissected prostate carcinomas reveals a high frequency of allelic loss on chromosome 8p12-21. *Cancer Res. 56*:2411–2416.

Wang, S.I., Parsons, R., and Ittmann, M. 1998. Homozygous deletion of the PTEN tumor suppressor gene in a subset of prostate adenocarcinomas. *Clin. Cancer Res. 4*:811–815.

Zitzelsberger, H., Engert, D., Walch, A., Kulka, U., Aubele, M., Hofler, H., Bauchinger, M., and Werner, M. 2001. Chromosomal changes during development and progression of prostate adenocarcinomas. *Br. J. Cancer 84*:202–208.

This Page Intentionally Left Blank

3

Alterations of Genes and Their Expression in Prostate Carcinoma

Pedro L. Fernández and Timothy M. Thomson

Introduction

During the last years of the 20th and first years of the 21st centuries two great events in molecular biology (MB) studies have occurred: the publication of the sequence of the human genome and the development of the microtechnologies and nanotechnologies applied to MB. This has greatly modified the design of research projects and the productivity of MB. During the pregenome era, when DNA microarray and other high-throughput technologies (HTTs) were not available, there was relatively slow progress in the analysis and discovery of new molecular alterations in human tumors and other pathologies. Techniques such as conventional electrophoresis of nucleic acids and polymerase chain reaction (PCR)-derived procedures have thus until recently been key tools in MB research. There is no doubt that the latter are still valuable and unavoidable methods for the analysis of a number, if not all, of molecular alterations. Yet, the evaluation of the differential expression of genes has accomplished a gigantic step with the introduction of HTTs. Indeed, many research projects are now based on an initial broad screening of molecular alterations in many of the human genes by means of expression profiling on deoxyribonucleic acid (DNA) microchips, with subsequent focus on more restricted sets of genes of significance to the pathology under study, by validation of the genomic status, ribonucleic acid (RNA) expression, and correlations with clinical–pathologic data.

Because most of the current solid knowledge on molecular alterations in prostate carcinoma are still based on studies prior to HTTs, we feel that a comprehensive description of such abnormalities involved in prostate carcinogenesis must include a review of those findings accomplished during the pregenomic/premicrochip era. This will be followed by a review of more recent knowledge generated by such state-of-the-art procedures.

Pregenomic Era

One of the most important characteristics of malignant cells is their increased proliferative capability, most likely resulting from impaired control of the regulatory elements of the cell cycle. Cell-cycle regulators are subject to strict control in normal cells and their activities fluctuate according to external stimuli, whereas independence from such stimuli emerges in neoplastic cells. There are several checkpoints in the cell cycle, which are regulated by an increasingly better understood complex system of modulators including, among others, the retinoblastoma gene product (pRb), cyclins, cyclin-dependent kinases (CDKs), and CDK inhibitors (CDKIs). One of the most studied

pathways of cell-cycle regulation is that involving pRb, a negative modulator of the restriction point at the G1-S transition, whose inactivation by several mechanisms such as phosphorylation by upstream elements (CDK-cyclins complexes) leads to cell-cycle progression and proliferation (Figure 43) (for review see Sherr and Roberts, 1995). Abnormalities in many of the aforementioned regulators, as well as others more indirectly linked to cell proliferation modulation (e.g., p53), have been observed in prostate carcinoma and will be herein reviewed.

Tumor Suppressor Genes

The Retinoblastoma Gene

The retinoblastoma gene was the first tumor suppressor gene described, and its role in tumorigenesis derives from its critical inhibitory role at the G1-S phase transition when its product (pRb) is in a hypophosphorylated state (Goodrich *et al.*, 1991).

The retinoblastoma (Rb) tumor suppressor gene has been observed to be altered in a subpopulation of prostate cancers in which loss of heterozygosity (LOH) at 13q affects about one-third of the cases and whose reintroduction in cancer cells with mutated gene suppresses tumorigenicity. This LOH seems to occur in both low-stage and more advanced cancers and may, therefore, be important in prostate carcinogenesis. Nevertheless, the absence of *Rb* mutations and the poor correlation of absent protein expression with LOH found by several authors indicate that another gene may be the target of 13q deletions.

A possible mechanism for *Rb* involvement in the development of prostate cancer could be mediated by its role in hormone stimuli regulation. Indeed, it is becoming evident that overexpression of this tumor suppressor gene leads to increased transcriptional activity of the androgen receptor (AR), which has an important growth-promoting effect in prostate cells, and cotransfection of Rb and AR may increase AR transcriptional activity fourfold in DU145 cells, probably by forming a protein–protein complex in an androgen-independent manner. It has also been postulated that loss of *Rb* function, for instance by viral oncoprotein sequestering, may cause a decrease in the response to androgens of tumor cells. The immunohistochemical absence of pRb expression seems to vary widely among the different studies, and it has been proposed that this analysis of Rb protein status may have prognostic capability in multivariate analysis regarding disease-specific survival (Krupski *et al.*, 2000). Nonetheless, the prognostic capacity of immunohistochemical *Rb* evaluation has been far less studied than many other cell-cycle–related genes.

p53

p53 is the product of a gene located in 17p13 and is considered, so far, the most commonly altered gene in human neoplasms (Hollstein *et al.*, 1991; Levine *et al.*, 1991). The p53 protein, in its wild-type form, negatively regulates proliferation and derives genetically injured cells toward apoptosis. Thus, p53 is located in an upstream crossroad between the Rb regulatory pathway of the G1-S phase transition and the apoptotic
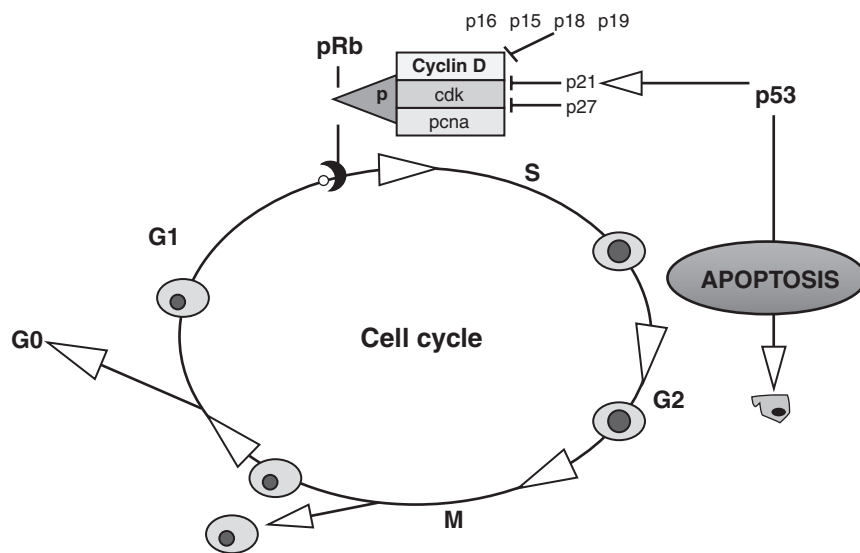
Figure 43 Scheme of cell-cycle regulation at G1.

cascade (see Figure 43). Different types of *p53* gene alterations lead to a stabilization of this usually short-lived protein, thus allowing its immunohistochemical detection within the nucleus, which frequently correlates with a mutated gene. Other methods to detect such abnormalities are single-strand conformational polymorphism (SSCP), reverse transcription (RT)-PCR, and sequencing of the coding regions of p53 mRNA, mainly spanning the most frequently mutated domains in exons 4 through 11. The overall frequency of gene abnormalities leading to altered protein expression in prostate cancer was 42% in the study by Chi *et al*. (1994), with nucleotide base-pair transitions of A-G or T-C being the most common abnormalities. However, the frequency of *p53* mutations is highly variable among authors and ranges between 1% and 42% (reviewed by Ruijter *et al*., 1999). The combined information obtained by immunohistochemical studies and microdissection, molecular analysis has provided useful information regarding the stage of neoplastic progression in which *p53* abnormalities seem to arise. Some authors have shown that *p53* mutations occur in high-grade prostatic intraepithelial neoplasia (PIN) and invasive carcinomas and that different types of mutations can coexist in different PIN and carcinoma foci within the same specimen of prostatectomy, indicating a multiclonal development of malignant prostate cancers. For other authors, this event is already observed in intact normal prostatic epithelium, but most authors claim that p53 overexpression is a rare and late event more easily identified in metastases. Possible explanations for these discrepancies are as follows: 1) the disparity of antibodies used, which may or may not detect the mutated protein only; 2) the different immunohistochemical protocols used, which cause wide variations in sensitivity; 3) the criteria and method of evaluation (absolute negativity versus some positivity, different cutoff percentages, morphometry versus naked eye); 4) variability in the size of the tested samples (needle biopsy, transurethral resection, prostatectomy specimens); and 5) etiopathogenetic differences among countries. It is therefore not surprising that different opinions are expressed regarding the usefulness of this marker as a prognostic factor in prostate pathology. Nevertheless, the association of p53 overexpression with tumor grade, advanced stage, metastatic potential, early prostate specific antigen (PSA) relapse, and survival have been consistent findings. A study in 2000 immunohistochemically analyzed p53 expression in 263 cases of prostate carcinoma followed for a mean period of 55 months (Quinn *et al*., 2000). This study has provided new insights into the problem by considering both percentage of positive cells and "clustering" of positivity, the latter being a good prognostic factor of poor evolution in positive cases. This study also allowed the authors to propose that p53 dysfunction within prostate carcinomas occurs in foci of tumor cells that are clonally expanded.

The potential usefulness of p53 evaluation as a predictor of therapy response is still under debate. For instance, it has been demonstrated that neoplastic cells with mutation in *p53* are more resistant to ionizing radiation, and the use of p53 evaluation has been proposed as a marker of resistance to this type of treatment or androgen ablation. Prediction of response to hormone therapy might also be indirectly evaluated by p53 status assessment given its proposed association with androgen-receptor amplification in refractory recurrent tumors. Upstream modulators of p53, such as MDM2 and ATM, are now being considered to be important in neoplastic development and treatment response in several tumor types, but their definitive involvement in prostate carcinogenesis remains unknown.

The INK4 Family

The INK4 (inhibitors of CDK4) family includes p16[INK4A], p15[INK4B], p18[INK4C], and p19[INK4D], which specifically inhibit the CDK4-6/cyclin D complexes (Sherr and Roberts, 1995). In addition to p16, the *INK4* locus encodes a second transcript called p14[ARF] ("Alternative Reading Frame") in humans and p19[ARF] in mice, which is derived from a different exon 1 (exon 1beta, centromeric to the first exon of p16/INK4, called alpha). INK4 cyclin kinase inhibitors inhibit cell-cycle progression at the G1-S transition by blocking pRb phosphorylation by CDK/cyclinD complexes. An increase in p16 expression and in its association to CDK4 and CDK6 has been observed in the normal prostate cell line human prostatic epithelial cells (HPECs) undergoing senescence, which might be involved in their inhibited proliferation, although inactivation of the p16/pRb pathway might not be sufficient to immortalize normal prostatic cells. Contradictory findings report both rarity of *p16* mutations and deletions in prostate cancer (Gaddipati *et al*., 1997; Manglod *et al*., 1997) and relatively frequent locus 9p21 homozygous deletion, as well as gene inactivation by promoter methylation (Cairns *et al*., 1995). With regard to expression levels, p16 up-regulation is more often considered than the opposite as a possible abnormality. Immunohistochemical overexpression of p16 has been observed in prostate carcinomas when compared to hyperplasia and in as many as 43% of tumors (Lee *et al*. 1999), in which high p16 expression was found to be an independent prognostic factor in multivariate analysis.

The CIP/KIP Family

$p21^{WAF1/CIP1}$, together with $p27^{KIP1}$ and $p57^{KIP2}$, belongs to the Cip/Kip family of CKIs. $p21^{WAF1/CIP1}$ is a tumor suppressor gene given its capacity to bind to and inhibit the kinase activity of a wider series of cyclin/CDK complexes than the INK4 family (Sherr and Roberts, 1995) (see Figure 43). However, this function depends on its concentration because low levels of the product can exert a stimulatory assembling effect on the cyclin D1/CDK4 complexes. P21 –/– cells show a deficient ability to arrest cell cycle in G1 in response to DNA damage. The expression of this gene is induced by native, but not mutant, *p53* in response to damaging agents, although *p21* modulation by p53-independent pathways has been proposed for several other tumor models. Although initially thought to be rarely altered at the genomic level in human neoplasms, LOH at its 6p locus and *p21* somatic mutations have been described in prostate cancers (Gao *et al.*, 1997). For some authors, *p21* expression abnormalities have failed to correlate with prostate carcinoma grade, stage, or cancer progression, whereas it might, alone or combined with *p53* determination, predict biochemical recurrences and survival for others (Sarkar *et al.*, 1999).

Contrary to p21, which seems to be a universal CKI acting on different types of cyclin/CDK complexes, *p27* exerts its inhibitory modulation on the cell cycle mainly through its binding to the cyclin E/CDK2 complex, thus blocking entry of cells in the S-phase. When sequestered from those complexes by cyclin D1/CDK4 complexes, *p27* detachment might allow cell-cycle progression. *p27* also seems to be involved in the regulation of drug resistance, apoptosis, and cell differentiation. *p27*-deficient mice develop endocrine tumors and display increased body size and multiple organ hyperplasia. Genomic alterations of the *p27* gene seem to be rare in human malignancies (Ponce-Castaneda *et al.*, 1995), and its protein expression is mainly regulated at the post-transcriptional level through protein translation and degradation. One study has shown LOH at 12p12-13 in 23% of the cases of primary carcinoma, 30% of lymph node metastases, and 47% of distant metastases and concludes that such genetic loss occurred prior to metastasis (Kibel *et al.*, 2000). Down-regulation of *p27* is frequently observed in prostate carcinomas, and this abnormality seems to arise in early neoplastic stages (PIN), in contrast to normal prostatic glands in which most luminal cells express this marker (De Marzo *et al*; 1998, Fernandez *et al.*, 1999). For some authors, decreased p27 immunohistochemical expression in prostate cancers correlates with markers of poor evolution, which could be useful to evaluate cases in terms of prognosis, although this is not unanimously supported. Again, the differences in antibodies and criteria of quantification may influence the conclusions of different studies.

Cyclins

Cyclin D1^{CCND1} is a critical regulator of the G1 checkpoint controlling cell-cycle progression, and there is important evidence that abnormal cyclin D1 is involved in tumorigenesis and tumor progression in different types of neoplasms. Cyclin D1 levels dramatically increase after androgen treatment in prostate proliferating cells from castrated rats. The relationship between cyclin D1 expression and steroid regulation is also found in human prostate tumors, in which there is a direct correlation between this expression and that of androgen receptors analyzed by immunohistochemistry (Kolar *et al.*, 2000). It is interesting that androgen deprivation therapy seems to cause an increased number of prostate tumors with increased *cyclin D1* copy number ("amplification") detected by fluorescence *in situ* hybridization (FISH) (Kaltz-Wittmer *et al.*, 2000).The immunohistochemical determination of cyclin D1 status in prostate cancers may provide prognostic information for some authors, who have observed increased expression in the most undifferentiated and advanced lesions. However, in a cohort of 213 patients followed up for a mean period of 12 years, despite finding a correlation of cyclins D and A expression with some histologic and cellular parameters such as differentiation, S-phase fraction, and perineural invasion, Altomaa *et al.* do not believe that these cyclins have independent prognostic value (1999). Regarding other cyclins, little is known about their possible role in prostate carcinogenesis. Nevertheless, it has been postulated that cyclin E functions as a coactivator of the androgen receptor and its aberrant expression might contribute to persistent activation of this receptor, even during anti-androgen therapy.

Many other cell-cycle regulatory genes may conceivably be subject to genomic alterations. Techniques such as conventional cytogenetics, LOH studies, FISH, and comparative genomic hybridization (CGH) have yielded interesting information on gross chromosomic alterations in prostate cancers (see Alers *et al.*, 1999; Bostwick and Foster, 2000, for review). Chromosomal gains involving cell-cycle–related genes are mainly found at 8q24, where the *MYC* oncogene is located. This gain is associated with high tumor grade and stage, and it has been found in a significant proportion of distant metastases. Moreover, *MYC* gene amplification has been detected in a subset of metastatic and recurrent prostate tumors and it seems to correlate with

the presence of regional lymph node metastases and poor prognosis. Chromosomal losses could also be important in prostate carcinogenesis, and they have been observed, for instance, at 6q21 where *CCNC* codifies for cyclin C. Finally, chromosomal losses in 10q23 may target the *PTEN* gene. PTEN protein negatively regulates cell migration and cell survival and induces a G1 cell-cycle block via negative regulation of the P13K/protein kinase B/Akt signaling pathway. It is interesting that loss of PTEN protein correlates with several pathologic markers of poor prognosis in prostate cancer and *PTEN* mutations and deletions have been detected in prostate carcinomas, particularly in metastatic cases.

Genomic Era: Markers of Prostate Epithelial Malignancy and Tumor Progression Identified by DNA Microarray Analysis

The application of recent HTTs allows the unbiased identification of molecules relevant to a given biologic or pathologic process. With these techniques, first markers for a particular biologic process are identified, and then the function of the corresponding molecules is studied. This conceptual approach is similar to that used for the characterization of antigens detected differentially by monoclonal antibodies, but is contrary to the more traditional approaches in which molecules of known function are studied in a given biologic context. Over the past few years, HTTS for the identification of transcripts and proteins have been developed. The comparison of complete, or near-complete, transcriptomes of two or more samples has been possible for several years, with techniques such as differential display, representational difference analysis, or serial analysis of gene expression (SAGE). However, a true HTT for the parallel and reproducible comparative analysis of multiple samples has not been available until the generalization of the DNA microarray technologies (Cole *et al.*, 1999). With the advent of the sequences of complete genomes, the latter technology permits faithful and reproducible comparisons of global transcriptomes.

When large repertoires of transcripts are compared, the results that are obtained are not mere individual markers that identify a given sample class, but are entire sets of transcripts that are characteristic of the process under study. These sets generally correspond to coregulated genes that are expressed in a coordinate fashion in response to the activation of specific biochemical pathways. Therefore a given set of transcripts that can be associated with a particular sample category

reflects a specific combination of ongoing biochemical processes that are predominantly activated in the samples that have been grouped under that category. The expectation is that the application of global transcriptome analysis in cancer will lead not only to the identification of markers of tumor progression but also to delineate with precision the biochemical pathways that are abnormally activated or suppressed in a given type and stage of a neoplastic process. Knowledge of such pathways and their regulatory molecules will permit the rational design and development of specific drugs. To fully achieve this goal improvements are still needed in predictive bioinformatics tools, as well as more complete databases relating genes, transcripts, proteins, structures, and pathways, and these predictions must be validated experimentally in appropriate cellular and animal models.

Several carefully designed studies for global transcriptome comparative analysis of prostate cancer, using microarray technology, have been reported. A number of issues need to be addressed to draw conclusions that apply to all of the studies. First, the pathologic diagnosis and the processing of the samples are not perfectly comparable between any two studies performed at different institutions. The variation in the length of time between surgery and cryopreservation, which causes tissue ischemia at different degrees, may introduce changes in expression patterns if the ischemia is maintained beyond certain limits (Dash *et al.*, 2002). Some studies use unrelated normal prostate tissue as the counterpart of cancerous tissue, whereas other studies use nonaffected prostate tissue from the same prostatectomy as that for the cancerous tissue. To date, very few published studies (for example, Ernst *et al.*, 2002) use laser microdissection to precisely select for normal and malignant epithelia, and therefore most tissues contain variable degrees of mixtures of epithelial cells with stromal and inflammatory cells, which may introduce a bias in the transcriptional repertoires under study. Also, accurate Gleason score assignments should be reflected in any study of prostate cancer, even if the goal of the study is to find transcriptional signatures common to all cancer samples with independence of their histologic differentiation because it has been shown that certain genes associate preferentially with either low or high Gleason scores (Singh *et al.*, 2002). Second, microarray platforms vary between studies, ranging from different types of complementary DNA (cDNA) arrays to the Affymetrix oligonucleotide arrays. These differences affect gene lists included in the platform, platform production process (deposition or on-site synthesis), probe labeling and hybridization, image acquisition, processing and filtering techniques, call criteria, and output data format.

Third, different statistical techniques are applied for the pretreatment of data and for the extraction of functionally meaningful sets of genes and sample grouping. One of the most widely used techniques, hierarchical clustering, behaves well when applied to relatively small datasets but appears to be less robust for the analysis of larger datasets. Many statistical techniques have been developed in the past few years for the analysis of data generated in microarray experiments that are intended to optimize the extraction of biologically meaningful correlations between samples and expressed genes (for a review, see Valafar, 2002).

The issue of how comparable two or more independent microarray analyses are has been addressed by the Chinnaiyan group (Rhodes *et al*., 2002). They performed a meta-analysis that included four transcriptional studies of prostate cancer, one by their own laboratory (Dhanasekaran *et al*., 2001) and three by other laboratories (Luo *et al*., 2001; Magee *et al*., 2001; Welsh *et al*., 2001). One study used oligonucleotide arrays (Welsh *et al*., 2002), whereas the other studies used spotted cDNA arrays. This analysis identified common sets of genes that were considered to be significantly overexpressed or underexpressed in prostate cancer in all the studies under consideration. Common overexpressed genes included some that were previously associated with prostate cancer, such as those for the membrane-associated proteases hepsin (Dhanasekaran *et al*., 2001; Luo *et al*., 2001; Magee *et al*., 2001; Welsh *et al*., 2001), the transcription factor Myc, the enzymes alpha-methyl malonyl CoA racemase (AMACR) and fatty acid synthase (FASN), or the translation initiation factor 3. Among genes commonly underrepresented in prostate cancer were some that had also been previously reported as down-regulated in cancer, for example, the genes for annexins, for Caveolin-2, or the insulin-like growth factor binding protein 3. The list of the genes that best distinguish malignant from nonmalignant prostate tissue in this meta-analysis differs somewhat from the list of most significantly overexpressed or underexpressed genes reported in each of the original reports. These differences may be a reflection of the statistical approaches used in the study by Rhodes *et al*. (2002) for the extraction of genes that showed patterns of overexpression and underexpression that were common to all the studies included in their meta-analysis. Therefore it is an example of how the application of a given statistical technique leads to the extraction of specific sets of genes that may not overlap completely with the sets of genes extracted by a different analytical procedure. In the following, we will briefly consider several new markers, identified in microarray studies, for which there is more than one source of evidence for their value to

distinguish malignant from nonmalignant prostate tissue. This selection favors those markers independently validated for discrimination of neoplastic versus normal states by additional techniques, such as immunohistochemistry, *in situ* hybridization, or real-time RT-PCR.

Genes Overexpressed in Prostate Cancer

Hepsin

The gene for hepsin has been reported as overexpressed in prostate cancer in several studies, and in all cases it has been found to be one of the markers that most significantly distinguishes malignant from nonmalignant prostate tissue (Dhanasekaran *et al*., 2001; Magee *et al*., 2001; Welsh *et al*., 2001). This overexpression has been subsequently validated by immunohistochemistry, *in situ* hybridization, and real-time RT-PCR, confirming the value of HPN as a marker for prostate cancer. Hepsin is overexpressed in all stages of prostate neoplasia, including PIN lesions, localized prostate carcinoma, and metastatic lesions, and no correlation has been found between expression and Gleason score, and it has been found to be overexpressed in neoplasias other than prostate cancer (Tanimoto *et al*., 1997). Hepsin is a protease localized at the cell surface of hepatocytes and has been suggested to be required for their growth (Torres-Rosado *et al*., 1993). It has been reported that hepsin plays a role in blood coagulation by proteolitic activation factor VII. However, mutant mice lacking hepsin do not show any discernible phenotype, except for increased serum levels of hepatic enzymes in the absence of visible damage to hepatocytes, and the mutant animals have normal embryogenesis, organ development, and liver regeneration and normal blood coagulation status (Wu *et al*., 1998). Somewhat contrary to what might have been expected from its high levels of expression in neoplasia, transfection and overexpression of hepsin into human PC-3 prostate cells cause arrest in G2-M, apoptosis, and diminished invasive capacity (Srikantan *et al*., 2002). These studies indicate that, despite the usefulness of the immunohistologic detection of hepsin as an indictor of prostate malignancy, its role in prostate cancer and other biologic processes remains to be determined.

Alpha-Methylacyl Coenzyme A Racemase

The gene for this enzyme was found overexpressed in prostate cancer in several microarray studies (Dhanasekaran *et al*., 2001; Jiang *et al*., 2001; Luo *et al*., 2001; Welsh *et al*., 2001) and validated by RT-PCR, Western Blotting, and immunohistochemistry (Jiang *et al*., 2002). AMACR is expressed at elevated

levels in atypical adenomatous hyperplasia (AHH) and PIN, and in localized and metastatic prostate cancer (Yang *et al*., 2002), and its value as a diagnostic aid in immunohistochemical analysis of prostatic fine needle biopsies has been evaluated, with very promising results (Jiang *et al*., 2002). AMACR is overexpressed in other tumor types, including colorectal and breast carcinomas and precursor lesions such as colon adenomas (Zhou *et al*., 2002). AMACR is a peroxisomal and mitochondrial enzyme that catalyzes the racemization of alpha-methyl-branched carboxylic coenzyme A thioesters. Although its role in cancer is just beginning to be studied (Zha *et al*., 2003), the high prevalence of its overexpression in different types of tumors converts AMACR into a potential therapeutic candidate.

Fatty Acid Synthase

Overexpression of the gene for FASN in prostate cancer was found in several microarray studies (Dhanasekaran *et al*., 2001; Welsh *et al*., 2001). FASN had been previously noted as a predictor of malignancy and progression in prostate cancer (Epstein *et al*., 1995), and it is overexpressed in other tumor types, such as breast, endometrium, ovarian, or colorectal cancers (Beveridge *et al*., 1988; Rashid *et al*., 1997). Molecular mechanisms have been explored to explain the overexpression of FASN in cancer, with evidence that it may be the result of excessive signaling in the Akt protein kinase pathway (van de Sande *et al*., 2002). These observations are relevant in that undue activation of Akt protein kinases is a common occurrence in androgen-independent prostate cancer cells, possibly as a result of the overexpression of the receptor tyrosine kinase HER-2 or other abnormal signaling, for example by loss of *PTEN* function, both of which occur in advanced prostate cancer. Inhibition of FASN leads to selective cytotoxic effects on cancer cells, and this enzyme has been proposed as a therapeutic target for cancer (Kuhajda *et al*., 2000).

Prostate-Specific Membrane Antigen

The gene for prostate-specific membrane antigen (PSMA) has long been known to be overexpressed in prostate cancer (Israeli *et al*., 1993; Reiter *et al*., 1998), although it is also present in benign prostate epithelium and endothelial cells in areas of neoangiogenesis associated with prostate tumor cells and other types of tumors (Chang *et al*., 1999). PSMA levels in prostate tumor cells increase in states of androgen deprivation or androgen independence (Wright *et al*., 1996). This protein is localized at the cell surface and has folate hydrolase and dipeptidase activities. In addition to prostate epithelium, PSMA is expressed in a number of other cell types, including duodenal columnar (brush border) epithelium, renal proximal tubular epithelium, benign breast epithelium, and a subset of skeletal muscle fibers (Chang *et al*., 1999). Detection of serum levels of PSMA is currently used by a number of laboratories to evaluate prostate cancer recurrence and metastasis in combination with PSA levels (Murphy *et al*., 1998). Because PSMA is a cell surface marker, it is also being evaluated for the radioimmunolocalization of prostate cancer metastases or residual disease, and as a target for tumor immunotherapy. No published studies have addressed the contribution of PSMA to the malignant phenotype of prostate cancer cells.

Myc

As discussed earlier, the Myc transcriptional regulator is a key participant in cellular processes associated with transformation and apoptosis (for recent reviews on the subject, see Hoffman *et al*., 2002; Pelengaris *et al*., 2002). High levels of MYC expression can occur as a consequence of increased transcription through amplification (Jenkins *et al*., 1997), chromosomal rearrangements that juxtapose a strong promoter to the MYC gene (Hoffman *et al*., 2002), or the activation of certain signaling pathways (e.g., the Wnt/β-catenin/Tcf pathway) (Gounari *et al*., 2002). In addition to transcriptional mechanisms, *MYC* message and protein can accumulate as a result of mutations that increase message stability or translation (Pelengaris *et al*., 2002). In prostate cancer, amplification and overexpression of *MYC* correlates with poor prognosis and more advanced disease (Jenkins *et al*., 1997). The 8q21-24 amplicon containing MYC also includes EIF3 (Nupponen *et al*., 1999) and PSCA, or prostate stem cell antigen (Reiter *et al*., 2000), two genes that are often overexpressed in prostate cancer, with higher levels associated with tumor progression (Nupponen *et al*., 1999; Reiter *et al*., 1998). The gene for the protein translation factor EIF3 (subunit 2) is one of the genes found to be overexpressed in malignant prostate epithelium in several microarray studies (Ernst *et al*., 2002; Rhodes *et al*., 2002). *Myc* suppresses the transcription of the cell-cycle/growth arrest genes *GAS1*, *p151NK4B*, *p21WAF1*, and *p27KIP*, among others, as well as the cell-cycle–modulated transcriptional regulators eIF4 and eIF2α. It activates the transcription of CCND2 (cyclin D2), CDK4, fatty acid synthase, ornithine decarboxylase, or NME1 (Mennsen and Hermeking, 2002; Watson *et al*., 2002). In the microarray analyses of prostate cancer described earlier, several of these targets of *Myc* transcriptional activity are up- or down-regulated in a pattern reminiscent of Myc-dependent regulation. This leaves open the possibility that advanced prostate cancer is a reflection, at least in part, of an "*Myc* overexpression" state.

Ezh2

The gene for Ezh2, a polycomb group protein regulating transcription through the modulation of chromatin architecture, is overexpressed in metastatic prostate cancer (LaTulippe *et al*., 2002; Varambally *et al*., 2002), and tumors with higher expression of its gene have poorer prognosis (Varambally *et al*., 2002). Overexpression of Ezh2 is also associated with prostate cancer recurrence, particularly when combined with a modest to strong expression of E-cadherin (Rhodes *et al*., 2003). Overexpression of Ezh2 was previously observed in lymphoid malignancies (Visser *et al*., 2001). Other genes coding for proteins that regulate chromatin architecture and global transcriptional state have been found abnormally expressed in cancer, such as Bmi-1 or Su(z)12, which are also polycomb group proteins (Kirmizis *et al*., 2003). Ezh2 is the human ortholog of *Drosophila* protein *enhancer of zeste* (LaJeunesse, 1996), and contains a suvar 3-9, enhancer-of-zeste, trithorax (SET) domain, through which it interacts with chromatin. SET domains are present in a number of proteins that associate with chromatin. Ezh2 shows histone methyl transferase activity (Cao *et al*., 2002) and, in association with the polycomb-group protein Eed, recruits histone deacetylases (van der Vlag and Otte, 1999). Ezh2 has been implicated in imprinted X chromosome inactivation. In overexpression studies in prostate cancer cells, Varambally *et al*. (2002) have shown that Ezh2 silences a specific set of genes that requires its histone deacetylase activity. They also observed that depletion of Ezh2 by siRNA caused growth inhibition and accumulation of cells in G2-M. This study was the first to imply a regulator of chromatin modeling in prostate cancer and poses the interesting questions whether transcriptional repression has a role in the origin and progression of this type of tumors, as has been suggested for other tumors (Jacobs and van Lohuizen, 2002), and the identity of the genes, that presumably control cell proliferation, survival, or invasion, that are the targets of this repression. The same study addressed the latter issue by comparing transcriptomes of cells overexpressing Ezh2 with the transcriptomes of parental cells, with the finding that the set of genes significantly down-regulated by this protein did not completely overlap sets of genes that are underexpressed in prostate tumors. More work will undoubtedly identify the target genes for Ezh2 that are most relevant for prostate cancer biology.

Other Genes

ERG, *MYBL2*, *PIM1*, *PTOV1*, *UBCH10*, and *IQGAP* are genes other than those described earlier that are found overexpressed in at least two microarray studies of prostate cancer or whose elevated expression in prostate cancer is supported by independent studies that use immunohistochemistry and other techniques for *in situ* expression analysis (Dhanasekaran *et al*., 2001; Ernst *et al*., 2002; LaTulippe *et al*., 2002; Santamaria *et al*., 2002; Welsh *et al*., 2001). Of these genes, the mitotic ubiquitin-conjugating enzyme UbcH10, which mediates the ubiquitination and degradation of cyclin B1 (Bastians *et al*., 1999), and IQGAP, a calmodulin-binding GTPase that modulates cytoskeletal architecture (Briggs and Sacks, 2003), are overexpressed in prostate cancer in several of the microarray studies (Ernst *et al*., 2001; LaTulippe *et al*., 2002; Welsh *et al*., 2001), but otherwise have not been implicated in cancer. Pim1, a serine/threonine kinase initially reported to confer susceptibility for the development of thymic lymphomas by retroviral targeting in a murine model, was shown by Dhanasekaran *et al*. (2001) to be overexpressed in prostate cancer and, to a lesser extent, PIN lesions. The same study, however, found that higher levels of expression correlate with improved survival (Dhanasekaran *et al*., 2001). PTOV1 is a mitogenic protein with unknown biochemical function that is overexpressed in PIN and in prostate cancer, with levels that correlate with proliferation index but not with Gleason score (Santamaria *et al*., 2002).

Genes Underexpressed in Prostate Cancer

Annexins

The annexins are a family of structurally related proteins that bind to phospholipids in a calcium-dependent manner. *ANX1*, *ANX2*, *ANX4*, and *ANX7* have been reported to be down-regulated in prostate cancer, most significantly in high-grade and hormone-independent tumors (Paweletz *et al*., 2000; Srivastava *et al*., 2001; Xin *et al*., 2003), and *ANX7* has been proposed as a tumor suppressor gene (Srivastava *et al*., 2001). Both overexpression and loss of expression of annexins have been reported in many types of tumors, including esophageal, lung, pancreas, lymphoid, and brain. Annexin 1 (ANX1) is a substrate of the epidermal growth factor receptor and regulates the activity of cytoplasmic phospholipase A2. Annexin 2 (ANX2) is a substrate of Src pp60 and protein kinase C, and its surface form functions as a coreceptor for tissue plasminogen activator. Annexin 4 (ANX4) interacts with glycosaminoglycans and may have a role in regulated secretion pathways. Annexin 7 (ANX7) is a substrate of phosphorylation by protein kinase C, has a GTPase activity, regulates IP3 receptor expression, and mediates exocytic membrane fusion. Thus, although all

annexins have very similar structures, each has distinct properties and functions. The functional significance of the simultaneous loss of several annexins in advanced cancer is not immediately obvious. This coordinate loss of expression in advanced prostate cancer may be the consequence of genetic alterations or common signals affecting transcription or other levels of expression of these annexins.

Caveolins

Caveolae are cholesterol-rich vesicular invaginations of the plasma membrane that require caveolins as critical scaffolding components. Caveolin-1 regulates the stability of caveolin-2, and, in turn, caveolin-2 regulates the formation of caveolae by caveolin-1. In microarray studies, levels of CAV2 expression are diminished in prostate cancer (Rhodes *et al.*, 2002). Although these results have not been confirmed by *in situ* expression techniques, they fit into what is known of the function of caveolins and their association with cancer. There is increasing evidence that caveolae may serve as platforms for integrating a number of signal-transduction machineries that are initiated at the cell surface. In particular, caveolin-1 binds to certain kinases in their catalytically active sites, thereby blocking their activity (Couet *et al.*, 1997). Based on the negative regulation of cell growth by caveolin 1 (Galbiati *et al.*, 1998), the tumor-prone phenotype of CAV1 null mice, and the frequent loss of expression in certain human tumors, CAV1 has been proposed as a tumor supressor gene (Razani *et al.*, 2001). The genes *CAV1* and *CAV2* colocalized to a fragile site on chromosome 7q31.1, a segment frequently lost in cancer, are also lost in a significant proportion of papillary thyroid carcinomas (Aldred *et al.*, 2003). Furthermore, a proportion of human breast cancers have mutations of the *CAV1* gene at a segment of the protein that functions in protein–protein interactions, presumably resulting in a diminished activity as an attenuator of positive growth signals (Hayashi *et al.*, 2001). Finally, the CAV1 promoter is hypermethylated in a large proportion of prostate cancer samples (Cui *et al.*, 2001). All these data support a role for *CAV1* as a tumor supresor. In observations that are seemingly in conflict with such a role, it has been reported that caveolin 1 levels are elevated in some cancers, including advanced prostate cancer (Yang *et al.*, 1998), and it has been suggested that elevated caveolin 1 may contribute to the androgen insensitive state of advanced prostate cancer (Nasu *et al.*, 1998). In view of these conflicting observations, and the finding of mutations in other cancers, it may be of interest to determine if the *CAV1* and *CAV2* genes expressed in advanced prostate tumors contain any inactivating mutations.

GAS1

The growth arrest–specific proteins are a heterogeneous group of proteins, operationally defined by virtue of their increased expression in cells that have exited the cell cycle. GAS1 is anchored to the cell surface through a glycosidyl phosphatidylinositol moiety, through which it associates with caveolae. Increased expression of GAS1 is stimulated on exit from cell cycle and senescence. GAS1 induces growth arrest that is dependent on *p53* but does not require its transactivation function (del Sal *et al.*, 1995). However, there are reports indicating that GAS1 may induce, rather than suppress, growth in certain cell types or conditions. Of interest in the context of other genes abnormally expressed in prostate cancer, it has been shown that GAS1 is transcriptionally repressed by *Myc* (Lee *et al.*, 1997). Therefore, a decreased expression of GAS1 in prostate cancer could be a consequence and an indicator of the altered expression and/or function of genes and proteins that regulate the Myc and/or Wnt/β-catenin/Tcf pathways (Lee *et al.*, 2001).

Glutathione-S-Transferases (GST)

The glutathione-S-transferase (GST) enzymes play an important role in detoxification by catalyzing the conjugation of many hydrophobic and electrophilic compounds with reduced glutathione. *GSTP1* is expressed at high levels in normal prostate gland basal cells but is lost in adenocarcinoma as a result of hypermethylation of the GSTP1 promoter (Lee *et al.*, 1994). Genetic studies have concluded that polymorphisms in the *GSTP1* gene are linked to susceptibility to prostate cancer (Harries *et al.*, 1997). Also, it has been reported that the probability of having prostate cancer is increased in men who have nondeleted (functional) genotypes at GSTT1 but not GSTM1 (Rebbek *et al.*, 1999). Thus, different GSTs appear to present different behaviors in prostate cancer. Their loss of expression in early stages of this neoplasia could result in increased susceptibility to the mutagenic action of certain agents, whereas increased expression in more advanced disease could be associated with resistance to chemotherapeutic agents.

Other Genes

In one microarray study (Dhanasekaran *et al.*, 2001), genes for several proteins of the transforming growth factor-beta (TGFβ) signaling pathways are underrepresented in prostate cancer. In physiologic conditions, activation of these pathways leads to growth arrest and loss-of-function mutations of genes, for regulators of this system are frequent in many types of tumors. However, functional interactions with the

RAS pathway subverts the TGFβ signaling, transforming it into positive stimuli for cell growth. In prostate cancer and other neoplasms, high levels of TGFβ ligands and their receptors are associated with a poor prognosis (reviewed in Bello-DeOcampo and Tindall, 2003). However, the expression of TGFβ ligands and receptors is down-regulated by androgen receptor (Evangelou *et al*., 2000). Therefore, it is possible that at early stages of prostate cancer progression, with high androgenic signaling, the TGFβ pathway is repressed, whereas at more advanced stages this repression is lost, concomitant with the conversion of the TGFβ signals into positive stimuli for growth, possibly because of the acquisition of novel mutations in proteins that interact with this pathway.

Additional genes, such as *FOSB* or *MEIS1*, appear to be down-regulated in prostate cancer as determined by two or more microarray studies, although the results require further validation. The protein FOSB, related to the transcriptional regulator c-FOS, has transforming activity. Its expression has been studied in multiple neoplasias, and it is generally associated with positive regulation of cell growth. Nevertheless, loss of expression of FOSB protein has been reported during breast cancer malignant progression possibly through post-transcriptional mechanisms (Milde-Langosch *et al*., 2003). MEIS1, a homebox protein with functions in normal development, was discovered by retroviral integration in a mouse model of leukemia (Moskow *et al*., 1995). Its gene has been found over-expressed in certain leukemias, but a more general role of MEI1 in cancer has not been explored.

Global Views of Prostate Cancer from Global Transcriptome Analysis

The power of the microarray technology is now well established for finding single markers or cohorts of genes associated with malignancy or specific aspects of the biology of prostate cancer, such as histologic appearance (Singh *et al*., 2002) or metastasis (LaTulippe *et al*., 2002; Ramaswamy *et al*., 2003). These sets of genes can be used in diagnostic applications but also for prognostic purposes (Singh *et al*., 2002). Beyond these applications, the microarray technology offers new ways of looking at the problem of underlying biochemical processes and mechanisms in cancer. The coordinated expression of genes reflects common transcriptional regulation, which is a result of the activation of specific signaling pathways. The significant differential cooccurrence of genes for proteins participating in a common biochemical pathway can be taken as a predominant activation of that pathway. From their meta-analysis study, Rubin *et al*. (2002)

have concluded that the pathways for polyamine and adenine monophosphate biosynthesis are overactivated in prostate cancer. However, the association of groups of coregulated genes that are overexpressed or underexpressed with other biochemical or signaling pathways (that may lead to indications of aberrant activities underlying the process of neoplastic transformation in prostate epithelium) has not been reported. For example, many studies have emphasized the importance of excessive or dysregulated signaling that originates at the cell surface in the development of androgen-independent states (for example, Craft *et al*., 1999; reviewed in Feldman and Feldman, 2001) or the crucial role played by signals mediated by the androgen receptor in early stages of prostate cancer. The microarray studies reviewed here do not convey unequivocal evidences for the concerted expression of genes that mark the predominant activation of either of these pathways in one stage or another in prostate cancer progression. This may be the result of the long-contended biologic heterogeneity of prostate cancer, which would hamper the discovery of global common traits. Should this be the case, microarray studies that include many more cases, preferably including microdissected samples, could provide the answer. Much needed are also improvements in algorithms and databases that permit the association of gene expression profiles with specific pathways, in the line of efforts such as KEGG (Kanehisa *et al*., 2002) and GenMAPP (Dahlquist *et al*., 2002).

CONCLUSIONS

A great number of genetic and epigenetic abnormalities have been reported in prostate neoplastic transformation and progression, many of them involving genes more or less closely related to cell-cycle regulation, and all the previously mentioned alterations reflect the great complexity of the oncogenic process that the prostate, like other organs, undergoes (reviewed in de Marzo *et al*., 2001; Lijovic and Frauman, 2003; Nwosu *et al*., 2001). The higher frequency of alterations in expression rather than at the gene level suggests that epigenetic mechanisms, increasingly demonstrated for different cell-cycle–related genes in different tumor types, will most likely be recognized to play a major role in prostate carcinogenesis. In this sense, expression profiling with HTTs is currently providing abundant information on the transcriptome status in prostate and other types of cancers, and it is becoming increasingly evident that it will be the transcriptomic and proteomic analysis of expression pathways, rather than the genomic status, which will help to clarify the carcinogenic mechanisms

and potential therapeutic approaches to cancer in the near future.

Acknowledgments

References

Aaltomaa, S., Eskelinen, M., and Lipponen, P. 1999. Expression of cyclin a and d proteins in prostate cancer and their relation to clinicopathological variables and patient survival. *Prostate* 38:175–182.

Aldred, M.A., Ginn-Pease, M.E., Morrison, C.D., Popkie, A.P., Gimm, O., Hoang-Vu, C., Krause, U., Dralle, H., Jhiang, S.M., Plass, C., and Eng C. 2003. Caveolin-1 and caveolin-2, together with three bone morphogenetic protein-related genes, may encode novel tumor suppressors down-regulated in sporadic follicular thyroid carcinogenesis. *Cancer Res. 63*:2864–2871.

Alers, J.C., Rochat, J., Krijtenburg, P-J., Hop, W.C.J., Kranse, R., Rosenberg, C., Tanke, H.J., Schröder, F.H., and van Dekken, H. 2000. Identification of genetic markers for prostatic cancer progression. *Lab. Invest. 80*:931–942.

Amler, L.C., Agus, D.V., DeDuc, C., Sapinoso, M.L., Fox, W.E., Kern, S., Lee, D., Wang, V., Laysens, M., Higgins, B., Martin, J., Gerald, W., Dracopoli, N., Cordon-Cardon, C., Scher, H.W., and Hampton, G.M. 2000. Dysregulated expression of androgen-responsive and nonresponsive genes in the androgen-independent prostate cancer xenograft model CWR22-R. *Cancer Res. 60*:6134–6141.

Bastians, H., Topper, L.M., Gorbsky, G.L., and Ruderman, J.V. 1999. Cell cycle-regulated proteolysis of mitotic target proteins. *Mol. Biol. Cell 10*:3927–3941.

Bello-DeOcampo, D., and Tindall, D.J. 2003. TGF-betal/Smad signaling in prostate cancer. *Curr. Drug Targets 4*:197–207.

Beveridge, R.A., Chan, D.W., Bruzek, D., Damron, D., Bray, K.R., Gaur, P.K., Ettinger, D.S., Rock, R.C., Shurbaji, M.S., and Kuhajda, F.P. 1988. A new biomarker in monitoring breast cancer: CA 549. *J. Clin. Oncol. 6*:1815–1821.

Bostwick, D.G., and Foster, C.S. 1999. Predictive factors in prostate cancer: Current concepts from the 1999 College of American Pathologists Conference on solid tumor prognostic factors and the 1999 World Health Organization Second International Consultation on prostate cancer. *Semin. Urol. Oncol. 17*:222–272.

Briggs, M.W., and Sacks, D.B. 2003. IQGAP proteins are integral components of cytoskeletal regulation. *EMBO Rep. 4*:571–574.

Cairns, P., Polascik, T.J., Eby, Y., Tokino, K., Califano, J., Merlo, A., Mao, L., Herath, J., Jenkins, R., Westra, W., and Bova, G.S. 1995. Frequency of homozygous deletion at p16/CDKN2 in primary human tumours. *Nat. Genet. 11*:210–212.

Cao. R., Wang, L., Wang, H., Xia, L., Erdjument-Bromage, H., Tempst, P., Jones, R.S., and Zhang, Y. 2002. Role of histone H3 lysine 27 methylation in Polycomb-group silencing. *Science 298*:1039–1043.

Chang, S.S., Reuter, V.E., Heston, W.D., Bander, N.H., Grauer, L.S., and Gaudin, P.B. 1999. Five different anti-prostate-specific membrane antigen (PSMA) antibodies confirm PSMA expression in tumor-associated neovasculature. *Cancer Res. 59*:3192–3198.

Chi, S-G., de Vere White, R.W., Meyers, F.J., Siders, D.B., Lee, F., and Gumerlock, P.H. 1994. P53 in prostate cancer: Frequent expressed transition mutations. *J. Natl. Cancer Inst. 86*:926–933.

Cole, K.A., Krizman, D.B., and Emmert-Buck, M.R. 1999. The genetics of cancer—a 3D model. *Nat. Genet. 21*:38–41.

Couet, J., Sargiacomo, M., and Lisanti, M.P. 1997. Interaction of a receptor tyrosine kinase, EGF-R, with caveolins. Caveolin binding negatively regulates tyrosine and serine/threonine kinase activities. *J. Biol. Chem. 272*:30429–30438.

Cui, J., Rohr, L.R., Swanson, G., Speights, V.O., Maxwell, T., and Brothman, A.R. 2001. Hypermethylation of the caveolin-1 gene promoter in prostate cancer. *Prostate 46*:249–256.

Craft, N., Shostak, Y., Carey, M., and Sawyers, C.L. 1999. A mechanism for hormone-independent prostate cancer through modulation of androgen receptor signaling by the HER-2/neu tyrosine kinase. *Nature Med. 5*:280–285.

Dahlquist, K.D., Salomonis, N., Vranizan, K., Lawlor, S.C., and Conklin, B.R. 2002. GenMAPP, a new tool for viewing and analyzing microarray data on biological pathways. *Nat. Genet. 31*:19–20.

Dash, A., Maine, I.P., Varambally, S., Shen, R., Chinnaiyan, A.M., and Rubin, M.A. 2002. Changes in differential gene expression because of warm ischemia time of radical prostatectomy specimens. *Am. J. Pathol. 161*:1743–1748.

del Sal, G., Ruaro, E.M., Utrera, R., Cole, C.N., Levine, A.J., and Schneider, C. 1995. Gas1-induced growth suppression requires a transactivation-independent p53 function. *Mol. Cell Biol. 15*:7152–7160.

De Marzo, A.M., Meeker, A.K., Epstein, J.I., and Coffey, D.S. 1998. Prostate stem cell compartments: Expression of the cell cycle inhibitor p27kip1 in normal, hyperplastic, and neoplastic cells. *Am. J. Pathol. 153*:911–919.

De Marzo, A.M., Putzi, M.J., and Nelson, W.G. 2001. New concepts in the pathology of prostatic epithelial carcinogenesis. *Urology 57*(Suppl 4A):103–114.

Dhanasekaran, S.M., Barrette, T.R., Ghosh, D., Shah, R., Varambally, S., Kurachi, K., Plenta, K.J., Rubin, M.A., and Chinnaiyan, A.M. 2001. Delineation of prognostic biomarkers in prostate cancer. *Nature 412*:822–826.

Epstein, J.I., Carmichael, M., and Partin, A.W. 1995. OA-519 (fatty acid synthase) as an independent predictor of pathologic state in adenocarcinoma of the prostate. *Urology 45*:81–86.

Ernst, T., Hergenhahn, M., Kenzelmann, M., Cohen, C.D., Bonrouhi, M., Weninger, A., Klaren, R., Grone, E.F., Wiesel, M., Gudemann, C., Kuster, J., Schott, W., Staehler, G., Kretzler, M., Hollstein, M., and Grone, H.J. 2002. Decrease and gain of gene expression are equally discriminatory markers for prostate carcinoma: A gene expression analysis on total and microdissected prostate tissue. *Am. J. Pathol. 160*:2169–2180.

Evangelou, A., Jindal, S.K., Brown, T.J., and Letarte, M. 2000. Down-regulation of transforming growth factor beta receptors by androgen in ovarian cancer cells. *Cancer Res. 60*:929–935.

Feldman, B.J., and Feldman, D. 2001. The development of androgen independent prostate cancer. *Nat. Rev. Cancer 1*:34–45.

Fernandez, P.L., Arce, Y., Farre, X., Martinez, A., Nadal, A., Rey, M.J., Peiro, N., Campo, E., and Cardesa, A. 1999. Expression of p27/kip1 is down-regulated in human prostate carcinoma progression. *J. Pathol. 187*:563–566.

Gaddipati, J.P., McLeod, D.G., Sesterhenn, I.A., Hussussian, C.J., Seth, P., Dracopoli, N.C., Moul, J.W., and Srivastava, S. 1997. Mutations of the p16 gene product are rare in prostate cancer. *Prostate 30*:188–194.

Galbiati, F., Volonte, D., Engelman, J.A., Watanabe, G., Burk, R., Pestell, R.G., and Lisanti, M.P. 1998. Targeted downregulation of caveolin-1 is sufficient to drive cell transformation and hyperactivate the p42/44 MAP kinase cascade. *EMBO. J. 17*: 6633–6648.

Gao, X., Chen, Y.Q., Wu, N., Grignon, D.J., Sakr, W., Porter, A.T., and Honn, K.V. 1997. Somatic mutations of the waf1/cip1 gene in primary prostate cancer. *Oncogene 11*:1395–1398.

Goodrich, D.W., Wang, N.P., Qian, Y.W., Lee, E.Y., and Lee, W.H. 1991. The retinoblastoma gene product regulates progression through the G1 phase of the cell cycle. *Cell 67*: 293–302.

Gounari, F., Signoretti, S., Bronson, R., Klein, L., Sellers, W.R., Kum, J., Siermann, A., Taketo, M.M., von Boehmer, H. and Khazaie, K. 2003. Stabilization of beta-catenin induces lesions reminiscent of prostatic intraepithelial neoplasia, but terminal squamous transdifferentiation of other secretory epithelia. *Oncogene 21*:4099–4107.

Harries, L.W., Stubbins, M.J., Forman, D., Howard, G.C., and Wolf, C.R. 1997. Identification of genetic polymorphisms at the glutathione S-transferase Pi locus and association with susceptibility to bladder, testicular and prostate cancer. *Carcinogenesis 18*:641–644.

Hayashi, K., Matsuda, S., Machida, K., Yamamoto, T., Fukuda, Y., Nimura, Y., Hayakawa, T,. and Hamaguchi, M. 2001. Invasion activating caveolin-1 mutation in human scirrhous breast cancers. *Cancer Res. 61*:2361–2364.

Hoffman, B., Amanullah, A., Shafarenko, M., and Liebermann, D.A. 2002. The proto-oncogene c-myc in hematopoietic development and leukemogenesis. *Oncogene 21*:3414–3421.

Hollstein, M., Sidransky, D., Vogelstein, B., and Harris, C.C. 1991. P53 mutations in human cancer. *Science 253*:49–53.

Israeli, R.S., Powell, C.T., Fair, W.R., and Heston, W.D. 1993. Molecular cloning of a complementary DNA encoding a prostate-specific membrane antigen. *Cancer Res. 53*:227–230.

Jacobs, J.J. and van Lohuizen, M. 2002. Polycomb repression: from cellular memory to cellular proliferation and cancer. *Biochim. Biophys. Acta 1602*:151–161.

Jenkins, R.B., Qian, J., Lieber, M.M., and Bostwick, D.G. 1997. Detection of c-*myc* oncogene amplification and chromosomal anomalies in metastatic prostatic carcinoma by fluorescence *in situ* hybridization. *Cancer Res. 57*:524–531.

Jiang, Z., Woda, B.A., Rock, K.L., Xu, Y., Savas, L., Khan, A., Pihan, G., Cai, F., Babcook, J.S., Rathanaswami, P., Reed, S.G., Xu, J., and Fanger, G.R. 2001. P504S: A new molecular marker for the detection of prostate carcinoma. *Am. J. Surg. Pathol. 25*:1397–1404.

Jiang, Z., Wu, C.L., Woda, B.A., Dresser, K., Xu, J., Fanger, G.R., and Yang, X.J. 2002. P504S/alpha-methylacyl-CoA racemase: A useful marker for diagnosis of small foci of prostatic carcinoma on needle biopsy. *Am. J. Surg. Pathol. 26*:1169–1174.

Kaltz-Wittmer, C., Klenk, U., Glaessgen, A., Aust, D.E., Diebold, J., Lohrs, U., and Baretton, G.B. 2000. FISH analysis of gene aberrations (MYC,CCND1,ERBB2,RB, and AR) in advanced prostatic carcinomas before and after androgen deprivation therapy. *Lab. Invest. 80*:1455–1464.

Kanehisa, M., Goto, S., Kawashima, S., and Nakaya, A. The KEGG databases at GenomeNet. *Nucleic Acids Res. 30*:42–46.

Kirmizis, A., Bartley, S.M., and Farnham, P.J. 2003. Identification of the Polycomb Group Protein SU(Z)12 as a potential molecular target for human cancer therapy. *Mol. Cancer Ther. 2*:113–121.

Kibel, A.S., Faith, D.A., Bova, G.S., and Isaacs, W.B. 2000. Loss of heterozygosity at 12P12-13 in primary and metastatic prostate adenocarcinoma. *J. Urol. 164*:192–196.

Kolar, Z., Murray, P.G., Scott, K., Harrison, A., Vojtesek, B., and Dusek, J. 2000. Relation of Bcl-2 expression to androgen receptor, p21WAF1/CIP1, and cyclin D1 status in prostate cancer. *Mol. Pathol. 53*:15–18.

Kuhajda, F.P., Pizer, E.S., Li, J.N., Mani, N.S., Frehywot, G.L., and Townsend, C.A. 2000. Synthesis and antitumor activity of an inhibitor of fatty acid synthase. *Proc. Natl. Acad. Sci USA 97*:3450–3454.

Krupski, T., Petroni, G.R., Frierson, H.F. Jr., and Theodorescu, J.U. 2000. Microvessel density, p53, retinoblastoma, and chromogranin a immunohistochemistry as predictors of disease-specific survival following radical prostatectomy for carcinoma of the prostate. *Urology 55*:743–749.

LaJeunesse, D., and Shearn, A., 1996. E(z): A polycomb group gene or a trithorax group gene? *Development 22*:2189–2197.

LaTulippe, E., Satagopan, J., Smith, A., Scher, H., Scardino, P., Reuter, V., and Gerald, W.L. 2002. Comprehensive gene expression analysis of prostate cancer reveals distinct transcriptional programs associated with metastatic disease. *Cancer Res. 62*:4499–4506.

Lee, C.S., Buttitta, L., and Fan, C.M. 2001. Evidence that the WNT-inducible growth arrest-specific gene 1 encodes an antagonist of sonic hedgehog signaling in the somite. *Proc. Natl. Acad. Sci. USA 98*:11347–11352.

Lee, C.T., Capodieci, P., Osman, I., Fazzari, M., Ferrara, J., Scher, H.I., and Cordon-Cardo, C. 1999. Overexpression of the cyclin-dependent kinase inhibitor p16 is associated with tumor recurrence in human prostate cancer. *Clin. Cancer Res. 5*:977–983.

Lee, T.C., Li, L., Philipson, L., and Ziff, E.B. 1997. Myc represses transcription of the growth arrest gene gas1. Myc represses transcription of the growth arrest gene gas1. *Proc. Natl. Acad. Sci. USA 94*:12886–12891.

Lee, W.H., Morton, R.A., Epstein, J.I., Brooks, J.D., Campbell, P.A., Bova, G.S., Hsieh, W.S., Isaacs, W.B., and Nelson, W.G. 1994. Cytidine methylation of regulatory sequences near the pi-class glutathione S-transferase gene accompanies human prostatic carcinogenesis. *Proc. Natl. Acad. Sci. USA 91*:11733–11737.

Levine, A.J., Momand, J., and Finlay, C.A. 1991. The p53 tumor suppressor gene. *Nature 351*:453–456.

Lijovic, M., and Frauman, A.G. 2003. Toward an understanding of the molecular genetics of prostate cancer progression. *J. Environ. Pathol. Toxicol. Oncol. 22*:1–15.

Luo, J., Duggan, D.J., Chen, Y., Sauvageot, J., Ewing, C.M., Bittner, M.L., Trent, J.M., and Issacs, W.B. 2001. Human prostate cancer and benign prostatic hyperplasia: Molecular dissection by gene expression profiling. *Cancer Res. 61*:4683–4688.

Magee, J.A., Araki, T., Patil, S., Ehrig, T., True, L., Humphrey, P.A., Catalona, W.J., Watson, M.A., and Milbrandt, J. 2001. Expression profiling reveals hepsin overexpression in prostate cancer. *Cancer Res. 61*:5692–5696.

Mangold, K.A., Takahashi, H., Brandigi, C., Wada, T., Wakui, S., Furusato, M., Boyd, J., Chandler, F.W., and Allsbrook, W. Jr. 1997. P16 (cdkn2/mts1) gene deletions are rare in prostatic carcinomas in the United States and Japan. *J. Urol. 157*:1117–1120.

Menssen, A., and Hermeking, H. 2002. Characterization of the c-MYC-regulated transcriptome by SAGE: Identification and analysis of c-MYC target genes. *Proc. Natl. Acad. Sci. USA 99*:6274–6279.

Milde-Langosch, K., Kappes, H., Riethdorf, S., Loning, T., and Bamberger, A.M. 2003. FosB is highly expressed in normal mammary epithelia, but down-regulated in poorly differentiated breast carcinomas. *Breast Cancer Res. Treat.* TT:265–275.

Moskow, J.J., Bullrich, F., Huebner, K., Daar, I.O., and Buchberg, A.M. 1995. Meisl, a PBX1-related homeobox gene involved in myeloid leukemia in BXH-2 mice. *Mol. Cell Biol. 15*:5434–5443.

Murphy, G.P., Kenny, G.M., Ragde, H., Wolfert, R.L., Boynton, A.L., Holmes, E.H., Misrock, S.L., Bartsch, G., Klocker, H., Pointner, J., Reissigl, A., McLeod, D.G., Douglas, T., Morgan, T., and Gilbaugh, J. Jr. 1998. Measurement of serum prostate-specific membrane antigen, a new prognostic marker for prostate cancer. *Urology 51(5A Suppl)*:89–97.

Nasu, Y., Timme, T.L., Yang, G., Bangma, C.H., Li, L., Ren, C., Park, S.H., DeLeon, M., Wang, J., and Thompson, T.C. 1998. Suppression of caveolin expression induces androgen sensitivity in metastatic androgen-insensitive mouse prostate cancer cells. *Nat. Med. 4*:1062–1064.

Nupponen, N.N., Porkka, K., Kakkola, L., Tanner, M., Persson, K., Borg, A., Isola, J., and Visakorpi, T. 1999. Amplification and overexpression of p40 subunit of eukaryotic translation initiation factor 3 in breast and prostate cancer. *Am. J. Pathol. 154*:1777–1783.

Nwosu, V., Carpten, J., Trent, J.M., and Sheridan, R. 2001. Heterogeneity of genetic alterations in prostate cancer: Evidence of the complex nature of the disease. *Hum. Mol. Genet. 10*:2313–2318.

Paweletz, C.P., Ornstein, D.K., Roth, M.J., Bichsel, V.E., Gillespie, J.W., Calvert, V.S., Vocke, C.D., Hweitt, S.M., Duray, P.H., Herring, J., Wang, Q.H., Hu, N., Linehan, W.M., Taylor, P.R., Liotta, L.A., Emmert-Buck, M.R., and Petricoin, E.F. 3rd. 2000. Loss of annexin I correlates with early onset of tumorigenesis in esophageal and prostate carcinoma. *Cancer Res. 60*:6293–6297.

Pelengaris, S., Khan, M., and Evan. G. 2002. c-MYC: More than just a matter of life and death. *Nat. Rev. Cancer 2*:764–776.

Ponce-Castaneda, M.V., Lee, M.H., Latres, E., Polyak, K., Lacombe, L., Montogomery, K., Mathew, S., Krauter, K., Sheinfeld, J., and Massague, J. 1995. P27/kip1: Chromosomal mapping to 12p12-12p13.1 and absence of mutations in human tumors. *Cancer Res. 55*:1211–1214.

Quinn, D.I., Henshall, S.M., Head, D.R., Golovsky, D., Wilson, J.D., Brenner, P.C., Turner, J.J., Delprado, W., Finlayson, J.F., Stricker, P.D., Grygiel, J.J., and Sutherland, R.L. 2000. Prognostic significance of p53 nuclear accumulation in localized prostate cancer treated with radical prostatectomy. *Cancer Res. 60*:1585–1594.

Ramaswamy, S., Ross, K.N., Lander, E.S., and Golub, T.R. 2003. A molecular signature of metastasis in primary solid tumors. *Nat. Genet. 33*:49–54.

Rashid, A., Pizer, E.S., Moga, M., Milgraum, L.Z., Zahurak, M., Pasternack, G.R., Kuhajda, F.P., and Hamilton, S.R. 1997. Elevated expression of fatty acid synthase and fatty acid synthetic activity in colorectal neoplasia. *Am. J. Pathol. 150*:201–208.

Razani, B., Engelman, J.A., Wang, X.B., Schubert, W., Zhang, X.L., Marks, C.B., Macaluso, F., Russell, R.G., Li, M., Pestell, R.G., Di Vizio, D., Hou, H. Jr., Kneitz, B., Lagaud, G., Christ, G.J., Edelmann, W., and Lisanti, M.P. 2001. Caveolin-1 null mice are viable but show evidence of hyperproliferative and vascular abnormalities. *J. Biol. Chem. 276*:38121–38138.

Rebbeck, T.R., Walker, A.H., Jaffe, J.M., White, D.L., Wein, A.J., and Malkowicz, S.B. 1999. Glutathione S-transferase-mu (GSTM1) and –theta (GSTT1) genotypes in the etiology of prostate cancer. *Cancer Epidemiol. Biomarkers Prev. 8*:283–287.

Reiter, R.E., Gu, Z., Watabe, T., Thomas, G., Szigeti, K., Davis, E., Wahl, M., Nisitani, S., Yamashiro, J., Le Beau, M.M., Loda, M., and Witte, O.N. 1998. Prostate stem cell antigen: A cell surface marker overexpressed in prostate cancer. *Proc. Natl. Acad. Sci. USA 95*:1735–1740.

Reiter, R.E., Sato, I., Thomas, G., Qian, J., Gu, Z., Watabe, T., Loda, M., and Jenkins, R.B. 2000. Coamplification of prostate stem cell antigen (PSCA) and MYC in locally advanced prostate cancer. *Genes Chromos. Cancer 27*:95–103.

Rhodes, D.R., Barrette, T.R., Rubin, M.A., Ghosh, D., and Chinnaiya, A.M. 2002. Meta-analysis of microarrays: Interstudy validation of gene expression profiles reveals pathway dysregulation in prostate cancer. *Cancer Res. 62*:4427–4433.

Rhodes, D.R., Sanda, M.G., Otte, A.P., Chinnaiyan, A.M., and Rubin, M.A. 2003. Multiplex biomarket approach for determining risk of prostate-specific antigen-defined recurrence of prostate cancer. *J. Natl. Cancer. Inst. 95*:661–668.

Ruijter, E., van de Kaa, C., Miller, G., Ruiter, D., Debruyne, F., and Schalken, J. 1999. Molecular genetics and epidemiology of prostate carcinoma. *Endocr. Rev. 20*:22–45.

Santamaria, A., Fernandez, P.L., Farre, X., Benedit, P., Reventos, J., Morote, J., Paciucci, R., and Thomson, T.M. 2003. PTOV-1, a novel protein overexpressed in prostate cancer, shuttles between the cytoplasm and the nucleus and promotes entry into the S phase of the cell division cycle. *Am. J. Pathol. 162*:897–905.

Sarkar, F.H., Li, Y., Sakr, W.A., Grignon, D.J., Madan, S.S., Wood, D.P. Jr., and Adsay, V. 1999. Relationship of p21(waf1) expression with disease-free survival and biochemical recurrence in prostate adenocarcinomas (pca). *Prostate 40*:56–260.

Sherr, C.J., and Roberts, J.M. 1995. Inhibitors of mammalian g1 cyclin-dependent kinases. *Genes Dev. 9*:1149–1163.

Singh, D., Febbo, P.G., Ross, K., Jackson, D.G., Manola, J., Ladd, C., Tamayo, P., Renshaw, A.A., D'Amico, A.V., Richie, J.P., Lander, E.S., Loda, M., Kantoff, P.W., Golub, T.R., and Sellers, W.R. 2002. Gene expression correlates of clinical prostate cancer behaviour. *Cancer Cell 1*:203–209.

Srikantan, V., Vallaqdares, M., Rhim, J.S., Moul, J.W., and Srivastava, S. 2002. HEPSIN inhibits cell growth/invasion in prostate cancer cells. *Cancer Res. 62*:6812–6816.

Srivastava, M., Bubendorf, L., Srikantan, V., Fossom, L., Nolan, L., Glasman, M., Leighton, X., Fehrle, W., Pittaluga, S., Raffeld, M., Koivisto, P., Willi, N., Gasser, T.C., Kononen, J., Sauter, G., Kallioniemi, O.P., Srivastava, S., and Pollard, H.B. 2001. ANX7, a candidate tumor suppressor for prostate cancer. *Proc. Natl. Acad. Sci. USA 98*:4575–4780.

Tanimoto, H., Yan, Y., Clarke, J., Korourian, S., Shigemasa, K., Parmley, T.H., Parham, G.P., and O'Brien, T.J. 1997. Hepsin, a cell surface serine protease indentified in hepatoma cells, is overexpressed in ovarian cancer. *Cancer Res. 57*: 2884–2887.

Torres-Rosado, A., O'Shea, K.S., Tsuji, A., Chou, S.H., and Kurachi, K. 1993. Hepsin, a putative cell-surface serine protease, is required for mammalian cell growth. *Proc. Natl. Acad. Sci. USA 90*:7181–7185.

Valafar, F. 2002. Pattern recognition techniques in microarray data analysis. *Ann. N.Y. Acad. Sci. 980*:41–64.

Van de Sande, T., De Schrijver, E., Heyns, W., Verhoeven, G., and Swinnen, J.V. 2002. Role of the phosphatidylinositol 3′-kinase/PTEN/Akt kinase pathway in the overexpression of fatty acid synthase in LNCaP prostate cancer cells. *Cancer Res. 62*:642–646.

van der Vlag, J., and Otte, A.P. 1999. Transcriptional repression mediated by the human polycomb-group protein EED involves histone deacetylation. *Nat. Genet. 23*:474–478.

Varambally, S., Dhanasekaran, S.M., Zhou, M., Barrette, T.R., Kumar-Sinha, C., Sanda M.G., Ghosh, D., Pienta, K.J.,

Sewalt, R.G., Otte, A.P., Rubin, M.A., and Chinnaiyan, A.M. 2002. The polycomb group protein EZH2 is involved in progression of prostate cancer. *Nature 419*:624–629.

Visser, H.P., Gunster, M.J., Kluin-Nelemans, H.C., Manders, E.M., Raaphorst, F.M., Meijer, C.J., Willemze, R., and Otte, A.P. 2001. The Polycomb group protein EZH2 is upregulated in proliferating, cultured human mantle cell lymphoma. *Br. J. Haematol. 112*:950–958.

Watson, J.D., Oster, S.K., Shago, M., Khosravi, F., and Penn, L.Z. 2002. Identifying genes regulated in a Myc-dependent manner. *J. Biol. Chem. 277*:36921–36930.

Welsh, J.B., Sapinoso, L.M., Su, A.I., Kern, S.G., Wang-Rodriguez, J., Moskaluk, C.A., Frierson, H.F., Jr., and Hampton, G.M. 2001. Analysis of gene expression identifies candidate markers and pharmacological targets in prostate cancer. *Cancer Res. 61*:5974–5978.

Wright, G.L., Grob, B.M., Haley, C., Grossman, K., Newall, K., Petrylak, D., Troyer, J., Konchuba, A., Schellhammer, P.F., and Moriarty, R. 1996. Upregulation of prostate-specific membrane antigen after androgen-deprivation therapy. *Urology 48*:326–334.

Wu, Q., Yu, D., Post, J., Halks-Miller, M., Sadler, J.E., and Morser, J. 1998. Generation and characterization of mice deficient in

hepsin, a hepatic transmembrane serine protease. *J. Clin. Invest. 101*:321–326.

Xin, W., Rhodes, D.R., Ingold, C., Chinnaiyan, A.M., and Rubin, M.A. 2003. Dysregulation of the annexin protein family is associated with prostate cancer progression. *Am. J. Pathol. 162*:255–261.

Yang, G., Truong, L.D., Timme, T.L., Ren, C., Wheeler, T.M., Park, S.H., Nasu, Y., Bangma, C.H., Kattan, M.W., Scardino, P.T., and Thompson, T.C. 1998. Elevated expression of caveolin is associated with prostate and breast cancer. *Clin. Cancer Res. 4*:1873–1880.

Yang, X.J., Wu, C.L., Woda, B.A., Dresser, K., Tretiakova, M., Fanger, G.R., and Jiang, Z. 2002. Expression of alpha-Methylacyl-CoA racemase (P504S) in atypical adenomatous hyperplasia of the prostate. *Am. J. Surg. Pathol. 26*:921–925.

Zha, S., Ferdinandusse, S., Denis, S., Wanders, R.J., Ewing, C.M., Luo, J., De Marzo, A.M., and Isaacs, W.B. 2003. Alpha-methylacyl-CoA racemase as an androgen-independent growth modifier in prostate cancer. *Cancer Res. 63*:7365–7376.

Zhou, M., Chinnaiyan, A.M., Kleer, C.G., Lucas, P.C., and Rubin, M.A. 2002. Alpha-Methylacyl-CoA racemase: A novel tumor marker over-expressed in several human cancers and their precursor lesions. *Am. J. Surg. Pathol. 26*:926–931.

4

In situ Hybridization of Human Telomerase Reverse Transcriptase mRNA in Prostate Carcinoma

Bernd Wullich, Jörn Kamradt, Volker Jung, and Thomas Fixemer

Introduction

There is strong experimental evidence that the maintenance of functional telomeres, and thus telomerase activity, is critical to a wide variety of cancers. Telomerase is expressed in ~90% of all human malignancies, including nearly 95% of prostate carcinomas, making it one of the most widespread molecular cancer markers (Shay and Bacchetti, 1997). In prostate cancer, the most common malignancy in elderly men in Western countries, increased telomerase activity is already evident at the very early stages of the disease, namely high-grade prostatic intraepithelial neoplasia (HGPIN) (Koeneman *et al.*, 1998; Zhang *et al.*, 1998).

Because it is found in almost all prostate cancers, telomerase is a candidate for improved diagnostic and therapeutic strategies. Its clinical use, however, is still limited because of several reasons. The telomerase regulatory mechanisms during cancer development are still largely undefined, based on both transcriptional and post-transcriptional mechanisms. The existence of different regulatory mechanisms possibly occurring in either a tissue-specific or tumor-specific manner are likely. We showed in prostate carcinomas that the two human telomerase core components (human telomerase ribonucleic acid [RNA] [hTR] and human telomerase reverse transcriptase [hTERT]) are not sufficient to determine telomerase activity (Kamradt *et al.*, 2003).

This at least holds true for the transcription product of hTERT because our studies were performed at the messenger RNA (mRNA) level.

At the protein level, chaperones-mediated telomerase assembly and function and the role of telomerase inhibitors have been focused by most recent studies (Akalin *et al.*, 2001; Nishimoto *et al.*, 2001). Furthermore, it remains unclear what high and low telomerase activities represent at the cellular level in clinical cancer specimens. On the one hand, variation in telomerase activity among cancer tissues might either reflect different levels of telomerase expression in each tumor cell or might be the result of numeric differences of telomerase expressing tumor cells within a tumor. However, although repressed during embryonic development in most tissues, telomerase activity remains detectable in some nonmalignant cells such as germline cells, hematopoietic progenitor cells, activated lymphocytes, a subset of epidermal and intestinal cells, and even in normal human fibroblasts (Hiyama *et al.*, 1995; Hiyama *et al.*, 1996; Masutomi *et al.*, 2003; Taylor *et al.*, 1996). This must be considered when interpreting telomerase determination studies because the *telomeric repeat amplification protocol (TRAP)* assay for sensitive detection of telomerase activity is usually applied to whole tissue samples, which are composed of a mixture of different cell types. *In situ* technologies are, therefore, required

Handbook of Immunohistochemistry and *in situ* Hybridization of Human Carcinomas, Volume 2: Molecular Pathology, Colorectal Carcinoma, and Prostate Carcinoma

321

to determine the cellular origin of telomerase in clinical specimens.

Visualization of hTERT mRNA Expression In Prostate Cancer Tissue Sections by *in situ* Hybridization

MATERIALS AND METHODS

hTERT cDNA Probe

For hTERT mRNA detection, a previously described 1261-bp cDNA fragment (from nucleotides 1895-3155) cloned into a polymerase chain reaction (PCR) II vector was used as probe (Liu *et al*., 1999). The 1261-bp fragment was a kind gift from Dr. Nan-Ping Weng (Laboratory of Immunology, Gerontology Research Center, National Institute on Aging, National Institutes of Health, Baltimore, MD). Sense and antisense mRNA hTERT probes were synthesized by *in vitro* transcription using T7 Transcription Kit (MBI Fermentas, St. Leon-Roth, Germany) and labeled with digoxigenin-dUTP (Roche Diagnostics, Mannheim, Germany). The sense probe served for negative control.

Preparation of Tissue Sections and Prehybridization

Formalin-fixed and paraffin-embedded tissue sections (5-µm thick) were deparaffinized in xylene (2 × 15 min) and rehydrated in graded series of alcohols. The slides were rinsed in deionized water and equilibrated in phosphate buffer saline (PBS) for further enzymatic treatment in 400 µg/ml proteinase K (Merck, Darmstadt, Germany) at 37°C for 15 min. After digestion, the sections were fixed with 4% paraformaldehyde in PBS for 5 min at room temperature and washed twice in 2X saline-sodium citrate (SSC) (Merck). For prehybridization, the slides were covered with 40 µl of the hybridization buffer without labeled mRNA antisense probe containing 2X SSC, 1X Denhardt's solution (50X Denhardt's stock solution: 1% polyvinylchloride, 1% pyrrolidone, 2% bovine serum albumin [BSA] (Oncor, Heidelberg, Germany), 10% dextran sulfate (Roche Diagnostics), 50 mM phosphate buffer (pH 7.0), 50 mM 1,4-dithiothreitol (Roche Diagnostics), 250 µg/ml yeast transfer RNA (tRNA) (Roche Diagnostics), 100 µg/ml polyadenylic acid (Roche Diagnostics), 500 µg/ml denatured and sheared DNA from fish sperm (Roche Diagnostics), and 40% deionized formamide (Oncor) and were incubated for 2 hr at 41°C in a humid chamber.

Hybridization and Immunodetection

The sections were hybridized overnight at 41°C with 40 µl hybridization mixture containing the hybridization buffer and 10 pM labeled mRNA hTERT probe per slide. After washing in graded concentrations of SSC (e.g., 2X, 1X, 0.1X for 30 min each) at 37°C, the sections were preincubated with 2% BSA solution for 20 min and then incubated with antiDig-POD FAB fragments (Roche Diagnostics). A signal amplification method based on the deposition of homemade biotinylated tyramine (dilution 1:500) (Jacobs *et al*., 1998) was used to enhance immunodetection. After precipitation of the biotinylated tyramine (10 min at room temperature) through the enzymatic action of horseradish peroxidase (HRP) and H_2O_2 (0.1%), the biotin precipitate was detected with an additional application of the HRP-labeled avidin–biotin complex (ABComplex/HRP; Dako) for 30 min in a humid chamber. The peroxidase reaction was developed with 3,3'-diaminobenzidine (Sigma). Finally, the slides were dehydrated, permanent mounted, and coverslipped for further microscopic analysis.

Control Experiments

In each hybridization experiment, labeled sense mRNA probes and RNase A-treated slides served as negative controls. The RNA digestion was performed by incubating the slides for 30 min at 37°C in a digestion buffer (0.5 M NaCl, 10 mM Tris-HCl, 1 mM ethylenediaminetetra-acetic acid [EDTA], pH 7.2) containing 10 µg/µl RNase A (Roche Diagnostics). Only RNase-sensitive signals were considered positive for hTERT mRNA expression.

Detection of hTERT mRNA in Malignant and Nonmalignant Prostate Tissue Specimens

RESULTS AND DISCUSSION

Using *in situ* hybridization, we demonstrated strong hTERT mRNA expression in the tumor glands, as shown in Figure 44 (Kamradt *et al*., 2003). A homogeneous staining distribution pattern is observed irrespective of varying Gleason grades between different tumor areas. At the cellular level, positive staining of hTERT is localized almost exclusively in the cytoplasm. It is interesting that we also recognized strong expression of hTERT mRNA in the epithelial cells of HGPIN foci (Figure 45), a finding that was similarly
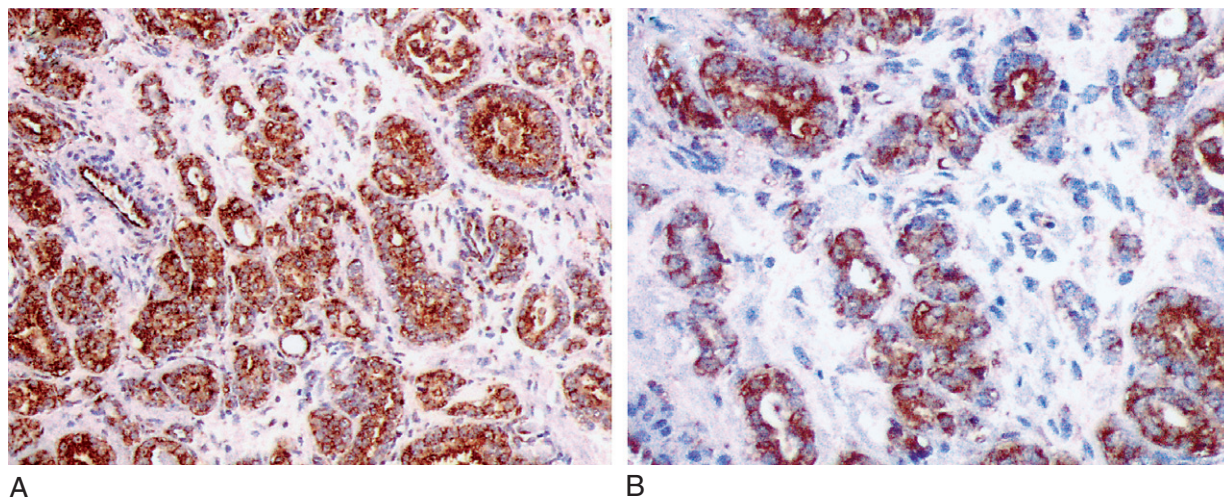
Figure 44 Human telomerase reverse transcriptase (hTERT) messenger ribonucleic acid (mRNA) expression in primary prostate cancer, Gleason 3. Labeling is observed in all tumor glands revealing a homogeneous distribution pattern. Note hTERT mRNA expression also in endothelial cells of the tumor microvessels. The stromal tissue is unlabeled (magnification 100X **(A)** 200X **(B)**).

described for hTR expression (Paradis *et al.*, 1999). Because it is generally accepted that HGPIN is a precursor of prostate cancer, this finding indicates that hTERT is expressed early in prostate carcinogenesis. Concerning cellular heterogeneity of clinical tissue specimens, it is of particular importance that endothelial cells and inflammatory cells also reveal hTERT mRNA expression as did the mucosal cells of the prostatic urethra. No staining of the surrounding stromal cells is detected.

It is important to note that we detected hTERT mRNA expression also in normal prostate tissue and benign prostatic hyperplasia (BPH). Labeling is restricted to the basal cell layer of normal glands (Figure 46). The secretory luminal cells are found to be hTERT negative, supporting experimental models that have shown basal cells to behave as stem cells that differentiate into secretory cells (Bonkhoff and Remberger, 1996). The low number of hTERT-expressing cells in the whole tissue of the BPH samples corresponds to the low overall levels of hTERT mRNA, which were measured in BPH by real-time reverse transcription (RT)-PCR (Kamradt *et al.*, 2003).

Comparing the *in situ* hTR expression patterns in benign and malignant prostate tissue sections, which were reported by Paradis *et al.* (1999), with our
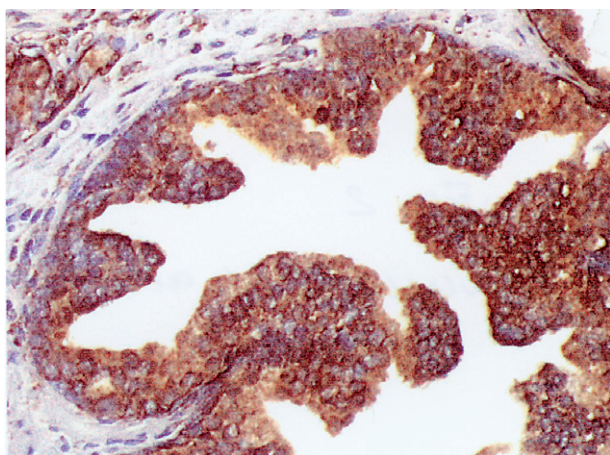
Figure 45 Human telomerase reverse transcriptase (hTERT) messenger ribonucleic acid (mRNA) expression in high-grade prostatic intraepithelial neoplasia (HGPIN) lesion. All epithelial cells of the HGPIN lesion express hTERT mRNA (magnification, 200X).
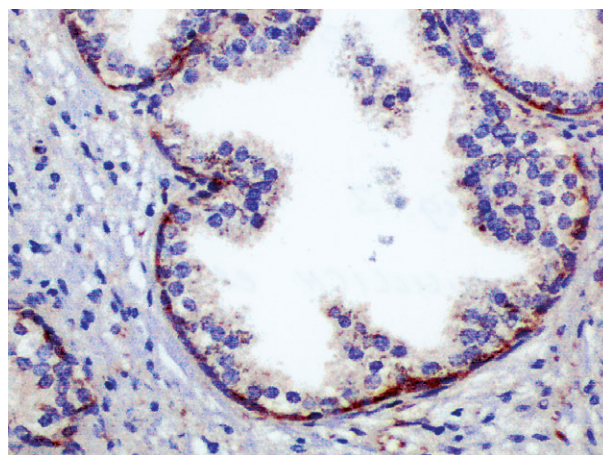
Figure 46 Human telomerase reverse transcriptase (hTERT) messenger ribonucleic acid (mRNA) expression in normal prostate gland. Labeling is restricted to the basal cell layer (magnification, 200X). No labeling is observed in the secretory cells and stromal tissue.

findings, the concordance of hTR and hTERT expression on the cellular level is remarkable, indicating some common mechanisms in the up-regulation of hTR and hTERT expression in prostate cells. This observation fits double labeling studies on sections from normal human testis, which reveal many cells with only hTR signals, some cells with both hTERT and hTR signals, but no cells with hTERT signals without hTR expression (Hiyama *et al.*, 2001). Cell culture experiments further indicate an overlap in the transcriptional regulatory control of the two genes (Yi *et al.*, 1999).

Only recently, anti-serum to telomerase became available, allowing immunohistochemical detection of the hTERT protein in clinical tissue specimens (Hiyama *et al.*, 1999; Iczkowski *et al.*, 2002). The distribution of hTERT protein paralleled that of hTERT mRNA. Like hTERT mRNA, hTERT protein is present in luminal cells of HGPIN foci, in cancerous lesions, and in the basal cell layer of normal prostate. The restricted hTERT protein expression in normal prostate tissue corresponds to the low-level telomerase activity in normal prostate gland and BPH, which was measured by the TRAP assay (Kamradt *et al.*, 2003; Zhang *et al.*, 1998).

Concerning subcellular distribution, there is a difference between mRNA and protein expression with the hTERT mRNA in the located cytoplasm and the hTERT protein mainly in the nucleus. This evidence documents the shift of the hTERT protein into the nucleus after translation of the mRNA in the cytoplasm.

In summary, hTERT mRNA seems to be overexpressed in the majority of prostate cancers and cancer cells within this tumor. More systematic studies, however, are still necessary investigating many cases with diverse pathologic characteristics. In terms of early diagnosis on prostate needle biopsy, few validated markers of prostate cancer have been identified that are overexpressed consistently such that they might be of diagnostic use in a large percentage of cases. Although basal cell–specific cytokeratins are a useful aid for diagnosis, these markers are lost in prostate cancer, limiting their diagnostic value because of possibly artifactual loss of immunostaining. In addition to markers such as α-methylacyl-CoA racemase (AMACR) (Luo *et al.*, 2002) and DD3 (Bussemakers *et al.*, 1999), detection of hTERT expression by means of *in situ* hybridization or immunohistochemistry may have important implications in future prostate cancer diagnostics. We have begun to use clinical needle biopsies in prospective studies comparing AMACR, basal cell-specific cytokeratins, and hTERT.

References

Akalin, A., Elmore, L.W., Forsythe, H.L., Amaker, B.A., McCollum, E.D., Nelson, P.S., Ware, J.L., and Holt, S.E. 2001. A novel mechanism for chaperone-mediated telomerae regulation during prostate cancer progression. *Cancer Res. 61*: 4791–4796.

Bonkhoff, H., and Remberger, K. 1996. Differentiation pathways and histogenetic aspects of normal and abnormal prostatic growth: A stem cell model. *Prostate 28*:98–106.

Bussemakers, M.J.G., Bokhoven, van A., Verhaegh, G.W., Smit, F.P., Karthaus H.F.M., Schalken, J.A., Debruyne, F.M.J., Ru, N., and Issacs, W.B. 1999. DD3: A new prostate-specific gene, highly overexpressed in prostate cancer. *Cancer Res. 59*:5975–5979.

Hiyama, E., Hiyama, K., Tatsumoto, N., Kodama, T., Shay, J.W., and Yokoyama, T. 1996. Telomerase activity in human intestine. *Int. J. Oncol. 9*:453–458.

Hiyama, E., Hiyama, K., Yokoyama, T., and Shay, J.W. 2001. Immunohistochemical detection of telomerase (hTERT) protein in human cancer tissues and a subset of cells in normal tissues. *Neoplasia 3*:17–26.

Hiyama, K., Hirai, Y., Kyoizumi, S., Akiyama, M., Hiyama, E., Piatyszek, M.A., and Shay, J.W. 1995. Activation of telomerase in human lymphocytes and hematopoietic progenitor cells. *J. Immunol. 155*:3711–3715.

Iczkowski, K.A., Pantazis, C.G., McGregor, D.H., Wu, Y., and Tawfik, O.W. 2002. Telomerase reverse transcriptase subunit immunoreactivity: A marker for high-grade prostate carcinoma. *Cancer 95*:2487–2493.

Jacobs, W., Dhaene, K., and van Marck, E. 1998. Tyramine-amplified immunohistochemical testing using "homemade" biotinylated tyramine is highly sensitive and cost-effective. *Arch. Pathol. Lab. Med. 122*:642–643.

Kamradt, J., Drosse, C., Kalkbrenner, S., Rohde, V., Lensch, R., Lehmann, J., Fixemer, T., Bonkhoff, H., Stoeckle, M., and Wullich, B, 2003. Telomerase activity and telomerase subunit gene expression levels are not related in prostate cancer: A real-time quantification and in situ hybridization study. *Lab. Invest. 83*:623–633.

Koeneman, K.S., Pan, C.X., Jin, J.K., Pyle, J.M. 3rd, Flanigan, R.C., Shankey, T.V., and Diaz, M.O. 1998. Telomerase activity, telomere length, and DNA ploidy in prostatic intraepithelial neoplasia (PIN). *J. Urol. 160*:1533–1539.

Liu, K., Schoonmaker, M. M., Levine, B.L., June, C.H., Hodes, R.J., and Weng, N.P. 1999. Constitutive and regulated expression of telomerase reverse transcriptase (hTERT) in human lymphocytes. *Proc. Natl. Acad. Sci. USA 96*:5147–5152.

Luo, J., Zha, S., Gage, W.R., Dunn, T.A., Hicks, J.L., Bennett, C.J., Ewing, C.M., Platz, E.A., Ferdinandusse, S., Wanders, R.J., Trent, J.M., Isaacs, W.B., and De Marzo, A.M. 2002. Alpha-methylacyl-CoA-racemase: A new molecular marker for prostate cancer. *Cancer Res. 62*:2220–2226.

Masutomi, K., Yu, E.Y., Khurts, S., Ben-Porath, I., Currier, J.L., Metz, G.B., Brooks, M.W., Kaneko, S., Murakami, S., DeCaprio, J.A., Weinberg, R.A., Stewart, S.A., and Hahn, W.C. 2003. Telomerase maintains telomere structure in normal human cells. *Cell 114*:241–253.

Nishimoto, A., Miura, N., Horikawa, I., Kugoh, H., Murakami, Y., Hirohashi, S., Kawasaki, H., Gazdar, A.F., Shay, J.W., Barrett, J.C., and Oshimura, M. 2001. Functional evidence for a telomerase repressor gene on human chromosome 10p15.1. *Oncogene 20*:828–835.

Paradis, V., Dargere, D., Laurendeau, I., Benoit, G., Vidaud, M., Jardin, A., and Bedossa, P. 1999. Expression of the RNA component of human telomerase (hTR) in prostate cancer, prostatic intraepithelial neoplasia, and normal prostate tissue. *J. Pathol.* *189*:213–218.

Shay, J.W., and Bacchetti, S. 1997. A survey of telomerase activity in human cancer. *Eur. J. Cancer 33*:787–791.

Taylor, R.S., Ramirez, R.D., Ogoshi, M., Chaffins, M., Piatyszek, M.A., and Shay, J.W. 1996. Detection of telomerase activity in malignant and nonmalignant skin condition. *J. Invest. Dermatol.* *196*:756–765.

Yi, X., Tesmer, V.M., Savre-Train, I., Shay, J.W., and Wright, W.E. 1999. Both transcriptional and posttranscriptional mechanisms regulate human telomerase template RNA-levels. *Mol. Cell Biol. 19*:3989–3997.

Zhang, W., Kapusta, L.R., Slingerland, J.M., and Klotz, L.H. 1998. Telomerase activity in prostate cancer, prostatic intraepithelial neoplasia, and benign prostatic epithelium. *Cancer Res. 58*:619–621.

This Page Intentionally Left Blank

5

Detection of Genetic Abnormalities Using Comparative Genomic Hybridization in Prostate Cancer Cell Lines

Lisa W. Chu and Jan C. Liang

Introduction

Comparative genomic hybridization (CGH) is a genome-wide method for screening changes in relative copy number of deoxyribonucleic acid (DNA) sequences (Kallioniemi *et al*., 1992). In CGH, genomic DNAs extracted from clinical samples or cell lines are used as probes (test DNA) and are hybridized against normal genomic DNA (reference DNA) onto normal metaphase spreads (target). Chromosomes from the metaphase spreads are then analyzed using a CGH image analysis system. The imaging system measures the intensity of signals from both the test and the reference probes along the axis of each chromosome. Ratios of test to reference intensities are then calculated along the chromosomal axis and visualized on a histogram of intensity ratios as a function of distance along the chromosomal axis. Regions of chromosomes that are more abundant in the test sample will have a ratio of greater than 1, whereas a ratio of less than 1 signifies decrease in DNA copy number in the test sample as compared to the reference.

As a result of its methodology, CGH offers advantages over many commonly used techniques. Specifically, gains and losses of specific chromosomal regions can be identified without the need for metaphase spread from patient samples or cell lines, which is necessary in conventional cytogenetics as well as multicolor karyotyping (i.e., Spectral Karyotyping, etc.). This feature of CGH also allows for the analysis of archival tissues (Isola *et al*., 1994). In addition, the use of tumor-cell genomic DNA as probe onto normal metaphase spreads in CGH eliminates the need for specific DNA probes and sequences that are necessary for techniques such as fluorescence *in situ* hybridization (FISH), polymerase chain reaction (PCR)-based methods, and restriction fragment length polymorphisms (RFLPs). These advantages also make CGH highly suitable for the analysis of solid tumors that are not easily cultured and for analyzing tumor cell lines that have complex chromosomal rearrangements.

Prostate cancer is one example of a cancer whose tumors are difficult to grow in culture and whose (very few) established cell lines have highly complex cytogenetic abnormalities. This disease is the most commonly diagnosed cancer and the second leading cause of cancer death among men in the United States (*Cancer Facts and Figures*, 2003). Because most prostate cancers are detected at an early stage, the challenge for clinicians is to determine which patients will progress

to have a more serious and life-threatening disease and thus need more aggressive treatment at the earliest stage possible. To this end, established prostate cancer cell lines have been used extensively to investigate tumor progression because they can be manipulated *in vitro* and in xenografts *in vivo*.

To emulate the progression of prostate tumors, Pettaway *et al*. (1996) created two *in vivo* models of prostate tumor progression using established prostate cancer cell lines, PC3M and LNCaP. Successive orthotopic implantation of these two cell lines into nude mice generated several variants of different growth characteristics and metastatic potential. The PC3M cell line was originally derived from liver metastases produced in nude mice subsequent to intrasplenic injection of the well-known PC3 cell line (Kaighn *et al*., 1979; Koslowski *et al*., 1984). Model PC3M and its selected variant sublines, PC3M–Pro4 and PC3M–LN4, were all tumorigenic and metastatic. However, orthotopic implantation of PC3M–Pro4 into nude mice produced significantly larger prostate tumors than either the parental or PC3M–LN4 lines. In contrast, PC3M–LN4 produced significantly larger lymph node tumors and was more metastatic to distant sites after orthotopic injection as compared to PC3M or PC3M–Pro4.

The model LNCaP and its selected variant sublines, LNCaP–Pro5 and LNCaP–LN3, represent a less aggressive prostate tumor progression model than the PC3M variant lines (Pettaway *et al*., 1996). Although all three sublines were tumorigenic, LNCaP–Pro5 was able to grow into significantly larger prostate tumors after orthotopic implantation into nude mice as compared to the other two lines. In contrast, LNCaP–LN3 had significantly higher incidences of lymph node metastases and produced significantly larger metastatic tumors in the lymph nodes.

In this chapter, we will describe how we used CGH to analyze genetic alterations in the six prostate cancer cell lines discussed earlier (Chu *et al*., 2001). Cytogenetics on two (LNCaP and LNCaP–LN3) of the six cell lines show that both cell lines had highly complex karyotypes, with chromosome numbers ranging from 71–97. The LNCaP model had a median chromosome number of 88 with 7 marker chromosomes, whereas LNCaP–LN3 had a median of 92 chromosomes with 8 marker chromosomes (Pettaway *et al*., 1996). These markers have been tentatively identified, but the exact chromosomal origins could not be determined. With CGH, we more precisely identified chromosomal gains and losses of the cell lines. We then compared the chromosomal abnormalities of the parental versus their respective variant cell lines to determine if unique abnormalities could contribute to the different biologic behaviors of the different sublines.

MATERIALS

1. High-molecular–weight (>4 kb) whole-genomic DNA from a normal male donor (reference DNA).
2. High-molecular–weight (>4 kb) whole-genomic DNA from each cell line (test DNA).
3. 10X Nick translation reaction buffer: 200 μM dATP, 200 μM dCTP, 200 μM dGTP, 500 μM Tris (pH 7.2), 200 μM MgCl$_2$, 100 μM beta-mercaptoethanol, 100 μg/ml bovine serum albumin (BSA) in ddH$_2$O (double distilled H$_2$O). Store at –20°C.
4. 1 mM Fluorescein–12–dUTP (DuPont NEN).
5. 1 mM TexasRed–5–dUTP (DuPont NEN).
6. 5–10 U/μl DNA Polymerase I (Invitrogen Corp., Carlsbad, CA).
7. BioNick 10X enzyme: obtained from BioNick Labeling System (Invitrogen).
8. 1 mg/ml Human Cot-1 DNA (Invitrogen Carlsbad, CA).
9. Normal human male metaphases prepared from lymphocytes on microscope slides (pre-prepared CGH slides can be obtained from Vysis, Inc., Downer's Grove, IL).
10. 3 M Sodium acetate, pH 5.2.
11. 75%, 85%, and 100% ethanol.
12. 20X saline-sodium citrate (SSC): Add 87.66 g of NaCl and 44.115 g citrate (citric acid) to 400 ml ddH$_2$O. pH to 7.0. Add up to 500 ml with ddH$_2$O.
13. 2X SSC: Add 50 ml 20X SSC to 450 ml ddH$_2$O. Place 50 ml in each of 2 coplin jars for post-hybridization slide washing. Change after every use. Store at room temperature.
14. Master hybridization solution (50% formamide/10% dextran sulfate/2X SSC): Add together 5 ml formamide (deionized and redistilled), 1 ml 20X SSC, and 1 g dextran sulfate. Heat at 70°C for 1–2 hours to dissolve the dextran sulfate. Let solution cool to room temperature before adjusting the pH to 7.0 with HCl. Bring volume up to 7 ml with ddH$_2$O. Aliquot and store at –20°C.
15. Slide denaturing solution (70% formamide/2X SSC): Add 35 ml of formamide (deionized and redistilled) and 5 ml 20X SSC, pH 7.0. Adjust the pH to 7.0 with HCl. Bring final volume up to 50 ml with ddH$_2$O. Place solution in coplin jar. Store at 4°C.
16. Post-hybridization slide-washing buffer, 50% formamide/2X, SSC: add 75 ml of formamide, 15 ml 20X SSC, pH 7.0, and 40 ml ddH$_2$O. pH to 7.0 with HCl. Bring final volume up to 150 ml with ddH$_2$O. Place 50 ml in each of three coplin jars. Store at 4°C.
17. 0.1 M Dibasic PN stock: Add 26.807 g Na$_2$HPO$_4$–7H$_2$O, 1 ml NP–40 and up to 1 L with ddH$_2$O. Autoclave to sterilize. Store at room temperature.
18. 0.1 M Monobasic PN stock: Add 13.799 g NaH$_2$PO$_4$–H$_2$O, 1 ml NP–40, and up to 1 L with ddH$_2$O. Autoclave to sterilize. Store at room temperature.

19. PN buffer: Add 0.1 M Monobasic PN stock to the desired volume of 0.1 M Dibasic PN stock to obtain pH 8.0. Place 50 ml in each of two coplin jars for post-hybridization slide washing. Change after every use. Store at room temperature.

20. Anti-fade mounting medium: Add 100 mg p-phenylenediamine dihybrochloride in 10 ml phosphate buffer saline (PBS). Adjust to pH 8.0 with 0.5 M carbonate–bicarbonate buffer (0.42 g $NaHCO_3$ in 10 ml ddH_2O, pH 9.0 with NaOH). Filter through 0.22 μ filter. Add 90 ml glycerol. Mix and store in aliquots in the dark at −20°C.

21. Stock 4,6-diamidino-2-phenylindole (DAPI; 100 μg/ml): Dissolve 1 mg DAPI in 10 ml ddH_2O. Add a few drops of methanol before adding H_2O to help dessolve DAPI. Store at −20°C and protect from light. This solution is stable for more than 1 year.

22. 0.1 μg/ml DAPI in anti-fade: Add 1 μl stock DAPI solution to 1 ml anti-fade mounting medium. Store at −20°C and protect from light. Replace when solution darkens.

23. Fluorescence microscope equipped with a 63X high-NA oil-immersion objective, single band-pass filters for fluorescein, TexasRed, and DAPI, and a black and white cooled CCD camera.

24. CGH image analysis system that is attached to the cooled CCD camera and has appropriate software for capturing and analyzing CGH images. As of this writing, commercial systems are available only from a few companies (i.e., Applied Imaging and MetaSystems).

METHODS

Labeling DNA Probes with Nick Translation

1. Prepare 15°C and 73°C waterbaths.

2. For each sample, mix the following in a 0.5 ml microcentrifuge tube on ice for 50 μl reaction:

> 1 μg high-molecular–weight genomic DNA.
> 1 μl 1 μM fluoroscein-12-dUTP for test DNA probes (or 1 mM TexasRed-5-dUTP for reference DNA probes).
> 5 μl 10X Nick translation reaction buffer.
> 1 μl DNA polymerase I (to optimize nucleotide incorporation).
> 2 μl BioNick 10X enzyme (adjustable depending on the quality of starting DNA and resulting probe size).
> ddH_2O for a final volume of 50 μl.

3. Mix well and microcentrifuge quickly to bring down reaction mix.

4. Incubate mix at 15°C for 60 min.

5. Stop reaction by heating reaction mix for 10 min at 73°C. Electrophorese 5 μl of the reaction mix on a nondenaturing 1% agarose gel for visualization. CGH probes should be in the range of 300–3000 bps for best results.

Comparative Genomic Hybridization

Preparation of Probe Mix

1. Combine the following in a 1.5 ml microcentrifuge tube:

> 10 μl fluorescein-labeled test DNA probe.[a]
> 10 μl TexasRed-labeled reference DNA probe.[a]
> 20 μl 1 μg/μl Human Cot–1 DNA.

2. Add 1/10 volume of 3M sodium acetate, pH 5.2. Mix well.

3. Add 2.5 volume of 100% ethanol to precipitate the DNA.

4. Microcentrifuge for 30 min at 14,000 rpm and 4°C to pellet the DNA.

5. Decant the supernatant and allow the pellet to air-dry for 10 min.

6. Add 10 μl master hybridization solution and resuspend pellet gently with pipet.

Preparation of Target Metaphase Slides

7. Prewarm the slide denaturation solution to 73°C in a waterbath.

8. Etch the glass slide on the backside to indicate region of the slide with metaphase targets. Commercially available slides usually come with two spots on each slide.

9. Prewarm slides on a 37°C slide warmer and then place into the denaturation solution for 2–10 minutes. Denaturing time may vary because of age of slide and batch variation on the metaphase preparation. Optimal time is when chromosome morphology is maintained (e.g., banding patterns exist for identification of chromosomes after DAPI staining) while adequate hybridization occurs.

10. Dehydrate slides by immersing them successively in coplin jars containing 70%, 85%, and 100% ethanol at room temperature for 2 min each.

11. Let slides air-dry.

12. Place slides on 37°C slide warmer.

---

[a]The amounts of test and reference probes can be increased if signals appear too dim.

Probe Denaturing and Hybridization

13. Denature probe mix (**Step 6**) by heating for 5 min at 73°C.

14. Apply 10 μl probe mix to area of slide containing metaphases.

15. Cover with 22 mm² coverslip and seal coverslip edges with rubber cement.

16. Incubate in moist chamber 2–3 days at 37°C.

Post-Hybridization Slide Processing

17. Prewarm three post-hybridization slide-washing buffers and one 2X SSC at 45°C in coplin jars.

18. Peel off rubber cement and gently remove coverslips.

19. Immerse slides in the three post-hybridization slide-washing buffers successively for 10 min each wash at 45°C.

20. Immerse slides in 2X SSC for 10 min at 45°C.

21. Immerse slides in 2X SCC for 10 min at room temperature.

22. Immerse slides in two changes of PN buffer for 5 min each at room temperature.

23. Immerse slides in ddH₂O for 5 min at room temperature.

24. Let slides air-dry.

25. Apply 30 μl 0.1 μg/ml DAPI in anti-fade (for counterstaining the DNA) per slide and cover with a 22 × 50 mm² (No. 1) coverslip.

26. Let DAPI incorporate into DNA for at least 2 hr at room temperature or overnight at 4°C before visualization and analysis.

Comparative Genomic Hybridization Microscopy, Imaging, and Image Analysis

The CGH slides were analyzed using the Olympus AX-70 fluorescence microscope equipped with single band-pass filters for Fluorescein, TexasRed, and DAPI and with a black and white cooled CCD camera (COHU). The MacProbe version 4.0 imaging software (Perceptive Scientific Instruments, Inc., now part of Applied Imaging) was used for CGH image analysis. For detailed instructions on how to use the imaging system, please refer to the user's manual because the procedures differ from system to system. At least 10 chromosome homologues of each chromosome from 5 to 10 normal metaphase spreads per hybridization were used for the mean test to reference ratios, and

the resulting profile was plotted next to chromosome ideograms of 400-band resolution for visual reference. A ratio threshold of 0.80 and 1.20 for detection of losses and gains, respectively, was used. Excluded from the analysis were chromosomes 19, 22, and Y; heterochromatic regions of chromosomes 1, 9, and 16; and acrocentric regions of chromosomes 13, 14, 15, and 21. Regions of loss or gain were included in the final CGH analysis if they were confirmed by dye swap experiments (e.g., test DNA labeled in TexasRed and reference DNA labeled in Fluorescein).

RESULTS AND DISCUSSION

We have performed CGH analysis on two *in vivo* models of prostate cancer progression as an example of how CGH analysis can aid in defining the genetic aberrations in cell lines (Chu *et al.*, 2001). An example of the CGH analysis, or the mean test to reference ratio profiles of the PC3M–LN4 cell line, is shown in Figure 47. Chromosomal regions of gains and losses were then determined from the ratio profiles for each cell line.

The first *in vivo* prostate tumor progression model with the parental cell line, PC3M, and its selected variant cell lines, PC3M–Pro4 and PC34M–LN4, represent an aggressive tumor progression model (Pettaway *et al.*, 1996). All cell lines in this model were tumorigenic and metastatic to lymph nodes. CGH analysis shows that the parental and variant cell lines shared four chromosomal aberrations (gains of 8q22–qter, 10q21–q22, and Xq27–qter and loss of 13q33-qter), suggesting that all cell lines have a common clonal origin. Unique to the parental PC3M was −15q, −17p, and +20q, which may not have been retained in the variant lines because of selective pressure during the establishment of the variants. It is interesting that PC3M and PC3M–Pro4 shared +1q32–q41, whereas PC3M and PC3M–LN4 shared +17q22–q23. Because these clones were derived after four generations of successive orthotopic injection in nude mice, we speculate that retention of +1q32–q41 and +17q22–q23 by PC3M–Pro4 and PC3M–LN4, respectively, is a result of selective pressure of growth in the prostate and the lymph node, respectively, after orthotopic injection into nude mice.

The emergence of the specific gain on 3q13 in PC3M–Pro4, which grew into a large prostate tumor after orthotopic injection as compared to the parental, may contribute to the growth characteristic of PC3M–Pro4. Although there are no previous reports of the involvement of this region in prostate cancer, abnormalities involving 3q13 have been reported in small and non–small-cell lung cancer (Balsara *et al.*, 1997; Dennis and Stock, 1999).
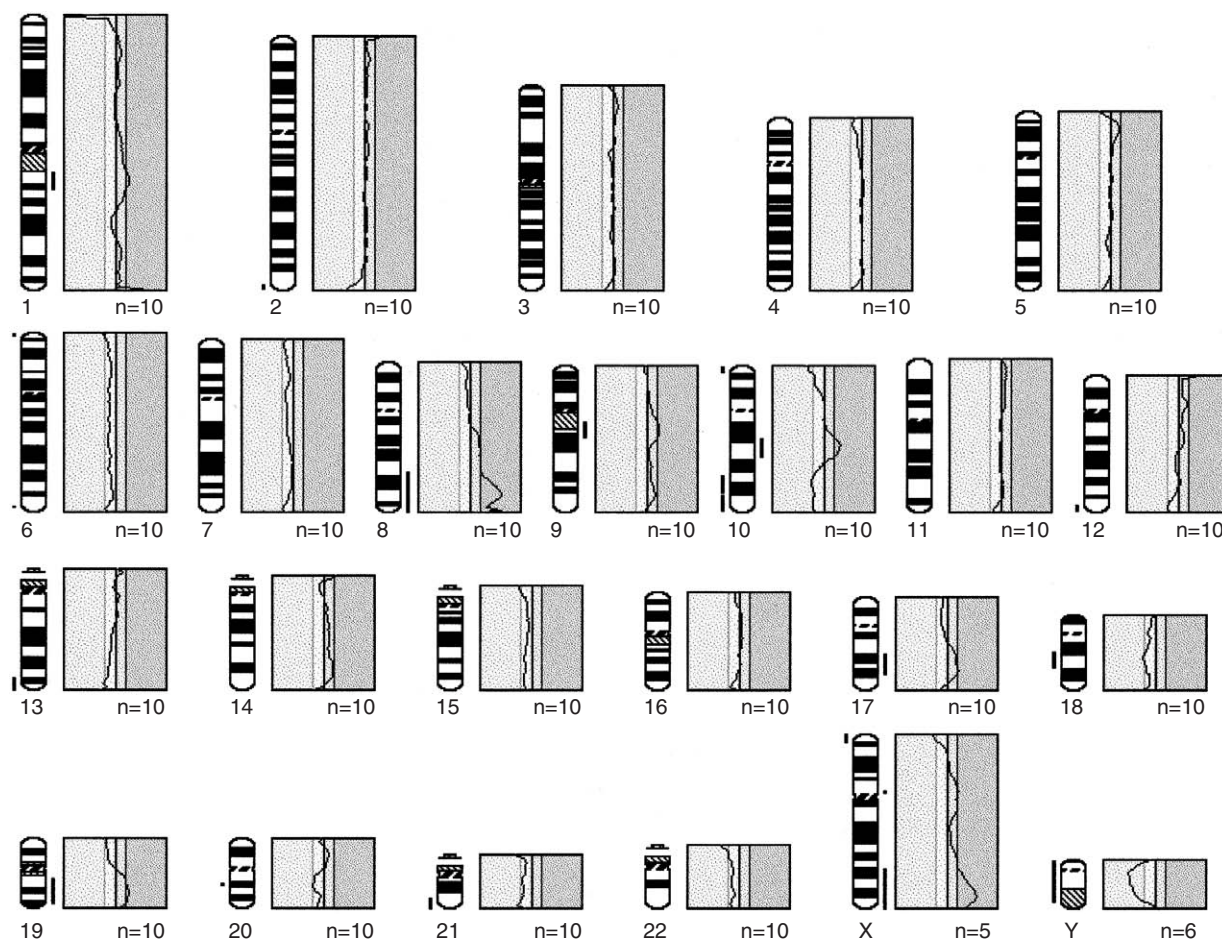
Figure 47 Comparative genomic hybridization analysis, or the mean test to reference ratio profiles, of the PC3M-LN4 cell line. For each graph profile, the middle line represents the ratio of 1, whereas the line to the left represents the ratio of 0.8 (threshold for loss) and the line to the right represents the ratio 1.2 (threshold for gain). To the left of each graph is an ideogram of the respective chromosome for approximate visual reference. Bars to the left and right of the ideogram mark regions of loss and gain, respectively.

The ability to grow into large metastatic tumors in the lymph nodes and to metastasize more readily to distant sites by PC3M–LN4 may be the result of the appearance of a gain on 1q21–q22, and losses of 10q23–qter and 18q12–q21 seen uniquely in this derivative line. All of these three regions of chromosomes have been suggested to play a role in the aggressiveness in cancer. Gain of 1q21 was found in metastatic prostate cancer (Alers *et al.*, 2000) and several other tumor types and has been associated with drug resistance in several cancers (Bieche *et al.*, 1995a; Kudoh *et al.*, 1999; Tarkkanen *et al.*, 1999). Chromosome arm 10q, and especially 10q23–qter, is one of the most frequent sites of loss reported in prostate cancer (Ittmann, 1998). The 10q23 region harbors the *PTEN/MMAC1* gene that has been shown to play a role in metastatic disease in many cancer types (El-Deiry, 2003). The loss of *PTEN/MMAC1* expression has been shown

to correlate with high Gleason score and advanced-stage primary prostate cancer (McMenamin *et al.*, 1999). Loss of the 18q12–q21 region has been reported in a variety of cancers including those of the colon (Laurent-Puig *et al.*, 1999), brain (Sehgal *et al.*, 1998) and breast (Bieche *et al.*, 1995b) and has been associated with poor prognosis in advanced stage prostate tumors (Bostwick *et al.*, 1998; Jenkins *et al.*, 1998; Ueda *et al.*, 1997; Verma *et al.*, 1999). The importance of 1q21–q22, 10q23–qter, and 18q12–q21 regions, as reported in the literature, suggests that these three regions may be responsible for the increased incidence of distant metastases and/or larger lymph node tumors of PC3M–LN4 after orthotopic implantantion as compared to PC3M and PC3M–Pro4.

In contrast to the first *in vivo* prostate tumor progression model, the second model derived from LNCaP represents a less aggressive prostate tumor

progression model (Pettaway *et al*., 1996). The LNCaP, LNCaP–Pro5, and LNCaP–LN3 cell lines all shared the gain of 3q27–qter and loss of 13q21–qter, again suggesting common clonal origin. In addition, the two variant lines shared gains of 2p23–pter and whole chromosome 3 with a loss of 6p21–q16, suggesting not only common clonal origin but also selective pressure during the establishment of the derivative lines following orthotopic implantantion.

The LNCaP–Pro5 cell line, similar to the PC3M–Pro4 cell line, is a derivative line selected for its ability to produce significantly larger tumors in the prostate after orthotopic injection into nude mice. This growth characteristic in LNCaP–Pro5 may be the result of the specific gain of 13q12–q13. The 13q12–q13 region harbors the *BRCA2* gene (Wooster *et al*., 1995). The *BRCA2* gene and the 13q12–q13 region in general have been suggested to be a marker of poor prognosis and tumor progression of some breast cancers (Eiriksdottir *et al*., 1998; Van den Berg *et al*., 1996; Wooster *et al*., 1995). Loss of heterozygosity studies on primary prostate tumors showed that there were many markers on 13q that are frequently deleted (Li *et al*., 1998; Melamed *et al*., 1997). However, markers tightly linked to *BRCA2* were not as frequently lost as other markers (Li *et al*., 1998; Melamed *et al*., 1997). This may indicate that there may be other genes of interest in this region that need to be elucidated. It is interesting that Geck *et al*. (2000) recently identified a gene (*AS3*) distal to *BRCA2* that may be a mediator of the androgen-induced proliferative shutoff and is consistent with the characteristic of LNCaP–Pro5 being receptive to androgen deprivation (Pettaway *et al.*, 1996).

In comparison, LNCaP–LN3, a derivative line that had significantly higher incidences of lymph node metastases and produced significantly larger metastatic tumors in the lymph nodes, had unique losses on 16q23–qter and 21q. Chromosomal band 16q23 has been associated with metastatic and aggressive behavior of prostate cancer, although no specific gene in this region has been identified (Bostwick *et al*., 1998; Elo *et al*., 1999; Latil *et al*., 1997; Li *et al*., 1999; Saric *et al*., 1999). Loss of heterozygosity of the 21q22 locus has been reported in one study to be important in the progression of prostate cancer from primary to metastatic tumors (Saric *et al*., 1999). Hyytinen *et al*. (1997) also reported the acquisition of this abnormality in a similar *in vivo* model of prostate cancer progression using the LNCaP cell line. These findings suggest that both losses of 16q23-qter and 21q may be responsible for the increased metastatic ability of LNCaP–LN3 as compared to LNCaP and LNCaP–Pro5.

One distinct advantage of CGH analysis is the ease of detecting chromosomal gains and losses without the need for metaphase spreads as in cytogenetics. Previously, karyotypes of two of the six cell lines (LNCaP and LNCap–LN13) were reported (Pettaway *et al*., 1996). Both the LNCaP and LNCaP–LN3 cell lines shared two copies of del(1p) (designated M1), del(2)(p22) (M2), del(6)(p21) (M3), del(10)(q24) (M4), t(1;15)(p22;q23) (M6), and t(6;16)(p21;q22) (M7), one copy of (M5) der(13)(p+), and two copies of chromosome X. In addition, LNCaP–LN3 had some chromosome X material on one of the M6 (M6+) and a der(14). The CGH data may aid in explaining some of the possible origins of the abnormal chromosomes identified by karyotype analysis. A CGH analysis of both LNCaP and LNCaP-LN3 showed no loss of 1p material as seen in M1, suggesting that the 1p chromosomal material at 1p22 was translocated to another chromosome, most likely chromosome 15 at 15q23, resulting in M6. Also, no loss of chromosome 15 material was seen by CGH of either cell lines, suggesting that t(1;15) is a reciprocal translocation. Loss of 2p22–pter, as indicated by M2, was not seen in CGH analysis in either parental or variant line, although LNCaP–LN3 showed a gain of 2p23–pter. One speculation of this discrepancy between karyotype and CGH analysis could be that the 2p chromosomal material was translocated to a cryptic location. There could then be an increase in copy number of this modified chromosome with the extra 2p23–pter material during the selection for LNCaP–LN3, resulting in a gain of chromosome 2p23–pter seen in the subline. CGH also showed no loss of 6p, as indicated by M3, suggesting that this chromosomal material was translocated elsewhere, perhaps to chromosome 16q22, resulting in M7. It is interesting that CGH of LNCaP–LN3 showed loss of 16q23–qter with a loss of 6p21–q16, suggesting that the 16q23–qter material may have reciprocally translocated to 6p21 resulting in M3. The selection for LNCaP-LN3 may have resulted in the loss of M3 chromosome, thus giving rise to a subline with both losses of 6p21–q16 and 16q23–qter. None of the LNCaP or its variant cell lines showed loss of 10q24–qter after CGH analysis, as indicated by M4 of the karyotype. This could suggest that the fragment may have translocated to a cryptic site or that this abnormality was present in less than 50% of the cells and thus is beyond the detection of CGH (Kallioniemi *et al*., 1992). Perhaps some of the unexplained deleted chromosomal material may be contained in M5, a derivative 13 chromosome. Specific to LNCaP–LN3, no copy number abnormalities were seen involving the specific abnormal chromosomes, M6+ and der(14), seen in the karyotype. However, CGH showed LNCaP–LN3 to differ from

LNCaP by the additional gains on 2p23–pter and the whole chromosome 3 as well as losses on 6p21–q16, 16q23–qter, and 21q. The relationship between the specific abnormalities seen by the CGH and the marker chromosomes seen uniquely in the karyotype of LNCaP–LN3 need to be further analyzed by other methods such as spectral karyotyping and FISH.

As demonstrated in the previous examples, CGH is an effective genome-wide screening method that is able to identify areas of the genome that have increased or decreased copy numbers. The distinguishing chromosomal abnormalities of each cell line as revealed by CGH analysis may contribute to their different biologic behaviors. To further study the unique regions of gains or losses identified by CGH in these cell lines, more specific techniques (e.g., loss of heterozygosity or FISH) need to be used. Because many of these abnormalities detected by CGH have also been found in primary and metastatic prostate tumors (Alers *et al.*, 2000; Chu *et al.*, 2003; Kim *et al.*, 2000; Mattfeldt *et al.*, 2003), these cell lines are important models for future studies of the progression of prostate cancer.

Acknowledgment

References

Alers, J.C., Rochat, J., Krijtenburg, P.J., Hop, W.C., Kranse, R., Rosenberg, C., Tanke, H.J., Schroder, F.H., and van Dekken, H. 2000. Identification of genetic markers for prostatic cancer progression. *Lab. Invest.* 80:931–942.

Balsara, B.R., Sonoda, G., du Manoir, S., Siegfried, J.M., Gabrielson, E., and Testa, J.R. 1997. Comparative genomic hybridization analysis detects frequent, often high-level, over-representation of DNA sequences at 3q, 5p, 7p, and 8q in human non-small cell lung carcinomas, *Cancer Res. 57*:2116–2120.

Bieche, I., and Lidereau, R. 1995a. Genetic alterations in breast cancer. *Genes Chromosomes Cancer 14*:227–251.

Bieche, I., Champeme, M.H., and Lidereau, R. 1995. Loss and gain of distinct regions of chromosome 1q in primary breast cancer. *Clinc. Cancer Res. 1*:123–127.

Bostwick, D.G., Shan, A., Qian, J., Darson, M., Maihle, NJ., Jenkins, R.B., and Cheng, L. 1998. Independent origin of multiple foci of prostatic intraepithelial neoplasia: Comparison with matched foci of prostate carcinoma. *Cancer 83*:1995–2002.

Cancer Facts & Figures 2003. American Cancer Society (publication 98-300M-No. 5008.98). Atlanta, GA.

Chu, L.W., Pettaway, C.A., and Liang, J.C. 2001. Genetic abnormalities specifically associated with varying metastatic potential of prostate cancer cell lines as detected by comparative genomic hybridization. *Cancer Genet. Cytogenet. 127*:161–167.

Chu, L.W., Troncoso, P., Johnston, D.A., and Liang, J.C. 2003. Genetic markers useful for distinguishing between organ-confined and locally advanced prostate cancer. *Genes Chromos. Cancer 36*:303–312.

Dennis, T.R., and Stock, A.D. 1999. A molecular cytogenetic study of chromosome 3 rearrangements in small cell lung cancer: Consistent involvement of chromosome band 3q13.2 *Cancer Genet. Cytogenet. 113*:134–140.

Eiriksdottir, G., Johannesdottir, G., Ingvarsson, S., Bjornsdottir, I.B., Jonasson, J.G., Agnarsson, B.A., Hallgrimsson, J., Gudmundsson, J., Egilsson, V., Sigurdsson, H., and Barkardottir, R.B. 1998. Mapping loss of heterozygosity at chromosome 13q: Loss at 13q12-q13 is associated with breast tumour progression and poor prognosis. *Eur. J. Cancer 34*:2076–2081.

El-Deiry, W.S. (ed) 2003. *Tumor Suppressor Genes Volume 1: Pathways and Isolation Strategies.* Humana Press, Totowa, N.J.

Elo, J.P., Harkonen, P., Kyllonen, A.P., Lukkarinen, O., and Vihko, P. 1999. Three independently deleted regions at chromosome arm 16q in human prostate cancer: Allelic loss at 16q24.1-q24.2 is associated with aggressive behaviour of the disease, recurrent growth, poor differentiation of the tumour and poor prognosis for the patient. *Br. J. Cancer 79*:156–160.

Geck, P., Maffini, M.V., Szelei, J., Sonnenschein, C., and Soto, A.M. 2000. Androgen-induced proliferative quiescence in prostate cancer cells: The role of AS3 as its mediator. *Proc. Natl. Acad. Sci. USA 97*:10185–10190.

Hyytinen, E.R., Thalmann, G.N., Zhau, H.E., Karhu, R., Kallioniemi, O.P., Chung, L.W., and Visakorpi, T. 1997. Genetic changes associated with the acquisition of androgen-independent growth, tumorigenicity and metastatic potential in a prostate cancer model. *Br. J. Cancer 75*:190–195.

Isola, J., DeVries, S., Chu, L., Ghazvini, S., and Waldman, F. 1994. Analysis of changes in DNA sequence copy number by comparative genomic hybridization in archival paraffin-embedded tumor samples. *Am. J. Pathol. 145*:1301–1308.

Ittmann, M.M. 1998. Chromosome 10 alterations in prostate adenocarcinoma (review). *Oncol. Rep. 5*:1329–1335.

Jenkins, R., Takahashi, S., DeLacey, K., Bergstralh, E., and Lieber, M. 1998. Prognostic significance of allelic imbalance of chromosome arms 7q, 8p, 16q, and 18q in stage T3N0M0 prostate cancer. *Genes Chromos. Cancer 21*:131–143.

Kaighn, M.E., Narayan, K.S., Ohnuki, Y., Lechner, J.F., and Jones, L.W. 1979. Establishment and characterization of a human prostate carcinoma cell line (PC-3). *Invest. Urol. 17*:16–23.

Kallioniemi, A., Kallioniemi, O.P., Sundar, D., Rutovitz, D., Gray, J.W., Waldman, F., and Pinkel, D. 1992. Comparative genomic hybridization for molecular cytogenetic analysis of solid tumors. *Science 258*:818–821.

Kim, S.H., Kim, M.S., and Jensen, R.H. 2000. Genetic alterations in microdissected prostate cancer cells by comparative genomic hybridization. *Prostate Cancer Prostatic Dis. 3*:110–114.

Koslowski, J.M., Fidler, I.J., Campbell, D., Xu, Z., Kaighn, M.E., and Hart, I.R. 1984. Metastatic behavior of human tumor cell lines grown in the nude mouse. *Cancer Res. 44*:3522–3529.

Kudoh, K., Takano, M., Koshikawa, T., Hirai, M., Yoshida, S., Mano, Y., Yamamoto, K., Ishii, K., Kita, T., Kikuchi, Y., Nagata, I., Miwa, M., and Uchida, K. 1999. Gains of 1q21-q22 and 13q12-q14 are potential indicators for resistance to cisplatin-based chemotherapy in ovarian cancer patients. *Clin. Cancer Res. 5*:2526–2531.

Latil, A., Cussenot, O., Fournier, G., Driouch, K., and Lidereau, R. 1997. Loss of heterozygosity at chromosome 16q in prostate adenocarcinoma: Identification of three independent regions. *Cancer Res. 57*:1058–1062.

Laurent-Puig, P., Blons, H., and Cugnenc, P.H. 1999. Sequence of molecular genetic events in colorectal tumorigenesis. *Eur. J. Cancer Prev. 8 Supplement 1*:S39–S47.

Li, C., Berx, G., Larsson, C., Auer, G., Aspenblad, U., Pan, Y., Sundelin, B., Ekman, P., Nordenskjold, M., van Roy, F., and

Bergerheim, U.S. 1999. Distinct deleted regions on chromosome segment 16q23-24 associated with metastases in prostate cancer. *Genes Chromos. Cancer 24*:175–182.

Li, C., Larsson, C., Futreal, A., Lancaster, J., Phelan, C., Aspenblad, U., Sundelin, B., Liu, Y., Ekman, P., Auer, G., and Bergerheim, U.S. 1998. Identification of two distinct deleted regions of chromosome 13 in prostate cancer. *Oncogene 16*:481–487.

Mattfeldt, T., Wolter, H., Trijic, D., Gottfried, H.W., Kestler, H.A. 2003. Chromosomal regions in prostatic carcinomas studied by comparative genomic hybridization, hierarchical cluster analysis and self-organizing feature maps. *Anal. Cell. Pathol. 24*:167–179.

McMenamin, M.E., Sound, P., Perera, S., Kaplan, I., Loda, M., and Sellers, W.R. 1999. Loss of PTEN expression in paraffin-embedded primary prostate cancer correlates with high Gleason score and advanced stage. *Cancer Res. 59*:4291–4296.

Melamed, J., Einhorn, J.M., and Ittmann, M.M. 1997. Allelic loss on chromosome 13q in human prostate carcinoma. *Clin. Cancer Res. 3*:1867–1872.

Pettaway, C.A., Pathak, S., Greene, G., Ramirez, E., Wilson, M.R., Killion, J.J., and Fidler, I.J. 1996. Selection of highly metastatic variants of different human prostatic carcinomas using orthotopic implantation in nude mice. *Clin. Cancer Res. 2*:1627–1636.

Saric, T., Brkanac, Z., Troyer, D.A., Padalecki, S.S., Sarosdy, M., Williams, K., Abadesco, L., Leach, R., and O'Connell, P. 1999. Genetic pattern of prostate cancer progression. *Intl. J. Cancer 81*:219–224.

Sehgal, A. 1998. Molecular changes during the genesis of human gliomas. *Semin. Surg. Oncol. 14*:3–12.

Tarkkanen, M., Huuhtanen, R., Virolainen, M., Asko-Seljavaara, S., Tukiainen, E., Lepantalo, M., Elomaa, I., and Knuutila, S., 1999. Comparison of genetic changes in primary sarcomas and their pulmonary metastases. *Genes Chromos. Cancer 25*:323–331.

Ueda, T., Komiya, A., Emi, M., Suzuki, H., Shiraishi, T., Yatani, R., Masai, M., Yasuda, K., and Ito, H. 1997. Allelic losses on 18q21 are associated with progression and metastasis in human prostate cancer. *Genes Chromos. Cancer 20*:140–147.

Van den Berg, J., Johannsson, O., Hakansson, S., Olsson, H., and Borg, A. 1996. Allelic loss at chromosome 13q12-q13 is associated with poor prognosis in familial and sporadic breast cancer. *Br. J. Cancer 74*:1615–1619.

Verma, R.S., Manikal, M., Conote, R.A., and Godec, C.J. 1999. Chromosomal basis of adenocarcinoma of the prostate. *Cancer Invest. 17*:441–447.

Wooster, R., Bignell, G., Lancaster, J., Swift, S., Seal, S., Mangion, J., Collins, N., Gregory, S., Gumbs, C., and Micklem, G. 1995. Identification of the breast cancer susceptibility gene BRCA2. *Nature 378*:789–792.

6

Markers for the Development of Early Prostate Cancer

Michael D. Slater, Christopher Lauer,
Angus Gidley-Baird, and Julian A. Barden

Introduction

To become invasive, prostate cancer cells must first penetrate histologic barriers such as the acinar basement membrane proteins and extracellular matrix adhesive glycoproteins. In prostatic intraepithelial neoplasia (PIN), neoplastic acinar epithelial cells are prevented from invading the interstitium by basement membrane components such as collagen IV, laminin, fibronectin, CD44, and heparan sulfate proteoglycan (perlecan) (Kammerer *et al.*, 1998). Other proteins may also be involved in the prevention of interstitial invasion. Tenascin is an adhesive glycoprotein found in both the extracellular matrix and the acinar basement membrane. E-cadherin is another adhesion protein that surrounds each acinar epithelial cell. These proteins have been proposed as markers for the invasive process (Kedeshian *et al.*, 1998). However, inconsistent results have been obtained when expression levels have been measured, possibly as a result of epitope masking.

The tenascin literature is ambiguous. Some workers have proposed that tenascin is involved in the maintenance of normal prostatic stromal-epithelial homeostasis (Xue *et al.*, 1998) and protects against the effects of neoplasia. This view is supported by studies that show that tenascin is secreted by stromal cells and fibroblasts but not by prostate cancer cells (Pilch *et al.*, 1999). In this scenario, tenascin acts as a defense mechanism against the degradation of basement membrane components by

neoplastic metalloproteases (Davidson *et al.*, 1998; Kusagawa *et al.*, 1998). Similarly, studies have shown that patients with high tenascin expression have better long-term survival than patients with weak or absent tenascin expression (Iskaros *et al.*, 1997). Conversely, other studies indicate that tenascin is secreted by cancer cells and that tenascin expression is required for stromal invasion (Phillips *et al.*, 1998; Yoshida *et al.*, 1999). Another study suggested that tenascin immunoreactivity does not appear to correlate with currently used prognostic indictors at all (Tokes *et al.*, 1999). Perhaps these contradictory results reflect the inherent difficulty in reliably labeling the tenascin epitope. This may be because of the incorporation of tenascin in fibronectin matrix fibrils, under the control of heparan sulfate glycosaminoglycans and its proteoglycan core perlecan, causing masking of the epitope in both the basement membrane and the extracellular matrix (Chung *et al.*, 1997).

Similarly, reports of E-cadherin expression in cancer have been contradictory. Cadherins are a family of glycoproteins that act as "glue" between adjacent epithelial cells. Suggestions have been made that prostate cancer cells induce de-expression of E-cadherin, which is associated with de-differentiation, invasion, and metastasis (Bussemakers *et al.*, 2000). The prostate carcinoma cell line PC-3N also demonstrates loss of E-cadherin (Tran *et al.*, 1999). Another study found consistent loss of E-cadherin expression with increasing tumor grade (Murant *et al.*, 1997). Conversely, other

studies have shown that E-cadherin expression is increased in metastatic prostate cancer (De Marzo *et al.*, 1999). In view of these contradictory reports, the use of E-cadherin as a prognostic indicator has been questioned (Kuczyk *et al.*, 1998).

Telomerase is a ribonucleoprotein enzyme that can synthesize telomeres, restoring chromosomal length after cell division and leading to cellular immortalization. It has long been associated with carcinogenesis, although the nature of this relationship is not entirely clear. In at least one study, immortalization of cells by telomerase does not appear to confer other changes associated with malignancy (Morales *et al.*, 1999). In fact, low levels of activity have been noted in normal lung, oral mucosa, skin, esophagus, stomach, colon–rectum, pancreas, prostate, bladder, kidney, cervix, and vulva. However, these normal tissue samples were often taken adjacent to tumors, (Matthews *et al.*, 2001) suggesting that there may be a "field effect" of biochemical changes associated with transformation that is not detectable using common histologic stains. The authors have described a similar field effect in prostate cancer, using the three patterns of purinergic receptor translocation (PRT) (Slater *et al.*, 2001). Similarly, another study found telomerase activity in prostate cores diagnosed with benign prostatic hyperplasia where a focus of established cancer existed elsewhere in the same prostate (Lin *et al.*, 1998). Other studies have noted telomerase activity in epithelial cell cancers, premalignant lesions, and sun-exposed skin (Ueda *et al.*, 1997). Conversely, a study in breast cancer found that only 24 of 34 (71%) infiltrating breast carcinomas (type not stated) were positive for telomerase and that no activity was seen in adjacent tissue areas or in benign lesions (Mokbel *et al.*, 1999). The telomerase antibodies used in all these studies were raised against a sequence in human telomerase reverse transcriptase (hTERT). In an effort to clarify the role of telomerase, we used an antibody raised against a novel segment of the telomerase-associated protein hTP_1.

In the current study, heat and enzymatic antigen retrieval techniques were used with a range of pH values to develop a protocol that enabled reliable labeling of tenascin and E-cadherin. Once the optimum protocol was established, serial sections of each block were immunolabeled for the neoplastic markers $P2X_{1-2}$ and hTP_1 as well as tenascin, E-cadherin, and the standard hematoxylin and eosin (H&E) stain. Labeling of $P2X_{1-2}$ was included because of its recent discovery as a consistently reliable marker for the initial biochemical changes indicating very early neoplastic transformation in the prostate (Slater *et al.*, 2001).

MATERIALS AND METHODS

We examined 2378 cores taken from different areas of the prostate from 289 patients. We have expressed the results by case rather than core by core because Gleason score takes into account all the examined cores, whereas PRT exhibits a field effect, with the same, PRT pattern being seen in many cores of the same case. A total of 23 cases were confirmed as normal; 77 were preneoplastic or very early neoplastic (by PRT assessment), including PIN; and 189 contained carcinoma. Of the Gleason scored cancer cases, 3% were low grade (Gleason score 4 or lower), 85% were medium grade (Gleason score 5–7), and 12% were high grade (Gleason score 8–10). Tissue samples were supplied as 4–5 μm paraffin-embedded sections from prostate core biopsies on glass slides. These were de-waxed in two changes of fresh Histoclear for 10 min each and rehydrated. The sections were incubated for 5 min in 0.3% hydrogen peroxide and in 1% bovine serum albumin (BSA) in phosphate buffer saline (PBS) and washed in PBS three times, 5 min per wash. Approximate serial sections from each case were labeled without antigen retrieval or with enzyme and heat antigen retrieval protocols at high (10), low (2), and physiologic (7) pH.

For enzymatic retrieval, the contents of one packet of pepsin (Dako Corp., Carpinteria, CA) was dissolved in 500 ml of 0.2 N HCl. This solution was preheated in coplin jars to 37°C in a convection oven. The de-paraffinized and H_2O_2-treated slides were placed in coplin jars for 15 minutes at 37°C. They were then removed and washed in distilled water.

Heat antigen retrieval (HAR) was carried out in Target Retrieval Solution (Dako Corp.). Solutions at pH 10.0, pH 7.0, and pH 2.0 were prepared. Slides were tested at 100°C for 10 min, 90°C for 30 min, 80°C for 50 min, and 70°C for 1 hr at each pH. The slides were allowed to cool to room temperature and were then washed in buffer. Thereafter, they were placed in a solution of 5% normal horse serum (0.5 ml horse serum in 10 ml PBS) and washed in PBS for 2 min to block nonspecific labeling.

Production of hTP1 Antiserum

The consensus sequence of human telomerase-associated protein (TP_1) (Harrington *et al.*, 1997) was examined for suitable epitopes. A segment in the C-terminal domain corresponding to the segment Cys2524-Glu2540 was chosen, and the peptide was synthesized using standard t-BOC chemistry on an

ABI synthesizer (Barden *et al.*, 1997). After high-performance liquid chromatography (HPLC) purification, the peptide was cross-linked to diphtheria toxin using maleimidocaproyl-N-hydroxysuccinimide and suspended in water at 5 mg/mL; aliquots were emulsified by mixing with Complete Freund's Adjuvant. Emulsion volumes of 1 mL containing 2 mg of peptide epitope were injected intramuscularly into a sheep, with second and subsequent boosts at intervals of 6 weeks, using Incomplete Freund's Adjuvant. Bleeds via venepuncture were obtained after 12 weeks, when adequate antibody titers had been obtained. Sera were tested with an enzyme linked immunosorbent assay (ELISA). Specificity of hTP_1 antibody was demonstrated by preincubating tissue slides otherwise found positively stained with 10 μM of the peptide epitope for 10 min prior to the normal addition of the primary antibody. All such slides were devoid of all stain of the type shown in Figure 49B compared with positive stain of the type shown in Figure 48C.
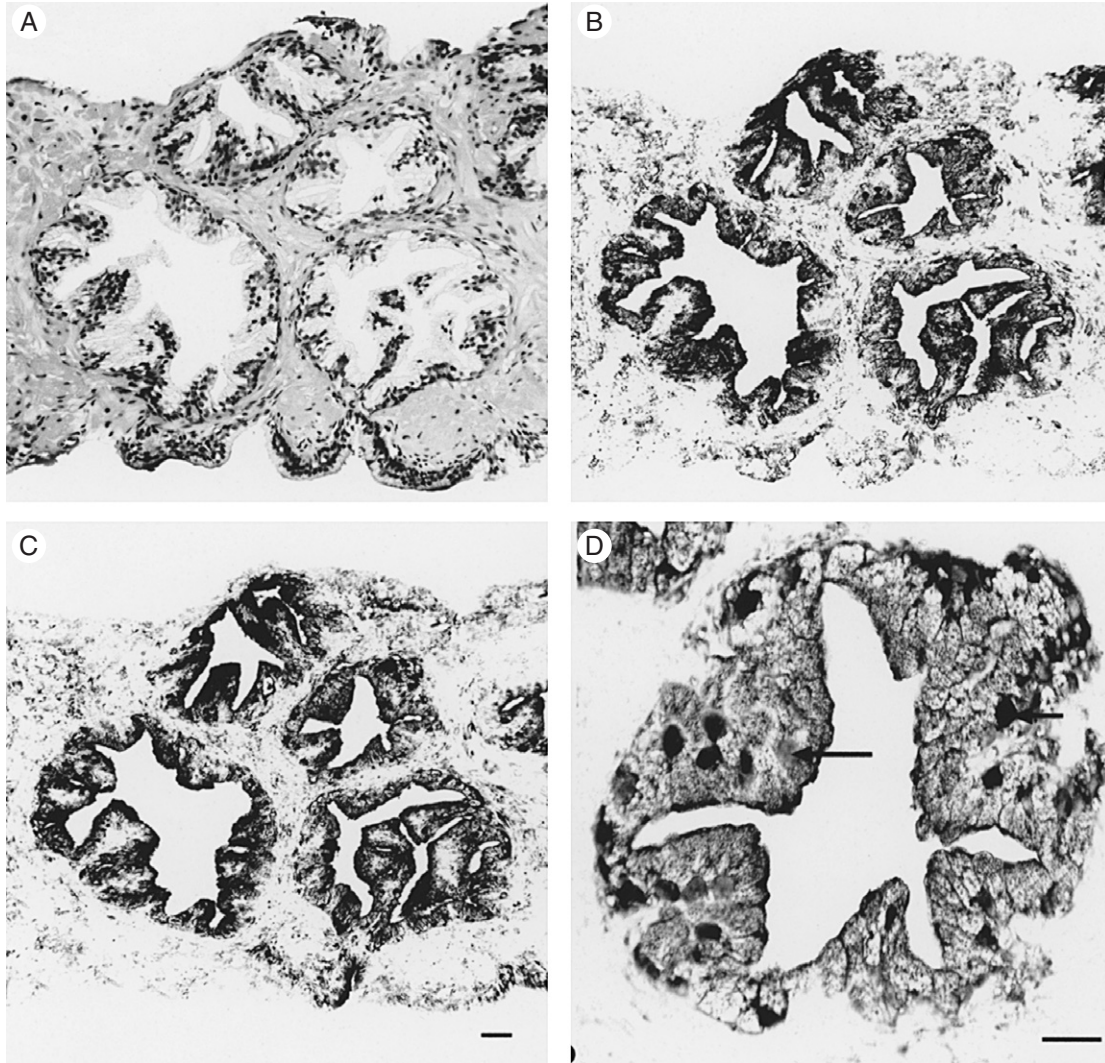
Figure 48 A: One of three cores taken from a 47-year-old patient diagnosed as normal. In this core no neoplastic features are evident. Hematoxylin and eosin (H&E) stain. **B**: The same histologic area in approximate serial section, labeled with anti-$P2X_{1-2}$. The labeling features are those of purinergic receptor translocation (PRT) 2, as the anti-$P2X_{1-2}$ label is translocating through the cytoplasm. **C**: The same histologic area in approximate serial section, labeled with anti-telomerase-associated protein antibody. The labeling features are similar to that of the PRT label in the previous micrograph. Bar 30 μm. **D**: High-power micrograph of an acinus from the same core, labeled with anti-$P2X_{1-2}$ antibody. Note that translocating P2X puncta are visible in the cytoplasm. Some nuclei have lost their label (*long arrow*), and some still retain a nuclear label (*short arrow*). Bar 20 μm.
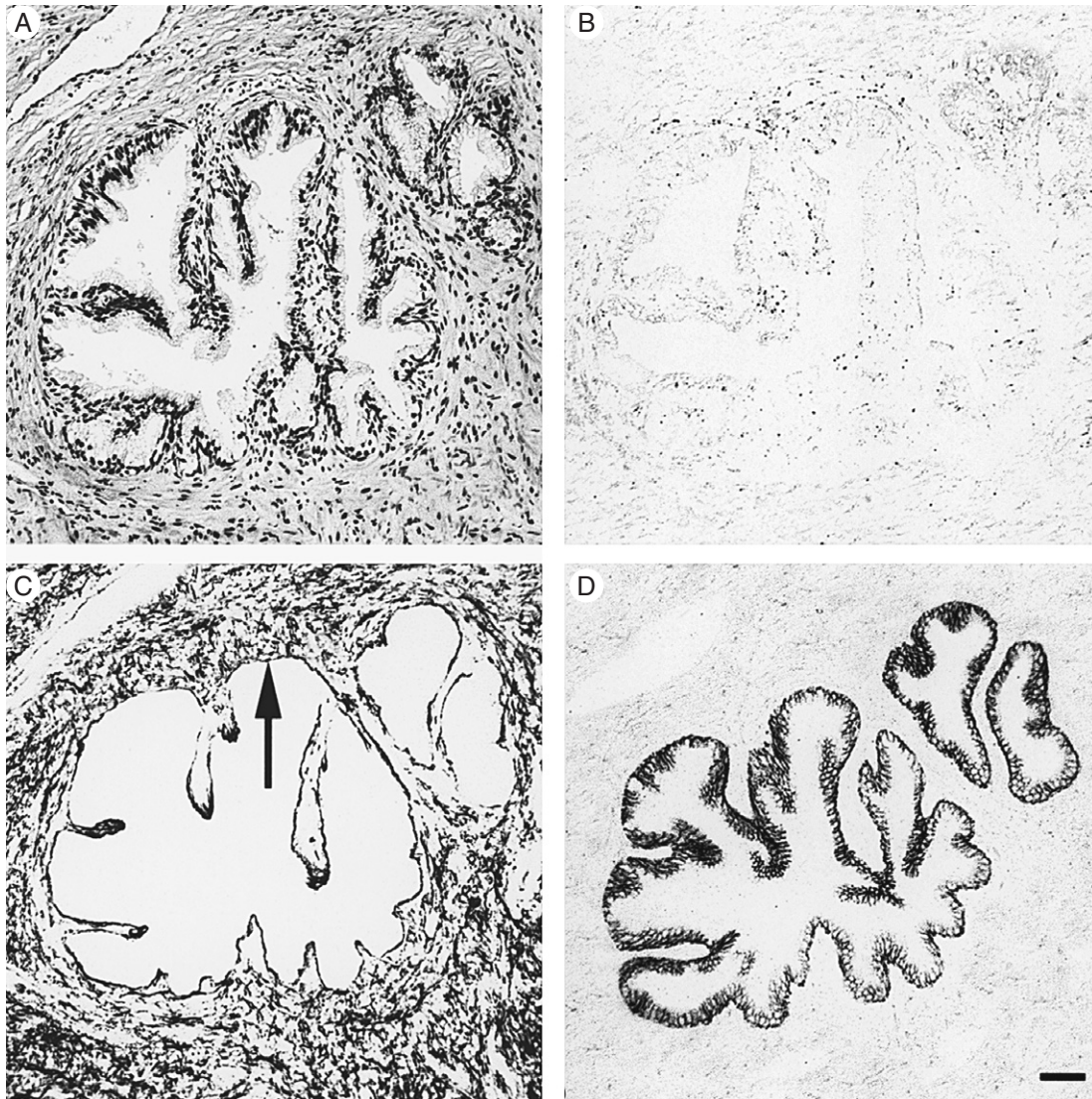
Figure 49 **A**: A prostatic epithelial acinus from a 76-year-old patient. This core biopsy was originally diagnosed as being normal with areas of benign prostatic hyperplasia (BPH). Hematoxylin and eosin (H&E) stain. **B**: The same acinus in approximate serial section, labeled with anti-P2X$_{1-2}$ antibody. No significant label was observed in epithelial cells, confirming the diagnosis. **C**: The same acinus in approximate serial section, labeled with anti-tenascin antibody. The stroma and epithelial basement membrane are strongly labeled. **D**: The same acinus in approximate serial section, labeled with anti-E-cadherin antibody. The plasma membrane of each epithelial cell is strongly labeled. Bar 50 μm.

The sections were then labeled with either an equal amount of rabbit anti-human P2X$_1$ and P2X$_2$ or sheep anti-human TP$_1$, respectively, at a concentration of 1:100 in PBS for 30 min. Sections labeled with monoclonal anti-human tenascin (clone BC-24, Sigma, St. Louis, MO) or monoclonal anti-E-cadherin (Zymed, San Francisco, CA) were treated with HAR at 90°C for 50 min. Slides were then washed three times in PBS for 10 min each, followed by a 30-min incubation with a 1:100 dilution of horseradish peroxidase (HRP)-conjugated rabbit anti-mouse or donkey anti-rabbit secondary antibody (Dako Corp.). All slides were then washed three times in PBS for 10 min each, visualized using a 0.05% solution of diaminobenzidine (DAB) for 10 min, washed, dried, and mounted in Entellan mounting medium (Merck). No counterstaining was used.

In addition, approximate serial sections were stained with a standard H&E protocol.

Control Methods

Tissue that was previously known to stain positively for each respective antibody was used as a positive control. Negative controls for each labeling parameter were established by incubation with mouse immunoglobulin G (IgG), mouse IgM, or either sheep or rabbit preimmune serum (1:25 dilution) in BSA in PBS and also by omission of the primary antibodies. In each case, this procedure resulted in a complete absence of labeling.

Labeling Intensity Quantitation

Actual levels of antigen were not quantified in this study, but rather relative differences in labeling intensity were determined using a standardized protocol. Differences in relative labeling density were measured using previously published methods (Slater, 1999).

RESULTS

Tenascin was abundant in the extracellular matrix and basement membrane in all normal tissues; tissue diagnosed with PIN and in all cores showed features of PRT 1, indicating early neoplastic change (Slater *et al.*, 2001), but was essentially absent in higher grade cancer tissue from Gleason sum score 4. Detection of tenascin in the basement membrane was unsurprising since its colocalization with fibronectin fibrils has been reported (Chung *et al.*, 1997) and is probably the source of the widely encountered epitope masking problems.

Routine immunoperoxidase protocols resulted in inconsistent and/or low levels of labeling for both tenascin and E-cadherin. Enzyme (pepsin) retrieval caused marked protein precipitation and unacceptable levels of damage to both the tenascin and the E-cadherin–labeled tissues. Reproducible labeling was only possible using an HAR protocol at 90°C for 50 min at pH 2.0. HAR at temperatures of 100°C or higher caused protein precipitation and tissue damage, although less than that with the enzymatic methods. Of the time and temperature ranges used, 90°C for 50 min produced optimal results. HAR at PH 10.0 or pH 7.0 did not improve labeling, but HAR at pH 2.0 dramatically improved the labeling intensity of both tenascin and E-cadherin, even where no label had been noted using routine protocols. Without the use of HAR, labeling was inconsistent or absent for both proteins. Controls demonstrated that these results were only the result of the combination of HAR and immunoperoxidase labeling, not to the HAR procedure itself.

In the current study, a significant reduction in tenascin expression was apparent in PRT 2 tissue and little or no tenascin labeling could be observed in PRT 3 tissue. We have previously demonstrated that P2X immunolabeling of prostate detected early neoplastic biochemical changes in apparently normal tissue (Slater *et al.*, 2001). This reduction in tenascin labeling did not correlate well with Gleason score because reduced expression was often already complete in tissue with low Gleason score. Both tenascin and PRT labeling exhibited a field effect in that, whereas the H&E appearance of the tissue varied in different locations of the prostate, both purinergic receptor expression and tenascin degradation were seen throughout the tissue. Telomerase-associated protein (TP$_1$) expression completely mimicked that of the P2X$_{1-2}$ receptors. In contrast, E-cadherin labeling around each epithelial cell remained intact in tissue that was normal, was BPH, or that showed evidence of PIN as well as in all prostate carcinomas, except those of the highest Gleason scores. An example of the PRT and TP$_1$ labeling is shown in Figure 48. An apparently normal core (by H&E stain, Figure 48A) is from a prostate that contained a tumor. The PRT staining (Figure 48B) of a serial section of the same core shows type 2 label (PRT 2) or cytoplasmic staining in the acinar epithelial cells. Normal cells are completely unstained. Similarly, TP$_1$ label of a serial section also shows the same cytoplasmic staining (Figure 48C). A higher power image in Figure 48D shows PRT labeling of several of the nuclei (*short arrow*) but with others unstained (*long arrow*) because the receptors have largely moved into the cytoplasm. Whereas BPH/normal tissue was entirely devoid of both P2X and TP$_1$ labeling, early cancer tissue produced labeling for both sets of markers that occurred in two well-defined patterns before the usual diagnostic histologic markers of cancer became evident by H&E stain. A third pattern (PRT 3) colocalized with obvious early prostate cancer and took the form of an apical membrane deposition of the label. Overall, PRT assessment involves P2X receptor expression first appearing within individual nuclei in the acini (type 1) before progressing to a cytoplasmic punctate label in the acinar epithelium, with an associated lack of nuclear stain (type 2). Finally, in advanced cases in which clear morphologic evidence of cancer was apparent by H&E stain, the P2X label condensed exclusively on the apical epithelium (type 3). Of these three types of purinergic receptor translocations, PRT 1 and PRT 2 can occur in the absence of identifiable morphologic change and thus appear as a

field effect, whereas PRT 3 always accompanies obvious cancer by H&E stain. Reduction in tenascin expression coincided with PRT 2 and was effectively de-expressed in tissue showing PRT 3. TP_1 expression exactly matched that of P2X receptors in the current study. In both normal tissue and PIN there was maximal expression of tenascin in the extracellular matrix and basement membrane and a strong label for E-cadherin surrounding each cell. Labeling for E-cadherin was uniformly strong along the borders of each adjoining prostatic epithelial cell in normal tissue, BPH, PIN, and all grades of prostate cancer except Gleason sum score 8–10, where acini were no longer identifiable.

Figure 49 shows serial sections from normal prostate tissue. No prostatic hyperplasia was present by H&E stain (Figure 49A). The complete lack of label for $P2X_{1-2}$ (Figure 49B) suggests that no early neoplasia was present. Tenascin label in this tissue was strong in the extracellular matrix and acinar basement membrane (Figure 49C, *arrow*), and the E-cadherin label surrounding each epithelial cell is continuous and intense (Figure 49D).

Figure 50 shows an apparently normal cluster of acini (by H&E stain, Figure 50A). A core from another location in this prostate revealed the presence of prostate cancer, Gleason score 5. Some mild hyperplasia is seen (Figure 50A, *arrow*). The presence of translocating $P2X_{1-2}$ receptors in the cytoplasm (Figure 50B, *arrow*) was found in all cores, representing a field effect that suggests the presence of a tumor somewhere in this prostate. These epithelial cells are unstained in normal tissue (compare with Figure 49B). Similarly, TP_1 label of a serial section also reveals the same cytoplasmic staining pattern (not shown). Figure 50C shows tenascin expression (*arrows*) that is only 38.4% (p < 0.0001) that of normal tissue (Figure 49C). This pattern was always accompanied by a PRT2 $P2X_{1-2}$ labeling pattern (Figure 50B) and an identical telomerase label. Figure 50D shows that cell-to-cell E-cadherin labeling remains intense.

Figure 51 shows serial sections from a core biopsy from an 81-year-old man diagnosed as having Gleason score 6 prostate cancer by H&E stain (Figure 51A). The $P2X_{1-2}$ receptor label type is PRT 3 (i.e., receptor expression condensed on the apical epithelium [Figure 51B, *arrow*], a labeling pattern only seen in obvious moderate-advanced cancer tissue). Figure 51C (*arrow*) shows that tenascin expression in the presence of PRT3 was only 19.0% (p <0.0001) that of normal tissue (Figure 49C). Despite the obvious presence of cancer, the E-cadherin label remained strong (Figure 51D), although the histologic architecture was itself degraded in this moderate-grade cancer tissue. These results are summarized in Table 10.

Correlation of prostate specific antigen (PSA) levels in each of the patients at the time of biopsy was made. A total of 23 cases were assigned normal status on the basis that there was no PRT or TP_1 label while tenascin was maximal and H&E staining appeared normal. The average PSA was 0.8 ± 0.1 ng/ml (mean ± SEM, range 0.1–1.8 ng/ml). Among the 77 cases found with PRT1 and similar nuclear TP_1 label, there was no reduction in tenascin label and the H&E staining always appeared normal in all tissue cores. These early neoplastic cases showed highly elevated PSA (13.2 ± 0.8 ng/ml, range 3.0–47.8 ng/ml) compared with the established normals. The bulk of the cases numbering 189 all exhibited cancer with Gleason scores from 3 to 9. Each exhibited PRT type 2 or 3 with similar TP_1 and greatly reduced tenascin. The PSA remained essentially unchanged in this cohort from the PRT1 cohort with a level of 13.7 ± 0.9 ng/ml with a range of 0.5–60.0 ng/ml. No differences were apparent as a result of patient age in the cohort.

DISCUSSION

One of the main tools of histologic diagnosis is the observation of cytologic and histologic change as revealed by stains like H&E. The current study adds to previous work (Slater *et al*., 2001) that details neoplastic biochemical changes that occur some time before the usual histologic markers are visible. The P2X, TP_1, and tenascin expression patterns described were consistent throughout each core from a particular case. This field effect suggests that a biopsy does not have to directly sample the few cells that exhibit visible cancer for the presence of the tumor to be detected. E-cadherin expression was not altered by neoplasia. All normally sampled areas of an affected prostate exhibit the changes described, with PRT1 present months to years before cancer becomes detectable by H&E staining.

Early markers of neoplasia are needed to improve the accuracy of diagnosis of prostate cancer. This disease is usually heterogeneous and multifocal, with diverse clinical and morphologic manifestations. Current understanding of the molecular basis for this heterogeneity is limited, particularly for PIN, the only putative precursor that can be identified according to morphologic criteria. It is conceivable that a stem cell of basal phenotype, or an amplifying cell, is the target of prostatic carcinogenesis. Prominent genetic heterogeneity is characteristic of both PIN and carcinoma, and multiple foci of PIN arise independently within the same prostate. The strong genetic similarities between PIN and cancer strongly suggest that evolution and clonal expansion of PIN, or other precursor lesions, may account for the multifocal etiology of carcinoma.
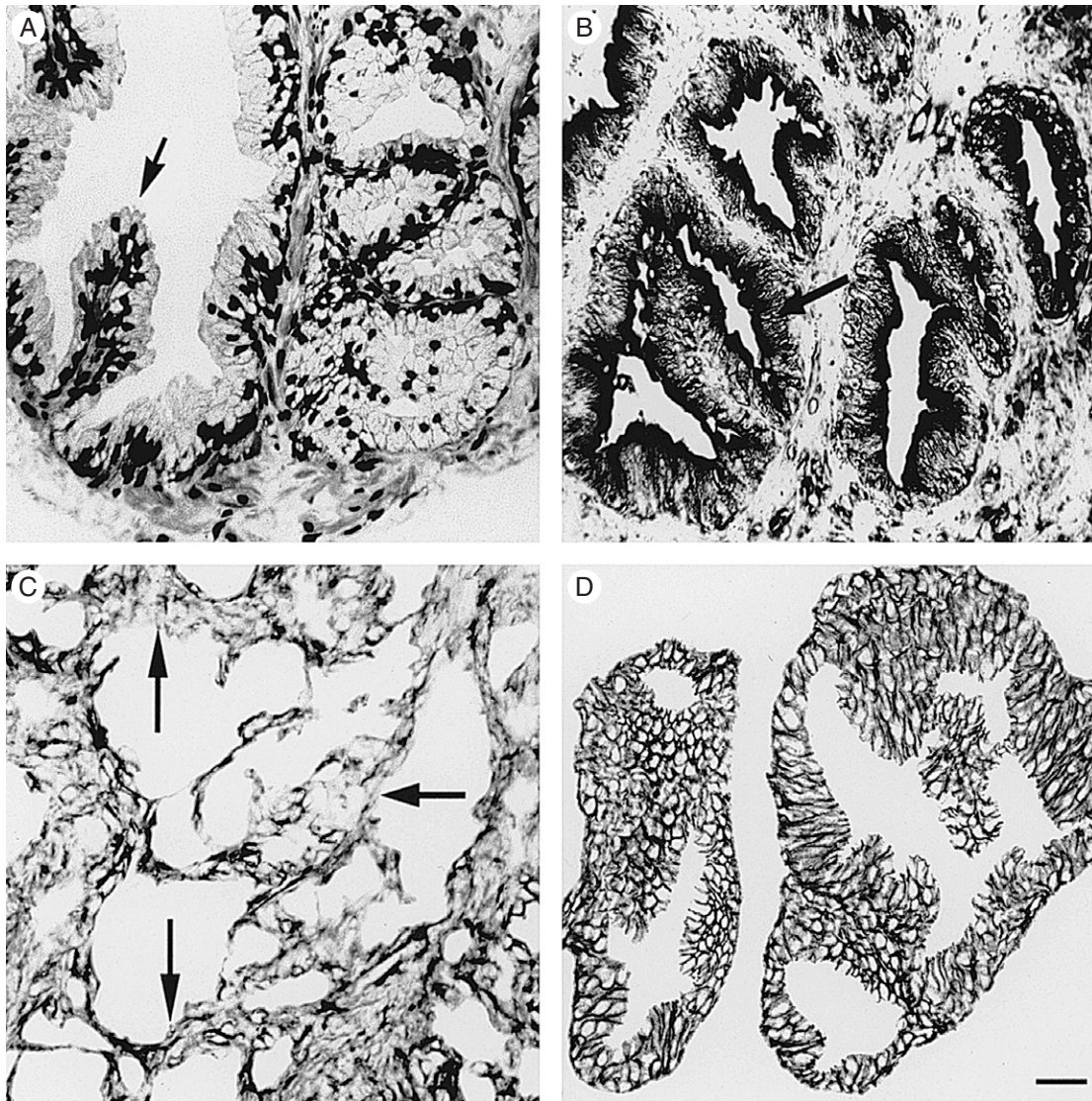
Figure 50 **A**: A photomicrograph of a prostate biopsy core from a 57-year-old patient diagnosed as having Gleason grade 3+3 = score 6 carcinoma with areas of benign prostatic hyperoplasia (BPH). The appearance of tissue in this particular core is normal with some mild hyperplasia (*arrow*). Hematoxylin and eosin (H&E) stain. **B**: The same histologic area in approximate serial section, labeled with anti-P2X$_{1-2}$ antibody. The features of purinergic receptor translocation (PRT) 2 (cytoplasmic puncta) are present in the acinar epithelium (*arrow*), indicating the presence of tumor in another area of the prostate. **C**: The same histologic area in approximate serial section, labeled with anti-tenascin antibody. The anti-tenascin label was only 38.4% (p < 0.0001) that of normal in the extracellular matrix compared with normal tissue, and there were extensive breaks in the continuity of the basement membrane (*arrow*). **D**: The same histologic area in approximate serial section, labeled with anti-E-cadherin antibody. The appearance is that of hyperplasia. The area of plasma membrane of each epithelial cell is strongly labeled. Bar 20 μm.

This observation suggests that a field effect probably underlies prostatic neoplasia. This was evident in the current study. It is well known that multiple foci of cancer often arise independently, lending additional support to this hypothesis (Foster *et al*., 2000). It has been further suggested that populations of secretory cells in a state of early neoplasia compound the absence of key genome protective mechanisms, thus setting the stage for an accumulation of genomic alterations and instability in high-grade PIN. This action occurs along with activation of telomerase, resulting in an immortal clone capable of developing into
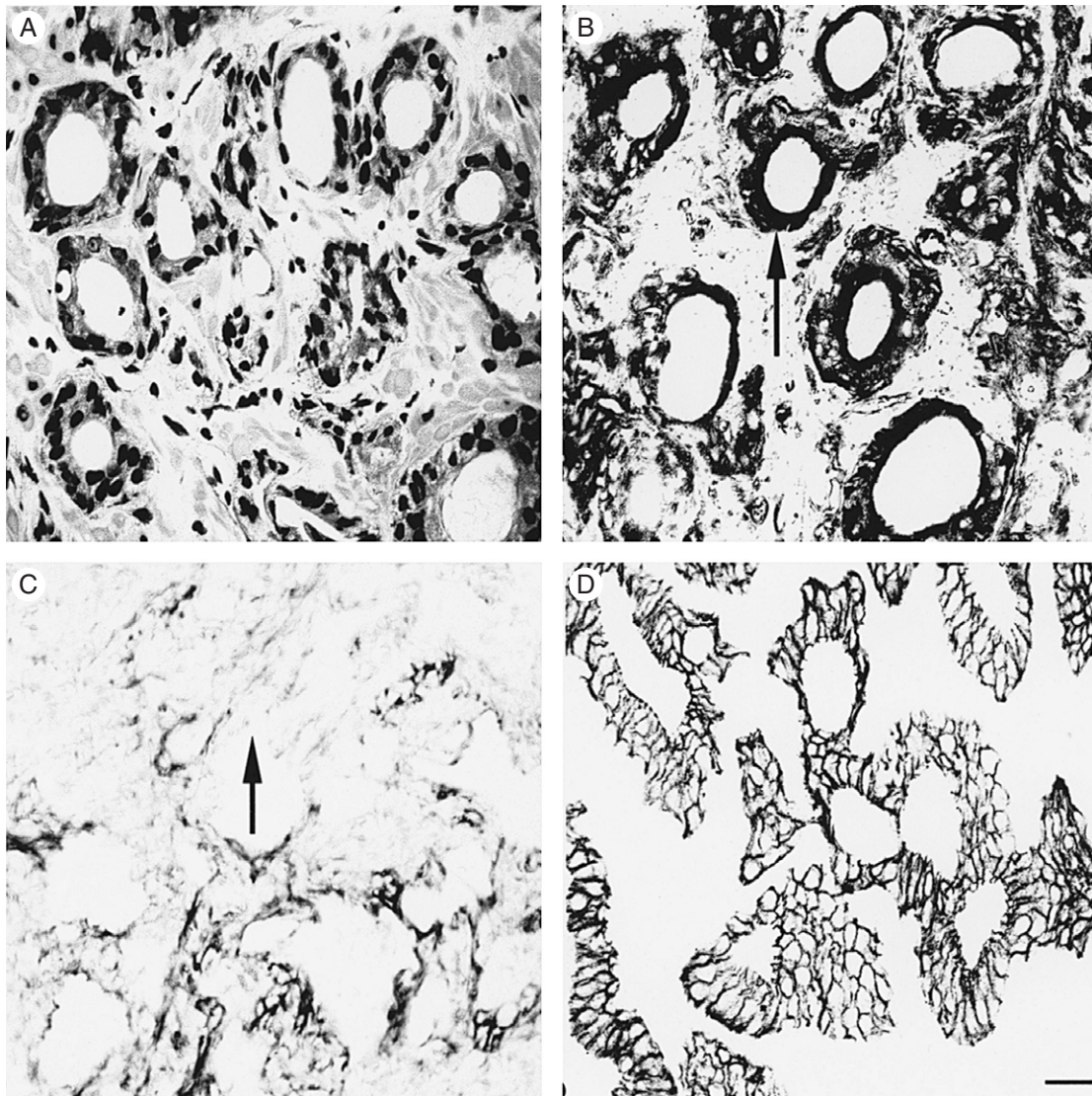
Figure 51 **A**: One of three cores taken from an 81-year-old patient also diagnosed as having Gleason grade 3+3 = score 6 carcinoma. In this core neoplastic features are evident by hematoxylin and eosin (H&E) stain. **B**: The same histologic area in approximate serial section, labeled with anti-P2X$_{1-2}$ antibody. The labeling features are those of purinergic receptor translocation (PRT) 3 because the anti-P2X$_{1-2}$ label is concentrated on the apical epithelium (*arrow*). **C**: The same histologic area in approximate serial section, labeled with anti-tenascin antibody. The anti-tenascin label is only 19.0% (p < 0.0001) that of normal in the extracellular matrix compared to normal and completely absent in the acinal basement membrane (*arrow*). **D:** The same histologic area in approximate serial section, labeled with anti-E-cadherin antibody. The area of the plasma membrane of each epithelial cell is strongly labeled. Bar 20 μm.

invasive carcinoma. Such a model predicts that genome protection remains intact in BPH, minimizing its malignant potential (De Marzo *et al.*, 1998).

Apoptosis, a type of programmed cell death, is a decisive mechanism in cell processes such as homeostasis, development, and many diseases, including cancer. The process of apoptosis is characterized by specific biochemical and morphologic changes. At present, there is convincing evidence that a sustained increase in intracellular Ca^{2+} can activate cytotoxic mechanisms in various cells and tissues. Among these ionic channels, the P2X purinoreceptors and the channels of capacitive entry of calcium have been described. Pro- and anti-apoptotic molecules such as bax and Bcl-2, respectively, have also been shown to participate in the process (Slater *et al.*, 2001). Direct injection of the rat prostate with an adenoviral vector that expresses Fas ligand (AdFasL/G) also results in rapid apoptosis in

Table 10 A Total of 289 Prostate Cases Comprising 2378 Cores*
Were Examined, Average Age 72 ± 9 Years

H&E, TP$_1$, and PRT Typing	Number of Cases	Tenascin Labeling	E-cadherin Labeling
Normal by H&E, PRT −ve, TP$_1$ −ve	23 (8%)	Maximal labeling	Maximal labeling
Normal by H&E, PRT 1, TP$_1$ +ve	77 (27%)	Maximal labeling	Maximal labeling
Gleason score 3–4, PRT 2-3, TP$_1$ +ve	6 (2%)	Only 38.4% that of normal; accompanied by PRT2	Maximal labeling
Gleason score 5–7, PRT 2-3, TP$_1$ +ve	160 (55%)	Only 19.0% that of normal; accompanied by PRT3	Maximal labeling
Gleason score 8–10, PRT 3, TP$_1$ +ve	23 (8%)	8.6-fold decrease with PRT 3	Architecture degraded = antibody de-expressed

H&E, hematoxylin and eosin; PRT, purinergic receptor translocation; TP$_1$, telomerase-associated protein.

*Each core was labeled for PRT, TP$_1$, H&E, tenascin, and E-cadherin.

primary prostate epithelial cells throughout the gland (Kirkman *et al.*, 2001).

Following damage to one or more of the four classes of regulatory genes—the growth promoting proto-oncogenes, cancer-suppressor genes (anti-oncogenes), apoptosis-regulating genes, or deoxyribonucleic acid (DNA) damage repair genes—neoplastic growth may occur. This process is often accompanied by abnormalities in the expression of oncoproteins such as platelet-derived growth factor, fibroblast growth factor, epidermal growth factor, colony stimulating factor 1, transcriptional activators, transducing proteins, cyclins, and their receptors (Cotran *et al.*, 1999). DNA damage repair is crucial to prevent the proliferation of neoplastic cells. The DNA base excision repair pathway is responsible for the repair of cellular alkylation and oxidative DNA damage. A crucial step in the base excision repair pathway involves the cleavage of baseless sites in DNA by an apurinic/apyrimidinic (AP), or baseless, endonuclease (Ape1/ref-1). Ape1/ref-1 is dramatically elevated in prostate cancer. The level of staining for Ape1/ref-1 increases from low in BPH to intense in PIN and cancer, and there is an increase in the amount of Ape1/ref-1 in the cytoplasm of PIN and cancer compared with BPH, with all tissues diagnosed by H&E stain. There was no correlation with PSA values (Kelley *et al.*, 2001). The use of complementary DNA (cDNA) microarrays with labeled cDNA from tumor samples obtained from transurethral resection of the prostate or radical prostatectomy have identified many up-regulated transcripts. Novel prostate cancer associations for several well-characterized genes of full-length cDNAs were identified, including *PLRP1*, *JM27*, human *UbcM2*, dynein light intermediate chain 2, and the human homologue of rat *sec61*. Novel associations with high-grade PIN included breast carcinoma

fatty acid synthase and cDNA *DKFZp434B0335* (Bull *et al.*, 2001). Tissue microarray technology also promises to greatly enhance clinical diagnosis and tissue-based molecular research by allowing improved conservation of tissue resources and experimental reagents, improved internal experimental control, and increased sample numbers per experiment (Bova *et al.*, 2001).

The current study demonstrates that P2X$_{1-2}$ and TP$_1$ in particular and tenascin expression to a lesser extent may prove to be reliable markers of early neoplastic transformation; E-cadherin is unsuitable for this purpose. Moreover, the increased accuracy of diagnosis of underlying prostate cancer using the PRT typing process suggests that PSA levels are actually far more accurate than has generally been supposed when the false-negative results arising from H&E-based diagnoses of sampled tissue that missed existing tumors are correctly categorized. New trials of the reagents are needed to further validate this approach.

In conclusion, biochemical and genetic changes have been shown to precede histologically identifiable changes accompanying cell transformation often by months or years. De-expression of the extracellular matrix adhesive glycoprotein tenascin and the cell-to-cell adherent protein E-cadherin have been suggested as markers of early neoplastic change in prostate epithelial cells. Previous studies have been inconclusive, probably because of epitope masking. We examined 2378 biopsy cores from 289 prostates using an HAR protocol at low pH to improve accuracy of detection. Tenascin and E-cadherin de-expression was correlated with purinergic receptor and telomerase-associated protein labeling and PSA levels and Gleason sum scores. E-cadherin was a poor marker because it was expressed in all lesions except carcinomas of the highest Gleason sum score. Tenascin was maximally

expressed in the extracellular matrix and acinar basement membrane in normal and prostatic intraepithelial neoplasia tissue. In prostate cancer tissue, tenascin expression did not correlate with Gleason sum score but was significantly de-expressed as purinergic receptor and telomerase associated protein expression increased. Marked changes in tenascin, telomerase-associated protein, and purinergic receptor expression were apparent well before any histologic abnormalities were visible by H&E stain, making these potential markers useful for early and developing prostate cancer. Moreover, the potential increased accuracy of diagnosis of underlying prostate cancer using PRT assessment suggests that PSA levels may be more accurate than has generally been supposed when the apparent false-negative results arising from H&E-based diagnoses are correctly categorized.

References

Barden, J.A., Cuthbertson, R.M., Jia-Zhen, W., Moseley, J.M., and Kemp, B.E. 1997. Solution structure of PTHrP(Ala15)(1-34). *J. Biol. Chem. 272*:29572–29578.

Bova, G.S., Parmigiani, G., Epstein, J.I., Wheeler, T., Mucci, N.R., and Rubin, M.A. 2001. Web-based tissue microarray image data analysis: Initial validation testing through prostate cancer Gleason grading. *Human Pathol. 32*:417–427.

Bull, J.H., Ellison, G., Patel, A., Muir, G., Walker, M., Underwood, M., Khan, F., and Paskins, L. 2001. Identification of potential diagnostic markers of prostate cancer and prostatic intraepithelial neoplasia using cDNA microarray. *Br. J. Cancer 84*:1512–1519.

Bussemakers, M.J., Van Bokhoven, A., Tomita, K., Jansen, C.F., and Schalken, J.A. 2000. Complex cadherin expression in human prostate cancer cells. *Int. J. Cancer 85*:446–450.

Chung, C., and Erickson, H. 1997. Glycosaminoglycans modulate fibronectin matrix assembly and are essential for matrix incorporation of tenascin-C. *J. Cell Sci. 110*:1413–1419.

Cotran, R., Kumar, V., and Collins, T. 1999. *Pathological Basis of Disease*, 6th ed. New York: WB Saunders Company.

Davidson, B., Goldberg, I., Gotlieb, W.H., Ben-Baruch, G., and Kopolovic, J. 1998. Expression of matrix proteins in uterine cervical neoplasia using immunohistochemistry. *Eur. J. Ob. Gyn. Reprod. Biol. 76*:109–114.

De Marzo, A.M., Knudsen, B., Chan-Tack, K., and Epstein, J.I. 1999. E-cadherin expression as a marker of tumour aggressiveness in routinely processed radical prostatectomy specimens. *Urology 53*:707–713.

De Marzo, A.M., Nelson, W.G., Meeker, A.K., and Coffey, D.S. 1998. Stem cell features of benign and malignant prostate epithelial cells. *J. Urol. 160*:2381–2392.

Foster, C.S., Bostwick, D.G., Bonkhoff, H., Damber, J.E., van der Kwast, T., Montironi, R., and Sakr, W.A. 2000. Cellular and molecular pathology of prostate cancer precursors. *Scand. J. Urol. Nephrol. Suppl.* 19–43.

Harrington, L., McPhail, T., Mar, V., Zhou, W., Oulton, R., Bass, M., Arruda, I., and Robinson, M. 1997. A mammalian telomerase-associated protein. *Science 275*:973–977.

Iskaros, B.F., Tanaka, K.E., Hu, X., Kadish, A.S., and Steinberg, J.J. 1997. Morphologic pattern of tenascin as a diagnostic biomarker in colon cancer. *J. Surg. Oncol. 64*:98–101.

Kammerer, R., Ehret, R., and von Kleist, S. 1998. Isolated extracellular matrix-based three-dimensional *in vitro* models to study orthotopically cancer cell infiltration and invasion. *Eur. J. Cancer 34*:1950–1957.

Kedeshian, P., Sternlicht, M.D., Nguyen, M., Shao, Z.M., and Barsky, S.H. 1998. Humatrix, a novel myoepithelial metrical gel with unique biochemical and biological properties. *Cancer Lett. 123*:215–226.

Kelley, M.R., Cheng, L., Foster, R., Tritt, R., Jiang, J., Broshears, J., and Koch, M. 2001. Elevated and altered expression of the multifunctional DNA base excision repair and redox enzyme Ape1/ref-1 in prostate cancer. *Clin. Cancer Res. 7*:824–830.

Kirkman, W. 3rd, Chen, P., Schroeder, R., Feneley, M.R., Rodriguez, R., Wickham, T.J., King, C.R., and Bruder, J.T. 2001. Transduction and apoptosis induction in the rat prostate, using adenovirus vectors. *Hum. Gene Ther. 12*:1499–1512.

Kuczyk, M., Serth, J., Machtens, S., Bokemeyer, C., Bathke, W., Stief, C., and Jonas, U. 1998. Expression of E-cadherin in primary prostate cancer: Correlation with clinical features. *Brit. J. Urol. 81*:406–412.

Kusagawa, H., Onoda, K., Namikawa, S., Yada, I., Okada, A., Yoshida, T., and Sakakura, T. 1998. Expression and degeneration of tenascin-C in human lung cancers. *Brit. J. Cancer 77*:98–102.

Lin, Y., Uemura, H., Fujinami, K., Hosaka, M., Iwasaki, Y., Kitamura, H., Harada, M., and Kubota, Y. 1998. Detection of telomerase activity in prostate needle-biopsy samples. *Prostate 36*:121–128.

Matthews, P., and Jones, C. 2001. Clinical implications of telomerase detection. *Histopathology 38*:485–498.

Mokbel, K., Parris, C., Ghilchik, M., Williams, G., and Newbold, R. 1999. The association between telomerase, histological parameters, and KI-67 expression in breast cancer. *Am. J. Surg. 178*:69–72.

Morales, C., Holt, S., and Ouellette, M. 1999. Absence of cancer-associated changes in human fibroblasts immortalized with telomerase. *Nat. Genet. 21*:115–118.

Murant, S.J., Handley, J., Stower, M., Reid, N., Cussenot, O., and Maitland, N.J. 1997. Co-ordinated changes in expression of cell adhesion molecules in prostate cancer. *Eur. J. Cancer 33*:263–271.

Phillips, G.R., Krushel, L.A., and Crossin, K.L. 1998. Domains of tenascin involved in glioma migration. *J. Cell Sci. 111*:1095–1104.

Pilch, H., Schaffer, U., Schlenger, K., Lautz, A., Tanner, B., Hockel, M., and Knapstein, P.G. 1999. Expression of tenascin in human cervical cancer-association of tenascin expression with clinicopathological parameters. *Gynecol. Oncol. 73*:415–421.

Slater, M. 1999. Mitochondrial DNA damage assessment using fluorescence microscopy quantitation. *J. Histotechnol.* 17–21.

Slater, M., Delprado, W.J., Murphy, C.R., and Barden, J.A. 2001. Detection of preneoplasia in histologically normal prostate biopsies. *Prostate Cancer Prost. Diseases 4*:92–96.

Tokes, A.M., Hortovany, I.E., Csordas, G., Kulka, J., Mozes, G., Hatalyak, A., and Kadar, A. 1999. Immunohistochemical localisation of tenascin in invasive ductal carcinoma of the breast. *Anticancer Res. 19*:175–179.

Tran, N.L., Nagle, R.B., Cress, A.E., and Heimark, R.L. 1999. N-Cadherin expression in human prostate carcinoma cell lines. An epithelial-mesenchymal transformation mediating adhesion with stromal cells. *Am. J. Pathol. 155*:787–798.

Ueda, M., Ouhtit, A., Bito, T., Nakazawa, K., Lubbe, J., Ichihashi, M., Yamasaki, H., and Nakazawa, H. 1997. Evidence for

UV-associated activation of telomerase in human skin. *Cancer Res*. 1997:370–374.

Xue, Y., Li, J., Latijnhouwers, M.A., Smedts, F., Umbas, R., Aalders, T.W., Debruyne, F.M., De La Rosette, J.J., and Schalken, J.A. 1998. Expression of periglandular tenascin-C and basement membrane laminin in normal prostate, benign prostatic hyperplasia and prostate carcinoma. *Brit. J. Urol.* *81*:844–851.

Yoshida, T., Yoshimura, E., Numata, H., Sakakura, Y., and Sakakura, T. 1999. Involvement of tenascin-C in proliferation and migration of laryngeal carcinoma cells. *Virch. Archiv.* *435*:496–500.

This Page Intentionally Left Blank

7

The Role of MUC18 in Prostate Carcinoma

Guang-Jer Wu

Introduction

The prostate is a tubuloalveolar gland that contains a simple, slowly renewing epithelium composed of three cell types: basal cells, secretory (luminal) cells, and neuroendocrine cells. Basal cells are interposed between luminal cells and the basement membrane. Secretory (luminal) cells surmount the basal cells. Neuroendocrine cells are rare and scattered throughout acini and ducts. All three types of epithelial cells may derive from the common stem cells, which reside in the basal cell compartment (Bonkhoff *et al.,* 1996).

Besides prostatitis, benign prostatic hyperplasia (BPH) and prostate carcinoma are the two major types of diseases associated with prostate gland. Basal epithelial cells are the principle proliferating epithelial population in the mature gland, and they are believed to be the precursor of BPH, which rarely becomes malignant (Grayhack *et al.,* 1998). Secretory cells are the predominant epithelial cells, and they are believed to be the major precursor of most prostate carcinomas, which are androgen-dependent (De Marzo *et al.,* 1998). However, under androgen ablation treatment, androgen-independent carcinomas may emerge from androgen-dependent secretory epithelial cells under the influence of paracrine growth factors and cytokines secreted from the surrounding stromal cells and neuropeptides secreted from the adjacent neuroendocrine cells. On rare occasion, some human prostate carcinomas may also originate from neuroendocrine cells, and the development of this type of carcinoma is also androgen-independent (DiSant' Agnese, 1992).

Prostate cancer is now the most commonly diagnosed cancer in American males and the second most common cause of cancer death among males in this country. One in 10 American men will develop prostate cancer in his lifetime (Brawley *et al.,* 1994). The majority of histologically localized prostate cancers remain subclinical and never require treatment. However, in some cases, prostate cancers rapidly metastasize, killing the patients within a year of the initial diagnosis. Once the cancer spreads outside of the glands, prostate cancer is nearly always fatal because there is no effective treatment.

The major challenge in controlling this disease is that it is impossible to predict when and which localized tumors will progress to become cancers. This poor prediction of the outcome of the disease partly reflects our lack of knowledge about the process by which a localized prostate cancer becomes metastatic (Wood *et al.,* 1994). An additional complication is that accurate clinical prognosis of the carcinoma in any individual case is difficult because 85% of prostatic carcinomas are multifocal and the cancer seen in the biopsy may not accurately reflect the entire biological potential (Catalona *et al.,* 1978). Furthermore, one of the present standard diagnostic tests for detecting prostate cancer metastases is to determine the elevated

Handbook of Immunohistochemistry and *in situ* Hybridization of Human Carcinomas, Volume 2: Molecular Pathology, Colorectal Carcinoma, and Prostate Carcinoma

347

serum level of prostate specific antigen (PSA). However, elevated serum PSA level is not always predictive of a pathologic state of the presence of metastatic prostate cancer because PSA is organ-specific rather than tumor-specific (Richie *et al.,* 1997). Other potential diagnostic markers for prostate cancer progression, such as α-catenin and KAI1, may not be a practical marker for diagnosis because of their absence or low expression in high-grade prostate carcinomas (Allan *et al.,* 1997). Thus, there is still an urgent need to search for an ideal marker for the early detection of the metastatic potential of prostate carcinomas. It would be of a greater advantage if these diagnostic molecular markers were also the key players in causing metastasis. Then they could also be targeted in designing an effective therapy.

Because the process of tumor metastasis is complex, this suggests that many genes are directly or indirectly involved in this process. The accumulation of the multiple intrinsic changes that lead to aberrant alterations of gene expression can be attributed to their metastatic phenotype; this is because the genome of metastatic tumor cells has greater instability than nonmetastatic tumor cells, and this renders metastatic tumor cells more prone to acquiring multiple mutations (Lengauer *et al.,* 1998). Many metastasis genes and metastasis suppressor genes have been identified (Ruddon, 1995) since the first successful demonstration of the conversion of the nonmetastatic Ha-ras-transformed NIH 3T3 fibroblast cells to metastatic tumor cells by transfection with the deoxyribonucleic acid (DNA) fragments isolated from a human metastatic tumor (Bernstein *et al.,* 1985). This also suggests that there are many alternative pathways for metastasis (Hanahan *et al.,* 2000). Some of these genes encode cell adhesion molecules (CAMs) such as *E-cadherin* (Umbas *et al.,* 1992), *integrins α2β1* (Zutter *et al.,* 1995) and *αVβ3* (Zheng *et al.,* 1999), *CD44* (Gao *et al.,* 1997), and *MUC18* (Wu *et al.,* 2001a; Xie *et al.,* 1997). The advent of modern state-of-the-art technologies such as serial analysis of gene expression (SAGE) analysis, DNA chip microarray analysis, and proteomics should rapidly lengthen the list of these two categories of genes in the near future. We should not be surprised if some of these genes are commonly shared by metastatic tumors derived from different tissues. As long as these genes render tumor cells, irrespective of their tissue origins, they will have the metastatic advantage over other tumor cells. It is also possible that some of the oncogenes or tumor suppressor genes may play some direct or indirect roles in tumor metastasis, as long as they directly or indirectly alter cytoskeleton structure, cellular motility, and invasiveness of tumor cells.

Fortunately, tumor metastasis is a rare event as a result of metastatic inefficiency because only a minute population of the metastatic cells can successfully intravasate or extravasate the vasculatures and survive the long, difficult journey to reach the target organs (Weiss, 1990). This hypothesis has been modified by results obtained by observing the process with the *in vivo* video microscopy. According to these results, the metastatic cells are better to dock themselves and thereafter establish secondary growth in distant organs than to have an increased migratory and invasive ability in the steps of intravasation or extravasation (Chambers *et al.,* 1995). The adept establishment of secondary growth by metastatic cells may be the outcome of a complex interaction between the tumor cells and the extracellular matrix. Many gene products could potentially affect this interaction; it is highly possible that altered expressions of CAMs in metastatic cells may increase their ability to establish secondary growth. We have focused our research on the effect of the expression of cell adhesion molecules on prostate cancer metastasis.

The social behaviors of the cells are governed by CAMs. The altered expression of CAMs affect the cell motility, cell–cell interactions, and cell–extracellular matrix interactions (Mohler, 1993). The metastatic potential of a tumor cell is the consequence of a complex interaction among many overexpressed or underexpressed CAMs, as documented in many carcinomas (Mohler, 1993). For example, *integrins αV, α4,* and *β3*; intercellular CAM (*I-CAM*); *MUC18*; and human leukocyte antigen-DR *(HLA-DR)* are overexpressed, whereas *E-cadherin*, *α-catenin*, and vascular CAM (*VCAM*) are underexpressed in metastatic melanomas (Herlyn, 1993). Overexpression of a CAM (such as *integrin α2β1*) abrogates the metastasis of breast carcinoma cells (Zutter *et al.,* 1995). However, overexpression of a CAM (such as integrin αVβ3) increases the metastatic ability of human prostate carcinoma cells (Zheng *et al.,* 1999).

Studies of the altered expression of CAMs in prostate cancers have been limited to *E-cadherin* (Umbas *et al.,* 1992), *CD44* (Gao *et al.,* 1997), carcinoembryonic antigen CAM (CEA-CAM) (Kleinerman *et al.,* 1995), and some integrins (Edlund *et al.,* 2001; Zheng *et al.,* 1999). Gaining expression of the standard form of *CD44* (Gao *et al.,* 1997) suppresses metastasis of prostate carcinoma. Gaining expression of CEA-CAM1 supresses tumor formation (Kleinerman *et al.,* 1995); however, its effect on metastasis has not been studied. Most of the effect of a single integrin is not as obvious, because many members of the integrin family are functionally compensatory to each other (Edlund *et al.,* 2001). Association of aberrant expression of other

CAMS with the malignant progression of prostate cancer has not been studied. To better understand the metastatic potential of prostate cancer, it is highly desirable to search for other CAMs, whose expression is increased in malignant prostate cancer, as opposed to its benign counterpart. We have focused our interest on the possible association of the altered expression of MUC18 in prostate cancer cell lines and tissues with the malignant progression of human prostate carcinoma.

Human MUC18 (huMUC18), a CAM in the immunoglobulin gene superfamily, is an integral membrane glycoprotein (Lehmann *et al.,* 1989). HuMUC18 has 646 amino acids that include an N-terminal extracellular domain of 558 amino acids, which has a 28 amino acids characteristic of a signal peptide sequence at its N-terminus, a transmembrane domain of 24 amino acids (amino acid #559-583), and a cytoplasmic domain of 64 amino acids at the C-terminus. Human MUC18 has eight putative N-glycosylation sites (Asn-X-Ser/Thr) and is heavily glycosylated and sialylated, resulting in an apparent molecular weight of 113,000–150,000. The extracellular domain of the protein comprises five immunoglobulin-like domains (V-V-C2-C2-C2) (Lehmann *et al.,* 1989) and an X domain (Wu *et al.,* 2001b). The cytoplasmic tail contains peptide sequences that will potentially be phosphorylated by protein kinase A (PKA), protein kinase C (PKC), and casein kinase II (Lehmann *et al.,* 1989). The structure of huMUC18 protein is depicted in Figure 52. From the intriguing protein structure, we predict that MUC18 protein probably has multiple functions in addition to cell-to-cell interaction, which actually triggers a cascade of signals that affects cytoskeleton structure and cellular motility and invasiveness. Other possible functions may include cooperating synergistically with growth factors (as a coreceptor) to modulate cell functions and to trigger an intracellular signaling pathway, activating matrix metalloproteinases (MMPs), serving as a coactivator for other cell functions, and serving as a cotransporter for extracellular small molecules (e.g., calcium ion influx).

Human MUC18 (huMUC18, Mel-CAM, CD146) was originally found to be abundantly expressed on the cellular surface of most malignant human melanomas and has been postulated to play a role in the progression of human melanoma (Lehmann *et al.,* 1989). Further studies show that the stable, ectopic expression of huMUC18 complementary DNA (cDNA) gene in three nonmetastatic human cutaneous melanoma cell lines increases the metastatic abilities of these cell lines in the immune-deficient mouse models (Xie *et al.,* 1997). Furthermore, the stable, ectopic expression of mouse *MUC18* (*moMUC18*) cDNA in two low-metastatic mouse melanoma cell lines increases the metastatic abilities of these cell lines in immune-competent syngeneic mice (Wu *et al.,* 2001a).

However, the overexpression of *MUC18* is not limited to melanoma as previously thought (Lehmann *et al.,* 1989). We have pioneered the study of possible *MUC18* expression in prostate cancer cells and tissues. We carried out molecular biologic and immunologic studies of the possible expression of MUC18 in three established prostate cancer cell lines and human prostate cancer tissues and in immunohistochemical studies of paraffin-embedded human prostate cancer tissue sections. From the results, we have suggested a hypothesis that overexpression of *MUC18* may be a new diagnostic marker for the metastatic potential of human prostate cancer and also that *MUC18* may be a determinant for mediating both tumorigenesis and metastasis of human prostate cancer cells (Wu *et al.,* 2001b). We have further tested the hypothesis by testing the effect of ectopic expression of *huMUC18* in human prostate LNCaP cells on their ability to form tumor in the prostate gland of and to increase metastasis in nude mice (Wu *et al.,* 2004).
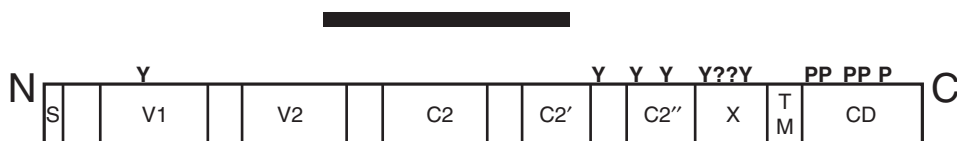
Figure 52 The structure of huMUC18 protein.

MATERIALS

1. Growth medium of the LNCaP cells: Modified RPMI 1640 medium containing 20 mM HEPES buffer (Cat. No. 22400-089, GIBCO/BRL/Invitrogen) and supplement with 2% glucose, 1 mM sodium phosphoenolpyruvate, and 10% fetal bovine serum.

2. Opti-MEM (Cat. No. 31985-070, GIBCO/BRL/ Life Technology).

3. Tris ethylenediaminetetraacetic acid (TE): 10 mM. Tris. HCl, pH 7.9, and 0.1 mM Na ethylenediamine tetraacetic acid (EDTA).

4. Na_3.Citrate buffer (7.14 mM, pH 6.0): 10X stock solution if prepared by dissolving 21 g of Na_3.Citrate. 2 H_2O (FW = 294.10) in 950 ml of deionized water, adjust the pH to 6.0 by addition of about 1.6–1.8 ml glacial acetic acid, and add water to a final volume of 1000 ml. 10X stock solution is kept at 4ºC. 1X solution is diluted freshly from 10X stock solution with water before use.

5. Phosphate buffer saline (PBS): 14.4 mM Na_2HPO_4, 0.56 mM NaH_2PO_4, and 0.1355 M NaCl (2.06 g of Na_2HPO_4 (FW = 141.96), 0.672 g of NaH_2PO_4 (FW = 120), 7.92 g of NaCl per 1000 ml of deionized water).

6. 1X Tris-buffered saline Tween (TBST) solution contains 10 mM Tris.HCl, pH 7.9, 150 mM NaCl, 0.05% Tween-20, which is diluted from the 10X stock solution by addition of deionized water before use. 10X stock solution contains 100 mM Tris.HCl, pH 7.9, 1.5 M NaCl, 0.5% of Tween-20 (5 ml per 1 liter of solution). Store the 10X stock solution at 4ºC.

7. ImmEdger pen (Cat. No. H-4000, Vector Laboratories, Burlingame, CA).

8. Biotinylated rabbit anti-chicken (immunoglobulin) IgY antibodies (Promega G289A or G2891).

9. Peroxidase-conjugated streptavidin solution (Dako Cat. No. K0675, LSAB2 bottle 2 or Dako Cat. #K1016, LSAB2).

10. 10X diaminobenzidine (DAB) buffer: 0.5 M Tris.HCl, pH 7.5–7.6, and 150 mM NaCl.

11. 5% (W/V) DAB stock solution: 500 mg of DAB (3,3-diaminobenzidine, Amresco, Cat. No. 0430) in 10 ml of 50 mM Tris.HCl buffer, pH 7.6.

12. DAB solution ready-to-use: 0.5 ml of 10X DAB buffer, 0.05 ml 5% (W/V) DAB, 0.005 ml of 30% hydrogen peroxide, and 4.45 ml of deionized water.

13. Hematoxylin staining solution: modified Harris formula (Cat. No. SL 90-16, Anapath product, Statlab Medical Products, Inc. Lewisville, TX) contains 0.5% (W/V) hematoxylin, 6.0% (W/V) ammonium aluminium sulfate dodecahydrate, 4.8% (V/V) ethanol, and 0.2% (V/V) methanol in water.

14. Eosin philoxine solution (Cat. No. S176, Polyscientific Research & Development Corp., Bayshore, NY).

15. Polymount (xylene-based synthetic resin) (Cat. No. S3153, Polyscientific Research & Development Corp.).

16. Lipofectamine (2 mg/ml, Cat. No. 18324-012, GIBCO/BRL, Life Technology) used without dilution.

17. DMRIE-C (2 mg/ml, Cat. No. 10459-014, GIBCO/BRL, Life Technology) used without dilution.

18. Anti-proteolytic cocktail: 1 mM benzamidine, 0.5 mM phenylmethylsulfonyl fluoride (PMSF), and 1 μg/ml each of antipain, leupeptin, chymostatin, and pepstatin (Sigma Chemical Co.): use 20 μl per ml of lysate.

19. BioRad protein assay dye reagent concentrate (Cat. No. 500-0006, BioRad Laboratories, Hercules, CA).

20. Human normal and prostate cancer tissue sections were obtained from the tissue archive of Emory University Hospital.

21. Five- to 6-week old male athymic (nu/nu) nude mice were from Harlan or male athymic nude mice (Cr1: NU/NU-nuBR) from Charles River.

22. Mouse tumors and tissues were from euthanized nude mice, which were injected with LNCaP clones.

METHODS

Overexpression and Purification of huMUC18 in *Escherichia coli* for Making Polyclonal Antibodies

1. Ligate the middle subfragment of the *huMUC18* cDNA gene (aa#211-376), which does not have any N-glycosylation sites, in-frame to the C-terminus of the *GST* (glutathione-S-transferase) gene in the plasmid vector pGEX-6P-1 (Pharmacia) and transform *E. coli* K-12 strain BL-21 cells.

2. Inoculate 1 L L-broth (supplemented with 0.1 mg/ml ampicillin and 0.2% glucose) with 5 ml of an overnight bacteria culture that contains the plasmid. Let it grow at 37ºC with vigorous shaking (250 rpm) for 2–3 hours, when A_{600} reaches to about 0.6. Add a freshly prepared isopropyl-D-thiogaloctopyranoside (IPTG) solution (0.5 M stock) to a final concentration of 0.1–0.2 mM to the culture to induce the overexpression of the GST fusion protein and continue the incubation and shaking for an additional 2 hours.

3. Pellet down the bacterial cells by centrifugation at 3000 rpm for 10 min in an HG-4L rotor in a Sorval RC-3 centrifuge. Pour off the medium and wash the pellet with 45 ml of ice-cold PBS. Resuspend the washed pellet by pipetting up and down in 15 ml of cold PBS

containing an anti-proteolytic cocktail. Pipet the cell suspension into a prechilled French Pressure cell (Cat. No. FA-031) mounted to a French Pressure Cell Press (American Instrument Co., Silver Spring, MD), increase the pressure to 800–1000 *psi*, and lyse the cells by releasing the pressure. Collect the lysate in a polycarbonate centrifuge tube, and centrifuge the lysate at 10,000 rpm for 30 min in a SS-34 rotor in an RC-2 centrifuge.

4. Determine the protein concentration of the clear supernatant of the lysate by the Bradford method (using the BioRad protein assay dye reagent) and adjust the protein concentration to about 10 mg/ml.

5. Mix the clear supernatant of the lysate with 1 ml bed volume of the Glutathione-Sepharose 4B (50% slurry of prewashed resin before use) and rotate the mixture at room temperature for 30 min to allow the GST-fusion protein to bind to the affinity resin.

6. Pellet the resin by centrifugation at 500X g for 5 min and discard the supernatant; wash the resin three times each with 40 ml of PBS and two times with 5 ml of cleavage buffer. Resuspend the resin in 20 ml of cleavage buffer, add 15 µl of PreScission protease (human rhinovirus type 14 3C protease), mix, and allow cleavage to take place at 4ºC overnight.

7. Centrifuge the resin down at 2000 rpm for 10 min and collect the supernatant (about 20 ml). Wash the resin twice with 20 ml PBS, and combine the supernatant and the two washes (total about 40 ml).

8. Concentrate the combined supernatant in an Amicon Centriprep-50 by centrifugation at 6000 rpm for 40 min twice until the volume is down to about 2–3 ml.

9. Apply the concentrated liquid to a Superdex-200 HR 10/30 column in a Pharmacia FPLC system to remove the contaminant 70 kDa protein, and collect 0.5 ml each fraction after 7 ml of void volume.

10. Determine the protein concentration of each fraction by using the Bradford method.

11. Check the purity of the recombinant middle fragment huMUC18 protein (about 22 kDa) by sodium dodecyl sulfate polyacrylamide gel electrophoresis (SDS-PAGE) and its reactivity with anti-huMUC18 antibodies.

12. The average yield of the final purified protein is about 2 mg per liter of IPTG-induced culture. Send 6 mg of protein to Lampire Biological Laboratories (Pipersville, PA) to immunize three egg-laying hens over a period of 3 months. After immunization, collect chicken sera for enzyme linked immunosorbent assay (ELISA) to determine the antibody titer.

13. Collect all the eggs laid immediately before and after immunization, but use only the eggs laid during the period when sera have a high titer of antibodies; pool the egg yolks, and purify the chicken IgY that contains the anti-huMUC18 antibodies.

Immunohistochemistry of Human Prostate Normal and Cancerous Tissues and Xenograft Tumors and Metastatic Lesions from Human huMUC18-Expressing LNCaP Cells.

1. Fix tumor specimen in 10% phosphate buffered formalin (Fisher #SF100-4, 4% (W/W) formaldehyde, 0.4% (W/V) monohydrate, monobasic sodium phosphate, 0.65% (W/V) anhydrous dibasic sodium phosphate, 1.5% (W/V) methanol, (pH 6.9–7.1) at room temperature for 1 week and then keep them at 4ºC until they are embedded with paraffin. Make 5 µm sections of paraffin-embedded tissues. Heat them at 58ºC for 60 min or 50–55ºC for 50 min to fix the tissue sections on the slides.

2. Deparafinize slides 3 times for 3 min each in xylene; remove xylene 3 times in 100% ethanol, and gradually rehydrate 3 min each with 95%, 80%, 70%, and 50% of ethanol; PBS; and water.

3. Retrieve antigen by putting the rehydrated slides in a gently boiling solution of sodium citrate (pH 6.0) (about 96ºC) for 10 min, and then let it cool at room temperature for 30–60 min.

4. Immerse the slides in PBS, and then quench the endogenous peroxidase with 3% hydrogen peroxide at room temperature for 10 min.

5. Wash the slides twice with PBS, blot dry, and circumscribe each tissue section on the same slide with a hydrophobic solution by using an ImmEdger pen because different adjacent sections on the same slide may be used for different concentrations of primary antibodies or control antibodies.

6. Blot each tissue section with 200–250 µl of a nonspecific blot solution of 5% nonfat milk in Tris-buffered saline Tween (TBST) with 0.02% Azide at 4ºC overnight.

7. Replace nonspecific blot solution with 200–250 µl of the primary antibody and let the immune reaction go on at room temperature for 30 min. Before use, preincubate the 1/300 to 1/600 diluted chicken anti-huMUC18 protein antibody with 5% nonfat milk in TBST-Azide for 15 min at room temperature.

8. Wash the slides 4 times with TBST, each time for 7–8 min, on a shaker.

9. React the tissue sections with a secondary antibody at room temperature for 30 min. Before use, preincubate the 1/250 to 1/500 diluted biotinylated rabbit anti-chicken IgY antibodies with 5% nonfat milk in TBST *without Azide*. Wash the slides as in **Step 8**.

10. Add about 5–7 drops of a streptavidin-horseradish peroxidase solution (Dako) per tissue section and let the reaction go on at room temperature for 45 min.

11. Wash the slides 3 times with PBS.

12. Stain each tissue section with 0.1–0.25 ml of DAB solution at room temperature for 20 min.

13. Wash twice with water.

14. Counterstain with hematoxylin solution for 2 min.

15. Wash the slides in subsequent order 3 times with deionized water, once with tap water for 5 min, and once with deionized water for 3 min. Gradually dehydrate the sections for 3 min each with 50%, 70%, 80%, and 95% ethanol, then 3 times with 100% ethanol; and then 3 times with xylene for 10 min, 60 min, and overnight, respectively.

16. Mount the slide with xylene-based Polymount, and let it dry in a fume hood for 3–7 days.

Selection of G418-Resistant Clones of LNCaP Cells

1. Seed 1×10^6 LNCaP cells to each 60-mm Petri dish (about 60% confluence) 1 day before lipofection. Wash the monolayer cells twice with Opti-MEM (GIBCO/Life Technology).

2. Precipitate 5 µg DNA to be used for transfection from a DNA solution after addition of 0.4 M NaCl (final concentration), mix with 2.5 volumes of 95% ethanol, and dissolve the DNA in 50 µl of sterile TE. Mix the DNA solution with 30 µg of DMRIE-C (Life Technology) or Lipofectamine (Life Technology) in 0.3 ml Opti-MEM. Allow the DNA-lipofecting reagent complexes to form at room temperature for at least 15 min and then mix it with 5 ml of Opti-MEM.

3. Add the DNA-Lipofectamine or DMRIE-C mixture (about 5.3 ml) to each Petri dish and allow the lipofection to proceed at 37ºC in a 5% CO_2 incubator for 6 hours. Remove the lipofection solution by suction and replace it with 5 ml of regular growth medium (modified RPMI1640 medium supplemented with 20 mM HEPES buffer, 1 mM Na pyruvate. 0.45% glucose, and 10% fetal bovine serum). Allow the culture to growth for 2 days at 37ºC in a 5% CO_2 inbutor.

4. Treat the culture with trypsin to detach the cells and split into two Petri dish plates. Add 5 ml of growth medium containing 0.25 mg/ml of G418 (active component 0.19 mg/ml, LD50) to each plate of culture and allow most of the cells to be killed by G418 for about 2 weeks. During the killing period, replace the culture medium containing G418 twice per week.

5. The G418-resistant ($G418^R$) colonies become visible with naked eyes. Treat each colony with 30 µl of 0.25% (W/V) trypsin in the incubator for 2–5 min to allow colonies to detach from Petri dish. Carefully transfer each clone with a sterile Eppendorf micropipet tip into a 24 well-plate, in which each well contains 1 ml of growth medium and G418.

6. Expand each colony gradually into 6-well plate, T-25, and T-75 tissue culture flasks.

7. Duplicate each set of colonies when colonies grow to cover completely each well of the 6-well plate. Use one set for making a Western Blot lysate by addition of 100 µl of Western Blot lysis buffer containing 2 µl of an antiproteolytic cocktail to each well. Determine the huMUC18 expression of each colony by a standard Western blot analysis (Wu et al., 2001b).

8. We find that transfection with DMRIE-C is 100 times more efficient than Lipofectamin. We obtain 75% of the $G418^R$ clones that express huMUC18 from DMRIE-C transfection. In contrast, we obtain only less than 10% of the G418-resistant clones that express huMUC18 from Lipofectamin transfection.

Assay of Tumorigenesis and Metastasis of Human Prostate LNCaP Cells in Nude Mice

1. Order 5–6-week-old male athymic nude mice from Harlan or from Charles River.

2. Follow the National Institutes of Health animal health care guidelines with the approved Institutional Animal Care and Use Committee protocol.

3. Surgically cut open the lower abdomen with a sterile technique after anesthetizing each mouse with 50 mg of Ketamine and 2 mg Xylazine per kg of body weight.

4. Inject 1×10^6 cells in 0.02 ml into one of the dorsolateral lobes of prostate gland (orthotopical injection). Close the wound with 9 mm metal wound clips (Mik Ron Autoclip, Cat. No. 42631, Clay Adam/ Beckton Dickinson and Co., Sparks, MD), which are sterilized in Cidex (glutaraldehyde 2.4% solution, Cat. No. 2245, reusable sterilizing and disinfecting solution, Johnson-Johnson Medical Inc.).

5. Observe the well-being of mice to ensure their recovery from surgery and check the wound healing daily for 1 week. Check the tumor growth by gently touching the lower abdomen of each mouse weekly.

6. Euthanize the mice after 4.5 or 5 to 5.5 months, and surgically open the lower abdomen. Check tumor in the prostate gland and possible metastasis to other organs such as seminal vesicles, ureter, kidney, periaortic lymph nodes, liver, brain, and lungs. Excise tumors and determine the tumor weight by a balance, fix a piece of tumor in formalin for hematoxylin and eosin (H&E) histology staining and immunohistochemistry, and homogenize the rest of the tumor to make protein lysate for Western Blot analysis and to make total

ribonucleic (RNA) for reverse transcription polymerase chain reaction (RT-PCR) analysis.

7. Excise the organs containing metastatic lesions, fix a small piece in formalin, and process the rest of the organs in the same way as the tumors in **Step 6**.

RESULTS AND DISCUSSION

Overexpression of Human MUC18 Correlates with the Development and Malignant Progression of Human Prostate Cancer

We carried out molecular biologic and immunologic studies of the possible expression of MUC18 in three established prostate cancer cell lines and human prostate cancer tissues and in immunohistochemical studies of paraffin-embedded human prostate cancer tissue sections. We found that MUC18 messenger RNA (mRNA) and protein were expressed in two metastatic prostate cancer cell lines (DU145 and PC-3) and in one metastatic bladder cancer cell line (TSU-PR1) but not in one nonmetastatic prostate cancer cell line (LNCaP.FGC) (Wu *et al.,* 2001b). Western Blot analysis shows that HuMUC18 protein is also expressed at high levels in the extracts prepared from tissue sections containing high-grade prostatic intraepithelial neoplasia (PIN), high-grade prostate carcinoma, and lung and lymph node metastases (Wu *et al.,* 2001b). In contrast, huMUC18 is weakly expressed in the extracts prepared from either the cultured primary normal prostatic epithelial cells or the normal prostate gland.

From immunohistochemical analysis we found that huMUC18 antigen was not expressed in most (90%) of the normal epithelial cells in the prostatic ducts/acini, nor in any (100%) of the epithelial cells of BPH. But huMUC18 was highly expressed in the majority (81%) of the neoplastic counterparts (high-grade PIN) and in the majority (80–84%) of the high-grade prostate adenocarcinomas and lung and lymph node metastatic lesions (Wu *et al.,* 2001b). Figure 53 shows a typical result of immunohistochemistry of human prostate cancer tissues. Taken together, we have provided the first evidence to show that the overexpression of MUC18 correlates with the malignant progression of human prostate cancer. From this, we suggest that it may be an ideal marker for monitoring the progression of prostate cancer from premalignant stage (PIN) to malignant stage and to metastasis to other organs. We also propose a hypothesis that MUC18 may be a possible mediator for the metastatic potential of prostate cancers.

The Presentation of huMUC18 in the Majority of Prostate Cancer Tissues is Different from that in Human Melanomas

Previously, two groups studied the possible expression of huMUC18 in prostate cancer cell lines and prostate cancer tissues and found that huMUC18 expression was not detectable (Putz *et al.,* 1999; Shih *et al.,* 1998). In contrast, we have found positive signals of Western Blot analysis and immunohistochemistry in both the prostate cancer cell lines and the tissues by using our chicken polyclonal antibodies; the results were confirmed by the RT-PCR analysis of huMUC18 mRNA (Wu *et al.,* 2001b). To reconcile these controversial results, we reason that the most likely cause for their negative results is that their mouse anti-huMUC18 monoclonal antibodies fail to recognize the huMUC18 epitopes presented in prostate cancer cell lines and tissues because we had similar experiences with monoclonal antibodies from a commercial source (Biocytex). The four Biocytex monoclonal antibodies could detect huMUC18 antigens in human melanoma sections by immunohistochemistry but not those in the tissue sections from human normal prostate gland and prostate carcinomas. In contrast, our chicken anti-huMUC18 polyclonal antibodies could recognize the huMUC18 antigens in both the tissue sections from human normal prostate gland and prostate carcinomas and cell lines as well as those from human melanomas and cell lines. We concluded that the presentation of huMUC18 antigens in human melanomas might be different from those in human prostate carcinomas (Wu *et al.,* 2001b).

Predominant Cytoplasmic Expression of huMUC18 Antigens May Correlate with the Malignant Progression of Human Prostate Carcinomas

In human cutaneous melanoma cells, huMUC18 antigen is predominantly expressed on the cytoplasmic membrane regardless of the stage of the tumor (Wu *et al.,* 2001b and in Figure 53A). In contrast, MUC18 expression in prostate cancer cells seems to change from a predominantly *cytoplasmic membrane* location in 80% of high-grade PIN to a predominantly *cytoplasmic* location as the prostate cancer progresses to a malignant stage (90% of the prostate carcinomas with Gleason scores of 6–8) (Wu *et al.,* 2001b and Figure 53). Thus the predominant cytoplasmic expression of huMUC18 antigen may also serve as an additional indicator for the malignant progression of human prostate cancer.
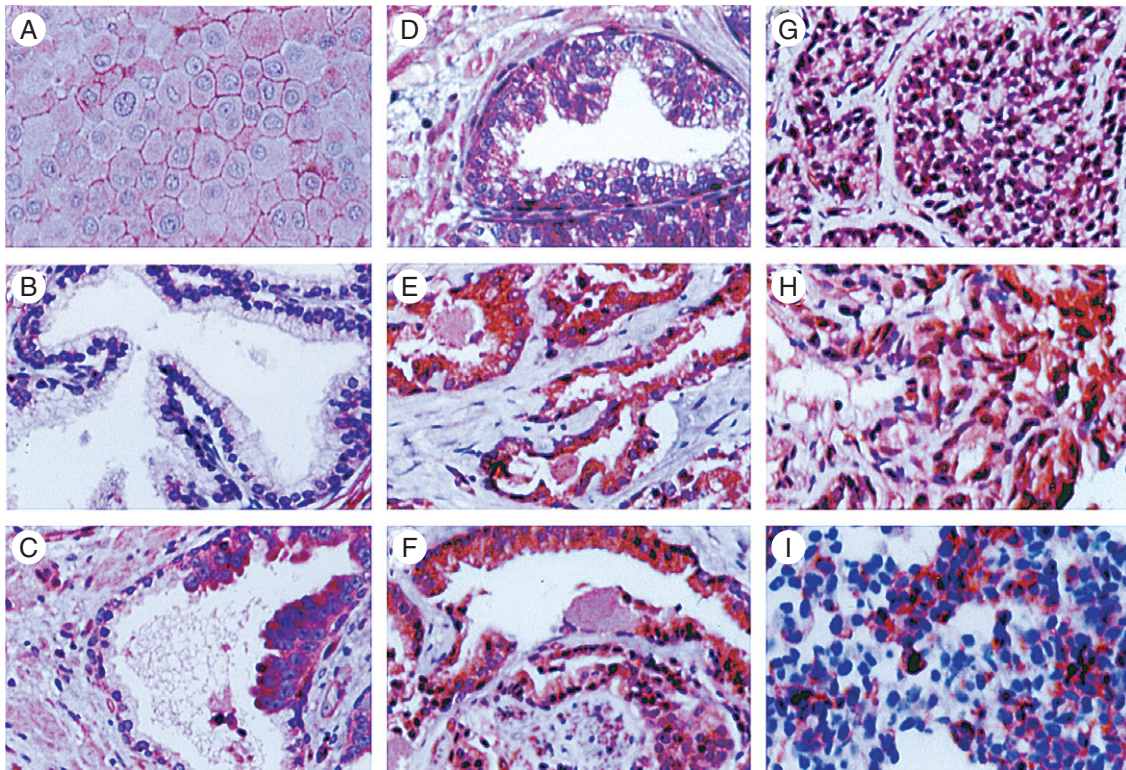
Figure 53 IHC of paraffin-embedded human prostate cancer tissue sections. All the tumor sections were immunohistochemically stained by using a 1/640 dilution of anti-huMUC18 antibodies except (**I**), in which a 1/320 dilution of the primary antibodies was used. All the pictures are of 500X magnification (observed with an oil-immersed 50X objectives). **A:** The staining of the human melanoma section (mostly in the cytoplasmic membranes, as a positive control). **B:** No staining of the normal epithelial cells. **C:** No staining of the normal epithelial cells in half of the acinus and staining of the cells with a high-grade prostatic intraepithelial neoplasia (PIN) in the other half of the same acinus. **D:** The membrane staining of a high-grade PIN. **E:** A strong staining of a prostate carcinoma with a Gleason score of about 6. **F:** A strong staining of a perineural invasion. **G:** A strong staining of a cribriform of prostatic adenocarcinoma. **H:** A strong staining of a ductal form of prostate carcinoma. **I:** A strong staining of the LNCaP cells of the LNS26 clone that has a positive expression of the transfected huMUC18 complementary deoxyribonuclecic acid (cDNA) gene.

Human MUC18 Expression Increases Tumor-Take and Determines the Metastasis of Human Prostate Cancer Cells

To test the hypothesis that huMUC18 may be an important determinant for human prostate cancer metastasis, we have studied the effect of MUC18 expression on tumor formation by the human prostate cancer LNCaP cells in the prostate gland of nude mice and metastasis of these MUC18-expressing cells to other organs. Because human prostate cancer cell line LNCaP did not express huMUC18 and had a minimal ability to metastasize, we transfected the huMUC18 cDNA gene into this cell line and selected the G418-resistant clones that expressed a high level of huMUC18.

We then tested the abilities of these clones to form tumors and to metastasize to other organs after ortho-topical injection into one of the dorsolateral lobes of the prostate. The increased huMUC18 expression in the prostate cancer cell line LNCaP (the clones of LNS-2-6, LNS-2-39, and LNS-3-5) results in an increased tumorigenic ability (tumor-take was increased from 20% to 60–75%). Expression also enables the cells to metastasize to seminal vesicles, the ureter, the kidney, and periaortic lymph nodes in a nude mouse model. One clone with a low expression level of huMUC18 (LNS-2-6 at a higher passage number of p64) still possessed the ability to metastasize but had a similar tumor-take to that of the two control clones, LNV-4-1 and LNV-5-1,

indicating that a low level of huMUC18 is sufficient to enable the LNCaP cells to metastasize. Cells of the parental LNCaP cell line and control clones (LNV-4-1 and LN-5-1 clones), which were transfected with the empty vector, caused only the formation of tumors (with a lower tumor-take of about 20% to about 30%) but no metastasis. We conclude that ectopically increased MUC18 expression increases the tumor-take and causes metastasis of LNCaP cells to various organs in a nude mouse system (Wu *et al.,* 2004).

We have further shown that the huMUC18-expressing LNCaP cells injected into the prostate gland are the cause of the metastatic lesions. This is because the tumors in mouse prostate glands and the metastatic lesions were of human origin, as shown by the positive results of the immunohistochemistry of the tissue sections from the primary tumors in the prostate gland and the metastatic lesions (Figure 54). As shown in Figure 54, the sections of primary tumors and various metastatic lesions were strongly stained by the anti-huMUC18 antibodies but very poorly stained by the anti-moMUC18 antibodies, or the control chicken IgY, or without any antibodies (Wu *et al.,* 2004).

Taken together, we have provided evidence to strongly support the hypothesis that MUC18 promotes the development and malignant progression of human prostate cancer. There seems to be a close association of metastasis with tumor, but not vice versa. Furthermore, we have also established a xenograft mouse model to further study how the huMUC18 mediates these processes. We did not study the possibility that MUC18 could also mediate the bone metastasis of the huMUC18-expressing LNCaP cells because we lack
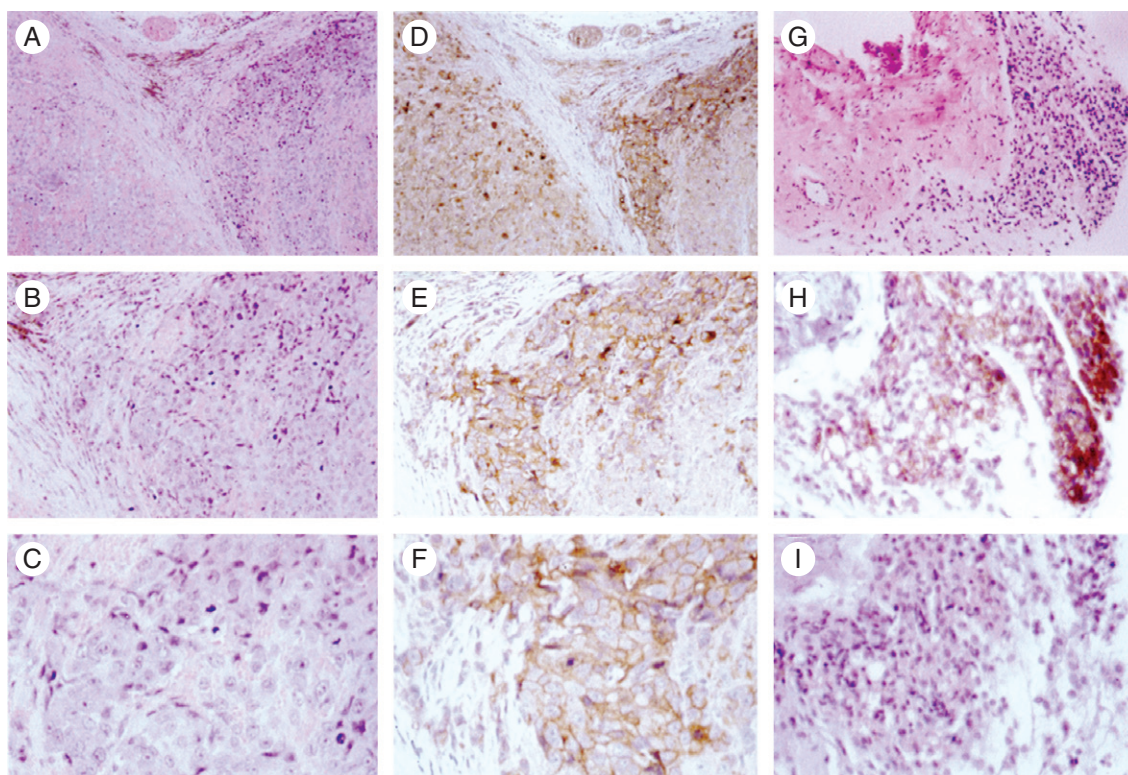
Figure 54 Histology and immunohistochemistry of LNCap tumor and metastasis lesions. The tumor sections were stained with hematoxylin and eosin or immunohistochemically stained with anti-huMUC18 antibodies. **A**, **B**, and **C** show the histology of a prostate tumor derived from the cells of the LNS35 clone at different magnifications— 100X(**A**), 200X(**B**), and 400X(**C**), respectively. **D**, **E**, and **F** show the immunohistochemistry of the same tumor in **A–C** at different magnifications (100X, 200X, and 400X, respectively) by using a 1/300 dilution of anti-huMUC18 antibodies to stain the huMUC18 antigen. **G** shows the histology of the metastatic lesion caused by the cells of the LNS239 clone in a periaortic lymph node (200X magnification). **H** shows a strong immunohistochemical staining of the same metastatic lesions in the lymph node in **G** by an 1/300 dilution of the anti-huMUC18 antibodies. **I** shows no staining of the same metastatic lesions in the lymph node in **G** by using the control immunoglobulin Y antibodies or without any antibodies. Both **H** and **I** are at a 400X magnification.

the expertise. This kind of analysis is now possible with the help from Dr. Leland Chung's group, who recently joined Emory University. We are in the process of comparing possible bone metastasis of the huMUC18-expressing LNCaP cells with the bone-metastasis–adapted LNCaP clone C42B.

MUC18 Expression Increases *in vitro* Motility and Invasiveness of the Human Prostate Cancer Cells, LNCaP

To further understand the mechanisms in MUC18-mediated metastasis, we have shown that increased MUC18 expression confers on LNCaP cells a higher motility (4–5 times) and invasiveness (4–5 times) *in vitro*. We have further shown that most of the increased motility and invasiveness of LNCaP clones is the result of expression of huMUC18, because both motility and invasiveness are significantly reduced in the presence of anti-huMUC18 antibodies (Wu *et al.,* 2004). From this result, we conclude that MUC18 expression profoundly affects many steps of the metastasis of LNCaP cells.

MUC18 Expression is Correlated with the Malignant Progression of Prostate Cancer in a Transgenic Mouse Model

The autochthonous TRAMP (transgenic adenocarcinoma mouse prostate) model established by Dr. Norman Greenberg (Greenberg *et al.,* 1995) is one of the two transgenic mouse models that have been established for studying the tumorigenesis and metastasis of prostate cancer. This model was created by the introduction of the SV40 T antigen (Tag) gene, which was fused to a rat probasin (PB) gene promoter and then transfected into the germ line of transgenic mice. In this way an independent transgenic autochthonous model of prostate cancer was generated in the C57BL/6 inbred strain of mice. The expression of the PB-Tag transgene is initially regulated by androgens and restricted to the prostatic epithelial cells of the dorsolateral and ventral lobes. By the time the mice are 12 weeks of age, TRAMP mice histologically display mild to severe hyperplasia with cribriform structures. Severe hyperplasia and adenocarcinoma is observed by 18 weeks of age. By 24–30 weeks of age, all TRAMP males display the primary tumors and metastasis that is commonly detected in the lymph nodes and lungs and less frequently in the bones, kidney, and adrenal glands. In this model the epithelial origin of the tumors and

metastatic deposits has been successfully demonstrated.

If the hypothesis of MUC18 expression in human prostate cancer is correct, it is possible that we may be able to further correlate the increased mouse MUC18 expression with the development and progression of prostate cancer in a transgenic mouse model. To test this hypothesis, we have collaborated with Dr. Norman Greenberg's group and used their TRAMP model for the experiment. The results of the expression of MUC18 during the progression of prostate cancer were obtained from 52 mice of this transgenic mouse model. When these reached the age of 181 days (25.9 weeks), they bore primary tumors in the prostate glands, and the expression of MUC18 mRNA and protein were detectable by RT-PCR and Western Blot analyses, respectively (Wu *et al.*, 2003). The tumors continued to grow until the mice were 227 days (32.4 weeks) of age, at which point some of the mice died. Metastasis of the tumor to periaortic lymph nodes was detectable in all the mice that bore primary tumors. When tumors were small (less than 0.5 g), MUC18 was expressed at a much lower level, although metastasis was also observed. There is a close association of metastasis with tumor formation. Positive expression of mouse MUC18 antigen in prostate tumors as well as in metastatic lesions in periaortic lymph nodes, liver, and lung was confirmed by immunohistochemistry. The control normal prostate did not have any detectable MUC18 expression. From this result we concluded that, like human prostate cancer patients, an increased MUC18 expression correlates with the metastasis of this mouse prostate cancer to periaortic lymph nodes as well as to liver and lungs in this transgenic mouse model (Wu *et al.,* 2003). We have not analyzed the bone samples of these transgenic mice. However, bone metastasis has been noticed in these transgenic mice (Foster, 2001).

CONCLUSIONS AND CLINICAL APPLICATIONS

We have provided immunologic evidence and molecular biologic evidence to show that MUC18 may be a possible diagnostic marker for monitoring the progression of prostate cancer from premalignant stage (PIN) to malignant stage and to metastasis to other organs. Because the prostate carcinomas are mostly heterogeneous, MUC18 is potentially a very useful diagnostic marker to detect the emergence of premalignant PIN lesions and prostate carcinomas at different stages. We have also provided biologic evidence to strongly suggest that MUC18 is one of the major players that increase the tumor-take and determine the metastatic potential of human prostate cancer cells. We also show

that there is a close association of metastasis with tumor, but not vice versa. The knowledge learned would be very useful for logically designing effective means, such as peptide vaccines, recombinant antibodies, or recombinant adenovirus vaccines, that can decrease, or even better, block the metastatic potential of this fatal cancer.

Acknowledgments

References

Allan, E.N., Luanda, M.E., and Abel, P.D. 1997. Molecular and cellular biology of prostate cancer. *Cancer and Metas. Rev. 16*:29–66.

Bernstein, S.C., and Weinberg, R.A. 1985. Expression of the metastatic phenotype of cells transfected with human metastatic tumor DNA. *Proc. Natl. Acad. Sci. USA 82*:1726–1730.

Bonkhoff, H., and Remberger, K. 1996. Differentiation pathways and histogenic aspects of normal and abnormal prostatic growth: A stem cell model. *Prostate 28*:98–106.

Brawley, O.W., and Kramer, B.S. 1994. The epidemiology and prevention of prostate cancer. In Dawson, N.A., and Vogelzang, N.J. (eds) *Prostate Cancer*. New York:Wiley-Liss, John Wiley & Sons, Inc., 47–64.

Catalona, W.J., and Scott, W.W. 1978. Carcinoma of the prostate; a review. *J. Urol. 119*:1–8.

Chambers, A.F., MacDonald, I.C., Schmidt, E.E., Koop, S., Morris, V.L., Khokha, R., and Groom, A.C. 1995. Step in tumor metastasis: New concepts from intravital video microscopy. *Cancer Metastasis Rev. 14*:279–301.

De Marzo, A.M., Nelson, W.M., Meeker, A.K., and Coffey, D.S. 1998. Stem cell features of benign and malignant prostate epithelial cells. *J. Urol. 160*:2381–2392.

DiSant' Agnese, P.A. 1992. Neuroendocrine differentiation in human prostatic carcinoma. *Human Path. 23*:287–296.

Edlund, M., Miyamoto, T., Sikes, R.A., Ogle, R., Laurie, G.W., Farach-Carson, M.C., Otey, C.A., Zhau, H.E., and Chung, L.W.K. 2001. Integrin expression and usage by prostate cancer cell lines on laminin substrata. *Cell Growth Diff. 12*:99–107.

Foster, B. 2001. New paradigms for prostate cancer research-TRAMP bone metastasis cell lines. In *Proceedings of the AACR special conference: New discoveries in prostate cancer biology and treatment*. At The Registry Resort, Naples, FL, Dec 5–9, 2001.

Gao, A.C., Lou, W., Dong, J.T., and Isaacs, J.T. 1997. CD44 is a metastasis suppressor gene for prostate cancer located on human chromosome 11p13. *Cancer Res. 57*:846–849.

Grayhack, J.T., Kozlowski, J.M., and Lee, C. 1998. The pathogenesis of benign prostatic hyperplasia: A proposed hypothesis and critical evaluation. *J. Urol. 160*:2375–2380.

Greenberg, N.M., DeMayo, F., Finegold, M.J., Medina, D., Tilley, W.D., Aspinall, J.O., Cunha, G.R., Donjacour, A.A., Matusik,

R.J., and Rosen, J.M. 1995. Prostate cancer in a transgenic mouse. *Proc. Natl. Acad. Sci. USA 92*:3439–3443.

Hanahan, D., and Weinberg, R.A. 2000. The hallmarks of cancer. *Cell 100*:57–70.

Herlyn, M. 1993. *Molecular and Cellular Biology of Melanoma*. Austin, TX: R.G. Landes Co., 1–97.

Kleinerman, D.I., Zhang, W., Lin, S., Van, N.T., von Eschenbach, A.C., and Hsieh, J.T. 1995. Application of a tumor suppressor (C-CAM1)-expressing recombinant adenovirus in androgen-independent human prostate cancer therapy: A preclinical study. *Cancer Res. 55*:2831–2836.

Lehmann, J.M., Reithmuller, G., and Johnson, J.P. 1989. MUC18, a marker of tumor progression in human melanoma. *Proc. Natl. Acad. Sci. USA 86*:9891–9895.

Lengauer, C., Kinzler, K.W., and Vogelstien, B. 1998. Genetic instabilities in human cancers. *Nature 396*:643–649.

Mohler, J.L. 1993. Cellular motility and prostate carcinoma metastases. *Cancer Metastasis Rev. 12*:53–67.

Putz, E.,Witter, K., Offner, S., Stosiek, P., Zippeliux, A., Johnson, J., Zahn, R., Reithmuller, G., and Pantel, K. 1999. Phenotypic characteristics of cell lines derived from disseminated cancer cells in bone marrow of patients with solid epithelial tumors: Establishment of working models for human micrometastases. *Cancer Res. 59*:241–248.

Richie, J.P., and Kaplan, I.D. 1997. Screening for prostate cancer: the horns of a dilemma. In Kantoff, P.W., Wishnow, K.I., and Loughlin, K.R. (eds) *Prostate Cancer: A Multidisciplinary Guide*. Malde, MA: Blackwell Science Inc., 1–10.

Ruddon R.W. 1995. Chapter 11: Biology of tumor metastasis. In *Cancer Biology, 3rd ed*. New York and Oxford: Oxford University Press, 402–427.

Shih, I.M., Nesbit, M., Herlyn, M., and Kurman, R.J. 1998. A new Mel-CAM (CD146)-specific monoclonal antibody, MN-4, on paraffin-embedded tissue. *Mod. Pathol. 11*:1098–1106.

Umbas, R., Schalken, J.A., Aalders, T.W., Carter, B.S., Karthaus, H.F.M., Schaafsma, H.E., Debruyene, F.M.J., and Isaacs, W.B. 1992. Expression of the cellular adhesion molecules E-cadherin is reduced or absent in high-grade prostate cancer. *Cancer Res. 52*:5104–5109.

Weiss, L. 1990. Metastatic inefficiency. *Adv. Cancer Res. 54*:159–211.

Wood, D.P. Jr., Banks, E.R., Humphreys, S., McRoberts, J.W., and Rangneker, V.M. 1994. Identification of bone marrow micrometastases in patients with prostate cancer. *Cancer 74*:2533–2540.

Wu, G.J., Chiang, C.F., Fu, P., Wang, S.W.C., Hess, W., Greenberg, N., and Wu, M.W.H. 2003. Correlation of MUC18 expression with the malignant progression of mouse prostate adenocarcinoma in the TRAMP mice. *Proceedings of the 94th Annual Meeting of American Association for Cancer Research. 44*:16, #298.

Wu, G.J., Peng, Q., Fu, P., Wang, S.W.C., Chiang, C.F., Dillehay, D.L., and Wu, M.W.H. 2004. Ectopical expression of human MUC18 increases metastasis of human prostate cancer cells. *Gene 327*:201–213.

Wu, G.J., Peng, Q., Wang, S.W., Yang, H., and Wu, M.W.H. 2001a. Effect of MUC18 expression on the in vitro invasiveness and in vivo tumorigenesis and metastasis of mouse melanoma cell lines in a syngeneic mouse model. *Proceedings of the 92nd Annual Meeting of American Association for Cancer Research. 42*:516. Abstract # 2776.

Wu, G.J., Wu, M.W.H., Wang, S.W., Liu, Z., Peng, Q., Qu, P., Yang, H., Varma, V.A., Sun, Q., Petros, J.A., Lim, S., and Amin, M.B. 2001b. Isolation and characterization of the major form of human MUC18 cDNA gene and correlation of MUC18 over-expression

in prostate cancer cells and tissues with malignant progression. *Gene 279*:17–31.

Xie, S., Luca, M., Huang, S., Gutman, M., Reich, R., Johnson, J.P., and Bar-Eli, M. 1997. Expression of MCAM/MCU18 by human melanoma cells leads to increased tumor growth and metastasis. *Cancer Res. 57*:2295–2303.

Zheng, D.Q., Woodard, A.S., Fornaro, M., Tallini, G., Languino, L.R. 1999. Prostatic carcinoma cell migration via αVβ3 integrin is modulated by a focal adhesion kinase pathway. *Cancer Res. 59*:1655–1664.

Zutter, M.M., Santoro, S.A., Staatz, W.D., and Tsung, Y.L. 1995. Re-expression of the α2β1 integrin abrogates the malignant phenotype of breast carcinoma cells. *Proc. Natl. Acad. Sci. USA 92*:7411–7415.

8

Role of Immunohistochemical Expression of PCNA and p53 in Prostate Carcinoma

**Francesco Cappello, Fabio Bucchieri,
and Giovanni Zummo**

Introduction

Prostate adenocarcinoma (PA) is the most prevalent diagnosed carcinoma and the second leading cause of cancer-related deaths in men in Western countries (Boring *et al.,* 1992), and this has determined a great interest in its pathogenesis and in the diagnostic and prognostic criteria and therapeutic approaches. Moreover, PA is a common finding at autopsy, depending on the age of the patient and the method of sampling because it is frequently clinically undiagnosable but histologically present (Sakr *et al.,* 1993a). Indeed, PA has a broad spectrum, ranging from a small insignificant tumor to advanced infiltrative cancer. As a consequence, the first and most important task for clinicians at the time of diagnosis is to establish its biologic aggressiveness.

The TNM (tumor–node–metastasis) cancer staging system is the most widely used clinical staging tool of PA, which is based on macroscopic extension of the tumor and the presence of metastasis in the lymph nodes or in distant organs. At a histologic level, the internationally used grading system of PA is the Gleason's system (GS), based on examining the tissue at a low magnification (Gleason, 1977). The score is obtained by identifying the predominant and the second most prevalent architectural pattern on the tissue and assigning a grade from 1 to 5, with 1 being the most differentiated and 5 being undifferentiated. The main advantages of GS are as follows: 1) it is easy to learn and apply and 2) it has been demonstrated to correlate well with prognosis (Kramer *et al.,* 1980). The most frequent disadvantages of the GS are as follows: 1) the underestimation of the malignancy of the biopsy material when a minimal amount of cancerous cells is present, and 2) multifocality of the PA with a simultaneous variety of differentiation, which causes difficulty in evaluating the neoplastic gland size and shape; this variability is especially important in identifying the grade 3.

Gleason 6 (3+3) is one of the most commonly used grades. In the past, Gleason grades from 5 to 7 were considered to be an intermediate grade of differentiation. However, it was demonstrated that Gleason 7 is more aggressive than grades 5 or 6 (Epstein *et al.,* 1996), and this finding has determined the clinical importance to keep the former grades separated from the latter. Moreover, Gleason 6 is histologically characterized by tubular and/or cribrous patterns of tumoral glands. Commonly, adenocarcinomas of most other

organs with a tubular pattern are more differentiated from the cribrous ones, the latter being considered an expression of intermediate differentiation. Instead, the presence of one (or both) of these patterns in the prostate adenocarcinoma implies an intermediate grade of differentiation. The research of discrepancies between these two patterns in terms of biologic characterization and behavior is a novel topic. Moreover, because the GS is a mathematical equation, the most accurate insight into the true nature of the tumor would be the combination of the tumoral grade and other prognostic variables. Indeed, a compilation of multiple prognostic indexes could allow greater precision in predicting the outcome (Kramer *et al.,* 1980).

To further complicate the spectrum of PA, we should be aware of the existence of prostatic intraepithelial neoplasm (PIN), a fundamental phase during prostate carcinogenesis (McNeal *et al.,* 1986). PINs are well-recognized premalignant lesions of the prostatic tissue, similar to cervical intraepithelial neoplasia or squamous intraepithelial lesion in cervical cancer and the grade of dysplasia of the tubular adenomas in large bowel carcinoma. PINs are frequently encountered in needle biopsy specimens, and are classified into three categories, depending on the level of dysplasia: mild (PIN-1), moderate (PIN-2), and severe ((PIN-3). More recently, a division in only two groups, low- and high-grade PIN (L-PIN and H-PIN), was proposed. Although several authors combine PIN-1 and PIN-2 as L-PIN (Jones *et al.,* 1994), the majority of authors agree that this distinction lacks clinical significance, and PIN-2 and PIN-3 should be considered H-PIN (Epstein *et al.,* 1995). Nevertheless, the distinction between L-PIN and H-PIN could be critical.

MATERIALS

1. Xylene.
2. Alcohol, absolute and 96º, and distilled water for appropriate dilutions.
3. Aqueous 3% H_2O_2.
4. Dulbecco's phosphate buffer saline (PBS).
5. 10% bovine serum albumin (BSA).
6. Primary antibodies diluted in appropriate normal serum or in diluent for antibodies.
7. Biotinylated secondary antibodies diluted in PBS.
8. Streptavidin-peroxidase complex diluted in PBS.
9. Aminoethylcarbazole (or diaminobenzidine), ready to use.
10. Aqueous hematoxylin.
11. Aqueous mounting.

METHODS

Immunohistochemical procedure to retrieve the presence of proliferating cell nuclear antigen (PCNA) and p53 on formalin-fixed and paraffin-embedded sections.

1. Dewax sections in xylene, clear in alcohol, and place in distilled water.
2. Blot excess water from slide with tissue and circle section with hydrophobic marker pen (PAP pen), apply aqueous 3% H_2O_2 to block endogenous peroxidase, and place in humid tray for 10 min.
3. Rinse with PBS.
4. Blot excess PBS from slide with tissue and apply 10% BSA (or protein blocking serum-free) for 10 min.
5. Do not rinse with PBS but, after blotting excess of blocking solution, apply primary antibody diluted in the appropriate normal serum or in diluent for antibodies, to the test and apply normal serum to the negative control sections. Simultaneously, run appropriate positive control, for example, for PSA.
6. Place lid on tray and keep for 1 hr.
7. Rinse with PBS, drain, and wipe.
8. Apply biotinylated link antibody to all sections for 15 min.
9. Rinse with PBS, drain, and wipe.
10. Apply streptavidin peroxidase complex to all sections for 15 min.
11. Rinse with PBS, drain, and wipe.
12. Apply AEC (3-amino-9-ethylcarbazole) or DAB (diaminobenzidine) substrate solution for 7 min.
13. Rinse off DAB into topped container, containing a few drops of solution hypochloride, in PBS.
14. Stack the slides into a slide rack in a jar of water.
15. Counterstain with hematoxylin for 1 min.
16. Rinse in two jars of tap water.
17. Quick dip in tap water to blue.
18. Rinse twice with tap water.
19. Mount with aqueous mounting.
20. Examine the slides microscopically: positive stain (presence of markers) brown or red and negative stain (absence of markers) blue.

RESULTS

Figure 55 shows morphologic differences between prostatic hyperplasia, dysplasia (PIN), and PA (low- and high-grade). Many researchers suggest that the tumoral progression from L-PIN to invasive carcinoma follows a predictable course (Brawer *et al.,* 1992), although the molecular mechanisms responsible for this progression remain unknown (Colanzi *et al.,* 1998). Indeed,

Hyperplasia   Dysplasia
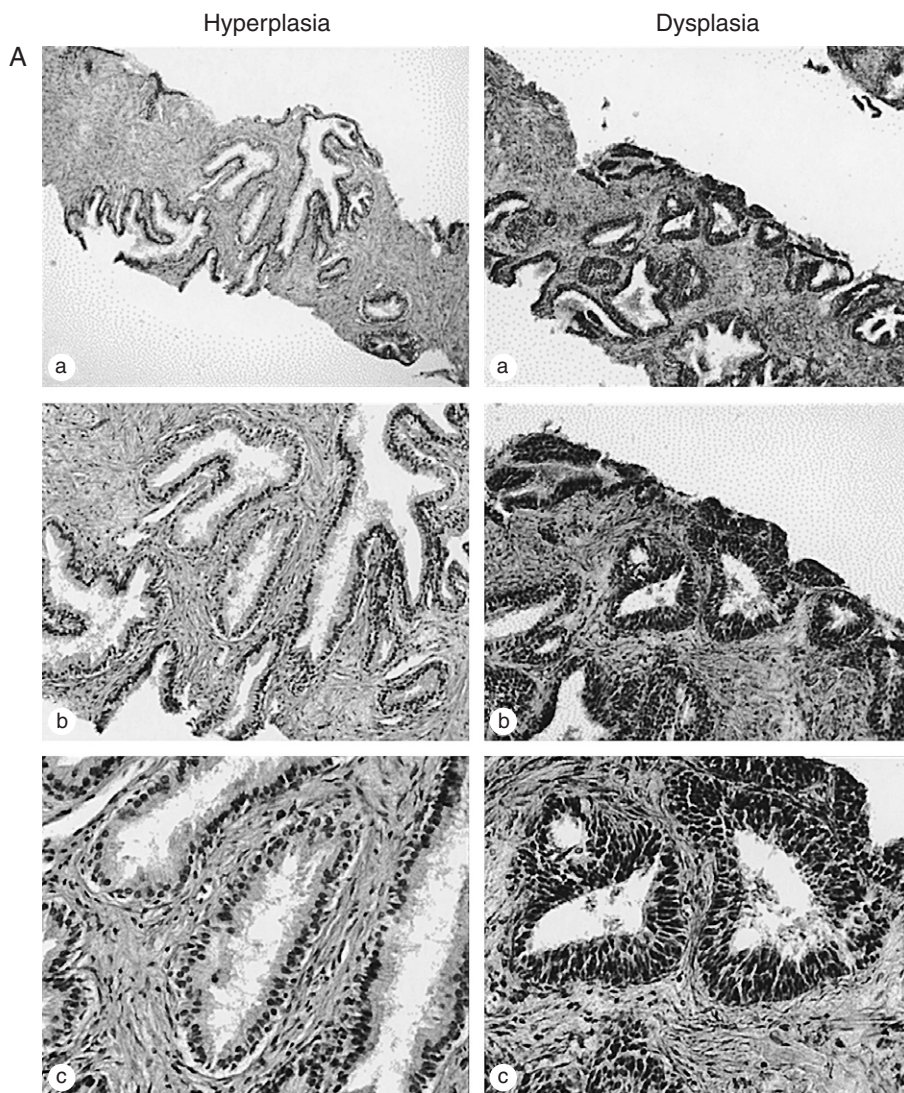
Figure 55 A, Morphologic aspects of prostatic hyperplasia and dysplasia. (Magnification: a: 4X; b: 20X; 40X.)

number of studies concentrate on the expression of different biologic markers expressed by PA to understand their role in carcinogenesis better and to test them as diagnostic and prognostic tools (Sakr *et al.,* 2001). A list of such markers is presented in Chapter 1 in Part III. In this chapter, we will focus on the clinical usefulness of two of them: PCNA and p53.

Figure 56A shows typical nuclear positivity for PCNA in low- and high-grade PA. The research of PCNA using immunohistochemical studies of PCNA are useful above all in needle biopsies, where limited tumoral tissue renders the assessment of grade difficult (Spires *et al.,* 1994).

Figure 56B shows nuclear immunopositivity of p53 in low- and high-grade PA. Although many authors

have demonstrated an association between p53 immunoreactivity and higher Gleason grade tumors (Kallakury *et al.,* 1994), this datum is still being debated (Karaburun-Parker *et al.,* 2001).

DISCUSSION

PCNA and p53: Role in Normal Cells

PCNA is a highly conserved eukaryotic protein that is essential for a number of deoxyribonucleic acid (DNA)-related processes, including DNA repair, replication, post-replication modification, and chromatin assembly. It is a trimeric protein formed by a sliding

Carcinoma low-grade   Carcinoma high-grade
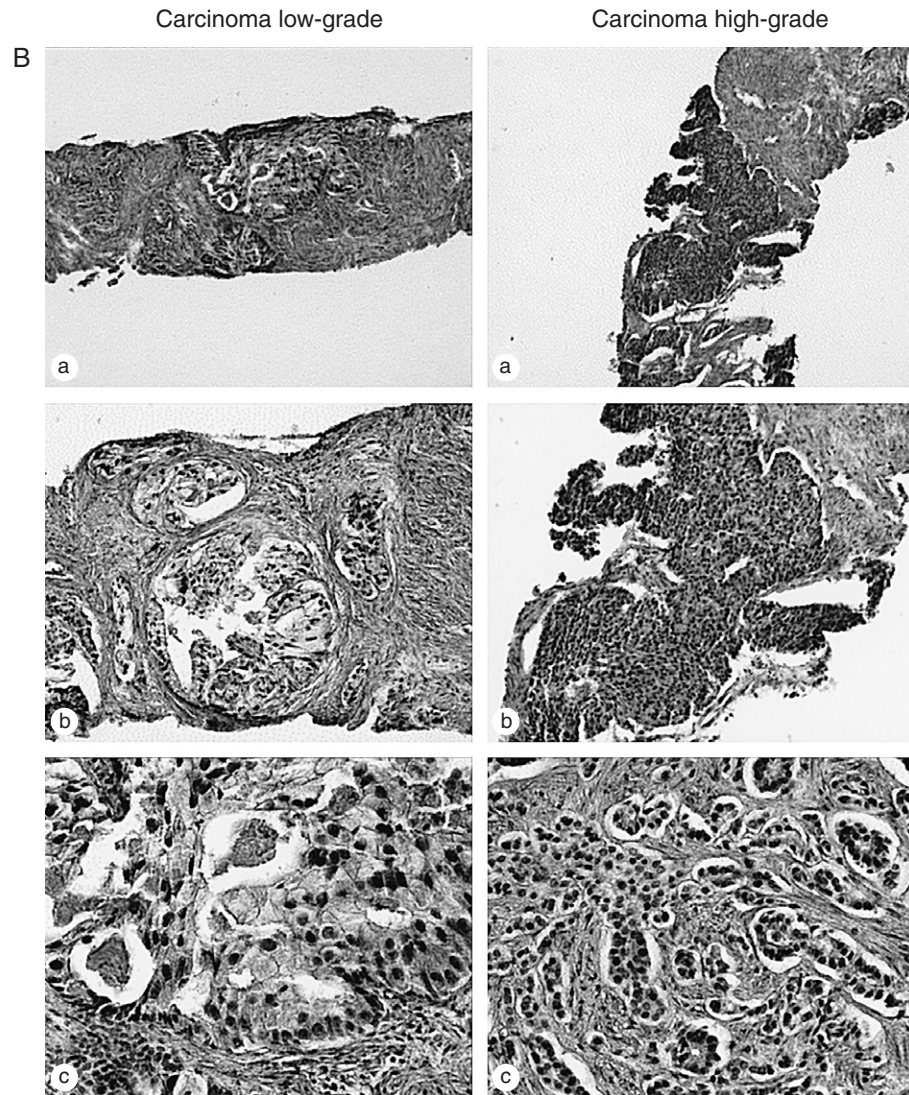
Figure 55 *Continued.* **B**, Low- and high-grade carcinoma. (Magnification: a: 4X; b: 20X; c: 40X.)

clamp that surrounds the DNA. Immunohistochemically, PCNA is positive in both G1 and G2 phases of the cell cycle. PCNA interacts with the eukaryotic replication DNA polymerase to form a replisome. The interaction of cell-cycle regulatory proteins that are part of the p53 response pathway, such as p21 with PCNA, may represent the link between DNA damage response and regulation of DNA replication and repair. In normal human cells, and in a few tumor cells, p21 exists in a quaternary complex with a cyclin, a cyclin-dependent kinase (CDK), and the PCNA. The protein p21 controls CDK activity, thereby affecting cell-cycle control, whereas PCNA functions in both DNA replication and repair. Furthermore, p21 blocks the ability of PCNA to activate DNA polymerase. This regulation results from a direct interaction between p21 and PCNA.

In response to DNA damage, cells will normally arrest cell-cycle progression to allow DNA repair to take place. If the mechanism coordinating these events fails, the resulting loss of genetic integrity can lead to the accumulation of mutations that may disrupt the

A   Carcinoma low-grade   Carcinoma high-grade
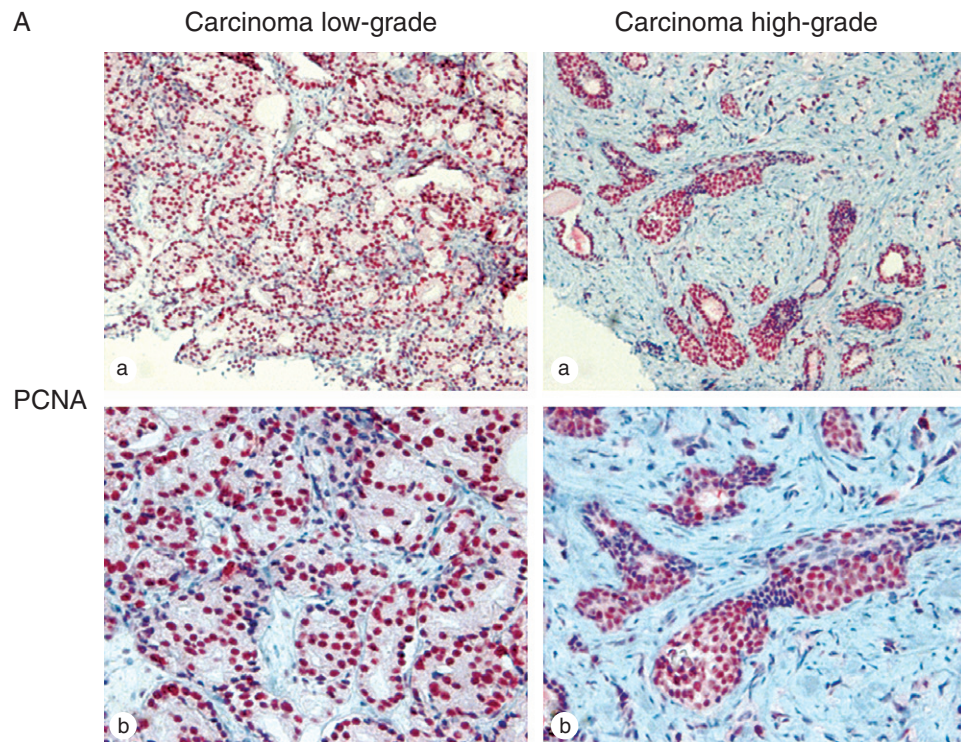
PCNA

Figure 56 A, Immunohistochemistry for proliferating cell nuclear antigen (PCNA) in carcinomas showing different levels of differentiation. (Magnification: a: 20X; b: 40X.)

normal growth and cell-cycle controls. One of the most interesting observations emerging from the study of PCNA-interacting proteins is that many of them, including p21, contain a conserved PCNA-binding motif.

The p53 tumor-suppressor protein controls the expression of the gene that encodes the p21 CDK regulator. Senescent cells have increased levels of the p21 protein, and its overexpression may block the growth of tumoral cells. During p53-mediated suppression of cell proliferation, p21 and PCNA may be important for coordinating the cell-cycle progression, DNA replication, and the repair of damaged DNA.

The tumor suppressor gene *p53* plays multiple roles in cells. Expression of high levels of the wild-type (but not mutant) *p53* has two outcomes: cell-cycle arrest or apoptosis. Although dispensable for viability in response to genotoxic stress, *p53* acts as an "emergency brake," inducing either arrest or apoptosis, protecting the genome from accumulating excess mutatitons. Consistent with this notion, cells lacking *p53* have been shown to be genetically unstable and thus more prone to tumors.

In particular, *p53* is frequently altered in malignant human tumors (Cappello *et al.,* 2002). In case of DNA damage, the functional (wild) *p53* may block cell-cycle progression in the late G1 phase or trigger an intrinsic mechanism of apoptosis (Levine *et al.,* 1991). The abnormal p53 protein, produced by a mutant gene, is ineffective and more stable than the wild-type protein; it becomes less sensitive to proteolysis and tends to accumulate in the nucleus, thus it is easily detected by immunohistochemistry (Bruner *et al.,* 1993). The monoclonal antibodies commonly used in immunohistochemistry for p53 recognize both the wild-type and the mutant p53; however, because the wild-type protein is rapidly degraded, its physiologic levels usually remain below the immunohistichemical detectability threshold. Therefore, the p53 immunoreactivity is likely to reflect *p53* gene mutations (Papadopoulos *et al.,* 1996).

PCNA and p53 in Prostate Carcinoma Diagnosis and Management

Because PA varies in its biologic behavior, we need markers to predict its outcome more accurately. Tumor differentiation and proliferative activity are thought to be important predictors of its biologic behavior

B   Carcinoma low-grade   Carcinoma high-grade

p53
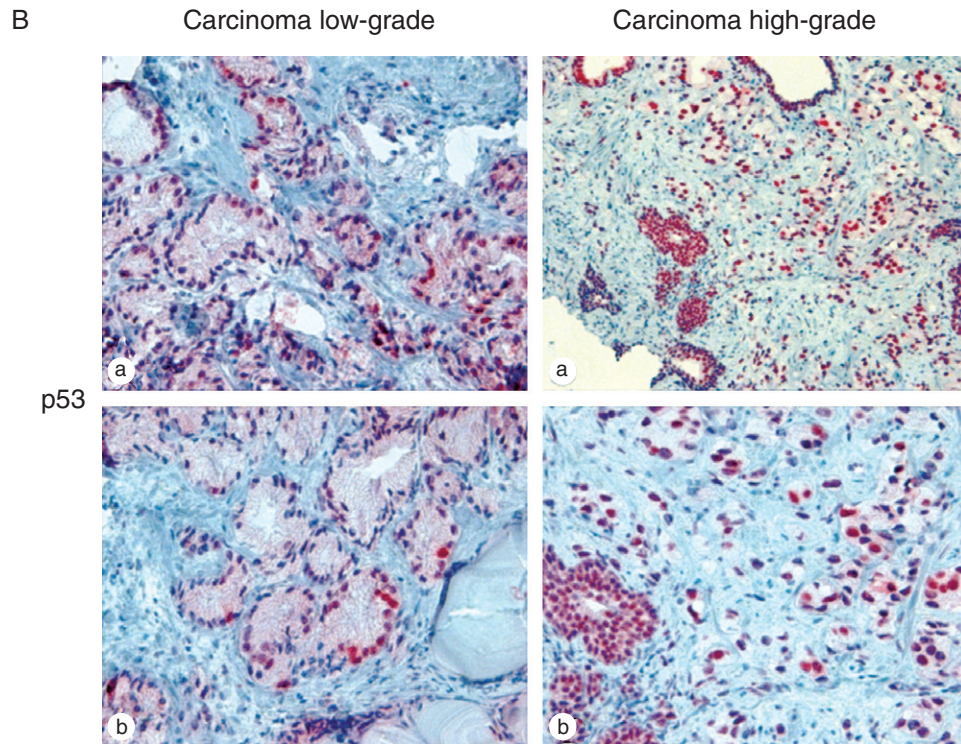
Figure 56 *Continued*. **B**, Immunohistochemistry for p53 in carcinomas showing different levels of differentiation (Magnification: a: 20X; b: 40X.)

(Sakr *et al.,* 1993b). As a consequence, the measurement of cellular proliferation by various methods has been shown to better correlate with the outcome in several human cancers, including prostate cancer (Cher *et al.,* 1995). The pattern of change in PCNA immunostaining may reflect certain aspects of the biologic nature of a malignant transformation (McNeal et al., 1995). Indeed, the PCNA expression seems to be related to the grade of progression of the cancer. In particular, it has been postulated that PCNA index can be an objective and quantitative means for evaluating the biologic malignancy of PA (Cappello *et al.,* 2003a).

PCNA may also be expressed in PIN, supporting the hypothesis that these are preinvasive lesions (Myers and Grizzle, 1997). In particular, PCNA and Ki-67 show an increased proliferative activity in H-PIN, the most likely precursor of PA, when compared to L-PIN and normal tissue (Xie *et al.,* 2000). PCNA overexpression could indicate an abnormal cellular growth in preneoplastic lesions because an increased proliferative potential of the dysplastic cells could be directly reflected in an increased expression of PCNA (Myers and Grizzle,

1996). In addition, the finding that the proliferative index of H-PIN lies between benign and carcinomatous prostate also supports the assertion that H-PIN is a biologic intermediate in the multistep process of transformation into carcinoma (Tamboli *et al.,* 1996).

Studies of the proliferation index for the peripheral and the transitional zone of the organ show a significant difference that can support the concept of a biologic difference between carcinomas arising in these zones (Grignon and Sark, 1994). Moreover, in the benign epithelium, 83% of PCNA positive cells are basal cells, whereas only 7% of PCNA-positive cells in dysplasia are basal cells. These findings support the hypothesis that dysplasia represents an evolutionary stage in the malignant transformation of the prostatic epithelium (McNeal *et al.,* 1995).

PCNA may help to predict prognosis. In fact, patients with lower PCNA expression are known to survive significantly longer than those with higher PCNA positivity (Spires *et al.,* 1994). In addition, PCNA has been tested in post-radiotherapy prostate biopsies by correlating the staining with the clinical outcome, discovering that PCNA negativity predicts

an eventual resolution of tumor, whereas PCNA positivity correlates with local failure (Crook *et al.,* 1994). Moreover, it has been demonstrated that the measurement of cell proliferation by PCNA immunolabeling also provides important prognostic information in T1-2M0 tumors, in addition to the GS (Vesalainen *et al.,* 1994).

Although the proliferative activity may be variable in prostate carcinoma, it seems to be correlated with p53 overexpression because PCNA expression is significantly higher in tumors with p53-positive cells (Cappello *et al.,* 2003b). Indeed, some authors support the concept that p53 mutation is an early change in at least a subset of PA (Al-Maghrabi *et al.,* 2001). However, the mutations of p53 tumor suppressor gene typically occur in an advanced stage of prostatic carcinoma and are commonly negative in PIN (Cappello *et al.,* 2003b; Myers and Grizzle, 1997). In contrast, some authors have found that p53 immunoreactivity in H-PIN is similar to that in the prostatic carcinoma but significantly different from that found in the benign prostate tissue (Tamboli *et al.,* 1998). These findings prove a closed relationship between H-PIN and PA in at least a subset of primary PA with a high-level of p53 protein accumulation (Humphrey and Swanson, 1995).

P53 expression is correlated with both the increased histologic grade and the presence of metastases, suggesting that *p53* gene may play a role in determining the behavior of a biologically aggressive subset of PA (Hughes *et al.,* 1995). In particular, *p53* gene mutation seems to be related to advanced (metastatic) stage, loss of differentiation, and transition from androgen-dependent to androgen-independent growth (Navone *et al.,* 1993). However, other authors have reported that *p53* mutations are infrequent in both primary and metastatic prostate tumors and that there is no strict correlation between *p53* mutation and tumor metastases (Dinjens *et al.,* 1994). In addition, p53 reactivity could be an independent prognostic indicator particularly valuable among the low- to intermediate-grade cancers (Shurbaji *et al.,* 1995). It is interesting that combined detection of *p53* and Bcl-2 overexpression may be useful in predicting hormone resistance in PA (Apakama *et al.,* 1996). Also, abnormal p53 findings between early and hormone refractory disease has been demonstrated to be related to PA progression (Heidenberg *et al.,* 1995). Moreover, the status of *p53* could also help in the evaluation of patients prior to radiotherapy because *p53* inactivation could produce radio-resistant tumors (Stattin *et al.,* 1996). In contrast, p53 protein overexpression is not predictive of outcome in patients treated with radiation therapy (Incognito *et al.,* 2000).

An accumulation of p53 nuclear protein detected by immunohistochemistry results in an independent adverse prognostic factor in patients with prostate cancer undergoing follow-up (Borre *et al.,* 2000). In a further study, p53 positivity was registered in 62.2% cases of prostate cancer, and the highest level of p53 accumulation in intermediate-grade carcinomas could predict the aggressiveness and risk of metastases, whereas no significant difference in the p53 positivity between low-grade and high-grade PA was noted.

Although many articles have investigated the predictive role of p53 for survival in PA, this argument is widely debated. In particular, it is still not clear how the p53 positivity influences the recommended course of treatment. The overexpression of p53 is associated with a poor prognosis in terms of progression and survival (Thomas *et al.,* 1993). Moreover, the highest level of *p53* accumulation in intermediate-grade carcinomas could predict the aggressive progression and risk of metastases (Sasor *et al.,* 2000), suggesting a potential utility of p53 as a preoperative prognostic indicator in localized prostate cancer (Stricker *et al.,* 1996). The high-grade PA shows a stronger expression of p53 than the low-grade PA (Karaburun *et al.,* 2001). In contrast, other studies have concluded that *p53* is rare in primary prostatic tumors (Voeller *et al.,* 1994), nonessential to the development of prostate cancer metastasis (Brooks *et al.,* 1996), and of limited use as a prognostic marker in primary or metastatic diseases (Cheng *et al.,* 1999). Some authors have found a significant correlation between p53 staining and grade of metastatis because patients with p53-positive tumors have a significantly shorter survival than the p53-negative group (Stattin *et al.,* 1996). Nevertheless, in the same study, in a Cox multiple regression analysis of the p53 status, tumor stage, grade, metastasis, and age of patient, p53 seemed to lose its significance as an independent predictor (Stattin *et al.,* 1996).

In another study, *p53* staining resulted in an independent predictor of disease-free survival in a multivariate analysis of p53, age and race of the patient, and stage, and grade of the tumor (Bauer *et al.,* 1995). The lower p53 expression in PA also seems to be related to a lower GS and to a lower expression of other markers of tumoral growth and behavior in both transition and peripheral zones (Erbersdobler *et al.,* 2002). In addition, although no correlation has been found between p53 protein expression and GS, pT stage, lymph node metastases, seminal vesicles invasion, positive or negative surgical resection margins, age of the patient, and p53 protein expression correlate significantly with capsular penetration; the patients with negative p53 neoplastic tissue in prostatic biopsy are likely to have a good prognosis in prolonged follow-up (Sulik *et al.,* 2002). Finally, p53 abnormalities are associated with

lymph node metastases derived from patients with PA who have not undergone hormonal therapy (Eastham *et al.,* 1995).

The wide discrepancy in the reported detection frequency of *p53* mutation in PA specimens could depend not only on the tumor type but also on the region of the tumors. Indeed, a heterogeneous topographic distribution of *p53* mutation has been observed because the analysis of topographic distribution of the mutant p53 allele shows remarkable differences between mutifocal tumors and intratumoral heterogeneity (Mirchandani *et al.,* 1995).

Positive nuclei of p53 have also been noted in the basal cells of benign glandular acini in regions flanking tumor, suggesting that the mutation of *p53* plays a role in the prostate carcinogenesis (Kallakury *et al.,* 1994). Moreover, mutation of *p53* may also be associated with an increased angiogenesis in PA (Yu *et al.,* 1997). In addition, studies of *p53* mutations in preneoplastic lesions have permitted the postulation that postatrophic hyperplasia (one of the patterns of prostatic atrophy) might be a precursor of PA (Tsujimoto *et al.,* 2002). The finding that sarcomatoid carcinoma developing from a high-grade PA is associated with a progressive accumulation of p53 (Delahunt *et al.,* 1999) supports the hypothesis that a clonal dominance of dedifferentiated cells carrying a *p53* mutation may be involved in the PA progression (Navone *et al.,* 1999).

In summary, although many studies have demonstrated a strong relationship between nuclear positivity for p53, relapse, and disease-specific mortality, these studies seem to be inconclusive. Nevertheless, we agree with Quinn *et al.* (2000), who hypothesize that the presence of cluster of p53-positive nuclei can be used for a group of patients with poor prognosis not identified by the traditional scoring methods. Moreover, they support the hypothesis that p53 dysfunction within PA could exist in foci of tumor cells clonally expanded in metastases. This is in agreement with Visakorpi *et al.* (1992), who propose that accumulation of p53 may confer a proliferative advantage for prostatic carcinoma cells and therefore define a small subgroup of highly malignant carcinomas. We also agree with Konishi *et al.* (1995), who report that *p53* mutation occasionally occurs in small foci of the tumor, and this genetic alteration could be closely associated with an invasive growth of heterogenous prostate carcinoma.

References

Al-Maghrabi, J., Vorobyova, L., Chapman, W., Jewett, M., Zielenska, M., and Squire, J.A. 2001. *P53* alteration and chromosomal instability in prostatic high-grade intraepithelial neoplasia and concurrent carcinoma: Analysis by immunohistochemistry, interphase in situ hybridization, and sequencing of laser-captured microdissected specimens. *Mod. Pathol. 14:*1252–1262.

Apakama, I., Robinson, M.C., Walter, N.M., Charlton, R.G., Royds, J.A., Fuller, C.E., Neal, D.E., and Hamdy, F.C. 1996. Bcl-2 overexpression combined with *p53* protein accumulation correlates with hormone-refractory prostate cancer. *Br. J. Cancer 74:*1258–1262.

Bauer, J.J., Sesterhenn, I.A., Mostofi, K.F., McLeod, D.G., Srivastava, S., and Moul, J.W. (1995). *P53* nuclear protein expression is an independent prognostic marker in clinically localized prostate cancer patients undergoing radical prostatectomy. *Clin. Cancer Res. 1:*1295–1300.

Boring, C.C., Squires, T.S., and Tong, T. 1992. Cancer statistics, 1992. *CA Cancer J. Clin. 42:*127–128.

Borre, M., Stausbol-Gron, B., and Overgaard, J. 2000. *P53* accumulation associated with bcl-2, the proliferation marker MIB-1 and survival in patients with prostate cancer subjected to watchful waiting. *J. Urol. 164:*716–721.

Brawer, M.K. 1992. Prostatic intraepithelial neoplasia: A premalignant lesion. *J. Cell Biochem. Suppl. 16G:*171–174.

Brooks, J.D., Bova, G.S., Ewing, C.M., Piantadosi, S., Carter, B.S., Robinson, J.C., Epstein, J.I., and Isaacs, W.B. 1996. An uncertain role for *p53* gene alterations in human prostate cancers. *Cancer Res. 56:*3814–3822.

Bruner, J.M., Connelly, J.H., and Saya, H. 1993. *P53* protein immunostaining in routinely processed paraffin-embedded sections. *Mod. Pathol. 6:*189–194.

Cappello, F., Bellafiore, M., Palma, A., and Bucchieri, F. 2002. Defective apoptosis and tumorigenesis. Role of p53 mutation and Fas-FasL system dysregulation. *Eur. J. Histochem. 46:*199–208.

Cappello, F., Palma, A., Martorana, A., Rappa, F., Cabibi, D., Barresi, E., Melloni, D., Farina, F., and Aragona, F. 2003a. Biological aggressiveness evaluation in prostate carcinomas: Immunohistochemical analysis of PCNA and *p53* in a series of Gleason 6 (3+3) adenocarcinomas. *Eur. J. Histochem. 47:*129–132.

Cappello, F., Rappa, F., and David, S., Anzalone, R., and Zummo, G. 2003b. Immunohistochemical evaluation of PCNA, p53, HSP60, HSP10 and MUC-2 presence and expression in prostate carcinogenesis. *Anticancer Res. 23:*1325–1331.

Cheng, L., Leibovich, B.C., Bergstralh, E.J., Scherer, B.G., Pacelli, A., Ramnani, D.M., Zincke, H., and Bostwick, D.G. 1999. P53 alteration in regional lymph node metastases from prostate carcinoma: A marker for progression? *Cancer 85:*2455–2459.

Cher, M.L., Chew, K., Rosenau, W., and Carroll, P.R. 1995. Cellular proliferation in prostatic adenocarcinoma as assessed by bromodeoxyuridine uptake and Ki-67 and PCNA expression. *Prostate 26:*87–93.

Colanzi, P., Santinelli, A., Mazzucchelli, R., Pomante, R., and Montironi, R. 1998. Prostatic intraepithelial neoplasia and prostate cancer: Analytical evaluation. *Adv. Clin. Path. 2:*271–284.

Crook, J., Robertson, S., and Esche, B. 1994. Proliferative cell nuclear antigen in postradiotherapy prostate biopsies. *Int. J. Radiat. Oncol. Biol. Phys. 30:*303–308.

Delahunt, B., Eble, J.N., Nacey, J.N., and Grebe, S.K. 1999. Sarcomatoid carcinoma of the prostate: Progression from adenocarcinoma is associated with p53 over-expression. *Anticancer Res. 19:*4279–4283.

Dinjens, W.N., van der Weiden, M.M., Schroeder, F.H., Bosman, F.T., and Trapman, J. 1994. Frequency and characterization of p53

mutations in primary and metastatic human prostate cancer. *Int. J. Cancer 56*:630–633.

Eastham, J.A., Stapleton, A.M., Gousse, A.E., Timme, T.L., Yang, G., Slawin, K.M., Wheeler, T.M., Scardino, P.T., and Thompson, T.C. 1995. Association of p53 mutations with metastatic prostate cancer. *Clin. Cancer Res. 1*:1111–1118.

Epstein, J.I., Grignon, D.J., Humphrey, P.A., McNeal, J.E., Sesterhenn, I.A., Troncoso, P., and Wheeler, T.M. 1995. Interobserver reproducibility in the diagnosis of prostatic intraepithelial neoplasia. *Am. J. Surg. Pathol. 19*:873–886.

Epstein, J.I., Partin, A.W., Sauvageot, J., and Walsh, P.C. 1996. Prediction of following radical prostatectomy: A multivariate analysis 721 men with long-term follow-up. *Am. J. Surg. Pathol. 20*:286–292.

Erbersdobler, A., Fritz, H., Schnoger, S., Graefen, M., Hammerer, P., Huland, H., and Henke, R.P. 2002. Tumour grade, proliferation, apoptosis, microvessel density, p53, and bcl-2 in prostate cancers: Differences between tumours located in the transition zone and in the peripheral zone. *Eur. Urol. 41*:40–46.

Gleason, D.F. 1977. Histologic grading and staging of prostatic carcinoma. In Tannenbaum M. (ed) *Urologic Pathology*: *The Prostate.* Philadelphia: Lea & Febiger, 171–197.

Grignon, D.J., and Sakr, W.A. 1994. Zonal origin of prostatic adenocarcinoma: Are there biologic differences between transition zone and peripheral zone adenocarcinomas of the prostate gland? *J. Cell. Biochem. Suppl. 19*:267–269.

Heidenberg, H.B., Sesterhenn, I.A., Gaddipati, J.P., Weghorst, C.M., Buzard, G.S., Moul, J.W., and Srivastava, S. 1995. Alteration of the tumor suppressor gene p53 in a high fraction of hormone refractory prostate cancer. *J. Urol. 154*:414–421.

Hughes, J.H., Cohen, M.B., and Robinson, R.A. 1995. P53 immunoreactivity in primary and metastatic prostatic adenocarcinoma. *Mod. Pathol. 8*:462:466.

Humphrey, P.A., and Swanson, P.E. 1995. Immunoreactive p53 protein in high-grade prostatic intraepithelial noeplasia. *Pathol. Res. Pract. 191*:881–887.

Incognito, L.S., Cazares, L.H., Schellhammer, P.F., Kuban, D.A., Van Dyk, E.O., Moriarty, R.P., Wright, G.L. Jr., and Somers, K.D. 2000. Overexpression of p53 in prostate carcinoma is associated with improved overall survival but not predictive of response to radiotherapy. *Int. J. Oncol. 17*:761–769.

Jones, E.C. and Young, R.H. 1994. The differential diagnosis of prostate carcinoma: Its distinction from premalignant and pseudocarcinomatous lesions of the prostate gland. *Am. J. Clin. Pathol. 101*:48–64.

Kallakury, B.V., Figge, J., Ross, J.S., Fisher, H.A., Figge, H.L., and Jennings, T.A. 1994. Association of p53 immunoreactivity with high Gleason tumor grade in prostatic adenocarcinoma. *Hum. Pathol. 25*:92–97.

Karaburun-Paker, S., Kilicarslan, B., Ciftcioglu, A.M., Oztekin, S., Sargin, F.C., Erdogru, T., and Baykara, M. 2001. Relationship between apoptosis regulator proteins (bcl-2 and p53) and Gleason score in prostate cancer. *Pathol. Oncol. Res. 7*:209–212.

Konishi, N., Hiasa, Y., Matsuda, H., Tao, M., Tsuzuki, T., Hayashi, I., Kitahori, Y., Shiraishi, T., Yatani, R., and Shimazaki, J. 1995. Intratumor cellular heterogeneity and alterations in ras oncogene and p53 tumor suppressor gene in human prostate carcinoma. *Am. J. Pathol. 147*:1112–1122.

Kramer, S.A., Spahr, J., Brendler, C.B., Glenn, J.F., and Paulson, D.F. 1980. Experience with Gleason's histopathologic grading in prostatic cancer. *J. Urol. 124*:223–225.

Levine, A.J., Momand, J., and Finlay, C.A. 1991. The p53 tumor suppressor gene. *Nature 351*:453–456.

McNeal, J.E., and Bostwick, D.G. 1986. Intraductal dysplasia: A premalignant lesion of the prostate. Hum. Pathol. 17:64–71.

McNeal, J.E., Haillot, O., and Yemoto, C. 1995. Cell proliferation in dysplasia of the prostate: Analysis by PCNA immunostaining. *Prostate 27*:258–268.

Mirchandani, D., Zheng, J., Miller, G.J., Ghosh, A.K., Shibata, D.K., Cote, R.J., and Roy-Burman, P. 1995. Heterogeneity in intratumor distribution of p53 mutions in human prostate cancer. *Am. J. Pathol. 147*:92–101.

Myers, R.B., and Grizzle, W.E. 1996. Biomarker expression in prostatic intraepithelial neoplasia. *Eur. Urol. 30*:153–160.

Myers, R.B., and Grizzle, W.E. 1997. Changes in biomarker expression in the development of prostatic adenocarcinoma. *Biotech. Histochem. 72*:86–95.

Navone, N.M., Troncoso, P., Pisters, L.L., Goodrow, T.L., Palmer, J.L., Nichols, W.W., von Eschenbach, A.C., and Conti, C.J. 1993. P53 protein accumulation and gene mutation in the progression of human prostate carcinoma. *J. Natl. Cancer Inst. 85*:1657–1669.

Navone, N.M., Labate, M.E., Troncoso, P., Pisters, L.L., Conti, C.J., von Eschenbach, A.C., and Logothetis, C.J. 1999. P53 mutations in prostate cancer bone metastases suggest that selected p53 mutants in the primary site define foci with metastatic potential. *J. Urol. 161*:304–308.

Papadopoulos, I., Rudolph, P., Wirth, B., and Weichert-Jacobsen, K. 1996. P53 expression, proliferation marker Ki-S5, DNA content and serum PSA: Possible biopotential markers in human prostatic cancer. *Urology 48*:261–268.

Quinn, D.I., Henshall, S.M., Head, D.R., Golovsky, D., Wilson, J.D. Brenner, P.C., Tumer, J.J., Delprado, W., Finlayson, J.F., Stricker, P.D., Grygiel, J.J., and Sutherland, R.L. 2000. Prognostic significance of p53 nuclear accumulation in localized prostate cancer treated with radical prostatectomy. *Cancer Res. 60*:1585–1594.

Sakr, W.A., and Partin, A.W. 2001. Histological margin of risk and the role of high-grade prostatic intraepithelial neoplasia. *Urology 57*:115–120.

Sakr, W.A., Haas, G.P., Cassin, B.F., Pontes, J.E., and Crissman, J.D. 1993a. The frequency of carcinoma and intraepithelial neoplasia of the prostate in young male patients. *J. Urol. 150*:379–385.

Sakr, W.A., Sarkar, F.H., Sreepathi, P., Drozdowicz, S., and Crissman, J.D. 1993b. Measurement of cellular proliferation in human prostate by AgNOR, PCNA, and SPF. *Prostate 22*:147–154.

Sasor, A., Wagrowska-Danilewicz, M., and Danilewicz, M. 2000. Ki-67 antigen and P53 protein expression in benign and malignant prostatic lesions. Immunohistochemical quantitative study. *Pol. J. Pathol. 51*:31–36.

Shurbaji, M.S., Kalbfleisch, J.H., and Thurmond, T.S. 1995. Immunohistochemical detection of p53 protein as a prognostic indicator in prostate cancer. *Hum. Pathol. 26*:106–109.

Spires, S.E., Banks, E.R., Davey, D.D., Jannings, C.D., Wood, D.P. Jr., and Cibull, M.L. 1994. Proliferating cell nuclear antigen in prostatic adenocarcinoma: Correlation with established prognostic indicators. *Urology 43*:660–666.

Stattin, P., Bergh, A., Karlberg, L., Nordgren, H., and Damber, J.E. 1996. P53 immunoreactivity as prognostic marker for cancer-specific survival in prostate cancer. *Eur. Urol. 30*:65–72.

Stricker, H.J., Jay, J.K., Linden, M.D., Tamboli, P., and Amin, M.B. 1996. Determining prognosis of clinically localized prostate cancer by immunohistochemical detection of mutant p53. *Urology 47*:366–369.

Sulik, M., and Guzinska-Ustymowicz, K. 2002. Expression of Ki-67 and PCNA as proliferating markers in prostate cancer. *Rocz. Akad. Med. Bialymst.* 47:262–269.

Tamboli, P., Amin, M.B., Schultz, D.S., Linden, M.D., and Kubus, J. 1996. Comparative analysis of the nuclear proliferative index (Ki-67) in benign prostate, prostatic intraepithelial neoplasia, and prostatic carcinoma. *Mod. Pathol.* 9:1015–1019.

Tamboli, P., Amin, M.B., Xu, H.J., and Linden, M.D. 1998. Immunohistochemical expression of retinoblastoma and p53 tumor suppressor genes in prostatic intraepithelial neoplasia: Comparison with prostatic adenocarcinoma and benign prostate. *Mod. Pathol. 11*:247–252.

Thomas, D.J., Robinson, M., King, P., Hasan, T., Charlton, R., Martin, J., Carr, T.W., and Neal, D.E. 1993. P53 expression and clinical outcome in prostate cancer. *Br. J. Urol.* 72:778–781.

Tsujimoto, Y., Takayama, H., Nonomura, N., Okuyama, A., and Aozasa, K. 2002. Postatrophic hyperplasia of the prostate in Japan: Histologic and immunohistochemical features and p53 gene mutation analysis. *Prostate 52*:279–287.

Vesalainen, S.L., Lipponen, P.K., Talja, M.T., Alhava, E.M., and Syrjanen, K.J. 1994. Proliferating cell nuclear antigen and p53 expression as prognostic factors in T1-2M0 prostatic adenocarcinoma. *Int. J. Cancer 58*:303–308.

Visakorpi, T., Kallioniemi, O.P., Heikkinen, A., Koivula, T., and Isola, J. 1992. Small subgroup of aggressive, highly proliferative prostatic carcinomas defined by p53 accumulation. *J. Natl. Cancer Inst. 84*:883–887.

Voeller, H.J., Sugars, L.Y., Pretlow, T., and Gelmann, E.P. 1994. P53 oncogene mutations in human prostate cancer specimens. *J. Urol. 151*:492–495.

Xie, W., Wong, Y.C., and Tsao, S.W. 2000. Correlation of increased apoptosis and proliferation with development of prostatic intraepithelial neoplasia (PIN) in ventral prostate of the Noble rat. *Prostate 44*:31–39.

Yu, E.Y., Yu, E., Meyer, G.E., and Brawer, M.K. 1997. The relation of p53 protein nuclear accumulation and angiogenesis in human prostatic carcinoma. *Prostate Cancer Prostatic Dis. 1*:39–44.

9

Role of the $p14^{ARF}$ and $p16^{INK4a}$ Genes in Prostate Cancer

Noboru Konishi

Introduction

Although prostate cancer is the second most lethal cancer in the Western world, its pathogenesis is relatively poorly understood at the genetic level. The biologic behavior of prostate carcinoma is extremely variable, ranging from an apparently innocuous tumor having no significant effect on life expectancy to a rapidly disseminating and lethal disease. In the realm of pathology, the most striking features of human prostate carcinoma are its heterogeneity and the disparity between biologic behavior and morphologic classification. Different grading systems have been proposed incorporating various histologic criteria such as the presence or absence of glandular architecture, the percentage of glandular formation, the degree of cellular anaplasia, and nuclear shape and appearance (Brawn *et al.,* 1982; Brooks *et al.,* 1986; Gaeta *et al.,* 1980; Mostofi, 1975). Advances in molecular biology have shown that an accumulation of genetic alterations does occur in the stepwise process of tumorigenesis, but the actual biologic basis of the disease is not, as yet, fully understood. Recent data have revealed that there is actually little direct proof to support genetic mutation as the primary and/or the only cause of prostate cancer, and it further appears that tumor initiation and tumor development or progression should be viewed as markedly separate biologic events.

Both genetic and epigenetic alterations of the *INK4a/ARF* locus may impair both the $p14^{ARF}$/*p53* and the $p16^{INK4a}$/RB pathways that appear important in the development and progression of prostate carcinomas. Epigenetic mechanisms such as hypermethylation are, in fact, suspected of being more responsible for tumor progression (Rennie *et al.,* 1998) than are gene mutations *per se,* whereas the $p16^{INK4a}$ gene, for example, was found to be mutated in one of the three prostate cancer cell lines (Liu *et al.,* 1995). This gene was methylated in three of the five other cell lines (Herman *et al.,* 1995). $p14^{ARF}$ may act as an upstream regulator of *p53* function in that it functions to confine MDM2 to a subsection of the nucleus, thus stabilizing intranuclear p53 protein and preventing its cytoplasmic transport (Pomerantz *et al.,* 1998; Stott *et al.,* 1998; Zhang *et al.,* 1998). Whereas homozygous deletion of $p14^{ARF}$ has been reported in ~40% of glioblastomas (Nakamura *et al.,* 2001a), the human $p14^{ARF}$ promoter contains a CpG island that is also aberrantly methylated in gliomas, colorectal adenomas, and carcinomas (Esteller *et al.,* 2001a; Esteller *et al.*, 2001b; Nakamura *et al.,* 2001a), and esophageal squamous cell carcinomas (Xing *et al.,* 1999). However, the possible silencing of $p14^{ARF}$ by methylation/deletion has not been studied specifically in prostate carcinomas. Inactivation of *RB* by mutation, deletion, and/or promoter hypermethylation may also provide alternative molecular mechanisms to $p16^{INK4a}$

Handbook of Immunohistochemistry and in situ Hybridization of Human Carcinomas,
Volume 2: Molecular Pathology, Colorectal Carcinoma, and Prostate Carcinoma

369

inactivation, *CDK4* amplification, or *CCND1* amplification/rearrangement in multiple human tumors, including prostate carcinomas (Konishi *et al.,* 1996).

The differing opinions concerning the significance of epigenetic mechanisms and mutational frequencies in prostate cancer may be the result, in part, of differences in histologic heterogeneity and in methodologies used to investigate the disease. Although the mosaic nature of prostate lesions is characteristic, little consideration has been given to the individual molecular events occurring in the intratumor polymorphic subpopulations that likely give rise to this histologic heterogeneity. Alterations in both *ras* and *p53* have been demonstrated in colon and lung cancers. (Fearon *et al.,* 1990; Vahakangas *et al.,* 1992), suggesting that aberrations in multiple genes may be related to the variable histogenesis of cell populations within a lesion. In the studies illustrated in this chapter, we used a combination of immunohistochemical and molecular genetic analyses to probe the interrelationship between alterations specifically in the *p14^{ARF}* and *p16^{INK4a}* genes and the histogenesis of intratumor cellular heterogeneity. Rather than analyzing large tumor masses as single entities, we examined focal areas within each tumor having different growth characteristics and were thus able to detect and show different patterns and types of gene alterations occurring, sometimes simultaneously, in human prostate cancers.

MATERIALS

1. Tissue fixative: 10% neutral buffered formalin (NBF) for histopathologic evaluation. In cases of heterogeneous tumors, three to five areas from each multifocal tumor were selected on the basis of histologic classification using the Gleason system.

2. Phosphate buffer saline (PBS): Mix 810 ml of 0.2 M disodium hydrogen phosphate $\times$ 12 H_2O and 190 ml of 0.2 M sodium dihydrogen phosphate $\times$ 2H_2O. Adjust the pH to 7.4 with HCl. Add 340 g of sodium chloride and bring volume to 2 L with distilled water. Store as the stock solution and dilute 1:20 with distilled water when used.

3. 10 mM sodium citrate buffer: Mix 9 ml of 0.1 M citrate acid $\times$ H_2O (2.1 g in 100 ml distilled water) and 41 ml of 0.1 M trisodium citrate $\times$ 2H_2O (14.7 g in 500 ml distilled water); bring volume to 500 ml with distilled water (pH 6.0).

4. Primary antibody diluted in PBS without calcium and magnesium.

5. Chromogen: 3,3'-diaminobenzidine tetrahydrochloride in 0.01% hydrogen peroxidase.

6. Tris EDTA (ethylenediamine tetra-acetic acid) buffer (TE): 10 mM Tris Cl, 0.1 mM EDTA (pH 7.5).

7. Primer sequences for *p14^{ARF}* methylation-specific PCR (MSP): for the unmethylated reaction, 5'-TTT TTG GTG TTAAAG GGT GGT GTA GT-3' (sense) and 5'-CAC AAA AAC CCT CAC TCA CAA CAA-3' (antisense), which amplify a 132-bp product; for the methylated reaction, 5'-GTG TTA AAG GGC GGC GTA GC-3' (sense) and 5'-AAA ACC CTC ACT CGC GAC GA-3' (antisense), which amplify a 122-bp product.

Primer sequences for *p16^{INK4a}* MSP: for the unmethylated reaction, 5'-TTA TTA GAG GGTGGG GTG GAT TGT-3' (sense) and 5'-CAA CCC CAA ACC ACA ACC ATA A-3' (antisense); for the methylated reaction, 5'-TTA TTA GAG GGT GGG GCG GAT CGC-3' (sense) and 5'-GAC CCC GAA CCG CGA CCG TAA-3' (antisense).

8. PCR mixture for MSP: PCR buffer (10 mM Tris, pH 8.3, 50 mM KCl), 1.5–2.0 mM MgCl$_2$, dNTPs (250 μM each), primers (0.5 μM each), 0.5 unit of Platinum *Taq* DNA polymerase (Invitrogen, Carlsbad, CA), approximately 40 ng bisulfite modified deoxyribonucleic acid (DNA).

9. Primer sequences for *p14^{ARF}* deletion: 5'-GAG TGA GGG TTT TCG TGG TT-3' (sense) and 5'-GCC TTT CCT ACC TGG TCT TC3' (antisense), which amplify a 149-bp product. Primer sequences for *p16^{INK4a}* deletion: 5'-GAG CAG CAT GGA GCC TTC-3' (sense) and 5'-AAT TCC CCT GCA AAC TTC GT-3' (antisense), which amplify a 204-bp product.

10. Primer sequences for loss of heterozygosity (LOH) assay of *RB* gene: 5'-AGC ATT GTT TCA TGT TGG TG-3' (sense) and 5'-CAG CAG TGA AGG TCT AAG CC-3' (antisense).

METHODS

Immunohistochemistry

1. After deparaffinization with xylene, incubate sections for 30 min in 0.3% hydrogen peroxidase in methanol.

2. Rinse the sections 3 times in PBS, and heat for 5 min in 10 mM sodium citrate buffer in a pressure cooker. For pRB immunostaining treat sections with 0.05% protease for 10 min at 37ºC.

3. Rinse sections 3 times in PBS and incubate at room temperature for 20 min with diluted 10% goat serum for p14^{ARF} immunostaining or with 10% rabbit serum for p16^{INK4a}, p53, and pRB immunostaining.

4. Incubate sections overnight at 4ºC with the primary antibodies at a dilution of 1:400 for p14^{ARF}, at 1:1000 for p16^{INK4a}, and at 1:20 for p53 and pRB.

5. Rinse sections 3 times in PBS and expose to biotin-labeled goat anti-rabbit immunoglobulin G (IgG) for p14^{ARF} and biotin-labeled rabbit anti-mouse IgG for p16^{INK4a}, p53, and pRB for 10 min at room temperature.

6. Rinse sections 3 times in PBS and incubate with peroxidase-labeled streptavidin for 5 min at room temperature.

7. Rinse sections 3 times in PBS and stain with the chromogen and counterstain with hematoxylin for microscopic evaluation.

Methylation–Specific PCR (MSP)

1. In each screw cap microcentrifuge tube add 7.0 µl of 3 M NaOH to 1.0 µg DNA in 100 µl of water (10 ng/µl) and mix.

2. Incubate the DNA mixture for 10 min at 37ºC.

3. Add 550 µl of freshly prepared DNA Modification Reagent I (CgGenome DNA modification kit, Intergen, Oxford, UK) and vortex, then incubate at 50ºC for 16–20 hr.

4. Add 5 µl of well-suspended DNA Modification Reagent III (CpGenome DNA modification kit) to the DNA solutions in the tubes.

5. Add 750 µl of DNA Modification Regent II (CpGenome DNA modification kit) to the tubes and mix briefly, then incubate at room temperature for 5 min.

6. Spin for 10 sec at 5000X g to pellet and discard supernatant.

7. Wash the pellet by adding 1.0 ml of 70% EtOH, vortex, centrifuge for 10 sec at 5000X g, and discard the resulting supernatant; repeat 3 times.

8. After the supernatant from the third wash has been removed, centrifuge the tube at high speed for 2–3 min, and remove the remaining supernatant.

9. Add 50 µl of a 20 mM NaOH/90% EtOH solution to the samples, vortex briefly, and incubate at room temperature for 5 min.

10. Spin for 10 sec at 5000X g to pellet the sample. Add 1.0 ml of 90% EtOH and vortex to wash the pellet. Spin again and remove the supernatant. Repeat the EtOH wash and spin steps.

11. After the supernatant from the second wash has been removed, centrifuge the sample at high speed for 5 min.

12. Remove the remaining supernatant and add 25–50 µl of TE. Vortex briefly to resuspend the pellet. The volume of TE added depends on the amount of starting DNA.

13. Incubated the sample for 15 min at 50–60ºC to elute the DNA.

14. Centrifuge at high speed for 2–3 min, and transfer the supernatant to a new tube.

15. Proceed to MSP or sequencing, or store at –15ºC to –25ºC.

16. PCR amplification is carried out in a DNA Thermal Cycler 480 with initial denaturing at 95ºC for 5 min, followed by 35 cycles of denaturing at 95ºC for 45 sec, annealing for 45 sec at 60ºC for the *p14^{ARF}* methylated/unmethylated reactions and for the *p16^{INK4a}* unmethylated reaction or at the *p14^{ARF}* methylated and unmethylated reactions or at 65ºC for the *p16^{INK4a}* methylated reaction, then extension for 1 min at 72ºC, followed by a final extension for 4 min at 72ºC.

17. Electrophorese the amplified products on 3% agarose gels, and visualize with ethidium bromide staining.

Differential PCR for p14^{ARF} and p16^{INK4a} Deletions

1. The PCR conditions are fundamentally the same as for MSP. DNA is amplified by 30 cycles of PCR at an annealing temperature of 60ºC for *p14^{ARF}* and by 29 cycles of PCR with an annealing temperature of 58ºC for *p16^{INK4a}*.

2. Analyze the PCR products on 8% acrylamide gels.

3. Photograph the gels using a DC290 Zoom Digital Camera (Kodak, Rochester, NY), and use the Kodak Digital Science ID Image Analysis Software (for densitometric analysis of the PCR fragments.

4. Samples presenting <20% of control signal are considered homozygously deleted.

LOH Assay for RB

1. PCR cycles include one cycle of 95ºC for 5 min followed by 26 cycles of denaturing at 95ºC for 45 sec each, annealing at 58ºC for 45 sec, extension at 72ºC for 1 min, and a final extension at 72ºC for 10 min.

2. Mix 1 µl aliquots of the PCR reactions with 12 µl deionized formamide and 0.5 µl GeneScan Internal Lane Size Standard (ABI, Foster City, CA) denatured formamide for 2 min at 94ºC, then perform capillary electrophoresis on 6% denaturing gels using the Genetic Analyzer 310 (ABI).

3. Data are automatically collected and analyzed with GeneScan software.

4. Samples heterozygous for a given locus are considered informative; homozygosity and microsatellite

instability prohibits evaluation of LOH or amplification at any affected locus.

PCR-Single-Strand Conformational Polymorphism

1. Exons 4–9 of *p53* are amplified in 35 cycles of PCR with denaturing at 95ºC for 30 sec, annealing at 57ºC for 30 sec, and extension at 72ºC for 1 min.

2. PCR mixture should contain 200 ng of DNA template, 22.7 pM of each primer pair, 1.5 mM $MgCl_2$, 250 pM/µl of each deoxyribonucleotide triphosphate, and 2.0 units of *Taq* polymerase.

3. Tag the PCR-amplified DNA fragments using primers end-labeled with [γ-^{32}P]-ATP (adenosine triphosphate).

4. Heat the aliquots at 95ºC for 2 min, chill on ice, then load onto 5% polyacrylamide gels containing 10 glycerol in 0.5X Tris-borate-EDTA.

5. Expose gels to X-ray film.

RESULTS AND DISCUSSION

The *INK4a/ARF* locus, located on chromosome 9p21, contains two tumor suppressor genes, *p14^ARF* and *p16^INK4a*. Both genes are characterized by two distinct promoters consisting of the first exon spliced to a common exon 2 in different reading frames (Quelle *et al.,* 1995). The *p16^INK4a* gene encodes an inhibitory protein of cyclin-dependent kinase 4 and 6 (CDK4/6), which functions to prevent pRB phosporylation and cell-cycle progression (Sherr, 1996). Therefore, the absence of *p16^INK4a* product results in pRB phosphory-lation, which stimulates the cell entry into S-phase and contributes to proliferation activity. In contrast, *p14^ARF* interacts with the oncogenic MDM2 protein, inducing stabilization of *p53* and enhancing *p53*-related function (Esteller *et al.,* 2001a). Thus, a single alteration in the *INK4a-ARF* locus can potentially disrupt the *p16^INK4a*/RB and *p14^ARF*/p53 tumor suppressor pathways and facilitate cancer development.

Initially it was believed that *p16^INK4a* homozygous deletions or mutations were rare in primary cancers, although ubiquitous and frequent inactivation of *p16^INK4a* was commonly detected in tumor cell lines (Nobori *et al.,* 1994). Subsequent studies revealed that a wide variety of tumors have small deletions of less than 200 Kb in both *p16^INK4a* alleles (Cheng *et al.,* 1994). More recent studies have identified hyper-methylation and homozygous deletion of the promoter region as a major mechanism of gene silencing (Herman *et al.,* 1995). Although numerous studies recognized a prominent tumor suppressor function of

p16^INK4a, *INK4a/ARF* locus alterations via homozygous deletion and hypermethylation appeared to be rare events in prostate carcinoma (Chen *et al.,* 1996; Gu, 1998).

We first studied the *p14^ARF*, *p16^INK4a*, *RB*, and *p53* gene status of 32 prostate carcinomas, looking not only for deletions and/or mutations but also for aberrant DNA methylation, using MSP, differential PCR, and single-strand conformational polymorphism (SSCP) (Konishi *et al.,* 2002a). We found hypermethylation of *p16^INK4a* exon 2 in ~66% (21/32) of the samples, within which three tumors demonstrated methylation of both the promoter and exon 2. Differential PCR also detected simultaneous homozygous deletion of *p14^ARF* and *p16^INK4a* in 13% (4/32) of samples, whereas simultaneous hypermethylation of both the *p14^ARF* and the *p16^INK4a* promoters was detected in only one case. In all, 25% of tumors (8/32) showed either *p16^INK4a* deletions, promoter methylation, or exon mutations; an additional specimen demonstrated concurrent *p16^INK4a* promoter methylation and an intron mutation.

As described earlier, *p14^ARF* plays a major role in the *p53* pathway by binding specifically to MDM2, resulting in stabilization of both *p53* and MDM2 (Stott *et al.,* 1998). We found that a mutually exclusive correlation between *p14^ARF* and *p53* mutations appears to exist in those cases of *p14^ARF* showing no *p53* mutations, as was previously reported (Konishi *et al.,* 2002a); in fact, only one tumor of the 32 studied showed any concurrent aberration—specifically, of both *p14^ARF* and *p53* a *p14^ARF* promoter methylation combined with a G→C transversion in exon 4 of *p53*. Reciprocal alterations between *p53* and *p14^ARF* have been observed by other investigators, including Esteller *et al.* (2001a), who reported that *p14^ARF* silencing by promoter hypermethylation mediates abnormal intracellular localization of MDM2. *p53* mutations may thus occur more rarely in tumors with inactivation of the *INK4a/ARF* locus than in tumors with wild-type genes (Pomerantz *et al.,* 1998). It is also possible that in cases where alterations of *p14^ARF* occur early in cancer development, the tumors may be able to retain wild-type *p53*. This pattern may apply to some of the prostate carcinomas in our series.

We then focused on analyzing the gene status of multiple individual areas within 16 histologically heterogeneous prostate carcinomas (Konishi *et al.,* 2002b) using immunohistochemistry, differential PCR, and *RB* LOH. Hypermethylation of exon 2 in *p16^INK4a* was found in all areas examined in 69% (11/16) of these heterogenous tumors. All focal areas examined had Gleason grades ranging from 1 to 5. Simultaneous homozygous deletion of the *p14^ARF* and *p16^INK4a* genes was detected by differential PCR in only 1 of 16 cases (Figure 57) and was found in only 2 of 5 foci
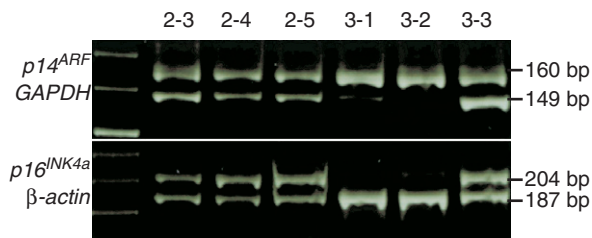
Figure 57 Differential polymerase chain reaction assessing *p14^ARF* and *p16^INK4a* homozygous deletions in prostate carcinomas. Tumor no. 2 and focus 3-3 have a normal gene status. Foci 3-1 and 3-2 show *p14^ARF* and *p16^INK4a* co-deletions.

individually analyzed within that tumor. In both foci 3-1 and 3-2, having Gleason grades of 5 and 4, respectively, homozygous deletion of *p14^ARF* exon 1 and of *p16^INK4a* exon 1α and the concurrent methylation of *p16^INK4a* exon 2 was observed, which is unusual because exon 1α and exon 2 are closely located. The same situation exists between exon 2 and exon 1β of *p14^ARF*. A somewhat higher frequency of *p14^ARF* than *p16^INK4α* deletions has been reported in other human neoplasms, including esophageal carcinomas, gliomas, and intracranial malignant lymphomas (Nakamura *et al.,* 2001a; Xing *et al.,* 1999); specific deletion of *p16^INK4a* exon 1α also occurs in some prostate cancers, although the mechanism is currently unknown.

Similar to the previously mentioned situation, only a single carcinoma (Figure 58), demonstrated simultaneous hypermethylation of the promoter regions of both *p14^ARF* and *p16^INK4a* in 2 of 5 focal areas. In the majority of human neoplasms, a clear correlation has been reported between promoter deletion/methylation and loss of gene expression as detected by immunohistochemistry (Nakamura *et al.,* 2001a; Nakamura *et al.,* 2001b); we also detected this association. The same two foci, 8-2 and 8-3, that demonstrated concurrent promotor hypermethylation also lacked any immunohistochemical expression of either *p14^ARF* or *p16^INK4a* (Figure 59). These two foci were Gleason graded as 3 and 4, respectively. It should be noted that other foci showed loss of protein expression without coinciding detectable alterations in the promoter regions, suggesting that mutations other than deletion or methylation may be operating in these cases.

We found a normal *p14^ARF* gene status in all 13 tumors immunopositive for *p14^ARF* expression. Three tumors had a total of seven individual foci lacking both p14^ARF and p16^INK4a expression, which correlated, in all but three instances, to homozygous promotor codeletion or promoter comethylation; these exceptional foci showed loss of both p14^ARF and p16^INK4a expression without simultaneous homozygous gene deletion or methylation. Another anomaly was that the remaining four individual foci examined were immunonegative for p16^INK4a expression without further alteration in the gene. Nuclear immunoreactivity of both p14^ARF and p16^INK4a was observed in normal prostate tissues.
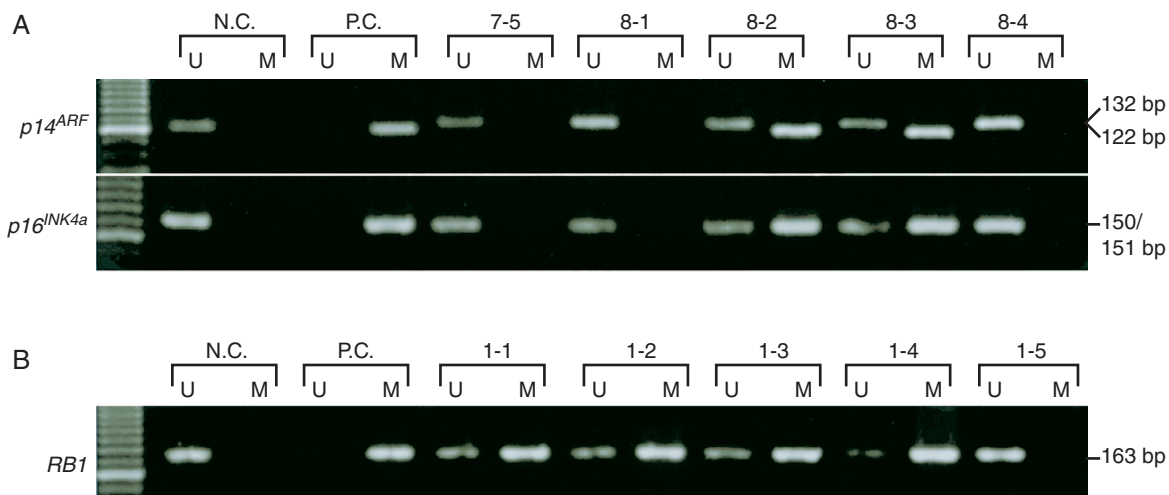
Figure 58 A: Methylation-specific polymerase chain reaction (PCR) of the *p14^ARF* and *p16^INK4a* promoter regions in prostate carcinomas. In foci 7-5, 8-1, and 8-4, only unmethylated DNA (U) is apparent. In tumor no. 8, *p14^ARF* and *p16^INK4a* methylation (*M*) was restricted to foci 8-2 and 8-3 lacking p14^ARF and p16^INK4a immunoreactivity. N.C., normal control DNA from a normal blood; P.C., positive control for methylated DNA; U, PCR product amplified by unmethylated-specific primers; M, PCR product amplified by methylated-specific primers. **B:** Methylation-specific PCR for *RB*. Hypermethylation of *RB* promoter was found in 4 of 5 foci in tumor no. 1 only.
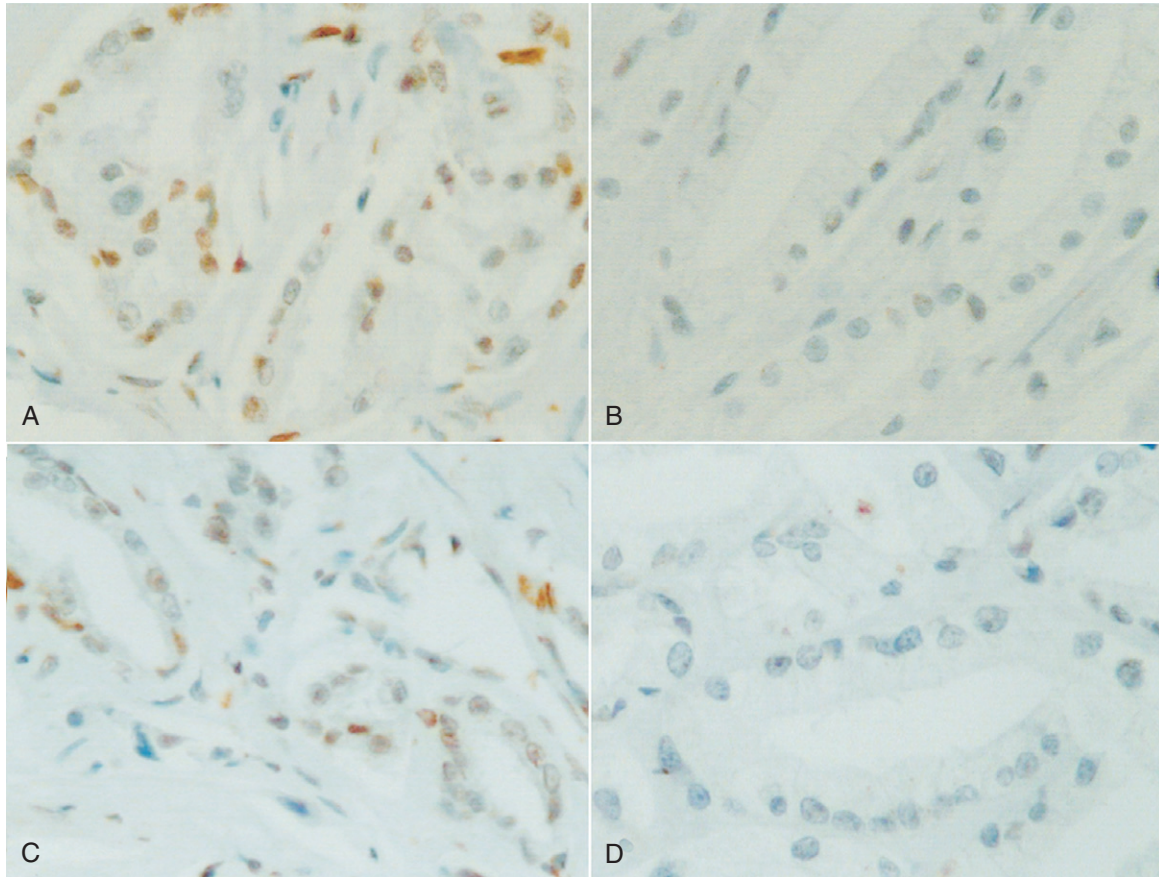
Figure 59 Loss of expression of p14^{ARF} and p16^{INK4a} was associated with promoter methylation. **A:** p14^{ARF} immunohistochemistry showing nuclear immunoreactivity in the majority of tumor cells from focus 8-1. **B:** A separate focus, 8-2, within the same tumor with no expression of p14^{ARF}. **C:** Focus 8-1 exihibits extensive and marked immunoreactivity for p16^{INK4a}. **D:** Within the same tumor, another focus, 8-2, shows no p16^{INK4a} immunoreactivity. Magnification, 300X; hematoxylin counterstain.

Nguyen *et al.* (2000) reported a high frequency of *p16^{INK4a}* exon 2 methylations in human prostate cancers (73%, or 8/11 cases), which correlated with up-regulated *p16^{INK4a}* transcripts. We similarly found frequent methylation of *p16^{INK4a}* exon 2 in the prostate carcinomas. Methylation patterns of *p16^{INK4a}* exon 2 in our evaluations were different from those of the other genes investigated in that methylation appeared to be an all-or-nothing event. The underlying mechanisms(s), however, are not clear because hyper-methylation of *p16^{INK4a}* exon 2 was not correlated with p16^{INK4a} immunohistochemical expression. This might relate to transcriptional inactivation and/or a more complex function for DNA methyltransferase. Similar situations occurred in abnormalities between *RB* and protein expression. A clear correlation was reported between *RB* homozygous deletion and/or promoter hypermethylation and loss of immunohistochemical

pRB expression in brain tumors (Nakamura *et al.,* 2001b); yet, in our prostate analyses, some nonmethy-lated foci were immunonegative for pRB. We did, however, find a correlation between pRB expression and *RB* LOH in that pRB expression was detected in the majority of foci showing retention of both alleles. We previously surveyed all 27 exons of *RB* in a series of prostate carcinomas (Konishi *et al.,* 1996); 16% (5/32) of cancers demonstrated mutations, but only one exonic mutation occurred. We therefore are led to conclude that *RB* alterations can occur in either introns or exons, possibly more frequently in the former, and may have no effect on amino acid composition. However, allelic loss of *RB* has been extensively inves-tigated and has been found in 27–67% of informative prostate cancers, suggesting that loss of pRB expres-sion is more likely the result of allelic loss of the gene. Mutational inactivation of the *RB* gene might, in a few

cases, be another mechanism, although we did not examine all exons of *RB* in these studies and cannot exclude the possibility of normal tissue contamination.

We now know that carcinoma of the prostate is genetically multicentric and histologically heterogeneous and multifocal (Konishi *et al.,* 1995b; Konishi *et al.*, 1997). Although the cases examined in this study were small in number and the significance of the observed specific genetic events is still speculative, the 16 highly heterogeneous prostate carcinomas analyzed showed multiple growth patterns, indicating subsets of cells with possibly separate factors directing their development. Although the overall incidence of promoter deletions and methylations seems to be infrequent in prostate cancers, we did find that these alterations can and do occur simultaneously. We could not detect any specific combination of methylation patterns or epigenetic changes occurring in representative focal areas within prostate tumors; however, the overall frequency of independent methylation events uncovered points to a role for methylation, possibly in progression, in prostate carcinogenesis. The combined effects of homozygous deletion and methylation of *p14^{ARF}* and/or *p16^{INK4a}* might function to deregulate both the *RB* and *p53* pathways; it is interesting, however, that our data clearly indicate that intratumor foci showing *RB* methylation or allelic loss have no coincidental methylation or deletion of *p16^{INK4a}*. Although mutation or methylation of *p16^{INK4a}* is evidently rare in prostate carcinoma, alterations in *RB* are not. Specific *p16^{INK4a}* gene mutations may occur only in a few foci within a larger tumor mass (Konsihi *et al.,* 1995a) but still be capable of impairing the *p16^{INK4a}/RB* pathway involved in the development and progression of the disease. Many contradictory reports on the role of genetic events in the histogenesis of prostate cancer may thus be due to this heterogeneous, multifocal nature. In other words, mutational heterogeneity may correlate to morphologic heterogeneity and molecular progression. We cannot presently say that these foci with specific *INK4a/ARF* locus alterations progress or predominate in the more aggressive forms of the disease, but we are getting closer to linking mutation type and location and histologic characteristics to specific genetic mechanisms.

References

Brawn, P.N., Ayala, A.G., von Eschenbach, A.C., Hassey, D.H., and Johnson, S.E. 1982. Histologic grading study of prostatic adenocarcinoma: The development of a new system and comparison with other methods—A preliminary study. *Cancer 49*:525–532.

Brooks, B., and Miller, G.L. 1986. Evaluation of prastatic cancer histology and grade distribution: Experience with the Colorado Central Cancer registry. *Prostate 8*:139–150.

Chen, W., Weghorst, C.M., Sabourin, C.L.K., Wang, Y., Wang, D., Bostwick, D.G., and Stoner, G.D., 1996. Absence of *p16/MTS1* gene mutations in human prostatic cancer. *Carcinogenesis 17*:2603–2607.

Cheng, J.Q., Jhanwar, S.C., Klein, W.M., Bell, D.W., Lee, W.C., Altomare, D.A., Nobori, T., Olopade, O.I., Buckler, A.J., and Testa, J.R., 1994. p16 alterations and deletion mapping of 9p21-p22 in malignant mesothelioma. *Cancer Res. 54*:5547–5551.

Esteller, M., Cordon-Cardo, C., Corn, P.G., Meltzer, S.J., Pohar, K.S., Watkins, D.N., Capella, G., Peinado, M.A., Matias-Guiu, X., Prat, J., Baylin, S.B., and Herman, J.G. 2001a. *p14^{ARF}* silencing by promoter hypermethylation mediates abnormal intracellular localization of MDM2. *Cancer Res. 61*:2816–2821.

Esteller, M., Corn, P.G., Baylin, S.B., and Herman, J.G. 2001b. A gene hypermethylation profile of human cancer. *Cancer Res. 61*:3225–3229.

Fearon, E.R., and Vogelstein, B. 1990. A genetic model for colorectal tumorigenesis. *Cell 61*:759–767.

Gaeta, J.F., Asirwatham, J.E., Miller, G., and Murphy, G.P. 1980. Histologic grading of primary prostatic cancer: A new approach to an old problem. *J. Urol. 123*:689–693.

Gu, K., Mes-Masson, A.M., Gauthier, J., and Saad, F. 1998. Analysis of the *p16* tumor suppressor gene in early-stage prostate cancer. *Mol. Carcinog. 21*:164–170.

Herman, J.G., Merlo, A., Mao, L., Lapidus, R.G., Issa, J.P., Davidson, N.E., Sidransky, D., and Baylin, S.B., 1995. Inactivation of the *CDKN2/p16/MTS1* gene is frequently associated with aberrant DNA methylation in all common human cancers. *Cancer Res. 55*:4525–4530.

Konishi, N., Hiasa, Y., Matsuda, H., Tao, M., Tsuzuki, T., Hayashi, I., Kitahori, Y., Shiraishi, T., Yatani, R., Shimazaki, J., and Lin, J.C. 1995b. Intratumor cellular heterogeneity and alterations in *ras* oncogene and p53 tumor suppressor gene in human prostate carcinoma. *Am. J. Pathol. 147*:1112–1122.

Konishi, N., Hiasa, Y., Nakamura, M., Kitahori, Y., Matsubara, K., and Nagai, H. 1997. Different patterns of DNA alterations detected by restriction landmark genomic scanning in heterogeneous prostate carcinomas. *Am. J. Pathol. 150*:305–314.

Konishi, N., Hiasa, Y., Tao, M., Matsuda, H., Nakamura, M., Yane, K., and Kitahori, Y. 1995a. Focal distribution of p16/CDKN2 gene mutations within individual prostate carcinomas. *Int. J. Oncol. 8*:549–554.

Konishi, N., Hiasa, Y., Tsuzuki, T., Matsuda, H., Tao, M., Nakamura, M., Naitho, H., Kitahori, Y., Shiraishi, T., Yatani, R., Shimazaki, J., and Lin, J.C. 1996. Detection of *pRB*, *p16/CDKN2* and *p15^{INK4B}* gene alterations with immunohistochemical studies in human prostate carcinomas. *Int. J. Oncol. 8*:107–112.

Konishi, N., Nakamura, M., Kishi, M., Nishiminne, M., Ishida, E., and Shimada, K. 2002a. DNA hypermethylation status of multiple genes in prostate adenocarcinoma. *Jpn. J. Cancer Res. 93*:767–773.

Konishi, N., Nakamura, M., Kishi, M., Nishiminne, M., Ishida, E., and Shimada, K. 2002b. Heterogeneous methylation and deletion patterns of the *INK4a/ARF* locus within prostate carcinomas. *Am. J. Pathol. 160*:1207–1214.

Liu, Q., Neuhausen, S., McClure, M., Frye, C., Weaver-Feldaus, J., Gruis, N.A., Eddington, K., Allalunis-Turner, M.J., Skolnick, M.H., Fujimura, F.K., and Kamb, A. 1995. CDKN2 (MTS1) tumor suppressor gene mutations in human tumor cell lines. *Oncogene 10*:1061–1067.

Mostofi. F.K. 1975. Grading of prostatic carcinoma. *Cancer Chemother. Rep. 59*:111–117.

Nakamura, M., Sakaki, T., Hashimoto, H., Nakase, H., Isida, E., Shimada, K., and Konishi, N. 2001b. Frequent alterations of the p14^ARF and p16^INK4a genes in primary central nervous system lymphomas. *Cancer Res. 61*:6335–6339.

Nakamura, M., Watanabe, T., Knangby, U., Asker, C., Wiman, K., Yonekawa, Y., Kleihues, P., and Ohgaki, H., 2001a. *p14^ARF* deletion and methylation in genetic pathways to glioblastomas. *Brain Pathol. 11*:159–168.

Nguyen, T.T., Nguyen, C.T., Goazales, F.A., Nicholas, P.W., Yu, M.C., and Jones, P.A., 2000. Analysis of cyclin-dependent kinase inhibitor expression and methylation patterns in human prostate cancers. *Prostate 43*:233–242.

Nobori, T., Miura, K., Wu, D.J., Lois, A., Takabayashi, K., and Carson, D.A. 1994. Deletions of the cyclin-dependent kinase-4 inhibitor gene in multiple human cancers. *Nature 368*:753–756.

Pomerantz, J., Schreiber-Agus, N., Leigeois, N.J., Silverman, A., Alland, L., Chin, L., Potes, J., Chen, K., Orlow, I., Lee, H.W., Cordon-Cardo, C., and DePinho, R.A. 1998. The *Ink4a* tumor suppressor gene product, p19^Arf, interacts with MDM2 and neutralizes MDM2's inhibition of p53. *Cell 92*:713–723.

Quelle, D.E., Zindy, F., Ashmun, R.A., and Sherr, C.J. 1995. Alternative reading frames of the *INK4a* tumor suppressor gene encode two unrelated proteins capable of including cell cycle arrest. *Cell 83*:993–1000.

Rennie, P.S., and Nelson, C.C. 1998. Epigenetic mechanisms for progression of prostate cancer. *Cancer Metastasis Rev. 17*:401–409.

Sherr, C.J., 1996. Cancer cell cycles. *Science 274*:1672–1677.

Stott, E.J., Bates, S., James, M.C., McConnell, B.B., Statborg, M., Brookes, S., Palmero, I., Ryan, K., Hara, E., Vousden, K.H., and Peters, G. 1998. The alternative product from the human CDKN2A locus, p14(ARF), participates in a regulatory feedback loop with p53 and MDM2. *EMBO. J. 17*:5001–5014.

Vahakangas, K.H., Samet, J.M., Metcalf, J.A., Welsh, J.A., Bannett, W.P., and Lane, D.P., 1992. Mutations of p53 and *ras* genes in radon-associated lung cancer from uranium miners. *Lancet 339*:576–580.

Xing, E.O., Nie, Y., Song, Y., Yang, G.Y., Cai, Y.C., Wang, I.D., and Yang, C.S., 1999. Mechanisms of inactivation of *P14^ARF*, *p15^INK4b*, and *p16^INK4a* genes in human esophageal squamous cell carcinoma. *Clin. Cancer Res. 5*:2704–2713.

Zhang, Y., Xiong, Y., and Yarbrough, W.G. 1998. ARF promoters MDM2 degradation and stabilizes p53: *ARF-INK4a* locus deletion impairs both the Rb and p53 tumor suppression pathways. *Cell 92*:725–734.

10

P504S/α-Methylacyl CoA Racemase: A New Cancer Marker for the Detection of Prostate Carcinoma

Zhong Jiang

Introduction

Prostate carcinoma is the most common form of cancer in men and the second leading cause of death accounting for men more than 37,000 deaths per year in the United States (Landis *et al.,* 1999). The wide use of serum prostate specific antigen (PSA) screening has resulted in an increased detection of patients with prostate cancer (DiGiuseppe *et al.,* 1997). A tissue diagnosis (prostate needle biopsy or transurethral resection of prostate (TuRP)) is mandatory for a patient with prostate cancer to receive appropriate therapy to minimize morbidity and mortality. However, tissue diagnosis can be difficult and inaccurate if the cancer is very limited because the establishment of a pathologic diagnosis requires the presence of a combination of multiple histologic features of tumor cells such as an infiltrating pattern, nuclear atypia, and the presence of characteristic extracellular material in malignant epithelium (Epstein and Yang, 2002; Epstein, 1995; Young *et al.,* 2000). No single dignostic feature of prostatic adnocarcinoma can be used reliably. In addition, many benign conditions can mimic the morphology of prostate cancer, despite their benign biologic behavior.

Overdiagnosis (false positivity) may cause unnecessary treatment of men without prostate cancer and lead to incontinence or impotency. Underdiagnosis (false negativity) may delay effective treatment to patients with prostate cancer and may lead to recognition of disease at a more advanced stage. Unfortunately, there is a significant error rate in pathologic diagnosis of prostate cancer in general practice because discrimination between benign and malignant glands can be difficult in the small biopsy, and this can be even more difficult for pathologists who are not specialized in urologic pathology. The accuracy of pathologic diagnosis of prostate cancer may be improved by the application of a more objective and reliable tumor specific marker. Therefore, a biochemical marker would be very useful in clinical practice.

Currently, PSA is the most commonly used biomarker for the diagnosis and prediction of prognosis in prostate cancer (Wand *et al.,* 1982). However, PSA is not a cancer specific marker, as it is present in both

Handbook of Immunohistochemistry and in situ Hybridization of Human Carcinomas,
Volume 2: Molecular Pathology, Colorectal Carcinoma, and Prostate Carcinoma

377

benign and malignant prostatic epithelial cells (Polascik *et al.,* 1999). Serum PSA levels are frequently elevated in benign conditions such as benign prostate hyperplasia (BPH) and prostatitis in addition to prostate cancer (Hasui *et al.,* 1994; Nadler *et al.,* 1995). Consequently, patients with elevated serum PSA must undergo a biopsy to confirm or exclude the presence of prostate cancer. Other biomarkers including prostate acid phosphatase (PAP) (Oesterling *et al.,* 1987), prostate-specific membrane antigen (Horoszewicz *et al.,* 1987), prostate inhibin peptide (Teni *et al.,* 1988), PCA-1 (Edwards *et al.,* 1982), PR92 (Kim *et al.,* 1989), prostate-associated glycoprotein complex (Wright *et al.,* 1991), PD41 (Beckett *et al.,* 1991), 12-lipoxygenase (Tang and Honn, 1994), p53 (Thomas *et al.,* 1993), and hepsin (Dhanasekaran *et al.,* 2001) are expressed in prostate carcinoma. However, none of the aforementioned markers could be used for tissue diagnosis because they either stained both benign and malignant glands or work poorly in formalin-fixed tissue with less sensitivity (Beckett *et al.*, 1991). Other prostate markers are discussed in this volume.

Benign prostate glands contain secretory epithelial cells with positive staining of PSA and PAP, and basal cells that lie beneath the secretory cells. Basal cell nuclei are oval shaped and are oriented parallel to the basement membrane. The cells may be inconspicuous in benign glands and may be difficult to distinguish from surrounding fibroblasts. It is very important to recognize basal cells and differentiate them from fibroblasts or two cell layers of cancer. Because basal cells are absent in prostate adenocarcinoma, high molecular cytokeratin (34βE12) and P63 immunostaining specific for basal cells have been used as an ancillary tool for diagnosis of prostate cancer. Positive staining for basal cells of prostate glands may render a definitive diagnosis of benign glands (Brawer *et al.*, 1985; Gown and Vogel, 1984; Signoretti *et al.,* 2000; Wojno and Epstein, 1995). However, a limitation of using this negative marker for diagnosis of the carcinoma is that basal cells have a patchy or discontinuous distribution in some benign lesions (i.e., adenosis and some atrophic glands). Consequently, negative staining for high molecular weight cytokeratin in a few glands suspicious for cancer is not proof of their malignancy (Wojno and Epstein, 1995).

Recent advances in molecular biology have already had a significant impact on the clinical practice of medicine. In particular, newly developed techniques such as ribonucleic acid (RNA) subtraction hybridization and complementary deoxyribonucleic acid (cDNA) microarrays allow the identification and comparison of genes differentially expressed between malignant and benign cells. Xu *et al.* (2000), using cDNA library subtraction in conjuction with high throughput microarray screening, found three proteins, including P503S, P504S, and P510S, from benign and malignant prostate tissue. P504S is a 1621-bp cDNA with an open reading frame that encodes a 382 amino acid protein that has been identified as human α-methylacyl-CoA racemase (AMACR) (Xu *et al*., 2000). α-Methylacyl-CoA racemase plays a role in the beta-oxidation of branched-chain fatty acids and fatty-acid derivatives (Ferdinandusse *et al.,* 2000). P504S messenger RNA (mRNA) was overexpressed in ~30% (microarray screening) to 60% (quantitative polymerase chain reaction [PCR] analysis) of prostate tumors and is low to undetectable levels in normal tissues (Xu *et al.,* 2000).

Using the immunohistochemical method, we demonstrated that P504S is a highly sensitive and specific positive tissue marker for prostate carcinoma (Jiang *et al*., 2001). We described a monoclonal antibody to P504S that shows preferential binding to all prostate carcinomas with no or limited reactivity to benign prostate glands on routine formalin-fixed and paraffin-embedded tissue sections. After our study, other groups have confirmed our findings by using polyclonal or monoclonal antibodies and also reported the extensive up-regulation of AMACR/P504S at the protein and transcript levels in prostate carcinoma (Beach *et al.,* 2002; Luo *et al,* 2002; Rubin *et al.,* 2002; Zhou *et al.,* 2002). Applications of P504S/AMACR as a diagnostic tissue marker for prostate carcinoma in clinical practice are discussed in this chapter.

MATERIALS

Cases

Specimens from prostatectomies, prostate needle biopsies, and TURPs were obtained from the surgical pathology files. The tissues were fixed in 10% neutral buffered formalin. Paraffin-embedded tissue blocks were cut into 5 μm-thick sections and transferred to glass slides.

Monoclonal Antibody to P504S

Full-length P504S was cloned into PTrcHisC (Invitrogen) and expressed in *Escherichia coli* with a histidine tag. The protein was purified by nickel chromatography, followed by ion exchange chromatography. Rabbit monoclonal antibody (MAb, 13H4) was generated from rabbits immunized with P504S protein.

Materials for
Immunohistochemical Staining

1. Phosphate buffer saline (PBS): 200 mg potassium chloride, 200 mg monobasic potassium phosphate, 8 g sodium chloride, and 2.16 g dibasic sodium phosphate 7 H_2O; bring volume to 1 L with distilled water (pH 7.4).

2. 0.01 mol/L citrate buffer: To make citrate buffer stock solution 0.1 M, disolve 21.01 g of citrate (citric acid monohydrate, Sigma C-7129) in deionized water to a final volume of 100 ml. Use this stock at a dilution of 1:100.

3. Primary rabbit MAb to P504S diluted in Dako (Carpinteria, CA) Antibody Diluent or PBS at 0.5 µg/ml dilution.

4. Primary mouse MAb (34βE12, Dako) to high molecular weight cytokeratin diluted in Dako Antibody Diluent or PBS at 1:50 dilution.

5. Cocktail of biotinylated anti-rabbit immunoglobulin G (IgG) and anti-mouse IgG/IgM (Ventana Medical Systems, Tucson, AZ). There are many available commercial kits for secondary antibody binding; in our case the Ventana Kit was used. Here, the provided cocktail of anti-mouse and anti-rabbit biotinylated antibodies was used without diluting. However, for special applications, when only anti-rabbit biotinylated antibody was required, the concentration of 5 µg/ml was used. To dilute the secondary antibody (if necessary) we used Dako Antibody Diluent or PBS.

6. Avidin/peroxidase complex (Ventana) forms complexes that will bind to the biotinylated secondary antibody. There are many available commercial kits for avidin/biotin/peroxidase staining. We used Ventana kit. The kit contains solutions of avidin and biotinyated peroxidase that are combined with PBS in precise ratios. For every 5 ml of required A/B/C solution, 176 µl of avidin solution and 176 µl of biotinylated peroxidase solution are added to 5 ml of PBS. This must be prepared 30 min prior to use.

7. Diaminobenzidine (DAB) and hydrogen peroxide (H_2O_2). The subsequent addition of the substrate DAB and H_2O_2 will allow the bound sites to be visualized. There are many commercially available kits for DAB visualization; we used the Ventana kit. This kit contains a solution of DAB and a solution of H_2O_2, which are combined in a kit-provided Tris buffer in precise ratios; For every 5 ml of required DAB working solution, 100 µl of DAB and 100 µl of H_2O_2 are added to 5 ml of Tris buffer. These molecules, when catalyzed by the peroxidase enzyme bound to the antibody (which is bound to the target site on the tissue), will produce a pigmented precipitate. This precipitate collects in the vicinity of the bound antibody site, thus visualizing the target in the tissue.

METHODS

1. Place formalin-fixed and paraffin-embedded tissue sections cut at 4 to 5 µm on charged slides for greater adhesion, and dry for 10 min at 65–70°C. Cool to room temperature, and check to see that all water has dried from slides.

2. Deparaffinize, clear, and rehydrate. Once slides have begun deparaffinization, the tissue sections should never be allowed to dry until the final step of staining has been completed.

Place dried slides in the following series of solutions:

Xylene	3 min
Xylene	3 min
100% ethanol	3 min
100% ethanol	3 min
95% ethanol	3 min
70% ethanol	3 min

Distilled water, rinse 3 times in fresh distilled water.

3. Antigen retrieval. For up to 24 slides make 200 ml of working solution by adding 2 ml of citrate stock solution to 198 ml of deionized water. Adjust final pH (using 10 M NaOH solution) to pH 6.0.

Place rinsed slides into a plastic staining bucket containing citrate working solution, and cover loosely with lid. Place the bucket in the center of the rotating platform and microwave slides for 5 min at 770 watts; add 50 ml of deionized water to ensure that the tissues remain wet, and microwave again for 5 min at 770 watts. Remove from microwave, and allow to cool at least for 20 min.

4. When slides have cooled (room temperature), rinse 3 times in distilled H_2O and place in PBS.

All remaining steps take place at room temperature. Volumes of all solutions applied to slides should be enough to cover all tissue areas.

5. Treat slides for 5 min with 3% H_2O_2, and rinse twice in PBS for endogenous peroxidase blocking.

6. Treat slides with Dako Serum-Free Protein Block for 5 min, and rinse twice in PBS for nonspecific protein blocking.

7. Incubate slides with P504S and 34βE12 antibodies for 45 min, and rinse twice in PBS.

8. Incubate slides with biotinylated secondary antibody for 30 min, and rinse twice in PBS.

9. Avidin/Biotin Complex (follow kit instructions for making this reagent): Apply to slides, incubate for 30 min, and rinse twice in PBS.

10. Apply DAB development to slides for 5–7 min, add another volume of DAB, allow to develop another 5–7 min, and rinse gently with distilled H_2O.

11. Place slides in hematoxylin solution for 1 min, and rinse in running tap water for 1–3 min for nuclear staining.

12. Dehydrate and place a coverslip.

RESULTS AND DISCUSSION

We have analyzed the pattern of expression of P504S in a large number of prostate carcinomas and benign prostate tissues, including 137 cases of prostate carcinoma and 70 cases of benign prostate, from prostatectomies (n = 77), prostate needle biopsies (n = 112), and TURP (n = 18) (Jiang *et al.*, 2001). P504S displays several features that make it an attractive marker for prostate carcinoma.

To determine the sensitivity and the pattern of expression of P504S in malignant prostate, we performed an immunohistochemical analysis with P504S MAb. Our data show that all 137 cases of prostate carcinomas show strongly positive expression of P504S. A diffuse staining pattern (>75% of tumor positive) was seen in 92% of cases regardless of the Gleason score. Positive P504S staining was defined as continuous dark cytoplasmic staining (Figure 60A) or apical granular staining patterns in the epithelial cells, which can be easily observed at low power magnification (<100X). Strong positivity for P504S was found in carcinomas but not in adjacent normal or atrophic glands (Figure 60B). P504S was also strongly positive in high-grade prostatic intraepithelial neoplasia (PIN). Furthermore, if high-grade PIN partially involved a prostatic gland, the expression of P504S was only present in the PIN but not in the normal epithelial cells of the same gland. High molecular weight cytokeratin is expressed in basal cells of benign glands but not in prostate carcinoma. It is interesting that the expression of high molecular weight cytokeratin and P504S appeared to be mutually exclusive.

In contrast to carcinomas, 88% of benign prostates including benign cases and benign prostate tissue adjacent to carcinomas were completely negative for P504S. The other 12% of cases showed only focal and *weak positivity* for P504S in the large normal or BPH glands. *Weak positivity* was defined as a single cell or groups of epithelial cells with a discontinuous and weakly granular staining pattern. In the later studies, scant fine granular background staining of epithelial and stromal cells (which cannot be seen at low power magnification [≤100X]) was considered negative. Moreover, small benign glands, which can mimic cancer, including atrophy, basal cell hyperplasia, inflammatory glands, urothelial epithelium/metaplasia and most of adenosis, did not show any expression of P504S. Therefore, when used in conjunction with histologic criteria, the P504S staining patterns should be a useful adjunct in distinguishing benign and malignant glands.
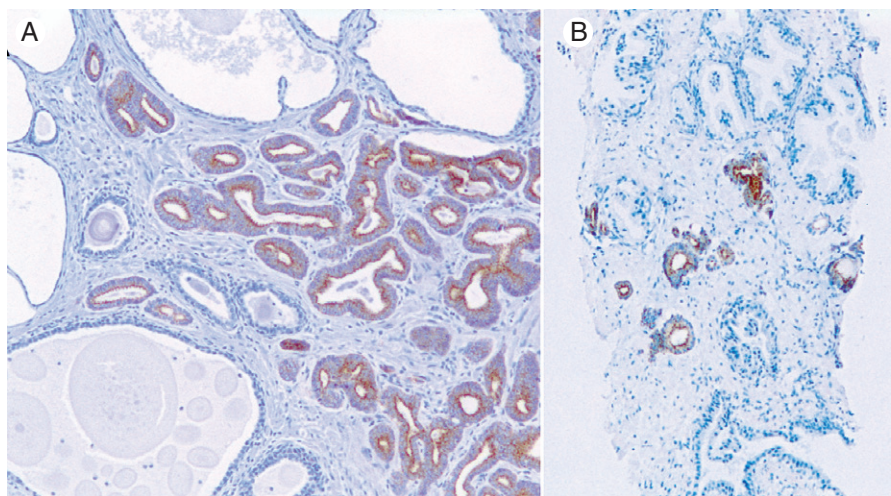
Figure 60 Immunohistochemical stain showing dark brown cytoplasmic P504S staining in malignant glands and negative staining in benign glands (**A**). Several small clusters of malignant glands in the prostate biopsy show positive staining for P504S but no staining in adjacent benign glands (**B**).

P504S/α-Methylacyl-CoA Racemase in High-Grade Prostatic Intraepithelial Neoplasia

High-grade PIN, which consists of architecturally benign prostatic acini or ducts lined by cytologic atypical cells, is considered a procursor of prostate cancer. Cytologic atypical cells show nuclear enlargement, hyperchromatism, and prominent nucleoli. Finding high-grade PIN is clinically significant because the risk of carcinoma on rebiopsy ranges from 27–79% (Davidson *et al.,* 1995; Keetch *et al.,* 1995; Kronz *et al.,* 2001; Shepherd *et al.,* 1996; Weinstein and Epstein, 1993). We have analyzed the expression of P504S in high-grade PIN from 138 cases of radical prostatectomy specimens. Lesions of high-grade PIN were divided as ones adjacent to cancer (HGPINadj, <5 mm) or ones away from cancer (HGPINaw, >5mm). P504S expression was detected in 94.2% (130/138) of HGPIN cases. Interestingly, in terms of percentage cases that are positive, HGPINadj showed a higher AMACR/P504S positive rate than HGPINaw (99.1% versus 86.9%). In terms of percentage of glands that are positive, HGPINadj also showed a higher AMACR/P504S positive rate than HGPINaw (58.6% versus 28.5%). Expression of P504S in high-grade PIN (Beach *et al.,* 2002, Jiang *et al.,* 2001; Luo *et al.,* 2002; Rubin *et al.,* 2002; Zhou *et al.,* 2002) demonstrated that P504S is present not only in the prostate carcinoma but also in its precursor lesion. Significance of studying P504S in high-grade PIN is its diagnostic value and its role in the early development of prostate cancer. First, the presence of P504S immunoreactivity in high-grade PIN suggests caution to exclude PIN before a diagnosis of cancer can be made. Because of the difference in the presence of basal cells in PIN but absence of basal cells in prostate cancer, a combination of P504S and a basal cell marker (34bE12 or p63) is recommended for differential diagnosis. Second, the presence of this enzyme suggests a biochemical link between high-grade PIN and prostate cancer. P504S may also serve as a molecular marker to monitor the early development of prostate cancer and its precursor lesions.

P504S/α-Methylacyl-CoA Racemase in Atypical Adenomatous Hyperplasia

Atypical adenomatous hyperplasia (AAH) is characterized by a well-circumscribed lobule of closely packed crowded small glands without significant cytologic atypia. Baron first described this lesion in 1941 (Baron and Angrist, 1941). Another synonym, "adenosis," was used to describe this entity by Brawn in 1982.

The prevalence of AAH has been reported to be 1.6% to 19.6% of TURP specimens and 23% of radical prostatectomy specimens (Bostwick *et al.,* 1993; Gaudin and Epstein, 1994; Qian and Bostwick, 1995). This wide range could be the result of variable diagnostic criteria used by different pathologists. Most cases of AAH are found in the prostatic transition zone where low-grade prostatic adenocarcinoma arises. The presence of pale cytoplasm and intraluminal crystalloids is also commonly found in both AAH and low-grade prostatic adenocarcinoma.

AAH can be difficult to distinguish from low-grade prostatic adenocarcinoma because of these similarities. AAH typically lacks significant cytologic atypia despite exhibiting abnormal architectural features similar to that of low-grade prostatic adenocarcinoma. Consequently, AAH can be confused with prostate cancer or a lesion suspicious for prostate cancer. However, the distinction between AAH and carcinoma is imperative because the prognosis and treatment are very different. The presence of patchy basal cells is a characteristic of AAH, which can be demonstrated by immunostaining for high molecular weight cytokeratins (34βE12). In contrast, prostatic adenocarcinoma usually lacks basal cells and rarely expresses high molecular weight keratin. However, basal cell staining alone might not be sufficient in some cases to make a definite disgnosis because patchy basal cell staining can be indistinguishable from negative staining, particularly if the material is limited. Therefore, a marker positive for prostate cancer will be valuable in making a definitive diagnosis.

We studied a total of 40 cases of AAH including 30 prostatectomies, 6 biopsies, and 4 transurethral resections to compare with 20 cases of prostatic carcinomas and 20 cases of BPH (Yang *et al.,* 2002). Immunohistochemistry for a prostate cancer marker P504S and a basal cell specific marker (high molecular cytokeratin, 34βE12) were performed in all the cases. High molecular cytokeratin staining confirmed the presence of patchy basal cells in all 40 cases of AAH. P504S was undetectable in the majority of AAH (33/40, 82.5%), focally expressed in 4/40 (10.0%), or diffusely positive only in 3/40 (7.5%) cases of AAH. It is interesting that two of seven P504S positive cases of AAH were found adjacent to adenocarcinoma. In contrast, all BPHs (20/20, 100%) were negative for P504S and all 20 cases of prostatic carcinomas (100%) showed a diffuse P504S staining pattern. These findings suggest that AAH is a heterogenous entity. The biologic significance of P504S expression in a small subset of AAH remains to be determined. Because 92.5% of AAH cases can be distinguished from prostatic adenocarcinoma in their P504S (negative or focal) expression

patterns, the combination of P504S and 34βE12 will help to distinguish AAH from prostatic adenocarcinoma, particularly in prostate needle biopsy specimens.

P504S/α-Methylacyl-CoA Racemase in Prostatic Carcinoma after Radiation

Radiation therapy can provide curative therapy for certain patients with prostate cancer. Six months after a successful radiation therapy, no residual cancer cells are expected to be found in a biopsy specimen. However, on sections stained with hematoxylin and eosin (H&E), benign epithelial cells in these irradiated glands show nuclear enlargement, prominent nuclear irregularity, and hyperchromasia, which mimic prostate adenocarcinoma (Bostwick *et al.,* 1982). It is critically important to confirm the presence of cancer in the irradiated prostate prior to initiating additional local therapy. It would be helpful to have a positive marker to facilitate the challenging distinction between post-radiation atypia from adenocarcinoma and thus increase diagnostic accuracy.

We studied 80 prostates including 40 radiated prostates (28 adenocarcinomas and 12 benign prostates) and 40 nonradiated prostate specimens (20 adenocarcinomas and 20 benign prostates) (Yang *et al.,* 2003). The specimens were obtained following salvage radical prostatectomy, transurethral resection, and needle biopsy. All 48 cases of carcinoma (28/28 radiated and 20/20 nonradiated specimens) showed strongly positive P504S immunostaining. P504S was negative for all radiated and nonradiated benign prostates and the radiated benign glands adjacent to carcinoma. Basal cell staining (34βE12) confirmed the presence of basal cells in all benign prostates and the absence of basal cells in carcinoma. The results demonstrate that P504S immunostaining facilitates the challenging differentiation between prostatic adenocarcinoma and radiation-induced atypia in benign prostatic epithelium.

P504S/α-Methylacyl-CoA Racemase: A Useful Marker for Diagnosis of Small Foci of Prostatic Carcinoma on Needle Biopsy

Needle biopsy is the most commonly used procedure for the definitive diagnosis of prostate cancer. Each year, millions of prostate needle biopsies are performed around the world. The diagnosis of prostate cancer based by morphologic examination is usually straightforward if the substantial tumor is present in the prostate needle biopsy, but it can be very difficult if there are only a few malignant or atypical glands. With increasing efforts to detect prostate cancer early by mass screening of men, there has been an increasing number of small foci of cancer encountered on prostate needle biopsies. Establishing a definitive diagnosis of malignancy in prostate needle biopsies with very small foci of adenocarcinoma is a major diagnostic challenge for surgical pathologists.

A positive diagnostic marker specific for prostatic adenocarcinoma may enhance our ability to detect limited prostate cancer and reduce errors in diagnosis. Whether small foci of carcinoma can be reliably detected by P504S is a crucial question for its clinical application. We studied 142 prostate needle biopsies, including 73 cases with a small focus of prostatic carcinoma and 69 benign prostates (Jiang *et al.,* 2002). A small focus of prostatic carcinomas was defined as a tumor focus of equal or less than 1 mm in diameter. P504S immunoreactivity was found in 69/73 cases (94.5%) of carcinoma but not in any benign prostates (0/69) or benign glands adjacent to malignant glands (Figure 60B). The 34βE12 immunostaining confirmed the absence of basal cells in the focus of carcinoma in all 73 cases.

The majority of diagnostic problems on prostate needle biopsies are related to small infiltrating malignant glands that are usually graded as Gleason score $3 + 3 = 6$. Several factors contribute to the difficulty in diagnosis of limited prostate cancer on needle biopsy. First, the malignant cells can be limited to a few glands that may be easily overlooked. Second, there is no single histologic feature specific and sufficient for the diagnosis of prostate cancer. The diagnosis is based on the combination of architectural, cytologic, and extracellular material change (Epstein, 1995). Third, many benign prostatic conditions, such as small-crowed glands, atrophy, inflammatory atypia, and basal cell hyperplasia, can mimic prostate cancer histologically (Gaudin and Reuter, 1997). Fourth, the consequences associated with incorrect diagnosis can be serious, such as unnecessary prostatectomy or radiation associated with adverse complications as a result of a false-positive diagnosis or delay of effective treatment as a result of a false-negative diagnosis. Finally, because of sampling variations, a small focus of prostate cancer on biopsy may not necessarily represent a tumor of insignificant volume (Cupp *et al.,* 1995) or the tumor may not be sampled on the rebiopsy. Therefore, it is important to make a definitive diagnosis using limited material if possible.

In our study, most of the cases (>95% of cases) with a minute focus of small infiltrating glands of cancer has a Gleason score $3 + 3 = 6$. Our results indicate that

P504S has potential diagnostic value in assisting pathologists to confirm the diagnosis of limited prostatic adenocarcinoma with Gleason score $3 + 3 = 6$. High-grade (Gleason score >7) prostate cancer with extensive involvement of the prostate can be easily recognized on needle biopsy tissue by routine H&E staining and rarely needs an adjunct study. However, small foci of high-grade prostate cancer occasionally can be seen in needle biopsy. In our study there were three cases of Gleason score >7. One of the cases with Gleason score 8 was negative for P504S. Therefore, the diagnostic value of P504S staining for detecting small foci of high-grade prostate carcinoma needs further investigation.

In summary, P504S immunohistochemistry detects minimal prostatic adenocarcinoma with high specificity and sensitivity in needle biopsy. Using P504S as a positive marker along with basal cell–specific 34βE12 as a negative marker could help to confirm the diagnosis of limited prostate cancer and reduce the chance of misdiagnosis in prostate needle biopsy (Jiang et al., 2002).

Our data showed that more than half of diagnostically uncertain foci were definitively classified when this combination of antibodies was used. Thirty-seven percent of the foci were diagnosed as cancer by at least two pathologists after analysis of the combination of P504S and 34βE12 stains (Jiang et al., 2004). Among the definitive malignant diagnostic foci, 53% of them were resolved by 34βE12 alone. In the remaining 47% of cases, the addition of P504S allowed a definitive diagnosis (Jiang et al., 2004). Our study demonstrated that these complementary immunostainings made a definitive diagnosis possible in the majority of prostatic needle biopsies with suspicious ASAPs by H&E staining. Ten thousand cases of rebiopsies can be avoided by determining their reduction based on the immunostaining of ASAP, even when there is only 1% reduction out of ~1 million needle biopsies performed each year in the United States. Considering the large number of prostate needle biopsies performed in the United States and around the world each year, this reduction rate of rebiopsy is considerable and could have a significant health and economic impact.

Utility of P504S and Basal Cell Immunostaining in Establishing Definite Diagnoses in Prostatic Needle Biopsies Suspicious for Malignancy

In view of the serious consequences of misdiagnosing prostatic adenocarcinoma, it is prudent to render a definite diagnosis only when histologic evidence is unequivocal. Cases with only limited atypia provide a major diagnostic challenge. The term "atypical small acinar proliferation (ASAP) suspicious for but not diagnostic of malignancy" applies to 1.5–9.0% of prostatic needle biopsies that show atypia insufficient for definite diagnosis (Bostwick et al., 1995; Orozco et al., 1998; Renshaw et al., 1998). Although it is not a discrete pathologic entity, ASAP is a valid diagnostic category implying "absolute uncertainty" regarding the diagnosis. Regardless of the rationale for its diagnosis, ASAP conveys a 42–45% predictive value for carcinoma in repeat biopsy (Iczkowski et al., 1998; Shepherd et al., 1996).

In recent studies, we assessed the ancillary utility of P504S/AMACR and keratin 34βE12 immunostaining for reaching definitive diagnosis in prostatic needle biopsies suspicious for malignancy (Jiang et al., 2004). Cases containing foci of ASAP based on H&E staining were immunostained with P504S/AMACR and cytokeratin 34βE12. Three urologic pathologists independently assigned diagnoses of cancer, ASAP, HGPIN, or benign.

Cautions for Using P504S in Clinical Diagnosis of Prostate Cancer

Although our findings suggest that P504S is an excellent marker for prostate adenocarcinoma, caution should be exercised in interpreting P504S immunohistochemical results for several reasons.

First, sensitivity of P504S immunostaining showed from 83% to 100% (Beach et al., 2002; Jiang et al., 2001; Luo et al., 2002; Rubin et al., 2002; Zhou et al., 2002). Negative P504S staining in small suspicious glands does not necessarily render a benign diagnosis. Although it is uncommon, focal nonreactivity of P504S has been previously reported in prostate cancer in prostatectomy specimens (Jiang et al., 2002). Our suggestion is to combine routine H&E staining with P504S and basal cell stains in difficult cases. We routinely cut five sections of the prostate biopsies. Levels of 1, 3, and 5 are stained with H&E, and levels of 2 and 4 are saved for immunostaining of P504S and high molecular weight cytokeratin.

Second, background P504S staining in smooth muscle and weak granular staining in benign glands have been reported (Jiang et al., 2002) and could lead to false-positive results. However, in our hands this pattern of staining can be readily distinguished from dark and circumferential positive staining pattern of malignant glands. Because benign glands are stained with basal cells, combination of P504S and high molecular weight

cytokeratin can easily rule out benign or PIN diagnoses if both markers are positive in the same gland.

Third, two possible premalignant lesions, high-grade PIN (Beach *et al.,* 2002; Jiang *et al.,* 2002; Luo *et al.,* 2002; Rubin *et al.,* 2002; Zhou *et al.,* 2002) and atypical adenomatous hyperplasia (Yang *et al.,* 2002), may exhibit some reactivity for P504S to less degree based on our recent studies. However, because both PIN and AAH retain basal cells, positive immunostaining for 34βE12 can help to distinguish PIN and AAH from prostate cancer.

Pathogenesis of P504S/α-Methylacyl CoA Racemase in Development of Prostate Carcinoma

Epidemiologic and animal studies have shown an association between dietary factors and increased risk for prostate cancer. Although increased fat content has been observed in prostate cancer cells, the molecular mechanism of this association is unclear. P504S/AMACR, an essential enzyme for the degradation of branched-chain fatty acids by β-oxidation, catalyzes the conversion of several (2*R*)-methyl-branched-chain fatty acyl-CoAs to their (*S*)-stereoisomers (Ferdinandusse *et al.,* 2000). High levels of branched-chain fatty acids have been found in some dietary sources such as beef, milk, and dairy products. Accumulation of branched-chain fatty acids in prostatic epithelium may lead to increased levels of AMACR. The discovery of P504S/AMACR overexpression in prostate cancer suggests that a role for P504S/AMACR and branched-chain fatty acids in the development of prostate cancer should be further investigated.

In conclusion, advances in molecular biology have been translated into significant progress in clinical medicine. One of the most powerful new techniques is genetic profiling using microarray (gene chip) technology. Our and other groups have demonstrated that P504S/AMACR is a sensitive and specific positive marker for prostate carcinoma in formalin-fixed and paraffin-embedded tissue sections using routine immunohistochemical procedure. It is the first gene identified from prostate cancer by cDNA microarrays to be suitable for clinical practice and to improve the diagnosis of prostate cancer.

References

Baron, E., and Angrist, A. 1941. Incidence of occult adenocarcinoma of the prostate after 50 years of age. *Arch. Pathol. 32*:787–793.

Beach, R., Gown, A.M., De Peralta-Venturina, M.N., Folpe, A.L., Yaziji, H., Salles, P.G., Grignon, D.J., Fanger, G.R., and Amin, M.B. 2002. P504S immunohistochemical detection in 405 prostatic specimens including 376 18-gauge needle biopsies. *Am. J. Surg. Pathol. 26*:1588–1596.

Beckett, M.L., Lipford, G.B., Haley, C.L., Schellhammer, P.F., and Wright, G.L., Jr. 1991. Monoclonal antibody PD41 recognizes an antigen restricted to prostate adenocarcinomas. *Cancer Res. 51*:1326–1333.

Bostwick, D.G., Egbert, B.M., and Fajardo, L.F. 1982. Radiation injury of the normal and neoplastic prostate. *Am. J. Surg. Pathol. 6*:541–551.

Bostwick, D.G., Qian, J., and Frankel, K. 1995. The incidence of high grade prostatic intraepithelial neoplasia in needle biopsies. *J. Urol. 154*:1791–1794.

Bostwick, D.G., Srigley, J., Grignon, D., Maksem, J., Humphrey, P., van der Kwast, T. H., Bose, D., Harrison, J., and Young R.H. 1993. Atypical adenomatous hyperplasia of the prostate: Morphologic criteria for its distinction from well-differentiated carcinoma. *Hum. Pathol. 24*:819–832.

Brawer, M.K., Peehl, D.M., Stamey, T.A., and Bostwick, D.G. 1985. Keratin immunoreactivity in the benign and neoplastic human prostate. *Cancer Res. 45*:3663–3667.

Brawn, P.N. 1982. Adenosis of the prostate: A dysplastic lesion that can be confused with prostate adenocarcinoma. *Cancer 49*:826–833.

Cupp, M.R., Bostwick, D.G., Myers, R.P., and Oesterling, J.E. 1995. The volume of prostate cancer in the biopsy specimen cannot reliably predict the quantity of cancer in the radical prostatectomy specimen on an individual basis. *J. Urol. 153*:1543–1548.

Davidson, D., Bostwick, D.G., Qian, J., Wollan, P.C., Oesterling, J.E., Rudders, R.A., Siroky, M., and Stilmant, M. 1995. Prostatic intraepithelial neoplasia is a risk factor for adenocarcinoma: Predictive accuracy in needle biopsies. *J. Urol. 154*:1295–1299.

Dhanasekaran, S.M., Barrette, T.R., Ghosh, D., Shah, R., Varambally, S., Kurachi, K., Pienta, K.J., Rubin, M.A., and Chinnaiyan, A.M. 2001. Delineation of prognostic biomarkers in prostate cancer. *Nature 412*:822–826.

DiGiuseppe, J.A., Sauvageot, J., and Epstein, J.I. 1997. Increasing incidence of minimal residual cancer in radical prostatectomy specimens. *Am. J. Surg. Pathol. 21*:174–178.

Edwards, J.J., Anderson, N.G., Tollaksen, S.L., von Eschenbach, A.C., and Guevara, J., Jr. 1982. Proteins of human urine. II. Identification by two-dimensional electrophoresis of a new candidate marker for prostatic cancer. *Clin. Chem. 28*:160–163.

Epstein, J., and Yang, X. 2002. *Prostate Biopsy Interpretation.* Philadelphia: Lippincott Williams & Wilkins, 64–91.

Epstein, J.I. 1995. Diagnostic criteria of limited adenocarcinoma of the prostate on needle biopsy. *Hum Pathol. 26*:223–229.

Ferdinandusse, S., Denis, S., IJlst, L., Dacremont, G., Waterham, H.R., and Wanders, R.J. 2000. Subcellular localization and physiological role of alpha-methylacyl-CoA racemase. *J. Lipid. Res. 41*:1890–1896.

Gaudin, P.B., and Epstein, J.I. 1994. Adenosis of the prostate. Histologic features in transurethral resection specimens. *Am. J. Surg. Pathol. 18*:863–870.

Gaudin, P.B., and Reuter, V.E. 1997. Benign mimics of prostatic adenocarcinoma on needle biopsy. *Anat. Pathol. 2*:111–134.

Gown, A.M., and Vogel, A.M. 1984. Monoclonal antibodies to human intermediate filament proteins. II. Distribution of filament proteins in normal human tissues, *Am. J. Pathol. 114*:309–321.

Hasui, Y., Marutsuka, K., Asada, Y., Ide, H., Nishi, S., and Osada, Y. 1994. Relationship between serum prostate specific antigen and histological prostatitis in patients with benign prostatic hyperplasia. *Prostate 25*:91–96.

Horoszewicz, J.S., Kawinski, E., and Murphy, G.P. 1987. Monoclonal antibodies to a new antigenic marker in epithelial prostatic cells and serum of prostatic cancer patients. *Anticancer Res. 7*:927–935.

Iczkowski, K.A., Bassler, T.J., Schwob, V.S., Bassler, I.C., Kunnel, B.S., Orozco, R.E., and Bostwick, D.G. 1998. Diagnosis of "suspicious for malignancy" in prostate biopsies: Predictive value for cancer. *Urology 51*:749–757; discussion 757–758.

Jiang, Z., Iczkowski, K.A., Woda, B.A., Tretiakova, M., and Yang, X.J. 2004. P504S immunostaining boosts diagnostic resolution of "suspicious" foci in prostatic needle biopsy specimens. *Am. J. Clin. Pathol. 121*:99–107.

Jiang, Z., Woda, B.A., Rock, K.L., Xu, Y., Savas, L., Khan, A, Pihan, G., Cai, F., Babcook, J.S., Rathanaswami, P., Reed, S.G., Xu, J., and Fanger, G.R. 2001. P504S: A new molecular marker for the detection of prostate carcinoma. *Am. J. Surg. Pathol. 25*:1397–1404.

Jiang, Z., Wu, C.L., Woda, B.A., Dresser, K., Xu, J., Fanger, G.R., and Yang, X.J. 2002. P504S/alpha-methylacyl-CoA racemase: A useful marker of diagnosis of small foci of prostatic carcinoma on needle biopsy. *Am. J. Surg. Pathol. 26*:1169–1174.

Keetch, D.W., Humphrey, P., Stahl, D., Smith, D.S., and Catalona, W.J. 1995. Morphometric analysis and clinical followup of isolated prostatic intraepithelial neoplasia in needle biopsy of the prostate. *J. Urol. 154*:347–351.

Kim, Y.D., Robinson, D.Y., Manderino, G.L., Tribby, II, and Tomita, J.T. 1989. Molecular characterization of the epitope in prostate and breast tumor-associated PR92 antigen. *Cancer Res. 49*:2379–2382.

Kronz, J.D., Allan, C.H., Shaikh, A.A., and Epstein, J.I. 2001. Predicting cancer following a diagnosis of high-grade prostatic intraepithelial neoplasia on needle biopsy: Data on men with more than one follow-up biopsy. *Am. J. Surg. Pathol. 25*:1079–1085.

Landis, S.H., Murray, T., Bolden, S., and Wingo, P.A. 1999. Cancer statistics, 1999. *CA Cancer J. Clin. 49*:8–31, 1.

Luo, J., Zha, S., Gaga, W. R., Dunn, T.A., Hicks, J.L., Bennett, C.J., Ewing, C.M., Platz, E.A., Ferdinandusse, S., Wanders, R.J., Trent, J.M., Isaacs, W.B., and De Marzo, A.M. 2002. Alpha-methylacyl-CoA racemase: A new molecular marker for prostate cancer. *Cancer Res. 62*:2220–2226.

Nadler, R.B., Humphrey, P.A., Smith, D.S., Catalona, W.J., and Ratliff, T.L. 1995. Effect of inflammation and benign prostatic hyperplasia on elevated serum prostate specific antigen levels. *J. Urol. 14*:407–413.

Oesterling, J.E., Brendler, C.B., Epstein, J.I., Kimball, A.W., Jr., and Walsh, P.C. 1987. Correlation of clinical stage, serum prostatic acid phosphatase and preoperative Gleason grade with final pathological stage in 275 patients with clinically localized adenocarcinoma of prostate. *J. Urol. 138*:92–98.

Orozco, R., O'Dowd, G., Kunnel, B., Miller, M.C., and Veltri, R.W. 1998. Observations on pathology trends in 62,537 prostate biopsies obtained from urology private practices in the United States. *Urology 51*:186–195.

Polascik, T.J., Oesterling, J.E., and Partin, A.W. 1999. Prostate specific antigen: A decade of discovery—what we have learned and where we are going. *J. Urol. 162*:293–306.

Qian, J., and Bostwick, D.G. 1995. The extent and zonal location of prostatic intraepithelial neoplasia and atypical adenomatous hyperplasia: Relationship with carcinoma in radical prostatectomy specimens. *Pathol. Res. Pract 191*:860–867.

Renshaw, A.A., Santis, W.F., and Richie, J.P. 1998. Clinicopathological characteristics of prostatic adenocarcinoma in men with atypical prostate needle biopsies. *J. Urol. 159*:2018–2021; discussion 2022.

Rubin, M.A., Zhou, M., Dhanasekaran, S.M., Varambally, S., Barrette, T.R., Sanda, M.G., Pienta, K.J., Ghosh, D., and Chinnaiyan, A.M. 2002. alpha-Methylacyl coenzyme A racemase as a tissue biomarker for prostate cancer. *JAMA 287*:1662–1670

Shepherd, D., Keetch, D.W., Humphrey, P.A., Smith, D.S., and Stahl, D. 1996. Repeat biopsy strategy in men with isolated prostatic intraepithelial neoplasia on prostate needle biopsy. *J. Urol. 156*:460–462; discussion 462–463.

Signoretti, S., Waltregny, D., Dilks, J., Isaac, B., Lin, D., Garraway, L., Yang, A., Montironi, R., McKeon, F., and Loda, M. 2000. p63 is a prostate basal cell marker and is required for prostate development. *Am. J. Pathol. 157*:1769–1775.

Tang, D.G., and Honn, K.V. 1994. 12-Lipoxygenase, 12(S)-HETE, and cancer metastasis. *Ann. N. Y. Acad. Sci. 744*:199–215.

Teni, T.R., Sheth, A.R., Kamath, M.R., and Sheth, N.A. 1988. Serum and urinary prostatic inhibin-like peptide in benign prostatic hyperplasia and carcinoma of prostate. *Cancer Lett. 43*:9–14.

Thomas, D.J., Robinson, M., King, P., Hasan, T., Charlton, R., Martin, J., Carr, T.W., and Neal, D.E. 1993. p53 expression and clinical outcome in prostate cancer. *Br. J. Urol. 72*:780–781.

Wang, M.C., Valenzuela, L.A., Murphy, G.P., and Chu, T.M. 1982. A simplified purification procedure for human prostate antigen. *Oncology 39*:1–5.

Weinstein, M.H., and Epstein, J.I. *1993* Significance of high-grade prostatic intraepithelial neoplasia on needle biopsy. *Hum. Pathol. 24*:624–629.

Wojno, K.J., and Epstein, J.I. 1995. The utility of basal cell-specific anti-cytokeratin antibody (34 beta E12) in the diagnosis of prostate cancer. A review of 228 cases. *Am. J. Surg. Pathol. 19*:251–260.

Wright, G.L., Jr., Beckett, M.L., Lipford, G.B., Haley, C.L., and Schellhammer, P.F. 1991. A novel prostate carcinoma-associated glycoprotein complex (PAC) recognized by monoclonal antibody TURP-27. *Int. J. Cancer 47*:717–725.

Xu, J., Stolk, J.A., Zhang, X., Silva, S.J., Houghton, R.L., Matsumura, M., Vedvick, T.S., Leslie, K.B., Badaro, R., and Reed, S.G. 2000. Identification of differentially expressed genes in human prostate cancer using subtraction and microarray. *Cancer Res. 60*:1677–1682.

Yang, X., Laven, R., Tretiakova, M., Steinberg, G., Blute, R.D. Jr., Woda, B., and Jiang, Z. 2003. Detection of alpha-methylacyl-CoA racemase/P540S in postradiation prostatic adenocarcinoma after radiation. *Urology 62*:282–286.

Yang, X.J., Wu, C.L., Woda, B.A., Dresser, K., Tretiakova, M., Fanger, G.R., and Jiang, Z. 2002. Expression of alpha-Methylacyl-CoA racemase (P504S) in atypical adenomatous hyperplasia of the prostate. *Am. J. Surg. Pathol. 26*:921–925.

Young, R., Sringley, J., and Amin, M. 2000. Tumors of the prostate glands, seminal vesicles, male urethra, and penis. Washington, D.C.: Armed Forces Institute of Pathology, 154–175, 289–344.

Zhou, M., Chinnaiyan, A.M., Kleer, C.G., Lucas, P.C., and Rubin, M.A. 2002. Alpha-Methylacyl-CoA racemase: A novel tumor marker over-expressed in several human cancers and their precursor lesions. *Am. J. Surg. Pathol. 26*:926–931.

This Page Intentionally Left Blank

11

Role of Somatostatin Receptors in Prostate Carcinoma

Jens Hansson

Introduction

Despite the high incidence of prostate cancer, knowledge and understanding of its pathophysiology remains rudimentary. The main treatment of advanced prostate cancer, androgen withdrawal, eventually is ineffective because virtually all tumors relapse as androgen-independent metastatic disease (Murphy *et al*., 1997). The prostate, however, is not only under androgen control; the homeostasis of the organ is maintained by several other regulatory factors. Knowledge of these other systems is necessary to arrive at an understanding about what causes prostate cells to become malignant and how to effectively treat the disease. Growth factors and neuropeptides can have a stimulatory or an inhibitory role to play in the regulation of cell proliferation, and alterations to their secretion, degradation, and receptor expression may be contributory factors to the development and progression of prostate cancer. Insight into the role of aberrantly regulated pathways during androgen-independent progression will supply crucial information regarding androgen-independent growth and may supply therapeutic possibilities. Evidence is now emerging that increased signaling through growth factors and neuropeptides may lead to aberrant regulation of kinase and phosphatase activity and contribute to the development of androgen indpendence (Culig *et al*., 1994; Jongsma *et al*., 2000a).

The regulatory peptide somatostatin may decrease secretion of mitogenic agents and block receptor and intracellular kinase activity, in part through activation of various phosphatases, resulting in repressed tumor growth. Investigations into the role of somatostatin in prostate biology may supply possibilities to interfere with androgen-independent proliferative and survival pathways, ultimately leading to better therapeutic treatment of refractory prostate cancer.

Somatostatin (SST) is expressed by a subset of neuroendocrine (NE) cells of the prostate (di Sant'Agnese and de Mesy Jensen, 1984), in addition to several other tissues where it has been found to function as an inhibitor of endocrine and exocrine secretory processes, neurotransmission, and proliferation, but also as a stimulator of apoptosis. These effects are mediated by five different G-protein coupled SST-receptors (SSTR1–5), which bind the naturally occurring peptides somatostatin-14 (SST-14) and somatostatin-28 (SST-28) with similar affinity, affecting a diversity of signaling pathways including adenylate cyclase and cyclic adenosine monophosphate (cAMP), protein phosphotases (PPs), potassium and calcium channels, and MAP-kinases such as Erk1/2 and p38 (Patel, 1999). SST-receptors are widely distributed throughout many tissues, ranging from the brain and pituitary to the pancreas, thyroid, and gut, where it controls the release of several compounds including growth

hormone (GH) and insulin. SST-receptors have been described in a variety of human tumors, including pituitary adenomas, gastroenteropancreatic tumors, breast and kidney tumors, and neuroblastomas. SSTR2-positive tumors may be visualized *in vivo* by the use of SST scintigraphy, using radiolabeled SSTR2-preferring analogs such as octreotide, and SST-analogs may control cell proliferation and apoptosis in several tumors (Schally, 1988).

The presence of SST binding sites in the prostate was shown as early as in the 1990s (Srkalovic *et al.*, 1990), and native SST inhibits proliferation of prostatic cancer cells *in vitro* (Brevini *et al.*, 1993). However, clinical trials using SST analogs, targeting the SSTR2 subtype, have demonstrated disparate results (Kalkner *et al.*, 1998; Logothetis *et al.*, 1994; Maulard *et al.*, 1995), and conflicting data regarding the occurrence of the specific receptor subtypes are found in the literature. The presence of messenger ribonucleic acid (mRNA) for *SSTR2* has been detected by reverse transcription polymerase chain reaction (RT-PCR) in cultured prostatic cell lines, and *SSTR1*, *2*, and *5* has been found in homogenates from prostate cancers (Halmos *et al.,* 2000; Munkelwitz *et al.*, 1997). However, by using SST-radioligand binding assays on prostate tissue sections, Reubi and collaborators (Reubi *et al.*, 1995) showed that primary prostatic cancer cells preferentially bind SST-28 rather than the synthetic peptide octreotide, which only binds to SSTR subtype 2 with high affinity and to SSTR subtype 5 and 3 with moderate affinity. This suggests that SSTR subtypes 1 and/or 4 are the predominately expressed subtypes in malignant epithelial cells. Indeed, although not able to detect *SSTR2* or *SSTR3*, Reubi and co-workers detected *SSTR1* mRNA in malignant primary prostate cells (Reubi *et al.*, 1995). To investigate possible *SSTR4* expression and localization, and to resolve the conflicting data found in the literature regarding *SSTR2*-expression, we performed nonradioactive *in situ* hybridization for *SSTR2* and *SSTR4* in prostatic tissues.

MATERIALS

1. Template deoxyribonucleic acid (DNA): Purified human DNA from healthy subjects (e.g., from blood samples) or plasmid clones containing full-length human *SSTR2* and *SSTR4* genes (SSTR complementary DNA [cDNA] clones may be available from Invitrogen or Clontech, for example).

2. Sense and antisense oligonucleotide primers (Invitrogen Ltd, UK) directed against *SSTR2* and *SSTR4*, with 5′ extensions containing sequences for T7 and T3 ribonucleic acid (RNA) polymerase promoters. The oligonucleotide sequence should be as follows: (bacteriophage promoters in italics) 5′*TTAACCCTCACTAAAGGG*TCATCAAGGT-GAAGTCCTCTGG3′ for *SSTR2/T3* sense, 5′*TAAT-ACGACTCACTATAGGG*AGATACTGGTTTGGAGG TCTCCA3′ for *SSTR2/T7* antisense, 5′*TTAACCCT-CACTAAAGGG*GGGCATGGTCGCTATCCAGTGC3′ for *SSTR4/T3* sense, and 5′*TAATACGACTCAC-TATAGGG*GACCAGGCCGGGTGTGG-CCACT-GCAG3′ for *SSTR4/T7* antisense. GenBank accession no. M81830 (*SSTR2*), L07833 (*SSTR4*).

3. PCR mixture: 50 μl reactions containing 10 ng template SSTR-plasmid (or 500 ng purified human DNA), 2.5 units HotStarTaq DNA polymerase (Qiagen, West Sussex, UK), 0.5 μM each of sense and antisense SSTR-primers, 200 μM each of dATP, dGTP, dCTP, dTTP, and 1.5 mM $MgCl_2$, and 1x HotStarTaq PCR buffer (Qiagen) in thin-walled 0.2 ml PCR tubes (Eppendorf).

4. Agarose gel, 1.5%: dissolve 1.5 g agarose in 100 ml 1X (TBE) buffer under heat, cool down to 60ºC, add 5 μl ethidium bromide (10 mg/ml stock solution), and cast the gel.

5. Tris-borate EDTA buffer (TBE): 5X stock contains 54 g Tris-base, 27.5 g boric acid, 20 ml 0.5 M EDTA (pH 8.0), and bring to 1 L.

6. EDTA, 0.5M: add 93.05 g $Na_2EDTA\times2H_2O$ to 300 ml distilled water, adjust to pH 8.0 by using 10 M NaOH, and bring to 500 ml.

7. Nucleic acids Precipitation Solution: a 0.1:2 (v/v) mixture of 5M ammonium acetate (pH 5.3):ethanol.

8. Ammonium acetate, 5M: mix 38.54 g of ammonium acetate with 50 ml water to dissolve, adjust the pH to 5.3, and bring to 100 ml.

9. GenElute spin columns (Sigma-Aldrich).

10. All buffers and reagents for RNA use should be made with diethyl pyrocarbonate (DEPC) or with DEPC-treated and autoclaved water. Make a 0.1% DEPC-solution in distilled water/buffer and allow to stand overnight at room temperature, then autoclave the solution.

11. 5M NaCl: dissolve 146.1 g NaCl in H_2O, and bring to 500 ml.

12. 1M $MgCl_2$: dissolve 40.66 g $MgCl_2\times6H_2O$ in H_2O, and bring to 200 ml.

13. Tris-Hcl, 1M (pH 7.5 and 9.5): dissolve 60.55 g Tris in 400 ml DEPC-water, adjust the pH to 9.5 or 7.5 with concentrated HCl, and bring to 500 ml with DEPC-water.

14. 1M $CaCl_2$: dissolve 29.4 g $CaCl_2\times2H_2O$ in H_2O, and bring to 200 ml.

15. Phosphate buffer saline (PBS): 10X contains 81.76 g NaCl, 12.46 g $Na_2HPO_4\times2H_2O$, 4.14 g $NaH_2PO_4\times H_2O$, bring to 1 L, and adjust the pH to 7.2–7.5.

16. Saline-sodium citrate (SSC): 20X stock contains 175 g NaCl, 88 g sodium citrate (Na$_3$ citrate). Dissolve in 800 ml H$_2$O, adjust the pH to 7.0 with 10 M NaOH, and adjust the volume to 1 L.

17. MOPS-buffer: 10X stock contains 41.86 g morpholino propane sulfonic acid (MOPS), 6.80 g sodium acetate, 3.72 g Na$_2$EDTA×2H$_2$O, 3.80 g ethylene glycol-bis (2-aminoethylether)-N,N,N′,N′-tetraacetic acid (EGTA). Mix with 850 ml H$_2$O, adjust pH to 7 with 10 M NaOH, and adjust final volume to 1 L. Store in the dark.

18. *In vitro* Transcription and Labeling Mixture: 20 μl reactions containing 25 units of either T3 or T7 RNA Polymerase (Roche Diagnostics, Bromma, Sweden); 1X transcription buffer (RNA Color kit; Amersham Pharmacia Biotech, Sweden) containing 40 mM Tris-HCl (pH 7.5), 6 mM MgCl$_2$, 2 mM spermidine, and 0.01% (w/v) bovine serum albumin (BSA); 1X nucleotide mixture containing fluorescein-11-UTP, UTP, ATP, CTP, and GTP, and 20 units of human placental ribonuclease inhibitor; and finally 10 mM fresh DTT.

19. Cold *in vitro* Transcription Mixture: as in **Step 18** but use 1X nucleotide mixture containing unlabeled UTP, ATP, CTP, and GTP (Roche Diagnostics) instead of the 1X labeled nucleotide mixture (Amersham).

20. RNase-free DNAse (Roche Diagnostics).

21. Hybond-N+ membrane (Amersham Pharmacia Biotech).

22. RNA gel, 2.0%: dissolve 2.0 g agarose in 100 ml 1X MOPS-buffer under heat, cool down, and cast the gel.

23. Tracking dye buffer: 50% glycerol, 1 mM EDTA, 0.6% bromophenol blue, 0.6% xylene cyanol.

24. Glyoxal sample buffer and GelStar (Bio Whitaker Molecular Applications, Vallensbaek, Denmark).

25. Tris EDTA buffer (TE-buffer): combine 500 μl 1M Tris-Cl (pH 7.5–8.0) with 10 μl 0.5 M EDTA, and bring to 50 ml.

26. Slot-blot: plasmid clones or PCR-derived DNA, containing full-length human *SSTR1-5* genes, flanked by phage promoters, or purified human RNA from tissues rich in *SSTR1-5*.

27. Hybridization buffer: 50 ml deionized formamide, 1 ml Tris-HCl (pH 7.5), 1X Denhardt's solution (BSA, polyvinylpyrrolidone, and ficoll, all at 0.2 mg/ml), 10 ml 20X SSC, and 40 μg salmon sperm, and bring to 100 ml. Filter through a 2 um nitrocellulose filter, and store at –20ºC.

28. Tris buffered saline (TBS): mix 100 ml 1M Tris-HCl (pH 7.5) with 80 ml 5M NaCl, and bring to 1 L.

29. Blocking solution: blocking reagent (from the RNA Color kit) 0.5% (w/v) in TBS-buffer.

30. Anti-fluorescein alkaline phosphatase conjugate solution: anti-fluorescein alkaline phosphatase conjugate (from the RNA Color kit), diluted 1:5000 (slot-blot) or 1:1000 (*in situ*) in TBS, and 0.5% BSA.

31. Detection buffer: mix 100 ml 1M Tris-HCl (pH 9.5) with 20 ml 5M NaCl and 50 ml 1M MgCl$_2$, and bring to 1 L.

32. Detection Solution: detection buffer containing 1 mmol/L levamisol, 0.33 mg/ml nitroblue tetrazolium chloride (NBT), and 0.175 mg/ml 5-bromo-4-chloro-3-indolyl phosphate (BCIP).

33. Stop buffer: mix 10 ml 1M Tris-HCl (pH 7.5) with 20 ml 0.5M EDTA and 30 ml 5M NaCl, and bring to 1 L.

34. Isopentane/2-methylbutene, flat pieces of cork, and Tissue-Tek (Sakura Finetek, Zoeterwoude, The Netherlands).

35. SuperFrost Plus slides (Menzel-Gläser, Germany).

36. Bouin's fixative: mix 75 ml saturated picric acid with 25 ml formaldehyde (37% w/w) and 5 ml glacial acetic acid.

37. 4% Paraformaldehyde-PBS (PF-PBS): dissolve 8 g paraformaldehyde in 100 ml H$_2$O under heat (60ºC). Add 10M NaOH until the solution becomes clear, and cool down. Add 20 ml 10X PBS and 80 ml H$_2$O, and filter through a 2 μm nitrocellulose filter. Store at 4ºC or in a freezer.

38. Digestion solution: dissolve 1 mg proteinase K in 10 ml 1M Tris-HCl (pH 7.5), 1 ml 1M CaCl$_2$, and bring to 500 ml.

39. Acetic anhydride solution: mix 5 ml 1M triethanolamine (TEA) with 1.5 ml 5M NaCl and 125 μl acetic anhydride, and bring to 50 ml. Make fresh in a vial protected from light.

40. Hematoxylin, Eosin and Faramount Mounting Medium (Dako A/S, Denmark).

Additional materials required include various glassware and plasticware, pipettes, thermal cycler (e.g., Mastercycler Gradient, Eppendorf, Bergman & Beving Instrument AB, Upplands Väsby, Sweden), 254 nm transilluminator (UVP, Upland, CA, spectrophotometer (e.g., GeneQuant; Amersham Pharmacia Biotech, Uppsala, Sweden), slot-blot apparatus (e.g., Minifold II, Schleicer and Schuells), cross-linker (UVP), hybridization oven (Hybaid, USA). All chemicals were from Sigma-Aldrich (Sigma-Aldrich Sweden AB, Stockholm, Sweden), unless otherwise stated. Plasmid clones for the full-length human SSTR1-5 genes were kindly provided by Dr. Graeme I. Bell, Chicago, IL, by Dr. Susumu Seino, Chiba, Japan, and by Dr. Friedrich Raulf, Basel, Switzerland (Rohrer *et al*., 1993; Yamada *et al*., 1992a; Yamada *et al*., 1992b; Yamada *et al*., 1993).

METHOD

In this report, we present a step-by-step protocol for nonradioactive *in situ* hybridization using fluorescein-labeled RNA probes. This protocol has been optimized to give strong and specific signals, enabling detection and discrimination between related sequences of low-copy mRNA. Choosing the right type of probe is essential for a good final result, as is tissue procurement including fixation method and duration. This protocol allows the researcher to detect low-copy mRNA not only in frozen tissues, but also in paraffin-embedded tissues. By incubating tissue intended for *in situ* hybridization in a buffer with active (not autoclaved) diethylpyrocarbonate, RNases present in the tissue are inactivated, enhancing low-copy mRNA detection (Braissant *et al*., 1996). Riboprobes are preferentially used for low-copy mRNA detection because RNA probes are inherently single stranded and have the highest stability of possible nucleic acid hybrids (Buvoli *et al*., 1987). Labeled RNA probes may be obtained by *in vitro* transcription of DNA in the presence of tagged nucleotides. Fluorescein-tagged nucleotides are preferable, because the incorporation of label can be directly monitored, and because chromogenic *in situ* detection can easily be applied using enzyme-conjugated anti-fluorescein antibodies. The riboprobe template DNA should contain sequences for the hybridizing probe but also flanking sequences for phage transcription promoters such as T3 or T7. This protocol generates DNA templates for *in situ* transcription of riboprobes, without the need to subclone into phage transcription vectors or culturing of bacteria, by utilizing phage promoter-primers in a PCR-reaction, allowing the researcher to adjust size and specificity of probes by choice of primers (Bales *et al*., 1993). This protocol further allows investigation of the specificity of synthesized riboprobes by hybridizing the antisense complementary RNA (cRNA) probes against full-length *SSTR1-5* RNA in a slot-blot. One may then use the same probes, buffers, and temperatures in the *in situ* hybridization experiments as in the slot-blots experiments, ensuring that the hybridization signals obtained are specific and not a consequence of cross-hybridization between closely related sequences. Negative and positive control tissues should also be used, together with antisense and sense riboprobes.

Template Generation

1. To synthesize human *SSTR2* and *SSTR4* cRNA probes of appropriate lengths and specificity, riboprobe templates may be generated by PCR from either purified human DNA (which naturally contains intron-less *SSTR2* and *SSTR4* genes) or from vectors carrying cloned *SSTR2* and *SSTR4* genes, using oligonucleotide primers directed against *SSTR2* or *SSTR4*, with 5′ extensions for T7 and T3 RNA polymerase promoters. Add template DNA and respective primer-pairs to thin-walled PCR tubes, together with the other components of the PCR mixture, bringing each reaction to 50 μl. Amplification should then be performed by using an initial denaturing/HotStarTaq activation step at 95ºC for 15 min, and then 30 cycles including denaturation at 94ºC for 30 sec, primer annealing at 68ºC for 45 sec, and primer extension at 72ºC for 1 min, followed by a final extension step at 72ºC for 7 min.

2. Subsequently analyze the PCR products on an 1.5% agarose gel (452 bp for *SSTR2* and 526 bp for *SSTR4*), excise the bands from the gel under ultraviolet (UV) light, and purify the DNA using the GenElute spin columns, removing agarose, unincorporated nucleotides, and enzymes.

3. Precipitate the purified DNA by adding three volumes ice-cold Nucleic Acid Precipitation Solution, put in freezer for 1 hr, and spin down in a tabletop centrifuge at 13000X g for 10 min to pellet the DNA.

4. Wash the DNA pellet by adding 500 μl ice-cold 70% ethanol, vortex, and spin down as in **Step 3**.

5. Discard the supernatant and air-dry the DNA pellet, then dissolve it in DEPC-treated water.

6. Take an aliquot and measure the DNA concentration in a spectrophotometer. Store the rest of the DNA at 4ºC or in freezer for long-time storage.

Riboprobe Synthesis

1. *In vitro* transcribe the PCR-derived riboprobe templates with fluorescein-labeled nucleotides and T7 or T3 RNA polymerase to synthesize nonradioactive *SSTR2* and *SSTR4* antisense or sense cRNA probes, respectively. To a 1.5 ml conical polypropylene tube in the dark, add the *in vitro* Transcription and Labeling Mixture and 1 μg PCR-derived template DNA, and bring to 20 μl using DEPC-water.

2. Mix gently, and incubate the reaction at 37ºC for 2 hr.

3. The synthesized cRNA may now either be stored at –20ºC, or the reaction may be treated with RNase-free DNAse, precipitated, and dissolved in formamide. Add 10 units DNAse to the labeled probe, and mix gently. Incubate at 37ºC for 10 min.

4. Stop the DNAse reaction by adding 1 μl 0.5M EDTA. Precipitate the RNA by adding three volumes ice-cold Nucleic Acid Precipitation Solution, put in freezer for 1 hr, and spin down in a tabletop centrifuge, at 13000X g for 10 min to pellet the cRNA.

5. Wash the cRNA pellet by adding 500 μl ice cold 70% ethanol, vortex, and spin down as in **Step 4.**

6. Discard the supernatant. Air-dry the cRNA pellet, and then dissolve it in 50 μl deionized formamide (protects the RNA from degradation).

7. Estimate fluorescein incorporation and amount of probe by spotting 2 μl aliquots of cRNA from **Step 2** onto a test strip of Hybond-N + membrane. Prepare a 1/5 dilution of the 1X nucleotide mixture as negative control, and spot 5 μl onto the test strip, next to the cRNA. Wash the test strip in 2X SSC at 60ºC for 30 min, then visualize the test strip on a transilluminator next to a TE-buffer-moistened reference strip, spotted with 1/10, 1/25, 1/50, 1/100, and 1/250 dilutions of the 1X nucleotide mixture. The cRNA probe should be equal or greater in intensity than the 1/50 (equals 125 ng/μl) spot on the reference strip, and the negative control spot should not be visible.

8. Determine the length (435bp for *SSTR2* and 509bp for *SSTR4*) and integrity of probes by glyoxal gel electrophoresis: mix up an aliquot (1 μg) of the cRNA with the glyoxal sample buffer (1:1), and incubate for 30 min at 50ºC. Chill on ice for 1 min, then add 1 μl tracking dye. Load the RNA samples into the wells of the gel, and run the gel. Either visualize directly on a UV table (by first soaking the gel in ethidium bromide), or preferably stain with GelStar, first removing the glyoxal by soaking the gel in 0.5 M ammonium acetate for 45 min and performing two washes in TE-buffer, then post-stain with GelStar in 1X MOPS.

9. Aliquote and store the probes in the dark, at –20ºC, until use.

Slot-Blot

1. The specificity of the synthesized *SSTR2* and *SSTR4* antisense riboprobes are evaluated by hybridization against synthesized sense *SSTR1-5* RNA in slot-blots (or use purified RNA from SSTR-rich tissues in Northern Blots) to verify that the hybridization signals are specific and not a consequence of cross-hybridization to related members of the SSTR family. If full-length *SSTR1-5* containing T3/T7-phage vectors are available, linearize them with appropriate restriction enzymes; if not, synthesize *SSTR1-5* riboprobe templates according to the Template Generation Protocol but using primers that give full-length gene products. After linearization of vectors (or synthesis of riboprobe templates), synthesize full-length sense *SSTR1-5* cRNA transcripts according to **Steps 1–8** in the Riboprobe Synthesis Protocol, but use the cold *in vitro* Transcription Mixture at **Step 1**, and omit **Step 7**.

2. Dilute each synthesized *SSTR1-5* cRNA sample in glyoxal sample buffer in tenfold dilution series (e.g., in 5×8 tubes). Heat each sample at 50ºC for 30 min, then chill on ice for 1 min.

3. Now blot the samples onto two separate Hybond-N+ membranes in five rows. A slot-blot apparatus may be used to ease the spacing of the dots in a regular manner. Cross-link the RNA to the membranes in a cross-linker, set at 120 mJ/cm², for 30 sec.

4. Place the membranes on top of a support mesh in a suitable tray containing 2X SSC. Roll up the piles into two tight rolls, inserting each membrane into a hybridization bottle. Add hybridization buffer and prehybridize at 55ºC for 1 hr in a rotating hybridization oven.

5. Add *SSTR2*-antisense riboprobe to one of the bottles, and *SSTR4*-antisense riboprobe to the other bottle, at a concentration of 10 ng/ml hybidiation buffer, and hybridize at 68ºC for *SSTR2*, and at 65ºC for *SSTR4*, for 16 hr. Place a thermometer inside the oven.

6. After hybridization, wash the membranes in preheated 1X SSC (2X 5 min), and then in 0.1X SSC (4X 15 min), at their respective hybridization temperature. Then perform a final wash in 1X SSC, this time at room temperature, on a shaker for 10 min. Subsequently equilibrate the membranes in a container filled with TBS for 10 min.

7. For detection of hybridization signals, incubate the membranes in the Blocking Solution for 1 hr at room temperature. Subsequently rinse the membranes in TBS, then incubate with the anti-fluorescein alkaline phosphatase conjugate solution, on a shaker for 1 hr at room temperature.

8. Wash the membranes in TBS for 5 min, then equilibrate them in Detection Buffer, 2X 5 min. Pour off, and develop the color reaction by adding fresh Detection Solution to the membranes.

9. Stop the reaction when the bands/spots are fully developed, by incubating the membranes in Stop Buffer for at least 10 min. Evaluate staining pattern and sensitivity. Each riboprobe should detect its corresponding receptor subtype sense RNA but not other RNA species. If necessary, adjust hybridization temperature and repeat the protocol.

Tissue Preparation

1. Collect fresh tissue specimens of human prostate, and pancreatic tissue for positive/negative control, working aseptically. It is then preferable to freeze the tissues because the paraffin-embedding procedure causes a loss of RNA.

2. To obtain frozen sections, immediately dissect the tissue into 3–4 mm cubes and place each piece onto a small square of cork, drench the piece in Tissue-Tek, and submerge it into a vial containing isopentane, surrounded and cooled by liquid nitrogen, until the tissue is completely frozen (a few minutes). This technique allows the tissue to retain most of the cellular structures, making pathologic evaluation possible. Transfer the frozen tissues to a –70ºC freezer until analyzed.

3. For paraffin embedding, immediately place 3–4 mm cubes of tissue in excess of Bouin's fixative (for 4–18 hr), then perform subsequent paraffin embedding according to standard procedures.

in situ Hybridization

1. Cut 6 μm thick sections of fresh-frozen, Tissue-Tek embedded specimens. Mount the still frozen sections onto SuperFrost Plus slides, then air-dry for 15 seconds at room temperature, and immediately fix the sections in, 4% PF-PBS (4ºC) on a shaker for 10 min.

2. Cut 4 μm thick sections of paraffin-embedded specimens, mount the sections onto SuperFrost Plus slides, and dry the sections for 2 hr at 65ºC. Then deparaffinize and rehydrate the sections by submerging the slides first in xylene (2X 15 min), then in 99.5% ethanol for 5 min, followed by 5 min in 95% ethanol, and finally in 70% ethanol for 5 min.

3. Incubate all specimens in PBS with 0.1% active (not-autoclaved) DEPC on a shaker for 15 min to inactivate RNases.

4. Repeat **Step 3**, then rinse the slides 2 times in PBS for 5 min.

5. Subsequently submerge the sections in 0.2 mol/L HCl on a shaker for 20 min, then rinse in PBS for 5 min.

6. Bouin-fixed specimens should now be digested with proteinase K (use the Digestion Solution) for 25 min at 37ºC, permeabilizing the tissue, allowing penetration of long riboprobes. Rinse the slides 3 times in PBS.

7. Incubate all slides in freshly prepared 0.25% acetic anhydride solution, blocking basic groups by acetylation and minimizing nonspecific adherence of probes to glass and tissue.

8. Equilibrate the slides on a shaker in 2X SSC.

9. Subsequently subject the slides to the same procedures and buffers as the membranes in the slot-blot protocol, changing only probe and anti-fluorescein alkaline phosphatase conjugate concentration. Cover the bottom of a humid chamber with 2X SSC, place two glass bars into the box, and prehybridize the slides by overlaying each section with hybridization buffer, incubating the slides on top of the glass bars at 55ºC for 1 hr.

10. Drain the hybridization buffer from the slides, and overlay each section with *SSTR2* or *SSTR4* (500 ng/ml for frozen specimens and 1000 ng/ml for Bouin-fixed specimens) antisense/sense riboprobe in hybridization buffer. Cover each section with a square of hydrophobic plastic coverslip (e.g., cut parafilm), and hybridize at 68ºC for *SSTR2*, and at 65ºC for *SSTR4*, for 16 hr. Place a thermometer inside the oven.

11. After hybridization, wash the slides in preheated 1X SSC (2X 5 min), and then in 0.1X SSC (4X 15 min), at their respective hybridization temperature. Then perform a final wash in 1X SSC, this time at room temperature, for 10 min. Subsequently, equilibrate the slides in TBS for 10 min.

12. For detection of hybridization signals, incubate the slides in the Blocking Solution for 1 hr at room temperature. Subsequently rinse the slides in TBS, drain off the fluid, and wipe with a tissue around the sections.

13. Cover and incubate each slide (100 μl) with anti-fluorescein alkaline phosphatase conjugate solution for 1 hr at room temperature.

14. Wash the slides 3 times in TBS for 5 min, then equilibrate them in Detection Buffer, 2X 5 min. Drain and wipe around the sections.

15. Develop the color reaction by adding, to each slide, 500 μl fresh Detection Solution (containing 1 mmo1/L fresh levamisol–inhibiting endogenous alkaline phosphatase activity). Coverslip with parafilm and incubate in the dark.

16. Monitor the reaction by viewing in a microscope. Stop the reaction by submerging the slides in Stop Buffer for 10 min.

17. Coverslip the slides with Faramount mounting medium and evaluate staining.

RESULTS AND DISCUSSION

To elucidate whether prostatic tissues express *SSTR2* and *SSTR4* in terms of mRNA for these receptor species, we performed a study on the distribution and localization of *SSTR2* and *SSTR4* transcripts by *in situ* hybridization. Nonradioactive antisense *SSTR2* and *SSTR4* riboprobes were hybridized to consecutive sections of benign prostatic hyperplasia (BPH) and prostate cancer tissue, generating positive hybridization signals in the cytoplasm of prostatic cells, giving a staining pattern independent of Gleason score. The specificity of the *in situ* hybridization experiments was

ensured by using the same buffers and temperatures as in the slot-blot control experiments, and the specificity of the antisense signals was further corroborated by the occurrence of positive *in situ* hybridization signals in the islets of Langerhans of pancreatic tissue, and negative signals in surrounding pancreatic tissue, whereas negative control sense riboprobes generated no signals in tissues investigated.

Our study showed that *SSTR4* positive signals emerged quickly in the detection solution and that they were confined to the exocrine epithelium of the prostate, giving a very strong cytoplasmic staining, whereas the *SSTR2* probe predominantly hybridized to stromal compartments such as smooth muscles and blood vessels, but also generated weak signals in the exocrine cells of several specimens after somewhat longer incubation in detection solution. In fact, more than 60% of BPH cases showed *SSTR2* positive staining of the secretory epithelium, and this number was increased to more than 80% in prostate cancer tissue, including metastatic lesions. *SSTR4* mRNA species was detected in the majority of BPH cases (75%) and in more

than 90% of malignant cases. Comparing adjacent tumor and BPH glands in the same tissue sections, both receptor forms were found to give stronger signals in cancer cells, *SSTR4* signals being the strongest (Hansson *et al*., 2002) as in Figure 61.

We also wanted to localize protein expression and corroborate the *in situ* data. Conflicting reports based on SST-binding, protein, and mRNA expression data are found in the literature. This may be the result of differential regulation of SST-receptor mRNA and protein, of cellular localization of protein, or in the sensitivity of the techniques. Reubi and co-workers found a lack of correlation between the *SSTR* mRNA amount and receptor density in pituitary adenomas (Schaer *et al*., 1997), and Schonbrunn reported a discrepancy of radioligand binding with immunohistochemical data in brain sections (Schonbrunn, 1999), suggesting receptor internalization. However, using well-characterized antibodies against SSTR1-5 (Helboe *et al*., 1997), we corroborated the *in situ* data for *SSTR2* and *SSTR4* with immunohistochemistry (Dizeyi *et al*., 2002), giving strong stromal but weak
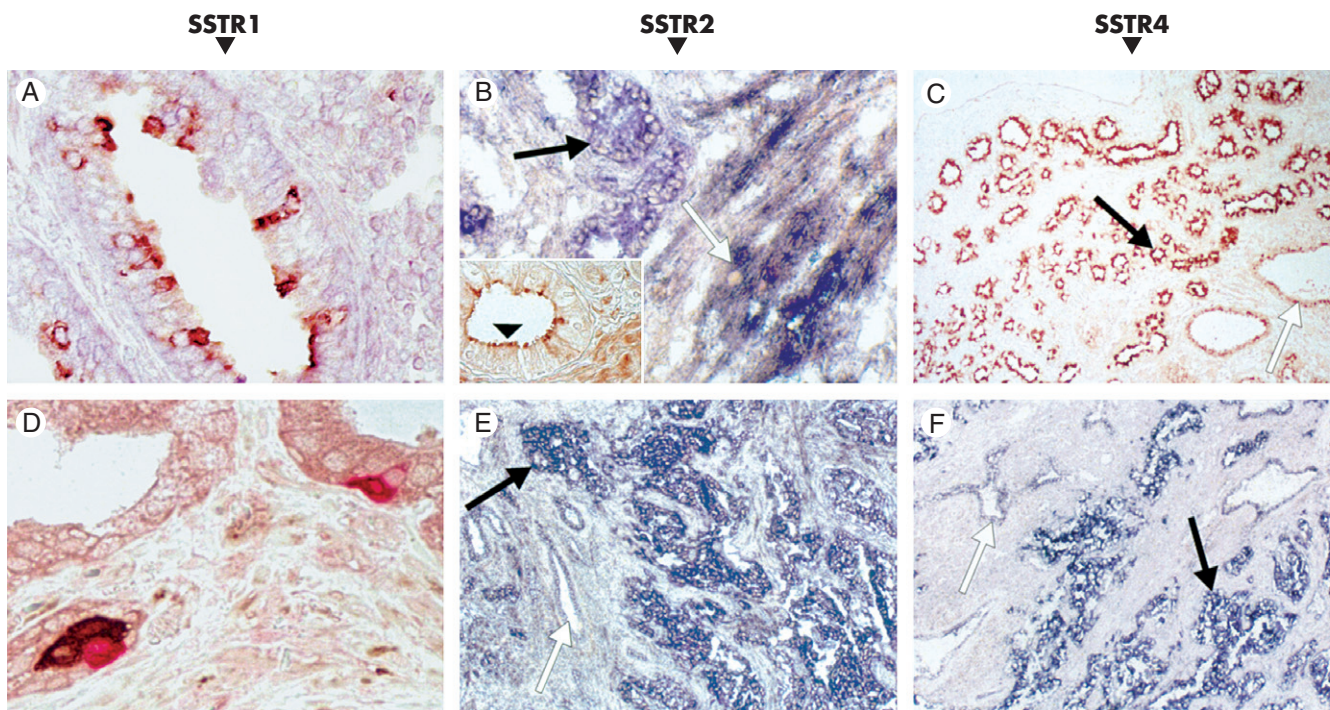
Figure 61 *In situ* hybridization and immunohistochemical localization of somatostatin receptors (SSTRs) in prostatic tissues. SSTR1 protein was detected in a subset of secretory cells (**A**) and was further localized to a subset of neuroendocrine cells (**D**), as visualized by co-localization of diaminobenzidine (DAB) (SSTR1) and Fast Red (CgA, a NE marker). SSTR2 transcripts (**B**) and protein (*inset in **B***) signals predominantly stained the stromal compartement (*white arrow in **B***), but moderate staining was also found in epithelial cells *(black arrow and arrowhead in **B**)*, visualized by NBT/BCIP (messenger ribonucleic acid [mRNA]) and DAB (protein). Note the stronger hybridization signal for SSTR2 in tumor cells *(black arrow in **E**)* than in adjacent benign cells *(white arrow in **E**)*. SSTR4-positive signals were confined to the exocrine epithelium of the prostate, giving the strongest (shortest developing time) SSTR signals in the prostate. SSTR4 protein (**C**) and mRNA (**F**) were found up-regulated in malignant cells *(black arrows in **C** and **F**)* when compared to benign areas *(white arrows in **C** and **F**)*.

epithelial SSTR2 expression and strong SSTR4 expression in the secretory cells with increased signals in cancer compared to BPH (see Figure 61). However, in two cases with poorly differentiated prostate cancer, tumor cells, but not benign cells, were found to be devoid of SSTR4 protein, suggesting that this receptor subtype may be lost in some cases. The SSTR1 specific antibodies supported the results of Reubi *et al.* (1995) that malignant exocrine cells express this receptor form. However, the staining pattern for SSTR1 protein was scattered, staining only a subpopulation of the secretory cells in any given gland, with no differences between benign and malignant areas. In addition, a subpopulation of the NE cells was also stained for SSTR1 protein (see Figure 61). Although antibodies directed against SSTR3 produced weak exocrine staining in a few cases, it was perinuclear and did not stain the plasma membranes and may thus be questioned, especially because RT-PCR has not been able to detect this receptor species in prostatic tissues. RT-PCR has, however, picked up *SSTR5* expression in the prostate (Halmos *et al.*, 2000), but we were unable to detect SSTR5 protein in either prostatic homogenates or tissue sections. This, together with poor octreotide binding, suggests that SSTR5 expression is low or absent in the prostate, and that subtypes 1 and 4 are the two predominant forms expressed by prostatic epithelium, and that SSTR2 is the predominant form in the stromal compartment.

Our results are in agreement with radioligand studies using SST-28 and RT-PCR studies on prostate cancer cell lines but are in contrast to binding data of octreotide of primary prostatic cancers (Reubi *et al.*, 1995). However, our results are in accordance with the findings of Nilsson *et al.* that the majority of prostatic metastatic lesions bind octreotide (Nilsson *et al.*, 1995), implicating SSTR2 expression. Our findings that both *SSTR2* and *SSTR4* are up-regulated in malignant prostate cells as compared to benign epithelium suggests that the discrepancies in octreotide binding may be the result of up-regulation of SSTRs in metastatic lesions as compared to primary cancers. Prostate cancers frequently produce osteoplastic bone metastases, probably in part because of an overexpression of urokinase (uPA) by prostate cancer cells as uPA is strongly mitogenic for osteoblasts. Osteoblasts express the uPA receptor, which activates pro-uPA, as does human kallikrein 2 (hK2). Cleavage of insulin-like growth factor (IGF)-binding proteins occur as a response to activation of uPA, and uPA further induces plasmin hydrolysis of transforming growth factor-beta (TGF-β)-binding proteins, also freeing TGF-β. IGF-I then acts on the tumor cells to stimulate proliferation and enhance their survival and antiapoptotic responses,

whereas TGF-β is a powerful stimulator of osteoblast proliferation (Luo *et al.*, 2002). Although TGF-β inhibits the proliferation of normal prostate cells, it promotes growth in transformed cells. Tumor cells become resistant to TGF-β repressed growth but retain TGF-β induced Smad signaling, enhancing migration and invasiveness. TGF-β induced Smad signaling is, however, also involved in the up-regulation of *SSTR2* transcription in mouse pituitary cells and in human pancreatic cancer cells (Puente *et al.*, 2001), and it is thus possible that SST-receptors are up-regulated in response to TGF-β signaling in prostate cancer, especially in metastatic lesions.

The binding of octreotide may furthermore be stronger *in vivo* than in *in vitro*, as suggested by the findings by Rocheville and co-workers. Their study showed that SSTRs are able to hetrodimerize with distantly related members of the G-protein-coupled receptor family, including the dopamine D2 receptor, as well as with other members of the SSTR family. Such dimerization, and binding of various ligands (e.g., dopamine), may alter the receptor-complex affinity for SST agonists and may also change intracellular signaling (Rocheville *et al.*, 2000a; Rocheville *et al.*, 2000b). It is possible that chimeric SST-dopamine agonists will be used in future treatments of prostate cancer and may increase the anti-tumoral effects. For example, both SST and dopamine are powerful inhibitors of growth hormone (GH) release, and thus GH-stimulated IGF-I release, but also of prolactin. IGF-I and prolactin have been shown to dramatically increase prostatic growth and to increase survival (Kindblom *et al.*, 2002; Ruffion *et al.*, 2003). Joint treatment with SST and dopamine agonists has been reported to exert additive effects on inhibition of prolactin secretion from rat prolactinomas, and in cultures of human acromegalic tumors, the chimeric SST-dopamine molecule BIM-23A387 has been shown to be 50 times more potent on GH inhibition than SST and dopamine analogs used either individually or combined (Saveanu *et al.*, 2002). What consequences this may have for possible treatment of PC with different SSTR targeting compounds remains to be determined, but it is feasible that chimeric SSTR2/D2-targeting molecules may enhance the inhibition of GH-dependent IGF-I release.

Transactivation of the androgen receptor (AR) may be a key event in the development of androgen-independent growth. Androgen independence may result from aberrant expression or activation of components of the AR pathway, including co-regulatory proteins and the AR itself. Evidence is emerging that increased signaling through neuropeptides, cytokines, and growth factors may aid in activation of the

androgen pathway in the absence of androgens or make the AR obliterate by stimulating alternative pathways, compensating for the loss of androgen-mediated proliferation and suppression of apoptosis. The progression to androgen independence appears to involve a switch between paracrine and autocrine stimulation of growth factors and/or NE differentiation (for a review, see Hansson and Abrahamsson, 2001; Hansson and Abrahamsson, 2003). In fact, androgen withdrawal may induce NE differentiation (Jongsma *et al*., 2000b) and may also increase levels of bioactive neuropeptides by down-regulating NEP, a metalloproteinase that cleaves and inactivates neuropeptides (Papandreou *et al.*, 1998). Various neuropeptides and growth factors, including bombesin and IGF-I, have indeed been reported to stimulate survival and proliferation of androgen-independent prostate cell lines and to induce androgen-independent growth and activation of AR-regulated genes (Culig *et al*., 1994; Jongsma *et al.*, 2000a; Hobisch, 1998). SST, however, may counteract growth factors and neuropeptides. Administration of SSTR2 agonists may decrease hepatic IGF-I release, affecting tumor cell growth. Lowered IGF-I levels may, however, not only have direct effects on the cancer cells but may also act to decrease the release of neuropeptides from NE cells because decreased IGF-I levels in patients with prostate cancer are associated with decreased serum levels of the NE marker CgA; IGF-I antibodies administrated to cultured human neuroendocrine carcinoid cells inhibit basal release of CgA (von Wichert *et al.,* 2000).

SST analogs may also act locally by binding to SSTR1-expressing NE cells and to SSTR2 receptors on stromal cells, decreasing paracrine stimulation, whereas autocrine stimulation may be diminished through epithelial-SSTR1 2, and 4 activation. SST may further inhibit mitogenic receptor activation and intracellular signal transduction. Stromal and NE growth factors are potent inducers of signal transduction pathways, including receptor tyrosine kinases and intracellular serine kinases such as PKA, MAPK, PI3-kinase, and Akt. There is now strong evidence that various kinases are involved in the growth of prostate cancer and that phosphorylation of the AR or co-regulatory proteins leads to androgen-independent proliferation and survival (Nazareth and Weigel 1996; Yeh *et al*., 1999). The activity regulated by phosphorylation is reversed by a variety of protein phosphatases, and SST is a known inducer of several different PPs, including tyrosine and threonine/serine PPs. Increased PP activity counteracts kinase activity and may lead to lower levels of phosphorylated AR and AR-pathway components, including coactivators, reducing proliferation and survival. Somatostatin has been shown to inhibit (Charland *et al*., 2001; Patel 1999) the Akt-kinase,

cAMP formation, and PKA activity; modulate the MAPK-pathway; and decrease cyclin E levels, all known activators of the AR (Yamamoto *et al*., 2000). The cyclin-dependent kinase (CDK) inhibitors p21 and p27 are up-regulated by SST (Medina *et al*., 2000; Pages *et al*., 1999), and this together with reduced cyclin levels may lead to repression of cyclin/CDK complex activity and G1/S transition.

Proliferation may also decrease as a consequence of diminished angiogenesis, mediated by activation of SSTR2 receptors expressed by endothelial cells and monocytes (Albini *et al*., 1999). Decreased release of NE-peptides through SSTR1 stimulation may also contribute to diminished formation of new blood vessels because NE cells produce vascular endothelial growth factor (VEGF) and are associated with angiogenetic prostate tumor areas (Borre *et al*., 2000; Dunn 2000). SST is further known to induce apoptosis through SSTR2 and SSTR3 receptors (Liu *et al*., 2000) but may also increase the apoptotic response by lowering secretion of survival factors from stromal and NE cells (Segal *et al*., 1994).

We have shown that human prostate cancers express multiple SSTR subtypes. However, low and differential expression of epithelial SSTR2 indicates that this subtype may not be optimal for direct targeting. However, SSTR4 is abundantly expressed in epithelial prostate cells and is further up-regulated in prostate cancer, suggesting that SSTR4 analogs may have a potential role in the treatment of prostate cancer. New SSTR4, but also SSTR1, analogs will have to be developed, enabling targeting of malignant and NE prostate cells. SSTR4 therapeutic schemes may further be enhanced by the use of cytotoxic or radioactive SST-analogs. Patients with hormone-refractory prostate cancer are often intolerant of aggressive cytotoxic therapies because of their age and poor performance. However, by using cytotoxic or radioactive compounds linked to SSTR4 analogs, adverse side effects would be minimized while increasing the apoptotic response in tumor cells.

Another approach would be to use combination therapy. For example, SSTR2-specific agents in combination with SSTR1 and SSTR4 agonists may be used to maximize both direct and indirect anti-proliferative effects. Chimeric SSTR2/D2-targeting analogs may enhance indirect effects. Giving maximal IGF-I blockade if used in combination with compounds that target the local synthesis of IGFs and/or the hydrolysis of IGF-binding proteins (IGFBPs). Growth hormone–releasing hormone (GHRH) antagonists have been shown to inhibit *IGF*-mRNA transcription in cultured prostatic cells (Plonowski *et al.*, 2002), and Koutsilieris *et al*. (2001) reported that by administrating both

octreotide and the uPA inhibitor dexamenthasone to patients with refractory prostate cancer (thus possibly lowering free IGFs through inhibition of both IGF release and IGFBP cleavage), up to 70% of refractory patients had an objective clinical response with decreasing prostate specific antigen (PSA) values more than 50% from baseline. Dexamenthasone may also increase SST-receptor expression because dexamenthasone has been reported to up-regulate TGF-β. Yet another inhibitor of this system may be antagonists of the NE-peptide bombesin because bombesin stimulates the release of uPA and bombesin antagonists have been reported to have anti-neoplastic effects in prostate cancer (Pinski *et al.*, 1993). SSTR1 agonists may directly decrease neuropeptide release from NE cells and, as discussed earlier, lower IGF-I levels may act to decrease the release of NE secretion, suggesting co-administration of SSTR1 and SSTR2 analogs. For maximal NE inhibition, various neuropeptide antagonists may also possibly be administered. Obviously, there is still a need to increase our understanding of the physiologic functions of the different SST-receptor subtypes and their receptor complexes in prostatic cells. Hopefully, such knowledge, together with the development of new SST analogs, will lead to improved therapeutic protocols for treatment of prostatic cancer.

CONCLUSION

Cancer research has for many years focused on mutational events that have their primary effect within the cancer cell. Recently, that focus has widened, with evidence of the importance of epigenetic events and of alterations in regulatory feedback loops for growth factors. Androgen ablation, introduced as an initial means of controlling the cancer, ultimately selects for a population of androgen-resistant cells, which become the dominant type in the tumor. Androgen-independent cells can use alternative signaling pathways to activate the androgen pathway or survive and proliferate in the absence of both androgen and AR. Several reports have shown that a switch between paracrine and autocrine stimulation of growth factors is associated with androgen independence, and NE differentiation has been linked to increased levels of mitogens and androgen-independent growth. Epigenetic loss of NEP expression may play an important role in NE differentiation and androgen independence. However, the genetic changes leading to unrestrained growth may not be uniform in the primary tumor, and this will result in phenotypically distinct cells with different cellular capabilities, with their own characteristic response to the microenvironment.

A single tumor may contain cells that use different mechanisms of androgen independence, and one or several different mechanisms may be in action in different cell populations. We have shown that SST-receptor subtypes 1 and 4 are the two predominant forms expressed by prostatic epithelium, including SSTR1-expressing NE cells, and that SSTR2 is the predominant form in the stromal compartment. SST-receptors may furthermore be up- or down-regulated, but one must also take into consideration that the intracellular machinery used by SST-receptors may be defective (e.g., specific PPs may be deleted or mutated in certain cell populations or tumors). SST-therapy may, however, be effective in several ways, including having direct and indirect effects; diminishing systemic, stromal, and NE growth factors; and inhibiting intracellular signal transduction pathways, potentially blocking cross-communication with the AR and compensating pathways. Combination therapy may include maximal IGF-I blockade or NE-inhibition, enhancing both direct and indirect effects, counteracting cell survival and proliferation in postate carcinoma, including androgen-independent disease. These potential mechanisms make SST analogs logical drug candidates in the therapy of prostate cancer.

References

Albini, A., Florio, T., Giunciuglio, D., Masiello, L., Carlone, S., Corsaro, A., Thellung, S., Cai, T., Noonan, D.M., and Schettini, G. 1999. Somatostatin controls Kaposi's sarcoma tumor growth through inhibition of angiogenesis. *FASEB 13*:647–655.

Bales, K.R., Hannon, K., Smith, C.K. II, and Santerre, R.F. 1993. Single-stranded RNA probes generated from PCR-derived DNA templates. *Mol. Cell. Probes 7*:269–275.

Borre, M., Nerstrom, B., and Overgaard, J. 2000. Association between immunohistochemical expression of vascular endothelial growth factor (VEGF), VEGF-expressing neuroendocrine-differentiated tumor cells, and outcome in prostate cancer patients subjected to watchful waiting. *Clin. Cancer. Res. 6*:1882–1890.

Braissant, O., Foufelle, F., Scotto, C., Dauca, M., and Wahli, W. 1996. Differential expression of peroxisome proliferator-activated receptors (PPARs): Tissue distribution of PPAR-alpha, -beta, and -gamma in the adult rat. *Endocrinology 137*:354–366.

Brevini, T.A., Bianchi, R., and Motta, M. 1993. Direct inhibitory effect of somatostatin on the growth of the human prostatic cancer cell line LNCaP: Possible mechanism of action. *J. Clin. Endocrinol. Metab. 77*:626–631.

Buvoli, M., Biamonti, G., Riva, S., and Morandi, C. 1987. Hybridization of oligodeoxynucleotide probes to RNA molecules: Specificity and stability of duplexes. *Nucleic Acids Res. 15*:9091.

Charland, S., Boucher, M.J., Houde, M., and Rivard, N. 2001. Somatostatin inhibits Akt phosphorylation and cell cycle entry, but not p42/p44 mitogen-activated protein (MAP) kinase activation in normal and tumoral pancreatic acinar cells. *Endocrinology 142*:121–128.

Culig, Z., Hobisch, A., Cronauer, M.V., Radmayr, C., Trapman, J., Hittmair, A., Bartsch, G., and Klocker, H. 1994. Androgen

receptor activation in prostatic tumor cell lines by insulin-like growth factor-I, keratinocyte growth factor, and epidermal growth factor. *Cancer Res. 54*:5474–5478.

Dizeyi, N., Konard, L., Bjartell, A., Wu, H., Gadaleanu, V., Hansson, J., Helboe, L., and Abrahamsson, P. 2002. Localization and mRNA expression of somatostatin receptor subtypes in human prostatic tissue and prostate cancer cell lines. *Urol. Oncol. 7*:91–98.

di Sant'Agnese, P.A., and de Mesy Jensen, K.L. 1984. Somatostatin and/or somatostatin-like immunoreactive endocrine-paracrine cells in the human prostate gland. *Arch. Pathol. Lab. Med. 108*:693–696.

Dunn, S.E. 2000. Insulin-like growth factor I stimulates angiogenesis and the production of vascular endothelial growth factor. *Growth. Horm. IGF Res. 10*:Suppl A:S41–42.

Halmos, G., Schally, A.V., Sun, B., Davis, R., Bostwick, D.G., and Plonowski, A. 2000. High expression of somatostatin receptors and messenger ribonucleic acid for its receptor subtypes in organ-confined and locally advanced human prostate cancers. *J. Clin. Endocrinol. Metab. 85*:2564–2571.

Hansson, J., and Abrahamsson, P.A. 2001. Neuroendocrine pathogenesis in adenocarcinoma of the prostate. *Ann. Oncol. 12*:Suppl 2:S145–152.

Hansson, J., and Abrahamsson, P.A. 2003. Neuroendocrine differentiation in prostatic carcinoma. *Scand. J. Urol. Nephrol. Suppl. 212*:28–34.

Hansson, J., Bjartell, A., Gadaleanu, V., Dizeyi, N., and Abrahamsson, P.A. 2002. Expression of somatostatin receptor subtypes 2 and 4 in human benign prostatic hyperplasia and prostatic cancer. *Prostate 53*:50–59.

Helboe, L., Moller, M., Norregaard, L., Schiodt, M., and Stidsen, C.E. 1997. Development selective antibodies against the human somatostatin receptor subtypes sst1-sst5. *Brain. Res. Mol. Brain. Res. 49*:82–88.

Hobisch, A., Eder, I.E., Putz, T., Horninger, W., Bartsch, G., Klocker, H., and Culig, Z. 1998. Interleukin-6 regulates prostate-specific protein expression in prostate carcinoma cells by activation of the androgen receptor. *Cancer Res. 58*:4640–4645.

Jongsma, J., Oomen, M.H., Noordzij, M.A., Romijn, J.C., van der Kwast, T.H., Schroder, F.H., and van Steenbrugge, G.J. 2000a. Androgen-independent growth is induced by neuropeptides in human prostate cancer cell lines. *Prostate 42*:34–44.

Jongsma, J., Oomen, M.H., Noordzij, M.A., Van Weerden, Martens, G.J., van der Kwast, T.H., Schroder, F.H., and van Steenbrugge, G.J. 2000b. Androgen deprivation of the PC-310 human prostate cancer model system induces neuroendocrine differentiation. *Cancer Res. 60*:741–748.

Kalkner, K.M., Nilsson, S., and Westlin, J.E. 1998. [111In-DTPA-D-Phe1]-octreotide scintigraphy in patients with hormone-refractory prostatic adenocarcinoma can predict therapy outcome with octreotide treatment: A pilot study. *Anticancer Res. 18*:513–516.

Kindblom, J., Dillner, K., Ling, C., Tornell, J., and Wennbo, H. 2002. Progressive prostate hyperplasia in adult prolactin transgenic mice is not dependent on elevated serum androgen levels. *Prostate 53*:24–33.

Koutsilieris, M., Mitsiades, C., Dimopoulos, T., Ioannidis, A., Ntounis, A., and Lambou, T. 2001. A combination therapy of dexamethasone and somatostatin analog reintroduces objective clinical responses to LHRH analog in androgen ablation-refractory prostate cancer in patients. *J. Clin. Endocrinol. 86*:5729–5736.

Lee, L.F., Guan, J., Qiu, Y., and Kung, H.J. 2001. Neuropeptide-induced androgen independence in prostate cancer cells: Roles

of nonreceptor tyrosine kinases Etk/Bmx, Src, and focal adhesion kinase. *Mol. Cell. Biol. 21*:8385–8397.

Liu, D., Martino, G., Thangaraju, M., Sharma, M., Halwani, F., Shen, S.H., Patel, Y.C., and Srikant, C.B. 2000. Caspase-8- mediated intracellular acidification precedes mitochondrial dysfunction in somatostatin-induced apoptosis. *J. Biol. Chem. 275*:9244–9250.

Logothetis, C.J., Hossan, E.A., and Smith, T.L. 1994. SMS 201-995 in the treatment of refractory prostatic carcinoma. *Anticancer Res. 14*:2731–2734.

Luo, X.H., Liao, E.Y., and Su, X. 2002. Progesterone upregulates TGF-b isoforms (b1, b2, and b3) expression in normal human osteoblast-like cells. *Calcif. Tissue. Int. 71*:329–334.

Maulard, C., Richaud, P., Droz, J.P., Jessueld, D., Dufour-Esquerre, F., and Housset, M. 1995. Phase I-II study of the somatostatin analogue lanreotide in hormone-refractory prostate cancer. *Cancer Chemother. Pharmacol. 36*:259–262.

Medina, D.L., Toro, M.J., and Santisteban, P. 2000. Somatostatin interferes with thyrotropin-induced G1-S transition mediated by cAMP-dependent protein kinase and phosphatidylinositol 3-kinase. Involvement of RhoA and cyclin E x cyclin-dependent kinase 2 complexes. *J. Biol. Chem. 275*:15549–15556.

Munkelwitz, R.A., Waltzer, W.C., Meek, A.G., and Hod, Y. 1997. Expression of somatostatin receptors in human prostatic cell lines. *J. Urol. 157*:9.

Murphy, G., Griffiths, K., Denis, L., Khoury, S., Chatelain, C., Cocklett, A.T.K. (eds). 1997. Epidemiology and natural history of prostate cancer: *Proceedings of the First International Consultation on Prostate Cancer,* June 20, 1996. Manchecourt Scientific Communication International.

Nazareth, L.V., and Weigel, N.L. 1996. Activation of the human androgen receptor through a protein kinase A signaling pathway. *J. Biol. Chem. 271*:19900–19907.

Nilsson, S., Reubi, J.C., Kalkner, K.M., Laissue, J.A., Horisberger, U., Olerud, C., and Westlin, J.E. 1995. Metastatic hormone-refractory prostatic adenocarcinoma expresses somatostatin receptors and is visualized *in vivo* by [111In]-labeled DTPA-D-[Phe1]-octreotide scintigraphy. *Cancer Res. 55*:5805s–5810s.

Pages, P., Benali, N., Saint-Laurent, N., Esteve, J.P., Schally, A.V., Tkaczuk, J., Vaysse, N., Susini, C., and Buscail, L. 1999. SST2 somatostatin receptor mediates cell cycle arrest and induction of p27(Kip1). Evidence for the role of SHP-1. *J. Biol. Chem. 274*:15186–15193.

Papandreou, C.N., Usmani, B., Geng, Y., Bogenrieder, T., Freeman, R., Wilk, S., Finstad, C.L., Reuter, V.E., Powell, C.T., Scheinberg, D., Magill, C., Scher, H.I., Albino, A.P., and Nanus, D.M. 1998. Neutral endopeptidase 24.11 loss in metastatic human prostate cancer contributes to androgen-independent progression. *Nat. Med. 4*:50–57.

Patel, Y.C. 1999. Somatostatin and its receptor family. *Front. Neuroendocrinol. 20*:157–198.

Pinski, J., Halmos, G., and Schally, A.V. 1993. Somatostatin analog RC-160 and bombesin/gastrin-releasing peptide antagonist RC-3095 inhibit the growth of androgen-independent DU-145 human prostate cancer line in nude mice. *Cancer Lett. 71*:189–196.

Plonowski, A., Schally, A.V., Letsch, M., Krupa, M., Hebert, F., Busto, R., Groot, K., and Varga, J.L. 2002. Inhibition of proliferation of PC-3 human prostate cancer by antagonists of growth hormone-releasing hormone: Lack of correlation with the levels of serum IGF-I and expression of tumoral IGF-II and vascular endothelial growth factor. *Prostate 52*:173–182.

Puente, E., Saint-Laurent, N., Torrisani, J., Furet, C., Schally, A.V., Vaysse, N., Buscail, L., and Susini, C. 2001. Transcriptional

activation of mouse sst2 somatostatin receptor promoter by transforming growth factor-beta. Involvement of Smad4. *J. Biol. Chem. 276*:13461–13468.

Reubi, J.C., Waser, B., Schaer, J.C., and Markwalder, R. 1995. Somatostatin receptors in human prostate and prostate cancer. *J. Clin. Endocrinol. Metab. 80*:2806–2814.

Rocheville, M., Lange, D.C., Kumar, U., Patel, S.C., Patel, R.C., and Patel, Y.C. 2000a. Receptors for dopamine and somatostatin: Formation of hetero-oligomers with enhanced functional activity. *Science 288*:154–157.

Rocheville, M., Lange, D.C., Kumar, U., Sasi, R., Patel, R.C., and Patel, Y.C. 2000b. Subtypes of the somatostatin receptor assemble as functional homo- and heterodimers. *J. Biol. Chem. 275*:7862–7869.

Rohrer, L., Raulf, F., Bruns, C., Buettner, R., Hofstaedter, F., and Schule, R. 1993. Cloning and characterization of a fourth human somatostatin receptor. *Proc. Natl. Acad. Sci. USA 90*:4196–4200.

Ruffion, A., Al-Sakkaf, K.A., Brown, B.L., Eaton, C.L., Hamdy, F.C., and Dobson, P.R. 2003. The survival effect of Prolactin on PC3 prostate cancer cells. *Eur. Urol. 43*:301–308.

Saveanu, A., Lavaque, E., Gunz, G., Barlier, A., Kim, S., Taylor, J.E., Culler, M.D., Enjalbert, A., and Jaquet, P. Demonstration of enhanced potency of a chimeric somatostatin-dopamine molecule, BIM-23A387, in suppressing growth hormone and prolactin secretion from human pituitary somatotroph adenoma cells. *J. Clin. Endocrinol. Metab.* 2002 Dec;87(12):5545–5552.

Segal, N.H., Cohen, R.J., Haffejee, Z., and Savage, N. 1994. BCL-2 proto-oncogene expression in prostate cancer and its relationship to the prostatic neuroendocrine cell. *Arch. Pathol. Lab. Med. 118*:616–618.

Schaer, J.C., Waser, B., Mengod, G., and Reubi, J.C. 1997. Somatostatin receptor subtypes sst1, sst2, sst3 and sst5 expression in human pituitary, gastroentero-pancreatic and mammary tumors: Comparison of mRNA analysis with receptor autoradiography. *Int. J. Cancer. 70*:530–537.

Schally, A.V. 1998. Oncological applications of somatostatin analogues. *Cancer Res. 48*:6977–6985.

Schonbrunn, A. 1999. Somatostatin receptors present knowledge and future directions. *Ann. Oncol. 10*:S17–21.

Srkalovic, G., Cai, R.Z., and Schally, A.V. 1990. Evaluation of receptors for somatostatin in various tumors using different analogs. *J. Clin. Endocrinol. Metab. 70*:195–204.

Von Wichert, G., Jehle, P.M., Hoeflich, A., Koschnick, S., dralle, H., Wolf, E., Wiedenmann, B., Boehm, B.O., Adler, G., and Seufferlein, T. 2000. Insulin-like growth factor-I is an autocrine regulator of chromogranin A secretion and growth in human neuroendocrine tumor cells. *Cancer Res. 60*:4573–4581.

Yamada, Y., Kagimoto, S., Kubota, A., Yasuda, K., Masuda, K., Someya, Y., Ihara, Y., Li, Q., Imura, H., and Seino, S. 1993. Cloning, functional expression and pharmacological characterization of a fourth (hSSTR4) and a fifth (hSSTR5) human somatostatin receptor subtype. *Biochem. Biophys. Res. Commun. 195*:844–852.

Yamada, Y., Post, S.R., Wang, K., Tager, H.S., Bell, G.I., and Seino, S. 1992a. Cloning and functional characterization of a family of human and mouse somatostatin receptors expressed in brain, gastrointestinal tract, and kidney. *Proc. Natl. Acad. Sci. USA. 89*:251–255.

Yamada, Y., Reisine, T., Law, S.F., Ihara, Y., Kubota, A., Kagimoto, S., Seino, M., Seino, Y., Bell, G.I., and Seino, S. 1992b. Somatostatin receptors, an expanding gene family: Cloning and functional characterization of human SSTR3, a protein coupled to adenylyl cyclase. *Mol. Endocrinol. 6*:2136–2142.

Yamamoto, A., Hashimoto, Y., Kohri, K., Ogata, E., Kato, S., Ikeda, K., and Nakanishi, M. 2000. Cyclin E as a coactivator of the androgen receptor. *J. Cell. Biol. 150*:873–880.

Yeh, S., Lin, H.K., Kang, H.Y., Thin, T.H., Lin, M.F., and Chang, C. 1999. From HER2/Neu signal cascade to androgen receptor and its coactivators: A novel pathway by induction of androgen target genes through MAP kinase in prostate cancer cells. *Proc. Natl. Acad. Sci. USA. 96*:5458–5463.

Role of Immunohistochemical Expression of Retinoid X Receptors in Prostate Carcinoma

Maria I. Arenas, Juan Alfaro, and Ricardo Paniagua

Introduction

It is known that retinoids, ligands for retinoic acid receptors (RAR) and retinoial X receptors (RXR), play an important role in regulating cellular proliferation and differentiation in many tissues. As a result of their properties, they are used for treatment of psoriasis, acne, and photoaging. Furthermore, retinoid-based therapy is usual in promyelocytic leukemia and is becoming increasingly important in cancer treatment. Nuclear retinoid receptors are proximate mediators in many effects of retinoids on gene expression, and their loss or diminished expression occurs in premalignant and malignant tissues.

Retinoid X Receptors

Retinoids are a group of chemical compounds that include both natural and synthetic vitamin A metabolites and analogs. These compounds are physiologic regulators of a large number of essential biologic processes such as embryonic development, vision, reproduction, bone formation, metabolism, hematopoiesis, differentiation, proliferation, and apoptosis (Nagy *et al*., 1998). Furthermore, it has been

shown that retinoids promote the differentiation of stem cells and neural stem cells (Calza *et al*., 2003). In addition to this capacities, they were shown to suppress carcinogenesis in variety of tissue types (e.g., oral cancer and skin, bladder, lung, prostate, and breast cancers) (Hansen *et al*., 2000). Considering that malignant transformation of the normal epithelium results from loss or disruption of the normal differentiation mechanisms, retinoids have been used for prevention and treatment of various epithelial cancers (Lotan *et al*., 1990).

Effects of retinoids are mainly mediated by retinoid nuclear receptors, which are members of the steroid hormone receptor superfamily (Mangelsdorf *et al*., 1995). There are two types of retinoid receptors: RARs and RXRs. Both receptor types are characterized by their ligand- and deoxyribonucleic acid (DNA)-binding abilities and also by their possible dimerization partners (Mangelsdorf and Evans, 1995). Each class of receptor is composed of three gene products (RAR-α, -β, -γ and RXR-α, -β, -γ), the transcription of which results in several isoforms as a result of the action of different promoters and messenger ribonucleic acid (mRNA) splicing (Brocard *et al*., 1996). Two forms of retinoic acid, named all-*trans*-retinoic acid (ATRA) and 9-*cis*-retinoic acid (9-*cis*-RA), can bind to RARs,

but only 9-*cis*-RA is able to bind to RXRs (Mangelsdorf and Evans, 1995).

In addition to the occurrence of different ligands and receptors, the complexity of retinoid signaling is increased by the possible formation of different homodimer and heterodimer receptors. Thus, RARs bind to their cognate response elements as heterodimers with RXRs; moreover, RXRs, which can also bind *in vitro* to certain DNA elements as homodimers, are heterodimeric partners for a number of nuclear receptors, such as thyroid hormone, vitamin D3, activated peroxisome proliferator, and nerve growth factor IB receptor (Mangelsdorf and Evans, 1995). Heterodimerization represents an important level of regulation for nuclear receptor–dependent signaling pathways (Kliewer *et al.*, 1992); for example, RXR homodimers were reported to preferentially form over RXR heterodimers following 9-*cis*-retinoic acid treatment (Zhang *et al.*, 1992). These dimers can bind to different hormone response elements (HREs) in the promoters of certain genes and act as transcription factors (Mangelsdorf and Evans, 1995). In general, when an HRE is bound to a nuclear hormone receptor, this may either activate or repress the transcription, depending on the presence of ligand, cell type, promoter, response element, and other signals (Vos *et al.*, 1997).

Because nuclear retinoid receptors are the proximate mediators of many effects of retinoids on gene expression, it is plausible to assume that changes in their expression and function may cause aberrations in the response of cells to retinoids and thereby alter the regulation of cell growth, differentiation, and the expression of a transformed phenotype. Indeed, it has been demonstrated that altered expression of retinoid nuclear receptors may be associated with malignant transformation of human cells (de The, 1996). Therefore, investigations of the expression patterns of retinoid receptors in normal, premalignant, and malignant tissues may provide important clues on the roles of these receptors in cancer development and in the response of these tissues to retinoid treatment (Sun and Lotan, 2002). Most of the reports about the expression of retinoid nuclear receptors have been performed in cultured untransformed and tumor cell lines in embryos and in premalignant lesions *in vivo* (Xu and Lotan, 1999), but studies about the expression of these receptors in human tissues are scarce, especially in the prostate. One of these reports (Lotan *et al.*, 2000) showed by *in situ* hybridization the presence of RXR-α and RXR-γ mRNAs in most of normal and cancerous prostates; however, RXR-β mRNA was expressed in four of eight benign prostates and in zero of 10 malignant prostates. Using immunohistochemistry,

Kikugawa *et al.* (2000) detected much more expression of RXR-α and RXR-γ than of RXR-β in human prostatic adenocarcinoma cells.

However, studies have demonstrated that RXR-selective retinoids represent promising agents for the prevention and treatment of cancer. Thus, 9-*cis* retinoic acid has shown a significant anti-proliferative and/or differentiating activity in prostate cancer cells (MoCormick *et al.*, 1999), and RXR-selective retinoids were more effective than *trans*-RA at inhibiting carcinogenesis in animals. It has also been observed than these RXR-selective ligands may exert their potent anti-cancer activity through inducing RAR-β expression in cancer cells that are resistant to classical retinoids (Wu *et al.*, 1997). Therefore, further studies are needed to investigate the possible role of these receptors (RXRs) in the physiologic behavior of human prostatic cells. Thus, the aim of this study was to evaluate the presence and the distribution of RXR-α, -β, -γ in normal prostate, benign prostatic hyperplasia (BPH), prostatic intraepithelial neoplasia (PIN), and prostatic carcinoma, using immunohistochemistry and Western Blot analysis, to elucidate the relationship among these receptors and the onset and development of prostatic adenocarcinoma.

MATERIALS

Western Blot

1. Extraction buffer (50 ml):
   1 M Tris-HCl: 1.576 g Tris-HCl; bring volume to 10 ml with deionized glass-distilled water, pH 7.6. Take 50 μl.
   4 M KCl: 2.982 g potassium chloride; bring volume to 10 ml with deionized glass-distilled water. Take 125 μl.
   1,4-Ditiho-L-threitol (DTT): Dissolve 8 mg DTT in 50 ml of extraction buffer.
   0.2 M Ethylenediamine tetra-acetic acid (EDTA): 0.584 g EDTA; bring volume to 10 ml with deionized glass-distilled water. Take 250 μl.
   1 M Phenylmethylsulfonyl fluoride (PMSF): Dissolve 1.742 g in 10 ml ethanol. Take 50 μl.
   Leupeptine: 10 mg leupeptine; bring volume to 1 ml with deionized glass-distilled water. Take 50 μl.
   Aprotinine: 1 mg aprotinine; bring volume to 1 ml with deionized glass-distilled water. Take 50 μl.
   0.5% Triton X-100: Dissolves 0.25 ml Triton X-100 in 50 ml extraction buffer.

10% sodium dodecyl sulphate (SDS): 2.884 g SDS; bring volume to 10 ml with deionized glass-distilled water. Take 500 µl.

1 M Sodium fluoride: 0.428 g in 10 ml with deionized glass-distilled water. Take 1 ml.

0.4 M Sodium orthovanadate: 0.736 g; bring volume to 10 ml with deionized glass-distilled water. Take 1 ml.

Add deionized glass-distilled water to raise 50 ml final volume.

2. 2X SDS-PAGE loading buffer (10 ml):

0.5M Tris-HCl: 0.788 g Tris-HCl; bring volume to 10 ml with deionized glass-distilled water, pH 6.8. Take 1.9 ml.

20% SDS: 2 g SDS; bring volume to 10 ml with deionized glass-distilled water. Take 2 ml.

Glycerol: Add 1 ml glycerol to 10 ml final volume SDS-PAGE loading buffer.

1% Bromophenol blue: 10 mg bromophenol blue in 1 ml absolute ethanol. Take 20 µl.

4% 2-Mercaptoethanol: 40 mg 2-mercaptoethanol in 1 ml. Take 0.6 ml.

SDS: Add 9 mg to 10 ml final volume SDS-PAGE loading buffer.

Add deionized glass-distilled water to raise 10 ml final volume. Adjust pH to 6.8 the SDS-PAGE loading buffer before rising with glass-distilled water.

3. Resolving gel (9%):

1.5 M Tris: 3.633 g Tris-HCl; bring volume to 20 ml with deionized glass-distilled water, pH 8.8. Take 2.5 ml.

30% Acrylamide: 30 g acrylamide, 0.8 g bis-acrylamide; bring volume to 100 ml with deionized glass-distilled water. Take 3 ml.

20% SDS: 2 g SDS bring volume to 10 ml with deionized glass-distilled water. Take 50 µl.

10% Ammonium persulphate: 0.5 g APS; bring volume to 5 ml with deionized glass-distilled water. Take 40 µl.

N,N,N',N'-Tetramethylethylendiamine (TEMED): take 20 µl.

Add 4.4 ml deionized glass-distilled water.

4. Stacking gel (3%):

0.5 M Tris: 6.05 g Tris-HCl bring volume to 5 ml with deionized glass-distilled water. Take 1.25 ml.

30% Acrylamide: 30 g acrylamide, 0.8 g bis-acrylamide; bring volume to 100 ml with deionized glass-distilled water. Take 0.5 ml.

20% SDS: 2 g SDS bring volume to 10 ml with deionized glass-distilled water. Take 25 µl.

10% APS: 0.5 g APS; bring volume to 5 ml with deionized glass-distilled water. Take 20 µl.

TEMED: Take 10 µl.

Add 3.2 ml deionized glass-distilled water.

5. 10X Running buffer (for 1 L):

0.25 M Tris: 30.28 g Trizma-base.

1.92 M Glycine: 144.12 g glycine.

20% SDS: 20 g SDS; bring to volume to 100 ml with deionized glass-distilled water. Take 5 ml.

Deionized glass-distilled water: 895 ml.

6. Nitrocellulose or polyvinylidene difluoride (PVDF) membranes.

7. Blotting buffer: 2 g sodium bicarbonate (10mM), 0.954 g sodium carbonate (3 mM), 600 ml methanol, 2400 ml deionized glass-distilled water.

8. Blocking buffer (for 50 ml):

5% nonfat dry milk. Take 2.5 g.

TBS: 10mM Tris, 150mM sodium chloride (NaCl): 0.6056 g Trizma-base, 1.749 g NaCl; bring volume to 500 ml with deionized glass-distilled water, pH 7.5. Take 49.975 ml.

0.05% Tween-20: Take 25 µl.

9. Washing buffer (for 100 ml):

TBS: 10mM Tris, 150 mM NaCl: 0.6056 g Trizma-base, 1.749 g NaCl; bring volume to 500 ml with deionized glass-distilled water, pH 7.5. Take 99.95 ml.

0.05% Tween-20: Take 50 µl.

10. Primary antibody (rabbit polyclonal antibody against RXR-α, mouse monoclonal immunoglobulin G_1 antibody against RXR-β, and rabbit polyclonal antibody against RXR-γ, all from Santa Cruz Biotechnologies, Santa Cruz, CA) diluted in TBS with 0.5% nonfat dry milk and 0.005% Tween-20.

11. Peroxidase-conjugated secondary antibodies (goat anti-rabbit or goat anti-mouse, Chemicon, Temecula, CA) diluted in TBS with 0.5% nonfat dry milk and 0.005% Tween-20.

12. Enhanced chemiluminescence (ECL) kit (Amersham, PRN 2109).

Immunohistochemistry

1. Dulbecco's phosphate buffer saline (PBS): 100 mg anhydrous calcium chloride, 200 mg potassium chloride, 200 mg monobasic potassium phosphate, 100 mg magnesium chloride•6H$_2$O; 8 g

sodium chloride, and 2.16 g dibasic sodium phosphate•7H$_2$O; bring volume to 1 L with deionized glass-distilled water, pH 7.4.

2. Fixative: 10% EM-grade formaldehyde in PBS.

3. 1% 3-aminopropyl-triethoxysilane (TESPA) solution: 1 mL TESPA and 99 ml acetone.

4. TESPA coated slides.

5. 0.3% H$_2$O$_2$ in methanol: 1 ml H$_2$O$_2$ (33%) and 99 ml methanol.

6. 0.01M citrate buffer: 2.941 g trisodium citrate •2 H$_2$O; bring volume to 1 L with deionized glass-distilled water, pH 6.

7. 0.05M TBS: 6.05 g Trizma-Base and 8.5 g NaCl; bring volume to 1 L with deionized glass-distilled water, pH 7.4.

8. 5% Bovine serum albumin (BSA): 5 g BSA and 100 ml TBS; 1 BSA to buffer with stirring.

9. 10% Normal donkey serum (NDS): 1 ml NDS and 9 ml TBS with 5% BSA.

10. Primary antibody diluted in TBS with 0.5% BSA and 1% NDS.

11. Biotinylated secondary antibody (swine anti-rabbit or rabbit anti-mouse biotinylated immunoglobulins from Dako, Barcelona, Spain) diluted in TBS with 0.5% BSA and 1% NDS.

12. Streptavidin-biotin peroxidase complex (Dako) diluted in TBS.

13. 0.2M Acetate buffer:

  16.4 g sodium acetate anhydrous; bring volume to 1 L with deionized glass-distilled water.

  12 ml acetic acid glacial; bring volume to 1 L with deionized glass-distilled water.

  452 ml solution A and 48 ml solution B, pH 5.6.

14. Developer solution:

  Ammonium nickel sulphate solution: 7.25 g ammonium nickel sulphate, 0.6 g glucose, 0.12 g ammonium chloride, bring volume to 150 ml with 0.2 M acetate buffer.

  3,3′-diaminobenzidine (DAB): 125 mg DAB in 150 ml deionized glass distilled water.

  150 ml solution A and 150 ml solution B plus 8 mg glucose oxidase.

METHODS

Western Blotting

1. Place the tissues on labeled aluminum foil and immediately place them in dry ice. It is imperative that the tissues stay cold, so that protease does not have time to act on the protein.

2. Place the tissues in a round bottom tube and add extraction buffer with protease and phosphatase inhibitors. Add 200 µl extraction buffer per each 100 mg tissue.

3. Homogenize immediately using a conventional rotor-status homogenizer until the sample is uniformly homogeneous (usually 1–5 min for prostatic tissues).

4. Place the homogenates on ice for 30 min. This step promotes the dissociation of nucleoprotein complexes.

5. Centrifuge the homogenate at 12,000 rpm for 15 min at 4ºC to remove insoluble material.

6. Transfer the supernatant to a new tube and discard the pellet.

7. Determinate the protein concentration (Bradford assay). We use the Bradford assay from Bio-Rad (Bio-Rad Laboratories, Hercules, CA).

8. Take x µl (= y µg protein) and mix with x µl of 2X sample buffer.

9. Boil for 5 min.

10. Cool at room temperature for 5 min.

11. Preparation of gel:

  Assemble the glass plates and spacers (1.5 mm thick).

  Pour the running gel to reach 5 cm from the glass bottom (~10 ml).

  Seal with 1 ml water-saturated 1-butanol.

  When gel has set, pour off the butanol and rinse with deionized water.

  Pour the stacking gel (~5 ml) and insert the comb immediately.

  When the stacking gel has set, place in gel rig and immerse in buffer.

  Prior to running the gel, flush the wells out thoroughly with running buffer.

12. After flash spinning the samples, load into the wells. Use molecular weight markers. We use Amersham LIFE SCIENCE Full Range Rainbow.

13. Running the gel at 160 V (constant voltage) for 1.5 hr.

14. Membrane transfer:

  If nitrocellulose membranes are used, they should be prewetted in distilled water for 1 min and equilibrated in blotting buffer for 10–15 min.

  If PVDF membranes are used, they should be prewetted in methanol for 1 min and rinsed in distilled water for 5 min to remove the methanol, then equilibrated in blotting buffer for 10–15 min.

  Cut out some whatman paper in a slightly bigger size than gel and membrane.

  Prewet the sponges and filter papers in 1X blotting buffer.

  Sandwich order:

▲ Sponge
▲ Two or three Whatman paper
▲ Membrane
▲ Gel
▲ Two or three Whatman paper
▲ Sponge
Assemble "sandwich" for Bio-Rad's
  Transblot. The sandwich should be put in the
  blotting machine so that the membrane is on
  the side of the cathode.
Transfer for 4 hr at 250 mA at 4ºC on a stir
  plate.

15. Antibodies and detection:
    When the transfer is finished, immerse mem-
      brane in blocking buffer for 1 hr.
    Incubate with primary antibody diluted in
      blocking buffer (RXR-β at 1:100, RXR-α
      and RXR-γ 1:200) overnight at 37ºC.
    Wash 3×10 min with 0.05% Tween-20 in TBS.
    Incubate with peroxidase-conjugated second-
      ary antibody diluted 1:4000 in blocking
      buffer (1:9 in TBS) for 1 hr at room
      temperature.
    Wash 3×10 min with 0.05% Tween-20 in TBS.
    Detect with Amersham ECL kit.

Immunohistochemistry

1. Rinse the samples twice in PBS, and fix for
24 hr at room temperature in 10% formaldehyde in PBS.

2. Following fixation, rinse the samples 3–5 times
over a period of 6 hr.

3. Dehydrate the samples, and embed in paraffin.

4. Cut 5-μm-thick sections with a stainless steel
blade, and mount the sections on TESPA-coated slides.

5. Dewax and rehydrate the sections.

6. Block endogenous peroxidase activity by incu-
bating the sections in 0.3% H_2O_2 for 20 min at room
temperature.

7. Rinse the samples for 5 min in TBS.

8. Locate slides in a plastic rack, fill empty spaces
with blank slides and place the rack in 0.01 M citrate
buffer (2 L) pH 6.0, in a conventional pressure cooker.

9. Heat for 5 min at highest pressure and let stand
for 20 min in the pressure cooker to retrieve the antigen.

10. Rinse the samples for 5 min twice in TBS.

11. Block nonspecific binding by incubating the
sections in TBS containing 10% NDS and 5% BSA for
30 min.

12. Add the primary antibody diluted 1:20 in TBS
containing 1% NDS and 0.5% BSA. Allow 50 μl per
slide, put on coverslip, and incubate overnight at 37ºC.

13. Rinse as in **Step 10**.

14. Incubate the sections in biotinylated secondary
antibody diluted 1:500 in TBS containing 1% NDS
and 0.5% BSA at room temperature for 1 hr.

15. Rinse as in **Step 10**.

16. Incubate the sections in streptavidin-biotin per-
oxidase complex diluted in TBS at room temperature
for 1 hr.

17. Rinse as in **Step 10**.

18. Rinse in 0.1 M acetate buffer for 3 min.

19. Develop using the glucose oxidase-DAB-nickel
intensification method, check staining under micro-
scope, and stop reaction in acetate buffer when strong
signal is obtained.

20. Dehydrate, clear in xylene, and mount.

RESULTS AND DISCUSSION

In the last years, the commercial availability of a
variety of antibodies has led to a faster and easier
immunohistochemical detection of numerous protein
in formalin-fixed and paraffin-embedded sections.
Some of them are actually used for clinical diagnosis;
thus, the expression of key altered proteins is studied
using specific antibodies to different markers depend-
ing on each pathology. This technique provides us the
possibility to exactly localize the *in vivo* expression of
RXR protein in prostates processed from total or
partial prostatectomies and needle biopsies.

Primarily, to use a new antibody, it is needed to
check its specificity using enzyme linked immunosor-
bent assay (ELISA) and Western Blot techniques.
With these procedures, it is possible to realize a semi-
quantitative study to detect the presence of an antigen
and its variation of expression in different samples or
pathologies. With Western Blot analysis, we have
detected only a single band for each antibody used at
the corresponding molecular weight: ~60 KDa for
RXR-α, -β, and –γ receptors. For RXR-α and RXR-γ,
the expression observed was similar in the three
sample types analyzed. However, for RXR-β, the
expression was weaker in prostate cancer than in
normal and hyperplastic prostates.

Effects of retinoic acid are mediated by specific
RAR and RXR subtypes and modulated by the cellular
levels of binding proteins (Giguere, 1994). These
receptors play a key role in controlling cell prolifera-
tion and apoptosis, and the aberrant expression of one
or more RARs and RXRs might result in abrogated
retinoid signaling and increased cell transformation in
several cancer types, including prostate, breast, and
lung (Campbell *et al.,* 1998). The identification of a
molecular alteration in the *RAR-α* gene in human acute
promyelocytic leukemia and the report of a decreased
expression of RAR-β in lung cancer (de The *et al*., 1990;

Gebert *et al.*, 1991) are in agreement to this hypothesis. To bind DNA, RARs require heterodimerization with RXRs; these latter can act as homodimers or heterodimers partners of a number of nuclear receptors (Mangelsdorf and Evans, 1995). As a result of the role of RXRs as pivotal mediator in several signaling pathways, the aim of this work was to study the presence and distribution of retinoid X receptors in normal and pathologic prostates.

In primary cultures of prostate cells it has been observed that ATRA is involved in the control of growth and the induction of apoptosis and that these effects are mediated by specific RAR subtypes including RAR-α and RAR-β. In these cells, the expression of mRAR-β was increased, whereas Bcl-2 protein levels were decreased (Pasquali *et al.*, 1999). However, in a clinical trial, Trump *et al.* (1997) concluded that ATRA was not active in patients with hormone-refractory prostate cancer. These authors proposed that the failure of this agent in these patients might be because of a failure of drug delivery, associated with enhanced mechanisms of ATRA clearance, which occur within a few days of beginning ATRA treatment. The synthetic retinoid *N*-(4-hydroxyphenyl) retinamide (4-HPR) has been shown to induce apoptosis in various malignant cells including human prostate carcinoma cell lines. This induction is mediated by retinoic nuclear acid receptors, by increasing the reactive oxygen species activity; expressing *p53*, *p21*, and *c-jun* genes; and decreasing the expression of *c-myc* gene (Sun *et al.*, 1999). However, in patients treated with 4-HPR for 28 days before radical prostatectomy, this synthetic retinoid was ineffective because its concentration in serum and in prostate was not significantly altered (Thaller *et al.*, 2000). Because the expression of the retinoid receptors can be up-regulated by retinoid therapy, the low level of this retinoid in prostate tissue can explain the ineffectiveness of 4-HPR treatment. Also Pasquali *et al.* (1996) reported that prostate cancer tissues have 5 to 8 times less retinoic acid than normal prostate or BPH. Therefore, the anti-cancer effects of conventional retinoids appear to be limited to androgen-dependent prostate cancer cells, whereas the more aggressive androgen-independent prostate cancer cells are refractory to these compounds (Campbell *et al.*, 1998).

In our study, the RXR-α was detected in almost all samples studied. In normal prostates, this receptor was located in the nucleus of both basal and secretory cells, showing a higher intensity of label in basal cells (Figure 62). In nodular and basal cell hyperplasia, RXR-α was found in the nuclear and cytoplasmic compartments, appearing almost exclusively in basal cells. However, in samples presenting atrophic hyper-
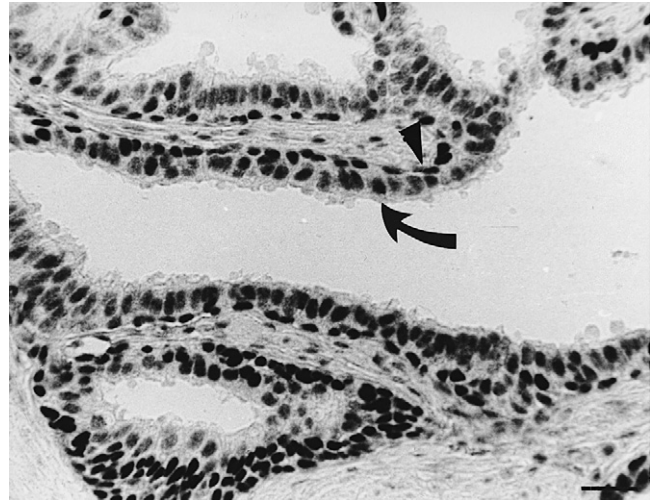
Figure 62 Positive immunoreaction to RXR-α in the nucleus of both basal cells (*arrowhead*) and secretory epithelial cells (*arrow*) of a normal prostate. Immunoreaction was more intense in basal cells. Bar: 25 μm.

plasia the percentage of positive cases to this receptor was lower, only reaching 22.2%. In this pathologic type, RXR-α was observed in a nuclear location.

All samples diagnosed with PIN, as low grade or as high grade, expressed RXR-α in the nucleus of basal and epithelial cells (Figure 63). A similar distribution was observed in the different carcinoma types, the only difference was that in samples diagnosed with low-grade Gleason (well-differentiated carcinomas), RXR-α expression was found in the cytoplasm (Figure 64).

It is known that retinoid receptors belong to the class of receptors (thyroid hormone receptors, vitamin D receptors, peroxisome proliferator activated receptors, etc.) that are constitutively found in the nucleus, regardless of whether the ligand is bound or not bound to the receptor, but we have found both nuclear and cytoplasmic location of the three types of receptors in some cases. Some studies suggest that the intracellular location of retinoic acid nuclear receptors may be regulated by retinoic acid and protein kinase C (Akmal *et al.*, 1998; Tahayato *et al.*, 1993). In this sense Akmal *et al.* (1998) reported that depletion of vitamin A in rat germ cells leads to a change in the location of RAR-α from the nucleus to the cytoplasm. Moreover, down-regulation of protein kinase C, a molecule that is not a ligand for these receptors, is able to increase the cytoplasmic location of RAR-α in COS-7 cells (Tahayato *et al.*, 1993). Also, Liu *et al.* (2000) have encountered, in LAPC-4 cells and PC3 cells, that RXR-α is present in both the cytoplasm and the
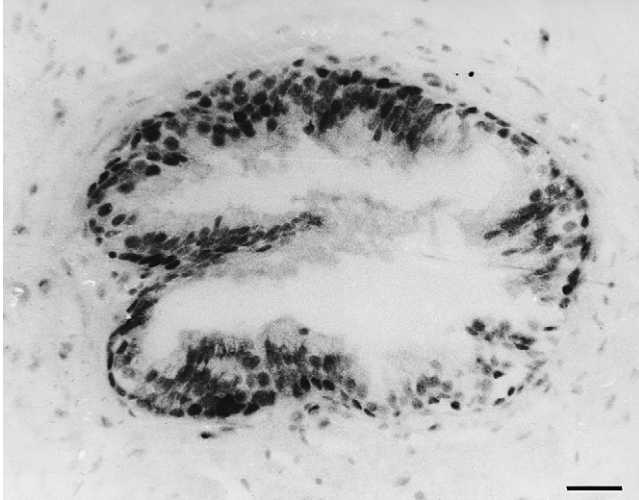
Figure 63 Nuclear immunostaining to RXR-α could be detected in low-grade prostatic intraepithelial neoplasia. Bar: 25 μm.

nucleus and, after treatment of the cells with the RXR synthetic ligand LG1069, cytoplasmic RXR-α translocated to the nucleus. In this regard, it has been reported that some nuclear receptors (steroid receptors) are found as an inactive cytoplasmic form in a complex with heat shock proteins (hsp) (Pratt and Toft, 1997). Thus, it is possible that either inactive retinoic acid nuclear receptors were forming a similar complex together with hsp or they were located in the absence of the ligand.

The retinoid X receptor β was detected in 8 of 15 (53.3%) normal prostates, showing a weaker expression
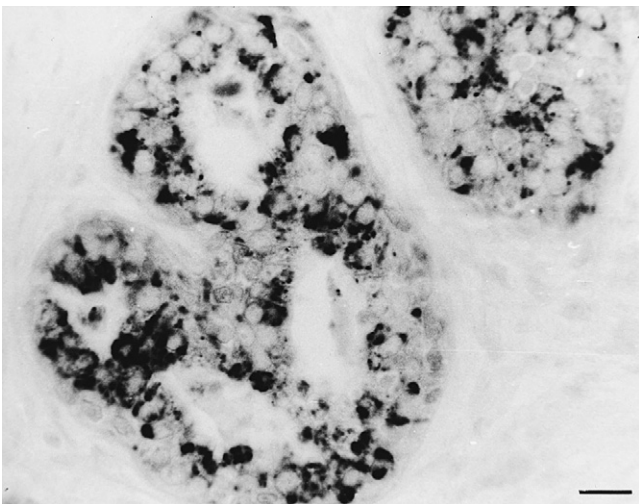
than the other retinoid receptors. This receptor was exclusively found in the nuclei and cytoplasm of basal cells. Of all BPH samples, only those presenting basal cell hyperplasia showed immunoreaction to RXR-β (Figure 65). The expression of this receptor was observed in the nucleus and the cytoplasm of basal cells and, in contrast to RXR-α, reactivity was more intense in the cytoplasm. Most of high-grade PIN foci (7 of 9) adjacent to well-differentiated carcinoma showed cytoplasmic immunoexpression to RXR-β antibody; however, in those glands adjacent to moderately and poorly differentiated carcinomas no immunoreaction in this antibody was found. Low-grade PIN foci presented a similar expression pattern to that of high-grade PIN but with higher label intensity. In prostatic adenocarcinoma, the percentage of samples positive to RXR-β was very low (3 of 25 cases, 12%). These three samples belong to well-differentiated carcinomas, and the RXR-β immunoexpression appeared in the cytoplasm (Figure 66).

Lotan *et al.* (2000), by *in situ* hybridization studies, reported a selective and significant reduction of *RXR-β* mRNA in prostate cancer and in normal prostate tissue adjacent to carcinoma. Also, Kikuwaga *et al.* (2000) detected a decrease of expression of RXR-β protein in prostatic cancer tissue. We have also observed a reduction of RXR-β protein (it was only expressed in three cases classified as well-differentiated carcinomas of 25 prostatic carcinoma samples); however, Kikuwaga *et al.* (2000) observed RXR-β expression in moderate- and poorly differentiated carcinomas. This reduced expression of RXR-β could be involved in the onset of prostate

Figure 64 Well-differentiated adenocarcinoma showing cytoplasmic labeling to RXR-α. Bar: 15 μm.
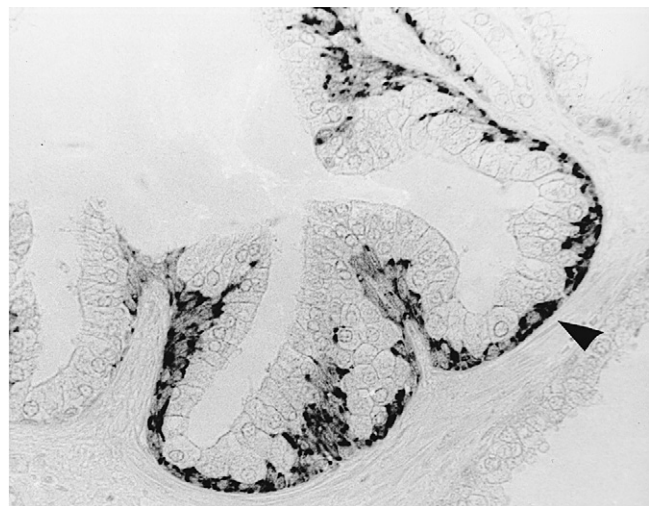
Figure 65 In glands presenting basal cell hyperplasia, the RXR-β labeling was more intense in the cytoplasm than in the nucleus (*arrowhead*). Bar: 25 μm.
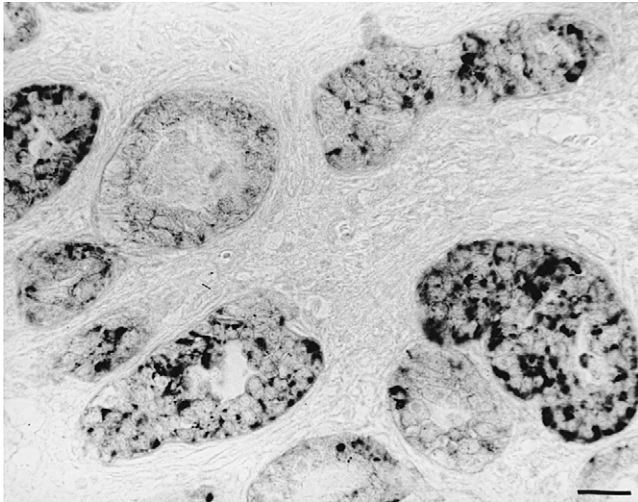
Figure 66 Cytoplasmic location of RXR-β in well-differentiated adenocarcinoma. Bar: 25 μm.
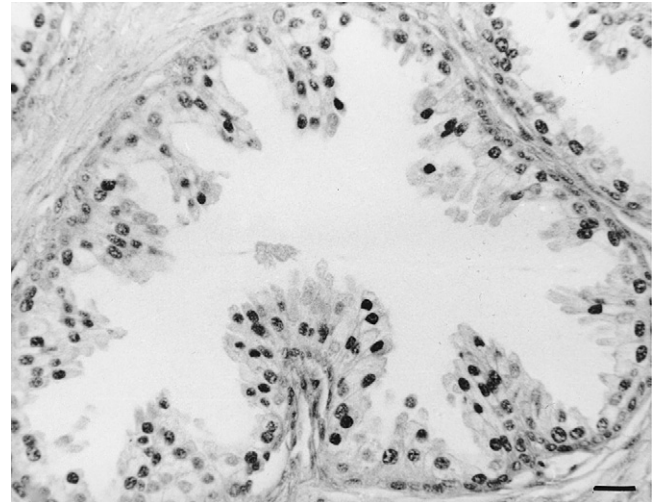
Figure 67 Low-grade prostatic intraepithelial neoplasia with papillary pattern. The nuclei of epithelial and still-present basal cells showed an intense immunolabeling to RXR-γ. Bar: 25 μm.

carcinogenesis because glands presenting PIN showed the same expression pattern as those positive samples with prostatic carcinoma. Also, this loss of expression could be related (in an advanced disease steady) to the ineffectiveness of retinoic acid treatment in some patients with androgen-independent or dependent prostate cancer (Trump *et al.*, 1997), but this hypothesis remains to be investigated.

The expression and distribution pattern of RXR-γ was similar to that found for RXR-α in most of the normal and pathologic samples (Figure 67). However, in prostates with nodular hyperplasia, the expression of RXR-γ was reduced to 87.5% of cases.

Taking these data together, it can be observed that expression of RXR-α and RXR-γ decreased in atrophic hyperplasia in comparison to that in normal

prostatic tissue. However, in nodular and basal cell hyperplasia, the expression was maintained. In prostatic adenocarcinoma, RXR-α and RXR-γ immunoexpression did not suffer variation in respect to that of normal tissue and is similar to that of PIN. The absence of changes in the expression of these receptors suggests that they do not play a significant role in prostate carcinogenesis. This hypothesis is in agreement with the weak inhibition of prostate cancer cell proliferation induced by RXR-α selective synthetic ligands (Vos *et al.*, 1997). However, RXR-β was expressed in 8 of 15 (53.3%) normal prostates and in 32% of the hyperplastic prostates studied, all of them diagnosed as basal cell hyperplasia. These data, together with those obtained for the other RXRs, lead to the suggestion that patients presenting with basal cell hyperplasia are potential

Table 11 Number of Prostates Showing Positive Immunostaining to the Three Retinoid X Receptor Types

| Receptor | Normal Prostates (n = 15) | Benign Hyperplastic Prostates | | | Prostatic Intraepithelial Neoplasia Foci (n = 40) | | Prostatic Adenocarcinoma (n = 25) | | |
		NH (n = 8)	BCH (n = 8)	AH (n = 9)	LG (n = 15)	HG (n = 25)	WDA (n = 9)	MDA (n = 8)	PDA (n = 8)
RXR-α	15 (100%)	8 (100%)	8 (100%)	2 (22.5%)	15 (100%)	25 (100%)	9 (100%)	8 (100%)	8 (100%)
RXR-β	8 (53.3%)	0 (0%)	8 (100%)	0 (0%)	9 (36%)	7 (28%)	3 (33.3%)	0 (0%)	0 (0%)
RXR-γ	15 (100%)	7 (87.5%)	8 (100%)	2 (22.5%)	15 (100%)	25 (100%)	9 (100%)	8 (100%)	8 (100%)

AH, atrophic hyperplasia; *BCH*, basal cell hyperplasia; *HG*, high-grade intraepithelial neoplasia; *LG*, low-grade prostatic intraepithelial neoplasia; *MDA*, moderate-differentiated adenocarcinoma; *NH*, Nodular hyperplasia; *PDA*, poorly differentiated adenocarcinoma; *WDA*, well-differentiated adenocarcinoma.

targets to receive treatment with retinoic acid as a result of the presence of the three types of receptors. However, in the patients that suffer atrophic and nodular hyperplasia, it is probable that this treatment is unsuccessful because of the low amount of the three types of RXRs (complete absence in the case of RXR-β).

At present, many of the markers used are not useful for a precise and early diagnosis of prostatic adenocarcinoma. In this case, the identification of reliable molecular markers indicating the potential development of a tumor or its later aggressiveness is an essential event in the oncology contest. Thus, Qiu *et al.* (1999) have proposed that the loss of RAR-β expression is an early event associated with esophageal carcinogenesis and the status of squamous differentiation. These authors also suggested that loss of this receptor is a common event across cancers of different types and etiologies.

Moreover, it has been reported that in several carcinoma types, such as head and neck squamous cell carcinomas and colorectal and cervical cancer, there is a loss or alteration at the chromosomal region 6p21.3 (Chatterjee *et al.*, 2001), where *RXR-β* gene is located (Fitzgibbon *et al.*, 1993). Also, Verhagen *et al.* (2000), studying high-risk prostate cancer pedigrees, observed a loss of 6p21.1-6p22 region, which was linked to the genetic region associated to prostatic carcinoma (*HPC-1*). However, it is known that the tumor necrosis factor-alpha (TNF-α) protein was strongly expressed in epithelial cells of prostate cancer tissue (Mizokami *et al.*, 2000), and this cytokine regulates negatively the *RXR-β* gene promoter diminishing the RXR-β mRNA and protein expression (Sugawara *et al.*, 1998). Therefore, the absence of RXR-β observed in this study in moderately and poorly differentiated carcinoma could be explained by these two mechanisms proposed earlier.

We propose that, for improving the usefulness in prostate cancer treatment with retinoids and other compounds related to the receptors that heterodimerize with RXRs, it would be necessary to study the loss or alteration of *RXR*s genes and the RXRs protein profile in prostatic specimens to clearly define the subsets of patients in whom retinoic acid–based therapies may be of clinical value.

References

Akmal, K.M., Dufour, J.M., Vo., M., Higginson, S., and Kim, K.H. 1998. Ligand dependent regulation of retinoic acid receptor α in rat testis: *in vivo* response to depletion and repletion of vitamin A. *Endocrinology 139*:1239–1248.

Brocard, J., Kastner, P., and Chambon, P. 1996. Two novel RXRa isoforms from mouse testis. Biochem. *Biophys. Res. Commun. 229*:211–218.

Calza, L., Giuliani, A., Fernandez, M., Pirondi, S., D'Intino, G., Aloe, L., and Giardino, L. 2003. Neural stem cells and cholinergic neurons: Regulation by immunolesion and treatment with mitogens, tetinoic acid, and nerve growth factor. *Proc. Natl. Acad. Sci. USA 100*:7325–7330.

Campbell, M.J., Park, S., Uskokovic, M.R., Dawson, M.L., and Koeffler, H.P. 1998. Expression of retinoic acid receptor-β sensitizes prostate cancer cells to growth inhibition mediated by combinations of retinoids and a 19-nor hexafluoride vitamin D_3 analog. *Endocrinology 139*:1972–1980.

Chatterjee, A., Pulido, H.A., Koul, S., Beleno, N., Perilla, A., Posso, H., Manusukhani, M., and Murty, V.V. 2001. Mapping the sites of putative tumor supresor genes at 6p25 and 6p21.3 in cervical carcinoma: Occurrence of allelic deletions in precancerous lesions. *Cancer Res. 61*:2119–2123.

de The, H. 1996. Altered retinoic acid receptors. *FASEB J. 10*:955–960.

de The, H., Chomienne, C., Lanotte, M., Degos, L., and Dejean, A. 1990. The t(15;17) translocation of acute promyelocytic leukaemia fuses the retinoic acid receptor alpha gene to a novel transcribed locus. *Nature 347*:558–561.

Fitzgibbon, J., Gillett, G.T., Woodward, K.J., Boyle, J.M., Wolfe, J., and Povey, S. 1993. Mapping of RXRB to human chromosome 6p21.3. *Ann. Hum. Genet. 57*:203–209.

Gebert, J.F., Moghal, N., Frangioni, J.V., Sugarbaker, D.J., and Neel, B.G. 1991. High frequency of retinoic acid beta abnormalities in human lung cancer. *Oncogene 6*:1859–1868.

Giguere, V. 1994. Retinoic acid receptors and cellular retinoid binding proteins: Complex interplay in retinoid signaling. *Endocr. Rev. 15*:61–79.

Hansen, L.A., Sigman, C.C., Andreola, F., Ross, S.A., Kelloff, G.J., and DeLuca, L.M. 2000. Retinoids in chemoprevention and differentiation therapy. *Carcinogenesis 21*:1271–1279.

Kikugawa, T., Tanji, N., Miyazaki, T., and Yokoyama, M. 2000. Immunohistochemical study of the receptors for retinoic acid in prostate adenocarcinoma. *Anticancer Res. 20*:3897–3902.

Kliewer, S.A., Umesomo, K., Mangelsdorf, D.J., and Evans, R.M. 1992. Retinoid X receptor interacts with nuclear receptors in retinoic acid, thyroid hormone and vitamin D3 signaling. *Nature 355*:446–449.

Liu, B., Lee, H-Y., Weinzimer, S.A., Powell, D.R., Cliford, I.L., Kane, J.M., and Cohen, P. 2000. Direct functional interactions between insulin-like growth factor-binding protein-3 and retinoid X receptor-α regulate transcriptional signaling and apoptosis. *J. Biol. Chem. 275*:33607–33613.

Lotan, B.Y., Xu, X.C., Shalev, M., Lotan, R., Williams, R., Wheeler, T.M., Thompson, T.C., and Kadmon, D. 2000. Differential expression of nuclear retinoid receptors in normal and malignant prostates. *J. Clin. Oncol. 18*:116–121.

Lotan, R., Lotan, D., and Sacks, P.G. 1990. Inhibition of tumour cell growth by retinoids. *Methods. Enzymol. 190*:100–110.

Mangelsdorf, D.J., and Evans, R.M. 1995. The RXR heterodimers and orphan receptors. *Cell 93*:841–850.

Mangelsdorf, D.J., Thummel, C., Beato, M., Herrlich, P., Schültz, G., Umesono, K., Blumberg, B., Kastner, P., Mark, M., Chambon, P., and Evans, R.M. 1995. The nuclear receptor superfamily: The second decade. *Cell 83*:835–839.

McCormiek, D.L., Rao, K.V., Steele, V.E., Lubet, R.A., Kelloff, G.J., and Bosland, M.C. 1999. Chemoprevention or rat prostate carcinogenesis by 9-cis-retinoic acid. *Cancer Res. 59*:521–524.

Mizokami, A., Gotoh, A., Yamada, H., Keller, E.T., and Matsumoto, T. 2000. Tumor necrosis factor-alpha represes androgen sensitivity in the LNCaP prostate cell line. *J. Urol. 164*:800–805.

Nagy, L., Thomazy, V.A., Heyman, R.A., and Davies, P.J. 1998. Retinoid-induced apoptosis in normal and neoplastic tissues. *Cell Death Differ.* 5:1–3.

Pasquali, D., Rossi, V., Prezioso, D., Gentile, V., Colantuoni, V., Lotti, T., Bellastella, A., and Sinisi, A.A. 1999. Changes in tissue transfiltaminase activity and expression during retinoic acid-induced growth arrest and apoptosis in primary cultures of human epithelial prostate cells. *J. Clin. Endocrinol. Metab.* 84:1463–1469.

Pasquali, D., Thaller, C., and Eichele, G. 1996. Abnormal level retinoic acid in prostate cancer tissues. *J. Clin. Endocrinol. Metab.* 8:2186–2191.

Pratt, W.B., and Toft, D.O. 1997. Steroid receptor interactions with heat sock proteins and immunophilin chaperones. *Endocrinol. Rev. 18*:306–360.

Qui, H., Zhang, W., El-Naggar, A.K., Lippman, S.M., Lin, P., Lotan, R., and Xu, X-C. 1999. Loss of retinoic acid receptor-ß is an early event during esophageal carcinogenesis. *Am. J. Phatol. 155*: 1519–1523.

Sugawara, A., Uruno, A., Nagata, r., Taketo, M.M. Takeuchi, K., and Ito, S. 1998. Characterization of mouse retinoid X receptor (RXR)-β gene promoter: Negative regulation bu tumor necrosis factor (TNF)-α. *Endocrinology 139*:3030–3033.

Sun, S-Y., and Lotan, R. 2002. Retinoids and their receptors in cancer development and chemoprevention. *Crit. Rev. Oncol. Hemato. 41*:41–55.

Sun, S-Y, Yue, P., and Lotan, R. 1999. Induction of apoptosis by *N*-(4-hydroxyphenyl)retinamide and its association with reactive oxygen species, nuclear retinoic acid receptors, and apoptosis-related genes in human prostate carcinoma cells. *Mol. Pharmacol. 55*:403–410.

Tahayato, A., Lefebvre, P., Fromstecher, P., and Dautrevaus, M. 1993. A protein kinase C-dependent activity modulates retinoic acid-induced transcription. *Mol. Endocrinol. 7*:1642–1653.

Thaller, C., Shalev, M., Frolov, A., Eichele, G., Thompson, T.C., Williams, R.H., Dillioglugil, O., and Kadmon, D. 2000. Fenretinide therapy in prostate cancer: Effects on tissue and serum retinoid concentration. *J. Clin. Oncol. 18*:3804–3808.

Trump, D.L., Smith, D.C., Stiff, D., Adedoyin, A., Day, R., Bahnson, R.R., Hofacker, J., and Branch, R.A. 1997. A phase II trial of all-trans-retinoic acid in hormone-refractory prostate cancer: A clinical trial with detailed pharmacokinetic analysis. *Cancer Chemother. Pharmacol. 39*:349–356.

Verghen, P.C.M.S., Zhu, X.L., Rohr, L.R., Cannon-Albright,L.A., Tavitgian, S.V., Skolnick, M.H., and Brothman, A.R. 2000. Microdissection, DOP-PCR, and comparative genomic hybridization of paraffin-embedded familial prostate cancers. *Cancer Gen. Cytogen. 122*:43–48.

Vos, S., Dawson, M.I., Holden, S., Le, T., Wang, A., Cho, S.K., Chen, D.L., and Koeffler, H.P. 1997. Effects of retinoid X receptor-selective ligands on proliferation of prostate cancer cells. *Prostate 32*:115–121.

Wu, Q., Dawson, M.I., Zheng, Y., Hobbs, P.D., Agadir, A., Jong, L., and Li, Y. 1997. Inhibition of trans-retinoic acid-resistant human breast cancer cell growth by retinoid X receptor-selective retinoids. *Mol. Cell. Biol. 17*:6598–6608.

Xu, X.C., and Lotan, R. 1999. Aberrant expression and function of retinoid receptors in cancer. In Nau, J., Blancer, W.S (eds) *Retinoids: The Biochemical and Molecular Basis of Vitamin A and Retinoid Action*. Berlin: Springer, 323–343.

Zhang, X.K., Lehmann, J., Hoffman, B., Dawson, M.I., Comeron, J., Graupner, G., Hermann, T., Tran, P., and Pfahl, M. 1992. Homodimer formation of retinoid X receptor induced by 9-cis retinoic acid. *Nature 358*:587–591.

13

Role of Androgen Receptor Cofactors in Prostate Cancer

Peng Lee and Zhengxin Wang

Introduction

The androgen receptor (AR) is a transcriptional activator that belongs to the steroid receptor superfamily and mediates androgen function in the development and maintenance of normal prostate tissue (Craft and Sawyers, 1998; Craft *et al.,* 1999a; Denmeade *et al.,* 1996; Jenster, 1999). Androgen causes increased cell proliferation in the prostate. Withdrawing androgen can inhibit prostatic cell growth and induce apoptosis (Denmeade *et al.,* 1996). However, results from tissue cultures and whole-animal studies suggest that androgens can also inhibit proliferation of prostate cells under certain circumstances. For example, cells from the PC3 cell line, derived from a human prostate carcinoma, do not express *AR* (Tilley *et al.,* 1990), but ectopic expression of AR complementary deoxyribonucleic acid (cDNA) led to slowed growth in PC3 cells in response to androgens (Yuan *et al.,* 1993). Immortalized nontumorigenic rat prostatic cells stably transfected with *AR* grew more slowly in the presence of androgens than those lacking *AR* (Whitacre *et al.,* 2002). Further analysis revealed that androgen-induced terminal cell differentiation caused growth inhibition (Whitacre *et al.,* 2002). The proliferation

rate of prostate cells in normal mice was shown to be very low. Testosterone injection into castrated animals increased prostate cell proliferation until a peak was reached (24–48 hr). After that point, the rate of cell proliferation gradually returned to the lower levels (Mirosevich *et al.,* 1999). This ability of androgens to mediate growth suppression indicates that they may have a dual role in cell proliferation and differentiation in the prostate gland.

Prostate cancer cells also appear to be dependent on AR. However, whereas prostate cancer usually begins as an androgen-dependent tumor that regresses in response to androgen ablation, tumors invariably and eventually reappear and progress in an androgen-independent manner (Craft and Sawyers, 1998; Craft *et al.,* 1999a; Denmeade *et al.,* 1996; Jenster, 1999). The continued expression (in most tumors) of both *AR* and diagnostic target genes that are normally androgen dependent (e.g., prostate specific antigen [PSA]) suggests that AR functions in the growth of advanced stage androgen-independent tumors (Balk, 2002; Bentel and Tilley, 1996; Culig *et al.,* 1998; Grossmann *et al.,* 2001). Studies with xenografts and cell lines have also implicated the role of AR in activation of the *PSA* gene and androgen-independent tumor growth despite the

Handbook of Immunohistochemistry and *in situ* Hybridization of Human Carcinomas, Volume 2: Molecular Pathology, Colorectal Carcinoma, and Prostate Carcinoma

409

absence of androgen (Balk, 2002; Craft *et al.,* 1999a; Craft *et al.,* 1999b; Zegarra-Moro *et al.,* 2002).

Although the molecular mechanisms that contribute to androgen-independent prostate cancer cell growth and expression of AR-dependent genes are not firmly established, one possibility is that AR mutations occurring in the ligand-binding domain of AR relax the ligand specificity and allow other steroid hormones (e.g., estrogenic or progestogenic) to activate the target genes (Bentel and Tilley, 1996; Culig *et al.,* 1998; Jenster, 1999). Another possibility is the activation of signaling pathways that synergize with the AR pathway by enhancing the levels (cellular concentrations) or activities (through functional modifications) of factors that regulate AR function on key target genes. Possible downstream targets include: 1) AR itself, 2) additional DNA-binding activators that synergize with AR, and 3) AR-interacting coactivators (see later) that directly or indirectly (via chromatin modifications) facilitate transcription.

In this regard, and consistent with similar findings for estrogen and progesterone receptors (Craft *et al.,* 1999b), it has been shown that 1) various factors (e.g., epidermal growth factor [EGF], insulin-like growth factor [IGF]-1, and keratinocyte growth factor [KGF]) (Culig *et al.,* 1994) and ectopic MEKK-1 (Abreu-Martin *et al.,* 1999) activate AR in an androgen-independent manner in prostate cancer cells; and 2) that androgen-independent prostatic cancer lines express the HER-2/neu receptor tyrosine kinase at higher levels than their androgen-dependent counterparts do and that, when ectopically expressed, HER-2/neu can facilitate the growth of androgen-independent cells and activate the AR pathway (Craft *et al.,* 1999b; Yeh *et al.,* 1999). It is interesting that a fraction of prostate cancer overexpresses *HER-2/neu* (Jorda *et al.,* 2002).

Like other members of the steroid receptor superfamily, AR contains a central DNA-binding domain, a C-terminal ligand-binding domain with an associated activation function-2 (AF-2) domain, and a N-terminal region containing the AF-1 domain (Brinkmann *et al.,* 1999). As is the case for other steroid receptors, ligand binding is generally believed to result in a conformational change in the AR with subsequent dissociation of heat shock proteins/chaperones; dimerization; binding to cognate androgen response elements (AREs) in target genes; and, through its AF-1 and AF-2 domains, interacting with various coactivators (later in this chapter) that facilitate transcription by the general transcriptional machinery (Brinkmann *et al.,* 1999).

Although the isolated AF-1 and AF-2 domains of the AR, like those of other receptors, can function independently with the p160 family of coactivators

(later), the AR interactions are more complex, and in the context of full-length AR, there appear to be pairwise interactions between AF-1 and AF-2, between AF-1 and a C-terminal part of p160, and (perhaps less significantly) between AF-2 and a distinct region (nuclear receptor interaction domain [NID]) of p160 (Alen *et al.,* 1999b; Berrevoets *et al.,* 1998; Ikonen *et al.,* 1997; Ma *et al.,* 1999). Distinct activation domains in p160 interact, in turn, with the coactivator p300/CBP (Aarnisalo *et al.,* 1998; Ma *et al.,* 1999), which also interacts directly with the AF-1 domain of the AR (Alen *et al.,* 1999b) and with as-yet-unknown factors.

As demonstrated in studies of other activators, AR requires the general initiation factors that form preinitiation complexes on common core promoter elements (e.g., TATA box) (Roeder, 1996) to activate genes as well as a variety of general and gene-specific coactivators that either modulate chromatin structure (Kingston and Narlikar, 1999; Workman and Kingston, 1998) or serve as direct adaptors between activators and general initiation factors (Roeder, 1998). General initiation factors include TFIID (TATA-binding factor), TFIIA, TFIIB, TFIIE, TFIIH, and ribonucleic acid (RNA) polymerase II (Pol II) (Roeder, 1996); general coactivators include upstream stimulatory activity (USA)-derived positive cofactors (PCs) and TATA binding protein-associated factor (TAF) subunits of TFIID (Roeder, 1998).

Various cofactors have been implicated more directly in AR function (Gelmann, 2002; Heinlein and Chang, 2002; Janne *et al.,* 2000). These include p300/CBP (Aarnisalo *et al.,* 1998), the p160 family (SRC-1, TIF-2/GRIP-1, and ACTR/P-CIP) (Alen *et al.,* 1999b; Berrevoets *et al.,* 1998; Ikonen *et al.,* 1997; Ma *et al.,* 1999), and protein arginine methyltransferases (PRMTs) (Stallcup *et al.,* 2000). They are all involved in histone acetyltransferase (HAT) or methyltransferase activities and are believed to act mainly through histone acetylation or methylation and consequent chromatin structural perturbations, but they can also act through functional acetylation or methylation of coactivators (Chen *et al.,* 1999; Xu *et al.,* 2001).

Another group includes thyroid hormone receptor-associated protein (TRAP) components of the TRAP/DRIP/SMCC/mediator complex (Malik and Roeder, 2000), which shows subunit-specific interactions with both nuclear receptors (TRAP220 with AR, thyroid receptor [TR], vitamin D receptor [VDR], peroxisome proliferator activated receptor [PPAR], retinoid acid receptor [RAR], retinoid X receptor [RXR], and estrogen receptor [ER], and TRAP170/DRIP150 with glucocorticoid receptor [GR]) (Wang *et al.,* 2002; Yuan *et al.,* 1998). This complex, in turn, interacts with the general initiation factors as well as RNA polymerase II and acts on DNA templates

during post-chromatin–remodeling steps (Malik and Roeder, 2000).

Other cofactors that have been variously implicated in the function of AR and, in most cases, other nuclear receptors include the ARA group (ARA24, ARA54, -55, -70, and -160), androgen receptor interacting protein (ARIP)-3, small nuclear RING finger protein (SNURF), β-catenin, FHL2, cyclin D1, and aminal-terminal enhancer of split (AES) (see http://ww2.mcgill.ca/androgendb/ARIPmap.gif for the list). Less is known about the mechanistic function of these factors; some show broader effects on basal transcription and other activators (Gelmann, 2002; Heinlein and Chang, 2002; Janne *et al.,* 2000).

Studies of diverse transcriptional activators from yeast to human have revealed increasingly complex activation mechanisms involving not only the very complicated general transcriptional machinery but also a large number of cofactors. Multisubunit cofactor complexes show gene- and cell-type specificities and functional redundancies in some cases. Given the role of the AR as a transcriptional activator, which is clearly functionally linked to prostate cancer, it is imperative to understand the molecular details of its action on key genes during prostate cancer development and progression. The study of cofactor expression profile in prostate cancer provides a leading step in understanding the involvement of these cofactors in prostate tumorigenesis and cancer progression. This knowledge ultimately will allow development of therapeutic agents that target a combination of specific DNA–protein and protein–protein interactions with AR-dependent genes.

MATERIALS

Radioactive *in situ* Hybridization on Formalin-Fixed, and Paraffin-Embedded Tissue (Using a ^{33}P-Labeled RNA Probe)

Note: All stock solutions should be made with sterile water (unless otherwise specified), and working solutions should be made with diethyl pyrocarbonate (DEPC)-treated water before day 2 procedures.

1. DEPC-treated water: Add 10 ml of DEPC to 10 L of H_2O, stir overnight, and autoclave.

2. 1M Tris-C1 (pH 8.0): Dissolve 121 g of Tris base in 800 ml of water, adjust the pH to 8.0 with concentrated HCl, then add H_2O to a final volume of 1 L.

3. 3X phosphate buffer saline (PBS) (pH 7.2): Dissolve 22.8 g of NaCl, 2.13 g of Na_2HPO_4, and 1.80 g of NaH_2PO_4 in H_2O to a final volume of 1 L.

4. 4% paraformaldehyde (PFA): Heat 66 ml of H_2O to 60ºC, add 4 g of PFA and 1–2 drops of 10 N NaOH to dissolve the PFA completely, add 1/3 of the 3X PBS, and adjust the pH to 7.2 with HCl and H_2O to a final volume of 100 ml. The solution should be made fresh and filtered before use.

5. Proteinase K solution (20 μg/ml proteinase K, 50 mM Tris [pH 8.0], 2 mM $CaCl_2$): Add 32 μl of proteinase K from a 25 mg/ml stock solution to a solution consisting of 38 ml of sterilized water, 2 ml of 1M Tris buffer (pH 8.0) and 80 μL of 1 M $CaCl_2$.

Note: Incubate at room temperature for 20 min and at 37ºC for 10 min before use.

6. 0.1 M triethanolamine (TEA) (pH 8.0): Add 1.4 g of TEA-Cl (Fluka, Ronkonkoma, NY) to DEPC-treated water to a final volume of 100 ml, and adjust the pH to 8.0 by adding NaOH.

7. 5 M NaCl: Dissolve 146 g of NaCl in H_2O to a final volume of 500 ml.

8. 20X saline-sodium citrate (SSC): Dissolve 175.3 g of NaCl and 88.2 g of sodium citrate in 800 ml of water, adjust the pH to 7.0 with a few drops of NaOH, and then add H_2O to a final volume of 1 L.

9. 50X Tris-acetic acid-ethylenediamine tetra-acetic acid (TAE) electrophoresis buffer: Dissolve 242 g of Tris base and 37.2 g of $Na_2EDTA-2H_2O$ in 800 ml of water, add 57.1 ml of glacial acetic acid, adjust the pH to 8.5, and add H_2O to a final volume of 1 L.

10. 100X Denhardt's solution: Dissolve 10 g of Ficoll 400, 10 g of polyvinylpyrolidone, and 10 g of bovine serum albumin (BSA) in H_2O to a final volume of 500 ml. Filter and store at –20ºC.

11. 1 M dithiothreitol (DTT): Dissolve 15.45 g of DTT in H_2O to a final volume of 100 ml, and then store at –20ºC.

12. 0.5 M Ethylenediamine tetra-acetic acid (EDTA): Dissolve 186.1 g of $Na_2EDTA-2H_2O$ in 800 ml H_2O by stirring vigorously, adjust the pH to 8.0 with about 20 g of NaOH, and then add H_2O to a final volume of 1 L.

13. 7.5 M ammonium acetate: 57.8 g of ammonium acetate in 100 ml of H_2O.

14. Prehybridization solution (50% formamide, 0.3 M NaCl, 10 mM Tris [pH 8.0], 1 mM EDTA, 500 μg/ml salmon sperm DNA, 500 μg/ml yeast transfer RNA [tRNA]): Add 1 ml of deionized formamide, 120 μl of 5 M NaCl, 20 μl of 1 M Tris (pH 8.0), 4 μl of 0.5 M EDTA, 250 μl of 4 mg/ml salmon sperm DNA, 200 μl of 5 mg/ml yeast tRNA and 406 μl of DEPC H_2O for 2 ml of prehybridization solution.

15. Hybridization solution (50% formamide, 0.3 M NaCl, 20 mM Tris [pH 8.0], 5 mM EDTA, 10 mM Na-phosphate buffer [pH 8.0], 10% dextran sulfate,

1X Denhardt's solution, 500 mg/ml yeast tRNA, and radioactive probe): Add 1 ml of deionized formamide, 120 µl of 5 M NaCl, 40 µl of 1 M Tris (pH 8.0), 20 µl of 0.5 M EDTA, 40 µl of 50X Denhardt's solution, 40 µl of 0.5 M Na-phosphate buffer (pH 8.0), 200 mg of dextran sulfate, 200 µl of 5 mg/ml yeast tRNA, and DEPC H_2O to 2 ml.

Note: Use $2–5 \times 10^6$ count per minute [cpm] probe/50 µl of hybridization solution. The hybridization solution should be placed at 65ºC for 1–2 hr before adding the probes because it takes time for dextran sulfate to dissolve. Boil the probe for 5 min, and chill on ice just before use.

16. Moist chamber solution: 2X SSC or 2X SSC in 50% formamide.

17. 5X SSC: Add 62.5 ml of 20X SSC with 187 ml H_2O for 250 ml of 5X SSC.

18. 2X SSC: Add 100 ml of 20X SSC to 900 ml H_2O.

19. 50% formamide/2X SSC solution: Add 125 ml of formamide, 25 ml of 20X SSC, and 100 ml of H_2O for 250 ml 50% formamide/2X SSC.

20. RNase buffer (0.3 M NaCl, 10 mM Tris [pH 8.0], 5 mM EDTA): Add 15 ml of 5 M NaCl, 2.5 ml of 1 M Tris, 2.5 ml of 0.5 M EDTA, 230 ml of ddH_2O for 250 ml RNase buffer.

21. RNase A solution (50 µg/ml RNase A, 0.3 M NaCl, 10 mM Tris [pH 8.0], 5 mM EDTA): Add 1.25 ml of 10 mg/ml RNase A, 15 ml of 5M NaCl, 2.5 ml of 1 M Tris (pH 8.0), 2.5 ml of 0.5 M EDTA, 228.75 ml of H_2O for 250 ml RNase A solution.

22. Sample mix: Add 40 µl 5X RNA gel running buffer (TAE), 70 µl of formaldehyde, and 200 µl of formamide.

23. Loading dye solution: 50% glycerol, 1 mM EDTA (pH 8.0), 0.25% BPP, 0.25% xylene cyanol FF.

24. 20% trichloroacetic acid (TCA), 7% TCA, 5% TCA.

25. 1.2% RNA agarose gel: Dissolve 1.2 g of agarose in 62.5 ml of DEPC H_2O, heat to 60ºC, and add 17.9 ml formaldehyde (under the hood) and 19.6 ml of 5X gel running buffer (TAE). Pour the mixture into a gel tray with a gel comb.

26. Histoclear or xylene.

27. 100% ethanol (EtOH), 95% EtOH, 85% EtOH, 70% EtOH.

28. Sephadex G-50 column.

29. Silicon spray.

30. Gill's hematoxylin.

31. Diluted eosin.

32. Scott's water.

33. Emulsion NTB-2 Kodak.

34. Kodak D-19 developer.

35. Kodak fixer.

Nonradioactive *in situ* Hybridization on Formalin-Fixed and Paraffin-Embedded Tissue (Using Digoxigenin-Labeled RNA Probe)

1. DEPC-treated water: Add 10 ml of DEPC to 10 L of H_2O, stir overnight, and autoclave.

2. 1 M Tris-Cl (pH 8.0): Dissolve 121 g of Tris base in 800 ml of water, adjust the pH to 8.0 with concentrated HCl, then add water to a volume of 1 L, and autoclave.

3. 3X PBS (pH 7.2): Add 22.8 g of NaCl, 2.13 g of Na_2HPO_4, and 1.80 g of NaH_2PO_4 to 1 L water.

4. 4% PFA: Heat 66 ml of water to 60ºC, add 4 g of PFA and 1–2 drops of 10 N NaOH to dissolve the PFA completely, add 1/3 of the 3X PBS, adjust the pH to 7.2 with HCl and add H_2O to a final volume of 100 ml. Filter it before use.

5. Proteinase K solution (20 µg/ML proteinase K, 50 mM Tris [pH 8.0], 2 mM $CaCl_2$): Add 32 µl of proteinase K from a 25 mg/ml stock solution to a solution consisting of 40 ml of sterilized water, 2 ml of 1 M Tris buffer (pH 8.0) and 80 µl of 1 M $CaCl_2$.

Note: Incubate at room temperature for 20 min and at 37ºC for 10 min before use.

6. 0.1 M TEA (pH 8.0): Add 1.4 g of TEA-Cl to DEPC-treated water to a final volume of 100 ml, adjust the pH to 8.0 by adding NaOH.

7. 1 M $CaCl_2$: Dissolve 147 g of $CaCl_2$ in H_2O to a final volume of 1 L.

8. 5 M NaCl: Dissolve 146 g of NaCl in H_2O to a final volume of 500 ml.

9. 1 M $MgCl_2$: Dissolve 19.4 g of $MgCl_2$ in H_2O to a final volume of 200 ml.

10. 4 M LiCl: Dissolve 170 g of LiCl in H_2O to a final volume of 1000 ml.

11. 20X SSC: Dissolve 175.3 g of NaCl and 88.2 g of sodium citrate in 800 ml of water, adjust the pH to 7.0 with a few drops of NaOH, and then add H_2O to a final volume of 1 L.

12. Prehybridization solution (50% deionized formamide, 1X Denhardt's solution, 10% dextran sulfate, 20 mM DTT, 250 µg/ml salmon sperm DNA, 500 µg/ml yeast tRNA in 2X SSC): Add 5 ml of 100% deionized formamide (Boehringer Mannheim Corp., Indianapolis, IN), 1 ml of 20X SSC; 100 µl of 100X Denhardt's solution, 1 g of dextran sulfate, 5 mg of yeast tRNA, 2.5 mg of salmon sperm DNA (predenatured), 200 µl of 1 M DTT, and DEPC-treated water to 10 ml, stir overnight, aliquot, and store at –80ºC.

13. Hybridization solution: Add 20 ng of the probe to µl of prehybridization solution.

14. 100X Denhardt's solution: Dissolve 10 g of Ficoll 400, 10 g of polyvinylpyrrolidone, and 10 g of

BSA in water to make up 500 ml. Filter and store at –20ºC.

15. 1 M DTT: Dissolve 15.45 g of DTT in H_2O to a final volume of 100 ml, and then store at –20ºC.

16. 0.5 M EDTA: Dissolve 186.1 g of Na_2EDTA-$2H_2O$ in 800 ml of water by stirring vigorously, adjust the pH to 8.0 with about 20 g of NaOH, and then add H_2O to a final volume of 1 l.

17. Buffer 1 (100 mM maleic acid, 150 mM NaCl): Dissolve 16 g of maleic acid and 8.77 g of NaCl in 900 ml of DEPC–H_2O, adjust the pH to 7.5 with HCl, and add DEPC–H_2O to a final volume of 1 L.

18. Buffer 2: Dissolve 10 g of the blocking reagent provided in the digoxigenin detection kit (Boehringer) in buffer 1 to a 1:10 dilution by heating and then store this at –20ºC.

19. Buffer 3 (100 mM Tris [pH 8.0], 100 mM NaCl, 50 mM $MgCl_2$): Add 100 ml of 1 M Tris-Cl, 20 ml of 5 M NaCl, and 50 ml of 1 M $MgCl_2$ to 800 ml of DEPC–H_2O, adjust the pH to 9.5, and add DEPC–H_2O to a volume of 1 L.

Note: The buffer can be filtered with Whatman No. 1 filter if precipitation occurs.

20. Buffer 4 (Tris-EDTA, TE): Add 10 ml of 1M Tris-Cl and 2 ml of 0.5 M EDTA in DEPC–H_2O to a final volume of 1 L, and then adjust the pH to 8.0.

21. 4 M LiCl: Dissolve 16.95 g of LiCl in DEPC–H_2O to a final volume of 100 ml.

22. Chromogenic substrate solution: Mix 45 µl of nitroblue tetrazolium (NBT) solution and 35 µl of X-phosphate solution in 10 ml buffer 3.

Note: The substrate solution should be prepared fresh before use.

23. 0.2 N HCl: Combine 10 ml of 1M HCl and 40 ml of DEPC–H_2O.

24. Moist chamber solution: 2X SSC or 2X SSC in 50% formamide.

25. Digoxigenin RNA labeling kit (Boehringer, Cat. No. 1175025).

26. Digoxigenin nucleic acid detection kit (Boehringer, Cat. No. 1175041).

27. 2X SSC/0.5% Triton/2% normal sheep serum (NSS): Use a vortex to mix 40 ml of 2X SSC, 200 µl of Triton X-100. Add 800 µl of NSS and invert to mix just prior to use.

28. Buffer 1/0.3% Triton/2% NSS: Use vortex to mix 40 ml of buffer 1, 120 µl of Triton X-100. Add 800 µl of NSS just prior to use.

29. Conjugate solution: Use vortex to mix 2 ml of buffer 1 and 6 µl of Triton X-100. Just prior to use, add 200 µl of NSS and 4 µl of antibody conjugate (tube from digoxigenin nucleic acid detection kit, Boehringer). Tap the tube to mix.

Radioactive *in situ* Hybridization on Formalin-Fixed and Paraffin-Embedded Tissue (Using ^{33}P-Labeled RNA Probe)

Day 1

Labeling the Probe

Note: Once labeled, the probe should be usable for a month at –70ºC.

1. High specific activity ^{33}P probe-labeling
   5 µl of 5X transcription buffer.
   1 µl of 100 mM DTT.
   1 µl of RNAsin.
   5 µl of rNTP (2.5 mM of GTP, ATP, CTP, and 15 mM of UTP).
   1 µl of DNA template (1 µg/ml, either plasmid or polymerase chain reaction [PCR] product).
   10 µl of α-^{33}P UTP (200 µCi, final concentration 0.4 µM).
   1 µl of RNA polymerase (either T7 or T3 polymerase).
   DEPC H_2O to a 25 ml reaction volume.

2. Incubate the probe for 2 hr at 37ºC.

3. Add 1 µl more of RNA polymerase to the probe and incubate for 30 more min.

4. Add 0.5 µl of RNase A-free DNAse I to the probe and incubate for 15 min at 37ºC.

5. Add 1 µl of 0.5M EDTA (pH 8.0) to the probe to stop the reaction.

6. Add 25 µl of TE (pH 8.0) to the probe, transfer the RNA probe solutions into the Sephadex G-50 columns, and purify by centrifuging at 1500 rpm for 3 min.

Note: Sephadex G-50 columns should be centrifuged at 1500 rpm for 3 min before the probe is added to remove the original buffer solutions in it.

7. Collecting the probe in a new Eppendorf tube, precipitate the probe with 1/10 of the 7.5 M ammonium acetate, 2.5 volumes of cold EtOH, and 10 mg of tRNA as the carrier overnight at –20ºC.

Day 2

8. Centrifuge the probe for 10 min, carefully aspirate out the liquid contents, and leave the tubes open to air-dry the RNA pellet for 15 min.

9. Resuspend the probe in 25 µl of DEPC H_2O.

Examining the Yield of the Probe by Scintillation Count

10. Dilute 1 µl of the probe with 9 µl of DEPC H$_2$O (1:10 dilution).

Note: Prepare two samples in parallel for the probe.

11. Mix 0.5 ml of H$_2$O, 5 µl 10 mg/ml BSA, 1 µl of the diluted probe, 0.5 ml of 20% TCA; leave on ice for 20 min.

12. Place a filter paper in a glass filter in the filtration unit, load the probe mixture, turn on the vacuum and wash the unit with 5% TCA.

13. Air-dry the filter on a paper towel for 5 min.

14. Place the filter into scintillation vials, and then add 5 ml of Hydrofluor fluid and read scintillation counts.

Checking the Probe on an RNA Gel (Agar Formaldehyde Gel) Using 1 Million and 0.5 Million Counts

Note: Prepare two samples and one control for the probe.

15. (a) Sample 1: Add 5 µl of DEPC H$_2$O, 18 µl of sample mix, 2 µl of loading buffer, and 1 µl of the probe.

(b) Sample 2: Add 5.5 µl of DEPC H$_2$O, 18 µl of sample mix, 2 µl of loading buffer, and 0.5 µl of the probe.

(c) As a control, use a mixture of tRNA (10 µg), 28S and 18S RNA (1 µg each) with ethidium bromide (EtBr) added.

Note: The samples must be boiled for 3 min and chilled on ice before being loaded into the gel. Meanwhile, the probe should be reprecipitated with 1/10 volume of the 7.5 M NH$_4$Ac and 2.5 volumes of cold 100% EtOH and incubated overnight at –20ºC.

16. Run the gel at 50 V until the dye comes out of the wells; then switch to 100 V. Leave the gel running for ~2 hr. Trace the wells in a darkroom for 28S, 18S, tRNA.

17. Soak and shake the gel in a siliconized glass tray in 2X SSC (250 ml) and then 7% TCA for 5 min each at speed 55 rpm.

18. Blot the gel between two pieces of blot paper surrounded by paper towels; periodically change the towels. Once dry, wrap the gel in plastic wrap, expose it to film in a darkroom, and leave it in a lightproof cassette for a few hours or overnight at room temperature for sufficient exposure.

Day 3

Wax Removal and Rehydration of the Paraffin-Embedded Tissue Sections

Note: The slides should be baked at 56ºC overnight the night before.

19. Rinse the slides in Histoclear or xylene 3 times for 5 min each.

20. Rinse the slides in 100% EtOH twice for 5 min each.

21. Rinse the slides in 95% EtOH once for 2 min.

22. Rinse the slides in 85% EtOH once for 2 min.

23. Rinse the slides in 70% EtOH once for 2 min.

24. Rinse the slides in DEPC H$_2$O once for 2 min.

Prehybridization Treatment

25. Incubate the slides in 4% PFA for 20 min.

26. Rinse the slides in PBS 3 times for 5 min each.

27. Incubate the slides in proteinase K solution for 15 min.

28. Rinse the slides 3 times in PBS for 2–5 min.

29. Incubate the slides in 4% PFA for 5 min.

30. Rinse the slides 3 times in PBS for 2–5 min.

31. Incubate the slides in 0.25% acetic anhydride (Ac-O-Ac)/0.1 M triethanolamine (pH 8.0) solution for 10 min.

Note: The triethanolamine must be freshly made. Add Ac-O-Ac after the slides are already inside the triethanolamine solution.

32. Rinse the slides twice briefly in 2X SSC.

33. Rinse the slide once briefly in DEPC H$_2$O.

Prehybridization and Hybridization

34. Prehybridize the slides with 125 µl of prehybridization solution per slide for 2–4 hr at 65ºC in a moist chamber.

Note: Cover the sections with a plastic coverslip and arrange the slides in moist dark boxes horizontally with the sections facing up.

35. Hybridize the slides with 70 µl of hybridization buffer overnight at 65ºC in a moist chamber sealed with tape or plastic wrap.

Note: Use 2–5×10^6 cpm probe per slide, heat the probe to 95–100ºC for 5 min, and chill on ice immediately after.

Day 4

Post-Hybridization Treatment

36. Remove the coverslip carefully in 5X SSC and rinse the slides once in 5X SSC at 55ºC for 10 min.

37. Rinse the slides once in 50% formamide/2X SSC solution at 65ºC for 20 min.

38. Incubate the slides in RNase buffer once at 37ºC for 10 min.

39. Incubate the slides in RNase A solution at 37ºC for 30 min.

40. Rinse the slides once in RNase buffer at 37ºC for 15 min.

41. Rinse the slides once in 50% formamide/2X SSC at 65ºC for 20 min.

42. Rinse the slides twice in 2X SSC at room temperature for 15 min.

43. Rinse the slides twice in 0.1X SSC at room temperature for 15 min.

Dehydration

44. Rinse the slides twice in 70% EtOH twice for 10 min.

45. Rinse the slides once in 95% EtOH for 5 min.

46. Rinse the slides once in 100% EtOH for 5 min.

47. Air-dry the slides at room temperature for 1 hr.

Autoradiography

Note: All procedures should be performed in the dark.

48. Melt the emulsion at 42ºC for 45 min.

49. Dip the slides by immersing them slowly and withdrawing them steadily (first dip blank test slides until no bubbles are present), drain them onto a paper towel for several seconds, and wipe off the excess emulsion on the back of the slides with tissue paper.

50. Dry the emulsion on the slides for a few hours in the dark, placing the slides horizontally on paper towels.

51. Arrange the slides in exposure boxes with the emulsion side down, seal the box with tape and wrap them in aluminum foil, and store them in a desiccator at 4ºC for 2–4 weeks.

Signal Development

52. Dip the slides in Kodak D-19 developer at 17ºC for 3 min.

53. Rinse the slides in tap H_2O at room temperature for 1 min.

54. Fix the slides in Kodak fixer at room temperature for 4 min.

55. Wash the slides 3 times in tap water at room temperature for 5 min each.

Counter Staining with Gill's Hematoxylin

56. Dip the slides in freshly filtered Gill's hematoxylin for 1.5 min.

57. Wash the slides in cold, overflowing tap water until the water runs clear, but make sure the water does not directly hit the slides.

58. Dip the slides in Scott's water for 2 min.

59. Quickly dip the slides a few times in cold running tap water (but do not directly hit the slides with the water).

60. Soak the slides in 80% EtOH for 2 min.

61. Quickly dip the slides in eosin (1:1 diluted working solution) for 15 seconds.

62. Soak the slides twice in 95% EtOH for 5 min.

63. Soak the slides twice in 100% EtOH for 10 min (using EtOH dehydrated wih beads).

64. Soak the slides 3 times in Histoclear dehydrated with beads for 10 min.

65. Mount the slides with Permount.

Nonradioactive in situ Hybridization on Formalin-Fixed and Paraffin-Embedded Tissue (Using a Digoxigenin-Labeled RNA Probe)

Day 1

Labeling the Probe

Note: Once labeled, the probe can be frozen and stored at -70ºC for up to 3 months.

1. Nonradioactive digoxigenin RNA probe labeling:
   2 µl of 10× transcription buffer.
   2 µl of NTP labeling mixture (Digoxigenin RNA labeling kit).
   1 µg of DNA.
   1 µl RNase inhibitor.
   2 µl of polymerase.
   Add DEPC H_2O to reach a 20 µl reaction volume.

2. Incubate for 2 hr at 37ºC (either T3 or T7 polymerase).

3. Add 1 µl of RNase-free DNAse I and incubate the probe for 15 min at 37ºC.

4. Add 1 µl of 0.5 M EDTA (pH 8.0) to stop the reaction.

5. Precipitate the labeled RNA at –70ºC at least 2 hr or overnight with 2.5 µl of 4 M LiCi and 75 µl of prechilled 100% EtOH.

Assessing the Yield of the Probe by Dot-Blot Assay

6. Centrifuge the probe 12,000 rpm at 4ºC for 20 min. Pour off the supernatant and wash the probe pellet with 1 ml of 70% ethanol. Centrifuge the probe again at 14,000 rpm at 4ºC for 30 min.

7. Pour off the supernatant carefully, turn the tube upside down on Kimwipe to dry, and place the tube at 42ºC for 5–7 min to finish drying.

Note: Do not overdry the pellet. Some water can remain on the pellet, but there should be no ethanol remaining.

8. Resuspended the pellet in 50 µl (or 100 µl for larger pellets) DEPC water (or TE buffer [pH 8.0]). Dissolve the pellet for 30 min at 37ºC and immediately place the solution on ice once the pellet has dissolved.

9. Add 0.5 µl of RNase inhibitor per 50 µl probe (on ice). Centrifuge the probe briefly at room temperature, and place it again on ice.

10. Serially dilute 2 µl of the probe and 2 µl of the control RNA (Digoxigenin labeling kit) in 1:10 dilution five times.

11. Spot 1 µl of the serially diluted probe on a nylon membrane and fix the RNA to the membrane by ultraviolet (UV) cross-linker or bake at 80ºC for 1 hr.

12. Incubate the membrane in buffer 2 for 10 min at room temperature and then in antidigoxigenin-conjugate solution (1:1000 in buffer 2) for 10–20 min at room temperature.

13. Wash the membrane twice in buffer.

14. Incubate the membrane briefly in buffer 3 and change to chromogenic substrate solution in the dark for up to 20 min to develop the color.

15. Stop the reaction by adding buffer 4. Judge the probe concentration against the control probe.

Day 2

Wax Removal and Rehydration of Paraffin-Embedded Tissue Sections

Note: The slides should be baked at 56ºC overnight the night before.

16. Rinse the slides 3 times in Histoclear or xylene for 5 min each.

17. Rinse the slides twice in 100% EtOH for 5 min each.

18. Rinse the slides once in 95% EtOH for 2 min.

19. Rinse the slides once in 85% EtOH for 2 min.

20. Rinse the slides once in 70% EtOH for 2 min.

Prehybridization Treatment

21. Treat the slides with 0.2 M HCl for 10 min at room temperature with agitation (shake at about 60 rpm).

22. Wash the slides 3 times with 1X PBS.

23. Predigest the contaminating RNase in Proteinase K solution for 15 min at 37ºC in a water bath.

24. Wash the slides 3 times with 1X PBS.

25. Post-fix the sections in 4% PFA for 5 min at room temperature.

26. Wash the slides 3 times with 1X PBS.

27. Add 50 ml 0.1 M TEA solution and 125 µl of active anhydride to the slides simultaneously. Incubate them at room temperature for 10 min with shaking.

28. Wash the slides three times with 1X PBS.

29. Treat the slides with graded ethanol sequentially: 70%, 80%, 95%, 100% (made in DEPC water).

30. Air-dry the sections on Kimwipe for 1 hr.

Prehybridization and Hybridization

31. Prehybridize the slides with 125 µl of prehybridization buffer per slide for 2–4 hr at 50ºC in a moist chamber.

Note: Cover the sections with a plastic coverslip and arrange the slides in moist boxes horizontally, with the sections facing up.

32. Wipe the prehybridization solution off the tissue edges with Kimwipe and hybridize the slides with 70 µl of hybridization solution overnight at 50ºC in a moist chamber, sealed with tape or plastic wrap.

Note: Using 40 ng of probe 100 µl of hybridization buffer, heat the probe to 95–100ºC for 5 min and chill it on ice immediately after.

Day 3

Post-Hybridization Treatment and Antibody Incubation

33. Wash off the plastic coverslip in 2X SSC.

34. Incubate the slides in container with 2X SSC at RT for 20 min with shaking.

35. Incubate the slides with 2X SSC/0.5% Triton/2% NSS for 1 hr 40 min at RT with shaking.

36. Wash the slides in buffer 1 and keep them in buffer 1 until ready to apply the next solution.

37. Incubate the slides in buffer 1/0.3% Triton/2% NSS solution at RT for 30 min with shaking.

38. After the 30 min incubation is complete, remove the slides individually and dry off the area surrounding the tissue as before with Kimwipe or a paper towel. Add 70 µl of conjugate solution to each slide. Cover the sections with a plastic coverslip and incubate them overnight at 4ºC in a moisture box.

Day 4

Signal Development

39. Warm up the slides at room temperature for 10 min and gently remove the coverslip of slides immersed in buffer 1.

40. Wash the slides twice in buffer 1 for 10 min each, while shaking.

41. Wash the slides once in buffer 3 for 1–2 min while shaking.

42. Add 300 µl of chromogenic substrate solution to each slide to cover the tissue.

Note: Keep the slides in buffer 3 until ready to add chromogenic substrate solution. For 20 slides, 7 ml chromogenic substrate solution is enough.

43. Place the slides in a humidified, light-tight box and check occasionally for color development. The color can develop up to 6 hr later.

44. Shake the slides in buffer 4 for a few minutes at room temperature to stop the color reaction.

45. Air-dry the slides and cover the slides using Aqua mount medium.

Note: Positive signal is purple/blue, and the negative cells are colorless/light pink.

RESULTS AND DISCUSSION

Analysis of Gene Expression in the Prostate by *in situ* Hybridization

Increasing numbers of AR-interacting proteins have been identified as AR cofactors (Glemann, 2002; Heinlein and Chang, 2002; Janne *et al.,* 2000). Although AR cofactors physically interact with AR and modulate AR-dependent transcription, the critical question is whether they play any roles in human prostate tumorigenesis and prostate cancer progression. To address this question, it is necessary to investigate whether expression profiles and functions of these cofactors change during prostate tumorigenesis and prostate cancer progression.

The techniques used to study gene expression in prostate tissues, such as reverse transcription polymerase chain reaction (RT-PCR) and DNA chip/array, require labor-intensive laser capture microdissection to collect homogeneous tissue or specific cell-type components. Immunohistochemistry can distinguish between the nuclear and cytoplasmic expressions of corresponding proteins, but it relies on antibodies with high specificity and sensitivity. However, *in situ* hybridization circumvents the previously mentioned problems and remains an effective tool for studying the temporal and spatial, tissue and cell-type specific expression of various genes (Manova *et al.,* 1990; Xu *et al.,* 1994).

To label the probe for *in situ* hybridization, fragments of corresponding genes (~500-bp DNA) can be amplified using PCR with two oligonucleotide primers containing T7 and T3 promoter sequences. Alternatively, the DNA fragment can be subcloned into a vector containing T7 and T3 promoter sequences at each side. ^{33}P-labeled radioactive or digoxigenin-labeled nonradioactive RNA probes were synthesized by incubation of the PCR-amplified DNA fragment or the plasmid DNA-containing gene of interest with T7 or T3 RNA polymerase. We observed that the specificity of the labeled probes varied dramatically in different regions of a gene. For example, probes generated with a 499-bp DNA fragment (from base pair 2263 to base pair 2762 of the *AR* cDNA) was tenfold stronger than

that generated with a 500-bp DNA fragment (from base pair 1 to base pair 500 of the *AR* cDNA) (Figure 68A, lanes 1 and 2 versus lanes 3 and 4). The difference in specificity could even be as great as 100-fold, as demonstrated when we used the nonradioactive method to label *ARA70* gene (Figure 68A, lanes 5–8, panels **c** and **d** versus panels **e** and **f**). However, although their specificities were somewhat different, all of these probes have been successfully used for *in situ* hybridization analysis. The weaker probes required longer exposure and sometimes resulted in higher background counts. It is sometimes difficult to discriminate the high background from the authentic signal when analyzing the signal for low abundance transcripts. Thus, it is advisable to change the region of DNA when the labeling signal is too low. Hybridization with the sense probes will serve as the negative controls. We were able to store the radioactive probe in a –80ºC freezer for up to 1 month and the nonradioactive probe for up to 3 months.

We have successfully examined the gene expression profiles of *AR* and various coactivators using radioactive (Figure 68B, C) and nonradioactive (Figure 68D) *in situ* hybridization in prostectomy specimen. All of the tissues used in the experiments were fixed in 10% formalin and paraffin embedded. We have also found that the sections yielded comparable results whether they were used immediately or within 3 months of the sectioning if stored at 4ºC. The sections should not be dried during prehybridization, hybridization, or antibody incubation. The hybridization temperature should be between 50–65ºC depending on the nature of the probe. We validated the *in situ* hybridization analysis (or specimen) by immunohistochemical analysis for proteins expressed in the prostate gland (such as AR and PSA). The messenger RNA expression levels from the *in situ* hybridization should be consistent with the protein levels from the immunohistochemistry of the same tissue, indicating that the specimen was suitable for *in situ* hybridization analysis.

For quantitative analysis, the signal (grain) of the *in situ* hybridization from the area of interest was captured with a microscope linked to a digital camera, counted, and then divided by the number of nuclei (cells) to obtain the grain number per cell. The nonradioactive *in situ* hybridization was scored semiquantitatively as negative (0), weakly positive (1+), moderately positive (2+), and strongly positive (3+). With the advance of a computer-aided automated scoring system, the staining density and percentage of nonradioactive *in situ* hybridization could eventually be scored quantitatively rather than semi-quantitatively.
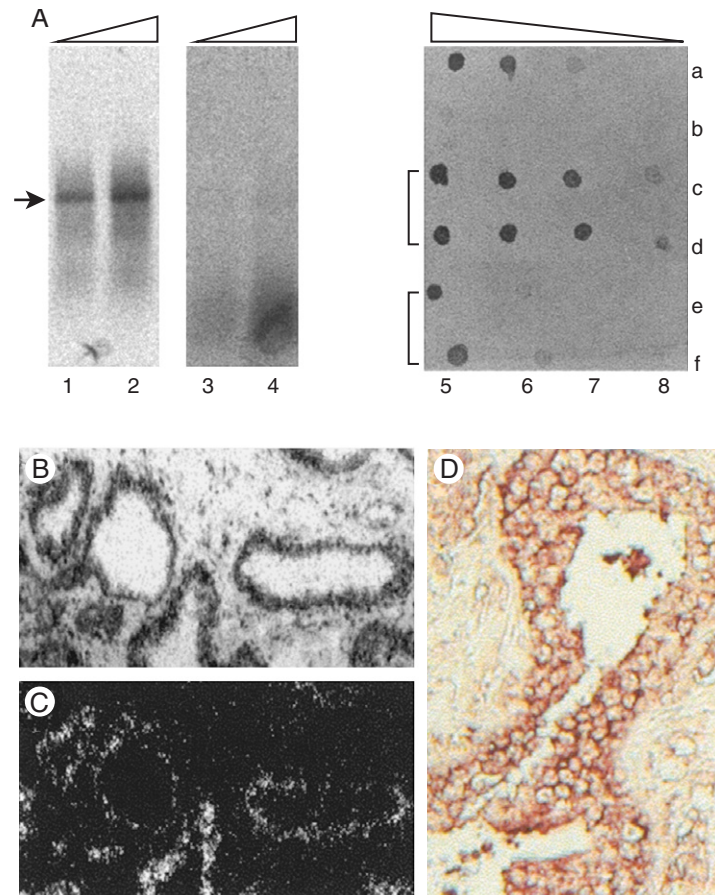
Figure 68 A: *Lanes 1–4* show autoradiography of the radioactive ribonucleic acid (RNA) probes labeled using T7 RNA polymerase with polymerase chain reaction–amplified deoxyribonucleic acid (DNA) fragments of androgen receptor (AR) complementary DNA (cDNA) from base pairs 2263–2762 (*lanes 1 and 2*) and from base pairs 1–500 (*lanes 3 and 4*). *Lanes 5–8* show Dot Blot of serial tenfold dilutions of the digoxigenin-labeled RNA probes. *Panel **a*** shows the control DNA (100 ng/μl) and *panel **b*** is blank. *Panels **c** and **d*** show probes labeled using T7 RNA polymerase with ARA70α cDNA from base pairs 901–1442 (the A of the ATG translation start codon was arbitrarily given the number 1) in pBluescrip II KS(-). *Panels **e** and **f*** show labeled ARA70 probes from base pairs 126–706 (the A of ATG translation start codon was arbitrarily given the number 1). **B:** Histology of benign prostate gland in bright field on an emulsifield slide. **C**: *In situ* hybridization signal (grain) of ARA70α in dark field. **D**: Nonradioactive *in situ* hybridization of ARA70α in benign prostate tissue.

Expression Profiles of Various
AR Cofactors in Prostate Cancer

Because the AR pathway is clearly indicated in prostate differentiation and proliferation as well as in prostate cancer, abnormal expressions of cofactors that positively or/and negatively modulate AR functions in the prostate might play important roles in prostate tumorigenesis and prostate cancer progression. Cyclin D1 strongly inhibits AR-driven gene expression in transient transfection assays (Petre *et al.*, 2002) (Figure 69), whereas overexpression of *cyclin D1* was shown to be associated with metastasis of prostate cancer to bone, and changed growth properties, increased tumorigenicity, and decreased requirement for androgen stimulation in LNCaP human prostate cancer cells both *in vitro* and *in vivo* (Chen *et al.,* 1998; Drobnjak *et al.,* 2000).

β-catenin is a key downstream effector in the Wnt/Wingless signaling pathway that governs the development process of cell fate specification, proliferation, polarity, and migration (Miller *et al.,* 1999). Activation of the Wnt/Wingless pathway was shown to lead to the formation of a free signaling pool of β-catenin that
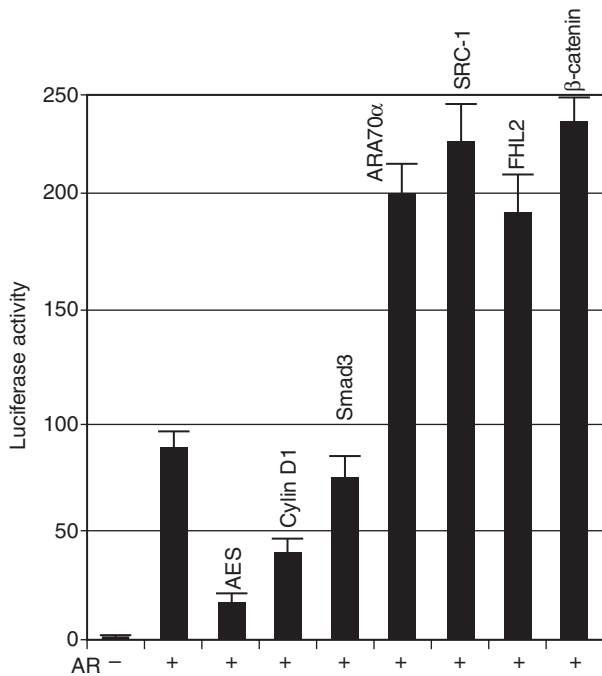
Figure 69 Cofactors affect androgen receptor (AR)-driven gene expression. PC3 cells were transfected with the following: 100 ng of ARE-E4-luc, 10 ng of pcDNA-AR, 50 ng of pcDNA-AES, 50 ng of pcDNA-cyclin D1, or 50 ng of pcDNA-Smad3; 150 ng of pcDNA-ARA70α, 150 ng of pcDNA-SRC-1, 150 ng of pcDNA-FHL2, or 150 ng of pcDNA-β-catenin expression plasmids as indicated. The cells were grown in the presence of 10 nM R 1881 for 48 hr after transfection, then harvested for luciferase activity assay.

enters the nucleus and forms a complex with members of the TCF/LEF family of transcription factors, initiating transcription of new genes (Morin, 1999). Studies showed that 5% of primary prostate cancers contained mutations in exon 3 of the β-catenin gene, a region that controls the stability of the protein (Voeller *et al.,* 1998). β-catenin strongly enhanced AR-driven gene expression (Figure 69) (Truica *et al.,* 2000). Mutant β-catenin can relieve the suppression of antiandrogens on androgen-dependent transcription and change AR sensitivity to ligands (Truica *et al.,* 2000).

Studies have described increased expression of *SRC-1* in clinical samples from androgen-independent prostate cancer and its function in androgen-independent activation of AR (Ueda *et al.,* 2002), and the increased expression of the FHL2 genes has been associated with prostatic carcinoma (Muller *et al.,* 2002).

The cofactors we have analyzed include Ran1/ARA24, ARA55/Hic-5, ARA54, ELE1/ARA70, TMF/ARA160, PIASI, AES, SRC1, and TRAP220 (Li et al., 2002). Among them, SRC-1 and TRAP220 are general cofactors that have been shown to interact ubiquitously with nuclear receptors such as AR, ER,

PR, GR, and TR (Malik and Roeder, 2000). The expression of most cofactors (ARA54, TMF/ARA160, SRC-1, and TRAP220) remained unchanged in both high-grade prostatic intraepithelial neoplasia (PIN) and prostate cancer, compared with adjacent benign prostate tissues. It remains to be determined whether there is a change in cellular distribution or modifications for these cofactors in prostate cancer.

Among the coactivatiors studied, ARA55 was the only one expressed uniquely in prostate stromal cells. We verified the stromal expression pattern of ARA55 by immunohistochemical stain. Its expression was decreased in prostate cancer. These results are consistent with published data using RT-PCR from prostatic cell lines and DNA microarray (Nessler-Menardi *et al.,* 2000). Given the well-documented evidence that the interaction between epithelial and stromal cells in the prostate gland (Cunha *et al.,* 1987; Gao *et al.,* 2001) is important for prostate growth and differentiation and for prostate tumorigenesis, it is interesting to know whether ARA55 plays any role in these processes.

AR cofactors ARA24 and PIASI are expressed in epithelial cells, and their expression are increased in both high-grade PIN and prostate cancer compared with adjacent benign prostate tissues, although the degrees and percentages of their increased expression vary (Li *et al.,* 2002). Expression of ARA24 was increased from twofold to tenfold with an average of 4.6 folds in 81% of cases. Although the expression of PIASI was increased in prostate cancer, the number of cases and degree of increase were not as dramatic as with ARA24; the expression was increased from twofold to 7.5-fold in 33% of cases. We also examined the levels of these cofactors in high-grade PIN by *in situ* hybridization. The results showed similar increases in the expression of these cofactors in high-grade PIN for ARA24 and PIASI.

Androgen-receptor coactivator ELE1/ARA70 was first identified as a factor fused to the *RET* protooncogene in thyroid neoplasia and as an androgen receptor coactivator that can enhance the transcriptional activity of AR in the presence of androgen (Yeh and Chang, 1996). There are two forms of ELE1/ARA70: the full-length ELEα/ARA70α and the c-terminal internally spliced short form, ELE1β/ARA70β (Alen *et al.,* 1999a). ARA70 was expressed in the prostate epithelium rather than in stromal cells (Li *et al.,* 2002). Surprisingly, the expression of ELEα/ARA70α was decreased twofold to thirtyfold (average of 7.5-fold) in 80% of prostate cancer cases. Similarly, it was expressed at a lower level in high-grade PIN. Our preliminary data indicate that the short form of ELE1/ARA70, ELE1β/ARA70β, is increased in prostate cancer (Lee and Wang, unpublished data).

Roles of AR Cofactors in Prostate Cancer

Nearly 50 cofactors have been shown to influence AR transactivation (Gelmann, 2002; Henlein and Chang, 2002; Janne *et al.,* 2000). Although identified through direct AR interactions, most of these factors have been tested slowly by transient transfection assay with synthetic ARE-containing luciferase reporters (see Figure 69). The abundance of cofactors was selected in part by tissue-specific expression of different cofactors (e.g., ARIP3) (Moilanen *et al.,* 1999), but co-expression of multiple cofactors in a single tissue appeared to be a general rule. Partial functional redundancy is known to exist among cofactors, the phenotype of the SRC-1$^{-/-}$ mouse being the most obvious example of this phenomenon (Weiss *et al.,* 2002). However, the striking functional diversity of AR cofactors characterized to date argues for alternative explanations for their abundance. Given the spatial constraints on the simultaneous interaction of these cofactors with a ligand AR dimmer, we may presume that the promoter and enhancer contexts determine the nature of AR-cofactor complexes that may be efficiently recruited (Robins *et al.,* 1994; Roche *et al.,* 1992). Such selectivity was illustrated by transcriptional regulation of positive and negative thyroid response elements (TREs) by TR and its cofactors (Sasaki *et al.,* 1999). Whereas the positive elements permit binding of TR and CBP in the presence of ligand, negative TREs selectively recruit TR-HADAC2 (histone deacetylase) complexes in a ligand-dependent manner. These results illustrate the ability of the promoter to discriminate between, and select for, the identity of cofactors bound to ligand-bound TR.

Because AR seems to regulate expression of a large number of genes in the prostate, the existence of the large number of AR cofactors would not be surprising if the specific AR-target gene selectively uses a distinct set of cofactors for its expression (Figure 70). We observed increased expression of some cofactors and decreased expression of others in prostate tumor tissues compared to adjacent benign prostate tissues (Li *et al.,* 2002). Our hypothesis was that cofactors with increased expression in cancer might be involved in transcription of a set of genes that are involved in cellular proliferation. In contrast, cofactors with decreased expression in tumor might be selectively recruited to a set of genes that are involved in differentiation (Figure 70). Therefore, changes in the levels of cofactors might change AR-target gene expression profiles in the prostate, shifting the balance between differentiation and proliferation of the normal prostate to the status preferable for proliferation in prostate cancer. Supporting this hypothesis, overexpression of
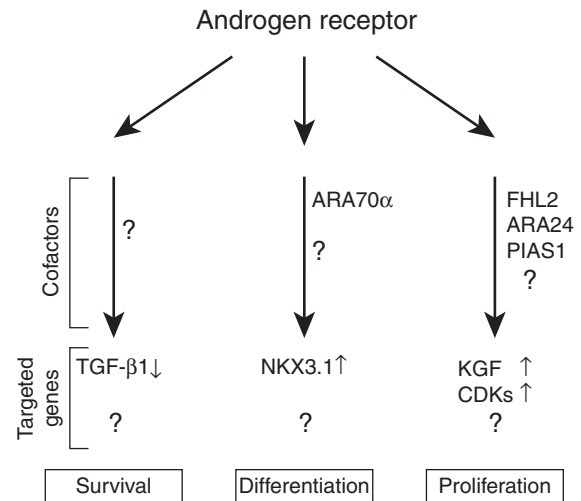
Figure 70 The androgen receptor (AR) performs multiple functions in the prostate gland through selective activation *(upper arrows)* or repression *(lower arrows)* of different AR direct target genes using a distinct set of cofactors. Question marks indicate unidentified potential cofactors that are important in these processes and genes that are targeted directly by the AR.

ELE1/ARA70 in the metastatic prostate cancer cell line LNCap, which expresses reduced levels of ELE1/ARA70 compared to normal primary prostate epithelial cells, dramatically suppressed the colony formation of LNCaP cells (Li *et al.,* 2002).

Perspectives

Given the fact that AR cofactors do not belong to a structurally conserved family of proteins and their functions converge with pathways involving signal transduction (PIAS1), cell-cycle regulation (cyclin D1 and E), and other functions, it is reasonable to speculate that their expressions, functions, and mechanisms in tumorigenesis are different. Although increasing numbers of AR cofactors have been identified, the biologic relevance of most of these factors to prostate cancer growth and progression remains to be tested. Future studies will focus on the effects of abnormal expression of some AR cofactors in the growth and progression of prostate tumors (LNCap xenografts) in nude nice. The other alternative would be to use knockout and transgenic mice to study the roles of AR cofactors in prostate tumorigenesis and prostate development. The androgen-independent growth of prostate cancer represents the major obstacle of current therapy for metastatic prostate cancer. Therefore, whether

abnormal expression or function of these cofactors contributes to androgen-independent growth of prostate cancer needs to be investigated.

Acknowledgements

References

Aarnisalo, P., Palvimo, J.J., and Janne, O.A. 1998. CREB-binding protein in androgen receptor-mediated signaling. *Proc. Acad. Sci. USA* 95:2122–2127.

Abreu-Martin, M.T., Chari, A., Palladino, A.A., Craft, N.A., and Sawyers, C.L. 1999. Mitogen-activated protein kinase kinase kinase 1 activates androgen receptor-dependent transcription and apoptosis in prostate cancer. *Mol. Cell. Biol. 19*:5143–5154.

Alen, P., Claessens, F., Schoenmakers, E., Swinnen, J.V., Verhoeven, G., Rombatus, W., and Peeters, B. 1999a. Interaction of the putative androgen receptor-specific coactivator ARA70/ELE1 alpha with multiple steroid receptors and identification of an internally deleted ELE1 beta isoform. *Mol. Endocarcinal. 13*:117–128.

Alen, P., Claessens, F., Verhoeven, G., Rombatus, W., and Peeters, B. 1999b. The androgen receptor amino-terminal domain plays a key role in p160 coactivator-stimulated gene transcription. *Mol. Cell. Biol. 19*:6085–6097.

Balk, S.P. 2002. Androgen receptor as a target in androgen-independent prostate cancer. *Urology 60*:132–138; discussion 138–139.

Bentel, J.M., and Tilley, W.D. 1996. Androgen receptors in prostate cancer. *J Endocrinol. 151*:1–11.

Berrevoets, C.A., Doesburg, P., Steketee, K., Trapman, J., and Brinkmann, A.O. 1998. Functional interactions of the AF-2 activation domain core region of the human androgen receptor with the amino-terminal domain and with the transcriptional coactivator TIF2 (transcriptional intermediary factor2). *Mol. Endocrinol. 12*:1172–1183.

Brinkmann, A.O., Blok, L.J., de Ruiter, P.E., Doesburg, P., Steketee, K., Berrevoets, C.A., and Trapman, J. 1999. Mechanisms of androgen receptor activation and function, *J. Steroid. Biochem. Mol. Biol. 69*:307–313.

Chen, H., Lin, R.J., Sie, W., Wilpitz, D., and Evans, R.M. 1999. Regulation of hormone induced histone hyperacetylation and gene activation via acetylation of an acetylase. *Cell 98*: 675–686.

Chen, Y., Martinez, L.A., LaCava, M., Coghlan, L., and Conti, C.J. 1998. Increased cell growth and tumorigenicity in human prostate LNCap cels by overexpression to cyclin D1. *Oncogene 16*:1913–1920.

Craft, N., and Sawyere, C.L. 1998. Mechanistic concepts in andro-gen-dependence of prostate cancer. *Cancer Metastasis Rev. 17*:421–427.

Craft, N., Chhor, C., Tran, C., Belldegrun, A., DeKernion, J., Witte, O.N., Said, J., Reiter, R.E., and Sawyers, C.L. 1999a. Evidence for clonal outgrowth of androgen-independent prostate cancer cells from androgen-dependent tumors through a two-step process. *Cancer Res. 59*:5030–5036.

Craft, N., Shostak, Y., M., and Sawyers, C.L. 1999b. A mechanism for hormone-independent prostate cancer through modulation of androgen receptor signaling by the HER-2/neu tyrosine kinase. *Nat. Med. 5*:280–285.

Culig, Z., Hobisch, A., Cronauer, M.V., Radmayr, C., Trapman, J., Hittmair, A., Bartsch, G., and Klocker, H., 1994. Androgen receptor activation in prostatic tumor cell lines by insulin-like growth factor-I, keratinocyte growth factor, and epidermal growth factor, *Cancer Res. 54*:5474–5478.

Culig, Z., Hobisch, A., Hittmair, A., Peterziel., H., Cato, A.C., Bartsch, G., and Klocker, H. 1998. Expression, structure, and function of androgen receptor in advanced prostatic carcinoma. *Prostate 35*:63–70.

Cunha, G.R., Donjacour, A.A., Cooke, P.S., Mee, S., Bigsby, R.M., Higgins, S.J., and Sugimura, Y., 1987. The endocriminology and development biology of the prostate. *Endocr. Rev. 8*:338–362.

Denmeade, S.R., Lin, X.S., and Isaacs, J.T. 1996. Role of pro-grammed (apoptotic) cell death during the progression and ther-apy for prostate cancer. *Prostate 28*:251–265.

Drobnjak, M., Osman, I., Scher, H.I., Fazari, M., and Cordon-Cardo, C. 2000. Overexpression of cyclin D1 is associated with metastatic prostate cancer to bone. *Clin. Cancer Res. 6*:1891–1895.

Gao, J., Arnold, J.T., and Isaacs, J.T. 2001. Conversion from a paracrine to an autocrine mechanism of androgen-stimulated growth during malignant transformation of prostatic epithelial cells. *Cancer Res. 61*:5038–5044.

Gelmann, E.P. 2002. Molecular biology of the androgen receptor. *J. Clin. Oncol. 20*:3001–3015.

Grossmann, M.E., Huang, H., and Tindall, D.J. 2001. Androgen receptor signaling in androgen-refractory prostate cancer. *J. Natl. Cancer Inst. 93*:1687–1697.

Heinlein, C.A., and Change, C. 2002. Androgen receptor (AR) coregulators: An overview. *Endocr. Rev. 23*:175–200.

Ikonen, T., Palvomo J.J., and Janne, O.A. 1997. Interaction between the amino- and carboxyl-terminal regions of the rat androgen receptor modulates transcriptionalactivity and is influenced by nuclear receptor coactivators. *J. Biol. Chem. 272*:29891–29828.

Janne, O.A., Moilanen, A.M., Poukka, H., Rouleau, N., Karvonen, U., Kotaja, N., Hakli, M., and Palvimo, J.J. 2000. Androgen-receptor-interacting nuclear proteins. *Biochem. Soc. Trans. 28*:401–405.

Jenster, G. 1999. The role of the androgen receptor in the develop-ment and progression of prostate cancer. *Semin. Oncol. 26*:407–421.

Jorda, M., Morales, A., Ghorab, Z., Fernandez, G., Nadji, M., and Block, N., 2002. Her2 expression in prostatic cancer: A comparison with mammary carcinoma. *J. Urol. 168*: 1412–1414.

Kingston, R.E., and Narlikar, G.J. 1999. ATP-dependent remodel-ing and accetylation as regulators of chromatin fluidity. *Genes Dev. 13*:2339–2352.

Li, P., Yu, X., Ge, K., Melamed, J., Roeder, R.G., and Wang, Z., 2002. Heterogeneous expression and functions of androgen receptors co-factors in primary prostate cancer. *Am. J. Pathol. 161*:1467–1474.

Ma, H., Hong, H., Huang, S.M., Irvine, R.A., Webb, P., Kushner, P.J., Coetzee, G.A., and Stallcup, M.R., 1999. Multiple signal input and output domains of the 160-kilodalton nuclear receptor coactivator proteins. *Mol. Cell. Biol. 19*:6164–6173.

Malik, S., and Roeder, R.G. 2000. Transcriptional regulation through Mediator-like coactivators in yeast and metazoan cells. *Trends Biochem. Sci. 25*:277–283.

Manova, K., Nocka, K., Besmer, P., and Bachvarova, R.F. 1990. Gonadal expression of c-kit encoded at the W locus of the mouse. *Development 110*:1057–1069.

Miller, J.R., Hicking, A.M., Brown, J.D., and Moon, R.T. 1999. Mechanism and function of signal transduction by the Wnt/Beta-catenin and Wnt/Ca2+ pathways. *Oncogene 18*:7860–7872.

Mirosevich, J., Bentel, J.M., Zeps, N., Redmond, S.L., D'Antuno, M.F., and Dawkins, H.J. 1999. Androgen receptor expression of proliferating basal and luminal cells in adult murine ventral prostate. *J. Endocrinoil. 162*:341–350.

Moilanen, A.M., Poukka, H., Karvonen, U., Hakli, M., Janne, O.A., and Palvimo, J.J. 1998. Identification of a novel RING finger protein as a coregulator in steroid receptor-mediated gene transcription. *Mol. Cell. Biol. 18*:5128–5139.

Morin, P.J. 1999. Beta-catenin signaling and cancer. *Bioessays 21*:1021–1030.

Muller, J.M., Metzger, E., Greschik, H., Bosserhoff, A.K., Mercep, L., Buettner, R., and Schule, R., 2002. The transcriptional coactivator FHL2 transmits Rho signals from the cell membrane into the nucleus. *EMBO. J. 21*:736–748.

Nessler-Menardi, C., Jtova, I., Culig, Z., Eder, I., Putz, T., Bartsch, G., and Klocker, H. 200. Expression of androgen receptor coregulatory proteins in prostate cancer and stroma-cell culture models. *Prostate 450*:124–131.

Petre, C.E., Wetherill, Y.B., Danielsen, M., and Kundsen, K.E., 2002. Cyclin D1: Mechanism and consequence of androgen receptor co-repressor activity. *J. Biol. Chem. 277*:207–2215.

Robins, D.M., Scheller, A., and Adler., A.J. 1994. Specific steroid response froma nonspecific DNA element. *J. Steroid Biochem. Mol. Biol. 49*:251–255.

Roche, P.J., Hoare, S.A., and Parker, M.G. 1992. A consensus DNA-binding site for the androgen receptor. *Mol. Endocrinol. 6*:2229–2235.

Roeder, L.T., 1998. Role of general and gene-specific cofactors in the regulation of eykaryotic transcription. *Cold Spring Harb. Symp. Quant. Biol. 63*:201–218.

Roeder, R.G. 1996. The role of general initiation factors in transcription by RNA polymerase II. *Trends Biochem. Sci. 21*:327–335.

Sasaki, S., Lesoon-Wood, L.A., Dey, A., Kuwata, T., Weintraub, B.D., Humphrey, G., Yang, W.M., Seto, E., Yen, P.M., Howard, B.H., and Ozato, K. 1999. Ligand-induced recruitment of a histone deactylase in the negative-feedback regulation of the thyrotropin beta gene. *Embo. J. 18*:5389–5398.

Stallcup, M.R., Chen, D., Hok, S.S., Ma, H., Lee, Y.H., Li, H., Schurter, B.T., and Aswad, D.W. 2000. Co-operation between protein-acetylating and protein-methylating co-activators in transcriptional activation. *Biochem. Soc. Trans. 28*:415–418.

Tilley, W.D., Wilson, C.M., Marcelli, M., and McPhaul, M.J. 1990. Androgen receptor gene expression in human prostate carcinoma cell lines. *Cancer Res. 50*:5382–5386.

Truica, C.I., Byers, S., and Gelmann, E.P. 2000. Beta-catenin affects androgen receptor transcriptional activity and ligand specificity. *Cancer Res. 60*:4709–4713.

Ueda, T., Mawji, N.R., Bruchosky, N., and Sadar, M.D., 2002. Ligand-independent activation of the androgen receptor by interleukin-6 and the role of steroid receptor coactivator-1 in prostate cancer cells. *J. Biol. Chem. 277*:38087–38094.

Voeller, H.J., Trucia, C.I., and Belmann, E.P. 1998. Beta-catenin mutations in human prostate cancer. *Cancer Res. 58*:2520–2523.

Wang, Q., Sharma, D., Ren, Y., and Fondell, J.D., 2002. A coregulatory role for the TRAP/Mediatopr complex in androgen receptor mediated gene expression. *J. Biol. Chem. 277*:42852–42858.

Weiss, R.S., Korcarz, C., Chassande, O., Cua, K., Sadow, P.M., Koo, E., Samarut, J., and Lang, R. 2002. Thyroid hormone and cardiac function in mice deficient in thyroid hormone receptor-alpha or –beta: An echocardiograph study. *Am. J. Physiol. Endocrinol. Metab. 283*:E428–E435.

Whitacre, D.C., Chauhan, S., Davis, T., Gordon, D., Cress, A.E., and Miesfeld, R.L. 2002. Androgen induction of *in vitro* prostate cell differentiation. *Cell Growth Differ. 13*:1–11.

Workman, J.L., and Kingston, R.E., 1998. Alteration of nucleosome structure as a mechanism of transcriptional regulation. *Annu. Rev. Biochem. 67*:545–579.

Xu, W., Chen, H., Du, K., Asahara, H., Tini, M., Emerson, B.M., Montminy, M., and Evans, R.M., 2001. A transcriptional switch mediated by cofactor methylation. *Science 294*:2507–2511.

Xu, X.C., Clifford, J.L., Hong, W.K., and Lotan, R. 1994. Detection of nuclear retinoic acid receptor mRNA in histological tissue sections using nonradioactive in situ hybridization histochemistry. *Diagn. Mol. Pathol. 3*:122–131.

Yeh, S., and Chang, C. 1996. Cloning and characterization of a specific coactivator, ARA70, for the androgen receptor in human aprostate cells. *Proc. Natl. Acad. Sci. USA 93*:5517–5521.

Yeh, S., Lin, H.K., Kang, H.Y., Thin, T.H., Lin, M.F., and Chang, C. 1999. From HER2/Neu signal cascade to androgen receptor and its coactivators: A novel pathway by induction of androgen target genes through MAP kinase in prostate cancer cells. *Proc. Natl. Acad. Sci. USA 96*:5458–5463.

Yuan, C.S., Ito, M., Fondell, J.D., Fu, Z.Y., and Roeder, R.G. 1998. The TRAP220 component of a thyroid hormone receptor-associated protein (TRAP) coactivator complex interacts directly with nuclear receptor in a ligand-dependent fashion. *Proc. Natl. Acad. Sci. USA 95*:7939–7944.

Yuan, S., Trachtenberg, J., Mills, G.B., Brown, T.J., Xu,, F., and Keating, A. 1993. Androgen-induced inhibition of cell proliferation in an androgen-insensitive prostate cancer cell line (PC-3) transfected with a human androgen receptor complementary DNA. *Cancer Res. 53*:1304–1311.

Zegarra-Moro, O.L., Schmidt, L.J., Huang, H., and Tindall, D.J. 2002. Disruption of androgen receptor function proliferation of androgen-refractory prostate cancer cells. *Cancer Res. 62*:1008–1013.

14

Role of Androgen Receptor Gene Amplification and Protein Expression in Hormone Refractory Prostate Carcinoma

Joanne Edwards and John M.S. Bartlett

Introduction

Prostate cancer is the second most frequent cause of male cancer-related deaths (Goktas *et al*., 1999). Androgens regulate prostate gland growth and differentiation by binding to the androgen receptor (AR), which regulates a network of androgen-responsive genes including prostate specific antigen (PSA). Prostate cancer growth is also stimulated by androgens and can be inhibited by AR antagonists (anti-androgens), surgical castration, or luteinizing hormone releasing hormone (LHRH) agonists (Avila *et al*., 2001). Approximately 70–80% of patients with prostate cancer treated with androgen deprivation therapy respond favorably in the first instance (Goktas *et al*., 1999). However, this effect is transient, with the majority of patients developing hormone refractory disease (Newling *et al*., 1997). The mechanisms involved in the development of hormone refractory disease are poorly understood. However, *AR* mutations (Avila *et al*., 2001), *AR* amplification (Edwards *et al*., 2001), increased AR expression (Edwards *et al*., 2003a), and activation of the AR by interaction with other signaling pathways have been implicated (Feldman and Feldman 2001, Edwards *et al*., 2003b).

Androgen receptors are present in all epithelial cells of the prostate. Down-regulation of AR expression during prostate cancer progression and increased expression with the development of hormone refractory disease (Edwards *et al*., 2003a; Segawa *et al*., 2001) have both been reported. AR expression levels have been reported to predict patient response to hormone therapy and to correlate with tumor grade, stage, and progression-free survival (Koivisto and Helin, 1999). It has been postulated that AR protein expression is increased as a result of *AR* amplification by a gene dosage effect resulting in the development of hormone refractory disease. *AR* amplification is associated with increased protein expression (Edwards *et al*., 2003a). When a quantitative study was conducted to compare AR protein expression and *AR* amplification, it was observed that AR protein expression was 50% higher in tumors with AR copy number; X-chromosome copy number ratio was greater than 1.5 (i.e., *AR* amplification was observed) (Ford *et al*., 2003). Although *AR* copy number can also be increased by polysomy of the X-chromosome, AR protein expression is not altered in this case (Brown *et al*., 2002; Edwards *et al*., 2003a). The incidence of X-chromosome polysomy ranges from 42–60%, whereas amplification of the

Handbook of Immunohistochemistry and *in situ* Hybridization of Human Carcinomas,
Volume 2: Molecular Pathology, Colorectal Carcinoma, and Prostate Carcinoma

423

AR gene ranges from 20–30% in hormone refractory prostate tumors (Edwards *et al*., 2003a; Koivisto *et al*., 1997). An increase in AR protein expression is also observed independently of *AR* amplification or increased *AR* copy number. This suggests that other mechanisms, such as increased protein stability or decreased AR degradation, may also be involved.

A study in 2004 demonstrated, using a prostate cancer xenograft model, that increased AR messenger ribonucleic acid (mRNA) expression was associated with the development of hormone refractory disease (Chen *et al*., 2004). Increasing AR protein expression *in vitro* and in xenograft studies via AR transfection promotes conversion from hormone sensitive to hormone refractory disease.

It is interesting that this study also demonstrated that hormone refractory disease remains ligand (DHT)-dependent and that phosphorylation of the receptor alone cannot activate the AR. However, high AR expression levels enabled antagonists, such as Bicalutamide, to activate rather than inhibit the AR (Chen *et al*., 2004). This chapter presents data on *AR* amplification and protein expression levels in paired hormone sensitive and hormone refractory tumors for the same patients, hence monitoring AR changes with the development of hormone refractory disease. In doing this we discuss how *AR* gene amplification and AR protein expression are best measured in human prostate tumors.

MATERIALS

1. Silane (3-aminopropyl-triethoysilane)-treated slides.
2. Xylene.
3. 95%, 80%, and 70% industrial methylated spirits (IMS).
4. 0.2 N HCl, used as a pretreatment to increase hybridization signal as acid deproteinases the tissue increasing probe penetration.
5. Pretreatment buffer (Vysis UK, Ltd.), 8% w/v sodium thiocyanate to reduce the protein disulfide bonds formed by fixation.
6. 0.5% pepsin (250 mg) diluted in 500 ml of protease buffer (0.2 N HCl; Vysis UK, Ltd.). This is used in conjunction with 0.2 N HCl and pretreatment buffer to digest protein and enhance probe penetration.
7. 10% formalin, used to fix the tissue following pretreatment.
8. 4,6-diamidino-2-phenylindole-2 hydrochloride (DAPI) in vestashield mounting medium (Vector, UK). Dilute 165 µl of DAPI (1.5 µg/ml) in vestashield mounting medium with 535 µl vestashield mounting medium (Vector).

9. Distilled water.
10. Probe, 1 µl X chromosome, SpectrumGreen labeled CEP X (Vysis UK, Ltd.), 1 µl AR, SpectrumOrange labeled probe locus Xq11-13 (Vysis UK, Ltd.), 1 µl CEP buffer (Vysis UK, Ltd.), and 7 µl of DNA/RNAse free water are combined for each slide to be hybridized.
11. Rubber cement (Halfords, UK).
12. Add 66 g of saline-sodium citrate (SSC) (3 M NaCl, 0.3 M Na citrate, pH 5.3; Vysis UK, Ltd.) to 250 ml with distilled water; this makes 20X SSC. Dilute 1:10 to make 2X SSC.
13. Post-hybridization wash buffer. Add 2 ml NP-40 (Vysis UK, Ltd.) to 100 ml of 20X SSC make up to 1 L with distilled water (pH 7–7.5). Store at room temperature.
14. Clear nail varnish.
15. Oil for use with oil immersion objectives.
16. 30% H_2O_2 diluted using distilled water to 0.3% (v/v).
17. Tris ethylenediamine tetra-acetic acid (EDTA) buffer (TE), 0.37 g sodium EDTA and 0.55 g Tris in 1 L distilled water (pH 8).
18. Vetor ABC elite kit (Vector).
19. Tris buffered saline (TBS), 10X TBS 60 g Tris base and 87.6 g NaCl, in 1 L distilled water. For working concentration dilute 10X TBS 1:10 with distilled water.
20. Avidin Biotin blocking kit (Vector).
21. AR primary antibody (NCL-AR-2F12, Vector, 1 mg/ml) diluted 1:100 using Dako diluent (Dako, Denmark).
22. DAB substrate kit (Vector).
23. Hematoxylin (Thermo Sandon, UK).
24. Scotts tap water (Thermo Sandon, UK).
25. Dibutlylphtalate in xylene (DPX; BDH Lab Supplies, UK).

METHODS

Tissue Preparation for Fluorescence *in situ* Hybridization and Immunohistochemistry

1. Prepare 3–5 µm thick sections from archival formalin-fixed and paraffin-embedded tissue using a microtome.
2. Place tissue sections onto silane-treated slides.
3. Bake overnight at 56°C.

Tissue section pretreatment for fluorescence *in situ* hybridization (FISH) analysis may be done manually or using a robotic procedure. We will discuss both methods in this chapter.

Pretreatment of Tissue Using Manual Method for FISH Analysis

Before this protocol begins, two water baths should be prepared; one water bath should be set for 80°C and the other for 37°C. These water baths are for stages 8 and 10, respectively. Alternatively, microwave water to bring up to temperature.

1. Dewax the slides in xylene for 5 min, and repeat using a fresh xylene bath.
2. Rehydrate in IMS 95% for min × 2.
3. Air-dry the sections.
4. Treat with 0.2 N HCl for 20 min.
5. Wash in distilled water for 3 min.
6. Wash in 2X SSC for 5 min.
7. Treat with 8% sodium thiocyanate at 80°C for 30 min.
8. Wash 2X briefly in SSC at room temperature.
9. Digest in protease solution (pepsin and protease buffer) at 37°C for 28 min. This step will vary as a result of tissue/fixation and is the most critical step in FISH.
10. Rinse slides in 2X SSC 5 times at room temperature.
11. Place in 10% neutral buffered formalin for 10 min.
12. Wash in 2X SSC for 5 min at room temperature.
13. Dehydrate in 70% IMS for 1 min.
14. Dehydrate in 85% IMS for 1 min.
15. Dehydrate in 95% IMS for 1 min.
16. Air-dry.

Pretreatment of Slides Using VP2000 Robot for FISH Analysis

1. Add 500 ml of pretreatment solution (8% iso-thiocyanate) to heated water bath 1; check pH (after each run, measure volume of pretreatment solution and make up to 500 ml with distilled water to correct for evaporation and check pH (pH 7). Discard pretreatment solution after 5 uses.
2. Measure 500 ml of protease buffer (use 5 times before discarding) and place in water bath 2.
3. Check the levels of each plastic basin in the VP2000 (Vysis UK, Ltd.). The plastic basins have a fine groove, to mark approximately 700 ml. Each basin should be topped up to the line, with the appropriate solution, every time the machine is run.
4. Place slides in VP2000 slide carrier and place on VP2000 (Vysis UK, Ltd.).
5. The protocol of the VP2000 is as follows:

a. Xylene for 5 min × 2.
b. 95% alcohol for 5 min × 2.
c. 0.2 N HCl for 20 min.
d. Water rinse for 3 min.
e. Pretreatment solution for 30 min at 80°C.
f. Water rinse for 3 min.
g. Protease buffer and protease for 28 min at 37°C.
h. Water rinse for 3 min.
i. Formalin fixation for 10 min.
j. Water rinse for 3 min.
k. 70% alcohol for 5 min.
l. 85% alcohol for 5 min.
m. 95% alcohol for 5 min.
n. Air-dry at 28°C for 3 min.
6. Switch on VP2000 before the computer.
7. Log on to the computer and select protocol for 28 min protease treatment.
8. Check protocol and start procedure by clicking of run on the computer screen.
9. Ensure water supply is turned on.
10. Top water bath up to ensure water is in the bath.
11. Add 250 mg protease to protease buffer just before protease treatment (about 1 hr after you start).
12. Treat in protease for 28 min for prostate tissue.

Note: From this point forward both the manual method and robotic method are the same.

Examination of Slides to Check if Tissue is Appropriately Digested

The pretreatment stage is designed to digest the protein from the tissue section. The extent of this depends on the original stroma of the tissue. Therefore, every tissue section may require slightly different digestion times (i.e., time spent in the protease). It is therefore important that before you proceed you examine the tissue section to ensure it is appropriately digested.

1. Place 20 µl of DAPI onto 22 mm × 26 mm coverslip.
2. Place slide on top of coverslip, ensuring that all tissue is covered.
3. Allow slide to stand for 5 min so DAPI can penetrate nucleus.
4. Place oil onto the coverslip if viewing using an oil objective.
5. Tissue is viewed at 400X and 1000X magnification using a Leica DMLB microscope incorporating an epifluorescence system with an 100W mercury arc lamp and triple band pass filter that spans the excitation and emission wavelengths of DAPI.
6. Samples with residual protein masking nuclei (underdigested) are redigested as appropriate, for a

maximum of a further 3 min. If samples are overdigested, then you need to select a new slide and begin again decreasing digestion time (see **Technical Note 1** at the end of this chapter).

7. Wash slides in distilled water for 5 min and air-dry in oven at 50°C.

Hybridization

1. Apply 10 µl of probe to 22 mm × 26 mm coverslip and place slide on top, ensuring there are no air bubbles (see **Technical Note 2** at the end of this chapter).

2. Seal coverslip using rubber cement.

3. Place slides on Omnislide at 72°C for 2 min to denature probe.

4. Incubate overnight at 37°C on Omnislide.

Post-Hybridization Wash

1. Peel off rubber cement and soak coverslips in post-hybridization wash buffer at room temperature.

2. Incubate in post-hybridization wash buffer for 2 min at 72°C.

3. Allow slides to air-dry in the dark.

Mounting

1. Apply 15 µl of DAPI in Vectashield to 22 mm × 26 mm coverslip, ensuring there are no air bubbles.

2. Seal coverslip with clear nail varnish.

3. Allow to dry for 15 min in the dark.

4. Store slides at 4°C in the dark (slides should be scored as soon as possible because fading occurs).

Visualization and Scoring of Tissue Sections

1. Slides are viewed using a Leica DMLB microscope incorporating an epifluorescence system with a 100W mercury arc lamp and triple band pass filter (DOG filter, Vysis UK, Ltd) that spans the excitation and emission wavelengths of Dapi, SpectrumGreen and SpectrumOrange fluorochromes. In addition, it is useful to have a single band pass filter for both SpectrumGreen and SpectrumOrange labeled probes.

2. Scan slides at 400X magnification to localize tumor areas.

3. Three areas should be identified and location should be noted.

4. Twenty nuclei per area should be assessed at 1000X by two independent observers, a total of 60 nuclei (see **Technical Note 3** at the end of this chapter).

5. The number of signals for X chromosome (green signals) and AR (orange signals) should be counted on a cell-by-cell basis and results should be recorded.

6. Calculate mean chromosomal copy number, by totaling the number of X chromosome signals counted in a specific area and dividing this figure by the number of nuclei assessed.

7. This calculation should be repeated for mean AR copy number.

8. An AR amplification is recorded if the ratio of the mean AR copy number/mean chromosomal copy number is greater than 1.5.

Immunohistochemistry

1. Cut 5 µm-thick sections and place them onto silane-coated slides.

2. Dewax the slides in xylene for 5 min, and repeat.

3. 2 × 5 min 100% alcohol.

4. 2 min 90% alcohol.

5. 2 min 70% alcohol.

6. Rinse in water for 3 min.

7. Treat with 0.3% H_2O_2 for 10 min on a stirrer (4 ml/400 ml) to destroy endogenous peroxidase.

8. Rinse in water for 3 min.

Antigen Retrieval

1. Place 1 L of TE buffer (pH 8.0) into plastic pressure cooker (A. Menarini Diagnostics, UK).

2. Microwave on full power for 13.5 min to warm the solution (850 watts).

3. Add the slides and put lid on, and microwave on full power for 2 min to bring to pressure (or until pressure is reached).

4. Microwave for 5 min under pressure.

5. Carefully remove weight to allow steam to escape; because of the high pressure steam being released at this stage, care should be taken and protective hand and face equipment should be worn.

6. Once all the steam has escaped, carefully remove lid.

7. Allow to cool for 20 min.

8. Wash in running tap water for 10 min.

9. Transfer to a staining dish with water.

Staining

1. Ring sections with Dako pen to create a barrier.
2. Blocking solution: (Vector ABC kit) add 15 µl of serum per ml of TBS buffer.
3. Cover the section with blocking solution and incubate for 20 min.
4. Blot serum from sections onto tissue.
5. Cover the section with avidin using a dropper and incubate for 5 min at room temperature.
6. Cover the section with biotin using a dropper and incubate for 5 min at room temperature.
7. Cover the section in primary antibody using dropper and incubate in a humidified chamber at 20°C for 30 min (AR diluted 1:100 in Dako diluent).
8. Wash 5 min in TBS twice at room temperature.
9. Cover sections in secondary antibody and incubate in humidified chamber at room temperature for 30 min (Vector biotinylated antibody, 15 µl serum + 5 µl antibody in 1 ml TBS).
10. Wash 5 min in TBS 2X.
11. While incubating in primary antibody make up Vector ABC reagent: 20 µl of A and 20 µl of B per ml of TBS, allow to stand for ~30 min.
12. Cover sections in ABC reagent and incubate in humidified chamber for 30 min at room temperature.
13. Wash twice for 5 min each in TBS.
14. Make DAB substrate (Vector): To 5 ml of distilled water add 2 drops buffer stock and mix, 4 drops of DAB stock and mix, 2 drops of hydrogen peroxide and mix.
15. Cover sections with substrate and incubate until brown color develops (2–10 min).
16. Wash in water 10 min.

Counterstain

1. Stain in hematoxylin for 90 sec.
2. Rinse in running tap water until water runs clear.
3. Blue with Scots tap water substitute.
4. Rinse in running tap water.

Dehydrate and Mount

1. Dehydrate through serial alcohols, 70% alcohol for 1 min.
2. 90% alcohol for 1 min.
3. 100% alcohol 2× for 1 min.
4. Xylene for 1 min.
5. Place DPX on coverslip and mount slide, ensuring no air bubbles are present.

Score Immunohistochemistry Slides

Staining should be scored blind by two independent observers using a weighted histoscore method (see **Technical Note 3** at the end of chapter).

1. The percentage and intensity of nuclei staining is evaluated for the whole tissue section.
2. Scan the slide using a light microscope at a magnification of 100X.
3. Note the percentage of tumor cell nuclei that stain weakly, moderately, and strongly.
4. Calculate histoscores from the sum of (0X percentage of cells with no staining) + (1X percentage of cells staining weakly positive) + (2X percentage of cells staining moderately positive) + (3X percentage of cells staining strongly positive).
5. The minimum histoscore using this method is 0 and the maximum is 300.
6. The mean of the two observers' scores should be used for analysis (See **Technical Note 3** at the end of this chapter).

RESULTS AND DISCUSSION

Using the previous methods, we analyzed *AR* gene amplification and protein expression in 51 patients with hormone refractory prostate cancer. Each patient investigated had a primary biopsy before androgen deprivation therapy and a paired biopsy following development of hormone refractory disease available for analysis.

AR gene amplifications are uncommon in hormone sensitive tumors and are present in 20–30% of hormone resistant tumors (Edwards *et al.*, 2001; Koivisto *et al.*, 1997). In the present study we investigated *AR* amplification and found that significantly more hormone resistant tumors had *AR* amplification (20%, 10/49) than hormone sensitive tumors (2%, 1/48) (p = 0.0085, Fisher's exact test). Figure 71 illustrates an example of a prostate cancer tumor with *AR* gene amplification. In the amplified tumors in our study the median AR:X chromosome ratio was 3.11 (interquartile range, 2.4–5.8). We also identified a patient with *AR* amplification in the hormone sensitive tumor, which responds fully to therapy, suggesting that *AR* amplification does not preclude a response to androgen deprivation therapy.

In 22 patients no abnormalities of either the X chromosome or the *AR* copy number were detected in either the biopsy taken before or after hormone relapse. Eighteen (38%) hormone sensitive tumors and 23 (47%) hormone relapsed tumors (p = 0.46, Fisher's exact test) had increased copies of the X chromosome.

Magnification × 1000
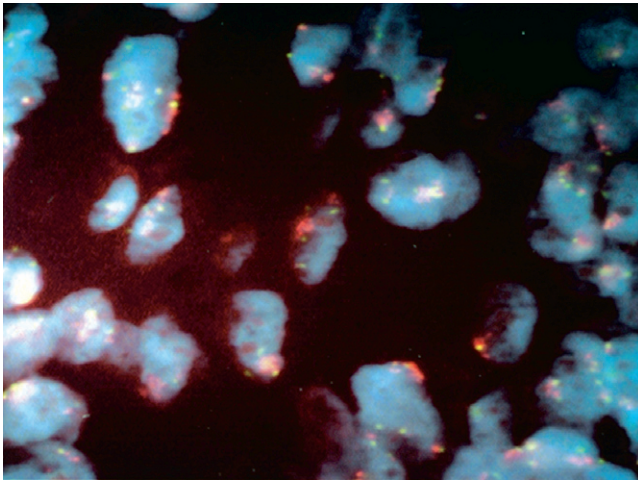
Figure 71 A prostate cancer tumor with androgen receptor (AR) gene amplification. AR amplification in prostate cancer nuclei (stained with DAPI, *blue*) showing increased copies of both AR (*red*) and chromosome X (*green*). Magnification 1000X.

Fifteen (31%) hormone sensitive tumors and 25 (51%) hormone relapsed tumors (p = 0.075, Fisher's exact test) showed evidence of increased *AR* gene copies. There was no significant difference in time to relapse in patients with *AR* amplifications (median 3.13 years, interquartile range 0.65–4.69 years) compared to those without *AR* amplifications (median 2.34 years, interquartile range 1.48–4.68 years). Therefore, although *AR* amplification is associated with hormone refractory disease, it does not influence time to relapse.

It is hypothesised that *AR* gene amplification is involved in the development of hormone resistant prostate cancer because amplification of *AR* is reported to result in an increase in AR protein expression (Visakorpi *et al*., 1995). Real-time reverse transcriptase-polymerase chain reaction (RT-PCR) demonstrated that even one additional copy of the *AR* gene may increase AR mRNA expression (Linja *et al*., 2001), suggesting that even a small increase in relative gene dosage could have biologic significance. An increase in AR protein expression is postulated to enable low circulating levels of androgens that are present following orchidectomy or treatment with LHRH agonists, to activate the AR even in the presence of anti-androgens (Koivisto *et al*., 1997) or to allow anti-androgens to act as agonists (Chen *et al*., 2004). We therefore measured AR protein expression and *AR* amplification status in our patient cohort. Because we have a unique data set of matched hormone sensitive and hormone refractory tumors from each patient, we were able to follow AR protein expression with the development of resistance in the

same patient and relate this to *AR* amplification status. Figure 72 illustrates an example of AR protein expression in hormone resistant prostate tumors. Our study demonstrates that the level of AR expression is significantly higher in hormone resistant tumors compared to matched hormone sensitive tumors (median 130, interquartile range, 55–167 versus median 94.5 interquartile range, 55–120, p = 0.019). We also noted that an increase in AR expression was seen in 80% (8/10) of cases with *AR* amplification. However, an increase in AR expression was also seen in 35% of cases that did not develop *AR* amplification. This suggests that although an increase in AR expression is associated with *AR* amplification, an increase in expression may also be the result of alternative mechanisms (e.g., decrease in protein degradation or an increase in protein stabilization).

Almost half of all patients in our cohort showed an increase in AR expression during the development of hormone refractory disease. An increase in AR protein expression therefore appears to be an import factor in the development of hormone refractory disease. However, in approximately 50% of patients, an increase in AR expression was not observed. Alternative routes to the development of hormone resistance must therefore be considered in these patients. We have reported that the development of hormone refractory prostate cancer is linked to gene amplification of members of both the MAP kinase and the P13K pathways (Edwards *et al*., 2003b). Evidence suggests that both of these pathways may sensitize the AR to low circulating levels of androgens via phosphorylation (Lin *et al*., 2001;

Magnification × 200
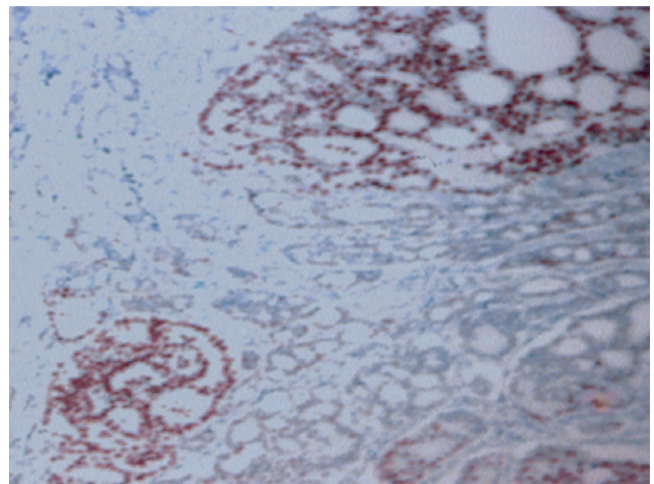
Figure 72 A prostate cancer tumor that expresses androgen receptor (AR) protein. AR protein expression is brown and is present in the tumor cell nuclei. Magnification 100X.

Magnification × 1000   Magnification × 400   Magnification × 400

A   B   C
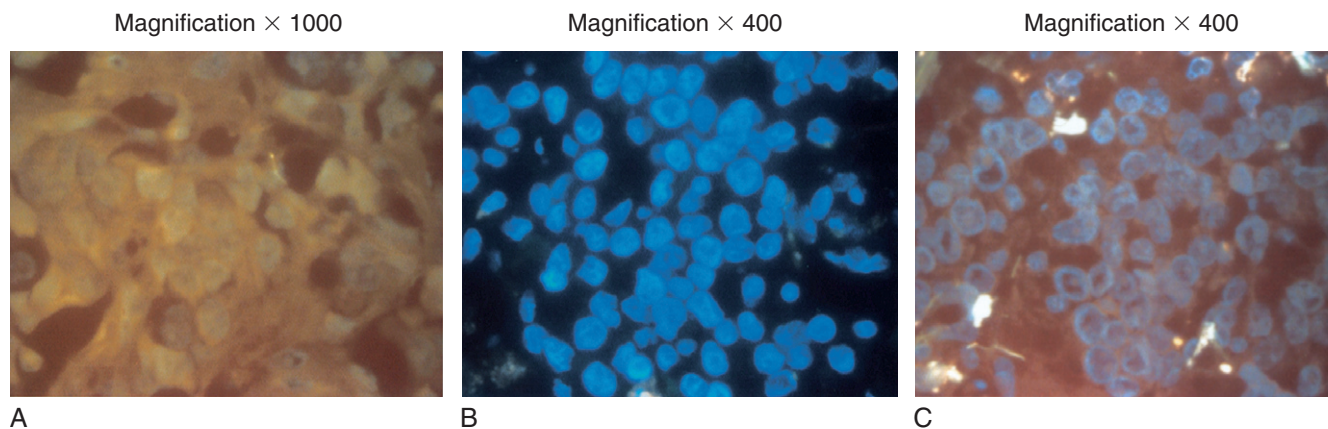
Figure 73 A: Tumor cells underdigested; note that the green protein obscures vision of the blue DAPI-stained nuclei. **B:** Digested; note that nuclei are clearly visible and membrane integrity remains. **C:** overdigested.

Zhu and Liu, 1997). It is also possible that hormone refractory prostate cancer develops via a mechanism that bypasses the AR (e.g., AP-1) (Henttu *et al.*, 1998; Krishna *et al.*, 2002).

In summary, we confirmed that *AR* gene amplification is associated with the development of hormone refractory prostate cancer in 20% of patients, and this is related to an increase in AR expression in the majority of cases. However, other mechanisms must also be involved in patients where an increase in AR protein expression is not observed.

Technical Notes

1. Tissue showing loss of nuclear boundaries (overdigestion) are discarded and duplicate slides are digested for a shorter period. Examples of digestion are shown in Figure 73. The important factor to be considered when assessing digestion is nuclear appearance. The nuclei should be evenly spread and not obscured by overlying protein.

2. If the tissue section is bigger than the coverslip and a larger coverslip is required, remember to increase volume of the probe appropriately.

3. For both FISH and IHC, tissue should always be scored by two independent observers. Analysis of agreement for each of these sets of measurements should be conducted using Bland and Altman. The mean difference between the two sets of measurements is obtained. This mean difference would be zero for optimal agreement between the measurements. Ninety-five percent confidence intervals for the mean is calculated to assess the precision of the estimate of mean difference. If these confidence intervals spanned zero, it is judged that there was no systematic bias in one set of measurements. This information is

displayed graphically by plotting the differences against the means of the two sets of measurements. The mean difference and 95% limits of agreement for the differences are displayed on the graphs. Ideally, the points should be randomly scattered above and below the zero line, reflecting no systematic bias in one or other method. The intra-class correlation coefficient (ICCC) between the two sets of measurements should also be calculated. ICCC is a true index of agreement between measurements reaching its maximum value of 1 if all the pairs of values fall on a straight line through the origin with slope unity. The criteria for assessing the degree of agreement are as follows: ICCC <0.4, poor; ICCC ≥0.4 but ≤0.59, fair; ICCC ≥0.6 but ≤0.74, good; and ICCC ≥0.75, excellent.

Acknowledgment

References

Avila, D.M., Soppi, S., and McPhaumh, P. 2001. The androgen receptor in syndromes of insensitivity and prostate cancer. *J. Steroid. Biochem. Mol. Biol. 76*:1435–1442.

Brown, R.S.D., Edwards, J., Dogan, A., Payne, H., Harland, S., Bartlett, J.M.S., and Masters, J.F.W. 2002. Amplification of the androgen receptor gene in bone metastases from hormone refractory prostate cancer. *J. Pathol. 198*:237–244.

Chen, C.D., Welsbie, D.S., Tran, C., Baek, S.H., Chen, R., Vessella, R., Rosenfeld, M.G., and Sawyers, C.L. 2004. Molecular determinants of resistance to antiandrogen therapy. *Nature Med. 10*:33–39.

Edwards, J. Krishna, N.S., Grigor, K.M., and Bartlett, J.M.S. 2003a. Androgen receptor gene amplification and protein expression in hormone refractory prostate cancer. *Br. J. Cancer 89*:522–556.

Edwards, J., Krishna, N.S., Mukherjee, R., Watters, A.D., Underwood, M.A., and Bartlett, J.M.S. 2001. Amplification of the androgen receptor may not explain the development of androgen-independent prostate cancer. *Br. J. Urol. Int. 88*:633–637.

Edwards, J., Krishna, N.S., Witton, C.J., and Bartlett, J.M.S. 2003b. Gene amplifications associated with the development of hormone resistant prostate cancer. *Clinical Cancer Res. 9*:5271–5281.

Feldman, B.J., and Feldman, D. 2001. The development of androgen independent prostate cancer. *Nature Med. Rev. 1*:34–45.

Ford, O.H., Gregory, C.W., Kin, D., Smitherman, A.B., and Mohler, J.L. 2003. Androgen receptor gene amplification and protein expression in recurrent prostate cancer. *J. Urol. 70*:1817–1821.

Goktas, S., Ziada, A., and Crawford, E.D. 1999. Combined androgen blockade for advanced prostatic carcinoma. *Prostate Cancer Prostatic Dis. 2*: 172–179.

Henttu, P., and Vihko, P. 1998. The protein kinase C activator, phorbol ester, elicits disparate functional responses in androgen-sensitive and androgen-independent human cancer cells. *Biochem. Biophyl. Res. Commun. 244*:167–171.

Koivisto, P., Kononen, J., Palmberg, C., Tammela, T., Hyytinen, E., Isola, J., Trapman, J., Cleutjens, K., Noordzij, A., Visakorpi, T., and Kallioniemi, O-P. 1997. Androgen receptor gene amplification: A possible molecular mechanism for androgen deprivation therapy failure in prostate cancer. *Cancer Res. 57*:314–419.

Krishna, N.S., Edwards, J., Underwood, M.A., Grigor, K.M., and Bartlett, J.M.S. 2002. AP-1 as a mediator of androgen refractory prostate cancer. *Br. J. Cancer 86*:s34.

Lin, H.K., Yeh, S., Kang, H.Y., and Chang, C. 2001. Akt suppresses androgen-induced apoptosis by phosphorylating and inhibiting androgen receptor. *Proc. Nat. Acad. Sci. USA. 98*: 7200–7205.

Linja, M.J., Savinainen, K.J., Saramaki, O.R., Tammela, T.L., Vessella, R.L., and Visakorpi, T. 2001. Amplification and over-expression of androgen receptor gene in hormone-refractory prostate cancer. *Cancer Res. 61*:3550–3555.

Newling, D., Fossa, S.D., Andersson, L., Abrahamsson, P.A., Aso, Y., Eisenberger, M.A., Khoury, S., Kozlowski, J.S., Kelly, K., Scher, H., and Hartley-Asp, B. 1997. Assessment of hormone refractory prostate cancer. *Urol. 49*:46–53.

Segawa, N., Mori, I., Utsunomiya, H., Nakamura, M., Nakamura, Y., Shan, L., Kakudo, K., and Katsuoka, Y. 2001. Prognostic significance of neuroendocrine differentiation, proliferation activity and androgen receptor expression in prostate cancer. *Pathol. Int. 51*:452–459.

Visakorpi, T., Hyytinen, E., Koivisto, P., Tanner, M., Keinanen, R., Palmberg, C., Palotie, A., Tammela, T., Isola, J., and Kallioniemi, O.P. 1995. In vivo amplification of the androgen receptor gene and progression of human prostate cancer. *Nat. Gen. 9*:401–406.

Zhu, X., and Liu, J.P. 1997. Steroid-independent activation of androgen receptor in androgen-independent prostate cancer: A possible role for the MAP kinase signal transduction pathway? *Mol. Cell. Endo. 134*:9–14.

15

Role of Immunohistochemical Loss of Bin1/Amphiphysin2 in Prostatic Carcinoma

James B. DuHadaway and George C. Prendergast

Introduction

The *Bin1* gene (also known as the *Amphiphysin2* gene) encodes several alternately spliced adapter proteins that have been implicated in both vesicle dynamics and nuclear processes. There is considerable evidence that nuclear-localized Bin1 proteins have tumor suppressor and proapoptotic activities in cancer cells. In the prostate, Bin1 proteins are expressed robustly in the nucleus of normal cells, but they are often absent or mislocalized in cases of primary prostate adenocarcinoma and invariably absent in metastases. *In vitro* investigations with prostate cancer cell lines show that ectopic expression of Bin1 proteins block proliferation and/or stimulate programmed cell death. Immunohistochemical analysis of Bin1 may have utility in discriminating the stage or prognosis of prostate cancers.

BAR Adapter Proteins Encoded by the *Bin1* Gene May Integrate Signaling and Trafficking Processes that Participate in Stress Signaling and Cancer Suppression

The human genome encodes at least four members of the Bin/Amphiphysin/Rvs (BAR) gene family, including *Bin1/Amphiphysin2, Bin2, Bin3*, and *Amphiphysin1*. BAR genes encode a set of adapter proteins that are marked by a unique N-terminal domain of undetermined function, termed the BAR domain. The *Bin1* and *Bin3* genes are highly conserved in evolution, with homologs found in fruit flies, nematodes, and yeast. *Bin1* and *Bin3* are expressed ubiquitously in mammalian cells, whereas *Bin2* and *Amphiphysin1* are expressed predominantly in hematopoetic cells and the central nervous system, respectively. BAR adapter proteins have been implicated in diverse cellular processes, including vesicle dynamics, actin organization, transcription, and proapoptotic stress signaling.

There is a broad body of evidence that nuclear-localized Bin1 proteins can mediate cancer suppression and cell suicide (DuHadaway *et al*., 2001; Elliott *et al*., 2000; Ge *et al*., 1999; Ge *et al.,* 2000a; Ge *et al*., 2000b; Sakamuro *et al*., 1996). Bin1 studies have been complicated by the fact that this gene encodes at least eight different splice isoforms that localize to different compartments of the cell (Butler *et al*., 1997; Wechsler-Reya *et al*., 1997b). Tissue-specific isoforms expressed mainly in the central nervous system have been linked to synaptic vesicle recycling (Wigge and McMahon, 1998). These isoforms lack cancer suppression or cell death activities, and their link to synaptic vesicle endocytosis is mediated through interactions with

Handbook of Immunohistochemistry and *in situ* Hybridization of Human Carcinomas, Volume 2: Molecular Pathology, Colorectal Carcinoma, and Prostate Carcinoma

431

Amphiphysin1, which is expressed predominantly in neurons. However, "gene knockout" experiments in the mouse have established that *Bin1/Amphiphysin2* is nonessential for endocytotic processes (Muller *et al.*, 2003). Similar findings have been made for the *Bin1* homolog in fission yeast (Routhier *et al.*, 2003). Moreover, although Amphiphysin1 has been reported to have a limited role in endocytosis in neurons, this role is only manifested under certain conditions of stimulus signaling (Di Paolo *et al.*, 2002). In the case of the muscle-specific and ubiquitous splice isoforms of Bin1, these proteins lack the alternately spliced sequences that are required for interactions with endocytotic proteins; moreover, these isoforms do not affect endocytosis (Elliott *et al.*, 2000). Instead, these isoforms are localized in both the cytosol and the nucleus, where they can mediate cancer suppression and cell death. Accordingly, *Bin1* may have multiple functions, perhaps distinguished by subcellular localization and integration of stress signals with vesicle dynamics and nuclear processes.

Based on the existing evidence, BAR adapter proteins have been suggested to serve as "bridging integrators" that couple signaling and trafficking processes in cells (Prendergast, 1999). Recent work on the homologs of *Bin1* and *Bin3* in fission yeast support an evolutionarily conserved role in stress signaling processes (Routhier *et al.*, 2003). Thus, rather than being involved in the "root" function of the variety of complexes in which they appear, Bin1 adapter proteins may instead act in these complexes to integrate signaling and trafficking processes in cells, in particular those related to stress signals and cancer suppression.

Bin1, C-Myc, and Cancer Cell Suicide

Bin1 isoform was identified initially as a c-Myc–interacting adapter protein with tumor suppressor properties. c-Myc is a central regulator of cell division that is frequently activated in diverse human cancers (Cole, 1986), including prostate cancer (Peehl, 1993). Although its exact function(s) is not entirely clear, Myc is thought to drive deoxyribonucleic acid (DNA) replication and cell division by regulating the transcription of cellular genes needed for those processes. Notably, when the expression of c-Myc is uncoupled from normal growth regulatory signals, c-Myc can trigger apoptosis or programmed cell death by diverse mechanisms (Prendergast, 1999).

The "death penalties" that are associated with inappropriate activation of c-Myc limit its oncogenic properties, and during neoplastic progression these "death penalties" are progressively suppressed or inactivated. Thus, these events cooperate with c-Myc activation and define important tumor suppression and progression mechanisms in the many aggressive cancers where Myc is activated, including prostate cancer. Studies in mesenchymal systems (e.g., fibroblasts, lymphocytes) show mutation of the tumor suppressor gene p53, suppression of signaling by the death receptor Fas, or up-regulation of the antiapoptotic proteins Bcl-2 or Bcl-XL that can limit c-Myc–induced cell death (Prendergast, 1999). However, in epithelial cell types c-Myc can drive cancer and trigger cell death by mechanisms that are independent of these molecules (Prendergast, 1999). Our laboratory has implicated *Bin1* in this setting (DuHadaway *et al.*, 2001), consistent with other evidence that *Bin1* promotes cancer cell suicide (Elliott *et al.*, 1999; Elliott *et al.*, 2000; Ge *et al.*, 1999; Ge *et al.*, 2000a; Hogarty *et al.*, 2000; Sakamuro *et al.*, 1996). In summary, *Bin1* losses may promote malignancy and tumor progression in part by abolishing a "death penalty" that is associated with c-Myc activation.

Bin1 Losses Occur Frequently in Prostate Cancer

Refinement of the chromosomal location of *Bin1* maps the gene to 2q14-21, within a midsection of chromosome 2q that is frequently deleted in metastatic prostate cancers (Cher *et al.*, 1996). No other tumor suppressor gene candidate has been identified other than *Bin1* in this region. Loss of heterozygosity (LOH) occurs in ~40% (6/15) of a panel of genomic DNAs isolated from tumor or matched adjacent normal prostate tissue (Ge *et al.*, 2000b). In contrast, no comparable LOH was detected in 18 DNAs from a control set of malignant or matched adjacent normal bladder tissues (Ge *et al.*, 2000b). The frequency of LOH is consistent with the report of frequent 2q21 deletions in metastatic prostate cancer (Cher *et al.*, 1996). Histochemical staining of normal prostate basal epithelial cells shows that *Bin1* is expressed robustly in a nuclear pattern seen in other cell types (DuHadaway *et al.*, 2003; Sakamuro *et al.*, 1996; Wechsler-Reya *et al.*, 1997a). In contrast, primary tumors and metastatic lesions exhibit frequent loss of expression in *Bin1* (DuHadaway *et al.*, 2003; Ge *et al.*, 2000b).

MATERIALS AND METHODS

Staining Frozen Tissue with Monoclonal Antibody 99D (Alternately Spliced Epitope)

MATERIALS

1. Distilled deionized water.

2. Dulbeccos's phosphate buffer saline (PBS): 100 mg anhydrous calcium chloride, 200 mg potassium chloride, 200 mg monobasic potassium phosphate, 100 mg magnesium chloride $\cdot$ 6H$_2$O; 8 g sodium chloride, and 2.16 g dibasic sodium phosphate $\cdot$ 7H$_2$O; bring volume to 1 L with deionized glass-distilled water (pH 7.4).

3. 4% paraformaldehyde (PFA)/PBS: Add 10 ml of a 16% PFA solution (15710, paraformaldehyde, 16% solution, Electron Microscopy Sciences, Ft. Washington, PA) to 30 ml PBS.

4. 0.1% Triton X-100/PBS solution: Add 100 µl of 100% Triton X-100 (BP151-500, Triton X-100, Fisher Scientific, Pittsburgh, PA) into 100 ml of PBS. Stir.

5. 3% hydrogen peroxide (H$_2$O$_2$): Add 20 ml of 30% H$_2$O$_2$ to 180 ml of water. Stir.

6. Normal horse serum blocker: Add 150 µl of horse serum (PK-4002, Peroxidase Mouse IgG, Vector Laboratories, Burlingame, CA) in 10 ml PBS, and mix.

7. Avidin D and Biotin Blocking Solution: (SP-2001, Avidin D and Biotin Blocking Solution, Vector Laboratories).

8. Anti-Bin1 clone 99D is commercially available.

9. Dilute Anti-Bin1 clone 99D to a concentration of 2 µg/ml in PBS.

10. Biotinylated secondary antibody: Add 150 µl of horse serum in 10 ml PBS, then add 50 µl of horse anti-mouse biotinylated antibody (PK-4002, Peroxidase Mouse IgG, Vector Laboratories), mix.

11. Vectastain ABC Reagent: Add 100 µl of reagent A to 50 ml of PBS, mix, then add 100 µl of reagent B, mix (PK-4002, Peroxidase Mouse IgG, Vector Laboratories).

Note: ABC reagent should stand for 30 min before it can be used.

12. Diaminobenzidine (DAB) Substrate Kit for peroxidases: Add two drops of Buffer Stock solution to 5 ml of water and mix well, add four drops of DAB stock solution and mix well, add two drops of H$_2$O$_2$ solution and mix well, and finally add two drops of the Nickel Solution and mix (SK-4100, DAB Substrate Kit for Peroxidase, Vector Laboratories, Burlingame, CA).

13. Dehydrate: Xylene, 100% ethanol, and 95% ethanol; use histologic grade reagents.

14. Mounting Media: Permount (SP15-100, Permount, Fisher Scientific).

METHODS

1. Allow the slides to warm to room temperature and air-dry (can be air-dried up to 24 hr) and wash twice in PBS.

2. Incubate in 4% paraformaldehyde/PBS (PFA) 30 min at 4ºC or 5 min at room temperature.

3. Rinse in water, then sequentially pass twice through PBS.

4. Permeabilize in 0.1% Triton-X-100/PBS for 10 min.

5. Wash slides twice in PBS for 5 min each. Remove slides from the water, wipe off excess water from around the tissue, add 3% H$_2$O$_2$ in water, and incubate for 5 min at room temperature.

6. Wash in water for 5 min followed by 5 min in PBS.

7. Remove slides from the PBS, wipe off excess PBS from around the tissue, add diluted normal horse blocking serum, place in humidified chamber, and incubate 30 min.

8. Blot excess serum from sections, add a drop of Avidin D blocking solution for 15 min. Rinse briefly with PBS, incubate for 15 min in a drop of the Biotin blocking solution, and blot excess solution from sections.

9. Incubate sections for 30 min with diluted 99 D antibody.

10. Wash slides 3 times for 5 min each in PBS.

11. Incubate sections for 30 min with the diluted biotinylated secondary antibody.

12. Wash slides 3 times for 5 min each in PBS.

13. Incubate section for 30 min with VECTASTAIN ABC reagent.

14. Wash slides 3 times for 5 min each in PBS.

15. Incubate sections in peroxidase substrate solution ~200 µl per section until desired staining intensity develops, avoiding background staining.

16. Rinse slide in water to stop the reaction.

17. Dehydrate slides by immersing in two changes of 95% ethanol and then two changes of 100% ethanol for 3 min each, and remove the ethanol by immersing the slides in two changes of xylene for 5 min each.

18. Add one to two drops of mounting medium and cover with coverslip.

Staining Formalin-Fixed and Paraffin-Embedded Tissues with Monoclonal Antibody 2F11 (Ubiquitous Epitope)

MATERIALS

1. Deparaffinization: Xylene, 100% ethanol, 95% ethanol, and 70% ethanol histologic grade reagents.

2. Distilled deionized water.

3. Pressure cooker (for antigen retrieval): Presto 4 quart stainless steel pressure cooker.

4. Antigen Unmasking Solution: Shake Antigen Unmasking Solution well and add 15 ml to 1600 ml of water (H-3300, Antigen Unmasking Solution, Vector Laboratories).

5. 3% H_2O_2: add 20 ml of 30% H_2O_2 to 180 ml of water, and mix.

6. Dulbeccos's PBS: 100 mg anhydrous calcium chloride, 200 mg potassium chloride, 200 mg mono-basic potassium phosphate, 100 mg magnesium chloride·6H_2O; 8 g sodium chloride, and 2.16 g diba-sic sodium phosphate·7H_2O; bring volume to 1 L with deionized glass-distilled water (pH 7.4).

7. Normal horse serum blocker: add 150 µl of horse serum to 10 ml PBS, mix.

8. Avidin D and Biotin Blocking Solution.

9. Anti-Bin1 clone 2F11 (available from Santa Cruz Biotechnology, Inc., Santa Cruz, CA).

10. Dilute Anti-Bin1 2F11 to a concentration of 2 µg/ml in PBS.

11. Biotinylated secondary antibody: add 150 µl of horse serum to 10 ml PBS, then add 50 µl of horse anti-mouse biotinylated antibody.

12. Vectastain ABC Reagent: add 100 µl of reagent A to 5 ml of PBS, then add 100 µl of reagent B, mix.

Note: ABC reagent should be allowed to stand for 30 min before using.

13. DAB Substrate Kit for peroxidases: Add two drops of Buffer Stock solution to 5 ml of water and mix well, add four drops of DAB stock solution and mix well, add two drops of H_2O_2 solution and mix well, and finally add two drops of the nickel solution and mix.

14. Dehydrate: xylene, 100% ethanol, and 95% ethanol histologic grade reagents.

15. Mounting Media: Permount (SP15-100, Permount, Fisher Scientific).

METHODS

1. Deparaffinize slides: immerse slides in two changes of xylene for 5 min each, then two changes of 100% ethanol for 3 min each, and finally in 70% ethanol for 3 min.

2. Transfer slides into water for 5 min to rehydrate.

3. Pour Antigen Unmarking Solution into the Presto 4 quart stainless steel pressure cooker.

4. Cover but do not lock lid. Bring solution to a boil.

5. Position slides into a metal staining rack (do not place slides close together) and lower rack into the cooker. Lock lid on the pressure cooker.

6. As soon as the pressure regulator begins to rock gently, indicating the cooker has pressurized, start timing.

7. After 1 min, remove the pressure cooker from heat source and run under cold water. Open lid, remove slide rack, and place in water bath.

8. Wash slides in water for 5 min.

9. Remove slides from the water, wipe off excess water from around the tissue, add 3% H_2O_2 in water, and incubate for 5 min at room temperature.

10. Wash for 5 min in water and then for 5 min in PBS.

11. Remove slides from the PBS and wipe off excess PBS from around the tissue. Add diluted normal horse blocking serum. Place in humidified chamber and incubate for 30 min.

12. Blot of excess serum from sections. Add a drop of Avidin D blocking solution and incubate for 15 min. rinse briefly with PBS, add a drop of the Biotin block-ing solution, and incubate for an additional 15 min. Blot excess solution from sections.

13. Add the diluted 2F11 antibody and incubate sections for 30 min.

14. Wash slides 3 times for 5 min each in PBS.

15. Add the diluted biotinylated secondary antibody and incubate sections for 30 min.

16. Wash slides 3 times for 5 min each in PBS.

17. Add VECTASTAIN ELITE ABC solution and incubate sections for 30 min.

18. Wash slides 3 times for 5 min each in PBS.

19. Add peroxidase substrate solution (~200 µl per section) and incubate until the desired staining inten-sity develops, avoiding background staining.

20. Stop the reaction by rinsing the slide in water.

21. Dehydrate slides by immersing in two changes of 95% ethanol and then two changes of 100% ethanol for 3 min each. Remove the ethanol by immersing the slides in two changes of xylene for 5 min each.

22. Add one or two drops of mounting medium and overlay with coverslip.

RESULTS

Analysis of primary and metastatic tumors indicated variable losses of expression in primary tumors but consistent losses in metastatic lesions. In an initial study using the Bin1 monoclonal antibody 99D

(Wechsler-Reya *et al*., 1997a), which recognizes an epitope within the c-Myc–binding domain of Bin1 splice isoforms, nuclear staining was documented in 30 cases of prostate cancer that included regions of neoplasia, benign hypertrophy, prostatic intraepithelial neoplasia (PIN), and atrophy (Ge *et al*., 2000b). Staining was consistently low in atrophic cells but readily detectable in all other cells. This study demonstrated positive staining of neoplastic cells in 29 of 30 cases studied.

A second study of three cases of normal prostate and 50 cases of primary prostate cancer of low- to mid-Gleason grade demonstrated much less frequent staining of neoplastic cells (DuHadaway *et al*., 2003). This

study was conducted with the Bin1 monoclonal antibody 2F11, which specifically recognizes an epitope in the BAR domain present in all splice isoforms of Bin1 (i.e., 2F11 is a "pan-Bin1 isoform" antibody). Using 2F11, the basal epithelial cells of all normal cases were strongly positive for Bin1 staining in the nucleus. In contrast, ~75% of primary cases of prostate cancer were negative for Bin1 (Figure 74). Of the 25% of primary tumors that scored positive for 2F11 staining, the pattern observed was strong nuclear and cytosolic staining of both tumor and stromal cells in the tumor (Figure 74). Although the basis for this pattern was not established, it was reminiscent of that produced in malignant melanoma by aberrant splice isoforms of

Bin1 mAb 2F11 (pan-Bin1)
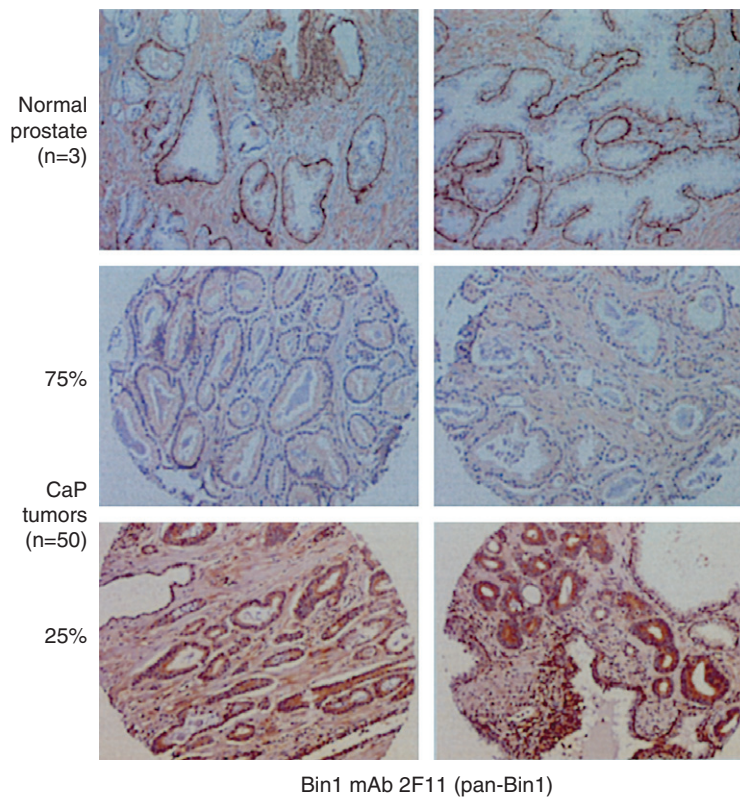
Figure 74 Immunohistochemical analysis of Bin1 in normal and malignant prostate cells. Strong nuclear staining of Bin1 with the monoclonal antibody 2F11 (DuHadaway *et al*., 2003) was detected in basal epithelial cells of normal parenchyma, whereas luminal columnar cells were uniformly negative (*top panels*). High-magnification images reveal that staining is predominately nuclear in character. Two examples of staining patterns are shown, which were observed in a tissue array of 50 cases of primary prostate adenocarcinoma. The major pattern observed (72% or 36/50 cases examined) was a general loss of staining in tumor cells (*middle panels*). An alternate pattern observed in positive cases (28% or 14/50 cases examined) was a strong nuclear and cytosolic staining throughout both tumor and stromal cells (*bottom panels*), possibly reflecting missplicing events (*see text*).

Bin1, termed Bin1 + 12A isoforms (Ge *et al*., 1999). The aberrant isoforms are also expressed by the androgen-independent human prostate tumor cell lines PC3 and Du145 (Ge *et al*., 2000b). Because the misspliced Bin1 + 12A isoforms lack the cancer suppression and proapoptotic activities of the ubiquitous isoforms expressed by normal prostate cells (Elliott *et al*., 2000), the altered staining pattern in some cases of prostate adenocarcinoma was interpreted to reflect a loss-of-function similar to that documented previously in melanoma (Ge *et al*., 1999).

DISCUSSION

Loss of the capability for programmed cell death is thought to have a major role in prostate cancer progression. Most prostate cancers are localized and indolent, but some tumors rapidly convert to a more aggressive status. Malignant conversion is tightly associated with acquisition of androgen independence: prostate cells that lose their susceptibility to androgen deprivation induced cell death are poorly managed in the clinic. Although the genetics of malignant conversion are not well understood, one of the most common abnormalities seen in tumors that have acquired invasive and metastatic potential is gain of chromosome 8q, where the c-Myc gene is located. Gains of 8q are well-correlated with disease progression, being found in 85% of lymph node metastases and 89% of recurrent hormone refractive tumors (Cher *et al*., 1996; Visakorpi *et al*., 1995). c-*Myc* amplification or overexpression is found in many prostate tumors, and it is associated with progression status (Buttyan *et al*., 1987). *Myc* activation delivers a powerful signal for malignant growth in many cells, including primary prostate cells (Thompson *et al*., 1989).

In prostate cancer, there is strong evidence that loss of the apoptotic response is associated with malignant conversion and progression to androgen independence (McDonnell *et al*., 1992). *p53* participates in a mechanism of apoptosis by *Myc* and is inactivated in many cancers including prostate cancers. However, *p53* is not required for Myc-induced death in epithelial cells (Sakamuro *et al*., 1995), nor is *p53* required for androgen deprival–induced death in prostate cells (Berges *et al*., 1993). Taken together, the results of *Bin1* studies support the hypothesis that loss of a *p53*-independent cell suicide program that involves Bin1 may be important for prostate cells to tolerate c-*Myc* activation.

In two comparatively small studies there was no apparent correlation between Bin1 status and Gleason grade. However, Bin1 losses were associated with high-grade cancers, based on Northern analysis of ribonucleic acid (RNA) isolated from 10 cases of metastatic prostate cancer (Ge *et al*., 2000b). In these metastatic cancers, Bin1 expression was universally undetectable, with losses extending beyond tumors where c-Myc was also overexpressed (Ge *et al*., 2000b). This observation suggested that there may be a benefit of Bin1 loss to tumor progression beyond settings that involve c-Myc activation. This possibility is consistent with evidence that Bin1 can also suppress cancer via *c*-Myc–independent mechanisms (Elliott *et al*., 1999). One skepticism is that the wide extent of losses of Bin1 expression or activity may merely reflect a loss of basal cells in prostate cancer. To rule out this possibility, our laboratory is using a conditional Bin1 "knockout" mouse model to confirm the expectation that Bin1 loss will be a sufficient cause to initiate or promote prostate tumor development in mice (study in progress).

An analysis of Bin1 status in the three most commonly studied prostate cancer cell lines (LNCaP, PC3, and DU145) offered additional support for the notion that Bin1 loss was associated with progression to androgen-independent status: Bin1 structure and expression patterns were unaffected in androgen-dependent LNCaP cells, but an abnormal, inactive splice isoform was expressed in androgen-independent PC3 and DU145 cells (Ge *et al*., 2000b). The abnormal splice isoforms seen in both cases were identical to that documented previously in human melanomas (Ge *et al*., 1999). Ectopic expression of Bin1 using an adenovirus vector triggered cell death in LNCaP and (to a lesser extent) in PC3 cells, but not in DU145 cells, which are refractory to many proapoptotic insults (Ge *et al*., 2000b). Taken together, these observations supported the hypothesis that Bin1 may have a role in prostate cancer suppression and that expression of the *Bin1* gene is attenuated or inactivated during prostate cancer progression. Further immunohistochemical analysis of Bin1 in prostate cancer may develop its potential as a prognostic marker or identifier for metastatic capacity.

References

Berges, R.R., Furuya, Y., Remington, L., English, H.F., Jacks, T., and Isaacs, J.T. 1993. Cell proliferation, DNA repair, and p53 function are not required for programmed death of prostatic glandular cells induced by androgen ablation. *Proc. Natl. Acad. Sci. USA 90*:8910–8914.

Butler, M.H., David, C., Ochoa, G.C., Freyberg, Z., Daniell, L., Grabs, D., Cremona, O., and De Camilli, P. 1997. Amphiphysin II (SH3P9; BIN1), a member of the amphiphysin/RVS family, is concentrated in the cortical cytomatrix of axon initial segments and nodes of Ravier in brain and around T tubules in skeletal muscle. *J. Cell. Biol. 137*:1355–1367.

Buttyan, R., Sawczuk, I.S., Benson, M.C., Siegal, J.D., and Olsson, C.A. 1987. Enhanced expression of the c-Myc protooncogene in high-grade human prostate cancers. *Prostate 11*:327–337.

Cher, M.L., Bova, G.S., Moore, D.H., Small, E.J., Carroll, P.R., Pin, S.S., Epstein, J.L., Isaacs, W.B., and Jensen, R.H. 1996. Genetic alterations in untreated metastases and androgen-independent prostate cancer detected by comparative genomic hybridization and allelotyping. *Cancer Res. 56*:3091–3102.

Cole, M.D. 1986. The myc oncogene: Its role in transformation and differentiation. *Ann. Rev. Genet. 20*:361–384.

Di Paolo, G., Sankaranarayanan, S., Wenk, M.R., Daniell, L., Perucco, E., Caldarone, B.J., Flavell, R., Picciotto, M.R., Ryan, T.A., Cremona, O., and De Camilli, P. 2002. Decreased synaptic vesicle recycling efficiency and cognitive deficts in amphiphysin 1 knockout mice. *Neuron 33*:789–804.

DuHadaway, J.B., Lynch, F.J., Brisbay, S., Bueso-Ramos, C., Troncoso, P., McDonnell, T., and Prendergast, G.C. 2003. Immunohistochemical analysis of Bin1/Amphiphysin II in human tissues: Diverse sites of nuclear expression and losses in prostate cancer. *J. Cell. Biochem. 88*:635–642.

DuHadaway, J.B., Sakamuro, D., Ewert, D.L., and Prendergast, G.C. 2001. Bin1 mediates apoptosis by c-Myc in transformed primary cells. *Cancer Res. 16*:3151–3156.

Elliott, K., Ge, K., Du, W., and Prendergast, G.C. 2000. The c-Myc-interacting adapter protein Bin1 activates a caspase-independent cell death program. *Oncogene 19*:4669–4684.

Elliott, K., Sakamuro, D., Basu, A., Du, W., Wunner, W., Staller, P., Gaubatz, S., Zhang, H., Prochownik, E., Eilers, M., and Prendergast, G.C. 1999. Bin1 functionally interacts with Myc in cells and inhibits cell proliferation by multiple mechanisms. *Oncogene 18*:3564–3573.

Ge, K., DuHadaway, J., Du, W., Herlyn, M., Rodeck, U., and Prendergast, G.C. 1999. Mechanism for elimination of a tumor suppressor: Aberrant splicing of a brain-specific exon causes loss of function of Bin1 in melanoma. *Proc. Natl. Acad. Sci. USA 96*:9689–9694.

Ge, K., DuHadaway, J., Sakamuro, D., Wechsler-Reya, R., Reynolds, C., and Prendergast, G.C. 2000a. Losses of the tumor suppressor Bin1 in breast carcinoma are frequent and reflect defits in a programmed cell death capacity. *Int. J. Cancer 85*:376–383.

Ge, K., Minhas, F., DuHadaway, J., Mao, N.C., Wilson, D., Sakamuro, D., Buccafusca, R., Nelson, P., Malkowicz, S.B., Tomaszewski, J.T., and Prendergast, G.C. 2000b. Loss of heterozygosity and tumor suppressor activity of Bin1 in prostate carcinoma. *Int. J. Cancer 86*:155–161.

Hogarty, M.D., Liu, X., Thompson, P.M., White, P.S., Sulman, E.P., Maris, J.M., and Brodeur, G.M. 2000. BIN1 inhibits colony formation and induces apoptosis in neuroblastoma cell lines with MYCN amplification. *Med. Pediatr. Oncol. 35*:559–562.

McDonnell, T.J., Troncoso, P., Brisbay, S.M., Logothetis, C., Chung, L.W., Hsieh, J.T., Tu, S.M., and Campbell, M.L. 1992. Expression of the protooncogene bcl-2 in the prostate and its association with emergence of androgen-independent prostate cancer. *Cancer Res. 52*:6940–6944.

Muller, A.J., Baker, J.F., DuHadaway, J.B., Ge, K., Du, W., Donover, P.S., Sharp, D.M., Farmer, G.E., Meade, R., Reid, C., Grzanna, R., Roach, A.H., and Prendergast, G.C. 2003. Targeted disruption of the murine Bin1/Amphiphysin II gene does not disable endocytosis but results in embryonic cardiomyopathy with aberrant myofibril formation. *Mol. Cell. Biol. 23*:4295–4306.

Peehl, D.M. 1993. Oncogenes in prostate cancer: An update. *Cancer 71*:1159–1164.

Prendergast, G.C. 1999. Mechanisms of apoptosis by c-Myc. *Oncogene 18*:2966–2986.

Routhier, E.L., Donover, P.S., and Prendergast, G.C. 2003. hob1+, the homolog of Bin1 in fission yeast, is dispensable for endocytosis but required for the response to starvation or genotoxic stress. *Oncogene 22*:637–648.

Sakamuro, D., Elliott, K., Wechsler-Reya, R., and Prendergast, G.C. 1996. BIN1 is a novel MYC-interacting protein with features of a tumor suppressor. *Nature Genet. 14*:69–77.

Sakamuro, D., Eviner, V., Elliott, K., Showe, L., White, E., and Prendergast, G.C. 1995. c-Myc induces apoptosis in epithelial cells by p53-dependent and p53-independent mechanisms. *Oncogene 11*:2411–2418.

Thompson, T.C., Southgate, J., Kitchener, G., and Land, H. 1989. Multistage carcinogenesis induced by ras and myc oncogenes in a reconstituted organ. *Cell 56*:917–930.

Visakorpi, T., Kallioniemi, A.H., Syvanen, A.C., Hyytinen, E.R., Karhu, R., Tammela, T., Isola, J.J., and Kallioniemi, O.P. 1995. Genetic changes in primary and recurrent prostate cancer by comparative genomic hybridization. *Cancer Res. 55*:342–347.

Wechsler-Reya, R., Elliott, K., Herlyn, M., and Prendergast, G.C. 1997a. The putative tumor suppressor BIN1 is a short-lived nuclear phosphoprotein whose localization is altered in malignant cells. *Cancer Res. 57*:3258–3263.

Wechsler-Reya, R., Sakamuro, D., Zhang, J., Duhadaway, J., and Prendergast, G.C. 1997b. Structural analysis of the human BIN1 gene: Evidence for tissue-specific transcriptional regulation and alternate RNA splicing. *J. Biol. Chem. 272*:31453–31458.

Wigge, P., and McMahon, H.T. 1998. The amphiphysin family of proteins and their role in endocytosis at the synapse. *Trends Neurosci. 21*:339–344.

This Page Intentionally Left Blank

16

Role of Prostate-Specific Glandular Kallikrein 2 in Prostate Carcinoma

Pirkko Vihko and Annakaisa Herrala

Introduction

Prostate cancer is the most frequently diagnosed malignancy among men in the Western countries. Human prostate specific antigen (hPSA, hK3) has been the cornerstone of prostate cancer diagnosis and follow-up for more than two decades, and human prostate specific glandular kallikrein 2 (hK2) is a new potential candidate for improving the diagnosis of the disease. There is high homology between these serine proteases (Henttu and Vihko, 1989; Henttu and Vihko, 1994; Lundwall, 1989). Both of them are expressed mainly in epithelial cells of prostate gland, and the messenger ribonucleic acid (mRNA) levels of hK2 have been reported to be 10–50% of those of hPSA (Henttu *et al*., 1990). The value of human prostate-specific glandular kallikrein (hK2) in prostate cancer diagnosis is under keen investigation. Many in-house methods for measuring serum hK2 are already in use (Becker *et al*., 2000; Black *et al*., 1999; Finlay *et al*., 2001; Klee *et al*., 1999), but commercial kits are not available yet, probably because of problems with assay standardization and the variation between different methods (Blijenberg *et al*., 2003). The mean hK2 concentration in sera of healthy men has been reported to be 26 ng/L, whereas the mean hK2 concentration in sera of patients with localized prostate was 72 ng/L, and in sera of patients with more

aggressive prostate cancer it was 116 ng/L, when measured with an ultrasensitive automated assay with a detection limit of 1.5 ng/L (Klee *et al*., 1999).

It has been shown with immunohistochemical studies that hK2 is more strongly expressed in prostate cancer than hPSA (Darson *et al*., 1997; Henttu *et al*., 1990). To study this phenomenon further, we measured the hK2 expression levels in benign and malignant prostate tissues from the same patient sample and compared them to hPSA expression at the mRNA level using an *in situ* hybridization technique and at the protein level with an immunohistochemical technique using specific monoclonal antibodies generated against hK2 (Herrala *et al*., 1997) and hPSA (Herrala *et al*., 2001; Vihko *et al*., 1990).

MATERIALS

Patient Tissue Specimens

The tissue specimens used in these experiments were collected from patients undergoing radical prostatectomy, biopsy, or transurethral resection of the prostate. Liver specimens were used as a negative control. The hematoxylin and eosin (H&E)-stained prostate tissue specimens were examined by a pathologist to ensure that they contained both benign (normal

or hyperplastic) and malignant tissue or malignant tissue only. The patients with prostate cancer were classified according to the Tumor-Node-Metastasis (TNM) classification system (Chisholm, 1988) and the prostate cancer tissue specimens were classified by the World Health Organization (WHO) histologic tumor grading system (Mostofi, 1980). The tissue sections adjacent to those checked by the pathologist were used for *in situ* hybridization and immunohistochemical studies.

1. Phosphate buffer saline (PBS) solution: 100 mg anhydrous calcium chloride, 200 mg potassium chloride, 200 mg monobasic potassium phosphate, 100 mg magnesium chloride $6 \times H_2O$; 8 g NaCl, and 2.16 g dibasic sodium phosphate $7 \times H_2O$; fill up to 1 L distilled H_2O, pH 7.2.

2. Fixative: 4% paraformaldehyde prepared in $1 \times$ PBS, pH 7.2; 40 g paraformaldehyde in 1 L $1 \times$ PBS, pH 7.2.

3. Glass slides (SuperFrost/Plus, Menzel-Gläser, Braunschweig, Germany).

4. Cole's hematoxylin stain: One portion: 1) hematoxylin solution 3 ml; 2) lugol solution 3 ml and; 3) alum solution 200 ml. Mix and let stand still for at least 15 minutes before use. Cole's hematoxylin stain can be eradicated by adding 4.5 ml of 5% sodium thiosulphate ($Na_2S_2O_3 \times H_2O$) into the staining mixture.

    a. Hematoxylin solution:

hematoxylin (Merck, Germany)	100 g
94% EtOH	1 L

    b. Lugol solution:

Iodine (I_2), p.a. (Merck)	20 g
Potassium iodide (KI) (Merck)	40 g
Distilled H_2O	1 L

    c. Alum solution:

Aluminium potassium sulphate, KAl(SO_4)$_2 \times H_2O$	12 g
Distilled H_2O	1 L

5. Eosin stain: 2.5 g eosin stain (Riedel de Häen, Germany), 200 ml distilled H_2O, 800 ml 94% EtOH, and 3.5 ml 100% acetic acid. First dissolve the eosin into water and then add EtOH. Before staining, add 700 µl of 100% acetic acid into 200 ml (one portion) of the eosin stain.

6. Pertex glue: Histolab, Gothenburg, Sweden.

7. DEPC-water: Add 1-2 ml diethylpyrocarbonate (DEPC) to 1 L of H_2O. Shake vigorously and leave overnight in a fume hood. Autoclave the DEPC water to inactivate the remaining DEPC. Store at room temperature. Wear gloves and use a fume hood when handling DEPC, which is a suspected carcinogen.

8. Transcription cocktail: 2 µl transcription buffer, 1 µl 0.2 *M* DTT (dithiothreitol), 0.5 µl 10 *nM* ATP (adenosine triphosphate), 0.5 µl 10 *nM* GTP (guanosine triphosphate), 0.5 µl 10 *nM* UTP (uridine triphosphatase), 0.5 µl RNasin (Promega), 0.5 µl transfer RNA (tRNA) (*Escherichia coli* 5 mg/ml, Boehringer, Mannheim, Germany), 2.5 µl linearized probe plasmid (= 1 µg), 1.5 µl ^{35}S-CTP (1250 Ci/mmol, PerkinElmer, Boston, MA), 0.5 µl suitable RNA polymerase (= 20U).

9. DNAse buffer: 0.01 *M* Tris-HCl, pH 7.9, 0.01 *M* NaCl, 0.006 *M* $MgCl_2$.

10. Quick spin columns: BioSpin 30/G50 Sephadex, Amersham Biosciences, UK.

11. 2 *M* Na acetate: 16.41 g sodium acetate, fill up to 0.1 L with H_2O.

12. 1 *M* DTT: 15.43 g DTT, fill up to 0.1 L with H_2O.

13. 0.1 *M* Glycine/0.2 *M* Tris-HCl, pH 7.4: 48.44 g Tris-HCl, 45 g glycine, fill up to 2 L with H_2O.

14. 0.1 *M* Tris-HCl, pH 8.0; 0.05 *M* EDTA (ethylenediamine tetra-acetic acid): 12.11 g Tris-HCl, 18.61 g EDTA, fill up to 1 L with H_2O.

15. $1 \times$ PBS, 4% paraformaldehyde: 4 g paraformaldehyde, fill up to 1 L with $1 \times$ PBS.

16. 0.1 *M* Triethanolamine (TEA), pH 8.0: 7.45 g TEA, fill up to 0.5 L with H_2O, autoclave.

17. $20 \times$ SSC (saline-sodium citrate): 3 *M* NaCl, 0.3 *M* Na citrate, 175.3 g sodium chloride, 88.23 g sodium citrate. Adjust the pH to 7.0 and fill up to 1 L with H_2O.

18. Adhesive border tape: Nitto No. 21, 0.2 mm $\times$ 50 mm $\times$ 20 mm, Nitto Denko Corp., Japan.

19. 1 *M* Tris-HCl, pH 8.0: 121.14 g Tris-HCl, fill up to 1 L with H_2O.

20 0.5 *M* EDTA: 18.61 g EDTA, fill up to 0.1 L with H_2O.

21. 50% dextran sulphate: 50 g dextran sulphate, fill up to 0.1 L with H_2O.

22. 100X Denhardt's solution: 10 g bovine serum albumin (BSA) (Sigma Fraction V), 10 g Ficol (400,000 mw), 10 g polyvinylpyrrolidone (PVP). Fill up to 500 ml with sterile H_2O. Dissolve the reagents in the following order: 1) Ficol, 2) BSA, and 3) PVP on magnetic stirrer, heat to 40°C, and filter-sterilize. Store in aliquots at –20°C.

23. 0.1 *M* DTT: Dissolve one part of 1 *M* DTT with 9 parts of H_2O.

24. Hybridization mix, HYBMIX: 702 mg NaCl (0.3 *M* at final concentration), 800 µl 1 *M* Tris-HCl, pH 8.0 (0.02 *M*), 400 µl 0.5 *M* EDTA (0.005 *M*), 6 ml 50% dextran sulphate (10%), 400 µl 100X Denhardt's solution (1X), 20 mg tRNA *E. coli* 0.5 mg/ml, 616.8 mg DTT (0.1 *M*). Mix NaCl first to 6 ml of H_2O and add all the ingredients in the order mentioned earlier. Mix thoroughly, and add water to a final volume of 16 ml. Divide into 500 µl aliquots.

25. Hydrophobic membrane: GelBond Film, agarose gel support medium, thickness 0.2 mm, Cambrex, Baltimore, MD.

26. 5 M NaCl: 146.1 g sodium chloride, fill up to 0.5 L H_2O.

27. TEN buffer: Mix 60 ml 5 M NaCl, 40 ml 1 M Tris-HCl, pH 8.0, and 20 ml 0.5 M EDTA, fill up to 1 L with H_2O.

28. Stringent wash buffer: 100 ml TEN buffer, 100 ml formamide, 3.08 g DTT.

29. RNAse buffer: 0.4 M NaCl, 0.01 M Tris-HCl, pH 8.0, 0.005 M EDTA. 10X stock: 100 ml 1 M Tris-HCl, pH 8.0, 100 ml 0.5M EDTA, 234 g NaCl; bring volume to 1 L with H_2O.

30. Materials and equipment needed in the darkroom: waterbath at 45°C, styrox boxes with ice (pack the ice tightly and evenly, check with a spirit level) covered first with aluminum foil and then with filter paper (Whatman 3M), scissors, gloves, black plastic boxes for slides, and nonsparking tape.

31. 0.6 M ammonium acetate: 23.12 g ammonium acetate, fill up to 0.5 L with H_2O.

32. Emulsion for autoradiography: Dilute the NTB2 emulsion (Kodak, Rochester, NY) to 50% solution with 0.6 M ammonium acetate; 19 ml is sufficient for 19 slides. The emulsion can be reused 3 times. Preheat the emulsion first at room temperature for 30 min and then to 45°C in a waterbath for 30 min. Fill the dipping chamber with emulsion and wait for at least 10 min to allow the air bubbles to go up. Keep the dipping chamber in a waterbath at 45°C.

33. Developer: D19, Kodak: Dissolve the reagents according to manufacturer's instructions.

34. Fixer: Unifix, Kodak: Dissolve the reagent according to manufacturer's instructions.

35. Fluorescent dye:1 mg Hoescht 33258 stain (Sigma-Aldrich, St. Louis, MO) in 250 ml 1 × PBS, pH 7.2. The solution remains stable for 1 month when stored in the dark at room temperature. Hoescht 33258 stain is carcinogenic. Gloves should be used during the procedure. The stain is reusable.

36. Immunoperoxidase method: Dako StreptABComplex/HRP Duet-kit, Mouse/Rabbit, Dako A/S, Denmark.

37. 3% hydrogen peroxide in distilled H_2O.

38. Tris buffered saline (TBS): 0.05 M Tris-HCl, 0.15 M NaCl, pH 7.6; 12.1 g Tris-HCl, 8.77 g NaCl, fill up to 2 L with H_2O.

39. 3% BSA blocking solution: 3 g BSA and 100 ml TBS. Add BSA to the buffer with stirring.

40. Primary antibody is diluted in TBS with 1% BSA.

41. Secondary antibody is diluted in TBS with 1% BSA.

42. Chromogenic substrate solution: To prepare a 1 mg/ml diaminobenzidine (DBA) chromogen solution (Dako AS), reconstitute one DAB tablet in 10 ml 0.05 M Tris-HCl, pH 7.6. The buffer must not contain sodium azide, which is an inhibitor of the peroxidase enzyme.

METHOD

Safety Points

All staining, dehydration, rehydration, and *in situ* hybridization procedures (steps before the darkroom) should be done in a fume hood. Notice that xylene is a toxic organic solvent. Always wear gloves and protective clothing. Follow the good laboratory practice and the rules of your laboratory and protect yourself appropriately when working with radioisotopes. Eradicate radioactive waste and all waste reagents and solutions in accordance with the regulations of your workplace.

Tissue Fixation and Embedding in Paraffin

1. Wash the tissue specimens once with 1 × PBS, and keep the specimens in 4% paraformaldehyde prepared in 1 × PBS for 16 hr or overnight at 4°C on a shaker with slow speed.

2. Wash the specimens for 2 × 5 min with 1 × PBS on a shaker.

3. Dehydrate the specimens at room temperature on shaker: 2 × 30 min 50% EtOH, 2 × 15 min 70% EtOH (you can leave the specimens here overnight or longer), 2 × 30 min 97% EtOH, 2 × 30 min 99% EtOH, 4 × 5 min xylene (for small specimens less than 1 cm in diameter), or 4 × 15 min xylene (for larger specimens).

4. Transfer the tissue specimens into melted paraffin and keep overnight at 58°C. Leave the caps open. Evaporate the xylene well, and if you can still smell xylene, replace the paraffin, keep the specimen tubes in the incubator, or transfer them into a vacuum chamber to remove the remaining xylene.

5. Transfer the specimens in paraffin to 4°C if you are not able to embed them immediately. When embedding the specimens in paraffin, pour the melted paraffin into a metal mold, drop the piece of tissue into the paraffin, place the plastic support onto the tissue and press it downward, add more paraffin, remove air bubbles by pressing again the plastic support, and let the tissue blocks solidify at room temperature.

6. Remove the paraffin block from the mold (keep the mold at –20°C for a short time to loosen the block) and trim the edges of the block for cutting with a microtome.

7. Cut 6-µm–thick sections and place them onto sterile glass slides.

8. Dry the samples on the slides for 1–4 days at 42°C, and then store the sample slides at 4°C.

Hematoxylin and Eosin Staining of Tissue Slides

Stain one slide from each patient specimen with H&E for histologic examination. Transfer the specimen slides onto a glass rack and dip the racks with the slides into the jar containing solutions.

1. Hydration of the paraffin-embedded sample slides: Place the slides into glass racks and perform the following procedure to hydrate the samples in glass dishes at room temperature: xylene 2×10 min, 97% EtOH 2×5 min, 70% EtOH 1×5 min, 30% EtOH 2×5 min, and H_2O 2×5 min.

2. Perform staining in the following order: Cole's hematoxylin stain 1 min, running tap water 5 min, eosin stain 1 min, 70% EtOH 10 sec, 95% EtOH 10 sec, absolute EtOH 1 min, 1) xylene solution 1 min, and 2) xylene solution 1 min. The flow of tap water should be moderate, so as not to loosen the tissue specimens from the glass slides. The last time in xylene is not so accurate because after that the slides are covered with coverslips.

3. Apply 4–6 drops of Pertex glue (Histolab, Sweden) onto the slides and place a coverslip on the slide, press gently to remove air bubbles, and dry overnight at room temperature. The slides are then ready for microscopic examination.

Specific hK2 and hPSA Probes

The probes for hK2 and hPSA *in situ* hybridization were a 250 bp fragment (nt 1198–1448) of hPSA complementary deoxyribonucleic acid (cDNA) (Henttu and Vihko, 1989) and a 300 bp fragment (nt 820–1120) of hK2 (Schedlich *et al.*, 1987). The fragments were amplified by polymerase chain reaction (PCR) using oligonucleotides with T7 or SP6 binding sites. The specificities of ^{32}P-labeled PCR products were checked by DNA blotting (1 µg of hPSA and hK2 DNA per slot). The anti-sense and sense RNA probes were transcribed from PCR products by using SP6 or T7 RNA polymerases (Promega, Madison, WI) as follows: Sterile plastics were used along DEPC-water.

The buffer used for labeling was from Promega's Riboprobe system (#P1121).

Generation of Anti-Sense and Sense RNA Probes

1. Incubate the transcription cocktail for 1 hr at 39°C. Add 0.7 µl H_2O + 0.5 µl buffer + 0.5 µl RNA polymerase. Incubate for an additional 30 min at 39°C. The plasmid is degraded from the transcription cocktail by adding 85 µl DNAse buffer and 2.5 µl RQ1 DNAse (Promega), now V_{Tot} = 100 µl, and incubating for 30 min at 39°C.

2. Add 100 µl of H_2O to the mixture and extract it by adding 200 µl of Mopod phenol/chloroform (1:1) (Sigma, St. Louis, MO) and vortexing. Separate the phases by centrifuging briefly. Transfer the water phase from the top to a clean tube and re-extract the organic phase with 100 µl of water.

3. Combine the water phases and precipitate RNA by adding 20 µl tRNA, 40 µl 2 *M* Na-acetate, pH 4.0, 40 µl 1 *M* DTT, and 950 µl 100% ethanol and incubate at –70°C for at least 1 hr.

4. Centrifuge the probe RNA after precipitation at 10,000 rpm for 30 min and dry it. Dissolve the probe RNA with 50 µl of H_2O.

5. Purify the RNA probe with a quick spin column. Centrifuge the quick spin column first inside a 15 ml tube, with an Eppendorf tube at the bottom, for 2 min at 2300 rpm to empty the quick spin column. Replace the Eppendorf tube with an empty one, pipette the sample on top of the dry gel matrix of the quick spin column, and centrifuge for 4 min at 2300 rpm. The sample volume is ~50 µl.

6. Precipitate the RNA probe by adding 20 µl tRNA, 9 µl 2 *M* Na-acetate (10% final concentration), 9 µl 1 *M* DTT (100 *mM* final concentration), and 2.5 vol/220 µl 100% EtOH and incubate the mixture at –70°C for at least 1 hr.

7. Centrifuge for 10 min at 10,000 rpm. Dry and dissolve the RNA probe into 5 µl 1 *M* DTT, 10 µl tRNA, and 35 µl H_2O.

8. Measure the activity from 1 µl + 4 ml of scintillation solution (e.g., OptiPhase, PerkinElmer) mixed well. There should be at least $1–3 \times 10^6$ cpm/µl.

9. Divide the probe into 20 µl aliquots at –70°C. The probe expires after 2 months.

In situ Hybridization

The *in situ* hybridization reactions for hK2 and hPSA were performed according to Chotteau-Lelievre *et al.* (1994) and Mustonen *et al.* (1998) with our own adjustments.

Things to Be Noted Before Starting the in situ Hybridization Procedure

Always use RNase-free glass dishes, racks, and water to avoid contamination with RNases. All durations are exact, and all dishes and liquids must be sterile at **Steps 1–6**. Pass the samples slides in glass racks through the following steps. Do not stop between **Steps 1–6**. All steps should be done with gentle agitation. Wear gloves all the time. Perform all steps in a fume hood.

Hydration of the Samples

1. Place the slides into glass racks and put the following procedure to hydrate the samples in glass dishes at room temperature: xylene 2×10 min, 97% EtOH 2×5 min, 70% EtOH 1×5 min, 30% EtOH 2×5 min, and H_2O 2×5 min.

2. Thaw the post-fixation solutions in a water bath at this point.

Elimination of Paraformaldehyde

Incubate slides in 0.1 M glycine/0.2 M Tris-HCl, pH 7.4 for 10 min at room temperature. This procedure eliminates reactive groups and reduces background signal.

Proteinase K Digestion

Proteinase K digestion is performed to ensure better access to the target mRNAs in the cells.

All buffers must be prewarmed at 37°C.

1. Incubate the slides in 0.1 M Tris-HCl, pH 8.0, 0.05 M EDTA for 5 min at 37°C.

2. Add proteinase K at a final concentration of 1 mg/ml in 0.1 M Tris-HCl, pH 8.0, 0.05 M EDTA and incubate slides in this solution for 15 min at 37°C.

3. Dip the slide rack into H_2O for 30 sec at room temperature.

Post-Fixation

Post-fixation is performed for better adhesion of the sections to glass slides. The solutions are thawed and preheated to 37°C during the hydration step. The post-fixation solution should be prepared in advance.

1. Incubate the slides in $1 \times$ PBS, 4% paraformaldehyde for 15 min at room temperature.

2. Wash the slides in $1 \times$ PBS for 5 min at room temperature.

Acetylation Step

Acetylation reduces the probe's binding to chromosomal DNA.

1. Incubate the slides in 0.1 M TEA, pH 8.0, for 10 min at room temperature.

2. Add 1 ml acetic anhydride to 400 ml TEA, transfer slides into this buffer, and incubate for 10 min at room temperature (add acetic anhydride just before use).

3. Incubate the slides in $2 \times$ SSC for 30 sec at room temperature.

4. Wash the slides in H_2O for 2×5 min at room temperature.

Dehydration of Samples and Outlining of the Samples

1. Dehydrate the samples at room temperature with the following ethanol solutions: 30% EtOH for 5 min, 70% EtOH for 5 min, 97% EtOH for 5 min, and 100% EtOH for 5 min.

2. Air-dry the slides in a dust-free environment for at least 30 min. It is possible to have a break at this point.

3. It is possible to hybridize different probes (sense and anti-sense) on the same slides. To avoid mixing the probes, delineate the probe areas with adhesive border tape.

Hybridization

Hybridization is a modification of different procedures (Angerer *et al.*, 1987; Angerer *et al.*, 1989; Fontaine *et al.*, 1988; Schmid *et al.*, 1989).

1. Dilute the probe in nuclease-free water. At a higher concentration, background noise will increase, whereas a lower concentration will limit the saturation of target mRNAs. The concentration of the probe ought to be double-checked by counting two 1-µl aliquots with the scintillation counter, especially when the labeled probe is older than 2 weeks.

2. Prepare the hybridization mixture by mixing 4 parts of HYBMIX, 5 parts of deionized formamide, and 1 part of probe (1000 to 20,000 cpm/µl). The optimal concentration of the probe is 20,000 cpm/µl. Use 500,000 cpm/25 µl for the half of a slide and 1,000,000 cpm/50 µl for the whole slide.

3. Prior to adding onto the slides, heat the probe to denature possible secondary structures, which could inhibit the hybridization. Heat the probe for 2 min at 80°C and then place it on ice.

4. Apply the hybridization mixture onto the sample slides. Cover the slides with hydrophobic membrane and make sure that there are no air bubbles.

5. Store the slides in a "humid box." Line the bottom of the box with paper towels soaked in a mixture of 40 ml formamide, 16 ml $20 \times$ SSC, and 20 ml H_2O.

6. Seal the box with normal tape and incubate overnight **>55–60°C, max 16 hr.**

Washing

1. Keep the tissues moist. Transfer the slides from one solution to another in racks.

2. Transfer the slides to 200 ml of solution of $20 \times$ SCC, 1.55 g DTT filled up to 1 L with H_2O. DTT should be the last component added to the solutions just prior to use, while DTT is labile.

3. Wash the slides for 4×15 min at room temperature with gentle agitation. The covering membranes will become loose during the first washing step; remove them carefully at the end of the first wash.

Stringent Wash

1. Wash the slides in a waterbath in the stringent wash buffer, which does not need to be preheated, for 30 min at 60°C.

RNase Treatment

RNase treatment is done to digest the single-strand nonhybridized probe and to reduce background noise.

1. Incubate the slides for 2×10 min in $1 \times$ RNase buffer at 37°C prior to RNase treatment.

2. Add 0.8 ml RNase A (stock 5 mg/ml) to 200 ml preheated (37°C) $1 \times$ RNase buffer and incubate the slides in this solution for 30 min at 37°C.

3. Wash with $1 \times$ RNase buffer for 5 min at 37°C.

Washes after RNase Treatment

1. Preheat the buffers to 60°C. Place the slide racks into a big plastic container. Agitate occasionally. You will need 1 L of each buffer.

2. Incubate the slides in $2 \times$ SSC for 15 min at 60°C.

3. Transfer the slides in $0.1 \times$ SSC and incubate for additional 15 min at 60°C.

Dehydration of the Samples

1. Dehydrate the samples, as in previous dehydration step.

2. Air-dry the slides at 37°C or room temperature in a dust-free box. It is important to protect the slides from dust.

3. Remove the black barrier tapes.

Autoradiography

Autoradiography is carried out **under minimal red illumination**. You will need **the darkroom** for several hours.

1. Dip the slides one by one into the NTB2 emulsion. Turn them, if necessary, to completely cover the surface. Wipe clean the tissue-free side of the slide. Lay the slides horizontally on an ice bed.

2. Let the slides dry on the ice for 1 hour. Keep the waterbath on during this time, to keep the room air humid. Transfer the slides into a dark box and keep them there overnight. Switch off the waterbath.

3. On the following morning (still under minimal red light), transfer the slides to a rack in the black plastic box. On the top of the box, put silica gel in gauze to remove possible moisture from the box. Moisture will cause the signal to fade.

4. Close the box tightly with black nonsparking tape. Wrap it in aluminium foil and put it in a thick plastic bag.

5. Prior to exposure, store the slide boxes in a freezer (–20°C) for 15 days ± 1. Keep the slide boxes separate from other sources of radioactivity because ^{32}P, for example, will increase the background signal. In the case of hK2 and hPSA, the exposure time was only 3 days to prevent excess of label and background signal. The exposure times must be specified for each probe separately.

Development of the Slides

1. Development is done under minimum red light. One big and three black plastic boxes are needed for developing the slides. Place the boxes on ice and cool the liquids to exactly 12°C (you can start when the temperature is 12.5°C).

2. Dip the slides racks into the solutions in the following order and for the following times: 1) developer for 2.5 min; 2) sterile H_2O for 30 sec; 3) fixer for 5 min; and 4) distilled H_2O for 5 min. Gently rock the slide racks in the liquids. **The times are exact!**

3. Lift the slides from the last waterbath, wipe dry the back of each slide, and place the slides into a cardboard box. The slides are now bright, and you can handle them in normal light.

4. Let the slides dry completely.

Fluorescent Staining of Nuclei or Hematoxylin and Eosin Staining for *in situ* Hybridized Samples

1. Transfer the slides to a glass rack, dip the slide racks into the Hoescht 33 258 staining solution for 2 min (exact time), and keep the slides under aluminum foil. The fluorescent dye will complex with DNA and the nuclei will appear blue. The Hoescht 33 258 stain will bind covalently to DNA; it is carcinogenic. Gloves should be used during the procedure. Fluorescence: excitation = 340 nm and emission = 450 nm.

2. Wash in $1 \times$ PBS for 3×2 min (**exact times**).

3. Lift the slide rack from the last staining step, and while the slides are still wet, place 5–6 drops of glycergel (Dako A/S, Denmark) on the each slide and place a coverslip on the slide. Press gently to remove air bubbles. Let the glycergel dry overnight at room temperature.

4. Remove extra glycergel with a soft toothbrush and cold water. The slides are ready for microscopic examination.

5. The developed *in situ* hybridized slides may also be H&E stained for histologic examination. No drying of the slides is needed, but you can transfer the slides directly from the last development step into Cole's hematoxylin stain for staining as previously described.

Detection of hK2 and hPSA Expression from *in situ* Hybridized Specimens

The epithelial and stromal signal densities of both hK2 and hPSA were measured from *in situ* hybridized sections with an MCID M4 3.0 digital image analyzer (Imaging Research Inc., Ontario, Canada). Epithelial signal densities were measured separately from benign and malignant epithelium, using a method similar to that described by Kainu *et al*. (1996). Silver grains

were measured from 10 separate, randomly picked 40X objective fields of epithelium and stroma. The averages of the 10 values were taken as the respective transcript levels of hK2 and hPSA in the specimen. The silver grains counted from stromal areas represented background and were subtracted from the respective epithelial values.

Immunohistochemistry

Sections adjacent to those used for *in situ* hybridization of hK2 and hPSA were immunohistochemically stained using specific monoclonal antibodies for hK2 and hPSA, 151C (Herrala *et al*., 1997), and 7E7 (Vihko *et al*., 1990), respectively. An immunoperoxidase method (Dako StreptABComplex/HRP Duet, Mouse/Rabbit, Dako A/S, Denmark) with these antibodies was applied to the specimens.

Immunohistochemical Staining of Tissue Sections

1. To deparaffinize and hydrate the sample slides, place the slides on a glass rack and carry out the following procedure at room temperature: 1) Incubate the sample slides in xylene for 2×10 min; 2) 97% EtOH for 2×5 min; 3) 70% EtOH for 5 min; 4) 30% EtOH for 5 min; and distilled H_2O for 2×5 min.

2. Incubate the slides with 3% hydrogen peroxide in distilled water for 5 min to quench endogenous peroxidase activity.

3. Rinse the slides with distilled water and transfer them into TBS solution for 5 min.

4. Block the slides by incubating with 3% BSA in TBS for 30 min.

5. Incubate with a mouse primary antibody optimally diluted in 1% BSA in TBS solution for 30 min at room temperature. Apply the antibody solution directly onto tissue sections. Keep the slides in a humid box (put wet paper towels on the bottom of a plastic box) during the incubation to prevent evaporation and drying of the tissue sections.

6. Rinse the slides with TBS and incubate them in TBS bath for 5 min.

7. Incubate the slides with biotinylated goat anti-mouse antibody for 30 min at room temperature in a humid box and again apply the antibody directly onto tissue sections.

8. Rinse as in **Step 6**.

9. Incubate the slides with a prepared streptABComplex/HRP working solution (supplied

with the kit) for 30 min at room temperature in humid box as stated earlier.

10. Rinse as in **Step 6.**

11. Incubate the slides with a prepared chromogenic substrate solution for peroxidase for 5–15 min.

12. Rinse the slides after the color reaction with distilled water and counter-stain them with hematoxylin. Perform the staining in the following order: Cole's hematoxylin stain 1 min, running tap water 5 min, 70% EtOH 10 sec, 95% EtOH 10 sec, absolute EtOH 1 min, 1. xylene solution 1 min, and 2. xylene solution 1 min. The flow of tap water should be moderate, in order not to loosen the tissue specimens from the glass slides. Place the coverslips with Pertex glue and the slides are ready for microscopic examination.

The color reaction times with chromogenic substrate were much shorter for hK2 and hPSA proteins, 1–2 min, than recommended for the procedure. The intensity of immunostaining for hK2 and hPSA was determined visually, and each specimen was assigned to one of the following categories: no staining –; low staining +; moderate staining ++; and high/very high staining intensity +++. The evaluation of protein expression was done without knowledge of the respective mRNA levels.

Statistical Analyses

The expression levels of hK2 and hPSA in benign and malignant prostate tissues were compared with a paired sample t-test. Pearson's test was used to determine the correlation between the hK2 and hPSA mRNA levels. Kendall's two-tailed bivariant correlation test was used to compare the mRNA values and protein levels of the specimens. Statistical analyses were performed with the SPSS for Windows software (SPSS Inc., Chicago, IL).

RESULTS AND DISCUSSION

Expression of hK2 and hPSA at mRNA and Protein Levels

Human K2 and hPSA mRNAs were detected in the epithelium of both normal and benign prostatic hyperplasia (BPH) tissues as well as in prostate cancer tissue (Figure 75). This was also confirmed at the protein level with immunohistochemistry (Figure 75). The counting of silver grains per m^2 in the *in situ* hybridization analyses showed hPSA expression to be higher in benign than cancer tissues. The average expression levels (±SD) were 0.188 ± 0.95 and 0.168 ± 0.06 for benign and cancer tissue, respectively (P = 0.06). The hK2 mRNA level, however, was significantly increased in cancer tissue compared to benign prostate tissue, the respective expression values being 0.203 ± 0.09 and 0.146 ± 0.06 (P<0.0005). The hK2 expression in Gradus I-II prostate cancer tissue, 0.211 ± 0.11, was significantly higher than that in benign prostate tissue 0.15 ± 0.07 (P<0.001). The hK2 expression in Gradus III had a similar pattern,
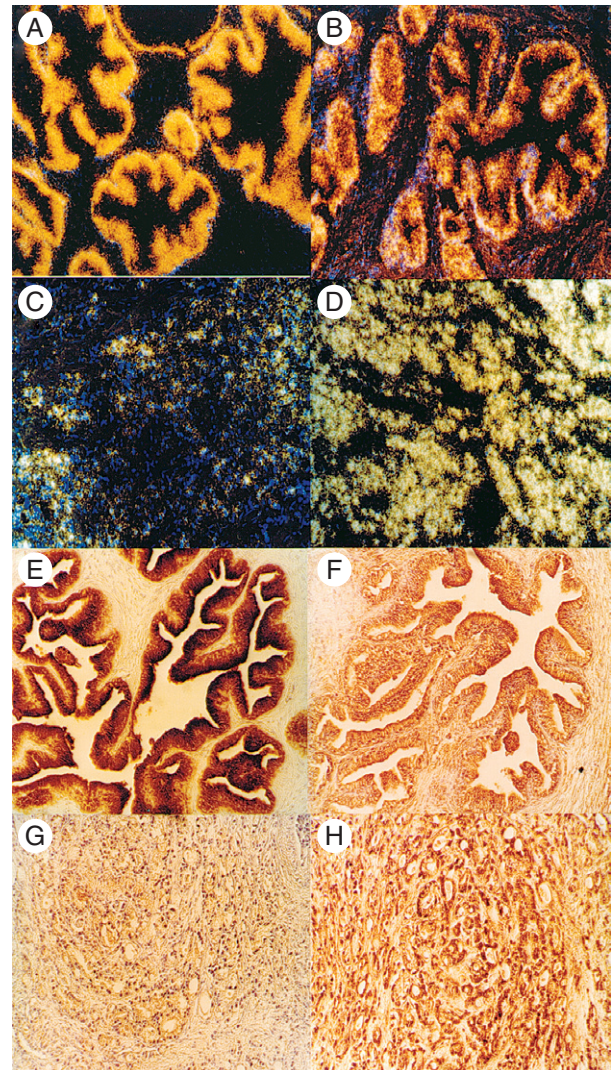
Figure 75 Expressions of hPSA (human prostate specific antigen) and hK2 (human prostate specific glandular kallikrein 2) at the messenger ribonucleic acid (mRNA) and protein levels in tissue samples from patients with benign prostatic hyperplasia (BPH) and prostate carcinoma. The levels of hPSA (**A, C**) and hK2 (**B, D**) mRNA in BPH (**A, B**) and carcinoma (**C, D**) tissue specimens were determined by using an *in situ* hybridization technique. The levels of hPSA (**E, G**) and hK2 (**F, H**) proteins in BPH (**E, F**) and carcinoma (**G, H**) tissue specimens were determined with an immunohistochemical technique. The *in situ* hybridization figures are dark-field microscopic images (magnification 125X). (*Cancer*, 2001, *92*:2975–2984). (Copyright 2001 *Cancer*).

the respective values being 0.19 ± 0.04 and 0.13 ± 0.03 (P<0.006). The hK2 expression in prostate cancer appears to increase along with the degree of malignancy.

The number of hPSA transcripts was higher than that of hK2 in 77.3% of benign tissues, whereas the respective value in cancer tissues was only 33.3%. In BPH tissue, the mean amount of hK2 mRNA was 82% of the respective value of hPSA (p<0.003), whereas in cancer tissue the mean hK2 expression level was 21% higher than that of hPSA (p<0.01). There was a correlation between the hPSA and hK2 mRNA levels in both benign (r=0.735, p<0.01) and malignant (r=0.767, p<0.01) tissues, indicating a possibility for coordinated expression of the genes in both normal and abnormal prostate gland. The liver specimens used as negative control did not exhibit any hybridizing reactivity in *in situ* hybridization, and no signal was detected in immunohistochemistry either. No signal was detected with *in situ* hybridization of sense probes.

The results at the protein level support the findings at the mRNA level: Most cancerous specimens showed a decrease in the hPSA protein content compared to that in benign tissue. Furthermore, an increase of hK2 protein in the cancerous areas compared to the benign areas of the same tissue sections was detected in a majority of the specimens. However, the consistency between the transcript and protein levels in some samples was not clear.

It has been shown that hK2 is more closely related to malignant prostate tumors than hPSA (Darson *et al*., 1997; Henttu *et al*., 1990). The immunoassays developed for hK2 show hK2 concentrations to be only about 1–3% of that of hPSA (Klee *et al*., 1999). We have shown that hK2 exists in two polymorphic forms, Arg^{226}hK2 and Trp^{226}hK2. Arg^{226}hK2 has chymotrypsin-like activity and is very labile when produced as a recombinant protein in insect cells, obviously inactivating itself. Trp^{226}hK2 is inactive (Herrala *et al*., 1997), and we suggest it to be a suitable protein for *in vitro* assay standardization.

The physiologic role of hK2 is unknown. It has been speculated that hK2 is involved in the regulation of hPSA because it has been shown that hK2 can activate the zymogen form of hPSA *in vitro* (Lovgren *et al*., 1997). The report demonstrating the anti-angiogenic activity of hPSA (Fortier *et al*., 1999) enables us to evaluate the results in view of the fact that hK2 is overproduced in prostate cancer tissue to prevent disease progression by activating hPSA. However, the amount of hPSA is decreasing.

We conclude that hK2 is expressed in higher (i.e., up to twofold) amounts in prostate cancer tissue compared to benign prostate tissue specimens for the same patient. The results for hPSA were reversed.

The immunohistochemistry results at the protein level supported the mRNA results. The correlation between the hK2 and hPSA expression levels indicates coordinated expression of the genes in normal and malignant prostate gland. Our results show that hPSA and hK2 give diverse information of prostate cancer development and progression, and that hK2 analysis at the mRNA and protein levels could be useful for the detection of prostate cancer because the increase of hK2 in tissue is cancer-specific.

References

Angerer, L.M., Cox, K.H., and Angerer, R.C. 1987. Demonstration of tissue-specific gene expression by in situ hybridization. *Methods Enzymol. 152*:649–661.

Angerer, L.M., Dolecki, G.J., Gagnon, M.L., Lum, R., Wang, G., Yang, Q., Humphreys, T., and Angerer, R.C. 1989. Progressively restricted expression of a homeo box gene within the aboral ectoderm of developing sea urchin embryos. *Genes Dev. 3*:370–383.

Becker, C., Piironen, T., Kiviniemi, J., Lilja, H., and Petterson, K. 2000. Sensitive and specific immunodetection of human glandular kallikrein 2 in serum. *Clin. Chem. 46*:198–206.

Black, M.H., Magklara, A., Obiezu, C.V., Melegos, D.N., and Diamandis, E.P. 1999. Development of an ultrasensitive immunoassay for human glandular kallikrein with no cross-reactivity from prostate-specific antigen. *Clin. Chem. 45*:790–799.

Blijenberg, B.G., Wildhagen, M.F., Bangma, C.H., Finlay, J.A., Väisänen, V., and Schröder, F.H., 2003. Comparison of two assays for human kallikrein 2. *Clin. Chem. 49*:243–247.

Chisholm, C.D. 1988. TMN classification of urologic tumours in 1988. *Br. J. Urol. 62*:501.

Chotteau-Lelievre, A., Desbiens, A., Pelczar, H., Defossez, P.-A., and de Launoit, Y. 1994. Differential expression patterns of the PEA3 group transcription factors through murine embryonic development. *Oncogene 5*:937–952.

Darson, M.F., Pacelli, A., Roche, P., Rittenhouse, H.G., Wolfert, R.L., Young, C.Y., Klee, G.G., Tindall, D.J., and Bostwick, D.G. 1997. Human glandular kallikrein 2 (hK2) expression in prostatic intraepithelial neoplasm and adenocarcinoma: A novel prosate cancer marker. *Urology 49*:857–862.

Finlay, J.A., Day, J.R., Evans, C.L., Carlson, R., Kuus-Reichel, K., Millar, L.S., Mikolajczyk, S.D., Goodmanson, M., Klee, G.G., and Rittenhouse, H.G. 2001. Development of dual monoclonal antibody immunoassay for total human kallikrein 2. *Clin. Chem. 47*:1218–1224.

Fontaine, B., Sassoon, D., Buckingham, M., and Changeux, J.P. 1988. Detection of the nicotinic acetylcholine receptor alpha-subunit mRNA by in situ hybridization at neuromuscular junctions of 15-day-old chick striated muscles. *EMBO J. 7*:603–609.

Fortier, A.H., Nelson, B.J., Grella, D.K., and Holaday, J.W. 1999. Antiangiogenic activity of prostate-specific antigen. *J. Natl. Cancer Inst. 91*:1635–1640.

Henttu, P., and Vihko, P. 1989. cDNA coding for the entire human prostate specific antigen shows high homologies to the human tissue kallikrein genes. *Biochem. Biophys. Res. Commun. 160*:903–910.

Henttu, P., and Vihko, P. 1994. Prostate-specific antigen and human glandular kallikrein: Two kallikreins of the human prostate. *Ann. Med. 26*:157–164.

Henttu, P., Lukkarinen, O., and Vihko, P. 1990. Expression of the gene coding for human prostate-specific antigen and related hGK-1 in benign and malignant tumors of the human prostate. *Int. J. Cancer 45*:654–660.

Herrala, A., Kurkela, R., Porvari, K., Isomäki, R., Henttu, P., and Vihko, P. 1997. Human prostate-specific glandular kallikrein is expressed as an active and inactive protein. *Clin. Chem. 43*:279–284.

Herrala, A., Porvari, K., Kyllönen, A., and Vihko, P. 2001. Comparison of human prostate specific glandular kallikrein 2 and human prostate specific antigen gene expression in prostate with gene amplification and over-expression of prostate specific glandular kallikrein 2 in tumor tissue. *Cancer 92*:2975–2984.

Kainu, T., Kononen, J., Johansson, O., Olsson, H., Borg, A., and Isola, J. 1996. Detection of germline BRCAI mutations in breast cancer patients by quantitative messenger RNA *in situ* hybridization. *Cancer Res. 56*:2912–2915.

Klee, G.G., Goodmanson, M.K., Jacobsen, S.J., Young, C.Y.F., Finlay, J.A., Rittenhouse, H.G., Wolfert, R.L., and Tindall, D.J. 1999. A highly sensitive automated chemiluminometric assay for measuring free human glandular kallikrein. *Clin. Chem. 45*:800–806.

Lovgren, J., Rajakoski, K., Karp, M., Lundwall, A., and Lilja, H. 1997. Activation of the zymogen form of prostate-specific antigen by human glandular kallikrein 2. *Biochem. Biophys. Res. Commun. 238*:549–555.

Lundwall, Å. 1989. Characterization of the gene for prostate-specific antigen, a human glandular kallikrein. *Biochem. Biophys. Res. Commun. 155*:1151–1159.

Mostofi, F.K. 1980. *Histological Typing of Prostate Tumours.* Geneva: World Heath Organization.

Mustonen, M.V.J., Poutanen, M.H., Kellokumpu, S., de Launoit, Y., Isomaa, V.V., Vihko, R.K., and Vihko, P.T. 1998. Mouse 17β-hydroxysteroid dehydrogenase type 2 mRNA is predominantly expressed in hepatocytes and in surface epithelial cells of the gastrointestinal and urinary tracts. *J. Mol. Endocrinol. 20*:67–74.

Schedlich, L., Bennets, B.H., and Morris, B.J. 1987. Primary structure of human glandular kallikrein gene. *DNA 6*:429–437.

Schmid, P., Schulz, W.A., and Hameister, H. 1989. Dynamic expression patterns of the myc protooncogene in midgestation mouse embryos. *Science 243*:226–229.

Vihko, P., Kurkela, R., Ramberg, J., Pelkonen, I., and Vihko, R. 1990. Time-resolved immunofluorometric assay of human prostate-specific antigen. *Clin. Chem. 36*:92–95.

17

Expression and Gene Copy Number Alterations of HER-2/neu (ERBB2) Gene in Prostate Cancer

Kimmo J. Savinainen and Tapio Visakorpi

Introduction

HER-2/neu gene (*ERBB2*) was initially identified as a transforming gene in chemically induced rat neuroblastomas (Schechter *et al.*, 1984). The gene, located at chromosomal region 17q21, encodes for a 185-kD transmembrane glycoprotein (Popescu *et al.,* 1989) that contains tyrosine kinase activity and belongs to the epidermal growth factor receptor family (Akiyama *et al.*, 1986). The human epidermal growth factor receptor (HER or ERBB) family consists of four distinct members, the epidermal growth factor (EGF) receptor (EGFR or HER-1, HER-2, HER-3, and HER-4). Ligands for this receptor family include EGF; transforming growth factor-α; amphiregulin; betacellulin; heparin-binding EGF-like growth factor; and epiregulin and neuregulins 1, 2, 3, and 4 (Holbro *et al.*, 2003; Sundaresan *et al.*, 1998). Specific ligand for HER-2 is not known, and it is believed that HER-2 is activated following its heterodimerization with another ligand bound HER receptor (Holbro *et al.,* 2003).

HER-2 is amplified and overexpressed in a wide variety of human tumors, mainly from epithelial origin (Scholl *et al.*, 2001). Especially-high amplification frequency, ~20–30%, has been found in breast cancer (Slamon *et al.*, 1989), and the amplification and/or overexpression are associated with poor prognosis

(Reese *et al.*, 1997). The finding of frequent amplification of *HER-2* in breast cancer has led to the development of anti-HER2 antibody, trastuzumab, therapy for breast cancer (Pegram *et al.*, 1999; Slamon *et al.*, 2001). It has now been demonstrated that a combination of trastuzumab with standard chemotherapy leads to a higher response rate and prolonged duration of response and to a lower death rate in metastatic breast cancer. For example, in a randomized trial of 469 women with metastatic breast cancer the median time to disease progression was 7.4 months for patients treated with chemotherapy plus trastuzumab compared to only 4.6 months for patients given chemotherapy alone (Slamon *et al.*, 2001). In addition, Seidman *et al.* (2001) have shown that weekly trastuzumab and paclitaxel therapy is active and relatively well tolerated in women with metastatic breast cancer. However, it seems that only tumors overexpressing the *HER-2* gene respond to trastuzumab (Ross *et al.*, 2003; Seidman *et al.*, 2001; Slamon *et al.*, 2001).

HER-2 Prostate Cancer Cell Lines and Xenografts

The most commonly studied human prostate cancer cell lines are LNCaP, PC-3, and DU-145. Of these,

PC-3 and DU145 are androgen-independent, whereas LNCaP is an androgen-sensitive cell line. The HER-2 protein is detected in all three cell lines (Zhau *et al*., 1992). In PC-3, the immunostaining of this protein is predominantly located at the plasma membrane, whereas cytoplasmic and perinuclear staining are also found in LNCaP and DU-145 cells, respectively. No evidence of *HER-2* gene amplification has been found in the cell lines by Southern Blotting (Zhau *et al*., 1992). We recently compared the expression of *HER-2* between the prostate cancer and breast cancer cell lines by using quantitative real-time reverse transcription polymerase chain reaction (RT-PCR). The expression levels in prostate cancer cell lines were similar to those in the breast cancer cell lines that do not contain *HER-2* gene amplification (Savinainen *et al*., 2002).

HER-2 is also expressed in androgen-independent 22Rv1 prostate cancer cell line. 22Rv1 cell line (Sramkoski *et al*., 1999) is derived from a human prostatic carcinoma xenograft, CWR22R, which has been established from tumors emerging in castrated mice inoculated with parental, androgen-dependent CWR22 xenograft. *HER-2* is expressed at low and similar levels in 22Rv1, CWR22, and CWR22R, suggesting that overexpression of *HER-2* does not drive transition of CWR22 from androgen dependence to independence (Mendoza *et al*., 2002; Sramkoski *et al*., 1999). In contrast, in prostate cancer xenograft models LNCaP and LAPC4, it has been shown that *HER-2* enhances signaling activity of the androgen receptor in the presence of low levels of androgens (Craft *et al*., 1999; Yeh *et al*., 1999). For example, the androgen-independent counterpart of the LAPC4 was shown to express more *HER-2* than the androgen-dependent one. In addition, forced overexpression of *HER-2* in the androgen-dependent cells caused androgen-independent growth in castrated animals. Thus, it was suggested that *HER-2* could be involved in the progression of prostate cancer toward androgen independence (Craft *et al*., 1999).

HER-2 Expression in Clinical Prostate Tumors

Although *HER-2* overexpression has been extensively investigated in prostate cancer, the results have been confusing and its significance has remained unclear. Some studies have reported that HER-2 is overexpressed in prostate cancer based on immunostaining (Gu *et al*., 1996; Myers *et al*., 1994; Signoretti *et al*., 2000), whereas others have not detected overexpression (Reese *et al*., 2001; Savinainen *et al*., 2002;

Visakorpi *et al*., 1992). In the studies that have demonstrated overexpression, the frequency of the tumors showing increased expression has varied from 7% to 100% (Table 12). Some studies have also reported that HER-2 overexpression is associated with advanced clinical stage, high histologic grade, poor prognosis (Fossa *et al*., 2002; Sadasivan *et al*., 1993), and progression toward androgen independence (Signoretti *et al*., 2000). However, not all studies have found such associations.

It seems that the main problem in the evaluation of HER-2 expression is poor reliability and quantitation of the immunostaining (Calvo *et al*., 2003; Sanchez *et al*., 2002). In 2003, Calvo *et al*. reviewed 18 studies, in which 9 different antibodies were used and no clear conclusions were made. We have analyzed untreated primary prostate tumors and metastases as well as hormone-refractory tumors for HER-2 expression by immunostaining using two antibodies, MAb1 and CB11 (Savinainen *et al*., 2002; Visakorpi *et al*., 1992). Our immunostaining protocols have been extensively validated by analyzing breast carcinomas. A strong correlation between positive immunostaining and gene amplification of *HER-2* gene using the protocols has been demonstrated in breast carcinomas (Tanner *et al*., 2000). However, in prostate cancer we have not found overexpression of HER-2 in any tumors stained (Savinainen *et al*., 2002; Visakorpi *et al*., 1992).

Another method to study expression of *HER-2* in clinical small samples is RT-PCR. Recent development of real-time RT-PCR has enabled reliable and quantitative analysis of gene expression (Helenius *et al*., 2001; Linja *et al*., 2001). We have measured the expression of *HER-2* in benign prostate hyperplasia and untreated and hormone-refractory prostate carcinomas by using the real-time RT-PCR (Savinainen *et al*., 2001). We compared the expression levels in prostate tumors and breast carcinomas with or without *HER-2* gene amplification. We found that the expression levels in prostate tumors were about equal to the expression levels in the breast carcinomas without gene amplification. Similar data have been published by Calvo *et al*. (2003).

Amplification of HER-2 Gene in Prostate Cancer

The majority of studies that have analyzed *HER-2* amplification, either by Southern Blotting, chromogenic *in situ* hybridization (CISH), or fluorescence *in situ* hybridization (FISH), show very clearly that

Table 12 Summary of the HER-2 Expression Studies in Prostate Cancer

Author	Year	Method	Tumor Type	Number of Samples	% OE	Comments
Calvo et al.	2003	IHC	AD	50	18	17/50 (1+), 8/50 (2+), and 1/50 (3+)
		IHC	HR	25	0	1/25 (1+)
Calvo et al.	2003	RT-PCR	benign	15	0	
		RT-PCR	AD	19	0	No overexpression in either AD or HR
		RT-PCR	HR	14	0	
Di Lorenzo et al.	2002	IHC	AD	58	36	21/58 (+2 or +3)
		IHC	HR	16	56	9/16 (+2 or +3)
Fossa et al.	2002	IHC	AD	112	37	41/112 showed ERBB2 expression
Jorda et al.	2002	IHC	AD	216	15	31/216 (weak positive; 2+); 2/216 (strong positive; 3+)
Lara et al.	2002	IHC	AD	62	8	4/62 (2+) and 1/62 (3+)
Morris et al.	2002	IHC	AD	84	7	
		IHC	HR	13	0	
		IHC	AD Met.	8	12	
		IHC	HR Met.	12	42	
Sanchez et al.	2002	IHC	AD	38	50	Modified Dako protocol. 10/38 (2+) and 9/38 (3+)
		IHC	AD	38	3	Standard Dako method. 1/38 (2+) and 0/38 (3+)
Savinainen et al.	2002	IHC	AD	54	0	
		IHC	HR	50	0	
		IHC	AD Met.	20	0	
Savinainen et al.	2002	RT-PCR	BPH	5	0	The level of expression was similar in all prostate tumor types
		RT-PCR	AD	21	0	
		RT-PCR	HR	8	0	
Liu et al.	2001	IHC/IF	PIN	6	0	
		IHC/IF	AD	30	0	0% by Dako protocol; 3% by monoclonal antibody
		IHC/IF	Met.	5	20	1/5 (3+) by IHC and IF
Osman et al.	2001	IHC	AD	83	39	32/83 (2+)
		IHC	Met.	20	80	Bone metastases; 10/20 (2+) and 6/20 (3+)
Reese et al.	2001	IHC	HR	39	36	9/39 (1+), 2/39 (2+), 2/39 (3+)
Shi et al.	2001	IHC	AD	31	29	
		IHC	AD	30	50	Short-term androgen ablation therapy before surgery
		IHC	HR	20	85	
Signoretti et al.	2000	IHC	AD	67	25	
		IHC	AD	34	59	Short-term androgen ablation therapy before surgery
		IHC	HR	18	78	
Haussler et al.	1999	IHC	Adenosis	48	2	Moderate/strong 1/48
		IHC	BPH	20	40	Moderate/strong 8/20
		IHC	PIN	30	60	Moderate/strong 20/30
		IHC	AD	38	0	
Morote et al.	1999	IHC	HR	70	64	
Mydlo et al.	1998	IHC	AD	14	0	2 of 13 revealed 20–50% of cells stained
		IHC	HR	3	0	1 of 3 revealed 20–50% of cells stained
Ross et al.	1997b	IHC	AD	113	29	

Table 12 Summary of the HER-2 Expression Studies in Prostate Cancer—cont'd

Author	Year	Method	Tumor Type	Number of Samples	% OE	Comments
Ross *et al.*	1997a	IHC	AD	62	29	
		IHC	PIN	6	17	
Gu *et al.*	1996	IHC	BPH	10	10	1/10 weak and 1/10 moderate
		IHC	AD	39	62	24/39 strong, 10/39 moderate, and 5/39 weak
Fox *et al.*	1994	IHC	AD	45	36	16/45 positively stained
Myers *et al.*	1994	IHC	BPH (basal)	23	100	23/23 moderate to strong
		IHC	BPH (luminal)	23	13	14/23 weak and 3/23 moderate to strong
		IHC	PIN	22	100	Moderate to strong both basal and luminal
		IHC	AD	29	93	2/29 weak and 27/29 moderate to strong
		IHC	AD Met.	16	94	1/16 weak and 15/16 moderate to strong
Veltri *et al.*	1994	IHC	AD	124	78	
Giri *et al.*	1993	IHC	BPH	36	94	34/36 positive stained
		IHC	AD	7	100	Moderate to strong immunoreactivity
Kuhn *et al.*	1993	IHC	BPH	9	0	
		IHC	AD	53	34	18/53 positive staining
Sadasivan *et al.*	1993	IHC	BPH	15	0	
		IHC	AD	25	36	9/25 positive staining
Mellon *et al.*	1992	IHC	BPH	34	18	6/34 positive staining
		IHC	AD	29	21	6/29 strong staining
Visakorpi *et al.*	1992	IHC	BPH	17	0	
		IHC	AD	147	0	11/147 showed low-level immunoreactivity
Zhau *et al.*	1992	IHC/1WB	BPH	6	0	2 by IHC and 4 by WB
		IHC/WB	AD	16	75	12/15 showed positive staining by IHC and 11/16 reacted positively by WB

AD, androgen dependent; BPH, benign prostatic hyperplasia; HR, hormone-refractory; IF, immunofluorescence; IHC, immunohistochemistry; Met, metastasis; OE, overexpression; PIN, prostatic intraepithelial neoplasia; RT-PCR, reverse transcription polymerase chain reaction; WB, Western Blotting.

HER-2 amplification is absent or at least rare in prostate cancer (Bubendorf *et al.*, 1999; Fournier *et al.*, 1995; Savinainen *et al.*, 2002). Approximately 500 prostate carcinomas have been analyzed for gene amplification in these studies (Table 13). For example, we screened 86 androgen-dependent and hormone-refractory prostate tumors for gene amplification by CISH (Savinainen *et al.*, 2001). Only one hormone-refractory tumor showed a borderline amplification (6–8 signals/cell). The tumor, however, did not over-express HER-2 based on immunostaining. Only one research group has reported high-level amplification *HER-2* gene (>5 copies/nucleus) in a substantial fraction of prostate cancer. Ross *et al.* (1997a, 1997b) studied 113 formalin-fixed and paraffin-embedded prostate cancer tumor specimens by FISH and found 5 or more copies of the gene in 41% of samples. Of the same samples, 29% overexpressed HER-2 protein by immunohistochemistry, but there was no correlation between HER-2 protein overexpression and the gene amplification. A few groups have reported low-level amplification of *HER-2* gene in prostate cancer. For example, Liu *et al.* (2001) and Kaltz-Wittmer *et al.* (2000) have reported low-level amplification on *HER-2* in 53% and 30% of cases, respectively. The most likely reasons why some research groups have reported that the *HER-2* gene is amplified in a subset of prostate cancer, whereas most other studies have not demonstrated the amplification, are technical variations and differences in the interpretation of the FISH analyses.

Table 13 Summary of the HER-2 Gene Copy Number Studies in Prostate Cancer

Author	Year	Method	Type	Number of Samples	% Amplification	Comments
Calvo *et al*.	2003	FISH	AD	20	0	
		FISH	HR	19	0	
Lara *et al*.	2002	FISH	AD	7	0	
Savinainen *et al*.	2002	CISH	AD	40	0	14/40 aneuploid, 0/40 high-level amplification
		CISH	AD Met.	14	0	8/14 aneuploid, 0/14 high-level amplification
		CISH	HR	32	3	8/32 aneuploid, 1/32 high-level amplification
Liu *et al*.	2001	FISH	PIN	15	0	
		FISH	AD	30	0	16/30 low-level amplification
		FISH	AD Met.	5	0	4/5 low-level amplification
Osman *et al*.	2001	FISH	AD	66	0	2/66 had ERBB2 amplification
Oxley *et al*.	2001	FISH	AD	114	0	2/114 aneuploid
Reese *et al*.	2001	FISH	HR	36	6	2/36 had ERBB2 amplification
Skacel *et al*.	2001	FISH	AD	39	0	10/39 aneuploid
Kaltz-Wittmer *et al*.	2000	FISH	AD	22	0	
		FISH	HR	63	3	19/63 with low-level amplification
Signoretti *et al*.	2000	FISH	AD/HR/Met.	21	0	All scorable tumor samples together
Bubendorf *et al*.	1999	FISH	BPH	31	0	
		FISH	AD/HR	262	0	All evaluable tumors together
Kallakury *et al*.	1998	FISH	AD	106	42	44/106 amplified tumors
Mark *et al*.	1998	FISH	AD	86	9	1/86 moderate and 7/86 low-level amplified
Ross *et al*.	1997b	FISH	AD	113	41	46/113 amplified tumors
Ross *et al*.	1997a	FISH	AD	62	44	27/62 amplified tumors
		FISH	PIN	6	17	1/6 amplified
Fournier *et al*.	1995	Southern	AD	15	0	
Latil *et al*.	1994	Southern	AD	21	0	
Zhau *et al*.	1992	Southern	AD	10	0	

AD, androgen dependent; BPH, benign prostatic hyperplasia; CISH, chromogenic *in situ* hybridization; FISH, fluorescence *in situ* hybridization; HR, hormone-refractory; Met, metastases; PIN, prostatic intraepithelial neoplasia.

Preclinical and Clinical Trials with Trastuzumab

Using androgen-dependent prostate cancer xenograft models CWR22 and LNCaP, grown in immunodeficient mice, Agus *et al*. (1999) demonstrated 60–90% growth inhibition with trastuzumab. However, no effect of trastuzumab was observed in the androgen-independent tumors. In combination with paclitaxel, however, trastuzumab showed an additive effect on growth in both androgen-dependent and androgen-independent tumors (Agus *et al*., 1999). Small *et al*. (2001) evaluated in a phase I setting safety of trastuzumab with docetaxel and estramustine in patients with prostate cancer with metastatic androgen-independent disease. The regimen was well tolerated, and a more than 50% decrease in prostate specific antigen (PSA) level was found in 9 of 13 patients. In phase II settings, Morris *et al*. (2002) treated 23 patients with trastuzumab alone. The drug showed no effect in the treatment of patients with androgen-independent disease. Presently, no randomized phase III prostate cancer clinical trials with trastuzumab have been published.

In conclusion, *HER-2* has been widely studied in many malignancies, including prostate cancer. However, the role of *HER-2* in prostate cancer

progression has remained unclear. Is *HER-2* gene amplified and does it lead to the protein overexpression? The published reports are contradictory. However, the studies that have used both immunohistochemistry and RT-PCR suggest that *HER-2* is not overexpressed in prostate cancer (Calvo *et al*., 2003; Savinainen *et al*., 2002). As a result of the difficulties to evaluate the expression level of *HER-2*, it has been suggested that detection of gene amplification is more useful. For example, it is now generally accepted that patients with breast cancer who are eligible for trastuzumab treatment should be identified based on gene amplification (Hammock *et al*., 2003; Sauer *et al*., 2003). The vast majority of the studies have shown that *HER-2* is not amplified in prostate cancer. Thus, it is highly unlikely that treatment strategies based on overexpression of *HER-2*, such as administration of trastuzumab, are effective in the treatment of prostate cancer.

The critical question is whether therapies directed against HER-2, which does not require the overexpression of *HER-2*, would be useful in treatment of this malignancy. For example, Agus *et al*. (2002) have demonstrated both *in vitro* and *in vivo* that the growth of several breast and prostate tumor models is inhibited by 2C4 anti-HER-2 monoclonal antibody regardless of the HER-2 expression level. Schwaab *et al*. (2001) have tested that bispecific antibody MDXH210, which has specificity for the non–ligand-binding site of the high-affinity immunoglobulin G receptor (Fc gamma RI) and the extracellular domain of the HER-2, in a phase I setting of patients with prostate cancer. The therapy caused a significant decrease in plasma HER-2 concentration on day 12 of treatment, which remained low throughout the study. No dose-limiting toxic effects were observed. Obviously, the efficacy of the therapy (phase II) needs also to be studied. In addition to antibodies, HER-2 can be targeted by small molecule inhibitors (Christensen *et al*., 2001). Mellinghoff and co-workers (2002) have shown that HER-1/HER-2 tyrosine kinase inhibitor PKI-166 showed profound growth-inhibitory effects on LAPC4 xenograft growth. Whether any of these strategies will be useful in the treatment of prostate cancer remains to be seen.

References

Agus, D.B., Akita, R.W., Fox, W.D., Lewis, G.D., Higgins, B., Pisacane P.I., Lofgren, J.A., Tindell, C., Evans, D.P., Maiese, K., Scher, H.I., and Sliwkowski, M.X. 2002. Targeting ligand-activated ErbB2 signaling inhibits breast and prostate tumor growth. *Cancer Cell 2*:127–137.

Agus, D.B., Scher, H.I., Higgins, B., Fox, W.D., Heller, G., Fazzari, M., Cordon-Cardo, C., and Golde, D.W. 1999. Response of prostate cancer to anti-Her-2/neu antibody in androgen-dependent and -independent human xenograft models. *Cancer Res. 59*:4761–4764.

Akiyama, T., Sudo, C., Ogawara, H., Toyoshima, K., and Yamamoto, T. 1986. The product of the human c-erbB-2 gene: A 185-kilodalton glycoprotein with tyrosine kinase activity. *Science 232*:1644–1646.

Bubendorf, L., Kononen, J., Koivisto, P., Schraml, P., Moch, H., Gasser, T.C., Willi, N., Mihatsch, M.J., Sauter, G., and Kallioniemi, O.P. 1999. Survey of gene amplifications during prostate cancer progression by high-throughout fluorescence in situ hybridization on tissue microarrays. *Cancer Res. 59*:803–806. Erratum in *Cancer Res.* 59:1388.

Calvo, B.F., Levine, A.M., Marcos, M., Collins, Q.F., Iacocca, M.V., Caskey, L.S., Gregory, C.W., Lin, Y., Whang, Y.E., Earp, H.S., and Mohler, J.L. 2003. Human epidermal receptor-2 expression in prostate cancer. *Clin. Cancer Res. 9*:1087–1097.

Christensen, J.G., Schreck, R.E., Chan, E., Wang, X., Yang, C., Liu, L., Cui, J., Sun, L., Wei, J., Cherrington, J.M., and Mendel, D.B. 2001. High levels of HER-2 expression alter the ability of epidermal growth factor receptor (EGFR) family tyrosine kinase inhibitors to inhibit EGFR phosphorylation in vivo. *Clin. Cancer. Res. 7*:4230–4238.

Craft, N., Shostak, Y., Carey, M., and Sawyers, C.L. 1999. A mechanism for hormone-independent prostate cancer through modulation of androgen receptor signaling by the HER-2/neu tyrosine kinase. *Nat. Med. 5*: 280–285.

DiLorenzo, G., Tortora, G., D'Armiento, F.P., De Rosa, G., Staibano, S., Autorino, R., D'Armiento, M., De Laurentiis, M., De Placido, S., Catalano, G., Biano, A.R., and Ciardiello, F. 2002. Expression of epidermal growth factor receptor correlates with disease relapse and progression to androgen-independence in human prostate Cancer. *Clin. Cancer Res. 8*:3438–3444.

Fournier, G., Latil, A., Amet, Y., Abalain, J.H., Volant, A., Mangin, P., Floch, H.H., and Lidereau, R. 1995. Gene amplifications in advanced-stage human prostate cancer. *Urol. Res. 22*:343–347.

Fossa, A., Lilleby, W., Fossa, S.D., Gaudernack, G., Torlakovic, G., and Berner, A. 2002. Independent prognostic significance of HER-2 oncoprotein expression in pN0 prostate cancer undergoing curative radiotherapy. *Int. J. cancer 99*:100–105.

Fox, S.B., Persad, R.A., Coleman, N., Day, C.A., Silcocks, P.B., and Collins, C.C. 1994. Prognostic value of c-erbB-2 and epidermal growth factor receptor in stage A1 (T1a) prostatic adenocarcinoma. *Br. J. Urol. 74*:214–220.

Giri, D.K., Wadhwa, S.N., Upadhaya, S.N., and Talwar, G.P. 1993. Expression of NEU/HER-2 oncoprotein (p185neu) in prostate tumors: An immunohistochemical study. *Prostate 23*:329–336.

Gu, K., Mes-Masson, A.M., Gauthier, J., and Saad, F. 1996. Overexpression of her-2/neu in human prostate cancer and benign hyperplasia. *Cancer Lett. 99*:185–189.

Hammock, L., Lewis, M., Phillips, C., and Cohen, C. 2003. Strong HER-2/neu protein overexpression by immunohistochemistry often does not predict oncogene amplification by fluorescence in situ hybridization. *Hum. Pathol. 34*:1043–1047.

Haussler, O., Epstein, J.I., Amin, M.B., Heitz, P.U., and Hailemariam, S. 1999. Cell proliferation, apoptosis, oncogene, and tumor suppressor gene status in adenosis with comparison to benign prostatic hyperplasia, prostatic intraepithelial neoplasia, and cancer. *Hum. Pathol. 30*:1077–1086.

Helenius, M.A., Saramaki, O.R., Linja, M.J., Tammela, T.L., and Visakorpi, T. 2001. Amplification of urokinase gene in prostate cancer. *Cancer Res. 61*:5340–5344.

Holbro, T., Civenni, G., and Hynes, N.E. 2003. The ErbB receptors and their role in cancer progression. *Exp. Cell. Res. 284*:99–110.

Jorda, M., Morales, A., Ghorab, Z., Fernandez, G., Nadji, M., and Block, N. 2002. Her2 expression in prostatic cancer: A comparison with mammary carcinoma. *J. Urol. 168*:1412–1414.

Kallakury, B.V., Sheehan, C.E., Ambros, R.A., Fisher, H.A., Kaufman, R.P. Jr., Muraca, P.J., and Ross, J.S. 1998. Correlation of p34cdc2 cyclin-dependent kinase overexpression, CD44s downregulation, and HER-2/neu oncogene amplification with recurrence in prostatic adenocarcinomas. *J. Clin. Oncol. 16*:1302–1309.

Kaltz-Wittmer, C., Klenk, U., Glaessgen, A., Aust, D.E., Diebold, J., Lohrs, U., and Baretton, G.B. 2000. FISH analysis of gene aberrations (MYC, CCND1, ERBB2, RB, and AR) in advanced prostatic carcinomas before and after androgen deprivation therapy. *Lab. Invest. 80*:1455–1464.

Kuhn, E.J., Kurnot, R.A., Sesterhenn, I.A., Chang, E.H., and Moul, J.W. 1993. Expression of the c-erbB-2 (HER-2/neu) oncoprotein in human prostatic carcinoma. *J. Urol. 150*:1427–1433.

Lara, P.N. Jr., Meyers, F.J., Gray, C.R., Edwards, R.G., Gumerlock, P.H., Kauderer C., Tichauer, G., Twardowski, P., Doroshow, J.H., and Gandara, D.R. 2002. HER-2/neu is overexpressed infrequently in patients with prostate carcinoma. Results from the California Cancer Consortium Screening Trial. *Cancer 94*:2584–2589.

Latil, A., Baron, J.C., Cussenot, O., Fournier, G., Boccon-Gibod, L., Le Duc, A., and Lidereau, R. 1994. Oncogene amplifications in early-stage human prostate carcinomas. *Int. J. Cancer 59*:637–638.

Linja, M.J., Savinainen, K.J., Saramaki, O.R., Tammela, T.L., Vessella, R.L., and Visakorpi, T. 2001. Amplification and overexpression of androgen receptor gene in hormone-refractory prostate cancer. *Cancer Res. 61*:3550–3555.

Liu, H.L., Gandour-Edwards, R., Lara, P.N. Jr., de Vere White, R., and LaSalle, J.M. 2001. Detection of low level HER-2/neu gene amplification in prostate cancer by fluorescence in situ hybridization. *Cancer J. 7*:395–403.

Mark, H.F., Feldman, D., Das, S., Kye, H., Mark, S., Sun, C.L., and Samy, M. 1999. Fluorescence in situ hybridization study of HER-2/neu oncogene amplification in prostate cancer. *Exp. Mol. Pathol. 66*:170–178.

Mellinghoff, I.K., Tran, C., and Sawyers, C.L. 2002. Growth inhibitory effects of the dual ErbB1/ErbB2 tyrosine kinase inhibitor PKI-166 on human prostate cancer xenografts. *Cancer Res. 62*:5254–5259.

Mellon, K., Thompson, S., Charlton, R.G., Marsh, C., Robinson, M., Lane, D.P., Harris, A.L., Horne, C.H., and Neal, D.E. 1992. p53, c-erbB-2 and the epidermal growth factor receptor in the benign and malignant prostate. *J. Urol. 147*:496–499.

Mendoza, N., Phillips, G.L., Silva, J., Schwall, R., and Wickramasinghe, D. 2002. Inhibition of ligand-mediated HER2 activation in androgen-independent prostate cancer. *Cancer Res. 62*:5485–5488.

Morote, J., de Torres, I., Caceres, C., Vallejo, C., Schwartz, S. Jr., and Reventos, J. 1999. Prognostic value of immunohistochemical expression of the c-erbB-2 oncoprotein in metastasic prostate cancer. *Int. J. Cancer 84*:421–425.

Morris, M.J., Reuter, V.E., Kelly, W.K., Slovin, S.F., Kenneson, K., Verbel, D., Osman, I., and Scher, H.I. 2002. HER-2 profiling and targeting in prostate carcinoma. *Cancer 94*:980–986.

Mydlo, J.H., Kral, J.G., Volpe, M., Axotis, C., Macchia, R.J., and Pertschuk, L.P. 1998. An analysis of microvessel density, androgen receptor, p53 and HER-2/neu expression and Gleason score in prostate cancer. Preliminary results and therapeutic implications. *Eur. Urol. 34*:426–432.

Myers, R.B., Srivastava, S., Oelschlager, D.K., and Grizzle, W.E. 1994. Expression of p160erbB-3 and p185erbB-2 in prostatic intraepithelial neoplasia and prostatic adenocarcinoma. *J. Natl. Cancer Inst. 86*:1140–1145.

Osman, I., Scher, H.I., Drobnjak, M., Verbel, D., Morris, M., Agus, D., Ross, J.S., and Cordon-Cardo, C. 2001. HER-2/neu (p185neu) protein expression in the natural or treated history of prostate cancer. *Clin. Cancer Res. 7*:2643–7.

Oxley, J.D., Winkler, M.H., Gillatt, D.A., and Peat, D.S. 2002. Her-2/neu oncogene amplification in clinically localized prostate cancer. *J. Clin. Pathol. 55*:118–120.

Pegram, M.D., and Slamon, D.J. 1999. Combination therapy with trastuzumab (Herceptin) and cisplatin for chemoresistant metastatic breast cancer: Evidence for receptor-enhanced chemosensitivity. *Semin. Oncol. 26*:89–95.

Popescu, N.C., King, C.R., and Kraus, M.H. 1989. Localization of the human erbB-2 gene on normal and rearranged chromosomes 17 to bands q12-21.32. *Genomics 4*:362–366.

Reese, D.M., Small, E.J., Magrane, G., Waldman, F.M., Chew, K., and Sudilovsky, D. 2001. HER2 protein expression and gene amplification in androgen-independent prostate cancer. *Am. J. Clin. Pathol. 116*:234–239.

Reese, D.M., and Slamon, D.J. 1997. HER-2/neu signal transduction in human breast and ovarian cancer. *Stem. Cells 15*:1–8.

Ross, J.S., Fletcher, J. A., Linette, G.P., Stec, J., Clark, E., Ayers, M., Symmans, W.F., Pusztai, L., and Bloom, K.J. 2003. The Her-2/neu gene and protein in breast cancer 2003: Biomarker and target of therapy. *Oncologist 8*:307–325.

Ross, J.S., Sheehan, C., Hayner-Buchan, A.M., Ambros, R.A., Kallakury, B.V., Kaufman, R., Fisher, H.A., and Muraca, P.J. 1997a. HER-2/neu gene amplification status in prostate cancer by fluorescence in situ hybridization *Hum. Pathol. 28*:827–833.

Ross, J.S., Sheehan, C.E., Hayner-Buchan, A.M., Ambros, R.A., Kallakury, B.V., Kaufman, R.P. Jr., Fisher, H.A., Rifkin, M.D., and Muraca, P.J. 1997b. Prognostic significance of HER-2/neu gene amplification status by fluorescence in situ hybridization of prostate carcinoma. *Cancer 79*:2162–2170.

Sadasivan, R., Morgan, R., Jennings, S., Austenfeld, M., Van Veldhuizen, P., Stephens, R., and Noble, M. 1993. Overexpression of Her-2/neu may be an indicator of poor prognosis in prostate cancer. *J. Urol. 150*:126–131.

Sanchez, K.M., Sweeney, C.J., Mass, R., Koch, M.O., Eckert, G.J., Geary, W.A. Baldridge, L.A., Zhang, S., Eble, J.N., and Cheng, L. 2002. Evaluation of HER-2/neu expression in prostatic adenocarcinoma: A requested for a standardized, organ specific methodology. *Cancer 95*:1650–1655.

Sauer, T., Wiedswang, G., Boudjema, G., Christensen, H., and Karesen, R. 2003. Assessment of HER-2/neu overexpression and/or gene amplification in breast carcinomas: Should in situ hybridization be the method of choice? APMIS *111*:444–450.

Savinainen, K.J., Saramaki, O.R., Linja, M.J., Bratt, O., Tammela, T.L., Isola, J.J., and Visakorpi, T. 2002. Expression and gene copy number analysis of ERBB2 oncogene in prostate cancer. *Am. J. Pathol. 160*:339–345.

Schechter, A.L., Stern, D.F., Vaidyanathan, L., Decker, S.J., Drebin, J.A., Greene, M.I., and Weinberg, R.A. 1984. The neu oncogene: An erb-B-related gene encoding a 185,000-Mr tumour antigen. *Nature 312*:513–516.

Scholl, S., Beuzeboc, P., and Pouillart, P. 2001. Targeting HER2 in other tumor types. *Ann. Oncol. 12 Suppl 1*:S81–S87.

Schwaab, T., Lewis, L.D., Cole, B.F., Deo, Y., Fanger, M.W., Wallace, P., Guyre, P.M., Kaufman, P.A., Heaney, J.A., Schned, A.R., Harris, R.D., and Ernstoff, M.S. 2001. Phase I pilot trial of the bispecific antibody MDXH210 (anti-Fc gamma RI X anti-HER-2/neu) in patients whose prostate cancer overexpresses HER-2/neu. *J. Immunother. 24*:79–87.

Seidman, A.D., Fornier, M.N., Esteva, F.J., Tan, L., Kaptain, S., Bach, A., Panageas, K.S., Arroyo, C., Valero, V., Currie, V., Gilewski, T., Theodoulou, M., Moynahan, M.E., Moasser, M., Sklarin, N., Dickler, M., D'Andrea, G., Cristofanilli, M., Rivera, E., Hortobagyi, G.N., Norton, L., and Hudis, C.A. 2001. Weekly trastuzumab and paclitaxel therapy for metastatic breast cancer with analysis of efficacy by HER2 immunophenotype and gene amplification. *J. Clin. Oncol. 19*:2587–2595.

Shi, Y., Brands, F.H., Chatterjee, S., Feng, A.C., Groshen, S., Schewe, J., Lieskovsky, G., and Cote, R.J. 2001. Her-2/neu expression in prostate cancer: High level of expression associated with exposure to hormone therapy and androgen independent disease. *J. Urol. 166*:1514–1519.

Signoretti, S., Montironi, R., Manola, J., Altimari, A., Tam, C., Bubley, G., Balk, S., Thomas, G., Kaplan, I., Hlatky, L., Hahnfeldt, P., Kantoff, P., and Loda, M. 2000. Her-2-neu expression and progression toward androgen independence in human prostate cancer. *J. Natl. Cancer Inst. 92*:1918–1925.

Skacel, M., Ormsby, A.H., Pettay, J.D., Tsiftsakis, E.K., Liou, L.S., Klein, E.A., Levin, H.S., Zippe, C.D., and Tubbs, R.R. 2001. Aneusomy of chromosomes 7, 8, and 17 and amplification of HER-2/neu and epidermal growth factor receptor in Gleason score 7 prostate carcinoma: A differential fluorescent in situ hybridization study of Gleason pattern 3 and 4 using tissue microarray. *Hum. Pathol. 32*:1392–1397.

Slamon, D.J., Godolphin, W., Jones, L.A., Holt, J.A., Wong, S.G., Keith, D.E., Levin, W.J., Stuart, S.G., Udove, J., Ullrich, A., and Press, M. F. 1989. Studies of the HER-2/neu proto-oncogene in human breast and ovarian cancer. *Science 244*:707–712.

Slamon, D.J., Leyland-Jones, B., Shak, S., Fuchs, H., Paton, V., Bajamonde, A., Fleming, T., Eiermann, W., Wolter, J., Pegram, M., Baselga, J., and Norton, L. 2001. Use of chemotherapy plus a monoclonal antibody against HER2 for metastatic breast cancer that overexpresses HER2. *New Engl. J. Med 344*:783–792.

Small, E.J., Bok, R., Reese, D.M., Sudilovsky, D., and Frohlich, M. 2001. Docetaxel, estramustine, plus trastuzumab in patients with metastatic androgen-independent prostate cancer. *Semin. Oncol. 28 (4 Suppl 15)*:71–76.

Sramkoski, R.M., Pretlow, T.G. 2nd, Giaconia, J.M., Pretlow, T.P., Schwartz, S., Sy M.S., Marengo, S.R., Rhim, J.S., Zhang, D., and Jacobberger, J.W. 1999. A new human prostate carcinoma cell line, 22Rv1. *In Vitro Cell. Dev. Biol. Anim. 35*:403–409.

Sundaresan, S., Roberts, P.E., King, K.L., Sliwkowski, M.X., and Mather, J.P. 1998. Biological response to ErbB ligands in non-transformed cell lines correlates with a specific pattern of receptor expression. *Endocrinology 139*:4756–4764.

Tanner, M., Gancberg, D., Di Leo, A., Larsimont, D., Rouas, G., Piccart, M.J., and Isola, J. 2000. chromogenic in situ hybridization: A practical alternative for fluorescence in situ hybridization to detect HER-2/neu oncogene amplification in archival breast cancer samples. *Am. J. Pathol. 157*:1467–1472.

Visakorpi, T., Kallioniemi, O.P., Koivula, T., Harvey, J., and Isola, J. 1992. Expression of epidermal growth factor receptor and ERBB2 (HER-2/Neu) oncoprotein in prostatic carcinomas. *Mod. Pathol. 5*:643–648.

Veltri, R.W., Partin, A.W., Epstein, J.E., Marley, G.M., Miller, C.M., Singer, D.S., Patton, K.P., Criley, S.R., and Coffey, D.S. 1994. Quantitative nuclear morphometry, Markovian texture descriptors, and DNA content captured on a CAS-200 Image analysis system, combined with PCNA and HER-2/neu immunohistochemistry for prediction of prostate cancer progression. *J. Cell Biochem. Suppl. 19*:249–258.

Yeh, S., Lin, H.K., Kang, H.Y., Thin, T.H., Lin, M.F., and Chang, C. 1999. From HER2/Neu signal cascade to androgen receptor and its coactivators: A novel pathway by induction of androgen target genes through MAP kinase in prostate cancer cells. *Proc. Natl. Acad. Sci. U S A 96*:5458–5463.

Zhau, H.E., Wan, D.S., Zhou, J., Miller, G.J., and von Eschenbach, A.C. 1992. Expression of c-erbB-2/neu proto-oncogene in human prostatic cancer tissues and cell lines. *Mol. Carcinog. 5*:320–327.

18

Combined Detection of Low Level HER-2/neu Expression and Gene Amplification in Prostate Cancer by Immunofluorescence and Fluorescence *in situ* Hybridization

Regina Gandour-Edwards and Janine LaSalle

Introduction

The *HER-2/neu* oncogene, located on chromosome 17q21, encodes a transmembrane tyrosine kinase receptor analogous to epidermal growth factor receptor (EGFR) (Schecter *et al.*, 1985). The receptor's role in oncogenesis can be derived from its action on cellular cascades involving proliferation and differentiation of epithelial cells. For instance, *HER-2/neu* induces metastatic capacity *in vitro* when transfected into a prostatic epithelial cell line (Zhau *et al.*, 1996). In human breast cancers, 20–30% of tumors demonstrate overexpression of the *HER-2/neu* protein, correlating with poor survival and recurrence (Jacobs *et al.*, 1999; Slamon *et al.*, 1989). *HER-2/neu* protein overexpression is not common in normal tissue but has been found in a variety of epithelial cancers, including bladder, prostate, ovarian, endometrial, gastric, and salivary

gland carcinomas (Moriyama *et al.*, 1991; Press *et al.*, 1997; Press *et al.*, 1994a; Ranzani *et al.*, 1990; Ross *et al.*, 1993; Saffari *et al.*, 1995; Zhau *et al.*, 1990).

To date, methods for detecting oncogene amplification and protein overexpression of *HER-2/neu* in epithelial cancers have shown variable results. Studies analyzing *HER-2/neu* overexpression by immunohistochemistry (IHC) have used a wide range of different antibodies, which result in either membrane or cytoplasmic localization (Morote *et al.*, 1999; Ross *et al.*, 1997). In breast cancer samples, *HER-2/neu* oncogene amplification by fluorescence *in situ* hybridization (FISH) has shown reasonable rates of concordance with IHC (Press *et al.*, 1994b). Pauletti *et al.* (1996) found that only 3% of breast cancer cases demonstrated overexpression of *HER-2/neu* protein without gene amplification identified by FISH.

Handbook of Immunohistochemistry and *in situ* Hybridization of Human Carcinomas,
Volume 2: Molecular Pathology, Colorectal Carcinoma, and Prostate Carcinoma

457
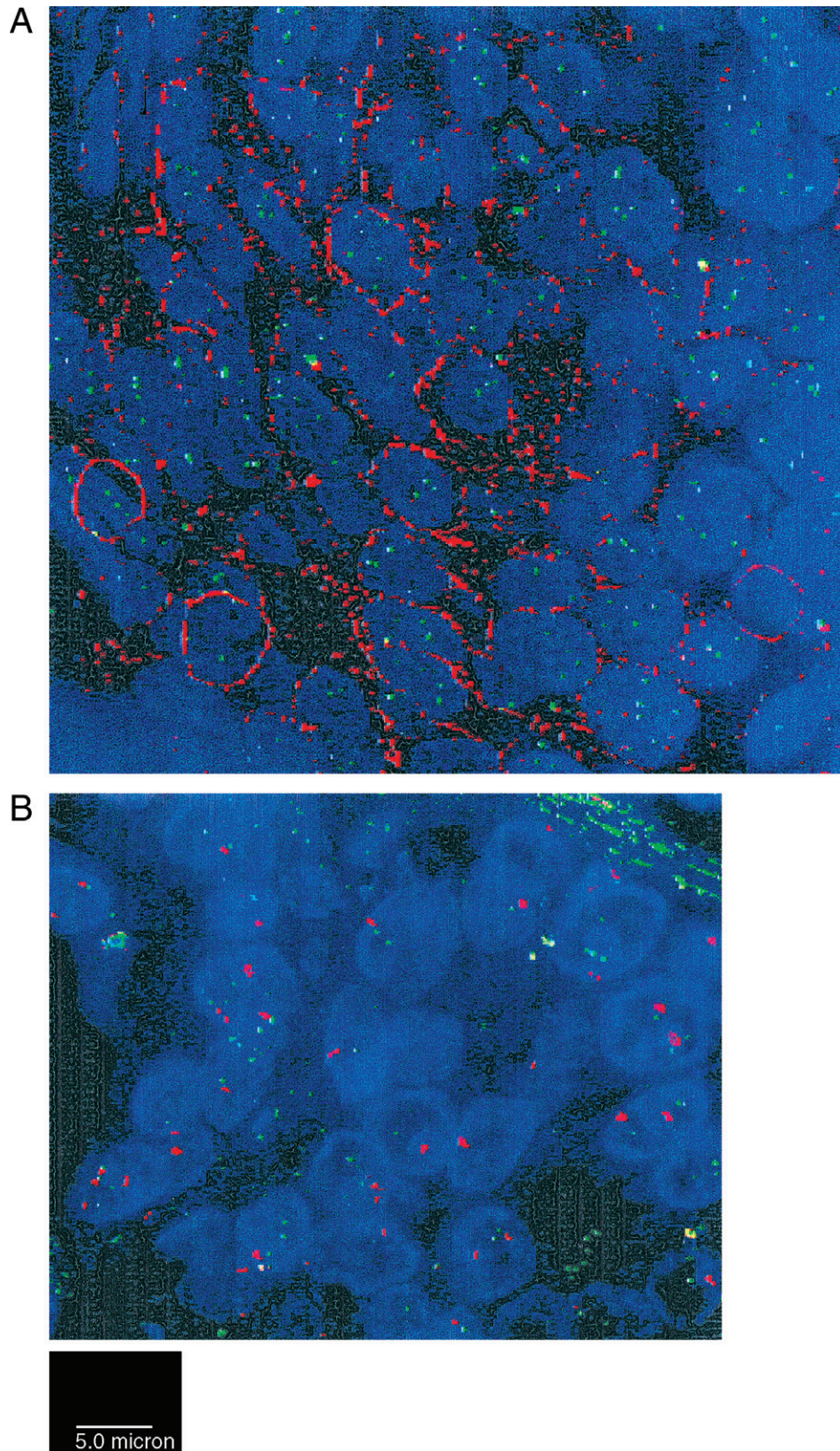
Figure 76 A: Combined detection of *HER-2/neu* amplification and overexpression by fluorescence *in situ* hybridization (FISH) and immuno-
fluorescence (IF). Lymph node tissue from metastasized prostate cancer showing the presence of membrane surface expression of *HER-2/neu*
(red fluorescence) and gene amplification by FISH *(green fluorescence)*. Blue fluorescence represents nuclei counterstained with DAPI.

MATERIALS

1. Paraffin sections of formalin-fixed human tumor tissue. Four micron–thick sections on coated "Plus" slides (Shandon-Lipshaw, Pittsburgh, PA).
2. Glass coplin jars (at least 4).
3. Xylene.
4. 50%, 70%, 90%, and 100% ethanol.
5. Temperature controlled slide block (Hybaid, Franklin, MA).
6. Dako hercep Test.
7. Dulbecco's phosphate buffer saline (PBS), 10X stock.
8. Blocking solution: 1X PBS, 10% fetal calf serum.
9. Wash solution: 1X PBS, 0.05% Tween-20.
10. Texas red goat anti-rabbit immunoglobulin (Molecular Probes, Eugene, OR).
11. Histochoice (Ameresco, Solon, OH).
12. SpectrumGreen labeled *HER-2/neu* DNA probe, SpectrumOrange labeled CEP17 probe (Vysis, Downer's Grove, IL).
13. Cover glasses, 18×18 mm and 20×30 mm.
14. Rubber cement.
15. Saline-sodium citrate (SSC), 20X stock.
16. Wash A: 2X SSC.
17. Wash B: 0.4X SSC, 0.3% Igepal.
18. Wash C: 2X SSC, 0.1% Igepal.
19. Mounting media: Vectashield (Vector Laboratories, Burlingame, CA), 1 g/ml DAPI (Molecular Probes, Eugene, OR).
20. Nail polish.

METHOD

Combined FISH and Immunofluorescence for *HER-2/neu*

1. Heat slides overnight at 56ºC on slide block.
2. Deparaffinize in xylene through 4 washes of 5 min in coplin jars under chemical hood with constant agitation.

3. Dehydrate with two 100% ethanol washes of 5 min each.
4. Dry slides for 5 min on 50ºC slide block.
5. In chemical hood, heat waterbath to 95–99ºC and immerse a coplin jar containing 1X antigen retrieval solution from Dako Hercep Test kit.
6. Place slides in coplin jar and incubate for 40 min.
7. Allow jar and slides to equilibrate to room temperature for 20 min.
8. Incubate slides with 200 µl of blocking solution, cover with a 20×50 mm coverslip, and incubate for 20 min at 37ºC in a humid chamber.
9. Remove coverslip and drain excess liquid.
10. Add 200 µl of a 1:100 dilution of the Dako anti-HER-2 primary antibody, cover with a 20×50 mm coverslip, and incubate 30 min at 37ºC in a humid chamber.
11. Wash in 1X PBS/0.05% Tween-20, 3 times for 5 min each.
12. Incubate slides with 200 µl of a 1:50 dilution of Texas red goat anti-rabbit immunoglobin in PBS, cover with a 20×50 mm coverslip, and incubate 30 min at 37ºC in a humid chamber.
13. Wash in 1X PBS/0.05% Tween-20, 3 times for 5 min.
14. Counterstain with 30 µl of 1 µg/ml of DAPI in Vectashield mounting media, and coverslip with a 20×30 mm glass.
15. Analyze by fluorescence microscopy for membrane staining of the HER-2 protein.
16. Wash slides 1X in PBS with agitation to gently remove coverslips.
17. Post-fix in Histochoice for 60 min.
18. Wash in 1X PBS for 5 min.
19. Dehydrate in 50%, 70%, 90%, and 100% ethanol for 5 min each.
20. Air-dry slides in darkness.
21. Add 10 µl of hybridization solution per slide, containing 7 µl hybridization solution (supplied with probe), 1 µl SpectrumGreen *HER-2/neu* probe, and 2 µl distilled water.

Figure 76—cont'd B: To assess the ploidy of chromosome 17 in addition to *HER-2/neu*, FISH was performed with a CEP 17 SpectrumOrange probe *(red fluorescence)* in addition to the *HER-2/neu* probe *(green fluorescence)*. Prostate cancer sample showing low copy number *HER-2/neu* amplification (2–4 spots per nucleus) compared to CEP 17 (1–2 spots per nucleus). Slides were analyzed on an Axioplan 2 fluorescence microscope (Carl Zeiss, Inc, NY) equipped with a Sensys CCD camera (Photometrics, Tucson, AZ), appropriate fluorescent filter sets, and automated xyz stage controls. The microscope and peripherals are controlled by a Macintosh Power Mac 9600/400 running IPLab Spectrum (Scanalytics, Vienna, VA) software with Multiprobe, Zeissmover, and three-dimensional extensions. Images were captured for blue, green, and red filters at one edge of the specimen and then repeated at 0.4 micron sections through the depth of the tissue (3–5 microns). Out-of-focus light was removed using HazeBuster software (Vaytek, Fairfield, IA). Image stacks for each fluorophore were merged and stacked to create a two-dimensional image representing all of fluorescence within the section.

22. Cover with a 18 × 18 mm coverslip, and seal with rubber cement.

23. On Hybaid or temperature-controlled heat block, denature slides for 85ºC for 1 min.

24. Hybridize in humid chamber for 4 hr to overnight at 37ºC.

25. Preheat Wash A solution (2X SSC) to 73 ± 1°C in waterbath.

26. Gently remove rubber cement, taking care not to disturb coverslips.

27. Immerse slides in 2X SSC and agitate to allow removal of coverslips.

28. Once coverslips have detached, immediately immerse slides in 73 ± 1ºC Wash A (2X SSC) for 2 min (time exactly from last slide immersed).

29. Immerse slides in Wash C solution (2X SSC, 0.1% Igepal) at room temperature for 1 min with agitation.

30. Blot excess liquid and air-dry slides in darkness.

31. Add 20 µl of mounting media per slide, cover with 18 × 18 mm coverslip, and seal with nail polish.

32. Analyze by fluorescent microscopy with appropriate filter sets for blue, green, and red fluorescence or by wide-field fluorescent microscopy and image analysis as in Figure 76A.

Dual FISH for HER-2/neu and Chromosome 17

1. Heat slides overnight at 56ºC on slide block.

2. Deparaffinize in xylene through 4 washes of 5 min in coplin jars under chemical hood with constant agitation.

3. Dehydrate with two 100% ethanol washes of 5 min each.

4. Dry slides for 5 min on 50ºC slide block.

5. In chemical hood, heat waterbath to 95–99ºC and immerse a coplin jar containing 1X antigen retrieval solution from Dako Hercep Test kit.

6. Place slides in coplin jar and incubate for 40 min.

7. Allow jar and slides to equilibrate to room temperature for 20 min.

8. Post-fix in Histochoice for 60 min.

9. Wash in 1X PBS for 5 min.

10. Dehydrate in 50%, 70%, 90%, and 100% ethanol for 5 min each.

11. Air-dry slides in darkness.

12. Add 10 µl of hybridization solution per slide, containing 7 I hybridization solution (supplied with probe), 1 µl distilled water.

13. Cover with a 18 × 18 mm coverslip, and seal with rubber cement.

14. On Hybaid or temperature-controlled heat block, denature slides for 85ºC for 1 min.

15. Hybridize in humid chamber for 4 hr to overnight at 37ºC.

16. Preheat Wash A solution (2X SSC) to 73 ± 1ºC in waterbath.

17. Gently remove rubber cement, taking care not to disturb coverslip.

18. Immerse slides in 2X SSC and agitate to allow removal of coverslips.

19. Once coverslips have detached, immediately immerse slides in 73 ± 1ºC Wash A (2X SSC) for 2 min (time exactly from last slide immersed).

20. Immerse slides in Wash C solution (2X SSC, 0.1% lgepal) at room temperature for 1 min with agitation.

21. Blot excess liquid and air-dry slides in darkness.

22. Add 20 µl of mounting media per slide, cover with 18 × 18 mm coverslip, and seal with nail polish.

23. Analyze by fluorescent microscopy with appropriate filter sets for blue, green, and red fluorescence or by wide-field fluorescent microscopy and image analysis as in Figure 76B.

FISH Amplification Scoring

1. Identify 100 prostate cancer cells by morphology.

2. Count *HER-2/neu* FISH (green) signals in each cancer cell.

3. Count at least 20 cells from surrounding normal prostate tissue to ensure efficient hybridization (2 signals/ nucleus should be observed in >80% of cells).

4. Score individual cells within each tissue as being diploid (two FISH signals per nucleus) or amplified (three or more FISH signals per nucleus) for *HER-2/neu*.

5. Record the range of *HER-2/neu* gene copy number for each sample.

6. For the CEP 17 plus *HER-2/neu* FISH slides, each cell was scored as follows:
   a. Amplified for *HER-2/neu* and diploid for CEP 17.
   b. Amplified for *HER-2/neu* and aneuploid for CEP 17 with copy numbers of each DNA probe equal.
   c. Amplified for *HER-2/neu* and aneuploid for CEP 17 with *HER-2/neu* gene copy number greater than CEP 17 copy number.
   d. Nonamplified for *HER-2/neu* and diploid for CEP 17.

RESULTS AND DISCUSSION

Our study compared FISH and IHC in determining the amplification and overexpression, respectively, of *HER-2/neu* in prostate cancer. In addition, we directly compared the *HER-2/neu* overexpression and gene amplification by combining immunofluorescence (IF) and FISH on the same tissue section. This novel method allows the direct comparison of gene amplification and protein overexpression on the same tissue section. Using this approach, we demonstrated discordance between the two methods and concluded that FISH can detect low level *HER-2/neu* amplification in prostate cancer specimens that do not overexpress *HER-2/neu* by IHC (Liu *et al*., 2001).

A recent clinical trial administered TRAS, a humanized monoclonal antibody to the *HER-2/neu* receptor, to patients with prostate cancer. However, infrequent expression of *HER-2/neu* was found in archival samples by IHC, FISH, or shed HER-2 antigen in serum (Lara *et al*., 2002), but the trial closed for nonfeasibility (Chee *et al*., 2003). Despite the results to date with *HER-2/neu* in prostate cancer, the methods outlined here are expected to be useful in analyzing *HER-2/neu* gene amplification and overexpression in other human cancers or for other relevant oncogenes (see also Part III, Chapter 17, in this volume).

References

Chee, K., Lara, P.N., Longmate, J., Meyers, F.J., Gray, C.R., Gandour-Edwards, R., Gumerlock, P.H., Twardowski, P., McNamara, M., Doroshow, J.H., and Gandara, D.R. 2003. TRAS and DOC in HER-2 (+) hormone refractory prostate cancer (HPRC): A California cancer consortium screening and phase II trial. *Am. Soc. Clin. Oncol.* Presentation.

Jacobs, T.W., Gown, A.M., Yaziji, H., Barnes, M.J., and Schnitt, S.J. 1999. Comparison of fluorescent in situ hybridization and immunohistochemistry for the evaluation of *HER-2/neu* in breast cancer. *J. Clin. Oncol. 17*:3690–3692.

Lara, P.N., Gray, C.R., Gandour-Edwards, R., Meyers, F.J., Gumerlock, P.H., Kauderer, C., Tichauer, G., Doroshow, J.H., and Gandara, D.R. *HER-2/neu* is infrequently overexpressed in prostate cancer: Results form the California Cancer Consortium screening trial. *Cancer 94*:2584–2589.

Liu, H.L., Gandour-Edwards, R., Lara, P.N., deVere-White, R., and LaSalle, J.M. 2001. Detection of low level *HER-2/neu* gene amplification in prostate cancer by fluorescent in situ hybridization (FISH). *Cancer J. 7*:395–403.

Moriyama, M., Akiyama, T., Yamamoto, T., Kawamoto, T., Kato, T., Sato, K., Watanuki, T., Hikage, T., Katsuta, N., and Mori, S. 1991. Expression of *c-erbB-2* gene product in urinary bladder cancer. *J. Urol. 45*:423–427.

Morote, J., de Torres, I., Caceres, C., Vallejo, C., Schwartz, S. Jr., and Reventos, J. 1999. Prognostic value of immunohistochemical expression of the *c-erbB-2* oncoprotein in metastatic prostate cancer. *Int. J. Cancer 84*:421–425.

Pauletti, G., Godolphin, W., Press, M.F., and Slamon, D.J. 1996. Detection and quantitation of *HER-2/neu* gene amplification in human breast cancer archival material using fluorescence in situ hybridization. *Oncogene 13*:63–72.

Press, M.F., Bernstein, L., Thomas, P.A., Meiner, L.F., Zhou, J.Y., Ma, Y., Hung, G., Robinson, R.A., Harris, C., E1-Naggar, A., Slamon, D.J., Phillips, R.N., Ross, J.S., Wolman, S.R., and Flom, K.J. 1997. *HER-2/neu* gene amplification characterized by fluorescence in situ hybridization: Poor prognosis in node-negative breast carcinomas. *J. Clin. Oncol. 715*: 2894–2904.

Press, M.F., Hung, G., Godolphin, W., and Slamon, D.J. 1994b. Sensitivity of *HER-2/neu* antibodies in archival tissue samples: Potential source of error in immunohistochemical studies of oncogene expression. *Cancer Res. 54*:2771–2777.

Press, M.F., Pike, M.C., Hung, G., Zhou, J.Y., Ma, Y., George, J., Dietz-Band, J., James, W., Slamon, D.J., and Batsakis, J.G. 1994a. Amplification and overexpression gene copy number of *HER-2/neu* in carcinomas of the salivary gland: Correlation with poor prognosis. *Cancer Res. 54*:5675–5682.

Ranzani, G.N., Pellegata, N.S., Previdere, C., Saragoni, A., Vio, A., Maltoni, M., and Amadori, D. 1990. Heterogeneous proto-oncogene amplification correlates with tumor progression and presence of metastases in gastric cancer patient. *Cancer Res. 50*:7811–7814.

Ross, J.S., Nazeer, T., Church, K., Amato, C., Figge, H., Rifkin, M.D., and Fisher, H.A. 1993. Contribution of *HER-2/neu* to tumor grade and DNA content analysis in the prediction of prostate carcinoma metastasis. *Cancer 72*:3020–3028.

Ross, J.S., Sheehan, C.E., Hayner-Buchan, A.M., Ambros, R.A., Kallakury, B.V., Kaufman, R., Fisher, H.A., and Muraca, P.J. 1997. Prognostic significance of *HER-2/neu* gene amplification status by fluorescence *in situ* hybridization of prostate carcinoma. *Cancer 79*:2162–2170.

Saffari, B., Jones, L.A., el-Naggar, A., Felix, J.C., George, J., and Press, M.F. 1995. Amplification and overexpression of *HER-2/neu* (c-erbB2) in endometrial cancers: Correlation with overall survival. *Cancer Res. 55*:5693–5698.

Schechter, A.L., Hung, M.C., Vaidnathan, L., Weinberg, R.A., Yang-Feng, T.L., Francke, U., Ullrich, A., and Coussens, L. 1985. The *neu* gene: An erbB-homologous gene distinct from and unlinked to the gene encoding the EGF receptor. *Science 229*:976–978.

Slamon, D.J., Godolphin, W., Jones, L.A., Holt, J.A., Wong, S.G., Keith, D.E., Levin, W.J., Stuart, S.G., Udove, J., and Ullrich, A. 1989. Studies of the *HER-2/neu* proto-oncogene in human breast and ovarian cancer. *Science 244*:707–712.

Zhau, H.E., Zhang, X., von Eschenbach, A.C., Scorsone, K., Babaian, R.J., Ro, J.Y., and Hung, M.C. 1990. Amplification and expression of the *c-erb B-2/neu* in proto-oncogene in human bladder cancer. *Mol. Carcinog. 3*:254–257.

Zhau, H.Y., Zhou, J., Symmans, W.F., Chen, B.Q., Chang, S.M., Sikes, R.A., and Chung, L.W. 1996. Transfected *neu* oncogene induces human prostate cancer metastasis. *Prostate 28*:73–83.

This Page Intentionally Left Blank

19

Calpain Proteases in Prostate Carcinoma

Alan Wells, Sourabh Kharait, Clayton Yates, and Latha Satish

Introduction

Tumor progression requires the disseminating cells to achieve four milestones: ability to detach from the primary tumor mass, migration to the ectopic site, avoidance of apoptosis in the foreign milieu, and proliferation. Although these cellular processes are under the control of numerous gene products and extracellular signals, the calpain family of intracellular limited proteases plays a central regulatory role at least in the first three steps (Goll *et al.*, 2003). Interest has grown in determining the role that these molecules might play in tumor progression as two developments have converged. First, there has been a recent burst in our understanding of the cell biologic and physiologic functions of calpains. Second, advances in medicinal chemistry have lead to the development of small molecule inhibitors of calpains.

The role of calpains in cell functioning has been reviewed (Goll *et al.*, 2003) and will only be briefly reiterated herein. Attachment to the primary cell mass is modulated by cadherin-mediated junctions. Calpain may directly target the cytoplasmic tail of cadherins to disrupt this homotypic adhesion (Rios-Doria *et al.*, 2002). During cell migration, calpains play a central role in forward spread and tail retraction (Glading *et al.*, 2002). These two cell behaviors appear regulated by membrane-associated calpains (Glading *et al.*, 2001; Tompa *et al.*, 2001). Cytosolic-, mitochondrial- and nuclear-localized calpains appear to contribute to survival and proliferation. Calpains were the first defined apoptosis mediators and are still found to induce apoptotic and necrotic cell death under certain circumstances (Wang, 2000). Last, the role of calpains in proliferation is more unsettled because conflicting reports claim calpains as either promoting or inhibiting cell cycling. Still, the central role of calpains in at least three key attributes of tumor progression is tantalizing for further evaluation.

Calpain Structure/Function

Calpains are a family of 13 distinct gene products with a general structure of a large subunit complexed to a single, shared 30-kDa small subunit (Goll *et al.*, 2003; Sorimachi and Suzuki, 2001). Of the 10 isoforms studied, most appear to be relatively cell- or tissue-type selective in expression. Two ubiquitous calpains, μ-calpain (*CAPN1*) and M-calpain (*CAPN2*), were named according to their relative requirement for calcium for activation *in vitro*, requiring micromolar and millimolar concentrations, respectively. It is these, the ubiquitous calpains, that have been implicated in

463

tumor progression in prostate and other carcinomas (Braun *et al.*, 1999; Mamoune *et al.*, 2003; Rios-Doria *et al.*, 2002).

External signals regulate the activities of the two ubiquitous calpains in cells. As such, simply determining tumor levels of calpains would yield little prognostic or theragnostic information. Even the one positive report (Rios-Doria *et al.*, 2002), relates only 1.2-fold to 1.4-fold changes in messenger ribonucleic acid (mRNA) levels—change levels that would be of little value in the evaluation of individual patients. The *in vitro* mechanism of activation is well described regarding calcium, with even the structural changes caused by calcium binding being defined (Moldoveanu *et al.*, 2002). However, the *in vivo* activation mechanisms have resisted ready dissection. μ-Calpain is thought to be activated by calcium fluxes downstream of various signals (Chaudhuri *et al.*, 2003; Glading *et al.*, 2002; Upadhya *et al.*, 2003). Calcium concentrations in sparks and puffs approach the levels required for at least partial activation of this calpain *in vitro* (Hirose *et al.*, 1999; Tompa *et al.*, 2002).

M-calpain is more of a challenge because the *in vitro* calcium levels for its activation are about 1000-fold higher. Reports have suggested that accessory proteins may contribute to activation of M-calpain (Glading *et al.*, 2002). However, there is scant evidence that these molecules directly activate M-calpain; nor does concomitantly localizing putative accessory molecules and M-calpain provide insight into activation status. Direct phosphorylation has been shown to modulate M-calpain activity in cells (Glading *et al.*, 2004; Shiraha *et al.*, 2002). Protein kinase A (PKA) mediated phosphorylation at amino acid 369/370 limits activation, whereas extracellularly regulated kinase (ERK)-mediated phosphorylation at serine 50 increases activity. These post-translational modifications hold promise for activation-specific antibodies that can be used in human tumor specimens, although phospho-serine/threonine-directed antibodies have yet to prove as specific or useful as phospho-tyrosine-directed antibodies.

Rapid autodegradation poses a further challenge for static analyses of calpain activity. Two small N-terminal clips present large subunit fragments of 78 kDa and 76 kDa (compared to the full-length 80 kDa). These specific cleavages might provide another static measure of activation, except that these are short-lived intermediaries that are not required for activity (Johnson and Guttmann, 1997).

Specific target fragments provide evidence of calpain activation during experimental challenges. Chief among these are talin, β–integrins, and focal adhesion kinase (FAK), along with various other adhesion and cell-cycle regulators. However, reagents to identify these and documentation that such fragments are calpain-specific are both lacking at present.

Calpain activity can be measured in live cells. Fluorescent molecules have been attached to quenching peptides that serve as targets for calpain (Glading *et al.*, 2000). Cells loaded with these permeant reporters can be evaluated for calpain-mediated fluorescence by controlling with calpain-selective inhibitors (with negative controls being proteosome inhibitors). An alternative method has been to load cells with a FRET (fluorescence resonance energy transfer) construct wherein the two fluorescent proteins are linked by a calpain-sensitive peptide sequence and one follows loss of FRET (Ono *et al.*, 2004; Vanderklish *et al.*, 2000).

MATERIALS AND METHODS

A number of methods have been derived to determine the presence and activation status of the two ubiquitous calpains. At the mRNA level, both gene microarray and *in situ* hybridization have been developed; the latter will be detailed herein. At the protein level, immunohistochemistry has been applied to tissues and immunoblotting and zymography has been applied to protein extracts; zymography will be described herein. Lastly, in living cells, such as freshly dispersed tumor cells, fluorescent substrates have been used to assess calpain activity and will be detailed herein. The other methods are simple derivatives of standard procedures and can be readily adapted from such procedures.

in situ Hybridization

MATERIALS

1. Digoxigenin (DIG) RNA labeling kit (Roche Molecular Diagnostics, Indianapolis, IN).
2. Qiagen mini-prep kit (Qiagen, Valencia, CA).
3. Ethanol.
4. Phosphate buffer saline (PBS).
5. Denhardt's Solution (Sigma, St. Louis, MO).
6. Dextran sulfate (Sigma).
7. 20X-SSC (saline-sodium chloride, 0.3 M; sodium citrate, 3 M).
8. Aurin tetra carboxylic acid (ATA) (Sigma).
9. Formamide (Sigma).
10. Herring sperm deoxyribonucleic acid (DNA) (Invitrogen, Carlsbad, CA).
11. Yeast transfer RNA (tRNA) (Invitrogen).

METHODS

In situ hybridization is a method to localize messenger RNA (mRNA) within the cell producing it by hybridizing the sequence of interest to a complementary strand of a nucleotide probe, performed on formalin-fixed and paraffin-embedded tissues.

1. The two different isoforms of calpain are cloned in either orientation into commercially available plasmoids DNA for subsequent DIG labeling.

2. Sense (control) and anti-sense RNA probes are obtained by using the DIG labeling RNA kit with SP6 RNA polymerase per manufacturer's instructions.

3. Labeled probes are purified by Qiagen miniprep kit.

4. The paraffin-embedded tissue sections are deparaffinized by standard procedures and then digested with 1 mg/ml of pronase for 10 min followed by washing in Tris/glycine buffer twice for 5 min.

5. After rinsing briefly in distilled water, the sections are dehydrated through 30%, 60%, 95%, and 100% ethanols for 1 min each step and air-dried.

6. Before hybridizing, the tissue sections are prehybridized with the prehybridization solution (1 M sodium phosphate solution, pH 7.6, 1% Denhardt's solution, dextran sulfate 5 g, ATA stock 50 mg/ml, 50 μl to a final volume of 50 ml) for at least 2–4 hr.

7. The prehybridization solution is drained and tissue sections are overlaid with 100 μl hybridization buffer (formamide/20% dextran sulfate; 1 M sodium phosphate, pH 7.4, 20X SSC, 1% Denhardt's solution, herring sperm DNA [10 mg/ml] and yeast tRNA [10 mg/ml], ATA stock [50 mg/ml]) containing 100 ng probe and incubated overnight at 37°C in a humidified chamber.

8. After hybridization, nonhybridized probes are removed using high-stringency washes.

9. The sections are incubated with anti-DIG–labeled secondary antibody conjugated with alkaline phosphatase. Staining reaction is performed using 5-bromo-4-chloro-3-indolyl phosphate/p-nitroblue tetrazolium chloride (BCIP/NBT) substrate and photographed.

Notes:

▲ If hybridization appears not to be isoform-specific, short oligonucleotide probes can be substituted for the full-length sense and anti-sense RNA probes. This will decrease sensitivity but improve specificity. Sequences that discriminate between human M-calpain and μ–calpain isoforms are ATGCCCGCCAT-GCTGCGT for CAPN2 and ATCTCCTCC-GACATCCTG for CAPN1.

▲ Platelets can act as a control for specificity because they express by and large only μ–calpain.

Calpain Zymography

MATERIALS

1. Purified porcine M-calpain and μ-calpain (Calbiochem, La Jolla, CA).

2. Calpain inhibitor I ALLN (Biomol, Plymouth Meeting, PA).

3. Casein (Sigma).

4. Gel casting reagents—acrylamide:bisacrylamide, TEMED (N, N, N′, N′-Tetramethylethylendiamine) ammonium per sulfate, 2-mercaptoethanol (2-ME), Tris buffer (Sigma).

5. Glycerol.

6. Bromophenol blue.

7. MOPS (morpholino propane sulfonic acid) (Sigma).

8. HEPES (*N*-2-hydroxyethyl-piperazine-*N*′-2-ethansulfonic acid) (Sigma).

9. Imidazole (Sigma).

10. EDTA (ethylenediamine tetra-acetic acid).

11. Calcium chloride.

12. Gel Code R Blue Stain Reagent (Coomassie blue) (Pierce, Rockford, IL).

METHODS

Casein zymography is used to determine the potential calpain activity in two ubiquitously expressed isoforms, M-calpain and μ-calpain.

1. Tumor specimen is either lysed directly as cells below (and insoluble debris removed by low speed centrifugation) or tumor cells are dissociated.

2. Following the appropriate treatments for experimental interventions (if desired for research), cells are lysed in 25 mM MOPS, pH 7.5; 10 mM ethyleneglycol-bis-N, N, N′, N′-tetra-acetic acid (EGTA), 10 mM EDTA, 5 mM 2-ME with 5 μg/ml of calpain-inhibitor-I to down-regulate the endogenous calpain production.

3. Equal volume of sample buffer (25 mM Tris pH 6.8, 25 mM EDTA, 50% glycerol, 50 mM 2-ME, 0.5% ([w/v] bromophenol blue) are added to the sample.

4. Gel casting:

   a. Separating Gel, 10% gel—1.8 ml of casein (7.5 mg/ml in 2X HEPES-imidazole buffer [HI buffer]) is copolymerized with 3.0 ml of 30% acrylamide:bisacrylamide (w/v), 1.08 ml 5X HI buffer, 100 μl 200 mM EGTA

with 3.02 ml water. 50 µl ammonium persulfate (10% w/v) and 10 µl TEMED were used to catalyze the polymerization.

  b. Stacking Gel

0.8 ml 30% acrylamide:bisacrylamide (w/v), 1.0 ml 5X HI buffer, 30 µl ammonium persulfate (10% w/v), and 6.0 µl TEMED with 3.2 ml water was poured into minigel casts (Bio Rad, Hercules, CA) (Croall *et al.*, 2002).

The casein gels are prerun with a buffer containing 1X HI, 5 mM EDTA, and 20 mM 2-ME for 15 min at 4°C.

5. Equal amounts of protein (~40 µg of sample) are loaded for each condition.

6. Samples are loaded with purified M-calpain and µ-calpain as migration controls in separate lanes, and the gels are run at 125 V for 3 hr in a cold room.

7. The gel is then removed and incubated in 20 mM MOPS (pH 7.5), 5 mM 2-ME with or without calcium (5 mM), for 24 hr at ambient temperature.

8. To visualize the areas of calpain proteolysis, the gel is stained with Coomassie blue.

9. Calpain activity is determined as white bands (loss of protein to bind Coomassie blue) in a blue background.

Note: This assay detects calpains that are activated by high levels of calcium. It does not detect any silenced calpains (mutated or post-translationally silenced). Furthermore, this does not measure calpain activity in the cell, only the potential pool of calpain that can be activated.

Fluorescent Reporters

BOC-LM-CMAC

MATERIALS

1. *t*-butoxycarbonyl-Leu-Met-chloromethyl-aminocoumarin (BOC-LM-CMAC) (Molecular Probes, Eugene, OR).
2. Fluoroscence microscopy.
3. Calpain inhibitor I (CI-I/ALLN) (Biomol).
4. Ionomycin (Sigma).
5. Human recombinant EGF (epidermal growth factor) (Collaborative Biomedical Products, Bedford, MA).

METHODS

BOC-LM-CMAC determines calpain activity in individual living cells for *in vivo* proteolysis (Glading *et al.*, 2000). This assay can be used to determine the calpain activity in cells both untreated and treated with factors, pharmacologic inhibitors, anti-sense oligonucleotides, and molecular constructs. The timing of this experimental treatments depends on the treatments used.

1. Tumors are dissociated and cells are plated on glass coverslips at 50–60% confluence.

2. Cells may be quiesced for treatment or examined directly.

3. The cells (drug-treated/transfected or controls) are then incubated for 20 min in the presence of 50 µM BOC-LM-CMAC. Positive control cells are treated with EGF (1 nM) for 10 min for M-calpain activation or ionomycin (10 µM) for 10 min for activation of both M-calpain and µ-calpain. Negative control cells are treated with CI-I/ALLN (5 µM) for 30 min.

4. After wet mounting of the coverslips on glass slides, the cells are observed for chloromethyl-aminocoumarin fluorescence using a fluorescent microscope (for Olympus, the filter is M-NUA filter).

5. Representative images of each slide are captured using a CCD camera. The image exposure settings are preset to remain identical within each experiment; thus one can directly compare fluorescence intensity within an experiment but not between experiments.

  Notes:

▲ The more confluent the cells are, the higher the background fluorescence.

▲ BOC-LM-CMAC is retained within the cells by conjugating with intracellular thiol groups. Cleavage of the substrate results in retention of the chloromethylaminocoumarin portion of the molecule in the cell and results in increased fluorescence.

▲ Initial test runs might be necessary to establish the exposure setting and camera gain settings to optimize discrimination between positive and negative fluorescence.

MAP2-DTAF

MATERIALS

1. MAP2 (microtubule associated protein 2) (Cytoskeleton, Denver, CO).
2. 5-([4,6-Dichlorotri-Azin-2-YL] Amino) Fluorescein (DTAF) (Sigma).
3. Prepacked Chromatography Columns (BioRad Laboratories Cat. No. 732-2010, Hercules, CA).
4. PIPES (piperazine-N,N′,-bis) (Sigma).
5. HEPES.
6. Calcium chloride.
7. Benzamidine (Sigma).

8. Dithioerythritol (DTE) (Sigma).
9. Dialysis cassettes (Pierce).
10. Spectrofluorometer.

METHODS

A second assay of calpain activity extant in live cells is the hydrolysis of MAP2-DTAF (microtubule associated protein 2) by cell lysates (Glading *et al.*, 2000; Tompa *et al.*, 1995).

1. Preparation of MAP2-DTAF

    a. Reconstitute the MAP2 vial in 100 µl of water and spin in microfuge tube.
    b. Remove 50 µl supernatant (can store the rest in –80°C for later preparation).
    c. To this 50 µl add 3.8 µl of pH buffer (2.65 g sodium carbonate, 0.125 g of benzamidine in 25 ml water).
    d. pH should be about 8.5.
    e. Add roughly 1 mg of DTAF and leave at 4°C for 30 min.
    f. Add 666 µl of equilibration buffer (0.26 g HEPES, 4 mg DTE, 0.9 mg PMSF, 0.8 mg benzamidine, 0.146 g sodium chloride in 50 ml) to the sample.
    g. Drain the size exclusion column and then add 15 ml of equilibration buffer and drain the column.
    h. Add sample and allow to enter the column.
    i. Add another 3 ml of equilibration buffer to the column and allow to run.
    j. Add another 1 ml of equilibration buffer and collect the fraction.
    k. Dialyze the collected fraction against the equilibration buffer overnight.

2. Wash cells twice with ice-cold PBS and lyse in 20 nM HEPES (pH 7.4), 10% glycerol, 0.1% Triton X-100, 500 mM sodium chloride, and 1 mM sodium vanadate.

3. After removing the cell debris by centrifugation, add 0.9 µg of DTAF-labeled MAP2 and 2 µl of 0.1 mM CaCl$_2$.

4. Measure fluorescence immediately at excitation and emission wavelength of 490 and 520 nm, respectively, for 3 min at room temperature. We use a Aminco-Bowman Series II spectrofluorometer (Spectronic Instruments Inc., Rochester, NY).

Notes:

▲ Extra DTAF-MAP2 can be stored at –20°C.
▲ Positive and negative controls can be attained as in the BOC assay mentioned earlier.

RESULTS AND DISCUSSION

The previous methods detect both presence of the calpains and their activation status. *In situ* hybridization denotes the presence of message for the two different isoforms dependent on detection sequence. Morphometric integration is most useful in determining the specific cells expressing these proteins because whole tissue determinations will mix normal cells with cancer cells. This information is particularly useful in demonstrating expression of either isoform in specific tumor cells.

Immunohistochemistry and immunofluorescence will demonstrate the presence of either isoform in the specific cells. The antibodies for both isoforms, but especially µ-calpain, must be optimized in each laboratory for best results because the antibodies are more robust for denatured forms. Localization of calpain isoforms may provide added information. Limiting the utility of this subcellular data is the pan-cellular distribution of both isoforms (Lane *et al.*, 1992) and the fact that localization-specified subsets of calpains can be activated in isolation (Glading *et al.*, 2001). Still the presence of calpains in cellular structures, such as adhesion plaques, suggests targets and functions. The new, intriguing question of exteriorized calpain (Dourdin *et al.*, 2001) is pursued best by morphometric calpain protein localization.

Combining message detection with protein determination is critical in evaluating activated calpains. Unactivated calpains are very long-lived with half-lives in excess of many days (Zhang *et al.*, 1996). However, on activation, calpains undergo autoproteolysis and subsequent rapid degradation (Glading *et al.*, 2000). Thus, lower protein levels of calpains may reflect either low expression or high level of activation; message levels best adjudicate these possibilities, with high message level in the presence of reduced protein levels, indicating ongoing calpain activation.

A newer method of calpain zymography (Croall *et al.*, 2002) readily distinguishes the two ubiquitous isoforms. This is one of the simplest means of determining the potential activatable calpain levels in cells. There are two caveats in using this method. First, this requires a sufficiently high level of protein at least 10^6 cells are required; for cancer specimens this means that the specimen will be mixed with stromal and other nontumor cell elements. Second, because the calpains must be activated in the gel, one cannot determine *in vivo* activation state. *Ex vivo* methods circumvent this latter limitation by determining the ability of cells or cell lysates to cleave reporters to their fluorescing states (Glading *et al.*, 2000; Glading *et al.*, 2002). However, these assays are semiquantitative at best and do not distinguish between different isoforms.

Calpain activity in individual cells can be detected by loading live cells with the cell-permeant fluorescent substrate BOC (Glading *et al*., 2000) (described earlier). Again, this is semi-quantitative at best (and only within an experimental series and not between series) and nondiscriminatory among the isoforms. The second assay described, the MAP2 assay that determines calpain activity *in vitro,* also does not distinguish between isoforms but rather is a semiquantitative assay; comparison between experiments requires normalization within each experiment. Both of these assays cannot be used on fixed or frozen tumor specimens, although it would be interesting to see if they can be adapted to live tumor sections to combine with morphometry. An advantage is that the fluorescence is scored for individual cells and can be performed on very small samples.

In sum, there are a number of methods which can be used to evaluate calpain presence and activity in cells and tumor tissues. Unfortunately, reagents have not been developed that can identify isoform-specific activation while preserving the tumor morphometry. Still, by combining these methods, one can approach functional tumor proteomics.

Calpain in Prostate Cancer Progression

Calpain has only recently been implicated in the progression of a number of tumors. Directly, increased calpain message levels have been shown in renal cell carcinoma (Braun *et al*., 1999), squamous cell carcinoma (Reichrath *et al*., 2003) (both μ-calpain), and prostate carcinoma (M-calpain) (Rios-Doria *et al*., 2002). Calpain activity and function were not pursued in these situations. Rather, calpains have been implicated due to their roles in adhesion, motility and survival/apoptosis.

Calpain activity leads to dissolution of focal adhesion and reduced adhesiveness to substratum (Glading *et al*., 2002). This can proceed through either M-calpain or μ-calpain (Bhatt *et al*., 2002; Satish *et al*., 2003). The diminished adhesiveness enables forward extension/ spreading as well as rear release during motility (Shiraha *et al*., 1999; Shiraha *et al*., 2002). Cell–cell adhesion (or cohesion) may also be modulated by calpain activity. In prostate and mammary epitheloid cells, calpain cleaves the cytosolic tail of E-cadherin proximal to (and releases) the catenin-binding motifs (Rios-Doria *et al*., 2002). This results in diminished cell–cell borders and subsequent separation. Although definitive data are still lacking, this molecular pathway may also occur in renal cells (Bush *et al*., 2000) and keratinocytes (Satish *et al*., 2003). Because motility and lessened cell–cell adhesion is required for tumor invasion and metastasis, calpain has been proposed as a key regulatory element in tumor invasion. One study addressed this by interfering with M-calpain activation using pharmacologic and molecular interventions (Mamoune *et al*., 2003). These inhibitory approaches limited tumor invasiveness *in vitro* and *in vivo*.

Calpain's role in apoptosis has been investigated in cancer as a point of exploitation (Nakagawa and Yuan, 2000; Wang, 2000). Blocking calpain prevents ischemia-induced apoptosis in hepatocellular carcinoma (Arora *et al*., 1996). This mirrors the findings of survival advantage by calpain inhibition during cerebral and other ischemic states (Wang, 2000). Recently, the question has become whether calpain can be activated in tumor cells to induce apoptosis. An initial study in a breast cancer cell line has been positive (Tagliarino *et al*., 2003). Obviously, because calpain is a pro-progression signaler via its effects on motility and adhesions, the apoptotic induction is qualitatively or quantitatively different. Further studies are needed to distinguish between these two options. A quantitative difference would have to be approached with caution because the lower end of the therapeutic window would be about the pro-progression activities. However, a qualitative distinction in calpain isoforms or mode of activation would open new avenues for rationale therapeutics.

The information on the involvement of calpain in the progression of tumors of the prostate and other solid organs is only in its infancy. Strong theoretic foundations are built on years of biochemical and cell biologic investigations that show the ubiquitous calpains as key regulators in the cellular behaviors critical to tumor progression and survival. The initial studies on calpains in tumor model systems or even human tumor biopsies are encouraging. It is expected that further investigations will soon determine whether calpains can be targeted to limit cancer spread or even to eliminate the tumors.

In conclusion, cancer progression to the invasive and metastatic state requires a tumor cell to detach from the primary mass, migrate to an ectopic site, and avoid apoptosis in its new environment. The limited intracellular proteases of the calpain family play roles in each of these cellular processes. Recent investigations have implicated modulation of calpain activity in prostate tumor progression. Detection of calpain signaling in human tumors provides a challenge in that calpain is regulated primarily in an epigenetic manner and thus is not readily amenable to static analyses of protein or message levels. Despite these obstacles, calpains should provide a novel target for adjuvant agents that seek to limit tumor dissemination. Thus, in the near future, the functioning of these proteases may need to be routinely determined in clinical specimens for personalized cancer therapy.

References

Arora, A.S., de Groen, P.C., Croall, D.E., Emori, Y., and Gores, G.J. 1996. Hepatocellular carcinoma cells resist necrosis during anoxia by preventing phospholipase-mediated calpain activation. *J. Cell. Physiol. 167*:434–442.

Bhatt, A., Kaverina, I., Otey, C., and Huttenlocher, A. 2002. Regulation of focal complex composition and disassembly by the calcium-dependent protease calpain. *J. Cell. Sci. 115*:3415–3425.

Braun, C., Engel, M., Seifert, M., Theisinger, B., Seitz, G., Zang, K.D., and Welter, C. 1999. Expression of calpain I messenger RNA in human renal cell carcinoma: Correlation with lymph node metastasis and histological type. *Intern. J. Cancer 84*:6–9.

Bush, K.T., Tsukamoto, T., and Nigam, S.K. 2000. Selective degradation of E-cadherin and dissolution of E-cadherin-catenin complexes in epithelial ischemia. *Am. J. Physiol. Renal Physiol. 278*:F847–852.

Chaudhuri, P., Colles, S.M., Damron, D.S., and Graham, L.M. 2003. Lysophosphatidylcholine inhibits endothelial cell migration by increasing intracellular calcium and activating calpain. *Arterioscl. Thromb. Vascul. Biol. 23*:218–223.

Croall, D.E., Moffett, K., and Hatch, H. 2002. Casein zymography of calpains using a 4-(2-hydroxyethyl)-1-piperazineethanesulfonic acid-imidazole buffer. *Analyt. Biochem. 304*:129–132.

Dourdin, N., Bhatt, A.K., Dutt, P., Greer, P.A., Arthur, J.S., Elce, J.S., and Huttenlocher, A. 2001. Myoblast fusion requires fibronectin degradation by exteriorized m-calpain. *J. Biol. Chem. 276*:48382–48388.

Glading, A., Bodnar, R.J., Reynolds, I.J., Shiraha, H., Satish, L., Potter, D.A., Blair, H.C. and Wells, A. 2004. Epidermal growth factor activates m-calpain (calpain 2), at least in part, by ERK-mediated phosphorylation. *Mol. Cell. Biol. 24*:2499–2512.

Glading, A., Chang, P., Lauffenburger, D.A., and Wells, A. 2000. Epidermal growth factor receptor activation of calpain is required for fibroblast motility and occurs via an ERK/MAP kinase signaling pathway. *J. Biol. Chem. 275*:2390–2398.

Glading, A., Lauffenburger, D.A., and Wells, A. 2002. Cutting to the chase: calpain proteases in cell migration. *Trends Cell Biol. 12*:46–54.

Glading, A., Uberall, F., Keyse, S.M., Lauffenburger, D.A., and Wells, A. 2001. Membrane proximal ERK signaling is required for M-calpain activation downstream of EGF receptor signaling. *J. Biol. Chem. 276*:23341–23348.

Goll, D.E., Thompson, V.F., Li, H., Wei, W., and Cong, J. 2003. The calpain system. *Physiol. Rev. 83*:731–801.

Hirose, K., Kadowaki, S., Tanabe, M., Takeshima, T., and Iino, M. 1999. Spatiotemporal dynamics of inositol 1,4,5-trisphosphate that underlies complex Ca^{2+} mobilization patterns. *Science 284*:1527–1530.

Johnson, G.V.W., and Guttmann, R.P. 1997. Calpains: Intact and active? *Bioessays 19*:1011–1018.

Lane, R.D., Allan, D.M., and Mellgren, R.L. 1992. A comparison of the intracellular distribution of μ-calpain, m-calpain,

and calpastatin in proliferating human A431 cells. *Exp. Cell Res. 203*:5–16.

Mamoune, A., Luo, J.-H., Lauffenburger, D.A., and Wells, A. 2003. m-Calpain as a target for limiting prostate cancer invasion. *Cancer Res. 63*:4632–4640.

Moldoveanu, T., Hosfield, C.M., Lim, D., Elce, J.S., Jia, Z., and Davies, P.L. 2002. A Ca(2+) switch aligns the active site of calpain. *Cell 108*:649–660.

Nakagawa, T., and Yuan, J. 2000. Cross-talk between two cysteine protease families. Activation of caspase-12 by calpain in apoptosis. *J. Cell Biol. 150*:887–894.

Ono, Y., Kakinuma, K., Torii, F., Irie, A., Nakagawa, K., Labeit, S., Abe, K., Suzuki, K., and Sorimachi, H. 2004. Possible regulation of conventional calpain system by skeletal muscle-specific calpain, p94. *J. Biol. Chem. 279*:2761–2771.

Reichrath, J., Welter, C., Mitschele, T., Classen, U., Meineke, V., Tilgen, W., and Seifert, M. 2003. Different expression patterns of calpain isozymes I and II (CAPN1 and 2) in squamous cell carcinomas (SCC) and basal cell carcinomas (BCC) of human skin. *J. Pathol. 199*:509–516.

Rios-Doria, J., Day, K.C., Kuefer, R., Rashid, M.G., Chinnaiyan, A.M., Rubin, M.A., and Day, M.L. 2002. The role of calpain in the proteolytic cleavage of E-cadherin in prostate and mammary epithelial cells. *J. Biol. Chem. 278*:1372–1379.

Satish, L., Yager, D., and Wells, A. 2003. ELR-negative CXC chemokine IP-9 as a mediator of epidermal-dermal communication during wound repair. *J. Invest. Dermatol. 120*:1110–1117.

Shiraha, H., Glading, A., Chou, J., Jia, Z., and Wells, A. 2002. Activation of m-calpain (calpain II) by epidermal growth factor is limited by PKA phosphorylation of m-calpain. *Mol. Cell. Biol. 22*:2716–2727.

Shiraha, H., Gupta, K., Glading, A., and Wells, A. 1999. IP-10 inhibits epidermal growth factor-induced motility by decreasing epidermal growth factor receptor-mediated calpain activity. *J. Cell Biol. 146*:243–253.

Sorimachi, H., and Suzuki, K. 2001. The structure of calpain. *J. Biochem. 129*:653–664.

Tagliarino, C., Pink, J.J., Reinicke, K.E., Simmers, S.M., Wuerzberger-Davis, S.M., and Boothman, D.A. 2003. μ-Calpain activation in β-lapachone-mediated apoptosis. *Cancer Biol. Ther. 2*:141–152.

Tompa, P., Emori, Y., Sorimachi, H., Suzuki, K., and Friedrich, P. 2001. Domain III of calpain is a Ca^{+2}-regulated phospholipid-binding domain. *Biochem. Biophys. Res. Comm. 280*:1333–1339.

Tompa, P., Mucsi, Z., Orosz, G., and Friedrich, P. 2002. Calpastatin subdomains A and C are activators of calpain. *J. Biol. Chem. 277*:9022–9026.

Tompa, P., Schad, E., Baki, A., Alexa, A., Batke, J., and Friedrich, P. 1995. An ultrasensitive, continuous fluorometric assay for calpain activity. *Analyt. Biochem. 228*:287–293.

Upadhya, G.A., Topp, S.A., Hotchkiss, R.S., Anagli, J., and Strasberg, S.M. 2003. Effect of cold preservation on intracellular calcium concentration and calpain activity in rat sinusoidal endothelial cells. *Hepatology 37*:313–323.

Vanderklish, P.W., Krushel, L.A., Holst, B.H., Gally, J.A., Crossin, K.I., and Edelman, G.M. 2000. Marking synaptic activity in dendritic spines with a calpain substrate exhibiting fluorescence resonance energy transfer. *Proc. Nat. Acad. Sci. USA 97*:2253–2258.

Wang, K.K. 2000. Calpain and caspase: Can you tell the difference? *Trends Neurosci. 23*:20–26.

Zhang, W., Lane, R.D., and Mellgren, R.L. 1996. The major calpain isozymes are long-lived proteins. Design of an antisense strategy for calpain depletion in cultured cells. *J. Biol. Chem. 271*:18825–18830.

This Page Intentionally Left Blank

20

Immunohistochemical Expression of Raf Kinase Inhibitor Protein in Prostate Carcinoma

Zheng Fu, Lizhi Zhang, and Evan T. Keller

Introduction

Prostate cancer is the most commonly diagnosed cancer in American men and is the second leading cause of cancer mortality in men older than age 50 years in the United States (Landis *et al*., 1998). Prostate cancer is a multifactorial disease with genetic and environmental components involved in its etiology (Steinberg *et al*., 1990). It is characterized by heterogeneous growth patterns that range from slow-growing tumors to very rapid-growing, highly metastatic tumors (Steinberg *et al*., 1990). The heterogeneity of prostate cancer makes it difficult to define genetic markers for this disease, although see Part III, Chapter 1, in this volume for additional information.

Standard therapy relies on removing or blocking the action of androgens (Koivisto *et al*., 1996). In most cases, this therapy results in a regression of the cancer. However, a portion of the cancer eventually relapses and metastasizes to other organs (Cude *et al*., 1999). Unfortunately, current medical therapy for metastatic prostate cancer is for the most part inefficient. As a result, the mortality rate of men with prostate cancer is still significant, second only to that of lung cancer among men in North America (Coffey, 1993; Cude *et al*., 1999). Clearly, detection of prostate cancer alone provides little prognostic value; the aggressiveness and

extent of the cancer must be measured as well before any treatment decisions can be made. In other words, it is critical to accurately distinguish those histologically localized cancers that will complete metastatic process from those that will remain indolent. Although we have abundant clinical and biologic information on prostate cancer, a large percentage of apparently resectable and theoretically curable lesions are found to be more advanced at the time of resection than envisaged, resulting in a substantial failure rate after attempted curative surgery, and relapse rate has approached 20–30% (Heimann and Hellman, 2000; Lerner *et al*., 1991; Schellhammer, 1988). To improve the ability to diagnose a potentially curable cancer or treat metastatic prostate cancer, an increasing understanding of the genes that regulate the metastatic ability of cells is required.

Metastasis is defined as the formation of progressively growing secondary tumor foci at sites discontinuous from the primary lesion (Welch and Rinker-Schaeffer, 1999). The metastatic process is a complex cascade. In brief, a metastatic cancer cell must escape from the primary tumor, enter the circulation, arrest in the microcirculation, invade a different tissue compartment, and then grow at that secondary site. Currently, metastasis is poorly understood at the molecular and mechanistic levels in most cancers,

Handbook of Immunohistochemistry and in situ Hybridization of Human Carcinomas,
Volume 2: Molecular Pathology, Colorectal Carcinoma, and Prostate Carcinoma

471

including prostate cancer. Theoretically, it should be possible to block metastasis by inhibiting a single gene that is required for the completion of any one of these steps in the metastatic cascade (Welch and Rinker-Schaeffer, 1999). In support of this possibility is the evidence that loss-of-function of specific genes called metastasis suppressor genes is an important event during the progression toward a malignant phenotype (Dong *et al.*, 1996; Steeg *et al.*, 1988; Yang *et al.*, 1997; Yoshida *et al.*, 2000).

We previously used gene array analysis to identify genes whose expression changes during the transition from nonmetastatic to metastatic prostate cancer by comparing the transcriptome (i.e., the complete collection of messenger ribonucleic acids [mRNAs] and their alternatively spliced forms) of a nonmetastatic human prostate cancer cell line (LNCaP) with that of a metastatic prostate cancer cell line that was derived from it (C4-2B) (Fu *et al.*, 2002). One gene product whose expression was lower in the metastatic cell line than in the nonmetastatic cell line was Raf kinase inhibitor protein (RKIP).

RKIP is a soluble 23-kDa basic cytosolic protein. It was initially characterized as phosphatidylethanolamine-binding protein (PEBP) expressed in brain tissue (Perry *et al.*, 1994; Tohdoh *et al.*, 1995). It has binding affinity for phosphatidylethanolamine (Bernier *et al.*, 1986), nucleotides like GTP (guanosine triphosphate) and GDP (guanosine diphosphate), small GTP-binding proteins, and other hydrophobic ligands (Bucquoy *et al.*, 1994). In the rat, PEBP was described to be involved in the differentiation of neurons (Ojika *et al.*, 2000). Besides the central nervous system, it is also expressed in a wide variety of tissues including spleen, testis, prostate, breast, ovary, muscle, and stomach (Bollengier and Mahler, 1988; Frayne *et al.*, 1999). In most cases the physiologic role of the protein *in vivo* is not yet understood. Recently, PEBP was assigned another name as Raf kinase inhibitor protein along with the novel function discovered lately (Yeung *et al.*, 1999). These authors discovered that RKIP suppressed the mitogen-activated protein kinase signaling by binding to Raf-1 and disrupted the physical interaction between Raf-1 and MEK. Later studies suggested additional roles of RKIP in the signaling machinery. For example, RKIP inhibited the signal transduction pathway that activated the transcription factor nuclear factor kappa B (NF-κB) (Yeung *et al.*, 2001).

This chapter reports on the molecular pathology we performed to characterize the function of RKIP in prostate cancer carcinoma. Particularly, the immuno-histochemistry (IHC) technology used to validate our observations in clinical setting will be discussed in detail. The role of RKIP in diagnostic and prognostic application will also be discussed.

MATERIALS

Immunohistochemistry on Frozen Sections

EQUIPMENT:

1. Slide holder.
2. Tissue-Tek container.
3. Microscope slides (FisherBrand, Cat. No. 12-550-19, Fisher Scientific, Pittsburgh, PA).
4. Dako Autostainer (DakoCytomation, Carpinteria, CA).

MATERIALS

1. Xylene. (Store stock in flammable cabinet.)
2. 100% Ethanol. (Store stock in flammable cabinet.)
3. 95% Ethanol. (Store stock in flammable cabinet.)
4. 70% Ethanol. Add 300 µl of deionized water to 700 µl of 100% ethanol. (Store stock in flammable cabinet.)
5. 10X Tris buffered saline with Tween-20 (TBST) (Dako, Cat. No. S3006) Add 1 L of TBST to 9 L of deionized water. Good for 5 days at room temperature. Otherwise, store TBST at 2–8ºC.
6. Biotin Blocking system (Dako, Cat. No. X0590).
7. Dako Envision + labeled polymer, peroxidase for use with rabbit antibody (Dako, Cat. No. K4003).
8. Peroxidase blocking reagent (Dako, Cat. No. S2001).
9. Liquid diaminobenzidine (DAB) + for enhanced sensitivity (Dako, Cat. No. K3468). Add 1 drop of the liquid DAB+ per ml of buffered substrate.
10. Protocol Harris hematoxylin-mercury free (acidified) (FisherBrand, Cat. No. 23-245-678).
11. Primary antibody rabbit polyclonal anti-RKIP antibody (1:400 dilution: Upstate, Cat. No. 07-137).
12. Permount (FisherBrand, Cat. No. SP15-100).

Immunohistochemistry on Permanent Formalin-Fixed and Paraffin-Embedded Sections

EQUIPMENT

1. DAKO Autostainer.
2. Slide holder.
3. Tissue-Tek container.
4. Microscope slides (FisherBrand, Cat. No. 12-550-19).
5. Tender pressure cooker (Nordicaware).

MATERIALS

1. Xylene. (Store stock in flammable cabinet.)

2. 100% Ethanol. (Store stock in flammable cabinet.)

3. 95% Ethanol. (Store stock in flammable cabinet.)

4. 70% Ethanol. Add 300 µl of deionized water to 700 µl of 100% ethanol. (Store stock in flammable cabinet.)

5. 10X TBST (Dako, Cat. No. S3006). Add 1 L of TBST to 9 L of deionized water. It is good for 5 days at room temperature. Otherwise, store TBST at 2–8ºC.

6. 10 mM Citrate buffer (pH 6.0) (FisherBrand, Cat. No. A104-500).

7. Dako Envision+ labeled polymer, peroxidase for use with rabbit antibody (Dako, Cat. No. K4003).

8. Peroxidase blocking reagent (Dako, Cat. No. S2001).

9. Liquid DAB+ for enhanced sensitivity (Dako, Cat. No K3468). Add 1 drop of the liquid DAB+ per ml of buffered substrate.

10. Protocol Harris hematoxylin-mercury free (acidified) (FisherBrand, Cat. No. 23-245-678).

11. Primary antibody rabbit polyclonal anti RKIP antibody (1:400 dilution; Upstate, Cat. No. 07-137).

12. Permount (FisherBrand, Cat. No. SP15-100).

METHODS

Immunohistochemistry on Frozen Sections

1. Cut 6 µm thick sections in a cryochamber and place on microscope slides.

2. Place slides in cold acetone for 15 min.

3. Remove slides and allow to air-dry for 30 sec to 1 min and place in TBST buffer.

Note: Antigen retrieval procedures are not performed on frozen tissue sections. Formalin (fixatives) has not been used and antigen sites should be available.

4. Add peroxidase blocking reagent for 5 min.

5. Rinse with TBST.

6. Add Avidin from Biotin Blocking system for 10 min and rinse with TBST buffer.

7. Add Biotin from Biotin Blocking system for 10 min and rinse with TBST buffer.

8. Incubate slides in 4ºC refrigerator overnight with primary antibody (rabbit anti-RKIP at 1:600 dilution). TBST buffer only on negative control slide.

9. Rinse with TBST buffer.

10. Add Envision+ labeled polymer, peroxidase for use with rabbit antibody for 30 min.

9. Rinse with TBST buffer.

10. Cover slides with DAB+ chromagen for 5 min.

11. Rinse with water.

12. Counterstain with hematoxylin for 12–15 sec.

13. Rinse with water.

14. Dehyrate slides by running them through the following solutions:

    a. 70% Ethanol for 2 min.

    b. 95% Ethanol for 2 min.

    c. 100% Ethanol for 2 min.

17. Incubate 3 times in Xylene for 2 min each.

18. Coverslip in Permount and label slides.

Note: For a positive control, immunostain a frozen section of normal prostate previously used to optimize the procedure. For a negative control, TBST buffer replaces the primary antibody (anti-RKIP antibody).

Immunohistochemistry on Permanent Formalin-Fixed and Paraffin-Embedded Sections

1. Cut 6 µm thick sections with a microtome and place on microscope slides.

2. Place all slides in Tissue-Tek slide holder. Heat the slide in oven at 60ºC for 20 min, which allows the paraffin to melt.

3. Deparaffinize and rehydrate slides by running them through the following solutions:

    a. Xylene for 2 min.

    b. Xylene for 2 min.

    c. Xylene for 2 min.

    d. 100% Ethanol for 2 min.

    e. 95% Ethanol for 2 min.

    f. 70% Ethanol for 2 min.

    g. Deionized water for 2 min.

4. Place slides in TBST buffer until ready for antigen retrieval.

5. Transfer slides to 10 mM citrate buffer (pH 6.0) in the pressure cooker.

6. Microwave on high for 10 min and then let it cool down for 10 min.

7. Rinse with deionized water and place the slides in TBST buffer.

8. Add peroxidase blocking reagent for 5 min.

9. Rinse with TBST buffer.

10. Incubate slides in 4ºC refrigerator overnight with primary antibody (rabbit anti-RKIP at 1:400 dilution). TBST buffer only on negative control slide.

11. Rinse with TBST buffer.

12. Add Envision+ labeled polymer, peroxidase for use with rabbit antibody for 30 min.

13. Rinse with TBST buffer.

14. Cover slides with DAB+ chromagen for 5 min.
15. Rinse with water.
16. Counterstain with hematoxylin for 12–15 sec.
17. Rinse with water.
18. Dehydrate slides by running them through the following solutions:
   a. 70% Ethanol for 2 min.
   b. 95% Ethanol for 2 min.
   c. 100% Ethanol for 2 min.
19. Incubate 3 times in xylene for 2 min each.
20. Coverslip in Permount and label slides.

Note: For a positive control, immunostain a formalin-fixed and paraffin-embedded section of normal prostate previously used to optimize the procedure. For a negative control, TBST buffer replaces the primary antibody (anti-RKIP antibody).

RESULTS AND DISCUSSION

Our previous gene array findings revealed that RKIP expression is decreased in the human C4-2B metastatic prostate cancer cell line compared to its nonmetastatic parental LNCaP cell line (Fu *et al.*, 2002). We measured the levels of RKIP mRNA and protein in these cell lines to validate the previous observation. Real-time reverse transcription polymerase chain reaction (RT-PCR) demonstrated that *RKIP* mRNA level was fourfold to fivefold lower in C4-2B than that in LNCaP, whereas immunoblot showed that the protein level was ~threefold lower in the C4-2B cells compared to the LNCaP cells. These results validated our prior gene array findings that *RKIP* expression is decreased in metastatic prostate cancer cells.

To characterize the function of RKIP during prostate cancer progression, we modulated RKIP expression in prostate cancer cells. We stably transfected sense *RKIP* vector or empty expression vector for control) into C4-2B cells to increase endogenous *RKIP* expression and stably transfected LNCaP cells with antisense *RKIP* vector (or empty expression vector for control) to decrease *RKIP* level. As expected, the sense *RKIP* vector-transfected C4-2B cells demonstrated increased RKIP expression, and the antisense *RKIP* vector-transfected LNCaP cells showed decreased *RKIP* expression compared with the corresponding control vector-transfected cells.

To determine whether modulation of *RKIP* expression influenced the tumorigenic properties of the prostate cancer cells, we measured the *in vitro* proliferation rates and the ability to form colonies in soft agar of the various LNCaP and C4-2B transfected clones. There were no statistically significant differences in *in vitro* proliferation rates or colony-forming abilities between the control vector-transfected and sense *RKIP* vector-transfected (C4-2B) or antisense

RKIP vector-transfected (LNCaP) clones (one-way analysis of variance [ANOVA]). These data suggest that modulation of *RKIP* expression has no effect on these two primary tumorigenic properties of human prostate cancer cells.

Because invasion is one of the most important steps of the metastatic cascade, we next examined whether *RKIP* expression is associated with cancer cell invasiveness. Accordingly, we evaluated the invasive ability of the parental (i.e., untransfected) LNCaP and C4-2B cells and their stable transfectants using an *in vitro* invasion assay. Increasing the expression of RKIP with sense *RKIP* complementary deoxyribonucleic acid (cDNA) decreased *in vitro* invasive ability of C4-2B cells between 30% and 50%. In agreement with this observation, decreasing *RKIP* expression in LNCaP cells by stable transfection with the antisense *RKIP* vector increased their *in vitro* invasive ability by 30–100%. These results demonstrated that decreased *RKIP* expression is associated with the increased invasive capability of prostate cancer cells *in vitro*.

Based on the observation from *in vitro* studies that RKIP inhibits the invasiveness but not the growth of tumor cells, it is tempting to speculate that *RKIP* may function as a metastasis suppressor gene in prostate cancer. To test this hypothesis, we examined the effect of *RKIP* expression on the metastatic phenotype of C4-2B cells. Accordingly, we implanted pooled clones of C4-2B cells stably transfected with either control vector or sense *RKIP* vector into the dorsal lobes of the prostate in SCID mice and monitored prostate tumorigenesis over 10 weeks. Two independent experiments and their pooled results are reported in Table 14. Ten weeks after the orthotopic implantation of tumor cells into the mice, there was not a statistically significant difference in the mean size of the primary (i.e., prostate) tumors in mice injected with sense *RKIP* vector-transfected C4-2B cells and mice injected with control vector-transfected C4-2B cells (Table 14). However, restoring *RKIP* expression in the C4-2B cells resulted in a decreased number of animals with metastases compared to those animals receiving the control-transfected cells (Table 14). Furthermore, the average number of lung metastases among the three mice that received the C4-2B cells with *RKIP* cDNA and developed lung metastases was 85% (95% CI = 37.9–96.4%) lower than that among mice injected with control vector-transfected C4-2B cells (Table 14).

To confirm that RKIP expression was modulated as expected *in vivo*, we examined RKIP expression levels in the mouse primary tumors and metastases. In this case, Western Blot analysis would not be a beneficial approach to detect the differential expression of RKIP because RKIP is expressed in a wide variety of tissues, and any

Table 14 Metastatic Ability of C4-2B Cells after Stable Transfection with Human Raf Kinase Inhibitor Protein (RKIP) Complementary Deoxyribonucleic Acid[a]

Cell Lines	No. Mice With Primary Tumor Formation/Total No. Mice	Tumor Size (cm³)	No. of Mice with Lung Metastases/Total No. Mice	No. of Lung Metastases/Mouse
Experiment 1				
C4-2B-(+)	5/5	2.25, 1.69, 1.87, 1.61, 1.43	5/5	15, 79, 17, 12, 18
C4-2B-ssRKIP	5/5	2.14, 2.06, 2.36, 2.35, 1.59	2/5	0, 4, 0, 3, 0
Experiment 2				
C4-2B-(+)	5/5	1.71, 2.81, 2.17, 2.63, 1.80	5/5	12, 54, 18, 17, 21
C4-2B-ssRKIP	5/5	2.59, 2.20, 1.44, 2.49, 1.70	1/5	0, 5, 0, 0, 0
Total (95% CI)				
C4-2B-(+)	10/10	2.20 (1.89–2.51)[b]	10/10	26.30 (10.45–42.15)[c]
C4-2B-ssRKIP	10/10	2.09 (1.81–2.37)[d]	3/10[e]	4.00 (1.52–6.48)[f]

[a]Spontaneous metastatic ability was determined by orthotopic injections of 1×10^6 C4-2B cells stably transfected with either empty vector (C4-2B-(+)) or a vector that constitutively expressed RKIP (C4-2B-ssRKIP) into 10 mice each (five mice in two separate experiments) and quantification of the number of lung metastases that developed 10 weeks after injection. (Lung sections were stained for prostate specific antigen expression to identify lung metastases derived from the orthotopic prostate tumors.)

[b]Mean tumor size (95% confidence interval).

[c]Mean number of lung metastases per mice among those that developed lung metastases (95% confidence interval).

[d]$P = .4727$ compared with C4-2B-(+) cells (Wilcoxon rank sum test).

[e]$P = .0031$ compared with C4-2B-(+) cells (Fisher's exact test).

[f]$P = .0139$ compared with C4-2B-(+) cells (Wilcoxon rank sum test).

This table was excerpted from Fu, Z., Smith, P.C., Zhang, L., Rubin, M.A., Dunn, R.L., Yao, Z., and Keller, E.T. 2003. Effect of raf kinase inhibitor protein expression on suppression of prostate cancer metastasis. *J. Natl. Cancer Inst. 95*:878-888 by permission of Oxford University Press.

undesired lesion in the tumor tissue may affect the results significantly. Therefore, we used IHC to monitor the *in situ* expression of RKIP protein, which provided several advantages including: 1) increased sensitivity and 2) precise localization of the protein expression within the tissues. Primary tumors derived from sense *RKIP* vector-transfected C4-2B cells displayed more RKIP expression than primary tumors derived from control vector-transfected C4-2B cells. Because the lung normally expressed RKIP, we could identify RKIP expression in the lung sections. RKIP was not detectable in the lung metastases of mice bearing primary tumors derived from control vector-transfected C4-2B cells. Furthermore, although RKIP expression was readily detectable in the primary tumors derived from sense *RKIP* vector-transfected C4-2B cells, RKIP was not detectable in the few metastases that developed from those tumors. The latter observation demonstrates that RKIP expression was down-regulated in the metastases. Collectively, these results provide strong evidence that RKIP expression is associated with the suppression of prostate cancer metastasis in a mouse model.

Metastasis-suppressor genes encode proteins that suppress the formation of overt metastases without affecting the growth rate of the primary tumor (Yoshida *et al.*, 2000). These genes differ from tumor suppressor genes, which suppress the growth of primary tumors. In our studies, the results of two independent experiments demonstrated that increased RKIP expression is associated with the decreased development of metastases but not with any changes in the growth of the primary tumors. These key data suggest that RKIP functions as a suppressor of metastasis. This finding is further strongly supported by the identification, based on IHC studies, that all metastases that formed in the murine models had diminished RKIP expression compared with the primary tumor, even when the primary tumor overexpressed RKIP. In addition, these results are in agreement with the discovery of an unidentified prostate cancer metastasis suppressor gene on chromosome 12q24 (Ichikawa *et al.*, 2000) because *RKIP* is located at 12q24.22 (International Radiation Mapping Consortium) (Deloukas *et al.*, 1998).

To date, relatively few metastasis suppressor genes have been identified. For most, the mechanism through which they prevent metastasis is not clear. Our studies have identified a novel anti-metastatic function for RKIP, a protein that regulates a signaling transduction cascade (Raf/MEK/ERK cascade). This is the first study to document the association between a cancer progression-associated decreased expression of a molecule that inhibits signal transduction and increased metastasis. These results suggest that inhibition of the MEK/ERK pathway may prevent metastasis. Consistent with our findings, several other groups reported that activation of the MAP kinase signal transduction pathway is increased as prostate cancer progresses to a more advanced and androgen-independent disease (Brunet *et al*., 1994; Price *et al*., 1999).

To examine the potential relevance of these findings to clinical prostate cancer, we used an immunohistochemical approach to detect RKIP in human normal and cancerous prostate tissue samples. Cases of clinically localized prostate cancer were obtained from radical prostatectomy at the time of surgery from patients with prostate cancer treated at the University of Michigan. The fresh radical prostatectomy specimens were frozen in liquid nitrogen within 30 min after surgical excision, as previously described (Rashid *et al*., 2001). Histologic confirmation of both tumor and normal regions of each prostate gland and tumor grading was performed using a previously described protocol (Rubin *et al*., 2002). Cases of prostate cancer metastases were obtained from the Rapid Autopsy Program at the University of Michigan. Metastases found in a variety of tissues were obtained from patients who died of widely metastatic prostate cancer and were frozen in liquid nitrogen within 4 hr of the patient's death, using a rapid autopsy method, as previously described (Rubin *et al*., 2002). All samples were grossly trimmed to ensure that 95% of the sample represented the desired lesion. Histologic sections stained with hematoxylin and eosin (H&E) and prostate specific antigen (PSA) confirmed that they were of malignant nature and of prostate cancer origin. The tissues harvested from autopsies yielded high-quality tumor samples, as evidenced by excellent preservation seen by light microscopy, strong PSA immunostaining, and the successful development of xenografts (Rubin *et al*., 2002). All the samples were electronically registered using a relational database (Microsoft Access). This allowed for convenient and rapid access of all samples.

We examined 10 cases of noncancerous prostate tissue, 12 cases of localized primary prostate cancer, and 22 cases of prostate cancer metastases derived from a variety of organs including lymph node, liver, lung, bone, adrenal, dura, bladder, thyroid, and stomach.

Strong positive staining for RKIP was observed in the cytoplasm of the epithelial cells in the prostate. There was no staining for the stroma in the prostate. RKIP was detectable in all noncancerous prostate tissue (n = 10) and primary prostate cancers (n = 12) examined but was undetectable in all prostate cancer metastases examined (n = 22) (Figure 77 and Table 15). Specifically, RKIP expression level was highest in benign tissue, lower in cancerous tissue (declining with increasing Gleason score), and absent in metastases (p <.001, Mantel-Haneszel Chi-square test).

An important source for false-negative staining is the variability in tissue quality, including effects of tissue fixation and surgical procedures, which may cause protein denaturation and antigen loss. Prostate glands in transition zone are especially susceptible to such variability. However, in our studies IHC was performed on frozen specimens, which provided a high degree of sensitivity and specificity (Press *et al*., 1994). Furthermore, clinical samples of metastases were obtained by using a rapid autopsy method that allowed us to obtain high-quality tissues shortly after the patient's death. To further rule out the possibility that the inability to detect RKIP in the metastatic samples was the result of the quality of the sections, samples were stained for PSA, which showed positive staining. In addition to the ability to detect PSA in these metastatic samples using IHC, we could not detect RKIP in the cancer cells of a liver metastases; however, we could detect RKIP in the surrounding normal liver (Figure 77, metastasis), demonstrating that RKIP protein is detectable using IHC in these samples. Taken together, results from IHC staining on clinical prostate cancer samples provide clinical evidence of a strong correlation between diminished RKIP expression and the occurrence of metastasis, which confirms the validity of our novel findings that *RKIP* functions as a metastasis suppressor gene in prostate cancer in the true clinical situation.

IHC has wide application in research and clinical pathology. Particularly, IHC is valuable to oncology for many reasons including: 1) tumor classification, 2) identification of the origin of a metastasis, 3) establishment of the malignancy of a lesion in some cases, and 4) determination of prognostic and predictive factor in oncology. For example, IHC has been reported to be a reliable and valid method for assessing estrogen receptor status and predicting clinical outcome (Barnes *et al*., 1996; Harvey *et al*., 1999). Dhanasekaran *et al*. (2001) have used IHC to validate hepsin, a transmembrane serine protease, and pim-1, a serine/threonine kinase, as prognostic biomarkers in prostate cancer.

Our current studies provided another line of evidence showing that IHC is of great help in validating our
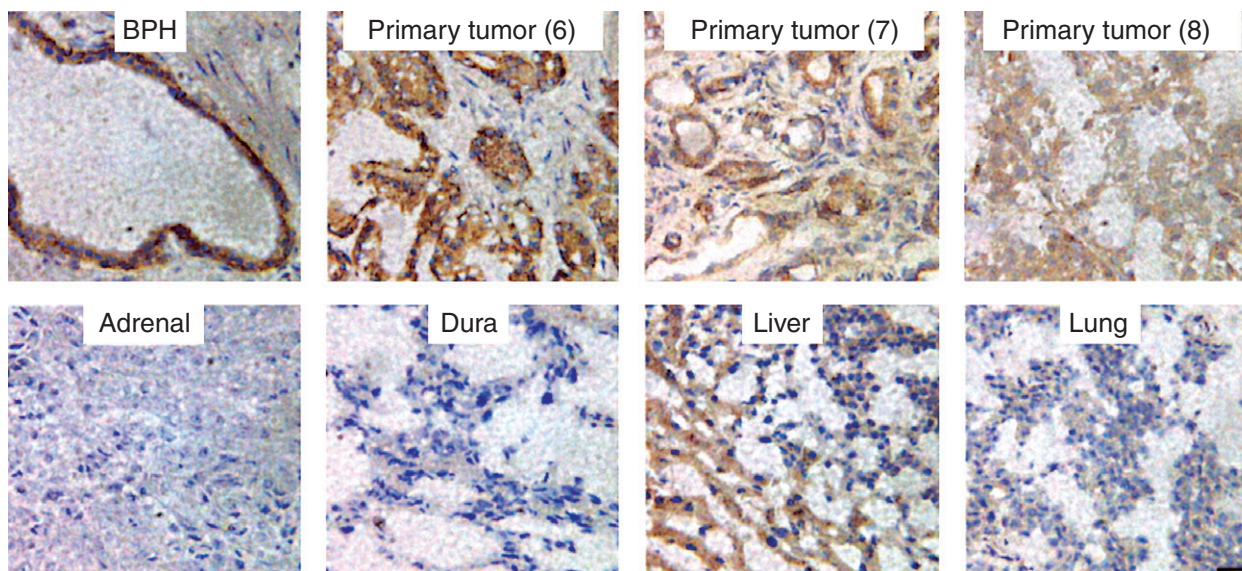
Figure 77 Immunohistochemical staining for Raf kinase inhibitor protein (RKIP) in human clinical tissue samples. Frozen samples of benign prostatic hyperplasia (BPH); primary prostate tumors (Gleason score indicated in parentheses); and prostate cancer metastases from the adrenal glands, duras, livers, and lungs were stained with a goat polyclonal antibody against RKIP (*brown*) and counterstained with hematoxylin. Note in the liver metastasis sample that the tumor (*upper right*) was negative for RKIP expression, whereas the normal surrounding liver tissue (*lower left*) was positive for RKIP expression. The scale bar indicates 50 μm. (This figure was excerpted from Fu, Z., Smith, P.C., Zhang, L., Rubin, M.A., Dunn, R.L., Yao, Z., and Keller, E.T. 2003. Effect of raf kinase inhibitor protein expression on suppression of prostate cancer metastasis. *J. Natl. Cancer Inst. 95*:878–888 by permission of Oxford University Press).

research findings in the clinical settings. In these studies, IHC of tissues from patients indicated RKIP expression in normal prostate and primary prostate cancers; however, its expression was undetectable in all metastases examined. It stands to reason that assessment of RKIP expression status may be used as both a prognostic and a predictive marker for metastatic prostate cancer. By combining this technology with clinical studies on the correlation of RKIP expression level with clinical outcomes, our findings will help

identify the ideal method for stratifying patients with prostate cancer into prognostic and optimal therapeutic groups.

After radical prostatectomy, prostate cancer recurs in an estimated 15–30% of patients, suggesting that undetected disease may have spread beyond the prostate gland before surgery (Han *et al.*, 2001; Roberts *et al.*, 2001). Kattan *et al.* (1998) have developed useful nomograms that use pretreatment clinical and pathologic parameters to help evaluate the likelihood

Table 15 Expression of Raf Kinase Inhibitor Protein (RKIP) in Human Prostate Tissues[a]

Tissue	Gleason Score	No. Samples Evaluated	RKIP Expression[b]
Noncancerous prostate	—	10	3.0 (3.0–3.0)
Primary prostate cancer	6	2	2.0 (2.0–2.0)
	7	6	1.75 (1.0–2.0)
	8	4	0.5 (0.0–1.0)
Prostate cancer metastases[c]	—	22	0.0 (0.0–0.0)

[a]The staining intensity was scored as follows: 0 (negative), 1 (weak), 2 (moderate), or 3 (strong); — = not applicable.

[b]Reported as median deviation (range).

[c]The metastases we examined were obtained from lymph nodes (three cases), bone (three cases), liver (seven cases), lung (two cases), adrenal (two cases), and other (five cases).

This table was excerpted from Fu, Z., Smith, P.C., Zhang, L., Rubin, M.A., Dunn, R.L., Yao, Z., and Keller, E.T. 2003. Effect of raf kinase inhibitor protein expression on suppression of prostate cancer metastasis. *J. Natl. Cancer Inst. 95*:878–888 by permission of Oxford University Press.

of disease-free survival after radical prostatectomy or brachytherapy (Ross *et al.*, 2001) for localized prostate cancer. However, these models demonstrated good but not excellent associations with outcomes, as reviewed by Ross *et al.* (2001). Therefore, given the limitations of current nomograms to accurately predict which patients have the greatest risk for developing aggressive prostate cancer, identifying and characterizing biomarkers for prostate cancer to aid the pretreatment evaluation of patients with clinically localized prostate cancer are in great demand. Such biomarkers could help identify patients at high risk for metastatic progression at early stages and thus enter into appropriate clinical trials for systemic therapies.

RKIP could be a potential candidate for such biomarkers. It would be interesting to evaluate RKIP expression level in conjunction with clinical and pathologic parameters associated with prostate cancer progression, including tumor stage, Gleason score, and PSA level to determine whether measuring RKIP amounts (in prostate specimens) might have potential as a molecular determinant of prostate cancer progression and metastasis. In addition, based on the knowledge obtained from this study, targeting MAP kinase signaling pathway may be a potential choice for treatment of metastatic prostate cancer. In conclusion, with the aid of IHC technology, we have identified *RKIP* as a clinical relevant novel prostate cancer metastasis suppressor gene that suppresses metastatic process in prostate cancer. Studies in the future will likely be directed toward use of RKIP in diagnostic, prognostic, and therapeutic ends.

Acknowledgments

References

Barnes, D.M., Harris, W.H., Smith, P., Millis, R.R., and Rubens, R.D. 1996. Immunohistochemical determination of oestrogen receptor: Comparison of different methods of assessment of staining and correlation with clinical outcome of breast cancer patients. *Br. J. Cancer 74*:1445–1451.

Bernier, I., Tresca, J.P., and Jolles, P. 1986. Ligand-binding studies with a 23 kDa protein purified from bovine brain cytosol. *Biochim. Biophys. Acta 871*:19–23.

Bollengier, F., and Mahler, A. 1988. Localization of the novel neuropolypeptide h3 in subsets of tissues from different species. *J. Neurochem. 50*:1210–1214.

Brunet, A., Pages, G., and Pouyssegur, J. 1994. Constitutively active mutants of MAP kinase kinase (MEK1) induce growth factor-relaxation and oncogenicity when expressed in fibroblasts. *Oncogene 9*:3379–3387.

Bucquoy, S., Jolles, P., and Schoentgen, F. 1994. Relationships between molecular interactions (nucleotides, lipids and proteins) and structural features of the bovine brain 21-kDa protein. *Eur. J. Biochem. 225*:1203–1210.

Coffey, D.S. 1993. Prostate cancer. An overview of an increasing dilemma. *Cancer 71*:880–886.

Cude, K.J., Dixon, S.C., Guo, Y., Lisella, J., and Figg, W.D. 1999. The androgen receptor: Genetic considerations in the development and treatment of prostate cancer. *J. Mol. Med. 77*:419–426.

Deloukas, P., Schuler, G.D., Gyapay, G., Beasley, E.M., Soderlund, C., Rodriguez-Tome, P., Hui, L., Matise, T.C., McKusick, K.B., Beckmann, J.S., Bentolila, S., Bihoreau, M., Birren, B.B., Browne, J., Butler, A., Castle, A.B., Chiannikulchai, N., Cleer, C., Day, P. J., Dehejia, A., Dibling, T., Drouot, N., Duprat, S., Fizames, C., and Bentley, D.R., 1998. A physical map of 30,000 human genes. *Science 282*:744–746.

Dhanasekaran, S.M., Barrette, T.R., Ghosh, D., Shah, R., Varambally, S., Kurachi, K., Pienta, K.J., Rubin, M.A., and Chinnaiyan, A.M. 2001. Delineation of prognostic biomarkers in prostate cancer. *Nature 412*:822–826.

Dong, J.T., Suzuki, H., Pin, S.S., Bova, G.S., Schalken, J.A., Isaaca, W.B., Barrett, J.C., and Isaaca, J.T. 1996. Downregulation of the KAI1 metastasis suppressor gene during the progression of human prostatic cancer infrequently involves gene mutation or allelic loss. *Cancer Res. 56*:4387–4390.

Frayne, J., Ingram, C., Love, S., and Hall, L. 1999. Localisation of phosphatidylethanolamine-binding protein in the brain and other tissues of the rat. *Cell Tissue Res. 298*:415–423.

Fu, Z., Dozmorov, I., and Keller, E.T. 2002. Osteoblasts produce soluble factors that induce a gene expression pattern in non-metastatic prostate cancer cells, similar to that found in bone metastatic prostate cancer cells. *Prostate 51 :*10–20.

Han, M., Partin, A.W., Pound, C.R., Epstein, J.I., and Walsh, P.C. 2001. Long-term biochemical disease-free and cancer-specific survival following anatomic radical retropubic prostatectomy. The 15-year Johns Hopkins experience. *Urol. Clin. North Am. 28 :*555–565.

Harvey, J.M., Clark, G.M., Osborne, C.K., and Allred, D.C. 1999. Estrogen receptor status by immunohistochemistry is superior to the ligand-binding assay for predicting response to adjuvant endocrine therapy in breast cancer. *J. Clin. Oncol. 17*:1474–1481.

Heimann, R., and Hellman, S. 2000. Clinical progression of breast cancer malignant behavior: What to expect and when to expect it. *J. Clin. Oncol. 18*:591–599.

Ichikawa, T., Hosoki, S., Suzuki, H., Akakura, K., Igarashi, T., Furuya, Y., Oshimura, M., Rinker-Schaeffer, C.W., Nihei, N., Barrett, J.C., Isaacs, J.T., and Ito, H. 2000. Mapping of metastasis suppressor genes for prostate cancer by microcell-mediated chromosome transfer. *Asian J. Androl. 2*:167–171.

Kattan, M.W., Eastham, J.A., Stapleton, A.M., Wheeler, T.M., and Scardino, P.T. 1998. A preoperative nomogram for disease recurrence following radical prostatectomy for prostate cancer. *J. Natl. Cancer. Inst. 90*:766–771.

Koivisto, P., Visakorpi, T., and Kallioniemi, O.P. 1996. Androgen receptor gene amplification: A novel molecular mechanism for endocrine therapy resistance in human prostate cancer. *Scand. J. Clin. Lab. Invest. Suppl. 226*:57–63.

Landis, S.H., Murray, T., Bolden, S., and Wingo, P.A. 1998. Cancer statistics, 1998. *CA Cancer J. Clin. 48*:6–29.

Lerner, S.P., Seale-Hawkins, C., Carlton, C.E., Jr., and Scardino, P.T. 1991. The risk of dying of prostate cancer in patients with clinically localized disease. *J. Urol. 146*:1040–1045.

Ojika, K., Mitake, S., Tohdoh, T., Appel, S.H., Otsuka, Y, Katada, E., and Matsukawa, N. 2000. Hippocampal cholinergic neu-rostimulating peptides (HCNP). *Prog. Neurobiol. 60*:37–83.

Perry, A.C., Hall, L., Bell, A.E., and Jones, R. 1994. Sequence analysis of a mammalian phospholipid-binding protein from testis and epididymis and its distribution between spermatozoa and extracellular secretions. *Biochem. J. 301*:235–242.

Press, M.F., Hung, G., Godolphin, W., and Slamon, D.J. 1994. Sensitivity of HER-2/neu antibodies in archival tissue samples: Potential source of error in immunohistochemical studies of oncogene expression *Cancer Res. 54*:2771–2777.

Price, D.T., Rocca, G.D., Guo, C., Ballo, M.S., Schwinn, D.A., and Luttrell, L.M. 1999. Activation of extracellular signal-regulated kinase in human prostate cancer. *J. Urol. 162*:1537–1542.

Rashid, M.G., Sanda, M.G., Vallorosi, Rios-Doria, J., Rubin, M.A., and Day, M.L. 2001. Posttranslational truncation and inactiva-tion of human E-cadherin distinguishes prostate cancer from matched normal prostate. *Cancer Res. 61*:489–492.

Roberts, S.G., Blutte, M.L. Bergstralh, E.J., Slezak, J.M., and Zincke, H. 2001. PSA doubling time as a predictor of clinical progression after biochemical failure following radical prosta-tectomy for prostate cancer. *Mayo Clin. Proc. 76*:576–581.

Ross, P.L., Scardino, P.T., and Kattan, M.W. 2001. A catalog of prostate cancer nomograms. *J. Urol. 165*:1562–1568.

Rubin, M.A., Zhou, M., Dhanasekaran, S.M., Varambally, S., Barrette, T.R., Sanda, M.G., Pienta, K.J., Ghosh, D., and Chinnaiyan, A.M. 2002. alpha-Methylacyl coenzyme A racemase as a tissue biomarker for prostate cancer. *JAMA 287*:1662–1670.

Schellhammer, P.F. 1988. Radical prostatectomy. Patterns of local failure and survival in 67 patients. *Urology 31*:191–197.

Steeg, P.S., Bevilacqua, G., Kopper, L., Thorgeirsson, U.P., Talmadge, J.E., Liotta, L.A., and Sobel, M.E. 1988. Evidence for a novel gene associated with low tumor metastatic potential. *J. Natl. Cancer. Inst. 80*:200–204.

Steinberg, G.D., Carter, B.S., Beaty, T.H., Childs, B., and Walsh, P.C. 1990. Family history and the risk of prostate cancer. *Prostate 17*:337–347.

Tohdoh, N., Tojo, S., Agui, H., and Ojika, K. 1995. Sequence homology of rat and human HCNP precursor proteins, bovine phosphatidylethanolamine-binding protein and rat 23-kDa pro-tein associated with the opioid-binding protein. *Brain Res. Mol. Brain Res. 30*:381–384.

Welch, D.R., and Rinker-Schaeffer, C.W. 1999. What defines a useful marker of metastasis in human cancer? *J. Natl. Cancer Inst. 91*:1351–1353.

Yang, X., Welch, D.R., Phillips, K.K., Weissman, B.E., and Wei, L.L. 1997. KAI1, a putative marker for metastatic potential in human breast cancer. *Cancer Lett. 119*:149–155.

Yeung K., Seitz, T., Li, S., Janosch, P., McFerran, B., Kaiser, C., Fee, F., Katsanakis, K.D., Rose, D.W., Mischak, H, Sedivy, J.M., and Kolch, W. 1999. Suppression of Raf-1 kinase activity and MAP kinase signaling by RKIP. *Nature 401*:173–177.

Yeung, K.C., Rose, D.W., Dhillon, A.S., Yaros, D., Gustafsson, M., Chatterjee, D., McFerran, B., Wyche, J., Kolch, W., and Sedivy, J.M. 2001. Raf kinase inhibitor protein interacts with NF-kappaB-inducing kinase and TAK1 and inhibits NF-kappaB activation. *Mol. Cell Biol. 21*:7207–7217.

Yoshida, B.A., Sokoloff, M.M., Dubauskas, Z., Chekmareva, M.A., Christiano, T.R., Stadler, W.M., and Rinker-Schaeffer, C.W. 2000. Metastasis-suppressor genes: A review and perspective on an emerging field. *J. Natl. Cancer Inst. 92*:1717–1730.

This Page Intentionally Left Blank

Index

481